

Gas Turbine Engineering Handbook

Second Edition

Gas Turbine Engineering Handbook

Second Edition

Meherwan P. Boyce

Managing Partner, The Boyce Consultancy

Fellow, American Society of Mechanical Engineers

Fellow, Institute of Diesel and Gas Turbine Engineers, U.K.



Gulf Professional Publishing
an imprint of Butterworth-Heinemann

Boston Oxford Auckland Johannesburg Melbourne New Delhi

Gulf Professional Publishing is an imprint of Butterworth–Heinemann.

Copyright © 2002 by Butterworth–Heinemann. Previously copyrighted © 1995. 1982 by Gulf Publishing Company, Houston, Texas

 A member of the Reed Elsevier group

All rights reserved.

No part of this publication may be reproduced, stored in a retrieval system, or transmitted in any form or by any means, electronic, mechanical, photocopying, recording, or otherwise, without the prior written permission of the publisher.

 Recognizing the importance of preserving what has been written, Butterworth–Heinemann prints its books on acid-free paper whenever possible.



Butterworth–Heinemann supports the efforts of American Forests and the Global ReLeaf program in its campaign for the betterment of trees, forests, and our environment.

Library of Congress Cataloging-in-Publication Data

Boyce, Meherwan P.

Gas turbine engineering handbook / Meherwan P. Boyce. – 2nd ed.
p. cm.

Includes bibliographical references and index.

ISBN 0-88415-732-6 (alk. paper)

1. Gas-turbines—Handbooks, manuals, etc. I. Title.

TJ778 .B67 2001
621.43'3—dc21

2001040520

British Library Cataloguing-in-Publication Data

A catalogue record for this book is available from the British Library.

Illustration Credit: Unless otherwise cited, the illustrations appearing in this book are supplied courtesy and used with the permission of the Turbomachinery Laboratories, Department of Mechanical Engineering, Texas A&M University, College Station, Texas 77843. These illustrations were published and are copyright © by the Turbomachinery Laboratories in the annual proceedings of their Turbomachinery Symposia.

The publisher offers special discounts on bulk orders of this book.

For information, please contact:

Manager of Special Sales

Butterworth–Heinemann

225 Wildwood Avenue

Woburn, MA 01801-2041

Tel: 781-904-2500

Fax: 781-904-2620

For information on all Gulf Professional Publishing publications available, contact our World Wide Web home page at: <http://www.gulfpp.com>

10 9 8 7 6 5 4 3 2 1

Printed in the United States of America

To the memory of my father, Phiroz H.J. Boyce

Contents

| | |
|--|------------|
| Preface | x |
| Preface to the First Edition | xii |
| Foreword to the First Edition | xiv |

Part I Design: Theory and Practice

| | |
|--|------------|
| 1 An Overview of Gas Turbines | 3 |
| Gas Turbine Cycle in the Combined Cycle or Cogeneration Mode. Gas Turbine Performance. Gas Turbine Design Considerations. Categories of Gas Turbines. Major Gas Turbine Components. Fuel Type. Environmental Effects. Turbine Expander Section. Materials. Coatings. Gas Turbine Heat Recovery. Supplementary Firing of Heat Recovery Systems. Bibliography. | |
| 2 Theoretical and Actual Cycle Analysis. | 58 |
| The Brayton Cycle. Actual Cycle Analysis. Summation of Cycle Analysis. A General Overview of Combined Cycle Plants. Compressed Air Energy Storage Cycle. Power Augmentation. Summation of the Power Augmentation Systems. Bibliography. | |
| 3 Compressor and Turbine Performance Characteristics | 112 |
| Turbomachine Aerothermodynamics. The Aerothermal Equations. Efficiencies. Dimensional Analysis. Compressor Performance Characteristics. Turbine Performance Characteristics. Gas Turbine Performance Computation. Bibliography. | |
| 4 Performance and Mechanical Standards. | 141 |
| Major Variables for a Gas Turbine Application. Performance Standards. Mechanical Parameters. Application of the Mechanical Standards to the Gas Turbine. Specifications. Bibliography. | |
| 5 Rotor Dynamics | 178 |
| Mathematical Analysis. Application to Rotating Machines. Critical Speed Calculations for Rotor Bearing Systems. Electromechanical Systems and Analogies. Campbell Diagram. Bibliography. | |

Part II Major Components

| | |
|--|------------|
| 6 Centrifugal Compressors. | 221 |
| Centrifugal Compressor Components. Centrifugal Compressor Performance. Compressor Surge. Process Centrifugal Compressors. Bibliography. | |
| 7 Axial-Flow Compressors | 275 |
| Blade and Cascade Nomenclature. Elementary Airfoil Theory. Laminar-Flow Airfoils. Cascade Test. Velocity Triangles. Degree of Reaction. Radial Equilibrium. Diffusion Factor. The Incidence Rule. The Deviation Rule. Compressor Stall. Performance Characteristics of an Axial-Flow Compressor. Stall Analysis of an Axial-Flow Compressor. Bibliography. | |
| 8 Radial-Inflow Turbines | 319 |
| Description. Theory. Turbine Design Considerations. Losses in a Radial-Inflow Turbine. Performance of a Radial-Inflow Turbine. Bibliography. | |

9 Axial-Flow Turbines337
Turbine Geometry. Impulse Turbine. The Reaction Turbine. Turbine Blade Cooling Concepts. Turbine Blade Cooling Design. Cooled-Turbine Aerodynamics. Turbine Losses. Bibliography.

10 Combustors370
Combustion Terms. Combustion. Combustion Chamber Design. Fuel Atomization and Ignition. Typical Combustor Arrangements. Air Pollution Problems. Catalytic Combustion. Bibliography.

Part III Materials, Fuel Technology, and Fuel Systems

11 Materials411
General Metallurgical Behaviors in Gas Turbines. Gas Turbine Materials. Compressor Blades. Forgings and Nondestructive Testing. Coatings. Bibliography.

12 Fuels436
Fuel Specifications. Fuel Properties. Fuel Treatment. Heavy Fuels. Cleaning of Turbine Components. Fuel Economics. Operating Experience. Heat Tracing of Piping Systems. Types of Heat-Tracing Systems. Storage of Liquids. Bibliography.

Part IV Auxiliary Components and Accessories

13 Bearings and Seals.469
Bearings. Bearing Design Principles. Tilting-Pad Journal Bearings. Bearing Materials. Bearing and Shaft Instabilities. Thrust Bearings. Factors Affecting Thrust-Bearing Design. Thrust-Bearing Power Loss. Seals. Noncontacting Seals. Mechanical (Face) Seals. Mechanical Seal Selection and Application. Seal Systems. Associated Oil System. Dry Gas Seals. Bibliography.

14 Gears521
Gear Types. Factors Affecting Gear Design. Manufacturing Processes. Installation and Initial Operation. Bibliography.

Part V Installation, Operation, and Maintenance

15 Lubrication541
Basic Oil System. Lubricant Selection. Oil Sampling and Testing. Oil Contamination. Filter Selection. Cleaning and Flushing. Coupling Lubrication. Lubrication Management Program. Bibliography.

16 Spectrum Analysis558
Vibration Measurement. Taping Data. Interpretation of Vibration Spectra. Subsynchronous Vibration Analysis Using RTA. Synchronous and Harmonic Spectra. Bibliography.

17 Balancing.584
Rotor Imbalance. Balancing Procedures. Application of Balancing Techniques. User's Guide for Multiplane Balancing. Bibliography.

18 Couplings and Alignment605
Gear Couplings. Metal Diaphragm Couplings. Metal Disc Couplings. Turbomachinery Uprates. Shaft Alignment. Bibliography.

19 Control Systems and Instrumentation634
 Control Systems. Condition Monitoring Systems. Monitoring Software. Implementation of a Condition Monitoring System. Life Cycle Costs. Temperature Measurement. Pressure Measurement. Vibration Measurement. Auxiliary System Monitoring. The Gas Turbine. Failure Diagnostics. Mechanical Problem Diagnostics. Summary. Bibliography.

20 Gas Turbine Performance Test692
 Introduction. Performance Codes. Flow Straighteners. Gas Turbine Test. Gas Turbine. Performance Curves. Performance Computations. Gas Turbine Performance Calculations. Plant Losses. Bibliography.

21 Maintenance Techniques.722
 Philosophy of Maintenance. Training of Personnel. Tools and Shop Equipment. Turbomachinery Cleaning. Hot-Section Maintenance. Compressor Maintenance. Bearing Maintenance. Coupling Maintenance. Rejuvenation of Used Turbine Blades. Repair and Rehabilitation of Turbomachinery Foundations. Large Machinery Startup Procedure. Typical Problems Encountered in Gas Turbines. Bibliography.

Appendix: Equivalent Units.778

Index.782

About the Author799

Preface

Gas Turbine Engineering Handbook discusses the design, fabrication, installation, operation, and maintenance of gas turbines. The second edition is not only an updating of the technology in gas turbines, which has seen a great leap forward in the 1990s, but also a rewriting of various sections to better answer today's problems in the design, fabrication, installation, operation, and maintenance of gas turbines. The new advanced gas turbines have firing temperatures of 2600°F (1427°C), and pressure ratios exceeding 40:1 in aircraft gas turbines, and over 30:1 in industrial turbines. Advances in materials, and coatings have spurred this technology, and the new edition has treated this new area in great detail. The emphasis on low NO_x emissions from gas turbines has led to the development of a new breed of dry low NO_x combustors, which are dealt in depth in this new edition. The second edition deals with an upgrade of most of the applicable codes both in the area of performance and mechanical standards.

The book has been written to provide an overall view for the experienced engineer working in a specialized aspect of the subject and for the young engineering graduate or undergraduate student who is being exposed to the turbomachinery field for the first time. The book will be very useful as a textbook for undergraduate turbomachinery courses as well as for in-house company training programs related to the petrochemical, power generation, and offshore industries.

The use of gas turbines in the petrochemical, power generation, and offshore industries has mushroomed in the past few years. In the past 10 years, the power industry has embraced the Combined Cycle Power Plants and the new high efficiency gas turbines are at the center of this growth segment of the industry. This has also led to the rewriting of chapters 1 and 2. It is to these users and manufacturers of gas turbines that this book is directed. The book will give the manufacturer a glimpse of some of the problems associated with his equipment in the field and help the user to achieve maximum performance efficiency and high availability of his gas turbines.

I have been involved in the research, design, operation, and maintenance of gas turbines since the early 1960s. I have also taught courses at the graduate and undergraduate level at the University of Oklahoma and Texas A&M University, and now, in general, to the industry. There have been over 3,000 students through my courses designed for the engineer in the field representing over 400 companies from around the world. Companies have

used the book, and their comments have been very influential in the updating of material in the second edition. The enthusiasm of the students associated with these courses gave me the inspiration to undertake this endeavor. The many courses I have taught over the past 25 years have been an educational experience for me as well as for the students. The Texas A&M University Turbomachinery Symposium, which I had the privilege to organize and chair for over eight years and be part of the Advisory Committee for 30 years, is a great contributor to the operational and maintenance sections of this book. The discussions and consultations that resulted from my association with highly professional individuals have been a major contribution to both my personal and professional life as well as to this book.

In this book, I have tried to assimilate the subject matter of various papers (and sometimes diverse views) into a comprehensive, unified treatment of gas turbines. Many illustrations, curves, and tables are employed to broaden the understanding of the descriptive text. Mathematical treatments are deliberately held to a minimum so that the reader can identify and resolve any problems before he is ready to execute a specific design. In addition, the references direct the reader to sources of information that will help him to investigate and solve his specific problems. It is hoped that this book will serve as a reference text after it has accomplished its primary objective of introducing the reader to the broad subject of gas turbines.

I wish to thank the many engineers whose published work and discussions have been a cornerstone to this work. I especially thank all my graduate students and former colleagues on the faculty of Texas A&M University without whose encouragement and help this book would not be possible. Special thanks go to the Advisory Committee of the Texas A&M University Turbomachinery Symposium and Dr. M. Simmang, Chairman of the Texas A&M University Department of Mechanical Engineering, who were instrumental in the initiation of the manuscript.

I wish to acknowledge and give special thanks to my wife, Zarine, for her readiness to help and her constant encouragement throughout this project.

I sincerely hope that this new edition will be as interesting to read as it was for me to write and that it will be a useful reference to the fast-growing field of turbomachinery.

Finally, I would like to add that the loss of my friend and mentor Dr. C.M. Simmang who has written the foreword to the first edition of this book is a deep loss not only to me but also to the engineering educational community and to many of his students from Texas A&M University.

Meherwan P. Boyce
Houston, Texas

Preface to the First Edition

Gas Turbine Engineering Handbook discusses the design, fabrication, installation, operation, and maintenance of gas turbines. The book has been written to provide an overall view for the experienced engineer working in a specialized aspect of the subject and for the young engineering graduate or undergraduate student who is being exposed to the turbomachinery field for the first time. The book will be very useful as a textbook for undergraduate turbomachinery courses as well as for in-house company training programs related to the petrochemical, power generation, and offshore industries.

The use of gas turbines in the petrochemical, power generation, and offshore industries has mushroomed in the past few years. It is to these users and manufacturers of gas turbines that this book is directed. The book will give the manufacturer a glimpse of some of the problems associated with his equipment in the field and help the user to achieve maximum performance efficiency and high availability of his gas turbines.

I have been involved in the research, design, operation, and maintenance of gas turbines since the early 1960s. I have also taught courses at the graduate and undergraduate level at the University of Oklahoma and Texas A&M University, and now, in general, to the industry. The enthusiasm of the students associated with these courses gave me the inspiration to undertake this endeavor. The many courses I have taught over the past 15 years have been an educational experience for me as well as for the students. The Texas A&M University Turbomachinery Symposium, which I had the privilege to organize and chair for seven years, is a great contributor to the operational and maintenance sections of this book. The discussions and consultations that resulted from my association with highly professional individuals have been a major contribution to both my personal and professional life as well as to this book.

In this book, I have tried to assimilate the subject matter of various papers (and sometimes diverse views) into a comprehensive, unified treatment of gas turbines. Many illustrations, curves, and tables are employed to broaden the understanding of the descriptive text. Mathematical treatments are deliberately held to a minimum so that the reader can identify and resolve any problems before he is ready to execute a specific design. In addition, the references direct the reader to sources of information that will help him to investigate and solve his specific problems. It is hoped that this book will

serve as a reference text after it has accomplished its primary objective of introducing the reader to the broad subject of gas turbines.

I wish to thank the many engineers whose published work and discussions have been a cornerstone to this work. I especially thank all my graduate students and former colleagues on the faculty of Texas A&M University without whose encouragement and help this book would not be possible. Special thanks go to the Advisory Committee of the Texas A&M University Turbomachinery Symposium and Dr. C.M. Simmang, Chairman of the Texas A&M University Department of Mechanical Engineering, who were instrumental in the initiation of the manuscript, and to Janet Broussard for the initial typing of the manuscript. Acknowledgment is also gratefully made of the competent guidance of William Lowe and Scott Becken of Gulf Publishing Company. Their cooperation and patience facilitated the conversion of the raw manuscript to the finished book. Lastly, I wish to acknowledge and give special thanks to my wife, Zarine, for her readiness to help and her constant encouragement throughout this project.

I sincerely hope that this book will be as interesting to read as it was for me to write and that it will be a useful reference to the fast-growing field of turbomachinery.

Meherwan P. Boyce
Houston, Texas

Foreword to the First Edition

The Alexandrian scientist Hero (circa 120 B.C.) would hardly recognize the modern gas turbine of today as the outgrowth of his aeolipile. His device produced no shaft work—it only whirled. In the centuries that followed, the principle of the aeolipile surfaced in the windmill (A.D. 900–1100) and again in the powered roasting spit (1600s). The first successful gas turbine is probably less than a century old.

Until recently, two principal obstacles confronted the design engineer in his quest for a highly efficient turbine: (1) the temperature of the gas at the nozzle entrance of the turbine section must be high, and (2) the compressor and the turbine sections must each operate at a high efficiency. Metallurgical developments are continually raising inlet temperatures, while a better understanding of aerodynamics is partly responsible for improving the efficiency of centrifugal and axial-flow compressors and radial-inflow and axial-flow turbines.

Today there are a host of other considerations and concerns which confront design and operating engineers of gas turbines. These include bearings, seals, fuels, lubrication, balancing, couplings, testing, and maintenance. *Gas Turbine Engineering Handbook* presents necessary data and helpful suggestions to assist engineers in their endeavors to obtain optimum performance for any gas turbine under all conditions.

Meherwan Boyce is no stranger to gas turbines. For more than a decade he has been highly active with the techniques of turbomachinery in industry, academics, research, and publications. The establishment of the annual Texas A&M University Turbomachinery Symposium can be numbered among his major contributions to the field of turbomachinery. Dr. Boyce subsequently directed the following seven prior to forming his own consulting and engineering company. The tenth symposium was held recently and attracted more than 1,200 engineers representing many different countries.

This important new handbook comes to us from an experienced engineer at a most opportune time. Never has the cost of energy been greater, nor is there a promise that it has reached its price ceiling. Dr. Boyce is aware of these concerns, and through this handbook he has provided the guide and means for optimum use of each unit of energy supplied to a gas turbine. The handbook should find its place in all the reference libraries of those

engineers and technicians who have even a small responsibility for design and operation of gas turbines.

*Clifford M. Simmang
Department of Mechanical Engineering
Texas A&M University
College Station, Texas*

Part I

Design: Theory and Practice

1

An Overview of Gas Turbines

The gas turbine is a power plant, which produces a great amount of energy for its size and weight. The gas turbine has found increasing service in the past 40 years in the power industry both among utilities and merchant plants as well as the petrochemical industry, and utilities throughout the world. Its compactness, low weight, and multiple fuel application make it a natural power plant for offshore platforms. Today there are gas turbines, which run on natural gas, diesel fuel, naphtha, methane, crude, low-Btu gases, vaporized fuel oils, and biomass gases.

The last 20 years has seen a large growth in Gas Turbine Technology. The growth is spearheaded by the growth of materials technology, new coatings and new cooling schemes. This, with the conjunction of increase in compressor pressure ratio, has increased the gas turbine thermal efficiency from about 15% to over 45%.

Table 1-1 gives an economic comparison of various generation technologies from the initial cost of such systems to the operating costs of these systems. Because distributed generation is very site specific the cost will vary and the justification of installation of these type of systems will also vary. Sites for distributed generation vary from large metropolitan areas to the slopes of the Himalayan mountain range. The economics of power generation depend on the fuel cost, running efficiencies, maintenance cost and first cost, in that order. Site selection depends on environmental concerns such as emissions, and noise, fuel availability, and size and weight.

Gas Turbine Cycle in the Combined Cycle or Cogeneration Mode

The utilization of gas turbine exhaust gases, for steam generation or the heating of other heat transfer mediums, or in the use of cooling or heating

**Table 1-1
Economic Comparison of Various Generation Technologies**

| Technology Comparison | Diesel Engine | Gas Engine | Simple Cycle Gas Turbine | Micro Turbine | Fuel Cell | Solar Energy Photovoltaic Cell | Wind | Bio Mass | River Hydro |
|---------------------------------------|----------------------|-------------------|---------------------------------|----------------------|------------------|---------------------------------------|-------------|-----------------|--------------------|
| Product Rollout | Available | Available | Available | Available | 1996–2010 | Available | Available | 2020 | Available |
| Size Range (kW) | 20–25,000+ | 50–7000+ | 500–450,000+ | 30–200 | 50–1000+ | 1+ | 10–2500 | NA | 20–1000+ |
| Efficiency (%) | 36–43% | 28–42% | 21–45% | 25–30% | 35–54% | NA | 45–55% | 25–35% | 60–70% |
| Gen Set Cost (\$/kW) | 125–300 | 250–600 | 300–600 | 350–800 | 1,500–3,000 | NA | NA | NA | NA |
| Turnkey Cost No-Heat Recovery (\$/kW) | 200–500 | 600–1000 | 300–650 | 475–900 | 1,500–3,000 | 5,000–10,000 | 700–1300 | 800–1500 | 750–1200 |
| Heat Recovery Added Cost (\$/kW) | 75–100 | 75–100 | 150–300 | 100–250 | 1,900–3,500 | NA | NA | 150–300 | NA |
| O & M Cost (\$/kWh) | 0.007–0.015 | 0.005–0.012 | 0.003–0.008 | 0.006–0.010 | 0.005–0.010 | 0.001–0.004 | 0.007–0.012 | 0.006–0.011 | 0.005–0.010 |

buildings or parts of cities is not a new concept and is currently being exploited to its full potential.

The Fossil Power Plants of the 1990s and into the early part of the new millennium will be the Combined Cycle Power Plants, with the gas turbine as being the centerpiece of the plant. It is estimated that between 1997–2006 there will be an addition of 147.7 GW of power. These plants have replaced the large Steam Turbine Plants, which were the main fossil power plants through the 1980s. The Combined Cycle Power Plant is not new in concept, since some have been in operation since the mid-1950s. These plants came into their own with the new high capacity and efficiency gas turbines.

The new marketplace of energy conversion will have many new and novel concepts in combined cycle power plants. Figure 1-1 shows the heat rates of these plants, present and future, and Figure 1-2 shows the efficiencies of the same plants. The plants referenced are the Simple Cycle Gas Turbine (SCGT) with firing temperatures of 2400°F (1315°C), Recuperative Gas Turbine (RGT), the Steam Turbine Plant (ST), the Combined Cycle Power Plant (CCPP), and the Advanced Combined Cycle Power Plants (ACCP) such as combined cycle power plants using Advanced Gas Turbine Cycles, and finally the Hybrid Power Plants (HPP).

Table 1-2 is an analysis of the competitive standing of the various types of power plants, their capital cost, heat rate, operation and maintenance costs, availability and reliability, and time for planning. Examining the capital cost and installation time, of these new power plants it is obvious that the gas turbine is the best choice for peaking power. Steam turbine plants are about 50% higher in initial costs \$800–\$1000/kW than combined cycle plants, which are about \$400–\$900/kW. Nuclear power plants are the most expensive. The high initial costs and the long-time in construction make such a plant unrealistic for a deregulated utility.

In the area of performance, the steam turbine power plants have an efficiency of about 35%, as compared to combined cycle power plants, which have an efficiency of about 55%. Newer Gas Turbine technology will make combined cycle efficiencies range between 60–65%. As a rule of thumb a 1% increase in efficiency could mean that 3.3% more capital can be invested. However one must be careful that the increase in efficiency does not lead to a decrease in availability. From 1996–2000 we have seen a growth in efficiency of about 10% and a loss in availability of about 10%. This trend must be turned around since many analysis show that a 1% drop in the availability needs about 2–3% increase in efficiency to offset that loss.

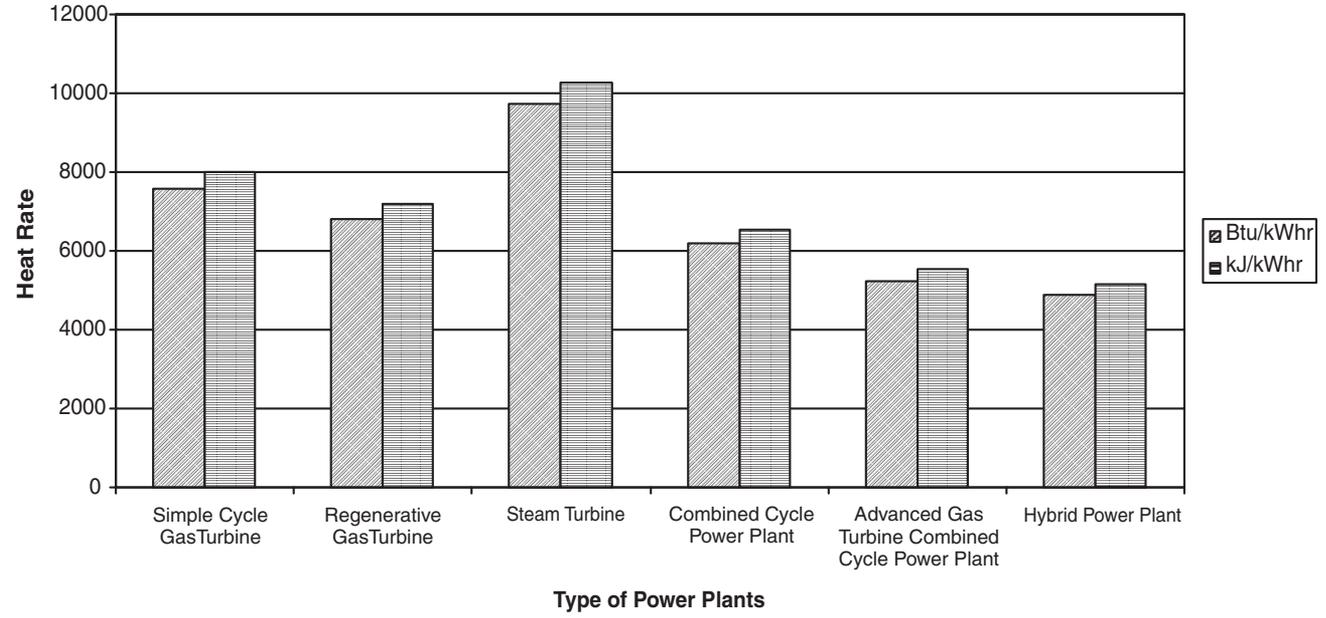


Figure 1-1. Typical heat rates of various types of plants.

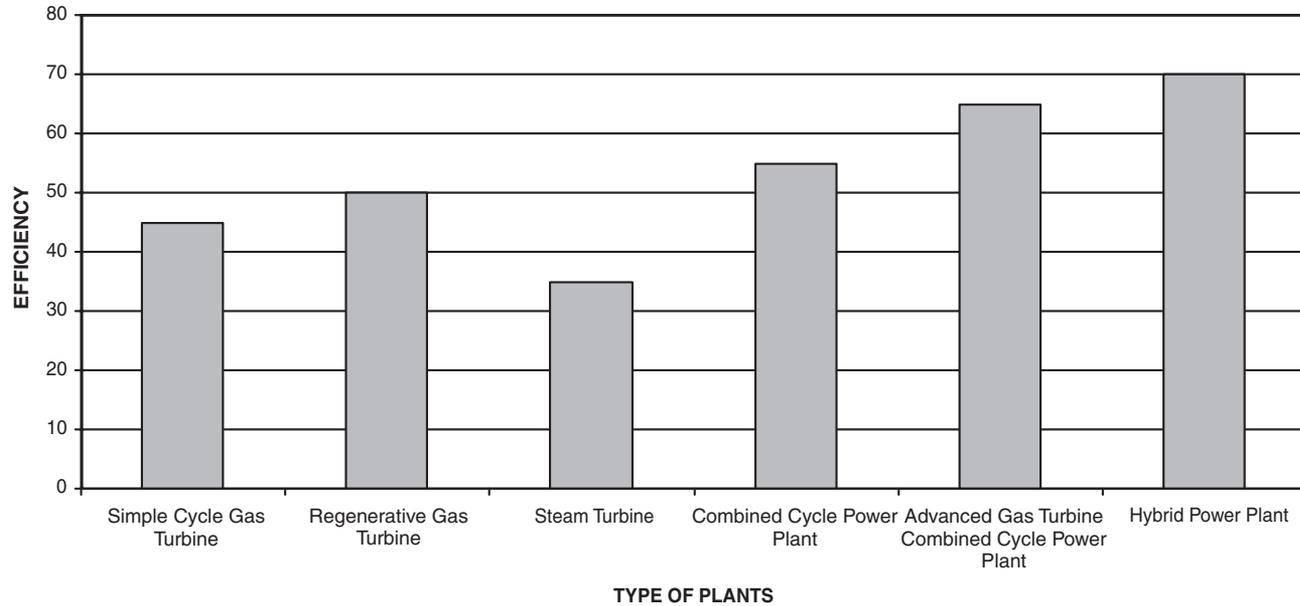


Figure 1-2. Typical efficiencies of various types of plants.

Table 1-2
Economic and Operation Characteristics of Plant

| Type of Plant | Capital Cost \$/kW | Heat Rate Btu/kWh kJ/kWh | Net Efficiency | Variable Operation & Maintenance (\$/MWh) | Fixed Operation & Maintenance (\$/MWh) | Availability | Reliability | Time from Planning to Completion Months |
|--|--------------------|-----------------------------|----------------|---|--|--------------|-------------|---|
| Simple cycle gas turbine (2500 °F/1371 °C) natural gas fired | 300–350 | 7582–8000 | 45 | 5.8 | 0.23 | 88–95% | 97–99% | 10–12 |
| Simple cycle gas turbine oil fired | 400–500 | 8322–8229 | 41 | 6.2 | 0.25 | 85–90% | 95–97% | 12–16 |
| Simple cycle gas turbine crude fired | 500–600 | 10662–11250 | 32 | 13.5 | 0.25 | 75–80% | 90–95% | 12–16 |
| Regenerative gas turbine natural gas fired | 375–575 | 6824–7200 | 50 | 6.0 | 0.25 | 86–93% | 96–98% | 12–16 |
| Combined cycle gas turbine | 600–900 | 6203–6545 | 55 | 4.0 | 0.35 | 86–93% | 95–98% | 22–24 |
| Advanced gas turbine combined cycle power plant | 800–1000 | 5249–5538 | 65 | 4.5 | 0.4 | 84–90% | 94–96% | 28–30 |
| Combined cycle coal gasification | 1200–1400 | 6950–7332 | 49 | 7.0 | 1.45 | 75–85% | 90–95% | 30–36 |
| Combined cycle fluidized bed | 1200–1400 | 7300–7701 | 47 | 7.0 | 1.45 | 75–85% | 90–95% | 30–36 |
| Nuclear power | 1800–200 | 10000–10550 | 34 | 8 | 2.28 | 80–89 | 92–98% | 48–60 |
| Steam plant coal fired | 800–1000 | 9749–10285 | 35 | 3 | 1.43 | 82–89% | 94–97% | 36–42 |
| Diesel generator-diesel fired | 400–500 | 7582–8000 | 45 | 6.2 | 4.7 | 90–95% | 96–98% | 12–16 |
| Diesel generator-power plant oil fired | 600–700 | 8124–8570 | 42 | 7.2 | 4.7 | 85–90% | 92–95% | 16–18 |
| Gas engine generator power plant | 650–750 | 7300–7701 | 47 | 5.2 | 4.7 | 92–96% | 96–98% | 12–16 |

The time taken to install a steam plant from conception to production is about 42–60 months as compared to 22–36 months for combined cycle power plants. The actual construction time is about 18 months, while environmental permits in many cases take 12 months and engineering 6–12 months. The time taken for bringing the plant on line affects the economics of the plant, the longer the capital employed without return, accumulates interest, insurance, and taxes.

It is obvious from this that as long as natural gas or diesel fuel is available the choice of combined cycle power plants is obvious.

Gas Turbine Performance

The aerospace engines have been the leaders in most of the technology in the gas turbine. The design criteria for these engines was high reliability, high performance, with many starts and flexible operation throughout the flight envelope. The engine life of about 3500 hours between major overhauls was considered good. The aerospace engine performance has always been rated primarily on its thrust/weight ratio. Increase in engine thrust/weight ratio is achieved by the development of high-aspect ratio blades in the compressor as well as optimizing the pressure ratio and firing temperature of the turbine for maximum work output per unit flow.

The Industrial Gas Turbine has always emphasized long life and this conservative approach has resulted in the Industrial Gas Turbine in many aspects giving up high performance for rugged operation. The Industrial Gas Turbine has been conservative in the pressure ratio and the firing temperatures. This has all changed in the last 10 years; spurred on by the introduction of the “Aero-Derivative Gas Turbine” the industrial gas turbine has dramatically improved its performance in all operational aspects. This has resulted in dramatically reducing the performance gap between these two types of gas turbines. The gas turbine to date in the combined cycle mode is fast replacing the steam turbine as the base load provider of electrical power throughout the world. This is even true in Europe and the United States where the large steam turbines were the only type of base load power in the fossil energy sector. The gas turbine from the 1960s to the late 1980s was used only as peaking power in those countries, it was used as base load mainly in the “developing countries” where the need of power was increasing rapidly that the wait of three to six years for a steam plant was unacceptable.

Figures 1-3 and 1-4 show the growth of the Pressure Ratio and Firing Temperature. The growth of both the Pressure Ratio and Firing Temperature

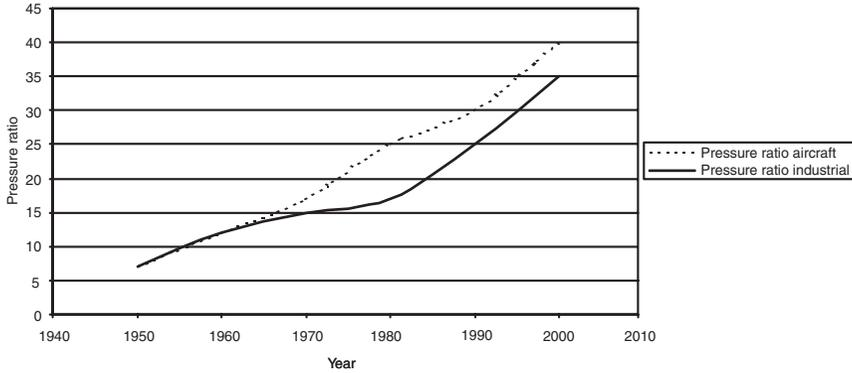


Figure 1-3. Development of engine pressure ratio over the years.

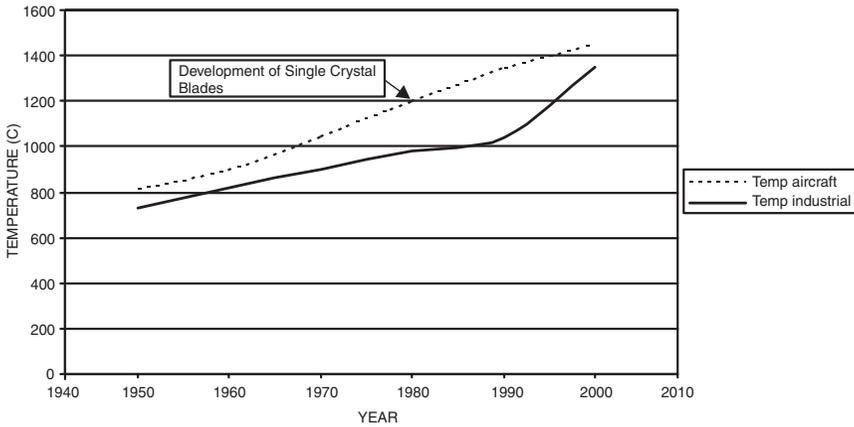


Figure 1-4. Trend in improvement in firing temperature.

parallel each other, as both growths are necessary to achieving the optimum thermal efficiency.

The increase in pressure ratio increases the gas turbine thermal efficiency when accompanied with the increase in turbine firing temperature. Figure 1-5 shows the effect on the overall cycle efficiency of the increasing pressure ratio and the firing temperature. The increase in the pressure ratio increases the overall efficiency at a given temperature, however increasing the pressure

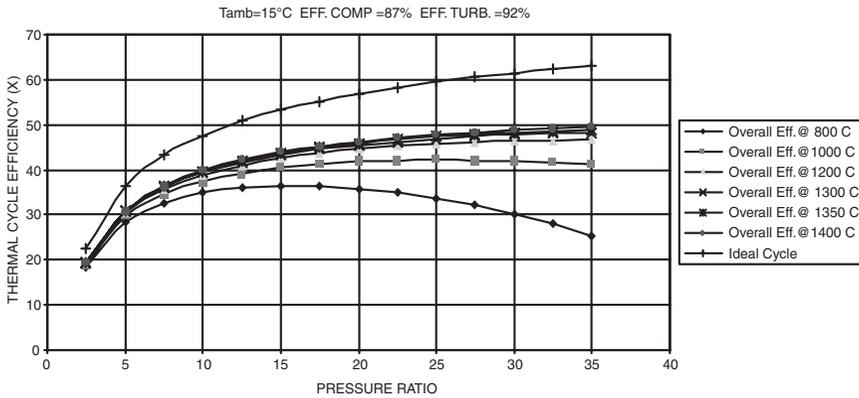


Figure 1-5. Overall cycle efficiency.

ratio beyond a certain value at any given firing temperature can actually result in lowering the overall cycle efficiency.

In the past, the gas turbine was perceived as a relatively inefficient power source when compared to other power sources. Its efficiencies were as low as 15% in the early 1950s, today its efficiencies are in the 45–50% range, which translates to a heat rate of 7582 Btu/kW-hr (8000 kJ/kW-hr) to 6824 BTU/kW-hr (7199 kJ/kW-hr). The limiting factor for most gas turbines has been the turbine inlet temperature. With new schemes of cooling using steam or conditioned air, and breakthroughs in blade metallurgy, higher turbine temperatures have been achieved. The new gas turbines have fired inlet temperatures as high as 2600 °F (1427 °C), and pressure ratios of 40:1 with efficiencies of 45% and above.

Gas Turbine Design Considerations

The gas turbine is the best suited prime mover when the needs at hand such as capital cost, time from planning to completion, maintenance costs, and fuel costs are considered. The gas turbine has the lowest maintenance and capital cost of any major prime mover. It also has the fastest completion time to full operation of any other plant. Its disadvantage was its high heat rate but this has been addressed and the new turbines are among the most efficient types of prime movers. The combination of plant cycles further increases the efficiencies to the low 60s.

The design of any gas turbine must meet essential criteria based on operational considerations. Chief among these criteria are:

1. High efficiency
2. High reliability and thus high availability
3. Ease of service
4. Ease of installation and commission
5. Conformance with environmental standards
6. Incorporation of auxiliary and control systems, which have a high degree of reliability
7. Flexibility to meet various service and fuel needs

A look at each of these criteria will enable the user to get a better understanding of the requirements.

The two factors, which most affect high turbine efficiencies, are pressure ratios and temperature. The axial flow compressor, which produces the high-pressure gas in the turbine, has seen dramatic change as the gas turbine pressure ratio has increased from 7:1 to 40:1. The increase in pressure ratio increases the gas turbine thermal efficiency when accompanied with the increase in turbine firing temperature. The increase in the pressure ratio increases the overall efficiency at a given temperature, however increasing the pressure ratio beyond a certain value at any given firing temperature can actually result in lowering the overall cycle efficiency. It should also be noted that the very high-pressure ratios tend to reduce the operating range of the turbine compressor. This causes the turbine compressor to be much more intolerant to dirt build-up in the inlet air filter and on the compressor blades and creates large drops in cycle efficiency and performance. In some cases, it can lead to compressor surge, which in turn can lead to a flameout, or even serious damage and failure of the compressor blades and the radial and thrust bearings of the gas turbine.

The effect of firing temperature is very predominant—for every 100 °F (55.5 °C) increase in temperature, the work output increases approximately 10% and gives about a 1–½ % increase in efficiency. Higher-pressure ratios and turbine inlet temperatures improve efficiencies on the simple-cycle gas turbine. Figure 1-6 shows a simple cycle gas turbine performance map as a function of pressure ratio and turbine inlet temperature.

Another way to achieve higher efficiencies is with regenerators. Figure 1-7 shows the effects of pressure ratio and temperatures on efficiencies and work for a regenerative cycle. The effect of pressure ratio for this cycle is opposite to that experienced in the simple cycle. Regenerators can increase efficiency as much as 15–20% at today's operating temperatures. The optimum pressure ratios are about 20:1 for a regenerative system compared to 40:1 for the

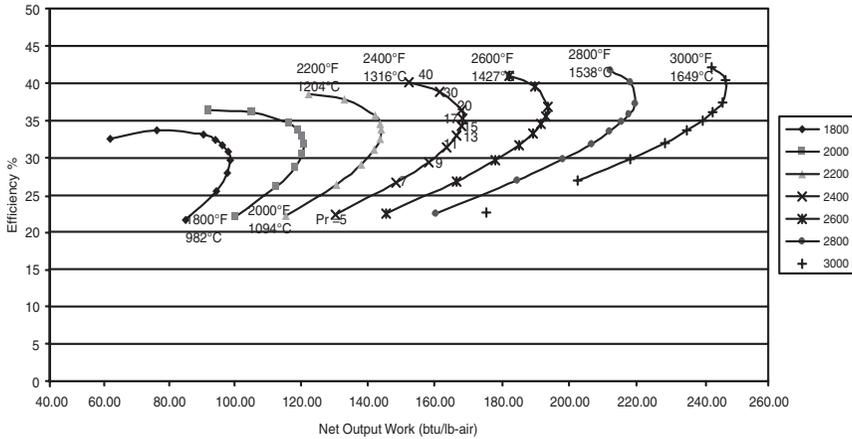


Figure 1-6. Performance map of a simple cycle gas turbine.

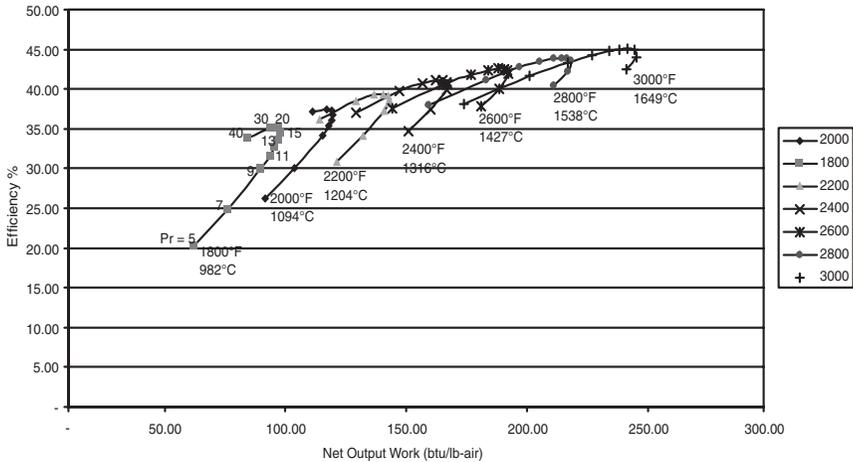


Figure 1-7. Performance map of a regenerative gas turbine.

simple-cycle at today’s higher turbine inlet temperatures that are starting to approach 3000 °F (1649 °C).

High availability and reliability are the most important parameters in the design of a gas turbine. The availability of a power plant is the percent of time the plant is available to generate power in any given period. The reliability of the plant is the percentage of time between planned overhauls.

The Availability of a power plant is defined as

$$A = (P - S - F)/P \quad (1-1)$$

where:

P = Period of time, hours, usually this is assumed as one year, which amounts to 8760 hours

S = Scheduled outage hours for planned maintenance

F = Forced outage hours or unplanned outage due to repair.

The Reliability of a power plant is defined as

$$R = (P - F)/P \quad (1-2)$$

Availability and reliability have a very major impact on the plant economy. Reliability is essential in that when the power is needed it must be there. When the power is not available it must be generated or purchased and can be very costly in the operation of a plant. Planned outages are scheduled for nonpeak periods. Peak periods are when the majority of the income is generated, as usually there are various tiers of pricing depending on the demand. Many power purchase agreements have clauses, which contain capacity payments, thus making plant availability critical in the economics of the plant.

Reliability of a plant depends on many parameters, such as the type of fuel, the preventive maintenance programs, the operating mode, the control systems, and the firing temperatures.

To achieve a high availability and reliability factor, the designer must keep in mind many factors. Some of the more important considerations, which govern the design, are blade and shaft stresses, blade loadings, material integrity, auxiliary systems, and control systems. The high temperatures required for high efficiencies have a disastrous effect on turbine blade life. Proper cooling must be provided to achieve blade metal temperatures between 1000 °F (537 °C), and 1300 °F (704 °C) below the levels of the onset of hot corrosion. Thus, the right type of cooling systems with proper blade coatings and materials are needed to ensure the high reliability of a turbine.

Serviceability is an important part of any design, since fast turnarounds result in high availability to a turbine and reduces maintenance and operations costs. Service can be accomplished by providing proper checks such as exhaust temperature monitoring, shaft vibration monitoring, and surge monitoring. Also, the designer should incorporate borescope ports for fast

visual checks of hot parts in the system. Split casings for fast disassembly, field balancing ports for easy access to the balance planes, and combustor cans, which can be easily disassembled without removing the entire hot section are some of the many ways that afford the ease of service.

Ease of installation and commissioning is another reason for gas turbine use. A gas turbine unit can be tested and packaged at the factory. Use of a unit should be carefully planned so as to cause as few start cycles as possible. Frequent startups and shutdowns at commissioning greatly reduce the life of a unit.

Environmental considerations are critical in the design of any system. The system's impact on the environment must be within legal limits and thus must be addressed by the designer carefully. Combustors are the most critical component, and great care must be taken to design them to provide low smoke and low NO_x output. The high temperatures result in increasing the NO_x emissions from the gas turbines. This resulted in initially attacking the NO_x problem by injecting water or steam in the combustor. The next stage was the development of Dry Low NO_x Combustors. The development of new Dry Low NO_x Combustors has been a very critical component in reducing the NO_x output as the gas turbine firing temperature is increased. The new low NO_x combustors increase the number of fuel nozzle and the complexity of the control algorithms.

Lowering the inlet velocities and providing proper inlet silencers can reduce air noise. Considerable work by NASA on compressor casings has greatly reduced noise.

Auxiliary systems and control systems must be designed carefully, since they are often responsible for the downtime in many units. Lubrication systems, one of the critical auxiliary systems, must be designed with a backup system and should be as close to failure-proof as possible. The advanced gas turbines are all digitally controlled and incorporate on-line condition monitoring to some extent. The addition of new on-line monitoring requires new instrumentation. Control systems provide acceleration-time, and temperature-time controls for startups as well as controls various anti-surge valves. At operating speeds they must regulate fuel supply and monitor vibrations, temperatures, and pressures throughout the entire range.

Flexibility of service and fuels are criteria, which enhance a turbine system, but they are not necessary for every application. The energy shortage requires turbines to be operated at their maximum efficiency. This flexibility may entail a two-shaft design incorporating a power turbine, which is separate and not connected to the Gasifier unit. Multiple fuel applications are now in greater demand, especially where various fuels may be in shortage at different times of the year.

Categories of Gas Turbines

The simple cycle gas turbine is classified into five broad groups:

1. *Frame Type Heavy-Duty Gas Turbines.* The frame units are the large power generation units ranging from 3 MW to 480 MW in a simple cycle configuration, with efficiencies ranging from 30–46%.
2. *Aircraft-Derivative Gas Turbines Aeroderivative.* As the name indicates, these are power generation units, which have origin in the aerospace industry as the prime mover of aircraft. These units have been adapted to the electrical generation industry by removing the bypass fans, and adding a power turbine at their exhaust. These units range in power from 2.5 MW to about 50 MW. The efficiencies of these units can range from 35–45%.
3. *Industrial Type-Gas Turbines.* These vary in range from about 2.5 MW–15 MW. This type of turbine is used extensively in many petrochemical plants for compressor drive trains. The efficiencies of these units is in the low 30s.
4. *Small Gas Turbines.* These gas turbines are in the range from about 0.5 MW–2.5 MW. They often have centrifugal compressors and radial inflow turbines. Efficiencies in the simple cycle applications vary from 15–25%.
5. *Micro-Turbines.* These turbines are in the range from 20 kW–350 kW. The growth of these turbines has been dramatic from the late 1990s, as there is an upsurge in the distributed generation market.

Frame Type Heavy-Duty Gas Turbines

These gas turbines were designed shortly after World War II and introduced to the market in the early 1950s. The early heavy-duty gas turbine design was largely an extension of steam turbine design. Restrictions of weight and space were not important factors for these ground-based units, and so the design characteristics included heavy-wall casings split on horizontal centerlines, sleeve bearings, large-diameter combustors, thick airfoil sections for blades and stators, and large frontal areas. The overall pressure ratio of these units varied from 5:1 for the earlier units to 35:1 for the units in present-day service. Turbine inlet temperatures have been increased and run as high as 2500 °F (1371 °C) on some of these units, this makes the gas turbine one of the most efficient prime mover on the market today reaching efficiencies of 50%. Projected temperatures approach 3000 °F (1649 °C) and,

if achieved, would make the gas turbine even a more efficient unit. The Advanced Gas Turbine Programs sponsored by the U.S. Department of Energy has these high temperatures as one of its goals. To achieve these high temperatures, steam cooling is being used in the latest designs to achieve the goals of maintaining blade metal temperatures below 1300°F (704°C), and prevent hot corrosion problems.

The industrial heavy-duty gas turbines employ axial-flow compressors and turbines. The industrial turbine consists of a 15–17 stage axial flow compressor; with multiple can-annular combustors each connected to the other by cross-over tubes. The cross-over tubes help propagate the flames from one combustor can to all the other chambers and also assures an equalization of the pressure between each combustor chamber. The earlier industrial European designs have single-stage side combustors. The new European designs do not use the side combustor in most of their newer designs. The newer European designs have can-annular or annular combustors since side (silo type) combustors had a tendency to distort the casing. Figure 1-8 is a cross-sectional representation of the GE Industrial Type Gas Turbine, with can-annular combustors, and Figure 1-9 is a cross-sectional representation of the Siemens Silo Type Combustor Gas Turbine. The turbine expander consists of a 2–4-stage axial flow turbine, which drives both the axial flow compressor and the generator.

The large frontal areas of these units reduce the inlet velocities, thus reducing air noise. The pressure rise in each compressor stage is reduced, creating a large, stable operating zone.

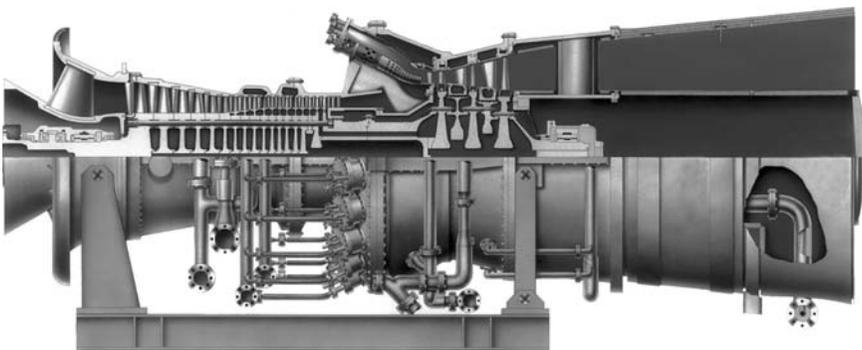


Figure 1-8. A frame-type gas turbine with can-annular combustors. (Courtesy GE Power Systems.)

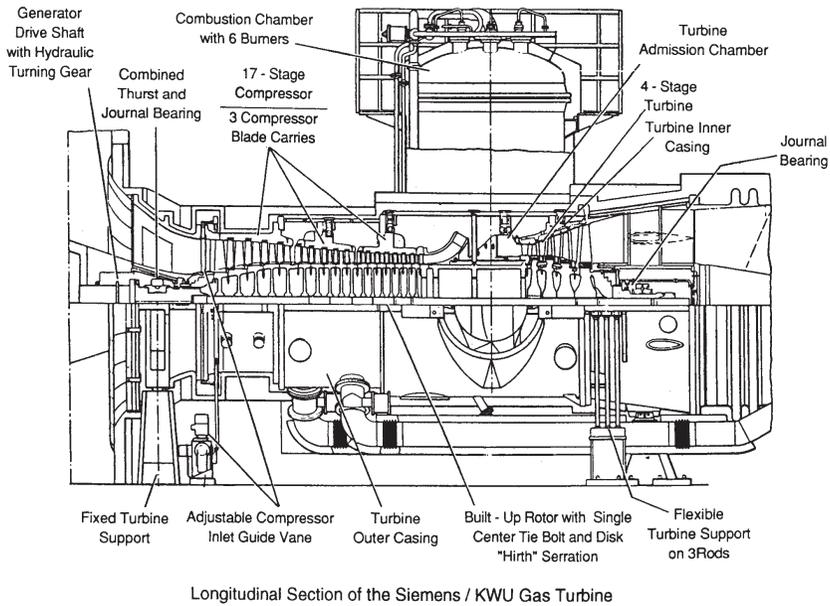


Figure 1-9. Frame-type gas turbine with silo type combustors. (Courtesy Siemens Power Generation.)

The auxiliary modules used on most of these units have gone through considerable hours of testing and are heavy-duty pumps and motors.

The advantages of the heavy-duty gas turbines are their long life, high availability, and slightly higher overall efficiencies. The noise level from this type of turbine is considerably less than an aircraft-type turbine. The heavy-duty gas turbine's largest customers are the electrical utilities, and independent power producers. Since the 1990s the industrial turbines have been the bulwarks of most combined cycle power plants.

The latest frame type units introduced are 480 MW units using steam cooling in the combined cycle mode, enabling the firing temperatures to reach 2600 °F (1427 °C). This enables efficiency in the combined cycle mode to reach 60% plus.

Aircraft-Derivative Gas Turbines

Aeroderivative gas turbines consist of two basic components: an aircraft-derivative gas generator, and a free-power turbine. The gas generator serves as a producer of gas energy or gas horsepower. The gas generator is derived

from an aircraft engine modified to burn industrial fuels. Design innovations are usually incorporated to ensure the required long-life characteristics in the ground-based environment. In case of fan jet designs, the fan is removed and a couple of stages of compression are added in front of the existing low-pressure compressor. The axial flow compressor in many cases is divided into two sections a low-pressure compressor followed by a high-pressure compressor. In those cases, there are usually a high-pressure turbine and a low-pressure turbine, which drives the corresponding sections of the compressor. The shafts are usually concentric thus the speeds of the high pressure and low-pressure sections can be optimized. In this case, the power turbine is separate and is not mechanically coupled; the only connection is via an aerodynamic coupling. In these cases, the turbines have three shafts, all operating at independent speeds. The gas generator serves to raise combustion gas products to conditions of around 45–75 psi (3–5 Bar) and temperatures of 1300–1700 °F (704–927 °C) at the exhaust flange. Figure 1-10 shows a cross section of an aeroderivative engine.

Both the Power Industry and the petrochemical industries use the aircraft-type turbine. The Power Industry uses these units in a combined cycle mode for power generation especially in remote areas where the power requirements are less than 100 MW. The petrochemical industry uses these types of turbines on offshore platforms especially for gas re-injection, and as power plants for these offshore platforms, mostly due to their compactness and the ability to be easily replaced and then sent out to be repaired. The aeroderivative gas turbine also is used widely by gas transmission companies and petrochemical plants, especially for many variable speed mechanical drives. These turbines are also used as main drives for Destroyers and Cruise Ships. The benefits of the aeroderivative gas turbines are:

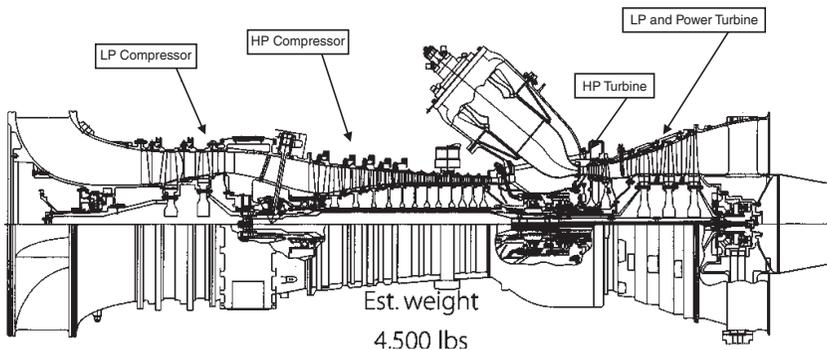


Figure 1-10. A cross section of an aeroderivative gas turbine engine.

1. *Favorable installation cost.* The equipment involved is of a size and weight that it can be packaged and tested as a complete unit within the manufacturer's plant. Generally, the package will include either a generator or a driven pipeline compressor and all auxiliaries and control panels specified by the user. Immediate installation at the job site is facilitated by factory matching and debugging.
2. *Adaptation to remote control.* Users strive to reduce operating costs by automation of their systems. Many new offshore and pipeline applications, today are designed for remote unattended operation of the compression equipment. Jet gas turbine equipment lends itself to automatic control, as auxiliary systems are not complex, water cooling is not required (cooling by oil-to-air exchanges), and the starting device (gas expansion motor) requires little energy and is reliable. Safety devices and instrumentation adapt readily for purposes of remote control and monitoring the performance of the equipment.
3. *Maintenance concept.* The off-site maintenance plan fits in well with these systems where minimum operating personnel and unattended stations are the objectives. Technicians conduct minor running adjustments and perform instrument calibrations. Otherwise, the aeroderivative gas turbine runs without inspection until monitoring equipment indicates distress or sudden performance change. This plan calls for the removal of the gasifier section (the aero-engine) and sending it back to the factory for repair while another unit is installed. The power turbine does not usually have problems since its inlet temperature is much lower. Downtime due to the removal and replacement of the Gasifier turbine is about eight hours.

Industrial Type Gas Turbines

Industrial Type Gas Turbines are medium-range gas turbines and usually rated between 5–15 MW. These units are similar in design to the large heavy-duty gas turbines; their casing is thicker than the aeroderivative casing but thinner than the industrial gas turbines. They usually are split-shaft designs that are efficient in part load operations. Efficiency is achieved by letting the gasifier section (the section which produces the hot gas) operate at maximum efficiency while the power turbine operates over a great range of speeds. The compressor is usually a 10–16 stage subsonic axial compressor, which produces a pressure ratio from about 5:1–15:1. Most American designs use can-annular (about 5–10 combustor cans mounted in a circular ring) or annular-type combustors. Most European designs use

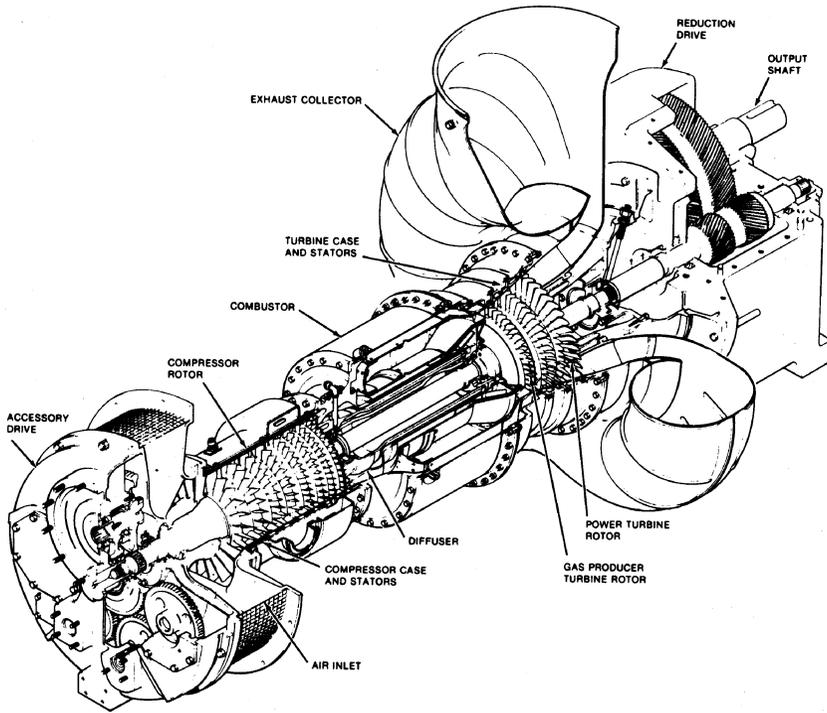


Figure 1-11. A medium size industrial gas turbine. (Courtesy Solar Turbines Incorporated.)

side combustors and have lower turbine inlet temperatures compared to their American counterparts. Figure 1-11 shows an Industrial Type Gas Turbine.

The gasifier turbine is usually a 2–3 stage axial turbine with an air-cooled first-stage nozzle and blade. The power turbine is usually a single- or two-stage axial-flow turbine. The medium-range turbines are used on offshore platforms and are finding increasing use in petrochemical plants. The straight simple-cycle turbine is low in efficiency, but by using regenerators to consume exhaust gases, these efficiencies can be greatly improved. In process plants this exhaust gas is used to produce steam. The combined-cycle (air-steam) cogeneration plant has very high efficiencies and is the trend of the future.

These gas turbines have in many cases regenerators or recuperators to enhance the efficiency of these turbines. Figure 1-12 shows such a new recuperated gas turbine design, which has an efficiency of 38%.

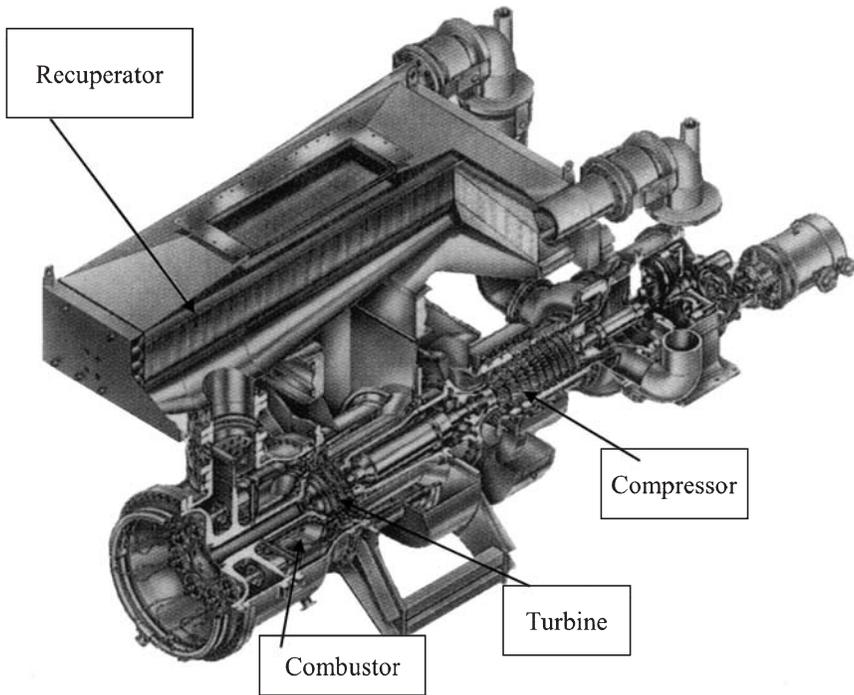


Figure 1-12. A recuperative medium-sized industrial gas turbine. (Courtesy Solar Turbines Incorporated.)

The term “regenerative heat exchanger” is used for this system in which the heat transfer between two streams is affected by the exposure of a third medium alternately to the two flows. (The heat flows successively into and out of the third medium, which undergoes a cyclic temperature.) In a recuperative heat exchanger each element of heat-transferring surface has a constant temperature and, by arranging the gas paths in contraflow, the temperature distribution in the matrix in the direction of flow is that giving optimum performance for the given heat-transfer conditions. This optimum temperature distribution can be achieved ideally in a contraflow regenerator and approached very closely in a cross-flow regenerator.

Small Gas Turbines

Many small gas turbines which produce below 5 MW are designed similar to the larger turbines already discussed; however, there are many designs

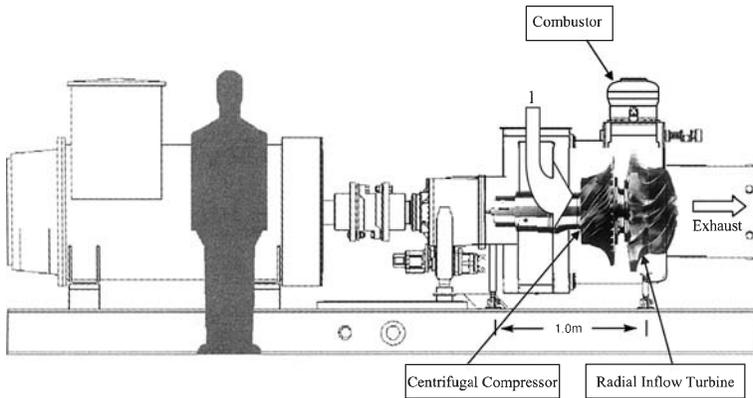


Figure 1-13. A small radial flow gas turbine cutaway showing the turbine rotor.

that incorporate centrifugal compressors or combinations of centrifugal and axial compressors as well as radial-inflow turbines. A small turbine will often consist of a single-stage centrifugal compressor producing a pressure ratio as high as 6:1, a single side combustor where temperatures of about 1,800 °F (982 °C) are reached, and radial-inflow turbines. Figure 1-13 shows a schematic of such a typical turbine. Air is induced through an inlet duct to the centrifugal compressor, which rotating at high speed, imparts energy to the air. On leaving the impeller air with increased pressure and velocity passes through a high-efficiency diffuser, which converts the velocity energy to static pressure. The compressed air, contained in a pressure casing, flows at low speed to the combustion chamber, which is a side combustor. A portion of the air enters the combustor head, mixes with the fuel and burns continuously. The remainder of the air enters through the wall of the combustor and mixes with the hot gases. Good fuel atomization and controlled mixing ensure an even temperature distribution in the hot gases, which pass through the volute to enter the radial inflow turbine nozzles. High acceleration and expansion of the gases through the nozzle guide vane passages and turbine combine to impart rotational energy, which is used to drive the external load and auxiliaries on the cool side of the turbine. The efficiency of a small turbine is usually much lower than a larger unit because of the limitation of the turbine inlet temperature and the lower component efficiencies. Turbine inlet temperature is limited because the turbine blades are not cooled. Radial-flow compressors and impellers inherently have lower efficiencies than their axial counterparts. These units are rugged and their simplicity in design assures many hours of trouble-free operation. A way to

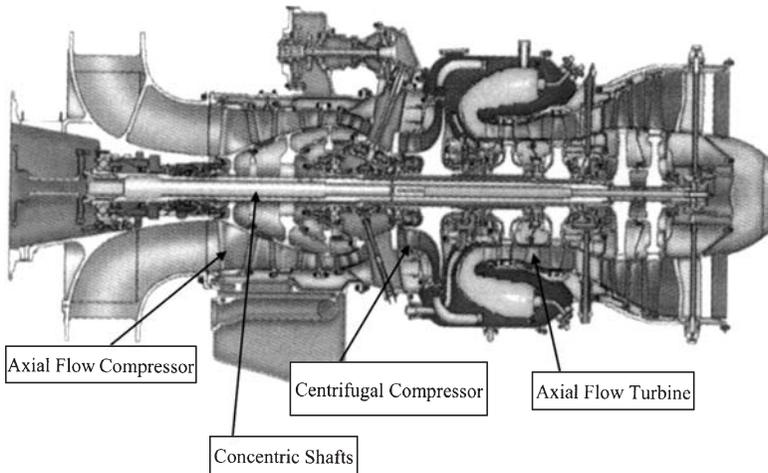


Figure 1-14. A small aeroderivative gas turbine. (Courtesy Pratt & Whitney Canada Corp.)

improve the lower overall cycle efficiencies, 18–23%, is to use the waste heat from the turbine unit. High thermal efficiencies (30–35%) can be obtained, since nearly all the heat not converted into mechanical energy is available in the exhaust, and most of this energy can be converted into useful work. These units when placed in a combined Heat power application can reach efficiencies of the total process as high as 60–70%.

Figure 1-14 shows an aeroderivative small gas turbine. This unit has three independent rotating assemblies mounted on three concentric shafts. This turbine has a three-stage axial flow compressor followed by a centrifugal compressor, each driven by a single stage axial flow compressor. Power is extracted by a two-stage axial flow turbine and delivered to the inlet end of the machine by one of the concentric shafts. The combustion system comprises of a reverse flow annular combustion chamber with multiple fuel nozzles and a spark igniter. This aeroderivative engine produces 4.9 MW and has an efficiency of 32%.

Micro-Turbines

Micro-turbines are usually referred to units of less than 350 kW. These units are usually powered by either diesel fuel or natural gas. They utilize technology already developed. The micro-turbines can be either axial flow or centrifugal-radial inflow units. The initial cost, efficiency, and emissions will be the three most important criterias in the design of these units.

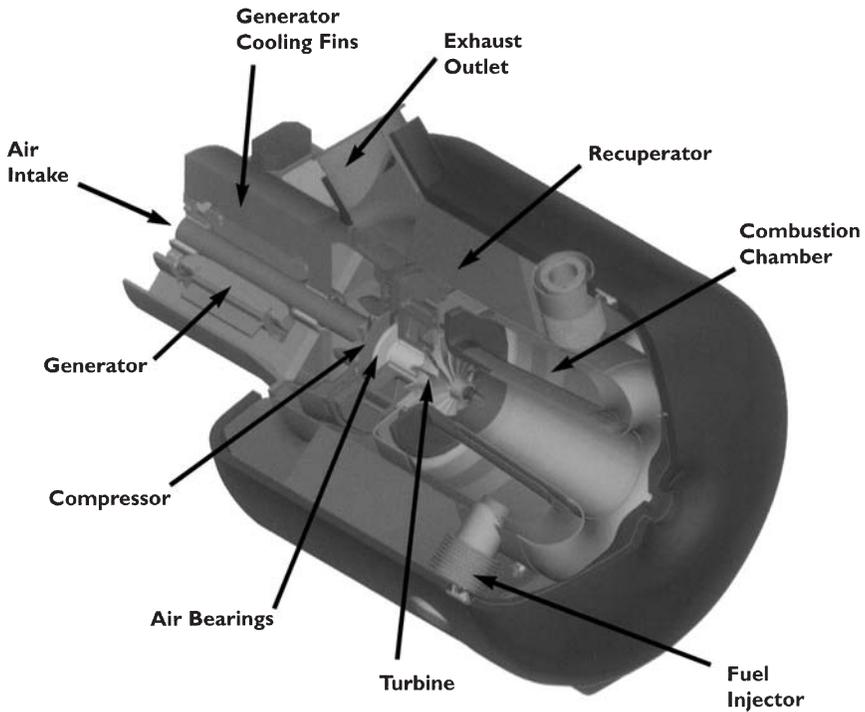


Figure 1-15. A compact micro-turbine schematic. (Courtesy Capstone Corporation.)

The micro-turbines to be successful must be compact in size, have low manufacturing cost, high efficiencies, quiet operation, quick startups, and minimal emissions. These characteristics, if achieved, would make micro-turbines excellent candidates for providing base-load and cogeneration power to a range of commercial customers. The micro-turbines are largely going to be a collection of technologies that have already been developed. The challenges are in economically packaging these technologies.

The micro-turbines on the market today range from about 20–350 kW. Today's micro-turbine are using radial flow turbines and compressors, as seen in Figure 1-15. To improve the overall thermal efficiency regenerators are used in the micro-turbine design, and in combination with absorption coolers, or other thermal loads very high efficiencies can be obtained. Figure 1-16 shows a typical cogeneration system package using a micro-turbine. This compact form of distributed power systems has great potential in the years to come.

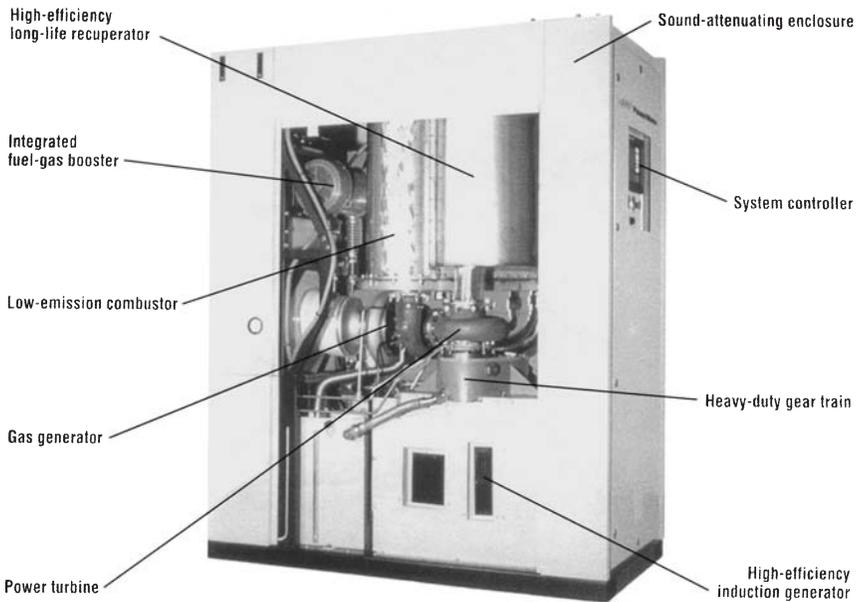


Figure 1-16. A cogeneration micro-turbine system package. (Courtesy Ingersoll Rand Corporation.)

Major Gas Turbine Components

Compressors

A compressor is a device, which pressurizes a working fluid. The types of compressors fall into three categories as shown in Figure 1-17. The positive displacement compressors are used for low flow and high pressure (head), centrifugal compressors are medium flow and medium head, and axial flow compressors are high flow and low pressure. In gas turbines the centrifugal flow, and axial flow compressors, which are continuous flow compressors, are the ones used for compressing the air. Positive displacement compressors such as the gear type units are used for lubrication systems in the gas turbines.

The characteristics of these compressors are given in Table 1-3. The pressure ratio of the axial and centrifugal compressors have been classified into three groups, industrial, aerospace and research. The aircraft gas turbines because of their thrust to weight ratio considerations have very high loading for each compressor stage. The pressure ratio per each stage

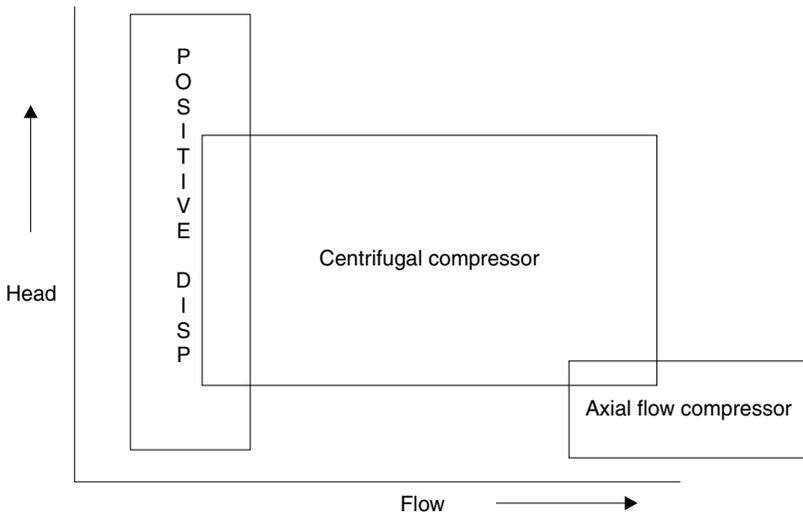


Figure 1-17. Performance characteristics of different types of compressors.

Table 1-3
Compressor Characteristics

| Types of Compressors | Pressure Ratio | | | Efficiency | Operating Range |
|-----------------------|----------------|-----------|----------|------------|-----------------|
| | Industrial | Aerospace | Research | | |
| Positive Displacement | Up to 30 | – | – | 75–82% | – |
| Centrifugal | 1.2–1.9 | 2.0–7.0 | 13 | 75–87% | Large 25% |
| Axial | 1.05–1.3 | 1.1–1.45 | 2.1 | 80–91% | Narrow 3–10% |

can reach as high as 1.4 per stage. In the industrial gas turbines, the loading per stage is considerably less and varies between 1.05–1.3 per stage. The adiabatic efficiency of the compressors has also increased and efficiencies in the high 80s have been achieved. Compressor efficiency is very important in the overall performance of the gas turbine as it consumes 55–60% of the power generated by the gas turbine.

The industrial pressure ratio is low for the reasons that the operating range needs to be large. The operating range is the range between the surge point and the choke point. Figure 1-18 shows the operating characteristics of a compressor. The surge point is the point when the flow is reversed in the compressor. The choke point is the point when the flow has reached a Mach = 1.0 the point where no more flow can get through the unit, a “stone

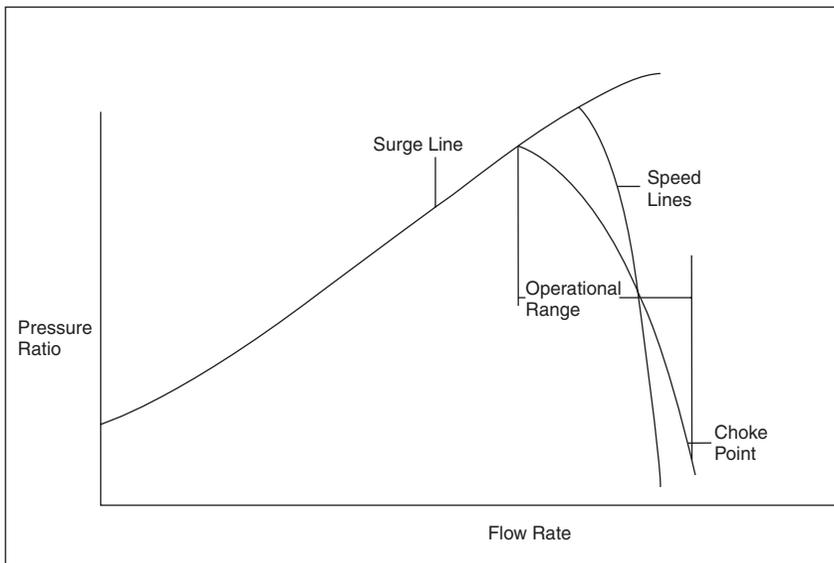


Figure 1-18. Schematic of a compressor performance map.

wall.” When surge occurs, the flow is reversed and so are all the forces acting on the compressor especially the thrust forces, which can lead to total destruction of the compressor. Thus, surge is a region that must be avoided. Choke conditions cause a large drop in efficiency, but do not lead to destruction of the unit.

It is important to note that with the increase in pressure ratio and the number of stages the operating range is narrowed.

The turbo-compressors discussed in this section transfer energy by dynamic means from a rotating member to the continuously flowing fluid. The two types of compressors used in gas turbines are axial and centrifugal. Nearly all gas turbines producing over 5 MW have axial flow compressors. Some small gas turbines employ a combination of an axial compressor followed by a centrifugal unit. Figure 1-19 shows a schematic of an axial-flow compressor followed by a centrifugal compressor, an annular combustor, and an axial-flow turbine, very similar to the actual engine depicted in Figure 1-14.

Axial-Flow Compressors. An axial-flow compressor compresses its working fluid by first accelerating the fluid and then diffusing it to obtain a pressure increase. The fluid is accelerated by a row of rotating airfoils or blades (the rotor) and diffused by a row of stationary blades (the stator). The

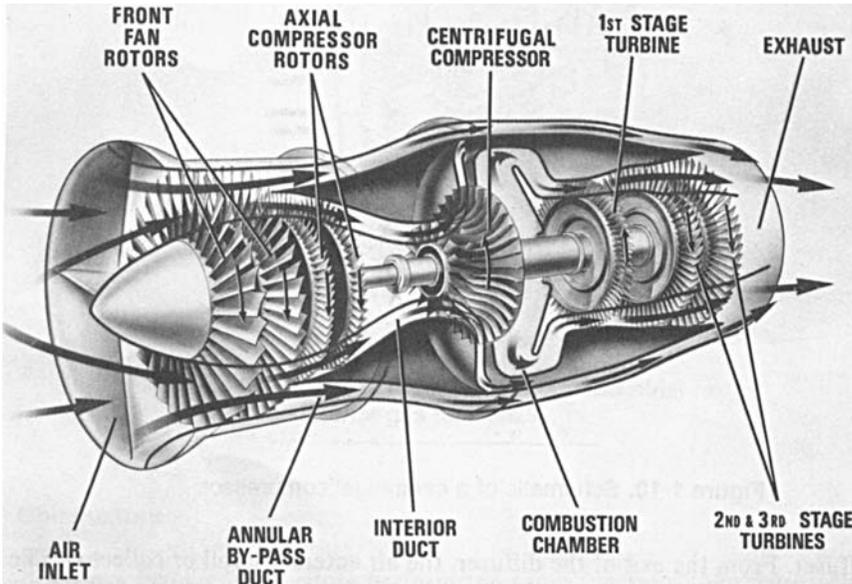


Figure 1-19. A schematic of a cutaway of a small gas turbine used in helicopter or vehicular applications.

diffusion in the stator converts the velocity increase gained in the rotor to a pressure increase. One rotor and one stator make up a stage in a compressor. A compressor usually consists of multiple stages. One additional row of fixed blades (inlet guide vanes) is frequently used at the compressor inlet to ensure that air enters the first-stage rotors at the desired angle. In addition to the stators, an additional diffuser at the exit of the compressor further diffuses the fluid and controls its velocity when entering the combustors.

In an axial flow compressor air passes from one stage to the next with each stage raising the pressure slightly. By producing low-pressure increases on the order of 1.1:1–1.4:1, very high efficiencies can be obtained. The use of multiple stages permits overall pressure increases up to 40:1. The rule of thumb for a multiple stage gas turbine compressor would be that the energy rise per stage would be constant rather than the pressure rise per stage.

Figure 1-20 shows multistage high-pressure axial flow turbine rotor. The turbine rotor depicted in this figure has a low-pressure compressor followed by a high-pressure compressor. There are also two turbine sections, and the

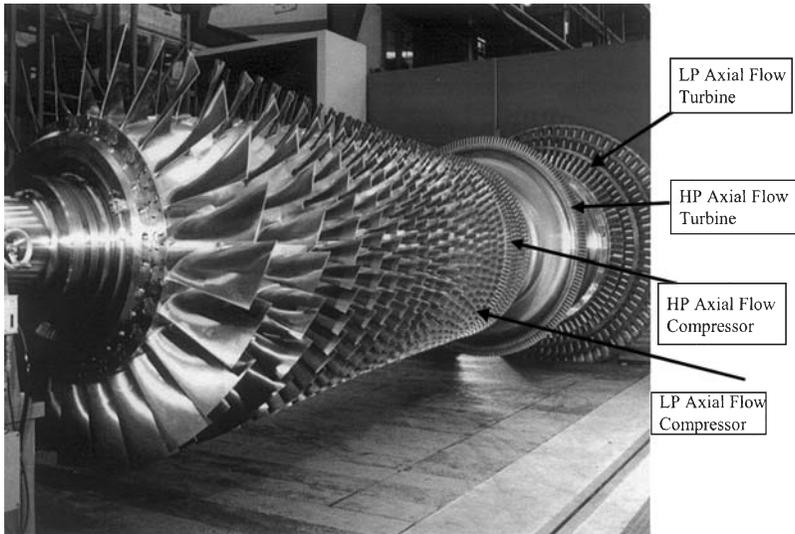


Figure 1-20. A high-pressure ratio turbine rotor. (Courtesy ALSTOM.)

reason there is a large space between the two turbine sections is that this is a reheat turbine and the second set of combustors are located between the high-pressure and the low-pressure turbine sections. The compressor produces 30:1 pressure in 22 stages. The low-pressure increase per stage also simplifies calculations in the design of the compressor by justifying the air as incompressible in its flow through an individual stage.

Centrifugal Flow Compressors. Centrifugal compressors are used in small gas turbines and are the driven units in most gas turbine compressor trains. They are an integral part of the petrochemical industry, finding extensive use because of their smooth operation, large tolerance of process fluctuations, and their higher reliability compared to other types of compressors. Centrifugal compressors range in size from pressure ratios of 1:3:1 per stage to as high as 13:1 on experimental models. Discussions here are limited to the compressors used in small gas turbines. This means that the compressor pressure ratio must be between 3–7:1 per stage. This is considered a highly loaded centrifugal compressor. With pressure ratios, which exceed 5:1, flows entering the diffuser from the rotor are supersonic in their mach number ($M > 1.0$). This requires a special design of the diffuser.

In a typical centrifugal compressor, the fluid is forced through the impeller by rapidly rotating impeller blades. The velocity of the fluid is converted to

pressure, partially in the impeller and partially in the stationary diffusers. Most of the velocity leaving the impeller is converted into pressure energy in the diffuser. The diffuser consists essentially of vanes, which are tangential to the impeller. These vane passages diverge to convert the velocity head into pressure energy. The inner edge of the vanes is in line with the direction of the resultant airflow from the impeller.

In the centrifugal or mixed-flow compressor the air enters the compressor in an axial direction and exists in a radial direction into a diffuser. This combination of rotor (or impeller) and diffuser comprises a single stage. The air enters into the centrifugal compressor through an intake duct and can be given a prewhirl by the IGVs as shown in Figure 1-21. The inlet guide vanes give circumferential velocity to the fluid at the inducer inlet. IGVs are installed directly in front of the impeller inducer or, where an axial entry is not possible, located radially in an intake duct. The purpose of installing the IGVs is usually to decrease the relative Mach number at the inducer-tip (impeller eye) inlet because the highest relative velocity at the inducer inlet is at the shroud. When the relative velocity is close to the sonic velocity or greater than it, a shock wave takes place in the inducer section. A shock wave produces shock loss and chokes the inducer. The air initially enters the

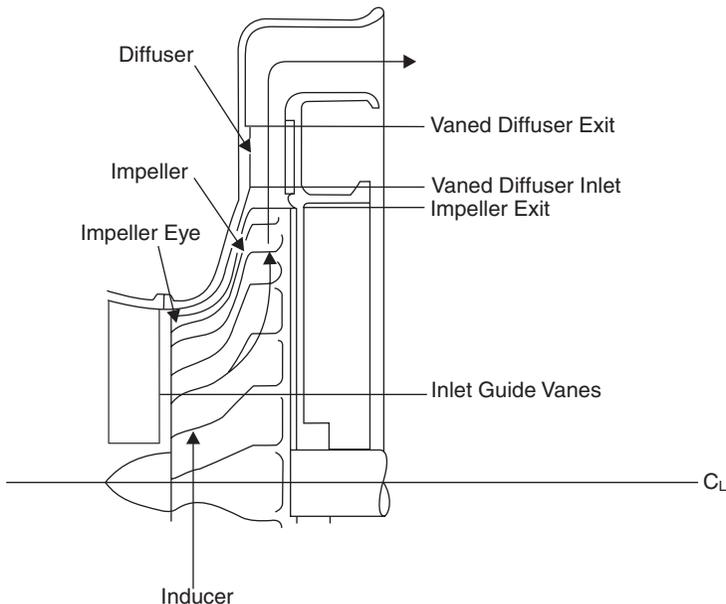


Figure 1-21. Schematic of a centrifugal compressor stage.

centrifugal impeller at the inducer. The inducer, usually an integral part of the impeller, is very much like an axial-flow compressor rotor. Many earlier designs kept the inducer separate. The air then goes through a 90° turn and exits into a diffuser, which usually consists of a vaneless space followed by a vaned diffuser. This is especially true if the compressor exit is supersonic as is the case with high-pressure ratio compressors. The vaneless space is used to reduce the velocity leaving the rotor to a value lower than Mach number = 1 ($M < 1$). From the exit of the diffuser, the air enters a scroll or collector. The centrifugal compressor is slightly less efficient than the axial-flow compressor, but it has a higher stability. A higher stability means that its operating range is greater (surge-to-choke margin).

Regenerators

Heavy-duty regenerators are designed for applications in large gas turbines in the 1–50 MW range. The use of regenerators in conjunction with industrial gas turbines substantially increases cycle efficiency and provides an impetus to energy management by reducing fuel consumption up to 30%. The term “regenerative heat exchanger” is used for this system in which the heat transfer between two streams is affected by the exposure of a third medium alternately to the two flows. The heat flows successively into and out of the third medium, which undergoes a cyclic temperature. In a recuperative heat exchanger each element of heat-transferring surface has a constant temperature and, by arranging the gas paths in contraflow, the temperature distribution in the matrix in the direction of flow is that giving optimum performance for the given heat-transfer conditions. This optimum temperature distribution can be achieved ideally in a contraflow regenerator and approached very closely in a cross-flow regenerator.

Figure 1-22 shows how a regenerator works. In most present-day regenerative gas turbines ambient air enters the inlet filter and is compressed to about 100 psi (6.8 Bar) and a temperature of 500 °F (260 °C). The air is then piped to the regenerator, which heats the air to about 900 °F (482 °C). The heated air then enters the combustor where it is further heated before entering the turbine. After the gas has undergone expansion in the turbine, it is about 1000 °F (538 °C) and essentially at ambient pressure. The gas is ducted through the regenerator where the waste heat is transferred to the incoming air. The gas is then discharged into the ambient air through the exhaust stack. In effect, the heat that would otherwise be lost is transferred to the air, decreasing the amount of fuel that must be consumed to operate the turbine. For a 25 MW turbine, the regenerator heats 10 million pounds of air per day.

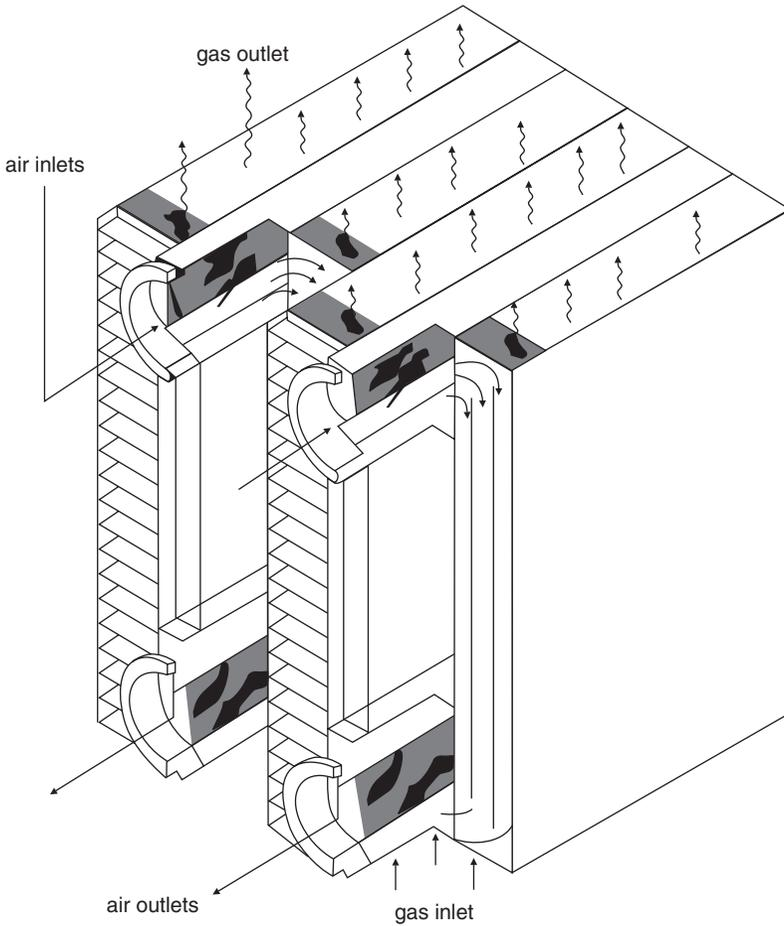


Figure 1-22. A typical plate and fin type regenerator for an industrial gas turbine.

Combustors

All gas turbine combustors perform the same function, they increase the temperature of the high-pressure gas. The gas turbine combustor uses very little of its air (10%) in the combustion process. The rest of the air is used for cooling and mixing. New combustors are also circulating steam for cooling purpose. The air from the compressor must be diffused before it enters the

combustor. The velocity of the air leaving the compressor is about 400–600 ft/sec (122–183 m/sec) and the velocity in the combustor must be maintained below 50 ft/sec (15.2 m/sec). Even at these low velocities care must be taken to avoid the flame to be carried on downstream.

The combustor is a direct-fired air heater in which fuel is burned almost stoichiometrically with one-third or less of the compressor discharge air. Combustion products are then mixed with the remaining air to arrive at a suitable turbine inlet temperature. Despite the many design differences in combustors, all gas turbine combustion chambers have three features: (1) a recirculation zone, (2) a burning zone (with a recirculation zone, which extends to the dilution region), and (3) a dilution zone, as seen in Figure 1-23. The air entering a combustor is divided so that the flow is distributed between three major regions (1) Primary Zone, (2) Dilution Zone and (3) Annular space between the liner and casing.

The combustion in a combustor takes place in the Primary Zone. Combustion of natural gas is a chemical reaction that occurs between carbon, or hydrogen, and oxygen. Heat is given off as the reaction takes place. The products of combustion are carbon dioxide and water. The reaction is Stoichiometric, which means that the proportions of the reactants are such that there are exactly enough oxidizer molecules to bring about a complete reaction to stable molecular forms in the products. The air enters the combustor in a straight through flow, or reverse flow. Most aero-engines have straight through flow type combustors. Most of the large frame type units have reverse flow. The function of the recirculation zone is to evap-

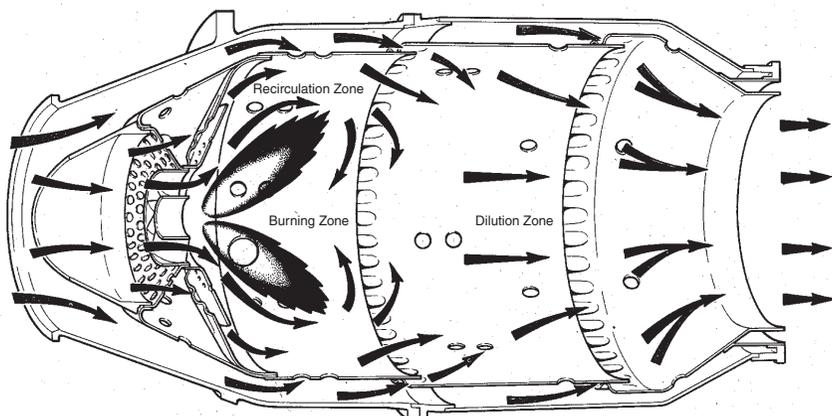


Figure 1-23. A typical combustor can with straight through flow.

orate, partly burn, and prepare the fuel for rapid combustion within the remainder of the burning zone. Ideally, at the end of the burning zone, all fuel should be burnt so that the function of the dilution zone is solely to mix the hot gas with the dilution air. The mixture leaving the chamber should have a temperature and velocity distribution acceptable to the guide vanes and turbine. Generally, the addition of dilution air is so abrupt that if combustion is not complete at the end of the burning zone, chilling occurs which prevents completion. However, there is evidence with some chambers that if the burning zone is run over-rich, some combustion does occur within the dilution region. Figure 1-24 shows the distribution of the air in the various regions of the combustor. The Theoretical or Reference Velocity is the flow of combustor-inlet air through an area equal to the maximum cross section of the combustor casing. The flow velocity is 25 fps (7.6 mps) in a reverse-flow combustor; and between 80 fps (24.4 mps) and 135 fps (41.1 mps) in a straight-through flow turbojet combustor.

Combustor inlet temperature depends on engine pressure ratio, load and engine type, and whether or not the turbine is regenerative or nonregenerative especially at the low-pressure ratios. The new industrial turbine pressure ratios are between 17:1, and 35:1, which means that the combustor inlet temperatures range from 850 °F (454 °C) to 1200 °F (649 °C). The new aircraft engines have pressure ratios, which are in excess of 40:1.

Combustor performance is measured by efficiency, the pressure decrease encountered in the combustor, and the evenness of the outlet temperature profile. Combustion efficiency is a measure of combustion completeness. Combustion completeness affects fuel consumption directly, since the heating value of any unburned fuel is not used to increase the turbine inlet

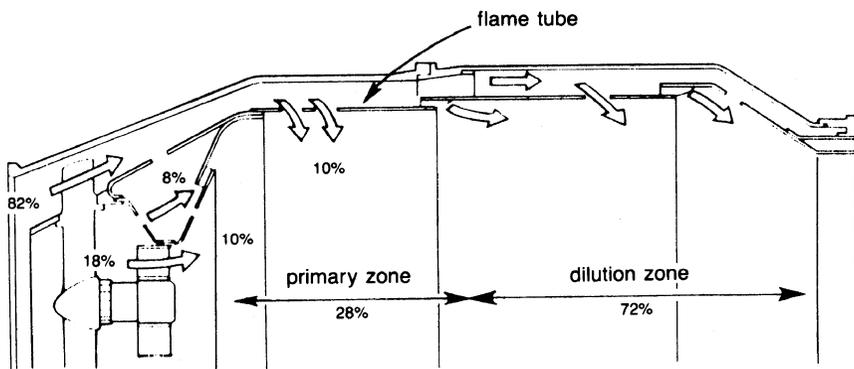


Figure 1-24. Air distribution in a typical combustor.

temperature. Normal combustion temperatures range from 3400°F (1871°C) to 3500°F (1927°C). At this temperature, the volume of nitric oxide in the combustion gas is about 0.01%. If the combustion temperature is lowered, the amount of nitric oxide is substantially reduced.

Typical Combustor Arrangements

There are different methods to arrange combustors on a gas turbine. Designs fall into four categories:

1. Tubular (side combustors)
2. Can-annular
3. Annular
4. External (experimental)

Can-annular and Annular. In aircraft applications where frontal area is important, either can-annular or annular designs are used to produce favorable radial and circumferential profiles because of the great number of fuel nozzles employed. The annular design is especially popular in new aircraft designs; however, the can-annular design is still used because of the developmental difficulties associated with annular designs. Annular combustor popularity increases with higher temperatures or low-Btu gases, since the amount of cooling air required is much less than in can-annular designs due to a much smaller surface area. The amount of cooling air required becomes an important consideration in low-BTU gas applications, since most of the air is used up in the primary zone and little is left for film cooling. Development of a can-annular design requires experiments with only one can, whereas the annular combustor must be treated as a unit and requires much more hardware and compressor flow. Can-annular combustors can be of the straight-through or reverse-flow design. If can-annular cans are used in aircraft, the straight-through design is used, while a reverse-flow design may be used on industrial engines. Annular combustors are almost always straight-through flow designs. Figure 1-25 shows a typical Can Annular combustor used in Frame type units, with reverse flow. Figure 1-26 is a tubo-annular combustor used in aircraft-type combustors, and Figure 1-27 is a schematic of an annular combustor in an aircraft gas turbine.

Tubular (side combustors). These designs are found on large industrial turbines, especially European designs, and some small vehicular gas turbines. They offer the advantages of simplicity of design, ease of maintenance, and long-life due to low heat release rates. These combustors may be of the

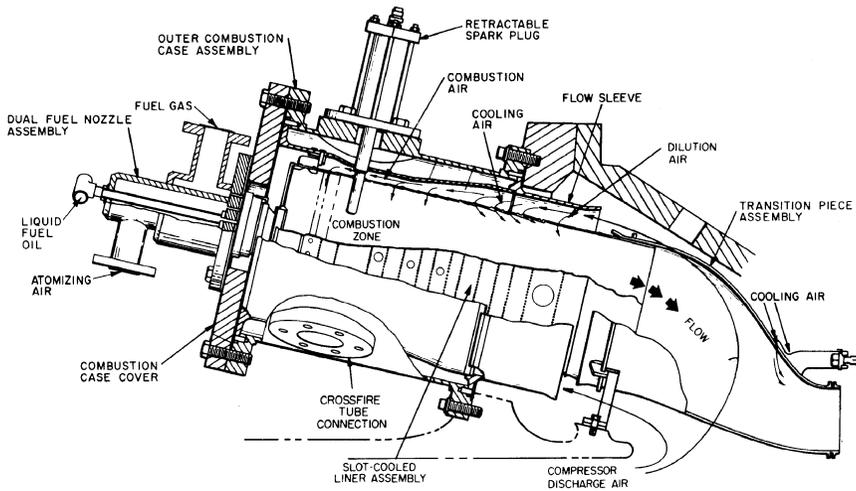


Figure 1-25. A typical reverse flow can-annular combustor.

“straight-through” or “reverse-flow” design. In the reverse-flow design air enters the annulus between the combustor can and its housing, usually a hot-gas pipe to the turbine. Reverse-flow designs have minimal length. Figure 1-28 shows one such combustor design.

External Combustor (experimental). The heat exchanger used for an external-combustion gas turbine is a direct-fired air heater. The air heater’s goal is to achieve high temperatures with a minimum pressure decrease. It consists of a rectangular box with a narrow convection section at the top. The outer casings of the heater consist of carbon steel lined with lightweight blanket material for insulation and heat re-radiation.

The inside of the heater consists of wicket-type coils (inverted “U”) supported from a larger-diameter inlet pipe, and a return header running along the two lengths of the heater. The heater can have a number of passes for air. The one shown in Figure 1-29 has four passes. Each pass consists of 11 wickets, giving a total of 44 wickets. The wickets are made of different materials, since the temperature increases from about 300–1,700 °F. Thus, the wickets can range from 304 stainless steel to RA330 at the high-temperature ends. The advantage of the wicket design is that the smooth transition of “U” tubes minimizes pressure drops. The U-shaped tubes also allow the wicket to freely expand with thermal stress. This feature eliminates the need for stress relief joints and expansion joints. The wickets are usually

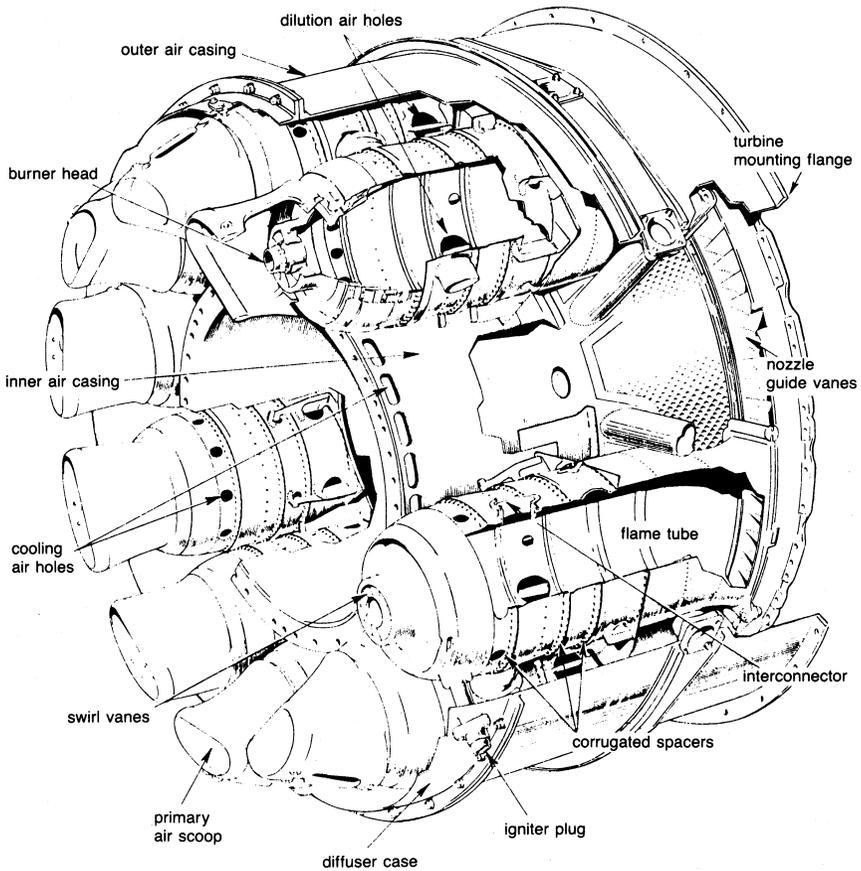


Figure 1-26. Turbo-annular combustion chamber for aircraft-type gas turbines.

mounted on a rollaway section to facilitate cleaning, repairs, or coil replacement after a long period of use.

A horizontally fired burner is located at one end of the heater. The flame extends along the central longitudinal axis of the heater. In this way the wickets are exposed to the open flame and can be subjected to a maximum rate of radiant heat transfer. The tubes should be sufficiently far away from the flame to prevent hot spots or flame pinching.

The air from the compressor enters the inlet manifold and is distributed through the first wicket set. A baffle in the inlet prevents the air flow from continuing beyond that wicket set. The air is then transferred to the return

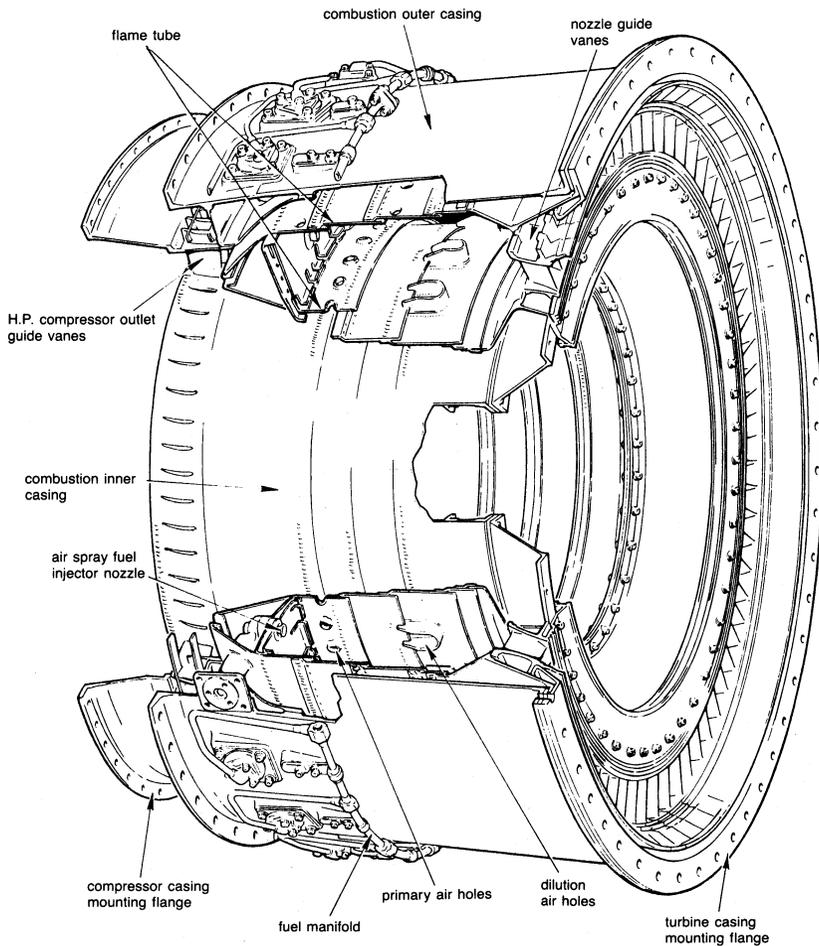


Figure 1-27. Annular combustion chamber.

header and proceeds further until it encounters a second baffle. This arrangement yields various passes and helps to minimize the pressure drop due to friction. The air is finally returned to the end section of the inlet manifold and exits to the inlet gas turbine.

The burner should be designed for handling preheated combustion air. Preheated combustion air is obtained by diverting part of the exhaust from the gas turbine. The air from the turbine is clean, hot air. To recover additional heat energy from the exhaust flue gases, a steam coil is placed

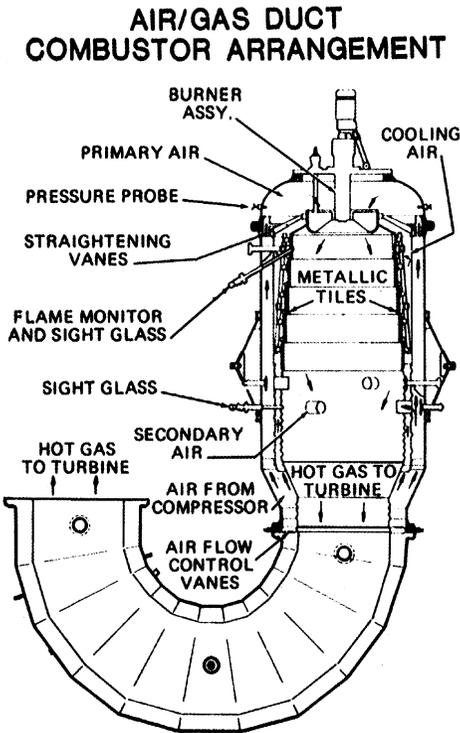


Figure 1-28. A typical single can side combustor.

in the convection section of the heater. The steam is used for steam injection into the compressor discharge or to drive a steam turbine. The flue gas temperature exiting from the heater should be around 600 °F (316 °C).

Fuel Type

Natural gas is the fuel of choice wherever it is available because of its clean burning and its competitive pricing as seen in Figure 1-30. Prices for Uranium, the fuel of nuclear power stations, and coal, the fuel of the steam power plants, have been stable over the years and have been the lowest. Environmental, safety concerns, high initial cost, and the long time from planning to production has hurt the nuclear and steam power industries. Whenever oil or natural gas is the fuel of choice, gas turbines and combined cycle plants are the power plant of choice as they convert the fuel into electricity very

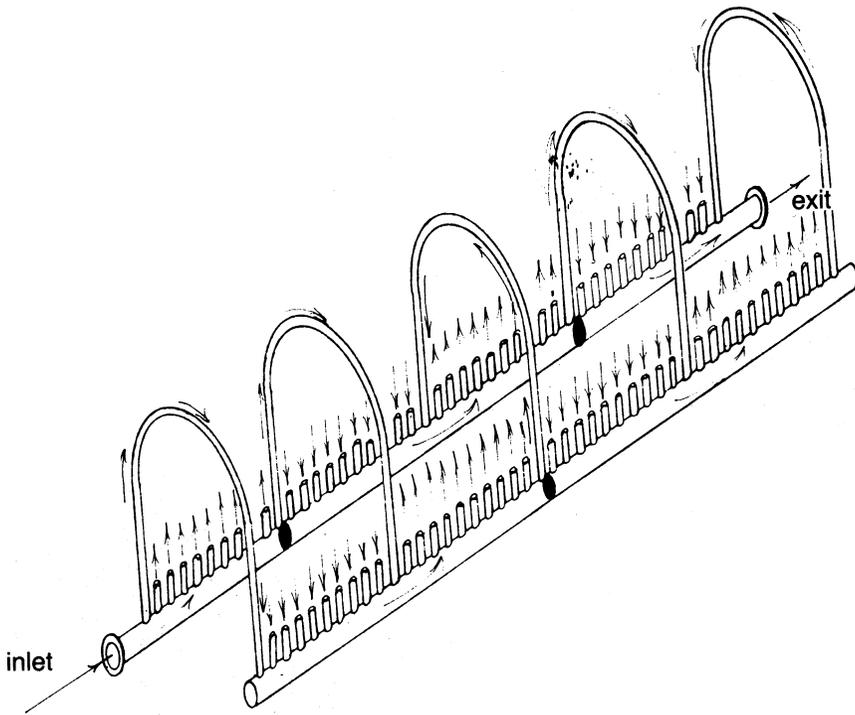


Figure 1-29. An external fired combustor with four passes.

efficiently and cost effectively. It is estimated that from 1997–2006 23% of the plants will be combined cycle power plants, and that 7% will be gas turbines. It should be noted that about 40% of gas turbines are not operated on natural gas.

The use of natural gas has increased and in the year 2000, has reached prices as high as US\$4.50 in certain parts of the U.S. This will bring other fuels onto the market to compete with natural gas as the fuel source. Figure 1-31 shows the growth of the natural gas as the fuel of choice in the United States, especially for power generation. This growth is based on completion of a good distribution system. This signifies the growth of combined cycle power plants in the United States.

Figure 1-32 shows the preference of natural gas throughout the world. This is especially true in Europe where 71% of the new power is expected to be fueled by natural gas, Latin America where 73% of the new power is expected to be fueled by natural gas, and North America where 84% of the

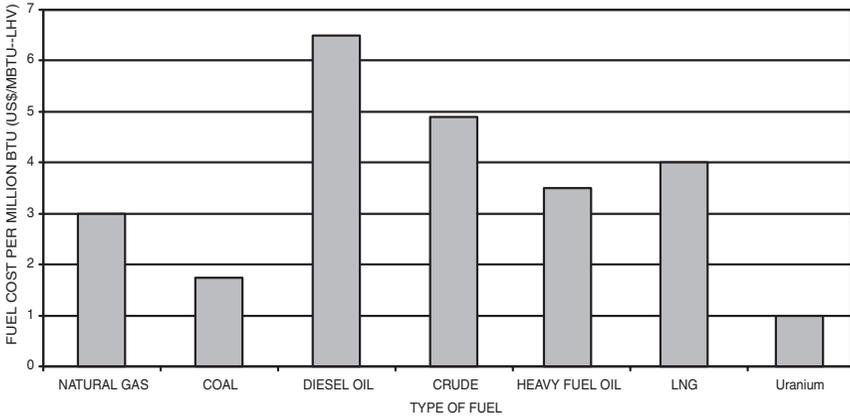


Figure 1-30. Typical fuel costs per million BTUs.

new power is expected to be fueled by natural gas. This means a substantial growth of combined cycle power plants.

The new gas turbines also utilize Low NO_x combustors to reduce the NO_x emissions, which otherwise would be high due to the high firing temperature of about 2300 °F (1260 °C). These low NO_x combustors require careful calibration to ensure an even firing temperature in each combustor. New types of instrumentation such as dynamic pressure transducers have been found to be effective in ensuring steady combustion in each of the combustors.

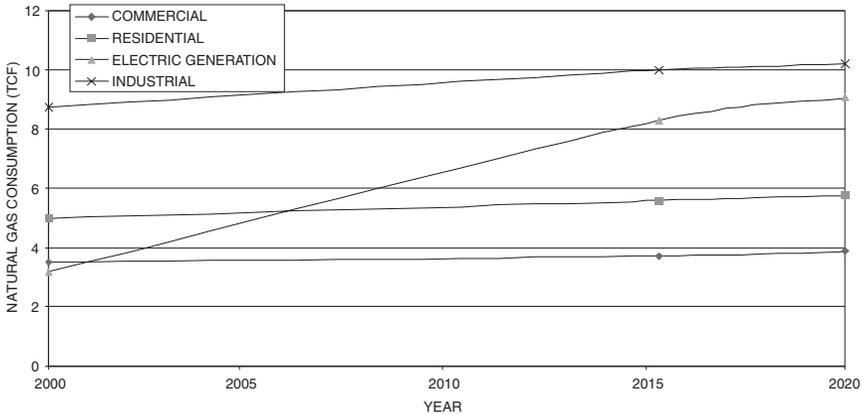


Figure 1-31. Projected natural gas consumption 2000–2020.

Environmental Effects

The use of natural gas and the use of the new dry low NO_x combustors have reduced NO_x levels below 10 ppm. Figure 1-33 shows how in the past 30 years the reduction of NO_x by first the use of steam (wet combustors) injection in the combustors, and then in the 1990s, the dry low NO_x

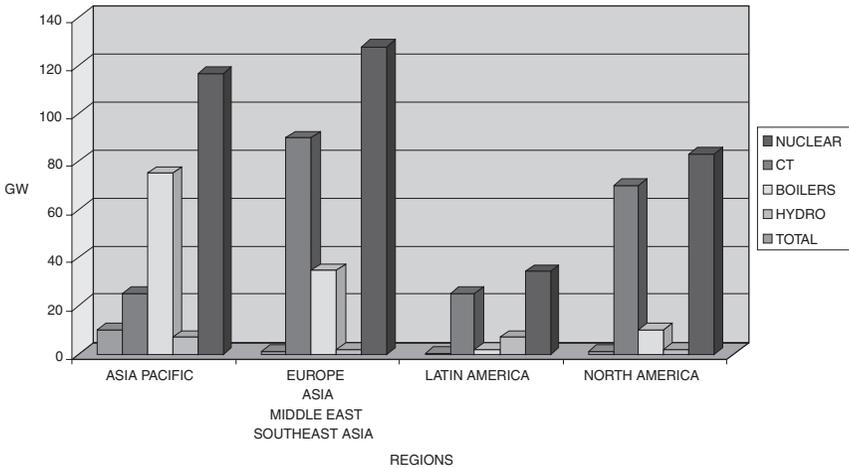


Figure 1-32. Technology trends indicate that natural gas is the fuel of choice.

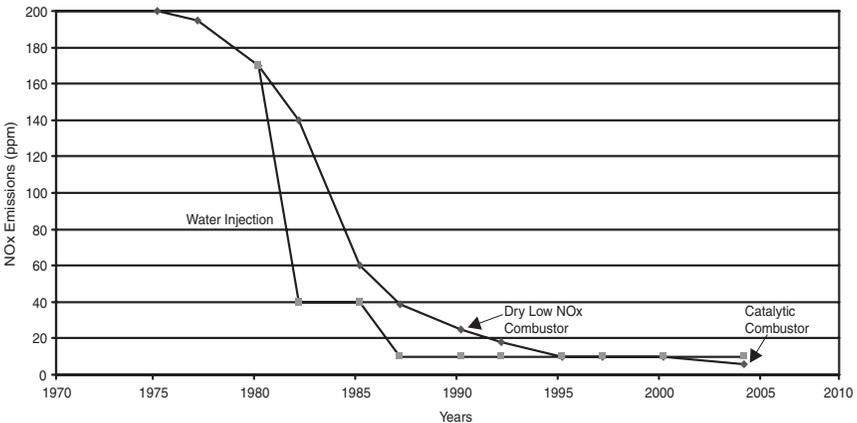


Figure 1-33. Control of gas turbine NO_x emissions over the years.

combustors have greatly reduced the NO_x output. New units under development have goals, which would reduce NO_x levels below 9 ppm. Catalytic converters have also been used in conjunction with both these types of combustors to even further reduce the NO_x emissions.

New research in combustors such as catalytic combustion have great promise, and values of as low as 2 ppm can be attainable in the future. Catalytic combustors are already being used in some engines under the U.S. Department of Energy's (DOE), Advanced Gas Turbine Program, and have obtained very encouraging results.

Turbine Expander Section

There are two types of turbines used in gas turbines. These consist of the axial-flow type and the radial-inflow type. The axial-flow turbine is used in more than 95% of all applications.

The two types of turbines—axial-flow and radial-inflow turbines—can be divided further into impulse or reaction type units. Impulse turbines take their entire enthalpy drop through the nozzles, while the reaction turbine takes a partial drop through both the nozzles and the impeller blades.

Radial-Inflow Turbine

The radial-inflow turbine, or inward-flow radial turbine, has been in use for many years. Basically a centrifugal compressor with reversed flow and opposite rotation, the inward-flow radial turbine is used for smaller loads and over a smaller operational range than the axial turbine.

Radial-inflow turbines are only now beginning to be used because little was known about them heretofore. Axial turbines have enjoyed tremendous interest due to their low frontal area, making them suited to the aircraft industry. However, the axial machine is much longer than the radial machine, making it unsuited to certain applications. Radial turbines are used in turbochargers and in some types of expanders.

The inward-flow radial turbine has many components similar to a centrifugal compressor. There are two types of inward-flow radial turbines: the cantilever and the mixed-flow. The cantilever type in Figure 1-34 is similar to an axial-flow turbine, but it has radial blading. However, the cantilever turbine is not popular because of design and production difficulties.

Mixed-Flow Turbine. The turbine as shown in Figure 1-35, is almost identical to a centrifugal compressor—except its components have different functions. The scroll is used to distribute the gas uniformly around the periphery of the turbine.

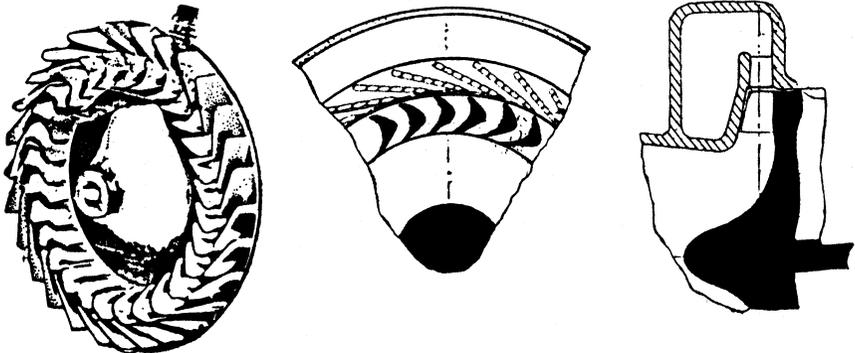


Figure 1-34. Cantilever-type radial inflow turbine.

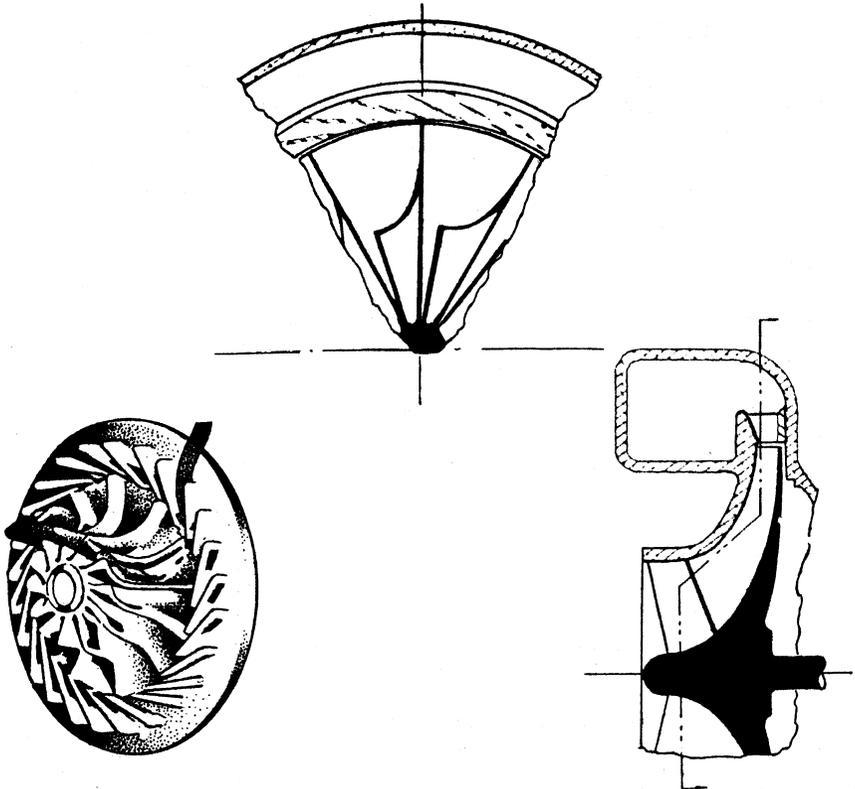


Figure 1-35. Mixed flow type radial inflow turbine.

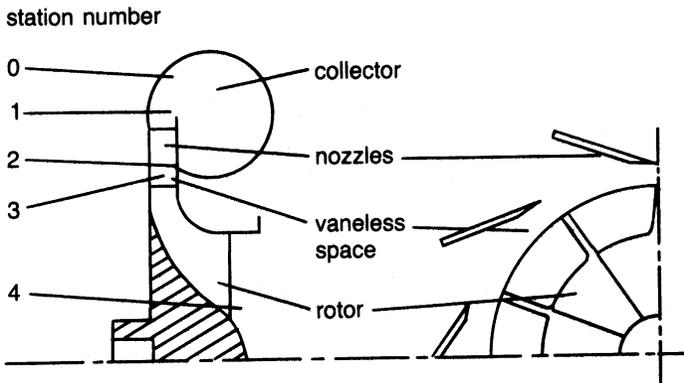


Figure 1-36. Components of a Radial Inflow Turbine.

The nozzles, used to accelerate the flow toward the impeller tip, are usually straight vanes with no airfoil design. The vortex is a vaneless space and allows an equalization of the pressures. The flow enters the rotor radially at the tip with no appreciable axial velocity and exits the rotor through the exducer axially with little radial velocity.

The nomenclature of the Inward-Flow Radial Turbine is shown in Figure 1-36. These turbines are used because of lower production costs, in part because the nozzle blading does not require any camber or airfoil design.

Axial-Flow Turbines

The axial-flow turbine, like its counterpart the axial-flow compressor, has flow, which enters and leaves in the axial direction. There are two types of axial turbines: (1) impulse type, and (2) reaction type. The impulse turbine has its entire enthalpy drop in the nozzle; therefore it has a very high velocity entering the rotor. The reaction turbine divides the enthalpy drop in the nozzle and the rotor. Figure 1-37 is a schematic of an axial-flow turbine, also depicting the distribution of the pressure, temperature and the absolute velocity.

Most axial flow turbines consist of more than one stage, the front stages are usually impulse (zero reaction) and the later stages have about 50% reaction. The impulse stages produce about twice the output of a comparable 50% reaction stage, while the efficiency of an impulse stage is less than that of a 50% reaction stage.

The high temperatures that are now available in the turbine section are due to improvements of the metallurgy of the blades in the turbines.

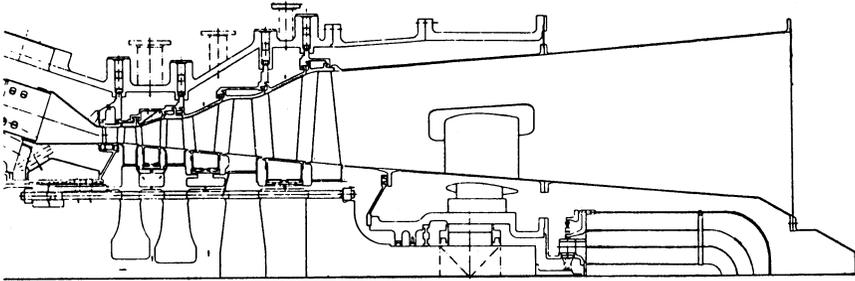


Figure 1-37. Schematic of an axial flow turbine.

Development of directionally solidified blades as well as the new single crystal blades, with the new coatings, and the new cooling schemes, are responsible for the increase in firing temperatures. The high-pressure ratio in the compressor also causes the cooling air used in the first stages of the turbine to be very hot. The temperatures leaving the gas turbine compressor can reach as high as 1200 °F (649 °C). Thus, the present cooling schemes need revisiting and the cooling passages are in many cases also coated. The cooling schemes are limited in the amount of air they can use, before there is a negating an effort in overall thermal efficiency due to an increase in the amount of air used in cooling. The rule of thumb in this area is that if you need more than 8% of the air for cooling you are loosing the advantage from the increase in the firing temperature.

The new gas turbines being designed, for the new millennium, are investigating the use of steam as a cooling agent for the first and second stages of the turbines. Steam cooling is possible in the new combined cycle power plants, which is the base of most of the new High Performance Gas Turbines. Steam as part of the cooling as well as part of the cycle power will be used in the new gas turbines in the combined cycle mode. The extra power obtained by the use of steam is the cheapest MW/\$ available. The injection of about 5% of steam by weight of air amounts to about 12% more power. The pressure of the injected steam must be at least 60 psi (4 Bar) Bar above the compressor discharge. The way steam is injected must be done very carefully so as to avoid compressor surge. These are not new concepts and have been used and demonstrated in the past. Steam cooling for example was the basis of the cooling schemes proposed by the team of United Technology and Stal-Laval in their conceptual study for the U.S. Department study on the High Turbine Temperature Technology Program, which was investigating Firing Temperatures of 3000 °F (1649 °C), in the early 1980s.

Materials

The development of new materials as well as cooling schemes has seen the rapid growth of the turbine firing temperature leading to high turbine efficiencies. The stage 1 blade must withstand the most severe combination of temperature, stress, and environment; it is generally the limiting component in the machine. Figure 1-38 shows the trend of firing temperature and blade alloy capability. Since 1950, turbine bucket material temperature capability has advanced approximately 850°F (472°C), approximately 20°F/10°C per year. The importance of this increase can be appreciated by noting that an increase of 100°F (56°C) in turbine firing temperature can provide a corresponding increase of 8–13% in output and 2–4% improvement in simple-cycle efficiency. Advances in alloys and processing, while expensive and time-consuming, provide significant incentives through increased power density and improved efficiency.

The increases in blade alloy temperature capability accounted for the majority of the firing temperature increase until air-cooling was introduced, which decoupled firing temperature from the blade metal temperature. Also, as the metal temperatures approached the 1600°F (870°C) range, hot corrosion of blades became more life limiting than strength until the introduction of protective coatings. During the 1980s, emphasis turned toward two major areas: improved materials technology, to achieve greater blade alloy capability without sacrificing alloy corrosion resistance; and advanced, highly

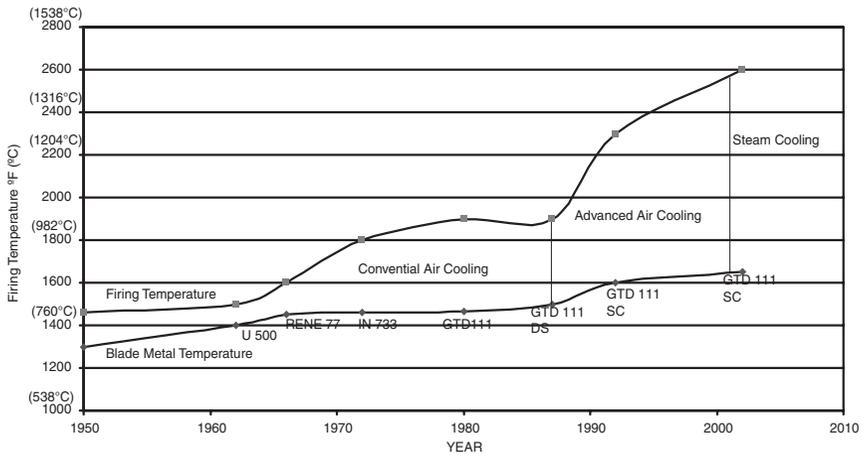


Figure 1-38. Firing temperature increase with blade material improvement.

sophisticated air-cooling technology to achieve the firing temperature capability required for the new generation of gas turbines. The use of steam cooling to further increase combined-cycle efficiencies in combustors was introduced in the mid to late 1990s. Steam cooling in blades and nozzles will be introduced in commercial operation in the year 2002.

In the 1980s, IN-738 blades were widely used. IN-738, was the acknowledged corrosion standard for the industry. Directionally Solidified (DS) blades, first used in aircraft engines more than 25 years ago, were adapted for use in large airfoils in the early 1990s and were introduced in the large industrial turbines to produce advanced technology nozzles and blades. The directionally solidified blade has a grain structure that runs parallel to the major axis of the part and contains no transverse grain boundaries, as in ordinary blades. The elimination of these transverse grain boundaries confers additional creep and rupture strength on the alloy, and the orientation of the grain structure provides a favorable modulus of elasticity in the longitudinal direction to enhance fatigue life. The use of directionally solidified blades results in a substantial increase in the creep life, or substantial increase in tolerable stress for a fixed life. This advantage is due to the elimination of transverse grain boundaries from the blades, the traditional weak link in the microstructure. In addition to improved creep life, the directionally solidified blades possess more than 10 times the strain control or thermal fatigue compared to equiaxed blades. The impact strength of the directionally solidified blades is also superior to that of equiaxed, showing an advantage of more than 33%.

In the late 1990s, single-crystal blades have been introduced in gas turbines. These blades offer additional, creep and fatigue benefits through the elimination of grain boundaries. In single-crystal material, all grain boundaries are eliminated from the material structure and a single crystal with controlled orientation is produced in an airfoil shape. By eliminating all grain boundaries and the associated grain boundary strengthening additives, a substantial increase in the melting point of the alloy can be achieved, thus providing a corresponding increase in high-temperature strength. The transverse creep and fatigue strength is increased, compared to equiaxed or DS structures. The advantage of single-crystal alloys compared to equiaxed and DS alloys in low-cycle fatigue (LCF) life is increased by about 10%.

Coatings

There are three basic types of coatings, thermal barrier coatings, diffusion coatings, and plasma sprayed coatings. The advancements in coating have also been essential in ensuring that the blade base metal is protected at these

high temperatures. Coatings ensure that the life of the blades are extended and in many cases are used as sacrificial layer, which can be stripped and recoated. Life of coatings depends on composition, thickness, and the standard of evenness to which it has been deposited. The general type of coatings is very little different from the coatings used 10–15 years ago. These include various types of diffusion coatings such as Aluminide Coatings originally developed nearly 40 years ago. The thickness required is between 25–75 μm thick. The new aluminide coatings with Platinum increase the oxidation resistance, and also the corrosion resistance. The thermal barrier coatings have an insulation layer of 100–300 μm thick, and are based on $\text{ZrO}_2\text{-Y}_2\text{O}_3$ and can reduce metal temperatures by 120–300 $^\circ\text{F}$ (50–150 $^\circ\text{C}$). This type of coating is used in combustion cans, transition pieces, nozzle guide vanes, and also blade platforms.

The interesting point to note is that some of the major manufacturers are switching away from corrosion protection biased coatings over towards coatings, which are not only oxidation resistant, but also oxidation resistant at higher metal temperatures. Thermal barrier coatings are being used on the first few stages in all the advanced technology units. The use of internal coatings is getting popular due to the high temperature of the compressor discharge, which results in oxidation of the internal surfaces. Most of these coatings are aluminide type coatings. The choice is restricted due to access problems to slurry based, or gas phase/chemical vapor deposition. Care must be taken in production, otherwise internal passages may be blocked. The use of pyrometer technology on some of the advanced turbines has located blades with internal passages blocked causing that blade to operate at temperatures of 95–158 $^\circ\text{F}$ (35–70 $^\circ\text{C}$).

Gas Turbine Heat Recovery

The waste heat recovery system is a critically important subsystem of a cogeneration system. In the past, it was viewed as a separate “add-on” item. This view is being changed with the realization that good performance, both thermodynamically and in terms of reliability, grows out of designing the heat recovery system as an integral part of the overall system.

The gas turbine exhaust gases enter the Heat Recovery Steam Generating (HRSG), where the energy is transferred to the water to produce steam. There are many different configurations of the HRSG units. Most HRSG units are divided into the same amount of sections as the steam turbine. In most cases, each section of the HRSG has a Pre-heater, an Economizer and Feed-water, and then a Superheater. The steam entering the steam turbine is superheated.

The most common type of an HRSG in a large Combined Cycle Power is the drum type HRSG with forced circulation. These types of HRSGs are vertical, the exhaust gas flow is vertical with horizontal tube bundles suspended in the steel structure. The steel structure of the HRSG supports the drums. In a forced circulation HRSG, the steam water mixture is circulated through evaporator tubes using a pump. These pumps increase the parasitic load and thus detract from the cycle efficiency. In this type of HRSG the heat transfer tubes are horizontal, suspended from un-cooled tube supports located in the hot gas path. Some vertical HRSGs are designed with evaporators, which operate without the use of circulation pumps.

The Once Through Steam Generators (OTSG) are finding quick acceptance due to the fact that they have smaller foot prints, and can be installed in a much shorter time and lower price. The Once Through Steam Generators unlike other HRSGs do not have defined economizer, evaporator, or superheater sections. Figure 1-39 is the schematic of an OTSG system, and a drum-type HRSG. The OTSG is basically one tube; water enters at one end and steam leaves at the other end, eliminating the drum and circulation pumps. The location of the water to steam interface is free to move, depending on the total heat input from the gas turbine, and flow rates and pressures of the Feedwater, in the tube bank. Unlike other HRSGs, the once-through units have no steam drums.

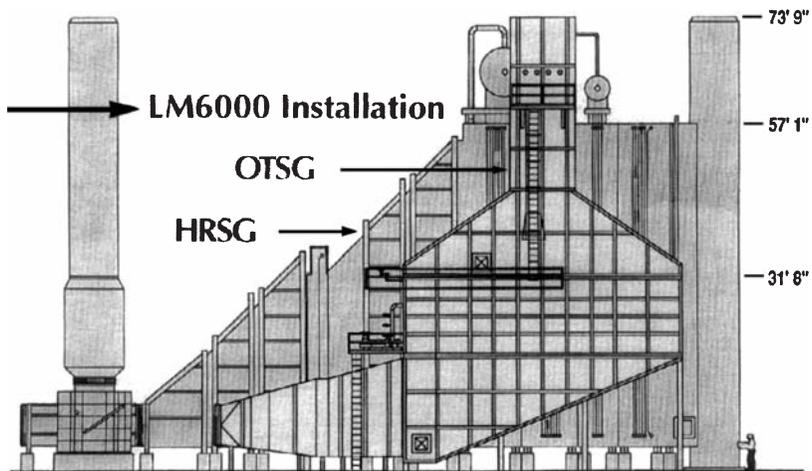


Figure 1-39. Comparison of a drum type HRSG to a once through steam generator. (Courtesy Innovative Steam Technologies.)

Some important points and observations relating to gas turbine waste heat recovery are:

Multipressure Steam Generators—These are becoming increasingly popular. With a single pressure boiler, there is a limit to the heat recovery because the exhaust gas temperature cannot be reduced below the steam saturation temperature. This problem is avoided by the use of multipressure levels.

Pinch Point—This is defined as the difference between the exhaust gas temperature leaving the evaporator section and the saturation temperature of the steam. Ideally, the lower the pinch point, the more heat recovered, but this calls for more surface area and, consequently, increases the back-pressure and cost. Also, excessively low pinch points can mean inadequate steam production if the exhaust gas is low in energy (low mass flow or low exhaust gas temperature). General guidelines call for a pinch point of 15–40°F (8–22°C). The final choice is obviously based on economic considerations.

Approach Temperature—This is defined as the difference between the saturation temperatures of the steam and the inlet water. Lowering the approach temperature can result in increased steam production, but at increased cost. Conservatively high-approach temperatures ensure that no steam generation takes place in the economizer. Typically, approach temperatures are in the 10–20°F (5.5–11°C) range. Figure 1-40 is the temperature energy diagram for a system and also indicates the approach and pinch points in the system.

Off-Design Performance—This is an important consideration for waste heat recovery boilers. Gas turbine performance is affected by load, ambient conditions, and gas turbine health (fouling, etc.). This can affect the exhaust gas temperature and the air flow rate. Adequate considerations must be given to bow steam flows (low pressure and high pressure) and superheat temperatures vary with changes in the gas turbine operation.

Evaporators—These usually utilize a fin-tube design. Spirally finned tubes of 1.25 in to 2 in outer diameter (OD) with three to six fins per inch are common. In the case of unfired designs, carbon steel construction can be used and boilers can run dry. As heavier fuels are used, a smaller number of fins per inch should be utilized to avoid fouling problems.

Forced Circulation System—Using forced circulation in a waste heat recovery system allows the use of smaller tube sizes with inherent increased heat transfer coefficients. Flow stability considerations must be addressed. The recirculating pump is a critical component from a reliability standpoint and standby (redundant) pumps must be considered. In any event, great care must go into preparing specifications for this pump.

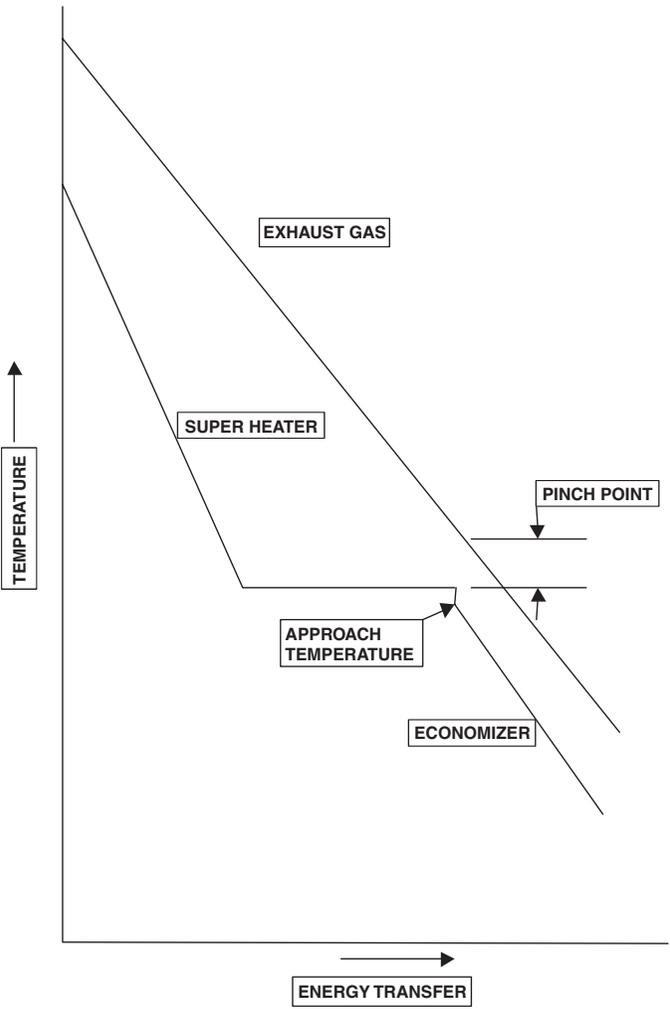


Figure 1-40. Energy transfer diagram in an HRSG of a combined cycle power plant.

Back Pressure Considerations (Gas Side)—These are important, as excessively high back-pressures create performance drops in gas turbines. Very low-pressure drops would require a very large heat exchanger and more expense. Typical pressure drops are 8–10 inches of water.

Supplementary Firing of Heat Recovery Systems

There are several reasons for supplementary firing a wasteheat recovery unit. Probably the most common is to enable the system to track demand (i.e., produce more steam when the load swings upwards, than the unfired unit can produce). This may enable the gas turbine to be sized to meet the base load demand with supplemental firing taking care of higher load swings. Figure 1-41 shows a schematic of a supplementary fired exhaust gas steam generator.

Raising the inlet temperature at the waste heat boiler allows a significant reduction in the heat transfer area and, consequently, the cost. Typically, as the gas turbine exhaust has ample oxygen, duct burners can be conveniently used.

An advantage of supplemental firing is the increase in heat recovery capability (recovery ratio). A 50% increase in heat input to the system increases the output 94%, with the recovery ratio increasing by 59%. Some important design guidelines to ensure success include:

- Special alloys may be needed in the superheater and evaporator to withstand the elevated temperatures.
- The inlet duct must be of sufficient length to ensure complete combustion and avoid direct flame contact on the heat transfer surfaces.

FPO

Figure 1-41. Supplementary fired exhaust gas steam generator.

- If natural circulation is utilized, an adequate number of risers and feeders must be provided as the heat flux at entry is increased.
- Insulation thickness on the duct section must be increased.

Instrumentation and Controls

The advanced gas turbines are all digitally controlled and incorporate on-line condition monitoring. The addition of new on-line monitoring requires new and smart instrumentation. The use of pyrometers to sense blade metal temperatures are being introduced. The blade metal temperatures are the real concern not the exit gas temperature. The use of dynamic pressure transducers for detection of surge and other flow instabilities in the compressor and also in the combustion process especially in the new Low NO_x Combustors, are being introduced. Accelerometers are being introduced to detect high-frequency excitation of the blades, this prevents major failures in the new highly loaded gas turbines.

The use of pyrometers in control of the advanced gas turbines is being investigated. Presently, all turbines are controlled based on gasifier turbine exit temperatures, or power turbine exit temperatures. By using the blade metal temperatures of the first section of the turbine the gas turbine is being controlled at its most important parameter, the temperature of the first stage nozzles and blades. In this manner, the turbine is being operated at its real maximum capability.

The use of dynamic pressure transducers gives early warning of problems in the compressor. The very high pressure in most of the advanced gas turbines cause these compressors to have a very narrow operating range between surge and choke. Thus, these units are very susceptible to dirt and blade vane angles. The early warning provided by the use of dynamic pressure measurement at the compressor exit can save major problems encountered due to tip stall and surge phenomenon.

The use of dynamic pressure transducer in the combustor section, especially in the Low NO_x Combustors ensures that each combustor can be burning evenly. This is achieved by controlling the flow in each combustor until the spectrums obtained from each combustor can match. This technique has been used and found to be very effective and ensures smooth operation of the turbine.

Performance monitoring not only plays a major role in extending life, diagnosing problems, and increasing time between overhauls, but also can provide major savings on fuel consumption by ensuring that the turbine is being operated at its most efficient point. Performance monitoring requires

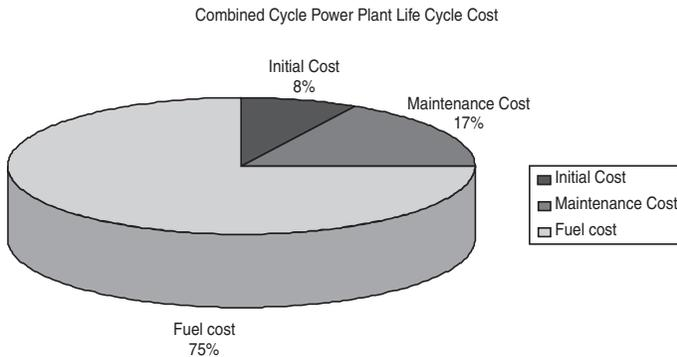


Figure 1-42. Plant life cycle cost for a combined cycle power plant.

an in-depth understanding of the equipment being measured. The development of algorithms for a complex train needs careful planning, understanding of the machinery and process characteristics. In most cases, help from the manufacturer of the machinery would be a great asset. For new equipment this requirement can and should be part of the bid requirements. For plants with already installed equipment a plant audit to determine the plant machinery status is the first step. Figure 1-42 shows the cost distribution over the life cycle of gas turbine plant. It is interesting to note that the initial cost runs about 8% of the total life cycle cost, and the operational and maintenance cost is about 17%, and the fuel cost is about 75%.

Bibliography

- Barker, Thomas, "Siemens' New Generation," *Turbomachinery International*, January–February 1995.
- Boyce, M.P., "Cutting Edge Turbine Technology," *Middle East Electricity*, August 1999.
- Boyce, M.P., "Turbo-Machinery for the Next Millennium," *Russia Gas Turbo-Technology Publication*, September–October 2000.
- Boyce, M.P., "Cogeneration and Combined Cycle Power Plants," Chapter 1, ASME Press 2001.
- Capstone Micro Turbine Sales Literature, "Simple Cycle Micro Turbine Power Generation System," 2000, Chatsworth, California.
- Distributed Power Editorial, "Distributed Generation: Understanding The Economics", May–June, 2000.

- Farmer, R., "Design 60% Net Efficiency in Frame 7/9H Steam Cooled CCGT," *Gas Turbine World*, May–June 1995.
- Hawthorne, W.R., and Olsen, W.T., Eds., *Design and Performance of Gas Turbine Plants*, Vol. 2, Princeton Univ. Press, 1960, pp. 563–590.
- Horner, M.W., "GE Aeroderivative Gas Turbines—Design and Operating Features," 39th GE Turbine State-of-the-Art Technology, Seminar, August 1996.
- Ingersoll-Rand Corporation, "Cogeneration System Package for Micro-Turbines," Sales Literature—2000, Portsmouth, New Hampshire.
- Leo, A.J., Ghezel-Ayagh, H., and Sanderson, R., Ultra High Efficiency Hybrid Direct Fuel Cell/Turbine Power Plant, ASME 2000-GT-0552, October–November 1999
- Modern Power Systems, Ed., "Steam cooled 60 Hz W501G generates 230 MW," August 1994.
- Paul, T.C., Schonewald, R.W., and Marolda, P.J., "Power Systems for the 21st Century—"H" Gas Turbine Combined Cycles" 39th GE Turbine State-of-the-Art Technology, Seminar, August 1996.
- United Nations Framework Convention on Climate Change, "Kyoto Protocol of 1997," United Nations 1997, N.Y.
- United States Environmental Protection Agency, "1990 Clean Air Act," Washington, D.C., 1990.
- Valenti, Michael, "A Turbine for Tomorrows Navy," ASME Mechanical Engineering, September 1998.

2

Theoretical and Actual Cycle Analysis

The thermodynamic analysis presented here is an outline of the air-standard Brayton cycle and its various modifications. These modifications are evaluated to examine the effects they have on the basic cycle. One of the most important is the augmentation of power in a gas turbine, this is treated in a special section in this chapter.

The Brayton Cycle

The Brayton cycle in its ideal form consists of two isobaric processes and two isentropic processes. The two isobaric processes consist of the combustor system of the gas turbine and the gas side of the HRSG. The two isentropic processes represent the compression (Compressor) and the expansion (Turbine Expander) processes in the gas turbine. Figure 2-1 shows the Ideal Brayton Cycle.

A simplified application of the first law of thermodynamics to the air-standard Brayton cycle in Figure 2-1 (assuming no changes in kinetic and potential energy) has the following relationships:

Work of compressor

$$W_c = \dot{m}_a(h_2 - h_1) \quad (2-1)$$

Work of turbine

$$W_t = (\dot{m}_a + \dot{m}_f)(h_3 - h_4) \quad (2-2)$$

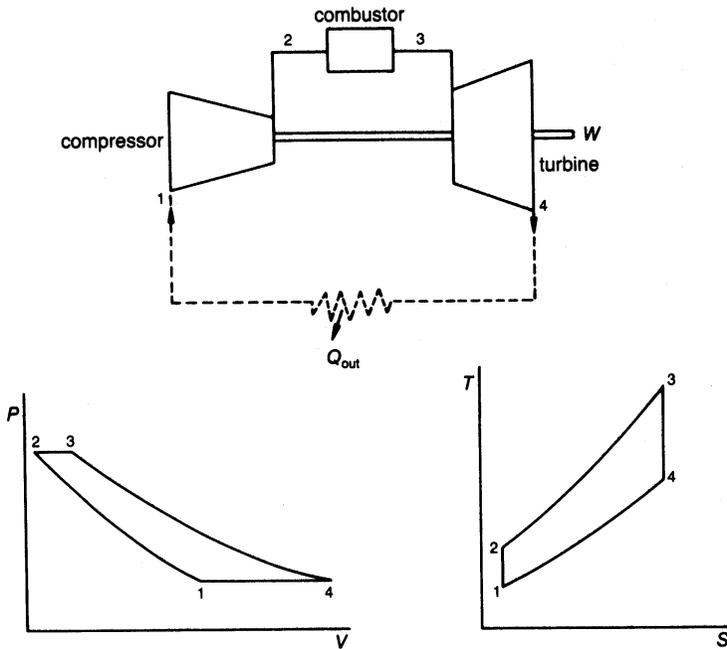


Figure 2-1. The air-standard Brayton cycle.

Total output work

$$W_{cyc} = W_t - W_c \tag{2-3}$$

Heat added to system

$$Q_{2,3} = \dot{m}_f \times LHV_{fuel} = (\dot{m}_a + \dot{m}_f)(h_3) - \dot{m}_a h_2 \tag{2-4}$$

Thus, the overall cycle efficiency is

$$\eta_{cyc} = W_{cyc} / Q_{2,3} \tag{2-5}$$

Increasing the pressure ratio and the turbine firing temperature increases the Brayton cycle efficiency. This relationship of overall cycle efficiency is based on certain simplification assumptions such as: (1) $\dot{m}_a \gg \dot{m}_f$, (2) the gas is calorically and thermally perfect, which means that

the specific heat at constant pressure (c_p) and the specific heat at constant volume (c_v) are constant thus the specific heat ratio γ remains constant throughout the cycle, (3) the pressure ratio (r_p) in both the compressor and the turbine are the same, and (4) all components operate at 100% efficiency. With these assumptions the effect on the ideal cycle efficiency as a function of pressure ratio for the ideal Brayton cycle operating between the ambient temperature and the firing temperature is given by the following relationship:

$$\eta_{\text{ideal}} = \left(1 - \frac{1}{r_p^{\frac{\gamma-1}{\gamma}}} \right) \quad (2-6)$$

where Pr = Pressure Ratio; and γ is the ratio of the specific heats. The above equation tends to go to very high numbers as the pressure ratio is increased.

Assuming that the pressure ratio is the same in both the compressor and the turbine the following relationships hold using the pressure ratio in the compressor:

$$\eta_{\text{ideal}} = 1 - \frac{T_1}{T_2} \quad (2-7)$$

and using the pressure ratio in the turbine

$$\eta_{\text{ideal}} = 1 - \frac{T_4}{T_3} \quad (2-8)$$

In the case of the actual cycle the effect of the turbine compressor (η_c), and expander (η_t) efficiencies must also be taken into account, to obtain the overall cycle efficiency between the firing temperature T_f and the ambient temperature T_{amb} of the turbine. This relationship is given in the following equation:

$$\eta_{\text{cycle}} = \left(\frac{\eta_t T_f - \frac{T_{\text{amb}} r_p^{\frac{(\gamma-1)}{\gamma}}}{\eta_c}}{T_f - T_{\text{amb}} - T_{\text{amb}} \left(\frac{r_p^{\frac{(\gamma-1)}{\gamma}} - 1}{\eta_c} \right)} \right) \left(1 - \frac{1}{r_p^{\frac{(\gamma-1)}{\gamma}}} \right) \quad (2-9)$$

Figure 2-2 shows the effect on the overall cycle efficiency of the increasing pressure ratio and the firing temperature. The increase in the pressure ratio increases the overall efficiency at a given firing temperature; however, increasing the pressure ratio beyond a certain value at any given firing temperature can actually result in lowering the overall cycle efficiency. It should also be noted that the very high-pressure ratios tend to reduce the operating range of the turbine compressor. This causes the turbine compressor to be much more intolerant to dirt build up in the inlet air filter and on the compressor blades and creates large drops in cycle efficiency and performance. In some cases, it can lead to compressor surge, which in turn can lead to a flameout, or even serious damage and failure of the compressor blades and the radial and thrust bearings of the gas turbine.

To obtain a more accurate relationship between the overall thermal efficiency and the inlet turbine temperatures, overall pressure ratios, and output work, consider the following relationships. For maximum overall thermal cycle efficiency, the following equation gives the optimum pressure ratio for fixed inlet temperatures and efficiencies to the compressor and turbine:

$$(r_p)_{\text{opt}} = \left\{ \frac{1}{T_1 T_3 \eta_t - T_1 T_3 + T_1^2} [T_1 T_3 \eta_t - \sqrt{(T_1 T_3 \eta_t)^2 - (T_1 T_3 \eta_t - T_1 T_3 + T_1^2)(T_3^2 \eta_c \eta_t - T_1 T_3 \eta_c \eta_t + T_1 T_3 \eta_t)}] \right\}^{\frac{\gamma}{\gamma-1}} \tag{2-10}$$

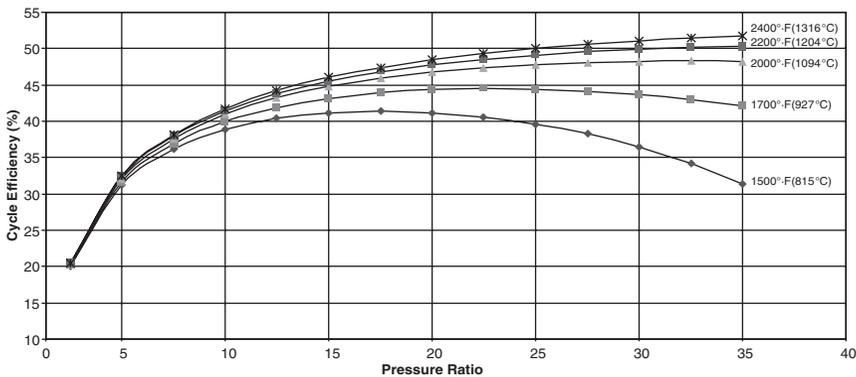


Figure 2-2. Overall cycle efficiency as a function of the firing temperature and pressure ratio. Based on a compressor efficiency of 87% and a turbine efficiency of 92%.

the above equation for no losses in the compressor and turbine ($\eta_c = \eta_t = 1$) reduces to:

$$(r_p)_{\text{opt}} = \left(\frac{T_1 T_3}{T_1^2} \right)^{\frac{\gamma}{\gamma-1}} \tag{2-11}$$

The optimum pressure ratio for maximum output work for a turbine taking into account the efficiencies of the compressor and the turbine expander section can be expressed by the following relationship:

$$r_{p_{\text{wopt}}} = \left[\left(\frac{T_3 \eta_c \eta_t}{2 T_1} \right) + \frac{1}{2} \right]^{\frac{\gamma}{\gamma-1}} \tag{2-12}$$

Figure 2-3 shows the optimum pressure ratio for maximum efficiency or work per lb (kg) of air. The optimum pressure ratio based on work occurs at a lower pressure ratio than the point of maximum efficiency at the same firing Temperature.

Thus, a cursory inspection of the efficiency indicate that the overall efficiency of a cycle can be improved by increasing the pressure ratio, or increasing the turbine inlet temperature, and the work per lb (kg) of air can be increased by increasing the pressure ratio, or increasing the turbine inlet temperature, or by decreasing the inlet temperature.

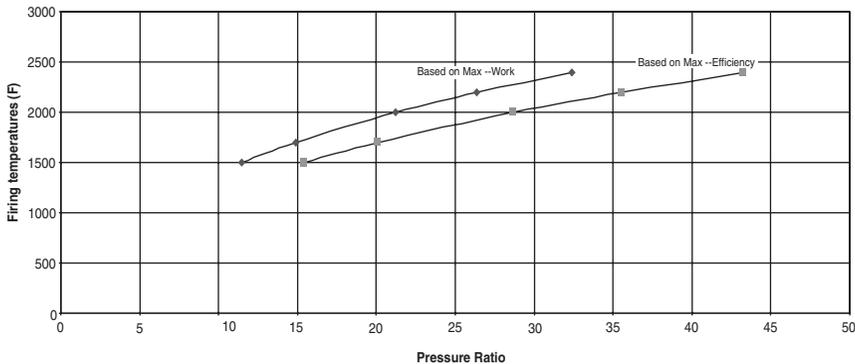


Figure 2-3. Pressure ratio based on maximum efficiency or work at various firing temperatures. Based on a compressor efficiency of 87% and a turbine efficiency of 92%.

Regeneration Effect

In a simple gas turbine cycle the turbine exit temperature is nearly always appreciably higher than the temperature of the air leaving the compressor. Obviously, the fuel requirement can be reduced by the use of a regenerator in which the hot turbine exhaust gas preheats the air between the compressor and the combustion chamber. Figure 2-4 shows a schematic of the regenerative cycle and its performance in the T-S diagram. In an ideal case the flow through the regenerator is at constant pressure. The regenerator effectiveness is given by the following relationship:

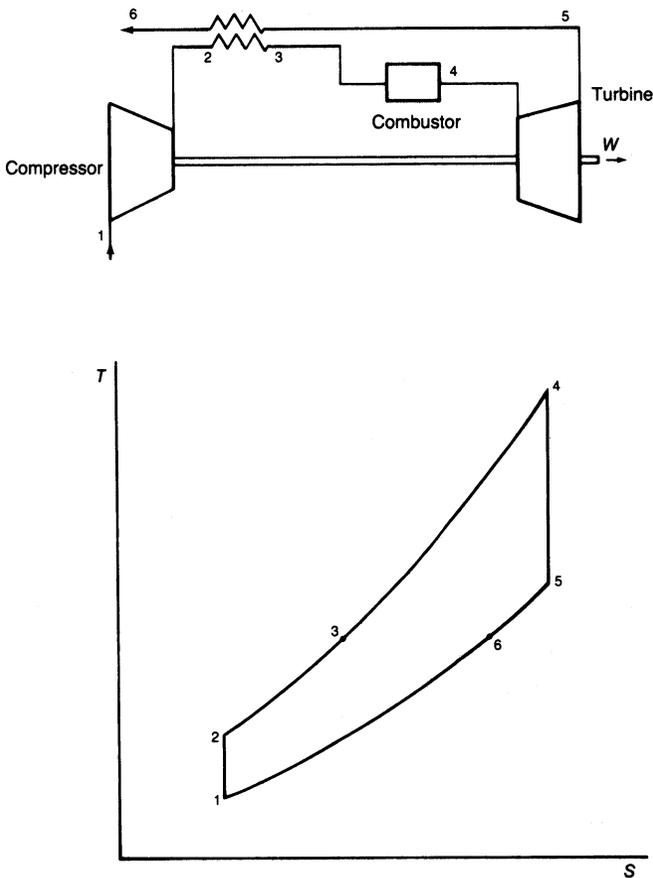


Figure 2-4. The regenerative gas turbine cycle.

$$\eta_{\text{reg}} = \frac{T_3 - T_2}{T_5 - T_2} \quad (2-13)$$

Thus, the overall efficiency for this system's cycle can be written as

$$\eta_{\text{RCYC}} = \frac{(T_4 - T_5) - (T_2 - T_1)}{(T_4 - T_3)} \quad (2-14)$$

Increasing the effectiveness of a regenerator calls for more heat transfer surface area, which increases the cost, the pressure drop, and the space requirements of the unit.

Figure 2-5 shows the improvement in cycle efficiency because of heat recovery with respect to a simple open-cycle gas turbine of 4.33:1 ratio pressure and 1,200 °F inlet temperature. Cycle efficiency drops with an increasing pressure drop in the regenerator.

There are two types of heat exchangers Regenerative and Recuperative. The term "regenerative heat exchanger" is used for a system in which the

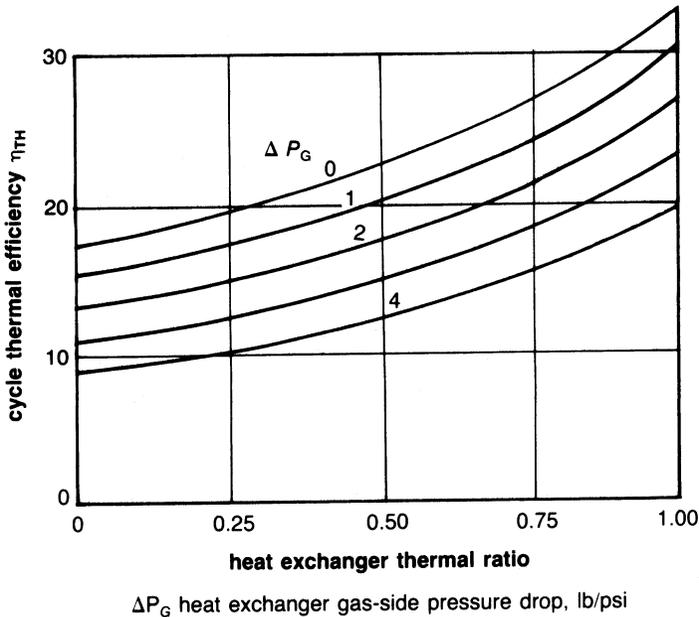


Figure 2-5. Variation of a gas turbine cycle efficiency with heat exchanger performance.

heat transfer between two streams is affected by the exposure of a third medium alternately to the two flows. The heat flows successively into and out of the third medium, which undergoes a cyclic temperature. These types of heat exchangers are widely used where compactness is essential. The automotive regenerators consisted of a large circular drum with honey-combed ceramic passages. The drum was rotated at a very low rpm (10–15 rpm). The drum surface was divided into two halves by an air seal. The hot air would pass through one half of the circular drum heating the honeycombed passages the air would encounter, then the cooler air would pass through these same passages as the drum was rotated and would be heated.

In a recuperative heat exchanger, each element of heat-transferring surface has a constant temperature and, by arranging the gas paths in contra-flow, the temperature distribution in the matrix in the direction of flow is that giving optimum performance for the given heat-transfer conditions. This optimum temperature distribution can be achieved ideally in a contra-flow regenerator and approached very closely in a cross-flow regenerator.

The matrix permitting the maximum flow per unit area will yield the smaller regenerator for a given thermal and pressure drop performance. A material with a high heat capacity per unit volume is preferred, since this property of the material will increase the switching time and tend to reduce carry-over losses. Another desirable property of the arrangement is low thermal conductivity in the direction of the gas flow. All leakages within the regenerator must be avoided. A leakage of 3% reduces the regenerator effectiveness from 80–71%.

Increasing the Work Output of the Simple Cycle Gas Turbine

The way to enhance the power output of a gas turbine can be achieved by intercooling and reheat.

Intercooling and Reheat Effects. The net work of a gas turbine cycle is given by

$$W_{\text{cyc}} = W_t - W_c \quad (2-15)$$

and can be increased either by decreasing the compressor work or by increasing the turbine work. These are the purposes of intercooling and reheating, respectively.

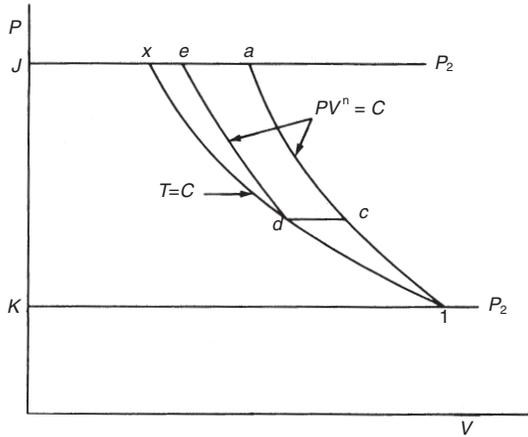


Figure 2-6. Multistages compression with intercooling.

Multi-staging of compressors is sometimes used to allow for cooling between the stages to reduce the total work input. Figure 2-6 shows a polytropic compression process 1-a on the P - V plane. If there is no change in the kinetic energy, the work done is represented by the area 1-a-j-k-1. A constant temperature line is shown as 1-x. If the polytropic compression from State 1 to State 2 is divided into two parts, 1-c and d-e with constant pressure cooling to $T_d = T_1$ between them, the work done is represented by area 1-c-d-e-I-k-1. The area c-a-e-d-c represents the work saved by means of the two-stage compression with intercooling to the initial temperature. The optimum pressure for intercooling for specified values P_1 and P_2 is:

$$P_{OPT} = \sqrt{P_1 P_2} \tag{2-16}$$

Therefore, if a simple gas turbine cycle is modified with the compression accomplished in two or more adiabatic processes with intercooling between them, the net work of the cycle is increased with no change in the turbine work.

The thermal efficiency of an ideal simple cycle is decreased by the addition of an intercooler. Figure 2-7 shows the schematic of such a cycle. The ideal simple gas turbine cycle is 1-2-3-4-1, and the cycle with the intercooling added is 1-a-b-c-2-3-4-1. Both cycles in their ideal form are reversible and can be simulated by a number of Carnot cycles. Thus, if the simple gas turbine cycle 1-2-3-4-1 is divided into a number of cycles like m -n-o-p-m,

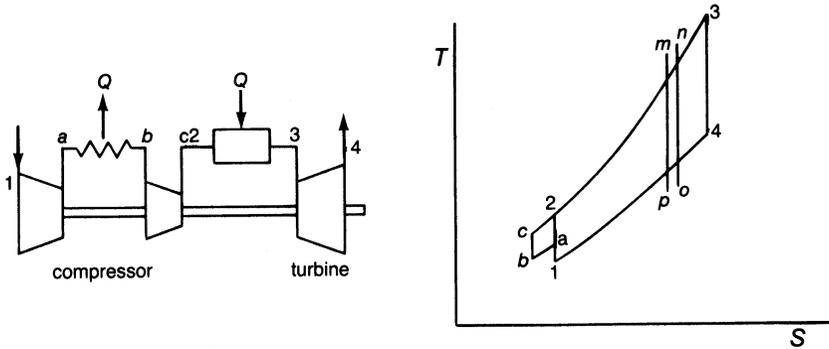


Figure 2-7. The intercooled gas turbine cycle.

these little cycles approach the Carnot cycle as their number increases. The efficiency of such a Carnot cycle is given by the relationship

$$\eta_{\text{CARNOT}} = 1 - \frac{T_m}{T_p} \quad (2-17)$$

Notice that if the specific heats are constant, then

$$\frac{T_3}{T_4} = \frac{T_m}{T_p} = \frac{T_2}{T_1} = \left(\frac{P_2}{P_1} \right)^{\frac{\gamma-1}{\gamma}} \quad (2-18)$$

All the Carnot cycles making up the simple gas turbine cycle have the same efficiency. Likewise, all of the Carnot cycles into which the cycle $a-b-c-2-a$ might similarly be divided have a common value of efficiency lower than the Carnot cycles which comprise cycle $1-2-3-4-1$. Thus, the addition of an intercooler, which adds $a-b-c-2-a$ to the simple cycle, lowers the efficiency of the cycle.

The addition of an intercooler to a regenerative gas turbine cycle increases the cycle's thermal efficiency and output work because a larger portion of the heat required for the process $c-3$ in Figure 2-7 can be obtained from the hot turbine exhaust gas passing through the regenerator instead of from burning additional fuel.

The reheat cycle increases the turbine work, and consequently the net work of the cycle, can be increased without changing the compressor work or the turbine inlet temperature by dividing the turbine expansion into two

or more parts with constant pressure heating before each expansion. This cycle modification is known as reheating as seen in Figure 2-8. By reasoning similar to that used in connection with Intercooling, it can be seen that the thermal efficiency of a simple cycle is lowered by the addition of reheating, while the work output is increased. However, a combination of regenerator and reheater can increase the thermal efficiency.

Actual Cycle Analysis

The previous section dealt with the concepts of the various cycles. Work output and efficiency of all actual cycles are considerably less than those of the corresponding ideal cycles because of the effect of compressor, combustor, and turbine efficiencies and pressure losses in the system.

The Simple Cycle

The simple cycle is the most common type of cycle being used in gas turbines in the field today. The actual open simple cycle as shown in Figure 2-9 indicates the inefficiency of the compressor and turbine and the loss in pressure through the burner. Assuming the compressor efficiency is η_c and the turbine efficiency is η_t , then the actual compressor work and the actual turbine work is given by:

$$W_{ca} = \dot{m}_a(h_2 - h_1)/\eta_c \quad (2-19)$$

$$W_{ta} = (\dot{m}_a + \dot{m}_f)(h_{3a} - h_4)\eta_t \quad (2-20)$$

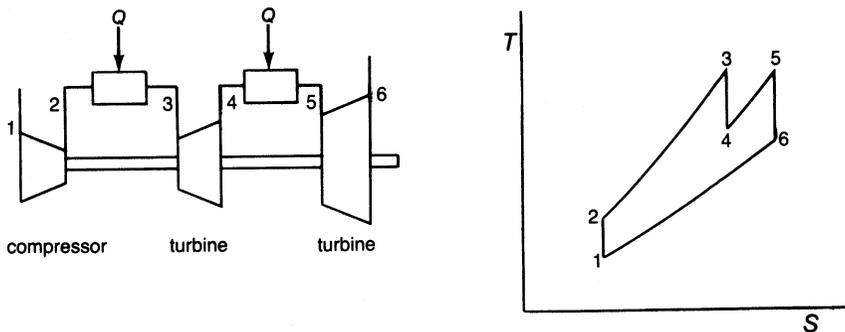


Figure 2-8. Reheat cycle and T-S diagram.

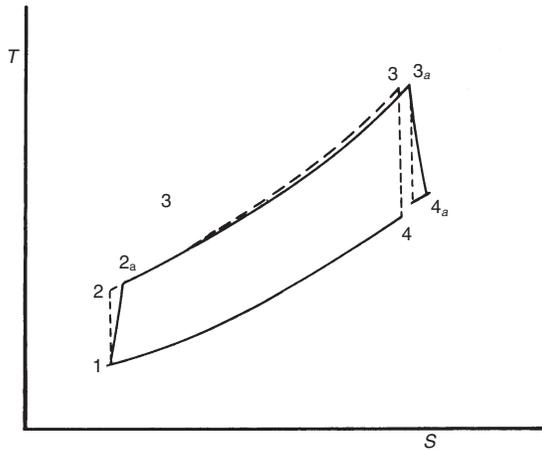


Figure 2-9. T-S diagram of the actual open simple cycle.

Thus, the actual total output work is

$$W_{\text{act}} = W_{\text{ta}} - W_{\text{ca}} \quad (2-21)$$

The actual fuel required to raise the temperature from 2a to 3a is

$$\dot{m}_f = \frac{h_{3a} - h_{2a}}{(LHV)\eta_b} \quad (2-22)$$

Thus, the overall adiabatic thermal cycle efficiency can be calculated from the following equation:

$$\eta_c = \frac{W_{\text{act}}}{\dot{m}_f(LHV)} \quad (2-23)$$

Analysis of this cycle indicates that an increase in inlet temperature to the turbine causes an increase in the cycle efficiency. The optimum pressure ratio for maximum efficiency varies with the turbine inlet temperature from an optimum of about 15.5:1 at a temperature of 1500°F (816°C) to about 43:1 at a temperature of about 2400°F (1316°C). The pressure ratio for maximum work, however, varies from about 11.5:1 to about 35:1 for the same respective temperatures.

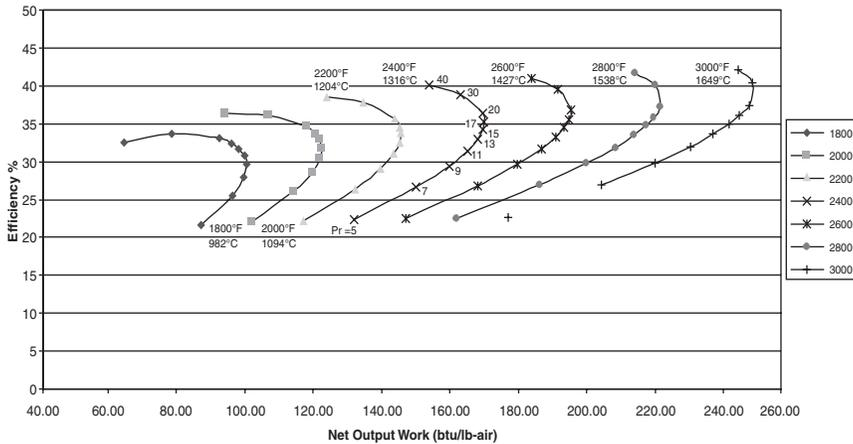


Figure 2-10. The performance map of a simple cycle gas turbine.

Thus, from Figure 2-10, it is obvious that for maximum performance, a pressure ratio of 30:1 at a temperature of 2800 °F (1537 °C) is optimal. Use of an axial-flow compressor requires 16–24 stages with a pressure ratio of 1.15–1.25:1 per stage. A 22-stage compressor producing a 30:1 pressure ratio is a relatively conservative design. If the pressure ratio were increased to 1.252:1 per stage, the number of stages would be about 16. The latter pressure ratio has been achieved with high efficiencies. This reduction in number of stages means a great reduction in the overall cost. Turbine temperatures increases give a great rise in efficiency and power, so temperatures in the 2400 °F (1316 °C) range at the turbine inlet are becoming the state-of-art.

The Split-Shaft Simple Cycle

The split-shaft simple cycle is mainly used for high torque and large load variant. Figure 2-11 is a schematic of the two-shaft simple cycle. The first turbine drives the compressor; the second turbine is used as a power source. If one assumes that the number-of-stages in a split-shaft simple cycle are more than that in a simple shaft cycle, then the efficiency of the split-shaft cycle is slightly higher at design loads because of the reheat factor, as seen in Figure 2-12. However, if the number-of-stages are the same, then there is no change in overall efficiency. From the H–S diagram one can find some

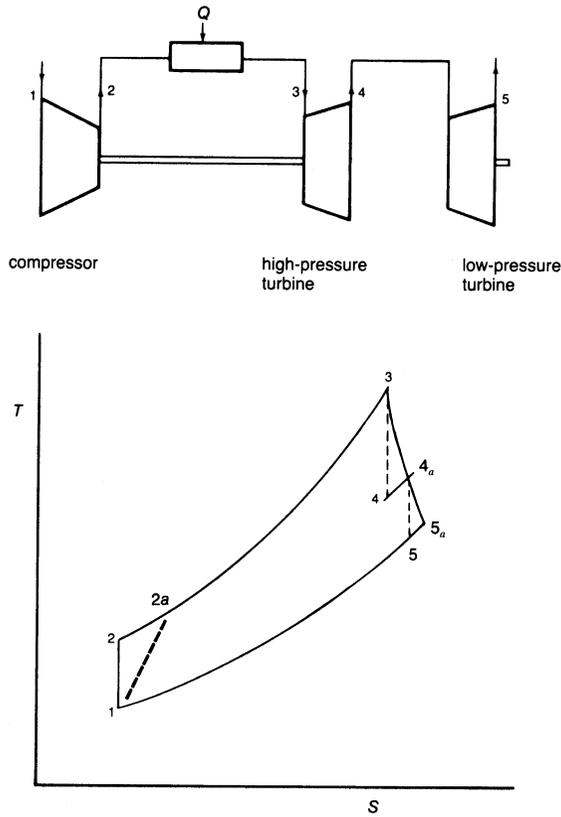


Figure 2-11. The split-shaft gas turbine cycle.

relationships between turbines. Since the job of the high-pressure turbine is to drive the compressor, the equations to use are:

$$h_{4a} = h_3 - W_{ca} \quad (2-24)$$

$$h_4 = h_3 - (W_{ca}/\eta_t) \quad (2-25)$$

Thus, the output work can be represented by the relationship:

$$W_a = (\dot{m}_a + \dot{m}_f)(h_{4a} - h_5)\eta_t \quad (2-26)$$

In the split-shaft cycle the first shaft supports the compressor and the turbine that drives it, while the second shaft supports the free turbine that drives the load. The two shafts can operate at entirely different speeds. The

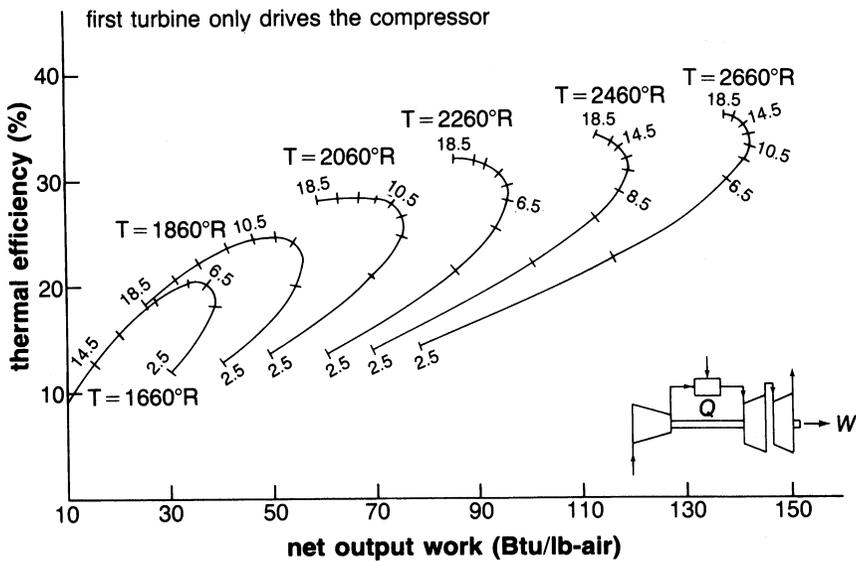


Figure 2-12. Performance map showing the effect of pressure ratio and turbine inlet temperature on a split shaft cycle.

advantage of the split-shaft gas turbine is its high torque at low speed. A free-power turbine gives a very high torque at low rpm. Very high torque at low rpm is convenient for automotive use, but with constant full-power operation, it is of little or no value. Its use is usually limited to variable mechanical-drive applications.

The Regenerative Cycle

The regenerative cycle is becoming prominent in these days of tight fuel reserves and high fuel costs. The amount of fuel needed can be reduced by the use of a regenerator in which the hot turbine exhaust gas is used to preheat the air between the compressor and the combustion chamber. From Figure 2-4 and the definition of a regenerator, the temperature at the exit of the regenerator is given by the following relationship:

$$T_3 = T_{2a} + \eta_{reg}(T_5 - T_{2a}) \tag{2-27}$$

Where T_{2a} is the actual temperature at the compressor exit. The regenerator increases the temperature of the air entering the burner, thus reducing the fuel-to-air ratio and increasing the thermal efficiency.

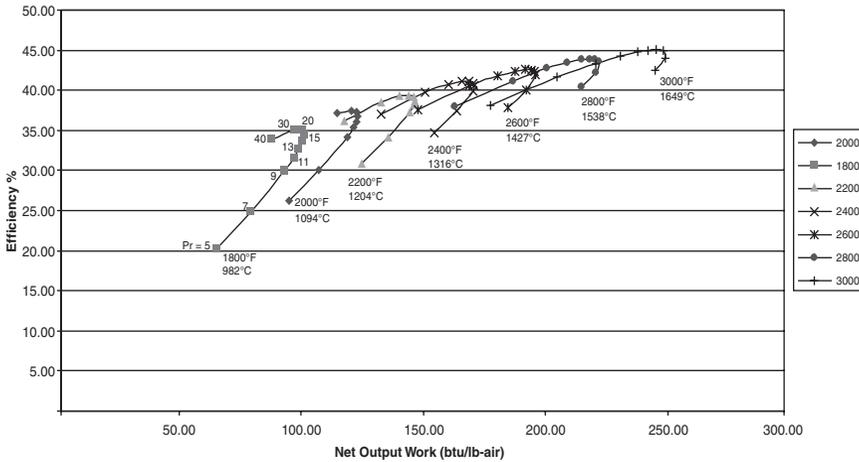


Figure 2-13. The performance map of a regenerative gas turbine cycle.

For a regenerator assumed to have an effectiveness of 80%, the efficiency of the regenerative cycle is about 40% higher than its counterpart in the simple cycle, as seen in Figure 2-13. The work output per pound of air is about the same or slightly less than that experienced with the simple cycle. The point of maximum efficiency in the regenerative cycle occurs at a lower pressure ratio than that of the simple cycle, *but the optimum pressure ratio for the maximum work is the same in the two cycles*. Thus, when companies are designing gas turbines, the choice of pressure ratio should be such that maximum benefit from both cycles can be obtained, since most offer a regeneration option. It is not correct to say that a regenerator at off-optimum would not be effective, but a proper analysis should be made before a large expense is incurred.

The split-shaft regenerative turbine is very similar to the split-shaft cycle. The advantage of this turbine is the same as that mentioned before; namely, high torque at low rpm. The cycle efficiencies are also about the same. Figure 2-14 indicates the performance that may be expected from such a cycle.

The Intercooled Simple Cycle

A simple cycle with intercooler can reduce total compressor work and improve net output work. Figure 2-7 shows the simple cycle with intercooling between compressors. The assumptions made in evaluating this

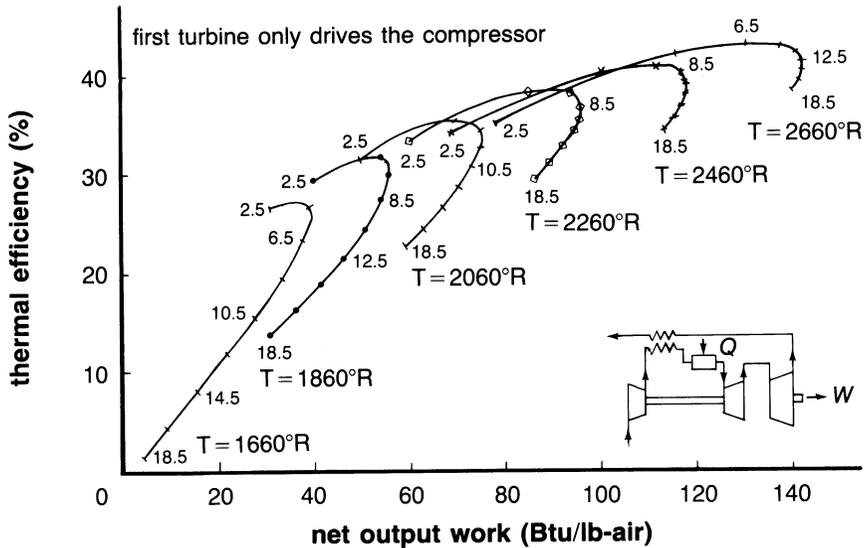


Figure 2-14. Performance map showing the effect of pressure ratio and turbine inlet temperature on a regenerative split shaft cycle.

cycle are: (1) compressor interstage temperature equals inlet temperature, (2) compressor efficiencies are the same, (3) pressure ratios in both compressors are the same and equal to $\sqrt{(P_2/P_1)}$.

The intercooled simple cycle reduces the power consumed by the compressor. A reduction in consumed power is accomplished by cooling the inlet temperature in the second or other following stages of the compressor to the same as the ambient air and maintaining the same overall pressure ratio. The compressor work then can be represented by the following relationship:

$$W_c = (h_a - h_1) + (h_c - h_1) \tag{2-28}$$

This cycle produces an increase of 30% in work output, but the overall efficiency is slightly decreased as seen in Figure 2-15. An intercooling regenerative cycle can increase the power output and the thermal efficiency. This combination provides an increase in efficiency of about 12% and an increase in power output of about 30%, as indicated in Figure 2-16. Maximum efficiency, however, occurs at lower pressure ratios, as compared with the simple or reheat cycles.

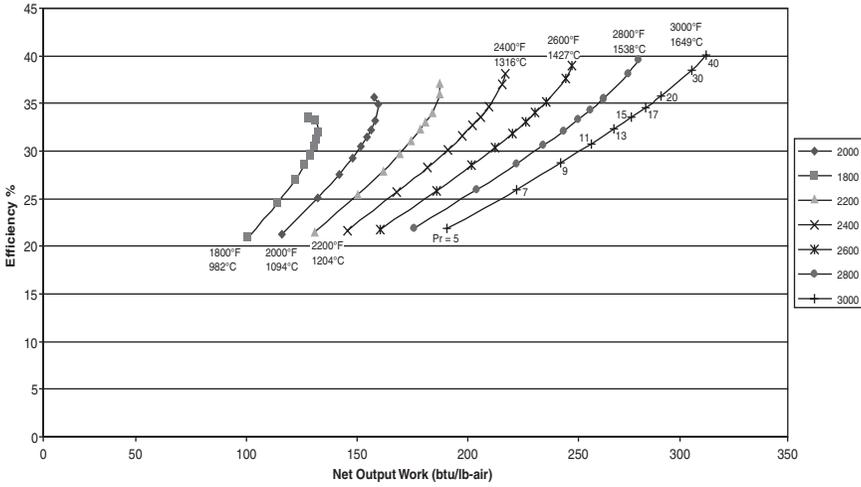


Figure 2-15. The performance map of an intercooled gas turbine cycle.

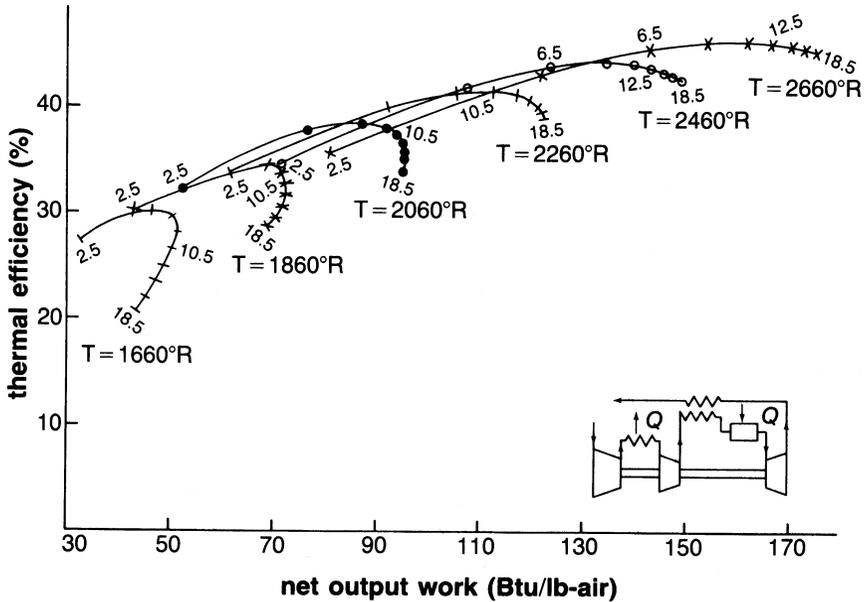


Figure 2-16. Performance map showing the effect of pressure ratio and turbine inlet temperature on an intercooled regenerative cycle.

The Reheat Cycle

The regenerative cycles improve the efficiency of the split-shaft cycle, but do not provide any added work per pound of air flow. To achieve this latter goal, the concept of the reheat cycle must be utilized. The reheat cycle, as shown in Figure 2-8, consists of a two-stage turbine with a combustion chamber before each stage. The assumptions made in this chapter are that the high-pressure turbine's only job is to drive the compressor and that the gas leaving this turbine is then reheated to the same temperature as in the first combustor before entering the low-pressure or power turbine. This reheat cycle has an efficiency which is less than that encountered in a simple cycle, but produces about 35% more shaft output power, as shown in Figure 2-17.

The Intercooled Regenerative Reheat Cycle

The Carnot cycle is the optimum cycle and all cycles incline toward this optimum. Maximum thermal efficiency is achieved by approaching the isothermal compression and expansion of the Carnot cycle, or by intercooling in compression and reheating in the expansion process. Figure 2-18 shows the intercooled regenerative reheat cycle, which approaches this optimum cycle in a practical fashion.

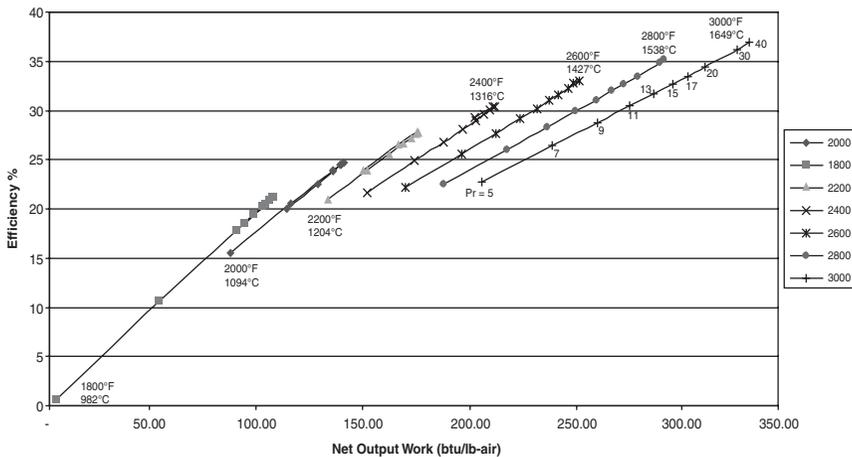


Figure 2-17. The performance of a reheat gas turbine cycle.

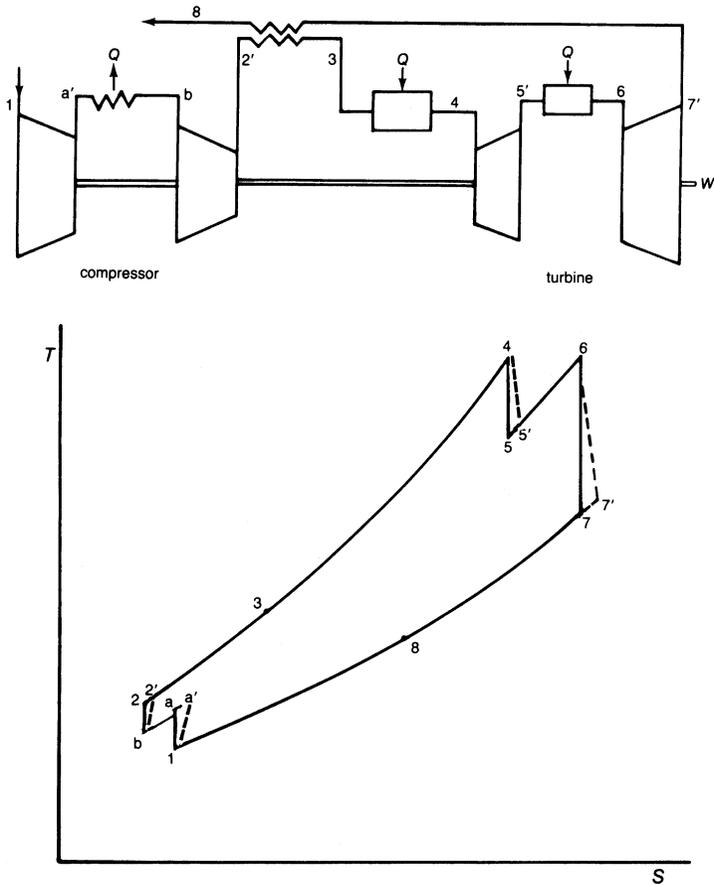


Figure 2-18. The intercooled regenerative reheat split-shaft gas turbine cycle.

This cycle achieves the maximum efficiency and work output of any of the cycles described to this point. With the insertion of an intercooler in the compressor, the pressure ratio for maximum efficiency moves to a much higher ratio, as indicated in Figure 2-19.

The Steam Injection Cycle

Steam injection has been used in reciprocating engines and gas turbines for a number of years. This cycle may be an answer to the present concern

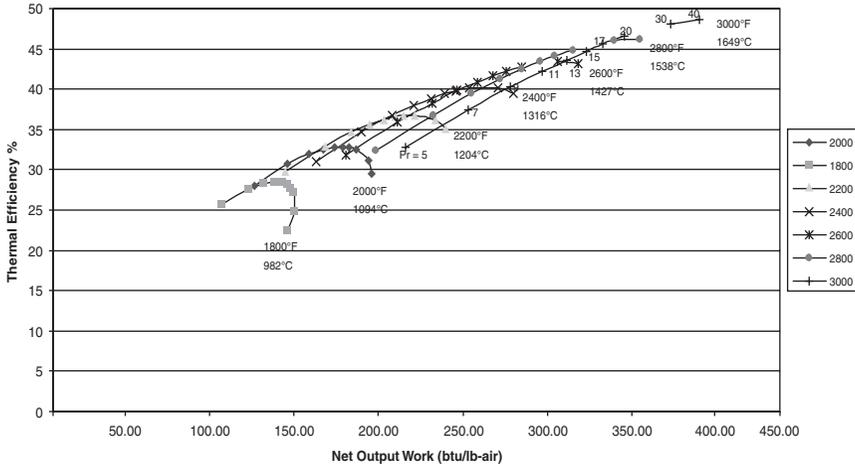


Figure 2-19. The performance of an inter-cooled, regenerative, reheat cycle.

with pollution and higher efficiency. Corrosion problems are the major hurdle in such a system. The concept is simple and straightforward: water is injected into the compressor discharge air and increases the mass flow rate through the turbine, as shown in the schematic in Figure 2-20. The steam being injected downstream from the compressor does not increase the work required to drive the compressor.

The steam used in this process is generated by the turbine exhaust gas. Typically, water at 14.7 psia (1 Bar) and 80 °F (26.7 °C) enters the pump and regenerator, where it is brought up to 60 psia (4 Bar) above the compressor discharge and the same temperature as the compressor discharged air. The steam is injected after the compressor but far upstream of the burner to create a proper mixture which helps to reduce the primary zone temperature in the combustor and the NO_x output. The enthalpy of State 3 (h_3) is the mixture enthalpy of air and steam. The following relationship describes the flow at that point:

$$h_3 = (\dot{m}_a h_{2a} + \dot{m}_s h_{3a}) / (\dot{m}_a + \dot{m}_s) \tag{2-29}$$

The enthalpy entering the turbine is given by the following:

$$h_4 = ((\dot{m}_a + \dot{m}_f) h_{4a} + \dot{m}_s h_{4s}) / (\dot{m}_a + \dot{m}_f + \dot{m}_s) \tag{2-30}$$

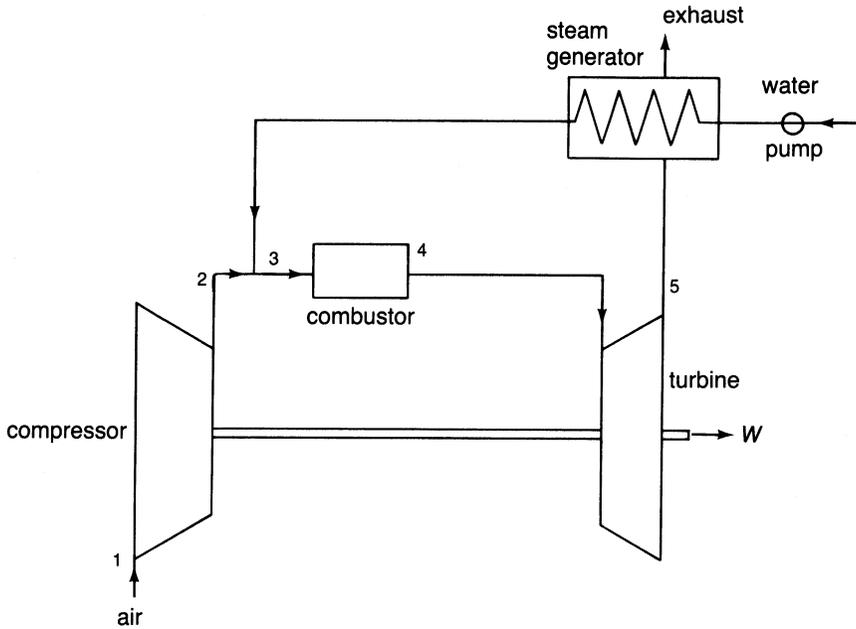


Figure 2-20. The steam injection cycle.

with the amount of fuel needed to be added to this cycle as

$$\dot{m}_f = \frac{h_4 - h_3}{\eta_b(LHV)} \quad (2-31)$$

The enthalpy leaving the turbine is

$$h_5 = ((\dot{m}_a + \dot{m}_f)h_{5a} + \dot{m}_s h_{5s}) / (\dot{m}_a + \dot{m}_f + \dot{m}_s) \quad (2-32)$$

Thus, the total work by the turbine is given by

$$W_t = (\dot{m}_a + \dot{m}_s + \dot{m}_f)(h_4 - h_5)\eta_t \quad (2-33)$$

And the overall cycle efficiency is

$$\eta_{cyc} = \frac{W_t - W_c}{\dot{m}_f(LHV)} \quad (2-34)$$

The cycle leads to an increase in output work and an increase in overall thermal efficiency.

Figure 2-21 show the effect of 5% by weight of steam injection at a turbine inlet temperature of 2400 °F (1316 °C) on the system. With about 5% injection at 2400 °F (1316 °C) and a pressure ratio of 17:1, an 8.3% increase in work output is noted with an increase of about 19% in cycle efficiency over that experienced in the simple cycle. The assumption here is that steam is injected at a pressure of about 60 psi (4 Bar) above the air from the compressor discharge and that all the steam is created by heat from the turbine exhaust. Calculations indicate that there is more than enough waste heat to achieve these goals.

Figure 2-22 shows the effect of 5% steam injection at different temperatures and pressures. Steam injection for power augmentation has been used for many years and is a very good option for plant enhancement. This cycle's great advantage is in the low production level of nitrogen oxides. That low level is accomplished by the steam being injected in the compressor discharge diffuser wall, well upstream from the combustor, creating a uniform mixture of steam and air throughout the region. The uniform mixture reduces the oxygen content of the fuel-to-air mixture and increases its heat capacity, which in turn reduces the temperature of the combustion zone and the NO_x formed. Field tests show that the amount of steam equivalent to the fuel flow by weight will reduce the amount of NO_x emissions to acceptable levels. The major problem encountered is corrosion. The corrosion problem is being

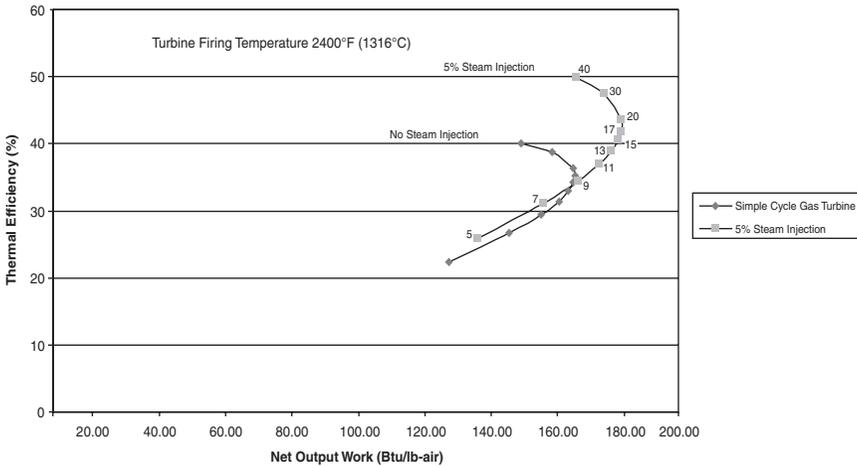


Figure 2-21. Comparison between 5% steam injection and simple cycle gas turbine.

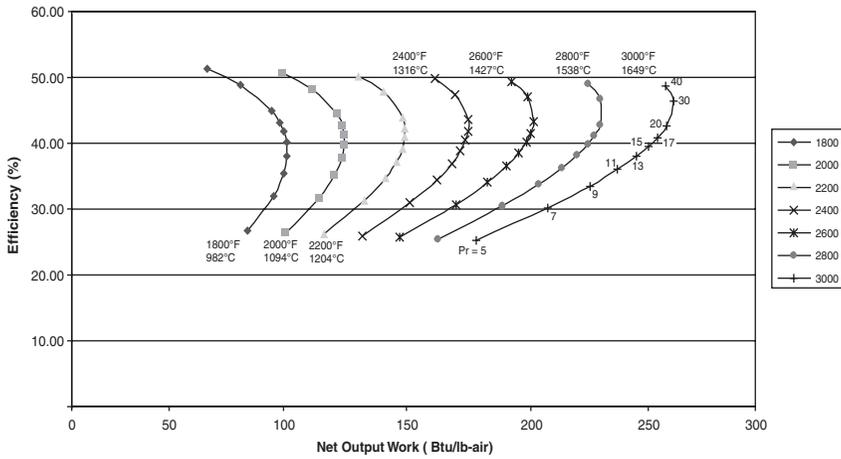


Figure 2-22. The performance map of a steam injected gas turbine.

investigated, and progress is being made. The attractiveness of this system is that major changes are not needed to add this feature to an existing system. The location of the water injector is crucial for the proper operation of this system and cycle.

The Evaporative Regenerative Cycle

This cycle, as shown in Figure 2-23, is a regenerative cycle with water injection. Theoretically, it has the advantages of both the steam injection and regenerative systems reduction of NO_x emissions and higher efficiency. The work output of this system is about the same as that achieved in the steam injection cycle, but the thermal efficiency of the system is much higher.

A high-pressure evaporator is placed between the compressor and the regenerator to add water vapor into the air steam and in the process reduce the temperature of this mixed stream. The mixture then enters the regenerator at a lower temperature, increasing the temperature differential across the regenerator. Increasing the temperature differential reduces the temperature of the exhaust gases considerably so that these exhaust gases, otherwise lost, are an indirect source of heat used to evaporate the water. Both the air and the evaporated water pass through the regenerator, combustion chamber, and turbine. The water enters at 80 °F (26.7 °C) and 14.7 psia (1 Bar) through a pump into the evaporator, where it is discharged as steam at the same temperature as the compressor discharged air and at a pressure of 60 psia (4 Bar) above the compressor discharge. It is then injected into the air

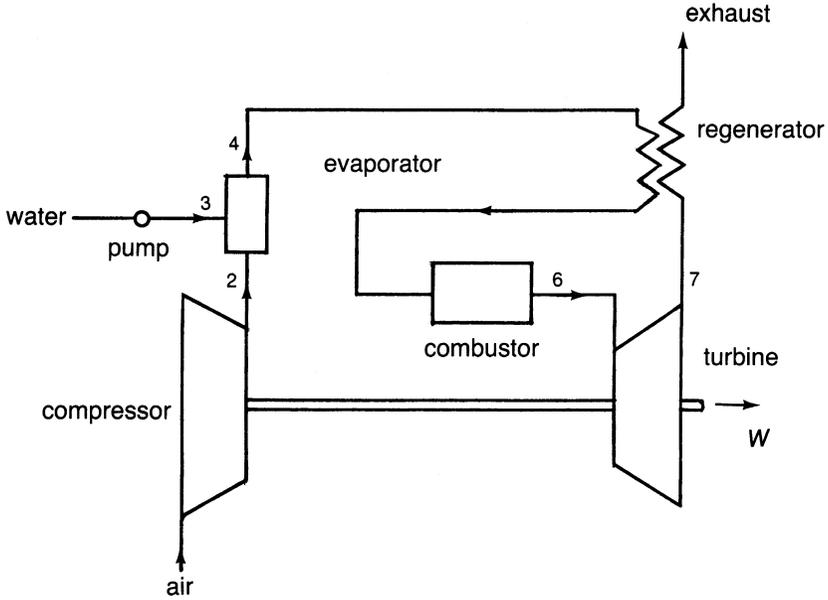


Figure 2-23. The evaporative regenerative cycle.

stream in a fine mist where it is fully mixed. The governing equations are the same as in the previous cycle for the turbine section, but the heat added is altered because of the regenerator. The following equations govern this change in heat addition. From the first law of thermodynamics, the mixture temperature (T_4) is given by the relationship:

$$T_4 = \frac{\dot{m}_a c_{pa} T_2 + \dot{m}_s c_{pw} (T_s - T_3) - \dot{m}_s h_{fg}}{\dot{m}_a c_{pa} + \dot{m}_s c_{ps}} \quad (2-35)$$

The enthalpy of the gas leaving the regenerator is given by the relationship

$$h_5 = h_4 + \eta_{\text{reg}} (h_7 - h_4) \quad (2-36)$$

Similar to the regenerative cycle, the evaporative regenerative cycle has higher efficiencies at lower pressure ratios. Figures 2-24 and 2-25 show the performance of the system at various rates of steam injection and turbine inlet temperatures. Similar to the steam injection cycle, the steam is injected

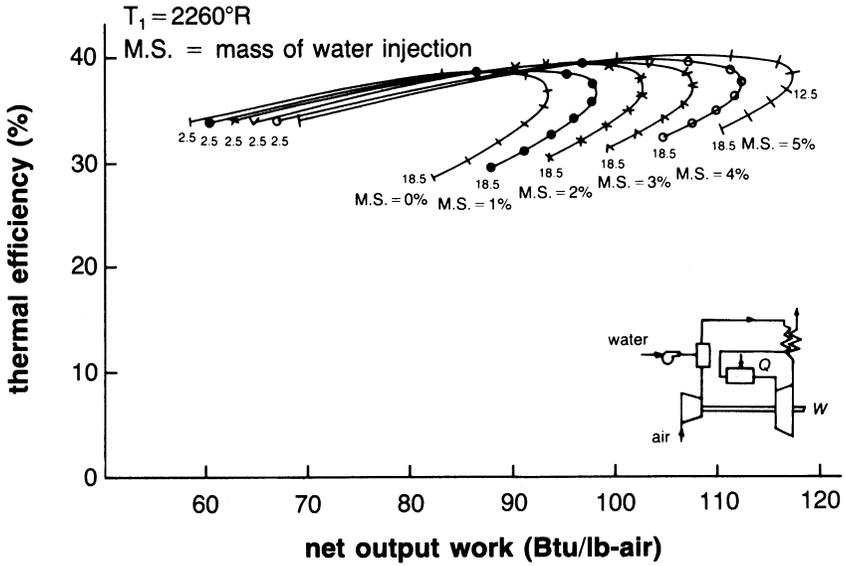


Figure 2-24. Performance map showing the effect of pressure ratio and steam flow rate on an evaporative regenerative cycle.

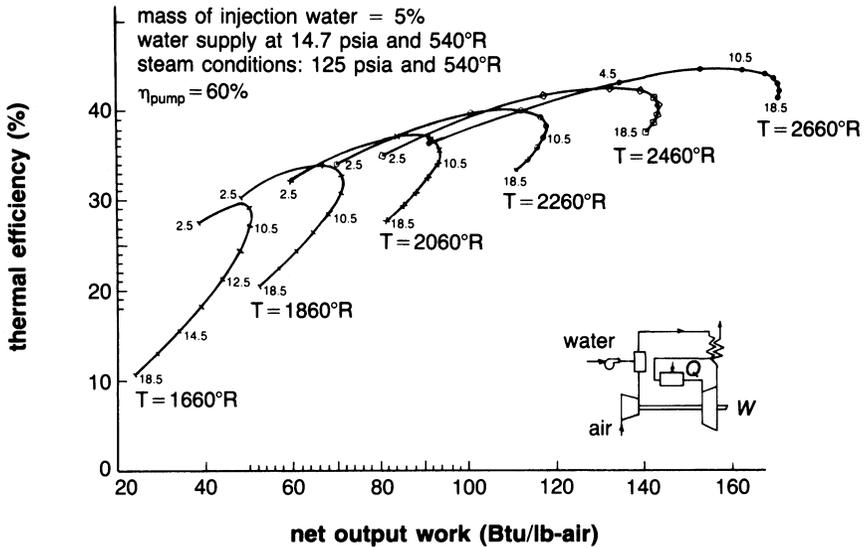


Figure 2-25. Performance map showing the effect of pressure ratio and steam flow rate on afixed steam rate evaporative regenerative cycle.

at 60 psi (4 Bar) higher than the air leaving the compressor. Corrosion in the regenerator is a problem in this system. When not completely clean, regenerators tend to develop hot spots that can lead to fires. This problem can be overcome with proper regenerator designs. This NO_x emission level is low and meets EPA standards.

The Brayton-Rankine Cycle

The combination of the gas turbine with the steam turbine is an attractive proposal, especially for electric utilities and process industries where steam is being used. In this cycle, as shown in Figure 2-26, the hot gases from the turbine exhaust are used in a supplementary fired boiler to produce superheated steam at high temperatures for a steam turbine.

The computations of the gas turbine are the same as shown for the simple cycle. The steam turbine calculations are:

Steam generator heat

$${}_4Q_1 = h_{1s} - h_{4s} \quad (2-37)$$

Turbine work

$$W_{ts} = \dot{m}_s (h_{1s} - h_{2s}) \quad (2-38)$$

Pump work

$$W_p = \dot{m}_s (h_{4s} - H_{3s}) / \eta_p \quad (2-39)$$

The combined cycle work is equal to the sum of the net gas turbine work and the steam turbine work. About one-third to one-half of the design output is available as energy in the exhaust gases. The exhaust gas from the turbine is used to provide heat to the recovery boiler. Thus, this heat must be credited to the overall cycle. The following equations show the overall cycle work and thermal efficiency:

Overall cycle work

$$W_{\text{cyc}} = W_{\text{ta}} + W_{\text{ts}} - W_c - W_p \quad (2-40)$$

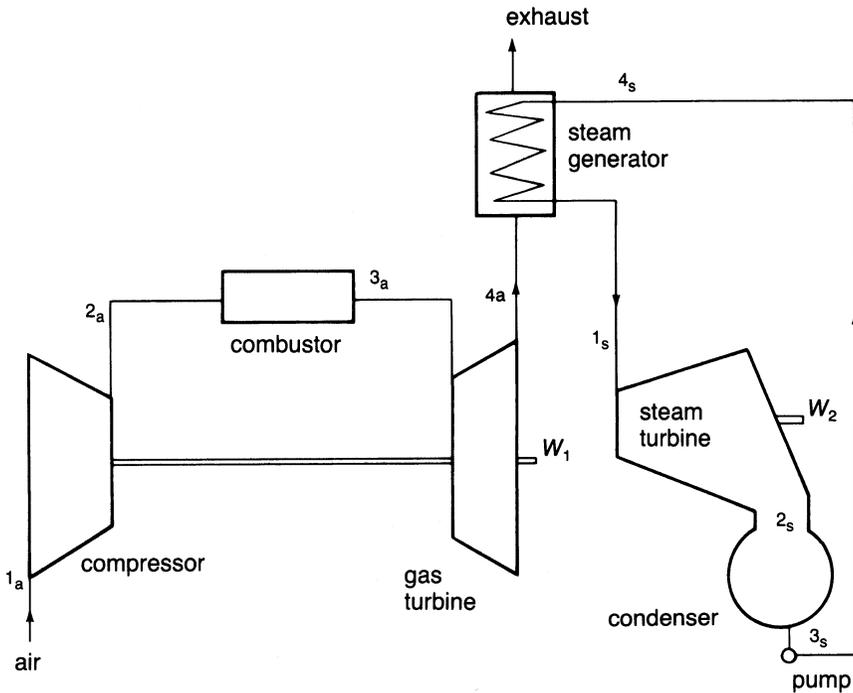


Figure 2-26. The Brayton-Rankine combined cycle.

Overall cycle efficiency

$$\eta = \frac{W_{cyc}}{\dot{m}_f(LHV)} \tag{2-41}$$

This system, as can be seen from Figure 2-27, indicates that the net work is about the same as one would expect in a steam injection cycle, but the efficiencies are much higher. The disadvantages of this system are its high initial cost. However, just as in the steam injection cycle, the NO_x content of its exhaust remains the same and is dependent on the gas turbine used. This system is being used widely because of its high efficiency.

Summation of Cycle Analysis

Figure 2-28 and 2-29 give a good comparison of the effect of the various cycles on the output work and thermal efficiency. The curves are drawn for a

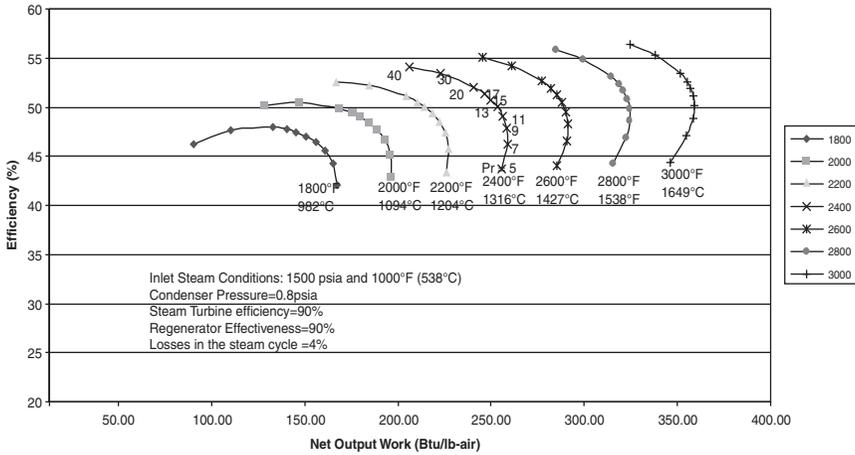


Figure 2-27. The performance map of a typical combined cycle power plant.

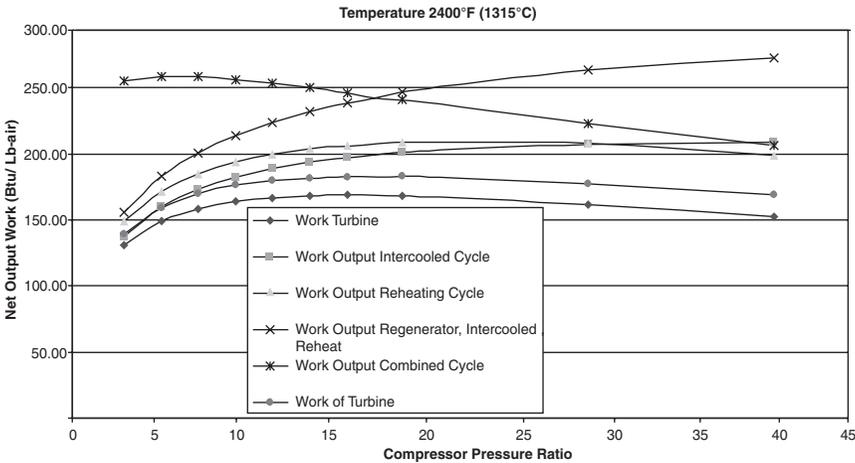


Figure 2-28. Comparison of net work output of various cycles temperature.

turbine inlet temperature of 2400 °F (1316 °C), which is a temperature presently being used by manufacturers. The output work of the regenerative cycle is very similar to the output work of the simple cycle, and the output work of the regenerative reheat cycle is very similar to that of the reheat cycle. The most work per pound of air can be expected from the intercooling, regenerative reheat cycle.

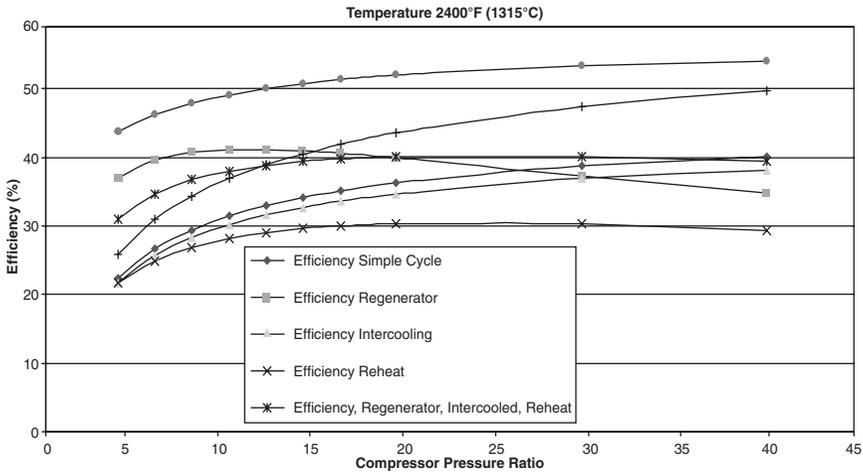


Figure 2-29. Comparison of thermal efficiency of various cycles temperature.

The most effective cycle is the Brayton-Rankine cycle. This cycle has tremendous potential in power plants and in the process industries where steam turbines are in use in many areas. The initial cost of this system is high; however, in most cases where steam turbines are being used this initial cost can be greatly reduced.

Regenerative cycles are popular because of the high cost of fuel. Care should be observed not to indiscriminately attach regenerators to existing units. The regenerator is most efficient at low-pressure ratios. Cleansing turbines with abrasive agents may prove a problem in regenerative units, since the cleansers can get lodged in the regenerator and cause hot spots.

Water injection, or steam injection systems, are being used extensively to augment power. Corrosion problems in the compressor diffuser and combustor have not been found to be major problems. The increase in work and efficiency with a reduction in NO_x makes the process very attractive. Split-shaft cycles are attractive for use in variable-speed mechanical drives. The off-design characteristics of such an engine are high efficiency and high torque at low speeds.

A General Overview of Combined Cycle Plants

There are many concepts of the combined cycle, these cycles range from the simple single pressure cycle, in which the steam for the turbine is generated at only one pressure, to the triple pressure cycles where the

steam generated for the steam turbine is at three different levels. The energy flow diagram Figure 2-30 shows the distribution of the entering energy into its useful component and the energy losses which are associated with the condenser and the stack losses. This distribution will vary some with different cycles as the stack losses are decreased with more efficient multilevel pressure Heat Recovery Steam Generating units (HRSGs). The distribution in the energy produced by the power generation sections as a function of the total energy produced is shown in Figure 2-31. This diagram shows that the load characteristics of each of the major prime-movers changes drastically

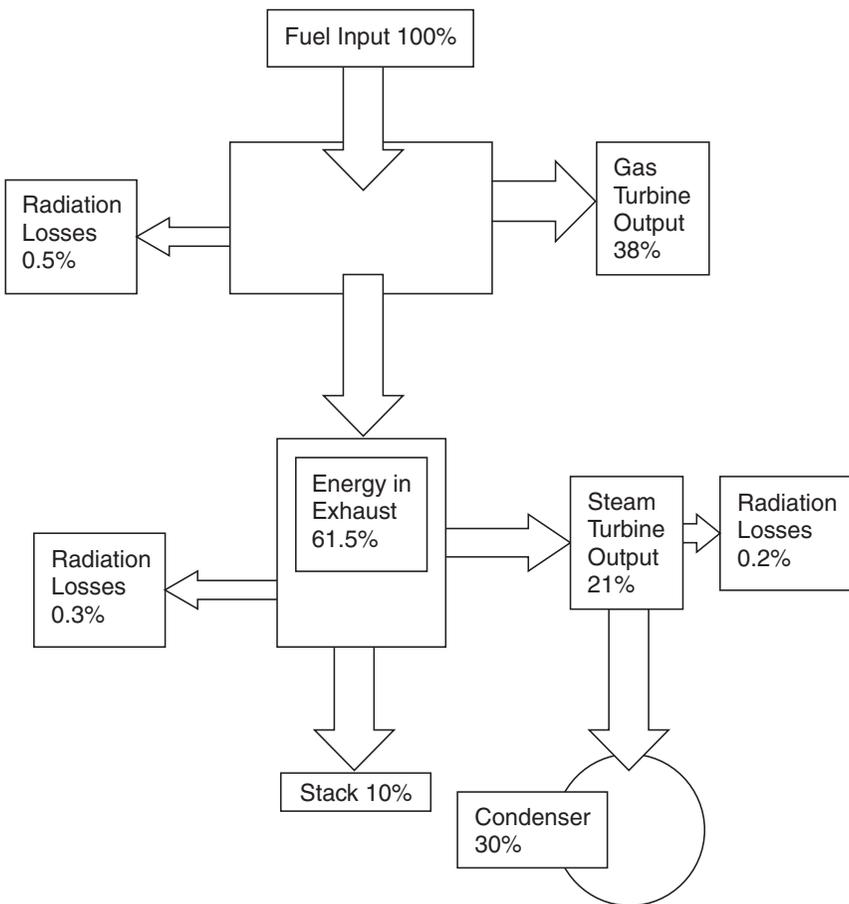


Figure 2-30. Energy distribution in a combined cycle power plant.

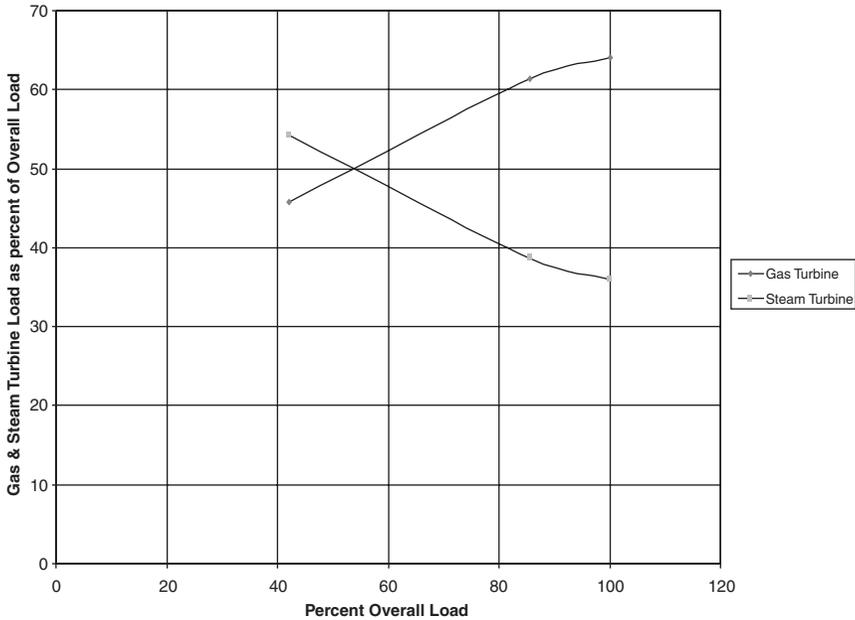


Figure 2-31. Load sharing between prime movers over the entire operating range of a combine cycle power plant.

with off-design operation. The gas turbine at design conditions supplies 60% of the total energy delivered and the steam turbine delivers 40% of the energy while at off-design conditions (below 50% of the design energy) the gas turbine delivers 40% of the energy while the steam turbine delivers 40% of the energy.

To fully understand the various cycles, it is important to define a few major parameters of the combined cycle. In most combined cycle applications the gas turbine is the topping cycle and the steam turbine is the bottoming cycle. The major components that make up a combined cycle are the gas turbine, the HRSG and the steam turbine as shown in Figure 2-32 a typical combined cycle power plant with a single pressure HRSG. Thermal efficiencies of the combined cycles can reach as high as 60%. In the typical combination the gas turbine produces about 60% of the power and the steam turbine about 40%. Individual unit thermal efficiencies of the gas turbine and the steam turbine are between 30–40%. The steam turbine utilizes the energy in the exhaust gas of the gas turbine as its input energy. The energy transferred to the Heat Recovery Steam Generator (HRSG) by

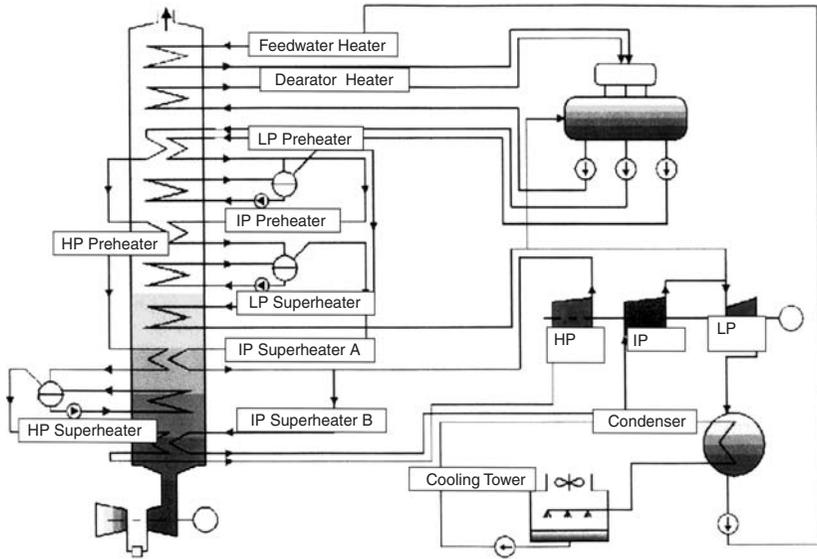


Figure 2-32. A typical large combined cycle power plant HRSG.

the gas turbine is usually equivalent to about the rated output of the gas turbine at design conditions. At off-design conditions the Inlet Guide Vanes (IGV) are used to regulate the air so as to maintain a high temperature to the HRSG.

The HRSG is where the energy from the gas turbine is transferred to the water to produce steam. There are many different configurations of the HRSG units. Most HRSG units are divided into the same amount of sections as the steam turbine, as seen in Figure 2-32. In most cases, each section of the HRSG has a pre-heater or economizer, an evaporator, and then one or two stages of superheaters. The steam entering the steam turbine is superheated.

The condensate entering the HRSG goes through a Deaerator where the gases from the water or steam are removed. This is important because a high oxygen content can cause corrosion of the piping and the components which would come into contact with the water/steam medium. An oxygen content of about 7–10 parts per billion (ppb) is recommended. The condensate is sprayed into the top of the Deaerator, which is normally placed on the top of the feedwater tank. Deaeration takes place when the water is sprayed and then heated, thus releasing the gases that are absorbed in the water/steam

medium. Deaeration must be done on a continuous basis because air is introduced into the system at the pump seals and piping flanges since they are under vacuum.

Deaeration can be either vacuum or over pressure deaeration. Most systems use vacuum deaeration because all the feedwater heating can be done in the feedwater tank and there is no need for additional heat exchangers. The heating steam in the vacuum deaeration process is a lower quality steam thus leaving the steam in the steam cycle for expansion work through the steam turbine. This increases the output of the steam turbine and therefore the efficiency of the combined cycle. In the case of the overpressure deaeration, the gases can be exhausted directly to the atmosphere independently of the condenser evacuation system.

Deaeration also takes place in the condenser. The process is similar to that in the Deaerator. The turbine exhaust steam condenses and collects in the condenser hotwell while the incondensable hot gases are extracted by means of evacuation equipment. A steam cushion separates the air and water so re-absorption of the air cannot take place. Condenser deaeration can be as effective as the one in a Deaerator. This could lead to not utilizing a separate Deaerator/feedwater tank, and the condensate being fed directly into the HRSG from the condenser. The amount of make-up water added to the system is a factor since make-up water is fully saturated with oxygen. If the amount of make-up water is less than 25% of the steam turbine exhaust flow, condenser deaeration may be employed, but in cases where there is steam extraction for process use and therefore the make-up water is large, a separate deaerator is needed.

The economizer in the system is used to heat the water close to its saturation point. If they are not carefully designed, economizers can generate steam, thus blocking the flow. To prevent this from occurring the feedwater at the outlet is slightly subcooled. The difference between the saturation temperature and the water temperature at the economizer exit is known as the approach temperature. The approach temperature is kept as small as possible between 10–20 °F (5.5–11 °C). To prevent steaming in the evaporator it is also useful to install a feedwater control valve downstream of the economizer, which keeps the pressure high, and steaming is prevented. Proper routing of the tubes to the drum also prevents blockage if it occurs in the economizer.

Another important parameter is the temperature difference between the evaporator outlet temperature on the steam side and on the exhaust gas side. This difference is known as the pinch point. Ideally, the lower the pinch point, the more heat recovered, but this calls for more surface area and, consequently, increases the back pressure and cost. Also, excessively low

pinch points can mean inadequate steam production if the exhaust gas is low in energy (low mass flow or low exhaust gas temperature). General guidelines call for a pinch point of 15–40 °F (8–22 °C). The final choice is obviously based on economic considerations.

The steam turbines in most of the large power plants are at a minimum divided into two major sections the High Pressure Section (HP) and the Low Pressure Section (LP). In some plants, the HP section is further divided into a High Pressure Section and an Intermediate Pressure Section (IP). The HRSG is also divided into sections corresponding with the steam turbine. The LP steam turbine's performance is further dictated by the condenser backpressure, which is a function of the cooling and the fouling.

The efficiency of the steam section in many of these plants varies from 30–40%. To ensure that the steam turbine is operating in an efficient mode, the gas turbine exhaust temperature is maintained over a wide range of operating conditions. This enables the HRSG to maintain a high degree of effectiveness over this wide range of operation.

In a combined cycle plant, high steam pressures do not necessarily convert to a high thermal efficiency for a combined cycle power plant. Expanding the steam at higher steam pressure causes an increase in the moisture content at the exit of the steam turbine. The increase in moisture content creates major erosion and corrosion problems in the later stages of the turbine. A limit is set at about 10% (90% steam quality) moisture content.

The advantages for a high steam pressure, is that the mass flow of the steam is reduced and that the turbine output is also reduced. The lower steam flow reduces the size of the exhaust steam section of the turbine thus reducing the size of the exhaust stage blades. The smaller steam flow also reduces the size of the condenser and the amount of water required for cooling. It also reduces the size of the steam piping and the valve dimensions. This all accounts for lower costs especially for power plants which use the expensive and high-energy consuming air-cooled condensers.

Increasing the steam temperature at a given steam pressure lowers the steam output of the steam turbine slightly. This occurs because of two contradictory effects: first the increase in enthalpy drop, which increases the output; and second the decrease in flow, which causes a loss in steam turbine output. The second effect is more predominant, which accounts for the lower steam turbine amount. Lowering the temperature of the steam also increases the moisture content.

Understanding the design characteristics of the dual or triple pressure HRSG and its corresponding steam turbine sections (HP, IP, and LP turbines) is important. Increasing pressure of any section will increase the work output of the section for the same mass flow. However, at higher

pressure, the mass flow of the steam generated is reduced. This effect is most significant for the LP Turbine. The pressure in the LP evaporator should not be below about 45 psia (3.1 Bar) because the enthalpy drop in the LP steam turbine becomes very small, and the volume flow of the steam becomes very large thus the size of the LP section becomes large, with long expensive blading. Increase in the steam temperature brings substantial improvement in the output. In the dual or triple pressure cycle, more energy is made available to the LP section if the steam team to the HP section is raised.

There is a very small increase in the overall cycle efficiency between a dual pressure cycle and a triple pressure cycle. To maximize their efficiency, these cycles are operated at high temperatures, and extracting most heat from the system thus creating relatively low stack temperatures. This means that in most cases they must be only operated with natural gas as the fuel, as this fuel contains a very low to no sulfur content. Users have found that in the presence of even low levels of sulfur, such as when firing diesel fuel (No. 2 fuel oil) stack temperatures must be kept above 300 °F (149 °C) to avoid acid gas corrosion. The increase in efficiency between the dual and triple pressure cycle is due to the steam being generated at the IP level than the LP level. The HP flow is slightly less than in the dual pressure cycle because the IP superheater is at a higher level than the LP superheater, thus removing energy from the HP section of the HRSG. In a triple pressure cycle the HP and IP section pressure must be increased together. Moisture at the steam turbine LP section exhaust plays a governing role. At inlet pressure of about 1500 psia (103.4 Bar), the optimum pressure of the IP section is about 250 psia (17.2 Bar). The maximum steam turbine output is clearly definable with the LP steam turbine pressure. The effect of the LP pressure also effects the HRSG surface area, as the surface area increases with the decrease in LP steam pressure, because less heat exchange increases at the low temperature end of the HRSG. Figure 2-33 is the energy/temperature diagram of the triple pressure HRSG. The IP and LP flows are much smaller than the HP steam turbine flow. The ratio is in the neighborhood of 25:1.

Compressed Air Energy Storage Cycle

The Compressed Air Energy Storage Cycle (CAES) is used as a peaking system that uses off-peak power to compress air into a large solution-mined underground cavern and withdraws the air to generate power during periods of high system power demand. Figure 2-34 is a schematic of such a typical plant being operated by Alabama Electric Cooperative, Inc., with the plant heat and mass balance diagram, with generation-mode parameters at rated load and compression-mode parameters at average cavern conditions.

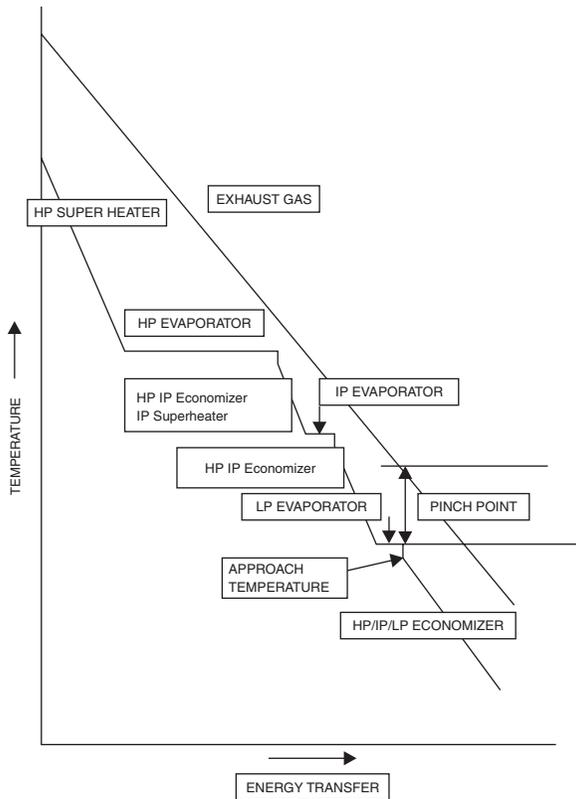


Figure 2-33. Energy/temperature diagram of the triple pressure HRSG.

The compressor train is driven by the motor/generator, which has a pair of clutches that enable it to act as a motor when the compressed air is being generated for storage in the cavern, declutches it from the expander train, and connects it to the compressor train. The compressor train consists of a three-section compressor each section having an intercooler to cool the compressed air before it enters the other section, thus reducing the overall compressor power requirements.

The power train consists of an HP and LP expander arranged in series that drives the motor/generator, which in this mode is declutched from the compressor train and is connected by clutch to the HP and LP expander train. The HP expander receives air from the cavern that is regeneratively heated in a recuperator utilizing exhaust gas from the LP expander, and then further combusted in combustors before entering the HP expander. The

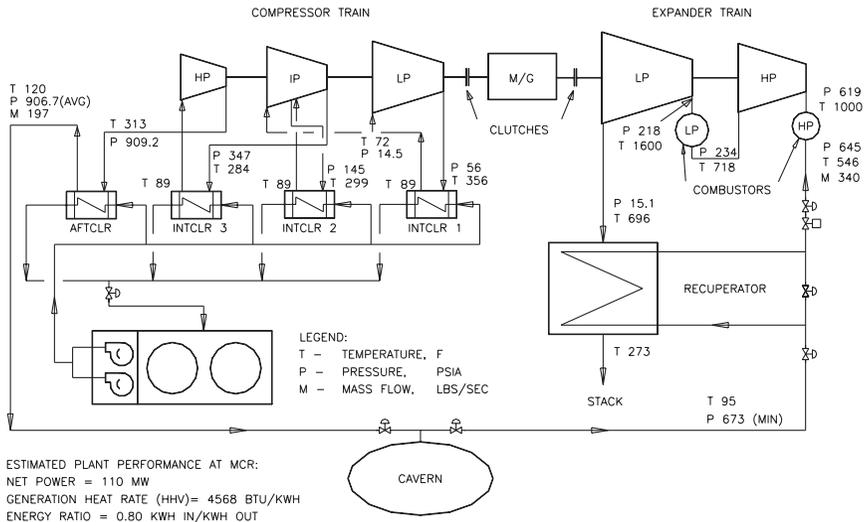


Figure 2-34. Schematic of a compressed air energy storage plant. (ASME Technical Paper 2000-GT-0595).

expanded air from the HP expander exhaust is reheated in combustors before entering the LP expander. Can-type combustors of similar design are employed in both the HP and LP expanders. The HP expander, which produces about 25% of the power, utilizes two combustors while the LP expander, producing 75% of the power, has eight. The plant is designed to operate with either natural gas or No. 2 distillate oil fuels and operates over a range of 10–110 MW.

The generator is operated as a motor during the compression mode. The system is designed to operate on a weekly cycle, which includes power generation five days per week, with cavern recharging during weekday nights and weekends.

Power Augmentation

The augmentation of power in a gas turbine is achieved by many different techniques. In this section, we are looking at techniques, which could be achieved on existing gas turbines. Thus, techniques such as additional combustors are not considered as being practical on an existing turbine. In other words, the concentration in this section is on practical solutions. Practical power augmentation can be divided into two main

categories. They range from the cooling of the inlet, to injection of steam or water into the turbine.

Inlet Cooling

- Evaporative methods—Either conventional evaporative coolers or direct water fogging
- Refrigerated inlet cooling systems—Utilizing absorption or mechanical refrigeration
- Combination of evaporative and refrigerated inlet systems—The use of evaporative coolers to assist the chiller system to attain lower temperatures of the inlet air.
- Thermal Energy Storage Systems—These are intermittent use systems where the cold is produced off-peak and then used to chill the inlet air during the hot hours of the day.

Injection of Compressed Air, Steam, or Water

- Injection of humidified and heated compressed air—Compressed air from a separate compressor is heated and humidified to about 60% relative humidity by the use of an HRSG and then injected into the compressor discharge.
- Steam Injection—Injection of the steam, obtained from the use of a low-pressure single stage HRSG, at the compressor discharge and/or injection in the combustor.
- Water Injection—Mid-compressor flashing is used to cool the compressed air and add mass flow to the system.

Inlet Cooling Techniques

Evaporative Cooling of the Turbine. Traditional evaporative coolers that use media for evaporation of the water have been widely used in the gas turbine industry over the years, especially in hot climates with low humidity areas. The low capital cost, installation, and operating costs make it attractive for many turbine-operating scenarios. Evaporation coolers consist of water being sprayed over the media blocks, which are made of fibrous corrugated material. The airflow through these media blocks, evaporates the water, as water evaporates, it consumes about 1059 BTU (1117 kJ) (latent heat of vaporization) at 60°F (15°C). This results in the reduction

of the air temperature entering the compressor from that of the ambient air temperature. This technique is very effective in low humidity regions.

The work required to drive the turbine compressor is reduced by lowering the compressor inlet temperature; thus increasing the output work of the turbine. Figure 2-35 is a schematic of the evaporative gas turbine and its effect on the Brayton cycle. The volumetric flow of most turbines is constant and therefore by increasing the mass flow, power increases in an inverse proportion to the temperature of the inlet air. The psychrometric chart shown shows that the cooling is limited especially in high humid conditions. It is a very low cost option and can be installed very easily. This technique does not however increase the efficiency of the turbine. The turbine inlet temperature is lowered by about 18°F (10°C), if the outside temperature is around 90°F (32°C). The cost of an evaporative cooling system runs around \$50/kw.

Direct inlet fogging, is a type of evaporative cooling method, where de-mineralized water is converted into a fog by means of high-pressure nozzles operating at 1000–3000 psi. (67–200 Bar) This fog then provides cooling

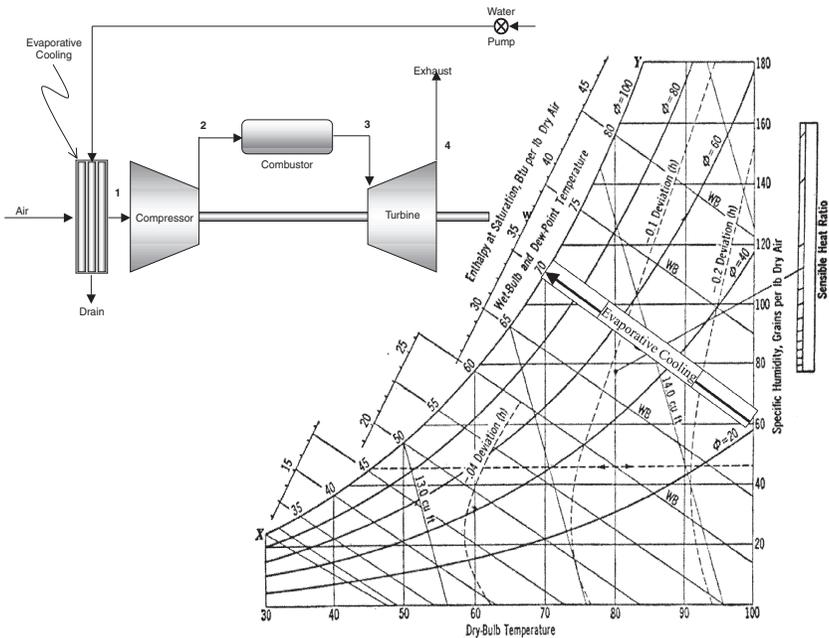


Figure 2-35. Schematic of evaporative cooling in a gas turbine.

when it evaporates in the air inlet duct of the gas turbine. The air can attain 100% relative humidity at the compressor inlet, and thereby gives the lowest temperature possible without refrigeration (the web bulb temperature). Direct high-pressure inlet fogging can also be used to create a compressor intercooling effect by allowing excess fog into the compressor, thus boosting the power output further.

Refrigerated Inlets for the Gas Turbines. The refrigerated inlets are more effective than the previous evaporative cooling systems as they can lower the temperatures by about 45–55 °F (25–30 °C). Two techniques for refrigerating the inlet of a gas turbine are vapor compression (mechanical refrigeration) and absorption refrigeration.

Mechanical Refrigeration. In a mechanical refrigeration system, the refrigerant vapor is compressed by means of a centrifugal, screw, or reciprocating compressor. Figure 2-36 is a schematic of a mechanical refrigeration intake for a gas turbine. The psychrometric chart included shows that refrigeration provides considerable cooling and is very well suited for hot humid climates.

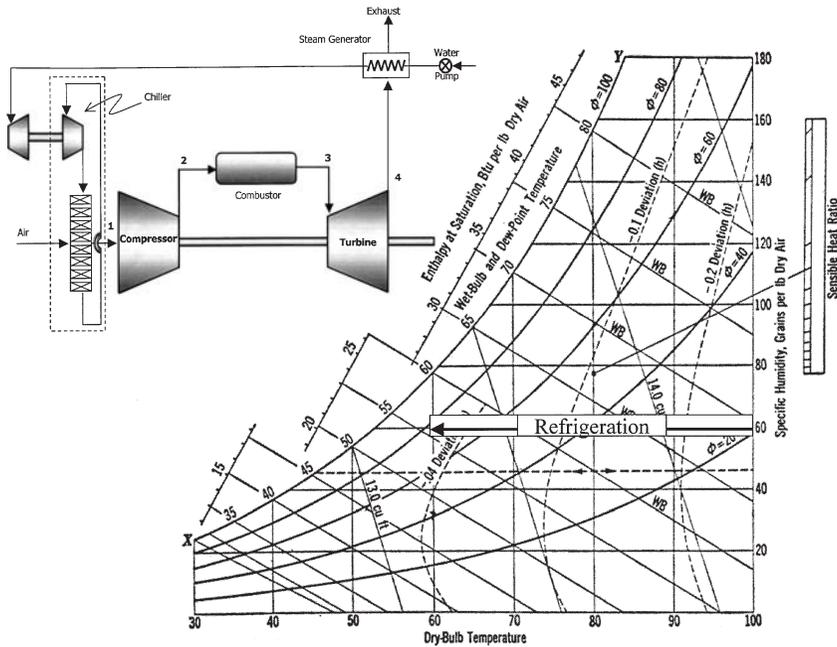


Figure 2-36. Mechanical refrigerated inlet system used to cool the inlet air of the gas turbine.

Centrifugal compressors are typically used for large systems in excess of 1,000 tons (12.4×10^6 BTU/ 13.082×10^6 kJ) and would be driven by an electric motor. Mechanical refrigeration has significantly high auxiliary power consumption for the compressor driver and pumps required for the cooling water circuit. After compression, the vapor passes through a condenser where it gets condensed. The condensed vapor is then expanded in an expansion valve and provides a cooling effect. The evaporator chills cooling water that is circulated to the gas turbine inlet chilling coils in the air stream. Chlorofluorocarbon (CFC) based chillers are now available and can provide a large tonnage for a relatively smaller plot space and can provide cooler temperature than the lithium-bromide (Li-Br) absorption based cooling systems. The drawbacks of mechanical chillers are high capital and operation and maintenance (O&M) cost, high power consumption, and poor part load performance.

Direct expansion is also possible wherein the refrigerant is used to chill the incoming air directly without the chilled water circuit. Ammonia, which is an excellent refrigerant, is used in this sort of application. Special alarm systems would have to be utilized to detect the loss of the refrigerant into the combustion air and to shut down and evacuate the refrigeration system.

Absorption Cooling Systems. Absorption systems typically employ lithium-bromide (Li-Br) and water, with the Li-Br being the absorber and the water acting as the refrigerant. Such systems can cool the inlet air to 50°F (10°C). Figure 2-37 is a schematic of an absorption refrigerated inlet system for the gas turbine. The cooling shown on the psychometric chart is identical to the one for the mechanical system. The heat for the absorption chiller can be provided by gas, steam, or gas turbine exhaust. Absorption systems can be designed to be either single or double effect. A single effect system will have a coefficient of performance (COP) of 0.7–0.9, and a double effect unit, a COP of 1.15. Part load performance of absorption systems is relatively good, and efficiency does not drop off at part load like it does with mechanical refrigeration systems. The costs of these systems are much higher than the evaporative cooling system, however refrigerated inlet cooling systems in hot humid climates are more effective due to the very high humidity.

Combination of Evaporative and Refrigerated Inlet Systems

Depending on the specifics of the project, location, climatic conditions, engine type, and economic factors, a hybrid system utilizing a combination of the above technologies may be the best. The possibility of using fogging

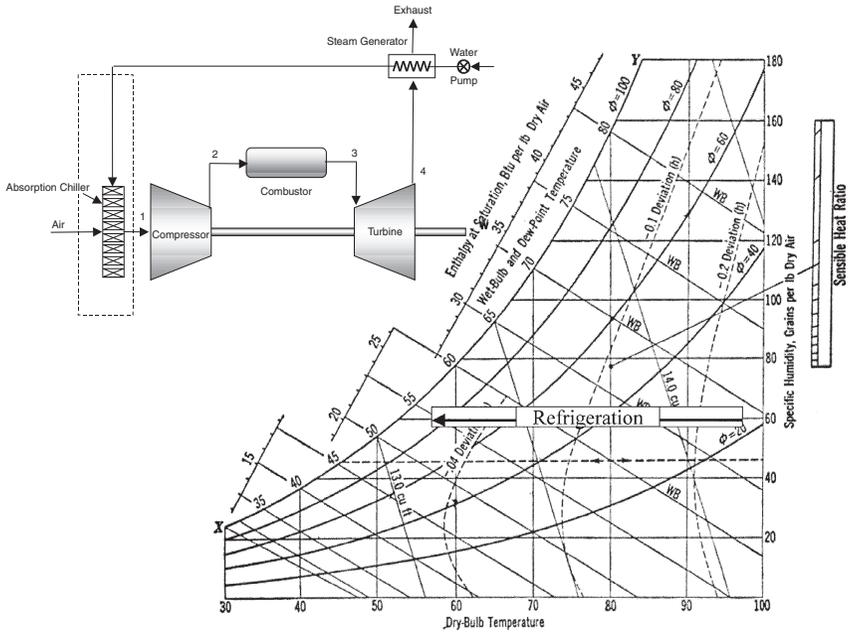


Figure 2-37. Absorption refrigerated inlet cooling system.

systems ahead of the mechanical inlet refrigeration system should be considered as seen in Figure 2-38. This may not always be intuitive, since evaporative cooling is an adiabatic process that occurs at constant enthalpy. When water is evaporated into an air stream, any reduction in sensible heat is accompanied by an increase in the latent heat of the air stream (the heat in the air stream being used to effect a phase change in the water from liquid to the vapor phase). If fog is applied in front of a chilling coil, the temperature will be decreased when the fog evaporates, but since the chiller coil will have to work harder to remove the evaporated water from the air stream, the result would yield no thermodynamic advantage.

To maximize the effect, the chiller must be designed in such a manner that in combination with evaporative cooling the maximum reduction in temperature is achieved. This can be done by designing a slightly undersized chiller, which is not capable of bringing the air temperature down to the ambient dew point temperature; but in conjunction with evaporative cooling the same effect can be achieved, thus taking the advantage of evaporative cooling to reduce the load of refrigeration.

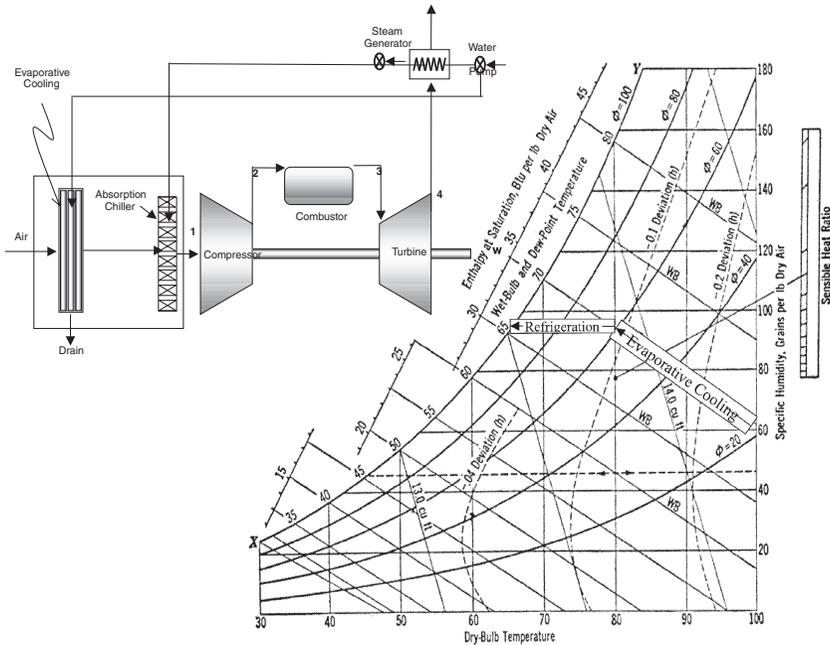


Figure 2-38. Evaporative and refrigerated inlet systems.

Thermal Energy Storage Systems

These systems are usually designed to operate the refrigeration system at off-peak hours and then use the refrigerated media at peak hours. The refrigerated media in most cases is ice and the gas turbine air is then passed through the media, which lowers its inlet temperature as seen in Figure 2-39. The size of the refrigeration system is greatly reduced as it can operate for 8–10 hours at off-peak conditions to make the ice, which is then stored, and air passed through it at peak operating hours that may only be for about 4–6 hours.

The cost for such a system runs about \$90–\$110/kW. And have been successfully employed for gas turbines producing 100–200 MW.

Injection of Compressed Air, Steam, or Water for Increasing Power

Mid-Compressor Flashing of Water. In this system, the water is injected into the mid-stages of the compressor to cool the air and approach an

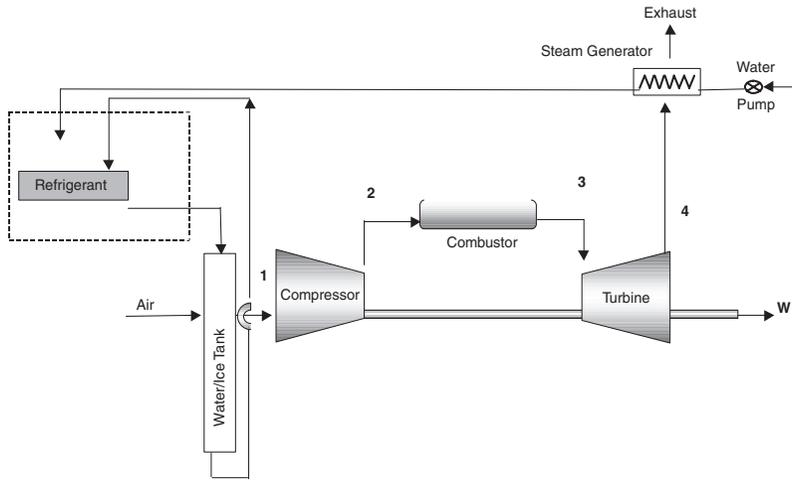


Figure 2-39. Thermal storage inlet system.

isothermal compression process as shown in Figure 2-40. The water injected is usually mechanically atomized so that very fine droplets are entered into the air. The water is evaporated as it comes in contact with the high pressure and temperature air stream. As water evaporates, it consumes about 1058 BTU (1117 kJ) (latent heat of vaporization) at the higher pressure and temperature resulting in lowering the temperature of the air stream entering the next stage. This lowers the work required to drive the compressor.

The intercooling of the compressed air has been very successfully applied to high-pressure engines. This system can be combined with any of the previously described systems.

Injection of Humidified and Heated Compressed Air. Compressed air from a separate compressor is heated and humidified to about 60% relative humidity by the use of an HRSG and then injected into the compressor discharge. Figure 2-41 is a simplified schematic of a compressed air injection plant, which consists of the following major components:

1. A commercial combustion turbine with the provision to inject, at any point upstream of the combustor, the externally supplied humidified and preheated supplementary compressed air. Engineering and mechanical aspects of the air injection for the compressed air injection plant concepts are similar to the steam injection for the power augmentation, which has accumulated significant operating experience.

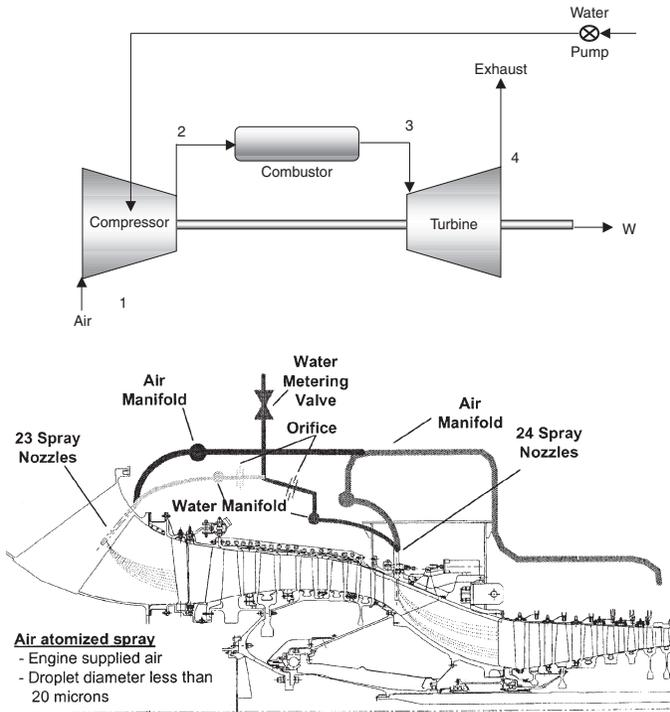


Figure 2-40. Mid-compressor cooling showing a schematic as well as an actual application in a GE LM 6000 Engine. (Courtesy GE Power Systems.)

2. A supplementary compressor (consisting of commercial off-the-shelf compressor or standard compressor modules) to provide the supplementary airflow up-stream of combustors.
3. A saturation column for the supplementary air humidification and preheating.
4. Heat recovery water heater and the saturated air preheater.
5. Balance-of-plant equipment and systems, including interconnecting piping, valves, controls, etc.

Injection of Water or Steam at the Gas Turbine Compressor Exit. Steam injection or water injection has been often used to augment the power generated from the turbine as seen in Figure 2-42. Steam can be generated from the exhaust gases of the gas turbine. The HRSG for such a unit is very elementary as the pressures are low. This technique augments power and also increases the turbine efficiency. The amount of steam is limited to about

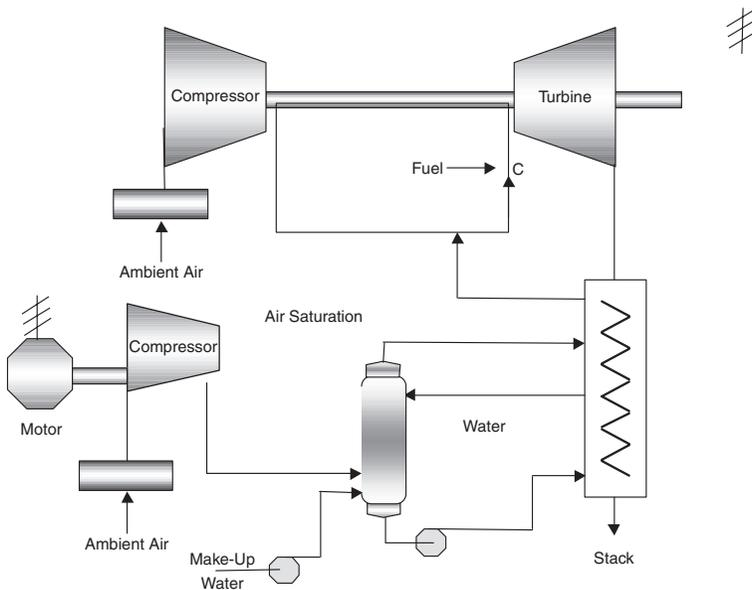


Figure 2-41. Heated and humidified compressed air injection system for power augmentation of a gas turbine.

12% of the airflow, which can result in a power increase of about 25%. The limits of the generator may restrict the amount of power, which can be added. The cost for such systems runs around \$100/kW.

Injection of Steam in the Combustor of the Gas Turbines Utilizing Present Dual Fuel Nozzles. Steam injection in the combustor has been commonly used for NO_x control as seen in Figure 2-43. The amount of steam, which can be added, is limited due to combustion concerns. This is limited to about 2–3% of the airflow. This would provide an additional 3–5% of the rated power. The dual fuel nozzles on many of the industrial turbines could easily be retrofitted to achieve the goal of steam injection. The steam would be produced using an HRSG. Multiple turbines could also be tied into one HRSG.

Combination of Evaporative Cooling and Steam Injection. The combination of the above techniques must also be investigated as none of these techniques is exclusive of the other techniques and can be easily used in conjunction with each other. Figure 2-44 is a schematic of combining the inlet evaporative cooling with injection of steam in both the compressor exit and the combustor. In this system, the power is augmented benefiting from

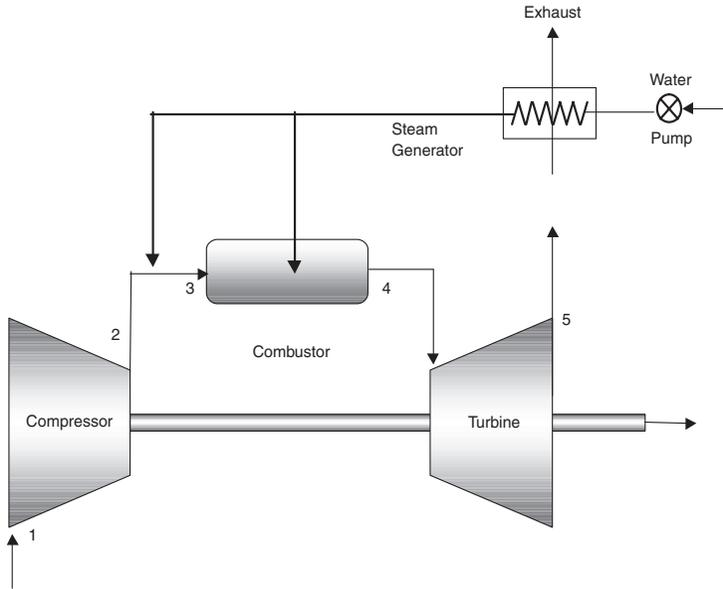


Figure 2-42. Steam injection at exit of compressor and in the combustor of the gas turbine.

the cooling of the air, and then augmented further by the addition of the steam.

Summation of the Power Augmentation Systems

The analysis of the different cycles examined here, which range from the simplest cycle such as evaporative cooling to the more complex cycles such as the humidified and heated compressed air cycle, are rated to their effectiveness and to their cost is shown in Table 2-1. The cycles examined here have been used in actual operation of major power plants, thus there are no cycles evaluated that are only conceptual in nature. The results show addition from 3–21% in power and the increase in efficiency from 0.4–24%

The cooling of the inlet air using an evaporative cycle, the simplest of the cycles, and which can be put into operation with the least outlay in capital is not very useful in operation in high humidity areas. The system would cost between \$300,000–\$500,000 per turbine thus amounting to a cost of \$135 per KW.

Refrigerated inlet cooling is much more effective in humid areas and can add about 12.8% to the power output of the simple cycle gas turbine. The

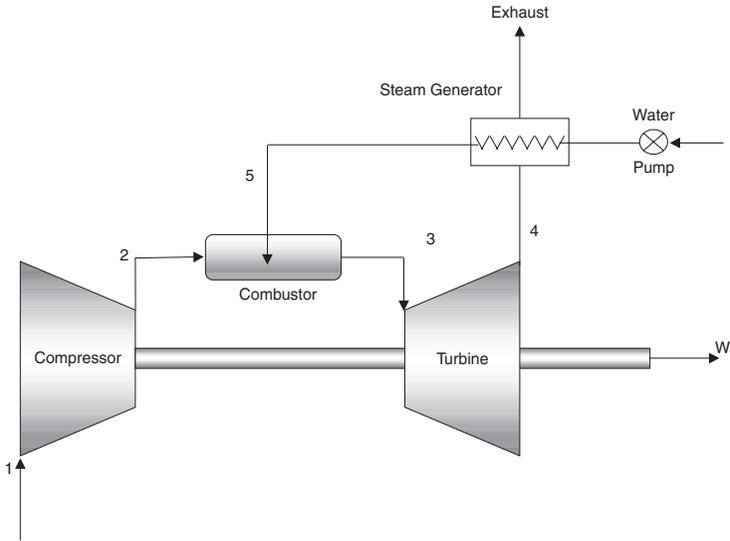


Figure 2-43. Steam injection in the gas turbine combustor.

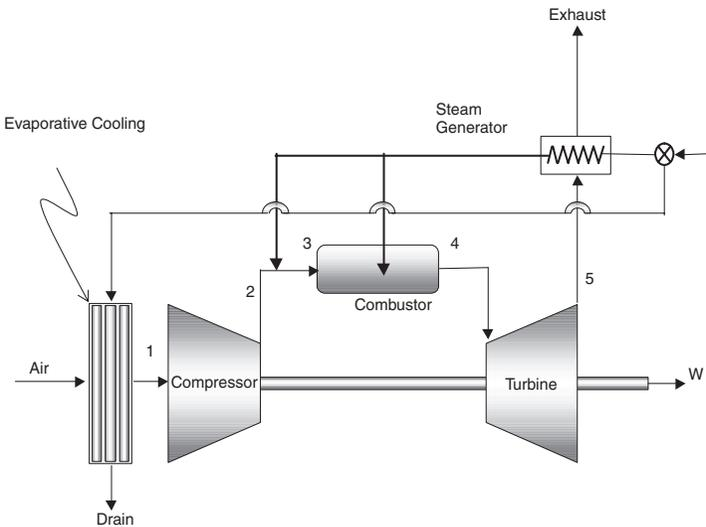


Figure 2-44. Evaporative cooling and steam injection in a gas turbine.

Table 2-1
Evaluation of Various Techniques to Enhance the Operation of the Simple Cycle Gas Turbine

| Based on Gas Turbine Operating at Power=110MW Inlet Temp=32°C Efficiency=32.92 Heat Rate 10935 KJ/KW-HR | | | | | | | | | |
|---|------------------------|-------------------------------|------------------------------------|--------------------|--------------------|-----------------|----------------------------|---|---------------------|
| Types of Process | Increase in Power (MW) | Percent Increase in Power (%) | Percent Increase in Efficiency (%) | Heat Rate kJ/kW-hr | Cost US\$ Millions | Cost/KW US\$/KW | Fuel Savings per year US\$ | Increase in Sales Revenue per Year US\$ | Total Earnings US\$ |
| Evaporative cooling | 3.69 | 3.32 | 0.39 | 10,891 | 0.5 | 135.67 | 515,264 | 396,755 | 912,019 |
| Refrigeration inlet cooling | 12.77 | 11.51 | 2.5 | 10,672 | 2.5 | 195.74 | 605,075 | 1,379,901 | 1,984,977 |
| Ice storage cooling | 12.77 | 11.51 | 2.5 | 10,672 | 1.5 | 117.44 | 201,692 | 459,967 | 661,659 |
| Inter-stage compressor cooling | 17.41 | 15.69 | 14.19 | 9,576 | 2.5 | 143.56 | 3,743,308 | 2,291,365 | 6,034,672 |
| Heated and humidified compressed air injection | 23.44 | 21.12 | 21.23 | 9,020 | 3.7 | 157.84 | 5,597,388 | 3,368,355 | 8,965,744 |
| Steam injection | 10.11 | 9.11 | 22.13 | 8954 | 1.7 | 168.19 | 5,220,193 | 1,466,792 | 6,686,985 |
| Evaporative cooling + Steam injection | 13.97 | 12.59 | 24.02 | 8817 | 2.1 | 150.34 | 5,770,444 | 2,068,616 | 7,839,060 |

cost outlay of such a system is among the costliest per KW of the cycles evaluated. The Concept here would be to have a single HRSG supply enough steam to provide cooling for three turbines. The steam would be used to power a steam turbine, which would then operate a refrigeration compressor or use the steam to provide absorption cooling for the three turbines. The concept was to reduce the turbine inlet temperature by about 30–50 °F (17–27 °C). The refrigeration unit could also be supplanted by the use of an ice storage system whose effect would be the same on the performance of the turbine except for the fact that it would operate for about eight hours in a day, the other 16 hours would be used to produce the ice used for cooling the air. In this manner, the refrigeration system could be much smaller than the system required for refrigeration of the inlet air 24 hours a day.

The cooling of the inter-stage compressor air by injecting water is also another very effective way for getting more power from the gas turbine. The problem in most units is that there is no convenient place to inject the water. The gas turbines would require substantial modification to install such a system. Care would have to be taken that any modification would not affect the integrity of the system. This type of a system is very effective in units where there is a low and high-pressure compressor, providing a very convenient place to inject the water. This type of compressor are mostly available in aeroderivative units.

The concept of injecting humidified and heated compressed air just after the gas turbine compressor is another very interesting way to increase power and efficiency. In this system, compressed air is added to the compressed discharge air. The compressed air is about 5% of the main gas turbine air and this air after it has been compressed using an external compressor is then injected into an air saturation device where steam obtained from the HRSG unit is then injected into the device to saturate the air with water and the saturated air then is further heated in the HRSG before it is injected into the compressor discharge of the gas turbine.

The injection of steam in the compressor discharge has been utilized over the years and has been found to be very effective. The amount of steam to be injected can vary from 5–15%. The injection of steam created from properly treated water does not affect the life of the hot section of the turbines. This is based on a large number of units where steam injection has been used. Steam injection, with an evaporative cooling inlet system would be best suited for hot humid areas this application based on the efficiency and cost as shown in Figure 2-45.

The additional costs for incorporating the systems are also shown in Figure 2-45. The cost per KW for the steam injection and the Heated and

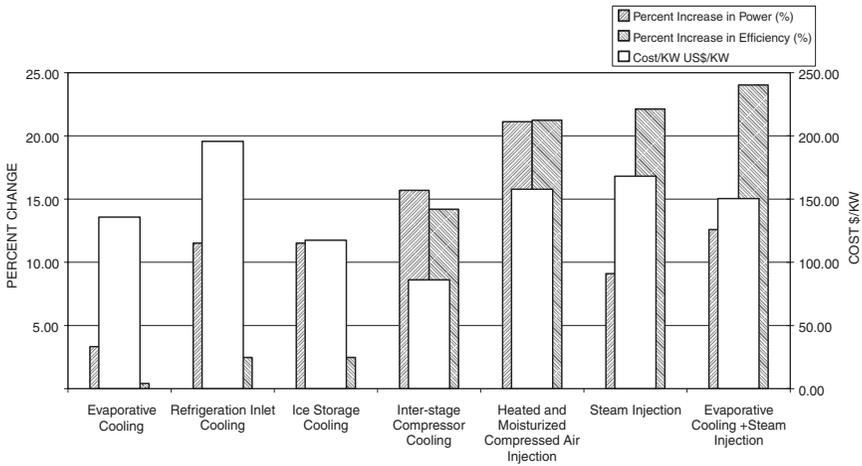


Figure 2-45. Comparison of various cycles based on percent change in power and efficiency and cost \$/KW.

Humidified Compressed Air Injection System are about the same. This is due to the fact that though the initial cost to install the Compressed Air System, for a turbine of about 100 MW, is about \$3.7 million as compared to about \$1.7 million for a steam injection system, the power generated by the Heated and Humidified Compressed Air Injection System is much higher.

The rate of return on the steam injection system is higher than the Compressed Air Injection System. This is due to the fact that though the efficiency of the steam injection system and the compressed air injection system is about the same, however, the initial cost of the steam injected system being over 50% lower than the compressed air injection system accounts for the difference.

The calculations for fuel gas savings have been based on an international price of fuel, at about US\$2.50 per million BTU (US\$2.64 per million KJ). The plant availability was taken at 97%, which is the availability throughout industry for most frame type plants. The cost of sale of new power was based on the average price of US\$0.04 per KW-Hr.

Some of the major restrictions in putting these cycles on existing units can be described as follows:

1. *Generator Power Output Capacity.* The generator, as a general rule of thumb is oversized by about 20% above the turbine rated load. The changes have to be limited to that region by limiting the steam or Compressed Air Injection.

2. *Turbine Firing Temperature.* The turbine firing temperature, the temperature of the gas measured at the inlet of the first stage nozzles, is limited to the design firing temperatures as increase in firing temperatures would greatly reduce the life of the turbine hot section.
3. *Injection Pressure.* The injection pressure must be between 75–100 psia (5–7 Bar) above the Compressor Discharge Pressure. In the case of the Heated and Humidified Compressed Air injected system, the air must be saturated.
4. *Nozzle Area of the First Turbine Stage (Expander Stage).* This is a very critical parameter and limits the total airflow into the turbine section, thus this limits the amount of steam injection or the amount of the heated and humidified compressed air injection.
5. *Surge Control.* The injection systems will all require major modifications to the control system to prevent injection till the units have reached full load and stabilized operation. During shutdown, the system must first shut off the injection system. These changes are very necessary to prevent the units from surging.
6. *NO_x Emissions.* The amount NO_x emissions is very critical in most regions where gas turbines are being utilized for power generation. The present cap is about 22 ppm; the aim is to go down to as low as 9 ppm. The techniques offered here all are NO_x emission friendly, in that they do not increase the present levels of NO_x, in fact in the case of the injection systems, both steam, and heated and humidified compressed air will lower the NO_x emissions making the plant even more environmentally friendly, especially in this critical location.
7. *Control Systems.* The costs in all these systems have taken into account modifications of the control systems. The control systems in most of these cases will have to be new to take into account the injection of steam, and the heated and humidified compressed air, the HRSG, and all its associated equipments such as pumps.

Bibliography

- Boyce, M.P., Meher-Homji, C.B., and Lakshminarasimha, A.N., "Gas Turbine and Combined Cycle Technologies for Power and Efficiency Enhancement in Power Plants," ASME 94-GT-435.
- Boyce, M.P., "Turbo-Machinery for the Next Millennium," *Russia Gas Turbo-Technology Publication*, September–October 2000.
- Boyce, M.P., "Advanced Cycles for Combined Cycle Power Plants," *Russia Gas Turbo-Technology Publication*, November–December 2000.

- Chodkiewicz, R., Porochnicki, J., and Potapczyk, A., "Electric Power and Nitric Acid Coproduction—A New Concept in Reducing The Energy Costs," *Powergen Europe '98*, Milan, Italy, 1998, Vol. 3, pp. 611–625.
- Chodkiewicz, R. "A Recuperated Gas Turbine Incorporating External Heat Sources in the Combined Gas-Steam Cycle," ASME Paper No. 2000-GT-0593.
- Cyrus, B., Meher-Homji, T.R., and Mee III, "Gas Turbine Power Augmentation by Fogging of Inlet Air," 28th Turbomachinery 28 Symposium Proceedings; p. 93; 1999.
- Kehlhofer, R.H., et al., "Combined Cycle Gas & Steam Turbine Power Plants," 2nd Edition, PennWell, Tulsa, Oklahoma, 1999.
- Lane, A.W., and Hoffman, P.A., "The U.S. Dept. of Energy Advanced Turbine System Program", ISROMAC-7, Hawaii, 1998.
- Miller, H.F., "Blade Erosion—FCCU Power Recovery Expanders," D-R Turbo Products Division, Olean, N.Y., 1989.
- Nakhamkin, M. "Increasing Gas Turbine or Combined Cycle Power Production with Compressed Air to Meet Peak Power Demands," ASME Paper No. 2000-GT-0596.
- Narula, R.G., "The Single-Shaft Combined Cycle Myth," ASME Paper No. 2000-GT-0594
- Holden, P., Moen, D., and DeCorso, M., "Alabama Electric Cooperative Compressed Air Energy Storage (CAES) Plant Improvements," ASME Paper No. 2000-GT-0595.
- "Ullman Encyclopaedia of Industrial Chemistry," 1991, Vol. A17.
- Wieler, C.L., "WR-21 Intercooled Recuperated Gas Turbine," U.S. DOE Advanced Turbine Systems Meeting, 1998.

3

Compressor and Turbine Performance Characteristics

This chapter examines the overall performance characteristics of compressors and turbines. This material is presented here to familiarize the reader with the behavior of these machines, classified under the broad term “turbomachinery.” Pumps and compressors are used to produce pressure; turbines produce power. These machines have some common characteristics. The main element is a rotor with blades or vanes, and the path of the fluid in the rotor may be axial, radial, or a combination of both.

There are three methods of studying the elements of turbomachinery operation. First, by examining forces and velocity diagrams, it is possible to discover some general relationships between capacity, pressure, speed, and power. Second, comprehensive experimentation can be undertaken to study relationships between different variables. Third, without considering the actual mechanics, one can use dimensional analysis to derive a set of factors whose grouping can shed light on overall behavior. The analysis presented in this chapter shows the typical performance diagrams one can expect from turbomachines. Off-design performance is also important in understanding trends and operating curves.

Turbomachine Aerothermodynamics

The motion of a gas can be studied in two different ways: (1) the motion of each gas particle can be studied to determine its position, velocity, acceleration, and state variation with time; (2) each particle can be studied to determine its *variation* in velocity, acceleration, and the state of various particles at every location in space and in time. In studying the movement

of each fluid particle, we are studying *Lagrangian motion*; in studying the spatial system we are studying *Eulerian motion*. This book will examine the Eulerian motion of the flow. The flow will be considered fully described if the magnitude, direction, and thermodynamic properties of the gas at every point in space are determined.

To understand the flow in turbomachines, an understanding of the basic relationships of pressure, temperature, and type of flow must be acquired. Ideal flow in turbomachines exists when there is no transfer of heat between the gas and its surroundings, and the entropy of the gas remains unchanged. This type of flow is characterized as a *reversible adiabatic flow*. To describe this flow, the total and static conditions of pressure, temperature, and the concept of an ideal gas must be understood.

Ideal Gas

Ideal gas obeys the equation of state $PV = MRT$ or $P/\rho = MRT$, where P denotes the pressure, V the volume, ρ the density, M the mass, T the temperature of the gas, and R the gas constant per unit mass independent of pressure and temperature. In most cases the ideal gas laws are sufficient to describe the flow within 5% of actual conditions. When the perfect gas laws do not apply, the gas compressibility factor Z can be introduced:

$$Z(P, T) = \frac{PV}{RT} \quad (3-1)$$

Figure 3-1 shows the relationship between the compressibility factor and pressure and temperature, couched in terms of reduced pressure and temperature:

$$P_r = \frac{P}{P_c} \quad T_r = \frac{T}{T_c} \quad (3-2)$$

P_c and T_c are the pressure and temperature of the gas at the critical point.

Static pressure is the pressure of the moving fluid. The static pressure of a gas is the same in all directions and is a scalar point function. It can be measured by drilling a hole in the pipe and keeping a probe flush with the pipe wall.

Total pressure is the pressure of the gas brought to rest in a reversible adiabatic manner. It can be measured by a pitot tube placed in the flow

FPO

Figure 3-1. Generalized compressibility factor for simple fluid. (Adapted with permission from *Journal of the American Chemical Society*, © 1955, American Chemical Society.)

stream. The gas is brought to rest at the probe tip. The relationship between total and static pressure is given in the following relationship:

$$P_t = P_s + \frac{\rho V^2}{2g_c} \quad (3-3)$$

where $\rho V^2/2g_c$ is the dynamic pressure head that denotes the velocity of the moving gas.

Static temperature is the temperature of the flowing gas. This temperature rises because of the random motion of the fluid molecules. The static temperature can only be measured by a measurement at rest relative to the moving gas. The measurement of the static temperature is a difficult, if not impossible, task.

Total temperature is the temperature rise in the gas if its velocity is brought to rest in a reversible adiabatic manner. Total temperature can be measured by the insertion of a thermocouple, *RTD* or thermometer in the fluid stream. The relationship between the total temperature and static temperature can be given:

$$T_t = T_s + \frac{V^2}{2c_p g_c} \quad (3-4)$$

Compressibility Effect

The effect of compressibility is important in high mach number machines. *Mach number* is the ratio of velocity to the acoustic speed of a gas at a given temperature $M \equiv V/a$. *Acoustic speed* is defined as the ratio change in pressure of the gas with respect to its density if the entropy is held constant:

$$a^2 \equiv \left(\frac{\partial P}{\partial \rho} \right)_{s=c} \quad (3-5)$$

With incompressible fluids, the value of the acoustic speed tends toward infinity. For isentropic flow, the equation of state for a perfect gas can be written:

$$P/\rho^\gamma = \text{const}$$

Therefore,

$$\ln P - \gamma \ln \rho = \text{const} \quad (3-6)$$

Differentiating the previous equation, the following relationship is obtained:

$$\frac{dP}{P} - \gamma \frac{d\rho}{\rho} = 0 \quad (3-7)$$

For an isentropic flow, the acoustic speed can be written:

$$a^2 = dP/d\rho$$

Therefore,

$$a^2 = \gamma P / \rho \quad (3-8)$$

Substituting the general equation of state and the definition of the acoustic velocity, the following equation is obtained:

$$a^2 = \gamma g_c R T_s \quad (3-9)$$

where T_s (static temperature) is the temperature of the moving gas stream.

Since the static temperature cannot be measured, the value of static temperature must be computed using the measurements of static pressure, and total pressure and temperature. The relationship between static temperature and total temperature is given by the following relationship:

$$\frac{T_t}{T_s} = 1 + \frac{V^2}{2g_c c_p T_s} \quad (3-10)$$

where the specific heat c_p at constant volume can be written:

$$c_p = \frac{\gamma R}{\gamma - 1} \quad (3-11)$$

and where γ is the ratio of the specific heats

$$\gamma = \frac{c_p}{c_v}$$

Combining Equations (3-10) and (3-11) gives the following relationship:

$$\frac{T_t}{T_s} = 1 + \frac{\gamma - 1}{2} M^2 \quad (3-12)$$

The relationship between the total and static conditions is isentropic; therefore,

$$\frac{T_t}{T_s} = \left(\frac{P_t}{P_s} \right)^{\frac{\gamma-1}{\gamma}} \quad (3-13)$$

and the relationship between total pressure and static pressure can be written:

$$\frac{P_t}{P_s} = \left(1 + \frac{\gamma - 1}{2} M^2\right)^{\frac{\gamma}{\gamma - 1}} \quad (3-14)$$

By measuring the total and static pressure and using Equation (3-14), the Mach number can be calculated. Using Equation (3-12), the static temperature can be computed, since the total temperature can be measured. Finally, using the definition of Mach number, the velocity of the gas stream can be calculated.

The Aerothermal Equations

The gas stream can be defined by the three basic aerothermal equations: (1) continuity, (2) momentum, and (3) energy.

The Continuity Equation

The continuity equation is a mathematical formulation of the law of conservation of mass of a gas that is a continuum. The law of conservation of mass states that the mass of a volume moving with the fluid remains unchanged

$$\dot{m} = \rho AV$$

where:

\dot{m} = mass flow rate

ρ = fluid density

A = cross-sectional area

V = gas velocity

The previous equation can be written in the differential form

$$\frac{dA}{A} + \frac{dV}{V} + \frac{d\rho}{\rho} = 0 \quad (3-15)$$

The Momentum Equation

The momentum equation is a mathematical formulation of the law of conservation of momentum. It states that the rate of change in linear momentum of a volume moving with a fluid is equal to the surface forces and body forces acting on a fluid. Figure 3-2 shows the velocity components in a generalized turbomachine. The velocity vectors as shown are resolved into three mutually perpendicular components: the axial component (V_a), the tangential component (V_θ), and the radial component (V_m).

By examining each of these velocities, the following characteristics can be noted: the change in the magnitude of the axial velocity gives rise to an axial force which is taken up by a thrust bearing, the change in radial velocity gives rise to a radial force which is taken up by the journal bearing. The tangential

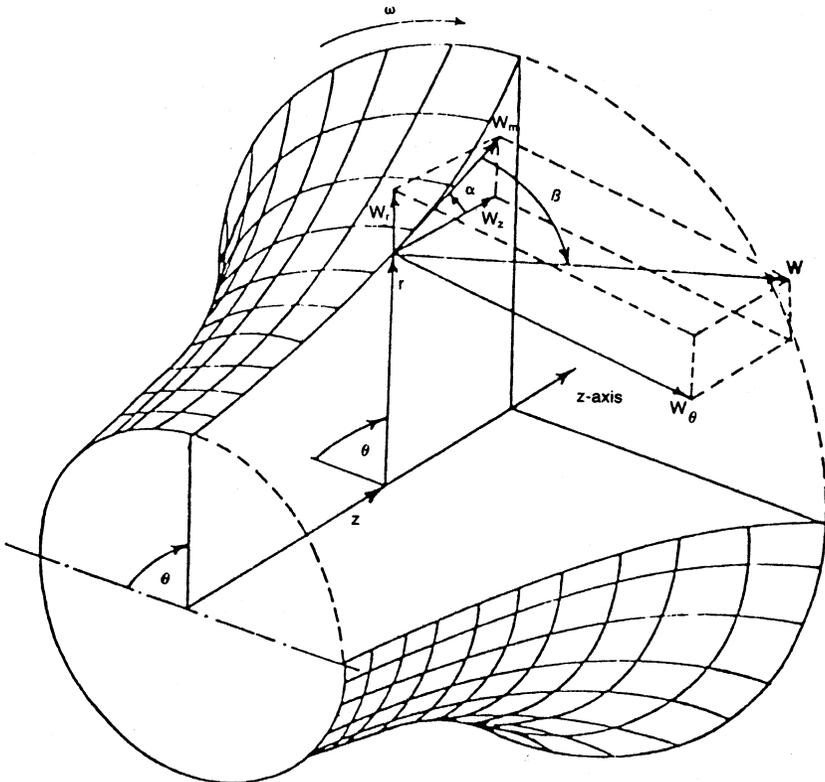


Figure 3-2. Velocity vectors in compressor rotor flow.

component is the only component that causes a force that corresponds to a change in angular momentum; the other two velocity components have no effect on this force—except for what bearing friction may arise.

By applying the conservation of momentum principle, the change in angular momentum obtained by the change in the tangential velocity is equal to the summation of all the forces applied on the rotor. This summation is the net torque of the rotor. A certain mass of fluid enters the turbomachine with an initial velocity V_{θ_1} , at a radius r_1 , and leaves with a tangential velocity V_{θ_2} at a radius r_2 . Assuming that the mass flow rate through the turbomachine remains unchanged, the torque exerted by the change in angular velocity can be written:

$$\tau = \frac{\dot{m}}{g_c}(r_1 V_{\theta_1} - r_2 V_{\theta_2}) \quad (3-16)$$

The rate of change of energy transfer (ft-lb_f/sec) is the product of the torque and the angular velocity (ω)

$$\tau\omega = \frac{\dot{m}}{g_c}(r_1\omega V_{\theta_1} - r_2\omega V_{\theta_2}) \quad (3-17)$$

Thus, the total energy transfer can be written:

$$E = \frac{\dot{m}}{g_c}(U_1 V_{\theta_1} - U_2 V_{\theta_2}) \quad (3-18)$$

where U_1 and U_2 are the linear velocity of the rotor at the respective radii. The previous relation per unit mass flow can be written:

$$H = \frac{1}{g_c}(U_1 V_{\theta_1} - U_2 V_{\theta_2}) \quad (3-19)$$

where H is the energy transfer per unit mass flow ft-lb_f/lb_m or fluid pressure. Equation (3-19) is known as the Euler turbine equation.

The equation of motion as given in terms of angular momentum can be transformed into other forms that are more convenient to understanding some of the basic design components. To understand the flow in a turbomachine, the concepts of absolute and relative velocity must be grasped. *Absolute velocity* (V) is gas velocity with respect to a stationary coordinate system. *Relative velocity* (W) is the velocity relative to the rotor. In turbomachinery,

the air entering the rotor will have a relative velocity component parallel to the rotor blade, and an absolute velocity component parallel to the stationary blades. Mathematically, this relationship is written:

$$\vec{V} = \vec{W} + \vec{U} \quad (3-20)$$

where the absolute velocity (V) is the algebraic addition of the relative velocity (W) and the linear rotor velocity (U). The absolute velocity can be resolved into its components, the radial or meridional velocity (V_m) and the tangential component V_θ . From Figure 3-3, the following relationships are obtained:

$$\begin{aligned} V_1^2 &= V_{\theta 1}^2 + V_{m1}^2 \\ V_2^2 &= V_{\theta 2}^2 + V_{m2}^2 \\ W_1^2 &= (U_1 - V_{\theta 1})^2 + V_{m1}^2 \\ W_2^2 &= (U_2 - V_{\theta 2})^2 + V_{m2}^2 \end{aligned} \quad (3-21)$$

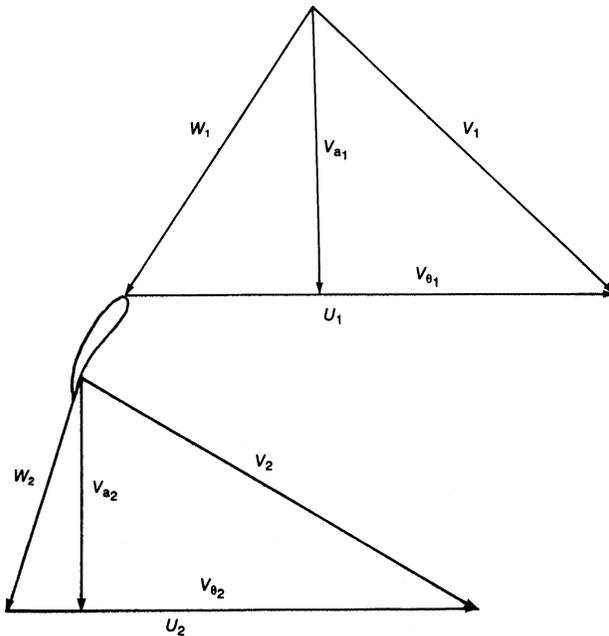


Figure 3-3. Velocity triangles for an axial-flow compressor.

By placing these relationships into the Euler turbine equation, the following relationship is obtained:

$$H = \frac{1}{2g_c} \left[(V_1^2 - V_2^2) + (U_1^2 - U_2^2) + (W_2^2 - W_1^2) \right] \quad (3-22)$$

The Energy Equation

The energy equation is the mathematical formulation of the law of conservation of energy. It states that the rate at which energy enters the volume of a moving fluid is equal to the rate at which work is done on the surroundings by the fluid within the volume and the rate at which energy increases within the moving fluid. The energy in a moving fluid is composed of internal, flow, kinetic, and potential energy

$$\epsilon_1 + \frac{P_1}{\rho_1} + \frac{V_1^2}{2g_c} + Z_1 + {}_1Q_2 = \epsilon_2 + \frac{P_2}{\rho_2} + \frac{V_2^2}{2g_c} + Z_2 + {}_1(\text{Work})_2 \quad (3-23)$$

For isentropic flow, the energy equation can be written as follows, noting that the addition of internal and flow energies can be written as the enthalpy (h) of the fluid:

$${}_1(\text{Work})_2 = (h_1 - h_2) + \left(\frac{V_1^2}{2g_c} - \frac{V_2^2}{2g_c} \right) + (Z_1 - Z_2) \quad (3-24)$$

Combining the energy and momentum equations provides the following relationships:

$$(h_1 - h_2) + \left(\frac{V_1^2}{2g_c} - \frac{V_2^2}{2g_c} \right) + (Z_1 - Z_2) = \frac{1}{g_c} [U_1 V_{\theta_1} - U_2 V_{\theta_2}] \quad (3-25)$$

Assuming that there is no change in potential energies, the equation can be written:

$$\left(h_1 + \frac{V_1^2}{2g_c} \right) - \left(h_2 + \frac{V_2^2}{2g_c} \right) = h_{1t} - h_{2t} = \frac{1}{g_c} [U_1 V_{\theta_1} - U_2 V_{\theta_2}] \quad (3-26)$$

Assuming that the gas is thermally and calorifically perfect, the equation can be written:

$$T_{1t} - T_{2t} = \frac{1}{C_p g_c} [U_1 V_{\theta_2} - U_2 V_{\theta_2}] \quad (3-27)$$

For isentropic flow,

$$\frac{T_{2t}}{T_{1t}} = \left(\frac{P_{2t}}{P_{1t}} \right)^{\frac{\gamma-1}{\gamma}} \tag{3-28}$$

By combining Equations (3-27) and (3-28),

$$T_{1t} \left[1 - \left(\frac{P_{2t}}{P_{1t}} \right)^{\frac{\gamma-1}{\gamma}} \right] = \frac{1}{C_p g_c} [U_1 V_{\theta_1} - U_2 V_{\theta_2}] \tag{3-29}$$

Efficiencies

Adiabatic Efficiency

The work in a compressor or turbine under ideal conditions occurs at constant entropy as shown in Figures 3-4 and 3-5, respectively. The actual

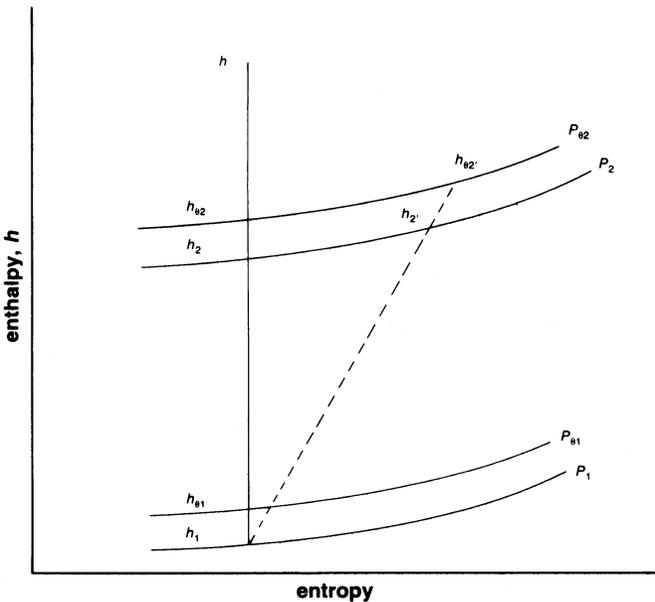


Figure 3-4. Entropy-enthalpy diagram of a compressor.

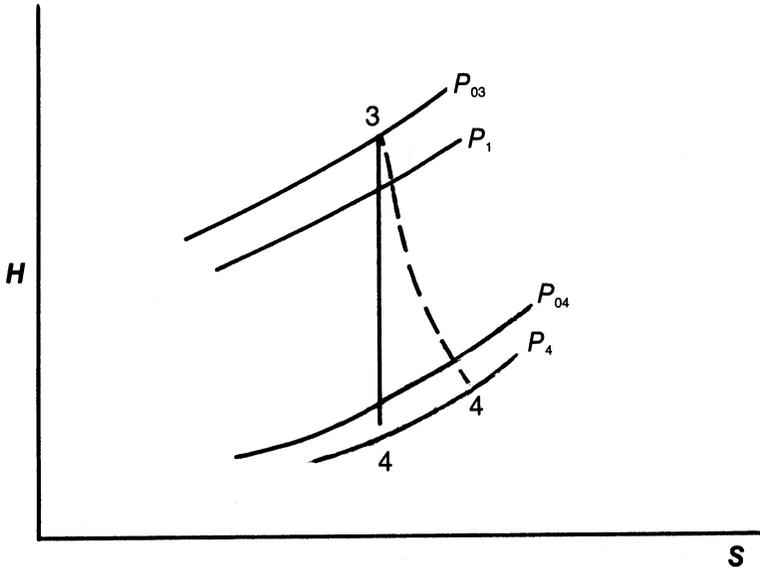


Figure 3-5. Entropy-enthalpy diagram of a turbine.

work done is indicated by the dotted line. The isentropic efficiency of the compressor can be written in terms of the total changes in enthalpy

$$\eta_{ad_c} = \frac{\text{Isentropic work}}{\text{Actual work}} = \frac{(h_{2t} - h_{1t})_{id}}{(h_{2t} - h_{1t})_{act}} \tag{3-30}$$

This equation can be rewritten for a thermally and calorifically perfect gas in terms of total pressure and temperature as follows:

$$\eta_{ad_c} = \left[\left(\frac{P_{2t}}{P_{1t}} \right)^{\frac{\gamma-1}{\gamma}} - 1 \right] / \left[\frac{T_{2t}}{T_{1t}} - 1 \right] \tag{3-31}$$

The process between 1 and 2' can be defined by the following equation of state:

$$\frac{P}{\rho^n} = \text{const} \tag{3-32}$$

where n is some polytropic process. The adiabatic efficiency can then be represented by

$$\eta_{ad_c} = \left[\left(\frac{P_{2t}}{P_{1t}} \right)^{\frac{\gamma-1}{\gamma}} - 1 \right] / \left[\left(\frac{P_{2t}}{P_{1t}} \right)^{\frac{n-1}{n}} - 1 \right] \quad (3-33)$$

The isentropic efficiency of the turbine can be written in terms of the total enthalpy change

$$\eta_{ad_t} = \frac{\text{Actual work}}{\text{Isentropic work}} = \frac{h_{3t} - h_{4t}}{h_{3t} - h_{4t}} \quad (3-34)$$

This equation can be rewritten for a thermally and calorifically perfect gas in terms of total pressure and temperature

$$\eta_{ad_t} = \frac{\left[1 - \frac{T_{4t}}{T_{3t}} \right]}{1 - \left(\frac{P_{4t}}{P_{3t}} \right)^{\frac{\gamma-1}{\gamma}}} \quad (3-35)$$

Polytropic Efficiency

Polytropic efficiency is another concept of efficiency often used in compressor evaluation. It is often referred to as small stage or infinitesimal stage efficiency. It is the true aerodynamic efficiency exclusive of the pressure-ratio effect. The efficiency is the same as if the fluid is incompressible and identical with the hydraulic efficiency

$$\eta_{pc} = \frac{\left[1 + \frac{dP_{2t}}{P_{1t}} \right]^{\frac{\gamma-1}{\gamma}} - 1}{\left[1 + \frac{dP_{2t}}{P_{1t}} \right]^{\frac{n-1}{n}} - 1} \quad (3-36)$$

which can be expanded assuming that

$$\frac{dP_{2t}}{P_{1t}} \ll 1$$

Neglecting second-order terms, the following relationship is obtained:

$$\eta_{pc} = \frac{\frac{\gamma-1}{n-1}}{n} \quad (3-37)$$

From this relationship, it is obvious that polytropic efficiency is the limiting value of the isentropic efficiency as the pressure increase approaches zero, and the value of the polytropic efficiency is higher than the corresponding adiabatic efficiency. Figure 3-6 shows the relationship between adiabatic and polytropic efficiency as the pressure ratio across the compressor increases. Figure 3-7 shows the relationship across the turbine.

Another characteristic of polytropic efficiency is that the polytropic efficiency of a multistage unit is equal to the stage efficiency if each stage has the same efficiency.

Dimensional Analysis

Turbomachines can be compared with each other by *dimensional analysis*. This analysis produces various types of geometrically similar parameters. Dimensional analysis is a procedure where variables representing a physical situation are reduced into groups, which are dimensionless. These dimensionless groups can then be used to compare performance of various types of machines with each other. Dimensional analysis as used in turbomachines can be employed to: (1) compare data from various types of machines—it is a useful technique in the development of blade passages and blade profiles, (2) select various types of units based on maximum efficiency and pressure head required, and (3) predict a prototype's performance from tests conducted on a smaller scale model or at lower speeds.

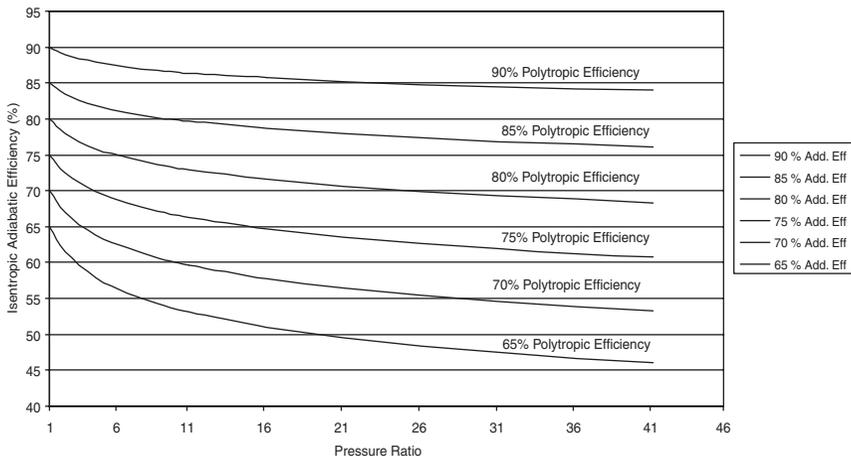


Figure 3-6. Relationship between adiabatic and polytropic efficiency.

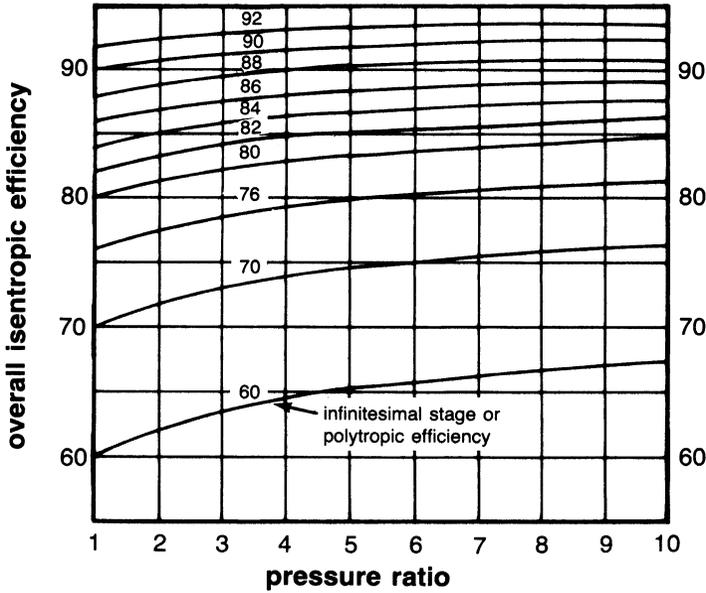


Figure 3-7. Overall and polytropic efficiency expansion.

Dimensional analysis leads to various dimensionless parameters, which are based on the dimension's mass (M), length (L), and time (T). Based on these elements, one can obtain various independent parameters such as density (ρ), viscosity (μ), speed (N), diameter (D), and velocity (V). The independent parameters lead to forming various dimensionless groups, which are used in fluid mechanics of turbomachines. Reynolds number is the ratio of the inertia forces to the viscous forces

$$Re = \frac{\rho V D}{\mu} \tag{3-38}$$

where ρ is the density of the gas, V the velocity, D the diameter of the impeller, and μ the viscosity of the gas.

The specific speed compares the head and flow rate in geometrically similar machines at various speeds

$$N_s = \frac{N \sqrt{Q}}{H^{3/4}} \tag{3-39}$$

where H is the adiabatic head, Q is the volume rate, and N the speed.

The specific diameter compares head and flow rates in geometrically similar machines at various diameters

$$D_s = \frac{DH^{1/4}}{\sqrt{Q}} \quad (3-40)$$

The flow coefficient is the capacity of the flow rate expressed in dimensionless form

$$\phi = \frac{Q}{ND^3} \quad (3-41)$$

The pressure coefficient is the pressure or pressure rise expressed in dimensionless form

$$\psi = \frac{H}{N^2D^2} \quad (3-42)$$

The previous equations are some of the major dimensionless parameters. For the flow to remain dynamically similar, all the parameters must remain constant; however, constancy is not possible in a practical sense, so one must make choices.

In selecting turbomachines the choice of specific speed and specific diameter determines the most suitable compressor (Figure 3-8a) and turbine (Figure 3-8b). It is obvious from Figure 3-8a that high-head and low-flow require a positive displacement unit, a medium-head and medium-flow require a centrifugal unit, and high-flow and low-head require an axial-flow unit. Figure 3-8a also shows the efficiency of the various types of compressors. This comparison can be made with the different compressors. While results from Figures 3-8a and 3-8b may vary with actual machines, the results do give a good indication of the type of turbomachine required for the head at the highest efficiency.

Flow coefficients and pressure coefficients can be used to determine various off-design characteristics. Reynolds number affects the flow calculations for skin friction and velocity distribution.

When using dimensional analysis in computing or predicting performance based on tests performed on smaller-scale units, it is not physically possible to keep all parameters constant. The variation of the final results will depend on the scale-up factor and the difference in the fluid medium. It is important in any type of dimensionless study to understand the limit of the parameters and that the geometrical scale-up of similar parameters must remain constant.

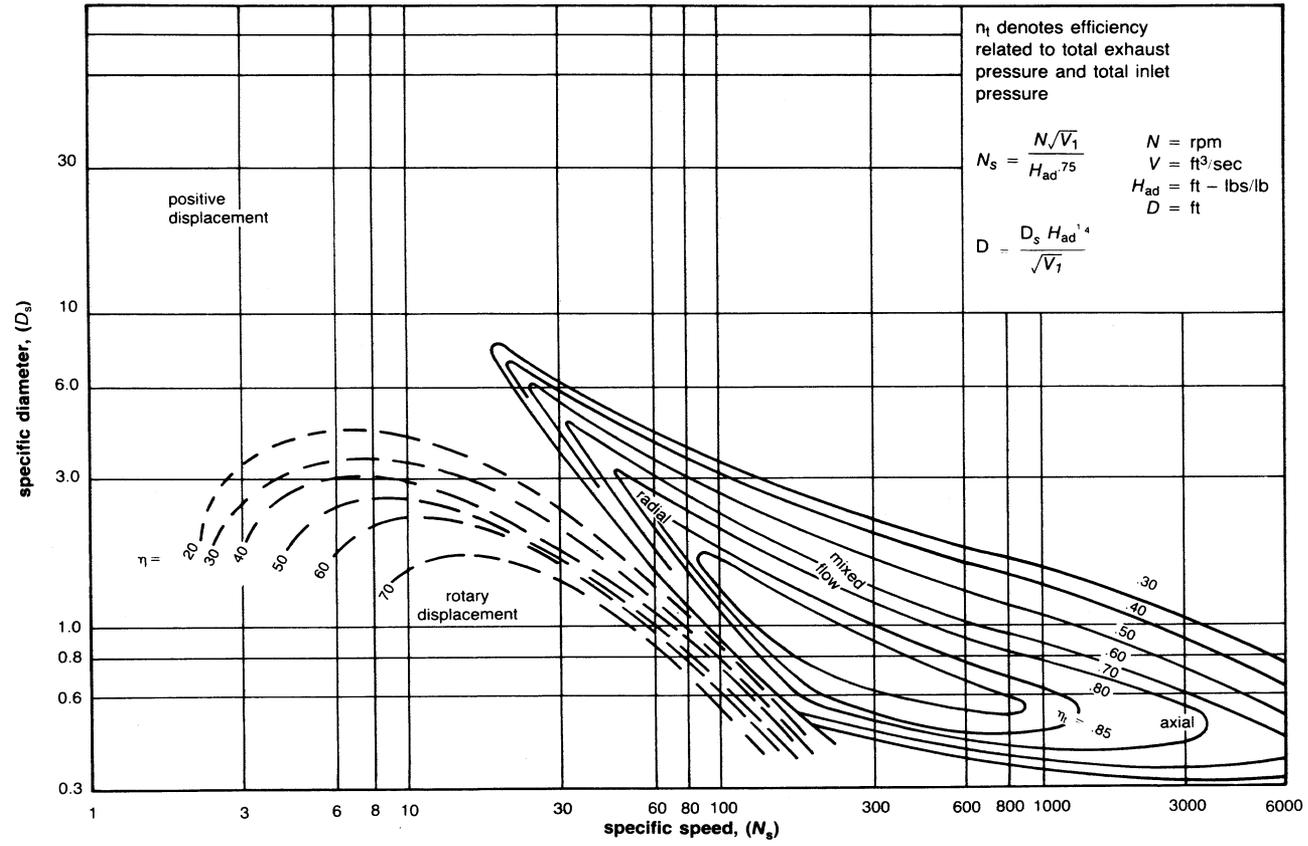


Figure 3-8a. Compressor map.

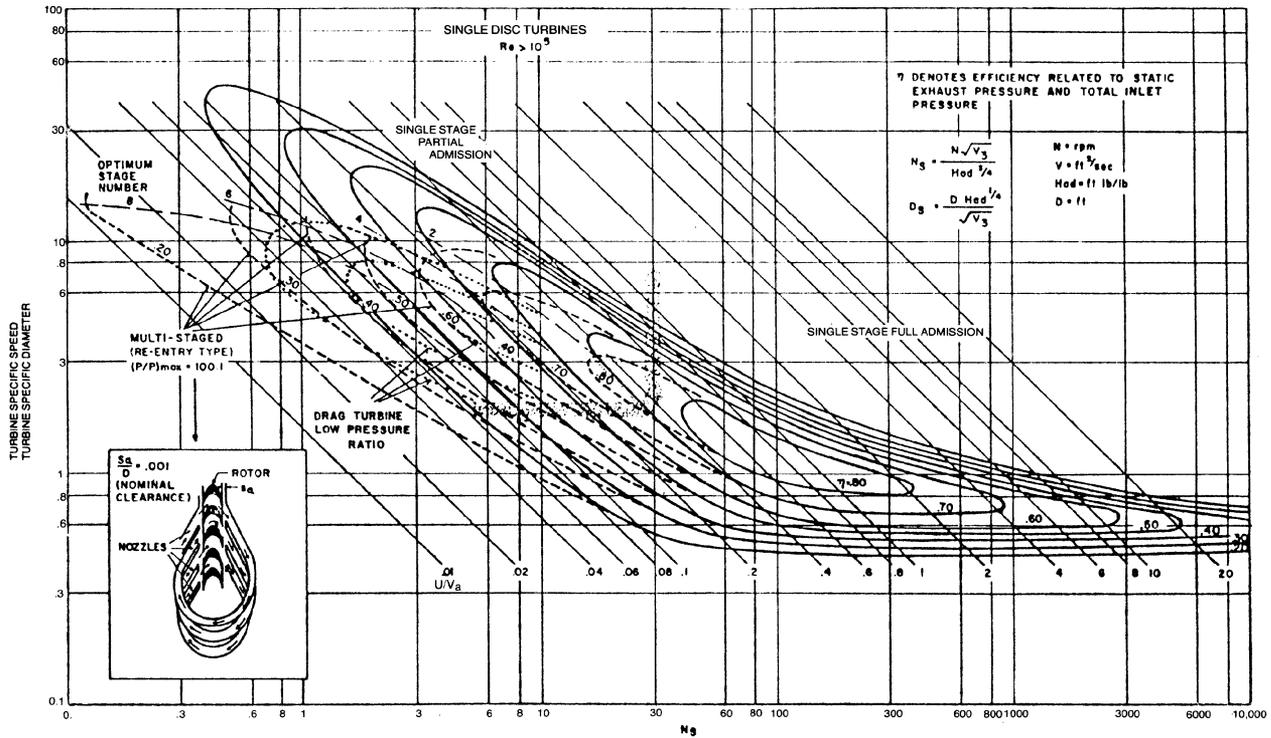


Figure 3-8b. Turbine map. (Balje, O.E., "A Study of Reynolds Number Effects in Turbomachinery," *Journal of Engineering for Power*, ASME Trans., Vol. 86, Series A, p. 227.)

Many scale-ups have developed major problems because stress, vibration, and other dynamic factors were not considered.

Compressor Performance Characteristics

Compressor performance can be represented in various ways. The commonly accepted practice is to plot the speed lines as a function of the pressure delivered and the flow. Figure 3-9 is a performance map for a centrifugal compressor. The constant speed lines shown in Figure 3-9 are constant aero-dynamic speed lines, not constant mechanical speed lines.

The actual mass flow rates and speeds are corrected by factor $(\sqrt{\theta}/\delta)$ and $(1/\sqrt{\theta})$ respectively, reflecting variations in inlet temperature and pressure. The surge line joins different speed lines where the compressor's operation becomes unstable. A compressor is in surge when the main flow through a compressor reverses direction for short time intervals, during which the back

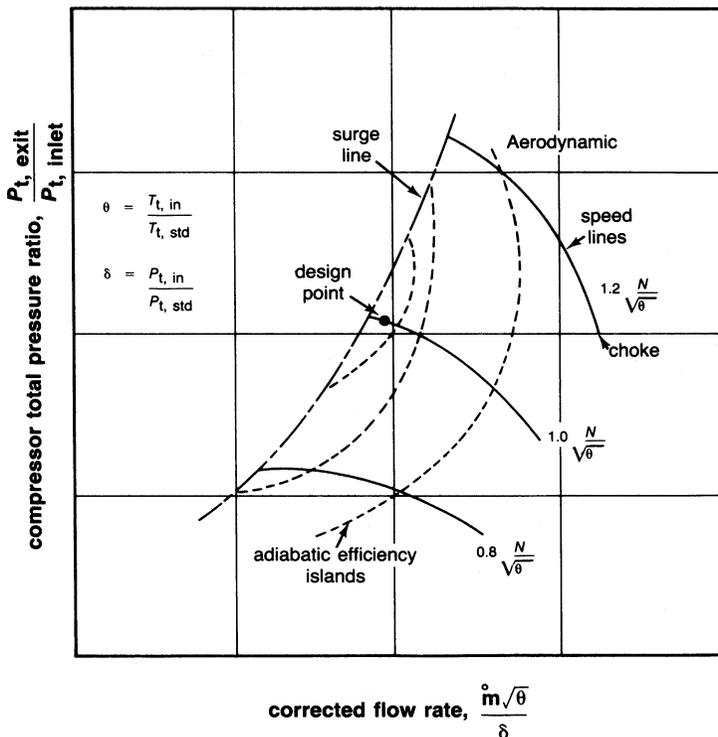


Figure 3-9. Typical centrifugal compressor performance characteristics.

(exit) pressure drops and the main flow assumes its proper direction. This process is followed by a rise in back-pressure, causing the main flow to reverse again. If allowed to persist, this unsteady process may result in irreparable damage to the machine. Lines of constant adiabatic efficiency (sometimes called efficiency islands) are also plotted on the compressor map. A condition known as “choke” indicates the maximum mass flow rate possible through a compressor at operating speed (Figure 3-9). Flow rate cannot be increased, since at this point it is beyond Mach one at the minimum area of the compressor, or a phenomenon known as “stone walling” occurs, causing a rapid drop in efficiency and pressure ratio.

Figure 3-10 shows a similar performance map for an axial-flow compressor. Note the smaller operational flow range for the axial-flow compressor as compared to the centrifugal compressor. Figure 3-11 shows a typical compressor map presented from a slightly different viewpoint. On this map,

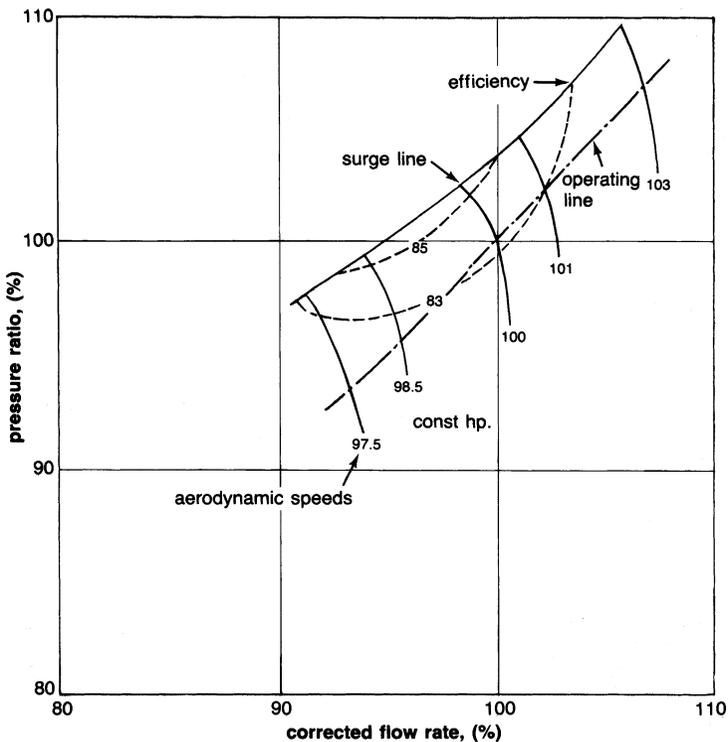


Figure 3-10. Typical flow map for an axial-flow compressor.

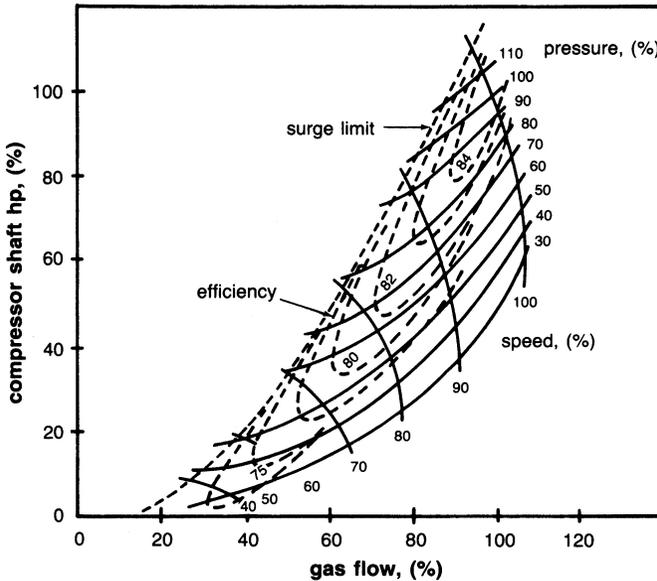


Figure 3-11. Typical compressor map where speedlines are a function of horsepower and flow rate.

the constant aerodynamic speed lines are functions of the power and flow rate. Constant pressure lines and efficiency islands are also shown on the same map.

Turbine Performance Characteristics

The two types of turbines—axial-flow and radial-inflow turbines—can be divided further into impulse or reaction type units. Impulse turbines take their entire enthalpy drop through the nozzles, while the reaction turbine takes a partial drop through both the nozzles and the impeller blades.

The two conditions that vary the most in a turbine are the inlet pressure and temperature. Two diagrams are needed to show their characteristics. Figure 3-12 is a performance map that shows the effect of turbine inlet temperature and pressure, while power is dependent on the efficiency of the unit, the flow rate, and the available energy (turbine inlet temperature). The effect of efficiency with speed is shown in Figure 3-13. Figure 3-13 also shows the difference between an impulse and a 50% reaction turbine. An impulse turbine is a zero-reaction turbine.

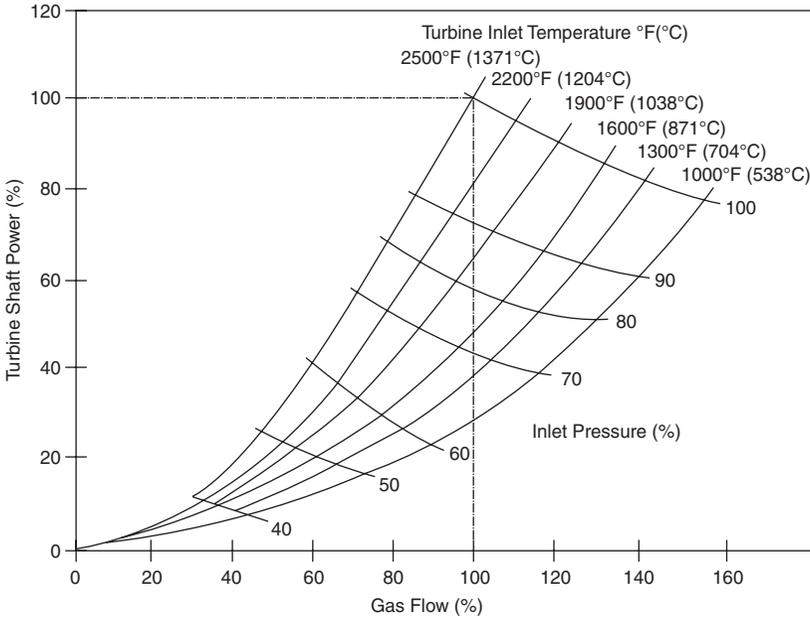


Figure 3-12. Turbine performance map.

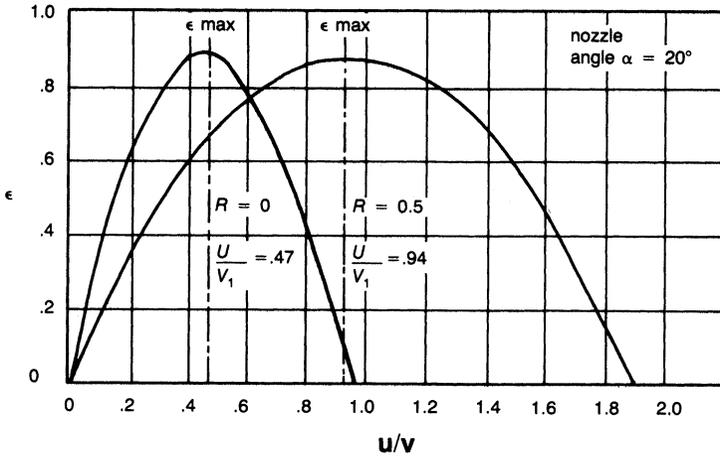


Figure 3-13. Variation of utilization factor with U/V_1 for $R = 0$ and $R = 0.5$. (From *Principles of Turbomachinery* by Dennis G. Shepherd, © 1956 by Macmillan Publishing Co., Inc.)

Gas Turbine Performance Computation

The following is a sample computation of the techniques used to determine the performance of a gas turbine. A test was run on a G.E. Frame 5 simple-cycle single-shaft unit as shown in Figure 3-14. The exhaust energy from this unit was recovered in a heat recovery boiler, which with supplementary gas firing, delivered 175,000 lbs/hr (79,545 kg/hr) of steam at 655 psia (44.8 Bar) and 750 °F (398 °C). It has a small steam turbine that acts as a starter unit. Figure 3-15 is a schematic of the system. The gas turbine was operated from about 25% load to full load. Full load was determined to

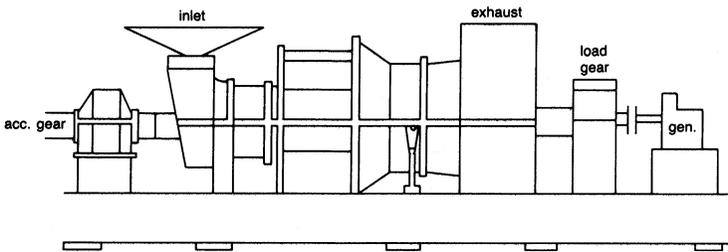


Figure 3-14. Typical industrial gas turbine.

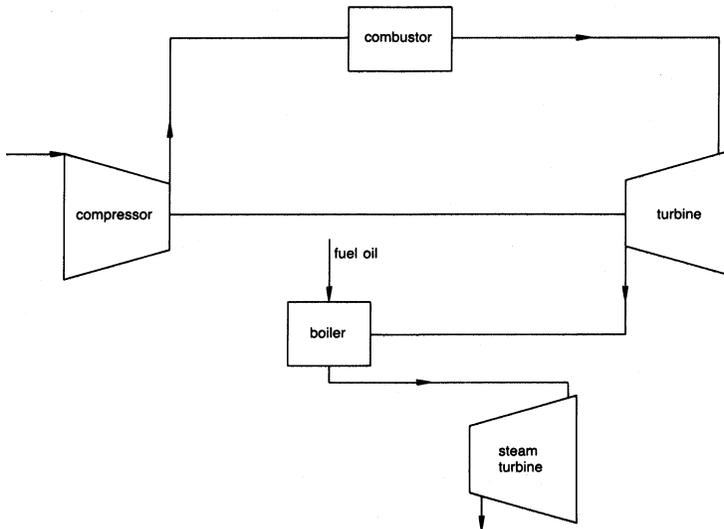


Figure 3-15. Schematic of combined cycle gas turbine.

be when the turbine's automatic controls took over. These controls are actuated by the exhaust temperature.

Figure 3-16 shows the effect of efficiency as a function of the load for both the compressor and turbine. Part-load turbine efficiencies are affected more than compressor efficiencies. The discrepancy results from the compressor operating at a relatively constant inlet temperature, pressure, and pressure ratio, while the turbine inlet temperature is greatly varied (Figure 3-17).

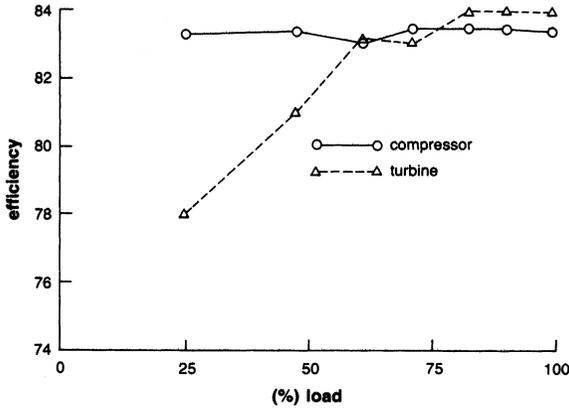


Figure 3-16. Compressor and turbine efficiency as a function of load.

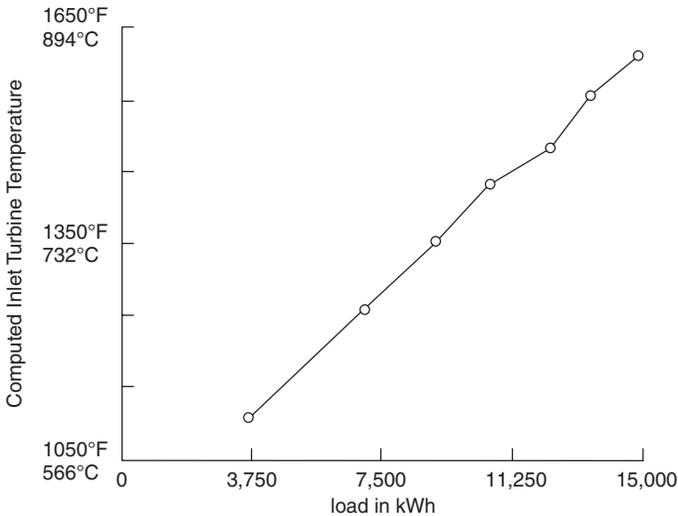


Figure 3-17. Turbine inlet temperature as a function of turbine load.

The turbine pressure ratio, however, remains relatively constant. The back-pressure on the turbine was measured at a relatively constant value of 30.25 inches Hg abs (1.02 Bar). This value creates about a 9-inch H₂O (228 mm H₂O) back-pressure on the turbine. The efficiency of the compressor is based on the following equation:

$$\eta_c = \frac{T_{t1} \left[\left(\frac{P_{t2}}{P_{t1}} \right)^{\frac{\gamma-1}{\gamma}} - 1 \right]}{\Delta T_{act}} \quad (3-43)$$

where:

T_{t1} = inlet temperature

P_{t2} = pressure at compressor outlet

P_{t1} = pressure at compressor inlet

ΔT_{act} = actual temperature rise in the compressor

γ = specific heat ratio; average value between inlet and outlet temperature was used

The turbine efficiency calculation is more complex. The first part is the calculation of the turbine inlet temperature. The calculation is based on the following equation:

$$T_{t3} = \frac{\dot{m}_a c_{p2} T_{t2} + n_b \dot{m}_f (LHV \text{ natural gas})}{c_{p3} c_{p3} (\dot{m}_f + \dot{m}_a)} \quad (3-44)$$

where:

T_{t2} = temperature at the outlet of the compressor

c_p = specific heat at constant pressure

\dot{m}_f = mass flow rate for the fuel

\dot{m}_a = mass flow rate of the air

η_b = combustion efficiency

(*LHV*) = lower heating value of the natural gas supplied

(950 Btu/cu ft [(35,426 kJ/cu m)] and specific gravity 0.557)

The mass flow value of the air was obtained by measuring the flow at the inlet of the gas turbine using an ion-gun velocimeter. Figure 3-18 shows the values obtained across the inlet. These values give an average flow rate of 720,868 lbs/hr (327,667 kg/hr). This flow rate is within experimental accuracy. The temperature drop in the turbine is based on an energy balance and is given by the following equation:

$$\Delta T_{\text{tact}} = \frac{W_{\text{load}}}{\eta_{\text{gen}}(m_f + \dot{m}_a)c_{P_{\text{avg}}}} + \frac{\dot{m}_a}{(\dot{m}_f + \dot{m}_a)} \frac{c_{P_{\text{cavg}}}}{c_{P_{\text{tavg}}}} \Delta T_{\text{cact}} \tag{3-45}$$

where:

W_{load} = generator output in kilowatts

η_{gen} = generator efficiency

$c_{P_{\text{tavg}}}$ = turbine average specific heat

$c_{P_{\text{cavg}}}$ = compressor average specific heat

ΔT_{tact} = temperature drop in turbine

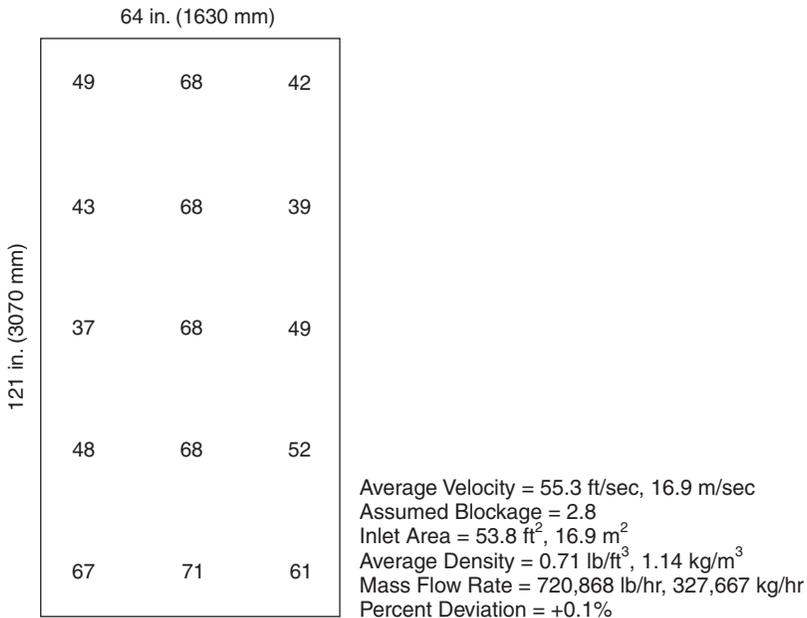


Figure 3-18. Typical inlet velocity profile for an industrial gas turbine.

The temperature drop calculated in this manner was compared to the drop calculated by subtracting the measured average exhaust temperature reading from the inlet temperature as obtained by the previous equation. The difference between these two methods was about 20° at the high-temperature exit. The second method gives a smaller drop, indicating that the temperature recorded is lower than the actual temperature. This result is expected, since the thermocouples are placed a distance downstream from the turbine blades and are not measuring the actual gas exhaust temperature. This comment is not a criticism of the control package, since that operates on a base exhaust temperature.

The turbine efficiency can now be calculated with the use of the following relationship:

$$\eta_t = \frac{\Delta T_{\text{tact}}}{T_{t3} \left\{ \left[1 - \frac{1}{\left(\frac{P_{t3}}{P_{t4}} \right)^{\frac{\gamma-1}{\gamma}}} \right] \right\}} \tag{3-46}$$

where the value of γ was an average value in the turbine.

The gas turbine is coupled with a steam recovery boiler. The exhaust gas from the turbine is used to supplement fire the boiler. The thermal efficiency of the gas turbine alone was calculated by using the following relationship:

$$\eta_{\text{ad}} = \frac{W_{\text{load}} \times K}{(LHV) \times Q} \tag{3-47}$$

where:

$$K = 3,412 \text{ Btu/kW-Hr (3,600 KJ/kW-hr)}$$

$$LHV = \text{heating value, Btu/ft}^3(\text{kJ/cu m})$$

$$Q_{\text{ft}} = \text{volume flow rate of fuel to turbine, ft}^3/\text{hr (cu m/hr)}$$

The overall system efficiency is based on the following equation:

$$\eta_{\text{sad}} = \frac{W_{\text{load}} \times K}{(LHV) \times Q - \dot{m}_{\text{sb}}(h_s - h_{\text{fw}}) + (LHV)Q_{\text{fb}}} \tag{3-48}$$

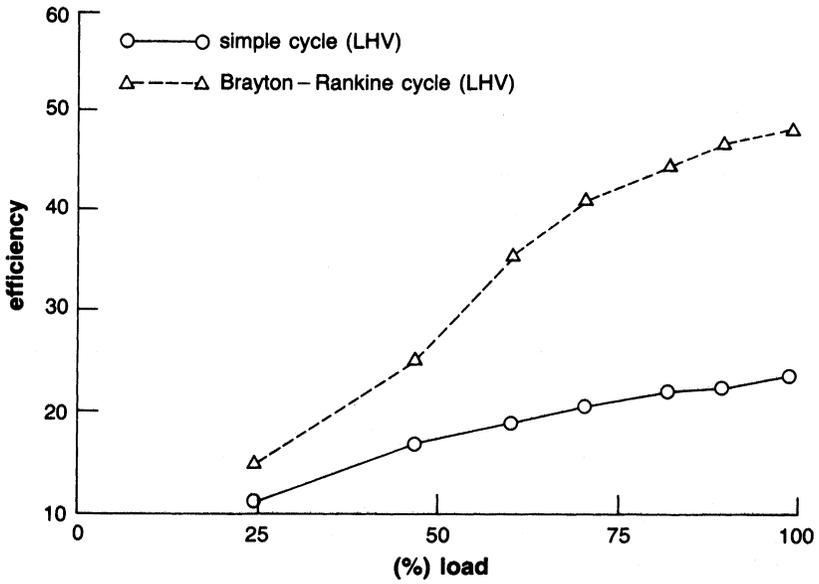


Figure 3-19. Combined cycle and simple cycle efficiency as a function of gas turbine load.

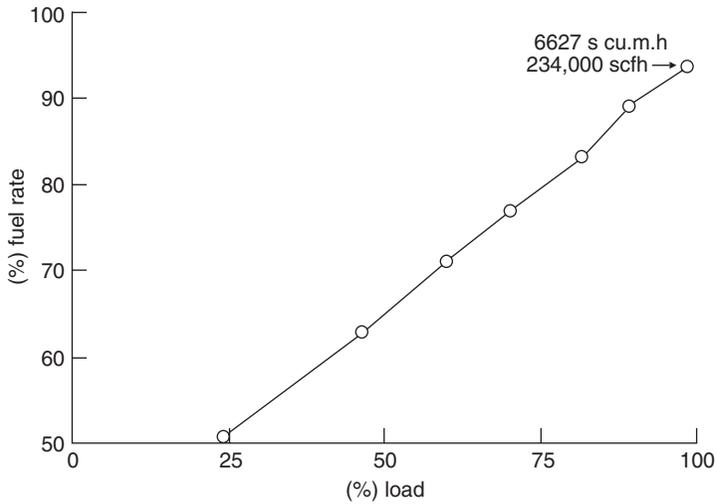


Figure 3-20. Fuel consumption as a function of gas turbine load.

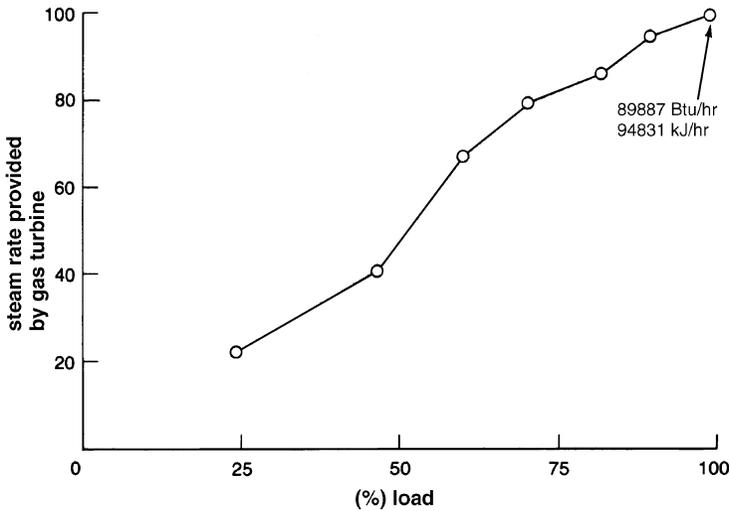


Figure 3-21. Steam generated by exhaust gases of gas turbine as a function of gas turbine load.

where:

\dot{m}_{sb} = mass flow of steam from recovery boiler

h_s = enthalpy of the superheated steam

h_{fw} = enthalpy of the feedwater

Q_{fb} = volume flow rate of fuel to boiler

Figure 3-19 shows the thermal efficiency of the gas turbine and the Brayton-Rankin cycle (gas turbine exhaust being used in the boiler) based on the *LHV* of the gas. This figure shows that below 50% of the rated load, the combination cycle is not effective. At full load, it is obvious the benefits one can reap from a combination cycle. Figure 3-20 shows the fuel consumption as a function of the load, and Figure 3-21 shows the amount of steam generated by the recovery boiler.

Bibliography

Balje, O.I., "A Study of Reynolds Number Effects in Turbomachinery," *Journal of Engineering for Power*, ASME Trans., Vol. 86, Series A, 1964, p. 227.

4

Performance and Mechanical Standards

The gas turbine is a complex machine, and its performance and reliability are governed by many standards. The American Society of Mechanical Engineers (ASME) performance test codes have been written to ensure that test, are conducted in a manner that guarantees that all turbines are tested under the same set of rules and conditions to ensure that the test results can be compared in a judicious manner. The reliability of the turbines depend on the mechanical codes that govern the design of many gas turbines. The mechanical standards and codes have been written by both ASME and the American Petroleum Institute (API).

Major Variables for a Gas Turbine Application

The major variables that affect the gas turbines are the following factors:

1. Type of application
2. Plant location and site configuration
3. Plant size and efficiency
4. Type of fuel
5. Enclosures
6. Plant operation mode; base or peaking
7. Start-up techniques

Each of the above points are discussed in the following sections.

Type of Application

The gas turbine is used in many applications, and the application determines in most parts the type of gas turbine best suited. The three major types of applications are aircraft propulsion, power generation, and mechanical drives.

Aircraft Propulsion. The aircraft propulsion gas turbines can be subdivided into two major categories, the jet propulsion and turboprop engines. The jet engine consists of a gasifier section and a propulsive thrust section as shown in Figure 4-1. The gasifier section is the section of the turbine, which produces high pressure and temperature gas for the power turbine. This comprises of a compressor section and a turbine section. the sole job of the gasifier turbine section is to drive the gas turbine compressor. This section has one or two shafts. The two-shaft gasifier section usually exists in the new high pressure type gas turbine where the compressor produces a very high pressure ratio, and has two different sections. Each section is comprised many stages. The two different compressor sections consist of the low pressure compressor section, followed by a high-pressure section. Each section may have between 10 to 15, stages. The jet engine has a nozzle following the gasifier turbine, which produces the thrust for the

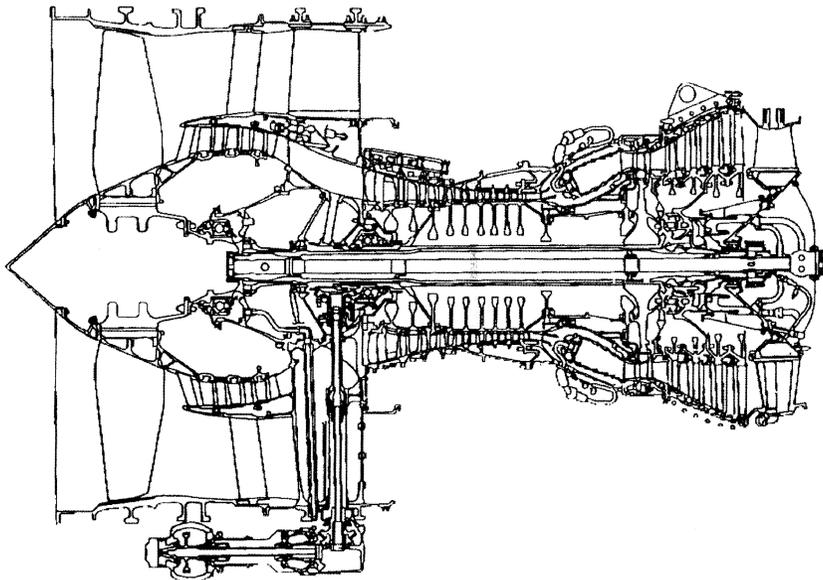


Figure 4-1. A schematic of a fan jet engine with a by-pass fan.

engine. In the newer jet turbines the compressor also has a fan section ahead of the turbine and a large amount of the air from the fan section by-passes the rest of the compressor and produces thrust. The thrust from the fan amounts to more than the thrust from the exhaust.

The jet engine has lead the field of gas turbines in firing temperatures. Pressure ratio of 40:1 with firing temperatures reaching 2500 °F (1371 °C), is now the mode of operation of these engines.

The turboprop engine has a power turbine instead of the nozzle as seen in Figure 4-2. The power turbine drives the propeller. The unit shown schematically is a two-shaft unit, this enables the speed of the propeller to be better controlled, as the gasifier turbine can then operate at a nearly constant speed. Similar engines are used in helicopter drive applications and many have axial flow compressors with a last stage as a centrifugal compressor as shown in Figure 1-14.

Mechanical Drives. Mechanical drive gas turbines are widely used to drive pumps and compressors. Their application is widely used by offshore and petrochemical industrial complexes. These turbines must be operated at various speeds and thus usually have a gasifier section and a power section. These units in most cases are aero-derivative turbines, turbines, which were originally designed for aircraft application. There are some smaller frame type units, which have been converted to mechanical drive units with a gasifier and power turbine.

Power Generation. The power generation turbines can be further divided into three categories:

1. Small standby power turbines less than 2-MW. The smaller size of these turbines in many cases have centrifugal compressors driven by radial inflow turbines, the larger units in this range are usually axial

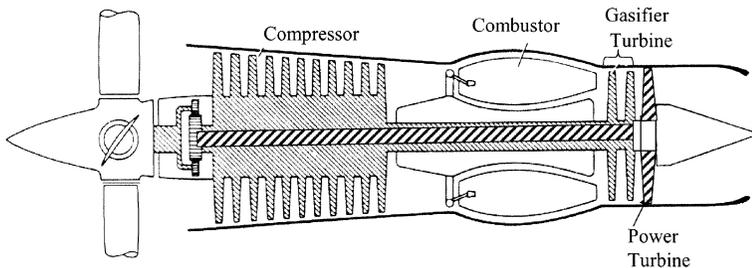


Figure 4-2. Schematic of a turboprop engine.

flow compressors sometimes combined with a centrifugal compressor as the last stage, operated by axial turbines.

2. Medium-sized gas turbines between 5–50 MW are a combination of aero-derivative and frame type turbines. These gas turbines have axial flow compressors and axial flow turbines.
3. Large power turbines over 50–480 MW, these are frame-type turbines, the new large turbines are operating at very high firing temperatures about 2400 °F (1315 °C) with cooling provided by steam, at pressure ratios approaching 35:1.

Plant Location and Site Configuration

The location of the plant is the principal determination of the type of plant best configured to meet its needs. Aero-derivatives are used on offshore platforms. Industrial turbines are mostly used in petrochemical applications, and the frame type units are used for large power production.

Other important parameters that govern the selection and location of the plant are distance from transmission lines, location from fuel port or pipe lines, and type of fuel availability. Site configuration is generally not a constraint. Periodically, sites are encountered where one plant configuration or another is best suited.

Plant Type. The determination to have an aero-derivative type gas turbine or a frame-type gas turbine is the plant location. In most cases if the plant is located off-shore on a platform then an aero-derivative plant is required. On most on-shore applications, if the size of the plant exceeds 100 MW then the frame type is best suited for the gas turbine. In smaller plants between 2–20 MW, the industrial type small turbines best suit the application, and in plants between 20–100 MW, both aero-derivative or frame types can apply. Aero-derivatives have lower maintenance and have high heat-recovery capabilities. In many cases, the type of fuel and service facilities may be the determination. Natural gas or diesel no. 2 would be suited for aero-derivative gas turbines, but heavy fuels would require a frame type gas turbine.

Gas Turbine Size and Efficiency

Gas turbine size is important in the cost of the plant. The larger the gas turbine the less the initial cost per kW. The aero-derivative turbines have traditionally been higher in efficiency however, the new frame type turbines have been closing the gap in efficiency. Figure 4-3 shows typical gas

turbine cost and efficiency as a function of gas turbine output for an industrial type turbine. Industrial turbines range from micro-turbines of 20 kW at an installed cost of nearly \$1000/kW and an efficiency of about 15–18%, to turbines rated at about 10 MW at a cost of \$500/kW and an efficiency of about 28–32%. The efficiency in these figures is a simple cycle gas turbine efficiency. These efficiencies can be increased by regeneration or other techniques dealt with in detail in Chapter 3. Figure 4-4 shows the aero-derivative turbines rated between 10 MW to 40 MW with an installed

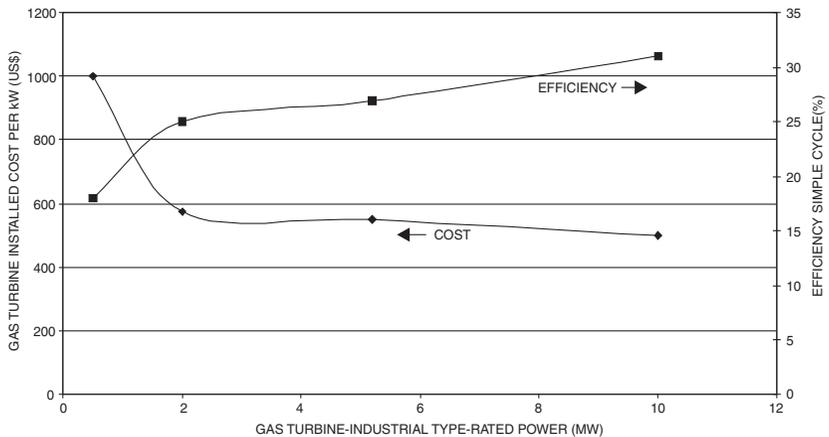


Figure 4-3. Installed cost and efficiency of industrial type turbines.

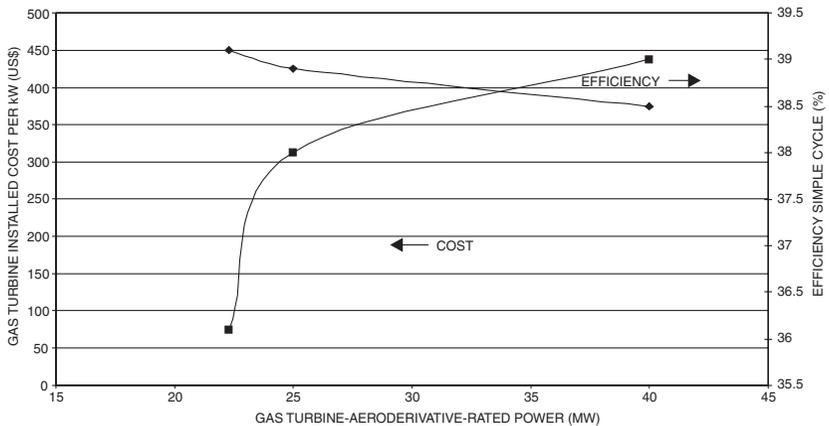


Figure 4-4. Installed cost and efficiency of aero-derivative type turbines.

cost of \$400/kW and an efficiency of about 40%. Figure 4-5 is for a frame type turbines. These turbines range from about 10 MW to about 250 MW with an installed cost for the larger units at \$350/kW, and efficiencies of the newer units reaching 40%.

Type of Fuel

The type of fuel is one of the most important aspects that govern the selection of a gas turbine. Chapter 12 handles the type of fuels and their effect in detail. Natural gas would be the choice of most operators if natural gas was available since its effects on pollution is minimal and maintenance cost would also be the lowest. Table 4-1 shows how the maintenance cost would increase from natural gas to the heavy oils.

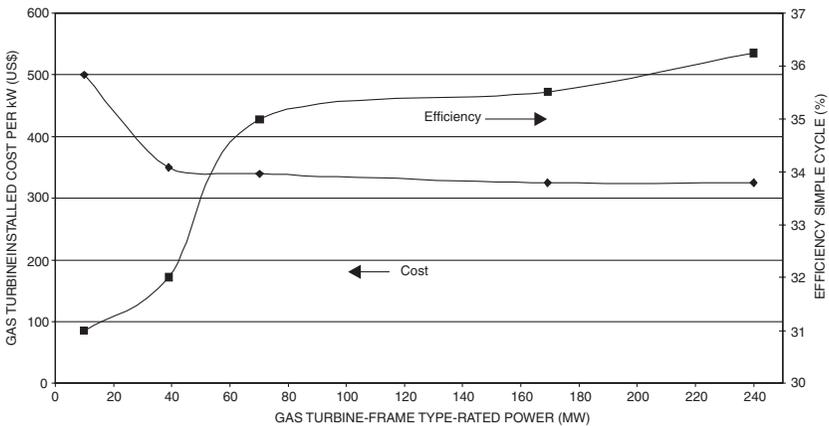


Figure 4-5. Installed cost and efficiency of frame type turbines.

Table 4-1
Typical Gas Turbine Maintenance Cost Based on Type of Fuel

| Type of Fuel | Expected Actual Maintenance Cost | Relative Maintenance Cost Factor |
|----------------------|----------------------------------|----------------------------------|
| Natural gas | 0.35 | 1.0 |
| No. 2 Distillate Oil | 0.49 | 1.4 |
| Typical Crude Oil | 0.77 | 2.2 |
| No. 6 Residual Oil | 1.23 | 3.5 |

Aero-derivative gas turbines cannot operate on heavy fuels, thus if heavy fuels was a criteria then the frame type turbines would have to be used. With heavy fuels, the power delivered would be reduced after about a weeks of operation by about 10%. On-line turbine wash is recommended for turbines with high vanadium content in their fuel, since to counteract vanadium magnesium salts have to be added. These salts cause the vanadium when combusted in the turbine to be turned to ashes. This ash settles on the turbine blades and reduces the cross sectional area, thus reducing the turbine power.

Enclosures

Gas turbines usually come packaged in their own enclosures. These enclosures are designed so that they limit the noise to 70dB at a 100ft (30 meters) from the gas turbine. In the case of a combined cycle power plant consisting of the gas turbine, HRSG, and the steam turbine can be either inside or outside. While open plants are less expensive than enclosed plants, some owners prefer to enclose their steam turbines in a building and use permanent cranes for maintenance. Thus leaving the gas turbine and the HRSG in the open environment. In severe climate areas, the entire plant is enclosed in a building. Single-shaft combined cycle power plant with the generator in the middle require a wider building to allow the generator to be moved to facilitate rotor removal and inspection. Plant arrangements that do not use axial or side exhaust steam turbines result in a taller building and higher building costs.

Plant Operation Mode: Base or Peaking

Gas turbines in the petrochemical industries are usually used under base load conditions powering compressors or pumps. In the power industry, the gas turbine has traditionally been used in peaking service, especially in the U.S. and Europe. In the developing world, the gas turbine has been used as a base loaded plant since the 1960s. Since the 1990s, the gas turbine, being the prime mover in combined cycle power plants, has been developed to operate at high pressures and temperatures, consequently high efficiencies have been achieved. Combined cycle power plants are not as were originally planned base loaded plants. It is not uncommon for the plant to be cycled from 40–100% load in a single day, every day of the year. This type of cycling effects the life of many of the hot section components in the gas turbine.

Start-up Techniques

The start-up of a gas turbine is done by the use of electrical motors, diesel motors, and in plants where there is an independent source of steam by a steam turbine. New turbines use the generator as a motor for start-up. After combustion occurs and the turbine reaches a certain speed, the motor declutches and becomes a generator. Use of a synchronous clutch between two rotating pieces of equipment is not new. It is very common in use with start-up equipment. In the case of single-shaft combined cycle power plants, a synchronous clutch can be used to connect the steam turbine to the gas turbine. However, use of a clutch in transmitting over 100 MW of power is new and has not found unequivocal customer acceptance. While use of a synchronous clutch leads to additional space requirements, additional capital and O&M costs, and potentially reduced availability, it does offer the tangible benefit of easy and fast plant startup. A major drawback of a single-shaft combined cycle power plant with a clutch is that the generator installation and maintenance and power evacuation are more complex and costly because the generator is located in the middle.

Performance Standards

The purpose of the ASME performance test codes is to provide standard directions and rules for the conduct and report of tests of specific equipment and the measurement of related phenomena. These codes provide explicit test procedures with accuracies consistent with current engineering knowledge and practice. The codes are applicable to the determination of performance of specific equipment. They are suitable for incorporation as part of commercial agreements to serve as a means to determine fulfillment of contract obligations. The parties to the test should agree to accept the code results as determined or, alternatively, agree to mutually acceptable limits of uncertainty established by prior agreement of the principal parties concerned.

The performance tests must be run as much as possible to meet the ASME performance codes. These codes are very well written and fully delineate the tests required. Meetings should be held in advance with the vendors to decide which part of the code would not be valid and what assumptions and correction factors must be undertaken to meet the various power and efficiency guarantees. The determination of special data or verification of particular guarantees, which are outside the scope of the codes, should be made only after written agreement of both parties to the test, especially regarding methods of measurement and computation, which should be completely described in the test report.

**ASME, Performance Test Code on Overall Plant Performance,
ASME PTC 46 1996**

This code is written to establish the overall plant performance. Power plants, which produce secondary energy output such as cogeneration facilities are included within the scope of this code. For cogeneration facilities, there is no requirement for a minimum percentage of the facility output to be in the form of electricity; however, the guiding principles, measurement methods, and calculation procedures are predicated on electricity being the primary output. As a result, a test of a facility with a low proportion of electric output may not be capable of meeting the expected test uncertainties of this code. This code provides explicit procedures for the determination of power plant thermal performance and electrical output. Test results provide a measure of the performance of a power plant or thermal island at a specified cycle configuration, operating disposition and/or fixed power level, and at a unique set of base reference conditions. Test results can then be used as defined by a contract for the basis of determination of fulfillment of contract guarantees. Test results can also be used by a plant owner, for either comparison to a design number, or to trend performance changes over time of the overall plant. The results of a test conducted in accordance with this code will not provide a basis for comparing the thermoeconomic effectiveness of different plant design.

Power plants are comprised of many equipment components. Test data required by this code may also provide limited performance information for some of this equipment; however, this code was not designed to facilitate simultaneous code level testing of individual equipment. ASME PTCs, which address testing of major power plant equipment provide a determination of the individual equipment isolated from the rest of the system. PTC 46 has been designed to determine the performance of the entire heat-cycle as an integrated system. Where the performance of individual equipment operating within the constraints of their design-specified conditions are of interest, ASME PTCs developed for the testing of specific components should be used. Likewise, determining overall thermal performance by combining the results of ASME code tests conducted on each plant component is not an acceptable alternative to a PTC 46 test.

**ASME, Performance Test Code on Test Uncertainty:
Instruments and Apparatus PTC 19.1 1988**

This test code specifies procedures for evaluation of uncertainties in individual test measurements, arising from both random errors and systematic errors, and for the propagation of random and systematic uncertainties

into the uncertainty of a test results. The various statistical terms involved are defined. The end result of a measurement uncertainty analysis is to provide numerical estimates of systematic uncertainties, random uncertainties, and the combination of these into a total uncertainty with an approximate confidence level. This is especially very important when computing guarantees in plant output and plant efficiency.

ASME, Performance Test Code on Gas Turbines, ASME PTC 22 1997

The object of the code is to detail the test to determine the power output and thermal efficiency of the gas turbine when operating at the test conditions, and correcting these test results to standard or specified operating and control conditions. Procedures for conducting the test, calculating the results, and making the corrections are defined.

The code provides for the testing of gas turbines supplied with gaseous or liquid fuels (or solid fuels converted to liquid or gas prior to entrance to the gas turbine). Test of gas turbines with water or steam injection for emission control and/or power augmentation are included. The tests can be applied to gas turbines in combined-cycle power plants or with other heat recovery systems.

Meetings should be held with all parties concerned as to how the test will be conducted and an uncertainty analysis should be performed prior to the test. The overall test uncertainty will vary because of the differences in the scope of supply, fuel(s) used, and driven equipment characteristics. The code establishes a limit for the uncertainty of each measurement required; the overall uncertainty is then calculated in accordance with the procedures defined in the code and by ASME PTC 19.1.

Mechanical Parameters

Some of the best standards from a mechanical point of view have been written by the American Petroleum Institute (API) and the American Society of Mechanical Engineers, as part of their mechanical equipment standards. The ASME and the API mechanical equipment standards are an aid in specifying and selecting equipment for general petrochemical use. The intent of these specifications is to facilitate the development of high-quality equipment with a high degree of safety and standardization. The user's problems and experience in the field are considered in writing these specifications. The task force, which writes the specifications, consists of members from the user, the contractor, and the manufacturers. Thus, the task-force team brings together both experience and know-how.

The petroleum industry is one of the largest users of gas turbines as prime movers for drives of mechanical equipment and also for power generation equipment. Thus the specifications written are well suited for this industry, and the tips of operation and maintenance apply for all industries. This section deals with some of the applicable API and ASME standards for the gas turbine and other various associated pieces.

It is not the intent here to detail the API or ASME standards, but to discuss some of the pertinent points of these standards and other available options. It is strongly recommended that the reader obtain from ASME and API all mechanical equipment standards.

API Std 616, Gas Turbines for the Petroleum, Chemical, and Gas Industry Services, 4th Edition, August 1998

This standard covers the minimum requirements for open, simple, and regenerative-cycle combustion gas turbine units for services of mechanical drive, generator drive, or process gas generation. All auxiliary equipment required for starting and controlling gas turbine units, and for turbine protection is either discussed directly in this standard or referred to in this standard through references to other publications. Specifically, gas turbine units that are capable of continuous service firing gas or liquid fuel or both are covered by this standard. In conjunction with the API specifications the following ASME codes also supply significant data in the proper selection of the gas turbine.

ASME Basic Gas Turbines B 133.2 Published: 1977 (Reaffirmed Year: 1997)

This standard presents and describes features that are desirable for the user to specify in order to select a gas turbine that will yield satisfactory performance, availability, and reliability. The standard is limited to a consideration of the basic gas turbine including the compressor, combustion system, and turbine.

ASME Gas Turbine Fuels B 133.7M Published: 1985 (Reaffirmed Year: 1992)

Gas turbines may be designed to burn either gaseous or liquid fuels, or both with or without changeover while under load. This standard covers both types of fuel.

ASME Gas Turbine Control and Protection Systems B133.4 Published: 1978 (Reaffirmed Year: 1997)

The intent of this standard is to cover the normal requirements of the majority of applications, recognizing that economic trade-offs and reliability implications may differ in some applications. The user may desire to add, delete, or modify the requirements in this standard to meet his specific needs, and he has the option of doing so in his own bid specification. The gas turbine control system shall include sequencing, control, protection, and operator information, which shall provide for orderly and safe start-up of gas turbine, control of proper loading, and an orderly shutdown procedure. It shall include an emergency shutdown capability, which can be operated automatically by suitable failure detectors or which can be operated manually. Coordination between gas turbine control and driven equipment must be provided for startup, operation, and shutdown.

ASME Gas Turbine Installation Sound Emissions B133.8 Published: 1977 (Reaffirmed Year: 1989)

This standard gives methods and procedures for specifying the sound emissions of gas turbine installations for industrial, pipeline, and utility applications. Included are practices for making field sound measurements and for reporting field data. This standard can be used by users and manufacturers to write specifications for procurement, and to determine compliance with specification after installation. Information is included, for guidance, to determine expected community reaction to noise.

ASME Measurement of Exhaust Emissions from Stationary Gas Turbine Engines B133.9 (Published: 1994)

This standard provides guidance in the measurement of exhaust emissions for the emissions performance testing (source testing) of stationary gas turbines. Source testing is required to meet federal, state, and local environmental regulations. The standard is not intended for use in continuous emissions monitoring although many of the online measurement methods defined may be used in both applications. This standard applies to engines that operate on natural gas and liquid distillate fuels. Much of this standard also will apply to engines operated on special fuels such as alcohol, coal gas, residual oil, or process gas or liquid. However, these methods may require

modification or be supplemented to account for the measurement of exhaust components resulting from the use of a special fuel.

**ASME Procurement Standard for Gas Turbine Electrical Equipment
B133.5 (Published: 1978) (Reaffirmed Year: 1997)**

The aim of this standard is to provide guidelines and criteria for specifying electrical equipment, other than controls, which may be supplied with a gas turbine. Much of the electrical equipment will apply only to larger generator drive installations, but where applicable this standard can be used for other gas turbine drives. Electrical equipment described here, in almost all cases, is covered by standards, guidelines, or recommended practices documented elsewhere. This standard is intended to supplement those references and point out the specific areas of interest for a gas turbine application. For a few of the individual items, no other standard is referenced for the entire subject, but where applicable a standard is referenced for a sub-item. A user is advised to employ this and other more detailed standards to improve his specification for a gas turbine installation. In addition, regulatory requirements such as OSHA and local codes should be considered in completing the final specification. Gas turbine electrical equipment covered by this standard is divided into four major areas: Main Power System, Auxiliary Power System, Direct Current System, Relaying. The main power system includes all electrical equipment from the generator neutral grounding connection up to the main power transformer or bus but not including a main transformer or bus. The auxiliary power system is the gas turbine section AC supply and includes all equipment necessary to provide such station power as well as motors utilizing electrical power. The DC system includes the battery and charger only. Relaying is confined to electric system protective relaying that is used for protection of the gas turbine station itself.

**ASME Procurement Standard for Gas Turbine Auxiliary Equipment
B133.3 (Published: 1981) (Reaffirmed Year: 1994)**

The purpose of this standard is to provide guidance to facilitate the preparation of gas turbine procurement specifications. It is intended for use with gas turbines for industrial, marine, and electric power applications. The standard also covers auxiliary systems such as lubrication, cooling, fuel (but not its control), atomizing, starting, heating-ventilating, fire protection, cleaning, inlet, exhaust, enclosures, couplings, gears, piping, mounting, painting, and water and steam injection.

API Std 618, Reciprocating Compressors for Petroleum, Chemical, and Gas Industry Services, 4th Edition, June 1995

This standard could be adapted to the fuel compressor for the natural gas to be brought up to the injection pressure required for the gas turbine. Covers the minimum requirements for reciprocating compressors and their drivers used in petroleum, chemical, and gas industry services for handling process air or gas with either lubricated or nonlubricated cylinders. Compressors covered by this standard are of moderate-to-low speed and in critical services. The nonlubricated cylinder types of compressors are used for injecting fuel in gas turbines at the high pressure needed. Also covered are related lubricating systems, controls, instrumentation, intercoolers, after-coolers, pulsation suppression devices, and other auxiliary equipment.

API Std 619, Rotary-Type Positive Displacement Compressors for Petroleum, Chemical, and Gas Industry Services, 3rd Edition, June 1997

The dry helical lobe rotary compressors nonlubricated cylinder types of compressors are used for injecting of the fuel in gas turbines at the high pressure needed. The gas turbine application requires that the compressor be dry. This standard is primarily intended for compressors that are in special purpose application and covers the minimum requirements for dry helical lobe rotary compressors used for vacuum, pressure, or both in petroleum, chemical, and gas industry services. This edition also includes a new inspector's checklist and new schematics for general purpose and typical oil systems.

API Std 613 Special Purpose Gear Units for Petroleum, Chemical, and Gas Industry Services, 4th Edition, June 1995

Gears, wherever used, can be a major source of problem and downtime. This standard specifies the minimum requirements for special-purpose, enclosed, precision, single- and double-helical one- and two-stage speed increasers and reducers of parallel-shaft design for refinery services. Primarily intended for gears that are in continuous service without installed spare equipment. These standards apply for gears used in the power industry.

API Std 677, General-Purpose Gear Units for Petroleum, Chemical, and Gas Industry Services, 2nd Edition, July 1997 (Reaffirmed March 2000)

This standard covers the minimum requirements for general-purpose, enclosed single- and multi-stage gear units incorporating parallel-shaft

helical and right angle spiral bevel gears for the petroleum, chemical, and gas industries. Gears manufactured according to this standard are limited to the following pitchline velocities: helical gears shall not exceed 12,000 feet per minute 60 meters per second (60 meters per second) and spiral bevel gears shall not exceed 8,000 feet per minute 40 meters per second (40 meters per second). This standard includes related lubricating systems, instrumentation, and other auxiliary equipment. Also included in this edition is new material related to gear inspection.

API Std 614, Lubrication, Shaft-Sealing, and Control-Oil Systems and Auxiliaries for Petroleum, Chemical, and Gas Industry Services, 4th Edition, April 1999

Lubrication, besides providing lubrication, also provides cooling for various components of the turbine. This standard covers the minimum requirements for lubrication systems, oil-type shaft-sealing systems, and control-oil systems for special-purpose applications. Such systems may serve compressors, gears, pumps, and drivers. The standard includes the systems' components, along with the required controls and instrumentation. Data sheets and typical schematics of both system components and complete systems are also provided. Chapters include general requirements, special purpose oil systems, general purpose oil systems and dry gas seal module systems. This standard is well written and the tips detailed are good practices for all types of systems.

API Std 671, Special Purpose Couplings for Petroleum Chemical and Gas Industry Services, 3rd Edition, October 1998

This standard covers the minimum requirements for special purpose couplings intended to transmit power between the rotating shafts of two pieces of refinery equipment. These couplings are designed to accommodate parallel offset, angular misalignment, and axial displacement of the shafts without imposing excessive mechanical loading on the coupled equipment.

ANSI/API Std 670 Vibration, Axial-Position, and Bearing-Temperature Monitoring Systems, 3rd Edition, November 1993

Provides a purchase specification to facilitate the manufacture, procurement, installation, and testing of vibration, axial position, and bearing temperature monitoring systems for petroleum, chemical, and gas industry services. Covers the minimum requirements for monitoring radial shaft

vibration, casing vibration, shaft axial position, and bearing temperatures. It outlines a standardized monitoring system and covers requirements for hardware (sensors and instruments), installation, testing, and arrangement. Standard 678 has been incorporated into this edition of standard 670. This is well-documented, standard, and widely used in all industries.

Application of the Mechanical Standards to the Gas Turbine

An examination of the above standards as they apply to the gas turbine and its auxiliaries are further examined in this section. The ASME B 133.2 basic gas turbines and the API standard 616, gas turbines for the petroleum, chemical, and gas industry services are intended to cover the minimum specifications necessary to maintain a high degree of reliability in an open-cycle gas turbine for mechanical drive, generator drive, or hot-gas generation. The standard also covers the necessary auxiliary requirements directly or indirectly by referring to other listed standards.

The standards define terms used in the industry and describe the basic design of the unit. It deals with the casing, rotors and shafts, wheels and blades, combustors, seals, bearings, critical speeds, pipe connections and auxiliary piping, mounting plates, weather-proofing, and acoustical treatment.

The specifications call preferably for a two-bearing construction. Two-bearing construction is desirable in single-shaft units, as a three-bearing configuration can cause considerable trouble, especially when the center bearing in the hot zone develops alignment problems. The preferable casing is a horizontally split unit with easy visual access to the compressor and turbine, permitting field balancing planes without removal of the major casing components. The stationary blades should be easily removable without removing the rotor.

A requirement of the standards is that the fundamental natural frequency of the blade should be at least two times the maximum continuous speed, and at least 10% away from the passing frequencies of any stationary parts. Experience has shown that the natural frequency should be at least four times the maximum continuous speed. Care should be exercised on units where there is a great change in the number of blades between stages.

A controversial requirement of the specifications is that rotating blades or labyrinths for shrouded rotating blades be designed for slight rubbing. A slight rubbing of the labyrinths is usually acceptable, but excessive rubbing can lead to major problems. New gas turbines use "squealer blades" some manufacturers suggest using ceramic tips, but whatever is done, great care should be exercised, or blade failure and housing damage may occur.

Labyrinth seals should be used at all external points, and sealing pressures should be kept close to atmospheric. The bearings can be either rolling element bearings usually used in aero-derivative gas turbines and hydrodynamic bearings used in the heavier frame type gas turbines. In the area of hydrodynamics bearings, tilting pad bearings are recommended, since they are less susceptible to oil whirl and can better handle misalignment problems.

Critical speeds of a turbine operating below its first critical should be at least 20% above the operating speed range. The term commonly used for units operating below their first critical is that the unit has a “stiff shaft,” while units operating above their first critical are said to have a “flexible shaft.” There are many exciting frequencies that need to be considered in a turbine. Some of the sources that provide excitation in a turbine system are:

1. Rotor unbalance
2. Whirling mechanisms such as:
 - a. Oil whirl
 - b. Coulomb whirl
 - c. Aerodynamic cross coupling whirl
 - d. Hydrodynamic whirl
 - e. Hysteretic whirl
3. Blade and vane passing frequencies
4. Gear mesh frequencies
5. Misalignment
6. Flow separation in boundary layer exciting blades
7. Ball/race frequencies in antifriction bearings usually used in aero-derivative gas turbines

Torsional criticals should be at least 10% away from the first or second harmonics of the rotating frequency. Torsional excitations can be excited by some of the following:

1. Start up conditions such as speed detents
2. Gear problems such as unbalance and pitch line runout
3. Fuel pulsation especially in low NO_x combustors

The maximum unbalance is not to exceed 2.0 mils (0.051 mm) on rotors with speeds below 4000 rpm, 1.5 mils (0.04 mm) for speeds between 4000–8000 rpm, 1.0 mil (0.0254 mm) for speeds between 8000–12,000 rpm, and 0.5 mils (0.0127 mm) for speeds above 12,000 rpm. These requirements are to

be met in any plane and also include shaft runout. The following relationship is specified by the API standard:

$$L_v = \sqrt{\frac{12000}{N}} \quad (4-1)$$

where:

L_v = Vibration Limit mils (thousandth of an inch), or mm (mils \times 25.4)

N = Operating speed (RPM)

The maximum unbalance per plane (journal) shall be given by the following relationships:

$$U_{\max} = 4W/N \quad (4-2)$$

where:

U_{\max} = Residual unbalance ounce-inches (gram-millimeters)

W = Journal static weight Lbs (kg)

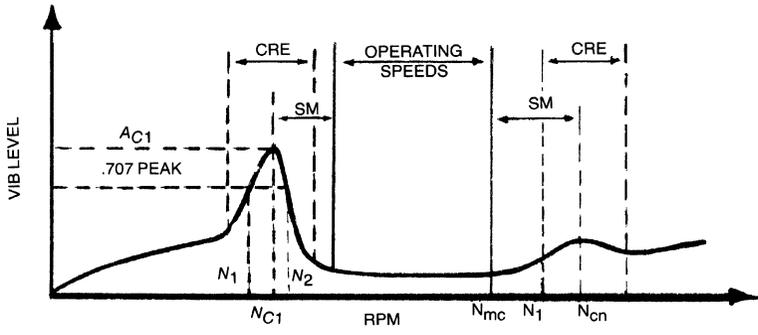
A computation of the force on the bearings should be calculated to determine whether or not the maximum unbalance is an excessive force.

The concept of an Amplification Factor (AF) is introduced in the new API 616 standard. Amplification factor is defined as the ratio of the critical speed to the speed change at the root mean square of the critical amplitudes.

$$AF = \frac{N_{c1}}{(N_2 - N_1)} \quad (4-3)$$

Figure 4-6 is an amplitude-speed curve showing the location of the running speed to the critical speed, and the amplitude increase near the critical speed. When the rotor amplification factor, as measured at the vibration probe, is greater than or equal to 2.5, that frequency is called critical and the corresponding shaft rotational frequency is called a critical speed. For the purposes of this standard, a critically damped system is one in which the amplification factor is less than 2.5.

Balancing requirement in the specifications require that the rotor with blades assembled must be dynamically balanced without the coupling, but



- | | |
|---|------------------------------------|
| N_{C1} = Rotor 1st critical, center frequency, cycles per minute | AF = Amplification Factor |
| N_{cn} = Critical speed, nth | $= \frac{N_{C1}}{N_2 - N_1}$ |
| N_t = Trip speed | SM = Separation Margin |
| N_{mc} = Maximum continuous speed, 105 percent | CRE = Critical Response Envelope |
| N_1 = Initial (lesser) speed at $.707 \times$ peak amplitude (critical) | N_{c1} = Amplitude @ N_{c1} |
| N_2 = Final (greater) speed at $.707 \times$ peak amplitude (critical) | A_{cn} = Amplitude @ N_{cn} |
| $N_2 - N_1$ = Peak width at the "half-power" point | |

Figure 4-6. Rotor response plot.

with the half key, if any, in place. The specifications do not discuss whether this balancing is to be done at high-speeds or low-speeds. The balancing conducted in most shops is at low-speed. A high-speed balancing should be used on problem shafts, and any units, which operate above the second critical. Field balancing requirements should be specified.

The lubrication system for the turbine is designed to provide both lubrication and cooling. It is not unusual that in the case of many gas turbines the maximum temperatures reached in the bearing section is about 10–15 minutes after the unit has been shutdown. This means that the lubrication system should continue to operate for a minimum of 20 minutes after the turbine has been shutdown. This system closely follows the outline in API Standard 614, which is discussed in detail in Chapter 15. Separate lubrication systems for various sections of the turbine and driven equipment may be supplied. Many vendors and some manufacturers provide two separate lubrication systems: One for hot bearings in the gas turbines and another for the cool bearings of the driven compressor. These and other lubrication systems should be detailed in the specifications.

The inlet and exhaust systems in gas turbines are described. The inlet and exhaust systems consist of an inlet filter, silencers, ducting, and expansion joints. The design of these systems can be critical to the overall design of a gas turbine. Proper filtration is a must, otherwise problems of blade contamination and erosion ensue. The standards are minimal for specifications,

calling for a coarse metal screen to prevent debris from entering, a rain or snow shield for protection from the elements, and a differential pressure alarm. Most manufacturers are now suggesting so-called high-efficiency filters that have two stages of filtration, an inertia stage to remove particles above five microns followed by one or more filter screens, self cleaning filters, pad type pre-filters, or a combination of them, to remove particles below five microns. Differential pressure alarms are provided by manufacturers, but the trend among users has been to ignore them. It is suggested that more attention be paid to differential pressure, than in the past, to assure high-efficiency operation.

Silencers are also minimally specified. Work in this area has progressed dramatically in the past few years with the NASA quiet engine program. There are some good silencers now available on the market, and inlets can be acoustically treated.

Starting equipment will vary, depending on the location of the unit. Starting drives include electric motors, steam turbines, diesel engines, expansion turbines, and hydraulic motors. The sizing of a starting unit will depend on whether the unit is a single-shaft turbine or a multiple-shaft turbine with a free-power turbine. The vendor is required to produce speed-torque curves of the turbine and driven equipment with the starting unit torque superimposed. In a free-power turbine design, the starting unit has to overcome only the torque to start the gas generator system. In a single-shaft turbine, the starting unit has to overcome the total torque. Turning gears are recommended in the specifications, especially on large units to avoid shaft bowing. They should always be turned on after the unit has been "brought down" and should be kept operational until the rotor is cooled.

The gears should meet API Standard 613. Gear units should be double-helical gears provided with thrust bearings. Load gears should be provided with a shaft extension to permit torsional vibration measurements. On high-speed gears, proper use of the lubricant as a coolant should be provided. Spraying oil as a coolant on the teeth and face of the units is recommended to prevent distortion. Chapter 14 details the design and operation characteristics of gears.

Couplings should be designed to take the necessary casing and shaft expansion. Expansion is one reason for the wide acceptance of the dry flexible coupling. A flexible diaphragm coupling is more forgiving in angular alignment; however, a gear-type coupling is better for axial movement access for hot alignment checks must be provided. The couplings should be dynamically balanced independently of the rotor system. Chapter 18 deals with the various types of couplings and the alignment techniques for gas turbines.

Controls, instrumentation, and electrical systems in a gas turbine are defined. The outline in the standard is the minimum a user needs for safe

operation of a unit. More details of the instrumentation and controls are given in Chapter 19.

The starting system can be manual, semiautomatic, or automatic, but in all cases should provide controlled acceleration to minimum governor speed and then, although not called for in the standards, to full speed. Units that do not have controlled acceleration to full speed have burned out first- and second-stage nozzles when combustion occurred in those areas instead of in the combustor. Purging the system of the fuel after a failed start is mandatory, even in the manual operation mode. Sufficient time for the purging of the system should be provided so that the volume of the entire exhaust system has been displaced at least five times.

Alarms should be provided on a gas turbine. The standards call for alarms to be provided to indicate malfunction of oil and fuel pressure, high exhaust temperature, high differential pressure across the air filter, excessive vibration levels, low oil reservoir levels, high differential pressure across oil filters, and high oil drain temperatures from the gearings. Shutdown occurs with low oil pressure, high exhaust temperature, and combustor flameout. It is recommended that shutdown also occur with high thrust bearing temperatures and with a temperature differential in the exhaust temperature. Vibration detectors suggested in the standards are noncontacting probes. Presently, most manufacturers provide velocity transducers mounted on the casing, but these are inadequate. A combination of noncontacting probes and accelerometers are needed to ensure the smooth operation and diagnostic capabilities of the unit.

Fuel systems can cause many problems, and fuel nozzles are especially susceptible to trouble. A gaseous fuel system consists of fuel filters, regulators, and gauges. Fuel is injected at a pressure of about 60 psi (4 Bar) above the compressor discharge pressure for which a gas compression system is needed. Knockout drums or centrifuges are recommended, and should be implemented to ensure no liquid carry-overs in the gaseous system.

Liquid fuels require atomization and treatment to inhibit sodium and vanadium content. Liquid fuels can drastically reduce the life of a unit if not properly treated. A typical fuel system is shown in Figure 4-7. The effect of fuels on gas turbines and the details of types of fuel handling systems is given in Chapter 12.

Recommended materials are outlined in the standards. Some of the recommendations in the standard are carbon steel for base plates, heat-treated forged steel for compressor wheels, heat-treated forged alloy steel for turbine wheels, and forged steel for couplings. The growth of materials technology has been so rapid especially in the area of high temperature materials the standard does not deal with it. Details of some of the materials

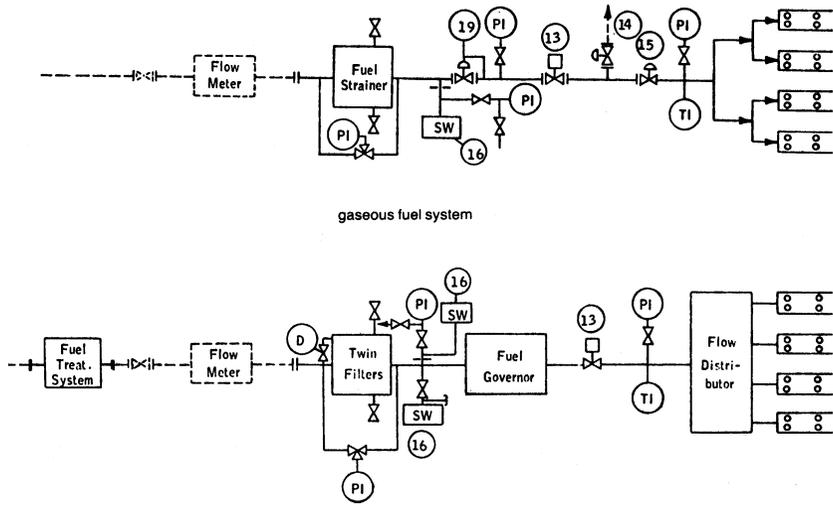


Figure 4-7. Fuel systems for gas turbines.

technology of the high temperature alloys and single crystal blades are dealt with in Chapters 9 and 11. However, the standards call for blading, which must have at least 8,000 trouble-free operating hours in similar operating conditions.

The vendor is required to present Campbell and Goodman diagrams for the blading backed by demonstrated experience in the application of identical blades operating with the same source or frequency of excitation that is present in the unit. The vendor shall indicate on the Goodman diagrams the standard acceptance margins. Chapter 11 deals with the Goodman diagram for materials. All Campbell diagrams shall show the blade frequencies that have been corrected to reflect actual operating conditions. Where applicable, the diagrams for shrouded blades shall show frequencies above and below the blade lock-up speed and shall specify the speed at which blade lock-up occurs. Chapter 5 goes into details of the Campbell diagram, and Chapter 16 deals with the types of signals emitted by the resonance of blades.

The tips of rotating blades and the labyrinths of shrouded rotating blades shall be designed to allow the unit to start up at any time in accordance with the vendor's requirements. When the design permits rubbing during normal start up, the component shall be designed to be rub tolerant and the vendor shall state in his proposal if rubbing is expected.

The blade natural frequencies shall not coincide with any source of excitation from 10% below minimum governed speed to 10% above

maximum continuous speed. If this is not feasible, blade stress levels developed at any specified driven equipment operation shall be low enough to allow unrestricted operation for the minimum service life. Blades shall be designed to withstand operation at resonant frequencies during normal warm-up. Speeds below the operation range corresponding to such blade resonance should be clearly specified.

Excitation sources, which should be included in the Campbell diagrams, should include fundamental and first harmonic passing frequencies of rotating and stationary blades upstream and downstream of each blade row, gas passage splitters, irregularities in vane and nozzle pitch at horizontal casing flanges, the first 10 rotor speed harmonics, meshing frequencies in gear units, and periodic impulses caused by the combustor arrangement.

The turbine undergoes three basic tests, these are hydrostatic, mechanical, and performance. Hydrostatic tests are to be conducted on pressure-containing parts with water at least one-and-a-half times the maximum operating pressure. The mechanical run tests are to be conducted for at least a period of four hours at maximum continuous speed. This test is usually done at no-load conditions. It checks out the bearing performance and vibration levels as well as overall mechanical operability. It is suggested that the user have a representative at this test to tape record as much of the data as possible. The data are helpful in further evaluation of the unit or can be used as base-line data. Performance tests should be conducted at maximum power with normal fuel composition. The tests should be conducted in accordance with ASME PTC-22, which is described in more detail in Chapter 20.

Gears

This standard API Standard 613 covers special purpose gears. They are defined as gears, which have either or both actual pinion speeds of more than 2900 rpm and pitchline velocities of more than 5000 ft/min (27 meters/sec). The standard applies to helical gears employed in speed-reducer or speed-increaser units.

The scope and terms used are well defined and includes a listing of standards and codes for reference. The purchaser is required to make decisions regarding gear-rated horsepower and rated input and output speeds.

This standard includes basic design information and is related to AGMA Standard 421. Specifications for cooling water systems are given as well as information about shaft assembly designation and shaft rotation. Gear-rated power is the maximum power capability of the driver. Normally, the horsepower rating for gear units between a driver and a driven unit would be

110% of the maximum power required by the driven unit or 110% of the maximum power of the driver, whichever is greater.

The tooth pitting index or K factor is defined as

$$K = \frac{W_t}{F \times d} \times \frac{(R + 1)}{R} \quad (4-4)$$

where:

W_t = transmitted tangential load, in pounds at the operating pitch diameter

$$W_t = \frac{12,600 \times \text{Gear rated horse power}}{\text{Pinion rpm} \times d}$$

F = net face width, inches

d = pinion pitch diameter, inches

R = ratio (number teeth in gear divided by number teeth in pinion)

The allowable K factor is given by

$$\text{Allowable } K = \text{Material index number} / \text{Service factor} \quad (4-5)$$

Service factors and material index number tabulation are provided for various typical applications, allowing the determination of the K factor. Gear tooth size and geometry are selected so that bending stresses do not exceed certain limits. The bending stress number is given by

$$\begin{aligned} S_t &= \text{Bending stress number} \\ &= \left(\frac{W_t \times P_{nd}}{F} \right) \times (SF) \times \left(\frac{1.8 \cos \psi}{J} \right) \end{aligned} \quad (4-6)$$

where:

W_t = as defined in Equation (4-4)

P_{nd} = normal diametral pitch

F = net face width, inches

ψ = helix angle

J = geometry factor (from AGMA 226)

SF = service factor

Design parameters on casings, joint supports, and bolting methods. Some service and size criteria are included.

Critical speeds correspond to the natural frequencies of the gears and the rotor bearings support system. A determination of the critical speed is made by knowing the natural frequency of the system and the forcing function. Typical forcing functions are caused by rotor unbalance, oil filters, misalignment, and a synchronous whirl.

Gear elements must be multiplane and dynamically balanced. Where keys are used in couplings, half keys must be in place. The maximum allowable unbalanced force at maximum continuous speed should not exceed 10% of static weight load on the journal. The maximum allowable residual unbalance in the plane of each journal is calculated using the following relationship

$$F = mr\omega^2 \quad (4-7)$$

Since the force must not exceed 10% of the static journal load,

$$mr = \frac{0.1 W}{\bar{\omega}^2} \quad (4-8)$$

Taking the correction constants, the equation can be written

$$\text{Max. unbalanced force} = \frac{56,347 \times \text{Journal static weightload}}{(\text{rpm})^2} \quad (4-9)$$

The double amplitude of unfiltered vibration in any plane measured on the shaft adjacent to each radial bearing is not to exceed 2.0 mils (0.05 mm) or the value given by

$$\text{Amplitude} = \sqrt{\frac{12,000}{\text{rpm}}} \quad (4-10)$$

where rpm is the maximum continuous speed. It is more meaningful for gears to be instrumented using accelerometers. Design specifications for bearings, seals, and lubrication are also given.

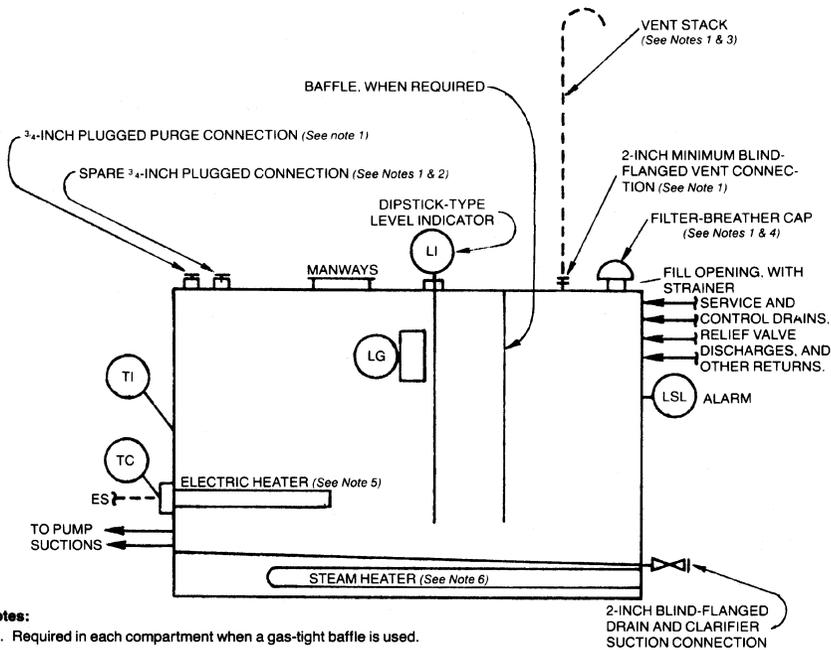
Accessories such as couplings, coupling guards, mounting plates, piping, instrumentation, and controls are described. Inspection and testing procedures are detailed. The purchaser is allowed to inspect the equipment during manufacture after notifying the vendor. All welds in rotating parts must receive 100% inspection. To conduct a mechanical run test, the unit must be operated at maximum continuous speed until bearing and lube oil

temperatures have stabilized. Then the speed is increased to 110% of maximum continuous speed and run for four hours.

Lubrication Systems

This API Standard 614 standard covers the minimum requirements for lubrication systems, oil shaft sealing systems, and related control systems for special purpose applications. The terms are fully defined, references are well documented and basic design is described. Details of the lubrication system are presented in Chapter 15.

Lubrication systems should be designed to meet continuously all conditions for a nonstop operation of three years. Typical lubricants should be hydrocarbon oils with approximate viscosities of 150 SUS at 100°F



Notes:

1. Required in each compartment when a gas-tight baffle is used.
2. The purchaser may specify a particular clarifier return in addition to the spare top connection.
3. To be furnished by the purchaser if required.
4. An optional tight cap shall be substituted when specified by the purchaser.
5. The purchaser may specify an electric heater.
6. The purchaser may specify a steam heater.

Figure 4-8. Standard oil reservoir.

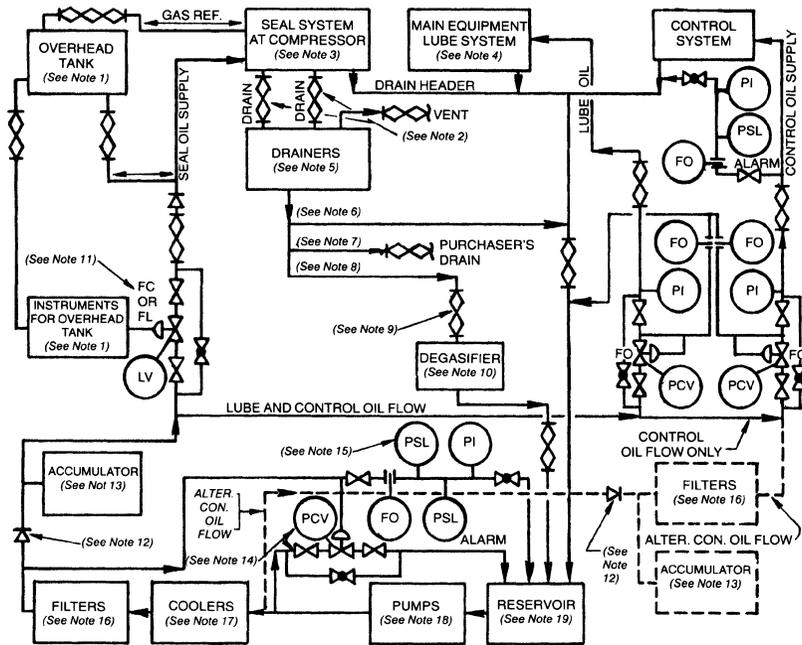
(37.8°C). Oil reservoirs should be sealed to prevent the entrance of dirt and water and sloped at the bottom to facilitate drainage. The reservoir working capacity should be sufficient for at least a five minute flow. A typical reservoir is shown in Figure 4-8. The oil system should include a main oil pump and a standby oil pump. Each pump must have its own driver sized according to API Standard 610. Pump capacities should be based on the systems' maximum usage plus a minimum of 15%. For seal oil systems, the pump capacity should be maximum capacity plus 20% or 10 gpm, whichever is greater. The standby oil pump should have an automatic startup control to maintain safe operation if the main pump fails. Twin oil coolers should be provided, and each should be sized to accommodate the total cooling load. Full-flow twin oil filters should be furnished downstream of the coolers. Filtration should be 10 microns nominal. The pressure drop for clean filters should not exceed 5 psi (0.34 Bar) at 100°F (37.8°C) operating temperature during normal flow.

Overhead tanks, purifiers, and degasing drums are covered. All pipe welding is to be done according to Section IX of the ASME code, and all piping must be seamless carbon steel, minimum schedule 80 for sizes 1½ inches (38.1 mm) and smaller, and a minimum of schedule 40 for pipe sizes 2 inches (50.8 mm) or greater.

The lubrication control system should enable orderly startup, stable operation, warning of abnormal conditions, and shutdown of main equipment in the event of impending damage. A list of required alarm and shutdown devices is provided. Figure 4-9 is a schematic of a seal lube and control oil system. The purchaser has the right to inspect the work and testing of subcomponents if he informs the vendor in advance. Each cooler, filter, accumulator, and other pressure vessels should be hydrostatically tested at one and one-half times design pressure. Cooling water jackets and other water-handling components should be tested at one and one-half times design pressure. The test pressure should not be less than 115 psig (7.9 Bar). Tests should be maintained for durations of at least 30 minutes.

Operational tests should:

1. Detect and correct all leaks.
2. Determine relief pressures and check for proper operation of each relief valve.
3. Accomplish a filter cooler changeover without causing startup of the standby pump.
4. Demonstrate that control valves have suitable capacity, response, and stability.
5. Demonstrate the oil pressure control valve can control oil pressure.



This arrangement is valid only when the pressure of the seal oil supply is higher than the pressure of the control oil supply

Notes:

- | | |
|--|--|
| <ol style="list-style-type: none"> 1. Overhead tank with instrumentation. 2. Connections by vendor when drainers are mounted on compressor baseplate. 3. Seal oil system at compressor only. 4. Lubrication system at main equipment only. 5. Float-controlled inner-seal drainers for transmitter-controlled inner-seal drainers. 6. Drain to reservoir. 7. Drain to purchaser's drains. 8. Drain to degassing drum. 9. Connections by vendor if degasifier is mounted on compressor baseplate. 10. Degassing drum. | <ol style="list-style-type: none"> 11. The purchaser must specify the desired failure action for the LV. 12. Omit check valve if accumulator is not used. 13. Direct-contact-type accumulator or bladder-type accumulator when required. 14. Omit the bypass PCV circuit if centrifugal pumps are used. 15. Switch to start standby pump. 16. Single oil filter or twin oil filters. 17. Single oil cooler or twin oil coolers. 18. Primary pumps. 19. Oil reservoir. |
|--|--|

Figure 4-9. Combined seal, lube, and control oil system.

Vibration Measurements

The API Standard 670 covers the minimum requirements for noncontacting vibration in an axial-position monitoring system.

The accuracy for the vibration channels should meet a linearity of $\pm 5\%$ of 200 millivolts per mil (0.001 inch, 0.0254 mm) sensitivity over a minimum operating range of 80 mils (2.032 mm). For the axial position, the channel linearity must be $\pm 5\%$ of 200 millivolts per mil sensitivity and a ± 1.0 mil of a straight line over a minimum operating range of 80 mils (2.032 mm). Temperature should not affect the linearity of the system by more than 5% over a temperature range of -30 to $+350$ °F (-34.4 to $+176.7$ °C) for the

probe and extension cable. The oscillator demodulator is a signal conditioning device powered by -24 volts of direct current. It sends a radio frequency signal to the probe and demodulates the probe output. It should maintain linearity over the temperature range of -30 to $+150^\circ\text{F}$ (-34.4 to $+65.6^\circ\text{C}$). The monitors and power supply should maintain their linearity over a temperature range of -20 to $+150^\circ\text{F}$ (-28.9 to $+65.6^\circ\text{C}$). The probes, cables, oscillator demodulators, and power supplies installed on a single train should be physically and electrically interchangeable.

The noncontacting vibration and axial position monitoring system, consisting of probe, cables, connectors, oscillator demodulator, power supply, and monitors. The probe tip diameters should be 0.190 – 0.195 inches (4.8 – 4.95 mm) with body diameters of $1/4$ (6.35 mm) -28 UNF $-2A$ threaded, or 0.3 – 0.312 inches (7.62 – 7.92 mm) with a body diameter of $3/8$ (9.52 mm) -24 UNF $-24A$ threaded. The probe length is about 1 inch long. Tests conducted on various manufacturer's probes indicate that the 0.3 – 0.312 -inch (7.62 – 7.92 mm) probe has a better linearity in most cases. The integral probe cables have a cover of tetra-flouroethylene, a flexible stainless steel armoring, which extends to within four inches of the connector. The overall physical length should be approximately 36 inches (914.4 mm) measured from probe tip to the end of the connector. The electrical length of the probe and integral cable should be six feet. The extension cables should be coaxial with electrical and physical lengths of 108 inches (2743.2 mm). The oscillator demodulator will operate with a standard supply voltage of -24 volts dc and will be calibrated for a standard electrical length of 15 feet (5 meters). This length corresponds to the probe integral cable and extension. Monitors should operate from a power supply of 117 volts $\pm 5\%$ with the linearity requirements specified. False shutdown from power interruption will be prevented regardless of mode or duration. Power supply failure should actuate an alarm.

The radial transducers should be placed within three inches of the bearing, and there should be two radial transducers at each bearing. Care should be taken not to place the probe at the nodal points. The two probes should be mounted 90° apart ($\pm 5^\circ$) at a 45° ($\pm 5^\circ$) angle from each side of the vertical center. Viewed from the drive end of the machine train, the x probe will be on the right side of the vertical, and the y probe will be on the left side of the vertical. Figures 4-10 and 4-11 show protection systems for a turbine and a gear box respectively.

The axial transducers should have one probe sensing the shaft itself within 12 inches (305 mm) of the active surface of the thrust collar with the other probe sensing the machined surface of the thrust collar. The probes should be mounted facing in opposite directions. Temperature probes embedded in the bearings are often more useful in preventing thrust-bearing failures than

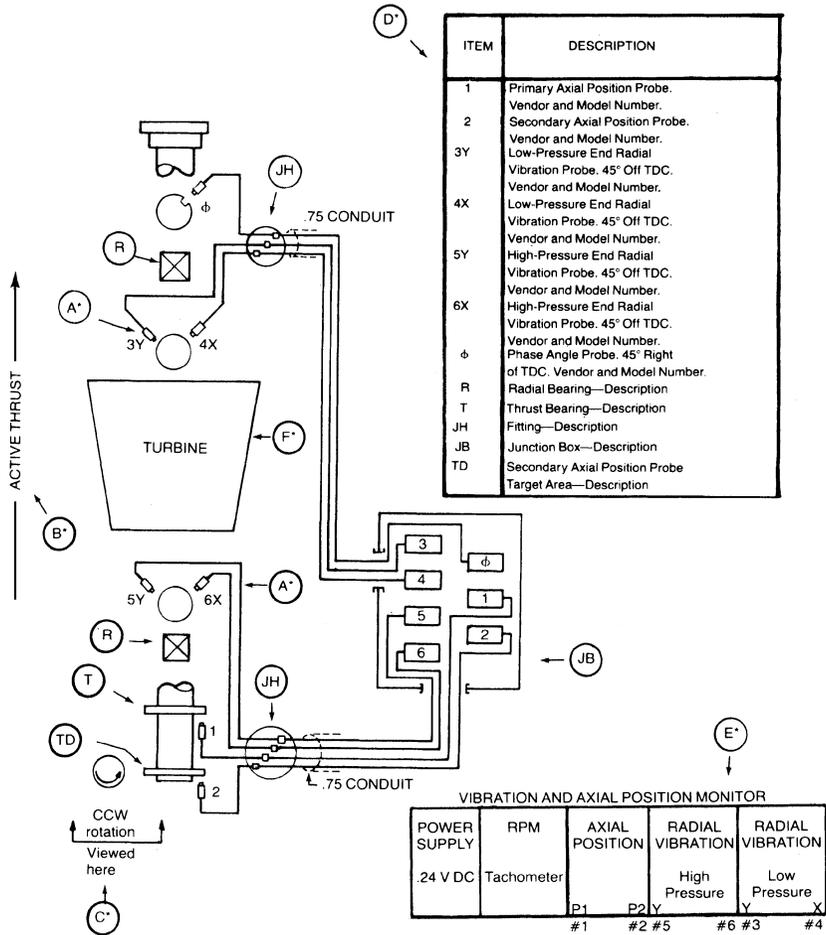


Figure 4-10. Typical protection system for a turbine.

the proximity probe. This is because of the expansion of the shaft casing and the probability that the probe is located far from the thrust collar.

When designing a system for thrust bearing protection, it is necessary to monitor small changes in rotor axial movement equal to oil film thickness. Probe system accuracy and probe mounting must be carefully analyzed to minimize temperature drift. Drift from temperature changes can be unacceptably high.

A functional alternative to the use of proximity probes for bearing protection is bearing temperature, bearing temperature rise (bearing temperature

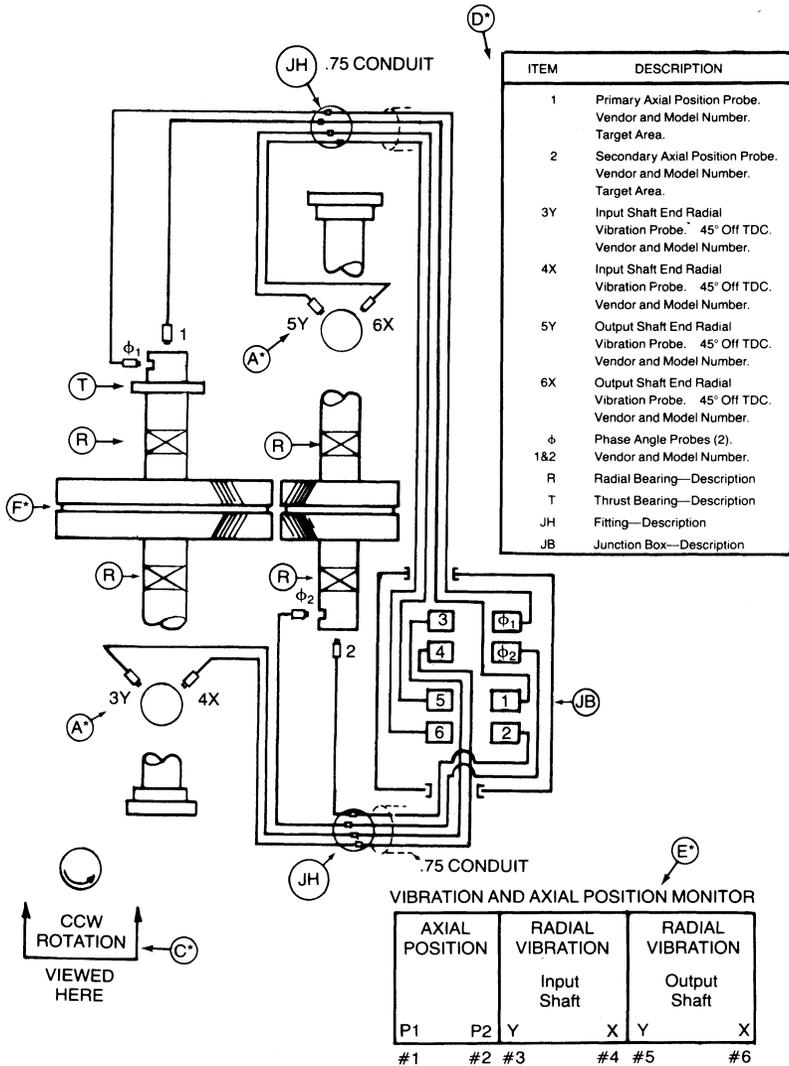


Figure 4-11. Typical protection system for a gearbox.

minus bearing oil temperature), and rate of change in bearing temperature. A matrix combining these functions can produce a positive indication of bearing distress.

A phase angle transducer should also be supplied with each train. This transducer should record one event per revolution. Where intervening

gear-boxes are used, a mark and phase angle transducer should be provided for each different rotational speed.

Specifications

The previous API standards are guidelines to information regarding machine train applications. The more pertinent the information obtained during the evaluation of the proposal, the better the selection for the problem. The following list contains items the user should consider in his attempt to properly evaluate the bid. Some of these points are covered in the API standards.

Table 4-2 indicates the main points an engineer must consider in evaluating different gas turbine units. Table 4-3 lists the important points that must

Table 4-2
Point to Consider in a Gas Turbine

| | |
|-----|---|
| 1. | Type of turbine: |
| | a. Aero-derivative |
| | b. Frame type |
| 2. | Type of fuel |
| 3. | Type of compressor |
| 4. | No. of stages and pressure ratio |
| 5. | Types of blades, blade attachment, and wheel attachment |
| 6. | No. of bearings |
| 7. | Type of bearings |
| 8. | Type of thrust bearings |
| 9. | Critical speed |
| 10. | Torsional criticals |
| 11. | Campbell diagrams |
| 12. | Balance planes |
| 13. | Balance pistons |
| 14. | Type of combustor |
| 15. | Wet and dry combustors |
| 16. | Types of fuel nozzles |
| 17. | Transition pieces |
| 18. | Type of turbine |
| 19. | Power transmission curvic coupling |
| 20. | No. of stages |
| 21. | Free-power turbine |
| 22. | Turbine inlet temperature |
| 23. | Type of fuels |
| 24. | Fuel additives |
| 25. | Types of couplings |
| 26. | Alignment data |

table continued on next page

Table 4-2 continued

-
- 27. Exhaust diffuser
 - 28. Performance map of turbine and compressor
 - 29. Gearing
 - 30. Drawings

Accessories

- 1. Lubrication systems
 - 2. Intercoolers
 - 3. Inlet filtration system
 - 4. Control system
 - 5. Protection system
-

Table 4-3
Vendor Requirements to be Provided by the User for a Compressor Train

-
- 1. *The Gas to Be Handled (Each Stream)*
 Composition by mol%, volume %, or weight %. To what extent does composition vary?
 Corrosive effects. Limits to discharge temperature, which may cause problems with the gas.
 - 2. *Quantity to Be Handled for Each Stage*
 Stage quantity and unit of measurement.
 If by volume, show: a. Whether wet or dry.
 b. Pressure and temperature reference points.
 - 3. *Inlet Conditions for Each Stage*
 Barometer.
 Pressure at compressor flange.
 State whether gauge or absolute.
 Temperature at compressor flange.
 Relative humidity.
 Ratio of specific heats.
 Compressibility.
 - 4. *Discharge Conditions*
 Pressure at compressor flange.
 State whether gauge or absolute.
 Compressibility.
 State temperature reference.
 - 5. *Interstage Conditions*
 Temperature difference between gas out of cooler and water into cooler.
 Is there interstage removal or addition of gas?
 Between what pressures may this be done? Advise permissible range.
 If gas is removed, treated, and returned between stages, advise pressure loss.
 What quantity change is involved?
 If this changes gas composition, a resultant analysis (ratio of specific heats, relative humidity, and compressibility at specific interstage pressure and temperature) must be provided.
 - 6. *Variable Conditions*
 State expected variation in intake conditions—pressure, temperature, relative humidity, MW, etc.
 State expected variation in discharge pressure.
-

table continued on next page

Table 4-3 continued

| | |
|-----|---|
| | <p>It is extremely important that changing conditions be related to each other. If relative humidity varies from 50 to 100% and inlet temperature varies from 0 to 100°F does 100% RH correspond with 100°F? Variations in conditions are best shown in tabular form with all conditions included in each column.</p> |
| 7. | <p><i>Flow Diagram</i> Provide a schematic flow sheet showing controls involved.</p> |
| 8. | <p><i>Regulation</i> What is to be controlled—pressure, flow, or temperature? Advise permissible variation in controlled item. Is regulation manual or automatic? If automatic, are operating devices and/or instruments to be included? How many control steps are desired on a reciprocator?</p> |
| 9. | <p><i>Cooling Water</i> Temperature: maximum and minimum Pressure at inlet and back pressure, if any. Whether open or closed cooling system desired. Source of water. Fresh, salt, or brackish. Silty or corrosive.</p> |
| 10. | <p><i>Driver</i> Specify type of driver. Electric motor: type, current conditions, power factor, enclosure, service factor, temperature rise, ambient temperature. Steam: inlet and exhaust pressure, inlet temperature and quality, importance of minimum water rate. Fuel gas: gas analysis, available pressure, low heating value of gas. Geared: AGMA rating if special.</p> |
| 11. | <p><i>General</i> Acceptability of petroleum lubricants? Indoor or outdoor installation? Floor space, special shape? Provide a sketch. Soil character. List accessories desired and advise which are to be spared. Pulsation dampeners or intake or discharge silencers to be supplied.</p> |
| 12. | <p><i>Specifications</i> Provide each bidder with three copies of any specification for the particular project. Complete information enables all manufacturers to bid competitively on the same basis and assists the purchaser in evaluating bids.</p> |

be supplied to the vendor, while the important points to consider in evaluating centrifugal compressors are listed in Table 4-4. These tables will enable the engineer to make a proper evaluation of each critical point and ensure that he is purchasing units of high reliability and efficiency.

Table 4-4
Points to Consider in a Centrifugal Compressor

-
1. Number of stages
 2. Pressure ratio and mass flow (per casing)
 3. Type of gas seals (inner seal) and oil seals
 4. Type of bearings (radial)
 5. Bearing stiffness coefficients
 6. Types of thrust bearings (Tapered land, nonequalizing tilting pad and Kingsbury)
 7. Thrust float
 8. Temperature for journal and thrust bearings (operating temperature)
 9. Critical speed diagram (Speed versus bearing stiffness curve)
 10. Type of impeller
 - a. Shroud or unshrouded
 - b. Blading
 - c. Attachment of blades to hub and shroud
 11. Attachment of impellers to shaft
 - a. Shrink fit
 - b. Key fit
 - c. Other
 12. Campbell diagrams of impellers
 - a. No. of blades (impellers)
 - b. No. of blades (diffuser)
 - c. No. of blades (guide vanes)
 13. Balance piston
 14. Balance planes (location)
 - a. How is it balanced (detail)
 15. Weight of toros (assembled)
 - a. Split casing
 - b. Barrel
 16. Data on torsional vibration (Bending criticals)
 17. Alignment data
 18. Type of coupling between tandems
 19. Performance curves (separate casings)
 - a. Surge margin
 - b. Surge line
 - c. Aerodynamic speed
 - d. Efficiency
 20. Intercooling type of cooler
 - a. Temperature drop
 - b. Pressure drop
 - c. Efficiency
 21. Horsepower curves
-

Bibliography

- ASME, Performance Test Code on Overall Plant Performance, ASME PTC 46 1996.
- ASME, Performance Test Code on Test Uncertainty: Instruments and Apparatus PTC 19.1, 1988.
- ASME, Performance Test Code on Gas Turbines, ASME PTC 22 1997, American Society of Mechanical Engineers 1997.
- ASME, Performance Test Code on Gas Turbine Heat Recovery Steam Generators, ASME PTC 4.4 1981, American Society of Mechanical Engineers Reaffirmed 1992.
- ASME, Performance Test Code on Steam Turbines, ASME PTC 6 1996.
- ASME, Performance Test Code on Steam Condensing Apparatus, ASME PTC 12.2 1983, American Society of Mechanical Engineers 1983.
- ASME, Performance Test Code on Atmospheric Water Cooling Equipment PTC 23, 1997.
- ASME Gas Turbine Fuels B 133.7M Published: 1985 (Reaffirmed year: 1992).
- ISO, Natural Gas—Calculation of Calorific Value, Density and Relative Density International Organization for Standardization ISO 6976-1983(E).
- Table of Physical Constants of Paraffin Hydrocarbons and Other Components of Natural Gas—Gas Producers Association Standard 2145-94.

Mechanical Specifications

- ANSI/API Std 610 Centrifugal Pumps for Petroleum, Heavy Duty Chemical and Gas Industry Services, 8th Edition, August 1995.
- ANSI/API Std 670 Vibration, Axial-Position, and Bearing-Temperature Monitoring Systems, 3rd Edition, November 1993.
- API Std 611, General Purpose Steam Turbines for Petroleum, Chemical, and Gas Industry Services, 4th Edition, June 1997.
- API Std 613 Special Purpose Gear Units for Petroleum, Chemical, and Gas Industry Services, 4th Edition, June 1995.
- API Std 614, Lubrication, Shaft-Sealing, and Control-Oil Systems and Auxiliaries for Petroleum, Chemical, and Gas Industry Services, 4th Edition, April 1999.
- API Std 616, Gas Turbines for the Petroleum, Chemical, and Gas Industry Services, 4th Edition, August 1998.
- API Std 617, Centrifugal Compressors for Petroleum, Chemical, and Gas Industry Services, 6th Edition, February 1995.
- API Std 618, Reciprocating Compressors for Petroleum, Chemical, and Gas Industry Services, 4th Edition, June 1995.

- API Std 619, Rotary-Type Positive Displacement Compressors for Petroleum, Chemical, and Gas Industry Services, 3rd Edition, June 1997.
- API Publication 534, Heat Recovery Steam Generators, 1st Edition, January 1995.
- API RP 556, Fired Heaters & Steam Generators, 1st Edition, May 1997.
- API Std 671, Special Purpose Couplings for Petroleum Chemical, and Gas Industry Services, 3rd Edition, October 1998.
- API Std 672, Packaged, Integrally Geared Centrifugal Air Compressors for Petroleum, Chemical, and Gas Industry Services, 3rd Edition, September 1996.
- API Std 677, General-Purpose Gear Units for Petroleum, Chemical, and Gas Industry Services, 2nd Edition, July 1997, Reaffirmed March 2000.
- API Std 681, Liquid Ring Vacuum Pumps and Compressors, 1st Edition, February 1996.
- ASME Basic Gas Turbines B 133.2 Published: 1977 (Reaffirmed year: 1997).
- ASME Gas Turbine Control and Protection Systems B133.4 Published: 1978 (Reaffirmed year: 1997).
- ASME Gas Turbine Installation Sound Emissions B133.8 Published: 1977 (Reaffirmed: 1989).
- ASME Measurement of Exhaust Emissions from Stationary Gas Turbine Engines B133.9 Published: 1994.
- ASME Procurement Standard for Gas Turbine Electrical Equipment B133.5 Published: 1978 (Reaffirmed year: 1997).
- ASME Procurement Standard for Gas Turbine Auxiliary Equipment B133.3 Published: 1981 (Reaffirmed year: 1994).
- ISO 10436:1993 Petroleum and Natural Gas Industries—General purpose Steam Turbine for Refinery Service, 1st Edition.

5

Rotor Dynamics

The present trend in rotating equipment is toward increasing design speeds, which increases operational problems from vibration; hence the importance of vibration analysis. A thorough appreciation of vibration analysis will aid in the diagnoses of rotor dynamics problems.

This chapter is devoted to vibration theory fundamentals concerning undamped and damped freely oscillating systems. Application of vibration theory to solving rotor dynamics problems is then discussed. Next, critical speed analysis and balancing techniques are examined. The latter part of the chapter discusses important design criteria for rotating machinery, specifically bearing driver types, and design and selection procedures.

Mathematical Analysis

The study of vibrations was confined to musicians until classical mechanics had advanced sufficiently to allow an analysis of this complex phenomenon. Newtonian mechanics provides an approach which, conceptually, is easy to understand. Lagrangian mechanics provides a more sophisticated approach, but it is intuitively more difficult to conceive. Since this book uses some basic concepts, we will approach the subject using Newtonian mechanics.

Vibration systems fall into two major categories: forced and free. A free system vibrates under forces inherent in the system. This type of system will vibrate at one or more of its natural frequencies, which are properties of the elastic system. Forced vibration is vibration caused by external force being impressed on the system. This type of vibration takes place at the frequency of the exciting force, which is an arbitrary quantity independent of the natural frequencies of the system. When the frequency of the exciting force

and the natural frequency coincide, a resonance condition is reached, and dangerously large amplitudes may result. All vibrating systems are subject to some form of damping due to energy dissipated by friction or other resistances.

The number of independent coordinates, which describe the system motion, are called the degrees of freedom of the system. A single degree of freedom system is one that requires a single independent coordinate to completely describe its vibration configuration. The classical spring mass system shown in Figure 5-1 is a single degree of freedom system.

Systems with two or more degrees of freedom vibrate in a complex manner where frequency and amplitude have no definite relationship. Among the multitudes of unorderly motion, there are some very special types of orderly motion called principal modes of vibration.

During these principal modes of vibration, each point in the system follows a definite pattern of common frequency. A typical system with two or more degrees of vibration is shown in Figure 5-2. This system can be a

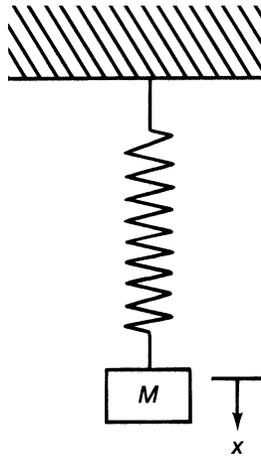


Figure 5-1. System with single degree of freedom.

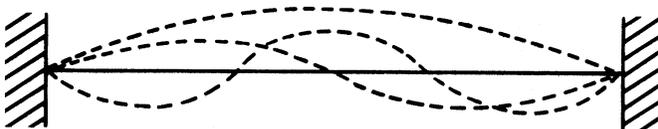


Figure 5-2. System with infinite number of degrees of freedom.

string stretched between two points or a shaft between two supports. The dotted lines in Figure 5-2 show the various principal vibration modes.

Most types of motion due to vibration occur in periodic motion. Periodic motion repeats itself at equal time intervals. A typical periodic motion is shown in Figure 5-3. The simplest form of periodic motion is harmonic motion, which can be represented by sine or cosine functions. It is important to remember that harmonic motion is always periodic; however, periodic motion is not always harmonic. Harmonic motion of a system can be represented by the following relationship:

$$x = A \sin \omega t \quad (5-1)$$

Thus, one can determine the velocity and acceleration of that system by differentiating the equation with respect to t

$$\text{Velocity} = \frac{dx}{dt} = A\omega \cos \omega t = A\omega \sin\left(\omega t + \frac{\pi}{2}\right) \quad (5-2)$$

$$\text{Acceleration} = \frac{d^2x}{dt^2} = -A\omega^2 \sin \omega t = A\omega^2 \sin(\omega t + \pi) \quad (5-3)$$

The previous equations indicate that the velocity and acceleration are also harmonic and can be represented by vectors, which are 90° and 180° ahead of the displacement vectors. Figure 5-4 shows the various harmonic motions of displacement, velocity, and acceleration. The angles between the vectors are called phase angles; therefore, one can say that the velocity leads displacement

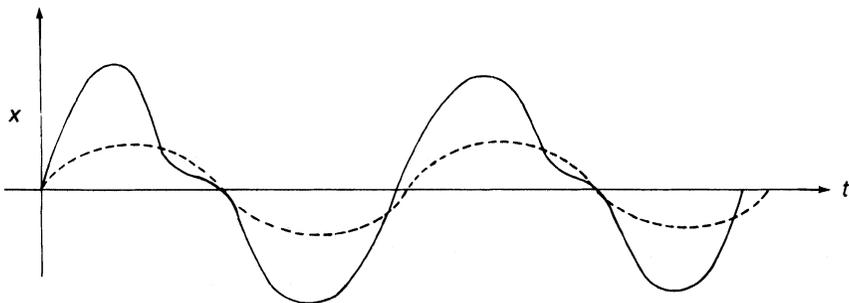


Figure 5-3. Periodic motion with harmonic components.

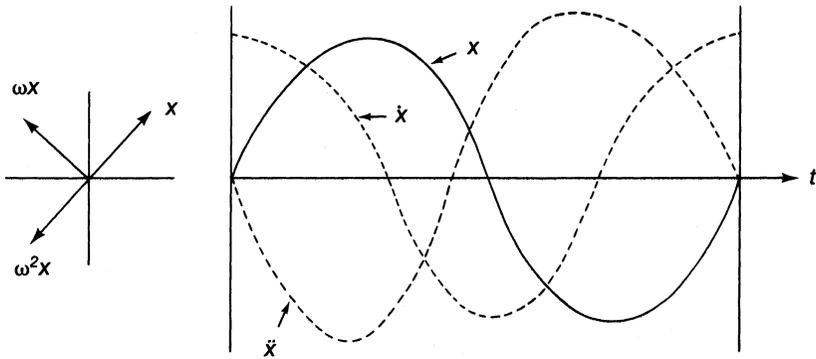


Figure 5-4. Harmonic motion of displacement, velocity, and acceleration.

by 90° , and that the acceleration acts in a direction opposite to displacement, or that it leads displacement by 180° .

Undamped Free System

This system is the simplest of all vibration systems and consists of a mass suspended on a spring of negligible mass. Figure 5-5 shows this simple, single

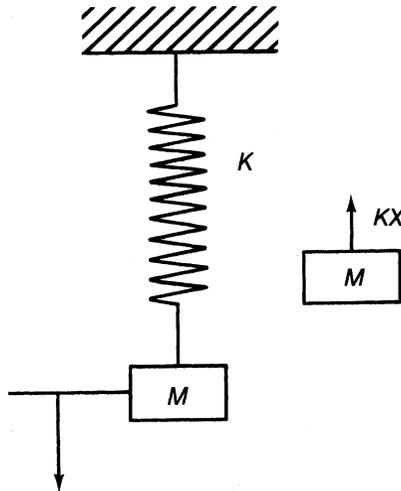


Figure 5-5. Single degree of freedom system (spring mass system).

degree of freedom system. If the mass is displaced from its original equilibrium position and released, the unbalanced force, the restoring ($-Kx$) of the spring, and acceleration are related through Newton's second law. The resulting equation can be written as follows:

$$m\ddot{x} = -Kx \quad (5-4)$$

This equation is called the motion equation for the system, and it can be rewritten as follows:

$$\ddot{x} + \frac{K}{m}x = 0 \quad (5-5)$$

Assuming that a harmonic function will satisfy the equation, let the solution be in the form

$$x = C_1 \sin \omega t + C_2 \cos \omega t \quad (5-6)$$

Substituting Equation (5-6) into Equation (5-5), the following relationship is obtained:

$$\left(-\omega^2 + \frac{K}{M}\right)x = 0$$

which can be satisfied for any value of x if

$$\omega = \sqrt{\frac{K}{M}} \quad (5-7)$$

Thus, the system has a single natural frequency given by the relationship in Equation (5-7).

Damped System

Damping is the dissipation of energy. There are several types of damping—viscous damping, friction or coulomb damping, and solid damping. Viscous damping is encountered by bodies moving through a fluid. Friction damping usually arises from sliding on dry surfaces. Solid damping, often called structural damping, is due to internal friction within the material itself. An example of a free vibrating system with viscous damping is given here.

As shown in Figure 5-6, viscous damping force is proportional to velocity and is expressed by the following relationship:

$$F_{\text{damp}} = -c\dot{x}$$

where c is the coefficient of viscous damping.

The Newtonian approach gives the equation of motion as follows:

$$m\ddot{x} = -kx - c\dot{x} \tag{5-8}$$

or it can be written as

$$m\ddot{x} + c\dot{x} + kx = 0$$

The solution to this equation is found by using the trial solution

$$x = c(e^{rt}) \tag{5-9}$$

which when substituted in Equation (5-8) yields the following characteristic equation:

$$\left(r^2 + \frac{c}{m}r + \frac{k}{m}\right)e^{rt} = 0 \tag{5-10}$$

This equation is satisfied for all values of t when

$$r_{1,2} = \frac{-c}{2m} \pm \sqrt{\frac{c^2}{4m^2} - \frac{k}{m}} \tag{5-11}$$

from which the general solution is obtained as follows:

$$x = e^{\frac{-c}{2m}t} \left[C_1 e^{\sqrt{\frac{c^2}{4m^2} - \frac{k}{m}}(t)} + C_2 e^{-\sqrt{\frac{c^2}{4m^2} - \frac{k}{m}}(t)} \right] \tag{5-12}$$

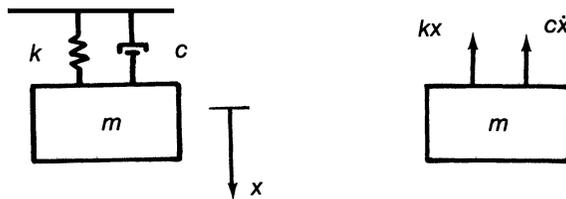


Figure 5-6. Free vibration with viscous damping.

The nature of the solution given by Equation (5-19) depends upon the nature of the roots, r_1 and r_2 . The behavior of this damped system depends upon whether the root is real, imaginary, or zero. The critical damping coefficient c_c can now be defined as that which makes the radical zero. Thus,

$$\frac{c^2}{4m^2} = \frac{k}{m}$$

which can be written as

$$\frac{c}{2m} = \sqrt{\frac{k}{m}} = \omega_n \quad (5-13)$$

One can therefore specify the amount of damping in any system by the damping factor

$$\zeta = \frac{c}{c_c} \quad (5-14)$$

Overdamped system. If $c^2/4m^2 > k/m$, then the expression under the radical sign is positive and the roots are real. If the motion is plotted as a function of time, the curve in Figure 5-7 is obtained. This type of nonvibratory motion is referred to as aperiodic motion.

Critically damped system. If $c^2/4m^2 = k/m$, then the expression under the radical sign is zero, and the roots r_1 and r_2 are equal. When the radical is zero and the roots are equal, the displacement decays the fastest from its initial value as seen in Figure 5-8. The motion in this case also is aperiodic.

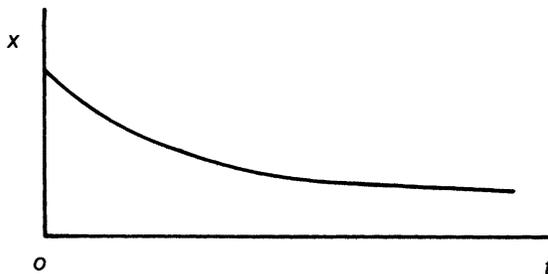


Figure 5-7. Overdamped decay.

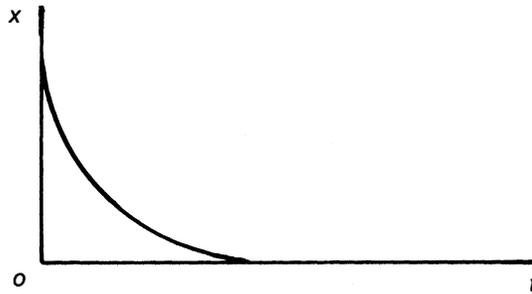


Figure 5-8. Critical damping decay.

This very special case is known as critical damping. The value of c for this case is given by:

$$\frac{c_{cr}^2}{4m^2} = \frac{k}{m}$$

$$c_{cr}^2 = 4m^2 \frac{k}{m} = 4mk$$

Thus,

$$c_{cr} = \sqrt{4mk} = 2m\sqrt{\frac{k}{m}} = 2m\omega_n$$

Underdamped system. If $c^2/4m^2 < k/m$, then the roots r_1 and r_2 are imaginary, and the solution is an oscillating motion as shown in Figure 5-9. All the previous cases of motion are characteristic of different oscillating systems, although a specific case will depend upon the application. The underdamped system exhibits its own natural frequency of vibration. When $c^2/4m^2 < k/m$, the roots r_1 and r_2 are imaginary and are given by

$$r_{1,2} = \pm i\sqrt{\frac{k}{m} - \frac{c^2}{4m^2}} \quad (5-15)$$

Then the response becomes

$$x = e^{-(c/2m)t} \left[C_1 e^{i\sqrt{\frac{k}{m} - \frac{c^2}{4m^2}}t} + C_2 e^{-i\sqrt{\frac{k}{m} - \frac{c^2}{4m^2}}t} \right]$$

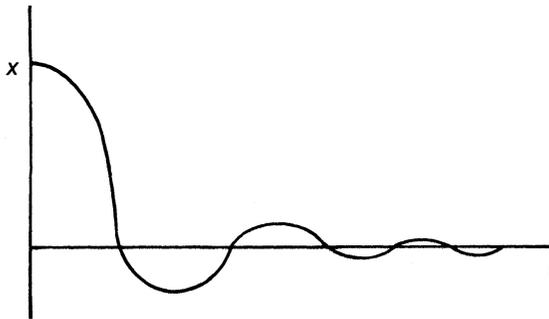


Figure 5-9. Underdamped decay.

which can be written as follows:

$$x = e^{-(c/2m)t} [A \cos \omega_d t + B \sin \omega_d t] \quad (5-16)$$

Forced Vibrations

So far, the study of vibrating systems has been limited to free vibrations where there is no external input into the system. A free vibration system vibrates at its natural resonant frequency until the vibration dies down due to energy dissipation in the damping.

Now the influence of external excitation will be considered. In practice, dynamic systems are excited by external forces, which are themselves periodic in nature. Consider the system shown in Figure 5-10.

The externally applied periodic force has a frequency ω , which can vary independently of the system parameters. The motion equation for this system may be obtained by any of the previously stated methods. The Newtonian approach will be used here because of its conceptual simplicity. The freebody diagram of the mass m is shown in Figure 5-11.

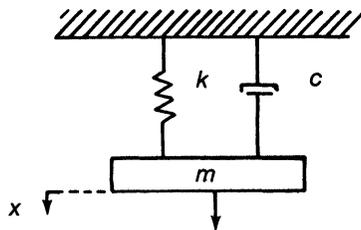


Figure 5-10. Forced vibration system.

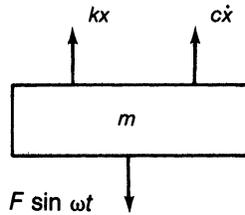


Figure 5-11. Free body diagram of mass (M).

The motion equation for the mass m is given by:

$$m\ddot{x} = F \sin \omega t - kx - c\dot{x} \quad (5-17)$$

and can be rewritten as

$$m\ddot{x} + c\dot{x} + kx = F \sin \omega t$$

Assuming that the steady-state oscillation of this system is represented by the following relationship:

$$x = D \sin (\omega t - \theta) \quad (5-18)$$

where:

D = amplitude of the steady-state oscillation

θ = phase angle by which the motion lags the impressed force

The velocity and acceleration for the system are given by the following relationships:

$$v = \dot{x} = D\omega \cos (\omega t - \theta) = D\omega \sin \left(\omega t - \theta + \frac{\pi}{2} \right) \quad (5-19)$$

$$a = \ddot{x} = D\omega^2 \sin (\omega t - \theta) = D\omega^2 \sin \left(\omega t - \theta + \frac{\pi}{2} \right) \quad (5-20)$$

Substituting the previous relationships into motion equation (5-17), the following relationship is obtained:

$$mD\omega^2 \sin (\omega t - \theta) - cD\omega \sin \left(\omega t - \theta + \frac{\pi}{2} \right) - D \sin (\omega t - \theta) + F \sin \omega t = 0 \quad (5-21)$$

Inertia force + Damping force + Spring force + Impressed force = 0

From the previous equation, the displacement lags the impressed force by the phase angle θ , and the spring force acts opposite in direction to

displacement. The damping force lags the displacement by 90° and is therefore in the opposite direction to the velocity. The inertia force is in phase with the displacement and acts in the opposite direction to the acceleration. This information is in agreement with the physical interpretation of harmonic motion. The vector diagram as seen in Figure 5-12 shows the various forces acting on the body, which is undergoing a forced vibration with viscous damping. Thus, from the vector diagram, it is possible to obtain the value of the phase angle and the amplitude of steady oscillation

$$D = \frac{F}{\sqrt{(k - m\omega^2)^2 + c\omega^2}} \quad (5-22)$$

$$\tan \theta = \frac{c\omega}{k - m\omega^2} \quad (5-23)$$

The nondimensional form of D and θ can be written as

$$D = \frac{F/k}{\sqrt{\left(1 - \frac{\omega^2}{\omega_n^2}\right)^2 + \left(2\zeta \frac{\omega}{\omega_n}\right)^2}} \quad (5-24)$$

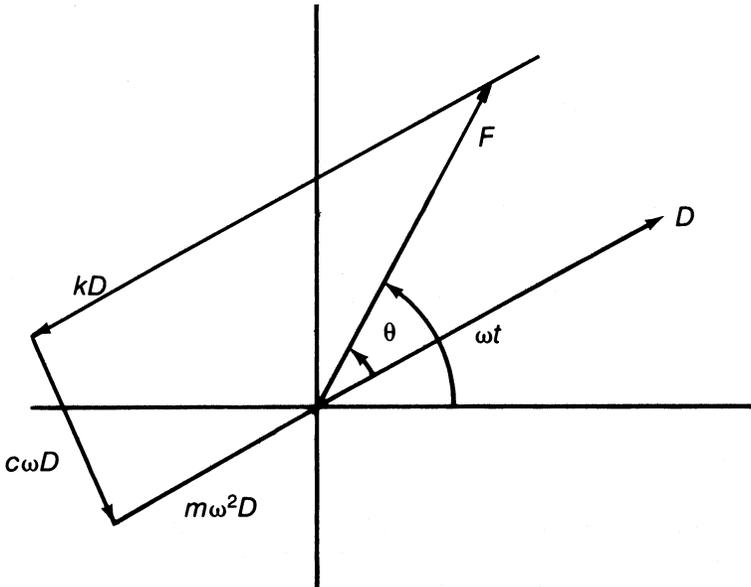


Figure 5-12. Vector diagram of forced vibration with viscous damping.

$$\tan \theta = \frac{2\zeta \frac{\omega}{\omega_n}}{1 - \left(\frac{\omega}{\omega_n}\right)^2} \quad (5-25)$$

where:

$$\omega_n = \sqrt{k/m} = \text{natural frequency}$$

$$\zeta = \frac{c}{c_c} = \text{damping factor}$$

$$c_c = 2 m\omega_n = \text{critical damping coefficient.}$$

From these equations, the effect on the magnification factor ($D/F/k$) and the phase angle (θ) is mainly a function of the frequency ratio ω/ω_n and the damping factor ζ . Figures 5-13a and 5-13b show these relationships. The damping factor has great influence on the amplitude and phase angle in the region of resonance. For small values of $\omega/\omega_n \ll 1.0$, the inertia and damping force terms are small and result in a small phase angle. For a value of $\omega/\omega_n = 1.0$, the phase angle is 90° . The amplitude at resonance approaches infinity as the damping factor approaches zero. The phase angle undergoes nearly a 180° shift for light damping as it passes through the critical frequency ratio. For large values of $\omega/\omega_n \gg 1.0$, the phase angle approaches 180° , and the impressed force is expended mostly in overcoming the large inertia force.

Design Considerations

Design of rotating equipment for high-speed operation requires careful analysis. The discussion in the preceding section presents elementary analysis of such problems. Once a design is identified as having a problem, it is an altogether different matter to change this design to cure the problem. The following paragraphs discuss some observations and guidelines based on the analysis presented in the previous sections.

Natural frequency. This parameter for a single degree of freedom is given by $\omega_n = \sqrt{k/m}$. Increasing the mass reduces ω_n , and increasing the spring constant k increases it. From a study of the damped system, the damped natural frequency $\omega_d = \omega_n \sqrt{1 - \zeta^2}$ is lower than ω_n .

Unbalances. All rotating machinery is assumed to have an unbalance. Unbalance produces excitation at the rotational speed. The natural frequency of the system ω_n is also known as the critical shaft speed. From the study of the forced-damped system, the following conclusions can be drawn:

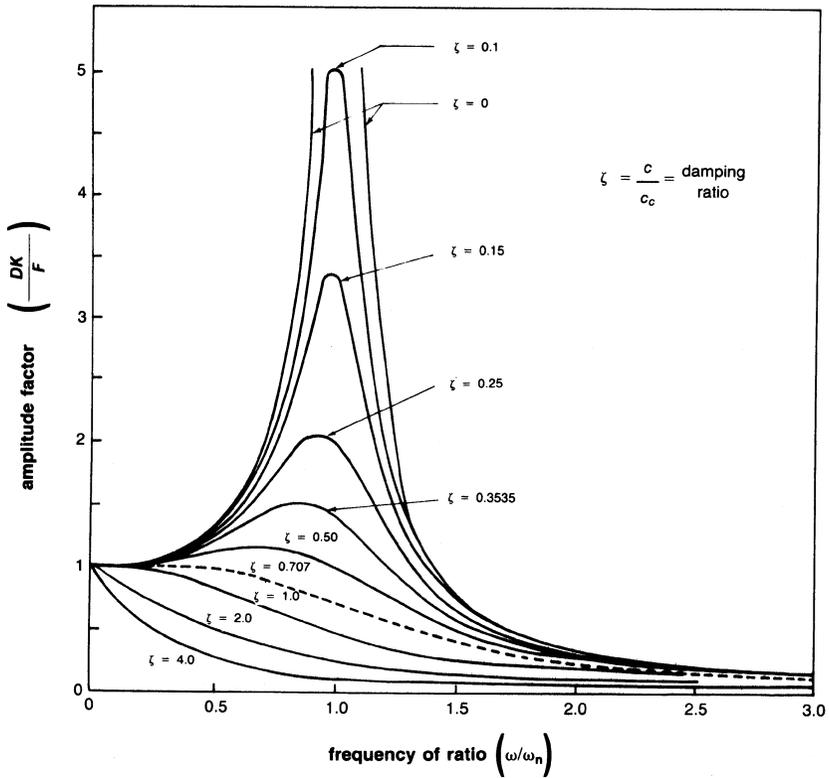


Figure 5-13a. Amplitude factor as a function of the frequency ratio r for various amounts of viscous damping.

(1) the amplitude ratio reaches its maximum values at $\omega_m = \omega_n \sqrt{1 - 2\zeta^2}$, and (2) the damped natural frequency ω_d does not enter the analysis of the forced-damped system. The more important parameter is ω_n , the natural frequency of the undamped system.

In the absence of damping the amplitude ratio becomes infinite at $\omega = \omega_n$. For this reason, the critical speed of a rotating machine should be kept away from its operating speed.

Small machinery involves small values of mass m and has large values of the spring constant k (bearing stiffness). This design permits a class of machines, which are small in size and of low speed in operation, to operate in a range below their critical speeds. This range is known as subcritical operation, and it is highly desirable if it can be attained economically.

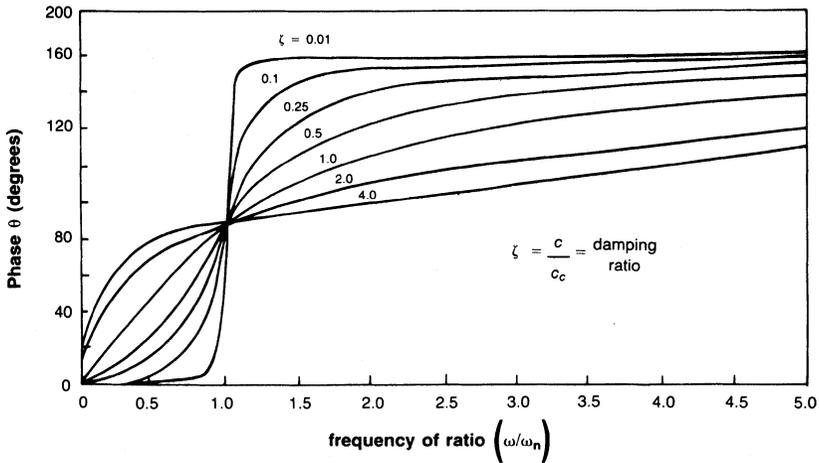


Figure 5-13b. Phase angle as a function of the frequency ratio for various amounts of viscous damping.

The design of large rotating machinery—centrifugal compressors, gas and steam turbines, and large electrical generators—poses a different problem. The mass of the rotor is usually large, and there is a practical upper limit to the shaft size that can be used. Also, these machines operate at high speeds.

This situation is resolved by designing a system with a very low critical speed in which the machine is operated above the critical speed. This is known as supercritical operation. The main problem is that during start-up and shut-down, the machine must pass through its critical speed. To avoid dangerously large amplitudes during these passes, adequate damping must be located in the bearings and foundations.

The natural structural frequencies of most large systems are also in the low-frequency range, and care must be exercised to avoid resonant couplings between the structure and the foundation. The excitation in rotating machinery comes from rotating unbalanced masses. These unbalances result from four factors:

1. An uneven distribution of mass about the geometric axis of the system. This distribution causes the center of mass to be different from the center of rotation.
2. A deflection of the shaft due to the weight of the rotor, causing further distance between the center of mass and the center of rotation. Additional discrepancies can occur if the shaft has a bend or a bow in it.

3. Static eccentricities are amplified due to rotation of the shaft about its geometric center.
4. If supported by journal bearings, the shaft may describe an orbit so that the axis of rotation itself rotates about the geometric center of the bearings.

These unbalance forces increase as a function of ω^2 , making the design and operation of high-speed machinery a complex and exacting task. Balancing is the only method available to tame these excitation forces.

Application to Rotating Machines

Rigid Supports

The simplest model of a rotating machine consists of a large disc mounted on a flexible shaft with the ends mounted in rigid supports. The rigid supports constrain a rotating machine from any lateral movement, but allow free angular movement. A flexible shaft operates above its first critical. Figures 5-14a and 5-14b show such a shaft. The mass center of the disc “ e ” is displaced from the shaft centerline or geometric center of the disc due to manufacturing and material imperfections. When this disc is rotated at a rotational velocity ω , the mass causes it to be displaced so that the center of

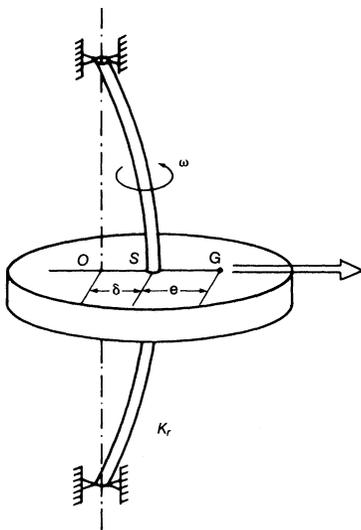


Figure 5-14a. Rigid supports.

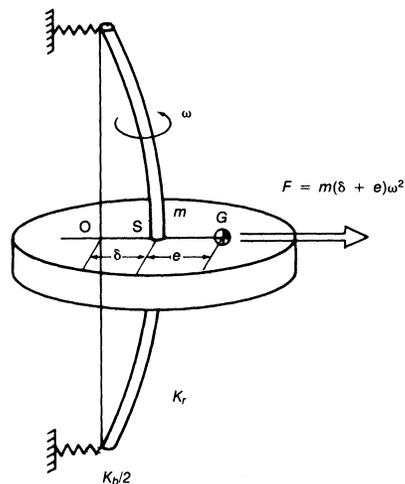


Figure 5-14b. Flexible supports.

the disc describes an orbit of radius δ_r , from the center of the bearing centerline. If the shaft flexibility is represented by the radial stiffness (K_r), it will create a restoring force on the disc of $K_r\delta_r$ that will balance the centrifugal force equal to $m\omega^2(\delta_r + e)$. Equating the two forces obtains

$$K_r\delta = m\omega^2(\delta_r + e)$$

Therefore,

$$\delta_r = \frac{m\omega^2 e}{K_r - m\omega^2} = \frac{(\omega/\omega_n)^2 e}{1 - (\omega/\omega_n)^2} \quad (5-26)$$

where $\omega_n = K_r/m$, the natural frequency of the lateral vibration of the shaft and disc at zero speed.

The previous equation shows that when $\omega < \omega_n$, δ_r is positive. Thus, when operating below the critical speed, the system rotates with the center of mass on the outside of the geometric center. Operating above the critical speed ($\omega > \omega_n$), the shaft deflection δ_r tends to infinity. Actually, this vibration is damped by outside forces. For very high speeds ($\omega \gg \omega_n$), the amplitude δ_r equals $-e$, meaning that the disc rotates about its center of gravity.

Flexible Supports

The previous section discussed the flexible shaft with rigid bearings. In the real world, the bearings are not rigid but possess some flexibility. If the flexibility of the system is given by K_b , then each support has a stiffness of $K_b/2$. In such a system, the flexibility of the entire lateral system can be calculated by the following relationship:

$$\begin{aligned} \frac{1}{K_t} &= \frac{1}{K_r} + \frac{1}{K_b} = \frac{K_b + K_r}{K_r K_b} \\ K_t &= \frac{K_r K_b}{K_b + K_r} \end{aligned} \quad (5-27)$$

Therefore, the natural frequency

$$\begin{aligned} \omega_{nt} &= \sqrt{\frac{K_t}{m}} = \sqrt{\frac{K_r K_b}{K_b + K_r}} / m \\ &= \sqrt{\frac{K_r}{m}} \times \sqrt{\frac{K_b}{K_b + K_r}} \\ &= \omega_n \sqrt{\frac{K_b}{K_b + K_r}} \end{aligned} \quad (5-28)$$

It can be observed from the previous expression that when $K_b \ll K_r$ (very rigid support), then $\omega_{nt} = \omega_n$ or the natural frequency of the rigid system. For a system with a finite stiffness at the supports, or $K_b \approx K_r$, then ω_n is less than ω_{nt} . Hence, flexibility causes the natural frequency of the system to be lowered. Plotting the natural frequency as a function of bearing stiffness on a log scale provides a graph as shown in Figure 5-15.

When $K_b \ll K_r$, then $\omega_{nt} = \omega_n K_b / K_r$. Therefore, ω_{nt} is proportional to the square root of K_b , or $\log \omega_{nt}$ is proportional to one-half $\log K_b$. Thus, this relationship is shown by a straight line with a slope of 0.5 in Figure 5-15. When $K_b \gg K_r$, the total effective natural frequency is equal to the natural rigid-body frequency. The actual curve lies below these two straight lines as shown in Figure 5-15.

The critical speed map shown in Figure 5-15 can be extended to include the second, third, and higher critical speeds. Such an extended critical speed map can be very useful in determining the dynamic region in which a given system is operating. One can obtain the locations of a system's critical speeds by superimposing the actual support versus the speed curve on the critical speed map. The intersection points of the two sets of curves define the locations of the system's critical speeds.

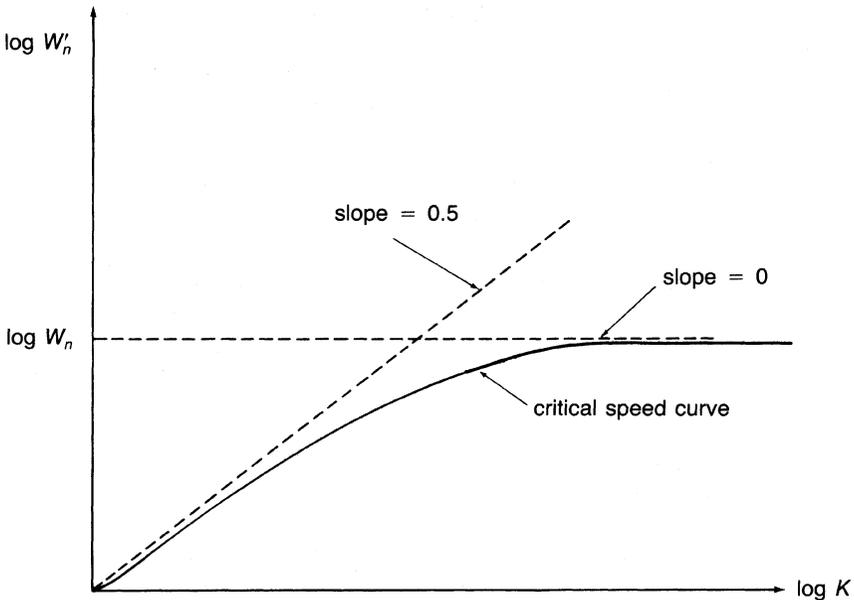


Figure 5-15. Critical speed map.



Figure 5-16a. Rigid supports and a flexible rotor.

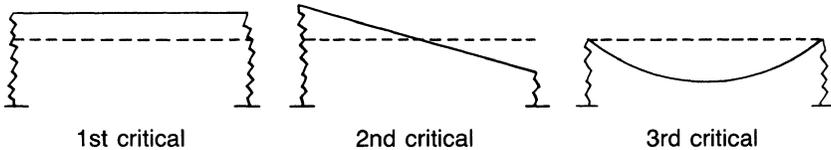


Figure 5-16b. Flexible supports and rigid rotors.

When the previously described intersections lie along the straight line on the critical speed map with a slope of 0.5, the critical speed is bearing controlled. This condition is often referred to as a “rigid-body critical.”

When the intersection points lie below the 0.5 slope line, the system is said to have a “bending critical speed.” It is important to identify these points, since they indicate the increasing importance of bending stiffness over support stiffness.

Figures 5-16a and 5-16b show vibration modes of a uniform shaft supported at its ends by flexible supports. Figure 5-16a shows rigid supports and a flexible rotor. Figure 5-16b shows flexible supports and rigid rotors.

To summarize the importance of the critical speed concept, one should bear in mind that it allows an identification of the operation region of the rotor-bearing system, probable mode shapes, and approximate locations of peak amplitudes.

Critical Speed Calculations for Rotor Bearing Systems

Methods for calculating undamped and damped critical speeds that closely follow the works of Prohl and Lund, respectively, are listed herein. Computer programs can be developed that use the equations shown in this section to provide estimations of the critical speeds of a given rotor for a range of bearing stiffness and damping parameters.

The method of calculating critical speeds as suggested by Prohl and Lund has several advantages. By this method, any number of orders of critical frequencies may be calculated, and the rotor configuration is not limited in the number of diameter changes or in the number of attached discs. In addition, shaft supports may be assumed rigid or may have any values of damping or stiffness. The gyroscopic effect associated with the moment of

attached disc inertia may also be taken into account. Perhaps the greatest advantage of the technique, however, is the relative simplicity with which all the capabilities are performed.

The rotor is first divided into a number of station points, including the ends of the shafting, points at which diameter changes occur, points at which discs are attached, and bearing locations. The shafting connecting the station points are modeled as massless sections which retain the flexural stiffness associated with the section's length, diameter, and modulus of elasticity. The mass of each section is divided in half and lumped at each end of the section where it is added to any mass provided by attached discs or couplings.

The critical-speed calculation of a rotating shaft proceeds with equations to relate loads and deflections from station $n - 1$ to station n . The shaft shear V can be computed using the following relationship:

$$V_n = V_{n-1} + M_{n-1}\omega^2 Y_{n-1} \quad (5-29)$$

and the bending moment

$$M_n = M_{n-1} + V_n Z_n$$

The angular displacement can be computed using the following relationship:

$$\theta_n = \beta_n \left[\frac{M_{n-1}}{2} + \frac{M_n}{2} \right] + \theta_{n-1} \quad (5-30)$$

where β = flexibility constant.

The vertical linear displacement is

$$Y_n = \beta_n \left[\frac{M_{n-1}}{3} + \frac{M_n}{6} \right] Z_n + \theta_{n-1} Z_n + Y_{n-1} \quad (5-31)$$

When crossing a flexible bearing at station n from the left side to the right side, the following relationships hold:

$$K_{xx} Y_n = -[(V_n)_{\text{Right}} - (V_n)_{\text{Left}}] \quad (5-32)$$

$$K_{\theta\theta} \theta_n = [(M_n)_{\text{Right}} - (M_n)_{\text{Left}}] \quad (5-33)$$

$$(\theta_n)_{\text{Right}} = (\theta_n)_{\text{Left}} \quad (5-34)$$

$$(Y_n)_{\text{Right}} = (Y_n)_{\text{Left}} \quad (5-35)$$

The initial boundary conditions are $V_1 = M_1 = 0$ for a free end and, to assign initial values for Y_1 and θ_1 , the calculation proceeds in two parts with the assumptions given as

$$\text{Pass 1} \quad Y_1 = 1.0 \quad \theta_1 = 0.0$$

$$\text{Pass 2} \quad Y_1 = 0.0 \quad \theta_1 = 1.0$$

For each part, the calculation starts at the free end and, using Equations (5-29) through (5-35), proceeds from station to station until the other end is reached. The values for the shear and moment at the far end are dependent on the initial values by the relationship:

$$\begin{aligned} V_n &= V_{n' \text{ Pass 1}} Y_1 + V_{n' \text{ Pass 2}} \theta_1 \\ M_n &= M_{n' \text{ Pass 1}} Y_1 + M_{n' \text{ Pass 2}} \theta_1 \end{aligned} \quad (5-36)$$

The critical speed is the speed at which both $V_n = M_n = 0$, which requires iterating the assumed rotational speed until this condition is observed.

If structural damping is to be considered, then a revised set of relationships must be used. For a system allowing vertical and horizontal shaft motion, the change in shear and moment across a station is given by:

$$\begin{bmatrix} -V'_x \\ -V'_y \\ M'_x \\ M'_y \end{bmatrix}_n = \begin{bmatrix} -V_x \\ -V_y \\ M_x \\ M_y \end{bmatrix}_n + \begin{bmatrix} s^2 m X \\ s^2 m Y \\ s^2 J_T \theta + s\omega J_P \phi \\ s^2 J_T \phi - s\omega J_P \theta \end{bmatrix}_n + (K + sB)_n \begin{bmatrix} X \\ Y \\ \phi \\ \theta \end{bmatrix}_n \quad (5-37)$$

The calculation of parameters between stations utilizes the following relationships:

$$X_{n+1} = X_n + Z_n \theta_n + C_1 [Z_n^2 (M'_{xn} - \epsilon M'_{yn})/2 + C_2 (V'_{yn} + \epsilon V'_{xn})]$$

$$Y_{n+1} = Y_n + Z_n \phi_n + C_1 [Z_n^2 (M'_{yn} + \epsilon M'_{xn})/2 + C_2 (V'_{yn} - \epsilon V'_{xn})]$$

$$\theta_{n+1} = \theta_n + C_1 [Z_n (M'_{xn} - \epsilon M'_{yn}) + Z_n^2 (V'_{xn} - \epsilon V'_{yn})/2]$$

$$\phi_{n+1} = \phi_n + C_1 [Z_n (M'_{yn} + \epsilon M'_{xn}) + Z_n^2 (V'_{yn} + \epsilon V'_{xn})/2]$$

$$M_{x,n+1} = M'_{xn} + Z_n V'_{xn}$$

$$M_{y,n+1} = M'_{yn} + Z_n V'_{yn}$$

$$V_{x,n+1} = V'_{xn}$$

$$V_{y,n+1} = V'_{yn}$$

where:

$$C_1 = 1/(EI)_n \sqrt{1 + \epsilon^2}$$

$$C_2 = \frac{Z_n^2}{6} - \frac{(Z EI)_n}{(\alpha GA)_n} \quad (5-38)$$

where:

E = Young's modulus of elasticity

I = sectional moment of inertia

G = shear modulus

ϵ = logarithmic decrement of internal shaft damping divided
by shaft vertical position

α = cross-sectional shape factor ($\alpha = .75$ for circular cross section)

Electromechanical Systems and Analogies

Where physical systems are so complex that mathematical solutions are not possible, experimental techniques based on various analogies may be one type of solution. Electrical systems that are analogous to mechanical systems are usually the easiest, cheapest, and fastest solution to the problem. The analogy between systems is a mathematical one based on the similarity of the differential equations. Thomson has given an excellent treatise on this subject in his book on vibration. Some of the highlights are given here.

A forced-damped system is shown in Figure 5-17. This system has a mass M , which is suspended on a spring K with a spring constant and a dash pot to produce damping. The viscous damping coefficient is c

$$M \frac{dv}{dt} + cv + K \int_0^t v dt = f(t) \quad (5-39)$$

A force-voltage system can be designed to represent this mechanical system as shown in Figure 5-18.

The equation representing this system when $e(t)$ is the voltage and represents the force, while inductance (L), capacitance C , and resistance R

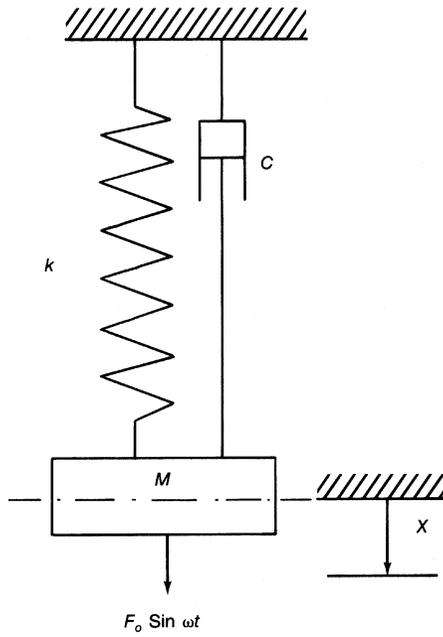


Figure 5-17. Forced vibration with viscous damping.

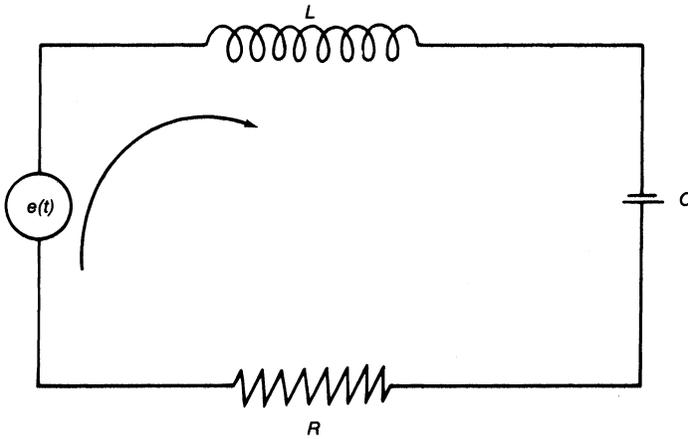


Figure 5-18. A force-voltage system.

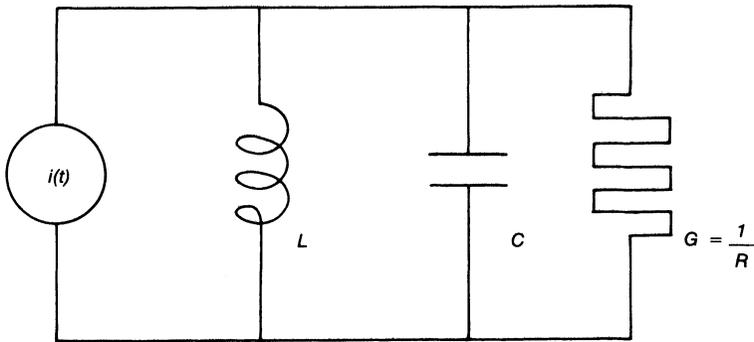


Figure 5-19. Force-current analogy.

represent the mass, spring constant, and the viscous damping, respectively, can be written as follows:

$$L \frac{di}{dt} + Ri + \frac{1}{C} \int_0^t i dt = e(t) \quad (5-40)$$

A force-current analogy can also be obtained where the mass is represented by capacitance, the spring constant by the inductance, and the resistance by the conductance as shown in Figure 5-19. The system can be represented by the following relationship:

$$C \frac{de}{dt} + Ge + \frac{1}{L} \int_0^t e dt = i(t) \quad (5-41)$$

Comparing all these equations shows that the mathematical relationships are all similar. These equations convey the analogous values. For convenience, Table 5-1 also shows these relationships.

Forces Acting on a Rotor Bearing System

There are many types of forces that act on a rotor-bearing system. The forces can be classified into three categories: (1) casing and foundation forces, (2) forces generated by rotor motion, and (3) forces applied to a rotor. Table 5-2 by Reiger is an excellent compilation of these forces.

Forces transmitted to casing and foundations. These forces can be due to foundation instability, other nearby unbalanced machinery, piping strains, rotation in gravitational or magnetic fields, or excitation of casing or

Table 5-1
Electromechanical System Analogies

| Mechanical Parameters | Electrical Parameters | |
|----------------------------------|----------------------------|----------------------------|
| | Force-Voltage Analogy | Force-Current Analogy |
| Force (F) | Voltage e current i | Current i Voltage e |
| Velocity \dot{x} or v | | |
| Displacement $x = \int_0^t v dt$ | Charge $q = \int_0^t i dt$ | |
| Mass M | Inductance L | Capacitance C |
| Dashpot c | Resistance R | Conductance G |
| Coefficient | | |
| Spring Constant k | Capacitance C | Inductance L |

foundation natural frequencies. These forces can be constant or variable with impulse loadings. The effect of these forces on the rotor-bearing system can be great. Piping strains can cause major misalignment problems and unwanted forces on the bearings. Operation of reciprocating machinery in the same area can cause foundation forces and unduly excite the rotor of a turbomachine.

Forces generated by rotor motion. These forces can be classified into two categories: (1) forces due to mechanical and material properties, and (2) forces caused by various loadings of the system. The forces from mechanical and material properties are unbalanced and are caused by a lack of homogeneity in materials, rotor bow, and elastic hysteresis of the rotor. The forces caused by loadings of the system are viscous and hydrodynamic forces in the rotor-bearing system, and various blade loading forces, which vary in the operational range of the unit.

Forces applied to a rotor. Rotor-applied forces can be due to drive torques, couplings, gears, misalignment, and axial forces from piston and thrust unbalance. They can be destructive, and they often result in the total destruction of a machine.

Rotor Bearing System Instabilities

Instabilities in rotor-bearing systems may be the result of different forcing mechanisms. Ehrich, Gunter, Alford, and others have done considerable work to identify these instabilities. One can divide these instabilities into two general yet distinctly different categories: (1) the forced or resonant instability dependent on outside mechanisms in frequency of oscillations;

Table 5-2
Forces Acting on Rotor Bearing Systems

| Source of Force | Description | Application |
|---|---|---|
| 1. Forces transmitted to foundations, casing, or bearing pedestals. | Constant, unidirectional force | Constant linear acceleration. |
| | Constant force, rotational | Rotation in gravitational or magnetic field. |
| 2. Forces generated by rotor motion. | Variable, unidirectional | Impressed cyclic ground or foundation-motion. |
| | Impulsive forces | Air blast, explosion, or earthquake. Nearby unbalanced machinery. Blows, impact. |
| | Random forces | Present in all rotating machinery. |
| | Rotating unbalance: residual, or bent shaft. | |
| | Coriolis forces | Motion around curve of varying radius. Space applications. Rotary-coordinated analyses. |
| | Elastic hysteresis of rotor | Property of rotor material, which appears when rotor is cyclically deformed in bending, torsionally or axially. |
| | Coulomb friction | Construction damping arising from relative motion between shrunkfitted assemblies. Dry-friction bearing whirl. |
| | Fluid friction | Viscous shear of bearings. Fluid entrainment in turbomachinery. Windage. |
| | Hydrodynamic forces, static. | Bearing load capacity. Volute pressure forces. |
| | Hydrodynamic forces, dynamic. | Bearing stiffness and damping properties. |
| 3. Applied to rotor | Dissimilar elastic beam Stiffness reaction forces | Rotors with differing rotor lateral stiffnesses. Slotted rotors, electrical machinery, Keyway. Abrupt speed change conditions |
| | Gyroscopic moments | Significant in high-speed flexible rotors with discs. |
| | Drive torque | Accelerating or constant-speed operation |
| | Cyclic forces | Internal combustion engine torque and force components. |
| | Oscillating torques | Misaligned couplings. Propellers. Fans. Internal combustion engine drive. |

table continued on next page

Table 5-2 continued

| Source of Force | Description | Application |
|-----------------|--|---|
| | Transient torques | Gears with indexing or positioning errors. |
| | Heavy applied rotor force | Drive gear forces. Misaligned 3-or-more rotor-bearing assembly. |
| | Gravity | Nonvertical machines. Nonspatial applications. |
| | Magnetic field: stationary or rotating | Rotating electrical machinery. |
| | Axial forces | Turbomachine balance piston Cyclic forces from propeller, or fan. Self-excited bearing forces. Pneumatic hammer |

and (2) the self-excited instabilities that are independent of outside stimuli and independent of the frequency. Table 5-3 is the characterization of the two categories of vibration stimuli.

Forced (resonant) vibration. In forced vibration the usual driving frequency in rotating machinery is the shaft speed or multiples of this speed.

This speed becomes critical when the frequency of excitation is equal to one of the natural frequencies of the system. In forced vibration, the system is a function of the frequencies. These frequencies can also be multiples of rotor speed excited by frequencies other than the speed frequency such as blade passing frequencies, gear mesh frequencies, and other component frequencies. Figure 5-20 shows that for forced vibration, the critical frequency remains constant at any shaft speed. The critical speeds occur at one-half, one, and two times the rotor speed. The effect of damping in forced vibration reduces the amplitude, but it does not affect the frequency at which this phenomenon occurs.

Typical forced vibration stimuli are as follows:

1. *Unbalance.* This stimulus is caused by material imperfections, tolerances, etc. The mass center of gravity is different from the geometric case, leading to a centrifugal force acting on the system.
2. *Asymmetric flexibility.* The sag in a rotor shaft will cause a periodic excitation force twice every revolution.
3. *Shaft misalignment.* This stimulus occurs when the rotor center line and the bearing support line are not true. Misalignment may also be

Table 5-3
Characteristics of Forced and Self-Excited Vibration

| | Forced or Resonant Vibration | Self-Excited or Instability Vibration |
|----------------------------|---|---|
| Frequency/rpm relationship | $N_F = N_{rpm}$ or N or rational fraction | Constant and relatively independent of rotating speed. |
| Amplitude/rpm relationship | Peak in narrow bands of rpm | Blossoming at onset and continue to increase with increasing rpm. |
| Influence of damping | Additional damping Reduce amplitude No change in rpm at which it occurs | Additional damping may defer to a higher rpm. Will not materially affect amplitude. |
| System geometry | Lack of axial sym. External forces | Independent of symmetry. Small deflection to an axisymmetric system. Amplitude will self-propagate. |
| Vibration frequency | At or near shaft critical or natural frequency | Same. |
| Avoidance | 1. Critical freq. Above running speed 2. Axisymmetric 3. Damping | 1. Operating rpm below onset. 2. Eliminates instability. Introduce damping. |

caused by an external piece such as the driver to a centrifugal compressor. Flexible couplings and better alignment techniques are used to reduce the large reaction forces.

Periodic loading. This type of loading is caused by external forces that are applied to the rotor by gears, couplings, and fluid pressure, which is transmitted through the blade loading.

Self-Excited Instabilities

The self-excited instabilities are characterized by mechanisms, which whirl at their own critical frequency independent of external stimuli. These types of self-excited vibrations can be destructive, since they induce alternating stress that leads to fatigue failures in rotating equipment. The whirling motion, which characterizes this type of instability, generates a tangential force normal to the radial deflection of the shaft, and a magnitude proportional to that deflection. The type of instabilities, which fall under this category, are usually called whirling or whipping. At the rotational speed where such a force is started, it will overcome the external stabilizing damp-

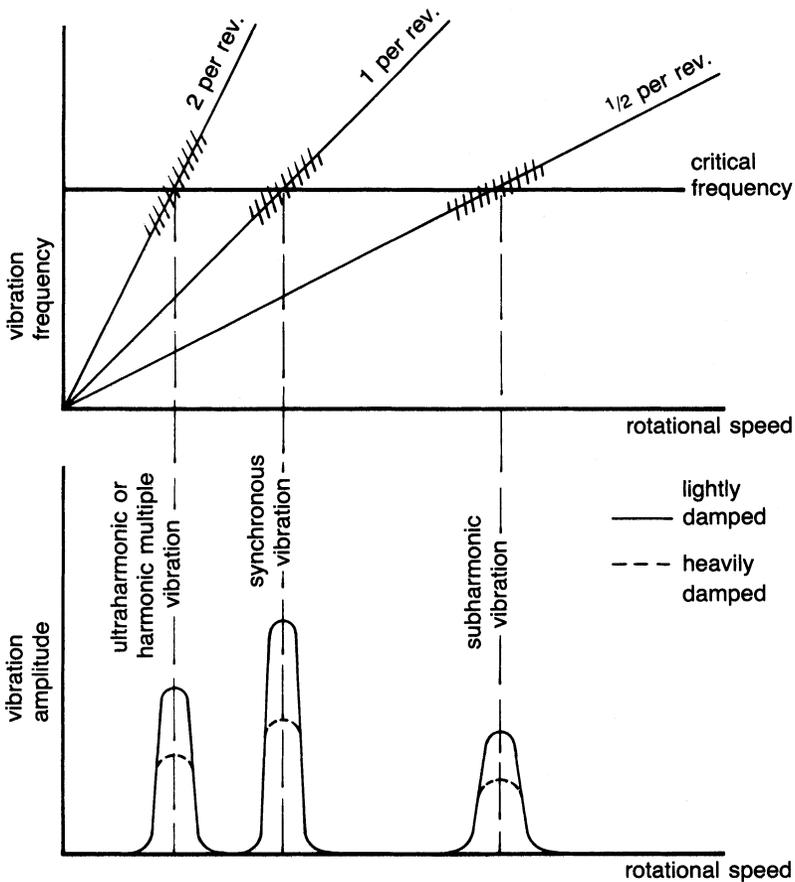


Figure 5-20. Characteristic of forced vibration or resonance in rotating machinery. (Ehrich, F.F., "Identification and Avoidance of Instabilities and Self-Excited Vibrations in Rotating Machinery," Adopted from ASME Paper 72-DE-21, General Electric Co., Aircraft Engine Group, Group Engineering Division, May 11, 1972.)

ing force and induce a whirling motion of ever-increasing amplitude. Figure 5-21 shows the onset speed. The onset speed does not coincide with any particular rotation frequency. Also, damping results from a shift of this frequency, not in the lowering of the amplitude as in forced vibration. Important examples of such instabilities include hysteretic whirl, dry-friction whip, oil whip, aerodynamic whirl, and whirl due to fluid trapped in the rotor. In a self-excited system, friction or fluid energy dissipations generate the destabilizing force.

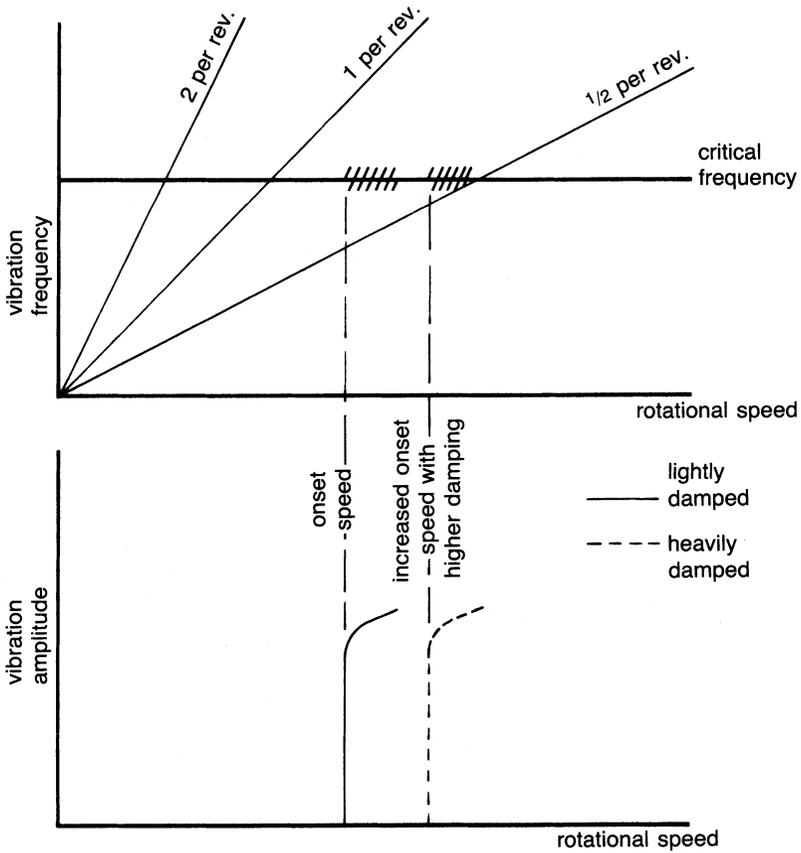


Figure 5-21. Characteristics of instabilities or self-excited vibration in rotating machinery. (Ehrich, F.F., "Identification and Avoidance of Instabilities and Self-Excited Vibrations in Rotating Machinery," Adopted from ASME Paper 72-DE-21, General Electric Co., Aircraft Engine Group, Group Engineering Division, May 11, 1972.)

Hysteretic whirl. This type of whirl occurs in flexible rotors and results from shrink fits. When a radial deflection is imposed on a shaft, a neutral-strain axis is induced normal to the direction of flexure. From first-order considerations, the neutral-stress axis is coincident with the neutral-strain axis, and a restoring force is developed perpendicular to the neutral-stress axis. The restoring force is then parallel to and opposing the induced force. In actuality, internal friction exists in the shaft, which causes a phase shift in the stress. The result is that the neutral-strain axis and neutral-stress axis are displaced so that the resultant force is not parallel to the deflection. The

tangential force normal to the deflection causes whirl instability. As whirl begins, the centrifugal force increases, causing greater deflections—which result in greater stresses and still greater whirl forces. This type of increasing whirl motion may eventually be destructive as seen in Figure 5-22a.

Some initial impulse unbalance is often required to start the whirl motion. Newkirk has suggested that the effect is caused by interfaces of joints in a rotor (shrink fits) rather than defects in rotor material. This type of whirl phenomenon occurs only at rotational speeds above the first critical. The phenomenon may disappear and then reappear at a higher speed. Some success has been achieved in reducing this type of whirl by reducing the number of separate parts, restricting the shrink fits, and providing some lockup of assembled elements.

Dry-friction whirl. This type of whip is experienced when the surface of a rotating shaft comes into contact with an unlubricated stationary guide. The effect takes place because of an unlubricated journal, contact in radial clearance of labyrinth seals, and loss of clearance in hydrodynamic bearings.

Figure 5-22b shows this phenomenon. When contact is made between the surface and the rotating shaft, the coulomb friction will induce a tangential force on the rotor. This friction force is approximately proportional to the

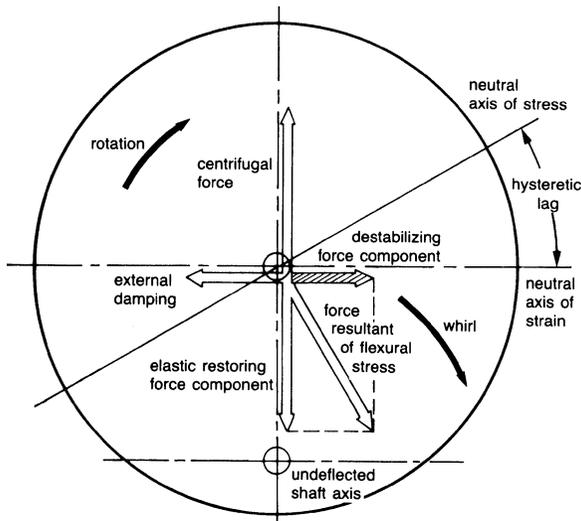


Figure 5-22a. Hysteretic whirl. (Ehrich, F.F., "Identification and Avoidance of Instabilities and Self-Excited Vibrations in Rotating Machinery," Adopted from ASME Paper 72-DE-21, General Electric Co., Aircraft Engine Group, Group Engineering Division, May 11, 1972.)

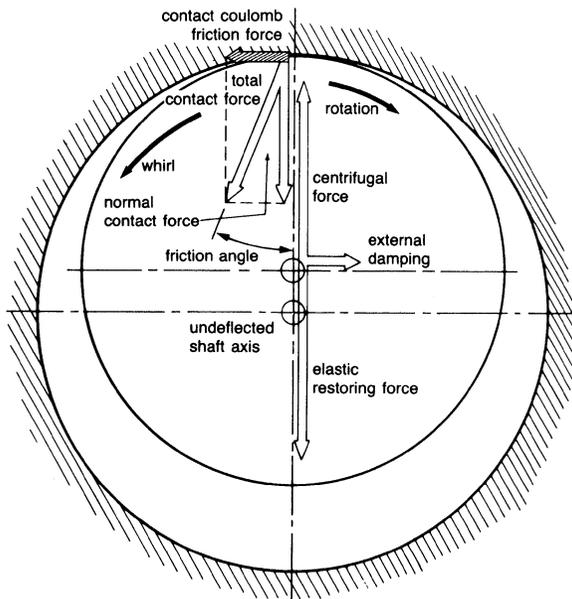


Figure 5-22b. Dry friction whirl. (Ehrich, F.F., "Identification and Avoidance of Instabilities and Self-Excited Vibrations in Rotating Machinery," Adopted from ASME Paper 72-DE-21, General Electric Co., Aircraft Engine Group, Group Engineering Division, May 11, 1972.)

radial component of the contact force, creating a condition for instability. The whirl direction is counter to the shaft direction.

Oil whirl. This instability begins when fluid entrained in the space between the shaft and bearing surfaces begins to circulate with an average velocity of one-half of the shaft surface speed. Figure 5-23a shows the mechanism of oil whirl. The pressures developed in the oil are not symmetric about the rotor. Because of viscous losses of the fluid circulating through the small clearance, higher pressure exists on the upstream side of the flow than on the downstream side. Again, a tangential force results. A whirl motion exists when the tangential force exceeds any inherent damping. It has been shown that the shafting must rotate at approximately twice the critical speed for whirl motion to occur. Thus, the ratio of frequency to rpm is close to 0.5 for oil whirl. This phenomenon is not restricted to the bearing, but it also can occur in the seals.

The most obvious way to prevent oil whirl is to restrict the maximum rotor speed to less than twice its critical. Sometimes oil whip can be reduced or eliminated by changing the viscosity of the oil or by controlling the oil

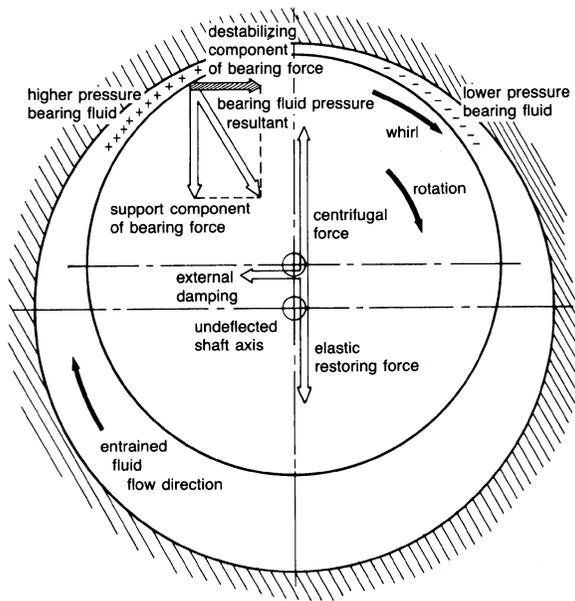


Figure 5-23a. Oil whirl. (Ehrich, F.F., "Identification and Avoidance of Instabilities and Self-Excited Vibrations in Rotating Machinery," Adopted from ASME Paper 72-DE-21, General Electric Co., Aircraft Engine Group, Group Engineering Division, May 11, 1972.)

temperature. Bearing designs that incorporate grooves or tilting pads are also effective in inhibiting oil-whirl instability.

Aerodynamic whirl. Although the mechanism is not clearly understood, it has been shown that aerodynamic components, such as compressor wheels and turbine wheels, can create cross-coupled forces due to the wheel motion. Figure 5-23b is one representation of how such forces may be induced.

The acceleration or deceleration of the process fluid imparts a net tangential force on the blading. If the clearance between the wheel and housing varies circumferentially, a variation of the tangential forces on the blading may also be expected, resulting in a net destabilizing force as shown in Figure 5-23b. The resultant force from the cross-coupling of angular motion and radial forces may destabilize the rotor and cause a whirl motion.

The aerodynamic cross-coupling effect has been quantified into equivalent stiffness. For instance, in axial-flow machines

$$K_{xy} = -K_{yx} = \frac{\beta T}{D_p H} \quad (5-42)$$

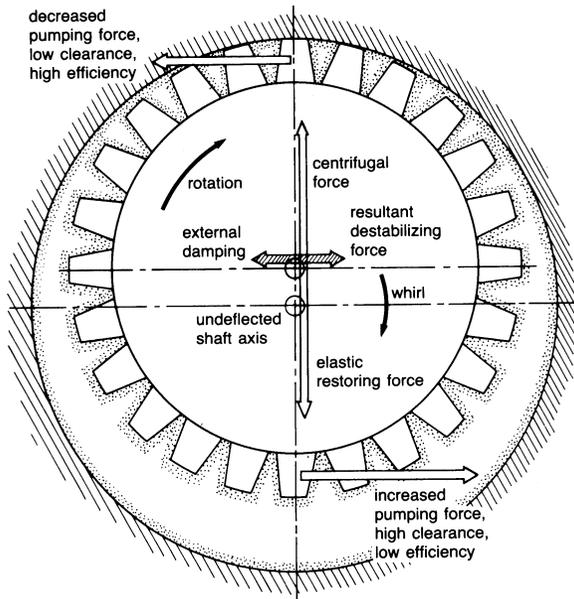


Figure 5-23b. Aerodynamic cross-coupling. (Ehrich, F.F., "Identification and Avoidance of Instabilities and Self-Excited Vibrations in Rotating Machinery," Adopted from ASME Paper 72-DE-21, General Electric Co., Aircraft Engine Group, Group Engineering Division, May 11, 1972.)

where:

β = efficiency slope versus displacement over blade-height curve

T = stage torque

D_P = average pitch diameter

H = average blade height

The stiffness that results from the previous quantification may be used in a critical-speed program in much the same manner as bearing coefficients.

Whirl from fluid trapped in the rotor. This type of whirl occurs when liquids are inadvertently trapped in an internal rotor cavity. The mechanism of this instability is shown in Figure 5-24. The fluid does not flow in a radial direction but flows in a tangential direction. The onset of instability occurs between the first and second critical speeds. Table 5-4 is a handy summary for both avoidance and diagnosis of self-excitation and instabilities in rotating shafts.

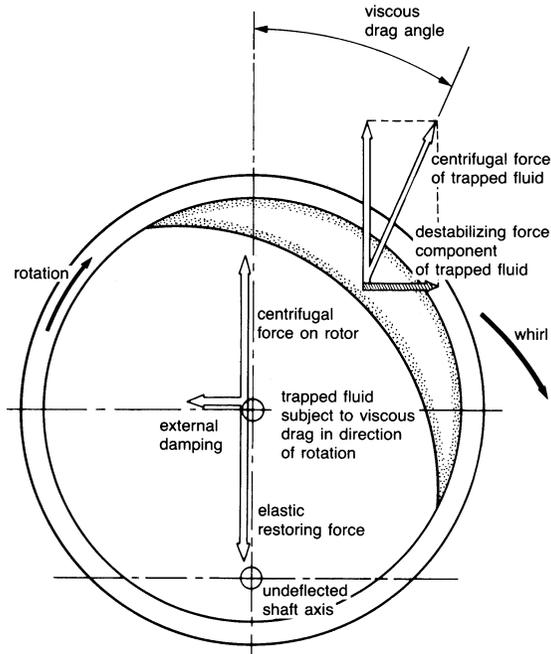


Figure 5-24. Whirl from fluid trapped in the rotor. (Ehrich, F.F., "Identification and Avoidance of Instabilities and Self-Excited Vibrations in Rotating Machinery," Adopted from ASME Paper 72-DE-21, General Electric Co., Aircraft Engine Group, Group Engineering Division, May 11, 1972.)

Campbell Diagram

The Campbell diagram is an overall or bird's-eye view of regional vibration excitation that can occur on an operating system. The Campbell diagram can be generated from machine design criteria or from machine operating data. A typical Campbell diagram plot is shown in Figure 5-25. Engine rotational speed is along the X axis. The system frequency is along the Y axis. The fan lines are engine-order lines: one-half engine order, one times engine order, two times engine order, three times engine order, four times engine order, five times engine order, 10 times engine order, etc. This form of design study is necessary, especially when designing an axial compressor to determine if a natural blade frequency is excited by a running frequency, its harmonics, or subharmonics. For example, take the second-stage blade of a hypothetical compressor. Its first flexural natural frequency is calculated and found to be 200 Hz. From the Campbell diagram figure, it

Table 5-4
Characteristics of Rotor Instabilities

| Type of Instability | Onset | Frequency Response | Caused by |
|-------------------------------|----------------|----------------------------------|---|
| <i>Forced Vibration</i> | | | |
| Unbalance | Any speed | $N_f = N$ | Nonhomogeneous material |
| Shaft misalignment | Any speed | $N_f = 2N$ | Driver and driven equipment misaligned |
| <i>Self-Excited Vibration</i> | | | |
| Hysteretic whirl | $N > N_1$ | $N_f \approx N_1$ $N_f = .5N$ | Shrink fits and built-up parts |
| Hydrodynamic whirl (Oil Whip) | $N > 2N_1$ | $N_f \leq .5N$ | Fluid film bearings and seals |
| Aerodynamic whirl | $N > N_1$ | $N_f = N_1$ | Compressor or turbine, tip clearance effects, balance pistons |
| Dry-friction whirl | Any speed | $N_{f1} = -nN$ | Shaft in contact with stationary guide |
| Entrained fluid | $N_1 < N < 2N$ | $N_f = N_1$ $.5N < N_f < N$ | Liquid or steam entrapped in rotor |

is apparent that a forcing frequency of 12,000 rpm produced by operating the compressor at 12,000 rpm will excite the 200-Hz first flexural frequency of the blade ($200 \text{ Hz} \times 60 = 12,000 \text{ rpm}$). Also, there are five inlet guide vanes ahead of the second-stage blade row. Operating the compressor at 2400 rpm will excite the 200 Hz natural frequency of the blade. ($200 \text{ Hz} \times 60 = 5 \times 2400 \text{ rpm}$.)

Following a calculation of the blade natural frequency and a Campbell diagram study of possible excitation sources, it is usual practice to check for the natural frequency band spread by testing the blades on a shaker table. This natural frequency band spread by testing the blades on a shaker table. This natural frequency band spread plotted on the Campbell diagram now indicates that operating the compressor between 11,700 rpm and 12,600 rpm should be prohibited. When there are several blade rows on the compressor and several sources of excitation, the designer can be confronted with the difficult task of designing the blade and guide vane rows to meet structural and aerodynamic criteria. Natural blade frequency will be affected by rotational and aerodynamic loading, and it needs to be factored in. In most axial compressors there are specific operational speed ranges, which are restricted to avoid blade failure from fatigue.

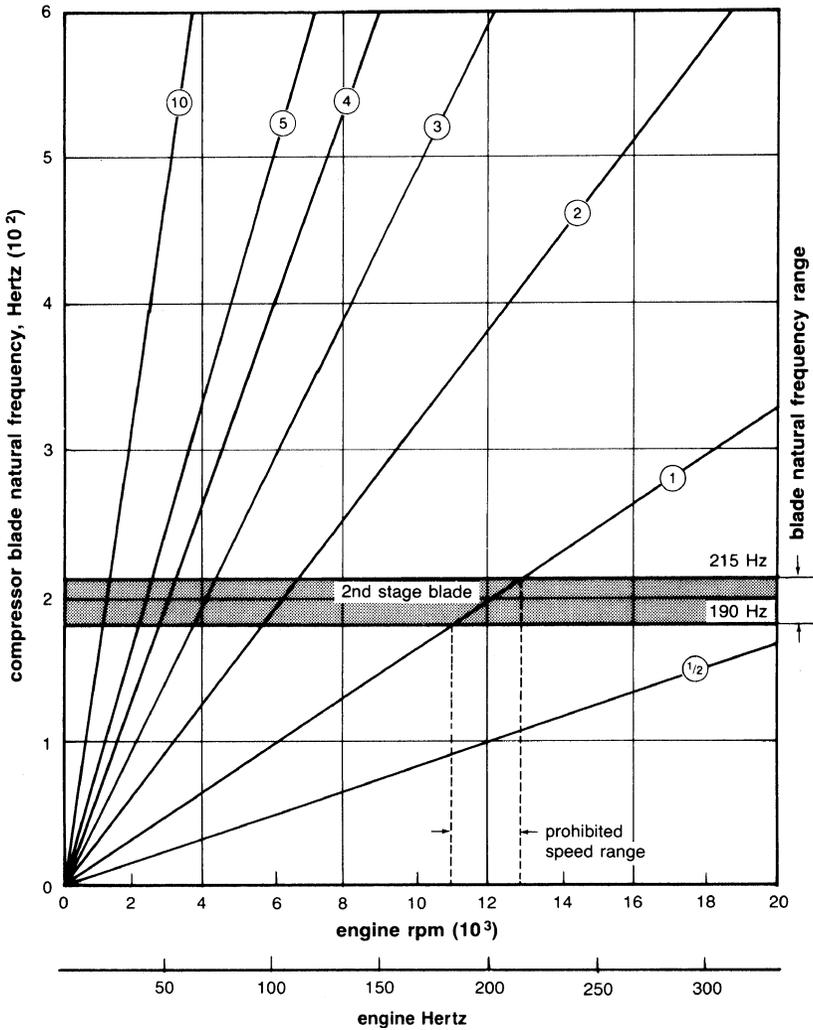


Figure 5-25. Campbell diagram.

To ensure that blade stress levels are within the fatigue life requirements of the compressor, it is usual practice to strain-gauge the blading on one or two prototype machines, measure the stress levels, and generate a Campbell diagram showing the plotted test data. To measure data, an impeller can also be mounted on a shaker table with a variable frequency output (0–10,000 Hz). Accelerometers can be mounted at various positions on the

impeller to obtain the frequency responses in conjunction with a spectrum analyzer (Figure 5-26).

Initially, tests are run to identify the major critical frequencies of the impeller. Mode shapes are then determined visually at each of the critical frequencies. To obtain these mode visualizations, salt is sprinkled evenly on the disc surface. The shaker is maintained at a particular frequency, at which value a given critical frequency is excited for a certain length of time so that the salt particles display the mode shape. The salt accumulates in the nodal regions. Photographs are taken at lower values of these critical frequencies. Photography allows a qualitative identification of the appropriate mode shapes corresponding to each frequency. Figure 5-27 shows an impeller with the mode shapes.

The next step in the testing procedure is to record accelerometer readings at various disc, blade, and shroud locations at lower critical frequencies. The objective of this test is to quantitatively identify the high and low excitation regions. For this test, a six- or five-blade region is considered sufficiently large to be representative of the entire impeller. The results of these tests are plotted on a Campbell diagram, as shown for one such impeller in Figure 5-28. Lines of excitation frequencies are then drawn vertically on the Campbell diagram, and a line corresponding to the design speed is drawn horizontally. Where the lines of excitation frequencies and multiples of running speed intersect near the line of design rpm, a problem area may exist. If, for instance, an impeller has 20 blades, a design speed of 3000 rpm (50 Hz), and a critical frequency of 1000 Hz, the impeller is very likely to be severely excited, since the critical is exactly $20N$. On a Campbell diagram the previous

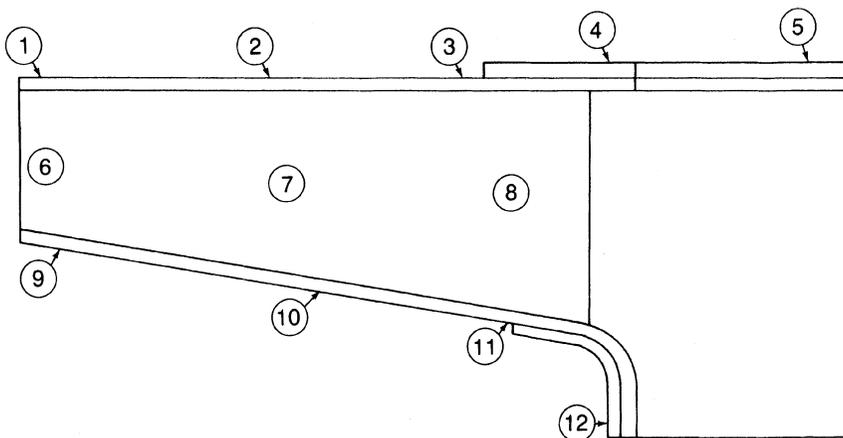


Figure 5-26. Accelerometer locations on impeller tested.

FPO

Figure 5-27. Impeller showing nodal points.

example will correspond to an exact intersect of the running speed line, 1000 Hz frequency line, and the line of slope $20N$.

A shrouded impeller was tested containing 12 blades and a design speed of 3000 rpm. The 12-bladed impeller's first excitation mode occurred at a frequency of 150 Hz, resulting in a single-umbrella mode occurring at the contact point between the two back shrouds. At 350 Hz a coupled mode existed. At these two frequencies it is the back shroud that is the exciting force. At 450 Hz a two-diameter mode existed. This mode is characterized by four nodal radial lines and in many instances can be the most troublesome mode. This mode is excited by the front shroud and the impeller eye. A double-umbrella mode occurred at 600 Hz. At the last two frequencies, the blade eye experienced high excitation. The Campbell diagram (Figure 5-28) showed that at design speed this frequency coincided with the $12N$ line. This coincidence is undesirable, since the number of blades is 12 and may be the exciting force needed to cause a problem. At 950 Hz, a three-diameter mode existed, and at 1100 Hz a four-diameter mode existed. At 1100 Hz the blade-tip frequency is the predominant forcing function. This impeller seemed to be in trouble at 600 Hz, since this frequency coincided with the number of blades. To remove this problem, it was recommended that either the number of blades should be increased to 15 or the blades should be made out of a thicker stock. This type of analysis is useful mostly in the design stages so that problems may be prevented. An analysis may also be helpful in the field. If a problem exists, the machine can be run at a different speed to avert a catastrophe.

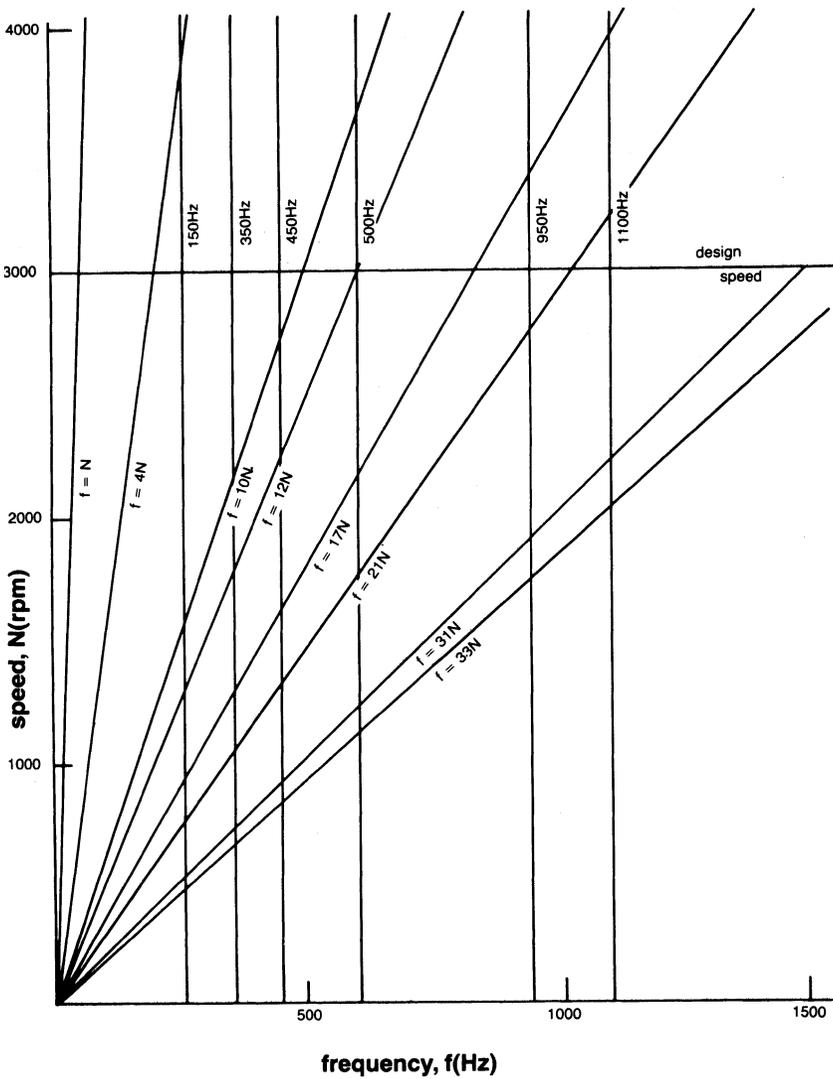


Figure 5-28. Campbell diagram of tested impeller.

Bibliography

- Alford, J.S., "Protecting Turbomachinery from Self-Excited Rotor Whirl," *Journal of Engineering for Power*, ASME Transactions, October, 1965, pp. 333–344.
- Ehrich, F.F., "Identification and Avoidance of Instabilities and Self-Excited Vibrations in Rotating Machinery," Adopted from ASME Paper 72-De-21, General Electric Co., Aircraft Engine Group, Group Engineering Division, May 11, 1972.
- Gunter, E.J., Jr., "Rotor Bearing Stability," Proceedings of the 1st Turbomachinery Symposium, Texas A&M University, October, 1972, pp. 119–141.
- Lund, J.W., "Stability and Damped Critical Speeds of a Flexible Rotor in Fluid-Film Bearings," ASME No. 73-DET-103.
- Newkirk, B.L., "Shaft Whipping," *General Electric Review*, Vol. 27, (1924), p. 169.
- Nicholas John, C., and Moll Randall, W., "Shifting Critical Speeds Out of the Operating Range by Changing From Tilting Pad to Sleeve Bearings" Proceedings of the 22nd Turbomachinery Symposium, Texas A&M University. p. 25, 1993.
- Prohl, M.A., "General Method of Calculating Critical Speeds of Flexible Rotors," *Trans. ASME, J. Appl. Mech.*, Vol. 12, No. 3, September 1945, pp. A142–A148.
- Reiger, D., "The Whirling of Shafts," *Engineer*, London, Vol. 158, 1934, pp. 216–228.
- Thomson, W.T., *Mechanical Vibrations*, 2nd edition, Prentice-Hall, Inc., Englewood Cliffs, N.J., 1961.

Part II

Major Components

6

Centrifugal Compressors

Centrifugal compressors are used in small gas turbines and are the driven units in most gas turbine compressor trains. They are an integral part of the petrochemical industry, finding extensive use because of their smooth operation, large tolerance of process fluctuations, and their higher reliability compared to other types of compressors. Centrifugal compressors range in size from pressure ratios of 1:3 per stage to as high as 12:1 on experimental models. Discussion here will be limited to pressure ratios below 3.5:1, since this type is prevalent in the petrochemical industry. The proper selection of a compressor is a complex and important decision. The successful operation of many plants depends on smooth and efficient compressor operations. To ensure the best selection and proper maintenance of a centrifugal compressor, the engineer must have a knowledge of many engineering disciplines.

In a typical centrifugal compressor the fluid is forced through the impeller by rapidly rotating impeller blades. The velocity of the fluid is converted to pressure, partially in the impeller and partially in the stationary diffusers. Most of the velocity leaving the impeller is converted into pressure energy in the diffuser as shown in Figure 6-1. It is normal practice to design the compressor so that half the pressure rise takes place in the impeller and the other half in the diffuser. The diffuser consists essentially of vanes, which are tangential to the impeller. These vane passages diverge to convert the velocity head into pressure energy. The inner edges of the vanes are in line with the direction of the resultant airflow from the impeller as shown in Figure 6-2.

Centrifugal compressors in general are used for higher-pressure ratios and lower-flow rates compared to lower-stage pressure ratios and higher-flow rates in axial compressors. Figure 6-3 is a map for centrifugal compressors that shows the effect of specific speed (N_s) and specific diameter (D_s) on their

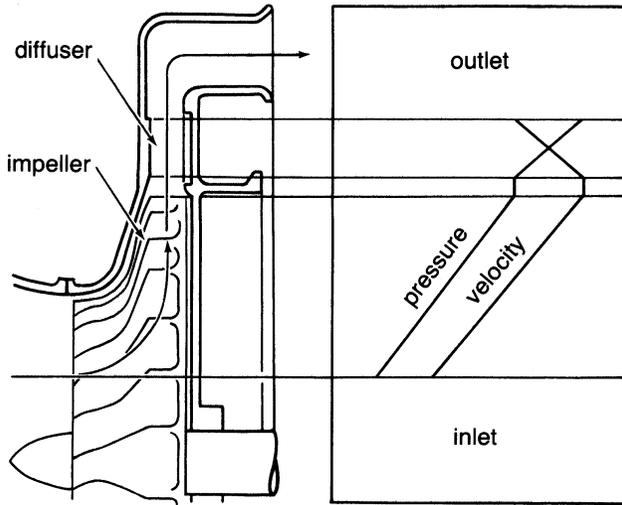


Figure 6-1. Pressure and velocity through a centrifugal compressor.

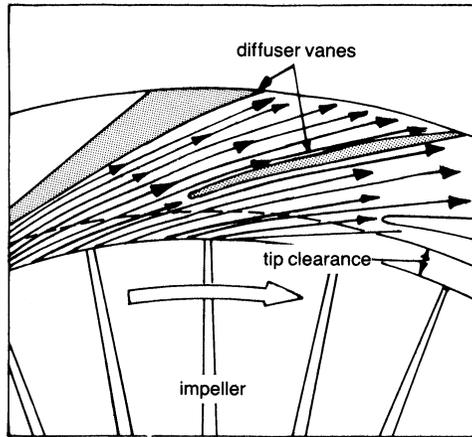


Figure 6-2. Flow entering a vaned diffuser.

efficiency. The most efficient region for centrifugal compressor operation is in a specific speed range between $60 < N_s > 1500$. Specific speeds of more than 3000 usually require an axial-flow-type compressor. In a centrifugal compressor the angular momentum of the gas flowing through the impeller is increased partly because the impeller's outlet diameter is significantly

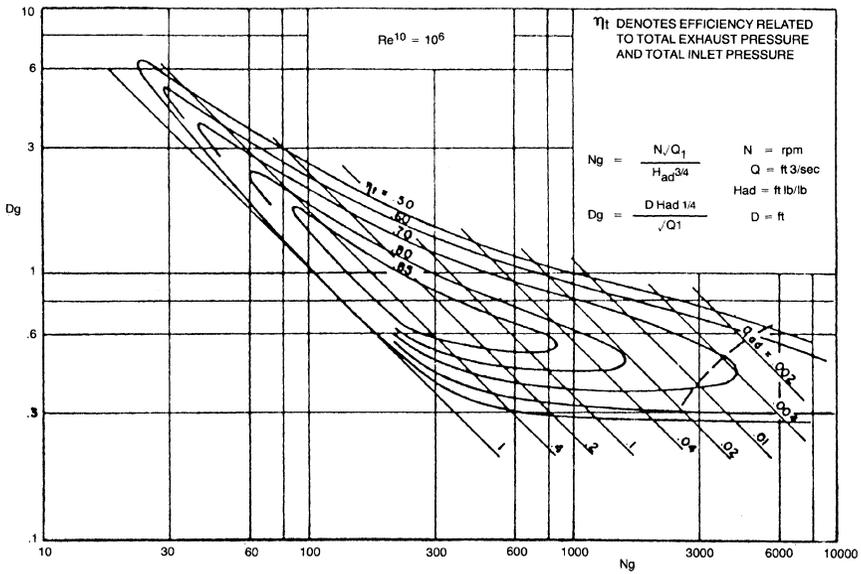


Figure 6-3. Centrifugal compressor map. (Balje, O.E., "A Study of Reynolds Number Effects in Turbomachinery," *Journal of Engineering for Power*, ASME Trans., Vol. 86, Series A, p. 227.)

greater than its inlet diameter. The major difference between axial and centrifugal compressors is the variance in the diameters of the inlet and the outlet. The flow leaving the centrifugal compressor is usually perpendicular to the axis of rotation.

Centrifugal Compressor Components

The terminology used to define the components of a centrifugal compressor is shown in Figure 6-4. A centrifugal compressor is composed of inlet guide vanes, an inducer, an impeller, a diffuser, and a scroll. The inlet guide vanes (IGVs) are used in only a high-pressure ratio transonic compressor. Centrifugal compressor impellers are either shrouded or unshrouded as seen in Figures 6-5 and 6-6.

The fluid comes into the compressor through an intake duct and is given prewhirl by the IGVs. It then flows into an inducer without any incidence angle, and its flow direction is changed from axial to radial. The fluid is given energy at this stage by the rotor as it goes through the impeller while compressing. It is then discharged into a diffuser, where the kinetic energy is

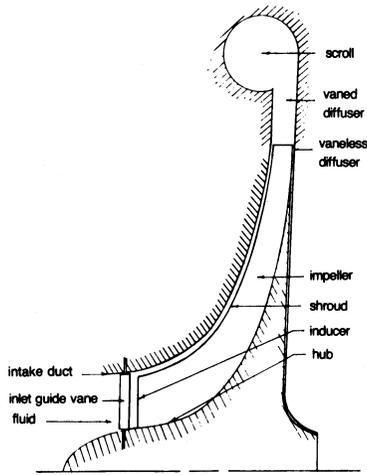


Figure 6-4. Schematic of a centrifugal compressor.

FPO

Figure 6-5. Closed impeller. (Courtesy Elliott Company, Jeannette, PA.)

FPO

Figure 6-6. Open-faced impeller.

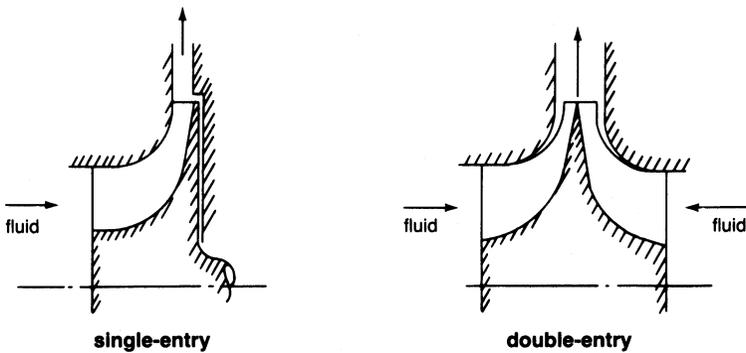


Figure 6-7. Types of entry-inducer systems.

converted into static pressure. The flow enters the scroll from which the compressor discharge is taken. Figure 6-1 shows the variations in pressure and velocity through a compressor.

There are two kinds of energy inducer systems: a single-entry inducer and a double-entry inducer as shown in Figure 6-7.

A double-entry inducer system halves the inlet flow so that a smaller inducer-tip diameter can be used, reducing the inducer-tip Mach number; however, the design is difficult to integrate into many configurations.

There are three impeller vane types, as shown in Figure 6-8. These are defined according to the exit blade angles. Impellers with exit blade angle

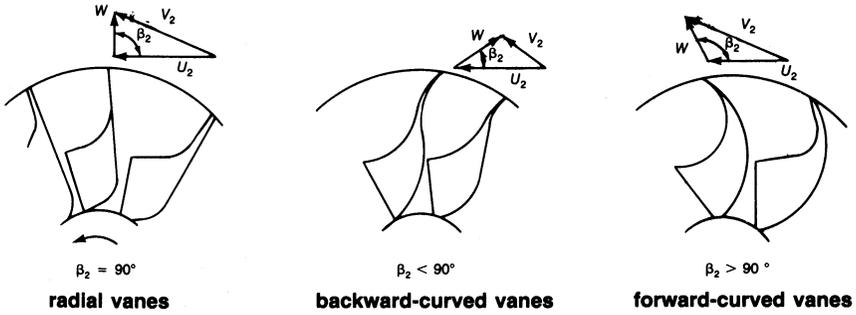


Figure 6-8. Various types of impeller blading.

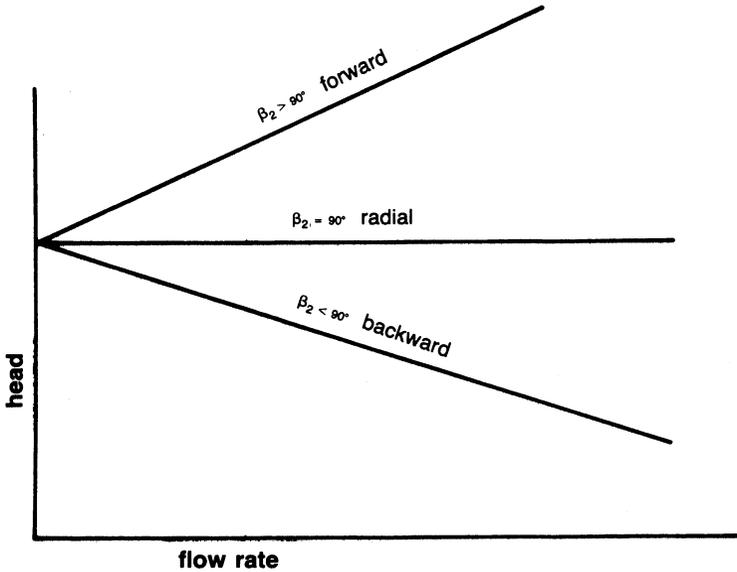


Figure 6-9. Head flow-rate characteristics for various outlet blade angles.

$\beta_2 = 90^\circ$ are radial vanes. Impellers with $\beta_2 < 90^\circ$ are backward-curved or backward-swept vanes, and for $\beta_2 > 90^\circ$, the vanes are forward-curved or forward-swept. They have different characteristics of theoretical head-flow relationship to each other, as shown in Figure 6-9. Although in Figure 6-9 the forward-curved head is the largest, in actual practice the head characteristics of all the impellers are similar to the backward-curved impeller. Table 6-1 shows the advantages and disadvantages of various impellers.

Table 6-1
The Advantages and Disadvantages of Various Impellers

| Types of Impellers | Advantages | Disadvantages |
|------------------------------|---|---|
| <i>Radial vanes</i> | <ol style="list-style-type: none"> 1. Reasonable compromise between low energy transfer and high absolute outlet velocity 2. No complex bending stress 3. Easy manufacturing | <ol style="list-style-type: none"> 1. Surge margin is relatively narrow |
| <i>Backward-curved vanes</i> | <ol style="list-style-type: none"> 1. Low-outlet kinetic energy = low-diffuser inlet mach number 2. Surge margin is wide | <ol style="list-style-type: none"> 1. Low-energy transfer 2. Complex bending stress 3. Hard manufacturing |
| <i>Forward-curved vanes</i> | <ol style="list-style-type: none"> 1. High-energy transfer | <ol style="list-style-type: none"> 1. High-outlet kinetic energy = High-diffuser inlet mach number. 2. Surge margin is less than radial vanes 3. Complex bending stress 4. Hard manufacturing |

The Euler equation, assuming simple one-dimensional flow theory, is the theoretical amount of work imparted to each pound of fluid as it passes through the impeller, and it is given by

$$H = \frac{1}{g_c} [U_1 V_{\theta 1} - U_2 V_{\theta 2}] \quad (6-1)$$

where:

H = work per lb of fluid

U_2 = impeller peripheral velocity

U_1 = inducer velocity at the mean radial station

$V_{\theta 2}$ = absolute tangential fluid velocity at impeller exit

$V_{\theta 1}$ = absolute tangential air velocity at inducer inlet

For the axial inlet,

$$V_{\theta 1} = 0$$

Then

$$H = -\frac{1}{g_c} (U_2 V_{\theta 2}) \quad (6-2)$$

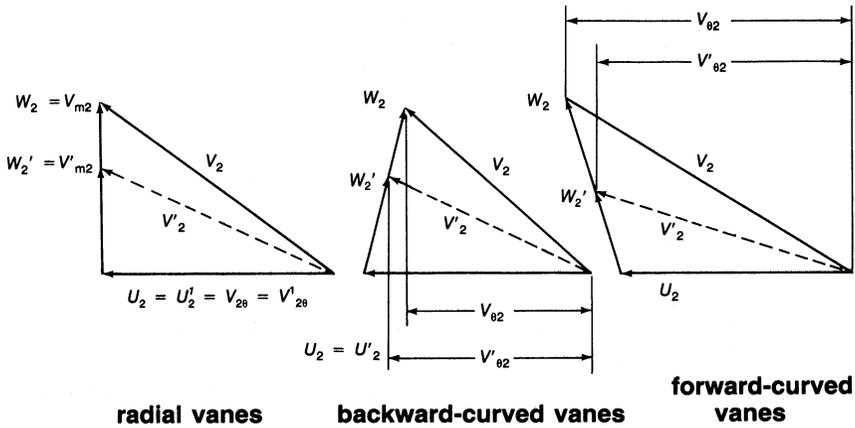


Figure 6-10. Velocity triangles.

Supposing constant rotational speeds, no slip, and an axial inlet, the velocity triangles are as shown in Figure 6-10. For the radial vane, the absolute tangential fluid velocity at the impeller exit is constant—even if the flow rate is increased or decreased.

Therefore,

$$H \approx \underbrace{U_2 V''_{\theta 2}}_{\substack{\text{flow} \\ \text{decrease}}} \approx \underbrace{U_2 V_{\theta 2}}_{\substack{\text{flow} \\ \text{increase}}} \approx \underbrace{U_2 V'_{\theta 2}}_{\substack{\text{flow} \\ \text{increase}}} \quad (6-3)$$

For backward-curved vanes, the absolute tangential fluid velocity at the impeller exit increases with the reduction of flow rates and decreases with the increase in flow rate as shown in the following equation:

$$H \approx \underbrace{-U_2 V''_{\theta 2}}_{\substack{\text{flow} \\ \text{decrease}}} > \underbrace{-U_2 V_{\theta 2}}_{\substack{\text{flow} \\ \text{increase}}} < \underbrace{-U_2 V'_{\theta 2}}_{\substack{\text{flow} \\ \text{increase}}} \quad (6-4)$$

For forward-curved vanes, the absolute tangential fluid velocity at the impeller exit decreases with the reduction of flow rates and increases with the decrease in flow rate as shown in the following equation:

$$H \approx \underbrace{-U_2 V''_{\theta}}_{\substack{\text{flow} \\ \text{decrease}}} < \underbrace{U_2 V_{\theta 2}}_{\substack{\text{flow} \\ \text{increase}}} > \underbrace{U_2 V'_{\theta}}_{\substack{\text{flow} \\ \text{increase}}} \quad (6-5)$$

Inlet Guide Vanes

The inlet guide vanes give circumferential velocity to the fluid at the inducer inlet. This function is called prewhirl. Figure 6-11 shows inducer inlet velocity diagrams with and without IGVs.

IGVs are installed directly in front of the inducer or, where an axial entry is not possible, located radially in an intake duct.

A positive vane angle produces prewhirl in the direction of the impeller rotation, and a negative vane angle produces prewhirl in the opposite direction. The disadvantage of positive prewhirl is that a positive inlet whirl velocity reduces the energy transfer. Since $V_{\theta 1}$ is positive according to the Euler equation defined by

$$H = \frac{1}{g_c} [U_1 V_{\theta 1} - U_2 V_{\theta 2}] \tag{6-6}$$

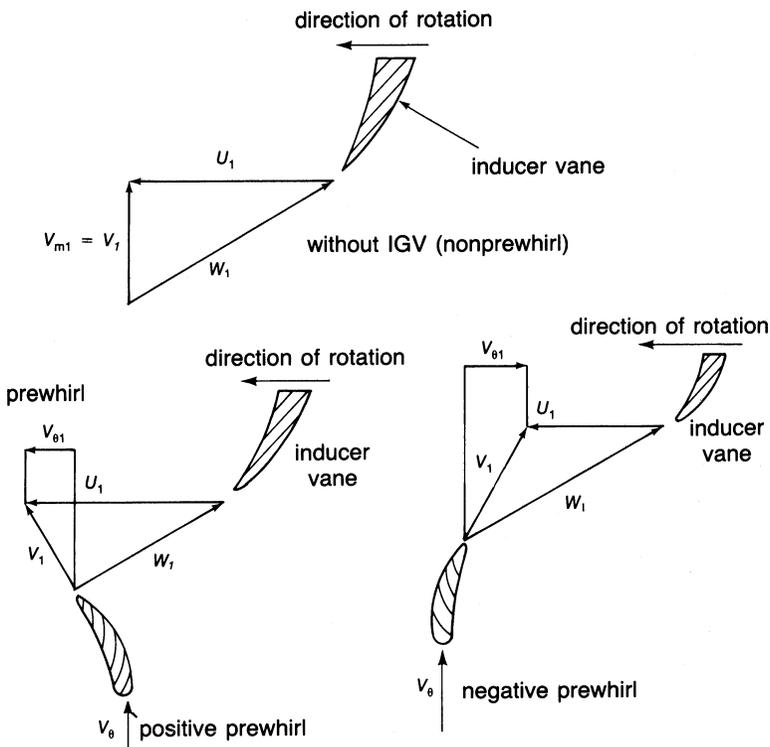


Figure 6-11. Inducer inlet velocity diagrams.

For nonprewhirl (without IGVs axial entry), $V_{\theta 1}$ is equal to zero. Then the Euler work is $H = -U_2 V_{\theta 2}$.

With positive prewhirl, the first term of the Euler equation remains $H = U_1 V_{\theta 1} - U_2 V_{\theta 2}$. Therefore, Euler work is reduced by the use of positive prewhirl. On the other hand, negative prewhirl increases the energy transfer by the amount $U_1 V_{\theta 1}$. This results in a larger pressure head being produced in the case of the negative prewhirl for the same impeller diameter and speed.

The positive prewhirl decreases the relative Mach number at the inducer inlet. However, negative prewhirl increases it. A relative Mach number is defined by

$$M_{rel} = \frac{W_1}{a_1} \tag{6-7}$$

where:

M_{rel} = relative Mach number

W_1 = relative velocity at an inducer inlet

a_1 = sonic velocity at inducer inlet conditions

The purpose of installing the IGVs is to decrease the relative Mach number at the inducer-tip (impeller eye) inlet because the highest relative velocity at the inducer inlet is at the tip section. When the relative velocity is

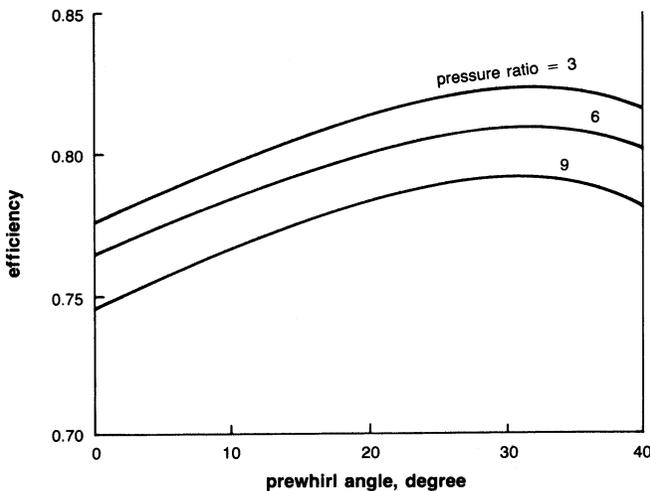


Figure 6-12. Estimated effect of inlet prewhirl. (Rodgers, C. and Shapiro, L., “Design Considerations for High-Pressure-Ratio Centrifugal Compressors,” ASME Paper No.: 73-GT-31.)

close to the sonic velocity or greater than it, a shock wave takes place in the inducer section. A shock wave produces shock loss and chokes the inducer. Figure 6-12 shows the effect of inlet prewhirl on compressor efficiency.

There are three kinds of prewhirl:

1. *Free-vortex prewhirl.* This type is represented by $r_1 V_{\theta 1} = \text{constant}$ with respect to the inducer inlet radius. This prewhirl distribution is shown in Figure 6-13. $V_{\theta 1}$ is at a minimum at the inducer inlet shroud radius. Therefore, it is not effective in decreasing the relative Mach number in this manner.
2. *Forced-vortex prewhirl.* This type is shown as $V_{\theta 1}/r_1 = \text{constant}$. This prewhirl distribution is also shown in Figure 6-14. $V_{\theta 1}$ is at a maximum at the inducer inlet shroud radius, contributing to a decrease in the inlet relative Mach number.

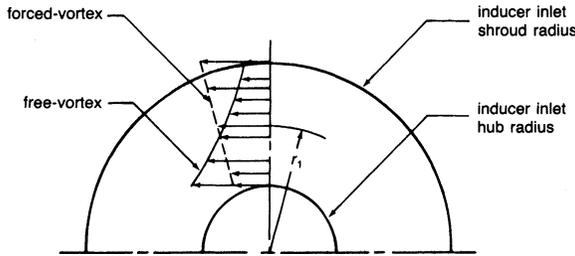


Figure 6-13. Prewhirl distribution patterns.

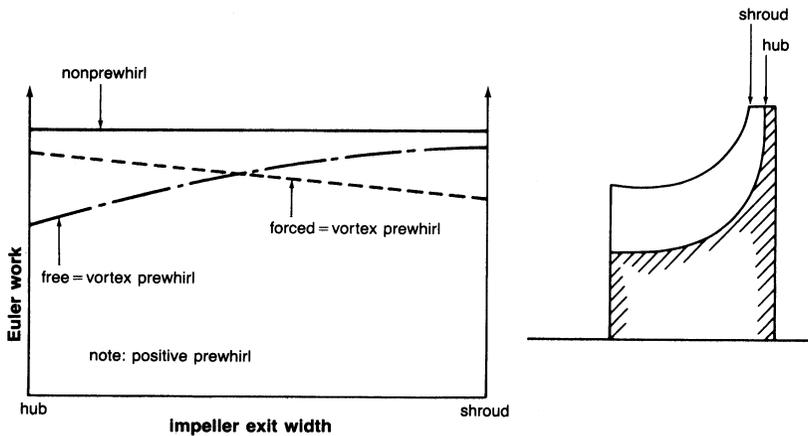


Figure 6-14. Euler work distribution at an impeller exit.

3. *Control-vortex prewhirl.* This type is represented by $V_{\theta 1} = AR_1 + B/r_1$, where A and B are constants. This equation shows the first type with $A = 0$, $B \neq 0$, and the second type with $B = 0$, $A \neq 0$.

Euler work distributions at an impeller exit, with respect to the impeller width, are shown in Figure 6-14. From Figure 6-14, the prewhirl distribution should be made not only from the relative Mach number at the inducer inlet shroud radius, but also from Euler work distribution at the impeller exit. Uniform impeller exit flow conditions, considering the impeller losses, are important factors in obtaining good compressor performance.

Impeller

An impeller in a centrifugal compressor imparts energy to a fluid. The impeller consists of two basic components: (1) an inducer like an axial-flow rotor, and (2) the radial blades where energy is imparted by centrifugal force. Flow enters the impeller in the axial direction and leaves in the radial direction. The velocity variations from hub to shroud resulting from these changes in flow directions complicate the design procedure for centrifugal compressors. C.H. Wu has presented the three-dimensional theory in an impeller, but it is difficult to solve for the flow in an impeller using the previous theory without certain simplified conditions. Others have dealt with it as a quasi-three-dimensional solution. It is composed of two solutions, one in the meridional surface (hub-to-shroud), and the other in the stream surface of revolution (blade-to-blade). These surfaces are illustrated in Figure 6-15.

By the application of the previous method using a numerical solution to the complex flow equations, it is possible to achieve impeller efficiencies of more than 90%. The actual flow phenomenon in an impeller is more complicated than the one calculated. One example of this complicated flow is shown in Figure 6-16. The stream lines observed in Figure 6-16 do not cross, but are actually in different planes observed near the shroud. Figure 6-17 shows the flow in the meridional plane with separation regions at the inducer section and at the exit.

Experimental studies of the flow within impeller passages have shown that the distribution of velocities on the blade surfaces are different from the distributions predicted theoretically. It is likely that the discrepancies between theoretical and experimental results are due to secondary flows from pressure losses and boundary-layer separation in the blade passages. High-performance impellers should be designed, when possible, with the aid of theoretical methods for determining the velocity distributions on the blade surfaces.

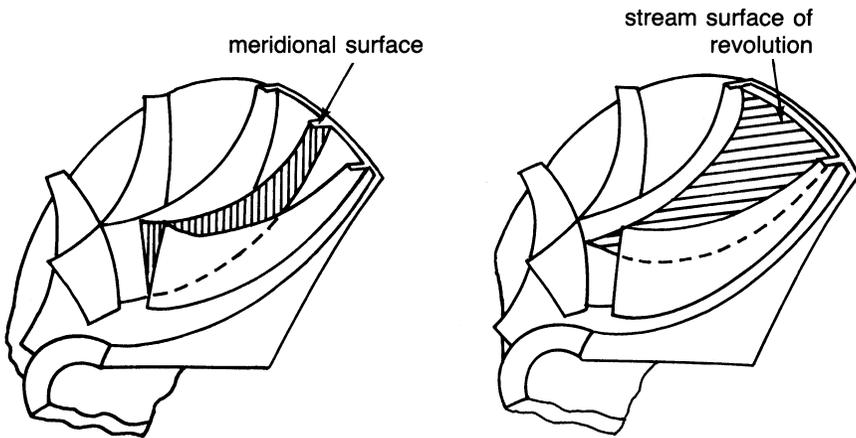


Figure 6-15. Two-dimensional surface for a flow analysis.

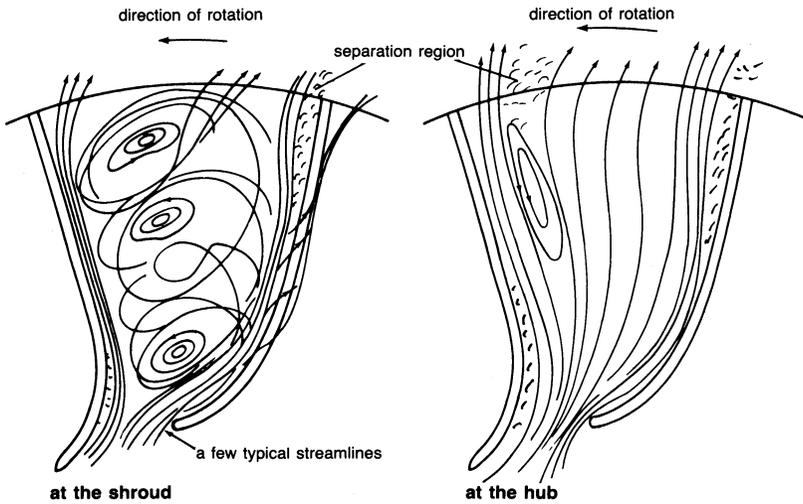


Figure 6-16. Flow map of impeller plane.

Examples of the theoretical velocity distributions in the impeller blades of a centrifugal compressor are shown in Figure 6-18. The blades should be designed to eliminate large decelerations or accelerations of flow in the impeller that lead to high losses and separation of the flow. Potential flow solutions predict the flow well in regions away from the blades where

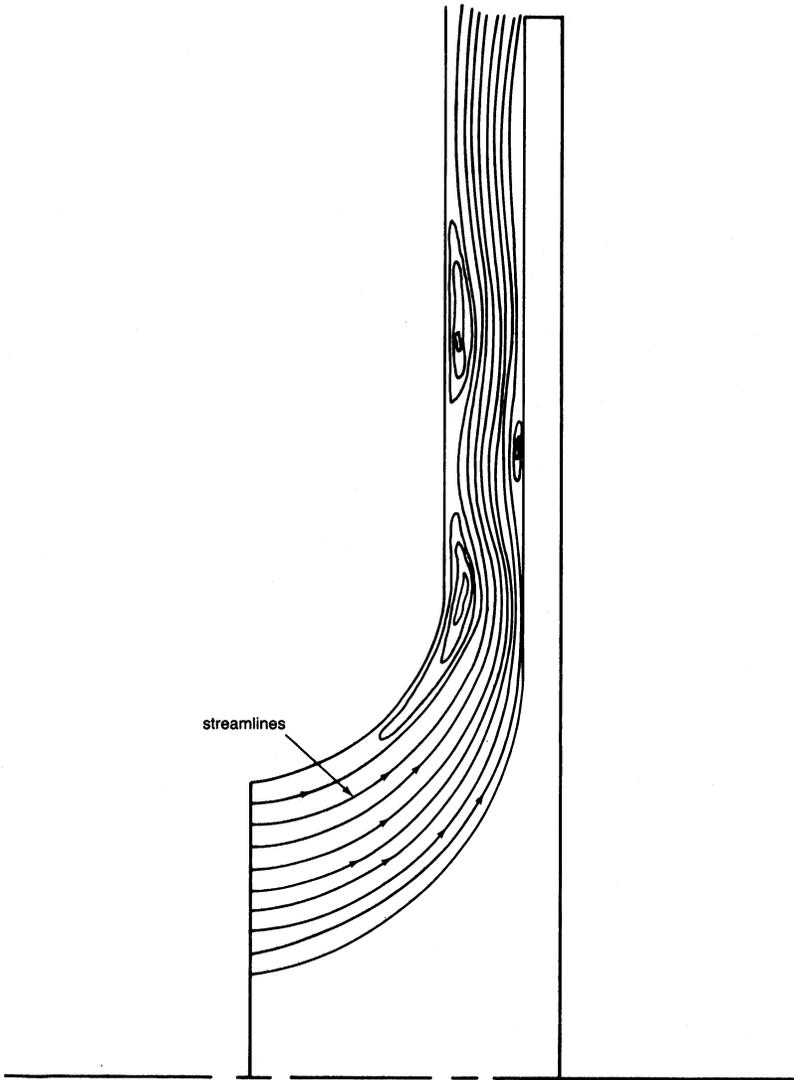


Figure 6-17. Flow map as seen in meridional plane.

boundary-layer effects are negligible. In a centrifugal impeller the viscous shearing forces create a boundary layer with reduced kinetic energy. If the kinetic energy is reduced below a certain limit, the flow in this layer becomes stagnant, then it reverses.

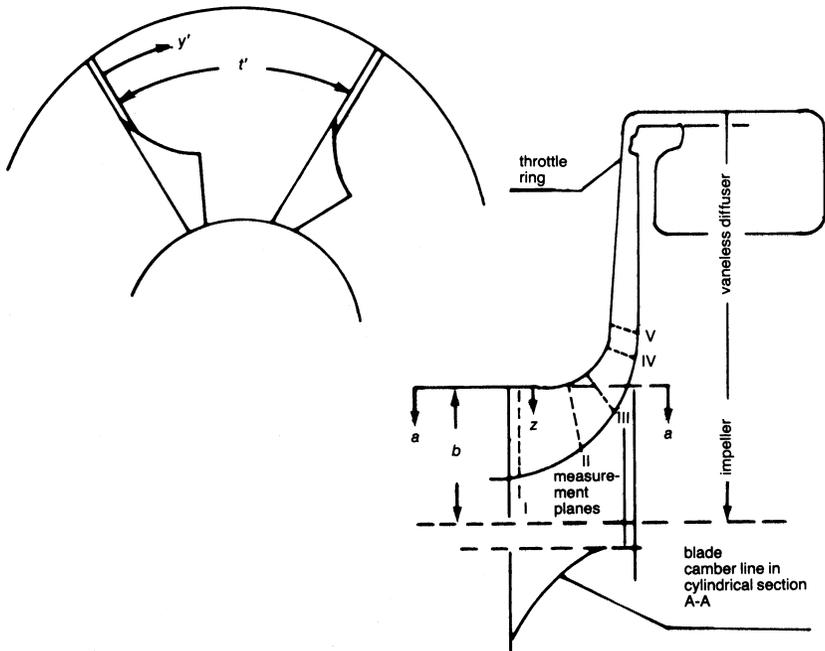
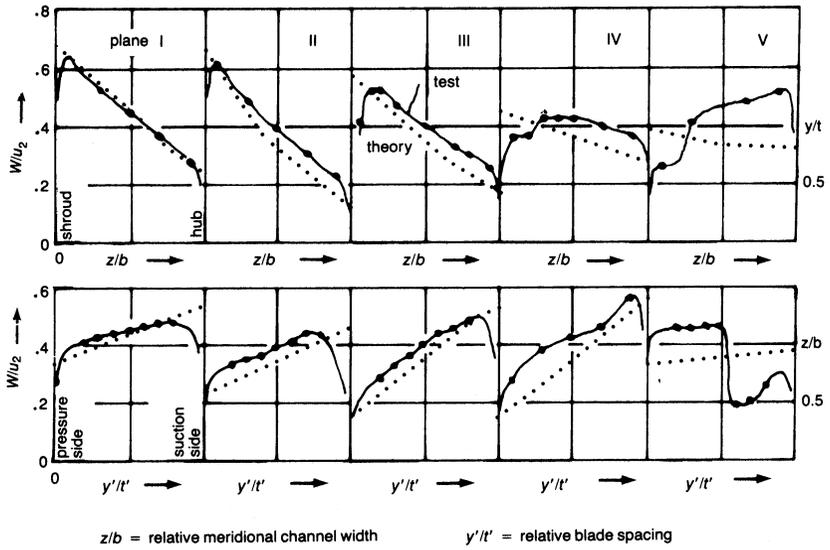


Figure 6-18. Velocity profiles through a centrifugal compressor.

Inducer

The function of an inducer is to increase the fluid's angular momentum without increasing its radius of rotation. In an inducer section the blades bend toward the direction of rotation as shown in Figure 6-19. The inducer is an axial rotor and changes the flow direction from the inlet flow angle to the axial direction. It has the largest relative velocity in the impeller and, if not properly designed, can lead to choking conditions at its throat as shown in Figure 6-19.

There are three forms of inducer camber lines in the axial direction. These are circular arc, parabolic arc, and elliptical arc. Circular arc camber lines are used in compressors with low pressure ratios, while the elliptical arc produces good performance at high pressure ratios where the flow has transonic mach numbers.

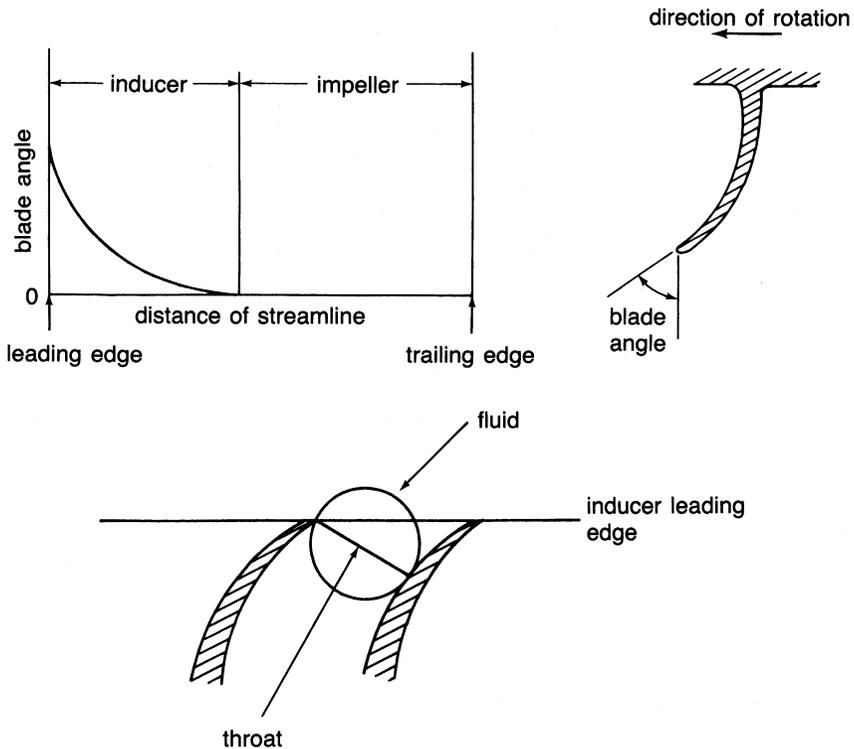


Figure 6-19. Inducer centrifugal compressor.

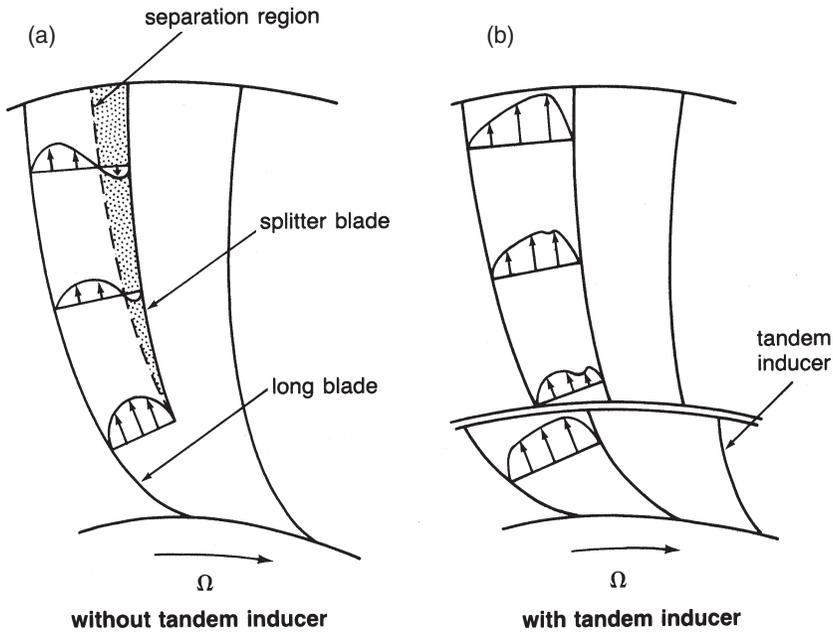


Figure 6-20. Impeller channel flow.

Because of choking conditions in the inducer, many compressors incorporate a splitter-blade design. The flow pattern in such an inducer section is shown in Figure 6-20a. This flow pattern indicates a separation on the suction side of the splitter blade. Other designs include tandem inducers. In tandem inducers the inducer section is slightly rotated as shown in Figure 6-20b. This modification gives additional kinetic energy to the boundary, which is otherwise likely to separate.

Centrifugal Section of an Impeller

The flow in this section of the impeller enters from the inducer section and leaves the impeller in the radial direction. The flow in this section is not completely guided by the blades, and hence the effective fluid outlet angle does not equal the blade outlet angle.

To account for flow deviation (which is similar to the effect accounted for by the deviation angle in axial-flow machines), the slip factor is used:

$$\mu = \frac{V_{\theta 2}}{V_{\theta 2\infty}} \quad (6-8)$$

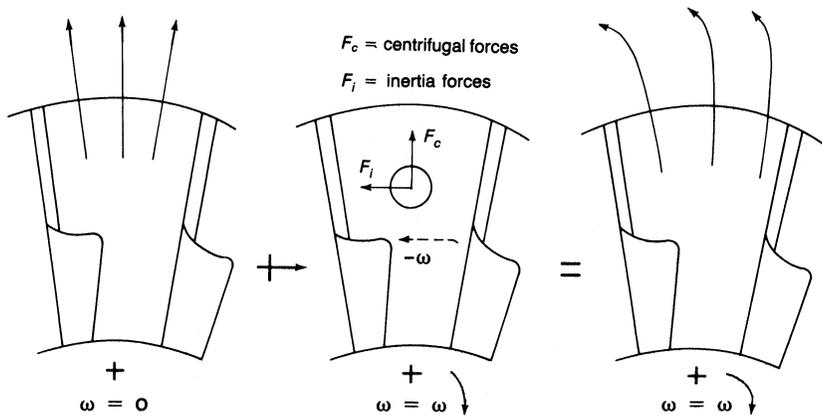


Figure 6-21. Forces and flow characteristics in a centrifugal compressor.

where $V_{\theta 2}$ is the tangential component of the absolute exit velocity with a finite number of blades, and $V_{\theta 2\infty}$ is the tangential component of the absolute exit velocity, if the impeller were to have an infinite number of blades (no slipping back of the relative velocity at outlet).

With radial blades at the exit,

$$\mu = \frac{V_{\theta 2}}{U_2} \tag{6-9}$$

Flow in a rotating impeller channel (blade passage) will be a vector sum of flow with the impeller stationary and the flow due to rotation of the impeller as seen in Figure 6-21.

In a stationary impeller, the flow is expected to follow the blade shape and exit tangentially to it. A high adverse pressure gradient along the blade passage and subsequent flow separation are not considered to be general possibilities.

Inertia and centrifugal forces cause the fluid elements to move closer to and along the leading surface of the blade toward the exit. Once out of the blade passage, where there is no positive impelling action present, these fluid elements slow down.

Causes of Slip in an Impeller

The definite cause of the slip phenomenon that occurs within an impeller is not known. However, some general reasons can be used to explain why the flow is changed.

Coriolis circulation. Because of the pressure gradient between the walls of two adjacent blades, the Coriolis forces, the centrifugal forces, and the fluid follow the Helmholtz vorticity law. The combined gradient that results causes a fluid movement from one wall to the other and vice versa. This movement sets up circulation within the passage as seen in Figure 6-22. Because of this circulation, a velocity gradient results at the impeller exit with a net change in the exit angle.

Boundary-layer development. The boundary layer that develops within an impeller passage causes the flowing fluid to experience a smaller exit area as shown in Figure 6-23. This smaller exit is due to small flow (if any) within the boundary layer. For the fluid to exit this smaller area, its velocity must increase. This increase gives a higher relative exit velocity.

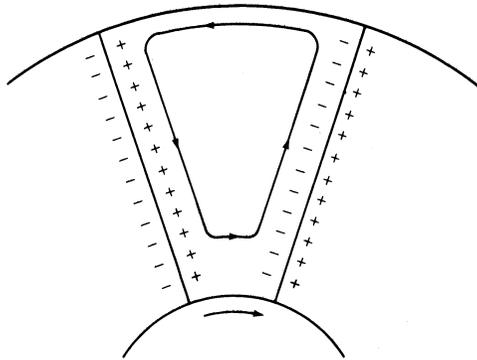


Figure 6-22. Coriolis circulation.

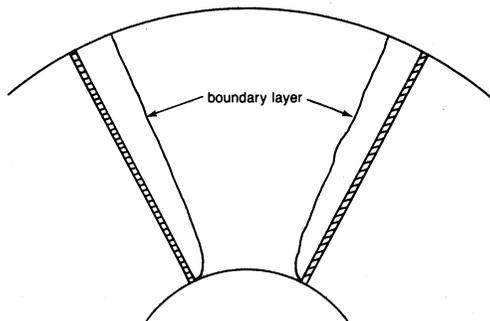


Figure 6-23. Boundary-layer development.

Since the meridional velocity remains constant, the increase in relative velocity must be accompanied with a decrease in absolute velocity.

Although it is not a new approach, boundary-layer control is being used more than ever before. It has been used with success on airfoil designs when it has delayed separation, thus giving a larger usable angle of attack. Control of the flow over an airfoil has been accomplished in two ways: by using slots through the airfoil and by injecting a stream of fast-moving air.

Separation regions are also encountered in the centrifugal impeller as shown previously. Applying the same concept (separation causes a loss in efficiency and power) reduces and delays their formation. Diverting the slow-moving fluid away lets the separation regions be occupied by a faster stream of fluid, which reduces boundary-layer build-up and thus decreases separation.

To control the boundary layer in the centrifugal impeller, slots in the impeller blading at the point of separation are used. To realize the full capability of this system, these slots should be directional and converging in a cross-sectional area from the pressure to the suction sides as seen in Figure 6-24. The fluid diverted by these slots increases in velocity and attaches itself to the suction sides of the blades. This results in moving the separation region closer to the tip of the impeller, thus reducing slip and losses encountered by the formation of large boundary-layer regions. The slots must be located at the point of flow separation from the blades. Experimental results indicate improvement in the pressure ratio, efficiency, and surge characteristics of the impeller as seen in Figure 6-24.

Leakage. Fluid flow from one side of a blade to the other side is referred to as leakage. Leakage reduces the energy transfer from impeller to fluid and decreases the exit velocity angle.

Number of vanes. The greater the number of vanes, the lower the vane loading, and the closer the fluid follows the vanes. With higher vane loadings, the flow tends to group up on the pressure surfaces and introduces a velocity gradient at the exit.

Vane thickness. Because of manufacturing problems and physical necessity, impeller vanes are thick. When fluid exits the impeller, the vanes no longer contain the flow, and the velocity is immediately slowed. Because it is the meridional velocity that decreases, both the relative and absolute velocities decrease, changing the exit angle of the fluid.

A backward-curved impeller blade combines all these effects. The exit velocity triangle for this impeller with the different slip phenomenon changes is shown in Figure 6-25. This triangle shows that actual operating conditions are far removed from the projected design condition.

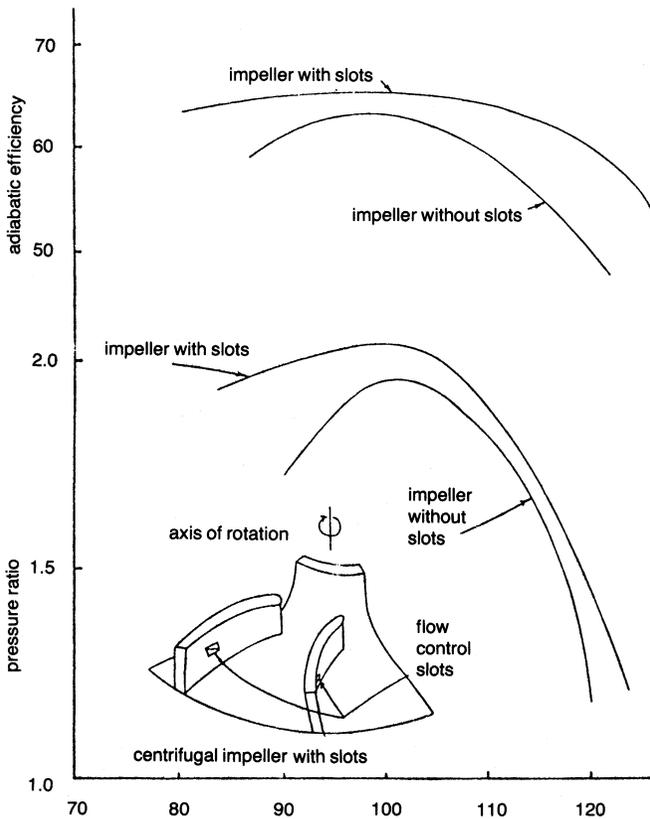
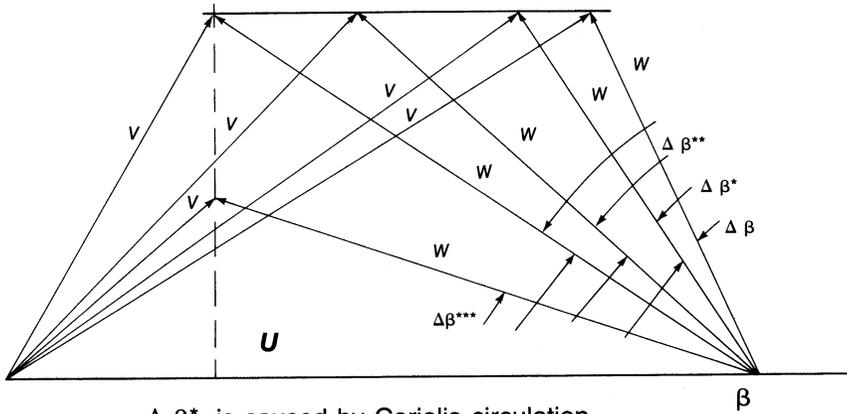


Figure 6-24. Percent design flow—laminar flow control in a centrifugal compressor.

Several empirical equations have been derived for the slip factor (see Figure 6-26). These empirical equations are limited. Two of the more common slip factors are presented here.

Stodola Slip Factor

The second Helmholtz law states that the vorticity of a frictionless fluid does not change with time. Hence, if the flow at the inlet to an impeller is irrotational, the absolute flow must remain irrotational throughout the impeller. As the impeller has an angular velocity ω , the fluid must have an angular velocity— ω relative to the impeller. This fluid motion is called the relative eddy. If there were no flow through the impeller, the fluid in the



- $\Delta \beta^*$ is caused by Coriolis circulation
- $\Delta \beta^{**}$ is caused by boundary-layer effects
- $\Delta \beta^{***}$ is caused by the blade thickness

Figure 6-25. Effect on exit velocity triangles by various parameters.

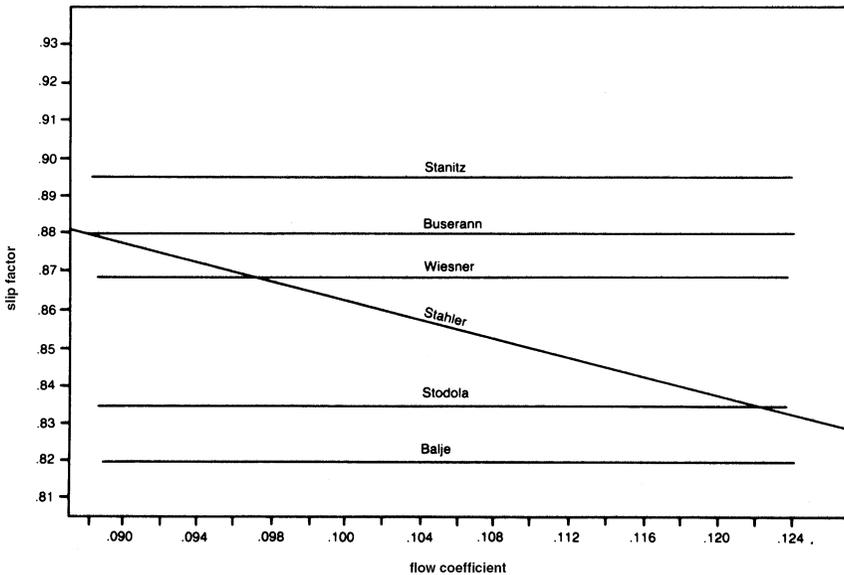


Figure 6-26. Various slip factors as a function of the flow coefficient.

impeller channels would rotate with an angular velocity equal and opposite to the impeller's angular velocity.

To approximate the flow, Stodola's theory assumes that the slip is due to the relative eddy. The relative eddy is considered as a rotation of a cylinder of fluid at the end of the blade passage at an angular velocity of $-\omega$ about its own axis. The Stodola slip factor is given by

$$\mu = 1 - \frac{\pi}{Z} \left[1 - \frac{\sin \beta_2}{\frac{V_{m2} \cot \beta_2}{U_2}} \right] \quad (6-10)$$

where:

- β_2 = the blade angle
- Z = the number of blades
- V_{m2} = the meridional velocity
- U_2 = blade tip speed.

Calculations using this equation have been found to be lower than experimental values.

Stanitz Slip Factor

Stanitz calculated blade-to-blade solutions for eight impellers and concluded that for the range of conditions covered by the solutions, U is a function of the number of blades (Z), and the blade exit angle (β_2) is approximately the same whether the flow is compressible or incompressible

$$\mu = 1 - \frac{0.63\pi}{Z} \left[1 - \frac{1}{\frac{W_{m2}}{U_2} \cot \beta_2} \right] \quad (6-11)$$

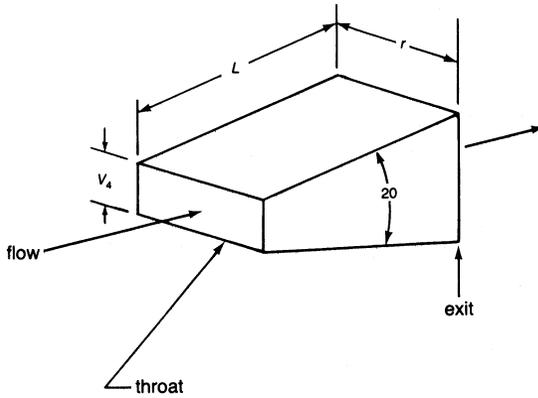
Stanitz's solutions were for $\pi/4 < \beta_2 < \pi/2$. This equation compares well with experimental results for radial or near-radial blades.

Diffusers

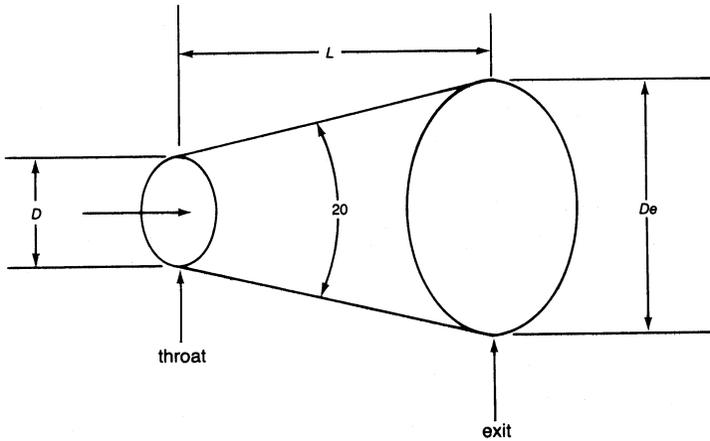
Diffusing passages have always played a vital role in obtaining good performance from turbomachines. Their role is to recover the maximum possible kinetic energy leaving the impeller with a minimum loss in total pressure. The efficiency of centrifugal compressor components has been steadily improved by advancing their performance. However, significant

further improvement in efficiency will be gained only by improving the pressure recovery characteristics of the diffusing elements of these machines, since these elements have the lowest efficiency.

The performance characteristics of a diffuser are complicated functions of diffuser geometry, inlet flow conditions, and exit flow conditions. Figure 6-27



(a) straight-wall rectangular diffuser



(b) straight-wall conical diffuser

Figure 6-27. Geometric classification of diffusers.

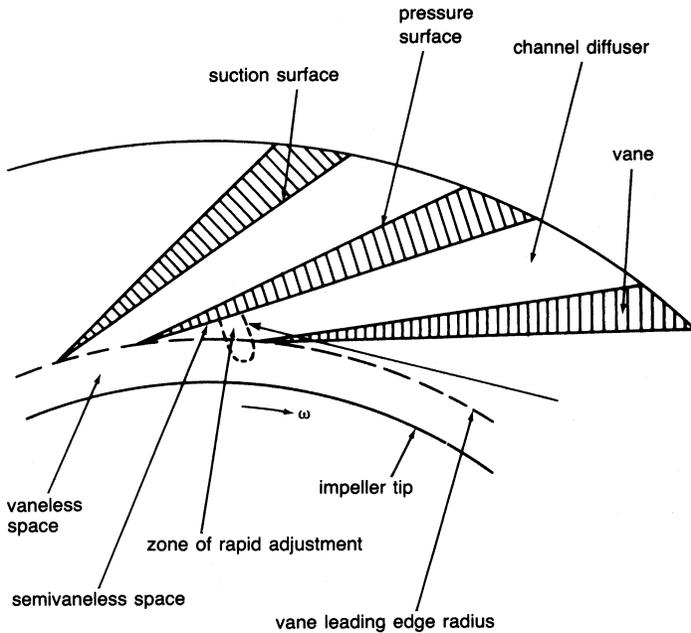


Figure 6-28. Flow regions of the vane diffuser.

shows typical diffusers classified by their geometry. The selection of an optimum channel diffuser for a particular task is difficult, since it must be chosen from an almost infinite number of cross-sectional shapes and wall configurations. In radial and mixed-flow compressors the requirement of high performance and compactness leads to the use of vane diffusers as shown in Figure 6-28. Figure 6-28 also shows the flow regime of a vane-island diffuser.

Matching the flow between the impeller and the diffuser is complex because the flow path changes from a rotating system into a stationary one. This complex, unsteady flow is strongly affected by the jet-wake of the flow leaving the impeller, as seen in Figure 6-29. The three-dimensional boundary layers, the secondary flows in the vaneless region, and the flow separation at the blades also affects the overall flow in the diffuser.

The flow in the diffuser is usually assumed to be of a steady nature to obtain the overall geometric configuration of the diffuser. In a channel-type diffuser the viscous shearing forces create a boundary layer with reduced kinetic energy. If the kinetic energy is reduced below a certain limit, the flow in this layer becomes stagnant and then reverses. This flow reversal causes

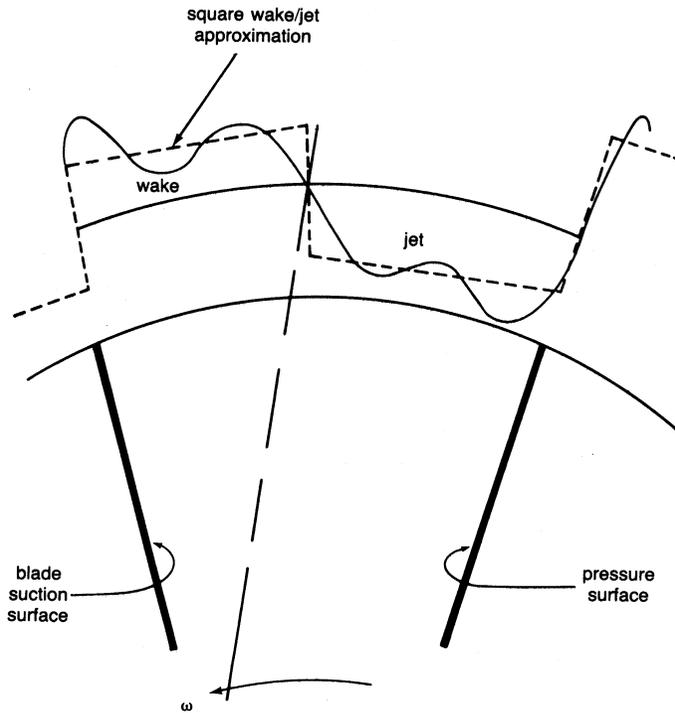


Figure 6-29. Jet-wake flow distribution from an impeller.

separation in a diffuser passage, which results in eddy losses, mixing losses, and changed-flow angles. Separation should be avoided or delayed to improve compressor performance.

The high-pressure-ratio centrifugal compressor has a narrow yet stable operating range. This operating range is due to the close proximity of the surge and choke flow limits. The word “surge” is widely used to express unstable operation of a compressor. Surge is the flow breakdown period during unstable operation. The unsteady flow phenomena during the onset of surge in a high-pressure-ratio centrifugal compressor causes the mass flow throughout the compressor to oscillate during supposedly “stable” operations. The throat pressure in the diffuser increases during the precursor period up to collector pressure P_{col} at the beginning of surge. All pressure traces (except plenum pressure) suddenly drop at the surge point. The sudden change of pressure can be explained by the measured occurrence of backflow from the collector through the impeller during the period between the two sudden changes.

Scroll or Volute

The purpose of the volute is to collect the fluid leaving the impeller or diffuser, and deliver it to the compressor outlet pipe. The volute has an important effect on the overall efficiency of the compressor. Volute design embraces two schools of thought. First, the angular momentum of the flow in the volute is constant, neglecting any friction effects. The tangential velocity $V_{5\theta}$ is the velocity at any radius in the volute. The following equation shows the relationship if the angular momentum is held constant

$$V_{5\theta}r = \text{constant} = K \quad (6-12)$$

Assuming no leakage past the tongue and a constant pressure around the impeller periphery, the relationship of flow at any section Q_θ to the overall flow in the impeller Q is given by

$$Q_\theta = \frac{\theta}{2\pi} Q \quad (6-13)$$

Thus, the area distribution at any section θ can be given by the following relationship:

$$A_\theta = Qr \times \frac{\theta}{2\pi} \times \frac{L}{K} \quad (6-14)$$

where:

r = radius to the center of gravity

L = volume width

Second, design the volute by assuming that the pressure and velocity are independent of θ . The area distribution in the volute is given by

$$A_\theta = K \frac{Q}{V_{5\theta}} \frac{\theta}{2\pi} \quad (6-15)$$

To define the volute section at a given θ , the shape and area of the section must be decided. Flow patterns in various types of volute are shown in Figure 6-30. The flow in the asymmetrical volute has a single-vortex instead of the double-vortex in the symmetrical volute. Where the impeller is discharging directly into the volute, it is better to have the volute width larger than the impeller width. This enlargement results in the flow from the

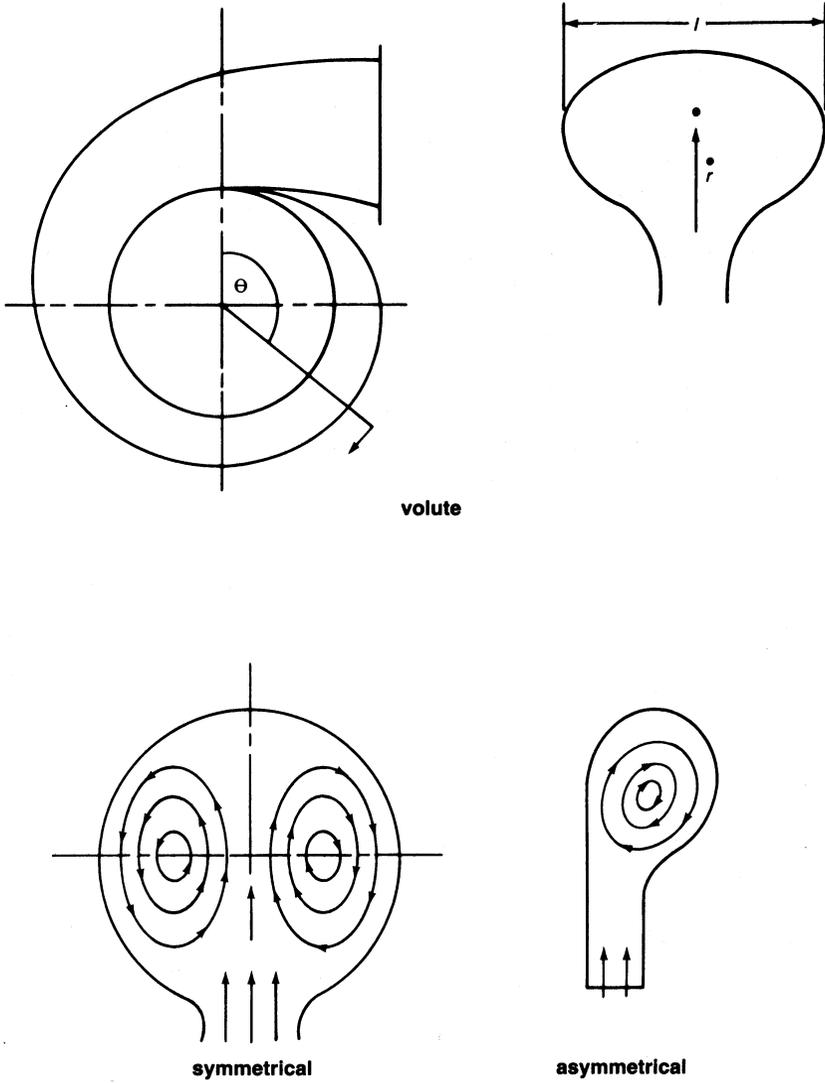


Figure 6-30. Flow patterns in volute.

impeller being bounded by the vortex generated from the gap between the impeller and the casing.

At flows different from design conditions, there exists a circumferential pressure gradient at the impeller tip and in the volute at a given radius.

At low flows, the pressure rises with the peripheral distance from the volute tongue. At high flows, the pressure falls with distance from the tongue. This condition results because near the tongue the flow is guided by the outer wall of the passage. The circumferential pressure gradients reduce efficiency away from the design point. Nonuniform pressure at the impeller discharge results in unsteady flows in the impeller passage, causing flow reversal and separation in the impeller.

Centrifugal Compressor Performance

Calculating the performance of a centrifugal compressor in both design and off-design conditions requires a knowledge of various losses encountered in a centrifugal compressor.

The accurate calculation and proper evaluation of losses within a centrifugal compressor is as important as the calculation of the blade-loading parameters. If the proper parameters are not controlled, efficiency decreases. The evaluation of various losses is a combination of experimental results and theory. The losses are divided into two groups: (1) losses encountered in the rotor, and (2) losses encountered in the stator.

A loss is usually expressed as a loss of heat or enthalpy. A convenient way to express them is in a nondimensional manner with reference to the exit blade speed. The theoretical total head available (q_{tot}) is equal to the head available from the energy equation

$$q_{\text{th}} = \frac{1}{U_2^2} (U_2 V_{\theta 2} - U_1 V_{\theta 1}) \quad (6-16)$$

plus the head, which is lost because of disc friction (Δq_{df}) and resulting from any recirculation (Δq_{rc}) of the air back into the rotor from the diffuser

$$q_{\text{tot}} = q_{\text{th}} + \Delta q_{\text{df}} + \Delta q_{\text{rc}} \quad (6-17)$$

The adiabatic head that is actually available at the rotor discharge is equal to the theoretical head minus the heat from the shock in the rotor (Δq_{sh}), the inducer loss (Δq_{in}), the blade loadings (Δq_{bl}), the clearance between the rotor and the shroud (Δq_c), and the viscous losses encountered in the flow passage (Δq_{sf})

$$q_{\text{ia}} = q_{\text{th}} - \Delta q_{\text{in}} - \Delta q_{\text{sh}} - \Delta q_{\text{bl}} - \Delta q_c - \Delta q_{\text{sf}} \quad (6-18)$$

Therefore, the adiabatic efficiency in the impeller is

$$\eta_{\text{imp}} = \frac{q_{\text{ia}}}{q_{\text{tot}}} \quad (6-19)$$

The calculation of the overall stage efficiency must also include losses encountered in the diffuser. Thus, the overall actual adiabatic head attained will be the actual adiabatic head of the impeller minus the head losses encountered in the diffuser from wake caused by the impeller blade (Δq_w), the loss of part of the kinetic head at the exit of the diffuser (Δq_{ed}), and the loss of head from frictional forces (Δq_{osf}) encountered in the vaned or vaneless diffuser space

$$q_{\text{oa}} = q_{\text{ia}} - \Delta q_w - \Delta q_{\text{ed}} - \Delta q_{\text{osf}} \quad (6-20)$$

The overall adiabatic efficiency in an impeller is given by the following relationship:

$$\eta_{\text{ov}} = \frac{q_{\text{oa}}}{q_{\text{tot}}} \quad (6-21)$$

The individual losses can now be computed. These losses are broken up into two categories: (1) losses in the rotor, and (2) losses in the diffuser.

Rotor Losses

Rotor losses are divided into the following categories:

Shock in rotor losses. This loss is due to shock occurring at the rotor inlet. The inlet of the rotor blades should be wedgelike to sustain a weak oblique shock, and then gradually expanded to the blade thickness to avoid another shock. If the blades are blunt, a bow shock will result, causing the flow to detach from the blade wall and the loss to be higher.

Incidence loss. At off-design conditions, flow enters the inducer at an incidence angle that is either positive or negative, as shown in Figure 6-31. A positive incidence angle causes a reduction in flow. Fluid approaching a blade at an incidence angle suffers an instantaneous change of velocity at the blade inlet to comply with the blade inlet angle. Separation of the blade can create a loss associated with this phenomenon.

Disc friction loss. This loss results from frictional torque on the back surface of the rotor as seen in Figure 6-32. This loss is the same for a given

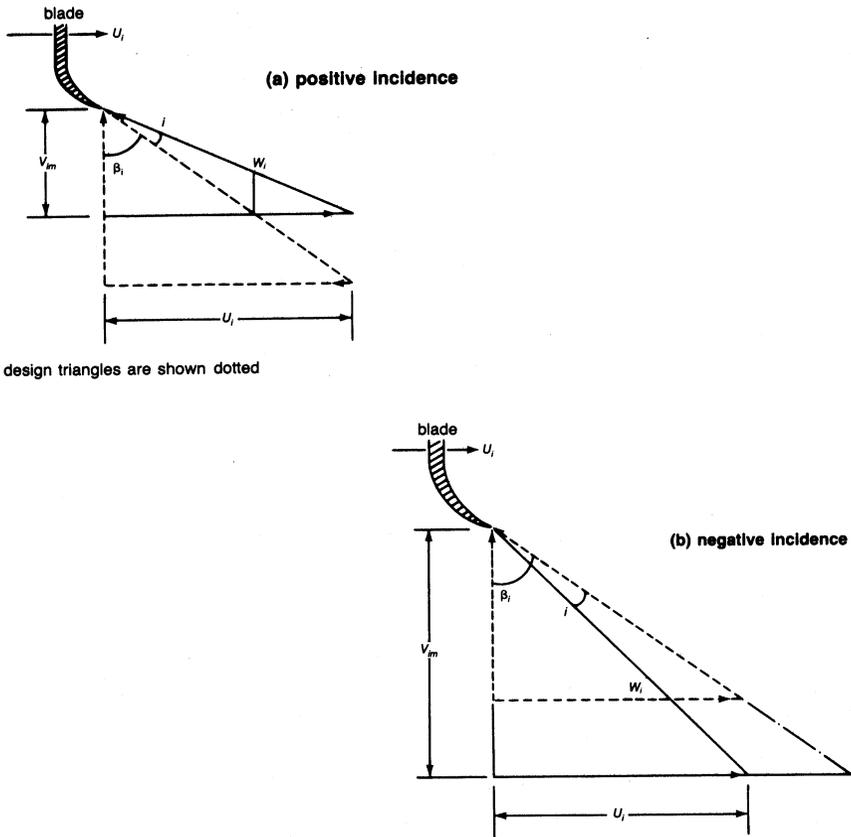


Figure 6-31. Inlet velocity triangles at nonzero incidents.

size disc whether it is used for a radial-inflow compressor or a radial-inflow turbine. Losses in the seals, bearings, and gear box are also lumped in with this loss, and the entire loss can be called an external loss. Unless the gap is of the magnitude of the boundary layer, the effect of the gap size is negligible. The disc friction in a housing is less than that on a free disc due to the existence of a “core,” which rotates at half the angular velocity.

Diffusion-blading loss. This loss develops because of negative velocity gradients in the boundary layer. Deceleration of the flow increases the boundary layer and gives rise to separation of the flow. The adverse pressure gradient that a compressor normally works against increases the chances of separation and causes significant loss.

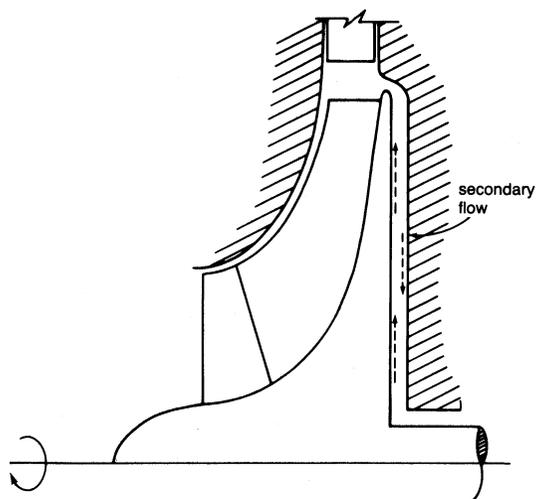


Figure 6-32. Secondary flow at the back of an impeller.

Clearance loss. When a fluid particle has a translatory motion relative to a noninertial rotating coordinate system, it experiences the Coriolis force. A pressure difference exists between the driving and trailing faces of an impeller blade caused by Coriolis acceleration. The shortest and least resistant path for the fluid to flow and neutralize this pressure differential is provided by the clearance between the rotating impeller and the stationary casing. With shrouded impellers, such a leakage from the pressure side to the suction side of an impeller blade is not possible. Instead, the existence of a pressure gradient in the clearance between the casing and the impeller shrouds, predominant along the direction shown in Figure 6-33, accounts for the clearance loss. Tip seals at the impeller eye can reduce this loss considerably.

This loss may be quite substantial. The leaking flow undergoes a large expansion and contraction caused by temperature variation across the clearance gap that affects both the leaking flow and the stream into which it discharges.

Skin friction loss. Skin friction loss is the loss from the shear forces on the impeller wall caused by turbulent friction. This loss is determined by considering the flow as an equivalent circular cross section with a hydraulic diameter. The loss is then computed based on well-known pipe flow pressure loss equations.

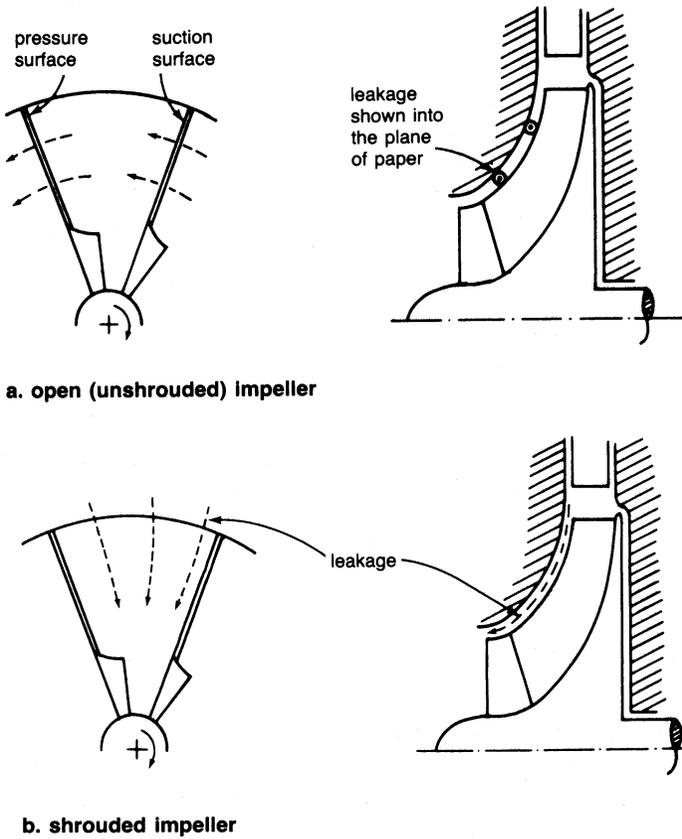


Figure 6-33. Leakage affecting clearance loss.

Stator Losses

Recirculating loss. This loss occurs because of backflow into the impeller exit of a compressor and is a direct function of the air exit angle. As the flow through the compressor decreases, there is an increase in the absolute flow angle at the exit of the impeller as seen in Figure 6-34. Part of the fluid is recirculated from the diffuser to the impeller, and its energy is returned to the impeller.

Wake-mixing loss. This loss is from the impeller blades, and it causes a wake in the vaneless space behind the rotor. It is minimized in a diffuser, which is symmetric around the axis of rotation.

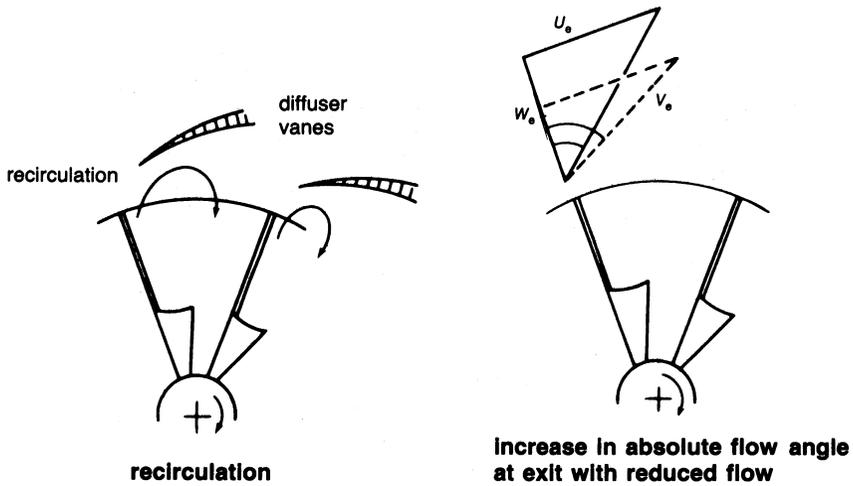


Figure 6-34. Recirculating loss.

Vaneless diffuser loss. This loss is experienced in the vaneless diffuser and results from friction and the absolute flow angle.

Vaned diffuser loss. Vaned diffuser losses are based on conical diffuser test results. They are a function of the impeller blade loading and the vaneless space radius ratio. They also take into account the blade incidence angle and skin friction from the vanes.

Exit loss. The exit loss assumes that one-half of the kinetic energy leaving the vaned diffuser is lost.

Losses are complex phenomena and as discussed here are a function of many factors, including inlet conditions, pressure ratios, blade angles, and flow. Figure 6-35 shows the losses distributed in a typical centrifugal stage of pressure ratio below 2:1 with backward-curved blades. This figure is only a guideline.

Compressor Surge

A plot showing the variation of total pressure ratio across a compressor as a function of the mass flow rate through it at various speeds is known as a performance map. Figure 6-36 shows such a plot.

The actual mass flow rates and speeds are corrected by factors $(\sqrt{\theta}/\delta)$ and $(1/\sqrt{\theta})$, respectively, to account for variation in the inlet conditions of temperature and pressure. The surge line joins the different speed lines where

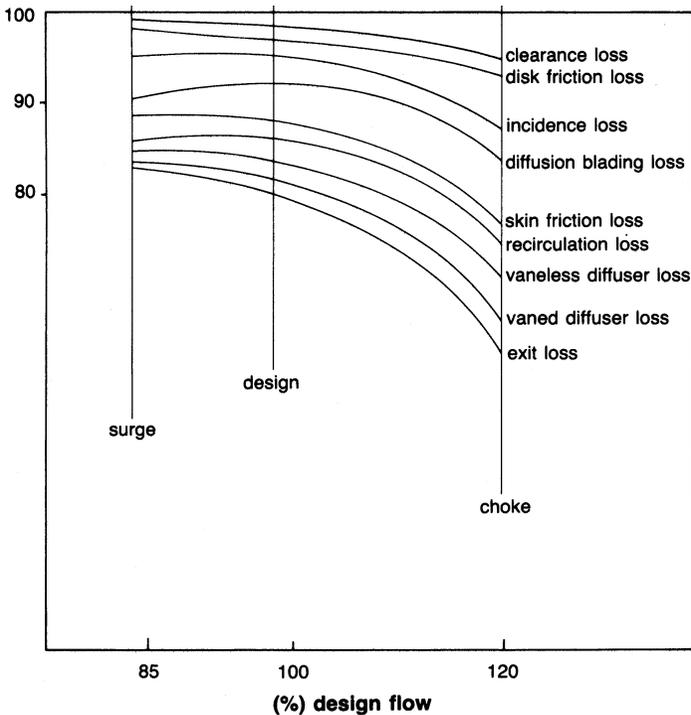


Figure 6-35. Losses in a centrifugal compressor.

the compressor's operation becomes unstable. A compressor is in "surge" when the main flow through the compressor reverses its direction and flows from the exit to the inlet for short time intervals. If allowed to persist, this unsteady process may result in irreparable damage to the machine. Lines of constant adiabatic efficiency (sometimes called efficiency islands) are also plotted on the compressor map. A condition known as "choke" or "stone walling" is indicated on the map, showing the maximum mass flow rate possible through the compressor at that operating speed.

Compressor surge is a phenomenon of considerable interest, yet it is not fully understood. It is a form of unstable operation and should be avoided in both design and operation. Surge has been traditionally defined as the lower limit of stable operation in a compressor and involves the reversal of flow. This reversal of flow occurs because of some kind of aerodynamic instability within the system. Usually a part of the compressor is the cause of the aerodynamic instability, although it is possible that the system arrangement could be capable of augmenting this instability. Figure 6-36 shows a typical

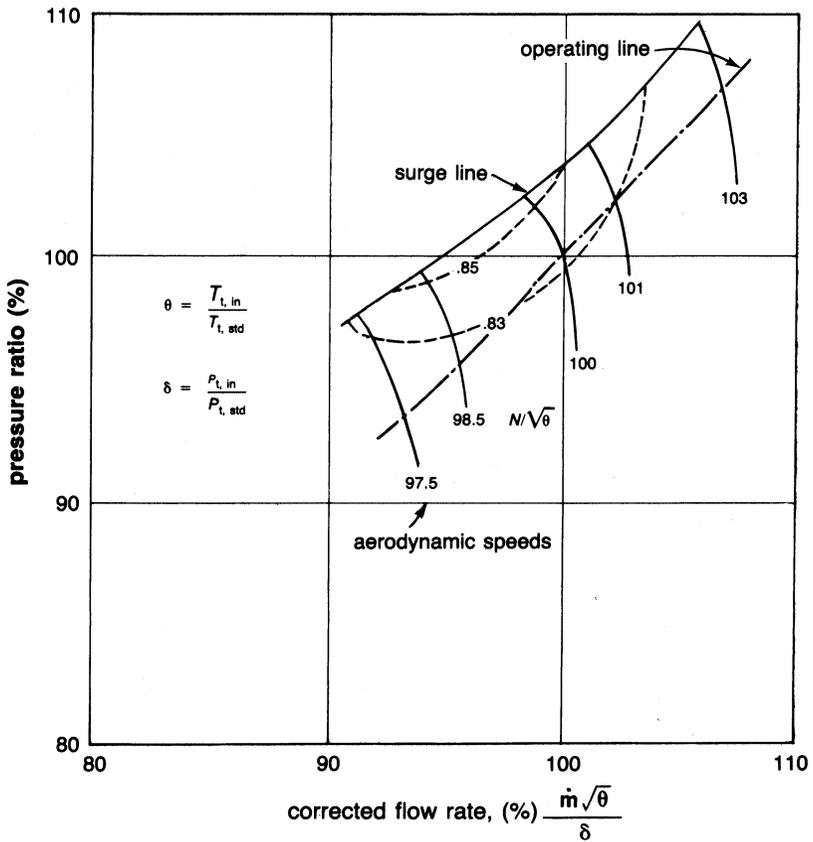


Figure 6-36. Typical compressor performance map.

performance map for a centrifugal compressor with efficiency islands and constant aerodynamic speed lines. The total pressure ratio can be seen to change with flow and speed. Compressors are usually operated at a working line separated by some safety margin from the surge line.

Surge is often symptomized by excessive vibration and an audible sound; however, there have been cases in which surge problems that were not audible have caused failures. Extensive investigations have been conducted on surge. Poor quantitative universality of aerodynamic loading capacities of different diffusers and impellers, and an inexact knowledge of boundary-layer behavior make the exact prediction of flow in turbomachines at the design stage difficult. However, it is quite evident that the underlying cause of surge is aerodynamic stall. The stall may occur in either the impeller or the diffuser.

When the impeller seems to be the cause of surge, the inducer section is where the flow separation begins. A decrease in the mass flow rate, an increase in the rotational speed of the impeller, or both can cause the compressor to surge.

Surge can be initiated in the diffuser by flow separation occurring at the diffuser entrance. A diffuser usually consists of a vaneless space with the prediffuser section before the throat containing the initial portion of the vanes in a vaned diffuser. The vaneless space accepts the velocity generated by the centrifugal impeller and diffuses the flow so that it enters the vaned diffuser passage at a lower velocity, avoiding any shock losses and resultant separation of the flow. When the vaneless diffuser stalls, the flow will not enter the throat. A separation occurs, causing the flow to finally reverse and surge the compressor. Stalling of the vaneless diffuser can be accomplished in two ways—by increasing impeller speed or decreasing the flow rate.

Whether surge is caused by a decrease in flow velocity or an increase in rotational speeds, either the inducer or vaneless diffuser can stall. Which stalls first is difficult to determine, but considerable testing has shown that for a low-pressure-ratio compressor, the surge initiates in the diffuser section. For units with single-stage pressure ratios above 3:1, surge is probably initiated in the inducer.

Most centrifugal compressors have for the most part impellers with backward leaning impeller blades. Figure 6-37 depicts the effects of impeller blade angle on the stable range and shows the variance in steepness of the slope of the head-flow curve.

The three curves are based on the same speed and show actual head. The relationship of ideal or theoretical head to inlet flow for different blade angles would be represented by straight lines. For backward leaning blades, the slope of the line would be negative. The line for radial blades would be horizontal. Forward leaning blades would have a positively sloped line. For the average petrochemical process plant application, the compressor industry commonly uses a backward-leaning blade with an angle (β_2) of between about 55–75° (or backward leaning angle of 15–35°), because it provides a wider stable range and a steeper slope in the operating range. This impeller design has proven to be about the best compromise between pressure delivered, efficiency, and stability. Forward leaning blades are not commonly used in compressor design, since the high exit velocities lead to large diffuser losses. A plant air compressor operating at steady conditions from day to day would not require a wide stable range, but a machine in a processing plant can be the victim of many variables and upsets. So more stability is highly desirable. Actually, the lower curve in Figure 6-37 appears to have a more gentle slope than either the middle or upper curve. This

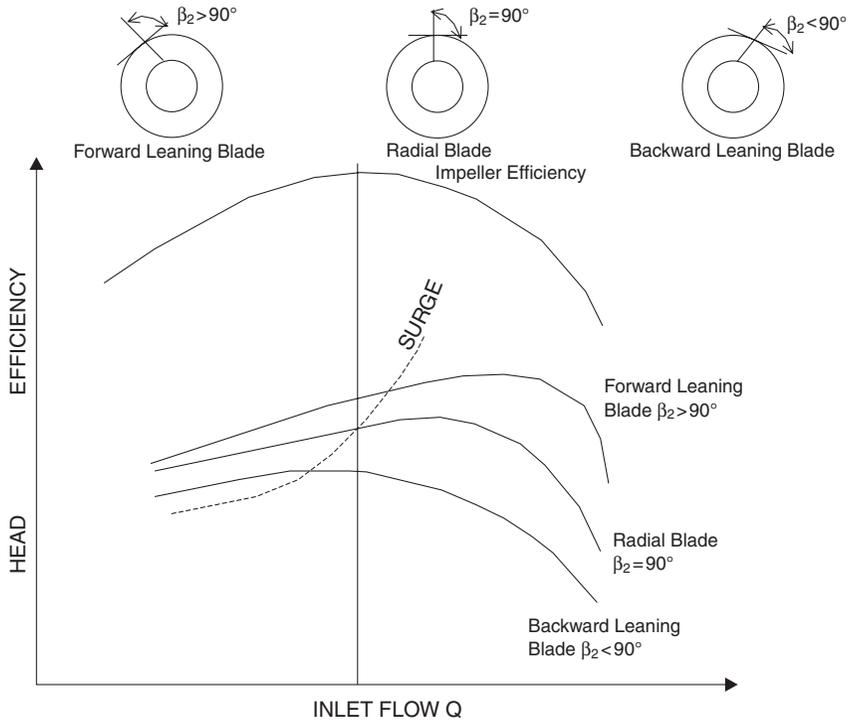


Figure 6-37. Effect of blade angle on stability.

comparison is true in the overall sense, but it must be remembered that the normal operating range lies between 100% flow (Q) and flow at surge, plus a safety margin of, usually, about 10%. The right-hand tail ends of all three curves are not in the operating range. The machine must operate with a suitable margin to the left of where these curves begin their steep decent or tail-off, and in the resultant operating range, the curve for backward leaning blades is steeper. This steeper curve is desirable for control purposes. Such a curve produces a meaningful change in pressure drop across the orifice for a small change in flow. The blade angle by itself does not tell the overall performance story. The geometry of other components of a stage will contribute significant effects also.

Most centrifugal compressors in service in petroleum or petrochemical processing plants use vaneless diffusers. A vaneless diffuser is generally a simple flow channel with parallel walls and does not have any elements inside to guide the flow.

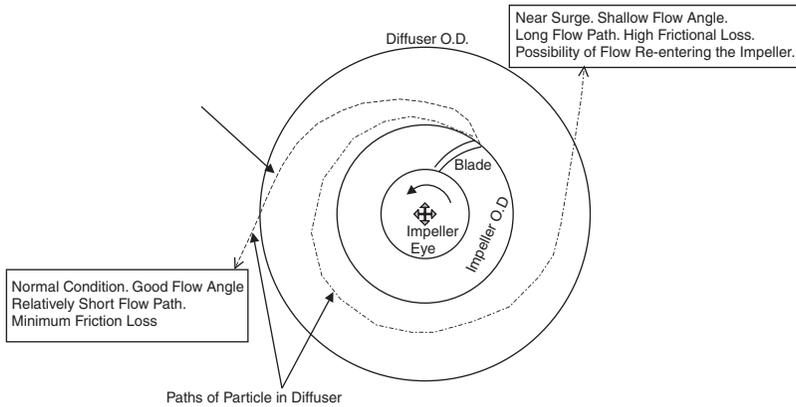


Figure 6-38. Flow trajectory in a vaneless diffuser.

When the inlet flow to the impeller is reduced while the speed is held constant, there is a decrease in the relative velocity leaving the impeller and the air angle associated with it. As the air angle decreases, the length of the flow path spiral increases. The effect is shown in Figure 6-38.

If the flow path is extended enough, the flow momentum at the diffuser walls is excessively dissipated by friction and stall. With this greater loss, the diffuser becomes less efficient and converts a proportionately smaller part of the velocity head to pressure. As this condition progresses, the stage will eventually stall. This could lead to a surge.

Vaned diffusers are used to force the flow to take a shorter, more efficient path through the diffuser. There are many styles of vaned diffusers, with major differences in the types of vanes, vane angles and contouring, and vane spacing. Commonly used vaned diffusers employ wedge-shaped vanes (vane islands) or thin-curved vanes. In high head stages, there can be two to four stages of diffusion. These usually consist of vaneless spaces to decelerate the flow, followed by two or three levels of vaned blades in order to prevent build-up of boundary layer, which causes separation and surging of the compressor. Figure 6-38 indicates the flow pattern in a vaned diffuser. The vaned diffuser can increase the efficiency of a stage by two to four percentage points, but the price for the efficiency gain is generally a narrower operating span on the head-flow curve with respect to both surge and stonewall. Figure 6-39 also shows the effect of off-design flows.

Excessive positive incidence at the leading edge of the diffuser vane occurs when the exit flow is too small at reduced flow, and this condition brings on a stall. Conversely, as flow increases beyond the rated point, excessive negative

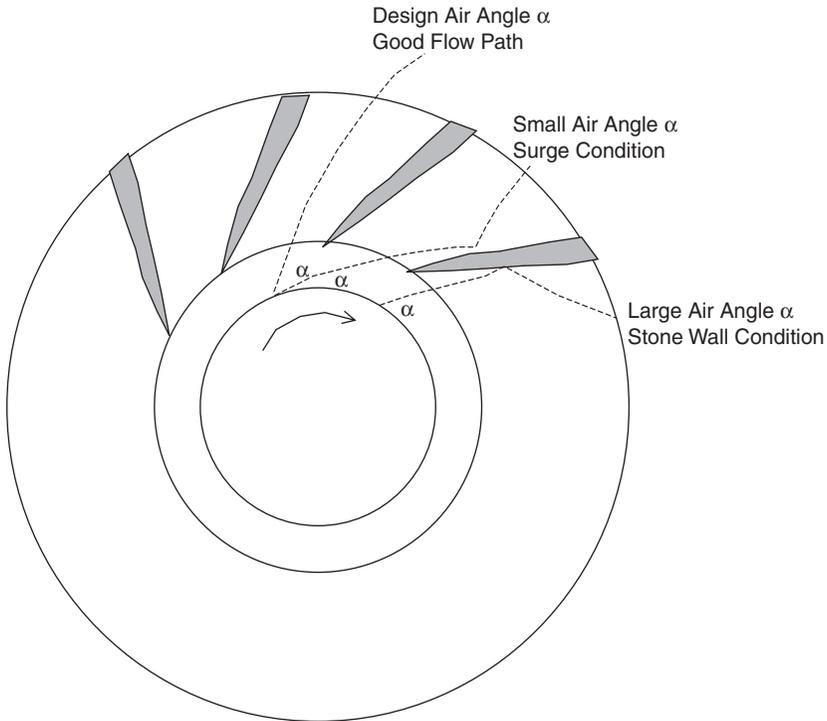


Figure 6-39. Vaned diffuser.

incidence can cause stonewall. Despite its narrowing effect on the usable operating range on the characteristic curve, the vaned diffuser has its application in situations where efficiency is of utmost importance. Although seldom used, movable diffuser vanes or vane islands can be used to alleviate the shock losses at off-design conditions. However, as the adjusting mechanisms required are quite complicated, they generally are applied only to single-stage machines.

It should be noted that the illustrations of the flow paths in Figures 6-37 through 6-39 are somewhat simplistic. Each flow path is indicated by a single streamline. The actual flow field is far more complex, with flow separation and recalculation present. Nevertheless, these figures should help with a practical understanding of the effects of changes in velocity triangles.

Stationary guide vanes direct the flow to the eye of the impeller in an orderly fashion. Depending upon the head requirements of an individual stage, these vanes may direct the flow in the same direction as the rotation

or tip speed of the wheel, an action known as positive pre-swirl. This is usually done to reduce the relative Mach number entering the inducer, in order to prevent shock losses. This, however, reduces the head delivered but improves the operating margin. The opposite action is known as counter-rotation or negative pre-swirl. This increases the head delivered but also increases the inlet relative mach number. Negative pre-swirl is rarely used, since it also decreases the operating range. Sometimes the guide vanes are set at zero degrees of swirl; these vanes are called radial guide vanes. Movable inlet guide vanes are occasionally employed on single-stage machines, or on the first stage of multi-stage compressors driven by electric motors at constant speed. The guide vane angle can be manually or automatically adjusted while the unit is on stream to accommodate off-design operating requirements. Because of the mechanical complexity of the adjusting mechanism and physical dimensional limitations, the variable feature can only be applied to the first wheel in almost all machine designs. Hence, the effect of changing vane angle is diluted in the stages downstream of the first. Although the flow to the entire machine is successfully adjusted by moving the first stage vanes, the remaining stages must pump the adjusted flow at a fixed guide vane angle.

Incidentally, a butterfly throttle valve in the suction line to the machine will produce nearly the same effects as moving the first stage guide vanes. However, throttling is not as efficient as moving the guide vanes, so that in many cases, the added cost of the movable vane mechanism can be justified by power savings.

Effects of Gas Composition

Figure 6-40 shows the performance of an individual stage at a given speed for three levels of gas molecular weight.

The heavy gas class includes gases such as propane, propylene, and standardized refrigerant mixtures. Air, natural gases, and nitrogen are typical of the medium class. Hydrogen-rich gases found in hydrocarbon processing plants are representative of the light class.

The following observations can be made with respect to the curve for heavy gas:

1. The flow at surge is higher.
2. The stage produces slightly more head than that corresponding to medium gas.
3. The right-hand side of the curve turns downward (approaches stone-wall) more rapidly.
4. The curve is flatter in the operating stage.

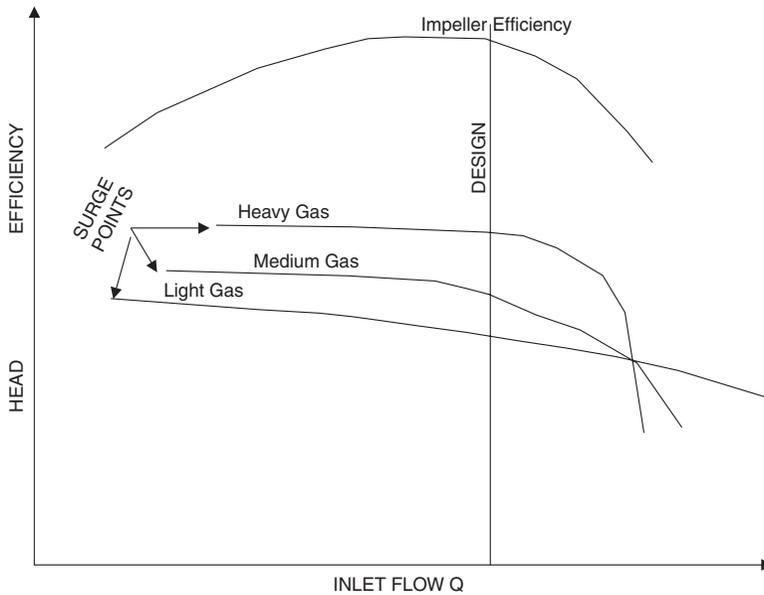


Figure 6-40. Effect of gas composition.

It is the last point (4) that often presents a problem to the designer of the antisurge control system. It should be noted that the flatness gets worse as stages are added in series. Since the RTS is small, there is a large change in flow corresponding to a small change in Head. The control system, therefore, must be more responsive. It should be obvious that curves for lighter gases have a more desirable shape.

External Causes and Effects of Surge

The following are some of the usual causes of surge that are not related to machine design:

1. Restriction in suction or discharge of a system.
2. Process changes in pressure, temperature, or gas composition.
3. Internal plugging of flow passages of compressor (fouling).
4. Inadvertent loss of speed.
5. Instrument or control valve malfunction.
6. Malfunction of hardware such as variable inlet guide vanes.
7. Operator error.

8. Maldistribution of load in parallel operation of two or more compressors.
9. Improper assembly of a compressor, such as a mispositioned rotor.

The effects of surge can range from a simple lack of performance to serious damage to the machine or to the connected system. Internal damage to labyrinths, diaphragms, the thrust bearing, and the rotor can be experienced. There has been a reported case of a bent rotor caused by violent surge. Surge often excites lateral shaft vibration and could produce torsional damage to such items as couplings and gears. Externally, devastating piping vibration can occur, causing structural damage, shaft misalignment, and failure of fittings and instruments.

The effects of the size and configuration of the connected system, as well as different operating conditions, on the intensity of surge can be astonishing. For example, a compressor system in a test set-up at the factory may exhibit only a mild reaction to surge. At the installation, however, the same compressor with a different connected system may react in a tumultuous manner. Surge can often be recognized by check valve hammering, piping vibration, noise, wriggling of pressure gauges or an ammeter on the driver, or lateral and/or axial vibration of the compressor shaft. Mild cases of surge sometimes are difficult to discern.

Surge Detection and Control

Surge-detection devices may be divided into two groups: (1) static devices, and (2) dynamic devices. To date, static surge-detection devices have been widely used; more research work needs to be done before dynamic detection devices are generally used. A dynamic device will probably meet the requirements and hopes of many engineers for a control device that can anticipate stall and surge, and prevent it. Obviously, detection devices must be linked to a control device that can prevent the unstable operation of a compressor.

Static surge-detection devices attempt to avoid stall and surge by the measurement of compressor conditions and ensure that a predecided value is not exceeded. When conditions meet or exceed the limit, control action is taken. A typical pressure-oriented anti-surge control system is shown in Figure 6-41. The pressure transmitter monitors the pressure and controls a device, which opens a blowoff valve. A temperature-sensing device corrects the readings of flow and speed for the effect of temperature. A typical flow-oriented device is also shown in Figure 6-42.

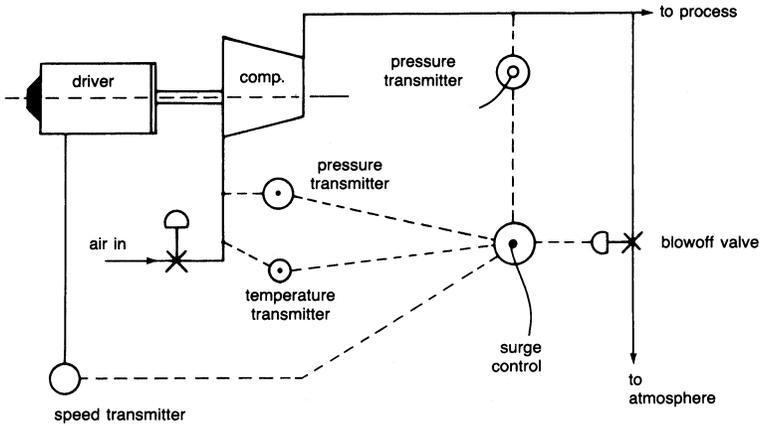


Figure 6-41. Pressure-oriented anti-surge control system.

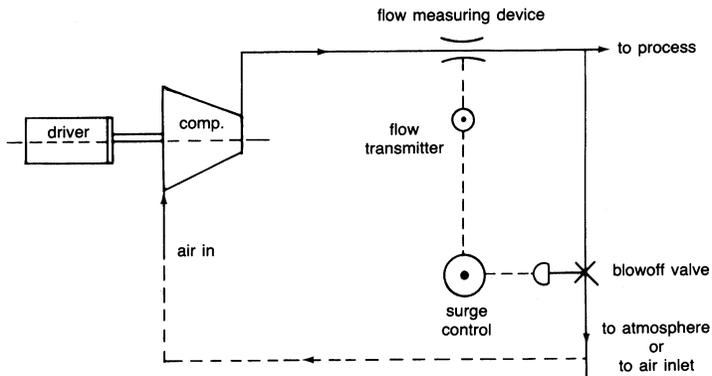


Figure 6-42. Flow-oriented anti-surge control system.

In all static surge-detection devices, the actual phenomenon of flow reversal (surge) is not directly monitored. What is monitored are other conditions related to surge. Control limits are set from past experience and a study of compressor characteristics.

Dynamic surge-detection and control methods are under study. They attempt to detect the *start* of a reversal of flow before it reaches the critical situation of surge. This procedure uses a boundary-layer probe.

The author has a patent for a dynamic surge-detection system, using a boundary-layer probe, presently undergoing field tests. This system consists of specially mounted probes in the compressor to detect boundary-layer flow

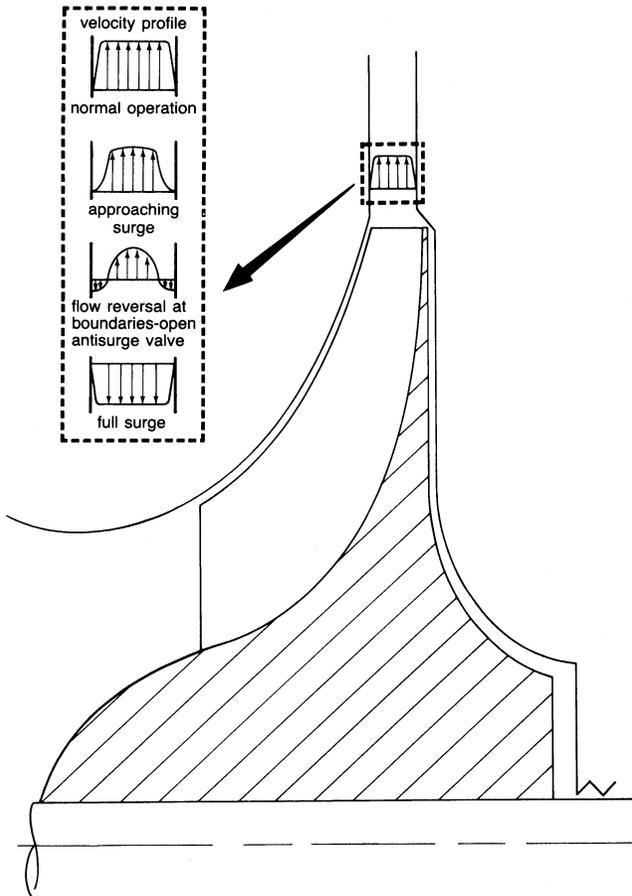


Figure 6-43. Boundary-layer surge prediction technique.

reversal, as shown in Figure 6-43. The concept assumes that the boundary layer will reverse before the entire unit is in surge. Since the system is measuring the actual onset of surge by monitoring the flow reversal, it is not dependent on the molecular weight of the gas and is not affected by the movement of the surge line.

The use of pressure transducers and casing accelerometers in the exit piping has been instrumental in detecting compressor surge. It has been found that as the unit approaches surge, the blade passing frequency (number of blades times rpm) and its second and third harmonic become excited. In a limited number of tests it has been noted that when the second harmonic

of the blade passing frequency reaches the same order of magnitude as the blade passing frequency, the unit is very close to surge.

Process Centrifugal Compressors

These compressors have impellers with a very low pressure ratio (1.1–1.3) and thus large surge-to-choke margins. Figure 6-44 shows a cross section of a typical multistage centrifugal compressor used in the process industries.

The common method of classifying process-type centrifugal compressors driven by gas turbines is based on the number of impellers and the casing design. Table 6-2 shows three types of centrifugal compressors. For each type of compressor, approximate maximum ratings of pressure, capacity, and brake horsepower are also shown. Sectionalized casing types have impellers, which are usually mounted on the extended motor shaft, and similar sections are bolted together to obtain the desired number of stages. Casing material is either steel or cast iron. These machines require minimum supervision and maintenance, and are quite economic in their operating range. The sectionalized casing design is used extensively in supplying air for combustion in ovens and furnaces.

The horizontally split types have casings split horizontally at the mid-section and the top. The bottom halves are bolted and doweled together as shown in Figure 6-45. This design type is preferred for large multistage units.

FPO

Figure 6-44. Cross section of a typical multistage centrifugal compressor. (Courtesy Elliott Company, Jeannette, PA.)

Table 6-2
Industrial Centrifugal Compressor Classification
Based on Casing Design

| Casing Type | Approximate Maximum Ratings | | |
|--|------------------------------------|---|--------------------------------------|
| | Approximate Pressure psig (Bar) | Approximate Inlet Capacity cfm (cmm) | Approximate Power Horsepower (kW) |
| 1. Sectionalized Usually multistage | 10 (0.7) | 20,000 (566) | 600 (447) |
| 2. Horizontally split Single stage (double-suction) | 15 (1.03) | 650,000 (18,406) | 10,000 (7,457) |
| Multistage | 1000 (69) | 200,000 (5,663) | 35,000 (26,100) |
| 3. Vertically split Single stage (single-suction) | | | |
| Overhung | 30 (2.07) | 250,000 (7,079) | 10,000 (7,457) |
| Pipeline | 1200 (82) | 25,000 (708) | 20,000 (14,914) |
| Multistage | More than 5500 (379) | 20,000 (566) | 15,000 (11,185) |

FPO

Figure 6-45. Horizontally split centrifugal compressor with shrouded rotors. (Courtesy of Elliott Company.)

FPO

Figure 6-46. Barrel-type compressor. (Courtesy Elliott Company, Jeannette, PA.)

The internal parts such as shaft, impellers, bearings, and seals are readily accessible for inspection and repairs by removing the top half. The casing material is cast iron or cast steel.

There are various types of barrel or centrifugal compressors. Low-pressure types with overhung impellers are used for combustion processes, ventilation, and conveying applications. Multistage barrel casings are used for high-pressures in which the horizontally split joint is inadequate. Figure 6-46 shows the barrel compressor in the background and the inner bundle from the compressor in front. Once the casing is removed from the barrel, it is horizontally split.

Compressor Configuration

To properly design a centrifugal compressor, one must know the operating conditions—the type of gas, its pressure, temperature, and molecular

weight. One must also know the corrosive properties of the gas so that proper metallurgical selection can be made. Gas fluctuations due to process instabilities must be pinpointed so that the compressor can operate without surging.

Centrifugal compressors for industrial applications have relatively low pressure ratios per stage. This condition is necessary so that the compressors can have a wide operating range while stress levels are kept at a minimum. Because of the low pressure ratios for each stage, a single machine may have a number of stages in one “barrel” to achieve the desired overall pressure ratio. Figure 6-47 shows some of the many configurations. Some factors to be considered when selecting a configuration to meet plant needs are:

1. Intercooling between stages can considerably reduce the power consumed.
2. Back-to-back impellers allow for a balanced rotor thrust and minimize overloading the thrust bearings.
3. Cold inlet or hot discharge at the middle of the case reduces oil-seal and lubrication problems.
4. Single inlet or single discharge reduces external piping problems.
5. Balance planes that are easily accessible in the field can appreciably reduce field-balancing time.
6. Balance piston with no external leakage will greatly reduce wear on the thrust bearings.
7. Hot and cold sections of the case that are adjacent to each other will reduce thermal gradients, and thus reduce case distortion.
8. Horizontally split casings are easier to open for inspection than vertically split ones, reducing maintenance time.
9. Overhung rotors present an easier alignment problem because shaft-end alignment is necessary only at the coupling between the compressor and driver.
10. Smaller, high-pressure compressors that do the same job will reduce foundation problems but will have greatly reduced operational range.

Impeller Fabrication

Centrifugal-compressor impellers are either shrouded or unshrouded. Open, shrouded impellers that are mainly used in single-stage applications are made by investment casting techniques or by three-dimensional milling. Such impellers are used, in most cases, for the high-pressure-ratio stages. The shrouded impeller is commonly used in the process compressor because

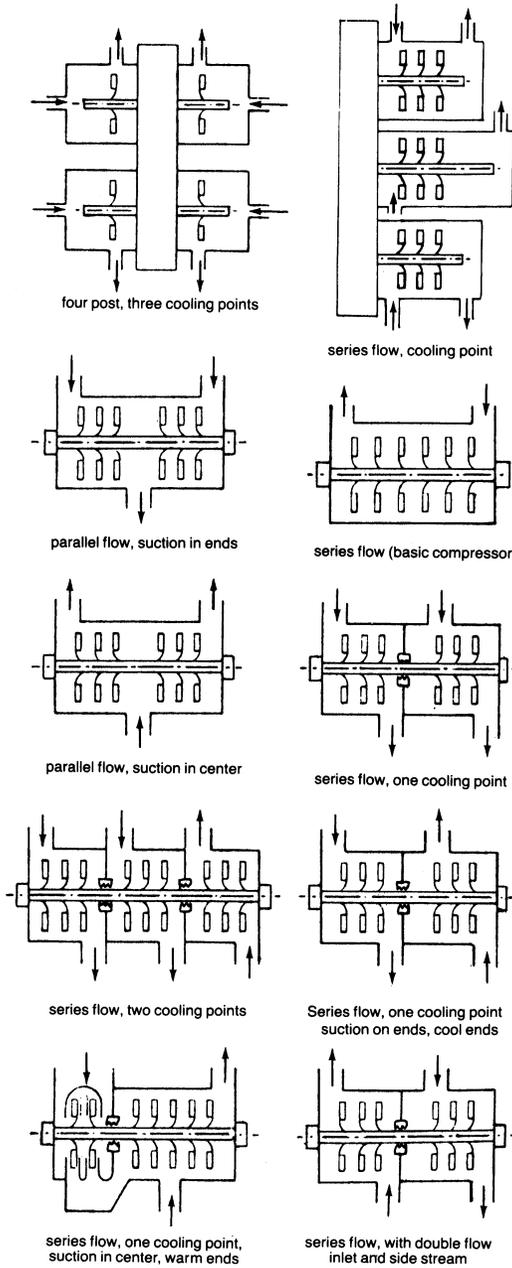


Figure 6-47. Various configurations of centrifugal compressors.

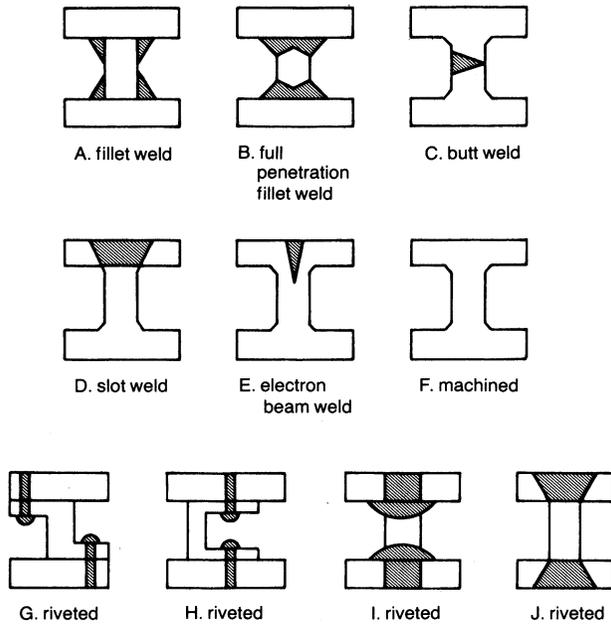


Figure 6-48. Several fabrication techniques for centrifugal impellers.

of its low pressure ratio stages. The low tip stresses in this application make it a feasible design. Figure 6-48 shows several fabrication techniques. The most common type of construction is seen in A and B where the blades are fillet-welded to the hub and shroud. In B the welds are full penetration. The disadvantage in this type of construction is the obstruction of the aerodynamic passage. In C, the blades are partially machined with the covers and then butt-welded down the middle. For backward lean-angled blades, this technique has not been very successful, and there has been difficulty in achieving a smooth contour around the leading edge.

D illustrates a slot-welding technique and is used where blade-passage height is too small (or the backward lean-angle too high) to permit conventional fillet welding. In E, an electron-beam technique is still in its infancy, and work needs to be done to perfect it. Its major disadvantage is that electron-beam welds should preferably be stressed in tension but, for the configuration of E, they are in shear. The configurations of G through J use rivets. Where the rivet heads protrude into the passage, aerodynamic performance is reduced.

Materials for fabricating these impellers are usually low-alloy steels, such as AISI 4140 or AISI 4340. AISI 4140 is satisfactory for most applications;

AISI 4340 is used for larger impellers requiring higher strengths. For corrosive gases, AISI 410 stainless steel (about 12% chromium) is used. Monel K-500 is employed in halogen gas atmospheres and oxygen compressors because of its resistance to sparking. Titanium impellers have been applied to chlorine service. Aluminum-alloy impellers have been used in great numbers, especially at lower temperatures (below 300°F). With new developments in aluminum alloys, this range is increasing. Aluminum and titanium are sometimes selected because of their low density. This low density can cause a shift in the critical speed of the rotor, which may be advantageous.

Bibliography

- Anderson, R.J., Ritter, W.K., and Dildine, D.M., "An Investigation of the Effect of Blade Curvature on Centrifugal Impeller Performance," NACA TN-1313, 1947.
- Balje, O.E., "Loss and Flow-Path Studies on Centrifugal Compressors, Parts I and II," ASME Paper Nos. 70-GT-1 2-A and 70-GT-1 2-B, June 1970.
- Balje, O.I., "A Study of Reynolds Number Effects in Turbomachinery," *Journal of Engineering for Power*, ASME Trans., Vol. 86, Series A, 1964, p. 227.
- Bammert, K., and Rautenberg, M., "On the Energy Transfer in Centrifugal Compressors," ASME Paper No. 74-GT-121.
- Boyce, M.P., "A Practical Three-Dimensional Flow Visualization Approach to the Complex Flow Characteristics in a Centrifugal Impeller," ASME Paper No. 66-GT-83, June 1983.
- Boyce, M.P., and Bale, Y.S., "A New Method for the Calculation of Blade Loadings in Radial-Flow Compressors," ASME Paper No. 71-GT-60, June 1971.
- Boyce, M.P., "New Developments in Compressor Aerodynamics," Proceedings of the 1st Turbomachinery Symposium, Texas A&M, October 1972.
- Boyce, M.P., and Bale, Y.S., "Diffusion Loss in a Mixed-Flow Compressor," Intersociety Energy conversion Engineering conference, San Diego, Paper No. 729061, September 1972.
- Boyce, M.P., and Desai, A.R., "Clearance Loss in a Centrifugal Impeller," Proceedings Of the 8th Intersociety Energy Conversion Engineering Conference, August 1973, Paper No. 7391 26, p. 638.
- Boyce, M.P., and Nishida, A., "Investigation of Flow in Centrifugal Impeller with Tandem Inducer," JSME Paper, Tokyo, Japan, May 1977.
- Boyce, M.P., "How to Achieve On-Line Availability of Centrifugal Compressors," *Chemical Weekly*, June 1978, pp. 115-127.
- Boyce, M.P., "Rerating of Centrifugal Compressors-Part I," *Diesel and Gas Turbine Worldwide*, October 1988, pp. 46-50.

- Boyce, M.P. "Rerating of Centrifugal Compressors-Part II," Diesel and Gas Turbine Worldwide, January-February 1989, pp. 8-20.
- Boyce, M.P., "Principles of Operation and Performance Estimation of Centrifugal Compressors." Proceedings of the 22nd Turbomachinery Symposium. Dallas, Texas, September 1993, pp. 161-78.
- Centrifugal Impeller Performance," NACA TN-1313, 1947.
- Coppage, J.E. et al., "Study of Supersonic Radial Compressors for Refrigeration and Pressurization Systems," WADC Technical Report 55-257, Astia Document No. AD 110467, 1956.
- Dallenback F., "The Aerodynamic Design and Performance of Centrifugal and Mixed-Flow Compressors," SAE International Congress, January 1961.
- Dawes, W., 1995, "A Simulation of the Unsteady Interaction of a Centrifugal Impeller with its Vaned Diffuser: Flows Analysis," ASME Journal of Turbomachinery, Vol. 117, pp. 213-222.
- Deniz, S., Greitzer, E. and Cumpsty, N., 1998, "Effects of Inlet Flow Field Conditions on the Performance of Centrifugal Compressor Diffusers Part 2: Straight-Channel Diffuser," ASME Paper No. 98-GT-474.
- Domercq, O., and Thomas, R., 1997, "Unsteady Flow Investigation in a Transonic Centrifugal Compressor Stage," AIAA Paper No. 97-2877.
- Eckhardt, D., "Instantaneous Measurements in the Jet-Wake Discharge Flow of a Centrifugal Compressor Impeller," ASME Paper No. 74-GT-90.
- Filipenco, V., Deniz, S., Johnston, J., Greitzer, E. and Cumpsty, N., 1998, "Effects of Inlet Flow Field Conditions on the Performance of Centrifugal Compressor Diffusers Part 1: Discrete Passage Diffuser," ASME Paper, No. 98-GT-473.
- Johnston, R. and Dean, R., 1966, "Losses in Vaneless Diffusers of Centrifugal Compressors and Pumps," *ASME Journal of Basic Engineering*, Vol. 88, pp. 49-60.
- Katsanis, T., "Use of Arbitrary Quasi-Orthogonals for Calculations Flow Distribution in the Meridional Plane of a Turbomachine," NASA TND-2546, 1964.
- Klassen, H.A., "Effect of Inducer Inlet and Diffuser Throat Areas on Performance of a Low-Pressure Ratio Sweptback Centrifugal Compressor," NASA TM X-3148, Lewis Research Center, January 1975.
- Owczarek, J.A., *Fundamentals of Gas Dynamics*, International Textbook Company, Pennsylvania, 1968, pp. 165-197.
- Phillips, M., 1997, "Role of Flow Alignment and Inlet Blockage on Vaned Diffuser Performance," Report No. 229, Gas Turbine Laboratory, Massachusetts Institute of Technology.
- Rodgers, C., "Influence of Impeller and Diffuser Characteristic and Matching on Radial Compressor Performance," SAE Preprint 268B, January 1961.

- Rodgers, C., and Sapiro, L., "Design Considerations for High-Pressure-Ratio Centrifugal Compressors," ASME Paper No. 73-GT-31.
- Rodgers, C., 1982, "The Performance of Centrifugal Compressor Channel Diffusers," ASME Paper No. 82-GT-10.
- Schlichting, H., *Boundary Layer Theory*, 4th edition, McGraw-Hill Book Co., 1962, pp. 547–550
- Senoo, Y., and Nakase, Y., "An Analysis of Flow Through a Mixed Flow Impeller," ASME Paper No. 71-GT-2.
- Senoo, Y., and Nakase, Y., "A Blade Theory of an Impeller with an Arbitrary Surface of Revolution," ASME Paper No. 71-GT-17.
- Shouman, A.R., and Anderson J.R., "The Use of Compressor-Inlet Prewirl for the Control of Small Gas Turbines," *Journal of Engineering for Power*, Trans ASME, Vol. 86, Series A, 1964, pp. 136–140.
- Stahler, A.F., "The Slip Factor of a Radial Bladed Centrifugal Compressor," ASME Paper No. 64-GTP-1.
- Stanitz, J.D., "Two-Dimensional Compressible Flow in Conical Mixed-Flow Compressors," NACA TN-1744, 1948.
- Stanitz, J.D. and Prian, V.D., "A Rapid Approximate Method for Determining Velocity Distribution on Impeller Blades of Centrifugal Compressors," NACA TN-2421, 1951.
- Stodola, A., *Steam and Gas Turbines*, McGraw-Hill Book Co., 1927.
- Wiesner, F.J., "A Review of Slip Factors for Centrifugal Impellers," *Journal of Engineering for Power*, ASME Trans., October 1967, p. 558.
- Woodhouse, H., "Inlet Conditions of Centrifugal Compressors for Aircraft Engine Superchargers and Gas Turbines," *J. Inst. Aeron. Sc.*, Vol. 15, 1948, pp. 403.
- Wu, C.H., "A General Theory of Three-Dimensional Flow in Subsonic and Supersonic Turbomachines of Axial, Radial, and Mixed-Flow Type," NACA TN-2604, 1952.

7

Axial-Flow Compressors

The axial-flow compressor compresses its working fluid by first accelerating the fluid and then diffusing it to obtain a pressure increase. The fluid is accelerated by a row of rotating airfoils (blades) called the rotor, and then diffused in a row of stationary blades (the stator). The diffusion in the stator converts the velocity increase gained in the rotor to a pressure increase. A compressor consists of several stages. One rotor and one stator make-up a stage in a compressor. One additional row of fixed blades (inlet guide vanes) is frequently used at the compressor inlet to ensure that air enters the first-stage rotors at the desired angle. In addition to the stators, another diffuser at the exit of the compressor further diffuses the fluid and controls its velocity entering the combustors. Although the working fluid can be any compressible fluid, only air will be considered here.

In an axial compressor air passes from one stage to the next, each stage raising the pressure slightly. By producing low-pressure increases on the order of 1.1:1 to 1.4:1, very high efficiencies can be obtained. The use of multiple stages permits overall pressure increases of up to 40:1. Figure 7-1 shows a multistage high-pressure axial compressor. The low-pressure increase per stage also simplifies calculations in the design of the compressor by justifying the air as incompressible in its flow through a stage.

As with other types of rotating machinery, an axial compressor can be described by a cylindrical coordinate system. The Z axis is taken as running the length of the compressor shaft, the radius r is measured outward from the shaft, and the angle of rotation θ is the angle turned by the blades in Figure 7-2. This coordinate system will be used throughout this discussion of axial-flow compressors.

Figure 7-3 shows the pressure, velocity, and total enthalpy variation for flow through several stages of an axial compressor. As indicated in Figure 7-3,

FPO

Figure 7-1. A multistage high-pressure axial compressor (Courtesy of Westinghouse Electric Corporation.)

the length of the blades, and the annulus area, which is the area between the shaft and shroud, decreases through the length of the compressor. This reduction in flow area compensates for the increase in fluid density as it is compressed, permitting a constant axial velocity. In most preliminary calculations used in the design of a compressor, the average blade height is used as the blade height for the stage.

Blade and Cascade Nomenclature

Since airfoils are employed in accelerating and diffusing the air in a compressor, much of the theory and research concerning the flow in axial compressors are based on studies of isolated airfoils. The nomenclature and methods of describing compressor blade shapes are almost identical to that of aircraft wings. Research in axial compressors involves several blades in a row to simulate a compressor rotor or stator. Such a row is called a cascade. When discussing blades, all angles, which describe the blade and its orientation, are measured with respect to the shaft (Z axis) of the compressor.

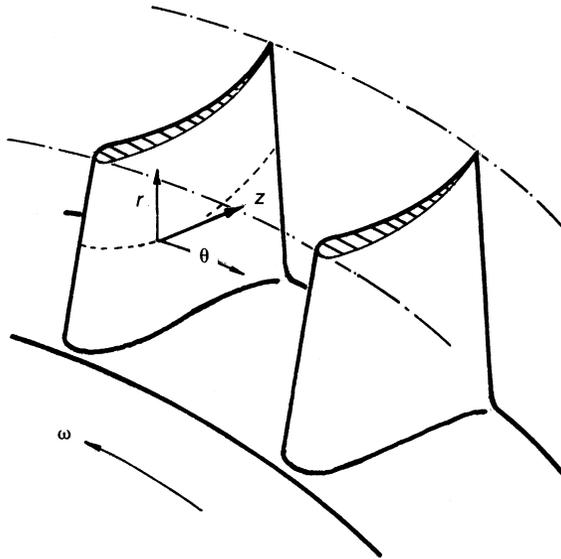


Figure 7-2. Coordinate system for axial-flow compressor.

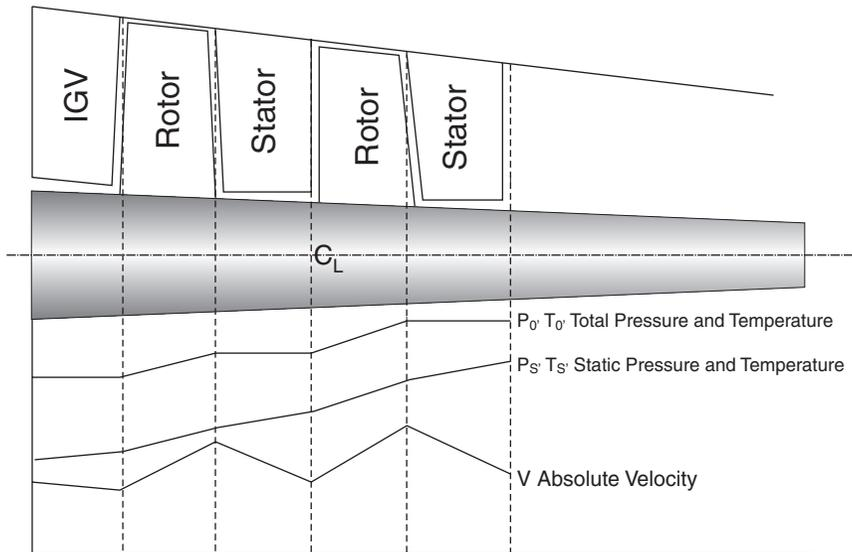


Figure 7-3. Variation of enthalpy, velocity, and pressure through an axial-flow compressor.

The airfoils are curved, convex on one side and concave on the other, with the rotor rotating toward the concave side. The concave side is called the pressure side of the blade, and the convex side is called the suction side of the blade. The chordline of an airfoil is a straight line drawn from the leading edge to the trailing edge of the airfoil, and the chord is the length of the chordline. (See Figure 7-4.) The camberline is a line drawn halfway between the two surfaces, and the distance between the camberline and the chordline is the camber of the blade. The camber angle θ is the turning angle of the camber line. The blade shape is described by specifying the ratio of the chord to the camber at some particular length on the chordline, measured from the leading edge. The aspect ratio AR is the ratio of the blade length to the chord length. The term “hub-to-tip ratio” is frequently used instead of aspect ratio. The aspect ratio becomes important when three-dimensional flow characteristics are discussed. The aspect ratio is established when the mass flow and axial velocity have been determined.

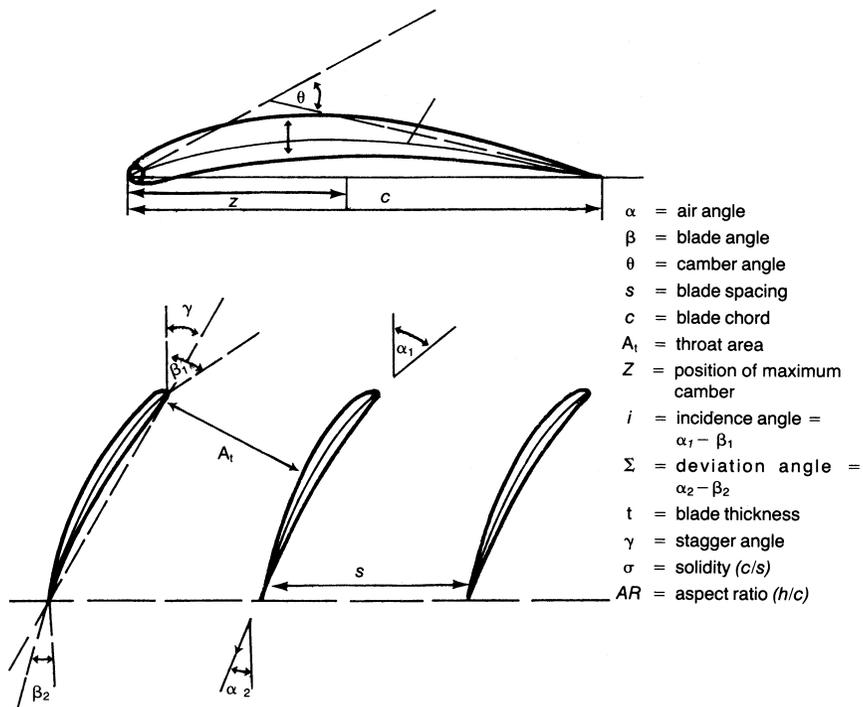


Figure 7-4. Blade profile nomenclature.

The pitch S_b of a cascade is the distance between blades, usually measured between the camberlines at the leading or trailing edges of the blades. The ratio of the chord length to the pitch is the solidity σ of the cascade. The solidity measures the relative interference effects of one blade with another. If the solidity is on the order of 0.5–0.7, the single or isolated airfoil test data, from which there are a profusion of shapes to choose, can be applied with considerable accuracy. The same methods can be applied up to a solidity of about 1.0 but with reduced accuracy. When the solidity is on the order of 1.0–1.5, cascade data are necessary. For solidity in excess of 1.5, the channel theory can be employed. The majority of present designs are in the cascade region.

The blade inlet angle β_1 is the angle formed by a line drawn tangent to the forward end of the camber line and the axis of the compressor. The blade outlet angle β_2 is the angle of a line drawn tangent to the rear of the camberline. Subtracting β_2 from β_1 gives the blade camber angle. The angle that the chordline makes with the axis of the compressor is γ , the setting or stagger angle of the blade. High-aspect ratio blades are often pretwisted so that at full operational speed the centrifugal forces acting on the blades will untwist the blades to the designed aerodynamic angle. The pretwist angle at the tip for blades with AR ratios of about four is between two and four degrees.

The air inlet angle α_1 , the angle at which incoming air approaches the blade, is different from β_1 . The difference between these two angles is the incidence angle i . The angle of attack α is the angle between the inlet air direction and the blade chord. As the air is turned by the blade, it offers resistance to turning and leaves the blade at an angle greater than β_2 . The angle at which the air does leave the blade is the air outlet angle α_2 . The difference between β_2 and α_2 is the deviation angle δ . The air turning angle is the difference between α_1 and α_2 and is sometimes called the deflection angle.

The original work by NACA and NASA is the basis on which most modern axial-flow compressors are designed. Under NACA, a large number of blade profiles were tested. The test data on these blade profiles is published. The cascade data conducted by NACA is the most extensive work of its kind. In most commercial axial-flow compressors NACA 65 series blades are used. These blades are usually specified by notation similar to the following: 65-(18) 10. This notation means that the blade has a lift coefficient of 1.8, a profile shape 65, and a thickness/chord ratio of 10%. The lift coefficient can be directly related to the blade camber angle by the following relationship for 65 series blades:

$$\Theta \approx 25 C_L \quad (7-1)$$

Elementary Airfoil Theory

When a single airfoil is parallel to the velocity of a flowing gas, the air flows over the airfoil as shown in Figure 7-5a. The air divides around the body, separates at the leading edge, and joins again at the trailing edge of the body. The main stream itself suffers no permanent deflection from the presence of the airfoil. Forces are applied to the foil by the local distribution of the stream and the friction of the fluid on the surface. If the airfoil is well designed, the flow is streamlined with little or no turbulence.

If the airfoil is set at the angle of attack to the air stream (as in Figure 7-5b), a greater disturbance is created by its presence, and the streamline pattern will change. The air undergoes a local deflection, though at some distance ahead of and behind the body the flow is still parallel and uniform. The upstream disturbance is minor compared to the downstream disturbance. The local deflection of the air stream can, by Newton's laws, be created only if the blade exerts a force on the air; thus, the reaction of the air must produce an equal and opposite force on the airfoil. These forces can appear only in the form of a pressure stream on the airfoil. The presence of

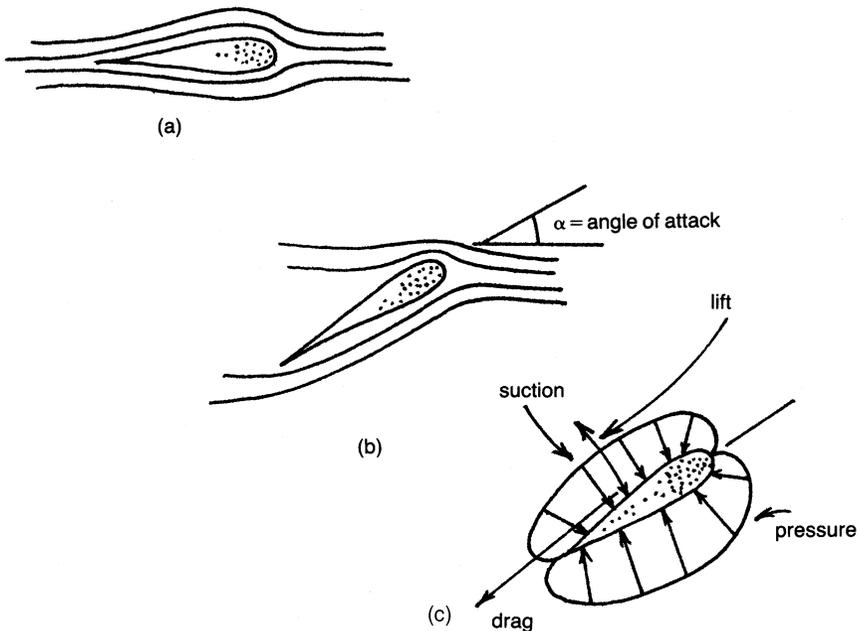


Figure 7-5. Flow around an airfoil at various angles of attack.

the airfoil has changed the local pressure distribution and, by the Bernoulli equation, the local velocities. Examination of the streamlines about the body shows that over the top of the airfoil, the lines approach each other, indicating an increase of velocity and a reduction in static pressure. On the underside of the airfoil, the action separates the streamlines, resulting in a static pressure increase.

Measurement of the pressure at various points on the surface of the airfoil will reveal a pressure distribution as shown in Figure 7-5c. The vectorial sum of these pressures will produce some resultant force acting on the blade. This resultant force can be resolved into a lift component L at right angles to the undisturbed air stream, and a drag component D , moving the airfoil in the direction of flow motion. This resultant force is assumed to act through a definite point located in the airfoil so that the behavior will be the same as if all the individual components were acting simultaneously.

By experimentation, it is possible to measure the lift and drag forces for all values of airflow velocity, angles of incidence, various airfoil shapes. Thus, for any one airfoil the acting forces can be represented as shown in Figure 7-6a. Using such observed values, it is possible to define relations between the forces

$$D = C_D A \rho \frac{V^2}{2} \quad (7-2)$$

$$L = C_L A \rho \frac{V^2}{2} \quad (7-3)$$

where:

- L = lift force
- D = drag force
- C_L = lift coefficient
- C_D = drag coefficient
- A = surface area
- ρ = fluid density
- V = fluid velocity

Two coefficients have been defined, C_L and C_D , relating velocity, density, area, and lift or drag forces. These coefficients can be calculated from wind-tunnel tests and plotted as shown in Figure 7-6b versus the angle of attack

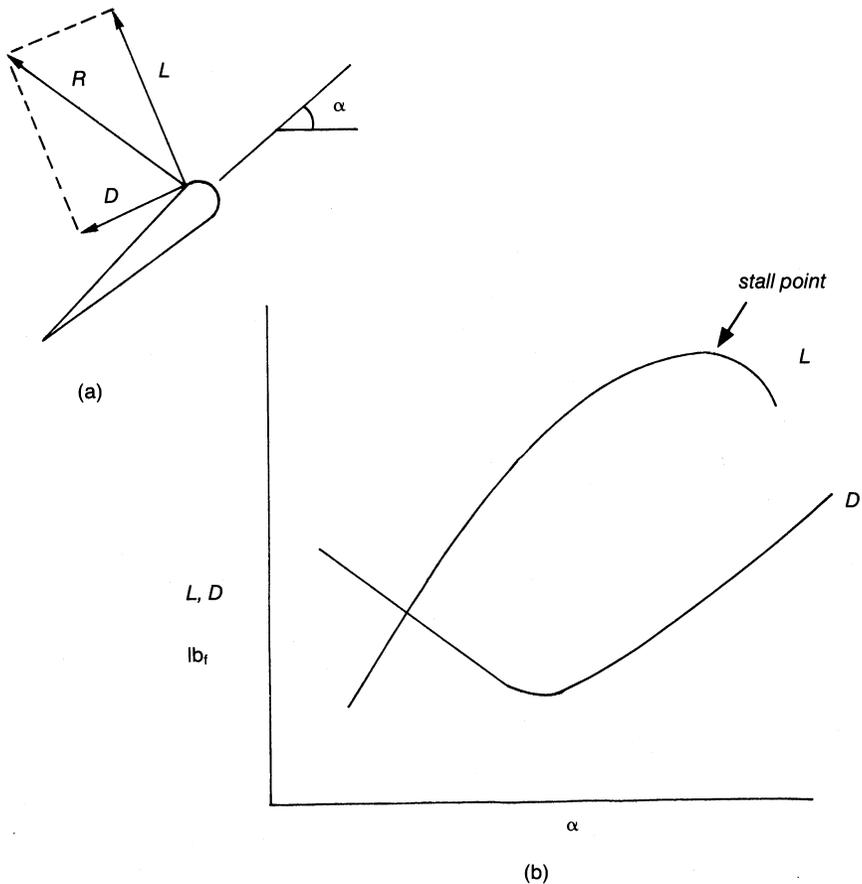


Figure 7-6. Characteristics of the lift and drag forces on an airfoil.

for any desired section. These curves can then be employed in all future predictions involving this particular foil shape.

Examination of Figure 7-6b reveals that there is an angle of attack that produces the highest lift force and lift coefficient. If this angle is exceeded, the airfoil "stalls" and the drag force increases rapidly. As this maximum angle is approached, a great percentage of the energy available is lost in overcoming friction, and a reduction in efficiency occurs. Thus, there is a point, usually before the maximum lift coefficient is reached, at which the most economical operation occurs as measured by effective lift for a given energy supply.

Laminar-Flow Airfoils

Just before and during World War II, much attention was given to laminar-flow airfoils. These airfoils are designed so that the lowest pressure on the surface occurs as far back as possible. The reason for this design is that the stability of the laminar boundary layer increases when the external flow is accelerated (in the flow with a pressure drop), and the stability decreases when the flow is directed against increasing pressure. A considerable reduction in skin friction is obtained by extending the laminar region in this way, provided that the surface is sufficiently smooth.

A disadvantage of this type of airfoil is that the transition from laminar to turbulent flow moves forward suddenly at small angles of attack. This sudden movement results in a narrow low-drag bucket, which means that the drag at moderate-to-large attack angles is much greater than an ordinary airfoil for the same attack angle as seen in Figure 7-7. This phenomenon can be attributed to the minimum pressure point moving forward; therefore, the point of transition between laminar and turbulent flow is also advanced toward the nose as shown in Figure 7-8. The more an airfoil is surrounded by turbulent airflow, the greater its skin friction.

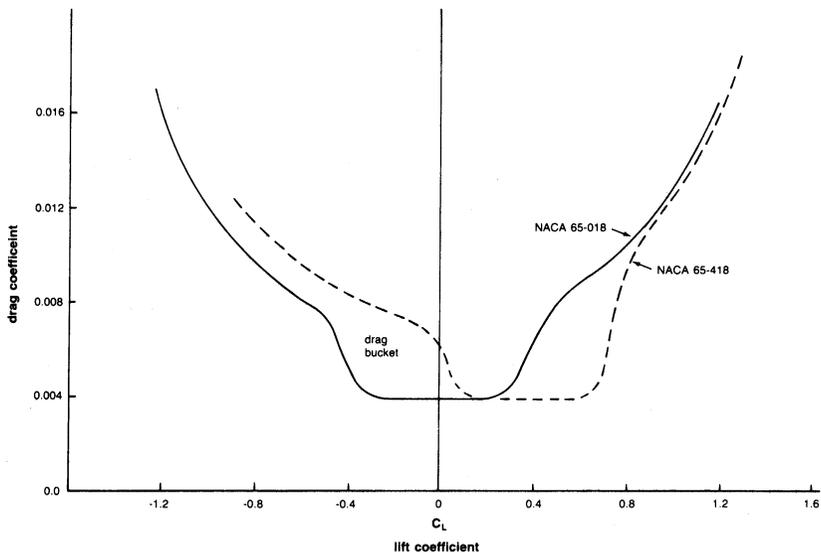


Figure 7-7. NACA measurements of drag coefficients for two laminar airfoils.

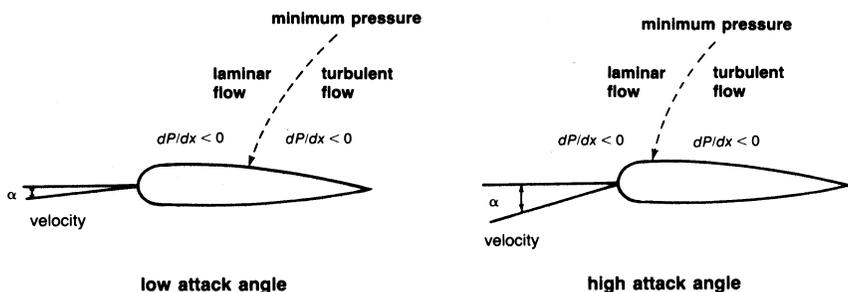


Figure 7-8. Laminar flow airfoils.

Cascade Test

The data on blades in an axial-flow compressor are from various types of cascades, since theoretical solutions are very complex, and their accuracy is in question because of the many assumptions required to solve the equations. The most thorough and systematic cascade testing has been conducted by NACA staff at the Lewis Research Center. The bulk of the cascade testing was carried out at low mach numbers and at low turbulence levels.

The NACA 65 blade profiles were tested in a systematic manner by Herrig, Emery, and Erwin. The cascade tests were carried out in a cascade wind tunnel with boundary-layer suction at the end walls. Tip effects were studied in a specially designed water cascade tunnel with relative motion between wall and blades.

Cascade tests are useful in determining all aspects of secondary flow. For better visualization, tests have been conducted in water cascades. The flow patterns are studied by injecting globules of dibutyl phthalate and kerosene in a mixture equal to the density of water. The mixture is useful in tracing secondary flow, since it does not coagulate.

An impeller designed for air can be tested using water if the dimensionless parameters, Reynolds number, and specific speed are held constant

$$R_e = \frac{\rho_{\text{air}} V_{\text{air}} D}{\mu_{\text{air}}} = \frac{\rho_{\text{water}} V_{\text{water}} D}{\mu_{\text{water}}} \quad (7-4)$$

$$N_s = \frac{Q_{\text{air}}}{N_{\text{air}} D^3} = \frac{Q_{\text{water}}}{N_{\text{water}} D^3} \quad (7-5)$$

where:

ρ = medium density

V = velocity

D = impeller diameter

μ = viscosity

N = speed

Using this assumption, one can apply this flow visualization method to any working medium.

One designed apparatus consists of two large tanks on two different levels. The lower tank is constructed entirely out of plexiglass and receives a constant flow from the upper tank. The flow entering the lower tank comes through a large, rectangular opening, which houses a number of screens so that no turbulence is created by water entering the lower tank. The center of the lower tank can be fitted with various boxes for the various flow visualization problems to be studied. This modular design enables a rapid interchanging of models and work on more than one concept at a time.

To study the effect of laminar flow, the blades were slotted as shown in Figure 7-9. For the blade treatment cascade rig experiment, a plexiglass cascade was designed and built. Figure 7-10 shows the cascade. This cascade

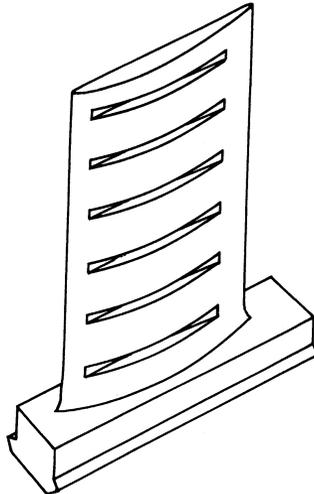


Figure 7-9. Perspective of compressor blade with treatment.

FPO

Figure 7-10. Cascade model in axial-flow test tank.

was then placed in the bottom tank and maintained at a constant head. Figure 7-11 shows the entire setup, and Figure 7-12 shows the cascade flow. Note the large extent of the laminar-flow regions on the treated center blades as compared to the untreated blades.

The same water tunnel was used for tests to study the effect of casing treatment in axial-flow compressors. In this study, the same Reynolds number and specific speeds were maintained as those experienced in an actual axial-flow compressor.

In an actual compressor the blade and the passage are rotating with respect to the stationary shroud. It would be difficult for a stationary observer to obtain data on the rotating blade passage. However, if that observer were rotating with the blade passage, data would be easier to acquire. This was accomplished by holding the blade passage stationary with respect to the observer and rotating the shroud. Furthermore, since casing treatment affects the region around the blade tip, it was sufficient to study only the upper portion of the blade passage. These were the criteria in the design of the apparatus.

The modeling of the blade passage required provisions for controlling the flow in and out of the passage. This control was accomplished by placing the blades, which partially form the blade passage, within a plexiglass tube. The tube had to be of sufficient diameter to accommodate the required flow through the passage without tube wall effect distorting the flow as it entered

FPO

Figure 7-11. Apparatus for testing axial-flow cascade model.

or left the blade passage. This allowance was accomplished by using a tube three times the diameter of the blade pitch. The entrance to the blades was designed so that the flow entering the blades was a fully developed turbulent flow. The flow in the passage between the blade tip and the rotating shroud was laminar. This laminar flow was expected in the narrow passage.

A number of blade shapes could have been chosen; therefore, it was necessary to pick one shape for this study which would be the most representative for casing treatment considerations. Since casing treatment is most effective from an acoustic standpoint in the initial stages of compression, the maximum point of camber was chosen toward the rear of the blade ($Z = .6$ chord). This type of blade profile is most commonly used for transonic flow and is usually in the initial stages of compression.

The rotating shroud must be in close proximity to the blade tips within the tube. To get this proximity, a shaft-mounted plexiglass disc was suspended from above the blades. The plexiglass disc was machined as shown in Figure 7-13. The plexiglass tube was slotted so that the disc could be centered on the center line of the tube and its stepped section lowered through the two slots in the tube. Clearances between the slot edges and the disc were minimized.

FPO

Figure 7-12. Treatments on center cascade blade.

One slot was cut directly above the blade passage emplacement. The other slot was sealed off to prevent leakage. As the disc was lowered into close proximity to the blade tips, the blade passage was completed. The clearance between disc and blade was kept at 0.035 of an inch. The disc, when spun from above, acted as the rotating shroud.

There are only two basic casing treatment designs other than a blank design—which corresponds to no casing treatment at all. The first type of casing treatment consists of radial grooves. A radial groove is a casing treatment design in which the groove is essentially parallel to the chordline of the blade. The second basic type is the circumferential groove. This type of casing treatment has its grooves perpendicular to the blade chordline. Figure 7-14 is a photograph of two discs showing the two types of casing

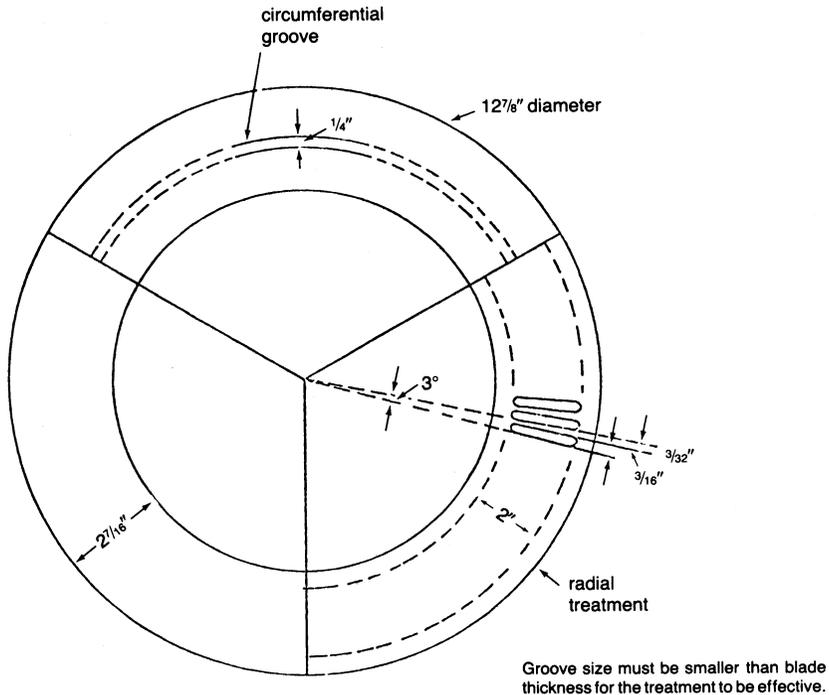


Figure 7-13. Details of the various casing treatments. Each treatment was on a separate disc.

treatment used. The third disc used is a blank, representing the present type of casing. The results indicate that the radial casing treatment is most effective in reducing leakage and also in increasing the surge-to-stall margin. Figure 7-15 shows the leakage at the tips for the various casing treatments. Figure 7-16 shows the velocity patterns observed by the use of various casing treatments. Note that for the treatment along the chord (radial), the flow is maximum at the tip. This flow maximum at the tip indicates that the chance of rotor tip stall is greatly reduced.

Energy Increases

In an axial flow compressor air passes from one stage to the next with each stage raising the pressure and temperature slightly. By producing low-pressure increases on the order of 1.1:1–1.4:1, very high efficiencies can be obtained. The use of multiple stages permits overall pressure increases up to

FPO

Figure 7-14. Two discs with casing treatment.

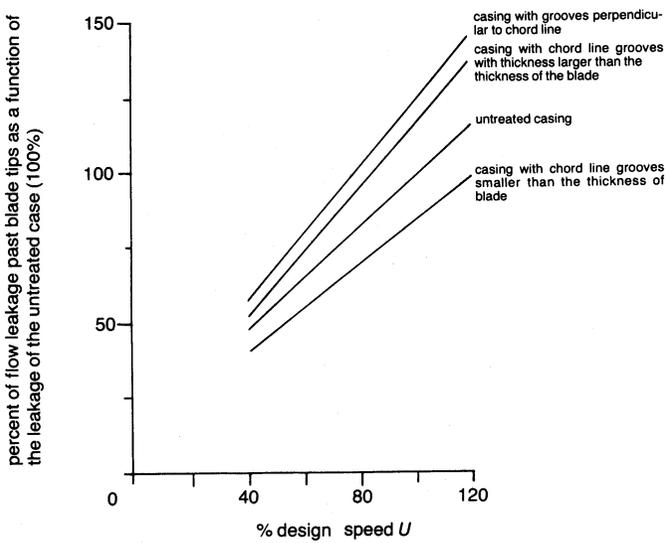


Figure 7-15. Mass flow leakage at tips for various casing treatments.

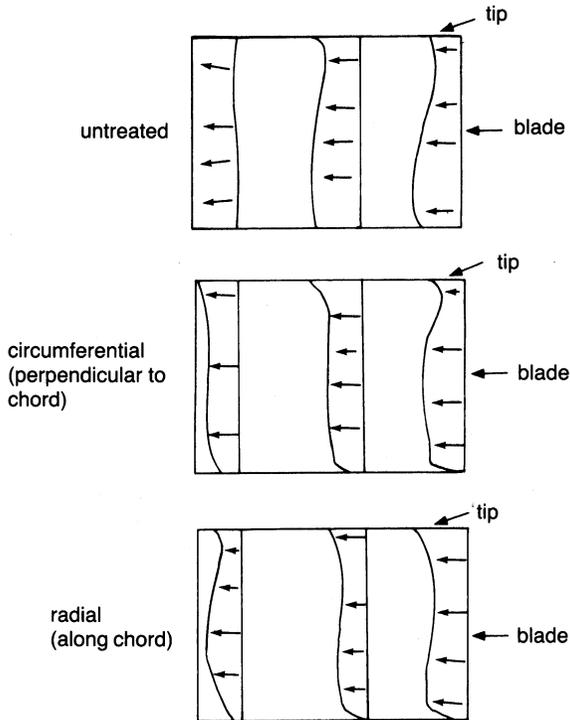


Figure 7-16. Velocity patterns observed in the side view of the blade passage for various casing treatments.

40:1. Figure 7-3 shows the pressure, velocity, and total enthalpy variation for flow through several stages of an axial flow compressor. It is important to note here that the changes in the *total* conditions for pressure, temperature, and enthalpy occur only in the rotating component where energy is inputted into the system. As seen also in Figure 7-3, the length of the blades, and the annulus area, which is the area between the shaft and shroud, decreases through the length of the compressor. This reduction in flow area compensates for the increase in fluid density as it is compressed, permitting a constant axial velocity. In most preliminary calculations used in the design of a compressor, the average blade height is used as the blade height for the stage.

The rule of thumb for a multiple stage gas turbine compressor would be that the energy rise per stage would be constant, rather than the commonly

held perception that the pressure rise per stage is constant. The energy rise per stage can be written as:

$$\Delta H = \frac{[H_2 - H_1]}{N_s} \quad (7-6)$$

where: H_1, H_2 = Inlet and Exit Enthalpy Btu/lb_m (kJ/kg)

N_s = number of stages

Assuming that the gas is thermally and calorically perfect (c_p , and γ are constant) equation 7-1 can be rewritten as:

$$\Delta T_{\text{stage}} = \frac{T_{\text{in}} \left[\left[\frac{P_2}{P_1} \right]^{\frac{\gamma-1}{\gamma}} - 1 \right]}{N_s} \quad (7-7)$$

where: T_{in} = Inlet Temperature (°F, °C)

P_1, P_2 = Inlet and Exit Pressure (psia, bar)

Velocity Triangles

As stated earlier, an axial-flow compressor operates on the principle of putting work into the incoming air by acceleration and diffusion. Air enters the rotor as shown in Figure 7-17 with an absolute velocity (V) and an angle α_1 , which combines vectorially with the tangential velocity of the blade (U) to produce the resultant relative velocity W_1 at an angle α_2 . Air flowing through the passages formed by the rotor blades is given a relative velocity W_2 at an angle α_4 , which is less than α_2 because of the camber of the blades. Note that W_2 is less than W_1 , resulting from an increase in the passage width as the blades become thinner toward the trailing edges. Therefore, some diffusion will take place in the rotor section of the stage. The combination of the relative exit velocity and blade velocity produce an absolute velocity V_2 at the exit of the rotor. The air then passes through the stator, where it is turned through an angle so that the air is directed into the rotor of the next stage with a minimum incidence angle. The air entering the rotor has an axial component at an absolute velocity V_{z1} and a tangential component $V_{\theta1}$.

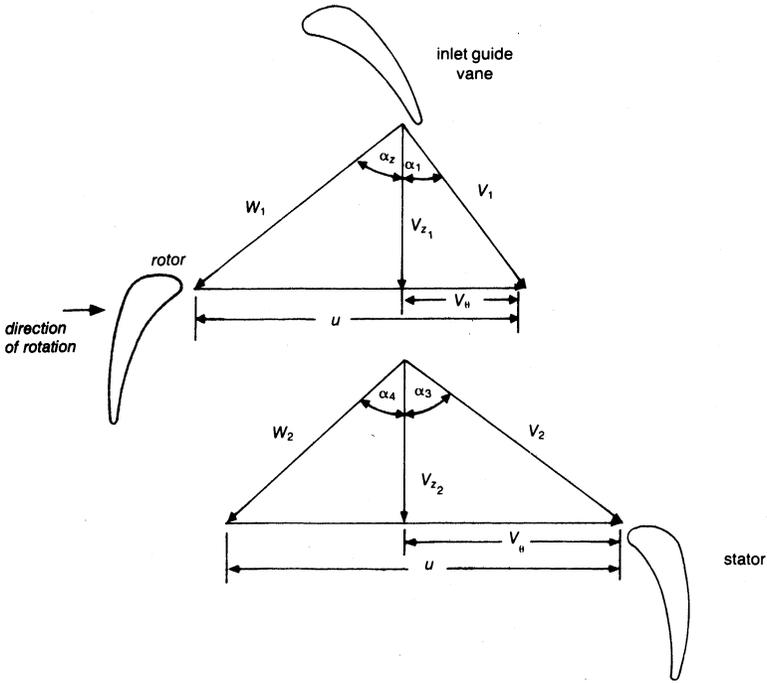


Figure 7-17. Typical velocity triangles for an axial-flow compressor.

Applying the Euler turbine equation

$$H = \frac{1}{g_c} [U_1 V_{\theta 1} - U_2 V_{\theta 2}] \quad (7-8)$$

and assuming that the blade speeds at the inlet and exit of the compressor are the same and noting the relationships,

$$V_{\theta 1} = V_{z1} \tan \alpha_1 \quad (7-9)$$

$$V_{\theta 2} = V_{z2} \tan \alpha_3 \quad (7-10)$$

Equation (7-1) can be written

$$H = \frac{U_1}{g_c} (V_{z1} \tan \alpha_2 - V_{z2} \tan \alpha_3) \quad (7-11)$$

Assuming that the axial component (V_z) remains unchanged,

$$H = \frac{UV_z}{g_c} (\tan \alpha_1 - \tan \alpha_3) \quad (7-12)$$

The previous relationship is in terms of the absolute inlet and outlet velocities. By rewriting the previous equation in terms of the blade angles or the relative air angles, the following relationship is obtained:

$$\begin{aligned} U_1 = U_2 = V_{z1} \tan \alpha_1 &= V_{z1} \tan \alpha_2 \\ &= V_{z2} \tan \alpha_3 + V_{z2} \tan \alpha_4 \end{aligned}$$

Therefore,

$$H = \frac{UV_z}{g_c} (\tan \alpha_2 - \tan \alpha_4) \quad (7-13)$$

The previous relationship can be written to calculate the pressure rise in the stage

$$c_p T_{in} \left[\left(\frac{P_2}{P_1} \right)^{\frac{\gamma-1}{\gamma}} - 1 \right] = \frac{UV_2}{g_c} (\tan \alpha_2 - \tan \alpha_4) \quad (7-14)$$

which can be rewritten

$$\frac{P_2}{P_1} = \left\{ \frac{UV_z}{g_c c_p T_{in}} [\tan \alpha_2 - \tan \alpha_4] + 1 \right\}^{\frac{\gamma}{\gamma-1}} \quad (7-15)$$

The velocity triangles can be joined together in several different ways to help visualize the changes in velocity. One of the methods is to simply join these triangles into a connected series. The two triangles can also be joined and superimposed using the sides formed by either the axial velocity, which is assumed to remain constant as shown in Figure 7-18a, or the blade speed as a common side, assuming that the inlet and exit blade speed are the same as shown in Figure 7-18b.

Degree of Reaction

The degree of reaction in an axial-flow compressor is defined as the ratio of the change of static head in the rotor to the head generated in the stage

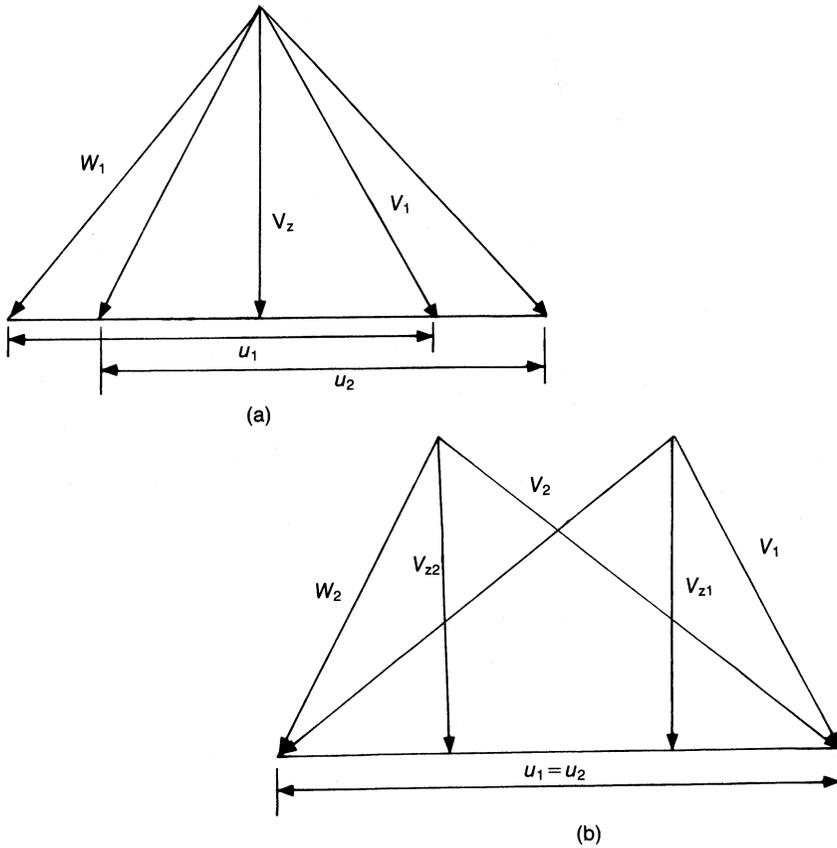


Figure 7-18. Velocity triangles.

$$R = \frac{H_{\text{rotor}}}{H_{\text{stage}}} \quad (7-16)$$

The change in static head in the rotor is equal to the change in relative kinetic energy:

$$H_r = \frac{1}{2g_c} (W_1^2 - W_2^2) \quad (7-17)$$

and

$$W_1^2 = V_{z1}^2 + (V_{z1} \tan \alpha_2)^2 \tag{7-18}$$

$$W_2^2 = V_{z2}^2 + (V_{z2} \tan \alpha_4)^2 \tag{7-19}$$

Therefore,

$$H_r = \frac{V_z^2}{2g_c} (\tan^2 \alpha_2 - \tan^2 \alpha_4)$$

Thus, the reaction of the stage can be written

$$R = \frac{V_z \tan^2 \alpha_2 - \tan^2 \alpha_4}{2U \tan \alpha_2 - \tan \alpha_4} \tag{7-20}$$

Simplifying the previous equation,

$$R = \frac{V_z}{2U} (\tan \alpha_2 + \tan \alpha_4) \tag{7-21}$$

In the symmetrical axial-flow stage, the blades and their orientation in the rotor and stator are reflected images of each other. Thus, a symmetrical axial-flow stage where $V_1 = W_2$ and $V_2 = W_1$ as seen in Figure 7-19, the

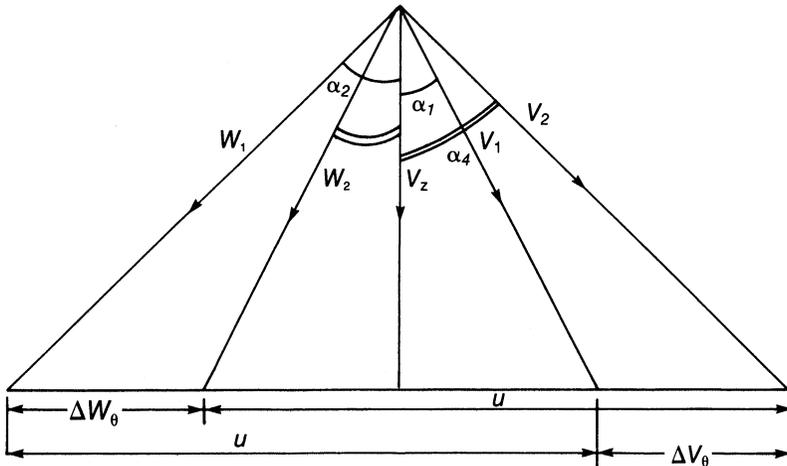


Figure 7-19. Symmetrical velocity triangle for 50% reaction stage.

head delivered in velocity as given by the Euler turbine equation can be expressed

$$H = \frac{1}{2g_c} [(U_1^2 - U_2^2) + (V_1^2 - V_2^2) + (W_2^2 - W_1^2)] \quad (7-22)$$

$$H = \frac{1}{2g_c} (W_2^2 - W_1^2) \quad (7-23)$$

The reaction for a symmetrical stage is 50%.

The 50% reaction stage is widely used, since an adverse pressure rise on either the rotor or stator blade surfaces is minimized for a given stage pressure rise. When designing a compressor with this type of blading, the first stage must be preceded by inlet guide vanes to provide prewhirl, and the correct velocity entrance angle to the first-stage rotor. With a high tangential velocity component maintained by each succeeding stationary row, the magnitude of W_1 is decreased. Thus, higher blade speeds and axial-velocity components are possible without exceeding the limiting value of .70–.75 for the inlet Mach number. Higher blade speeds result in compressors of smaller diameter and less weight.

Another advantage of the symmetrical stage comes from the equality of static pressure rises in the stationary and moving blades, resulting in a maximum static pressure rise for the stage. Therefore, a given pressure ratio can be achieved with a minimum number of stages, a factor in the lightness of this type of compressor. The serious disadvantage of the symmetrical stage is the high exit loss resulting from the high axial velocity component. However, the advantages are of such importance in aircraft applications that the symmetrical compressor is normally used. In stationary applications, where weight and frontal area are of lesser importance, one of the other stage types is used.

The term “asymmetrical stage” is applied to stages with reaction other than 50%. The axial-inflow stage is a special case of an asymmetrical stage where the entering absolute velocity is in the axial direction. The moving blades impart whirl to the velocity of the leaving flow which is removed by the following stator. From this whirl and the velocity diagram as seen in Figure 7-20, the major part of the stage pressure rise occurs in the moving row of blades with the degree of reaction varying from 60–90%. The stage is designed for constant energy transfer and axial velocity at all radii so that the vortex flow condition is maintained in the space between blade rows.

The advantage of a stage with greater than 50% reaction is the low exit loss resulting from lower axial velocity and blade speeds. Because of the

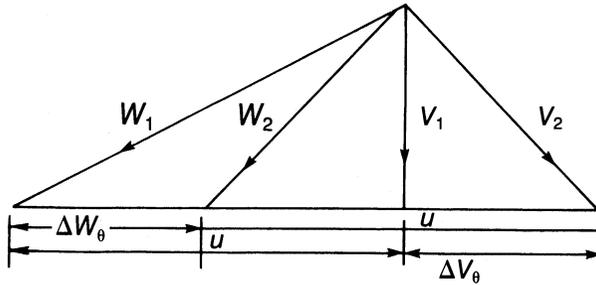


Figure 7-20. Axial-entry stage velocity diagram.

small static pressure rise in the stationary blades, certain simplifications can be introduced such as constant-section stationary blades and the elimination of interstage seals. Higher actual efficiencies have been achieved in this stage type than with the symmetrical stage—primarily because of the reduced exit loss. The disadvantages result from a low static pressure rise in the stationary blades that necessitates a greater number of stages to achieve a given pressure ratio and creating a heavy compressor. The lower axial velocities and blade speed, necessary to keep within inlet Mach number limitations, result in large diameters. In stationary applications where the increased weight and frontal area are not of great importance, this type is frequently used to take advantage of the higher efficiency.

The axial-outflow stage diagram in Figure 7-21 shows another special case of the asymmetrical stage with reaction greater than 50%. With this type of

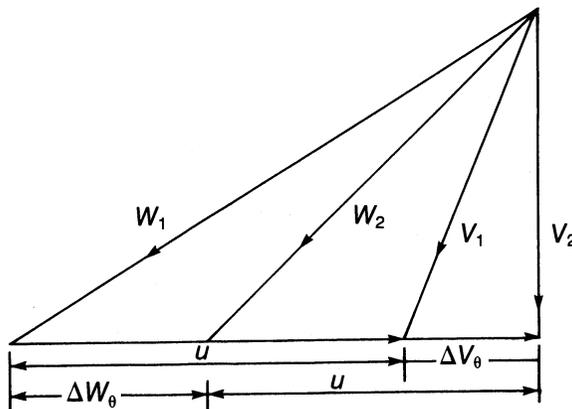


Figure 7-21. Axial-outflow stage velocity diagram.

design, the absolute exit velocity is in an axial direction, and all the static pressure rise occurs in the rotor. A static pressure decrease occurs in the stator so that the degree of reaction is in excess of 100%. The advantages of this stage type are low axial velocity and blade speeds, resulting in the lowest possible exit loss. This design produces a heavy machine of many stages and of large diameter. To keep within the allowable limit of the inlet Mach number, extremely low values must be accepted for the blade velocity and axial velocity. The axial-outflow stage is capable of the highest actual efficiency because of the extremely low exit loss and the beneficial effects of designing for free vortex flow. This compressor type is particularly well-suited for closed-cycle plants where smaller quantities of air are introduced to the compressor at an elevated static pressure.

While a reaction of less than 50% is possible, such a design results in high inlet Mach numbers to the stator row, causing high losses. The maximum total divergence of the stators should be limited to approximately 20° to avoid excessive turbulence. Combining the high inlet for the limiting divergence angles produces a long stator, thereby producing a longer compressor.

Radial Equilibrium

The flow in an axial-flow compressor is defined by the continuity, momentum, and energy equations. A complete solution to these equations is not possible because of the complexity of the flow in an axial-flow compressor. Considerable work has been done on the effects of radial flow in an axial-flow compressor. The first simplification used considers the flow axisymmetric. This simplification implies that the flow at each radial and axial station within the blade row can be represented by an average circumferential condition. Another simplification considers the radial component of the velocity as much smaller than the axial component velocity, so it can be neglected.

For the low-pressure compressor with a low-aspect ratio, and where the effect of streamline curvature is not significant, the simple radial equilibrium solution can be used. The simple radial equilibrium solution assumes that the change of the radial velocity component along the axial direction is zero ($\partial V_{\text{rad}}/\partial z = 0$) and the change of entropy in the radial direction is negligible ($\partial s/\partial r = 0$). The meridional velocity (V_m) is equal to the axial velocity (V_z), since the effect of streamline curvature is not significant. The radial gradient of the static pressure can be given

$$\frac{\partial P}{\partial r} = \rho \frac{V_\theta^2}{r} \quad (7-24)$$

Using the simple radial equilibrium equation, the computation of the axial velocity distribution can be calculated. The accuracy of the techniques depends on how linear V_{θ}^2/r is with the radius.

This assumption is valid for low-performance compressors, but it does not hold well for the high-aspect ratio, highly loaded stages where the effects of streamline curvature become significant. The radial acceleration of the meridional velocity and the pressure gradient in the radial direction must be considered. The radial gradient of static pressure for the highly curved streamline can be written

$$\frac{\partial P}{\partial r} = \rho \left(\frac{V_{\theta}^2}{r} \pm \frac{\rho V_m^2 \cos \epsilon}{r_c} \right) \quad (7-25)$$

where ϵ is the angle of the streamline curvature with respect to the axial direction and r_c is the radius of curvature.

To determine the radius of curvature and the streamline slope accurately, the configuration of the streamline through the blade row must be known. The streamline configuration is a function of the annular passage area, the camber and thickness distribution of the blade, and the flow angles at the inlet and outlet of the blade. Since there is no simple way to calculate the effects of all the parameters, the techniques used to evaluate these radial accelerations are empirical. By using iterative solutions, a relationship can be obtained. The effect of high radial acceleration with high-aspect ratios can be negated by tapering the tip of the compressor inward so that the hub curvature is reduced.

Diffusion Factor

The diffusion factor first defined by Lieblien is a blade-loading criterion

$$D = \left(1 - \frac{W_2}{W_1} \right) + \frac{V_{\theta 1} - V_{\theta 2}}{2\sigma W_1} \quad (7-26)$$

The diffusion factor should be less than .4 for the rotor tip and less than .6 for the rotor hub and the stator. The distribution of the diffusion factor throughout the compressor is not properly defined. However, the efficiency is less in the later stages due to distortions of the radial velocity distributions in the blade rows. Experimental results indicate that even though efficiency is less in the later stages, as long as the diffusion loading limits are not exceeded, the stage efficiencies remain relatively high.

The Incidence Rule

For low-speed airfoil design, the region of low-loss operation is generally flat, and it is difficult to establish the precise value of the incidence angle that corresponds to the minimum loss as seen in Figure 7-22. Since the curves are generally symmetrical, the minimum loss location was established at the middle of the low-loss range. The range is defined as the change in incidence angle corresponding to a rise in the loss coefficient equal to the minimum value.

The following method for calculation of the incidence angle is applicable to cambered airfoils. Work by NASA on the various cascades is the basis for the technique. The incidence angle is a function of the blade camber, which is an indirect function of the air-turning angle

$$i = ki_0 + m\zeta + \delta_m \tag{7-27}$$

where i_0 is the incidence angle for zero camber, and m is the slope of the incidence angle variation with the air-turning angle (ζ). The zero-camber incidence angle is defined as a function of inlet air angle and solidity as seen in Figure 7-23 and the value of m is given as a function of the inlet air angle and the solidity as seen in Figure 7-24.

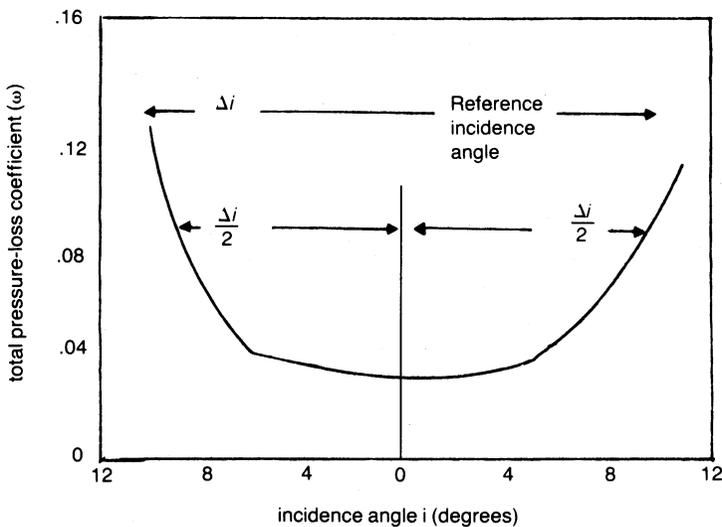


Figure 7-22. Loss as a function of incidence angle.

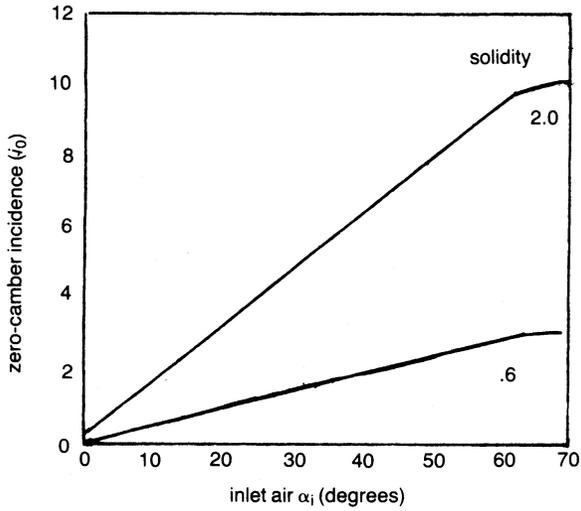


Figure 7-23. Incidence angle for zero-camber airfoil.

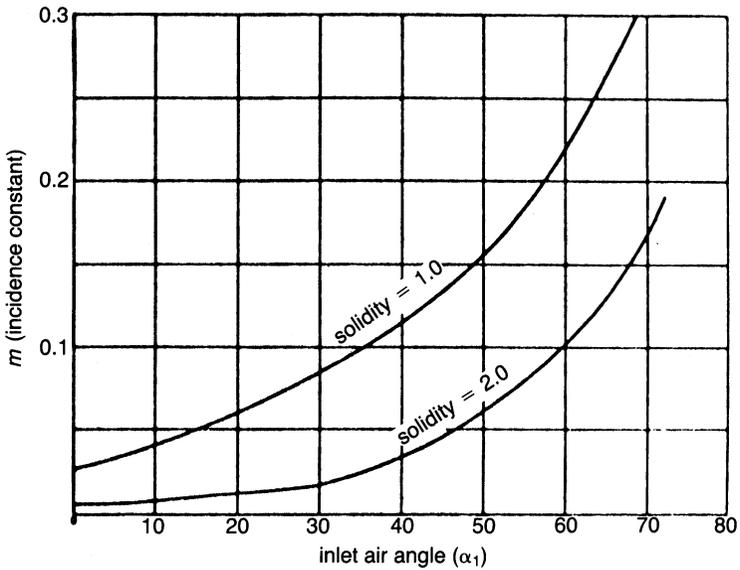


Figure 7-24. Slope of incidence angle variation with air angle.

The incidence angle i_0 is for a 10% blade thickness. For blades of other than 10% thickness, a correction factor K is used, which is obtained from Figure 7-25.

The incidence angle now must be corrected for the Mach number effect (δ_m). The effect of the Mach number on incidence angle is shown in Figure 7-26. The incidence angle is not affected until a Mach number of .7 is reached.

The incidence angle is now fully defined. Thus, when the inlet and outlet air angles and the inlet Mach number are known, the inlet blade angle can be computed in this manner.

The Deviation Rule

Carter's rule, which shows that the deviation angle is directly a function of the camber angle and is inversely proportional to the solidity ($\delta = m\theta\sqrt{1/\sigma}$) has been modified to take into account the effect of stagger, solidity, Mach number, and blade shape as shown in the following relationship:

$$\delta_f = m_f\theta\sqrt{1/\sigma} + 12.15 t/c(1 - \theta/8.0) + 3.33(M_1 - 0.75) \tag{7-28}$$

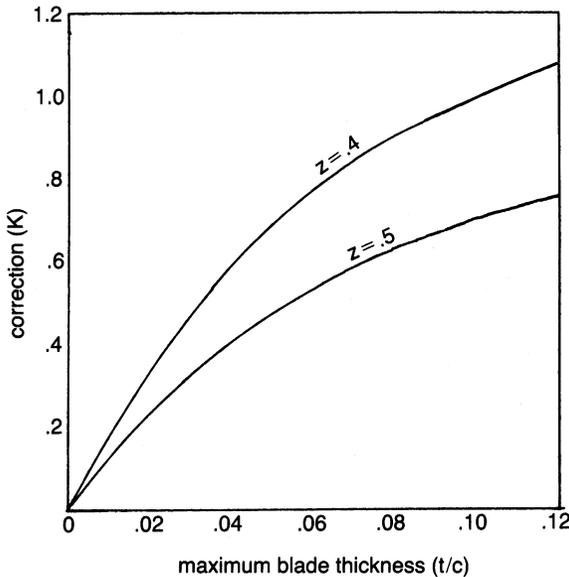


Figure 7-25. Correction factor for blade thickness and incidence angle calculation.

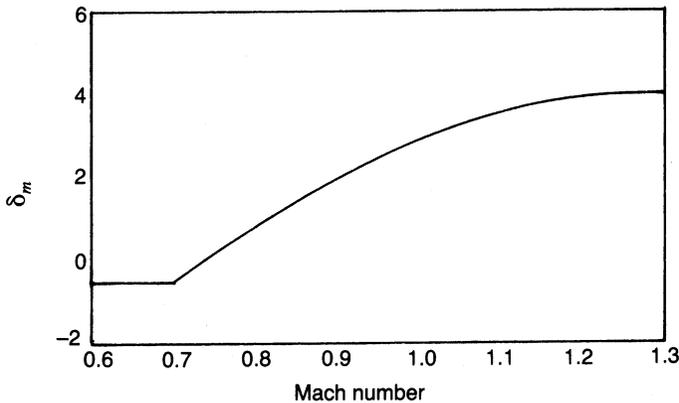


Figure 7-26. Mach-number correction for incidence angle.

where m_f is a function of the stagger angle, maximum thickness, and the position of maximum thickness as seen in Figure 7-27. The second term of the equation should only be used for camber angles $0 < \theta > 8$. The third term must be used only when the mach number is between $0.75 < M > 1.3$.

The use of NACA cascade data for calculating the exit air angle is also widely used. Mellor has replotted some of the low-speed NACA 65 series cascade data in convenient graphs of inlet air angle against exit air angle for blade sections of given lift and solidity set at various staggers. Figure 7-28 shows the NACA 65 series of airfoils.

The 65 series blades are specified by an airfoil notation similar to 65-(18) 10. This specification means that an airfoil has the profile shape 65 with a camber line corresponding to a lift coefficient (C_L) = 1.8 and approximate thickness of 10% of the chord length. The relationship between the camber angle and the lift coefficient for the 65 series blades is shown in Figure 7-29.

The low-speed cascade data have been replotted by Mellor in the form of graphs of α_2 against α_1 for blade sections of given camber and space-chord ratio but set at varying stagger γ , and tested at varying incidence ($i = \alpha_1 - \beta_1$) or angle of attack ($\alpha_1 - \gamma$) as seen in Figure 7-30. The range on each block of results is indicated with heavy black lines, which show the attack angle at which the drag coefficient increases by 50% over the mean unstalled drag coefficient.

NACA has given “design points” for each cascade tested. Each design point is chosen on the basis of the smoothest pressure distribution observed on the blade surfaces: if the pressure distribution is smooth at one particular incidence at low speed, it is probable that the section will operate efficiently

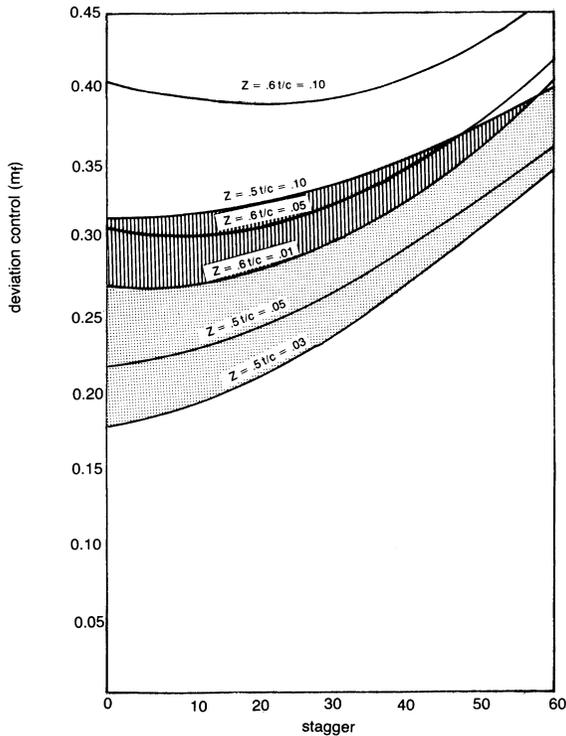


Figure 7-27. Position of maximum thickness effect on deviation.

at a higher Mach number at the same incidence, and that this same incidence should be selected as a design point.

Although such a definition appears somewhat arbitrary at first, the plots of such design points against solidity and camber give consistent curves. These design points are replotted in Figure 7-31, showing the angle of attack ($\alpha_1 - \gamma$) plotted against space-chord ratio for different cambers. The design attack angle of a cascade of given space-chord ratio and camber is independent of stagger.

If the designer has complete freedom to choose space-chord ratio, camber, and stagger, then a "design point" choice may be made by trial and error from the plots of Figure 7-30 and 7-31. For example, if an outlet angle (α_2) of 15 is required from an inlet angle of 35, a reference to the curves of the figures will show that a space-chord ratio of 1.0, camber 1.2, and stagger 23 will give a cascade operating at its design point. There are a limited variety of cascades of different space-chord ratios, but one cascade that will operate at

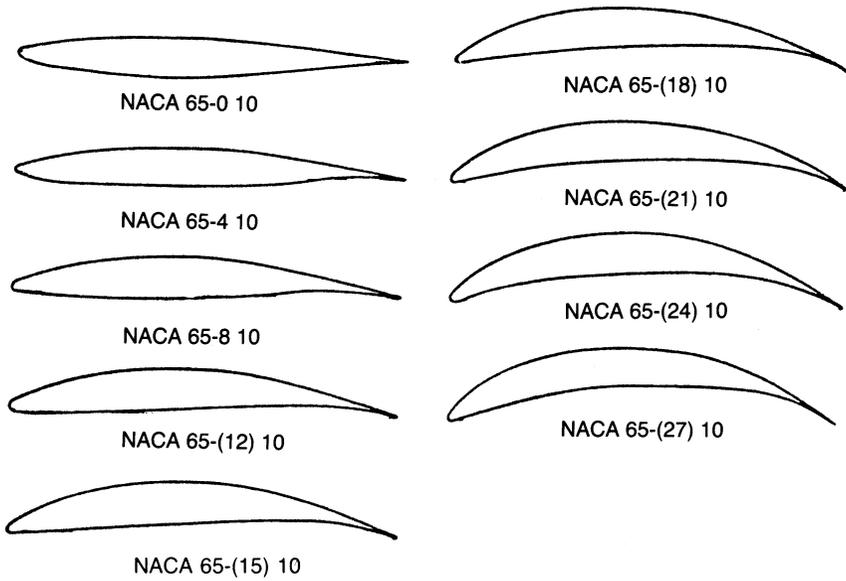


Figure 7-28. The NACA 65 series of cascade airfoils.

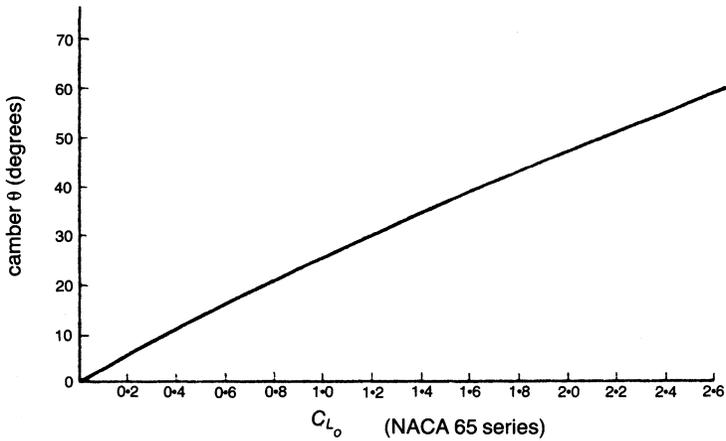


Figure 7-29. Approximate relation between camber (θ) and C_{L0} of NACA 65 series.

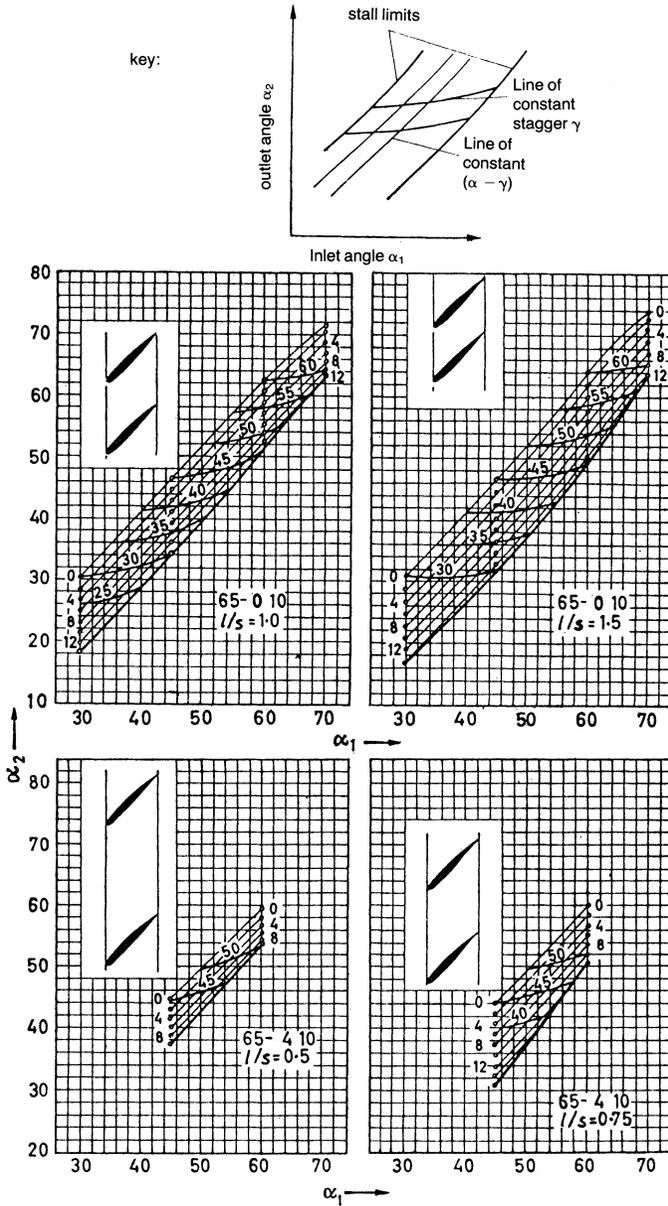


Figure 7-30. The NACA 65 series cascade data. (Courtesy of G. Mellor, Massachusetts Institute of Technology, Gas Turbine Laboratory Publication.)

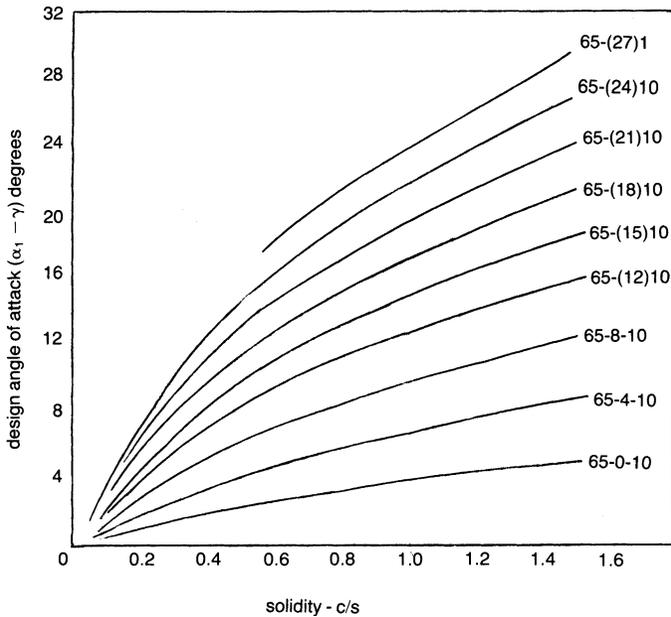


Figure 7-31. Design angles of attack ($\alpha_1 - \gamma$) for NACA 65 series.

“design point” at the specified air angles. For example, if the space-chord ratio were required to be 1.0 in the previous example, then the only cascade that will produce design point operation is that of camber 1.2, stagger 23.

Such a design procedure may not always be followed, for the designer may choose to design the stage to operate closer to the positive stalling limit or closer to the negative stalling (choking) limit at design operating conditions to obtain more flexibility at off-design conditions.

Compressor Stall

There are three distinct stall phenomena. Rotating stall and individual blade stall are aerodynamic phenomena. Stall flutter is an aeroelastic phenomenon.

Rotating Stall

Rotating stall (propagating stall) consists of large stall zones covering several blade passages and propagates in the direction of the rotor and at some fraction of rotor speed. The number of stall zones and the propagating rates vary considerably. Rotating stall is the most prevalent type of stall phenomenon.

The propagation mechanism can be described by considering the blade row to be a cascade of blades as shown in Figure 7-32. A flow perturbation causes blade 2 to reach a stalled condition before the other blades. This stalled blade does not produce a sufficient pressure rise to maintain the flow around it, and an effective flow blockage or a zone of reduced flow develops. This retarded flow diverts the flow around it so that the angle of attack increases on blade 3 and decreases on blade 1. The stall propagates downward relative to the blade row at a rate about half the block speed; the diverted flow stalls the blades below the retarded-flow zone and unstalls the blades above it. The retarded flow or stall zone moves from the pressure side to the suction side of each blade in the opposite direction of rotor rotation. The stall zone may cover several blade passages. The relative speed of propagation has been observed from compressor tests to be less than the rotor speed. Observed from an absolute frame of reference, the stall zones appear to be moving in the direction of rotor rotation. The radial extent of the stall zone may vary from just the tip to the whole blade length. Table 7-1 shows the characteristics of rotating stall for single and multistage axial-flow compressors.

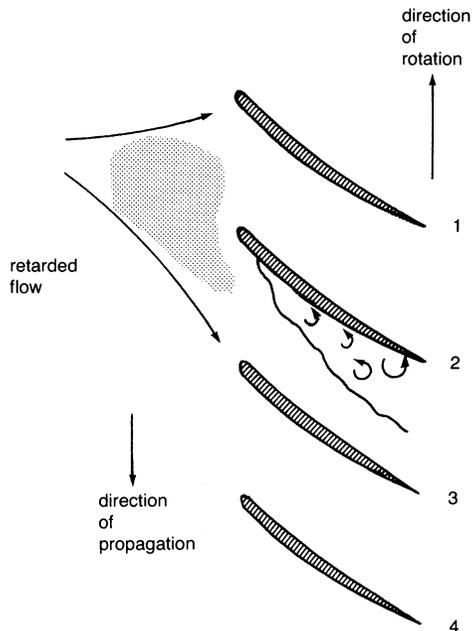


Figure 7-32. Propagating stall in a cascade.

Table 7-1
Summary of Rotating Stall Data

| Single-Stage Compressors | | | | | | |
|--------------------------|----------------------|-----------------------|---|--|-----------------------------|---------------|
| Type of Velocity Diagram | Hub-tip Radius Ratio | Number Of Stall Zones | Propagation Rate, Stall Speed, abs/ Rotor Speed | Weight-flow Fluctuation during stall, $\Delta_p V / \bar{V}$ | Radial Extent of Stall Zone | Type of Stall |
| Symmetrical | 0.50 | 3 | 0.420 | 1.39 | Partial | Progressive |
| | | 4 | 0.475 | 2.14 | | |
| | | 5 | 0.523 | 1.66 | ↓ | ↓ |
| | 0.90 | 1 | 0.305 | 1.2 | Total | Abrupt |
| | 0.80 | 8 | 0.87 | 0.76 | Partial | Progressive |
| | | 1 | 0.36 | 1.30 | Total | Abrupt |
| | 0.76 | 7 | 0.25 | 2.14 | Partial | Progressive |
| | | 8 | 0.25 | 1.10 | | |
| | | 5 | 0.25 | 1.10 | ↓ | ↓ |
| | | 3 | 0.23 | 2.02 | ↓ | |
| | | 4 | 0.48 | 1.47 | Total | |
| | | 3 | 0.48 | 2.02 | | |
| | | 2 | 0.49 | 1.71 | ↓ | |
| | 0.72 | 6, 8 | 0.245 | 0.71 = 1.33 | Total | Progressive |
| Free vortex | 0.60 | 1 | 0.48 | 0.60 | Partial | Progressive |
| | | 2 | 0.36 | 0.60 | Partial | Progressive |
| | | 1 | 0.10 | 0.68 | Total | Abrupt |
| Solid body | 0.60 | 1 | 0.45 | 0.60 | Partial | Progressive |
| | | 1 | 0.12 | 0.65 | Total | Abrupt |
| Vortex transonic | 0.50 | 3 | 0.816 | — | Partial | Progressive |
| | | 2 | 0.634 | — | Total | Progressive |
| | | 1 | 0.565 | — | Total | Abrupt |
| | | 0.40 | 2 | — | — | Partial |

| Multistage Compressors | | | | |
|------------------------|---|-----------------------------|--------------|---------------|
| Number of Stall Zones | Propagation Rate, Stall Speed, abs/ Rotor Speed | Radial Extent of Stall Zone | Periodicity | Type of Stall |
| 3 | 0.57 | Partial | Steady | Progressive |
| 4 | ↓ | ↓ | ↓ | ↓ |
| 5 | | | | |
| 6 | | | | |
| 7 | | | | |
| 4 | 0.55 | Partial | Intermittent | Progressive |
| 5 | ↓ | ↓ | ↓ | ↓ |
| 6 | | | | |

| | | | | |
|---|------|---------|--------------|-------------|
| 1 | 0.48 | Partial | Steady | Progressive |
| 1 | 0.57 | Partial | Steady | Progressive |
| 2 | | | | |
| 3 | ↓ | ↓ | ↓ | ↓ |
| 4 | | | | |
| 1 | 0.57 | Partial | Intermittent | Progressive |
| 2 | | | | |
| 3 | ↓ | ↓ | ↓ | ↓ |
| 4 | | | | |
| 5 | | | | |
| 1 | 0.47 | Total | Steady | Abrupt |
| 1 | 0.43 | Total | Steady | Abrupt |
| 1 | 0.53 | Total | Steady | Abrupt |

Individual Blade Stall

This type of stall occurs when all the blades around the compressor annulus stall simultaneously without the occurrence of a stall propagation mechanism. The circumstances under which individual blade stall is established are unknown at present. It appears that the stalling of a blade row generally manifests itself in some type of propagating stall and that individual blade stall is an exception.

Stall Flutter

This phenomenon is caused by self-excitation of the blade and is aero-elastic. It must be distinguished from classic flutter, since classic flutter is a coupled torsional-flexural vibration that occurs when the freestream velocity over a wing or airfoil section reaches a certain critical velocity. Stall flutter, on the other hand, is a phenomenon that occurs due to the stalling of the flow around a blade.

Blade stall causes Karman vortices in the airfoil wake. Whenever the frequency of these vortices coincides with the natural frequency of the airfoil, flutter will occur. Stall flutter is a major cause of compressor blade failure.

Performance Characteristics of an Axial-Flow Compressor

The calculation of the performance of an axial-flow compressor at both design and off-design conditions requires the knowledge of the various types of losses encountered in an axial-flow compressor.

The accurate calculation and proper evaluation of the losses within the axial-flow compressor are as important as the calculation of the blade-loading parameter, since unless the proper parameters are controlled, the efficiency drops. The evaluation of the various losses is a combination of experimental results and theory. The losses are divided into two groups: (1) losses encountered in the rotor, and (2) losses encountered in the stator. The losses are usually expressed as a loss of heat and enthalpy.

A convenient way to express the losses is in a nondimensional manner with reference to the blade speed. The theoretical total head available (q_{tot}) is equal to the head available from the energy equation ($q_{\text{th}} = q_{\text{tot}}$) plus the head, which is lost from disc friction.

$$q_{\text{tot}} = q_{\text{th}} + q_{\text{df}} \quad (7-29)$$

The adiabatic head that is actually available at the rotor discharge is equal to the theoretical head minus the head losses from the shock in the rotor, the incidence loss, the blade loadings and profile losses, the clearance between the rotor and the shroud, and the secondary losses encountered in the flow passage

$$q_{\text{ia}} = q_{\text{th}} - q_{\text{in}} - q_{\text{sh}} - q_{\text{bl}} - q_{\text{c}} - q_{\text{sf}} \quad (7-30)$$

Therefore, the adiabatic efficiency in the impeller is

$$\eta_{\text{imp}} = \frac{q_{\text{ia}}}{q_{\text{tot}}} \quad (7-31)$$

The calculation of the overall stage efficiency must also include the losses encountered in the stator. Thus, the overall actual adiabatic head attained would be the actual adiabatic head of the impeller minus the head losses encountered in the stator from wake caused by the impeller blade, the loss of part of the kinetic head at the exit of the stator, and the loss of head from the frictional forces encountered in the stator

$$q_{\text{oa}} = q_{\text{ia}} - q_{\text{w}} - q_{\text{ex}} - q_{\text{osf}} \quad (7-32)$$

Therefore, the adiabatic efficiency in the stage

$$\eta_{\text{stage}} = \frac{q_{\text{oa}}}{q_{\text{tot}}} \quad (7-33)$$

The losses as mentioned earlier can be further described:

1. *Disc friction loss.* This loss is from skin friction on the discs that house the blades of the compressors. This loss varies with different types of discs.
2. *Incidence loss.* This loss is caused by the angle of the air and the blade angle not being coincident. The loss is minimum to about an angle of $\pm 4^\circ$, after which the loss increases rapidly.
3. *Blade loading and profile loss.* This loss is due to the negative velocity gradients in the boundary layer, which gives rise to flow separation.
4. *Skin friction loss.* This loss is from skin friction on the blade surfaces and on the annular walls.
5. *Clearance loss.* This loss is due to the clearance between the blade tips and the casing.
6. *Wake loss.* This loss is from the wake produced at the exit of the rotary.
7. *Stator profile and skin friction loss.* This loss is from skin friction and the attack angle of the flow entering the stator.
8. *Exit loss.* This loss is due to the kinetic energy head leaving the stator.

Figure 7-33 shows the various losses as a function of flow. Note that the compressor is more efficient as the flow nears surge conditions. Figure 7-34 also shows a typical axial-flow compressor map. Note the steepness of the constant speed lines as compared with a centrifugal compressor. The axial-flow compressor has a much smaller operating range than its counterpart in the centrifugal compressor.

Stall Analysis of an Axial-Flow Compressor

A typical vibration analysis identified a surge condition in the fifth stage of an axial compressor. A pressure transducer with a voltage output was used to obtain the frequency spectra. In the first four stages of the compressor, no outstanding vibration amplitudes were recorded. A signal was noted at $48N$ (N being the running speed), but the amplitude was not high, and it did not fluctuate. A measurement at the low-pressure bleed chamber taken from the fourth stage showed similar characteristics. The compressor high-pressure bleed chamber occurs after the eighth stage. A measurement at this chamber showed a high, fluctuating $48N$ signal. As there are 48 blades on the fifth-stage wheel, a problem in the fifth stage was suspected. However, above the fifth stage are blade rows of $86N$ ($2 \times 48N$), so the analysis was not clearcut. It was found that the measurement at the high-pressure bleed chamber

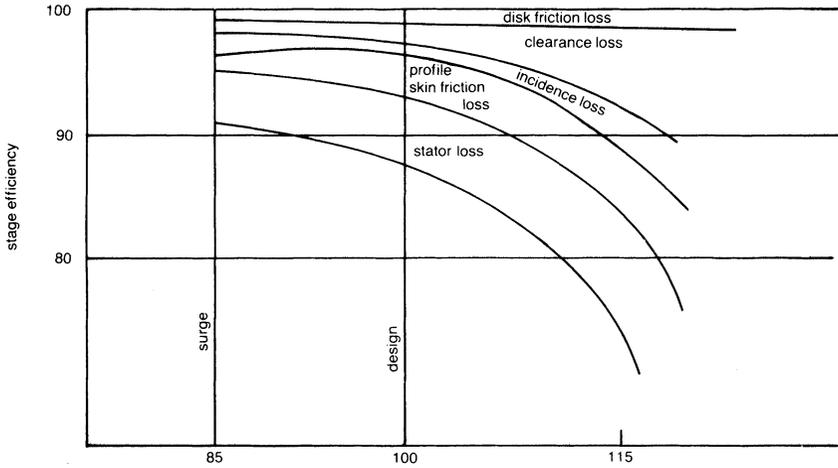


Figure 7-33. Losses in an axial-flow compressor stage.

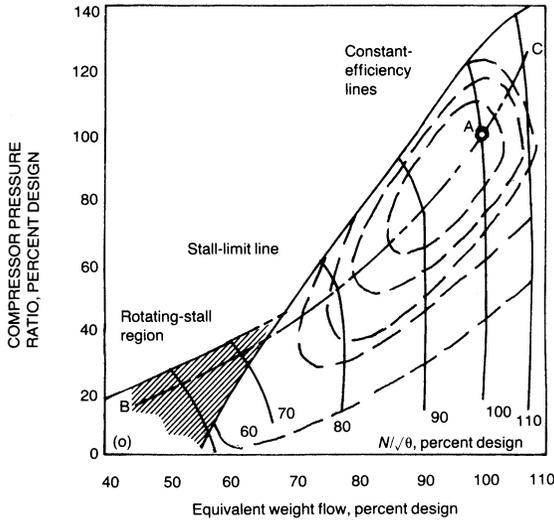


Figure 7-34. Performance map of an axial-flow compressor.

showed only a very small $86N$ amplitude compared to the high amplitude of the $48N$ frequency. Since blade rows of 86 blades were closer to the high-pressure bleed chamber, the expected high signal should have been $86N$ compared to $48N$ under normal operating conditions. This high amplitude

of $48N$ indicated that it was the fifth stage that caused the high, fluctuating signal; thus, a stall condition in that section was probable. Figures 7-35, 7-36, 7-37, and 7-38 show the spectrum at speeds of 4100, 5400, 8000, and 9400 rpm. At 9400 rpm, the second and third harmonics of $48N$ were also very predominant.

Next, the fifth-stage pressure was measured. Once again, a high amplitude at $48N$ was found. However, a predominant reading was also observed at 1200 Hz frequency. Figures 7-39 and 7-40 show the largest amplitudes at speeds of 5800 and 6800 rpm, respectively.

At the compressor exit, predominate frequencies of $48N$ existed up to speeds of 6800 rpm. At 8400 rpm, the $48N$ and $86N$ frequencies were of about equal magnitudes—the only signal where the $48N$ and $86N$ frequencies were the same. The pressure was measured from a static port in the

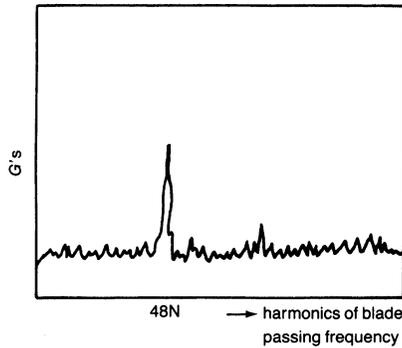


Figure 7-35. High-pressure bleed chamber—4100 rpm.

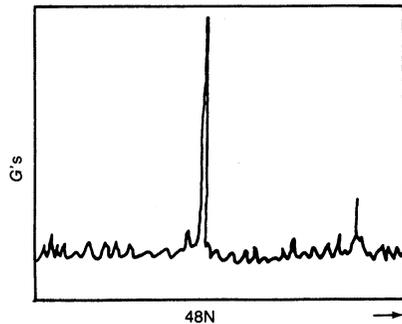


Figure 7-36. High-pressure bleed chamber—5400 rpm.

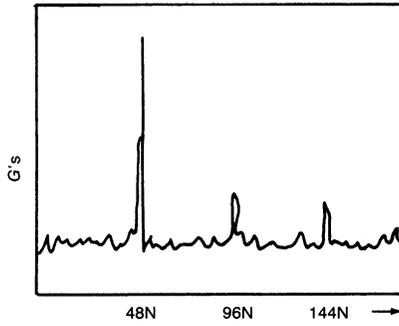


Figure 7-37. High-pressure bleed chamber—8000 rpm.

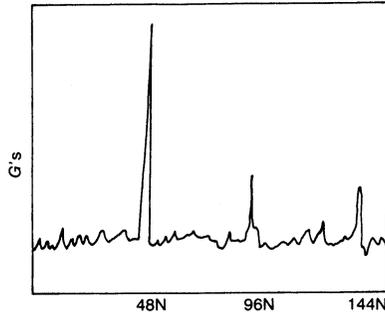


Figure 7-38. High-pressure bleed chamber—9400 rpm.



Figure 7-39. Fifth-stage bleed pressure—5800 rpm.

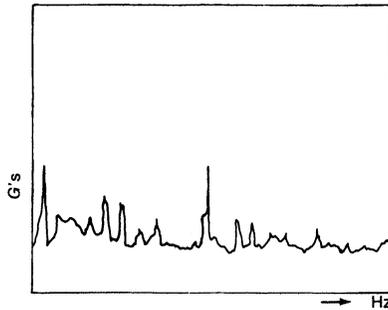


Figure 7-40. Fifth-stage bleed pressure—6800 rpm.

chamber. All other pressures were measured from the shroud, thus indicating the phenomena occurred at the blade tip. Since the problem was isolated to the fifth stage, the conclusion was that the stall occurred at the fifth-stage rotor tip. A subsequent inspection confirmed the suspicion when cracks at the blade hubs were noticed.

Bibliography

- Boyce, M.P., "Transonic Axial-Flow Compressor," ASME Paper No. 67-GT-47.
- Boyce, M.P., "Fluid Flow Phenomena in Dusty Air," (Thesis), University of Oklahoma Graduate College, 1969, p. 18.
- Boyce, M.P., Schiller, R.N., and Desai, A.R., "Study of Casing Treatment Effects in Axial-flow Compressors," ASME Paper No. 74-GT-89.
- Boyce, M.P., "Secondary Flows in Axial-flow Compressors with Treated Blades," AGARD-CCP-214 pp. 5-1 to 5-13, 1974.
- Carter, A.D.S., "The Low-Speed Performance of Related Aerofoils in Cascade," Rep. R.55, British NGTE, September, 1949.
- Giamati, C.C., and Finger, H.B., "Design Velocity Distribution in Meridional Plane," NASA SP 36, Chapter VIII (1965), p. 255.
- Graham, R.W. and Guentert, E.C., "Compressor Stall and Blade Vibration," NASA SP 36, (1965) Chapter XI, p. 311.
- Hatch, J.E., Giamati, C.C., and Jackson, R.J., "Application of Radial Equilibrium Condition to Axial-Flow Turbomachine Design Including Consideration of Change of Entropy with Radius Downstream of Blade Row," NACA RM E54A20 (1954).
- Herrig, L.J., Emery, J.C., and Erwin, J.R., "Systematic Two-Dimensional Cascade Tests of NACA 65 Series Compressor Blades at Low Speed," NACA R.M. E 55H11 (1955).

- Holmquist, L.O., and Rannie, W.D., "An Approximate Method of Calculating Three-Dimensional Flow in Axial Turbomachines" (Paper) Meeting Inst. Aero. Sci., New York, January 24-28, 1955.
- Horlock, J.H., "Axial Flow Compressors," Robert E. Krieger Publishing Company, 1973.
- Koller, U., Monig, R., Kusters, B., Schreiber, H-A, 1999, "Development of Advanced Compressor Airfoils for Heavy-Duty Gas Turbines. Part I: Design and Optimization," ASME 99-GT-95.
- Lieblein, S., Schwenk, F.C., and Broderick, R.L., "Diffusion Factor for Estimating Losses and Limiting Blade Loading in Axial-Flow Compressor Blade Elements," NACA RM #53001 (1953).
- Mellor, G., "The Aerodynamic Performance of Axial Compressor Cascades with Application to Machine Design," (Sc. D. Thesis), M.I.T. Gas Turbine Lab, M.I.T. Rep. No. 38 (1957).
- Stewart, W.L., "Investigation of Compressible Flow Mixing Losses Obtained Downstream of a Blade Row," NACA RM E54120 (1954).

8

Radial-Inflow Turbines

The radial-inflow turbine has been in use for many years. It first appeared as a practical power-producing unit in the hydraulic turbine field. Basically a centrifugal compressor with reversed flow and opposite rotation, the radial-inflow turbine was the first used in jet engine flight in the late 1930s. It was considered the natural combination for a centrifugal compressor used in the same engine. Designers thought it easier to match the thrust from the two rotors and that the turbine would have a higher efficiency than the compressor for the same rotor because of the accelerating nature of the flow.

The performance of the radial-inflow turbine is now being investigated with more interest by the transportation and chemical industries: in transportation, this turbine is used in turbochargers for both spark ignition and diesel engines; in aviation, the radial-inflow turbine is used as an expander in environmental control systems; and in the petrochemical industry, it is used in expander designs, gas liquefaction expanders, and other cryogenic systems. Radial-inflow turbines are also used in various small gas turbines to power helicopters and as standby generating units.

The radial-inflow turbine's greatest advantage is that the work produced by a single stage is equivalent to that of two or more stages in an axial turbine. This phenomenon occurs because a radial-inflow turbine usually has a higher tip speed than an axial turbine. Since the power output is a function of the square of the tip speed ($P \propto U^2$) for a given flow rate, the work is greater than in a single-stage axial-flow turbine.

The radial-inflow turbine has another advantage: its cost is much lower than that of a single or multistage axial-flow turbine. The radial-inflow turbine has a lower turbine efficiency than the axial-flow turbine; however, lower initial costs may be an incentive to choosing a radial-inflow turbine.

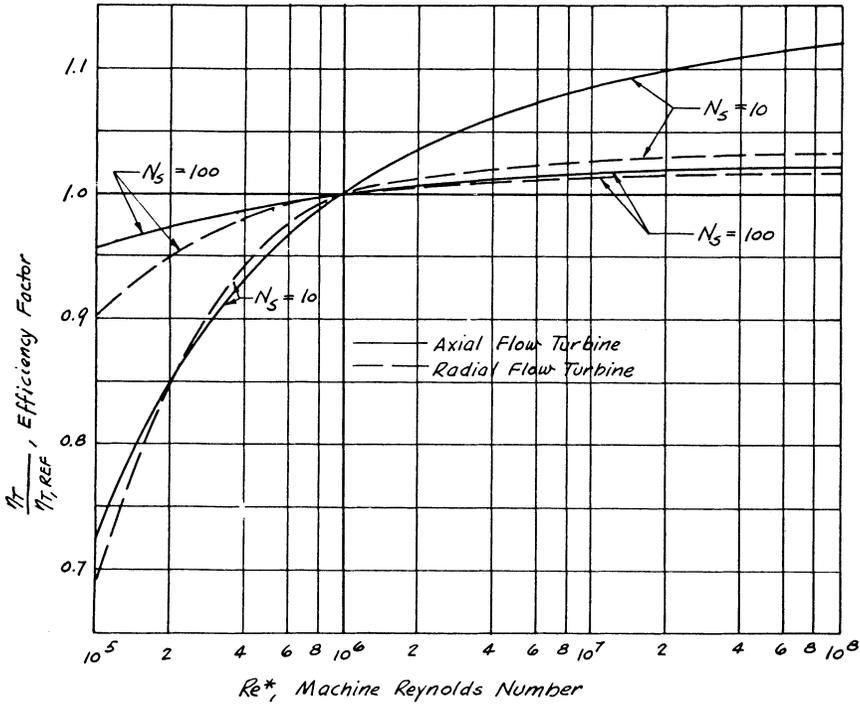


Figure 8-1. Influence of Reynolds number on turbine stage efficiency.

The radial-inflow turbine is especially attractive when the Reynolds number ($Re = \rho UD/\mu$) becomes low enough ($Re = 10^5 - 10^6$) that the efficiency of the axial-flow turbine is below that of a radial-inflow turbine, as shown in Figure 8-1. The effect of specific speed ($N_s = N\sqrt{Q}/H^{3/4}$) and specific diameter ($D_s = DH^{1/4}/\sqrt{Q}$) on the efficiency of a turbine is shown in Figure 8-2. Radial-inflow turbines are more efficient at a Reynolds number between 10^5 and 10^6 and specific speeds below $N_s = 10$.

Description

The radial-inflow turbine has many components similar to those of a centrifugal compressor. However, the names and functions differ. There are two types of radial-inflow turbines: the cantilever radial-inflow turbine and the mixed-flow radial-inflow turbine. Cantilever blades are often two-dimensional and use nonradial inlet angles. There is no acceleration of the

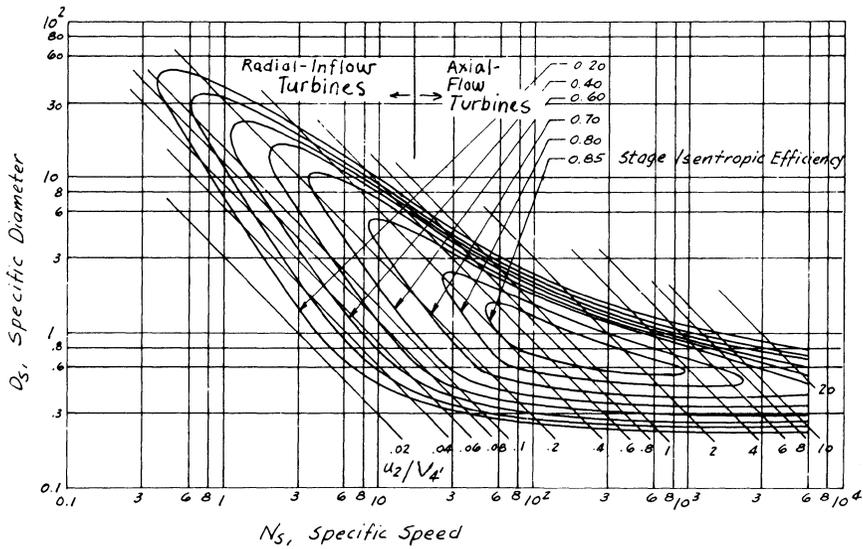


Figure 8-2. $N_s D_s$ diagram for a turbine stage. Efficiency is on a total-to-total basis; that is, it is related to inlet and exit stagnation conditions. Diagram values are suitable for machine Reynolds number $Re \geq 10^6$. (Balje, O.E., "A Study of Reynolds Number Effects in Turbomachinery," Journal of Engineering for Power, ASME Trans., Vol. 86, Series A, p. 227.)

flow through the rotor, which is equivalent to an impulse or low-reaction turbine. The cantilever-type radial-inflow turbine is infrequently used because of low efficiency and production difficulties. This type of turbine also has rotor blade flutter problems.

The radial-inflow turbine can be the cantilever type as shown in Figure 8-3, or the mixed-flow type as shown in Figure 8-4. The mixed-flow radial-inflow turbine is a widely used design. Figure 8-5 shows the components. The scroll or collector receives the flow from a single duct. The scroll usually has a decreasing cross-sectional area around the circumference. In some designs the scrolls are used as vaneless nozzles. The nozzle vanes are omitted for economy to avoid erosion in turbines where fluid or solid particles are trapped in the air flow. Frictional flow losses in vaneless designs are greater than in vanned nozzle designs because of the nonuniformity of the flow and the greater distance the accelerating air flow must travel. Vaneless nozzle configurations are used extensively in turbochargers where efficiency is not important, since in most engines the amount of energy in the exhaust gases far exceeds the energy needs of the turbocharger.

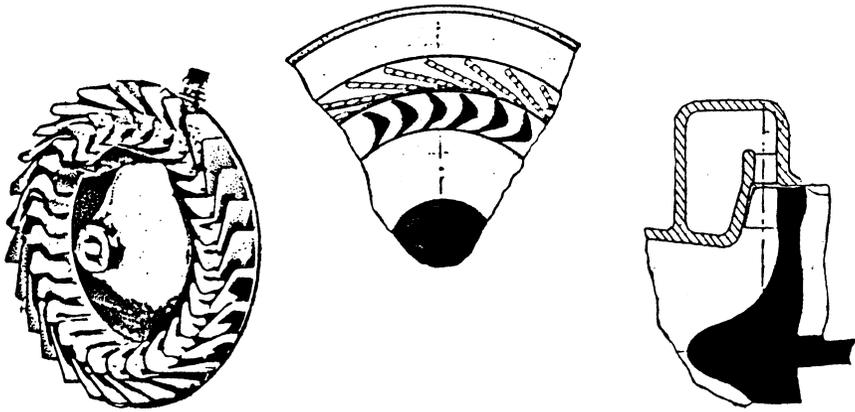


Figure 8-3. Cantilever-type radial-inflow turbine.

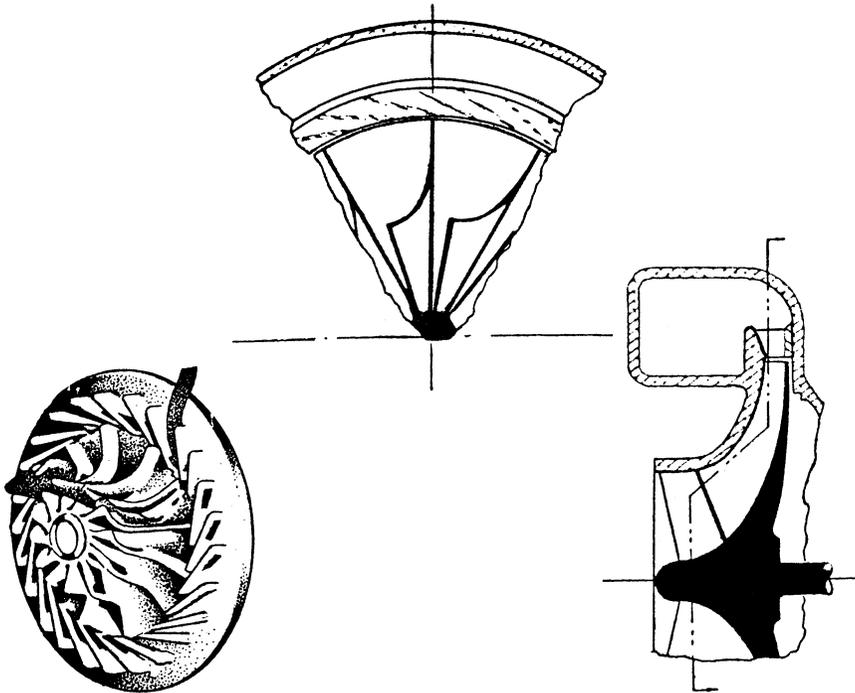


Figure 8-4. Mixed-flow-type radial-inflow turbine.

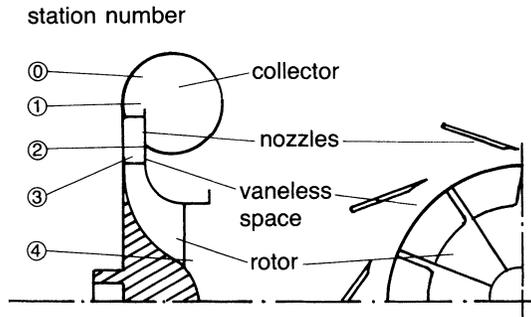


Figure 8-5. Components of a radial-inflow turbine.

The nozzle blades in a vaned turbine design are usually fitted around the rotor to direct the flow inward with the desired whirl component in the inlet velocity. The flow is accelerated through these blades. In low-reaction turbines the entire acceleration occurs in the nozzle vanes.

The rotor or impeller of the radial-inflow turbine consists of a hub, blades, and in some cases, a shroud. The hub is the solid axisymmetrical portion of the rotor. It defines the inner boundary of the flow passage and is sometimes called the disc. The blades are integral to the hub and exert a normal force on the flow stream. The exit section of the blading is called an exducer and it is constructed separately like an inducer in a centrifugal compressor. The exducer is curved to remove some of the tangential velocity force at the outlet.

The outlet diffuser is used to convert the high absolute velocity leaving the exducer into static pressure. If this conversion is not done, the efficiency of the unit will be low. This conversion of the flow to a static head must be done carefully, since the low-energy boundary layers cannot tolerate great adverse pressure gradients.

Theory

The general principles of energy transfer in a radial-inflow turbine are similar to those already outlined in the compressor section. Figure 8-6 shows the velocity vectors in turbine rotor flow.

The Euler turbine equation previously defined holds for flow in any turbomachine

$$H = \frac{1}{g_c} (U_3 V_{\theta 3} - U_4 V_{\theta 4}) \quad (8-1)$$

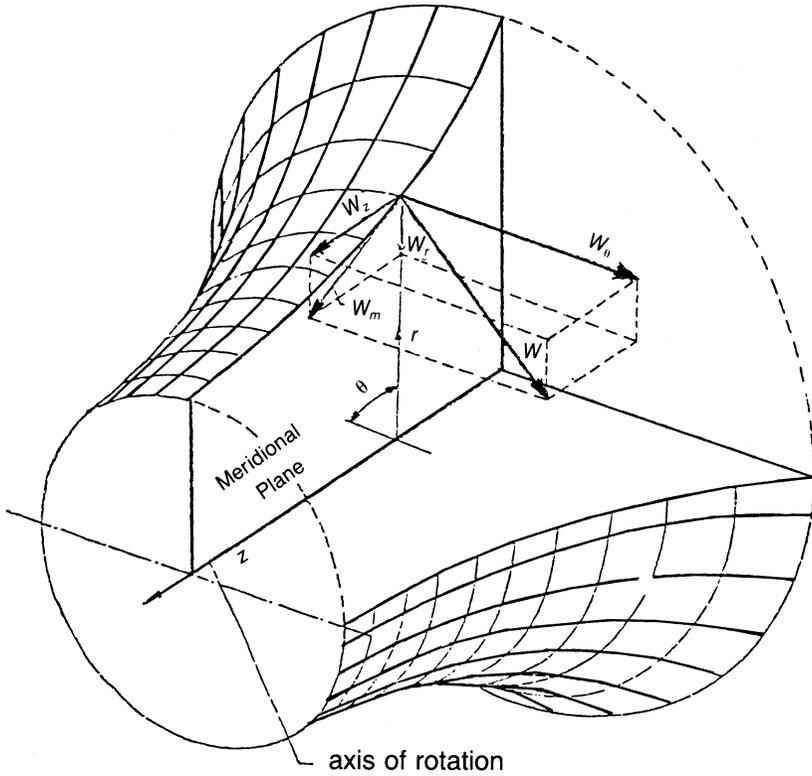


Figure 8-6. Velocity vectors in turbine rotor flow.

It may be written in terms of the absolute and relative velocities

$$H = \frac{1}{2g_c} [(U_3 - U_4)^2 + (V_3^2 - V_4^2) + (W_4^2 - W_3^2)] \tag{8-2}$$

For a positive power output, the blade tip speed and whirl velocity combination at the inlet must be greater than at the exit. From Equation (8-2), the flow must be radially inward so that centrifugal effects may be used. The velocity exiting from a turbine is considered to be unrecoverable; therefore, the utilization factor is defined as the ratio of the total head to the total head plus the absolute exit velocity.

$$\epsilon = \frac{H}{H + (\frac{1}{2} V_4^2)} \tag{8-3}$$

The relative proportions of energy transfers obtained by a change of static and dynamic pressure are used to classify turbomachinery. The parameter used to describe this relationship is called the degree of reaction. Reaction, in this case, is energy transfer by means of a change in static pressure in a rotor to the total energy transfer in the rotor

$$R = \frac{\frac{1}{2g} [(U_3^2 - U_4^2) + (W_4^2 - W_3^2)]}{H} \tag{8-4}$$

The overall efficiency of a radial-inflow turbine is a function of efficiencies from various components such as the nozzle and rotor. A typical turbine expansion enthalpy/entropy diagram is shown in Figure 8-7. The total enthalpy remains constant through the nozzle, since neither work nor heat is transferred to or from the fluid. Within the the rotor, the total enthalpy changes. Downstream of the rotor the total enthalpy remains constant.

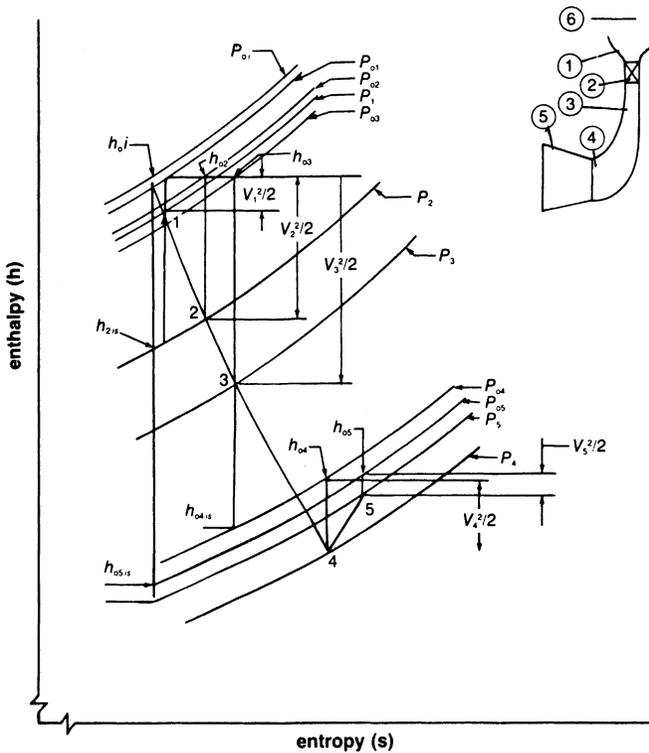


Figure 8-7. *h-s* diagram for turbine stage process.

Total pressure decrease in the nozzle and outlet diffuser are only from frictional losses. In an ideal nozzle or diffuser the total pressure drop is zero. Isentropic efficiency is defined as the ratio of the actual work to the isentropic enthalpy decrease, which is the expansion from the inlet total pressure to the outlet total pressure

$$\eta_{is} = \frac{h_{0i} - h_{05}}{h_{0i} - h_{05is}} \quad (8-5)$$

The nozzle efficiency can be calculated as shown in the following relationship:

$$\eta_{noz} = \frac{h_{0i} - h_2}{h_{0i} - h_{2is}} \quad (8-6)$$

The rotor efficiency can be defined as shown in the following relationship:

$$\eta_{rotor} = \frac{h_{0i} - h_4}{h_{0i} - h_{4is}} \quad (8-7)$$

Similar to the concept of small-stage efficiency in a compressor, the polytropic efficiency in a turbine is the small-stage efficiency in a turbine. The isentropic efficiency can be written in terms of the total pressure as follows:

$$\eta_{is} = \frac{1 - \left(\frac{P_{05}}{P_{oi}}\right)^{\frac{n-1}{n}}}{1 - \left(\frac{P_{05}}{P_{oi}}\right)^{\frac{\gamma-1}{\gamma}}} \quad (8-8)$$

where P/ρ_n equals constant and represents the polytropic process for any particular expansion process. The polytropic efficiency can be written

$$\begin{aligned} \eta_{poly} &= \frac{dh_{0act}}{dh_{0isen}} \\ &= \frac{1 - \left[1 - \frac{n-1}{n} \left(\frac{\Delta P_o}{P_{oi}}\right), \dots\right]}{1 - \left[1 - \frac{\gamma-1}{\gamma} \frac{\Delta P_{oi}}{P_{oi}}, \dots\right]} \\ &= \left(\frac{n-1}{n}\right) / \left(\frac{\gamma-1}{\gamma}\right) \end{aligned} \quad (8-9)$$

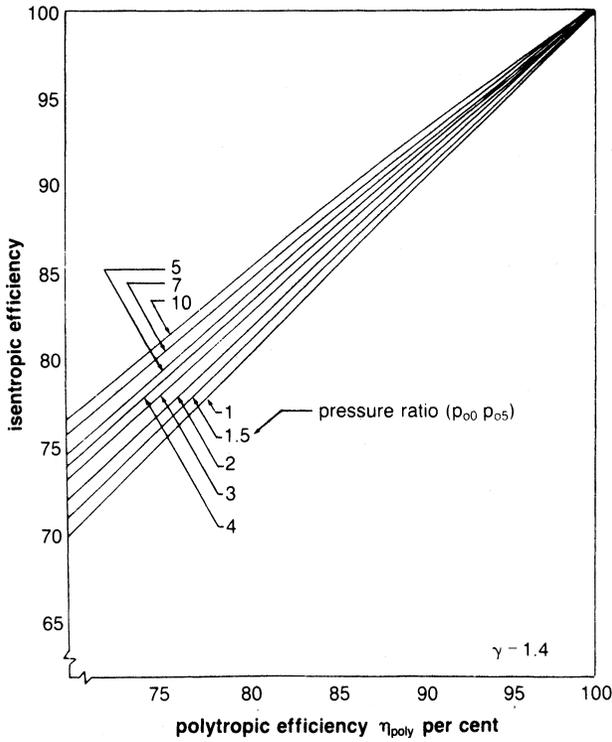


Figure 8-8. Relationship between polytropic and isentropic efficiency during expansion.

The polytropic efficiency in a turbine can be related to the isentropic efficiency and obtained by combining the previous two equations

$$\eta_{is} = \frac{1 - \left(\frac{P_{05}}{P_{oi}}\right)^{\frac{\eta_{poly} \gamma - 1}{\gamma}}}{1 - \frac{P_{05}}{P_{oi}}^{\frac{\gamma - 1}{\gamma}}} \tag{8-10}$$

or

$$\eta_{poly} = \frac{1n \left[1 - \eta_{is} + \eta_{is} \left(\frac{P_{05}}{P_{oi}}\right)^{\frac{\gamma - 1}{\gamma}} \right]}{\left(\frac{\gamma - 1}{\gamma}\right) 1n \left(\frac{P_{05}}{P_{oi}}\right)} \tag{8-11}$$

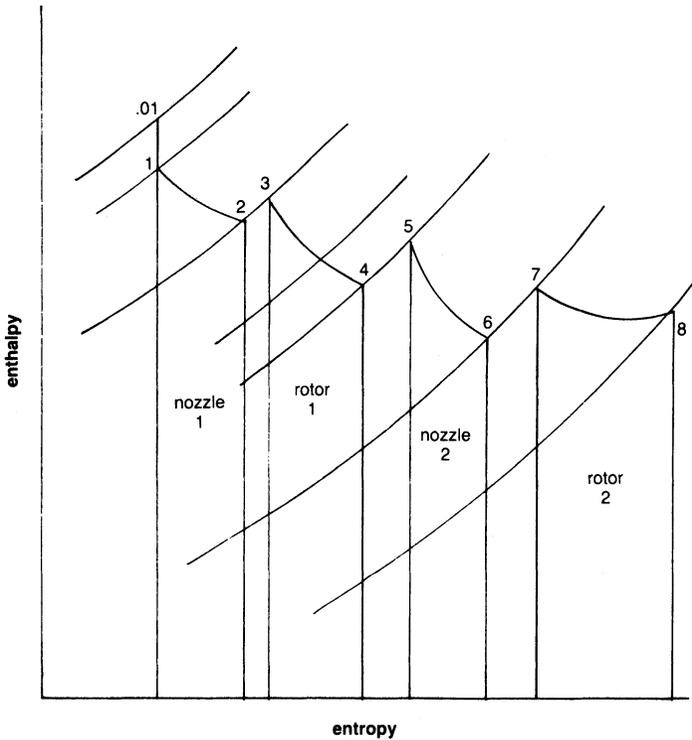


Figure 8-9. Enthalpy-entropy diagram for a multistage turbine.

The relationship between the two efficiencies is plotted in Figure 8-8. The multistage turbine on an enthalpy/entropy diagram is shown in Figure 8-9. Examining the characteristic of the multistage unit, the isentropic enthalpy decrease of the incremental stages as compared to the isentropic enthalpy decrease of a single, whole stage encompassing the multistages is defined as the reheat factor. Since the pressure lines diverge as entropy increases, the sum of the small-stage isentropic decreases are somewhat greater than the overall isentropic decrease for the same pressure. Hence, the reheat factor is greater than unity, and the turbine's isentropic efficiency is greater than its polytropic efficiency of the turbine.

The reheat factor can be given

$$R_f = \frac{\eta_{isen}}{\eta_{poly}} \quad (8-12)$$

Turbine Design Considerations

To design a radial-inflow turbine of the highest efficiency, the exit velocity leaving the turbine must be axial. If the exit velocity is axial, the Euler turbine equation reduces to

$$H = U_3 V_{\theta 3} \quad (8-13)$$

since $V_{\theta 4} = 0$ for an axial outlet velocity.

The flow entering the rotor of a radial-inflow turbine must have a certain incidence angle corresponding to the “slip flow” in a centrifugal impeller and not to zero incidence. By relating this concept to the radial-inflow turbine, the following relationship can be obtained for the ratio of whirl velocity to blade tip speed:

$$\frac{V_{\theta 3}}{U_3} = \left[1 - \frac{\pi}{2\eta_B} \frac{D_3}{D_3 - D_4} \right] \quad (8-14)$$

This ratio is usually in the neighborhood of 0.8. A ratio of D_3/D_4 for radial-inflow rotors is around 2.2, and η_B is the number of blades.

With the aid of the previous relationships, a velocity diagram for the flow entering a radial-inflow turbine can be drawn as shown in Figure 8-10.

The variation in stage efficiency can be shown as a function of the tip speed ratio. The tip speed ratio is a function of the blade speed and the theoretical spouting velocity if the entire enthalpy drop takes place in the nozzle as given by the following equation:

$$\phi = \frac{U}{V_o} \quad (8-15)$$

where

$$V_o = \sqrt{2g_c J \Delta H_o}$$

Figure 8-11 shows the efficiency variation with the tip speed ratio. This curve also shows the runaway speed. Runaway speed is achieved when turbine torque falls to zero at blade speeds higher than the design speed. If failure occurs above the tip speed, the rotor can be defined as a fail-safe rotor design.

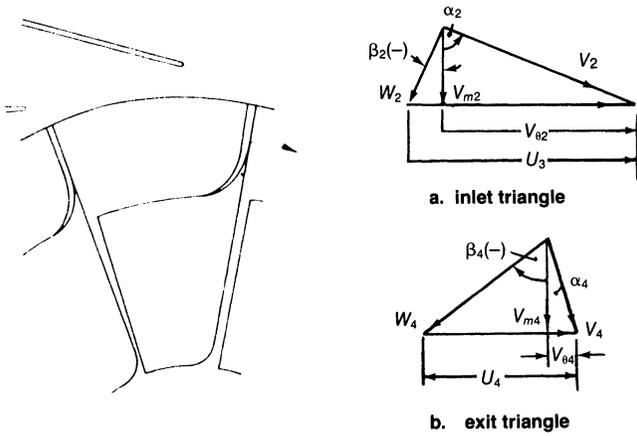


Figure 8-10. Velocity triangles for a radial-inflow turbine.

The inlet area at the blade tip can be calculated using the continuity equation

$$A_3 = \pi D_3 b_3 - \eta_{BT} t_3 b_3 = \frac{\dot{m}}{\rho V_3 \cos \beta_3} \tag{8-16}$$

where b_3 is the blade height and t_3 the blade thickness.

At the exit of the turbine, the absolute exit velocity is axial. Since the blade speed varies at the exit from hub to shroud, a series of blade diagrams are obtained as shown in Figure 8-12.

Losses in a Radial-Inflow Turbine

Losses in a radial-inflow turbine are similar to those in a centrifugal impeller. The losses can be divided into two categories: internal losses and external losses. Internal losses can be divided into the following categories:

1. *Blade loading or diffusion loss.* This loss is due to the type of loading in an impeller. The increase in momentum loss comes from the rapid increase in boundary-layer growth when the velocity close to the wall is reduced. This loss varies from around 7% at a high-flow setting to about 12% at a low-flow setting.

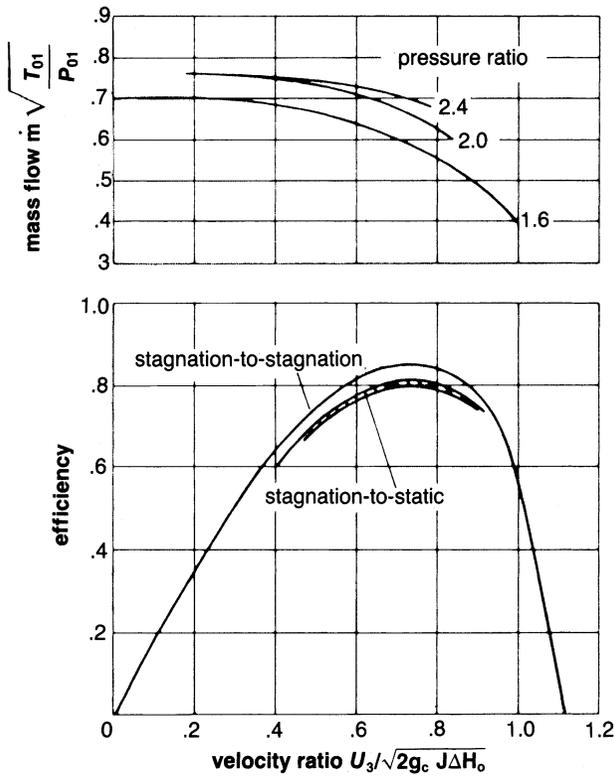


Figure 8-11. An example of a radial-inflow turbine characteristic. (Courtesy Institution of Mechanical Engineers.)

2. *Frictional loss.* Frictional loss is due to wall shear forces. This loss varies from about 1–2% as the flow varies from a low-flow to a high-flow setting.
3. *Secondary loss.* This loss is caused by the movement of the boundary layers in a direction different from the main stream. This loss is small in a well-designed machine and is usually less than 1%.
4. *Clearance loss.* This loss is caused by flow passing between the stationary shroud and the rotor blades and is a function of the blade height and clearance. The clearance is usually fixed by tolerances and, for smaller blade heights, the loss is usually a greater percentage. This loss varies between 1 and 2%.
5. *Heat loss.* This loss is due to heat lost to the walls from cooling.

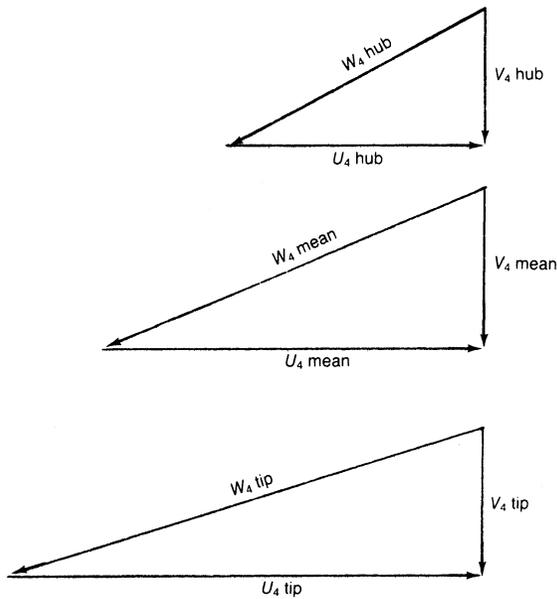


Figure 8-12. Exit velocity diagrams for a radial-inflow turbine.

6. *Incidence loss.* This loss is minimal at design conditions but will increase with off-design operation. These losses vary from about $\frac{1}{2}$ – $1\frac{1}{2}$ %.
7. *Exit loss.* The fluid leaving a radial-inflow turbine constitutes a loss of about one-quarter of the total exit head. This loss varies from about 2–5%.

The external losses are from disc friction, the seal, the bearings, and the gears. The disc friction loss is about 1/2%. The seal, bearings, and gear losses vary from about 5–9%.

Performance of a Radial-Inflow Turbine

A turbine is designed for a single operating condition called the design point. In many applications the turbine is required to operate at conditions other than the design point. The turbine work output can be varied by adjusting the rotative speed, pressure ratio, and turbine inlet temperature. Under these different running conditions, the turbine is operating at off-design conditions.

To predict turbine characteristics, it is necessary to compute flow characteristics throughout the turbine. To perform this computation, the flow must be analyzed inside the blade passage. This analysis is done by first examining the flow in the meridional plane, sometimes called the hub-to-shroud plane. A solution is then obtained for the flow in the blade-to-blade plane. Once this solution is obtained, the flows in the two planes can be combined to give the final quasi-three-dimensional flow. These surfaces are shown in Figure 8-13. The velocity distribution in the meridional plane varies between the hub and shroud as shown in Figure 8-14. The velocity distribution between the suction and pressure surfaces also varies. The velocity between the suction and pressure surfaces varies because the blades are working on the fluid and, as a result, there must be a pressure difference across the blade. The form of velocity distribution on the rotor blades at the hub and shroud and also between the pressure and suction sides is shown in Figure 8-15.

The boundary layer along the blade surfaces must be well energized so that no separation of the flow occurs. Figure 8-16 shows a schematic of the flow in a radial-inflow impeller. Off-design work indicates that radial-inflow turbine efficiency is not affected by changes in flow and pressure ratio to the extent of an axial-flow turbine.

In a radial-inflow turbine the problems of erosion and exducer blade vibration are prominent. The size of the particles being entrained decreases with the square root of the turbine wheel diameter. Inlet filtration is suggested for expanders in the petrochemical industry. The filter usually has to

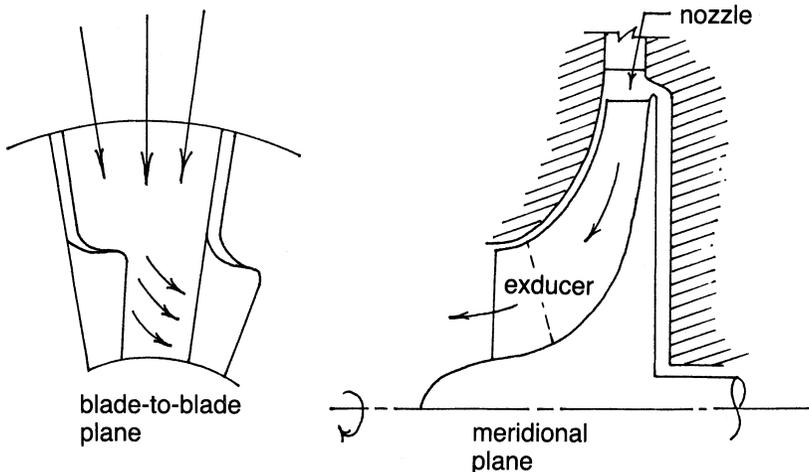


Figure 8-13. The two major flow planes in a radial-inflow turbine.

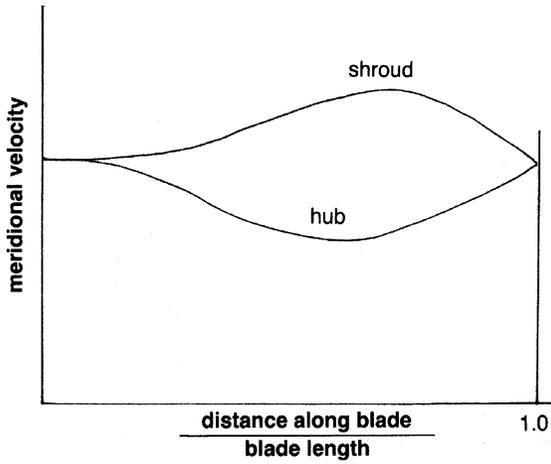


Figure 8-14. Meridional velocity distribution from hub to shroud along the blade length.

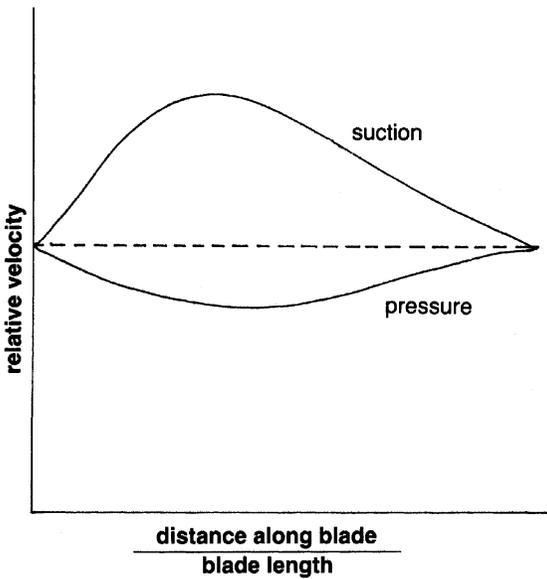


Figure 8-15. Relative velocity distribution of suction and pressure side along the blade length.

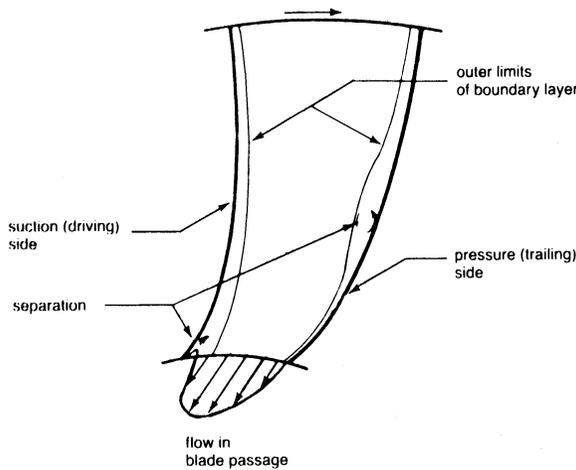


Figure 8-16. Boundary-layer formation in a radial-flow impeller.

be an inertia type to remove most of the larger particles. The exducer fatigue problem is serious in a radial turbine, although it varies with blade loading. The exducer should be designed so that it has a natural frequency four times above the blade passing frequency.

Noise problems in a radial-inflow turbine come from four sources:

1. Pressure fluctuations
2. Turbulence in boundary layers
3. Rotor wakes
4. External noise

Severe noise can be generated by pressure fluctuations. This noise is created by the passage of the rotor blades through the varying velocity fields produced by the nozzles. The noise generated by turbulent flow in boundary layers occurs on most internal surfaces. However, this noise source is negligible. Noise generated from rotor flow is due to the wakes generated downstream in the diffuser. The noise generated by the rotor exducer is considerable. The noise consists of high-frequency components and is proportional to the eighth power of the relative velocity between the wake and the free stream. Outside noise sources are many, but the gear box is the primary source. Intense noise is generated by pressure fluctuations that result from tooth interactions in gearboxes. Other noises may result from out-of-balance conditions and vibratory effects on mechanical components and casings.

Bibliography

- Abidat, M.I., Chen, H., Baines, N.C., and Firth, M.R., 1992. "Design of a Highly Loaded Mixed Flow Turbine," Proc. Inst. Mechanical Engineers, *Journal Power & Energy*, 206: 95–107.
- Arcoumanis, C., Martinez-Botas, R.F., Nouri, J.M., and Su, C.C., 1997. "Performance and Exit Flow Characteristics of Mixed Flow Turbines," *International Journal of Rotating Machinery*, 3(4): 277–293.
- Baines, N.A., Hajilouy-Benisi, A., and Yeo, J.H., 1994. "The Pulse Flow Performance and Modeling of Radial Inflow Turbines," IMechE, Paper No. a405/017.
- Balje, O.E., "A Contribution to the Problem of Designing Radial Turbomachines," Trans. ASME, Vol. 74, p. 451 (1952).
- Benisek, E., 1998. "Experimental and Analytical Investigation for the Flow Field of a Turbocharger Turbine," IMechE, Paper No. 0554/027/98.
- Benson, R.S., "A Review of Methods for Assessing Loss Coefficients in Radial Gas Turbines," *International Journal of Mechanical Sciences*, 12 (1970), pp. 905–932.
- Karamanis, N. Martinez-Botas, R.F., Su, C.C., "Mixed Flow Turbines: Inlet and Exit flow under steady and pulsating conditions," ASME 2000-GT-470.
- Knoernschild, E.M., "The Radial Turbine for Low Specific Speeds and Low Velocity Factors," *Journal of Engineering for Power*, Trans ASME, Serial A, Vol. 83, pp. 1–8 (1961).
- Rodgers, C., "Efficiency and Performance Characteristics of Radial Turbines," SAE Paper 660754, October, 1966.
- Shepherd, D.G., *Principles of Turbomachinery*, New York, The Macmillan Company, 1956.
- Vavra, M.H., "Radial Turbines," Pt 4., AGARD-VKI Lecture Series on Flow in Turbines (Series No. 6), March, 1968.
- Vincent, E.T., "Theory and Design of Gas Turbines and Jet Engines," New York, McGraw-Hill, 1950.
- Wallace, F.J., and Pasha, S.G.A., 1972, *Design, Construction and Testing of a Mixed-Flow Turbine*.
- Winterbone, D.E., Nikpour, B., and Alexander, G.L., 1990, "Measurement of the Performance of a Radial Inflow Turbine in Conditional Steady and Unsteady Flow," IMechE, Paper No. 0405/015.

9

Axial-Flow Turbines

Axial-flow turbines are the most widely employed turbines using a compressible fluid. Axial-flow turbines power most gas turbine units—except the smaller horsepower turbines—and they are more efficient than radial-inflow turbines in most operational ranges. The axial-flow turbine is also used in steam turbine design; however, there are some significant differences between the axial-flow turbine design for a gas turbine and the design for a steam turbine.

Steam turbine development preceded the gas turbine by many years. Thus, the axial-flow turbine used in gas turbines is an outgrowth of steam turbine technology. In recent years the trend in high turbine inlet temperatures in gas turbines has required various cooling schemes. These schemes are described in detail in this chapter with attention to both cooling effectiveness and aerodynamic effects. Steam turbine development has resulted in the design of two turbine types: the impulse turbine and the reaction turbine. The reaction turbine in most steam turbine designs has a 50% reaction level that has been found to be very efficient. This reaction level varies considerably in gas turbines and from hub to tip in a single-blade design.

Axial-flow turbines are now designed with a high work factor (ratio of stage work to square of blade speed) to obtain lower fuel consumption and reduce the noise from the turbine. Lower fuel consumption and lower noise requires the design of higher by-pass ratio engines. A high by-pass ratio engine requires many turbine stages to drive the high-flow, low-speed fan. Work is being conducted to develop high-work, low-speed turbine stages that have high efficiencies.

Turbine Geometry

The axial-flow turbine, like its counterpart the axial-flow compressor, has flow, which enters and leaves in the axial direction. There are two types of axial

turbines: (1) impulse type, and (2) reaction type. The impulse turbine has its entire enthalpy drop in the nozzle; therefore it has a very high velocity entering the rotor. The reaction turbine divides the enthalpy drop in the nozzle and the rotor. Figure 9-1 is a schematic of an axial-flow turbine, also depicting the distribution of the pressure, temperature, and the absolute velocity.

Most axial flow turbines consist of more than one stage, the front stages are usually impulse (zero reaction) and the later stages have about 50% reaction. The impulse stages produce about twice the output of a comparable 50% reaction stage, while the efficiency of an impulse stage is less than that of a 50% reaction stage.

The high temperatures that are now available in the turbine section are due to improvements of the metallurgy of the blades in the turbines. Development of directionally solidified blades as well as the new single crystal blades, with the new coatings, and the new cooling schemes, are responsible for the increase in firing temperatures. The high-pressure ratio in the compressor also causes the cooling air used in the first stages of the turbine to be very hot. The temperatures leaving the gas turbine compressor can reach as high as 1200°F (649°C). Thus the present cooling schemes need revisiting,

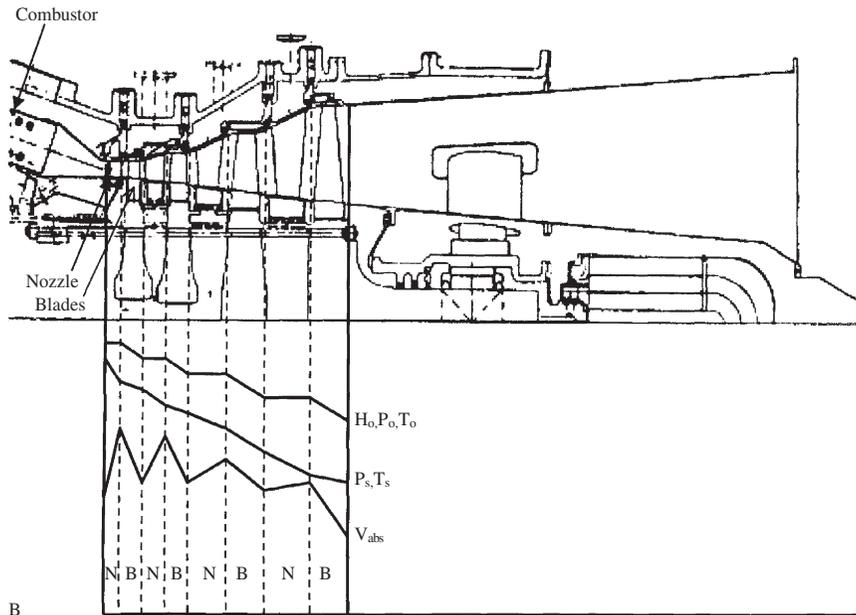


Figure 9-1. Schematic of an axial flow turbine flow characteristics.

and the cooling passages are in many cases also coated. The cooling schemes are limited in the amount of air they can use, before there is a negating an effort in overall thermal efficiency due to an increase in the amount of air used in cooling. The rule of thumb in this area is that if you need more than 8% of the air for cooling you are losing the advantage from the increase in the firing temperature.

The new gas turbines being designed, for the new millennium, are investigating the use of steam as a cooling agent for the first and second stages of the turbines. Steam cooling is possible in the new combined cycle power plants, which is the base of most of the new high performance gas turbines. Steam, as part of the cooling as well as part of the cycle power, will be used in the new gas turbines in the combined cycle mode. The extra power obtained by the use of steam is the cheapest MW/\$ available. The injection of about 5% of steam by weight of air amounts to about 12% more power. The pressure of the injected steam must be at least 40 Bar above the compressor discharge. The way steam is injected must be done very carefully so as to avoid compressor surge. These are not new concepts and have been used and demonstrated in the past. Steam cooling for example was the basis of the cooling schemes proposed by the team of United Technology and Stal-Laval in their conceptual study for the U.S. department study on the High Turbine Temperature Technology Program, which was investigating Firing Temperatures of 3000°F (1649°C), in the early 1980s.

There are three state points within a turbine that are important when analyzing the flow. They are located at the nozzle entrance, the rotor entrance, and at the rotor exit. Fluid velocity is an important variable governing the flow and energy transfer within a turbine. The absolute velocity (V) is the fluid velocity relative to some stationary point. Absolute velocity is important when analyzing the flow across a stationary blade such as a nozzle. When considering the flow across a rotating element or rotor blade, the relative velocity W is important. Vectorially, the relative velocity is defined

$$\vec{W} = \vec{V} - \vec{U} \quad (9-1)$$

where U is the tangential velocity of the blade.

This relationship is shown in Figure 9-2. The subscript z used in Figure 9-2 denotes the axial velocity, while θ denotes the tangential component.

Two angles are defined in Figure 9-2. The first angle is the air angle α , which is defined with respect to the tangential direction. The air angle α represents the direction of the flow leaving the nozzle. In the rotor, the air angle α represents the angle of the absolute velocity leaving the rotor. The blade angle β is the angle the relative velocity makes with the tangential

FPO

Figure 9-2. Stage nomenclature and velocity triangles.

direction. It is the angle of the rotor blade under ideal conditions (no incidence angle).

Degree of Reaction

The degree of reaction in an axial-flow turbine is the ratio of change in the static enthalpy to the change in total enthalpy

$$R = \frac{h_1 - h_4}{h_{01} - h_{04}} \quad (9-2)$$

A rotor with a constant radius and an axial velocity constant throughout can be written

$$R = \frac{(W_4^2 - W_3^2)}{(V_3^2 - V_4^2) + (W_4^2 - W_3^2)} \quad (9-3)$$

From the previous relationship, it is obvious that for a zero-reaction turbine (impulse turbine) the relative exit velocity is equal to the relative inlet velocity. Most turbines have a degree of reaction between 0 and 1; negative reaction turbines have much lower efficiencies and are not usually used.

Utilization Factor

In a turbine, not all energy supplied can be converted into useful work—even with an ideal fluid. There must be some kinetic energy at the exit that is discharged due to the exit velocity. Thus, the utilization factor is defined as the ratio of ideal work to the energy supplied

$$E = \frac{H_{id}}{H_{id} + \frac{V_4^2}{2g}} \quad (9-4)$$

and it can be written in terms of the velocity for a single rotor with constant radius

$$E = \frac{(V_3^2 - V_4^2) + (W_4^2 - W_3^2)}{V_3^2 + (W_4^2 - W_3^2)} \quad (9-5)$$

Work Factor

In addition to the degree of reaction and the utilization factor, another parameter used to determine the blade loading is the work factor

$$\Gamma \equiv \frac{\Delta h_\theta}{U^2} \quad (9-6)$$

and it can be written for a constant radius turbine

$$\Gamma = \frac{V_{\theta 3} - V_{\theta 4}}{U} \quad (9-7)$$

The previous equation can be further modified for the maximum utilization factor where the absolute exit velocity is axial and no exit swirl exists

$$\Gamma = \frac{V_{\theta 3}}{U} \quad (9-8)$$

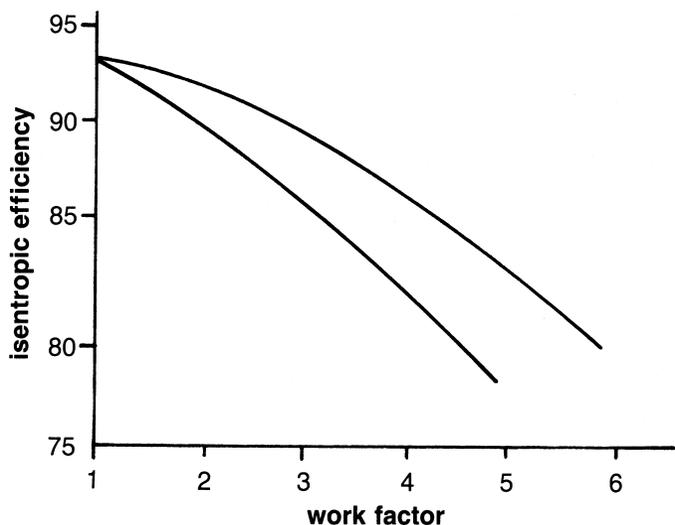


Figure 9-3. Effect of stage work on efficiency.

The value of the work factor for an impulse turbine (zero reaction) with a maximum utilization factor is two. In a 50% reaction turbine with a maximum utilization factor the work factor is one.

In recent years the trend has been toward high work factor turbines. The high work factor indicates that the blade loading in the turbine is high. The trend in many fan engines is toward a high by-pass ratio for lower fuel consumption and lower noise levels. As the by-pass ratio increases, the relative diameter of the direct-drive fan turbine decreases, resulting in lower blade tip speeds. Lower blade tip speeds mean that with conventional work factors, the number of turbine stages increases. Considerable research is being conducted to develop turbines with high work factors, high blade loadings, and high efficiencies. Figure 9-3 shows the effect of turbine stage work and efficiency. This diagram indicates that efficiency drops considerably as the work factor increases. There is little information on turbines with work factors over two.

Velocity Diagrams

An examination of various velocity diagrams for different degrees of reaction is shown in Figure 9-4. These types of blade arrangements with varying degrees of reaction are all possible; however, they are not all practical.

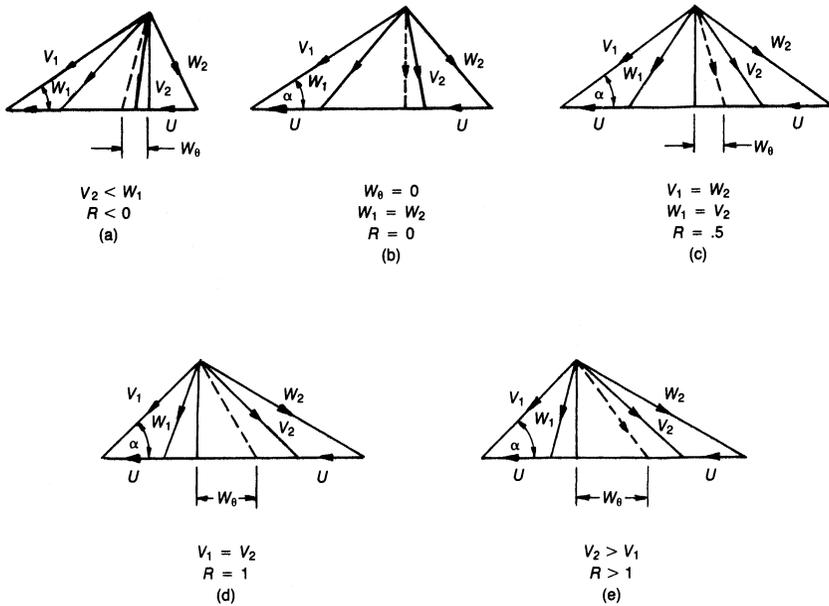


Figure 9-4. Turbine velocity triangles showing the effect of various degrees of reaction.

Examining the utilization factor, the discharge velocity ($V_4^2/2$), represents the kinetic energy loss or the unused energy part. For maximum utilization, the exit velocity should be at a minimum and, by examining the velocity diagrams, this minimum is achieved when the exit velocity is axial. This type of a velocity diagram is considered to have zero exit swirl. Figure 9-5 shows the various velocity diagrams as a function of the work factor and the turbine type. This diagram shows that zero exit swirl can exist for any type of turbine.

Zero exit swirl diagram. In many cases the tangential angle of the exit velocity ($V_{\theta 4}$) represents a loss in efficiency. A blade designed for zero exit swirl ($V_{\theta 4} = 0$) minimizes the exit loss. If the work parameter is less than two, this type of diagram produces the highest static efficiency. Also, the total efficiency is approximately the same as the other types of diagrams. If Γ is greater than 2.0, stage reaction is usually negative, a condition best avoided.

Impulse diagram. For the impulse rotor, the reaction is zero, so the relative velocity of the gas is constant, or $W_3 = W_4$. If the work factor is less than 2.0, the exit swirl is positive, which reduces the stage work. For this reason, an impulse diagram should be used only if the work factor is 2.0 or

| STAGE WORK FACTOR | DIAGRAM TYPE | | |
|-------------------|-----------------|---------|-------------|
| | ZERO EXIT SWIRL | IMPULSE | SYMMETRICAL |
| 1 | | | |
| 2 | | | |
| 4 | | | |

Figure 9-5. Effect of diagram type and stage work factor on velocity diagram shape.

greater. This type of diagram is a good choice for the last stage because for Γ greater than 2.0, an impulse rotor has the highest static efficiency.

Symmetrical diagram. The symmetrical-type diagram is constructed so that the entrance and exit diagrams have the same shape: $V_3 = W_4$ and $V_4 = W_3$. This equality means that the reaction is

$$R = 0.5 \tag{9-9}$$

If the work factor Γ equals 1.0, then the exit swirl is zero. As the work factor increases, the exit swirl increases. Since the reaction of 0.5 leads to a high total efficiency, this design is useful if the exit swirl is not counted as a loss as in the initial and intermediate stages.

Impulse Turbine

The impulse turbine is the simplest type of turbine. It consists of a group of nozzles followed by a row of blades. The gas is expanded in the nozzle, converting the high thermal energy into kinetic energy. This conversion can be represented by the following relationship:

$$V_3 = \sqrt{2\Delta h_0} \tag{9-10}$$

The high-velocity gas impinges on the blade where a large portion of the kinetic energy of the moving gas stream is converted into turbine shaft work.

Figure 9-6 shows a diagram of a single-stage impulse turbine. The static pressure decreases in the nozzle with a corresponding increase in the absolute velocity. The absolute velocity is then reduced in the rotor, but the static pressure and the relative velocity remain constant. To get the maximum energy transfer, the blades must rotate at about one-half the velocity of the gas jet velocity. Two or more rows of moving blades are sometimes used in conjunction with one nozzle to obtain wheels with low blade tip speeds and stresses. In-between the moving rows of blades are guide vanes that redirect the gas from one row of moving blades to another as shown in Figure 9-7. This type of turbine is sometimes called a Curtis turbine.

Another impulse turbine is the pressure compound or Rateau turbine. In this turbine the work is broken down into various stages. Each stage consists of a nozzle and blade row where the kinetic energy of the jet is absorbed into the turbine rotor as useful work. The air that leaves the moving blades enters the next set of nozzles where the enthalpy decreases further, and the velocity is increased and then absorbed in an associated row of moving blades.

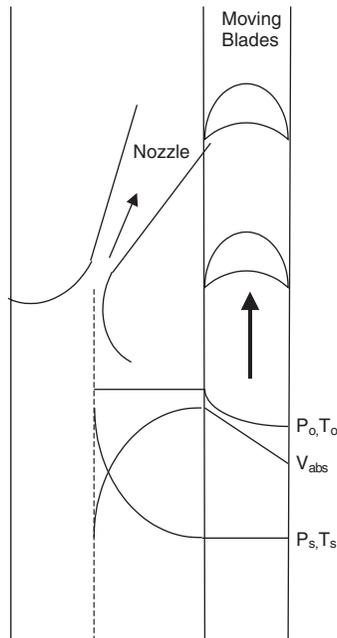


Figure 9-6. Schematic of an impulse turbine showing the variation of the thermodynamic and fluid mechanical properties.

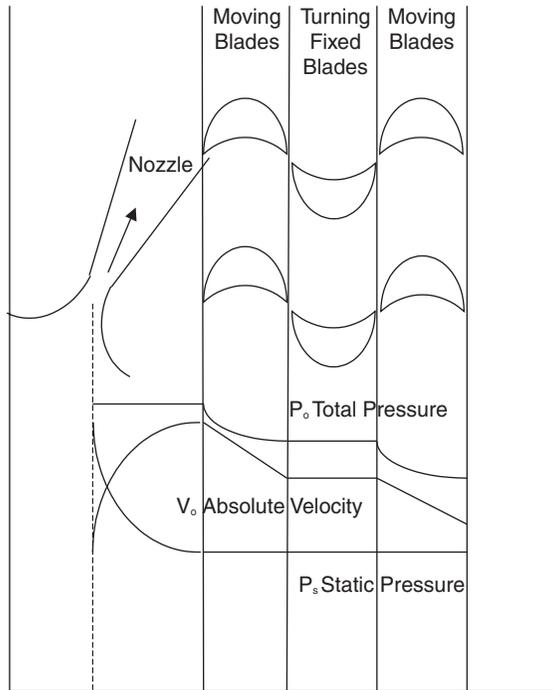


Figure 9-7. Pressure and velocity distributions in a Curtis-type impulse turbine.

Figure 9-8 shows the Ratteau turbine. The total pressure and temperature remain unchanged in the nozzles, except for minor frictional losses.

By definition, the impulse turbine has a degree of reaction equal to zero. This degree of reaction means that the entire enthalpy drop is taken in the nozzle, and the exit velocity from the nozzle is very high. Since there is no change in enthalpy in the rotor, the relative velocity entering the rotor equals the relative velocity exiting from the rotor blade. For the maximum utilization factor, the absolute exit velocity must be axial as shown in Figure 9-9. The air angle α for maximum utilization is

$$\cos \alpha_3 = \frac{2U}{V_3} \tag{9-11}$$

The air angle α is usually small, between 12° and 25° . The limit on this angle is placed by the throughflow velocity, $V_1 \sin \alpha$. If the limit is too small, the angle will require a longer blade length. The flow factor, which is a ratio

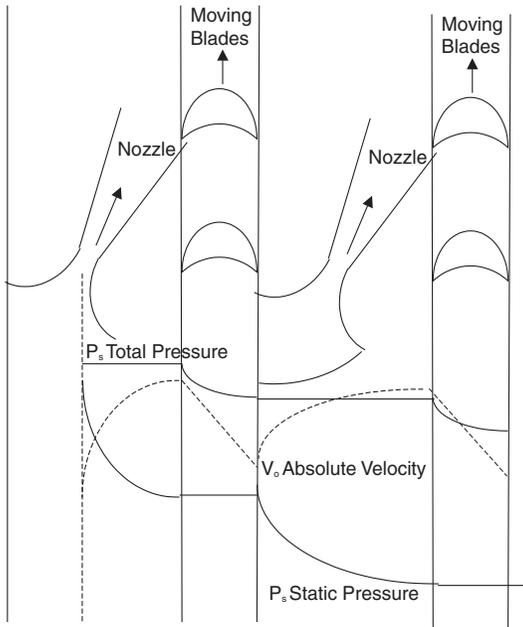


Figure 9-8. Pressure and velocity distributions in a Rateau-type impulse turbine.

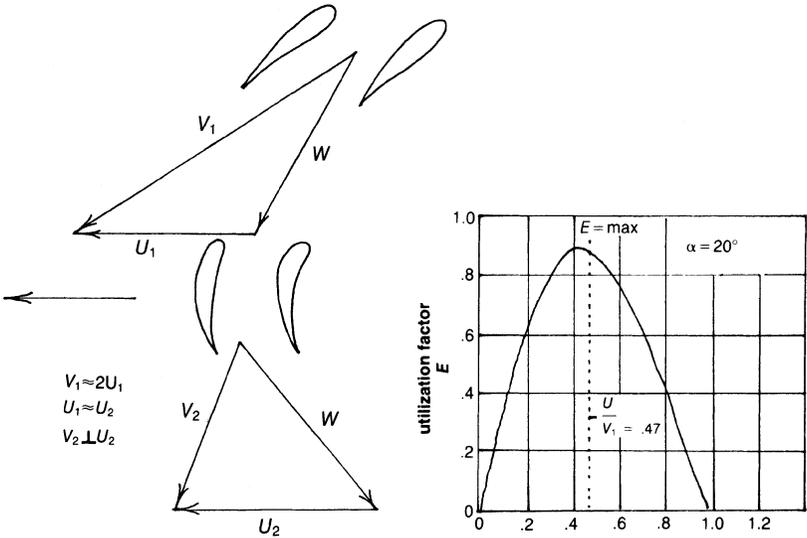


Figure 9-9. Effect of velocity and air angle on utilization factor.

of the blade speed to the inlet velocity, is a useful parameter to compare with the utilization factor (Figure 9-9).

The optimum value of U/V_3 is a criterion indicating the maximum energy transfer to the shaft work. It also represents the departure from the optimum design value of $\cos \alpha$, causing a loss of energy transfer. The losses will increase at off-design conditions because of the incorrect attack angle of the gas with respect to the rotor blade. The maximum efficiency of the stage will still occur at or near the value of $U/V_3 = \cos \alpha_3/2$

The power developed by the flow in an impulse turbine is given by the Euler equation

$$P = \dot{m}U(V_{\theta 3} - V_{\theta 4}) = U(V_{\theta 3} - v_{\theta 4}) \quad (9-12)$$

This equation, rewritten in terms of the absolute velocity and the nozzle angle α for maximum utilization, can be shown as

$$P = \dot{m}U(V_{\theta 3} \cos \alpha_3) \quad (9-13)$$

The relative velocity W remains unchanged in a pure impulse turbine, except for frictional and turbulence effect. This loss varies from about 20% for very high-velocity turbines (3000 ft/sec) to about 8% for low-velocity turbines (500 ft/sec). Since the blade speed ratio is equal to $(\cos \alpha)/2$ for maximum utilization, the energy transferred in an impulse turbine can be written

$$P = \dot{m}U(2U) = 2\dot{m}U^2 \quad (9-14)$$

The Reaction Turbine

The axial-flow reaction turbine is the most widely used turbine. In a reaction turbine both the nozzles and blades act as expanding nozzles. Therefore, the static pressure decreases in both the fixed and moving blades. The fixed blades act as nozzles and direct the flow to the moving blades at a velocity slightly higher than the moving blade velocity. In the reaction turbine, the velocities are usually much lower, and the entering blade relative velocities are nearly axial. Figure 9-10 shows a schematic view of a reaction turbine.

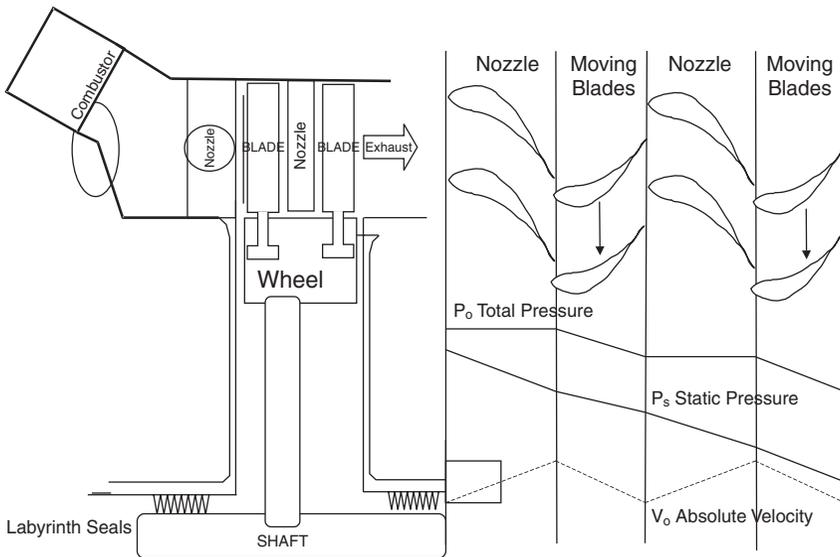


Figure 9-10. Schematic of a reaction-type turbine showing the distribution of the thermodynamic and fluid mechanic properties.

In most designs, the reaction of the turbine varies from hub to shroud. The impulse turbine is a reaction turbine with a reaction of zero ($R = 0$). The utilization factor for a fixed nozzle angle will increase as the reaction approaches 100%. For $R = 1$, the utilization factor does not reach unity but reaches some maximum finite value. The 100% reaction turbine is not practical because of the high rotor speed necessary for a good utilization factor. For reaction less than zero, the rotor has a diffusing action. Diffusing action in the rotor is undesirable, since it leads to flow losses.

The 50% reaction turbine has been used widely and has special significance. The velocity diagram for a 50% reaction is symmetrical and, for the maximum utilization factor, the exit velocity (V_4) must be axial. Figure 9-11 shows a velocity diagram of a 50% reaction turbine and the effect on the utilization factor. From the diagram $W_3 = V_4$, the angles of both the stationary and rotating blades are identical. Therefore, for maximum utilization,

$$\frac{U}{V_3} = \cos \alpha \quad (9-15)$$

The 50% reaction turbine has the highest efficiency of all the various types of turbines. Equation (9-15) shows the effect on efficiency is relatively small for a wide range of blade speed ratios (0.6–1.3).

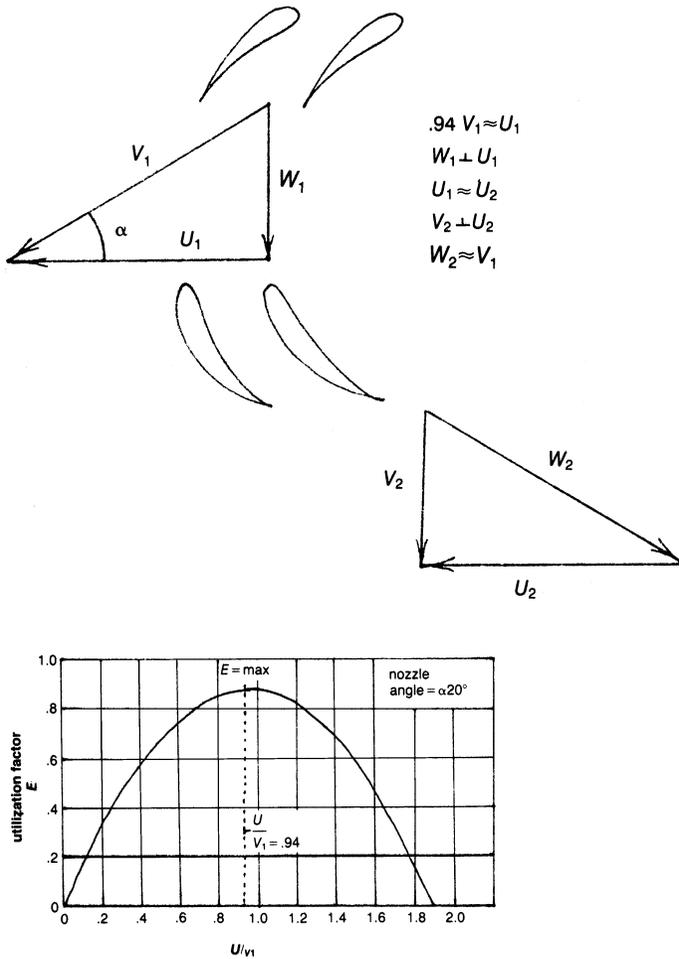


Figure 9-11. The effect of exit velocity and air angle on the utilization factor.

The power developed by the flow in a reaction turbine is also given by the general Euler equation. This equation can be modified for maximum utilization

$$P = \dot{m}U(V_3 \cos \alpha_3) \tag{9-16}$$

For a 50% reaction turbine, Equation (9-16) reduces to

$$P = \dot{m}U(U) = \dot{m}U^2 \tag{9-17}$$

The work produced in an impulse turbine with a single stage running at the same blade speed is twice that of a reaction turbine. Hence, the cost of a reaction turbine for the same amount of work is much higher, since it requires more stages. It is a common practice to design multistage turbines with impulse stages in the first few stages to maximize the pressure decrease and to follow it with 50% reaction turbines. The reaction turbine has a higher efficiency due to blade suction effects. This type of combination leads to an excellent compromise, since otherwise an all-impulse turbine would have a very low efficiency, and an all-reaction turbine would have an excessive number of stages.

Turbine Blade Cooling Concepts

The turbine inlet temperatures of gas turbines have increased considerably over the past years and will continue to do so. This trend has been made possible by advancement in materials and technology, and the use of advanced turbine blade cooling techniques. The development of new materials as well as cooling schemes has seen the rapid growth of the turbine firing temperature leading to high turbine efficiencies. The stage 1 blade must withstand the most severe combination of temperature, stress, and environment; it is generally the limiting component in the machine. Figure 9-12 shows the trend of firing temperature and blade alloy capability.

Since 1950, turbine bucket material temperature capability has advanced approximately 850°F (472°C), approximately 20°F (10°C) per year. The

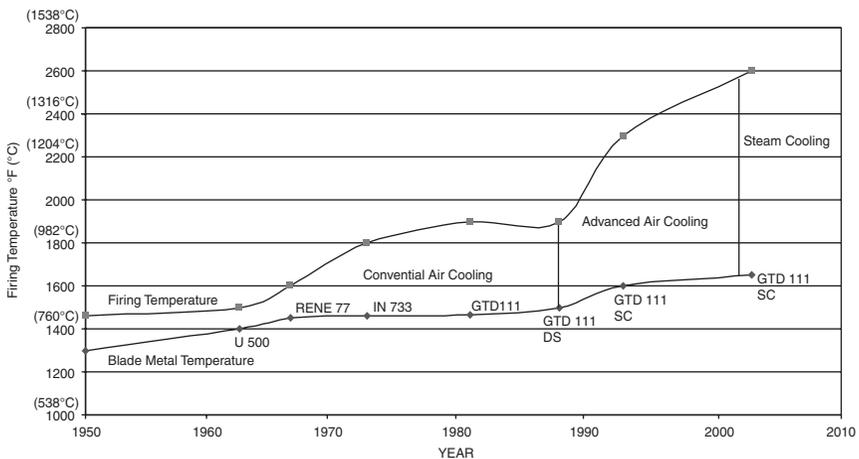


Figure 9-12. Firing temperature increase with blade material improvement.

importance of this increase can be appreciated by noting that an increase of 100°F (56°C) in turbine firing temperature can provide a corresponding increase of 8–13% in output and 2–4% improvement in simple-cycle efficiency. Advances in alloys and processing, while expensive and time-consuming, provide significant incentives through increased power density and improved efficiency. The cooling air is bled from the compressor and is directed to the stator, the rotor, and other parts of the turbine rotor and casing to provide adequate cooling. The effect of the coolant on the aerodynamics depends on the type of cooling involved, the temperature of the coolant compared to the mainstream temperature, the location and direction of coolant injection, and the amount of coolant. A number of these factors are being studied experimentally in annular and two-dimensional cascades.

In high-temperature gas turbines cooling systems need to be designed for turbine blades, vanes, endwalls, shroud, and other components to meet metal temperature limits. The concepts underlying the following five basic air-cooling schemes are (Figure 9-13):

1. Convection cooling
2. Impingement cooling

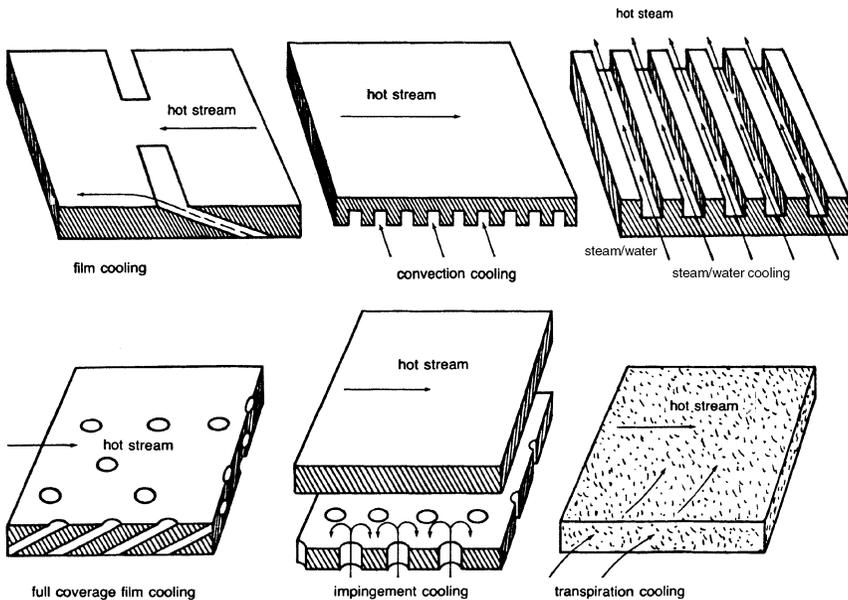


Figure 9-13. Various suggested cooling schemes.

3. Film cooling
4. Transpiration cooling
5. Water/Steam cooling

Until the late 1960s, convection cooling was the primary means of cooling gas turbine blades; some film cooling was occasionally employed in critical regions. Film cooling in the 1980s and 1990s was used extensively. In the year 2001, steam cooling is being introduced in the production of frame type engines used in combined cycle applications. The new turbines have very high-pressure ratios and this leads to compressor air leaving at very high temperatures, which affects their cooling capacity.

Convection Cooling

This form of cooling is achieved by designing the cooling air to flow inside the turbine blade or vane, and remove heat through the walls. Usually, the air flow is radial, making multiple passes through a serpentine passage from the hub to the blade tip. Convection cooling is the most widely used cooling concept in present-day gas turbines.

Impingement Cooling

In this high-intensity form of convection cooling, the cooling air is blasted on the inner surface of the airfoil by high-velocity air jets, permitting an increased amount of heat to be transferred to the cooling air from the metal surface. This cooling method can be restricted to desired sections of the airfoil to maintain even temperatures over the entire surface. For instance, the leading edge of a blade needs to be cooled more than the midchord section or trailing edge, so the gas is impinged.

Film Cooling

This type of cooling is achieved by allowing the working air to form an insulating layer between the hot gas stream and the walls of the blade. This film of cooling air protects an airfoil in the same way combustor liners are protected from hot gases at very high temperatures.

Transpiration Cooling

Cooling by this method requires the coolant flow to pass through the porous wall of the blade material. The heat transfer is directly between the

coolant and the hot gas. Transpiration cooling is effective at very high temperatures, since it covers the entire blade with coolant flow.

Water/Steam Cooling

Water is passed through a number of tubes embedded in the blade. The water is emitted from the blade tips as steam to provide excellent cooling. This method keeps blade metal temperatures below 1000 °F (537.8 °C).

Steam is passed through a number of tubes embedded in the nozzle or blades of the turbine. In many cases, the steam is bled from after the HP Steam Turbine of a combined cycle power plant and returned after cooling the gas turbine blades, where the steam gets heated in the process to the IP steam turbine. This is a very effective cooling scheme and keeps the blade metal temperature below 1250 °F (649 °C).

Turbine Blade Cooling Design

The incorporation of blade cooling concepts into actual blade designs is very important. There are five different blade cooling designs.

Convection and Impingement Cooling/Strut Insert Design

The strut insert design shown in Figure 9-14 has a midchord section that is convection-cooled through horizontal fins, and a leading edge that is impingement cooled. The coolant is discharged through a split trailing edge. The air flows up the central cavity formed by the strut insert and through holes at the leading edge of the insert to impingement cool the blade leading edge. The air then circulates through horizontal fins between the shell and strut, and discharges through slots in the trailing edge. The temperature distribution for this design is shown in Figure 9-15.

The stresses in the strut insert are higher than those in the shell, and the stresses on the pressure side of the shell are higher than those on the suction side. Considerably more creep strain takes place toward the trailing edge than the leading edge. The creep strain distribution at the hub section is unbalanced. This unbalance can be improved by a more uniform wall temperature distribution.

Film and Convection Cooling Design

This type of blade design is shown in Figure 9-16. The midchord region is convection-cooled, and the leading edges are both convection and film-cooled. The cooling air is injected through the blade base into two central

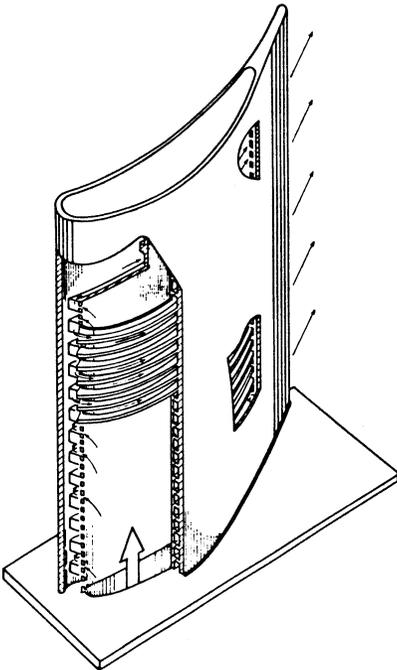


Figure 9-14. Strut insert blade.

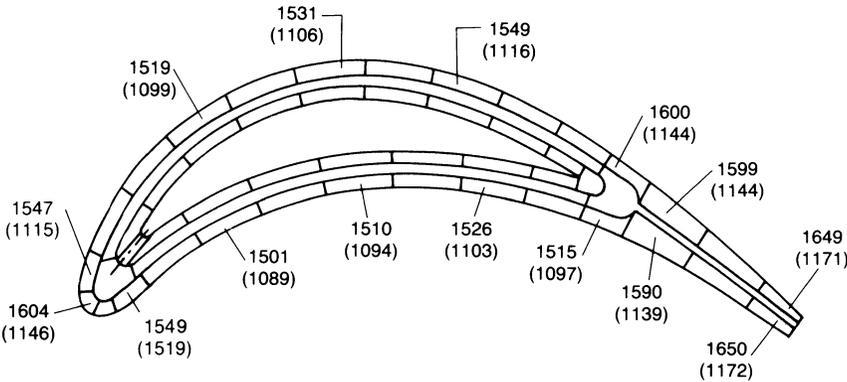


Figure 9-15. Temperature distribution for strut insert design, °F (cooled).

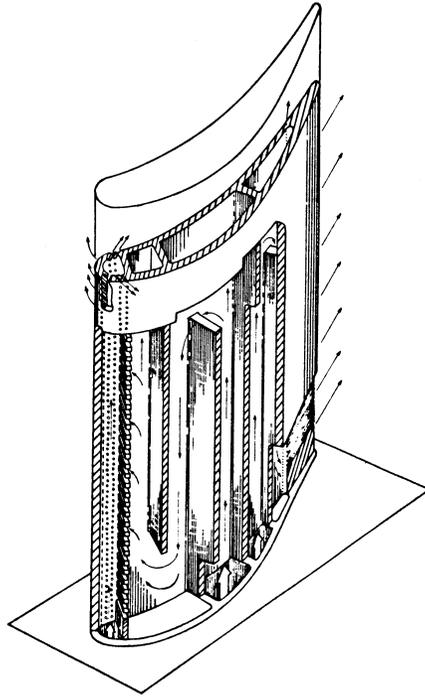


Figure 9-16. Film and convection-cooled blade.

and one leading edge cavity. The air then circulates up and down a series of vertical passages. At the leading edge, the air passes through a series of small holes in the wall of the adjacent vertical passages, and then impinges on the inside surface of the leading edge and passes through film cooling holes. The trailing edge is convection-cooled by air discharging through slots. The temperature distribution for film and convection cooling design is shown in Figure 9-17. From the cooling distribution diagram, the hottest section can be seen to be the trailing edge. The web, which is the most highly stressed blade part, is also the coolest part of the blade.

A similar cooling scheme with some modifications is used in some of the latest gas turbine designs. The firing temperature of GE FA units is about 2350 °F (1288 °C), which is the highest in the power generation industry. To accommodate this increased firing temperature, the FA employs advanced cooling techniques developed by GE Aircraft Engines. The first and second stage blades as well as all three-nozzle stages are air-cooled. The first stage blade is convectively cooled by means of an advanced aircraft-derived serpentine arrangement as shown in Figure 9-18.

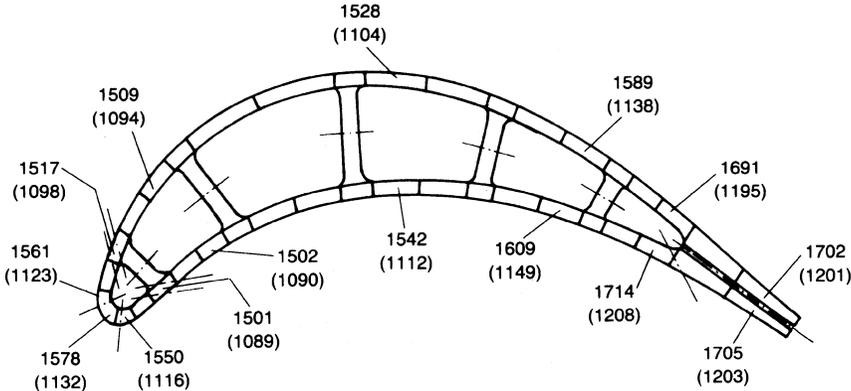


Figure 9-17. Temperature distribution for film convection-cooled design, °F (cooled).

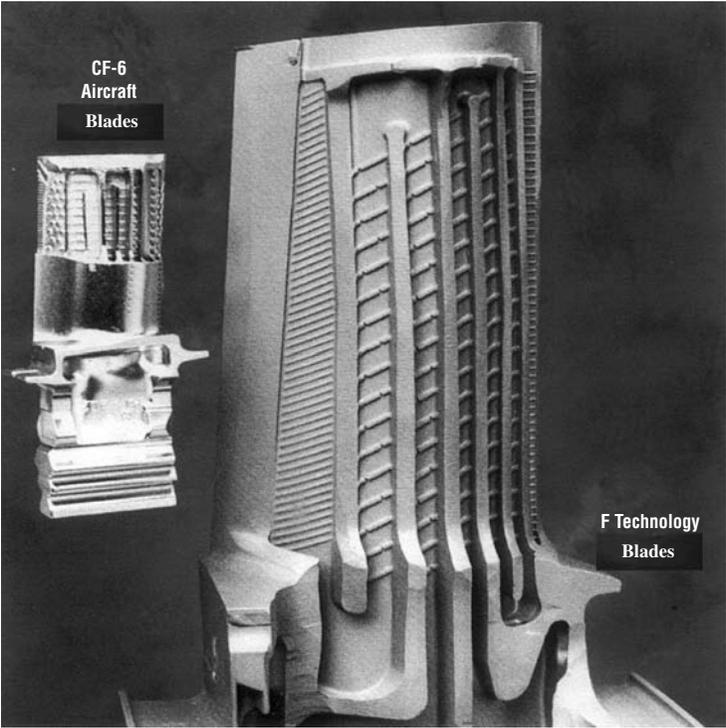


Figure 9-18. Internal of the frame FA blades, showing cooling passages. (Courtesy GE Power Systems.)

Cooling air exits through axial airways located on the bucket's trailing edge and tip, and also through leading edge and sidewalls for film cooling.

Transpiration Cooling Design

This design has a strut-supported porous shell (Figure 9-19). The shell attached to the strut is of wire from porous material. Cooling air flows up the central plenum of the strut, which is hollow with various-size metered holes on the strut surface. The metered air then passes through the porous shell. The shell material is cooled by a combination of convection and film cooling. This process is effective due to the infinite number of pores on the blade surface. The temperature distribution is shown in Figure 9-20.

The trailing edge of the strut develops the highest creep strain. This strain occurs despite the sharp stress relaxation at the trailing edge projection. The creep strain in the strut is well balanced. Transpiration cooling requires a material of porous mesh resistant to oxidation at a temperature of 1600 °F (871.1 °C) or more. Otherwise, the superior creep properties of this design

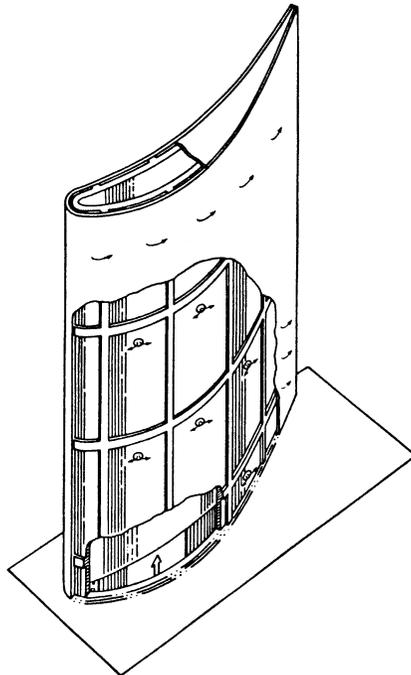


Figure 9-19. Transpiration-cooled blade.

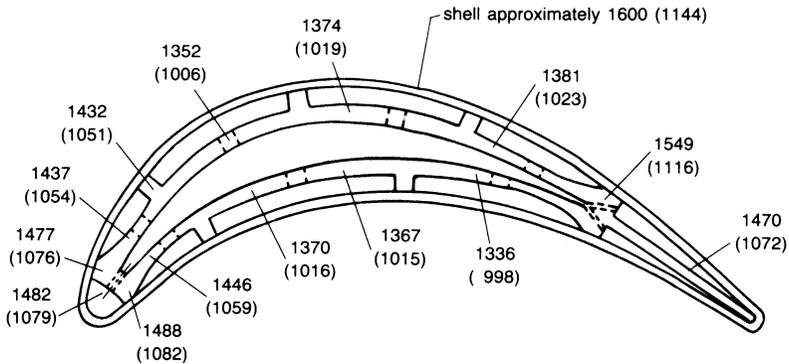


Figure 9-20. Temperature distribution for transpiration-cooled design, °F (cooled).

are insignificant. Since oxidation will close the pores, causing uneven cooling and high thermal stresses, the possibility of blade failure exists. The reason for superior creep property is a relatively low strut temperature 1400 °F average (760.0 °C), which more than compensates for the high level of centrifugal stress required to support the porous shell.

Multiple Small-Hole Design

With this particular design, primary cooling is achieved by film cooling with cold air injected through small holes over the airfoil surface (Figure 9-21). The temperature distribution is shown in Figure 9-22.

These holes are considerably larger than holes formed with porous mesh for transpiration cooling. Also, because of their larger size, they are less susceptible to clogging by oxidation. In this design, the shell is supported by cross ribs and is capable of supporting itself without a strut under engine operating conditions.

This design has the highest creep life next to a transpiration-cooled design, and it has the best strain distribution between leading and trailing edges. It is the closest to optimum.

Water-Cooled Turbine Blades

This design has a number of tubes embedded inside the turbine blade to provide channels for the water (Figure 9-23). In most cases, these tubes are constructed from copper for good heat-transfer conditions. The water, which is converted to steam by the time it reaches the blade tips, is then

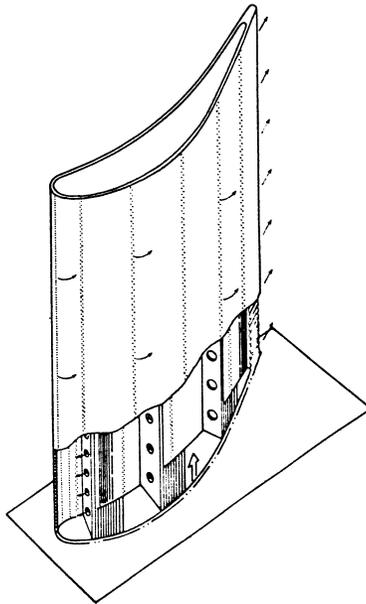


Figure 9-21. Multiple small hole transpiration-cooled blade.

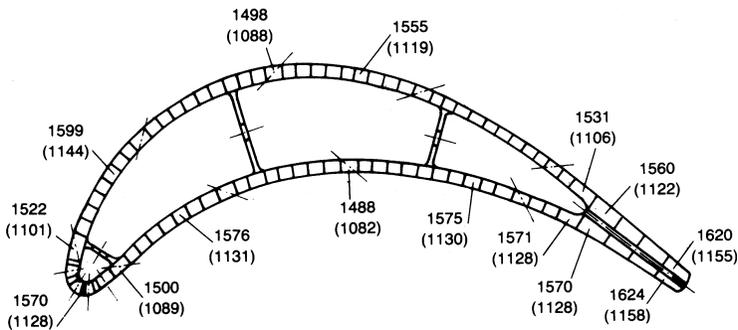


Figure 9-22. Temperature distribution for a multiple small-hole design, °F (cooled).

injected into the flow stream. These blades are presently in the experimental stage. They hold great promise for the turbine of the future in which turbine inlet temperatures of 3000 °F (1648.8 °C) are possible. This type of cooling should keep blade metal temperatures below 1000 °F (537.8 °C) so that there will be no hot-corrosion problems.

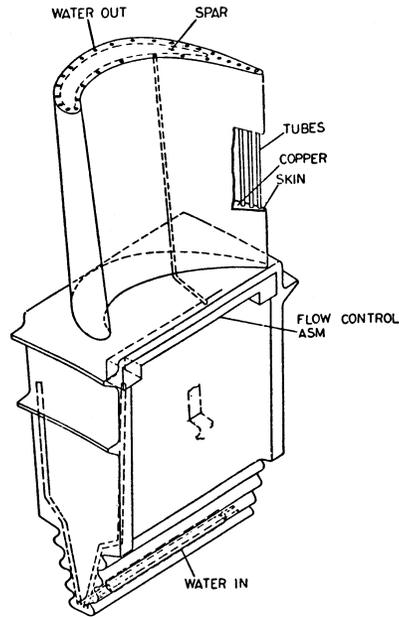


Figure 9-23. Water-cooled turbine blade. (Courtesy General Electric Company.)

Steam-Cooled Turbine Blades

This design has a number of tubes embedded inside the turbine blade to provide channels for steam. In most cases these tubes are constructed from copper for good heat-transfer conditions. Steam injection is becoming the prime source of cooling for gas turbines in a combined cycle application. The steam, which is extracted from the exit of the HP Turbine, is sent through the nozzle blades, where the steam is heated, and the blade metal temperature decreased. The steam is then injected into the flow stream entering the IP steam turbine. This increases the overall efficiency of the combined cycle.

In the case of the rotating blades, the steam, after it is used in the cooling of the blades, is returned through a series of specially designed slip rings to the steam flow entering the IP steam turbine. Steam cooling in combined cycle power plants holds great promise for the turbines of the future in which turbine inlet temperatures of 3000 °F (1649 °C) are possible. This type of cooling should keep blade metal temperatures below 1200 °F (649 °C) so that hot-corrosion problems will be minimized. It also will help increase the efficiency of the total combined cycle power plant by between 1% and 3%.

An evaluation of the six different blade designs is shown in Table 9-1.

Table 9-1
Summary of Creep Life Experiments

| Blade Cooling Design | Time to 1% Creep Strain (hrs) | |
|----------------------|-------------------------------|-----------------------------|
| | Based on Initial Conditions | Based on Average Conditions |
| Strut design | 2430 | 47,900 |
| Film convection | 186 | 46,700 |
| Transpiration | 2530 | Infinite |
| Multiple small-hole | 4800 | 33,500 |
| Water cooled | 150 | Infinite |
| Steam cooled | 150 | 35,000 |

Cooled-Turbine Aerodynamics

The injection of coolant air in the turbine rotor or stator causes a slight decrease in turbine efficiency; however, the higher turbine inlet temperature usually makes up for the loss of the turbine component efficiency, giving an overall increase in cycle efficiency. Tests by NASA on three different types of cooled stator blades were conducted on a specially built 30-inch turbine cold-air test facility. The outer shell profile of all three blade types was the same, as seen in Figure 9-24.

Total pressure surveys were made downstream of the stators in both the radial and circumferential directions to determine the effect of coolant on stator losses. The wake traces for the stator with discrete holes and the stator with trailing edge slots show that there is a considerable difference in total

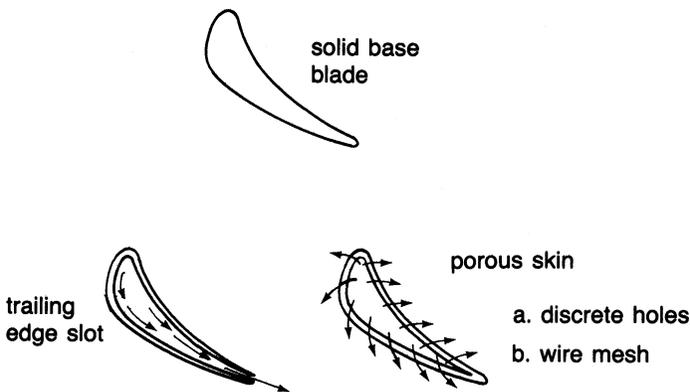


Figure 9-24. Cooled turbine blade types.

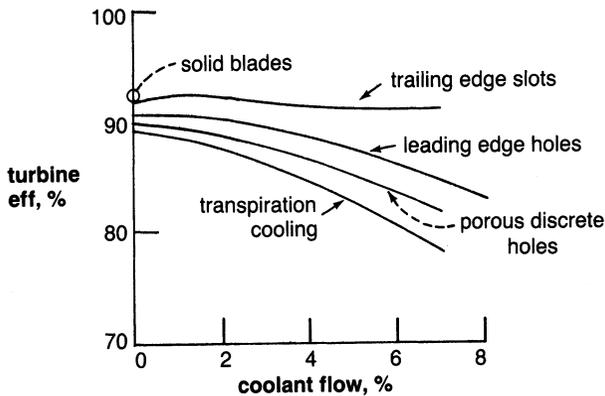


Figure 9-25. The effect of various types of cooling on turbine efficiency.

pressure loss patterns as a function of the type of cooling and the amount of cooling air supplied. As the coolant flow for the porous blades increases, the disturbance to the flow pattern and the wake thickness increases. Consequently, the losses increase. In a blade with trailing edge slots, the loss initially starts to increase with coolant flow as the wake thickens. However, as the coolant flow is increased, it tends to energize the wake and reduce losses. For a higher coolant flow, the coolant pressures must be higher, resulting in an energization of the flow.

By comparing the various cooling techniques, it becomes obvious that a blade with trailing edge slots is thermodynamically the most efficient, as shown in Figure 9-25. The porous stator blades decrease the stage efficiency considerably. This efficiency indicates losses in the turbine but does not take into account cooling effectiveness. As indicated earlier, the porous blades are more effective for cooling.

Turbine Losses

The primary cause of efficiency losses in an axial-flow turbine is the build-up of boundary layer on the blade and end walls. The losses associated with a boundary layer are viscous losses, mixing losses, and trailing edge losses. To calculate these losses, the growth of the boundary layer on a blade must be known so that the displacement thickness and momentum thickness can be computed. A typical distribution of the displacement and momentum thickness is shown in Figure 9-26. The profile loss from this type of boundary-layer build-up is due to a loss of stagnation pressure, which in turn is

caused by a loss of momentum in the viscous fluid. The blade shape and the pressure gradient to which the flow is subjected are major factors in this type of loss. The endwall losses are also due to a loss of momentum and, although they are also dependent on the profile and pressure gradient, the profile shape and pressure gradient are considerably different. Endwall losses are often combined with secondary losses, since adjacent blade profiles cause a pressure gradient from the pressure surface to the suction surface. The blade loading is thus produced by the different pressures on the opposite side of the same blade. The pressure gradient across the blade passage induces flow from the higher to the lower-pressure regions. This secondary flow causes losses and results in vorticity in the exit flow.

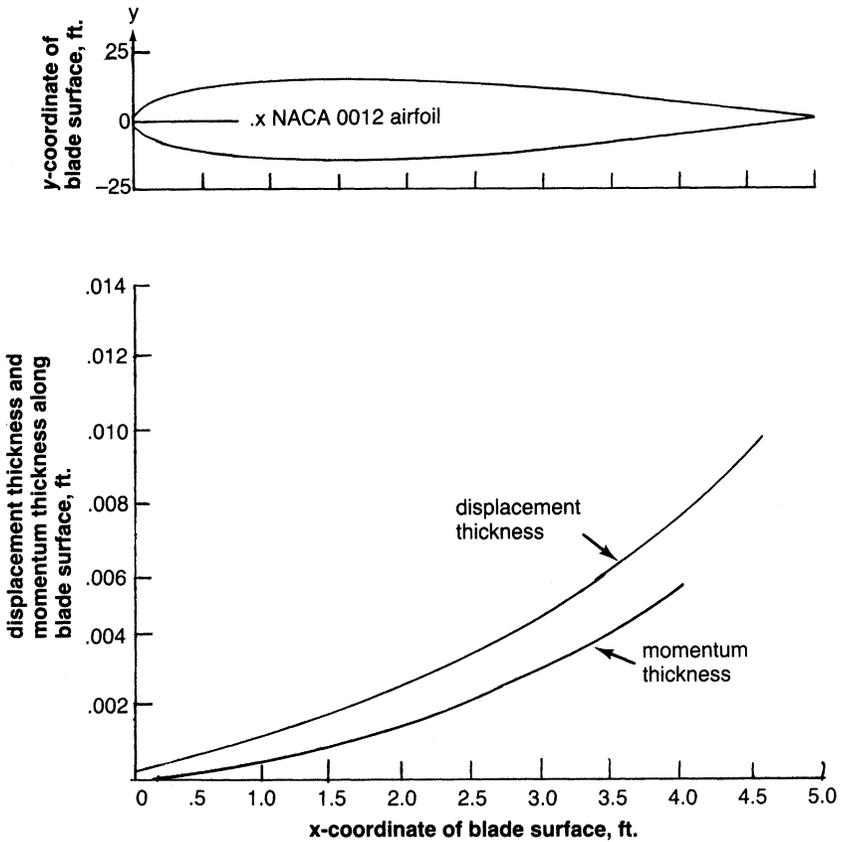


Figure 9-26. Growth of displacement and momentum thickness on an airfoil.

Table 9-2
Turbine Loss Values in the Overall Stage

| Loss Mechanics | Loss (%) |
|-----------------|----------|
| Profile | 2-4 |
| Endwall | 1 1/2-4 |
| Secondary flow | 1-2 |
| Rotor incidence | 1-3 |
| Tip clearance | 1 1/2-3 |
| Wheel disc | 1-2 |

Tip clearance loss occurs when the blade tip is mechanically free of the shroud casing, and the pressure gradient across the blade thickness induces flow leakage through the clearance space. This flow across the tip causes turbulence, a pressure drop, and interferes with the main stream flow. All of these effects contribute to tip clearance loss. Another loss is caused by flow incidence when the gas angle and the blade angle of the flow do not coincide, resulting in a disruption of the flow at the blade leading edge. Disc friction loss occurs in an axial-flow compressor because of the close clearances between the casing and the rotor disc. The entrapped fluid causes a viscous power dissipation when the fluid is dragged by the rotor. Table 9-2 shows the approximate value of these losses in the overall stage.

A simple but effective technique for calculating the loss in an axial-flow turbine has been developed. In the loss computation, the blade geometry, the spacing between the blades, the aspect ratio, the thickness ratio, and the effect of the Reynolds number are taken into account. However, those factors not taken into account are the stagger angle, the trailing edge thickness, and the effects of Mach number. Neglecting Mach number effects causes a problem in the highly loaded stages. The optimum solidity ($\sigma = c/s$) of the blades is computed from

$$\sigma = 2.5 (\cot \alpha_2 + \cot \alpha_1) \sin^2 \alpha_2 \quad (9-18)$$

The loss coefficient can now be computed

$$\omega = \left(\frac{10^5}{\text{Re}} \right)^{1/4} [(1 + \omega_\theta)(0.975 + 0.075/AR) - 1] \omega_i \quad (9-19)$$

where AR is the aspect ratio (h/c), ω_θ is the loss from blade geometry seen in Figure 9-27, ω_i is the loss due to the incidence angle seen in Figure 9-28, and $\text{Re} = V_3 D_n / \nu_3$ where $D_n = (2AR \sin \alpha_2) / (\sigma \sin \alpha_2 + AR)$

The change in enthalpy is given by

$$h_{2a} = h_{2s} + \omega V_3^2/2 \tag{9-20}$$

This loss is now to be recomputed for the rotor.

The off-design characteristics of a turbine are as important to define as the design-point characteristics. Figure 9-29 shows the effect of the speed-to-

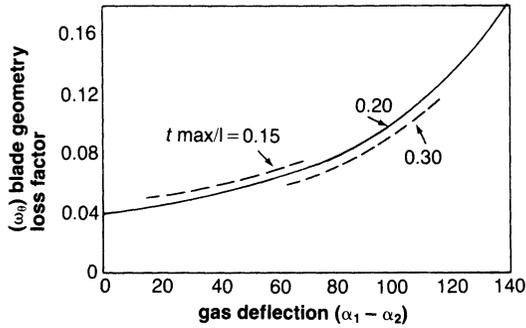


Figure 9-27. Blade geometry loss.

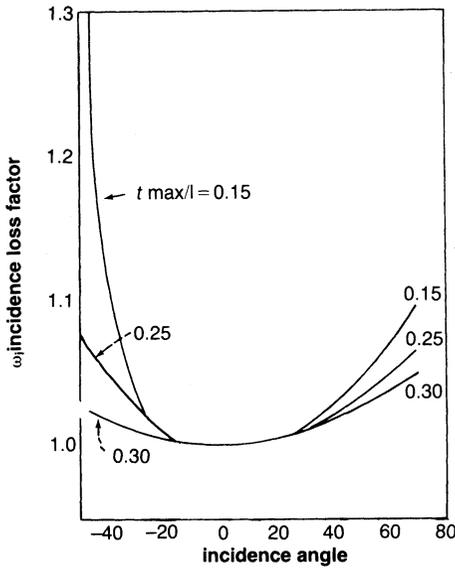


Figure 9-28. Incidence angle loss.

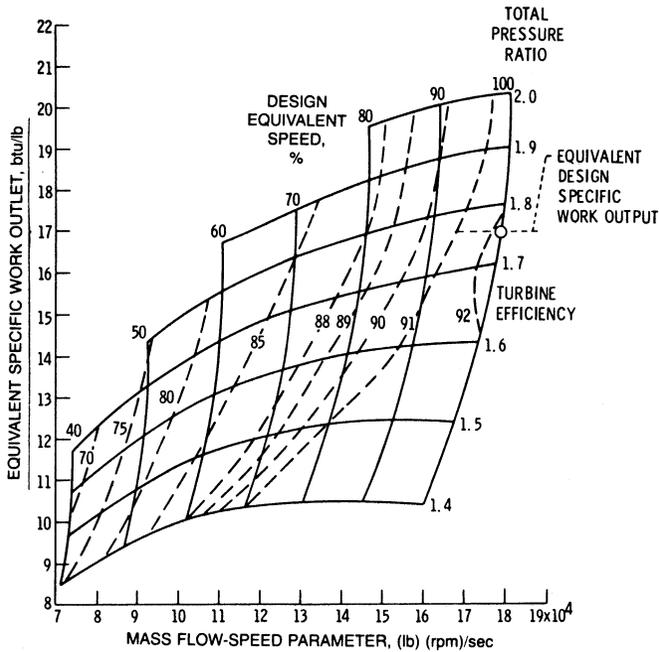


Figure 9-29. Turbine performance map.

pressure ratio on the work output. It is obvious from these diagrams that turbine inlet temperature and pressure ratio are the two factors that affect the turbine output most significantly. To obtain these off-design performance characteristics, it is necessary to study the effect of various dimensionless parameters, such as pressure and temperature coefficients, as a function of the flow coefficient. Other techniques used to study flow phenomena and distribution of the flow through the blade are also used for determining off-design conditions.

Bibliography

- Balje, O.E., and Binsley, R.L., "Axial Turbine Performance Evaluation," *Journal of Engineering for Power*, ASME Transactions, 90A, pp. 217–232, 1960.
- Balje, O.E., "Axial Cascade Technology and Application to Flow Path Designs," *Journal of Engineering for Power*, ASME Transactions 90A, pp. 309–340, 1968.
- Behning, F.P., Schum, H.J., and Szanca, E.M., "Cold-Air Investigation of a Turbine with Transpiration-Cooled Stator Blades, IV—Stage Performance with Wire-Mesh Shell Blading," NASA, TM X-2176, 1971.

- Benign, F., Rust, H. Jr., and Moffitt, T.P., "Cold-Air Investigation of a Turbine with Transpiration-Cooled Stator Blades, III—Performance of Stator with Wire-Mesh Shell Blading," NASA, TM X-2166, 1971.
- Brown, L.E., "Axial Flow Compressor and Turbine Loss Coefficients: A Comparison of Several Parameters," *Journal of Engineering for Power*, ASME Transactions 94A, pp. 193–201, 1972.
- Gehring, S., and Riess, W., "Through-Flow Analysis for Cooled Turbines." 3rd Conference on Turbomachinery-Fluid Dynamics and Thermodynamics, London March, 1999.
- Glassman, A.J., and Moffitt, T.P., "New Technology in Turbine Aerodynamics," Proceedings of the 1st, Turbomachinery Symposium, Texas A&M University, p. 105, 1972.
- Horlock, J.H., "Axial Flow Turbines," Butterworth and Company Ltd., London, 1966.
- Lakshminarayana, B., *Fluid Dynamics and Heat Transfer of Turbomachinery*, John Wiley & Sons Inc., New York, 1996.
- Moffitt, T.P., Prust, H.W. Jr., Szanca, E.M., and Schum, H.J., "Summary of Cold-Air Tests of a Single-Stage Turbine with Various Stator Cooling Techniques," NASA, TM X-52969, 1971.
- Petrovic, M., and Riess, W., "Through-Flow Calculation in Axial Turbines at Part Load and Low Load" Conference on Turbomachinery-Fluid Dynamics and Thermodynamics, Erlangen, 1995.
- Prust, H.W. Jr., Behning, F.P., and Bider, B., "Cold-Air Investigation of a Turbine with Stator Blade Trailing Edge Coolant Ejection, II—Detailed Stator Performance," NASA, TM X-1963, 1970.
- Prust, H.W. Jr., Schum, H.J., and Behning, F.P., "Cold-Air Investigation of a Turbine for High-Temperature Engine Application, II—Detailed Analytical and Experimental Investigation of Stator Performance," NASA, TN D-4418, 1968.
- Prust, H.W. Jr., Schum, H.J., and Szanca, E.M., "Cold-Air Investigation of a Turbine with Transpiration-Cooled Stator Blades, I—Performance of Stator with Discrete Hole Blading," NASA, TX X-2094, 1970.
- Shahpar S., "A Comparative Study of Optimization Methods for Aerodynamic Design of Turbomachinery Blades," 2000-GT-523.
- Shepherd, D.G., "Principles of Turbomachinery," The Macmillan Company, New York, 1956.
- Szanca, E.M., Schum, H.J., and Prust, H.W. Jr., "Cold-Air Investigation of a Turbine with Transpiration-Cooled Stator Blades, I—Performance of Stator with Discrete Hole Blading," NASA, TM X-2094, 1970.
- Szanca, E.M., Schum, H.J., and Behnong, F.P., "Cold-Air Investigation of a Turbine with Transpiration-Cooled Stator Blades, II—Stage Performance with Discrete Hole Stator Blades," NASA, TM X-2133, 1970.

- Talceishi, K., Matsuura, M., Aoki, S., and Sato, T., 1989, "An Experimental Study of Heat Transfer and Film Cooling on Low Aspect Ratio Turbine Nozzles," ASME paper 89-GT-187.
- Thompson, W.E., "Aerodynamics of Turbines," Proceedings of the 1st Turbomachinery Symposium, Texas A&M University, p. 90, 1972.
- Traupel, W., "Thermische Turbomaschinen," Vol. 1. Springer-Verlag, Berlin, 1988.
- Whitney, W.J., Szanca, E.M., Moffitt, T.P., and Monroe, D.E., "Cold-Air Investigation of a Turbine for High-Temperature Engine Application," I—Turbine Design and Overall Stator Performance, NASA, TN D-3751, 1967.
- Whitney, W.J., "Comparative Study of Mixed and Isolated Flow Methods for Cooled Turbine Performance Analysis," NASA, TM X-1572, 1968.
- Whitney, W.J., "Analytical Investigation of the Effect of Cooling Air on Two-Stage Turbine Performance," NASA, TM X-1728, 1969.
- Whitney, W.J., Szanca, E.M., and Behning, F.P., "Cold-Air Investigation of a Turbine with Stator Blade Trailing Edge Coolant-Ejection, I—Overall Stator Performance," NASA, TM X-1901, 1969.
- Whitney, W.J., Szanca, E.M., Bider, B., and Monroe, D.E., "Cold-Air Investigation of a Turbine for High-Temperature Engine Application III—Overall Stage Performance," NASA, TN D-4389, 1968.

10

Combustors

Heat input to the gas turbine Brayton cycle is provided by a combustor. The combustor accepts air from the compressor and delivers it at an elevated temperature to the turbine (ideally with no pressure loss). Thus, the combustor is a direct-fired air heater in which fuel is burned almost stoichiometrically with one-third or less of the compressor discharge air. Combustion products are then mixed with the remaining air to arrive at a suitable turbine inlet temperature. There are many types of combustors, but the three major types are tubular, tubo-annular, and annular. Despite the many design differences, all gas turbine combustion chambers have three features: (1) a recirculation zone, (2) a burning zone (with a recirculation zone which extends to the dilution region), and (3) a dilution zone. The function of the recirculation zone is to evaporate, partly burn, and prepare the fuel for rapid combustion within the remainder of the burning zone. Ideally, at the end of the burning zone, all fuel should be burnt so that the function of the dilution zone is solely to mix the hot gas with the dilution air. The mixture leaving the chamber should have a temperature and velocity distribution acceptable to the guide vanes and turbine. Generally, the addition of dilution air is so abrupt that if combustion is not complete at the end of the burning zone, chilling occurs and prevents completion. However, there is evidence with some chambers that if the burning zone is run overrich, some combustion does occur within the dilution region.

Combustor inlet temperature depends on engine pressure ratio, load and engine type, and whether or not the turbine is regenerative or nonregenerative especially at the low-pressure ratios. The new industrial turbine pressure ratios are between 17:1, and 35:1, which means that the combustor inlet temperatures range from 850 °F (454 °C) to 1200 °F (649 °C). The new aircraft engines have pressure ratios, which are in excess of 40:1.

Regenerative gas turbines have combustor inlet temperatures, which range from 700 °F (371 °C) to 1100 °F (593 °C). Combustor pressures for a full-load operation vary from 45 psia (3.1 Bar) for small engines to as much as 588 psia (40.5 Bar) in complex engines. Fuel rates vary with load, and fuel atomizers may be required for flow ranges as great as 100:1. However, the variation in the fuel-to-air ratio between idle and full-load conditions usually does not vary by more than a factor of three. During transient conditions, fuel-to-air ratios vary. At lightoff and during acceleration, a much higher fuel-to-air ratio is needed because of the higher temperature rise. On deceleration, the conditions may be appreciably leaner. Thus, a combustor that can operate over a wide range of mixtures without the danger of blowouts simplifies the control system.

Combustor performance is measured by efficiency, the pressure decrease encountered in the combustor, and the evenness of the outlet temperature profile.

Combustion efficiency is a measure of combustion completeness. Combustion completeness affects fuel consumption directly, since the heating value of any unburned fuel is not used to increase the turbine inlet temperature. To calculate combustion efficiency, the actual heat increase of the gas is ratioed to the theoretical heat input of the fuel (heating value).

Efficiency thus becomes

$$\eta_{\text{comb}} = \frac{\Delta h_{\text{actual}}}{\Delta h_{\text{theoretical}}} = \frac{(\dot{m}_a + \dot{m}_f) h_3 - \dot{m}_a h_2}{\dot{m}_f (LHV)} \quad (10-1)$$

where:

η_{comb} = efficiency

\dot{m}_a = mass flow of gas

\dot{m}_f = mass flow of fuel

h_3 = enthalpy of gas leaving combustor

h_2 = enthalpy of gas entering combustor

LHV = fuel heating value

The loss of pressure in a combustor is a major problem, since it affects both the fuel consumption and power output. Total pressure loss is usually in the range of 2–8% of static pressure. This loss is the same as a decrease in compressor efficiency. The result is increased fuel consumption and lower power output that affects the size and weight of the engine.

The uniformity of the combustor outlet profile affects the useful level of turbine inlet temperature, since the average gas temperature is limited by the peak gas temperature. This uniformity assures adequate nozzle life, which depends on operating temperature. The average inlet temperature to the turbine affects both fuel consumption and power output. A large combustor outlet gradient will work to reduce average gas temperature and consequently reduce power output and efficiency. Thus, the traverse number must have a lower value—between 0.05 and 0.15 in the nozzle.

Equally important are the factors that affect satisfactory operation and life of the combustor. To achieve satisfactory operation, the flame must be self-sustaining, and combustion must be stable over a range of fuel-to-air ratios to avoid ignition loss during transient operation. Moderate metal temperatures are necessary to assure long life. Also, steep temperature gradients, which cause warps and cracks, must be avoided. Carbon deposits can distort the liner and alter the flow patterns to cause pressure losses. Smoke is environmentally objectionable as well as a fouler of heat exchangers. Minimum carbon deposits and smoke emissions also help assure satisfactory operation.

Combustion Terms

Before proceeding with combustor design, a definition of some terms is necessary:

1. *Reference velocity*. The theoretical velocity for flow of combustor-inlet air through an area equal to the maximum cross section of the combustor casing (25 fps (8 mps) in a reverse-flow combustor; 80–135 fps (24–41 mps) in a straight-through flow turbojet combustor).
2. *Profile factor*. The ratio between the maximum exit temperature and the average exit temperature.
3. *Traverse number (temperature factor)*. (a) The peak gas temperature minus mean gas temperature divided by mean temperature rise in nozzle design. (b) The difference between the highest and the average radial temperature.
4. *Stoichiometric proportions*. Constituent proportions of the reactants are such that there are exactly enough oxidizer molecules to bring about a complete reaction to stable molecular forms in the products.
5. *Equivalence ratio*. The ratio of the oxygen content at stoichiometric conditions and actual conditions:

$$\phi = \frac{(\text{Oxygen/fuel at stoichiometric})}{(\text{Oxygen/fuel at actual condition})}$$

6. *Pressure drop.* A pressure loss occurs in a combustor because of diffusion, friction, and momentum. The pressure drop value is 2–10% of the static pressure (compressor outlet pressure). The efficiency of the engine will be reduced by an equal percent.
7. *Lower Heating Value.* The lower heating value of the gas is one in which the H₂O in the products has not condensed. The lower heating value is equal to the higher heating value minus the latent heat of the condensed water vapor.

Combustion

In its simplest form, combustion is a process in which some material or fuel is burned. Whether it is striking a match or firing a jet engine, the principles involved are the same, and the products of combustion are similar.

Combustion of natural gas is a chemical reaction that occurs between carbon, or hydrogen, and oxygen. Heat is given off as the reaction takes place. The products of combustion are carbon dioxide and water. The reaction is



(Methane + Oxygen) (Carbon dioxide + Water + Heat)

Four parts of oxygen are required to burn one part of methane. The products of combustion are one part of carbon dioxide and two parts of water. One cubic foot of methane will produce one cubic foot of carbon dioxide gas.

Oxygen used for combustion occurs in the atmosphere. The chemical composition of air is approximately 21% oxygen and 79% nitrogen, or one part oxygen to four parts nitrogen. In other words, for each cubic foot of oxygen contained in the air, there are about four cubic feet of nitrogen.

Oxygen and nitrogen molecules each contain two atoms of oxygen or nitrogen. Noting that one part, or molecule, of methane requires four parts of oxygen for complete combustion, and since the oxygen molecule contains two atoms, or two parts, the volumetric ratio of methane and oxygen is as follows:



The preceding equation is the true chemical equation for the combustion process. One cubic foot of methane actually requires two cubic feet of oxygen for combustion.

Since the oxygen is contained in air, which also has nitrogen, the combustion reaction can be written as follows:

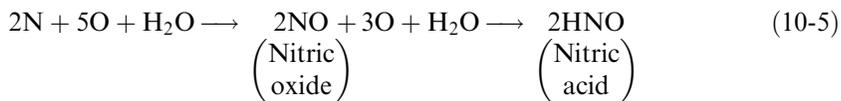


(Methane + Air) (Carbon dioxide + Nitrogen + Water + Heat)

One cubic foot (0.03 cu.m) of methane requires 10 cubic feet (0.28 cu.m) of air (2 cu.ft (0.06 cu.m) of oxygen and 8 cu.ft (0.23 cu.m) of nitrogen) for combustion. The products are carbon dioxide, nitrogen, and water. The combustion product of one cubic foot of methane yields a total of nine cubic feet of carbon dioxide gas. Also, the gas burned contains some ethane, propane, and other hydrocarbons. The yield of inert combustion gas from burning a cubic foot of methane will be 9.33 cubic feet (0.26 cu.m)

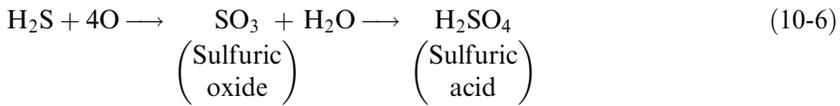
If the combustion process created only the reactions shown in the previous discussion, no provision would be necessary for control. Unfortunately, other reactions occur in which undesirable products are formed.

The chemical reaction that occurs in the formation of nitric acid during the combustion process is as follows:



The water required in the previous reaction comes from the water of combustion. The intermediate reaction shown previously (nitric acid formation) does not occur during the combustion process, but after the nitric oxide is further oxidized to nitrogen dioxide (NO_2) and cooled. Consequently, it is necessary to control the formation of nitric oxide during the combustion process to prevent its ultimate conversion to nitric acid. The formation of nitric oxide during combustion can be retarded by reducing the temperature at which combustion occurs. Normal combustion temperatures range from 3400°F to 3500°F (1871°C to 1927°C). At this temperature, the volume of nitric oxide in the combustion gas is about 0.01%. If the combustion temperature is lowered, the amount of nitric oxide is substantially reduced. By maintaining a temperature below 2800°F (1538°C) at the burner, the nitric oxide volume will be below the maximum limit of 20 parts per million (0.002%). This minimum is attained by injecting a noncombustible gas (flue gas) around the burner to cool the combustion zone.

Sulfuric acid is another common by-product of combustion. Its reaction is as follows:



The formation of sulfuric acid cannot be economically retarded in the combustion process. The best method of eliminating sulfuric acid as a combustion product is to remove sulfur from the incoming fuel gas. Two separate sweetening processes are used to remove all sulfur from the fuel gas that will be burned.

The amount of oxygen in the combustion gas is regulated by controlling the ratio of air to fuel in the primary section. As previously mentioned, the ideal volumetric ratio of air to methane is 10:1. If less than 10 volumes of air are used with one volume of methane, the combustion gas will contain carbon monoxide. The reaction is as follows:



In gas turbines there is plenty of air, so the carbon monoxide problem is not present.

Combustion Chamber Design

The most simple combustor is a straight-walled duct connecting the compressor and turbine as seen in Figure 10-1. Actually, this arrangement is impractical because of the excessive pressure loss resulting from combustion at high velocities. The fundamental pressure loss from combustion is proportional to the air velocity squared. Since compressor discharge

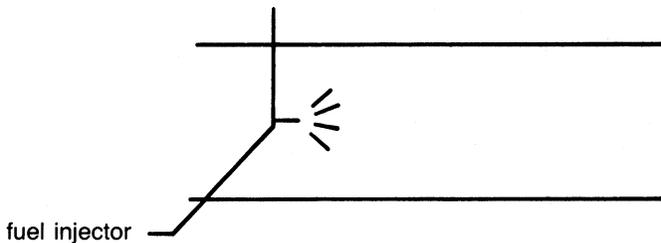


Figure 10-1. Simple straight-walled duct combustor.

velocities can be on the order of 500 ft/sec (152.4 m/sec), the combustion pressure loss can be up to one-quarter of the pressure rise produced by the compressor. For this reason, air entering the combustor is first diffused to lower the velocity. Still, up to half the combustor pressure loss can be caused by this diffusion.

Even with a diffuser, velocities are still too high to permit stable combustion. With flame speeds of a few fps, a steady flame cannot be produced by simple injection into an airstream with a velocity one to two orders of magnitude greater. Even if ignited initially, the flame will be carried downstream and cannot be sustained without continuous ignition. A baffle of some type needs to be added to create a region of low velocity and flow reversal for flame stabilization as seen in Figure 10-2. The baffle creates an eddy region in the flow continually drowning in gases to be burned, mixing them, and completing the combustion reaction. It is this steady circulation that stabilizes the flame and provides continuous ignition. The problem in combustion then becomes one of producing only enough turbulence for mixing and burning, and avoiding an excess, which results in increased pressure loss.

It is desirable to be able to analyze the controlling features of a stabilizing system so that a good combustion efficiency with respect to pressure loss is attained. Since combustor design involves the formation of turbulent zones with complicated fluid flow and chemical reaction effects, combustor designers must resort to empiricism. A simple bluff body, such as a baffle placed in the flow stream, is the simplest case of flame stabilization. Though the basic flow pattern in each combustor primary zone is similar (fuel and air mixed, ignited by recirculating flame, and burned in a highly turbulent region), there are various ways to create flame stability in the primary zone. However, they are more complicated and difficult to analyze than the simple baffle. Figures 10-3 and 10-4 show two such designs. In one, a strong vortex

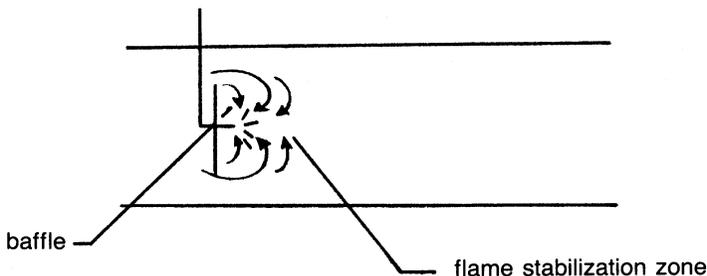


Figure 10-2. Baffle added to straight-walled duct to create flame stabilization zone.

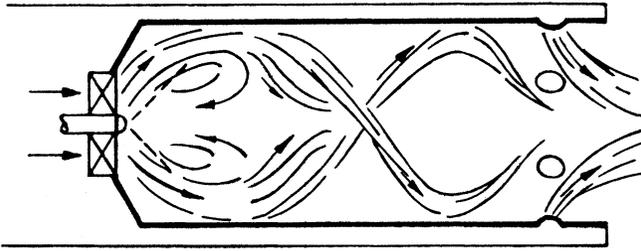


Figure 10-3. Flame stabilization region created by swirl vanes.

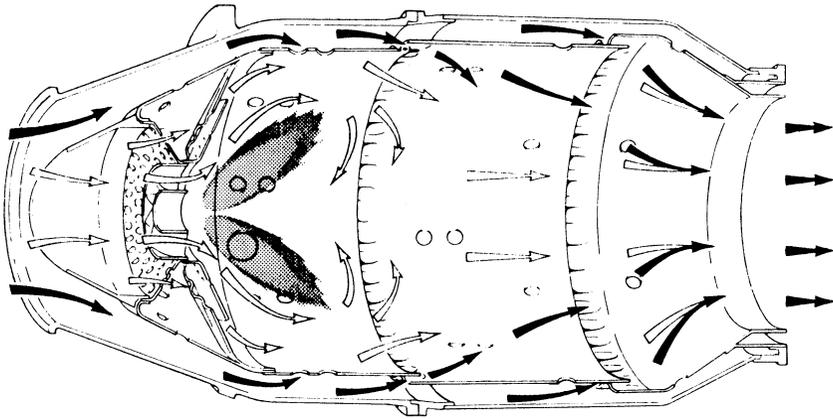


Figure 10-4. Flame stabilization created by impinging jets and general airflow pattern. (©Rolls-Royce Limited.)

is created by swirl vanes around the fuel nozzle. Another flow pattern is formed when combustor air is admitted through rings of radial jets. Jet impingement at the combustor axis results in upstream flow. The upstream flow forms a toroidal recirculation zone that stabilizes the flame.

Velocity is an important factor in primary zone design. A fixed velocity value in the combustor creates a limited range of mixture strength for which the flame is stable. Also, different flame stabilizing arrangements (baffles, jets, or swirl vanes) exhibit different ranges of burnable mixtures at a given velocity. Figure 10-5 is a general stability diagram that shows how the range of burnable mixtures decreases as velocity increases. Changing baffle size will affect the range of burnable limits as well as the pressure loss. To accommodate a wide operating range of fuel-to-air ratios, the combustor is designed to operate well below the blowout velocity. Gas turbine compress-

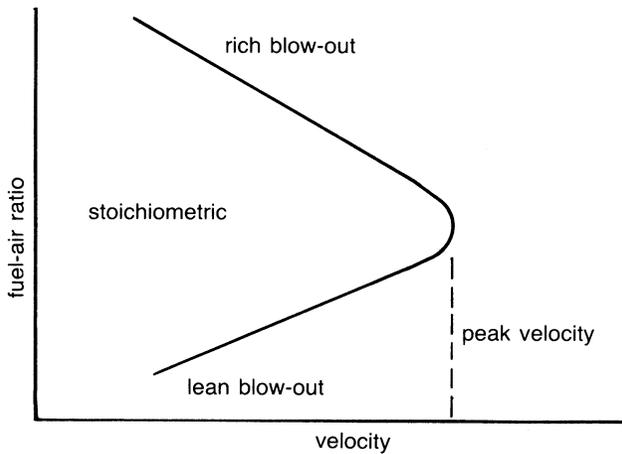


Figure 10-5. Range of burnable fuel-air ratios versus combustor gas velocity.

sors operate with nearly constant air velocities at all loads. This constant air velocity results from the compressor operating at a constant speed, and in the cases where the mass flow varies as a function of the load, the static pressure varies similarly; the volumetric air flow is nearly constant. Therefore, velocity can be used as a criterion in combustor design, especially with respect to flame stabilization.

The importance of air velocity in the primary zone is known. In the primary zone fuel-to-air ratios are about 60:1; the remaining air must be added somewhere. The secondary, or dilution, air should only be added after the primary reaction has reached completion. Dilution air should be added gradually so as not to quench the reaction. The addition of a flame tube as a basic combustor component accomplishes this, as shown in Figure 10-6. Flame tubes should be designed to produce a desirable outlet profile and to last a long time in the combustor environment. Adequate life is assured by film cooling of the liner.

Figure 10-7 shows a can-annular combustor. At the left is a transition zone in which high-velocity air from the compressor is diffused to a lower velocity and higher pressure, and distributed around the combustion liner.

The air enters the annular space between the liner and casing, and is admitted into the space within the liner through holes and slots because of the pressure difference. The design of these holes and slots divides the liner into distinct zones for flame stabilization, combustion, dilution, and provides film cooling of the liner.

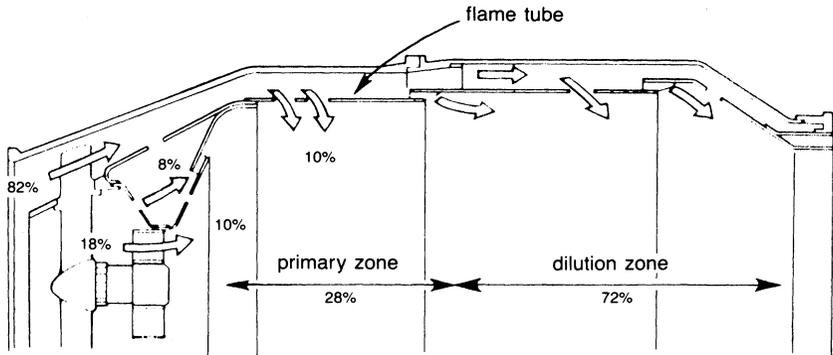


Figure 10-6. Addition of flame tube distributes flow between primary and dilution zone.

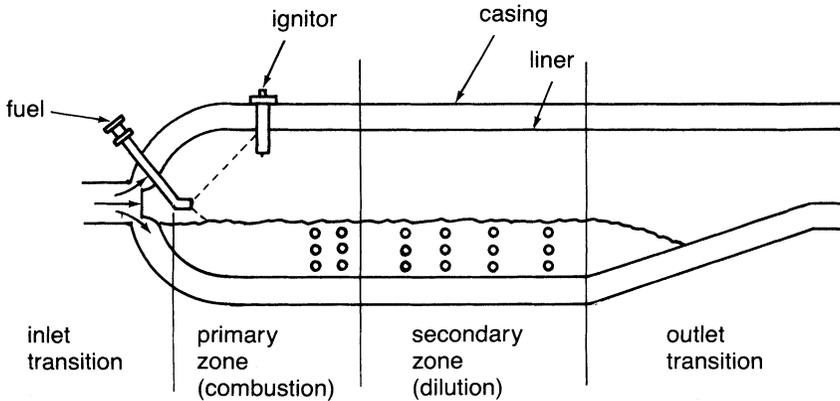


Figure 10-7. A can-annular combustor.

Flame Stabilization

With the aid of swirl vanes surrounding the fuel nozzle, strong vortex flow occurs in the combustion air in the combustion region. Figure 10-8 shows a suitable distribution of axial and rotational momentum. A low-pressure region is created at the combustor axis, which causes recirculation of the flame toward the fuel nozzle. At the same time, radial holes around the liner supply air to the center of the vortex, making the flame grow to some extent. Jet angles and penetration from the holes are such that jet impingement along the combustor axis results in upstream flow. The upstream flow forms a torroidal recirculation zone, which stabilizes the flame.

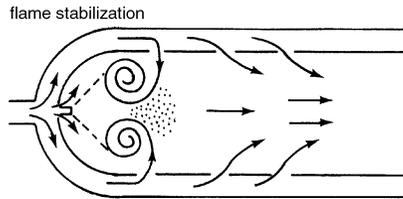


Figure 10-8. Flow pattern by swirl vanes and radial jets.

Combustion and Dilution

With torroidal air flow, combustors will operate without visible smoke when properly developed for a primary-zone equivalence ratio below 1.5. Visible smoke is an air-pollution problem.

After combustion, the rich burning mixture leaves the combustion zone and flows between the rows of air jets entering the liner. Each jet entrains air and burning fuel and carries it toward the combustor axis, forming torroidal recirculation patterns around each jet that result in intensive turbulence and mixing throughout the combustor.

This combustion product is diluted with air entering through holes on the liner to make the temperature appropriate for blade material and to have enough volume-flow in the dilution zone. Air is jet-penetrated mainly because of converging clearances and creates high local pressure.

Film Cooling of the Liner

The liner experiences a high temperature because of heat radiated by the flame and combustion. To improve the life of the liner, it is necessary to lower the temperature of the liner and use a material that has a high resistance to thermal stress and fatigue. The air film cooling method reduces the temperature both inside and outside the surface of the liner. This reduction is accomplished by fastening a metal ring inside the liner to leave a definite annular clearance. Air is admitted into this clearance space through rows of small holes in the liner and is directed by the metal rings as a film of cooling air along the liner inside. Figure 10-9a shows how the flow is induced by the static pressure drop across the liner surface. In high air mass flow combustors, this pressure drop may be too small to be effective. It may be necessary to use the total pressure difference in high air mass flow combustors. This type of arrangement is shown in Figure 10-9b.

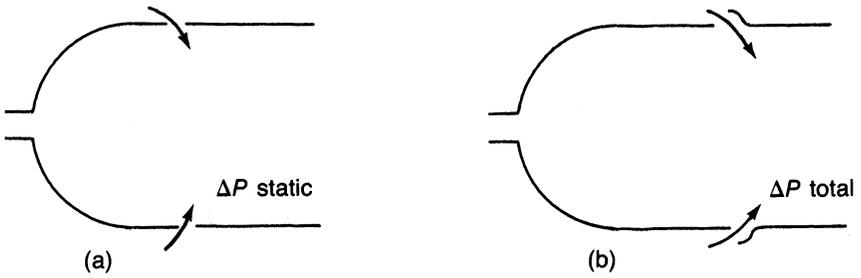


Figure 10-9. Film cooling of a combustor liner.

Fuel Atomization and Ignition

In most gas turbines, liquid fuel is atomized and injected into the combustors in the form of a fine spray. A typical low-pressure fuel atomization nozzle is shown in Figure 10-10. The fuel spray entrains air because of the

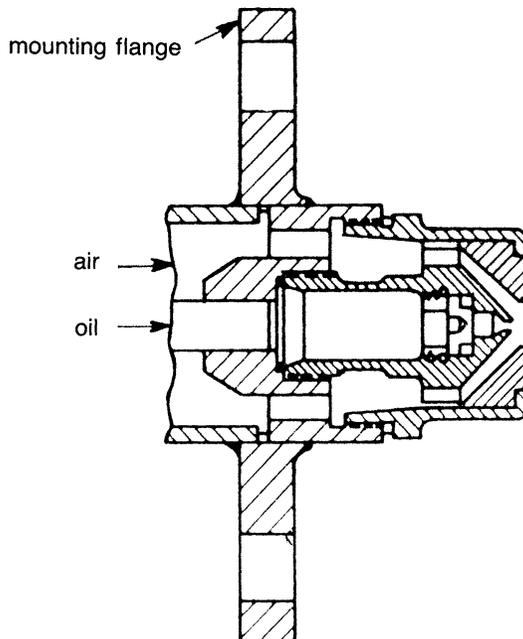


Figure 10-10. Low-pressure air atomizer. (Courtesy of General Electric Company.)

momentum and drag of fuel droplets; however, this process produces a low-pressure region inside the spray cone that causes it to converge downstream of the nozzle. This low-pressure region is counteracted by upstream axial flow of combustion products, preventing convergence in the combustion chamber.

In a simple pressure-atomizing fuel nozzle the flow rate varies as the square root of the pressure. Aircraft turbines operating over a wide range of altitudes and power levels require atomizers that have a capacity range of about 100:1 with a moderate range of fuel pressures. This wide range can be provided with dual-orifice nozzles, spill control nozzles, variable-area nozzles, or air-atomizing nozzles.

The dual-orifice nozzle consists of two concentric simplex fuel nozzles. The outer nozzle has two to ten times the flow capacity of the inner nozzle. Ignition is usually obtained from an ignitor interfaced with a high-energy capacitive discharge ignition system.

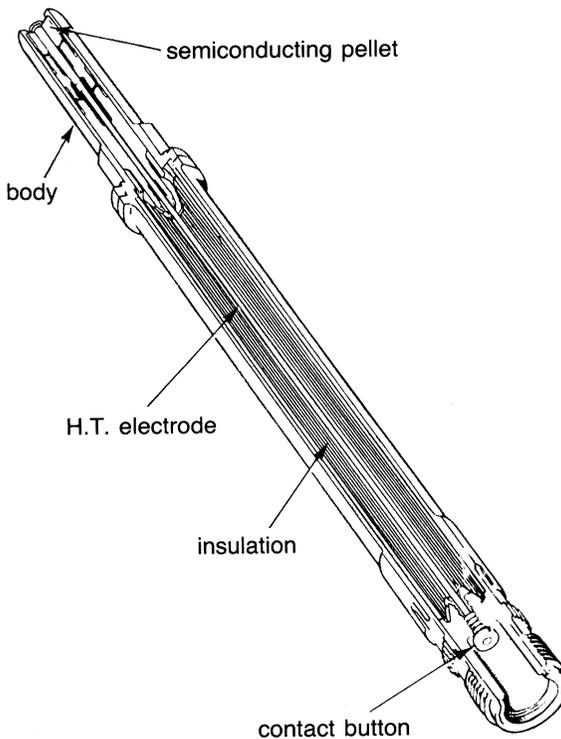


Figure 10-11. An ignitor plug. (©Rolls-Royce Limited.)

In multiple combustion installations all combustors are interconnected by tubes located near the upstream ring of perforations. Ignitors are provided in only some of the combustors. When one combustor lights, the sudden increase in pressure loss forces flame through the interconnecting tubes to the adjacent combustors, immediately lighting the other combustors.

An ignitor plug is shown in Figure 10-11. This plug is a surface discharge plug, thus energy does not have to jump an air gap. The plug end is covered by a semiconductive material and is formed by a pellet, permitting an electrical leakage from the central high-tension electrode to the body. The discharge takes the form of a high-intensity flash from the electrode to the body.

Combustor Design Considerations

Cross-sectional area. The combustor cross section can be determined by dividing the volumetric flow at the combustor inlet by a reference velocity which has been selected as being appropriate for the particular turbine conditions on the basis of proven performance in a similar engine. Another basis for selecting a combustor cross section comes from correlations of thermal loading per unit cross section. Thermal loading is proportional to the primary zone air flow because fuel and air mixtures are near stoichiometric in all combustors.

Length. Combustor length must be sufficient to provide for flame stabilization, combustion, and mixing with dilution air. The typical value of the length-to-diameter ratio for liners ranges from three to six. Ratios for casing range from two to four.

Wobbe Number. Wobbe Number is an indicator of the characteristics and stability of the combustion process.

$$W_b = \frac{LHV}{\sqrt{Sp \cdot Gr * T_{amb}}}$$

Increasing the Wobbe Number can cause the flame to burn closer to the liner. Decreasing the Wobbe Number can cause pulsations in the combustor.

Pressure drop. The minimum practical pressure drop—excluding diffuser loss—is about 14 times the reference velocity pressure. Higher values are frequently used. Some values for this pressure loss are: 100 fps (30 mps), 4%; 80 fps (24 mps), 2.5%; 70 fps (21 mps), 2%; 50 fps (15 mps), 1%.

Volumetric heat-release rate. The heat-release rate is proportional to the fuel-to-air ratio and the combustor pressure, and it is a function of

combustor capacity. Actual space required for combustion, as chemical limits are approached, varies with pressure to the 1.8 power.

Liner holes. Liner area to casing area and liner hold area to casing area are important to the performance of combustors. For example, the pressure loss coefficient has a minimum value in the range of 0.6 of the liner area/casing area ratio with a temperature ratio of 4:1.

In practice it has been found that the diameter of holes in the primary zone should be no larger than 0.1 of the liner diameter. Tubular liners with about 10 rings of eight holes each give good efficiency. As discussed before, swirl vanes with holes yield better combustor performance.

In the dilution zone, sizing of the holes can be used to provide a desired temperature profile.

Combustion Liners. Three major changes have occurred since the original AISI 309 stainless louver cooled liners. The first change was the adoption of better materials such as Hastelloy X/RA333 in the 1960s, and Nimonic 75 and the adoption of the slot-cooled liner in the early 1970s. This slot-cooled design offers considerably more liner cooling effectiveness, and, from a materials standpoint, presents a new area of processing challenges. Fabrication and repair of liners is primarily by a combination of brazing and welding. Earlier liners, on the other hand, were made using a welded construction with mechanically formed louvers.

For resistance against fatigue, Nimonic 75 has been used with Nimonic 80 and Nimonic 90. Nimonic 75 is an 80-20 nickel-chromium alloy stiffened with a small amount of titanium carbide. Nimonic 75 has excellent oxidation and corrosion resistance at elevated temperatures, a reasonable creep strength, and good fatigue resistance. In addition, it is easy to press, draw, and mold. As firing temperatures have increased in the newer gas turbine models, HA-188, a Cr, Ni-based alloy, has recently been employed in the latter section of some combustion liners for improved creep rupture strength.

Second, in addition to the base material changes, many of today's combustors also have Thermal Barrier Coatings (TBCs), which have an insulation layer of the total thickness used is 0.015–0.025 inch (0.4–0.6 mm) and are based on $ZrO_2\text{-}Y_2O_3$ and can reduce metal temperatures by 90–270 °F (50–150 °C).

TBCs consist of two different materials applied to the hot side of the component: a bond coat applied to the surface of the part, and an insulating oxide applied over the bond coat. Characteristics of TBCs are that the insulation is porous, and they have two layers. The first layer is a bond coat of NiCrAlY, and the second is a top coat of YTTRIA stabilized Zirconia.

Advantages of the TBCs are the reduction of metal temperatures of cooled components, by about 8–14 °F (4–9 °C) per mil (25.4 microns) of coating, the microstructure, and a coated liner. The primary benefit of the TBCs is to provide an insulating layer that reduces the underlying base material temperature and mitigates the effects of hot streaking or uneven gas temperature distributions. These coatings are now standard on most high-performance gas turbines and have demonstrated excellent performance in production machines.

The third major change was the introduction of steam cooling of the liners. This concept, especially in combined cycle application, has great potential.

Transition Pieces. Although technically not part of the combustor they are an important part of the combustion system. Less complicated than the liners, the transition pieces have probably been more challenging from a materials/processes standpoint. Therefore, new materials have tended to be first introduced on the transition piece. From a design standpoint, significant improvements have been made on advanced models through the use of heavier walls, single-piece aft ends, ribs, floating seal arrangements, and selective cooling. These design changes have been matched by material improvements. Early transition pieces were made from AISI 309 stainless steel. In the early 1960s, nickel base alloys Hastelloy-X and RA-333 were used in the more limiting parts. These alloys became standard for transition pieces by 1970.

In the early 1980s, a new material, Nimonic 263, was introduced into service for transition pieces. This material is a precipitation-strengthened, nickel-base alloy with higher strength capability than Hastelloy-X. Since the early 1980s, Thermal Barrier Coatings (TBCs) have been applied to the transition pieces of the higher firing temperature gas turbine models and to uprated machines. Field experience over thousands of hours of service has demonstrated good durability for this coating on transition pieces.

Improvement has also been made to increase the wear resistance of some transition pieces in the aft end or picture frame area. Cobalt-base hard coatings applied by thermal spray have been tested in field machines and the best spray has been shown to improve the wear life of sealing components by more than four times.

Reliability of Combustors. The heat from combustion, pressure fluctuation, and vibration in the compressor may cause cracks in the liner and nozzle. Also, there are corrosion and distortion problems. The edges of the holes in the liner are great concern because the holes act as stress concentrators for any mechanical vibrations and, on rapid temperature fluctuations, high-temperature gradients are formed in the region of the hole edge, giving rise to a corresponding thermal fatigue.

It is necessary to modify the edge of the hole in various ways to reduce these stress concentrations. Some methods of modification are priming, plunging, and standard radiusing and polishing methods. In the Dry Low NO_x Combustors, especially in the lean pre-mix chambers, pressure fluctuations can set up very high vibrations, which lead to major failures.

Typical Combustor Arrangements

All gas turbine combustors provide the same function; however, there are different methods to arrange combustors on the gas turbine. Designs fall into three major categories:

1. Tubular (single can)
2. Turbo-annular
3. Annular

FPO

Figure 10-12a. Top view of a large side combustor with special tiles. (Courtesy Brown Boveri Turbomachinery, Inc.)

FPO

Figure 10-12b. Special tiles for a large side combustor. (Courtesy Brown Boveri Turbomachinery, Inc.)

FPO

Figure 10-13. Single can combustor. (Courtesy Brown Boveri Turbomachinery, Inc.)

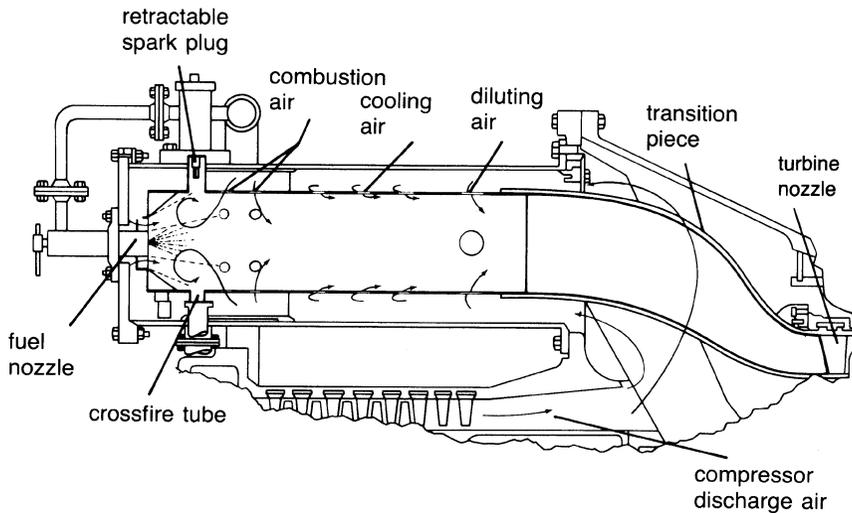


Figure 10-14. Turbo-annular or can-annular combustor for a heavy-duty gas turbine. (Courtesy of General Electric Company.)

Tubular or single-can designs are preferred by many European industrial gas turbine designers. These large single combustors offer the advantage of simplicity of design and long life because of low heat-release rates. These combustors are sometimes very large. They can range in size from small units of about 6 inches (15.24 cm) in diameter and a 1 ft (0.3 m) high to combustors, which are over 10 feet (3 m) in diameter and 30–40 feet (3–12 m) high. These large combustors use special tiles as liners. Any liner damage can be easily corrected by replacing the damaged tiles. Figure 10-12 shows such a liner. The tubular combustors can be designed as “straight-through” or “reverse-flow designs.” Most large single-can combustors are of the reverse-flow design. In this design, the air enters the turbine through the annulus between the combustor can and the hot gas pipe as seen in Figure 10-13. The air then passes between the liner and the combustor can and enters the combustion region at various points of entry. About 10% of the air enters the combustion zone, about 30–40% of the air is used for cooling purposes, the rest is used in the dilution zone. Reverse-flow designs are much shorter than the straight-through flow designs.

The tubular, or single-can, for large units usually has more than one nozzle. In many cases a ring of nozzles is placed in the primary zone area. The radial and circumferential distribution of the temperature to the turbine nozzles is not as even as in tubo-annular combustors.

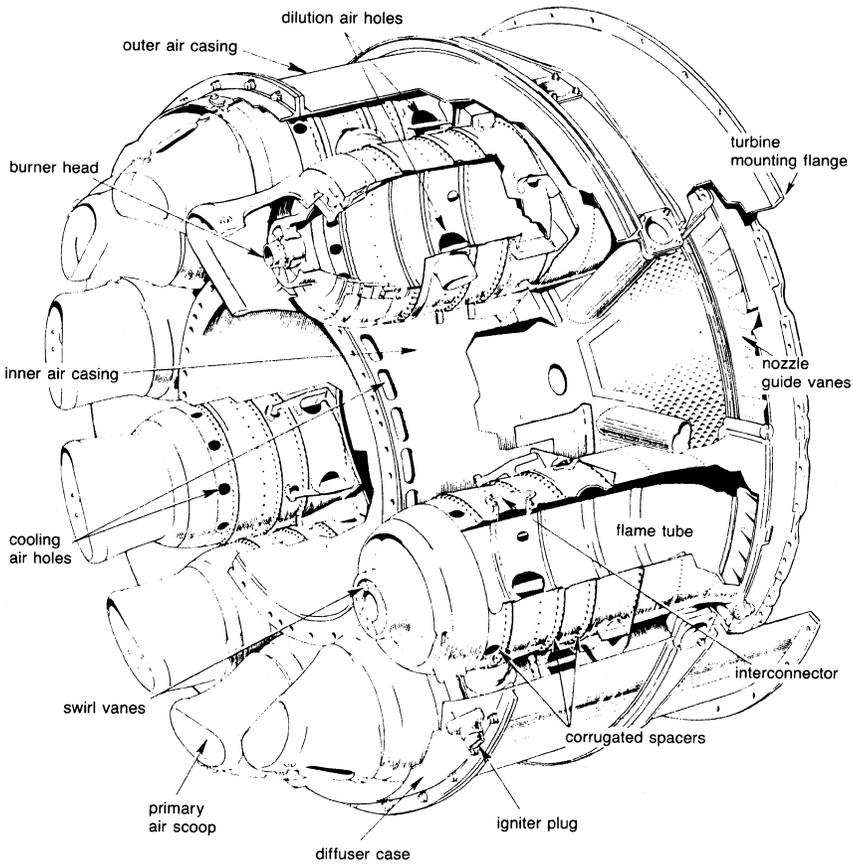


Figure 10-15. “Straight-through” flow-type can-annular combustors. (© Rolls-Royce Limited.)

Tubo-annular combustors are the most common type of combustors used in gas turbines. The industrial gas turbines designed by U.S. companies use the tubo-annular or can-annular type seen in Figure 10-14. The advantage to these types of combustors are the ease of maintenance. They also have a better temperature distribution than the side single-can combustor and can be of the straight-through or reverse-flow design. As with the single-can combustor, most of these combustors are of the reverse-flow design in industrial turbines.

In most aircraft engines the tubo-annular combustors are of the straight-through flow type seen in Figure 10-15. The straight-through flow type

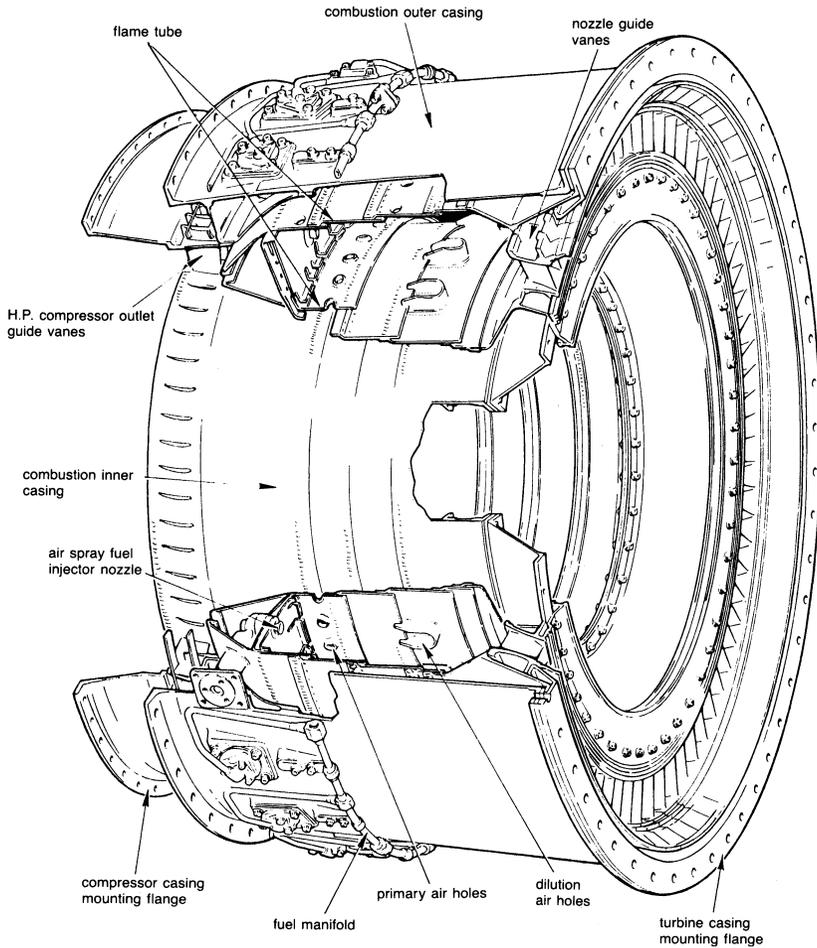


Figure 10-16. Aircraft-type annular combustion chamber. (© Rolls-Royce Limited.)

tubo-annular combustor requires a much smaller frontal area than the reverse-flow type tubo-annular combustor. The tubo-annular combustor also requires more cooling air flow than a single or annular combustor because the surface area of the tubo-annular combustor is much greater. The amount of cooling air is not much of a problem in turbines using high-Btu gas, but for low-Btu gas turbines, the amount of air required in the primary zone can be as high as 35% of the total air needed, thus reducing the amount of air available for cooling purposes.

FPO

Figure 10-17. Industrial-type can-annular combustor. (Courtesy of Solar Turbines Incorporated.)

Higher temperatures also require more cooling and, as temperatures increase, the single can or annular combustor design becomes more attractive. The tubo-annular combustor has a more even combustion because each can has its own nozzle and a smaller combustion zone, resulting in a much more even flow. Development of a tubo-annular combustor is usually less expensive, since only one can needs to be tested instead of an entire unit as in an annular or single-can combustor. Therefore, the fuel and air requirements can be as low as 8–10% of the total requirements.

Annular combustors are used mainly in aircraft-type gas turbines where frontal area is important. This type of combustor is usually a straight-through flow type. The combustor outside radius is the same as the compressor casing, thus producing the streamline design seen in Figure 10-16. The annular combustor mentioned earlier requires less cooling air than the tubo-annular combustor, and so it is growing in importance for high-temperature application. On the other hand, the annular combustor is much harder to get to for maintenance and tends to produce a less favorable

radial and circumferential profile as compared to the tubo-annular combustors. The annular combustors are also used in some newer industrial gas turbine applications as seen in Figure 10-17. The higher temperatures and low-Btu gases will foster more use of annular-type combustors in the future.

Air Pollution Problems

Smoke

In general, it has been found that much visible smoke is formed in small, local fuel-rich regions. The general approach to eliminating smoke is to develop leaner primary zones with an equivalence ratio between 0.9 and 1.5. Another supplementary way to eliminate smoke is to supply relatively small quantities of air to those exact, local, over-rich zones.

Unburnt Hydrocarbons and Carbon Monoxide

Unburnt hydrocarbon (UHC) and carbon monoxide (CO) are only produced in incomplete combustion typical of idle conditions. It appears probable that idling efficiency can be improved by detailed design to provide better atomization and higher local temperatures. CO₂ production is a direct function of the fuel burnt (3.14 times the fuel burnt) it is not possible to control the production of CO₂ in fossil fuel combustion, the best control is the increasing of the turbine efficiency, thus requiring less fuel to be burnt for the same power produced.

Oxides of Nitrogen

The main oxides of nitrogen produced in combustion are NO, with the remaining 10% as NO₂. These products are of great concern because of their poisonous character and abundance, especially at full-load conditions.

The formation mechanism of NO can be explained as follows:

1. Fixation of atmospheric oxygen and nitrogen at high-flame temperature.
2. Attack of carbon or hydrocarbon radicals of fuel on nitrogen molecules, resulting in NO formation.
3. Oxidation of the chemically bound nitrogen in fuel.

In 1977, the Environmental Protection Agency (EPA) in the U.S. issued proposed rules that limited the emissions of new, modified and reconstructed gas turbines to:

- 75 vppm NO_x at 15% oxygen (dry basis)
- 150 vppm SO_x at 15% oxygen (dry basis), controlled by limiting fuel sulfur content to less than 0.8% wt.

These standards applied to simple and regenerative cycle gas turbines, and to the gas turbine portion of combined cycle steam/electric generating systems. The 15% oxygen level was specified to prevent the NO_x ppm level being achieved by dilution of the exhaust with air.

Figure 10-18 shows how in the past 30 years the reduction of NO_x by first the use of steam (Wet Combustors) injection in the combustors, and then in the 1990s, the Dry Low NO_x Combustors have greatly reduced the NO_x output. New units under development have goals, which would reduce NO_x levels below 9 ppm.

In 1977 it was recognized that there were a number of ways to control oxides of nitrogen:-

1. Use of a rich primary zone in which little NO formed, followed by rapid dilution in the secondary zone.
2. Use of a very lean primary zone to minimize peak flame temperature by dilution.
3. Use of water or steam admitted with the fuel for cooling the small zone downstream from the fuel nozzle.
4. Use of inert exhaust gas recirculated into the reaction zone.
5. Catalytic exhaust cleanup.

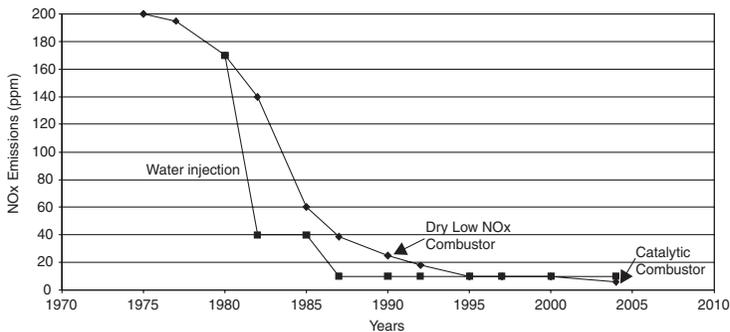


Figure 10-18. Control of gas turbine NO_x emissions over the years.

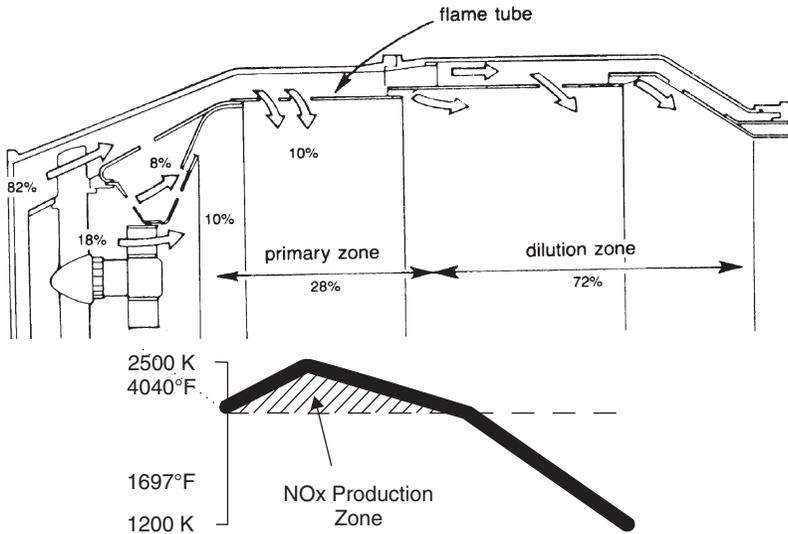


Figure 10-19. A typical combustor showing the NO_x production zone.

“Wet” control became the preferred method in the 1980s and most of 1990s since “dry” controls and catalytic cleanup were both at very early stages of development. The catalytic converters were used in the 1980s and are still being widely used; however the cost of rejuvenating the catalyst is very high.

There has been a gradual tightening of the NO_x limits over the years from 75 ppm down to 25 ppm, and now the new turbine goals are 9 ppm.

Advances in combustion technology now make it possible to control the levels of NO_x production at source, removing the need for “wet” controls. This of course opened up the market for the gas turbine to operate in areas with limited supplies of suitable quality water, e.g., deserts or marine platforms.

Although water injection is still used, “dry” control combustion technology has become the preferred method for the major players in the industrial power generation market. DLN (Dry Low NO_x) was the first acronym to be coined, but with the requirement to control NO_x without increasing carbon monoxide and unburned hydrocarbons this has now become DLE (Dry Low Emissions).

The majority of the NO_x produced in the combustion chamber is called “thermal NO_x .” It is produced by a series of chemical reactions between the nitrogen (N_2) and the oxygen (O_2) in the air that occur at the elevated temperatures and pressures in gas turbine combustors. The reaction rates are highly temperature dependent, and the NO_x production rate becomes significant above flame temperatures of about 3300 °F (1815 °C). Figure 10-19 shows schematically, flame temperatures and therefore NO_x production

zones inside a “conventional” combustor. This design deliberately burned all of the fuel in a series of zones going from fuel-rich to fuel-lean to provide good stability and combustion efficiency over the entire power range.

The great dependence of NO_x formation on temperature reveals the direct effect of water or steam injection on NO_x reduction. Recent research showed an 85% reduction of NO_x by steam or water injection with optimizing combustor aerodynamics.

In a typical combustor as shown in Figure 10-19, the flow entering the primary zone is limited to about 10%. The rest of the flow is used for mixing the combusted air and cooling the combustor can. The Maximum temperature is reached in the primary or stoichiometric zone of about 4040°F (2230°C) and after the mixing of the combustion process with the cooling air the temperature drops down to a low of 2500°F (1370°C).

Basis for NO_x Prevention. Emissions from turbines are a function of temperature and thus a function of the F/A ratio. Figure 10-20 shows that as the temperature is increased the amount of NO_x emissions are increased and the CO , and the unburnt hydrocarbons are decreased. The principal mechanism for NO_x formation is the oxidation of nitrogen in air when exposed to high temperatures in the combustion process, the amount of NO_x is thus dependent on the temperature of the combustion gases and also, to a lesser amount on the time the nitrogen is exposed to these high temperatures.

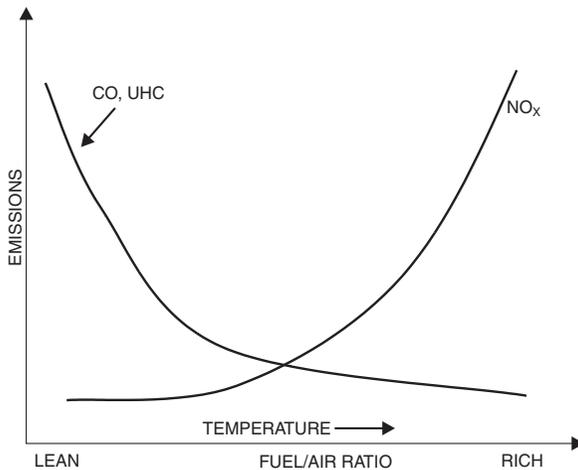
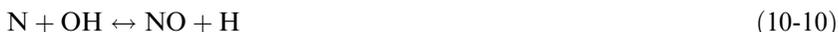


Figure 10-20. The effect of flame temperature on emissions.

The challenge in these designs is to lower the NO_x without degradation in unit stability. In the combustion of fuels that do not contain nitrogen compounds, NO_x compounds (primarily NO) are formed by two main mechanisms, thermal mechanism and the prompt mechanism. In the thermal mechanism, NO is formed by the oxidation of molecular nitrogen through the following reactions:

NO_x is primarily formed through high temperature reaction between Nitrogen and Oxygen from the air.



Hydrocarbon radicals, predominantly through the reaction, initiate the prompt mechanism



The HCN and N are converted rapidly to NO by reaction with oxygen and hydrogen atoms in the flame.

The prompt mechanism predominates at low temperatures under fuel-rich conditions, whereas the thermal mechanism becomes important at temperatures above 2732 °F (1500 °C). Due to the onset of the thermal mechanism the formation of NO_x in the combustion of fuel/air mixtures increases

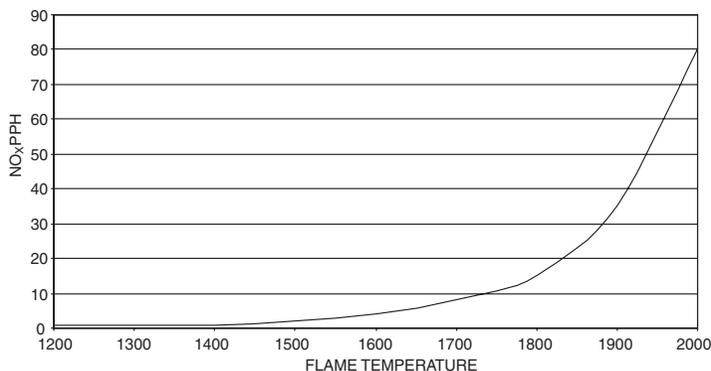


Figure 10-21. Correlation of adiabatic flame temperature with NO_x emissions.

rapidly with temperature above 2732 °F (1500 °C) and also increases with residence time in the combustor.

The production rate of NO can be given as follows:

$$\frac{d(NO)}{dt} = \frac{K}{\sqrt{T}} e^{\frac{E}{T}} \sqrt{O_2(N_2)} \tag{10-12}$$

The important parameters in the reduction of NO_x as seen in the above equation are the temperature of the flame, the nitrogen and oxygen content and the resident time of the gases in the combustor. Figure 10-21 is a correlation between the adiabatic flame temperature and the emission of NO_x. Reduction of any and all these parameters will reduce the amount of NO_x emitted from the turbine.

Dry Low NO_x Combustor

The gas turbine combustors have seen considerable change in their design as most new turbines have progressed to Dry Low Emission NO_x Combustors from the wet combustors, which were injected by steam in the primary zone of the combustor. The DLE approach is to burn most (at least 75%) of the fuel at cool, fuel-lean conditions to avoid any significant production of NO_x. The principal features of such a combustion system is the premixing of

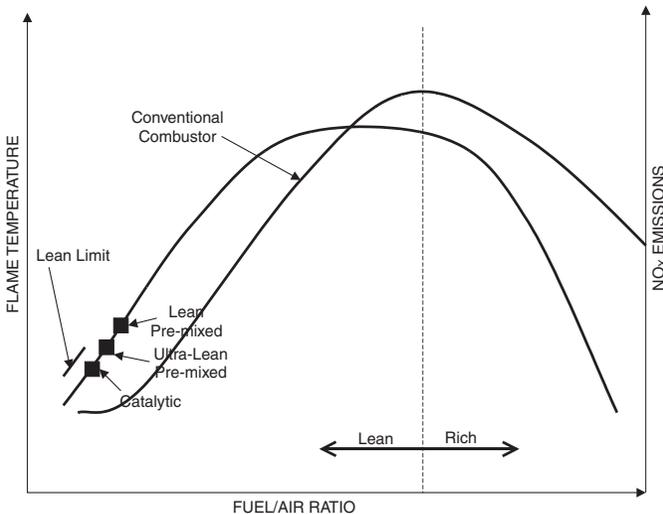


Figure 10-22. Effect of fuel /air ratio on flame temperature and NO_x emissions.

the fuel and air before the mixture enters the combustion chamber and leanness of the mixture strength in order to lower the flame temperature and reduce NO_x emission. This action brings the full load operating point down on the flame temperature curve as seen in Figure 10-22 and closer to the lean limit. Controlling CO emissions thus can be difficult and rapid engine off-loads bring the problem of avoiding flame extinction, which if it occurs cannot be safely reestablished without bringing the engine to rest and going through the restart procedure.

Figure 10-23 shows a schematic comparison of a typical dry low emission NO_x combustor and conventional combustors. In both cases, a swirler is used to create the required flow conditions in the combustion chamber to stabilize the flame. The DLE fuel injector is much larger because it contains the fuel/air premixing chamber and the quantity of air being mixed is large, approximately 50–60% of the combustion air flow.

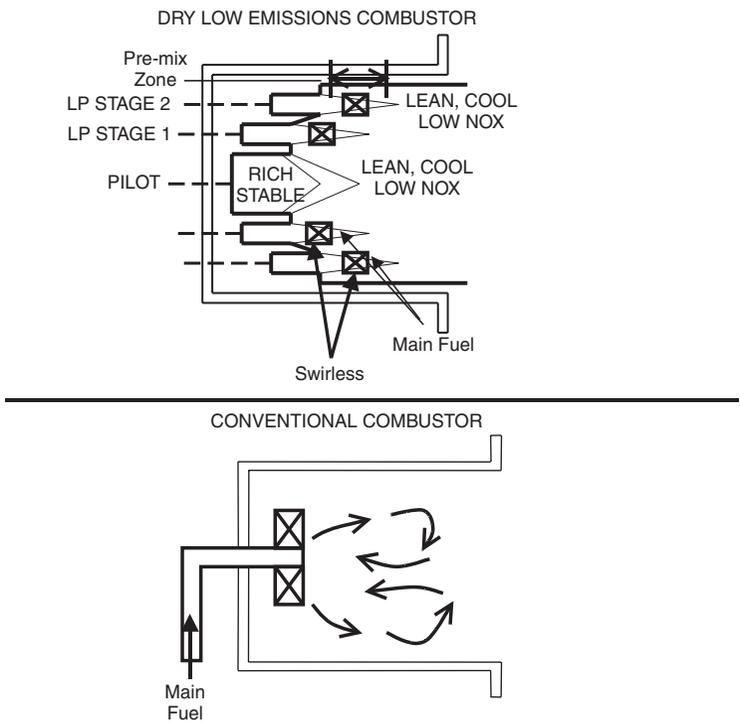


Figure 10-23. A schematic comparison of a typical dry low emission NO_x combustor and a conventional combustors.

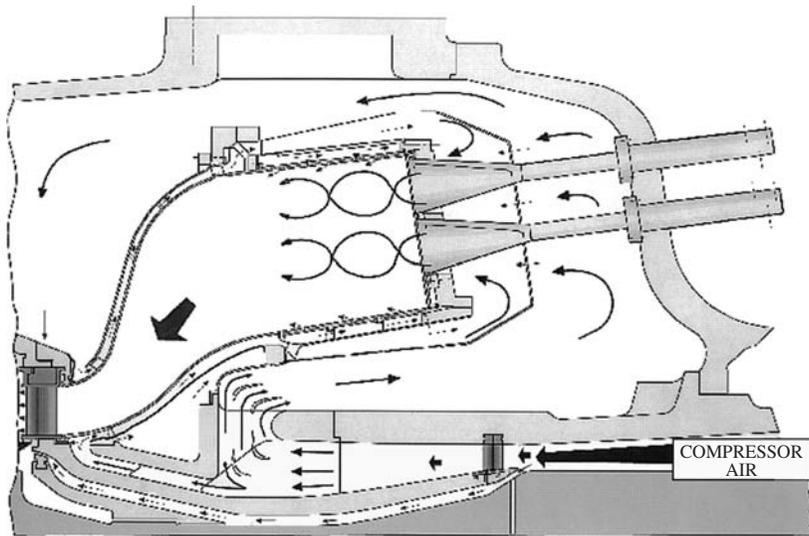


Figure 10-24. Schematic of a dry low emission NO_x combustor (Courtesy ALSTOM.)

The DLE injector has two fuel circuits. The main fuel, approximately 97% of the total, is injected into the air stream immediately downstream of the swirler at the inlet to the pre-mixing chamber. The pilot fuel is injected directly into the combustion chamber with little if any premixing. With the flame temperature being much closer to the lean limit than in a conventional combustion system, some action has to be taken when the engine load is reduced to prevent flame out. If no action were taken flame-out would occur since the mixture strength would become too lean to burn. A small proportion of the fuel is always burned richer to provide a stable “piloting” zone, while the remainder is burned lean. In both cases, a swirler is used to create the required flow conditions in the combustion chamber to stabilize the flame. The LP fuel injector is much larger because it contains the fuel/air pre-mixing chamber and the quantity of air being mixed is large, approximately 50–60% of the combustion air flow.

Figure 10-24 shows a schematic of an actual dry low emission NO_x combustor used by ALSTOM in their large turbines. With the flame temperature being much closer to the lean limit than in a conventional combustion system, some action has to be taken when the engine load is reduced to prevent flame out. If no action were taken flame-out would occur since the mixture strength would become too lean to burn.

One method is to close the compressor inlet guide vanes progressively as the load is lowered. This reduces the engine airflow and hence reduces the change in mixture strength that occurs in the combustion chamber. This method, on a single shaft engine, generally provides sufficient control to allow low emission operation to be maintained down to 50% engine load. Another method is to deliberately dump air overboard prior to or directly from the combustion section of the engine. This reduces the airflow and also increases the fuel flow required (for any given load) and hence the combustion fuel/air ratio can be held approximately constant at the full load value. This latter method causes the part load thermal efficiency of the engine to fall off by as much as 20%. Even with these air management systems lack of combustion stability range can be encountered particularly when load is rapidly reduced.

If the combustor does not feature variable geometry, then it is necessary to turn on the fuel in stages as the engine power is increased. The expected operating range of the engine will determine the number of stages, but typically at least 2 or 3 stages are used as seen in Figure 10-25. Some units have very complex staging as the units are started or operated at off-design conditions.

Gas turbines often experience problems with these DLE combustors, some of the common problems experienced are:

- auto-ignition and flash-back
- combustion instability

These problems can result in sudden loss of power because a fault is sensed by the engine control system and the engine is shutdown.

Auto-ignition is the spontaneous self-ignition of a combustible mixture. For a given fuel mixture at a particular temperature and pressure, there is a finite time before self-ignition will occur. Diesel engines (knocking) rely on it to work, but spark-ignition engines must avoid it

DLE combustors have pre-mix modules on the head of the combustor to mix the fuel uniformly with air. To avoid auto-ignition, the residence time of the fuel in the premix tube must be less than the auto-ignition delay time of the fuel. If auto-ignition does occur in the pre-mix module then it is probable that the resulting damage will require repair and/or replacement of parts before the engine is run again at full load.

Some operators are experiencing engine shutdowns because of auto-ignition problems. The response of the engine suppliers to rectify the situation has not been encouraging, but the operators feel that the reduced reliability cannot be accepted as the “norm.”

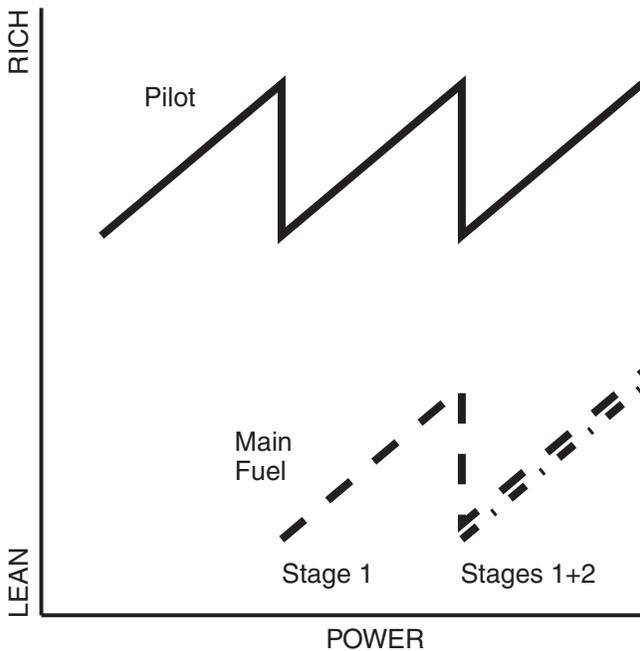


Figure 10-25. Shows the staging of dry low emissions combustor as the turbine is brought to full power.

If auto-ignitions occur, then the design does not have sufficient safety margin between the auto-ignition delay time for the fuel and the residence time of the fuel in the pre-mix duct. Auto-ignition delay times for fuels do exist, but a literature search will reveal that there is considerable variability for a given fuel. Reasons for auto-ignition could be classified as follows:

- long fuel auto-ignition delay time assumed
- variations in fuel composition reducing auto-ignition delay time
- fuel residence time incorrectly calculated
- auto-ignition triggered “early” by ingestion of combustible particles

Flashback into a pre-mix duct occurs when the local flame speed is faster than the velocity of the fuel/air mixture leaving the duct.

Flashback usually happens during unexpected engine transients, e.g., compressor surge. The resultant change of air velocity would almost certainly result in flashback. Unfortunately, as soon as the flame-front approaches

the exit of the pre-mix duct, the flame-front pressure drop will cause a reduction in the velocity of the mixture through the duct. This amplifies the effect of the original disturbance, thus prolonging the occurrence of the flashback.

Advanced cooling techniques could be offered to provide some degree of protection during a flashback event caused by engine surge. Flame detection systems coupled with fast-acting fuel control valves could also be designed to minimize the impact of a flashback. The new combustors also have steam cooling being provided.

High pressure burners for gas turbines use pre-mixing to enable combustion of lean mixtures. The stoichiometric mixture of air and fuel varies between 1.4 and 3.0 for gas turbines. The flames become unstable when the mixture exceeds a factor of 3.0 and below 1.4 the flame is too hot and NO_x emissions will rise rapidly. The new combustors are therefore shortened to reduce the time the gases are in the combustor. The number of nozzles is increased to give better atomization and better mixing of the gases in the combustor. The number of nozzles in most cases increases by a factor of 5–10, which does lead to a more complex control system. The trend now is to an evolution towards the can-annular burners. For example, ABB GT9 turbine had one combustion chamber with one burner, the new ABB 13 E2 has 12 can-annular combustors and 72 burners.

Combustion instability only used to be a problem with conventional combustors at very low engine powers. The phenomenon was called “rumble.” It was associated with the fuel-lean zones of a combustor, where the conditions for burning are less attractive. The complex 3D-flow structure that exists in a combustor will always have some zones that are susceptible to the oscillatory burning. In a conventional combustor, the heat release from these “oscillating” zones was only a significant percentage of the total combustor heat release at low power conditions.

With DLE combustors, the aim is to burn most of the fuel very lean to avoid the high combustion temperature zones that produce NO_x . So these lean zones that are prone to oscillatory burning are now present from idle to 100% power. Resonance can occur (usually) within the combustor. The pressure amplitude at any given resonant frequency can rapidly build up and cause failure of the combustor. The modes of oscillation can be axial, radial or circumferential, or all three at the same time. The use of dynamic pressure transducer in the combustor section, especially in the low NO_x combustors ensures that each combustor can be burning evenly. This is achieved by controlling the flow in each combustor can till the spectrums obtained from each combustor can match. This technique has been used and found to be very effective and ensures combustor stability.

The calculation of the fuel residence time in the combustor or the pre-mixing tube is not easy. The mixing of the fuel and the air to produce a uniform fuel/air ratio at the exit of the mixing tube is often achieved by the interaction of flows. These flows are composed of swirl, shear layers, and vortex. CFD modeling of the mixing tube aerodynamics is required to ensure the success of the mixing process and to establish that there is a sufficient safety margin for auto-ignition.

By limiting the flame temperature to a maximum of 2650 °F (1454 °C) single digit NO_x emissions can be achieved. To operate at a maximum flame temperature of 2650 °F (1454 °C), which is up to 250 °F (139 °C) lower than the LP system previously described, requires pre-mixing 60–70% of the air flow with the fuel prior to admittance into the combustion chamber. With such a high amount of the available combustion air flow required for flame temperature control, insufficient air remains to be allocated solely for cooling the chamber wall or diluting the hot gases down to the turbine inlet temperature. Consequently some of the air available has to do double duty, being used for both cooling and dilution. In engines using high turbine inlet temperatures, 2400–2600 °F (1316–1427 °C), although dilution is hardly necessary there is not enough air left over to cool the chamber walls. In this case, the air used in the combustion process itself has to do double duty and be used to cool the chamber walls before entering the injectors for pre-mixing with the fuel. This double duty requirement means that film or effusion cooling cannot be used for the major portion of the chamber walls. Some units are looking into steam cooling. Walls are also coated with thermal barrier coating (TBC), which has a low thermal conductivity and hence insulates the metal. This is a ceramic material that is plasma sprayed on during combustion chamber manufacture. The temperature drop across the TBC, typically by 300 °F (149 °C), means the combustion gases are in contact with a surface that is operating at approximately 2000 °F (1094 °C), which also helps to prevent the quenching of the CO oxidation.

Catalytic Combustion

Catalytic combustion is a process in which a combustible compound and oxygen react on the surface of a catalyst, leading to complete oxidation of the compound. This process takes place without a flame and at much lower temperatures than those associated with conventional flame combustion. Due partly to the lower operating temperature, catalytic combustion produces lower emissions of nitrogen oxides (NO_x) than conventional combustion. Catalytic combustion is now widely used to remove pollutants from

exhaust gases, and there is growing interest in applications in power generation, particularly in gas turbine combustors.

In catalytic combustion of a fuel/air mixture the fuel reacts on the surface of the catalyst by a heterogeneous mechanism. The catalyst can stabilize the combustion of ultra-lean fuel/air mixtures with adiabatic combustion temperatures below 1500 °C. Thus, the gas temperature will remain below 1500 °C and very little thermal NO_x will be formed, as can be seen in Figure 10-21. However, the observed reduction in NO_x in catalytic combustors is much greater than that expected from the lower combustion temperature. The reaction on the catalytic surface apparently produces no NO_x directly, although some NO_x may be produced by homogeneous reactions in the gas phase initiated by the catalyst.

Features of Catalytic Combustion

Surface Temperatures. At low temperatures, the oxidation reactions on the catalyst are kinetically controlled, and the catalyst activity is an important parameter. As the temperature increases, the build-up of heat on the catalyst surface due to the exothermic surface reactions produces ignition and the catalyst surface temperature jumps rapidly to the adiabatic flame temperature of the fuel/air mixture on ignition. Figure 10-26 shows a

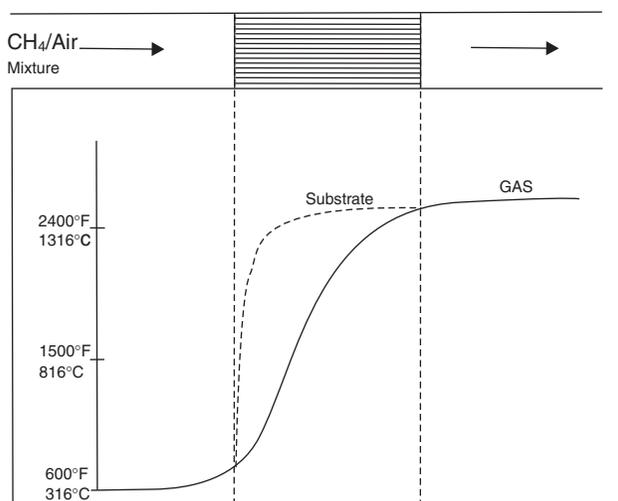


Figure 10-26. Schematic temperature profiles for catalyst (substrate) and bulk gas in a traditional catalytic combustor.

schematic of the temperature profiles for catalyst and bulk gas in a traditional catalytic combustor. At the adiabatic flame temperature, oxidation reactions on the catalyst are very rapid, and the overall steady state reaction rate is determined by the rate of mass transfer of fuel to the catalytic surface. The bulk gas temperature rises along the reactor because of heat transfer from the hot catalyst substrate and eventually approaches the catalyst surface temperature.

As the catalyst surface temperature is equal to the adiabatic flame temperature after ignition, it is independent of the overall conversion in the combustion reaction. It follows that the catalyst surface temperature cannot be reduced simply by limiting the conversion (by using a short reactor or a monolith with large cells, for example). Therefore, unless some other means of limiting the catalyst surface temperature is used, the catalyst materials must be able to withstand the adiabatic flame temperature of the fuel/air mixture during the combustion reaction. For the present generation of gas turbines this temperature will be equal to the required turbine inlet temperature of 1300°C, which presents severe problems for existing combustion catalyst.

Catalytica has developed a new approach to catalytic combustion, and Tanaka Kikinzoku Kogyo K.K. combines catalytic and homogeneous combustion in a multistage process. In this approach, shown schematically in Figure 10-27, the full fuel/air mixture required to obtain the desired combustor outlet temperature is reacted over a catalyst. However, a self-regulating chemical process limits the temperature rise over the catalyst. The catalyst temperature at the inlet stage therefore remains low and the catalyst can maintain very high activity over long periods of time. Because of the high catalyst activity at the inlet stage, ignition temperatures are low enough to allow operation at, or close to, the compressor discharge temperature, which minimizes the use of a preburner. The outlet stage brings the partially combusted gases to the temperature required to attain homogeneous combustion. Because the outlet stage operates at a higher catalyst temperature, the stable catalyst in this stage will have a lower activity than the inlet stage catalyst. However, as the gas temperature in this stage is higher, the lower activity is adequate. In the final stage, homogeneous gas phase reactions complete the combustion of the fuel and bring the gases to the required combustor outlet temperature.

The temperature rise in the inlet stage is limited by taking advantage of the unique properties of palladium combustion catalysts. Under combustion conditions, palladium can be either in the form of the oxide or the metal. Palladium oxide is a highly active combustion catalyst, whereas palladium metal is much less active. Palladium oxide is formed under oxidizing conditions

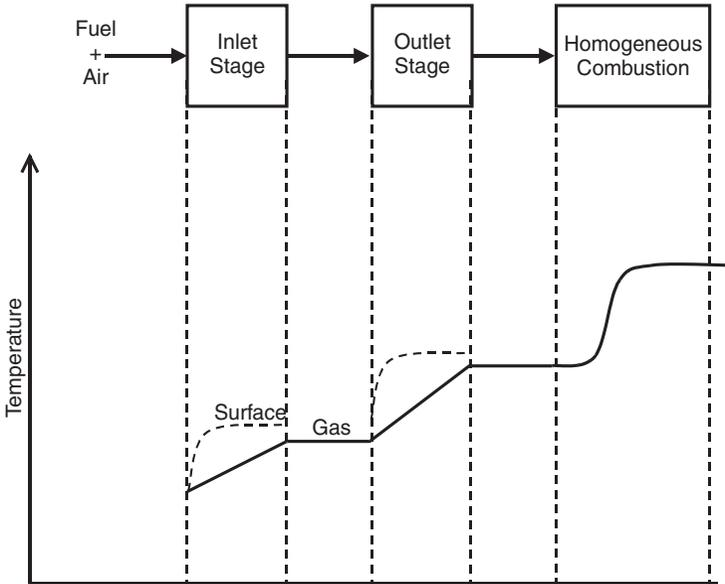


Figure 10-27. Schematic temperature profiles for catalytic combustion system in which the wall temperature is limited and complete combustion occurs after the catalyst.

at temperatures higher than 400°F (200°C), but decomposes to the metal at temperatures between 1436°F (780°C) and 1690°F (920°C), depending on the pressure. So when the catalyst temperature reaches about 1472°F (800°C) the catalytic activity will suddenly fall off due to the formation of the less active palladium metal, preventing any further rise in temperature. The catalyst essentially acts as a kind of chemical thermostat that controls its own temperature.

Catalytic Combustor Design

Testing at full scale has been done in a catalytic combustor system developed by GE for its MS9001E gas turbine. The MS9001E combustor operates with a full load firing temperature of 2020°F (1105°C) and a combustor exit temperature of about 2170°F (1190°C). The key components of the test stand at the GE Power Generation Engineering Laboratories in Schenectady, New York, are shown in Figure 10-28.

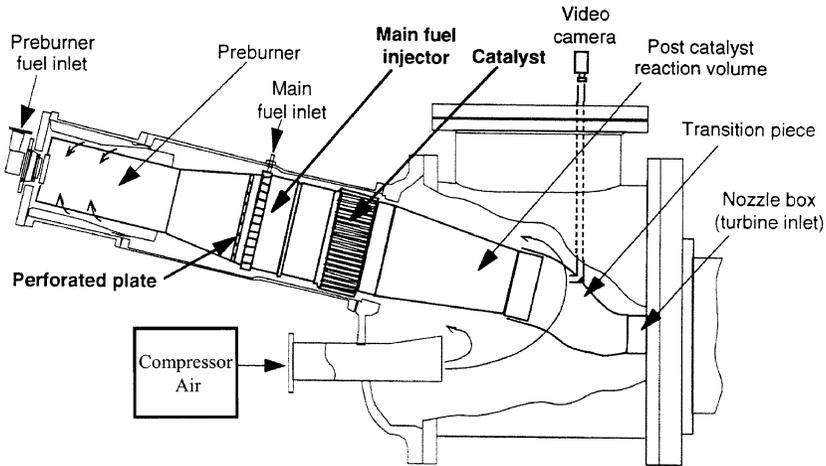


Figure 10-28. Schematic of a full scale catalytic combustor. Courtesy GE Power Systems and Catalytica Combustion Systems Inc.

There are four major subassemblies in the overall combustion system: the preburner, the main fuel injector, the catalytic reactor.

Preburner. The preburner carries the machine load at operating points where the conditions in the catalytic reactor are outside of the catalyst operating window. Most often, these are the low load points where the fuel required for turbine operation is insufficient for the catalyst to generate the necessary minimum exit gas temperature. As the turbine load is increased, progressively more fuel is directed through the main injector and progressively less goes to the preburner. Ultimately, the preburner receives only enough fuel to maintain the catalyst above its minimum inlet temperature.

Main fuel injector. This unit is designed to deliver a fuel-air mixture to the catalyst that is uniform in composition, temperature, and velocity. A multi-venturi tube (MVT) fuel injection system was developed by GE specifically for this purpose. It consists of 93 individual venturi tubes arrayed across the flow path, with four fuel injection orifices at the throat of each venturi.

Catalytic reactor. The role of the catalyst was described earlier; it must burn enough of the incoming fuel to generate an outlet gas temperature high enough to initiate rapid homogeneous combustion just past the catalyst exit.

The catalytic combustor has great potential in the application of gas turbines in new combined cycle power plants as the NO_x emissions in high attainment areas will have to be below 2 ppm.

Bibliography

- Ballal, D.R., and Lefebvre, A.H., "A Proposed Method for Calculating Film Cooled Wall Temperatures in Gas Turbine Combustor Chambers," ASME Paper #72-WA/HT-24, 1972.
- Clarke, J.S., and Lardge, H.E., "The Performance and Reliability of Aero-Gas Turbine Combustion Chambers," ASME 58-GTO-13, 1958.
- Dalla Betta, Ralph A., Nickolas, S.G., Weakley, C.K., Lundberg, K., Caron, T.J., Chamberlain, J., and Greeb, K., "Field Test of a 1.5 MW Industrial Gas Turbine with a Low Emissions Catalytic Combustion System," ASME 99-GT-295.
- Dutta, P., Cowell, L.H., Yee, D.K., and Dalla Betta, R.A., "Design and Evaluation of a Single-Can Full Scale Catalytic Combustion System for Ultra-Low Emissions Industrial Gas Turbines," ASME 97-GT-292.
- Faires, V.M., and Simmang, C.M., *Thermodynamics*, 6th ed., The Macmillan Co., New York, 1978, pp. 345–347.
- Grahman, J., Jones, R.E., Mayek, C.J., and Niedzwicki, R.W., *Aircraft Propulsion*, Chapter 4. NASA SP-259.
- Greenwood, S.A., "Low Emission Combustion Technology for Stationary Gas Turbine Engines," Proceedings of the 29th Turbomachinery Symposium, September 2000.
- Hilt, M.B., and Johnson, R.H., "Nitric Oxide Abatement in Heavy Duty Gas Turbine Combustors by Means of Aerodynamics and Water Injection," ASME Paper #72-GT-22, 1972.
- Maurice, L.Q.W., and Blust, J.W., "Emission from Combustion of Hydrocarbons in a Well Stirred Reactor," AIAA 1999.
- O'Brien, W.J., "Temperature Measurement for Gas Turbine Engines," SAE Paper #750207, 1975.
- Schlatter, J.C., Dalla Betta, R.A., Nickolas, S.G., Cutrone, M.B., Beebe, K.W., and Tsuchiya, T., "Single-Digit Emissions in a Full Scale Catalytic Combustor," ASME 97-GT-57.
- Yee, D.K., Lundberg, K., and Weakley, C.K., "Field Demonstration of a 1.5 MW Industrial Gas Turbine with a Low Emissions Catalytic Combustion System," ASME 2000-GT-88.

Part III

Materials, Fuel Technology, and Fuel Systems

11

Materials

Temperature limitations are the most crucial limiting factors to gas turbine efficiencies. Figures 11-1a and 11-1b show how increased turbine inlet temperatures decrease both specific fuel and air consumption while increasing efficiency. Materials and alloys that can operate at high temperatures are very costly—both to buy and to work on. Figure 11-1c shows relative raw material costs. Thus, the cooling of blades, nozzles, and combustor liners is an integral part of the total materials picture.

Since the design of turbomachinery is complex, and efficiency is directly related to material performance, material selection is of prime importance. Gas and steam turbines exhibit similar problem areas, but these problem areas are of different magnitudes. Turbine components must operate under a variety of stress, temperature, and corrosion conditions. Compressor blades operate at relatively low temperature but are highly stressed. The combustor operates at a relatively high temperature and low-stress conditions. The turbine blades operate under extreme conditions of stress, temperature, and corrosion. These conditions are more extreme in gas turbine than in steam turbine applications. As a result, the materials selection for individual components is based on varying criteria in both gas and steam turbines.

A design is only as efficient as the performance of the selected component materials. The combustor liner and turbine blades are the most critical components in existing high-performance, long-life gas turbines. The extreme conditions of stress, temperature, and corrosion make the gas turbine blade a materials challenge. Other turbine components present operational problem areas, but to a lesser degree. For this reason, gas turbine blade metallurgy will be discussed for solutions to problem areas. Definition of potential solutions will also relate to other turbine components.

The interaction of stress, temperature, and corrosion yields a complex mechanism that cannot be predicted by existing technology. The required

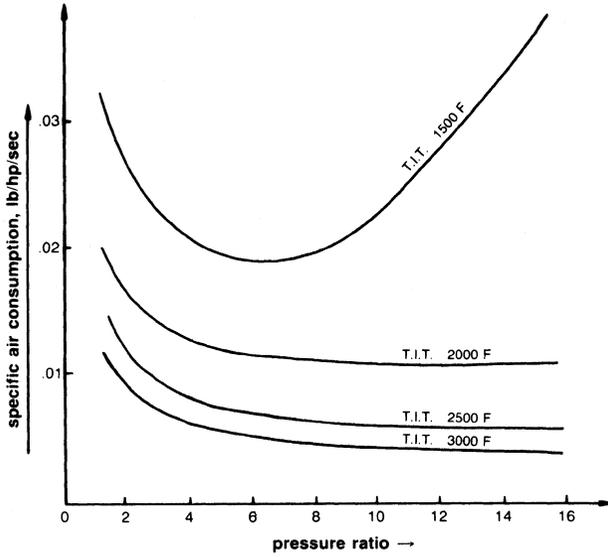


Figure 11-1a. Specific air versus pressure ratio and turbine inlet temperatures.

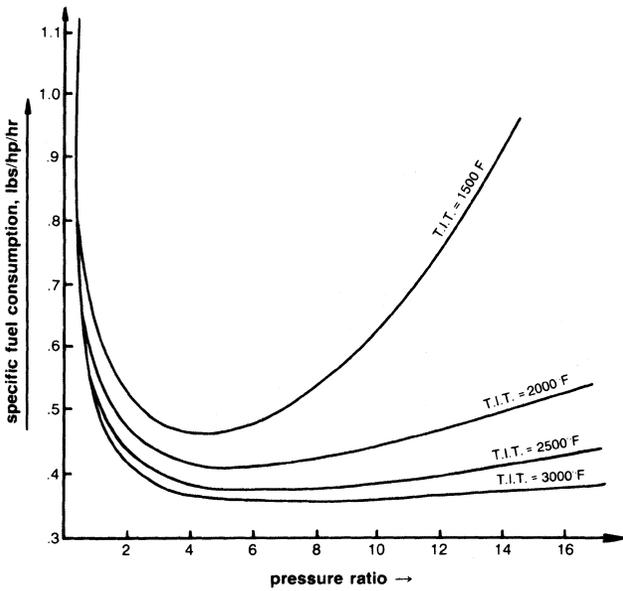


Figure 11-1b. Specific fuel consumption versus pressure ratio and turbine inlet temperature.

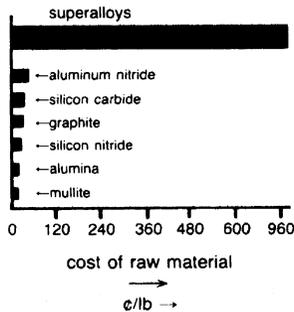


Figure 11-1c. A comparison of raw material costs.

material characteristics in a turbine blade for high performance and long life include limited creep, high-rupture strength, resistance to corrosion, good fatigue strength, low coefficient of thermal expansion, and high-thermal conductivity to reduce thermal strains. The failure mechanism of a turbine blade is related primarily to creep and corrosion and secondarily to thermal fatigue. Satisfying these design criteria for turbine blades will ensure high-performance, long life, and minimal maintenance.

The development of new materials as well as cooling schemes has seen the rapid growth of the turbine firing temperature leading to high turbine efficiencies. The stage 1 blade must withstand the most severe combination of temperature, stress and environment; it is generally the limiting component in the machine. Figure 11-2 shows the trend of firing temperature and blade alloy capability.

Since 1950, turbine bucket material temperature capability has advanced approximately 850 °F (472 °C), approximately 20 °F/10 °C per year. The importance of this increase can be appreciated by noting that an increase of 100 °F (56 °C) in turbine firing temperature can provide a corresponding increase of 8–13% in output and 2–4% improvement in simple-cycle efficiency. Advances in alloys and processing, while expensive and time-consuming, provide significant incentives through increased power density and improved efficiency. Before discussing some of these materials in depth it is important to understand the general behavior of metals.

General Metallurgical Behaviors in Gas Turbines

Creep and Rupture

The melting point of different metals varies considerably, and their strengths at various temperatures are different. At low temperatures all

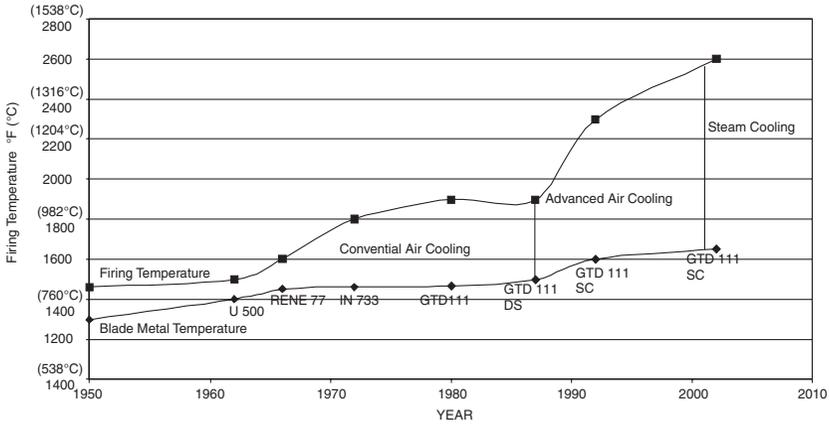


Figure 11-2. Firing temperature increase with blade material improvement.

materials deform elastically, then plastically, and are time independent. However, at higher temperatures, deformation is noted under constant load conditions. This high-temperature, time-dependent behavior is called creep-rupture. Figure 11-3 shows a schematic of a creep curve with the various stages of creep. The initial or elastic strain is the first region that proceeds into a plastic strain region at a decreasing rate. Then a nominally constant plastic strain rate is followed by an increasing strain rate to fracture.

The nature of this creep depends on the material, stress, temperature, and environment. Limited creep (less than 1%) is desired for turbine blade application. Cast superalloys fail with only a minimum elongation. These alloys fail in brittle fracture—even at elevated operating temperatures.

Stress-rupture data are often presented in a Larson–Miller curve, which indicates the performance of an alloy in a complete and compact graphical style. While widely used to describe an alloy’s stress-rupture characteristics over a wide temperature, life, and stress range, it is also useful in comparing the elevated temperature capabilities of many alloys. The Larson-Miller parameter is

$$P_{LM} = T(20 + \log t) \times 10^{-3} \tag{11-1}$$

where:

P_{LM} = Larson-Miller parameter

T = temperature, °R

t = rupture time, hr

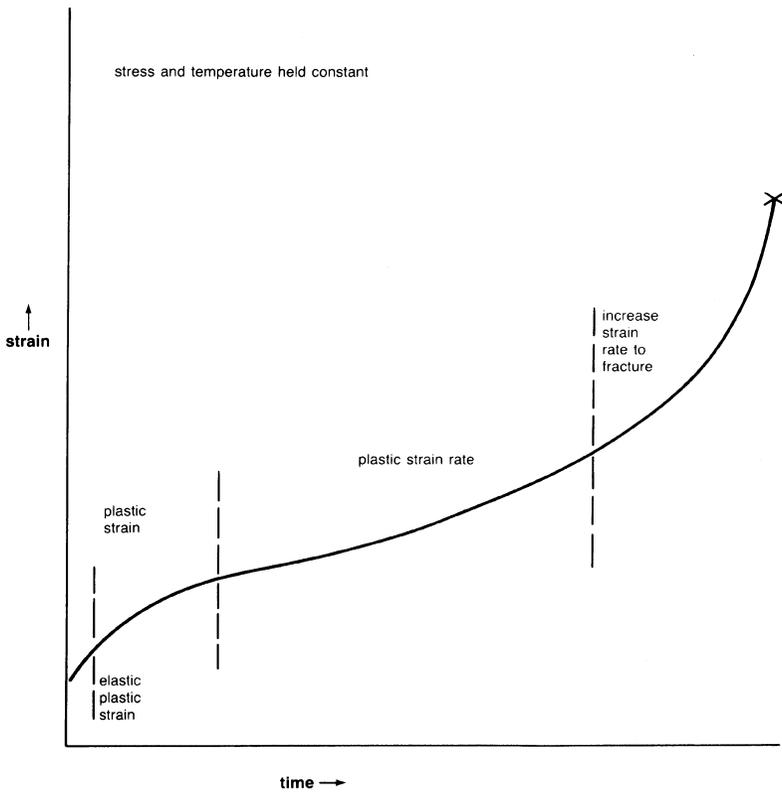


Figure 11-3. Time dependent strain curve under constant load.

The Larson-Miller parameters are plotted in Figure 11-4 for the specified turbine blade alloys. A comparison of A-286 and Udimet 700 alloy curves reveals the difference in capabilities. The operational life (hrs) of the alloys can be compared for similar stress and temperature conditions.

Ductility and Fracture

Ductility is commonly measured by elongation and reduction in area. In many cases, all three stages of creep shown in Figure 11-3 are not present. At high temperatures or stresses, very little primary creep is seen, while in the case of cast superalloys, failure occurs with just a small extension. This amount of extension is ductility. In a time-creep curve there are two elongations of interest. One elongation is from the plastic strain rate, and the second elongation is the total elongation or the elongation at fracture.

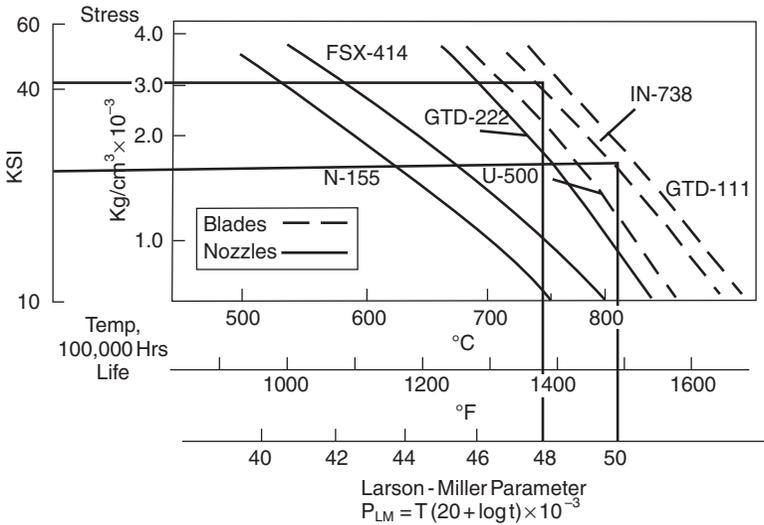


Figure 11-4. Larson-Miller parameter for various types of blades.

Ductility is erratic in its behavior and is not always repeatable—even under laboratory conditions. Ductility of a metal is affected by the grain size, the specimen shape, and the techniques used for manufacturing. A fracture that results from elongation can be of two types: brittle or ductile, depending on the alloy. A brittle fracture is intergranular with little or no elongation. A ductile fracture is transgranular and typical of normal ductile tensile fracture. Turbine blade alloys tend to indicate low ductility at operating temperatures. As a result, surface notches are initiated by erosion or corrosion, and then cracks are propagated rapidly.

Cyclic Fatigue

All materials would fail at a certain load if cycled over a large amount of cycles. A very common type of failure, which blades in turbines undergo is known as “high cycle fatigue.” This type of failure is caused when the blade is subjected repeatedly to an unsteady load. Most materials under these alternating loads would fail in about 10^7 cycles, assuming that the resonance frequency for a given blade is 10^3 Hz. This would tend to mean that the material would fail within 10^4 seconds, about 2.8 hours, if the blade was subjected to an alternating force, which would excite the blade resonance frequency. This type of failure would be depicted by a chevron type of markings on the failed surface, near the trailing edge of the blade.

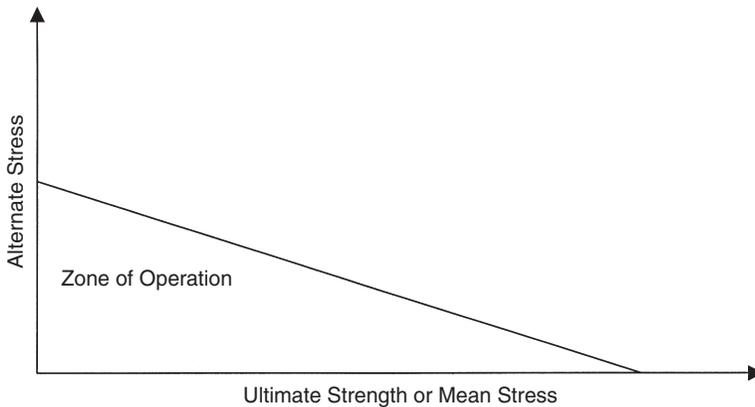


Figure 11-5. Goodman Diagram.

A Goodman diagram of the material is often used to determine the amount of alternating stress on the blades at different loadings. The Goodman Diagram is shown in Figure 11-5. The Goodman diagram is particularly helpful in determining the effectiveness of a material or component that will be subjected to a cyclic stress superimposed upon a non-zero mean stress. The horizontal axis is the Mean or Stress or Ultimate Strength of the material in psi or MPa, and the vertical axis is the Alternating Stress, which is half the ultimate strength or mean stress multiplied by any correction or safety factors.

Thermal Fatigue

Thermal fatigue of turbine blades is a secondary failure mechanism. Temperature differentials developed during starting and stopping of the turbine produce thermal stress. The cycling of these thermal stresses is thermal fatigue. Thermal fatigue is low-cycle and similar to a creep-rupture failure. The analysis of thermal fatigue is essentially a problem in heat transfer and properties such as modulus of elasticity, coefficient of thermal expansion, and thermal conductivity.

The most important metallurgical factors are ductility and toughness. Highly ductile materials tend to be more resistant to thermal fatigue. They also seem more resistant to crack initiation and propagation.

Research programs are underway to demonstrate that brittle materials can be successfully utilized in demanding, high-temperature structural applications. From the work already done, it has been established that silicon nitride and silicon carbide, in their variety of forms and fabrications, are the

two most likely candidates for the future ceramic engine. Both exhibit a suitable workability, the desired strength at high temperatures, and have specific resistance, availability, and manufacturing ease to make them likely prospects for gas turbine components.

The operating schedule of a gas turbine produces a low-frequency thermal fatigue. The number of starts per hours of operating time directly affects the blade life. Table 11-1 shows fewer starts per operating time increases turbine life.

Corrosion

The use of Ni-base superalloys as turbine blades in an actual end-use atmosphere produces deterioration of material properties. This deterioration can result from erosion or corrosion. Erosion results from hard particles impinging on the turbine blade and removing material from the blade surface. The particles may enter through the turbine inlet or can be loosened scale deposits from within the combustor.

Corrosion is described as hot corrosion and sulfidation processes. Hot corrosion is an accelerated oxidation of alloys caused by the deposition of Na_2SO_4 . Oxidation results from the ingestion of salts in the engine and sulfur from the combustion of fuel. Sulfidation corrosion is considered a form of hot corrosion in which the residue that contains alkaline sulfates. Corrosion causes deterioration of blade materials and reduces component life.

Hot corrosion is a rapid form of attack that is generally associated with alkali metal contaminants, such as sodium and potassium, reacting with sulfur in the fuel to form molten sulfates. The presence of only a few parts per million (ppm) of such contaminants in the fuel, or equivalent in the air, is sufficient to cause this corrosion. Sodium can be introduced in a number of ways, such as salt water in liquid fuel, through the turbine air inlet at sites near salt water or other contaminated areas, or as contaminants in water/steam injections. Besides the alkali metals such as sodium and potassium, other chemical elements can influence or cause corrosion on bucketing. Notable in this connection are vanadium, primarily found in crude and residual oils.

There are now two distinct forms of hot corrosion recognized by the industry, although the end result is the same. These two types are high-temperature (Type 1) and low-temperature (Type 2) hot corrosion.

High-temperature hot corrosion has been known since the 1950s. It is an extremely rapid form of oxidation that takes place at temperatures between $1500^\circ\text{F}/816^\circ\text{C}$ and $1700^\circ\text{F}/927^\circ\text{C}$ in the presence of sodium sulfate (Na_2SO_4). Sodium sulfate is generated in the combustion process as a result of the reaction between sodium, sulfur, and oxygen. Sulfur is present as a natural contaminant in the fuel.

**Table 11-1
Operation and Maintenance Life of an Industrial Turbine**

| Type of Application and Fuel | | Firing Temperature below 1700 °F (927 °C) | | | Firing Temperature above 1700 °F (927 °C) | | |
|--|-----------|--|---------------------|---------------------|--|---------------------|---------------------|
| | | Comb. Liners | 1st Stage Nozzle | 1st Stage Blades | Comb. Liners | 1st Stage Nozzle | 1st Stage Blades |
| BASE LOAD | Starts/hr | + | + | + | | | |
| Nat. gas | 1/1000 | 30,000 | 60,000 | 100,000 | 15,000 | 25,000 | 35,000 |
| Nat. gas | 1/10 | 7500 | 42,000 | 72,000 | 3,750 | 20,000 | 25,000 |
| Distillate oil | 1/1000 | 22,000 | 45,000 | 72,000 | 11,250 | 22,000 | 30,000 |
| Distillate oil | 1/10 | 6000 | 35,000 | 48,000 | 3,000 | 13,500 | 18,000 |
| Residual | 1/1000 | 3,500 | 20,000 | 28,000 | 2,500 | 10,000 | 15,000 |
| Residual | 1/10 | | | | | | |
| SYSTEM PEAKING | | | | | | | |
| Normal max. load of short duration and daily starts | | | | | | | |
| Nat. gas | 1/10 | 7,500 | 34,000 | 60,000 | 5,000 | 15,000 | 24,000 |
| Nat. gas | 1/5 | 3,800 | 28,000 | 40,000 | 3,000 | 12,500 | 18,000 |
| Distillate | 1/10 | 6,000 | 27,200 | 53,500 | 4,000 | 12,500 | 19,000 |
| Distillate | 1/5 | 3,000 | 22,400 | 32,000 | 2,500 | 10,000 | 16,000 |
| TURBINE PEAKING | | | | | | | |
| Operating Above 50 °F–100 °F (28 °C–56 °C) | | | | | | | |
| Firing Temperature | | | | | | | |
| Nat. gas | 1/5 | 2,000 | 12,000 | 20,000 | 2,000 | 12,500 | 18,000 |
| Nat. gas | 1/1 | 400 | 9,000 | 15,000 | 400 | 10,000 | 15,000 |
| Distillate | 1/5 | 1,600 | 10,000 | 16,000 | 1,700 | 11,000 | 15,000 |
| Distillate | 1/1 | 400 | 7,300 | 12,000 | 400 | 8,500 | 12,000 |

Low-temperature hot corrosion was recognized as a separate mechanism of corrosion attack in the mid-1970s. This attack can be very aggressive if the conditions are right. It takes place at temperatures in the 1100 °F (593 °C) to 1400 °F/760 °C range and requires a significant partial pressure of SO₂. It is caused by low melting eutectic compounds resulting from the combination of sodium sulfate and some of the alloy constituents such as nickel and cobalt. It is, in fact, somewhat analogous to the type of corrosion called Fireside Corrosion in coal-fired boilers.

The two types of hot corrosion cause different types of attack. High-temperature corrosion features intergranular attack, sulfide particles and a denuded zone of base metal. Metal oxidation occurs when oxygen atoms combine with metal atoms to form oxide scales. The higher the temperature, the more rapidly this process takes place, creating the potential for failure of the component if too much of the substrate material is consumed in the formation of these oxides.

Low-temperature corrosion characteristically shows no denuded zone, no intergranular attack, and a layered type of corrosion scale.

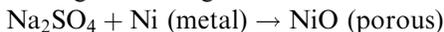
The lines of defense against both types of corrosion are similar. First, reduce the contaminants.

Second, use materials that are as corrosion-resistant as possible. Third, apply coatings to improve the corrosion resistance of the bucket alloy.

Hot corrosion includes two mechanisms:

1. *Accelerated Oxidation*

During initial stages—blade surface clean



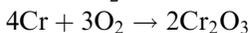
2. *Catastrophic Oxidation*

Occurs with Mo, W, and V present—reduces

NiO layer—increases oxidation rate

Reactions—Ni-Base Alloys

Protective oxide films

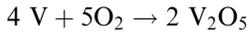
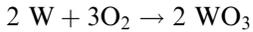
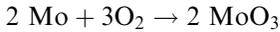


Sulfate

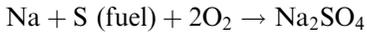


Na—from NaCl (salt)

S—from fuel

Other Oxides

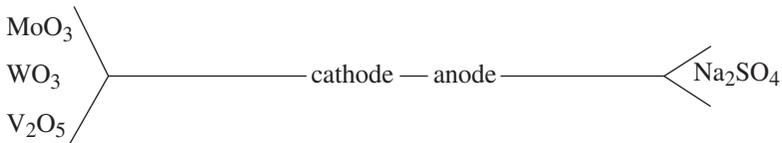
The Ni-base alloy surface is exposed to an oxidizing gas, oxide nuclei form, and a continuous oxide film forms (Ni) (Cr_2O_3 , etc.). This oxide film is a protective layer. The metal ions diffuse to the surface of the oxide layer and combine with the molten Na_2SO_4 to destroy the protective layer. Ni_2S and Cr_2S_3 results (*sulfidation*):



Cl—grain boundaries—*causes intergranular corrosion*

The extent of the corrosion depends on the amount of nickel and chromium in the alloy. The oxide films become porous and nonprotective, which increases the oxidation rate (accelerated oxidation).

Catastrophic oxidation requires the presence of Na_2SO_4 and Mo, W, and/or V. Crude oils are high in V; ash will be 65% V_2O_5 or higher. V can be alloyed in metal. A galvanic cell is generated:



The galvanic corrosion deletes the protective oxide film and increases the oxidation rate.

The corrosion problem includes: (1) erosion, (2) sulfidation, (3) intergranular corrosion, and (4) hot corrosion. The 20% Cr alloys increase oxidation resistance. Sixteen percent Cr alloys (Inconel 600) are less resistant. Cr in alloys reduces grain boundary oxidation, while high Ni alloys tend to oxidize along grain boundaries. Age-hardened gas turbine blades of 10–20% Cr will corrode (sulfidation) at more than 1400 °F. Ni_2S forms in the grain boundary. The addition of cobalt to the alloy increases the temperature at which the attack occurs. To reduce corrosion, either increase the Cr amount or apply a coating (Al or Al + Cr).

A high-nickel alloy is used for increased strength at elevated temperature, and a chromium content in excess of 20% is desired for corrosion resistance. An optimum composition to satisfy the interaction of stress, temperature, and corrosion has not been developed. The rate of corrosion is directly related to alloy composition, stress level, and environment. The corrosive atmosphere contains chloride salts, vanadium, sulfides, and particulate matter. Other combustion products, such as NO_x , CO, CO_2 , also contribute to the corrosion mechanism. The atmosphere changes with the type of fuel used. Fuels, such as natural gas, diesel #2, naphtha, butane, propane, methane, and fossil fuels, will produce different combustion products that affect the corrosion mechanism in different ways.

Gas Turbine Materials

The composition of the new and conventional alloys throughout the turbine are shown in Table 11-2. This table describes materials used in the GE line of turbines but the materials are common to all brands of high temperature turbine even though there may be some variations in the composition of the alloys. In the early years of turbine development, increases in blade alloy temperature capability accounted for the majority of the firing temperature increase until air-cooling was introduced, which decoupled firing temperature from the blade metal temperature. Also, as the metal temperatures approached the 1600 °F (870 °C) range, hot corrosion of blades became more life limiting than strength until the introduction of protective coatings. During the 1980s, emphasis turned toward two major areas: improved materials technology, to achieve greater blade alloy capability without sacrificing alloy corrosion resistance; and advanced, highly sophisticated air-cooling technology to achieve the firing temperature capability required for the new generation of gas turbines. The use of steam cooling to further increase combined-cycle efficiencies in combustors was introduced in the mid to late 1990s. Steam cooling in blades and nozzles will be introduced in commercial operation in the year 2002.

In the 1980s, IN 738 blades were widely used. IN-738, was the acknowledged corrosion standard for the industry. New alloys, such as GTD-111, were developed and patented by GE in the mid-1970s. GTD-111 possesses about a 35 °F (20 °C) improvement in rupture strength as compared to IN-738. GTD-111 is also superior to IN-738 in low-cycle fatigue strength.

The design of this alloy was unique in that it utilized phase stability and other predictive techniques to balance the levels of critical elements (Cr, Mo, Co, Al, and Ta), thereby maintaining the hot corrosion resistance of IN-738 at higher strength levels without compromising phase stability. Most

Table 11-2
High-Temperature Alloys (Courtesy GE Power Systems)

| Component | Cr | Ni | Co | Fe | W | Mo | Ti | Al | Cb | V | C | B | Ta |
|-------------------|-----------|-----------|-----------|-----------|----------|-----------|-----------|-----------|-----------|----------|----------|----------|-----------|
| Turbine Blades | | | | | | | | | | | | | |
| U500 | 18.5 | BAL | 18.5 | – | – | 4 | 3 | 3 | – | – | 0.07 | 0.006 | – |
| RENE 77 (U700) | 15 | BAL | 17 | – | – | 5.3 | 3.35 | 4.25 | – | – | 0.07 | 0.02 | – |
| IN738 | 16 | BAL | 8.3 | 0.2 | 2.6 | 1.75 | 3.4 | 3.4 | 0.9 | – | 0.10 | 0.001 | 1.75 |
| GTD111 | 14 | BAL | 9.5 | – | 3.8 | 1.5 | 4.9 | 3.0 | – | – | 0.10 | 0.01 | 2.8 |
| Turbine Nozzles | | | | | | | | | | | | | |
| X40 | 25 | 10 | BAL | 1 | 8 | – | – | – | – | – | 0.50 | 0.01 | – |
| X45 | 25 | 10 | BAL | 1 | 8 | – | – | – | – | – | 0.25 | 0.01 | – |
| FSX414 | 28 | 10 | BAL | 1 | 7 | – | – | – | – | – | 0.25 | 0.01 | – |
| N155 | 21 | 20 | 20 | BAL | 2.5 | 3 | – | – | – | – | 0.20 | – | – |
| GTD-222 | 22.5 | BAL | 19 | – | 2.0 | 2.3 | 1.2 | 0.8 | – | 0.10 | 0.008 | 1.00 | – |
| Combustors | | | | | | | | | | | | | |
| SS309 | 23 | 13 | – | BAL | – | – | – | – | – | – | 0.10 | – | – |
| HAST X | 22 | BAL | 1.5 | 1.9 | 0.7 | 9 | – | – | – | – | 0.07 | 0.005 | – |
| N-263 | 20 | BAL | 20 | 0.4 | – | 6 | 2.1 | 0.4 | – | – | 0.06 | – | – |
| HA-188 | 22 | 22 | BAL | 1.5 | 14.0 | – | – | – | – | – | 0.05 | 0.01 | – |
| Turbine Wheels | | | | | | | | | | | | | |
| Alloy 718 | 19 | BAL | – | 18.5 | – | 3.0 | 0.9 | 0.5 | 5.1 | – | 0.03 | – | – |
| Alloy 706 | 16 | BAL | – | 37.0 | – | – | 1.8 | – | 2.9 | – | 0.03 | – | – |
| Cr-Mo-V | 1 | 0.5 | – | BAL | – | 1.25 | – | – | – | 0.25 | 0.30 | – | – |
| A286 | 15 | 25 | – | BAL | – | 1.2 | 2 | 0.3 | – | 0.25 | 0.08 | 0.006 | – |
| M152 | 12 | 2.5 | – | BAL | – | 1.7 | – | – | – | 0.3 | 0.12 | – | – |
| Compressor Blades | | | | | | | | | | | | | |
| AISI 403 | 12 | – | – | BAL | – | – | – | – | – | – | 0.11 | – | – |
| AISI 403 + Cb | 12 | – | – | BAL | – | – | – | – | 0.2 | – | 0.15 | – | – |
| GTD-450 | 15.5 | 6.3 | – | BAL | – | 0.8 | – | – | – | – | 0.03 | – | – |

nozzle and blade castings are made by using the conventional equiaxed investment casting process. In this process, the molten metal is poured into a ceramic mold in a vacuum, to prevent the highly reactive elements in the super alloys from reacting with the oxygen and nitrogen in the air. With proper control of metal and mold thermal conditions the molten metal solidifies from the surface to the center of the mold, creating an equiaxed structure. Directional solidification (DS) is also being employed to produce advanced technology nozzles and blades. First used in aircraft engines more than 25 years ago, it was adapted for use in large airfoils in the early 1990s. By exercising careful control over temperature gradients, a planar solidification front is developed in the bade, and the part is solidified by moving this planar *front* longitudinally through the entire length of the part. The result is a blade with an oriented grain structure that runs parallel to the major axis of the part and contains no transverse grain boundaries, as in ordinary blades. The elimination of these transverse grain boundaries confers additional creep and rupture strength on the alloy, and the orientation of the grain structure provides a favorable modulus of elasticity in the longitudinal direction to enhance fatigue life. The use of directionally solidified blades results in a substantial increase in the creep life, or substantial increase in tolerable stress for a fixed life. This advantage is due to the elimination of transverse grain boundaries from the bucket, the traditional weak link in the microstructure. In addition to improved creep life, the directionally solidified blades possess more than 10 times the strain control or thermal fatigue compared to equiaxed blades. The impact strength of the DS blades is also superior to that of equiaxed, showing an advantage of more than 33%.

In the late 1990s, single-crystal blades have been introduced in gas turbines. These blades offer additional, creep and fatigue benefits through the elimination of grain boundaries. In single-crystal material, all grain boundaries are eliminated from the material structure and a single crystal with controlled orientation is produced in an airfoil shape. By eliminating all grain boundaries and the associated grain boundary strengthening additives, a substantial increase in the melting point of the alloy can be achieved, thus providing a corresponding increase in high-temperature strength. The transverse creep and fatigue strength is increased, compared to equiaxed or DS structures. The advantage of single-crystal alloys compared to equiaxed and DS alloys in low-cycle fatigue (LCF) life is increased by about 10%.

Blade life comparison is provided in the form of the stress required for rupture as a function of a parameter that relates time and temperature (the Larson-Miller Parameter). The Larson-Miller parameter is a function of

blade metal temperature and the time the blade is exposed to those temperatures. Figure 11-4 shows the comparison of some of the alloys used in blade and nozzle application. This parameter is one of several important design parameters that must be satisfied to ensure proper performance of the alloy in a blade application, especially for long service life. Creep life, high- and low-cycle fatigue, thermal fatigue, tensile strength and ductility, impact strength, hot corrosion and oxidation resistance, producibility, coatability and physical properties must also be considered.

Turbine Wheel Alloys

Alloy 718 Nickel-Based Alloy. This nickel-based, precipitation-hardened alloy is the newest being developed for the next generation of Frame type gas turbine machines. This alloy has been used for wheels in aircraft turbines for more than 20 years. Alloy 718 contains a high concentrations of alloying elements and is therefore difficult to produce in the very large ingot sizes needed for the large Frame type turbine wheel and spacer forgings. This effort requires close cooperation between the manufacturer, and its superalloy melters and large forging suppliers to conduct the solidification and forging flow studies that are necessary to bring into production a new wheel material for large wheels. This development effort has resulted in the production of the largest ingots ever made and forged into high-quality qualification turbine wheel and spacer forgings.

Alloy 706 Nickel-Based Alloy. This nickel-based, precipitation-hardened alloy is being used in the large frame type units by GE such as the frame 7FA, 9FA, 6FA, and 9EC turbine wheel and spacer alloy, and it offers a very significant increase in stress rupture and tensile yield strength compared to the other wheel alloys. Figures 11-6 and 11-7 show the stress rupture and tensile yield strength of the various alloys. This alloy is similar to Alloy 718, but contains somewhat lower concentrations of alloying elements, and is therefore easier to produce in the very large ingot sizes needed for the large frame type gas turbines.

Cr-Mo-V Alloy. Turbine wheels and spacers of most GE single shaft heavy-duty gas turbines are made of 1% Cr -1.25% Mo- 0.25% V steel. This alloy is used in the quenched and tempered condition to enhance bore toughness. Stress rupture strength of the dovetail region (periphery) is controlled by providing extra stock at the periphery to produce a slower cooling rate during quenching.

The stress rupture properties of this alloy are shown in Figure 11-6.

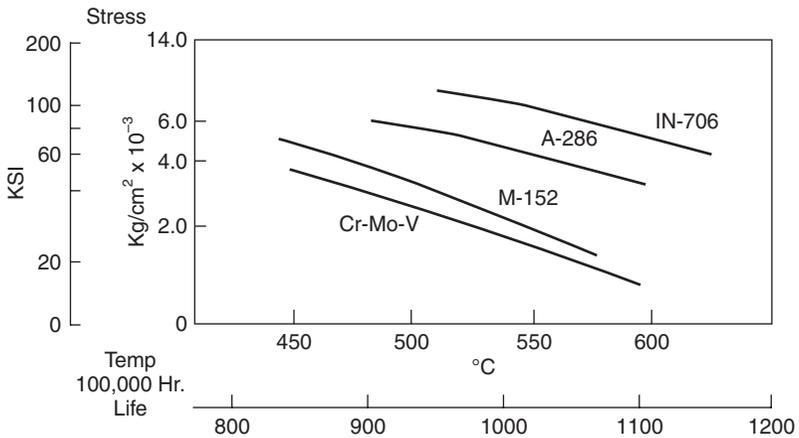


Figure 11-6. Turbine Wheel Alloys stress rupture comparison.

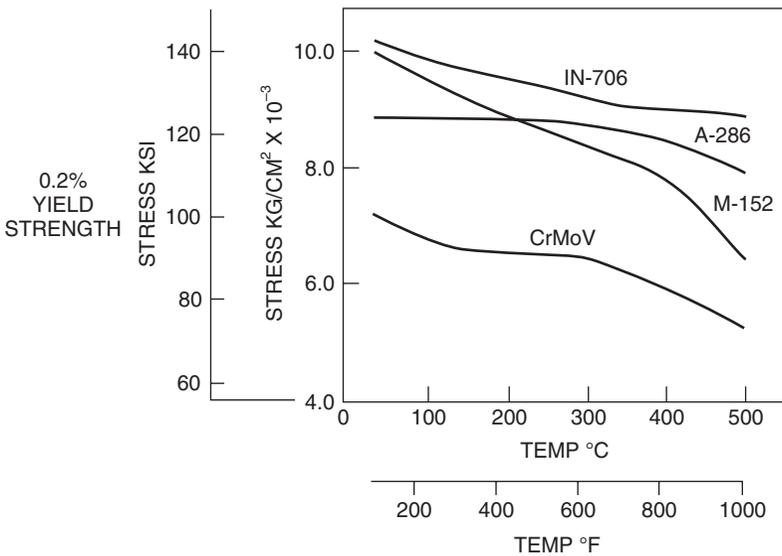


Figure 11-7. Turbine Wheel Alloys tensile yield strength comparison.

12 Cr Alloys. This family of alloys has a combination of properties that makes it especially valuable for turbine wheels. These properties include good ductility at high-strength levels, uniform properties throughout thick sections and favorable strength at temperatures up to about 900 °F (482 °C)

M-152 alloy is a 2–3% nickel-containing member of the 12 Cr family of alloys. Initially, it was used as an upgrade in gas turbines as a replacement for A286. It features outstanding fracture toughness, in addition to the properties common to other 12 Cr alloys. M-152 alloy is intermediate in rupture strength, between Cr–Mo–V and A286 alloy (Figure 11-6), and has higher tensile strength than either one. These features, together with its favorable coefficient of expansion and good fracture toughness, make the alloy attractive for use in gas turbine applications.

A286 Alloy. A286 is an austenitic iron base alloy that has been used for years in aircraft engine applications. Its use for industrial gas turbines started about 1965, when technological advances made the production of sound ingots sufficient in size to produce these wheels possible.

As knowledge of the capabilities of M-152 increased, production of the wheels was switched from A286 to M-152. A286 is currently being introduced in turbines as part of a composite aft shaft.

Compressor Blades

Compressor blading is variously made by forging, extrusion, or machining. All production blades, until recently, have been made from Type 403 or 403 Cb (both 12 Cr) stainless steels. During the 1980s, a new compressor blade material, GTD-450, a precipitation hardened, martensitic stainless steel, was introduced into production for advanced and uprated machines, as shown in Table 2. This material provides increased tensile strength without sacrificing stress corrosion resistance. Substantial increases in the high-cycle fatigue and corrosion fatigue strength are also achieved with this material, compared to Type 403. Superior corrosion resistance is also achieved due to high concentrations of chromium and molybdenum. Compressor corrosion are usually caused by moisture and salt ingested by the turbine. Coating of compressor blades is also highly recommended.

Forgings and Nondestructive Testing

Most other rotor parts in gas turbines are individually forged. This includes compressor wheels, spacers, distance pieces, and stub shafts. All are made from quenched and tempered low-alloy steels (Cr–Mo–V or Ni–Cr–Mo–V) with the material and heat treatment optimized for the specific part. The intent is to achieve the best balance of strength, toughness with ductility, processing and nondestructive evaluation capability, particularly when it is recognized that some

of these parts may be exposed to operating temperatures as low as -60°F (-51°C).

It is recommended that parts are sonic and magnetic particle tested. Many last-stage compressor wheels are spun in a manner analogous to turbine wheels as a means of proof testing and imparting bore residual stresses. This last-stage compressor wheel is probably the next most critical rotor component after the turbine wheels, especially in the new very high pressure ratio compressors.

New nondestructive techniques to inspect turbine forgings to greater levels of sensitivity than ever before possible have been developed. These new ultrasonic inspection techniques are being applied to all the turbine forgings to ensure an even greater level of confidence in these high strength forgings.

Additional development efforts continue to improve the current processing of other forgings by working with our suppliers on the further optimization of properties and forging quality. In-process, nondestructive evaluation of all rotor components continues to be emphasized as a critical aspect to produce quality forgings.

Ceramics

The day when turbines will operate at $2500\text{--}3000^{\circ}\text{F}$ ($1371\text{--}1649^{\circ}\text{C}$), yielding double the present horsepower at half the present engine size, may not be far off. This dream may turn into reality because of ceramics and unique cooling systems. Ceramics were, until recently, dismissed as being too brittle, hard to fabricate, and not suited to flight engines. However, the addition of aluminum to ceramics forms a compound that is more ductile.

Temperature limits of flight engine alloys have been steadily increasing about 20°F (11°C) per year since 1945. Transpiration and internally cooled metal blades have resulted in higher temperatures and more efficient operation. But the direct correlation between efficiency and fabrication cost has resulted in a situation of diminishing returns for the superalloys. As more and more cooling air is needed for the superalloy components, the efficiency of the engine drops to a point where turbine inlet temperatures around 2300°F (1260°C) are the optimum and, at that point, they are uneconomic for automotive use.

Increasing efficiency with the use of 2500°F (1371°C) tolerant uncooled ceramic blades provides an improvement in fuel consumption of more than 20% from an 1800°F (982°C) turbine inlet temperature. This rate represents almost a 50% improvement in specific air consumption. This improvement implies that for the same size engine, power almost doubles, or conversely

(and possibly more important to automakers), engine flow size could be cut in half and retain the same horsepower output.

Ceramics are quite tolerant of such contaminants as sodium and vanadium, which are present in low-cost fuels and highly corrosive to currently used nickel alloys. Ceramics are also up to 40% lighter than comparable high-temperature alloys—another plus in application. But the biggest plus is material cost. Ceramics cost around 5% the cost of super alloys.

Despite all the advantages of ceramics, they are brittle, and unless this problem is overcome, the use of ceramics in gas turbines will not be practical.

Coatings

Blade coatings were originally developed by the aircraft engine industry for aircraft gas turbines. Metal temperatures in heavy-duty gas turbines are lower than those in aircraft engines. However, heavy-duty gas turbines are generally subjected to excessive contamination or accelerated attack known as hot corrosion.

Blade coatings are required to protect the blade from corrosion, oxidation, and mechanical property degradation. As super alloys have become more complex, it has been increasingly difficult to obtain both the higher strength levels that are required and a satisfactory level of corrosion and oxidation resistance without the use of coatings. Thus, the trend toward higher firing temperatures increases the need for coatings. The function of all coatings is to provide a surface reservoir of elements that will form very protective and adherent oxide layers, thus protecting the underlying base material from oxidation and corrosion attack and degradation.

Experience has shown that the lives of both uncoated and coated blades depend to a large degree on the amount of fuel and air contamination, as well as the operating temperature of the blade. The effect of sodium, a common contaminant, on bucket life at 1600°F (871°C) is seen in Figure 11-8. When sodium sulfate (Na_2SO_4) is present, hot corrosion is greatly accelerated. Sodium sulfate is a product of combustion. The presence of only a few parts per million (ppm) of sodium and sulfate is sufficient to cause extensive hot corrosion damage. Sulfur is present as a natural contaminant in the fuel. Sodium can be introduced as a natural contaminant in the fuel, or in the atmosphere of sites located near salt water or contaminated areas.

The PT-Al coating is a precious metal applied by uniformly electroplating a thin layer (0.00025 inch) of platinum onto the bucket at the airfoil surface, followed by pack-diffusion steps to deposit a layer of aluminum and chromium. The resulting coating has an outer skin of an extremely corrosion resistant, platinum-aluminum intermetallic composition. As seen in Figure 11-8

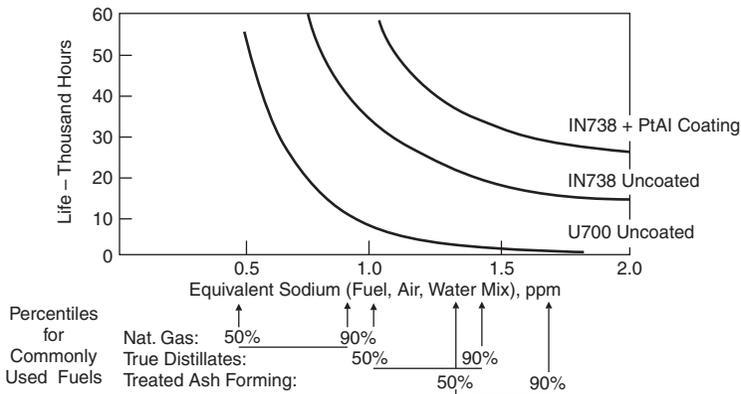


Figure 11-8. Effect of sodium corrosion on blade life.

test was conducted for comparative corrosion on coated and uncoated IN-738 blades. The blades were run side-by-side in the same machine under severe corrosive conditions. The two blades were removed for interim evaluation after 11,300 service hours (289 starts). The unit burnt sour natural gas containing about 3.5% ppm sulfur and was located in a region where the soil surrounding the site contains up to 3% sodium.

The uncoated blade showed an 0.005 inch corrosion attack over 50% of the airfoil concave face, with about 0.010 inch penetration at the base of the airfoil. Examination of the coated blade revealed no visual evidence of attack, except for one small roughened spot on the leading edge about 1 inch up from the platform, and a second spot in the middle of the convex side about 1 inch down from the tip.

Metallographic examination of other areas revealed similar degrees of corrosion on the two blades. At no point on the coated blade had the corrosion penetrated to the base metal, although in the two areas on the coated blade about 0.002 inch of the original 0.003 inch coating had been oxidized.

Experience with uncoated IN-738 blades in this very hostile environment indicates about 25,000 hours blade life can be attained. The coated blade life, based on this interim evaluation, should add an additional 20,000 hours of life.

Experience has shown that the lives of both uncoated and coated blades depend to a large degree on the amount of fuel and air contamination. This effect is shown in Figure 11-8, which illustrates the effect of sodium, a common contaminant, on blade life at 1600 °F (871 °C). The presence of increased levels of contaminants give rise to an accelerated form of attack called hot corrosion.

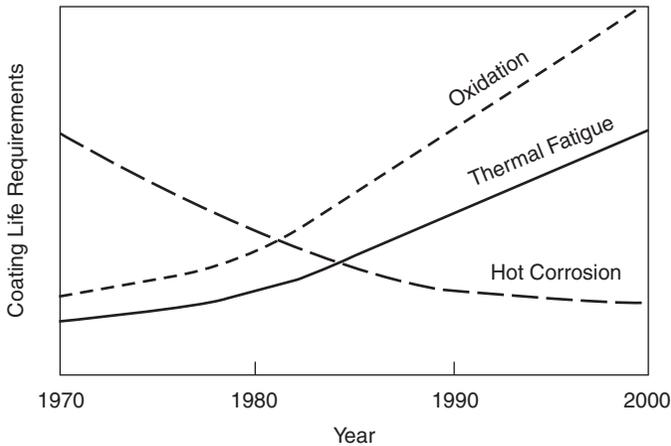


Figure 11-9. Blade coating requirements and coating evolution.

Hot corrosion is distinctly different from the pure oxidation of an aircraft environment; hence, coatings for heavy-duty gas turbines have different capabilities compared to coatings for aircraft engines. In addition to hot corrosion, high-temperature oxidation and thermal fatigue resistance have become important criteria in the higher firing gas turbines, as shown in Figure 11-9. In today's advanced machines, oxidation is of concern not only for external blade surfaces, but also for internal passages such as cooling holes, due to the high temperature of the cooling air, which in turn is due to the high pressure ratio in the compressor.

The main requirements of a coating are to protect blades against oxidation, corrosion, and cracking problems. Coatings are there to prevent the base metal from attack. Other benefits of coatings include thermal fatigue from cyclic operation, surface smoothness and erosion in compressor coatings, and heat flux loading when one is considering thermal barriers. A secondary consideration, but perhaps rather more relevant to thermal barriers, is their ability to tolerate damage from light impacts without spalling to an unacceptable extent because of the resulting rise in the local metal temperatures. Coatings also extend life, provide protection by enduring the operational conditions, and protect the blades by being sacrificial by allowing the coating to be restripped and recoated on the same base metal.

The past and future trends in the development of coatings are shown in Figure 11-10. Present-day coatings last 10–20 times longer than coatings used 10 years ago. Coated blades last up to two times longer than uncoated blades in the field. Figure 11-11 is a comparison between the various types of

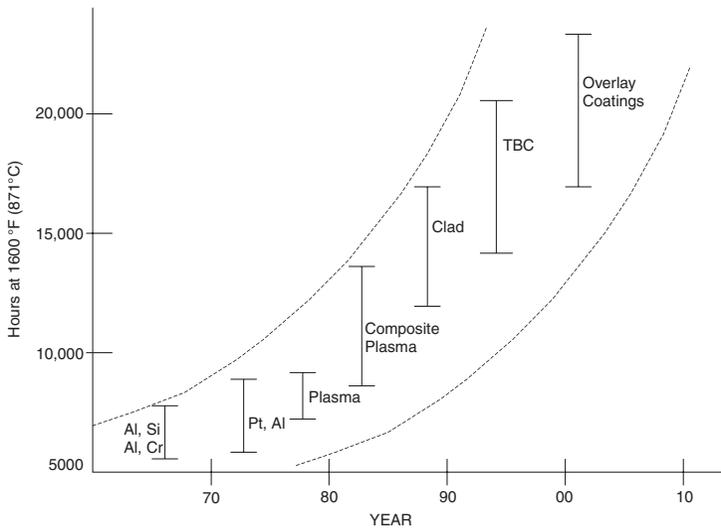


Figure 11-10. Developments of coatings.

coatings on the comparative resistance in the areas of Oxidation, Corrosion, and Cracking. To improve the oxidation protection an increase of aluminum content in the outer region of the coating matrix is needed. The higher aluminum content forms a more protective aluminum oxide layer that greatly improves the high-temperature oxidation resistance.

Life of coatings depends on Composition, Thickness, and the Standard of Evenness to which it has been deposited. Most of the new coatings are applied by vacuum Plasma Spray technique to ensure that the coating has been applied in a uniform and controlled manner. Coatings help extend the life of bladings by protecting them against Oxidation, Corrosion, Cracking, Thermal Fatigue, Temperature excursions, and foreign object damage (FOD) damage. Oxidation is a prime consideration in “clean fuel” regime, while corrosion is due to higher metal temperatures and emphasis in not so clean a fuel.

For a given combination of loadings, coating life is governed by:

1. Composition of the coating that includes environmental and mechanical properties such as thermal fatigue.
2. Coating Thickness that provides a greater protective reservoir if thicker. However, thicker coatings may have lower thermal fatigue resistance.
3. Standard of deposition such as thickness uniformity, or defined thickness variation and coating defects.

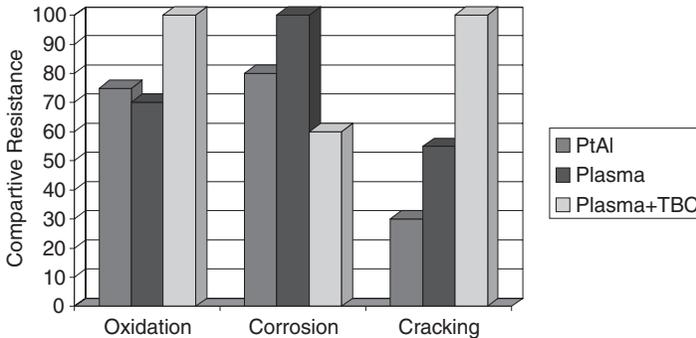


Figure 11-11. Comparative resistance in various types of coatings.

There are three basic types of coatings, thermal barrier coatings, diffusion coatings, and plasma sprayed coatings. The advancements in coating have also been essential in ensuring that the blade base metal is protected at these high temperatures. Coatings ensure that the life of the blades are extended and in many cases are used as sacrificial layer, which can be stripped and recoated. The general type of coatings is very little different from the coatings used 10–15 years ago. These include various types of diffusion coatings such as Aluminide Coatings originally developed nearly 40 years ago. The thickness required is between 25–75 μm thick, these coatings consisted of Ni/Co = about 30% Al. The new aluminide coatings with Platinum (Pt) increase the oxidation resistance, and also the corrosion resistance. Platinum in the coating increases the activity of aluminum in the coating, enabling a very protective and adherent Al_2O_3 scale to form on the surface.

Coatings developed some 30–35 years ago, commonly known as MCrAlY, have a wide range of composition tailored to the type of performance required and are Ni/Co based as shown in these three common types of coatings:

1. Ni, 18% Cr, 12% Al, 0.3% Y
2. Co, 29% Cr, 3% Al, 0.3% Y
3. Co, 25% Ni, 20% Cr, 8% Al, 0.3% Y

These coatings are usually 75–500 μm thick and sometimes have other minor element additions used to improve environmental resistance such as Pt, Hf, Ta, and Zr. Carefully chosen, these coatings can give very good performance.

The thermal barrier coatings have an insulation layer of 100–300 μm thick, and are based on $\text{ZrO}_2\text{--Y}_2\text{O}_3$ and can reduce metal temperatures by 90–270 $^\circ\text{F}$ (50–150 $^\circ\text{C}$). This type of coating is used in combustion cans, transition pieces, nozzle guide vanes, and also blade platforms.

The interesting point to note is that some of the major manufacturers are switching away from corrosion protection biased coatings to coatings that are not only oxidation resistant, but also oxidation resistant at higher metal temperatures. Thermal barrier coatings are being used on the first few stages in all the advanced technology units. The use of internal coatings is getting popular due to the high temperature of the compressor discharge, which results in oxidation of the internal surfaces. Most of these coatings are aluminide type coatings. The choice is restricted due to access problems to slurry based, or gas phase/chemical vapor deposition. Care must be taken in production otherwise internal passages may be blocked. The use of pyrometer technology on some of the advanced turbines has located blades with internal passages blocked causing that blade to operate at metal temperatures of 50–100 °F (28–56 °C) higher than the neighboring blades.

Shroud Coatings

New high temperature gas turbines operate at considerably higher temperatures than previous heavy-duty gas turbines. Therefore, to provide a durable stationary shroud component, coatings are being used to coat the surface of this high-temperature, inner shroud component. The coating of shrouds was developed and has been used extensively in aircraft engines. This provides an extremely oxidation-resistant surface and a rub-tolerant coating in the event that the blade tips rub against the stationary shroud. The coating also reduces the leakage between the blades and the shroud thus reducing tip losses.

Future Coatings

The investigation of even more corrosion-resistant coating materials has been an area of intensive research and development for the past few years. The goals of this research are to further improve the oxidation-resistance and thermal fatigue resistance of high-temperature bucket coatings. In addition to these environmentally resistant coating development efforts, work is also underway to develop advanced thermal barrier coatings (TBCs) for application to stationary and rotating gas path components. By careful process control, the structure of these TBCs may be made more resistant to thermal fatigue and their lives greatly extended.

The capabilities of new coatings are initially evaluated in the laboratory on specially designed rainbow rotor test rigs to determine their corrosion resistance and effect on mechanical properties.

Another area of research is the development of techniques to ensure that the application of the coatings are extremely even. The external deposition source can be electron beam vapor deposition, sputtering, plasma spray, cladding, or any number of other techniques. The technique for application of overlay coatings which appears to have the most promise is high-velocity plasma. For this technique, powder particles of the desired coating composition are accelerated through a plasma field to velocities as high as three times the speed of sound. The impact of the powder onto the workpiece results in a much stronger bond between the coating and workpiece than can be achieved by using conventional subsonic plasma spray deposition. In addition, much higher coating densities can be achieved using the high-velocity plasma.

One company has developed and patented a “detonation gun” to use for coating application. Basically, the gun detonates a metered mixture of oxygen, acetylene, and particles of the desired coating material and throws them at supersonic velocities at the workpiece surface. The workpiece itself remains at quite low temperatures, so its metallurgical properties are not modified.

Bibliography

- Bernstein, H.L., “High Temperature Coatings for Industrial Gas Turbine Users,” Proceedings of the 28th Turbomachinery Symposium, Texas A&M University; p. 179; 1999.
- Bernstien H.L., “Materials Issues for Users of Gas Turbines,” Proceedings of the 27th Texas A&M Turbomachinery Symposium, (1998).
- Lavoie, R., and McMordie, B.G., “Measuring Surface Finish of Compressor Airfoils Protected by Environmentally Resistant Coatings,” 30th Annual Aerospace/Airline Plating and Metal Finishing Forum, April 1994.
- McMordie, B.G., “Impact of Smooth Coatings on the Efficiency of Modern Turbomachinery,” 2000 Aerospace/Airline Plating & Metal Finishing Forum Cincinnati, Ohio, March 2000.
- Schilke, P.W., “Advanced Gas Turbine Materials and Coatings,” 39th GE Turbine State-of-the-Art Technology Seminar, August 1996.
- Warnes B.M., and Hampson L.M., “Extending the Service Life of Gas Turbine Hardware,” ASME 2000-GT-559.
- Wood, M.I., “Developments in Blade Coatings: Extending the Life of Blades? Reducing Lifetime Costs?,” CCGT Generation, March 1999, IIR Ltd.

12

Fuels

The gas turbine's major advantage has been its inherent fuel flexibility. Fuel candidates encompass the entire spectrum from gases to solids. Gaseous fuels traditionally include natural gas, process gas, low-Btu coal gas, and vaporized fuel oil gas. "Process gas" is a broad term used to describe gas formed by some industrial process. Process gases include refinery gas, producer gas, coke oven gas, and blast furnace gas among others. Natural gas is the fuel of choice and is usually the basis on which performance for a gas turbine is compared, since it is a clean fuel fostering longer machine life.

Vaporized fuel oil gas behaves very closely to natural gas because it provides high performance with a minimum reduction of component life. About 40% of the turbine power installed operates on liquid fuels. Liquid fuels can vary from light volatile naphtha through kerosene to the heavy viscous residuals. The classes of liquid fuels and their requirements are shown in Table 12-1.

The light distillates are equal to natural gas as a fuel, and between light distillates and natural gas fuels, 90% of installed units can be counted. Care must be taken in handling liquid fuels to avoid contamination, and the very light distillates like naphtha require special concern in the design of fuel systems because of their high volatility. Generally, a fuel tank of the floating head type with no area for vaporization is employed. The heavy true distillates like #2 distillate oil can be considered the standard fuel. The true distillate fuel is a good turbine fuel; however, because trace elements of vanadium, sodium, potassium, lead, and calcium are found in the fuel, the fuel has to be treated. The corrosive effect of sodium and vanadium is very detrimental to the life of a turbine.

Vanadium originates as a metallic compound in crude oil and is concentrated by the distillation process into heavy oil fractions. Sodium compounds

**Table 12-1
Comparison of Liquid Fuels for Gas Turbines**

| General Fuel Type | True Distillate & Naphthas | Blended Heavy Distillates & Low-Ash Crudes | Residuals & High-Ash Crude |
|---------------------------|--|--|--|
| Fuel pre-heat | No | Yes | Yes |
| Fuel atomization | Mech/LP air | HP/LP air | HP air |
| Desalting | No | Some | Yes |
| Fuel inhibition | Usually none | Limited | Always |
| Turbine washing | No | Yes, except distillate | Yes |
| Start-up fuel | With naphtha | Some fuels | Always |
| Base fuel cost | Highest | Intermediate | Lowest |
| Description | High-quality distillate essentially ash-free | Low-ash, limited contaminant levels | Low-volatility High-ash |
| Types of fuels included | True distillates (naphtha, kerosene, no. 2 diesel, no. 2 fuel oil, JP-4, JP-5) | High-quality crudes, slightly contaminated distillates Navy distillate | Residuals and low-grade crude (No. 5 fuel, No. 6 fuel, Bunker C) |
| ASTM designation | 1-GT, 2-GT, 3-GT | 3-GT | 4-GT |
| Turbine inlet temperature | Highest | Intermediate | Lowest |

are most often present in the form of salt water, which results from salty wells, transport over seawater, or mist ingestion in an ocean environment. Fuel treatments are costly and do not remove all traces of these metals. As long as the fuel oil properties fall within specific limits, no special treatment is required. Blends are residuals that have been mixed with lighter distillates to improve properties. The specific gravity and viscosity can be reduced by blending. About 1% of total installed machines can operate on blends.

A final fuels group contains high-ash crudes and residuals. These account for 5% of installed units. Residual fuel is the high-ash by-product of distillation. Low cost makes them attractive; however, special equipment must always be added to a fuel system before they can be utilized. Crude is attractive as a fuel, since in pumping applications it is burned straight from the pipeline. Table 12-2 shows data obtained from a number of users that

Table 12-2
Operation and Maintenance Life of an Industrial Turbine

| Type of Application and Fuel | | Firing Temperature below 1700 °F (927 °C) | | | Firing Temperature above 1700 °F (927 °C) | | |
|---|--------|--|------------------|------------------|--|------------------|------------------|
| | | Comb. Liners | 1st Stage Nozzle | 1st Stage Blades | Comb. Liners | 1st Stage Nozzle | 1st Stage Blades |
| | | BASE LOAD | Starts/hr | + | + | + | |
| Nat. gas | 1/1000 | 30,000 | 60,000 | 100,000 | 15,000 | 25,000 | 35,000 |
| Nat. gas | 1/10 | 7,500 | 42,000 | 72,000 | 3,750 | 20,000 | 25,000 |
| Distillate oil | 1/1000 | 22,000 | 45,000 | 72,000 | 11,250 | 22,000 | 30,000 |
| Distillate oil | 1/10 | 6,000 | 35,000 | 48,000 | 3,000 | 13,500 | 18,000 |
| Residual | 1/1000 | 3,500 | 20,000 | 28,000 | 2,500 | 10,000 | 15,000 |
| Residual | 1/10 | | | | | | |
| SYSTEM PEAKING | | | | | | | |
| Normal Max. Load of short duration and daily starts | | | | | | | |
| Nat. gas | 1/10 | 7,500 | 34,000 | 60,000 | 5,000 | 15,000 | 24,000 |
| Nat. gas | 1/5 | 3,800 | 28,000 | 40,000 | 3,000 | 12,500 | 18,000 |
| Distillate | 1/10 | 6,000 | 27,200 | 53,500 | 4,000 | 12,500 | 19,000 |
| Distillate | 1/5 | 3,000 | 22,400 | 32,000 | 2,500 | 10,000 | 16,000 |
| TURBINE PEAKING | | | | | | | |
| Operating Above 50 °F–100 °F (28–56 °C) | | | | | | | |
| Firing Temperature | | | | | | | |
| Nat. gas | 1/5 | 2,000 | 12,000 | 20,000 | 2,000 | 12,500 | 18,000 |
| Nat. gas | 1/1 | 400 | 9,000 | 15,000 | 400 | 10,000 | 15,000 |
| Distillate | 1/5 | 1,600 | 10,000 | 16,000 | 1,700 | 11,000 | 15,000 |
| Distillate | 1/1 | 400 | 7,300 | 12,000 | 400 | 8,500 | 12,000 |

indicates a considerable reduction in downtime, depending on the type of service and fuel used. This table also shows that natural gas is by far the best fuel. The effect of various fuels on the output work of the turbine can be seen in Figure 12-1. This figure shows that vaporized fuel oil gives a higher output. This high output results when steam is mixed with the hot fuel gas, which enters the combustor at (371 °C). Corrosion effects have not been detected with this fuel, since the steam is not allowed to condense in the turbine.

Assuming that natural gas is the base line fuel to obtain the same power using diesel fuel the gas turbine would have to be fired at a higher temperature, and for low Btu (400 Btu/cu ft, 14911 KJ/m³) gases at the same firing temperature the turbine would produce more power due to the fact that the amount of fuel could be increased by threefold, thus increasing the overall mass flow through the turbine. The limitation in using low Btu gases is that it takes about 30% of the air for combustion as compared to 10% of the air for natural gas leaving much less air for cooling the combustor liners. Because of this for low Btu gases it is easier to modify annular combustor turbines, which have less of a combustor liner surface area than can-annular combustors. Another problem is that in some cases the extra flow can choke the turbine nozzles. For turbines used in combined cycle

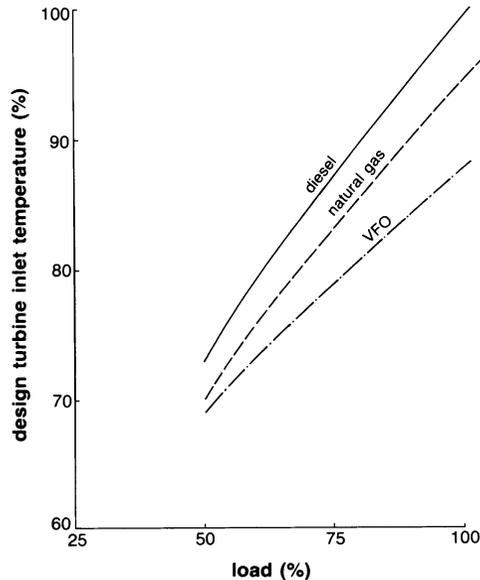


Figure 12-1. Effect of various fuels on turbine inlet temperature.

application there is a tendency to keep the same firing temperature at off-load conditions but with the use of the inlet guide vanes vary the airflow rate.

Fuel Specifications

To decide which fuel to use, a host of factors must be considered. The object is to obtain high efficiency, minimum downtime, and the total economic picture. The following are some fuel requirements that are important in designing a combustion system and any necessary fuel treatment equipment:

1. Heating value
2. Cleanliness
3. Corrosivity
4. Deposition and fouling tendencies
5. Availability

The heating of a fuel affects the overall size of the fuel system. Generally, fuel heating is a more important concern in connection with gaseous fuels, since liquid fuels all come from petroleum crude and show narrow heating-value variations. Gaseous fuels, on the other hand, can vary from 1100 Btu/ft³ (41,000 KJ/m³) for natural gas to (11,184 KJ/m³) or below for process gas. The fuel system will of necessity have to be larger for the process gas, since more is required for the same temperature rise.

Cleanliness of the fuel must be monitored if the fuel is naturally “dirty” or can pick up contaminants during transportation. The nature of the contaminants depends on the particular fuel. The definition of cleanliness here concerns particulates that can be strained out and is not concerned with soluble contaminants. These contaminants can cause damage or fouling in the fuel system and result in poor combustion.

Corrosion by the fuel usually occurs in the hot section of the engine, either in the combustor or the turbine blading. Corrosion is related to the amounts of certain heavy metals in the fuel. Fuel corrosivity can be greatly reduced by specific treatments discussed later in this chapter.

Deposition and fouling can occur in the fuel system and in the hot section of the turbine. Deposition rates depend on the amounts of certain compounds contained in the fuel. Some compounds that cause deposits can be removed by fuel treating.

Finally, fuel availability must be considered. If future reserves are unknown, or seasonal variations are expected, dual fuel capability must be considered.

Fuel requirements are defined by various fuel properties. By coincidence, the heating-value requirement is also a property and needs no further mention.

Cleanliness is a measure of the water and sediment and the particulate content. Water and sediment are found primarily in liquid fuels, while particulates are found in gaseous fuels. Particulates and sediments cause clogging of fuel filters. Water leads to oxidation in the fuel system and poor combustion. A fuel can be cleaned by filtration.

Carbon residue, pour point, and viscosity are important properties in relation to deposition and fouling. Carbon residue is found by burning a fuel sample and weighing the amount of carbon left. The carbon residue property shows the tendency of a fuel to deposit carbon on the fuel nozzles and combustion liner. Pour point is the lowest temperature at which a fuel can be poured by gravitational action. Viscosity is related to the pressure loss in pipe flow. Both pour point and viscosity measure the tendency of a fuel to foul the fuel system. Sometimes, heating of the fuel system and piping is necessary to assure a proper flow.

The ash content of liquid fuels is important in connection with cleanliness, corrosion, and deposition characteristics of the fuel. Ash is the material remaining after combustion. Ash is present in two forms: (1) as solid particles corresponding to that material called sediment, and (2) as oil or water soluble traces of metallic elements. As mentioned earlier, sediment is a measure of cleanliness. The corrosivity of a fuel is related to the amount of various trace elements in the fuel ash. Certain high-ash fuels tend to be very corrosive. Finally, since ash is the fuel element remaining after combustion, the deposition rate is directly related to the ash content of the fuel.

Table 12-3 is a summary of gaseous fuel specifications. The two major areas of concern are heating value with its possible variation and contaminants. Fuels outside a specification can be utilized if some modification is made.

Gas fuels with heating values between 300–1100 Btu/ft³ (11,184–41,000 KJ/m³) are in use today; however, future systems may use gas with heating values

Table 12-3
Gaseous Fuel Specifications

| | |
|---|---|
| Heating value | 300–1100 Btu/ft ³ (11,184–41,000 KJ/m ³) |
| Solid contaminants | < 30ppm |
| Flammability limits | 2.2:1 |
| Composition—S, Na, K, Li | < 5ppm |
| (Sulfur + sodium + potassium + lithium) | (When formed into alkali metasulfate) |
| H ₂ O (by weight) | < 25% |

below 100 Btu/ft³ (3728 KJ/m³). Although wide ranges of heating values can be accommodated with different fuel systems, the maximum variation that can be used in a given fuel system is $\pm 10\%$.

Sulfur content must be controlled in units with exhaust recovery systems. If sulfur condenses in the exhaust stack, corrosion can result. In units without exhaust recovery there is no problem, since stack temperatures are considerably higher than the dew point. Sulfur can, however, promote hot-section corrosion in combustion with certain alkali metals such as sodium or potassium. This type of corrosion is sulfidation or hot corrosion and is controlled by limiting the intake of sulfur and alkali metals. Contaminants found in a gas depend on the particular gas. Common contaminants include tar, lamp black, coke, sand, and lube oil.

Table 12-4 is a summary of liquid fuel specifications set by manufacturers for efficient machine operations. The water and sediment limit is set at 1% by maximum volume to prevent fouling of the fuel system and obstruction of the fuel filters. Viscosity is limited to 20 centistokes at the fuel nozzles to prevent clogging of the fuel lines. Also, it is advisable that the pour point be 20 °F (11 °C) below the minimum ambient temperature. Failure to meet this specification can be corrected by heating the fuel lines. Carbon residue should be less than 1% by weight based on 100% of the sample. The hydrogen content is related to the smoking tendency of a fuel. Lower

Table 12-4
Liquid Fuel Specifications

| | |
|--------------------|-----------------------------------|
| Water and sediment | 1.0% (V%) Max. |
| Viscosity | 20 centistokes at fuel nozzle |
| Pour point | About 20° below min. ambient |
| Carbon residue | 1.0% (wt) based on 100% of sample |
| Hydrogen | 11.% (wt) minimum |
| Sulfur | 1% (wt) maximum |

Typical Ash Analysis and Specifications

| Metal | Lead | Calcium | Sodium & Potassium | Vanadium |
|------------------------|-------------|----------------|-------------------------------|-----------------|
| Spec. max. (ppm) | 1 | 10 | 1 | 0.5 untreated |
| Naphtha | 0-1 | 0-1 | 0-1 | 500 treated |
| Kerosene | 0-1 | 0-1 | 0-1 | 0-.1 |
| Light distill. | 0-1 | 0-1 | 0-1 | 0-.1 |
| Heavy distill. (true) | 0-1 | 0-1 | 0-1 | 0-.1 |
| Heavy distill. (blend) | 0-1 | 0-5 | 0-20 | .1/80 |
| Residual | 0-1 | 0-20 | 0-100 | 5/400 |
| Crude | 0-1 | 0-20 | 0-122 | .1/80 |

hydrogen-content fuels emit more smoke than the higher-hydrogen fuels. The sulfur standard is to protect from corrosion those systems with exhaust heat recovery.

The ash analysis receives special attention because of certain trace metals in the ash that cause corrosion. Elements of prime concern are vanadium, sodium, potassium, lead, and calcium. The first four are restricted because of their contribution to corrosion at elevated temperatures; however, all these elements may leave deposits on the blading.

Sodium and potassium are restricted because they react with sulfur at elevated temperatures to corrode metals by hot corrosion or sulfurization. The hot-corrosion mechanism is not fully understood; however, it can be discussed in general terms. It is believed that the deposition of alkali sulfates (Na_2SO_4) on the blade reduces the protective oxide layer. Corrosion results from the continual forming and removing of the oxide layer. Also, oxidation of the blades occurs when liquid vanadium is deposited on the blade. Fortunately, lead is not encountered very often. Its presence is primarily from contamination by leaded fuel or as a result of some refinery practice. Presently, there is no fuel treatment to counteract the presence of lead.

Fuel Properties

Natural gas has a Btu content of about 1000–1100 Btu/ft³ (37,272–41,000 KJ/m³). By definition, low-Btu gases can vary between 100–350 Btu/ft³ (3728–13,048 KJ/m³). Presently, little success has been achieved in burning gases with a heating value lower than 200 Btu/ft³ (7456 KJ/m³). To provide the same energy as natural gas, a 150 Btu/ft³ (5592 KJ/m³) low-Btu gas must be utilized at the rate of seven times that of natural gas on a volumetric basis. Therefore, the mass flow rate to provide the same energy must be about 8–10 times that of natural gas. The flammability of low-Btu gases is very much dependent on the mixture of CH₄ and other inert gases. Figure 12-2 shows this effect by illustrating that a mixture of CH₄-CO₂ of less than 240 Btu/ft³ (8947 KJ/m³) is inflammable, and a CH₄-N₂ mixture of less than about 150 Btu/ft³ is less inflammable. Low-Btu gases near these values have greatly restricted flammability limits when compared to CH₄ in the air. Vaporized fuel oil gas is produced by mixing superheated steam with oil and then vaporizing the oil to provide a gas whose properties and heating value are close to natural gas.

Important liquid fuel properties for a gas turbine are shown in Table 12-5. The flash point is the temperature at which vapors begin combustion. The flash point is the maximum temperature at which a fuel can be handled safely.

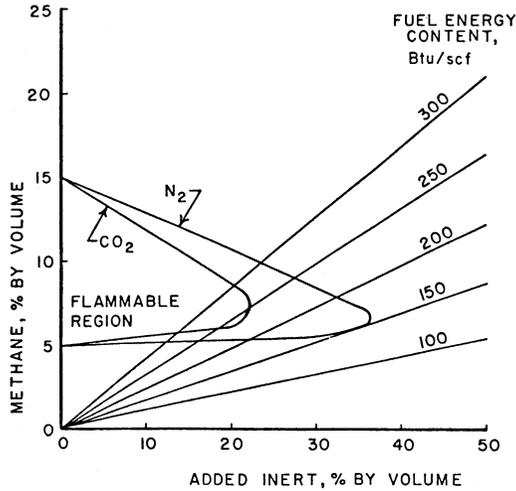


Figure 12-2. Flammable fuel mixtures of $\text{CH}_4\text{-N}_2$ and $\text{CH}_4\text{-CO}_2$ at one atm showing various energy levels.

The pour point is an indication of the lowest temperature at which a fuel oil can be stored and still be capable of flowing under gravitational forces. Fuels with higher pour points are permissible where the piping has been heated. Water and sediment in the fuel lead to fouling of the fuel system and obstruction in fuel filters.

The carbon residue is a measure of the carbon compounds left in a fuel after the volatile components have vaporized. Two different carbon residue tests are used, one for light distillates, and one for heavier fuels. For the light fuels, 90% of the fuel is vaporized, and the carbon residue is found in the remaining 10%. For heavier fuels, since the carbon residue is large, 100% of the sample can be used. These tests give a rough approximation of the tendency to form carbon deposits in the combustion system. The metallic compounds present in the ash are related to the corrosion properties of the fuel.

Viscosity is a measure of the resistance to flow and is important in the design of fuel pumping systems.

Specific gravity is the weight of the fuel in relation to water. This property is important in the design of centrifugal fuel washing systems. Sulfur content is important in connection with emission concerns and in connection with the alkali metals present in the ash. Sulfur reacting with alkali metals forms compounds that corrode by a process labeled sulfidation.

Luminosity is the amount of chemical energy in the fuel that is released as thermal radiation.

**Table 12-5
Fuel Properties**

| | Diesel Fuel Burner Fuel | | | | High-Ash Crude Heavy Residual | Typical Libyan Crude | Navy Distillate | Heavy Distillate | Low-Ash Crude |
|--|-------------------------|------------|---------------|-------------------|-------------------------------------|----------------------------|--------------------|---------------------|------------------|
| | Kerosene | #2 | Oil #2 | JP-4 | | | | | |
| Flash point °F | 130/160 | 118–220 | 150/200 | < RT | 175/265 | | 186 °F | 198 | 50/200 |
| Pour point °F | –50 | –55 to +10 | –10/30 | | 15/95 | 68 | 10 °F | | 15/110 |
| Visc. CS @ 100 °F | 1.4/2.2 | 2.48/2.67 | 2.0/4.0 | .79 | 100/1,800 | 7.3 | 6.11 | 6.20 | 2/100 |
| SSU | | 34.4 | | | | | 45.9 | | |
| Sulfur % | .01/.1 | .169/.243 | .1/.8 | .047 | .5/4 | .15 | 1.01 | 1.075 | .1/2.7 |
| API gr. | | 38.1 | 35.0 | 53.2 | | | 30.5 | | |
| Sp. gr. @ 100 °F | .78/.83 | .85 | .82–.88 | .7543@60 °F | .92/1.05 | .84 | .874 | .8786 | .80/.92 |
| Water & ded. | | | 0 | | | .1%wt | | | |
| Heating value $\frac{\text{Btu}}{\text{lb}}$ | 19,300/ 19,700 | 18,330 | 19,000/19,600 | 18,700/ 18,820 | 18,300/18,900 | 18,250 | | 18,239 | 19,000/19,400 |
| Hydrogen % | 12.8/14.5 | 12.83 | 12/13.2 | 14.75 | 10/12.5 | | | 12.40 | 12/13.2 |
| Carbon residue 10% bottoms | .01/.1 | .104 | .03/.3 | | | 2/10 | | | .3/3 |
| Ash ppm | 1/5 | .001 | 0/20 | | 100/1,000 | 36ppm | | | 20/200 |
| Na + K ppm | 01.5 | | 0/1 | | 1/350 | 2.2/4.5 | | | 0/50 |
| V | 0/.1 | | 0/.1 | | 5/400 | 0/1 | | | 0/15 |
| Pb | 0/.5 | | 0/1 | | 0/25 | | | | |
| Ca | 0/1 | 0/2 | 0/2 | | 0/50 | | | | |

Finally, the weight of a fuel, light or heavy, refers to volatility. The most volatile fuels vaporize easily and come out early in the distillation process. Heavy distillates will come out later in the process. What remains after distillation is referred to as residual. The ash content of residual fuels is high.

Catastrophic oxidation requires the presence of Na_2SO_4 and Mo, W, and/or V. Crude oils are high in V; ash will be 65% V_2O_5 or higher. The rate at which corrosion proceeds is related to temperature. At temperatures of more than 1500°F, attack by sulfidation takes place rapidly. At lower temperatures with vanadium-rich fuels, oxidation catalyzed by vanadium pentoxide can exceed sulfidation. The effect of temperature on IN 718 corrosion by sodium and vanadium is shown in Figure 12-3. The corrosive threshold is generally accepted to be in the range of 1100–1200°F, (593–649°C) and this cannot be considered a feasible firing temperature due to losses in efficiency and power output. Figure 12-4 shows the effect of sodium

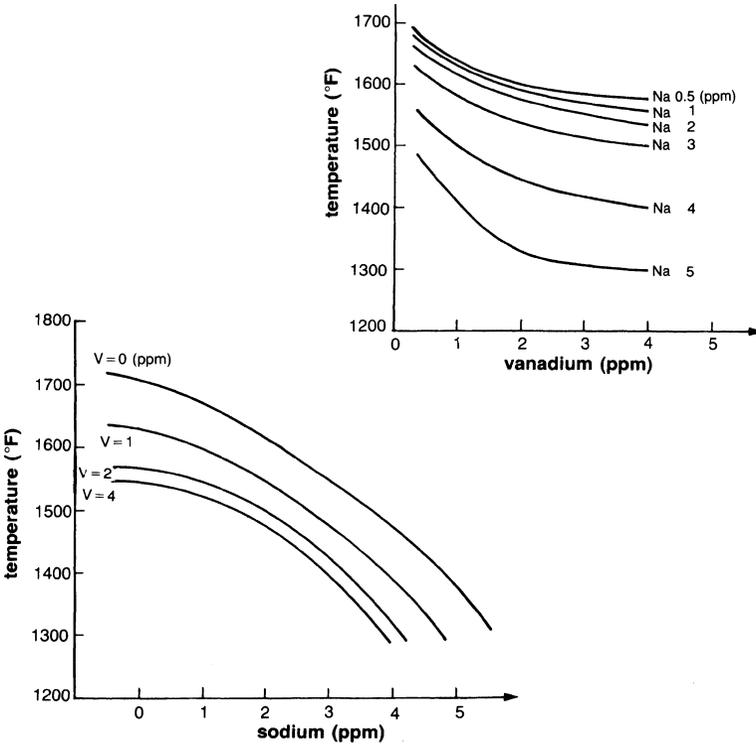


Figure 12-3. The effect of temperature on IN 718 corrosion by sodium and vanadium.

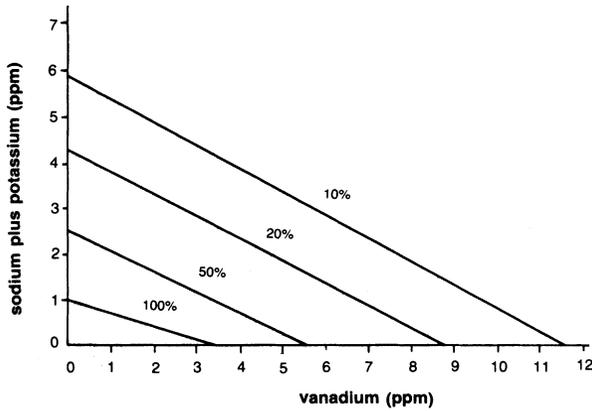


Figure 12-4. Effect of sodium, potassium, and vanadium on combustor life.

plus potassium and vanadium on life. Allowable limits for 100%, 50%, 20%, and 10% of normal life with uncontaminated fuel at standard firing temperatures are shown.

Fuel Treatment

Natural gas requires no fuel treatment; however, low-Btu gas, especially if derived from various coal gasification processes, requires various types of cleaners for use in a gas turbine. These cycles can get very complex as indicated by a typical system, which utilizes a steam bottoming cycle to achieve high efficiency. Vaporized fuel oil gas is already cleansed of its impurities in the vaporization process.

A corrosion-inhibiting fuel treatment has been developed for the use of lower-grade liquid fuels. Sodium, potassium, and calcium compounds are most often present in fuel in the form of seawater. These compounds result from salty wells and transportation over seawater, or they can be ingested by the compressor in mist form in ocean environments. Methods developed to remove the salt and reduce the sodium, potassium, and calcium rely on the water-solubility of these compounds. Removal of these compounds through their water-solubility is known as fuel washing. Fuel washing systems fall into four categories: centrifugal, DC electric, AC electric, and hybrids.

The centrifugal fuel-cleaning process consists of mixing 5–10% water with the oil plus an emulsion breaker to aid the separation of water and oil. Then a mixer dispenses the wash water into the oil stream to aid the impurities in forming a water solution. The centrifuges then separate this water from the

oil. A schematic of the system is shown in Figure 12-5. If the specific gravity of the fuel is above .96 or viscosity exceeds 3500 SSU @ 100°F (38°C), centrifugal separation is impractical, and the specific gravity of one of the components must be increased. Water weight can be increased by dissolving epsom salt in it. Specific gravity of the fuel can be decreased by fuel blending. Figure 12-6 shows the relation is linear, and the blend has a specific gravity

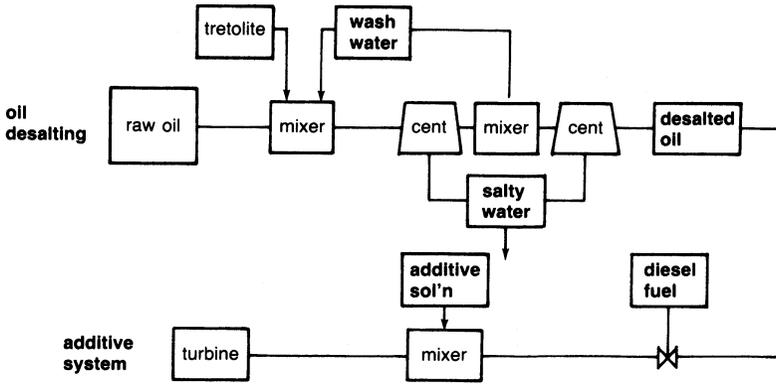


Figure 12-5. A typical residual fuel treatment system.

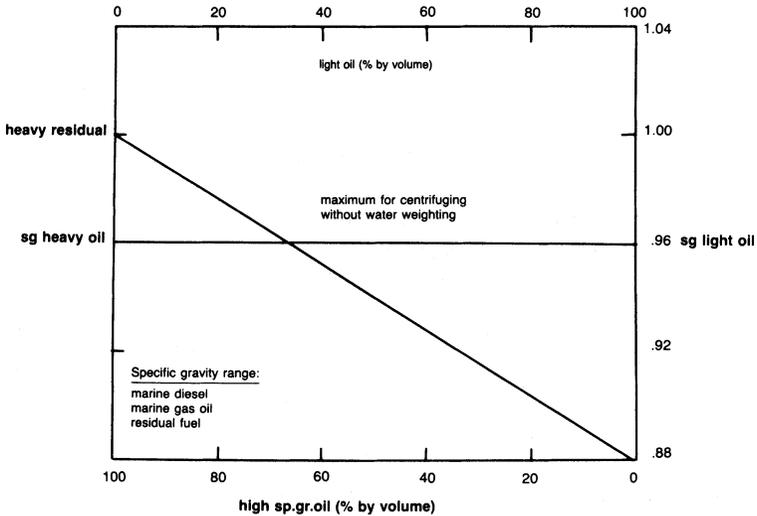


Figure 12-6. Fuel blending for specific gravity reduction. Specific gravity heavy oil = 1.0. Specific gravity light oil = .88.

which is the average of the constituents. However, viscosity blending is a logarithmic relation as shown in Figure 12-7. To reduce viscosity from 10,000 to 3000 SSU, a 3:1 reduction requires a dilution of only 1:10. An added advantage of the centrifugal process is that the sludge and particulates that can cause fuel system fouling are removed.

Electrostatic separators operate on a principle similar to centrifugal separation. The salt is first dissolved in the water, and the water is then separated. Electrostatic separators utilize an electric field to coalesce droplets of water for an increase in diameter and an associated increased settling rate. The DC separators are most efficient with light fuels of low conductivity, and AC separators are used with heavier, highly conductive fuels. Electrostatic separators are attractive because of safety considerations (no rotating machinery) and maintenance (few overhauls). However, sludge removal is more difficult. Water washing systems are summarized in Table 12-6.

Vanadium originates as a metallic compound in crude oil and is concentrated by the distillation process into the heavy-oil fractions. Blade oxidation occurs when liquid vanadium is deposited onto a blade and acts as a catalyst. Vanadium compounds are oil-soluble and are thus unaffected by fuel washing. Without additives, vanadium forms low-melting-temperature

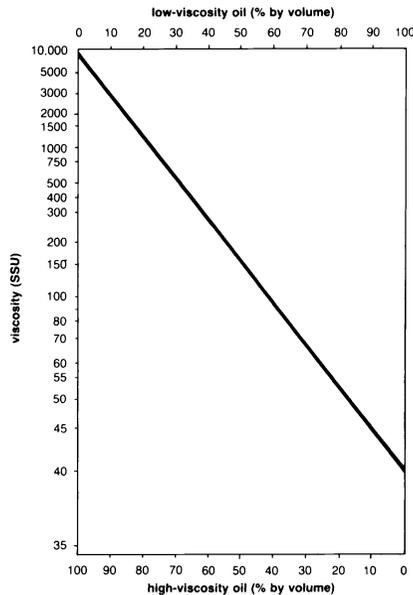


Figure 12-7. Fuel viscosity blending chart. High-viscosity oil = 10,000 SSU. Low-viscosity oil = 40 SSU.

Table 12-6
Selection of Fuel Washing Systems

| Fuel | Washing System |
|---------------------|--|
| Distillate | Centrifugal or DC electrostatic desalter |
| Heavy distillates | Centrifugal or AC electrostatic desalter |
| Light-medium crudes | Centrifugal or AC electrostatic desalter |
| Light residual | Centrifugal or AC electrostatic desalter |
| Heavy crudes | Centrifugal desalter and hybrid systems |
| Heavy residuals | Centrifugal desalter and hybrid systems |

compounds, which deposit on a blade in a molten slag state that causes rapid corrosion. However, by the addition of a suitable compound (magnesium, for example), the melting point of the vanadates is increased sufficiently to prevent them from being in the liquid state under service conditions. Thus, slag deposition on the blades is avoided. Calcium was initially selected as the inhibiting agent, as tests indicated it was more effective at 1750°F (954°C). Subsequent tests showed magnesium gave better protection at 1650°F (899°C) and below. However, at temperatures of 1750°F (954°C) and over, magnesium no longer inhibits but rather *accelerates* corrosion. Magnesium also provides more friable deposits than calcium inhibitors. A magnesium/vanadium ratio of 3:1 reduces corrosion by a factor of six between temperatures of 1550°F (843°C) and 1400°F (760°C).

The particular magnesium compound selected for inhibition is dependent upon fuel characteristics. For low-vanadium concentrations (below 50 ppm), an oil-soluble compound such as magnesium sulfonate is added in the correct proportion to the vanadium present. The cost of oil-soluble inhibitors becomes prohibitive above concentrations of 50 ppm.

At higher concentrations of vanadium, magnesium sulfate or magnesium oxide is used as an inhibitor. Both are approximately equal in material cost, but magnesium sulfate has proven itself, while magnesium oxide is still under study. Magnesium sulfate requires by far the most capital cost, as it must be first dissolved, then adjusted to a known concentration. It is mixed with an oil and an emulsifying agent to form an emulsion to suspend in the fuel. Two different injection procedures are used. One method is to mix the solution with desalted fuel in a dispersion mixer just prior to the combustion chamber. The inhibited oil is burned quickly, usually within a minute after mixing, because the solution has a tendency to settle out. Also, the solution can be dispersed in the fuel prior to the service tanks. To avoid settling out of the solution, the tanks are recirculated through distribution headers. Since a magnesium-to-vanadium ratio of $3.25 \pm 0.25 : 1$ is used in practice, the

second dispersion method is the standard practice as the tanks can be certified "within specification" before burning. Adequate knowledge of contaminants is essential for successful inhibition.

An alternate approach to fuel washing is to utilize a vaporized fuel oil system (VFO). This technology was developed as a method for converting natural gas fuel systems to liquid fuel. The process involves mixing steam with the liquid fuel and then vaporizing the mixture. The vaporized mixture exhibits the same combustion properties as natural gas.

VFO works well in gas turbines. In a nine-month test program, the combustion properties of VFO were studied in a combustion test module. A gas turbine was also operated on VFO. The tests were conducted to study the combustion characteristics of VFO, the erosive and corrosive effects of VFO, and the operation of a gas turbine on VFO. The combustion tests were conducted on a combustion test module built from a GE Frame 5 combustion can and liner. The gas turbine tests were conducted on a Ford model 707 industrial gas turbine. Both the combustion module and gas turbine were used in the erosion and corrosion evaluation. The combustion tests showed the VFO to match natural gas in flame patterns, temperature profile, and flame color. The operation of the gas turbine revealed that the gas turbine not only operated well on VFO, but its performance was improved. The turbine inlet temperature was lower at a given output with VFO than with either natural gas or diesel fuel. This phenomenon is due to the increase in exhaust mass flow provided by the addition of steam in the diesel for the vaporization process. Following the tests, a thorough inspection was made of materials in the combustion module and on the gas turbine, which came into contact with the vaporized fuel or with the combustion gas. The inspection revealed no harmful effects on any of the components due to the use of VFO.

The VFO technology provides a means of converting natural gas systems to liquid fuel without requiring new fuel liners, nozzles, and control systems. However, VFO also offers a method of treating contaminated fuel. The VFO process vaporizes only a portion of the liquid fuel; the contaminants stay in the remaining liquid fuel. The remaining liquid can be utilized either as fuel or as feedstock for other processes. It has been found that if 90% of the fuel is vaporized, the remaining 10% provides the heat required for vaporization. The heat required to vaporize the liquid fuel is recovered in the gas turbine as heat added into the combustion can, so the process is very efficient. The only loss is the energy in the heated gases leaving the vaporizer exhaust.

The overall costs for a VFO unit can be lower than the costs of conventional liquid fuel treatment plants. The U.S. Department of Energy conducted a survey that showed that the costs of operating a liquid fuel treatment system over a 20-year period is approximately \$0.50 MMBtu

output. This cost includes the initial capital investment, maintenance, and operating costs. The initial cost of a VFO unit with an output of 800 MMBtu/hr (required for a 60 MW gas turbine) is approximately \$1150/MMBtu/hr output (\$920,000 total). The operating costs of a VFO unit are very low, since the only power requirement is the electrical power needed to drive several small pumps. The energy required to vaporize the oil is obtained from burning the unvaporized oil. Any additional expense in operating a VFO system results from maintenance. Maintenance will be minimal with properly selected components.

Heavy Fuels

With heavy fuels, the ambient temperature and the fuel type must be considered. Even at warm environmental temperatures, the high viscosity of the residual could require fuel preheating or blending. If the unit is planned for operation in extremely cold regions, the heavier distillates could become too viscous. Fuel system requirements limit viscosity to 20 centistokes at the fuel nozzles.

Fuel system fouling is related to the amount of water and sediment in the fuel. A by-product of fuel washing is the desludging of the fuel. Washing rids the fuel of those undesirable constituents that cause clogging, deposition, and corrosion in the fuel system. The last part of treatment is filtration just prior to entering the turbine. Washed fuel should have less than .025% bottom sediment and water.

Frequently, no visible smoke and no carbon deposition are design parameters. Smoke is an environmental concern, while excessive carbon can impair the fuel spray quality and cause higher liner temperatures due to the increased radiation emissivity of the carbon particles as compared to the surrounding gases. Smoke and carbon are a fuel-related property. The hydrogen saturation influences smoke and free carbon. The less-saturated fuels like benzene (C_6H_6) tend to be smokers; the better fuels like methane (CH_4) are saturated hydrocarbons. This effect is shown in Figure 12-8. Boiling temperature is a function of molecular weight. Heavier molecules tend to boil at a higher temperature. Since a less-saturated molecule will weigh more (higher molecular weight), one can expect residuals and heavy distillates to be smokers. This expectation is founded in practice. The design solution pioneered by General Electric on its LM 2500, which has an annular combustor as shown in Figure 12-9, was to increase flow and swirl through the dome surrounding the fuel injector. The increased flow helped to avoid rich pockets and promoted good mixing. The axial swirler achieved a no-smoke condition and reduced liner temperature.

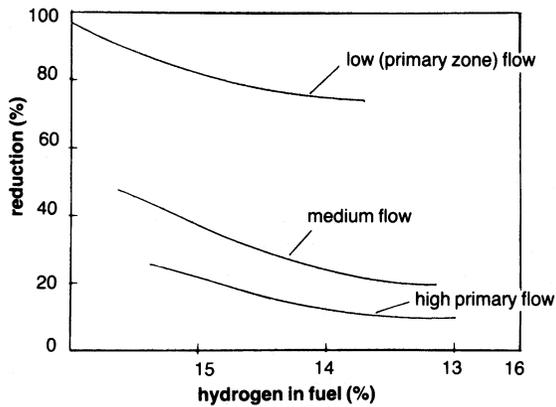


Figure 12-8. Effect of hydrogen saturation in primary flow on smoke.

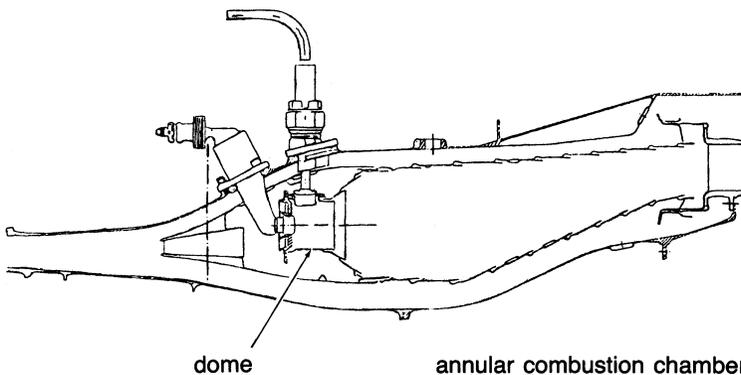


Figure 12-9. Cross section of an annular combustor showing high dome flow configuration. (Courtesy of General Electric Company.)

Special consideration must be afforded to the combustion chamber walls. Low-grade fuels tend to release a higher amount of their energy as thermal radiation instead of heat. This energy release, coupled with the large diameter of the single can and the formation of carbon deposits, can lead to an over-heating problem on the liner. One vendor advocates the use of metallic tiles as combustor liners. The tiles hook into the wall in slots provided for them. The tiles have fine-pitched fins cast on the back. The fins form a double-wall structure by bridging the gap between the flame-tube wall and the tile. This annulus is fed by air, thus providing a strong cooling action. The standard sheet metal design was abandoned due to warpage.

Cleaning of Turbine Components

A fuel treatment system will effectively eliminate corrosion as a major problem, but the ash in the fuel plus the added magnesium does cause deposits in the turbine. Intermittent operation of 100 hours or less offers no problem, since the character of the deposit is such that most of it sheds upon refiring, and no special cleaning is required. However, the deposit does not reach a steady-state value with continuous operation and gradually plugs the first-stage nozzle area at a rate of between 5% and 12% per 100 hours. Thus, at present, residual oil use is limited to applications where continuous operation of more than 1,000 hours is not required.

If the need exists to increase running time between shutdowns, the turbine can be cleaned by the injection of a mild abrasive into the combustion system. Abrasives include walnut shells, rice, and spent catalyst. Rice is a very poor abrasive, since it tends to shatter into small pieces. Usually, a 10% maximum blockage of the first-stage nozzle is tolerated before abrasive cleaning is initiated. Abrasive cleaning will restore 20–40% of the lost power by removing 50% of the deposits. If the frequency of abrasive injection becomes unacceptable and cannot prevent the nozzle blockage from becoming more than 10%, water washing becomes necessary. Water or solvent washing can effectively restore 100% of the lost power. A typical operating plot is shown in Figure 12-10.

Hot Section Wash

The water washing of the hot section of the turbine is required for fuels with high vanadium contents. The addition of magnesium salts to encounter the corrosive action of the vanadium creates ash, which deposits on the

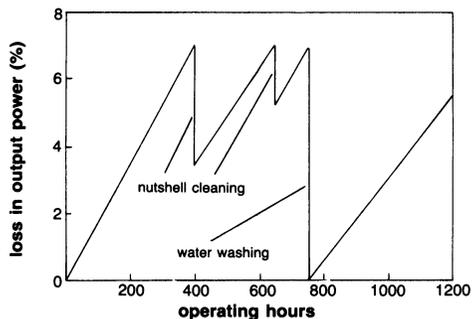


Figure 12-10. Effect of cleaning on power output.

blades reducing the flow area. This ash must be removed and in many cases this means that the hot section blades and nozzles must be washed every 100–120 hours. This is done by bringing the turbine down and running it on turning gear till the turbine blade temperatures are around 200 °F (93.3 °C), in most cases this is reached in about six to eight hours. The turbine hot expander section is then blasted by steam and most of the ash is removed. The turbine is then brought up to speed after the turbine blade section is dried. This whole process takes about 20 hours.

Compressor Washing

Compressor washing is also a very important part of turbine operations. Two approaches to compressor cleaning are abrasion and solvent cleaning. The use of abrasive cleaning has diminished due to erosion problems, liquid washing is primarily used. The new high-pressure compressors are very susceptible to dirt on the blades that not only can lead to a reduction in performance but can also lead to compressor surge. Washing efficacy is site-specific due to the different environmental conditions at each plant. There are many excellent techniques and systems for water washing. Operators must often determine the best approach for their gas turbines. This includes what solvents if any should be used, and the frequencies of wash. Many operators have found that water wash without any solvent is as effective as with the use of solvents. This is a complex technical-economical problem also depending on the service that the gas turbines are in and the plant surroundings. However the use of nondemineralized water could result in more harm than good.

Water washing (with or without detergents) cleans by water impact and by removing the water-soluble salts. The effect of water cleaning is usually not very effective after the first few stages. It is most important that the manufacturer's recommendations be followed with respect to water wash quality, detergent/water ratio, and other operating procedures. Water washing using a water-soap mixture is an efficient method of cleaning. This cleaning is most effective when carried out in several steps, which involve the application of a soap and water solution, followed by several rinse cycles. Each rinse cycle involves the acceleration of the machine to approximately 50 percent of the starting speed, after which the machine is allowed to coast to a stop. A soaking period follows during which the soapy water solution may work on dissolving the salt.

A fraction of airborne salt always passes through the filter. The method recommended for determining whether or not the foulants have a substantial salt base is to soap wash the turbine and collect the water from all drainage ports available. Dissolved salts in the water can then be analyzed.

Online washing is being widely used as a means to control fouling by keeping the problem from developing. Techniques and wash systems have evolved to a point where this can be done effectively and safely. Washing can be accomplished by using water, water-based solvents, petroleum-based solvents, or surfactants. The solvents work by dissolving the contaminants while surfactants work by chemically reacting with the foulants. Water-based solvents are effective against salt, but fare poorly against oily deposits. Petroleum-based solvents do not effectively remove salty deposits. With solvents, there is a chance of foulants being re-deposited in the latter compressor stages.

Even with good filtration, salt can collect in the compressor section. During the collection process of both salt and other foulants, an equilibrium condition is quickly reached, after which re-ingestion of large particles occurs. This re-ingestion has to be prevented by the removal of salt from the compressor prior to saturation. The rate at which saturation occurs is highly dependent on filter quality. In general, salts can safely pass through the turbine when gas and metal temperatures are less than 1000 °F. Aggressive attacks will occur if the temperatures are much higher. During cleaning, the actual instantaneous rates of salt passage are very high together with greatly increased particle size.

The following are some tips that should be followed by operators during water washes:

- The water used should be demineralized. The use of nondemineralized water would harm the turbine.
- On-line wash should be done whenever compressor performance diminishes by 2–3%. It would be imprudent to let foulants build up before commencing water wash.
- Stainless steel for tanks, nozzles, and manifolds are recommended to reduce corrosion problems.
- Spray nozzles should be placed where proper misting of the water would occur, and minimize the downstream disturbance of the flow. Care should be taken that a nozzle would not vibrate loose and enter the flow passage.
- After numerous water washes, the compressor performance will deteriorate and a crank wash will be necessary.

Fuel Economics

Because gas turbine fuel properties are not the ones that determine cost, in some instances the better gas turbine fuel will sell for less than the poorer one. The selection of the most economical fuel depends on many considerations,

of which fuel cost is but one. However, users should always burn the most *economical* fuel, which may not be the cheapest fuel.

Fuel properties must be known and economics considered before a fuel is selected. The properties of a fuel greatly affect the cost of a fuel treatment facility. A doubling of viscosity roughly doubles the cost of desalting equipment, and having a specific gravity of greater than .96 greatly complicates the washing system and raises costs. Trying to remove the last trace of a metallic element affects the cost of fuel washing approximately as shown in Table 12-7. The high cost of fuel treatment systems is the fuel washing system, since the ignition system costs about 10% of that amount. The fuel flow rate as well as the fuel type affect the fuel treatment system investment cost as shown in Figure 12-11.

Gas turbines, like other mechanical devices, require inspection, maintenance, and service. Maintenance costs include the combustion system, hot-gas path, and major inspections. (See Chapter 21.) The effect of fuel type on maintenance costs is shown in Table 12-8. A cost factor is shown using natural gas as unity. The cost of maintenance is subject to great variations. Recognizing the great difficulty in establishing expected maintenance costs

Table 12-7
Effect of Washed Fuel Quality on System Cost

| Sodium Reduction | Washing System Cost |
|------------------|---------------------|
| 100 → 5 ppm Na | x dollars |
| 100 → 2 ppm Na | 2x dollars |
| 100 → 1 ppm Na | 4x dollars |
| 100 → ½ ppm Na | 8x dollars |

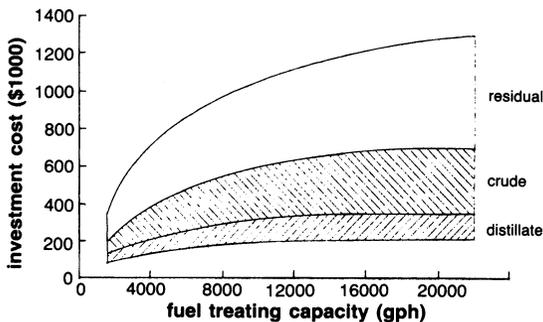


Figure 12-11. Gas turbine fuel treatment plant investment costs. (Courtesy of General Electric Company.)

Table 12-8
Average Total Maintenance and Cost Factor for a Gas Turbine

| Fuel | Expected Actual Maintenance Cost (mils/kWh) | Expected Maintenance Cost Factor |
|----------------------|--|---|
| Natural gas | 0.3 | 1.0 = Base line |
| No. 2 distillate oil | 0.4 | 1.25 |
| Typical crude oil | 0.6 | 2.0 |
| No. 6 residual oil | 1.0 | 3.33 |

Table 12-9
Economic Factors Influencing Fuel Selection

| |
|-----------------------------------|
| I. <i>Fuel Cost</i> |
| II. <i>Operation</i> |
| 1. Power output for given turbine |
| 2. Efficiency degradation |
| 3. Outstage (Downtime) |
| III. <i>Capital Investment</i> |
| 1. Fuel washing and inhibition |
| 2. Fuel quality monitoring |
| 3. Turbine wash and cleaning |
| IV. <i>Duty Cycle</i> |
| 1. Continuous duty required |
| 2. Total annual operation |
| 3. Starts and stops |

for different applications, Table 12-8 should be used as a rough guide in estimating costs. These data are based on actual maintenance costs for heavy-duty gas turbines.

As has been shown, the selection of the most economical fuel can depend on many factors besides cost. Table 12-9 summarizes the major economic considerations in fuel selection.

Operating Experience

Early U.S. experience in residual operation dates back to the early 1950s. Several companies adapted gas turbines to run on residual fuel for locomotive application. Operating with a low inlet temperature 1350 °F (732 °C), low-sulfur residual corrosion was limited; however, it was noted that any increase in firing temperature was accompanied by serious corrosion. Because of the advantage of increased firing temperatures, research on fuel

Table 12-10
Typical Manufacturer's Fuel Data on Total Installed Horsepower

| Fuel | Units % | % Hours of Operation | % Total hp |
|----------------|----------------|-----------------------------|-------------------|
| Natural gas | 60 | 80 | 90 |
| Dual fuel | 22.5 | 8 | 4.0 |
| Distillate oil | 15 | 6 | 0.6 |
| Residual oil | 2.0 | 5 | 5 |
| Crude oil | .2 | .5 | 0.4 |
| Other | 0.3 | .5 | – |

treatment was initiated. Eventually, the corrosion-causing materials were discovered, and a fuel treatment system to limit corrosion was developed.

Power plants in both peaking and standby modes achieved 30,000 hours between major overhauls. It was during these operations that the deposit problem on the turbine nozzles became apparent. Also, deposits developed on the fuel nozzles, a situation that could cause deviation in the fuel spray angle and related combustion problems. Therefore, both turbine and fuel nozzles needed frequent cleaning.

As discussed earlier, economic situations heavily dictate fuel selection. After the surge of interest in gas turbines in the early 1950s, use in the 1960s dwindled because of the cost, problems, and availability of natural gas. The 1990s have seen a tremendous growth in gas turbine usage with the advent of the high-efficiency gas turbines (40–45%), being used in Combined Cycle Power Plants, which have plant efficiencies between 55–60%. Most of these turbines were all driven by natural gas. In 2000–2001, gas turbines are backordered for the next three to five years. All this growth in the turbine has been fueled by cheap natural gas at \$3.50/mmBTU (\$3.32/mmkJ). The cost of natural gas in late 2001 is heading to \$9.0/mmBTU (\$8.53/mmkJ), this will make alternative fuels interesting once again. Table 12-10 is an estimate of the world population of gas turbines, and it reflects the growth of natural gas driven gas turbines in the late 1990s and early 2000s.

Heat Tracing of Piping Systems

As mentioned earlier, heavy fuels need to be kept at a temperature where the viscosity of the fuel is limited to 20 centistokes at the fuel nozzles. Heat tracing is used to maintain pipes and the material that pipes contain at temperatures above the ambient temperature. Two common uses of heat tracing are preventing water pipes from freezing and maintaining fuel oil pipes at high enough

temperatures such that the viscosity of the fuel oil will allow easy pumping. Heat tracing is also used to prevent the condensation of a liquid from a gas.

A heat-tracing system is often more expensive on an installed cost basis than the piping system it is protecting, and it will also have significant operation costs. A recent study on heat-tracing costs showed installed costs of \$31/ft (\$95/meter) to \$142/ft (\$430/meter) and yearly operating cost of \$1.40/ft (\$4.35/meter) to \$16.66/ft (\$50/meter). In addition to being a major cost, the heat-tracing system is an important component of the reliability of a piping system. A failure in the heat-tracing system will often render the piping system inoperable. For example, with a water freeze protection system; the piping system may be destroyed by the expansion of water as it freezes if the heat-tracing system fails.

The vast majority of heat-traced pipes are insulated to minimize heat loss to the environment. A heat input of 2 to 10 watts per foot (6 to 30 watts per meter) is generally required to prevent an insulated pipe from freezing. With high wind speeds, an un-insulated pipe could require well over 100 watts per foot (300 watts per meter) to prevent freezing. Such a high heat input would be very expensive.

Heat tracing for insulated pipes is generally only required for the period when the material in the pipe is not flowing. The heat loss of an insulated pipe is very small compared to the heat capacity of a flowing fluid. Unless the pipe is extremely long (several thousands of feet or meters), the temperature drop of a flowing fluid will not be significant.

The three major methods of avoiding heat tracing are:

1. Changing the ambient temperature around the pipe to a temperature that will avoid low-temperature problems. Burying water pipes below the frost line or running them through a heated building are the two most common examples of this method.
2. Emptying a pipe after it is used. Arranging the piping such that it drains itself when not in use, can be an effective method of avoiding the need for heat tracing. Some infrequently used lines can be pigged or blown out with compressed air. This technique is not recommended for commonly used lines due to the high labor requirement.
3. Arranging a process such that some lines have continuous flow can eliminate the need for tracing these lines. This technique is generally not recommended because a failure that causes a flow stoppage can lead to blocked or broken pipes.

Some combination of these techniques may be used to minimize the quantity of traced pipes. However, the majority of pipes containing fluids that must

be kept above the minimum ambient temperature are generally going to require heat tracing.

Types of Heat-Tracing Systems

Industrial heat-tracing systems are generally fluid systems or electrical systems. In fluid systems, a pipe or tube called the tracer is attached to the pipe being traced, and a warm fluid is put through it. The tracer is placed under the insulation. Steam is by far the most common fluid used in the tracer, although ethylene glycol and more exotic heat-transfer fluids are used. In electrical systems, an electrical heating cable is placed against the pipe under the insulation.

Stream Tracing Systems

Steam tracing is the most common type of industrial pipe tracing. In 1960, over 95 percent of industrial tracing systems were steam traced. By 1995, improvements in electric heating technology increased the electric share to 30 to 40 percent, but steam tracing is still the most common system. Fluid systems other than steam are rather uncommon and account for less than 5% of tracing systems.

Half-inch (12.7 mm) copper tubing is commonly used for steam tracing. Three-eighths-inch (9.525 mm) tubing is also used, but the effective circuit length is then decreased from 150 feet (50 meters) to about 60 feet (20 meters). In some corrosive environments, stainless steel tubing is used, and occasionally standard carbon steel pipe ($\frac{1}{2}$ –1 inch) is used as the tracer.

In addition to the tracer, a steam tracing system as seen in Figure 12-12, consists of steam supply lines to transport steam from the existing steam lines to the traced pipe, a steam trap to remove the condensate and hold back the steam, and in most cases a condensate return system to return the condensate to the existing condensate return system. In the past, a significant percentage of condensate from steam tracing was simply dumped to drains, but increased energy cost and environmental rules have caused almost all condensate from new steam tracing systems to be returned. This has significantly increased the initial cost of steam tracing systems.

Applications requiring accurate temperature control are generally limited to electric tracing. For example, chocolate lines cannot be exposed to steam temperatures or the product will degrade, and if caustic soda is heated above 150 °F (66 °C), it becomes extremely corrosive to carbon steel pipes.

For some applications, either steam or electricity is simply not available and this makes the decision. It is rarely economic to install a steam boiler

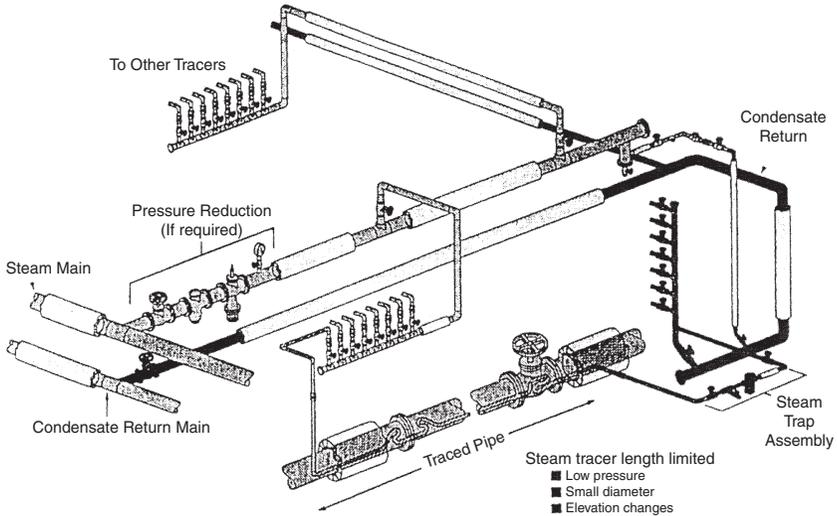


Figure 12-12. Steam tracing system.

just for tracing. Steam tracing is generally considered only when a boiler already exists or is going to be installed for some other primary purpose. Additional electric capacity can be provided in most situations for reasonable costs. It is considerably more expensive to supply steam from a long distance than it is to provide electricity. Unless steam is available close to the pipes being traced, the automatic choice is usually electric tracing.

Electric Tracing

An electric tracing system as seen in Figure 12-13 consists of an electric heater placed against the pipe under the thermal insulation, the supply of electricity to the tracer, and any control or monitoring system that may be used (optional). The supply of electricity to the tracer usually consists of an electrical panel and electrical conduit or cable trays. Depending on the size of the tracing system and the capacity of the existing electrical system, an additional transformer may be required.

Storage of Liquids

Atmospheric Tanks

The term atmospheric tank as used here applies to any tank that is designed to be used within plus or minus a few pounds per square foot (a few tenths of

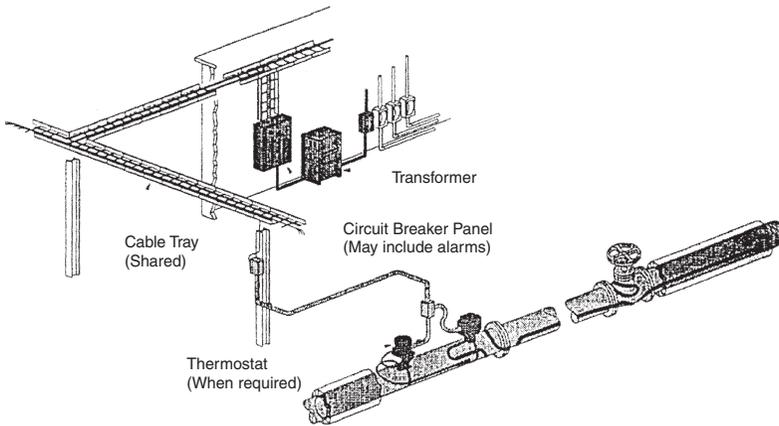


Figure 12-13. Electric heat tracing system.

a Bar) of atmospheric pressure. It may be either open to the atmosphere or enclosed. Minimum cost is usually obtained with a vertical cylindrical shape and a relatively flat bottom at ground level.

Elevated Tanks

These can supply a large flow when required, but pump capacities need be only for average flow. Thus, they may save on pump and piping investment. They also provide flow after pump failure, an important consideration for fire systems.

Open Tanks

These may be used to store materials that will not be harmed by water, weather, or atmospheric pollution. Otherwise, a roof, either fixed or floating, is required. Fixed roofs are usually either domed or coned. Large tanks have coned roofs with intermediate supports. Since negligible pressure is involved, snow and wind are the principal design loads. Local building codes often give required values.

Fixed Roof Tanks

Atmospheric tanks require vents to prevent pressure changes, which would otherwise result from temperature changes and the withdrawal or the addition of liquid. API Standard 2000, venting atmospheric and Low

Pressure Storage Tanks, gives practical rules for vent design. The principals of this standard can be applied to fluids other than petroleum products. Excessive losses of volatile liquids, particularly those with flash points below 100 °F (38 °C), may result from the use of open vents on fixed-roof tanks. Sometimes vents are manifolded and led to a vent tank, or the vapor may be extracted by a recovery system.

An effective way of preventing vent loss is to use one of the many types of variable-volume tanks. These are built under API Standard 650. They may have floating roofs of the double-deck or the single-deck type. There are lifter-roof types in which the roof either has a skirt moving up and down in an annular liquid seal or is connected to the tank shell by a flexible membrane. A fabric expansion chamber housed in a compartment on top of the tank roof also permits variation in volume.

Floating Roof Tanks

These tanks must have a seal between the roof and the tank shell. If not protected by a fixed roof, they must have drains for the removal of water, and the tank shell must have a “wind girder” to avoid distortion. An industry has developed to retrofit existing tanks with floating roofs. Much detail on the various types of tank roofs is given in manufacturers’ literature. Figure 12-14 shows types. These roofs cause less condensation build up and are highly recommended.

Pressure Tanks

Vertical cylindrical tanks constructed with domed or coned roofs, which operate at pressures above 15 psia (1 Bar) but are still relatively close to atmospheric pressure, can be built according to API Standard 650. The pressure force acting against the roof is transmitted to the shell, which may have sufficient weight to resist it. If not, the uplift will act on the tank bottom. The strength of the bottom, however, is limited, and if it is not

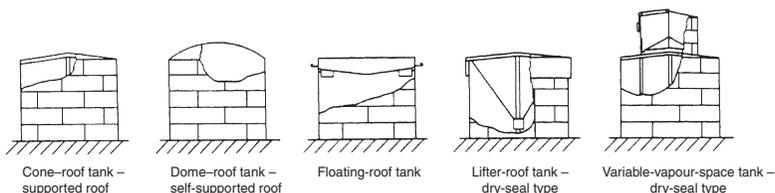


Figure 12-14. Some types of atmospheric storage tanks.

sufficient, an anchor ring or a heavy foundation must be used. In the larger sizes, uplift forces limit this style of tank to very low pressures.

Bibliography

- Bahr, D.W., Smith, J.R., and Kenworthy, N.J., "Development of Low Smoke Emission Combustors for Large Aircraft Turbine Engines," AIAA Paper Number 69-493.
- Boyce, M.P., "Chapter 10. Transport and Storage of Fluids-Process-Plant Piping," *Perry's Chemical Engineers' Handbook*, 7th Edition, 1997.
- Boyce, M.P., Trevillion, W., and Hoehing, W.W., "A New Gas Turbine Fuel," *Diesel & Gas Turbine Progress*, March 1978 (Reprint).
- Boyce, M.P., Trevillion, W., and Hoehing, W.W., "A New Gas Turbine Fuel," *Diesel & Gas Turbine Progress*, March 1978 (Reprint).
- Brown Boveri Turbomachinery, Inc., "MEGA PAK CT, The simple cycle combustion turbine plant designed for today's energy needs," Pub. No. 4875-BIO-7610.
- Combustors for Large Aircraft Turbine Engines, AIAA Paper Number 69-493.

Part IV

Auxiliary Components and Accessories

13

Bearings and Seals

Bearings

The bearings in gas and steam turbines provide support and positioning for the rotating components. Radial support is generally provided by journal, or roller bearings, and axial positioning is provided by thrust bearings. Some engines, mainly aircraft jet engines, use ball or roller bearings for radial support, but nearly all-industrial gas turbines use journal bearings.

A long service life, a high degree of reliability and economic efficiency are the chief aims when designing bearing arrangements. To reach these criteria, design engineers examine all the influencing factors:

1. Load and speed
2. Lubrication
3. Temperatures
4. Shaft arrangements
5. Life
6. Mounting and dismounting
7. Noise
8. Environmental conditions

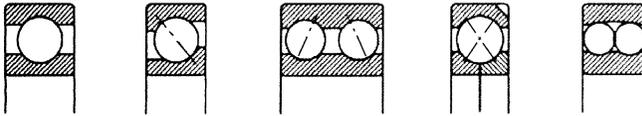
Rolling Bearings

The aeroderivative gas turbine design, with its low supported—weight rotors—for example, the LM 5000 HP rotor weighs 1,230 lbs (558 kg)—incorporates roller bearings throughout. These do not require the large lube oil reservoirs, coolers and pumps, or the pre- and post-lube cycle associated with journal bearing designs. Roller bearings have proven to be extremely

rugged and have demonstrated excellent life in industrial service. Most bearings provide reliable service for over 100,000 hours. In practice, it is advisable to replace bearings when exposed during major repairs, estimated at 50,000 hours for gas generators and 100,000 hours for power turbines.

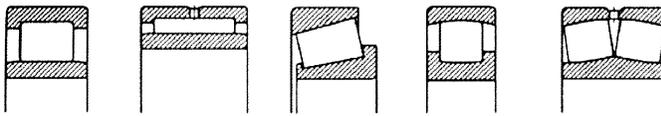
There are many roller bearing types. They are differentiated according to the direction of the main radial loads (radial bearings) or axial loads (thrust

Radial ball bearings



Deep groove ball bearing Angular contact ball bearing single row Angular contact ball bearing double row Four-point bearing Self-aligning ball bearing

Radial roller bearings



Cylindrical roller bearing Needle roller bearing Tapered roller bearing Barrel roller bearing Spherical roller bearing

Thrust ball bearings



Thrust ball bearing Angular contact thrust ball bearing double direction

Thrust roller bearings



Cylindrical roller thrust bearing Spherical roller thrust bearing

Figure 13-1. Types of rolling bearings. (Courtesy FAG bearings.)

bearings), and the type of rolling elements used, balls or rollers. Figure 13-1 shows the different types of bearings. The essential difference between ball bearings and roller bearings are that ball bearings have a lower carrying capacity and higher speeds, while the roller bearings have higher load carrying capacity and lower speeds.

The rolling elements transmit loads from one bearing ring to the other in the direction of the contact lines. The contact angle α is the angle formed by the contact lines and the radial plane of the bearing. α refers to the nominal contact angle, i.e., the contact angle of the load-free bearing as seen in Figure 13-2. Under axial loads, the contact angle of deep groove ball bearings, angular contact ball bearings, etc., increases. Under a combined load it changes from one rolling element to the next. These changing contact angles are taken into account when calculating the pressure distribution within the bearing. Ball bearings and roller bearings with symmetrical rolling elements have identical contact angles at their inner rings and outer rings. In roller bearings with asymmetrical rollers, the contact angles at the inner rings and outer rings are not identical. The equilibrium of forces in these bearings is

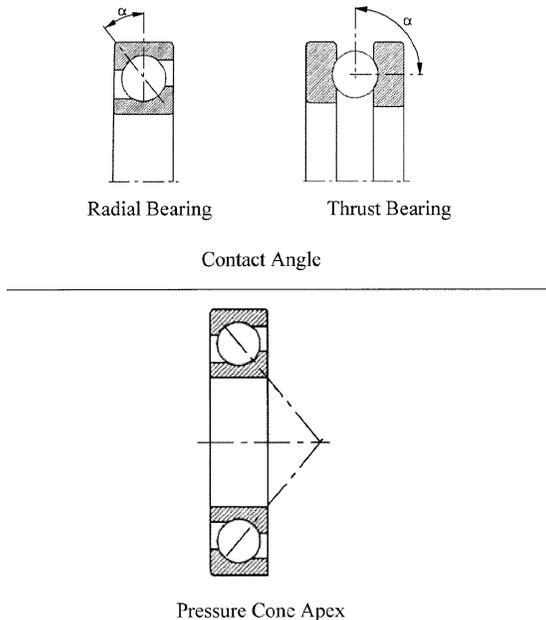
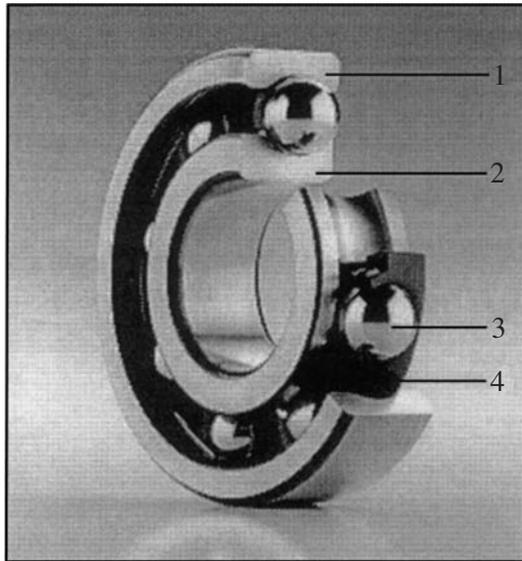


Figure 13-2. Rolling bearing terminology. (Courtesy FAG bearings.)

maintained by a force component, which is directed towards the lip. The pressure cone apex is that point on the bearing axis where the contact lines of an angular contact bearing (i.e., an angular contact ball bearing, a tapered roller bearing, or a spherical roller thrust bearing, intersect). The contact lines are the generatrices of the pressure cone apex. In angular contact bearings, the external forces act, not at the bearing center, but at the pressure cone apex.

Rolling bearings generally consist of bearing rings, inner ring and outer ring, rolling elements that roll on the raceways of the rings, and a cage that surrounds the rolling elements as seen in Figure 13-3. The rolling elements are classified according to their shapes. Into balls, cylindrical rollers, needle rollers, tapered rollers, and barrel rollers as shown in Figure 13-4.

The rolling elements' function is to transmit the force acting on the bearing from one ring to the other. For a high load carrying capacity it is important that as many rolling elements as possible, which are as large as possible, are accommodated between the bearing rings. Their number and size depend on the cross section of the bearing. It is just as important for load ability that the rolling elements within the bearing are of identical size. Therefore, they are sorted according to grades. The tolerance of one grade



1 Outer ring, 2 Inner ring, 3 Rolling element, 4 Cage

Figure 13-3. Roller bearing showing the various components. (Courtesy FAG Bearings.)

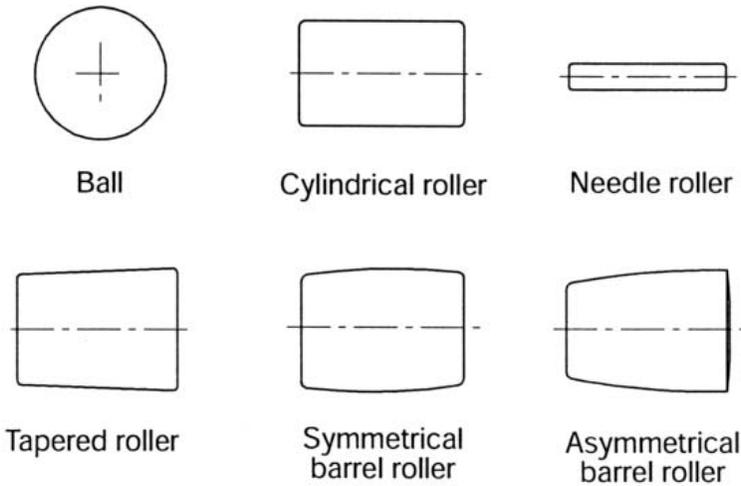


Figure 13-4. Various types of rollers used in a rolling bearing. (Courtesy FAG bearings.)

is very slight. The generatrices of cylindrical rollers and tapered rollers have a logarithmic profile. The center part of the generatrix of a needle roller is straight, and the ends are slightly crowned, this profile prevents edge stressing when under load.

The bearing rings comprise of an inner ring and an outer ring to guide the rolling elements in the direction of rotation. Raceway grooves, lips, and inclined running areas guide the rollers and transmit axial loads in transverse direction as seen in Figure 13-5. Cylindrical roller bearings and needle roller bearings, which need to accommodate shaft expansions have lips only on one bearing ring and are commonly known as floating bearings.

The functions of a cage are to keep the rolling elements apart so that they do not rub against each other, to keep the rolling elements evenly spaced for uniform load distribution, to prevent rolling elements from falling out of separable bearings and bearings that are swiveled out and to guide the rolling elements in the unloaded zone of the bearing. The transmission of forces is not one of the cage's functions.

Cages are classified into pressed cages, machined cages, and moulded cages. Pressed cages are usually made of steel, but sometimes of brass, too. They are lighter than machined metal cages. Since a pressed cage barely closes the gap between inner ring and outer ring, lubricant can easily penetrate into the bearing.

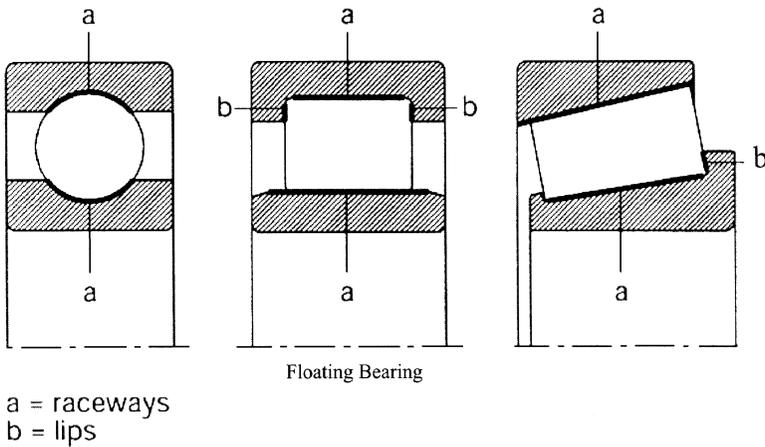


Figure 13-5. Raceway grooves and lips for typical roller bearings. (Courtesy FAG bearings.)

Machined cages of metal and textile laminated phenolic resin are made from tubes of steel, light metal or textile laminated phenolic resin, or cast brass rings. To obtain the required strength, large, heavily loaded bearings are fitted with machined cages. Machined cages are also used where lip guidance of the cage is required. Lip-guided cages for high-speed bearings are in many cases made of light materials such as light metal or textile laminated phenolic resin to keep the forces of gravity low.

Molded cages using injection molding techniques can realize designs with an especially high-load carrying capacity. Injection molding has made it possible to realize cage designs with an especially high-load carrying capacity. The elasticity and low weight of the cages are of advantage where shock-type bearing loads, great accelerations and decelerations as well as tilting of the bearing rings relative to each other have to be accommodated. Polyamide cages feature very good sliding and dry running properties.

There are a number of special rolling bearing designs and some series of cylindrical roller bearings without cages. By omitting the cage the bearing can accommodate more rolling elements. This yields an increased load rating, but, due to the increased friction, the bearing is suitable for lower speeds only.

Load ratings. The load rating of a bearing reflects its load carrying capacity and is an important factor in the dimensioning of rolling bearings. It is determined by the number and size of the rolling elements, the curvature ratio, the contact angle, and the pitch circle diameter of the bearing. Due to

the larger contact area between rollers and raceways the load ratings of roller bearings are higher than those of ball bearings.

The load rating of a radial bearing is defined by radial loads whereas that of a thrust bearing is defined by axial loads. Every rolling bearing has a dynamic load rating and a static load rating. The terms “dynamic” and “static” refer to the movement of the bearing but not to the type of load.

In all rolling bearings with a curved raceway profile, the radius of the raceway is slightly larger than that of the rolling elements. This curvature difference in the axial plane is defined by the curvature ratio x . The curvature ratio is the curvature difference between the rolling element radius and the slightly larger groove radius.

$$\text{radius curvature ratio } x = (\text{groove radius} - \text{rolling element}) / \text{rolling element radius}$$

Thrust ball bearings are used where purely axial loads have to be accommodated. The single direction (= single row) design is designed for loads from one direction, the double direction one (= double row) for reversing loads. Besides the design with flat washers, designs with spherical housing washers and seating washers are also available that can compensate for misalignment.

Spherical roller thrust bearings can accommodate high axial loads. They are suitable for relatively high speeds. The raceways, which are inclined toward the bearing axis, allow the bearings to accommodate radial loads as well. The radial load must not exceed 55% of the axial load.

The bearings have asymmetrical barrel rollers and compensate for misalignment. As a rule, spherical roller thrust bearings have to be lubricated with oil.

Wear. The life of rolling bearings can be terminated, apart from fatigue, as a result of wear. The clearance of a worn bearing gets too large.

One frequent cause of wear is that foreign particles penetrate into a bearing due to insufficient sealing and have an abrasive effect. Wear is also caused by starved lubrication and when the lubricant is used up.

Therefore, wear can be considerably reduced by providing good lubrication conditions (viscosity ratio $x > 2$ if possible) and a good degree of cleanliness in the rolling bearing. Where $x \leq 0.4$ wear will dominate in the bearing if it is not prevented by suitable additives (EP additives).

The kinematically permissible speed may be higher or lower than the thermal reference speed. The basis of the thermal reference speed for cases where the operating conditions (load, oil viscosity, or permissible

temperature) deviate from the reference conditions. Decisive criteria for the kinematically permissible speed are the strength limit of the bearing parts and the permissible sliding velocity of rubbing seals. Kinematically permissible speeds, which are higher than the thermal reference speeds, can be reached, for example, with specially designed lubrication, bearing clearance adapted to the operating conditions, and accurate machining of the bearing seats with special regard to heat dissipation.

The thermal reference speed is a new index of the speed suitability of rolling bearings. It is defined as the speed at which the reference temperature of 160 °F (70 °C) is established. For high temperature rolling bearings, the steel used for bearing rings and rolling elements is generally heat-treated so that it can be used at operating temperatures of up to 300 °F (150 °C). At higher temperatures, dimensional changes and hardness reductions result. Therefore, operating temperatures over 300 °F (150 °C) require special heat treatment.

Journal Bearings

The heavy frame type gas turbines use journal bearings. Journal bearings may be either full round or split; the lining may be heavy as used in large-size bearings for heavy machinery, or thin, as used in precision insert-type bearings in internal combustion engines. Most sleeve bearings are of the split type for convenience in servicing and replacement. Often in split bearings, where the load is entirely downward, the top half of the bearing acts only as a cover to protect the bearing and to hold the oil fittings. Figure 13-6 shows a number of different types of journal bearings. A description of a few of the pertinent types of journal bearings is given here:

1. *Plain journal.* Bearing is bored with equal amounts of clearance (on the order of $1\frac{1}{2}$ to two thousandths of an inch per inch of journal diameter) between the journal and bearing.
2. *Circumferential grooved bearing.* Normally has the oil groove at half the bearing length. This configuration provides better cooling, but reduces load capacity by dividing the bearing into two parts.
3. *Cylindrical bore bearings.* Another common bearing type used in turbines. It has a split construction with two axial oil-feed grooves at the split.
4. *Pressure or pressure dam.* Used in many places where bearing stability is required, this bearing is a plain journal bearing with a pressure pocket cut in the unloaded half. This pocket is approximately $1/32$ of an inch (.8 mm) deep with a width 50% of the bearing length.

| BEARING TYPE | LOAD CAPACITY | SUITABLE DIRECTION OF ROTATION | RESISTANCE TO HALF-SPEED WHIRL | STIFFNESS AND DAMPING |
|--|---------------|--|---------------------------------------|-----------------------|
| CYLINDRICAL BORE  | GOOD |  | WORST ↓ INCREASING ↓ BEST | MODERATE |
| CYLINDRICAL BORE WITH DAMMED GROOVE  | GOOD |  | | MODERATE |
| LEMON BORE  | GOOD |  | | MODERATE |
| THREE LOBE  | MODERATE |  | | GOOD |
| OFFSET HALVES  | GOOD |  | | EXCELLENT |
| TILTING PAD  | MODERATE |  | | GOOD |

Figure 13-6. Comparison of general bearing types.

This groove or channel covers an arc of 135° and terminates abruptly in a sharp-edge dam. The direction of rotation is such that the oil is pumped down the channel toward the sharp edge. Pressure dam bearings are for one direction of rotation. They can be used in conjunction with cylindrical bore bearings as shown in Figure 13-6.

5. *Lemon bore or elliptical.* This bearing is bored with shims at the split line, which are removed before installation. The resulting bore shape approximates an ellipse with the major axis clearance approximately twice the minor axis clearance. Elliptical bearings are for both directions of rotation.

6. *Three-lobe bearing*. The three-lobe bearing is not commonly used in turbomachines. It has a moderate load-carrying capacity and can be operated in both directions.
7. *Offset halves*. In principle, this bearing acts very similar to a pressure dam bearing. Its load-carrying capacity is good. It is restricted to one direction of rotation.
8. *Tilting-pad bearings*. This bearing is the most common bearing type in today's machines. It consists of several bearing pads posed around the circumference of the shaft. Each pad is able to tilt to assume the most effective working position. Its most important feature is self-alignment when spherical pivots are used. This bearing also offers the greatest increase in fatigue life because of the following advantages:
 - a. Self-aligning for optimum alignment and minimum limit.
 - b. Thermal conductivity backing material to dissipate heat developed in oil film.
 - c. A thin babbitt layer can be centrifugally cast with a uniform thickness of about 0.005 of an inch (0.127 mm). Thick babbitts greatly reduce bearing life. Babbitt thickness in the neighborhood of .01 in. (.254 mm) reduce the bearing life by more than half.
 - d. Oil film thickness is critical in bearing stiffness calculations. In a tilting-pad bearing, one can change this thickness in a number of ways: (1) changing the number of pads; (2) directing the load on or in-between the pads; (3) and changing axial length of pad.

The previous list contains some of the most common types of journal bearings. They are listed in the order of growing stability. All of the bearings designed for increased stability are obtained at higher manufacturing costs and reduced efficiency. The antiwhirl bearings all impose a parasitic load on the journal, which causes higher power losses to the bearings, and in turn, requires higher oil flow to cool the bearing. Many factors enter into the selection of the proper design for bearings. Some of the factors that affect bearing design follow:

1. Shaft speed range.
2. Maximum shaft misalignment that can be tolerated.
3. Critical speed analysis and the influence of bearing stiffness on this analysis.
4. Loading of the compressor impellers.
5. Oil temperatures and viscosity.

6. Foundation stiffness.
7. Axial movement that can be tolerated.
8. Type of lubrication system and its contamination.
9. Maximum vibration levels that can be tolerated.

Bearing Design Principles

The journal bearing is a fluid-film bearing. This description means that a full film of fluid completely separates the stationary bushing from the rotating journal—the two components that make up the bearing system. This separation is achieved by pressurizing the fluid in the clearance space to the extent that the fluid forces a balance in the bearing load. This balance requires the fluid to be continuously introduced into and pressurized in the film space. Figure 13-7 shows the four modes of lubrication in a fluid-film bearing. The hydrodynamic mode bearing is the most common bearing type used and is also often called the “self-acting” bearing.

As can be seen in Figure 13-7a, the pressure is self-induced by the relative motion between the two bearing member surfaces. The film is wedge-shaped in this type of lubrication mode. Figure 13-7b shows the hydrostatic mode of lubrication. In this type of a bearing, the lubricant is pressurized externally and then introduced in the bearing. Figure 13-7c shows the squeeze-film lubrication mode. This type of a bearing derives its load-carrying capacity and separation from the fact that a viscous fluid cannot be instantaneously

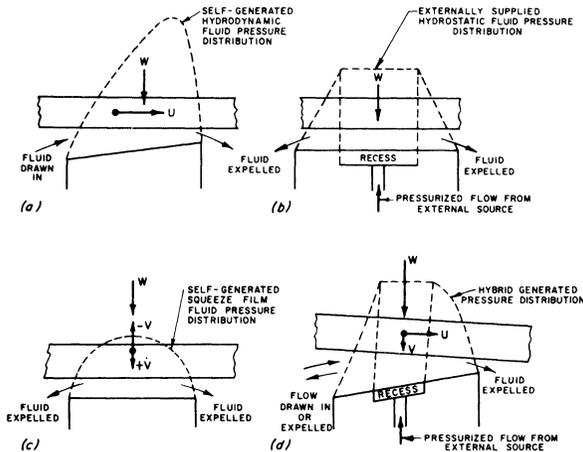


Figure 13-7. Modes of fluid-film lubrication: (a) hydrodynamic, (b) hydrostatic, (c) squeeze film, (d) hybrid.

squeezed out between two surfaces that are approaching each other. Figure 13-7d shows a hybrid-type bearing that combines the previous modes. The most common hybrid type combines the hydrodynamic and hydrostatic modes.

A further investigation of the hydrodynamic mode is warranted, since it is the most common type of lubrication mode employed. This type of lubrication depends on the bearing member velocity as well as the existence of a wedge-shaped configuration. The journal bearing forms a natural wedge as seen in Figure 13-8, which is inherent in its design. Figure 13-3 also shows the pressure distribution in the bearing. Fluid-film thickness depends on the mode, lubrication, and application and varies from .0001 to .01 inches (.00254–.254 mm.) For hydrostatic oil-lubricated bearings, the film thickness is .008 of an inch (.203 mm). In the special case of oil-squeeze film bearings where the capacity must be provided to take extremely high-revising loads with no bearing harm, the oil-film thickness could be below .0001 of an inch (.00254 mm). Since the film thickness is so very important, an understanding of the surface is very important.

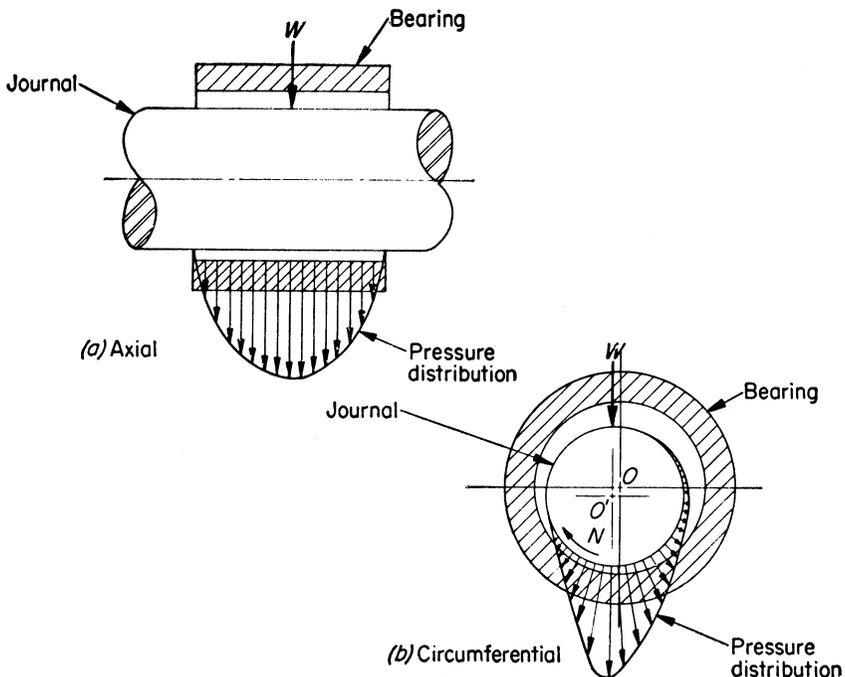


Figure 13-8. Pressure distribution in a full journal bearing.

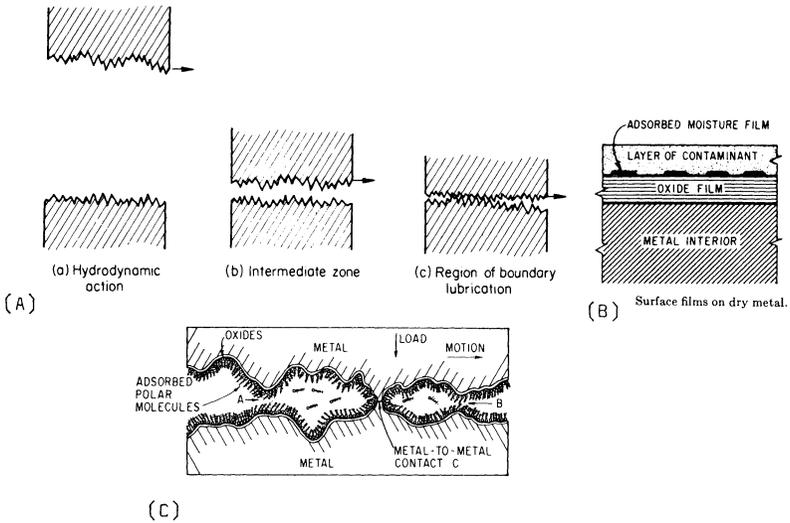


Figure 13-9. Enlarged views of bearing surfaces.

All surfaces, regardless of their finish, are made up of peaks and valleys, and in general, the average asperity height may be 5–10 times the RMS surface finish reading. When the surface is abraded, an oxide film will form almost immediately.

Figure 13-9a shows the relative separation of the full-film, mixed-film, and boundary. If a full-film exists, the bearing life is almost infinite. The limitation in the case of full-film is due to lubricant breakdown, shock load, bearing surface erosion, and fretting of bearing components. Figures 13-9b and 13-9c are cross sections showing the various contamination types. Oil additives are contaminants that form beneficial surface films.

The bearing health can be best described by plotting a ZN/P versus coefficient of friction curve. Figure 13-10 shows such a curve where Z is the lubricant viscosity in centipoise, N the rpm of the journal, and P is the projected area unit loading.

As the bearing speed is increased for a given lubricant and loading, the friction is at its lowest when full-film is achieved, after which the increase is due to the increasing lubricant shear force.

The bearing fluid film acts like a spring that is nonlinear. Figure 13-11 shows a curve of bearing load versus film thickness and eccentricity ratio. The bearing stiffness can then be obtained at any load value by drawing a line tangent to the curve at the load point. The film stiffness can then be used in determining the critical speed of the rotor.

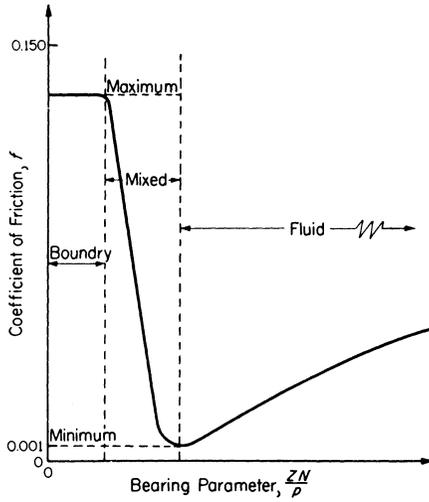


Figure 13-10. Classic ZN/P curve.

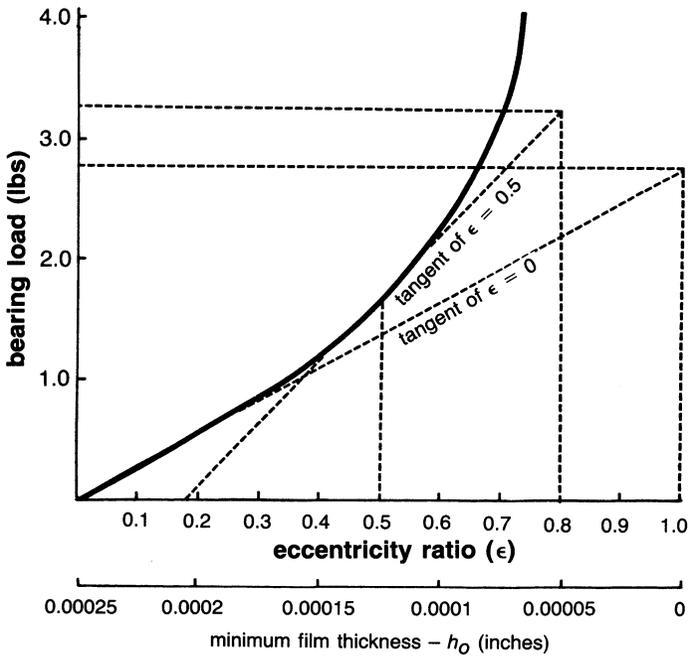


Figure 13-11. Journal bearing load capacity versus minimum film thickness and eccentricity ratio.

With higher speeds and unusual fluid lubricants, turbulence in the fluid film is no longer rare. Normally, thin film is thought of as being laminar, but with high speeds, low viscosity, and sometimes high-density fluids, the lubricant can be turbulent in the film space. This turbulence manifests itself as an abnormal increase in power loss. As compared to laminar-flow conditions, a Reynolds number, even in the transition region, can double the power and, deep in the turbulent region, can increase the power tenfold. Although this phenomenon, because of its random nature, is difficult to analyze, there is an unusual amount of theoretical work that has been done and some experimental work that is available. Just as a guide, one can assume that the transition point will occur at a Reynolds number of about 800. As to film thickness, there is evidence indicating that under turbulent conditions it is actually greater than calculated, based on laminar-flow theory.

Tilting-Pad Journal Bearings

Normally, the tilting-pad journal bearing is considered when shaft loads are light because of its inherent ability to resist oil whirl vibration. However, this bearing, when properly designed, has a very high load-carrying capacity. It has the ability to tilt to accommodate the forces being developed in the hydrodynamic oil film, and therefore operates with an optimum oil-film thickness for the given load and speed. This ability to operate over a large range of load is especially useful in high-speed gear reductions with various combinations of input and output shafts.

Another important advantage of the tilting-pad journal bearing is its ability to accommodate shaft misalignment. Because of its relatively short length-to-diameter ratio, it can accommodate minor misalignment quite easily.

As shown earlier, bearing stiffness varies with the oil-film thickness so that the critical speed is directly influenced to a certain degree by oil-film thickness. Again, in the area of critical speeds, the tilting-pad journal bearing has the greatest degree of design flexibility. There are sophisticated computer programs that show the influence of various load and design factors on the stiffness of tilting-pad journal bearings. The following variations are possible in the design of tilting-pad bearings:

1. The number of pads can be varied from three to any practical number.
2. The load can be placed either directly on a pad or to occur between pads.

3. The unit loading on the pad can be varied by either adjusting the arc length or the axial length of the bearing pad.
4. A parasitic pre-load can be designed into the bearing by varying the circular curvature of the pad with respect to the curvature of the shaft.
5. An optimum support point can be selected to obtain a maximum oil-film thickness.

On a high-speed rotor system, it is necessary to use tilting-pad bearings because of the dynamic stability of these bearings. A high-speed rotor system operates at speeds above the first critical speed of the system. It should be understood that a rotor system includes the rotor, the bearings, the bearing support system, seals, couplings, and other items attached to the rotor. The system's natural frequency is therefore dependent on the stiffness and damping effect of these components.

Commercial multipurpose tilting-pad bearings are usually designed for multidirectional rotation so that the pivot point is at pad midpoint. However, the design criteria generally applied for producing maximum stability and load-carrying capacity locates the pivot at two-thirds of the pad arc in the direction of rotation.

Bearing pre-load is another important design criterion for tilting-pad bearings. Bearing pre-load is bearing assembly clearance divided by machined clearance

$$\text{Pre-load ratio} = C'/C = \frac{\text{Concentric pivot film thickness}}{\text{Machined clearance}}$$

A pre-load of 0.5–1.0 provides for stable operation because a converging wedge is produced between the bearing journal and the bearing pads.

The variable C' is an installed clearance and is dependent upon the radial pivot position. The variable C is the machine clearance and is fixed for a given bearing. Figure 13-7 shows two pads of a five-pad tilting-pad bearing where the pads have been installed such that the pre-load ratio is less than one, and Pad 2 has a pre-load ratio of 1.0. The solid line in Figure 13-7 represents the position of the journal in the concentric position. The dashed line represents the journal in a position with a load applied to the bottom pads.

From Figure 13-12, Pad 1 is operating with a good converging wedge, while Pad 2 is operating with a completely diverging film, thus indicating that the pad is completely unloaded. Therefore, bearings with pre-load ratios of 1.0 or greater will be operating with some of their pads completely unloaded, thus reducing the overall stiffness of the bearing and decreasing its stability, since the upper pads do not aid in resisting cross-coupling influences.

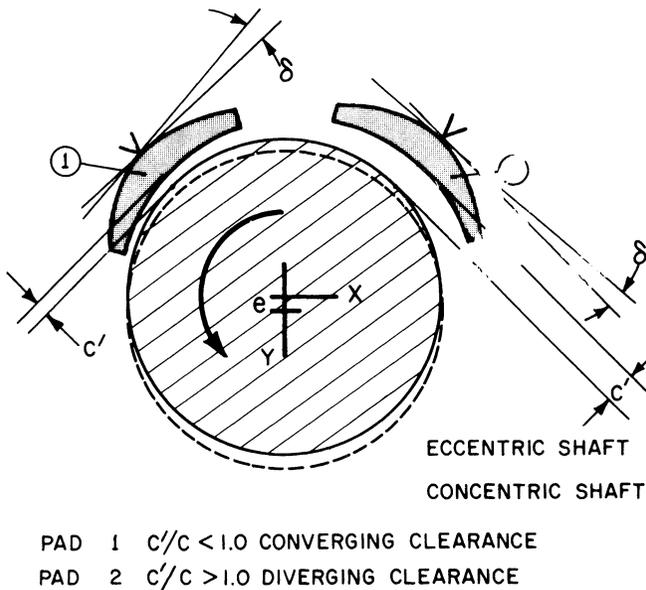


Figure 13-12. Tilting-pad bearing pre-load.

Unloaded pads are also subject to flutter, which leads to a phenomenon known as “leading-edge lock-up.” Leading-edge lock-up causes the pad to be forced against the shaft, and it is then maintained in that position by the frictional interaction of the shaft and the pad. Therefore, it is of prime importance that the bearings be designed with pre-load, especially for low-viscosity lubricants. In many cases, manufacturing reasons and the ability to have two-way rotation cause many bearings to be produced without pre-load.

Bearing designs are also affected by the transition of the film from a laminar to a turbulent region. The transition speed (N_t) can be computed using the following relationship:

$$N_t = 1.57 \times 10^3 \frac{\nu}{\sqrt{DC^3}}$$

where:

ν = viscosity of the fluid

D = diameter (inches)

C = diametrical clearance (inches)

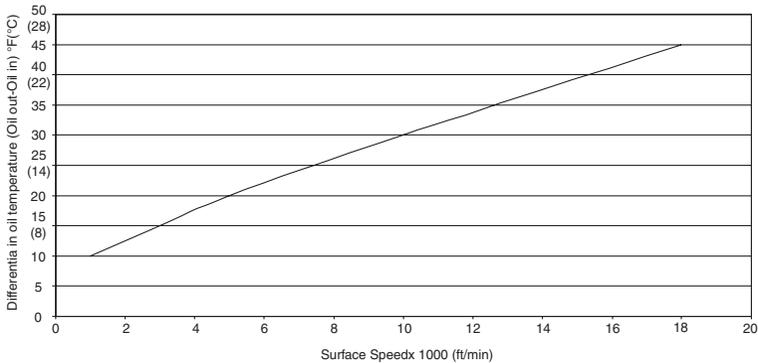


Figure 13-13. Oil discharge characteristics.

Turbulence creates more power absorption, thus increasing oil temperature that can lead to severe erosion and fretting problems in bearings. It is desirable to keep the oil discharge temperature below 170°F (77°C), but with high-speed bearings, this ideal may not be possible. In those cases, it is better to monitor the temperature difference between the oil entering and leaving as shown in Figure 13-13.

Bearing Materials

In all the time since Issaac Babbitt patented his special alloy in 1839, nothing has been developed that encompasses all of its excellent properties as an oil-lubricated bearing surface material. Babbitts have excellent compatibility and nonscoring characteristics and are outstanding in embedding dirt and conforming to geometric errors in machine construction and operation. They are, however, relatively weak in fatigue strength, especially at elevated temperatures and when the babbitt is more than about 0.015 of an inch (.381 mm) thick as seen in Figure 13-14. In general, the selection of a bearing material is always a compromise, and no single composition can include all desirable properties. Babbitts can tolerate momentary rupture of the oil film, and may well minimize shaft or runner damage in the event of a complete failure. Tin babbitts are more desirable than the lead-based materials, since they have better corrosion resistance, less tendency to pickup on the shaft or runner, and are easier to bond to a steel shell.

Application practices suggest a maximum design temperature of about 300°F (149°C) for babbitt, and designers will set a limit of about 50°F (28°C) less. As temperatures increase, there is a tendency for the metal to

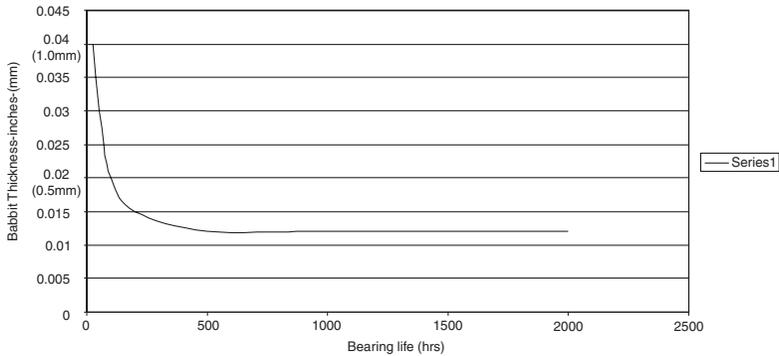


Figure 13-14. Babbitt fatigue characteristics.

creep under the softening influence of the rising temperature. Creep can occur with generous film thickness and can be observed as ripples on the bearing surface where flow took place. With tin babbitts, observation has shown that creep temperature ranges from 375 °F (190 °C) for bearing loads below 200 psi (13.79 Bar) to about 260–270 °F (127–132 °C) for steady loads of 1000 psi (69 Bar). This range may be improved by using very thin layers of babbitt such as in automotive bearings.

Bearing and Shaft Instabilities

One of the most serious forms of instability encountered in journal bearing operation is known as “half-frequency whirl.” It is caused by self-excited vibration and characterized by the shaft center orbiting around the bearing center at a frequency of approximately half of the shaft rotational speed as shown in Figure 13-15.

As the speed is increased, the shaft system may be stable until the “whirl” threshold is reached. When the threshold speed is reached, the bearing becomes unstable, and further increase in speed produces more violent instability until eventual seizure results. Unlike an ordinary critical speed, the shaft cannot “pass through,” and the instability frequency will increase and follow that half ratio as the shaft speed is increased. This type of instability is associated primarily with high-speed, lightly loaded bearings. At present, this form of instability is well understood, can be theoretically predicted with accuracy, and avoided by altering the bearing design.

It should be noted that the tilting-pad journal bearing is almost completely free from this form of instability. However, under certain conditions,

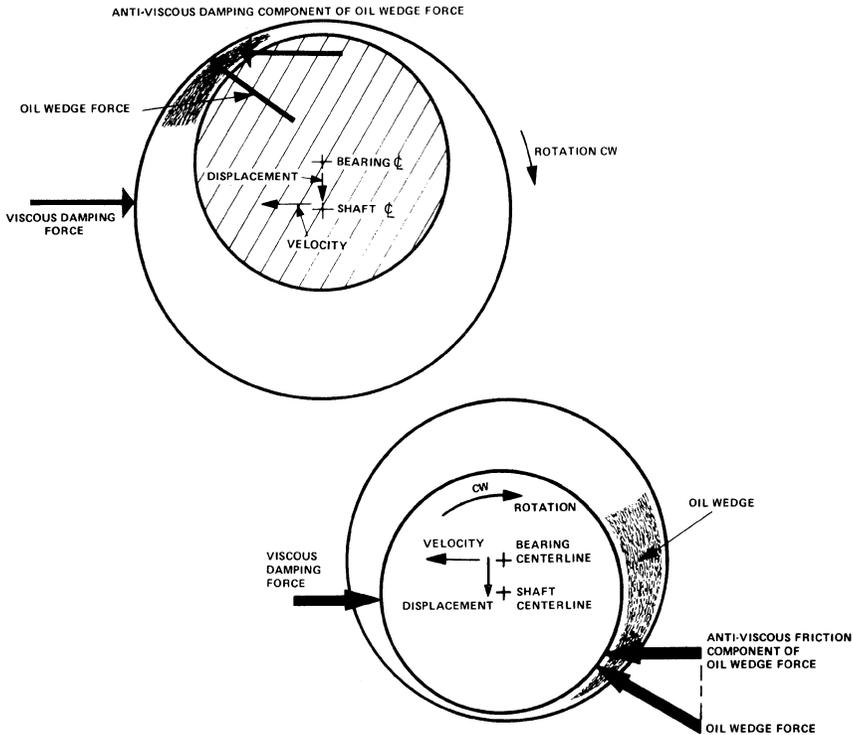


Figure 13-15. Oil whirl.

the tilting pads themselves can become unstable in the form of shoe (pad) flutter, as mentioned previously.

All rotating machines vibrate when operating, but the failure of the bearings is mainly caused by their inability to resist cyclic stresses. The level of vibration a unit can tolerate is shown in the severity charts in Figure 13-16. These charts are modified by many users to reflect the critical machines in which they would like to maintain much lower levels. Care must always be exercised when using these charts, since different machines have different size housings and rotors. Thus, the transmissibility of the signal will vary.

Thrust Bearings

The most important function of a thrust bearing is to resist the unbalanced force in a machine's working fluid and to maintain the rotor in its

position (within prescribed limits). A complete analysis of the thrust load must be conducted. As mentioned earlier, compressors with back-to-back rotors reduce this load greatly on thrust bearings. Figure 13-17 shows a number of thrust-bearing types. Plain, grooved thrust washers are rarely used with any continuous load, and their use tends to be confined to cases where the thrust load is of very short duration or possibly occurs at a standstill or low speed only. Occasionally, this type of bearing is used for light loads (less than 50 lb/in^2 [3.5 bar]), and in these circumstances the operation is probably hydrodynamic due to small distortions present in the nominally flat bearing surface.

When significant continuous loads have to be taken on a thrust washer, it is necessary to machine into the bearing surface a profile to generate a fluid film. This profile can be either a tapered wedge or occasionally a small step.

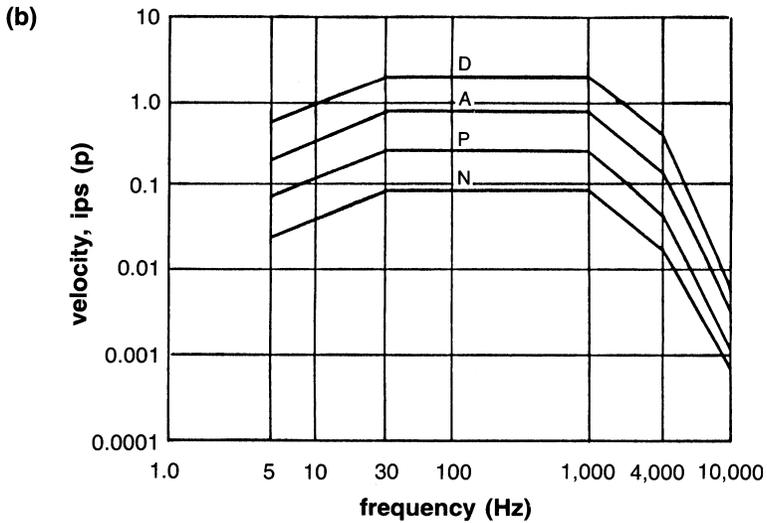
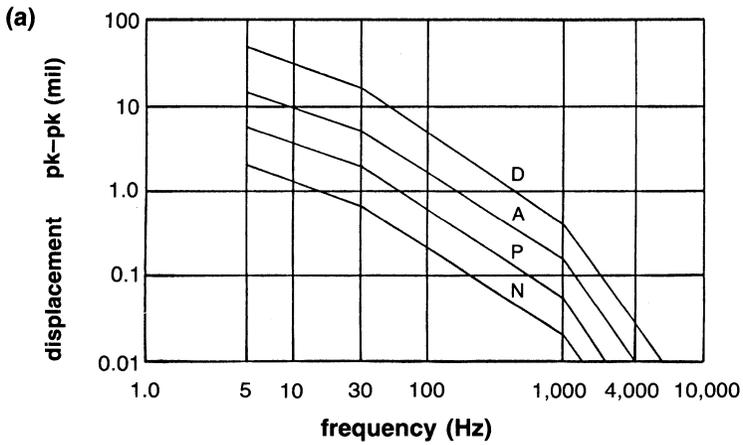
The tapered-land thrust bearing, when properly designed, can take and support a load equal to a tilting-pad thrust bearing. With perfect alignment, it can match the load of even a self-equalizing tilting-pad thrust bearing that pivots on the back of the pad along a radial line. For variable-speed operation, tilting-pad thrust bearings as shown in Figure 13-18 are advantageous when compared to conventional taper-land bearings. The pads are free to pivot to form a proper angle for lubrication over a wide speed range. The self-leveling feature equalizes individual pad loadings and reduces the sensitivity to shaft misalignments that may occur during service. The major drawback of this bearing type is that standard designs require more axial space than a nonequalizing thrust bearing.

Factors Affecting Thrust-Bearing Design

The principal function of a thrust bearing is to resist the thrust unbalance developed within the working elements of a turbomachine and to maintain the rotor position within tolerable limits.

After an accurate analysis has been made of the thrust load, the thrust bearing should be sized to support this load in the most efficient method possible. Many tests have proven that thrust bearings are limited in load capacity by the strength of the babbitt surface in the high load and temperature zone of the bearing. In normal steel-backed babbitted tilting-pad thrust bearings, this capacity is limited to between 250 and 500 psi (17 and 35 Bar) average pressure. It is the temperature accumulation at the surface and pad crowning that cause this limit.

The thrust-carrying capacity can be greatly improved by maintaining pad flatness and by removing heat from the loaded zone. By the use of



- D = Dangerous, shutdown.
- A = Abnormal, will deteriorate.
Inspect as early as possible.
- P = Problems, keep close watch.
- N = Normal.

Figure 13-16. Severity charts: (a) displacement, (b) velocity,

Figure continued on next page

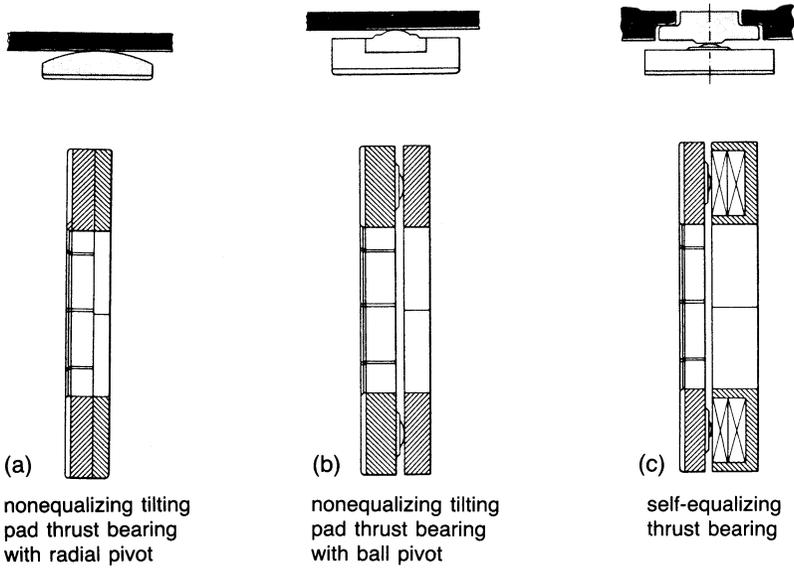


Figure 13-18. Various types of thrust bearings.

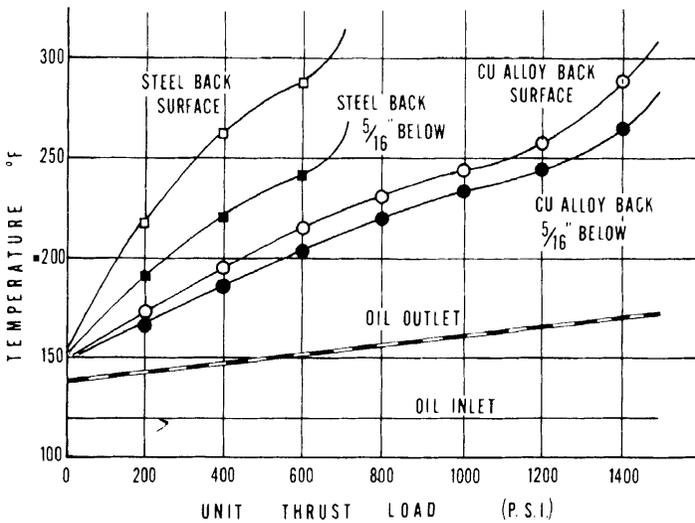


Figure 13-19. Thrust-bearing temperature characteristics.

high thermal conductivity backing materials with proper thickness and proper support, the maximum continuous thrust limit can be increased to 1000 psi or more. This new limit can be used to increase either the factor of safety and improve the surge capacity of a given size bearing or reduce the thrust bearing size and consequently the losses generated for a given load.

Since the higher thermal conductivity material (copper or bronze) is a much better bearing material than the conventional steel backing, it is possible to reduce the babbitt thickness to .010–.030 of an inch (.254–.762 mm). Embedded thermocouples and RTDs will signal distress in the bearing if properly positioned. Temperature monitoring systems have been found to be more accurate than axial position indicators, which tend to have linearity problems at high temperatures.

In a change from steel-backing to copper-backing a different set of temperature limiting criteria should be used. Figure 13-19 shows a typical set of curves for the two backing materials. This chart also shows that drain oil temperature is a poor indicator of bearing operating conditions because there is very little change in drain oil temperature from low load to failure load.

Thrust-Bearing Power Loss

The power consumed by various thrust bearing types is an important consideration in any system. Power losses must be accurately predicted so that turbine efficiency can be computed and the oil supply system properly designed.

Figure 13-20 shows the typical power consumption in thrust bearings as a function of unit speed. The total power loss is usually about 0.8–1.0% of the total rated power of the unit. New vectored lube bearings that are being tested show preliminary figures of reducing the power loss by as much as 30%.

Seals

Seals are very important and often critical components in turbomachinery, especially on high-pressure and high-speed equipment. This chapter covers the principal sealing systems used between the rotor and stator elements of turbomachinery. They fall into two main categories: (1) noncontacting seals, and (2) face seals.

Since these seals are an integral part of the rotor system, they affect the dynamic operating characteristics of the machine; for instance, both the

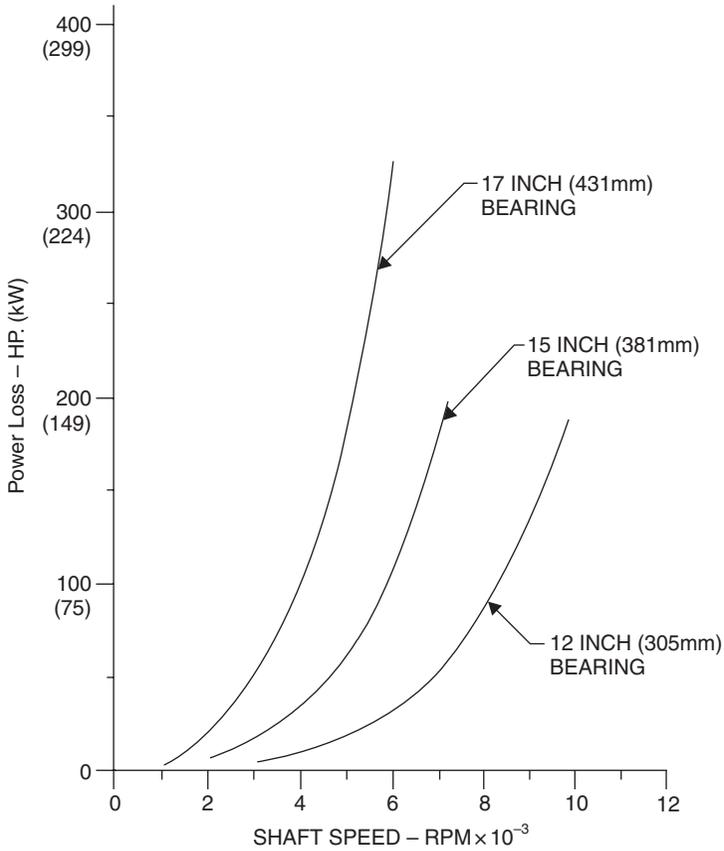


Figure 13-20. Total power loss in thrust bearings.

stiffness and damping factors will be changed by seal geometry and pressures. Hence, these effects must be carefully evaluated and factored in during the design of the seal system.

Noncontacting Seals

These seals are used extensively in high-speed turbomachinery and have good mechanical reliability. They are not positive sealing. There are two types of noncontacting seals (or clearance seals): labyrinth seals and ring seals.

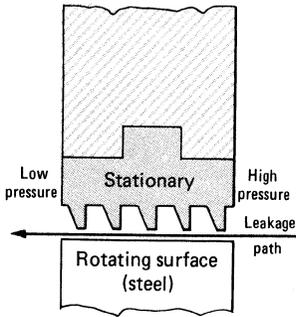
Labyrinth Seals

The labyrinth is one of the simplest of sealing devices. It consists of a series of circumferential strips of metal extending from the shaft or from the bore of the shaft housing to form a cascade of annular orifices. Labyrinth seal leakage is greater than that of clearance bushings, contact seals, or film-riding seals. Consequently, labyrinth seals are utilized when a small loss in efficiency can be tolerated. They are sometimes a valuable adjunct to the primary seal.

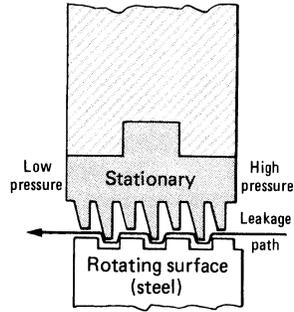
In large gas turbines labyrinth seals are used in static as well as dynamic applications. The essentially static function occurs where the casing parts must remain unjoined to allow for differences in thermal expansion. At this junction location, the labyrinth minimizes leakage. Dynamic labyrinth applications for both turbines and compressors are interstage seals, shroud seals, balance pistons, and end seals.

The major advantages of labyrinth seals are their simplicity, reliability, tolerance to dirt, system adaptability, very low shaft power consumption, material selection flexibility, minimal effect on rotor dynamics, back diffusion reduction, integration of pressure, lack of pressure limitations, and tolerance to gross thermal variations. The major disadvantages are the high leakage, loss of machine efficiency, increased buffering costs, tolerance to ingestion of particulates with resulting damage to other critical items such as bearings, the possibility of the cavity clogging due to low gas velocities or back diffusion, and the inability to provide a simple seal system that meets OSHA or EPA standards. Because of some of the foregoing disadvantages, many machines are being converted to other types of seals.

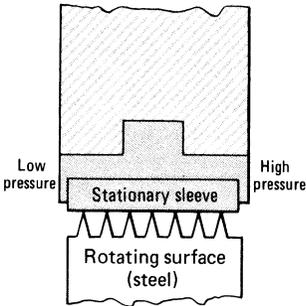
Labyrinth seals are simple to manufacture and can be made from conventional materials. Early designs of labyrinth seals used knife-edge seals and relatively large chambers or pockets between the knives. These relatively long knives are easily subject to damage. The modern, more functional, and more reliable labyrinth seals consist of sturdy, closely spaced lands. Some labyrinth seals are shown in Figure 13-21. Figure 13-21a is the simplest form of the seal. Figure 13-21b shows a grooved seal is more difficult to manufacture but produces a tighter seal. Figures 13-21c and 13-21d are rotating labyrinth-type seals. Figure 13-21e shows a simple labyrinth seal with a buffered gas for which pressure must be maintained above the process gas pressure and the outlet pressure (which can be greater than or less than the atmospheric pressure). The buffered gas produces a fluid barrier to the process gas. The eductor sucks gas from the vent near the atmospheric end. Figure 13-21f shows a buffered, stepped labyrinth. The step labyrinth



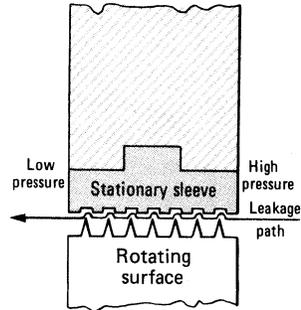
a. Simplest design. (Labyrinth materials: aluminum, bronze, babbitt or steel)



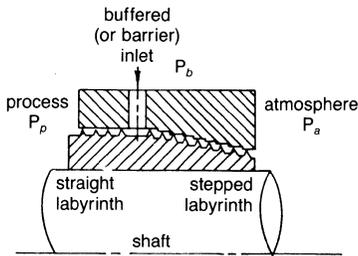
b. More difficult to manufacture but produces a tighter seal. (Same material as in a.)



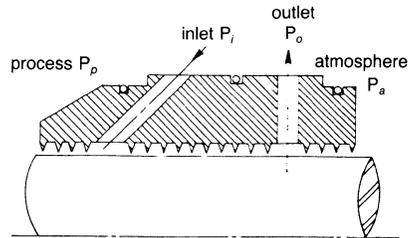
c. Rotating labyrinth type, before operation. (Sleeve material: babbitt, aluminum, nonmetallic or other soft material)



d. Rotating labyrinth, after operation. Radial and axial movement of rotor cuts grooves in sleeve material to simulate staggered type shown in b.



e. buffered combination labyrinth



f. buffered-vented straight labyrinth

Figure 13-21. Various configurations of labyrinth seals.

gives a tighter seal. The matching stationary seal is usually manufactured from soft materials such as babbitt or bronze, while the stationary or rotating labyrinth lands are made from steel. This composition enables the seal to be assembled with minimal clearance. The lands can therefore cut into the softer materials to provide the necessary running clearances for adjusting to the dynamic excursions of the rotor.

To maintain maximum sealing efficiency, it is essential that the labyrinth lands maintain sharp edges in the direction of the flow. This requirement is similar to that in orifice plates. A sharp edge provides for maximum vena contracta effect, and hence maximum restriction for the leakage flows. (Figure 13-22.)

High fluid velocities are generated at the throats of the constrictions, and the kinetic energy is then dissipated by turbulence in the chamber beyond each throat. Thus, the labyrinth is a device wherein there is a multiple loss of velocity head. With a straight labyrinth, there is some velocity carry-over that results in a loss of effectiveness, especially if the throats are closely spaced. To maximize the aerodynamic blockage effect of this carry-over, the diameters can be stepped or staggered to cause impingement of the expanding orifice jet on a solid, transverse surface. The leakage is approximately inversely proportional to the square root of the number of labyrinth lands. Thus, if leakage is to be cut in half at a four-point labyrinth, the number of

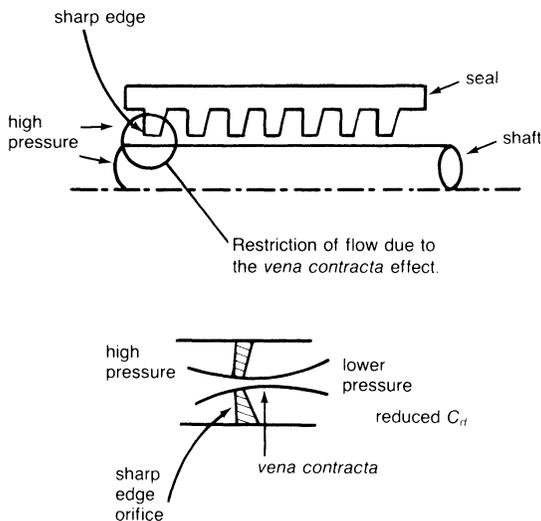


Figure 13-22. Theory behind the knife-edge arrangement.

lands would have to be increased to 16. The Elgi leakage formulae can be modified and written as

$$\dot{m}_l = 0.9A \left[\frac{\frac{g}{V_o} (P_o - P_n)}{n + \ln \frac{P_n}{P_o}} \right]^{1/2}$$

For staggered labyrinths, the equation can be written as

$$\dot{m}_l = 0.75A \left[\frac{\frac{g}{V_o} (P_o - P_n)}{n + \ln \frac{P_n}{P_o}} \right]^{1/2}$$

where:

\dot{m}_l = leakage, lb/sec

A = leakage area of single throttling, sq ft

P_o = absolute pressure before the labyrinth, lb/sq ft

V_o = specific volume before the labyrinth, cu ft/lb_m

P_n = absolute pressure after the labyrinth, lb_f/sq ft

n = number of lands

The leakage of a labyrinth seal can be kept to a minimum by providing: (1) minimum clearance between the seal lands and the seal sleeve, (2) sharp edges on the lands to reduce the flow discharge coefficient, and (3) grooves or steps in the flow path for reducing dynamic head carryover from stage to stage.

The labyrinth sleeve can be flexibly mounted to permit radial motion for self-aligning effects. In practice, a radial clearance of under 0.008 is difficult to achieve, except with very small high-precision machines. On larger turbines, clearances of 0.015–0.02 are generally used. During machine construction, it is important to measure and record these clearances because mechanical seizure or loss in aerodynamic efficiency can often be traced to incorrect labyrinth seal clearances.

The windback seal closely resembles the labyrinth but has an entirely different operational principle. A screw-thread device winds the oil, which is carried around the bore by the windage of the shaft, into an internal drain for return to the system as shown in Figure 13-23a.

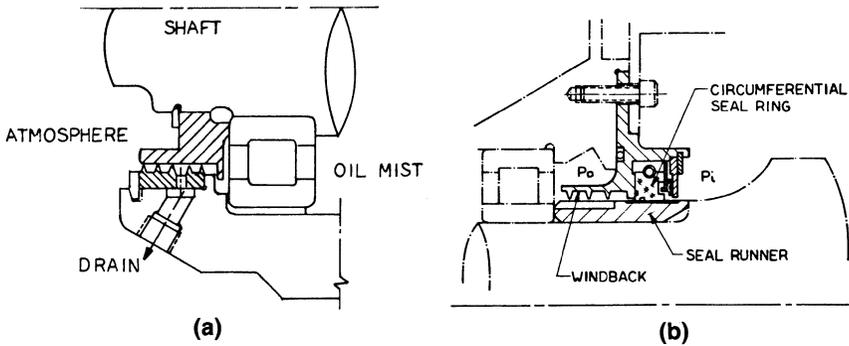


Figure 13-23. Windback seal.

Windback structures are extremely simple. Clearances about the shaft are ample, and the device has high reliability. When shaft speeds extend into the low regions where windage effects are inadequate for effective operation, augmentation of windage can be achieved by special configurations of the shaft surface. Windbacks are also used as adjuncts to other types of seals, as shown in Figure 13-23b. With circumferential seals, windbacks can be used to keep oil splash from reaching the seal carbons when coking problems exist. In oil-buffered seals for compressors they are used to direct the small internal leakage into a pressurized drain to effect practically complete recovery of the leakage.

Ring (Bushing) Seals

The restrictive ring seal is essentially a series of sleeves in which the bores form a small clearance around the shaft. Thus, the leakage is limited by the flow resistance in the restricted area and controlled by the laminar or turbulent friction. The API 617 codes characterize this type of seal. Most of the restrictive-type seals are of the floating type rather than the fixed type. The floating rings permit a much smaller leakage, and they can be of either the segmented type as shown in Figure 13-24a or the rigid type as shown in Figure 13-24b.

Because of the minimal contact between the stationary ring and the rotor, these seals, when properly designed, are ideal for high-speed rotating machinery.

When adequate lubrication and cooling fluid is available, the seal ring, manufactured from babbitt-lined steel, bronze, or carbon, will function satisfactorily. When the medium to be sealed is air or gas, carbon seal rings must be used. Carbon has self-lubricating properties. Cooling of the seal is provided by the leakage flow through the seal. Depending on the operating

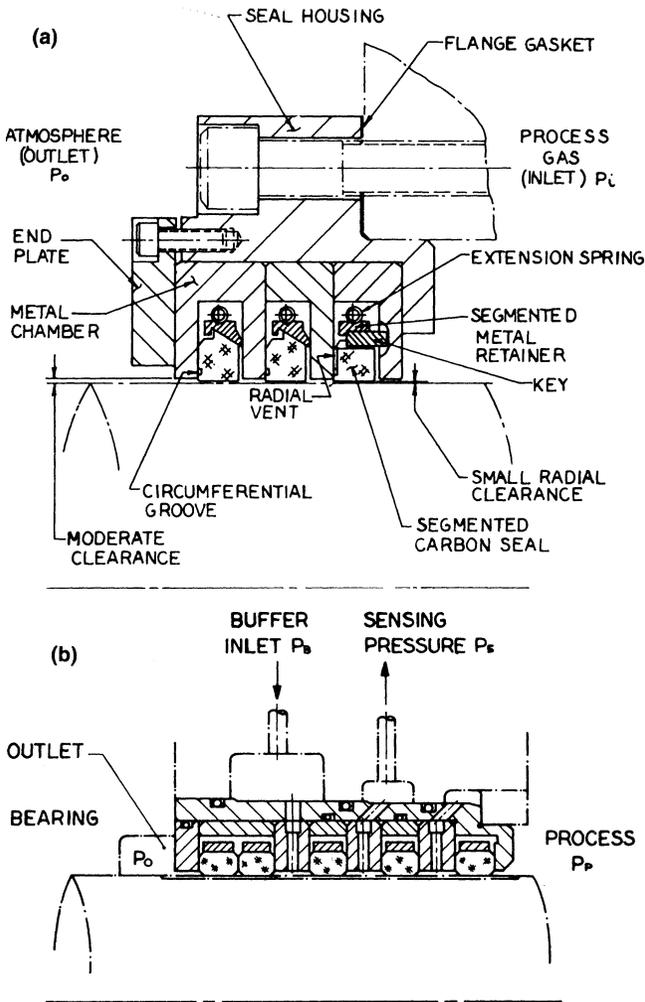


Figure 13-24. Floating-type restrictive ring seal.

temperature and environment, aluminum alloys and silver are also used in the manufacture of the seal rings. Leakage limitation depends upon the type of flow and type of bushing. There are four types of flow: compressible and incompressible, each of which may be either laminar or turbulent. Ring seals are divided into two categories: fixed breakdown rings and floating breakdown rings, according to whether or not they are fixed with respect to the stationary housing.

Fixed seal rings. The fixed seal ring consists of a long sleeve affixed to a housing in which the shaft rotates with small clearance. It is an inexpensive assembly. However, since it is fixed, the seal behaves like a redundant bearing when rubbing occurs and, like the labyrinth, requires large clearances. Therefore, long assemblies must be used to keep leakage within reasonable limits. Since long seal assemblies aggravate alignment and rubbing problems, sturdier shafts are required to keep operating speeds in a subcritical region. The fixed-bushing seal almost always operates with appreciable eccentricity. This, plus the combination of a large clearance and a large eccentricity ratio, produces large leakages per unit length. Fixed-seal rings are therefore impractical where leakage is undesirable.

Floating seal rings. Clearance seals, which are free to move in a radial direction relative to the shaft and machine housing, are known as floating seals. These seals have advantages that very close, annular clearance-type seals do not possess. The floating characteristic permits them to move freely with shaft motions and deflections, thereby avoiding the effects of severe rubbing.

Differential thermal expansion is a problem at high temperatures where the shaft and bushing are of dissimilar materials, or where there is any substantial temperature gradient between them. For example, the grades of carbon used commonly have a linear thermal expansion coefficient of one-third to one-fifth that of steel, necessitating the design of thermal expansion control into the carbon bushing. This is achieved by shrinking the carbon into a metallic retaining ring with a coefficient of expansion that equals or exceeds that of the shaft material.

It is good practice in critical applications to use bushings of a material with a slightly higher coefficient of thermal expansion than that of the shaft. Here, incipient seizure causes the bushings to grow away from the shaft. The large torque associated with high shearing intensity may necessitate locking the bushings against rotation if the unbalanced pressure forces seating them against the housing walls are insufficient to prevent rotation.

Build up of dirt or other foreign material between the seal ring and seat will result in damage to the journal and excessive seal spin on a floating seal ring unit. Soft materials, such as babbitt and silver, are notorious for trapping contaminants and causing shaft damage.

Mechanical (Face) Seals

This device forms a running seal between flat precision-finished surfaces. Its primary function is to prevent leakage. When used on rotating shafts, the

sealing surfaces are in a plane perpendicular to the shaft, and the forces that hold the contact faces together will consequently be parallel to the shaft axis. For a seal to function properly, four sealing points must function as shown in Figure 13-25. They are: (1) the stuffing-box face must be sealed, (2) leakage down the shaft must be sealed, (3) the mating ring in the gland plate must be sealed in a floating design, and (4) the dynamic faces (rotary to stationary) must seal. Basically, most mechanical seals have the following components:

1. Rotating seal ring
2. Stationary seal ring
3. Spring devices to provide pressure
4. Static seals

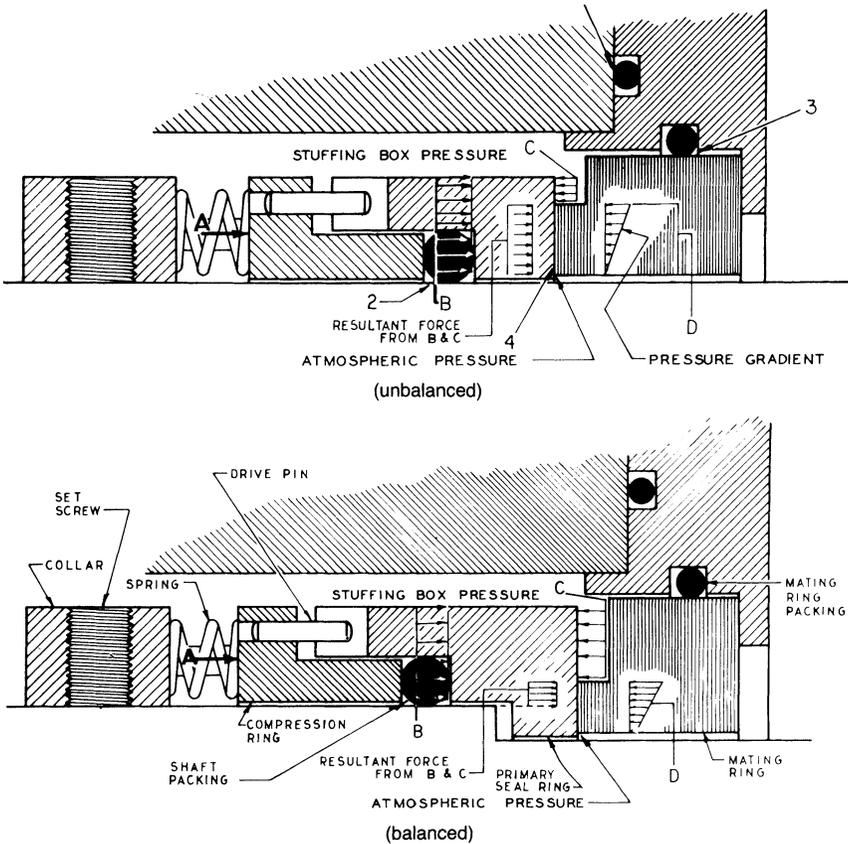


Figure 13-25. Unbalanced seal and balanced seal with step in shaft.

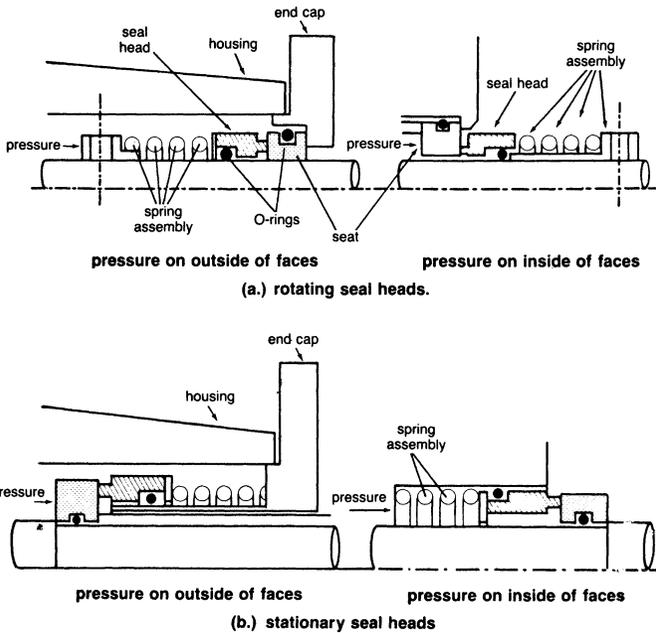


Figure 13-26. Rotating and stationary seal heads.

A complete seal has two basic units: the seal head unit and the seal seat. The seal head unit consists of the housing, the end-face member, and the spring assembly. The seal seat is the mating member that completes the precision-lapped face combination that provides the seal.

The seal head may either rotate or remain stationary (attached to the body). Either one (head or seat) may rotate, while the other remains stationary. The movement of the sealing action depends on the direction of the pressure. This is illustrated in Figure 13-26, which shows rotating and stationary heads.

Some form of mechanical loading device, usually a spring, is needed to ensure that in the event of a loss of hydraulic pressure, the sealing surfaces are kept closed. The amount of load on the sealing area is determined by the degree of "seal balance." Figure 13-27 shows what is meant by seal balance. A completely balanced combination occurs when the only force exerted on the sealing surfaces is the spring force, i.e., hydraulic pressure does not act on the sealing surfaces. The kind of spring that should be used depends upon a variety of factors: the space available, the loading characteristics required, the environment in which the seal is to operate, etc. Based on these considerations, either a single spring or a multiple-spring design can be utilized.

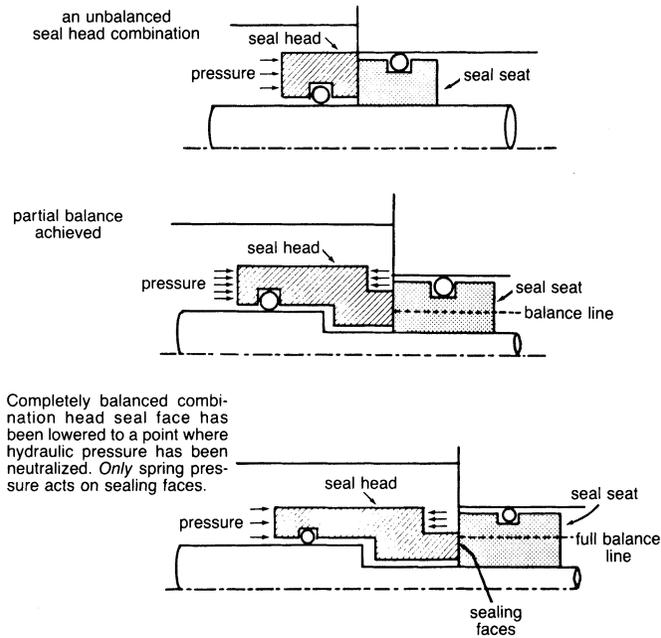


Figure 13-27. The seal balance concept.

When a very small axial space is available, belleville springs, finger washers, or curved washers may be used.

A somewhat recent development is the use of magnetic force to obtain a face-loading action. Magnetic seals have provided reliable service under a variety of fluids and severe operating conditions. Some of the design advantages claimed are that magnetic seals are compact and lighter, provide an even distribution of sealing force, and are easy to assemble. Figure 13-28 shows a simple magnetic seal.

Shaft sealing elements can be split up into two groups. The first may be called pusher-type seals and includes the O-ring, V-ring, U-cup, and wedge configurations. The second group are Bellow-type seals, which differ from the pusher-type seals in that they form a static seal between themselves and the shaft. Figure 13-29 shows some typical pusher-type seals.

A typical mechanical contact shaft seal has two major elements, as seen in Figure 13-30. These are the oil-to-pressure-gas seal and the oil-to-uncontaminated-seal-oil-drain seal or breakdown bushing. This type of seal will normally have buffering via a single ported labyrinth located inboard of the seal and a positive shutdown device, which will attempt to maintain gas

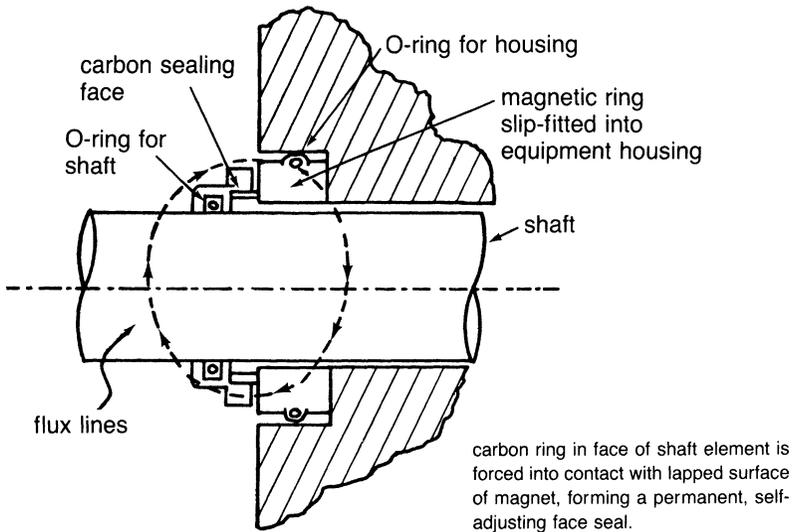


Figure 13-28. Simple magnetic-type seal.

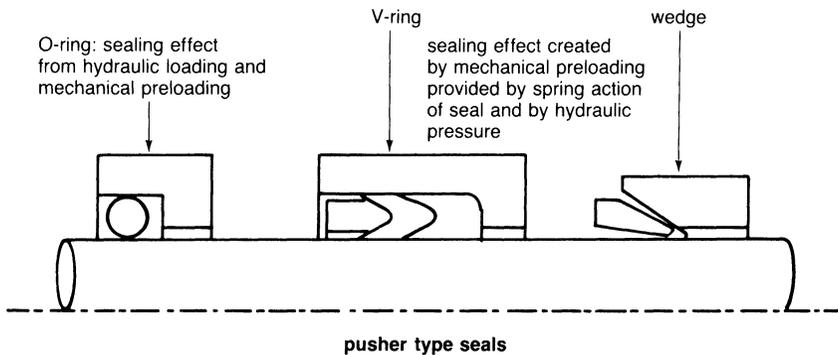
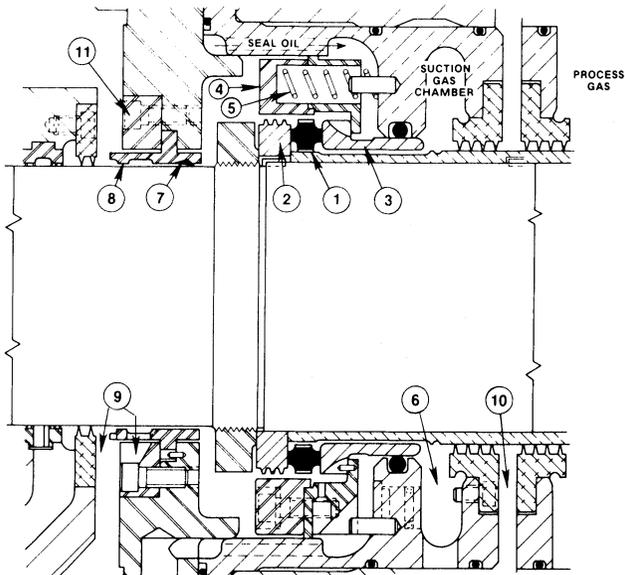


Figure 13-29. Various types of shaft sealing elements.

pressure in the casing when the compressor is at rest and seal oil is not being applied. For shutdown, the carbon ring is kept tightly sandwiched between the rotating seal ring and stationary sleeve with gas pressure to prevent gas from leaking out when no oil pressure is available.

In operation, seal oil pressure is held at a differential of 35–50 psid (2.4–3.5 bar) over the process gas pressure which the seal is sealing against. This high-pressure oil can be seen entering in the top in Figure 13-30 and



- | | |
|-----------------------------------|--------------------------------------|
| 1. ROTATING CARBON RING | 7. FLOATING BABBITT-FACED STEEL RING |
| 2. ROTATING SEAL RING | 8. SEAL WIPER RING |
| 3. STATIONARY SLEEVE | 9. SEAL OIL DRAIN LINE |
| 4. SPRING RETAINER | 10. BUFFER GAS INJECTION PORT |
| 5. SPRING | 11. BYPASS ORIFICE |
| 6. GAS AND CONTAMINATED OIL DRAIN | |

Figure 13-30. Mechanical contact shaft seal.

completely fills the seal cavity. Some of the oil (a relatively small percentage, ranging from 2 to 8 gpd per seal depending on machine size) is forced across the carbon ring seal faces, which are sandwiched between the rotating seal ring (rotating at shaft velocity) and the stationary sleeve (nonrotating and forced against the carbon ring by a series of peripheral springs). Therefore, the actual rotative speed of the carbon ring can be anywhere between zero rpm and full rotational speed. Oil crossing these seal faces contacts the process gas and is, thus, “contaminated oil.”

The majority of the oil flows out of the uncontaminated seal oil drain after taking a pressure drop from design seal oil pressure to atmospheric pressure across the breakdown bushing. An orifice is placed in parallel with the breakdown bushing to meter the proper amount of oil flow for cooling. The contaminated oil leaves through the drain to a degasifier for purification.

The bearing oil drain can be either combined with the uncontaminated seal oil drain or kept separate; however, a separate system will increase bearing span and lower critical speeds.

Mechanical Seal Selection and Application

The following is a list of factors that have proven to be helpful in seal system design and selection:

1. Product
2. Seal environment
3. Seal arrangement
4. Equipment
5. Secondary packing
6. Seal-face combinations
7. Seal gland plate
8. Main seal body

Product

The physical and chemical properties of the liquid being sealed will place constraints upon the type of seal arrangement, the materials of construction, and the seal design that can be used.

Pressure. The relative pressures of the material to be sealed affect the decision of whether to use a balanced or unbalanced seal design. Pressure also affects the choice of face material because of the seal-face loading.

If the service happens to be below atmospheric pressure, then special considerations are required to seal the material effectively. Most unbalanced seal designs are applicable up to 100 psig (7 Bar) stuffing-box pressure. At more than 100 psig (7 Bar), balanced seals should be used.

Seal manufacturers base their seal-face combination designs on PV ratings. These are the multiple of the face load (P) and the sliding velocity (V) of the faces. The maximum PV rating for an unbalanced seal is about 200,000 and about 2,250,000 for a balanced seal.

Temperature. The temperature of the liquid being pumped is important because it affects the seal-face material selection as well as face wear life. This is primarily a result of changes in lubricity of the fluid with changes in temperature.

Common seal designs may handle fluid temperatures in the 0°F to +200°F (−17°C–93°C) range. When temperatures are above the +200°F

(93 °C) range, special metal bellows seals may be used up to the +650 °F (343 °C) range. Low temperature (−100 °F to 0 °F) (−73 °C to −17 °C) also requires special arrangements, since most hydrocarbons have little lubricity in this range.

The most important consideration concerning temperature is to avoid operating close to a temperature, which will allow flashing of the liquid. Mechanical seals work well on many liquids; they work poorly on most gases.

Lubricity. In any mechanical seal design there is rubbing motion between the dynamic seal faces. This rubbing motion is most often lubricated by the fluid being pumped. Therefore, the lubricity of the pumped liquid at the given operating temperature must be considered to determine if the chosen seal design and face combination will perform satisfactorily.

Most seal manufacturers limit the speed of their seals to 90 fps (27.4 mps) with good lubrication of the faces. This is primarily due to the centrifugal forces acting on the seal which tend to restrict its axial flexibility.

Abrasion. When evaluating the possibility of installing a seal in a liquid that has entrained solids, several factors must be considered. Is the seal constructed in such a way that the dynamic motion of the seal will be restricted by fouling of the seal parts? The seal arrangement that is usually preferred when abrasives are present is a flushed single inside type with a face combination of very hard material. However, factors such as toxicity or corrosiveness of the material may dictate that other arrangements be used.

Corrosion. When considering the corrosiveness of the material being pumped, one must determine what metals will be acceptable for the seal body, what spring material may be used, what face material will be compatible with the liquid being pumped (that is, whether the binder or the carbon or tungsten carbide will be attacked, or whether the base metal of the plated seal-face will be attacked), and what type of elastomer or gasket material can be used. The corrosion rate will affect the decision of whether to use a single or multiple-spring design because the spring can tolerate a greater amount of corrosion without weakening it appreciably.

Toxicity. This factor is becoming an increasingly important consideration in the design of mechanical seals. Since the rubbing seal faces require liquid penetration to cool and lubricate them, it is reasonable to expect that there will be some vapor passing across the faces. This is in fact the case. A normal seal can be expected to “leak” from a few ppm to 10 cc/min. It is also generally accepted that the seal leakage rate will increase with speed.

Additional Product Considerations

1. Is the product thermosensitive? The heat generated by the seal faces may cause polymerization.
2. Is the product shear sensitive, i.e., will it harden due to turbulence?
3. If the product is highly flammable, be aware of possible ignition sources.
4. In-hazardous services plan for personnel protection in the event of seal leakage.
5. Products with dissolved gas must be properly vented. In most cases, vent the stuffing box back to pump action.
6. Seals in cold services are extremely sensitive to moisture. There must be a way to “dry out the system” after repair.
7. Consideration must be given to the pressure and temperature that the seal will see during normal operation, startup, shutdown, and upset conditions.
8. Vapor pressure of the product must be known to prevent vaporization in the stuffing box.

Seal Environment

Once an adequate definition of the product is made, the design of the seal environment can be selected. There are four general parameters that an environmental system may regulate or change:

1. Pressure control
2. Temperature control
3. Fluid replacement
4. Atmospheric air elimination

The most common environmental control systems include flushing, barrier fluids, quenching, and heating/cooling systems. Each has its use in regulating the parameters mentioned previously.

Seal Arrangement Considerations

There are four considerations:

1. Double seals have been the standard with toxic and lethal products, but maintenance problems and the seal design contribute to poor reliability. The double face-to-face seal should be looked at more closely.

2. Do not use a double seal in dirty service—the inside seal will hang up.
3. The API standard is a good guide to the use of balanced and unbalanced seals. Application of a balanced seal at too low a pressure may encourage face lift-off.
4. The number of arrangements and auxiliary features are more than 100. Regardless of the seal vendor, the arrangement will generally determine success.

Equipment

Too few people consider the equipment with the seal selection. In most cases, poor equipment will give poor seal performance, regardless of the seal or arrangement chosen. Also, beware that different pumps with the same shaft diameter and TDH may present different sealing problems. (Note: These same considerations may be used for troubleshooting.)

Secondary Packing

More emphasis should be placed on secondary packing than it receives, especially if these members involve Teflon. Most seal designs using an O-ring for shaft packing give similar performance. A wide variation in performance is seen between various seal vendor designs when Teflon shaft packing is used. Depending on the seal arrangement, there can be a difference in mating-ring (stationary) packing performance when Teflon is used.

Seal-Face Combinations

Choices of seal-face combinations have come a long way in the last 8–10 years. Stellite is being phased out in petroleum and petrochemical seal applications. Better grades of ceramic are being offered as the standard material. The cost of tungsten carbide has decreased considerably. Relap-ping services for tungsten are available near most industrial areas. Silicon carbide is gaining a hold on the market, especially in abrasive service. The technology of manufacturing tungsten carbide in a composite or overlay arrangement is offered by all of the major seal manufacturers. The dynamics of seal faces are better understood today.

Seal Gland Plate

The seal gland plate is an item that is caught in-between the pump vendor and the seal vendor. The pump vendors can furnish good, reasonably priced

alloy glands, but they are also limited because the gland is cast and must fit several seal designs. There are also some glands furnished by pump vendors that can be easily distorted by bolting. Special glands requiring heating, quench, and drain with a floating-throat bushing on ANSI pumps should be furnished by the seal vendor. Gland designs on several ANSI pumps are not that impressive.

Main Seal Body

Designs differ considerably from one manufacturer to another. The term “seal body” makes reference to all rotating parts on a pusher seal, excluding shaft packing and the seal ring. The configuration or options offered on the seal body may be the chief reason to avoid the design for that particular service.

Seal Systems

In recent years, these systems have become more sophisticated to meet modern chemical process requirements and government restrictions. A simple seal system is the buffered and educted restrictive-ring seal system. This type of system, as shown in Figure 13-31, must operate with buffering pressure greater than the process and eductor pressure. The eductor pressure must in turn be below the atmospheric pressure. Problems with these systems

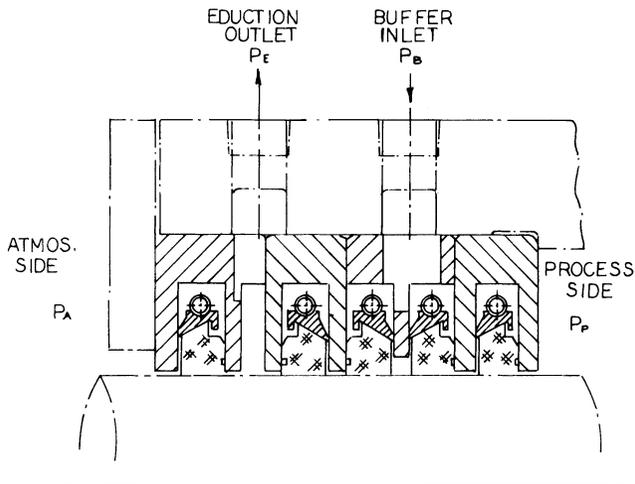


Figure 13-31. Restrictive ring seal system with both buffer and eduction cavities.

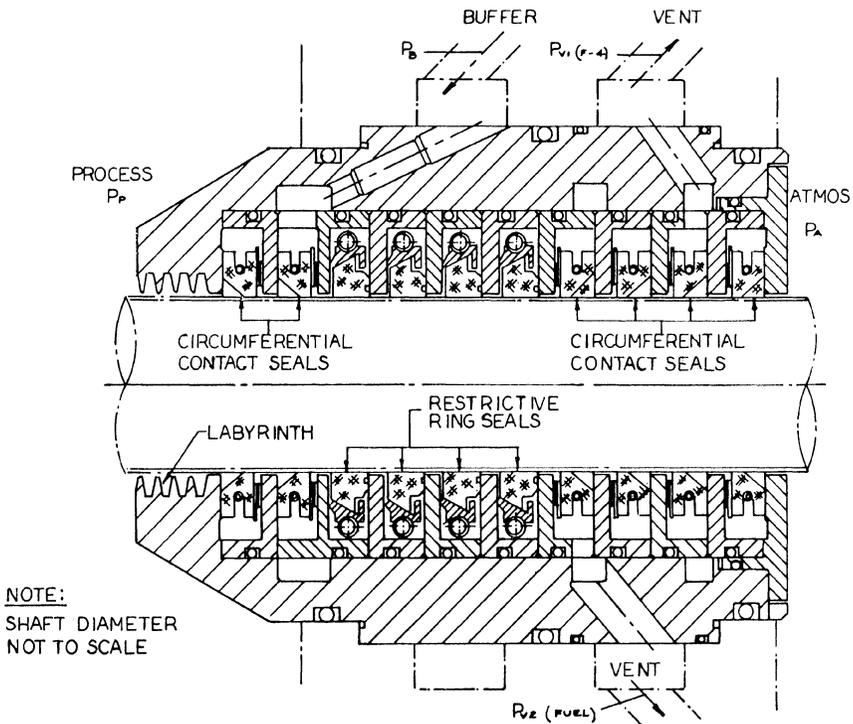


Figure 13-32. Multiple combination segmented gas seal system.

are common because the eductor system does not have a large enough capacity, the buffered gas pressure is not higher than the process pressure, and in many cases the rings are installed backward.

The complex seal systems incorporate many different types of components to provide the most efficient sealing. Figure 13-32 shows a system that includes three different types of seals. The labyrinth seal initially provides the restriction that prevents the polymers contained in the process gas from clogging the seal rings. The labyrinth seal is followed by the two segmented circumferential contact seals and the four segmented restrictive-ring seals, which are primary seals in this combination. The primary restrictive-ring seals are followed by four circumferential segmented seal rings. A buffer gas is also introduced at the first set of circumferential contact seals, and an eductor is situated in the middle of the rear circumferential seals. Thus, this sealing system is very efficient in preventing any leakage and also for utilizing educted gas in the process.

Gas compressors operating on highly toxic or flammable gases may require redundant systems to assure no leakages. In many applications, such as refrigeration gas, buffer seals are required with the liquid-buffered face seal. A popular technique is to use a buffered labyrinth seal with a liquid seal.

Associated Oil System

One of the advantages of mechanical contact seals is that the associated seal oil supply system may be relatively simple compared to the system required with other types of seals, as seen in Figure 13-33. The relatively high oil-to-gas differential and wide allowable range allow simple differential regulators to be used to control the oil supply system rather than a complex overhead tank arrangement. The dark lines in Figure 13-34 represent the seal oil system used for this type of seal. Seal oil is taken from a controlled header “A” and dropped to the required ΔP via a relatively inexpensive regulator control. The sensing point for this ΔP control is off the contaminated drain cavity on the high-pressure end of the compressor. By sensing off the high-pressure end, a minimum of ΔP of oil to gas is always held on both ends of the compressor. Any pressurizing of the contaminated drain cavity due to

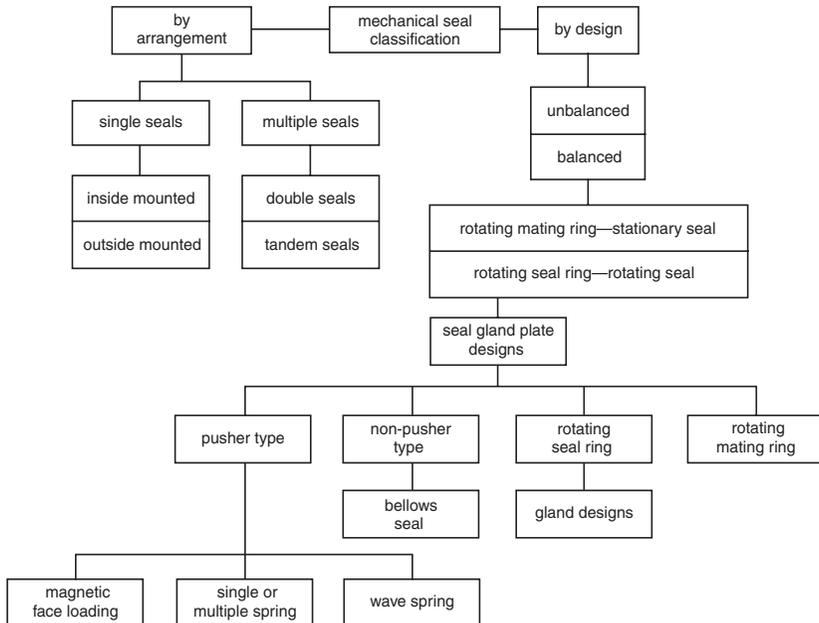


Figure 13-33. Mechanical seal classifications.

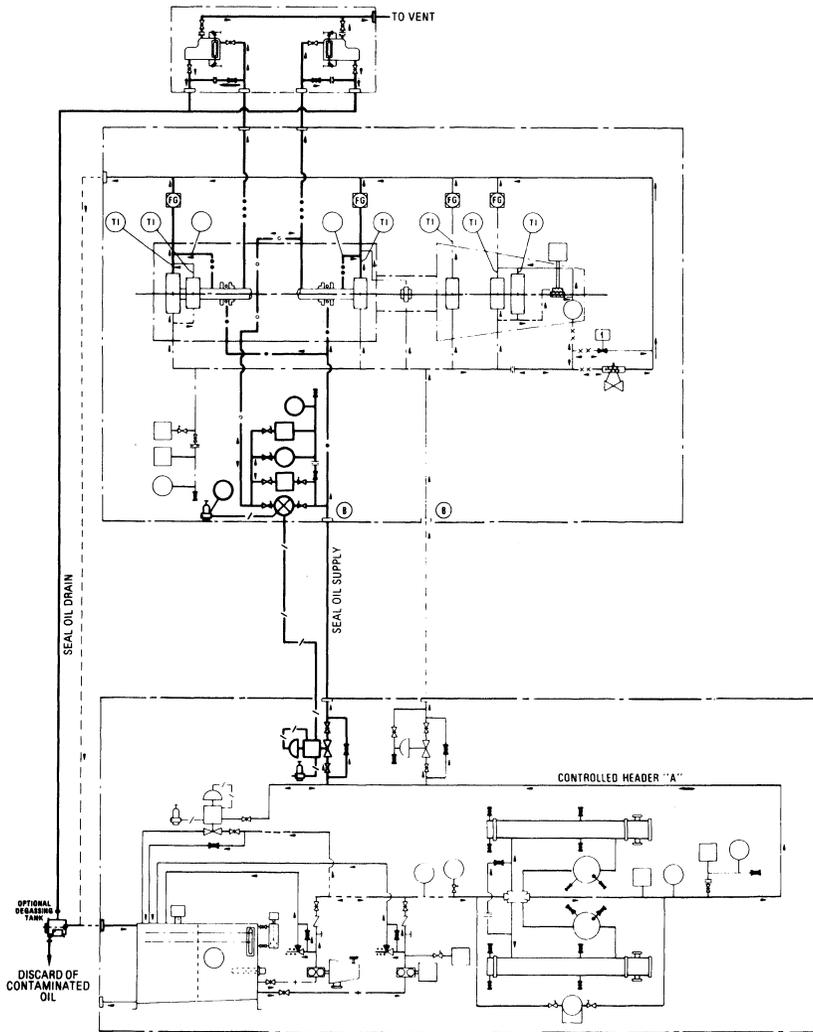


Figure 13-34. Mechanical contact seal and lube oil system.

buffer gas being used is also automatically followed by using a sensing point located in the contaminated drain oil cavity. In the system shown, the “uncontaminated oil” combines immediately with lube oil and returns to the reservoir where the “contaminated oil” can be trapped by a drainer and automatically drained to be optionally discarded or returned to the reservoir via a degassing tank.

Dry Gas Seals

The use of dry gas seals in process gas centrifugal compressors has increased over the last 30 years, replacing traditional oil film seals in most applications. Over 85% of centrifugal gas compressors manufactured today are equipped with dry gas seals.

Dry gas seals are basically mechanical face seals, consisting of a mating ring, which rotates and a primary ring, which is stationary. A cross-sectional view of a dry gas seal is shown in Figure 13-35. The rotating assembly consists of the mating ring (with spiral grooves) mounted on a shaft sleeve held in place axially with a clamp sleeve and a locknut. It is typically pin driven. The mating ring with spiral grooves and the primary ring are held within the retainer assembly. The stationary assembly consists of the primary ring mounted in a retainer assembly held stationary within the compressor housing. Under static conditions, the primary and mating rings are held in contact due to the spring load on the primary ring.

The spiral groove pattern, for a clockwise rotation, on the mating ring is shown in Figure 13-36. The operating principle of the spiral grooved gas seal is that of a hydrostatic and hydrodynamic force balance. As gas enters the grooves, it is sheared towards the center. The sealing dam acts as a restriction to the gas outflow, thereby raising the pressure upstream of the dam. This increased pressure causes the flexibly mounted, primary ring to separate

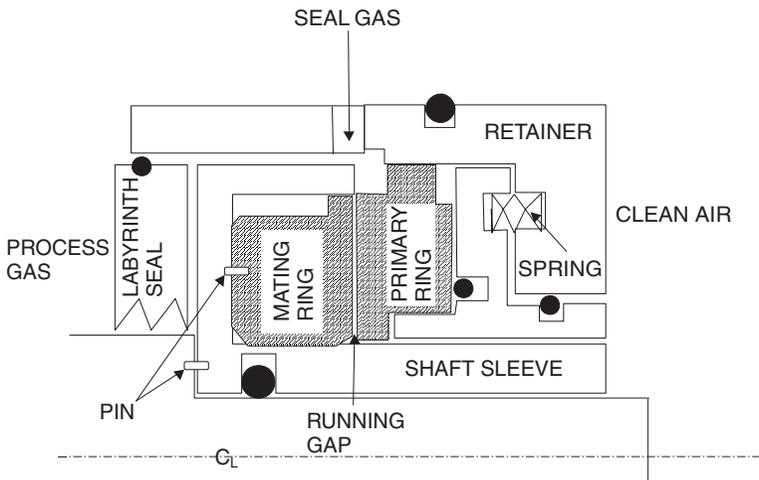


Figure 13-35. Single dry gas seal.

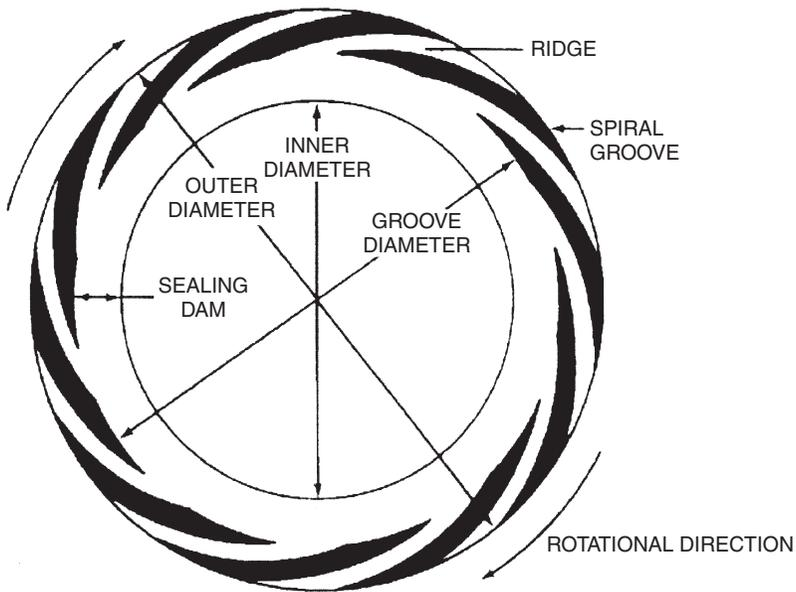


Figure 13-36. Spiral grooved mating ring. (Courtesy Proceedings Seventeenth Turbomachinery Symposium, Dry Gas Compressor Seals by Piyush Shah, John Crane Inc.)

from the mating ring. During normal operation, the running gap is approximately 3 microns. Under pressurization, the forces exerted on the seal are hydrostatic and are present whether the mating ring is stationary or rotating. Hydrodynamic forces are generated only upon rotation. The mating ring consisting of the logarithmic spiral grooves is the key to generating these hydrodynamic forces.

During operation, the grooves in the mating ring generate a hydrodynamic force that causes the primary ring to separate from the mating ring creating a “running gap” between the two rings, which effectively seals against the process gas. During normal operation, the running gap is approximately 3 microns. A sealing gas is injected into the seal, providing the working fluid, which establishes the running gap.

Operating Range of Dry Gas Seals

Gases ranging from inert gases such as nitrogen to highly toxic gaseous mixtures of natural gas and hydrogen sulfide can be sealed utilizing the

optimum seal arrangements. The operating range of the spiral grooved dry gas seals is as follows:

Sealed Pressure: 2,400 psi (165 Bar)
Temperature: 500 °F (260 °C)
Surface Speed: 500 ft./sec. (152 m/sec)
M.W.: 2–60

Dry Gas Seal Materials

The gas composition, contaminants in the gas stream, operating temperatures and process conditions dictate the choice of materials. The most common materials of construction are as follows:

Mating Ring: Tungsten Carbide, Silicon Carbide
Primary Ring: Carbon, Silicon Carbide
O-Rings: Elastomers (Viton, “Kalrez”)
Hardware: 300 or 400 series ss (Sleeves, discs, retainer rings)
Coil Springs: 316 ss, Hastelloy

Dry Gas Seal Systems

The use of dry gas seals requires a system designed to supply sealing gas to the seal as a working fluid for the running gap. These gas seal systems are normally supplied by the compressor OEM mounted on the compressor base plate. There are two basic types of gas seal systems, differential pressure (ΔP) control and flow control. Differential control systems control the supply of seal gas to the seal by regulating the seal gas pressure to a pre-determined value typically 15 psi (1 Bar) above the sealing pressure. This is accomplished through the use of a differential pressure control valve. Flow control systems control the supply of seal gas to the seal by regulating the seal gas flow through an orifice upstream of the seal. This is accomplished through the use of a differential pressure control valve monitoring pressures on either side of the orifice.

Dry Gas Seal Degradation

Contamination of the seal by foreign objects leads to seal failures. The running gap between the primary and mating gas seal rings is typically around 3 microns. Injection of any type of solids or liquids into this very

narrow seal running gap can cause degradation of seal performance. This would create excessive gas leakage to the vent and eventual failure of the seal.

Since the typical operating gaps between the two sealing surfaces range from 0.0001 in to 0.0003 in, the resultant leakage is very small in magnitude. Under conditions of static pressurization beyond 50–75 psi (3.4–5.17 bar), the seal leaks a very small amount. This leakage increases with increasing pressure and reduces with increasing temperature. Increased viscosity of gases at higher temperatures reduces the amount of seal leakage. For example, 4-in. (101.6 mm) shaft seal on a natural gas compressor statically pressurized to 1,000 psi (69 bar) will leak about 1 scfm (0.03 scmm). Under dynamic condition, due to the pumping effect of the spiral grooves, the leakage increases as well.

The power loss can also be increased with seal contamination. The seal surfaces being noncontacting under dynamic conditions the power loss associated with dry gas seals is very small. The power loss for a 10-in. (254 mm) seal operating at 1000 psi (69 Bar) and 10,000 rpm is about 12–14 kW. With damaged seal surfaces, these losses can be increased by 20–30%.

Foreign material within the seal results in increased shearing forces between the primary and mating rings, causing overheating of the seal components, leading to o-ring extrusion or some other mechanical form of seal failure. The major areas from which gas seals contamination occurs are:

- Process gas leakages from the inboard or high-pressure side of the seal.
- Bearing lubrication oil from the outboard or low-pressure side of the seal.
- The seal gas injected into the seal being contaminated upstream of the injection.

Contamination from Process Gas. Contamination from process gas can occur when there is insufficient supply of sealing gas into the seal, allowing process gas to come into direct contact with the seal ring faces. Contaminants existing within the process gas can then damage the seal.

Contamination from Bearing Lubrication Oil. A barrier seal is required on the outboard side of the dry gas seal, between the gas seal and the compressor bearing. The primary function of the barrier seal, typically buffered with air or nitrogen, is to prohibit the flow of bearing lubrication oil into the gas seal. Contamination of the dry gas seal from lube oil can occur when the barrier seal fails to function as intended.

Contamination from Seal Gas Supply. Contamination from the seal gas supply occurs when the sealing gas is not properly treated upstream of the dry gas seal. Gas seal manufacturers have stringent requirements for seal gas quality. Typically, the sealing gas must be dry and filtered of particles 3 micron and larger. Filters are normally provided in the gas seal system to meet this requirement.

Dry gas seals operate under extremely tight tolerances, which demand that special care be taken in the design of the gas seal environment, and in the operation of the compressor and gas seal system. While the threat of seal degradation and reduced seal life due to outside influences is real, the detrimental effects of these factors can be minimized.

The replacement of mechanical seals by dry gas seals must be closely examined. There have been many cases where the replacement has caused the compressor to operate in an unstable manner. This is due to the fact that removal of the mechanical seal causes a change in the damping of the rotor and can cause the rotor to operate closer to its critical speed.

Bibliography

- Abramovitz, S., "Fluid Film Bearings, Fundamentals and Design Criteria, and Pitfalls," Proceedings of the 6th Turbomachinery Symposium, December 1977, pp. 189–204.
- Childs, D.W., and Vance, J.M., "Annular Gas Seals and Rotordynamics of Compressors and Turbines" Proceedings of the 26th Turbomachinery Symposium, Texas A&M University, p. 201, 1997.
- "Effects of Compressible Annular Seals," Proceedings of the 24th Turbomachinery Symposium, Texas A&M University, p. 175, 1995.
- Egli, T., "The Leakage of Steam Through Labyrinth Seals," Trans. ASME, 1935, pp. 115–122.
- Evenson, R.S., Mason, B., Frederick, D.V., St. Onge, and Alain, G. "Development and Field Application of a Single Rotor Design Dry Gas Seal," Proceedings of the 24th Turbomachinery Symposium, Texas A&M University; p. 107; 1995.
- FAG "Rolling Bearing Damage," Publication No. WL 82 102/2 Esi 1995.
- FAG "Rolling Bearings, Fundamentals, Types, Design," Publication No. WL 43 1190 EA 1996.
- Garner, D.R., and Leopard, A.J., "Temperature Measurements in Fluid Film Bearings," Proceedings of the 13th Turbomachinery Symposium, Texas A&M University; p. 133; 1984.

- Herbage, B.S., "High Speed Journal and Thrust Bearing Design," Proceedings of the 1st. Turbomachinery Symposium, Texas A&M University, October 1972, pp. 56–61.
- Herbage, B., "High Efficiency Fluid Film Thrust Bearings for Turbomachinery," 6th Proceedings of the Turbomachinery Symposium, Texas A&M University, December 1977, pp. 33–38.
- Jackson, C., "Radial and Thrust Bearing Practices with Case Histories," Proceedings of the 14th Turbomachinery Symposium, Texas A&M University, p. 73, 1985.
- King, T.L., and Captao, J.W., "Impact on Recent Tilting Pad Thrust Bearing Tests on Steam Turbine Design and Performance," Proceedings of the 4th Turbomachinery Symposium, Texas A&M University, October 1975, pp. 1–8.
- Leopard, A.J., "Principles of Fluid Film Bearing Design and Application," Proceedings of the 6th Turbomachinery Symposium, Texas A&M University, December 1977, pp. 207–230.
- Mayeux, T., Paul, Feltman Jr., and Paul, L., "Design Improvements Enhance Dry Gas Seal's Ability to Handle Reverse Pressurization," Proceedings of the 25th Turbomachinery Symposium, Texas A&M University, p. 149, 1996.
- Richards, R.L., Vance, J.M., Paquette, D.J., Zeidan, F.Y., "Using a Damper Seal to Eliminate Subsynchronous Vibrations in Three Back-to-Back Compressors," Proceedings of the 24th Turbomachinery Symposium, Texas A&M University, p. 59, 1995.
- Salamone, D.J., "Journal Bearing Design Types and Their Applications to Turbomachinery," Proceedings of the 13th Turbomachinery Symposium, Texas A&M University, p. 179, 1984.
- Scharrer, J.K., Pelletti, and Joseph, M., "Leakage and Rotordynamic Effects of Compressible Annular Seals," Proceedings of the 24th Turbomachinery Symposium, Texas A&M University, p. 175, 1995.
- Shah, P., "Dry Gas Compressor Seals," Proceedings of the 17th Turbomachinery Symposium, Texas A&M University, p. 133, 1988.
- Shapiro, W., and Colsher, R., "Dynamic Characteristics of Fluid Film Bearings," Proceedings of the 6th Turbomachinery Symposium, Texas A&M University, December 1977, pp. 39–53.
- Southcott, J.F., Sweeney, J.M., Feltrnan Jr., and Paul, L., "Dry Gas Seal Retrofit," Proceedings of the 24th Turbomachinery Symposium, Texas A&M University, p. 221, 1995.
- Takeuchi, Takao, Kataoka, Tadashi, Nagasaka, Hiroshi, Kakutani, Momoko, Ito, Masanobu, Muraki, and Ryoji "Advanced Dry Gas Seal by the Dynamic Ion Beam Mixing Technique," Proceedings of the 27th Turbomachinery Symposium, Texas A&M University, p. 39, 1998.

14

Gears

Gearing is one of the most important components between prime movers and driven units. If gearing is not selected properly, it can cause many problems. Gearing transmits great power at high rotational speeds. Recent advances in turbomachinery technology, especially in turbines, compressors, couplings, and bearings, have required gearing to withstand high external forces. To design problem-free equipment, it is important to consider the effect of the external system on gearing. Thus, all the factors that influence design, application, and operation of gear drives should be considered in the design phase.

Since problems encountered with gears are complex, it is unfair to blame them on the gear manufacturers alone. The gear supplier is much less informed about the package than any other group. Problems should be handled as a team effort between manufacturers and users. One factor causing problems is that the system is not timed in terms of spring constants and masses. The gear is usually the only item required to operate with metal parts in such close contact with other components. This setup can result in early failure. Gearing is also subjected to cyclic loading varying from 0 to 55,000 cycles per minute.

With current materials and heat-treating techniques, the use of high-hardness gearing with tooth loads of 1500–2000 pounds per inch of face at pitchline velocities of 20,000–30,000 feet per minute (6096–9144 mpm) is not at all uncommon. In turbine-driven test equipment, gear drives have been built with pitchline velocities as high as 55,000 feet per minute (16,764 mpm) and rotational speeds approaching 100,000 rpm. The magnitude of internal forces and material stresses coupled with the high speeds has resulted in gear drives that are dynamically complicated and sensitive to influences from other components in the system.

The system characteristics of the entire train must be known so that the selection of the gear will be proper. The major points affecting the system are: (1) couplings, (2) vibration, (3) operation conditions, (4) thrust loads, and (5) mounting type.

Couplings are a constant source of unbalance vibration, and critical speed changes can be attributed to spacer shift and wear. Coupling lockkeys can also cause severe housing vibration, while shaft vibration can remain low. Therefore, it is important to monitor vibration with accelerometers in addition to proximity probes. Gear failure from high vibration is common when the gear and pinion teeth operate within a few hundred microinches of each other. Accelerometers can also monitor gear mesh frequencies and thus act as early warning devices. Operating conditions must be known in detail.

In many cases, the gear manufacturer is provided with only the design horsepower of the machine. Actual transmitted loads can be much higher due to the proximity of torsional or lateral critical speeds. Surge in centrifugal compressors can cause severe overload and result in failures.

External thrust loads are another major problem, and in many cases they lead to double-helical gear selection. The gear housing and the mounting type of the gear train are very important considerations in the overall life of the unit, since improper mounting and expansion of the gear housing can lead to misalignment problems.

A substantial structure to support the gear drive weight, thrust, and torque reactions with minimum load deflections must be provided. At least two dowels for locating each gear housing are required, and it is necessary to minimize housing vibration from whatever source. Ideally, the structures should be reinforced concrete or steel filled with grout. The inclusion of oil reservoirs in the structure supporting major train components should be avoided, since unavoidable thermal changes will have adverse effects on alignment. If a reinforced concrete or a filled structure cannot be provided, resonance due to train component mass and structure stiffness at system rotational frequencies or harmonics should be avoided.

Gear Types

The choice between single- and double-helical gearing is sometimes difficult. Both gearing types can be made to equal limits of accuracy as control of the gearing accuracy is only a function of the accuracy and maintenance of the gear-generating machines, machining techniques, and operator skill. A hobbled gear is generated in a continuous process by a simple and easily maintained rack from cutter, which will produce gearing of extremely high-profile accuracy with virtually immeasurable spacing errors and uniform

lead. Where both helices of a double-helical gear are cut at the same time, or sequentially without a change in setup, apex position error will be virtually unobservable in operation, and axial vibration excitation from the mesh will be negligible. The same basic equipment can be used for generating either single- or double-helical gears, although the continuous finishing processes used for double-helical gears produce a higher order of accuracy of lead and tooth spacing than does grinding if it is used for finishing a single-helical type.

Thrust loading is a significant problem in the design of any gear unit, and effects differ based on the choice of single- or double-helical gearing. In either case an accurate estimate of the thrust loading is required to make an intelligent compensation for it. With double-helical gearing, continuous axial loading can be accommodated by a slight increase in capacity to account for the helix load imbalance. API 613 and 617 specifications require that single-helical gears must have a thrust bearing. It is also recommended (but not required) that double-helical gears have thrust bearings.

The increase in cost and the reduction of efficiency thus caused is only a fraction of that incurred when a large-diameter, high-velocity thrust bearing must be mounted on a single-helical pinion shaft.

Intermittent loading, such as that from gear couplings mounted on thermally expanding shafting, is a different problem. This problem is accommodated in a double-helical unit by judicious selection of helix angle and coupling size so that axial coupling forces resulting from the transmission of torque are less than the thrust force produced by each helix of the gear. This design assures that the coupling will slip to relieve any axial loading and that the power balance on the two helices will be maintained.

High-speed gear couplings are selected in which the pitch diameter is substantially smaller than that of the pinion. Axial forces produced will be high, and the combination should be examined very closely as a potential trouble source.

Double-helical speed gear is the first choice in calculating the accuracy of loading and smoothness of operation. Predictable performance renders unnecessary any deviations from easily defined and measured geometry. These gear sets will be more efficient and have unmatched reliability if properly applied. Reasonable intelligence must be exercised in coupling selection. This discretion will assure vibration and noise levels that are often indistinguishable from that of the connected machinery.

In single-helical gearing, all forces externally generated must be added to the thrust produced by the gear itself, and the total is used on each shaft to select the high-speed shaft thrust bearing. An error in thrust or bearing capacity estimation will result in frequent failures of the thrust bearing or

the associated shafting. Single-helical gearing, due to asymmetrical loading from the helix, has two sources of design difficulty which do not exist in double-helical gear sets. The effective center of tooth pressure oscillates back and forth across the face, putting substantial alternating loads on the shaft bearings. This oscillation results in peak bearing loads substantially greater than those calculated, which can lead to early bearing failure. In addition, the helix-induced thrust force causes the gearing to try to skew in the housing, unbalancing the bearing loading and forcing the gearing to run out of parallel. Crowning of single-helical gearing is used to counter the effects of shaft misalignment.

Factors Affecting Gear Design

A transverse section through a gear and pinion mesh is shown in Figure 14-1 with some of the major points in gear and pinion interaction. Figure 14-2 shows the terminology used to describe helical gear. The major factors affecting gear performance are: (1) pressure angle, (2) helix angle, (3) tooth hardness, (4) scoring, (5) gear accuracy, (6) bearing types, (7) service factor, (8) gear housing, and (9) lubrication.

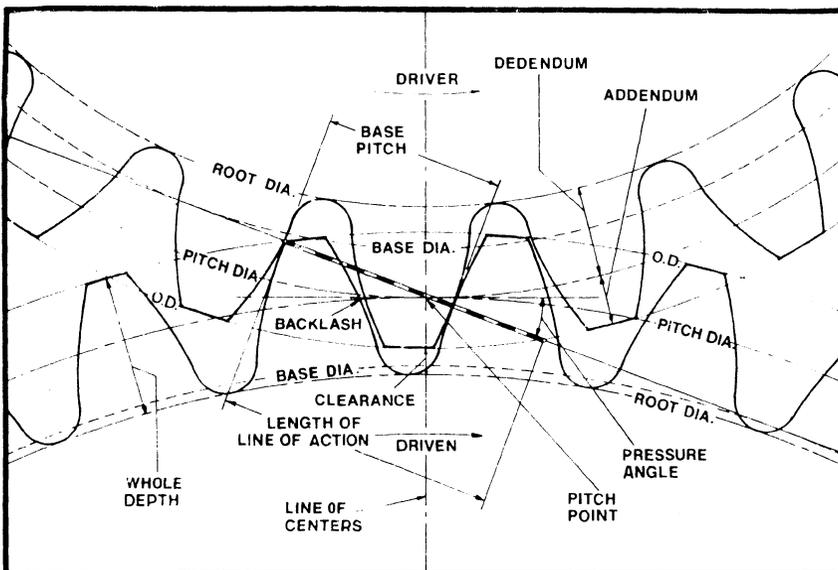


Figure 14-1. Transverse section through gear and pinion mesh.

Pressure Angle

The decision regarding the pressure angle is one that the designer has to make early in the design stage. Conventionally, pressure angles have ranged between 14.5° and 25° . Changes in the pressure angle affect both the contact ratio and the length of line of action. As the pressure angle increases, the contact ratio and the length of line of action decreases as seen in Figures 14-3 and 14-4. The contact ratio is an indication of the number of teeth in contact. As a general rule, the higher the contact ratio, the less noise the gears will generate.

The strength of the tooth is an important factor in the selection of the pressure angle. Figure 14-5 shows the variation of gear tooth geometry and pressure angle. The higher the pressure angle, the higher the tooth strength.

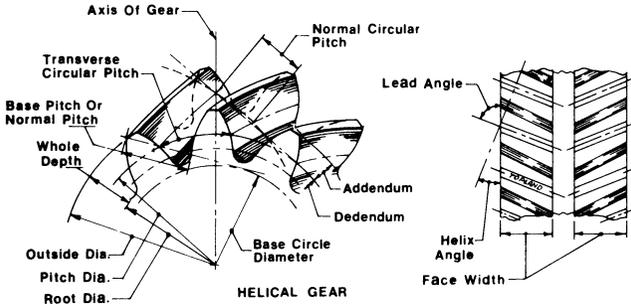


Figure 14-2. Helical gear terminology.

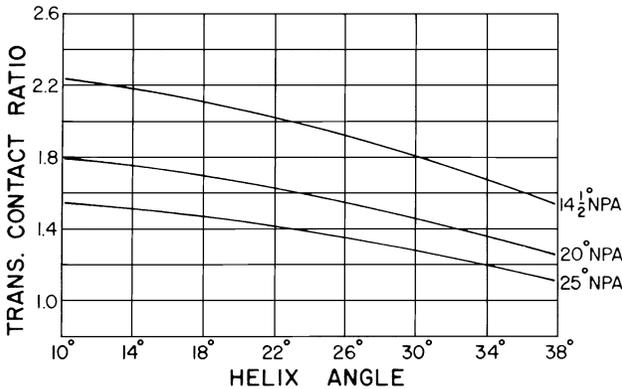


Figure 14-3. Variation of transverse contact ratio with pressure angle and helix angle. (Courtesy of Lufkin Industries, Inc.)

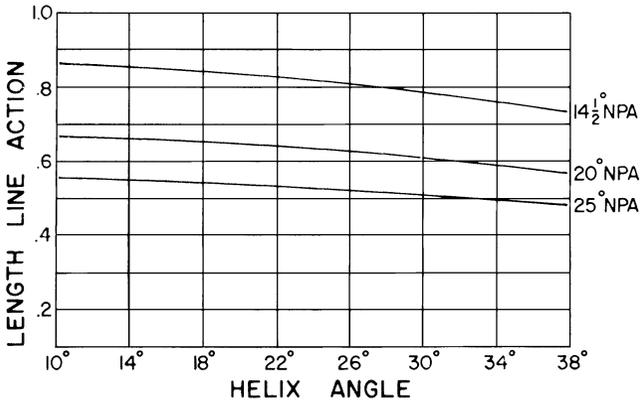


Figure 14-4. Length of line of action change with pressure angle and helix angle. (Courtesy of Lufkin Industries, Inc.)

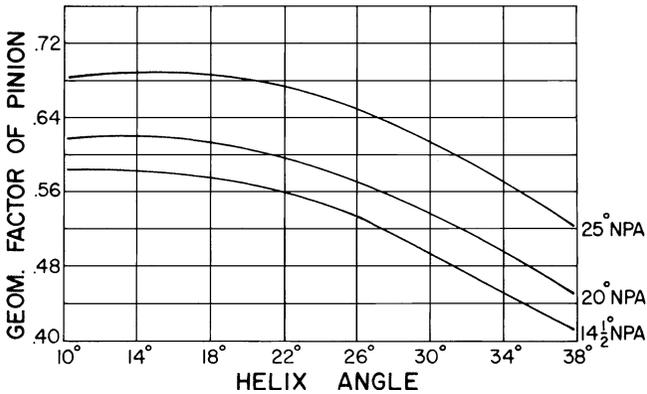


Figure 14-5. Variation of gear tooth geometry with pressure angle and helix angle. (Courtesy of Lufkin Industries, Inc.)

The noise that the gears generate decreases with a contact ratio increase. Thus, the selection of pressure angles involves many factors. Normal angles in use today are between 17.5° and 22.5°. Higher pressure angles increase the bearing loadings, but this increase is not a determining factor when selecting pressure angles.

Helix Angle

Helix angles vary from 5° to 45°. Single-helical angles fall between 5° and 20°, and double-helical angles fall between 20° and 45°. Helix angles are

selected to obtain a minimum overlap ratio and to provide good load sharing. Figure 14-6 shows the effect on overlap ratio with increasing helix angle. The thrust generated is also a function of the helix angle as shown in Figure 14-7. An increase in helix angle increases the thrust; thus, this increase is the main reason for the lower helix angles in single-helical gearing.

Both single- and double-helical gearing have advantages and disadvantages. The advantages of single-helical gearing are greater accuracy, less

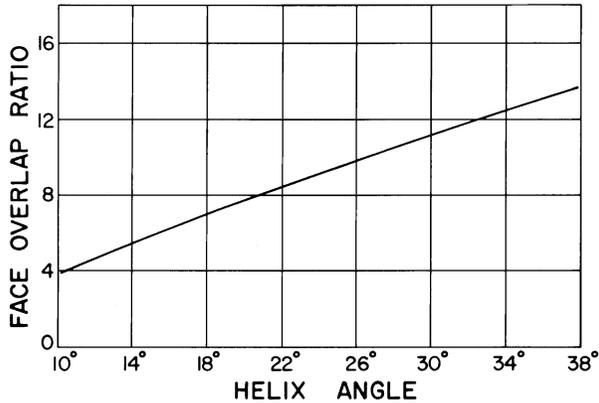


Figure 14-6. Face overlap (contact) ratio variation with helix angle. (Courtesy of Lufkin Industries, Inc.)

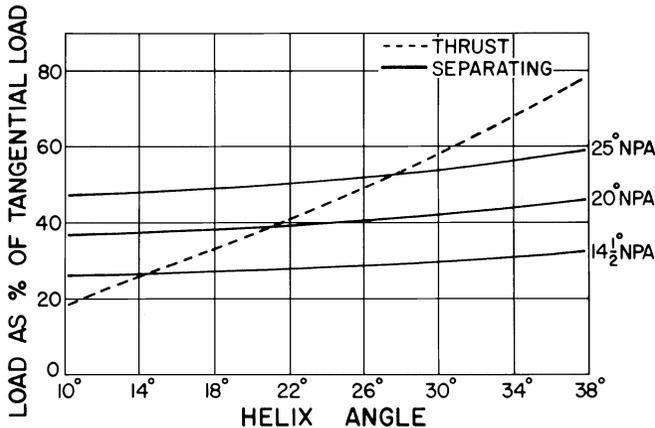


Figure 14-7. Thrust and separating load as a percentage of transmitted tangential load. (Courtesy of Lufkin Industries, Inc.)

sensitivity to coupling thrust, no measurable apex runout, and it is less expensive to cut teeth. The disadvantages of single-helical gears are that they require expensive thrust bearing and thrust faces, and are less efficient due to heat load on the thrust bearing.

Advantages of double-helical gears are that they are very simple to design and manufacture because of the absence of thrust faces and thrust bearings, very little thrust is produced by gearing, and they are more efficient than single-helical gears, which are subject to thrust bearing losses. Some disadvantages of double-helical gears: they are sensitive to coupling lockup, it is hard to modify the tooth longitudinally, and it is slightly more expensive to cut teeth because of setup and tool change.

Tooth Hardness

Gears available today have varying hardness, ranging from 225 BHN to 60 Rc. Each has advantages and disadvantages, so factors determining hardness must be carefully evaluated.

Medium-range gears are not too sensitive to operational errors and wear slightly before failing. Also, very hard gears are more susceptible to scoring due to high-lead intensity and sliding velocities. The noise levels on medium-hard gears increase with wear and give warning of gear failure. Heat treatment on medium-hard gears is simple compared to surface-hardened gearing. Hardened gearing is used mainly when weight and space are at a premium. When carbonized, case-hardened gearing must be subjected to a grinding operation to provide the finish. When nitriding is used, finish lapping or honing can be used. Hardened gears result in larger tooth deflections, thus resulting in noisier gears.

Scoring

For high-speed or high-load intensity, scoring must be evaluated. The probability of scoring is predicted using the flash temperature index. If the index value is below 275, it is considered to be a low-scoring risk. Values between 275 and 335 are considered high risks. Copper or silver plating is sometimes used on gear teeth to reduce failure during startups when the scoring probability increases. This plating acts as extreme-pressure lubricant to separate the tooth surface asperities until the teeth break in.

Figure 14-8 shows the effect of speed and load intensity on the flash temperature index. These curves are general in nature, since scoring is a function of pressure angle, lubrication, and tooth size.

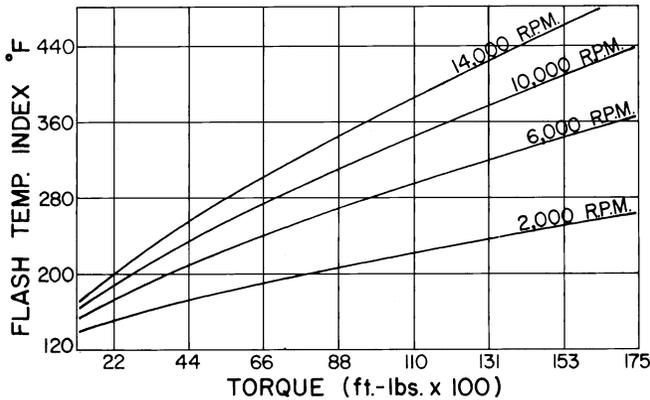


Figure 14-8. Scoring based on flash temperature index related to speed and torque. (Courtesy of Lufkin Industries, Inc.)

Gear Accuracy

There are no accuracy standards for high-speed enclosed gear drives. The AGMA 390 is the standard for gear accuracy and has tabulated allowable errors based on gear size for the different elements of gear teeth. This standard holds only for loose gearing and, if used for high-speed, wide-face width gears, will lead to early failure. As a general rule, manufacturers of high-speed gearing monitor the gears and pinions for involute, lead, runout, spacing, and surface finish. Light-load blue transfer checks are conducted to prove the accuracy of the system.

Types of Bearings

Bearings of all types can be used to support gears. Normally, gear drives proposed for turbine-driven applications, whether they are single- or double-helical, will be supported in sleeve-type bearings.

The most common type used are plain journal bearings. They have good load-carrying capacity, but they can also have oil whirl problems. To prevent oil whirl problems, pressure dam or tilting pad journal bearings are used. Gear motors have imposed operating loads and do not require the same degree of no-load bearing stability as compressor turbines, which have only the rotor weight applied to the bearings.

The exclusion of rolling-type bearings from drives of this class may be unwarranted. In the lower horsepower ranges, bearing ratings can be easily provided so that race and roller fatigue can be ignored as a source of failure.

Drives using rolling element bearings may sometimes provide additional design latitude for the gear manufacturer. The extensive use of rolling element bearings in contemporary light-weight gas turbine designs bears strong testimony for this point.

Thrust bearings vary from the ball bearing to the self-equalizing tilting pad-type. The most common type is the babbitt-lined, flat-face thrust bearing. The flat-face bearing is sometimes modified to add tapered lands, which double the load-carrying capacity. Tilting pad bearings are becoming more popular because of their high-thrust capacity and misalignment capabilities. Also, the tilting pad thrust bearing is more efficient because of the higher allowable loading and lower rubbing speeds.

Service Factor

When selecting gears, two major areas to consider are the service factor and type of drive to be employed. The service factor is defined as the minimum ratio between calculated capacity and average transmitted load for any component of the system. In general, one of three criteria will be the controlling influence in gear drives. These are failures due to tooth surface pitting, wear, or physical loss of teeth from breakage. Consequences of the three failure modes differ, particularly in regard to the time length involved. Wear can continue for a long period of time without affecting machinery serviceability or reliability. Pitting, if progressive, will eventually destroy the working profile of the teeth, altering their thermal characteristics, and often rendering the drive unsuitable because of high-vibration levels long before the teeth are incapable of carrying load. Loss of a portion of a tooth by breakage has immediate consequences. The balance is immediately and drastically affected and, with major tooth breakage, the gear will be incapable of further operation. Any evaluation of a service factor should determine which of the three modes is involved.

Current practice includes the automatic provision of an additional 50% margin when designing for gear tooth bending. This margin has the effect of eliminating gear tooth breakage as a primary cause of failure except with severe and unforeseen overloads.

Design against failure by wear under heavy tooth loads will result in the selection of heavy-bodied lubricants, generally 150 SSU or more at supply temperature. Pitting failures are the most difficult to provide a margin against as increasing gear size or hardness are the only means of improving capacity, and both entail an increase in cost.

The service factor itself is not an overload capacity per se, as it includes either empirical or theoretical estimates of the effect of such factors as length

of service life, torque fluctuations, and reliability level required. The service factors as established by the American Gear Manufacturers Association and published in their standards are intended for application to transmitted load requirements; if substantial overload capacity is planned or allowed (an oversize driver), additional gear rating must be included to provide for operation at those levels. Similarly, torque loads resulting from torsional oscillations or faulty operation are outside the scope of normally applied service factors and must be evaluated and provided for separately. Any torque fluctuations that result in a separation of gear teeth at speed will be most difficult to provide for. Impact loads occur during re-engagement, and very short service life is a frequent result of operation under these conditions.

Gear Housings

Gear housings are made from materials such as cast iron, steel, or aluminum. Before final matching, the gear housing must be stress-relieved for dimensional stability. Housing should also be rigid enough to resist misalignment. A sufficient clearance should be provided around the gears to prevent oil choking. To prevent thermal distortion, the design should be able to maintain uniform case temperatures. Gear housings can cause alignment problems from thermal distortion.

Lubrication

The oil furnished to high-speed gears has a dual purpose: tooth and bearing lubrication and cooling. Usually, only 10–30% of the oil is for lubrication, and 70–90% is for cooling.

A turbine oil with rust and oxidation inhibitors is preferred. This oil must be kept clean, cooled, and have the correct viscosity. Synthetic oils should not be used without the manufacturer's approval.

When selecting a high-speed gear unit, the possibility of using an AGMA No. 2 oil should be considered. In most cases, the sleeve bearings in the system can use this oil and, if not, a compromise 200 SSU at 100°F (38°C) oil should be considered.

When 150 SSU at 100°F (38°C) oil is necessary, inlet temperatures should be limited to 110–120°F (43–49°C) to maintain an acceptable viscosity. Oil should be supplied in the temperature and pressure range specified by the manufacturer. Up to a pitch-line speed of approximately 15,000 feet per minute (4572 mpm) the oil should be sprayed into the out-mesh. Spraying allows maximum cooling time for the gear blanks and applies the oil at the highest temperature area of the gears. Also, a negative

pressure is formed when the teeth come out of the mesh, pulling the oil into the tooth spaces.

At more than approximately 15,000 feet per minute, (4,572 mpm) 90% of the oil should be sprayed into the outmesh and 10% into the inmesh. This procedure is a safety precaution to assure the amount of oil required for lubrication is available at the mesh. When the speed ranges from 25,000 to 40,000 feet per minute (7,670–12,192 mpm), oil should be sprayed on the sides and gap area (on double-helical) of the gears to minimize thermal distortion.

Manufacturing Processes

Gear manufacturers use several methods for manufacturing good high-speed gearing. The most common are hobbing, hobbing and shaving, hobbing and lapping, and grinding.

High-speed gearing requires a finishing operation after cutting that involves shaving, lapping, or grinding. Shaved or lapped gears have been more widely used than ground gears. However, there are some advantages and disadvantages to each manufacturing process.

Hobbing

This process produces good tooth spacing and accurate lead. It cannot economically achieve a surface finish better than $40\ \mu\text{in}$ ($1016\ \mu\text{mm}$). The cutting tool, called the “hob gear,” is basically a worm gear that has been fluted and has form-relieved teeth. These flutes provide the cutting edges and can be sharpened to retain the original tooth profile. As the workpiece meshes with the hob, the teeth are formed by a series of cuts known as the generating process. To cut the helix angle, the rotation of the work is slightly retarded or advanced in relationship to the hob rotation, and the feed is held in a definite relationship with the work and hob. Very accurate gearing can be produced by this process.

Hobbing and Shaving

The shaving process improves surface finish, involute profile, and lead, and can be used to crown the teeth. Shaving with inaccurate cutters will reduce hobbled accuracy, and it cannot improve spacing or pitch-line runout. The shaving cutter has involute teeth and meshes with the part being shaved, thus improving the finish.

Hobbing and Lapping

The lapping process improves surface finish, involute profile, lead, and pitch-line runout. Absolute accuracy is not as good on lapped gears, but the mismatch error is generally as good as other production methods. Lapping is performed with the gears on an accurate mounting stand running at zero backlash with a cutting compound mixed with oil or grease performing the finishing operation. Lapping is also sometimes performed at the site. If site lapping is done, care must be taken to thoroughly clean the lubrication system before the system is put on-line. If the lubrication system is not clean, scoring of the bearing can take place.

Finish lapping of high-speed gears requires that the gear teeth be carefully hobbled to 40–50 microinches (1016–1270 μm) surface finish with good lead profile and tooth spacing. Lapping is required for surface finish and profile improvement only. When required, a surface finish of 8–15 microinches (200–380 μm) can be obtained but, as a general rule, 20–30 microinches (508–762 μm) is acceptable.

Grinding

Grinding produces the best absolute values of lead and involute profile. As a general rule, tooth spacing is not as good as gearing produced on a precision hobbing machine because of the smaller index wheel and the single-space indexing procedure. The disadvantage of the grinding process is the skill and patience required of the operator. Gears too large to be checked depend on a roll-in blue check for verification of lead and involute. Also, the grinding machines in current use have a reciprocating motion of the grinding head and require greater maintenance to produce good gears.

Gear Rating

The API, with help from gear manufacturers, has a 1977 standard (API 613) for rating gears. (See Chapter 4.) A common procedure for comparing and sizing gear is based on the tooth pitting index, the K factor

$$\text{Allowable } K = \frac{\text{Material index number}}{\text{Service factor}} \quad (14-1)$$

The material index is based on hardness and geometry parameters. The service factor takes into account the driving and the driven equipment characteristics. The AGMA 211 standard defines K as

$$K = \frac{126,000 \times P_{sc}}{N_p \times d^2 \times F} \times \frac{M_g + 1}{M_g} \quad (14-2)$$

where:

P_{sc} = transmitted horsepower

M_g = gear ratio

N_p = pinion rpm

d = pinion pitch diameter in inches

F = net face width of narrowest mating gears, or the sum of the face width of each helix of double-helical (inches)

API 613 is consistent with AGMA 211. However, API 613 is more conservative than the AGMA procedure, using service factors of 1.5 and 2.0.

The strength rating based on API 613 is

$$S_t = \frac{w_t \times P_n \times (SF)}{F} \times \frac{1.8 \cos \theta}{J} \quad (14-3)$$

where:

S_t = bending stress number

θ = helix angle

J = geometry factor

SF = service factor

P_n = normal diameter pitch

Gear Noise

Noise from an operating gear set is a function of roundness and concentricity of operating elements (both gearing and shafting), accurate balance and, in particular, control of tooth spacing errors and uniformity of mesh stiffness to reduce meshing frequency excitation. It is significant that for

submarine gears, where the ultimate in quietness is essential, the hallmarks are moderate tooth loading, fine pitch, high-helix angle, and low-pressure angle—all diametrically opposite from the usual and necessary practice for single-helical, hardened and ground gearing, which have low-helix angle (for minimum thrust), very coarse pitch teeth (to get adequate strength), and high loading (because of the carburized hardening).

Some factors causing gear noise can be attributed to, but not limited to, the following:

1. Tooth spacing or involute error
2. Contact ratio
3. Surface finish
4. Wear on tooth flanks or pitting
5. Excessive or too little backlash
6. Gear, shaft, or housing resonance
7. Tooth deflections
8. Pitch-line runout
9. Load intensity on gearing
10. Clutches and couplings
11. Lube oil pump and piping
12. Transmitted noise from driven or driving machinery

Installation and Initial Operation

The mounting of a gearbox into trains is a precision job and should be done carefully. Gear unit installation is one of the most important factors to be considered for long, trouble-free operation. No matter how accurately the gear unit is manufactured, it can be destroyed in a few hours of operation when improperly installed. The same care should be taken when installing a gearbox as with any high-speed machinery. The mounting surface should be a flat, level, single-plane surface of finished steel at a height that will permit the shimming necessary to align the gear unit properly to connecting shafts. The shims should be of a size at least equal to the width of the unit foot pad. Then the gear unit should be placed on the foundation in the approximate required position. Uneven supports can distort the gearbox and adversely affect the gear tooth contact.

Shaft alignment is very important for long gear life. Poor alignment can cause unequal distribution of tooth loads and distortion of the gear elements from overhung moments. A 2.0-mil shaft vibration level on the gear unit produced by misalignment is equivalent to a gear pitch-line runout of 2.0 mils.

The gear housing must be properly supported to maintain proper internal gear alignment. When a gear unit is installed, the support pads must be maintained in the same plane as used by the manufacturer during assembly when gear face contact was obtained in the plant. Before startup, gear face contact should be checked using high-spot bluing, and rotating or rocking the pinion or lighter element back and forth sharply within the confines of the backlash. Inspection of this blued area should show approximately 90% face contact. If this contact is not obtained, the gear housing can be shimmed under the proper corner until an acceptable face contact is achieved.

Many large, high-hardness or wide-face width gears are manufactured with helix angle modifications to account for torsional and bending deflection. When the helix angle has been modified, good face contact will not be obtained under light load. In this case, the gear supplier should furnish data on percent of face contact versus load to be used as a guide during installation and startup. Also, many gears have a short area of ease-off on each end of the teeth to prevent end-loading, and this area usually will not show contact under light load.

The larger the gear unit, the more important this check becomes, since large housings tend to be more flexible. Also, the use of baseplates furnished by the original equipment manufacturer does not eliminate face contact problems, and these inspection procedures should be carried out.

After the gear checks have been made, the foundation bolts should be uniformly tightened and the alignment rechecked. It may be necessary to repeat the shimming and tightening of foundation bolts to obtain final, correct cold alignment.

Alignment of high-speed gear units should always be hot-checked and adjustments made as necessary. Temperatures vary so greatly throughout the housing and shafting that it is impossible to calculate a thermal growth accurately and, therefore, an alignment check must be made in the hot condition.

When the alignment is complete, the baseplate or bed should be grouted in as close to the gear housing as possible. Journal bearings are used on the gear shafts and proper oil flow must be maintained. The oil system should therefore be checked thoroughly prior to startup. The gear lube system is normally flushed prior to any operations. The usual procedure is to seal off the gearbox components to which acid would be harmful, acid flush the system, and follow with a neutralizing flush before filling with the lube oil. Gear mesh spray nozzles should be checked to be sure dirt was not pumped through the system by observing the sprays or by introducing high-pressure air into the spray nozzle manifold.

When possible, gears should be run-in on initial startup. Speeds and loads should be increased in percentage increments. Lube oil temperature, and pressure and bearing temperatures should be observed and adjustments made to the lube system as required. The number of adjustments made will depend on the complexity of the system. Oil pressure is of primary importance. When an auxiliary pump has been provided, oil should be circulated before the actual start. If not, the pump should be primed, and the journals wetted with oil. Primer holes are sometimes provided or alternate journals can be oiled through the holes provided for bearing temperature detectors.

It is recommended that warning devices be provided to eliminate as much human error as possible, and the set points should be checked carefully. As with any startup, vibrations should be monitored and recorded. The vibration monitoring system should include at least one accelerometer to detect any vibrations generated at gearmesh frequency. The recorded data should be saved to provide baseline vibration data for future reference.

Shutdowns, as well as startups, require care and attention. Shutdown of a unit, which has been operating in a humid atmosphere, can result in considerable condensation and subsequent rusting of the gears, shaft journals, and housing in a very short time. When water contacts clean steel, it begins to etch the steel immediately. When shutdowns in such conditions are necessary, provisions to prevent condensation must be furnished.

Under normal operating conditions, the oil should be changed every 2,500 operating hours or every six months, whichever occurs first. Where operating conditions warrant, this period may be extended; conversely, severe operating conditions may make it necessary to change oil at more frequent intervals. Such conditions may occur with the rapid rise and fall in temperature, which produces condensation, when operating in moist or dusty atmospheres, or in the presence of chemical fumes. In any case, the lubrication supplier should be consulted when determining a lubricant maintenance program. It may be necessary to analyze the oil periodically until a reasonable program can be established.

Bibliography

- AGMA 211.02, "Surface Durability (Pitting) of Helical and Herringbone Gear Teeth," Washington, D.C., 1969.
- AGMA 390.03, "Gear Classification, Materials, and Measuring Methods of Unassembled Gears," *Gear Handbook*, Vol. 1, Washington, D.C., 1973.

API 613, *Special Purpose Gear Units for Refinery Services*, 2nd edition, Washington, D.C., 1977.

API 617, *Centrifugal Compressors for General Refinery Services*, Washington, D.C., 1979.

Partridge, J.R., "High-Speed Gears-Design and Application," Proceedings of the 6th Turbomachinery Symposium, Texas A&M University, December 1977, pp. 133-142.

Phinney, J.M., "Selection and Application of High-Speed Gear Drives," Proceedings of the 1st Turbomachinery Symposium, Texas A&M University, October 1972, pp. 62-66.

Part V

Installation, Operation, and Maintenance

15

Lubrication

For reliable turbomachine performance, it is vital to have a properly designed, installed, operated, and maintained lubrication system. The lubrication system of a turbomachine is the “lifeblood” for this complex and finely tuned piece of machinery. The oil must be pumped in continuous circulation, conditioned, drained, and returned to be pumped again. In some units there are independent and dedicated turbine lube oil, compressor lube oil, and turbine control oil systems. There are combined systems with turbine lube oil and control oil from one system and compressor lube oil from another, or with turbine and compressor lube oil from one system and turbine control oil from another. In most cases, one system will supply all lube and control oil.

This chapter deals with the principles involved in the operation and maintenance of a lubrication system, and it describes the main components of such a system, including the lubricant itself. The following topics are discussed:

1. Basic oil system
2. Lubricant selection
3. Oil sampling and testing
4. Oil contamination
5. Filter selection
6. Cleaning and flushing
7. Coupling lubrication

Basic Oil System

API Standard 614 covers in detail the minimum requirements for lubrication systems, oil-type shaft-sealing systems, and control-oil supply systems for special-purpose applications.

Lubrication Oil System

A typical lubrication oil system is shown in Figure 15-1. Oil is stored in a reservoir to feed the pumps and is then cooled, filtered, distributed to the end users, and returned to the reservoir. The reservoir can be heated for startup purposes and is provided with local temperature indication, a high-temperature alarm and high/low level alarm in the control room, a sight glass, and a controlled dry nitrogen purge blanket to minimize moisture intake.

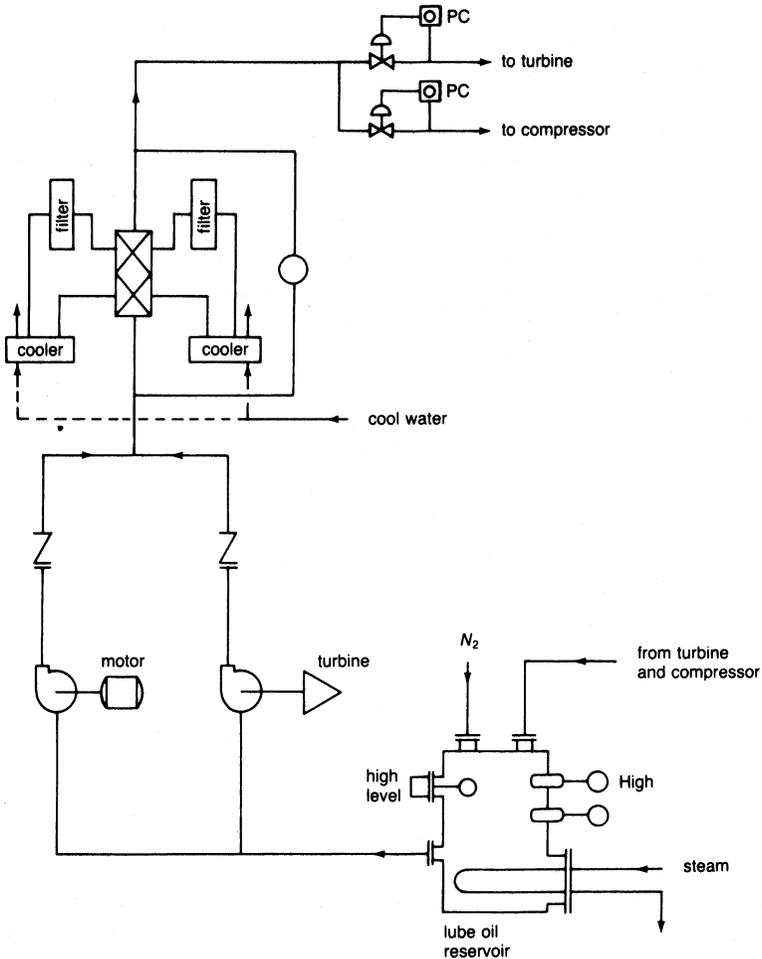


Figure 15-1. A typical lube oil system.

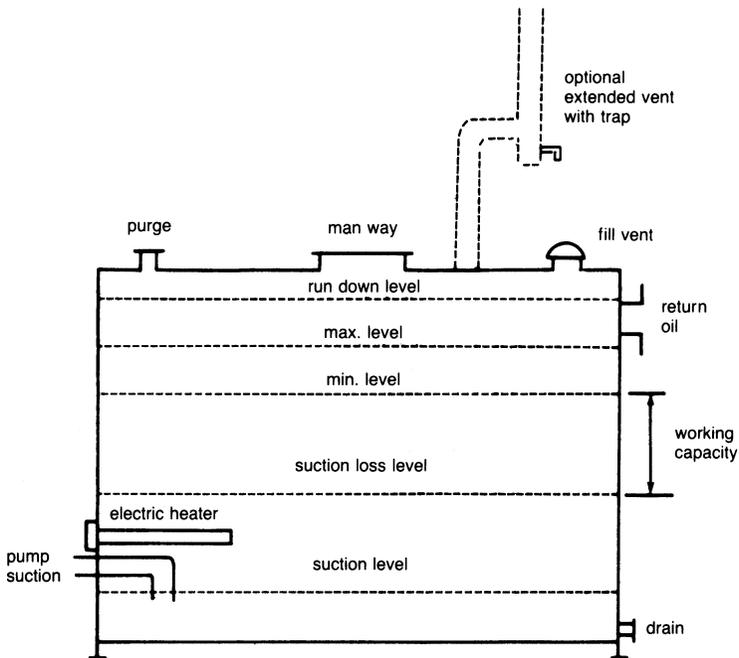


Figure 15-2. Lube oil reservoir.

The reservoir shown in Figure 15-2 should be separate from the equipment base plate and sealed against the entrance of dirt and water. The bottom should be sloped to the low drain point, and the return oil lines should enter the reservoir away from the oil pump suction to avoid disturbances of the pump suction. The working capacity should be at least five minutes based on normal flow. Reservoir retention time should be 10 minutes, based on normal flow and total volume below minimum operating level. Heating for the oil should also be provided. If thermostatically controlled electrical immersion heating is provided, the maximum watt density should be 15 watts per square inch (2.33 w/cm^2). When steam heating is used, the heating element should be external to the reservoir.

The rundown level, which is the highest level the oil in the reservoir may reach during system idleness, is computed by considering the oil contained in all components, bearing and seal housings, control elements, and furnished piping that drains back to the reservoir. The rundown capacity should also include a 10% minimum allowance for the interconnecting piping.

The capacity between the minimum and the maximum operating levels in an oil system that discharges seal oil from the unit should be enough for a minimum

operation of three days with no oil being added to the reservoir. The free surface should be a minimum of 0.25 sq ft/gpm (0.023m²/gpm) of normal flow.

The reservoir interior should be smooth to avoid pockets and provide an unbroken finish for any interior protection. Reservoir wall-to-top junctions may be welded from the outside by utilizing full-penetration welds.

Each reservoir compartment should be provided with two three-quarter-inch minimum size plugged connections above the rundown oil level. These connections may be used for such services as purge gas, makeup, oil supply, and clarifier return. One connection should be strategically located to ensure an effective sweep of purge gas toward the vents.

The oil system should be equipped with a main oil pump, a standby and, for critical machines, an emergency pump. Each pump must have its own driver, and check valves must be installed on each pump discharge to prevent reverse flow through idle pumps. The pump capacity of the main and standby pumps should be 10–15% greater than maximum system usage. The pumps should be provided with different prime movers.

The main pumps are usually steam turbine driven with an electric motor driven backup pump. A small mechanical-drive turbine is highly reliable as long as it is running, but it is undependable for starting automatically after long idle periods. A motor is thus the preferred backup pump driver. A “ready-to-run” status light is usually provided for the motor in the control room to give visible evidence that the electrical circuit is viable. Starting of the backup pump is initiated by multiple and redundant sources. The turbine drivers should be maintained for failure by either low-speed or low-steam chest pressure or both.

Low oil pressure switches are provided on the pumps and discharge header ahead of the coolers and filters, sometimes after the cooler and filters, and always at the end of the line where the reduced oil pressure feeds the various users. A signal from any of these should start the motor-driven pump and all alarms should be activated in the control room. The emergency oil pump can be driven with an AC motor but from a power source that is different to the standby pump. When dc power is available, DC electric motors can also be used. Process gas or air-driven turbines and quick-start steam turbines are often used to drive the emergency pumps.

The pump capacities for lube and control oil systems should be based upon the particular system’s maximum usage (including transients) plus a minimum of 15%. The pump capacity for a seal oil system should be based upon the system’s maximum usage plus either 10 gpm or 20%, whichever is greater. Maximum system usage should include allowance for normal wear. Check valves should be provided on each pump discharge to prevent reverse flow through the idle pump.

The pumps can be either centrifugal or positive displacement types. The centrifugal pumps should have a head curve continuously rising toward the shut-off point. The standby pump should be piped into the system in a manner that permits checking of the pump while the main pump is in operation. To achieve this, a restriction orifice is required with a test bleeder valve piped to the return oil line or the reservoir.

Twin oil coolers (Figure 15-3) should be provided and piped in parallel using a single multiport transflow valve to direct the oil flow to the coolers. The water should be on the tube side and the oil on the shell side. The oil-side pressure should be greater than the water-side pressure. This ratio is no assurance that water will not enter the system in the event of a tube leak, but it does reduce the risk. The oil system should be equipped with twin full-flow oil filters located downstream from the oil coolers. Since the filters are located downstream from the oil coolers, only one multiport transflow valve is required to direct the oil flow to the cooler-filter combinations. Do not pipe the filters and coolers with separate inlet and outlet block valves.

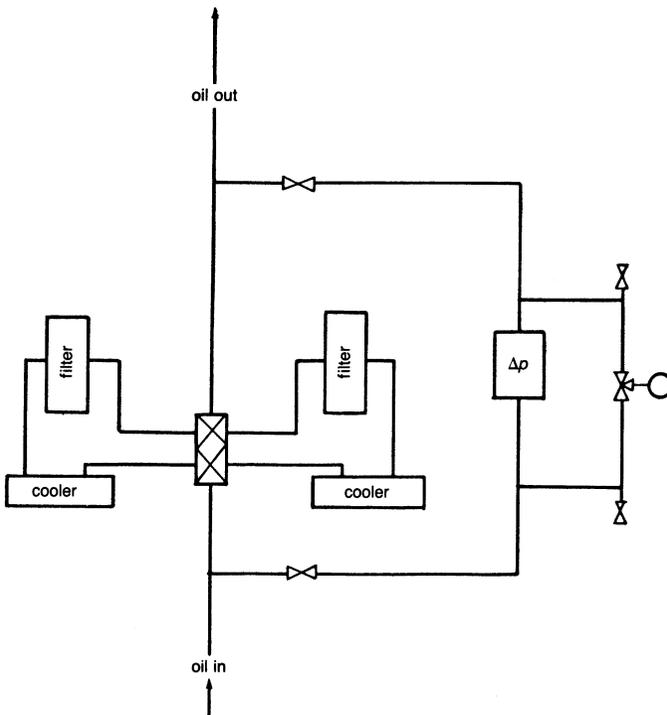


Figure 15-3. Cooler-filter arrangement.

Separate block valves can cause loss of oil flow from the possible human error of flow blockage during a filter switching operation.

Filtration should be 10 microns nominal. For hydrocarbon and synthetic oils, the pressure drop for clean filters should not exceed five psi at 100°F operating temperature at normal flow. Cartridges will have a minimum collapsing differential pressure of 50 psi (3.447379 Bars).

The system should have an accumulator to maintain sufficient oil pressure while the standby pump accelerates from an idle condition. An accumulator becomes a must if a steam turbine drives the standby pump. Overhead tanks are specified by many users to assure flow to critical machinery components. The sizing of the tanks varies depending on the application. In some gas turbine applications, the bearings reach maximum temperature as long as 20 minutes after shutdown.

The oil coolers and filters are controlled by a local temperature control loop with remote control room indication and high/low alarm. The coolers and filters also have an indicating differential pressure alarm. These usually feed into a common high alarm to pre-warn a need for switching and filter element replacement.

To ensure the required constant pressure, a local pressure control loop is provided on each system—turbine lube oil, compressor lube oil, and control oil. Each oil pressure system should be recorded in the control room to provide troubleshooting information. The success of the oil system depends upon not only the instrumentation, but upon proper instrument location.

The minimum alarms and trips recommended for each major driver and driven machine should be a low oil pressure alarm, a low oil pressure trip (at some point lower than the alarm point), a low oil level alarm (reservoir), a high oil filter differential pressure alarm, a high bearing metal temperature alarm, and a metal chip detector. See Table 15-1.

Each pressure- and temperature-sensing switch should be in separate housings. The switch type should be single-pole, double-throw, furnished

Table 15-1
Alarms and Trips

| | Alarm | Trip |
|---------------------------------------|--------------|-------------|
| Low oil pressure | x | x |
| Low oil level | x | |
| High oil filter | x | |
| High thrust bearing metal temperature | x | |
| High thrust bearing oil temperature | x | |
| Metal chip detector | x | |

as “open” (de-energized) to alarm and “close” (energize) to trip. The pressure switches for alarms should be installed with a “T”-connection pressure gauge and bleeder valve for testing the alarm.

Thermometers should be mounted in the oil piping to measure the oil at the outlet of each radial and thrust bearing and into and out of the coolers. It is also advisable to measure bearing metal temperatures.

Pressure gauges should be provided at the discharge of the pumps, the bearing header, the control oil line, and the seal oil system. Each atmospheric oil drain line should be equipped with steel nonrestrictive bull’s-eye-type flow indicators positioned for viewing through the side. Viewports in oil lines can be very useful in providing a visual check for oil contamination.

In the piping arrangement and layout it is very important to eliminate air pockets and trash collectors. Before starting a new or modified oil system, every foot of the entire system—right up to the final connection at the machine—should be methodically cleaned, flushed, drained, refilled and all instruments thoroughly checked.

Seal Oil System

The compressor seal oil system is designed and furnished with instrumentation similar to the lube oil system shown in Figure 15-4. The only essential difference is how the end-supply control is handled. Since much higher pressures (1500–2500 psi) (103.4214–172.3689 Bars) are often involved, the pumps are usually a positive displacement-type. This requires a pressure control valve spilling oil back to the reservoir. This oil supply is available to an elevated head tank that is provided for each shaft seal. The head tank is pressured by its own process-seal pressure connection, so the seal oil supply system pressure must be maintained at a level to supply the highest pressure seal. The oil rate to each seal is maintained by tank level control from the supply system. The tanks are provided with a high/low level alarm to the control room. The low alarm warns of excessive oil consumption by the seal and also calls for backup pump start along with the various pressure switches and primary pump turbine failure in a similar manner to the lube oil system.

A degassing facility is also provided to separate gas contaminants from the seal oil. Figure 15-5 shows a typical degassing drum arrangement. A gas-tight baffle and a liquid seal should divide the degassing drum into two sections to confine the separated gas to one side of the drum. The gas side of the drum should be vented and provided with an inert-gas purge. To assist in degassing the oil, the drum will be heated by electricity or steam.

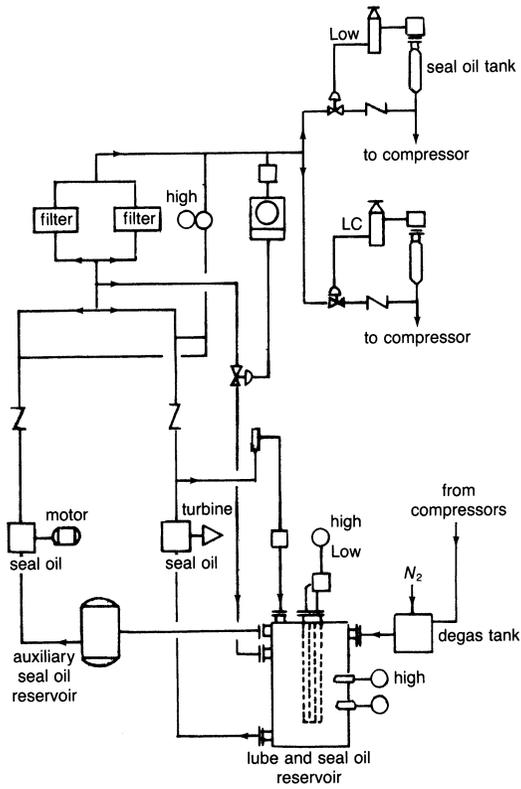


Figure 15-4. Seal oil system.

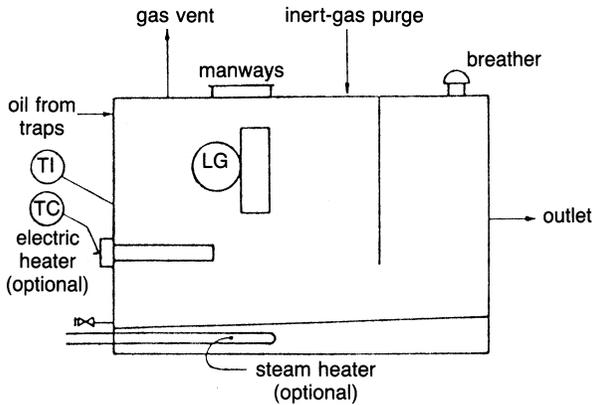


Figure 15-5. Typical degassing drum arrangement.

Lubricant Selection

A good turbomachinery oil must have a rust and oxidation inhibitor, good demulsibility and the correct viscosity, and be both nonsludging and form-resistant. Besides lubrication, the oil has to cool bearings and gears, prevent excessive metal-to-metal contact during starts, transmit pressure in control systems, carry away foreign materials, reduce corrosion, and resin degradation.

For gas turbines, especially the more advanced high-temperature gas turbines, the oil of choice should be synthetic oil, since synthetic oils have a high flash point. Gas turbine lubrication systems should be run for about 20 minutes after shutdown since maximum temperatures are reached after 10 minutes of shutdown especially in the bearing area. Most gas turbines are also on turning gear to avoid sagging in the shaft. Mineral oils can be used for the compressor. It is not uncommon to have two types of oil in a petrochemical plant. Mineral oil costs much less than the synthetic oil.

The selection of the correct lubricant must begin with the manufacturer. Refer to the operator's instruction manual for the oil required and the recommended viscosity range. The local environmental conditions should be seriously considered, including exposure to outside element conditions, acid gas, or steam leaks. As a general rule, most turbomachines are lubricated with premium-quality turbine-grade oil. However, under certain environmental conditions, it may be advantageous to consider another oil. For example, if a machine is subject to exposure to low concentrations of chlorine or anhydrous hydrochloric acid gases, it may be better to select another oil that will outperform the premium turbine oil. Good results have been recorded using oil containing alkaline additives. Certain automotive or diesel engine oils contain the optimum amount and type of alkaline additives to protect the base oil from reaction with chlorine and HCl. In services where the attack on the lubricant by the gas is unknown, laboratory tests are suggested.

Oil Sampling and Testing

Oils from turbomachinery should be tested periodically to determine their suitability for continued use; however, visual inspection of the oil can be useful in detecting contaminated oil when the appearance and odor is changed by the contaminant.

An oil sample should be withdrawn from the system and analyzed in the laboratory. The usual tests of the used oil include: (1) viscosity, (2) pH and neutralization number, and (3) precipitation. The test results will

indicate changes from the original specifications and, depending on how extensive these changes are, whether the oil can or cannot be used in the machines.

Oil Contamination

Oil contamination in a turbomachine is one of the major problems maintenance crews face. However, while contamination is a continuous problem, the *levels* of contamination are what cause the most concern.

The greatest source of contamination is extraneous matter. Atmospheric dirt, for example, is always a serious threat. It can enter the oil system through vents, breathers, and seals. Its primary effect is equipment wear, but plugging of oil lines and ports, and reduced oxidation stability of the oil are also serious effects.

Metal particles from wear and rust particles from reservoir and oil piping corrosion can lead to premature equipment failure and oil deterioration. It is important to provide suitable filtering equipment to remove these particles from the system.

Water contamination is a constant threat. The sources of water are many—atmospheric condensation, steam leaks, oil coolers, and reservoir leaks. Rusting of machine parts and the effects of rust particles in the oil system are the major results of water in oil. In addition, water forms an emulsion and, combined with other impurities, such as wear metal and rust particles, acts as a catalyst to promote oil oxidation.

Contamination from process gas can be a serious problem, particularly during startup. Every effort must be exercised to prevent and detect this type of contamination.

Most hydrocarbon gases are more soluble in cold oil than in hot oil and may lower the viscosity to a dangerous level. The problems of thrust-bearing failures during startup due to low-viscosity oil can be eliminated by equipping the reservoir with oil heaters to raise the oil to the normal operating temperatures before starting the machine.

Equipment in HCl and chlorine service must be protected against the exposure of these acid gases to the oil. Obviously, the first line of defense is to eliminate seal failures. However, as a secondary protection, these machines could be lubricated with an alkaline oil. The alkaline additives react to the low concentrations of the acid gases, thus eliminating the addition of these acids to the oil molecule.

To remove insoluble contaminants, various types of full-flow filters can be used. Two general types are usually selected: surface filters and depth filters. Both types of filters are effective for the removal of particulate matter.

Surface filters, if manufactured from the correct material, will not be affected by water in the oil. Water-resistant pleated-paper elements have much greater surface areas than the depth-type element and yield a much lower differential pressure when used as replacement elements in filters originally equipped with depth-type elements. Pleated-paper elements are available that will remove particle sizes down to a nominal one-half micron.

The depth-type filter elements are used when the oil is free from water, and when particles sizes to be removed are in the five-micron and greater range. Generally, the depth-type element is water-sensitive, and when oil is contaminated with moisture, this element type will absorb the water and produce a rapid increase in differential pressure across the filter. The desired maximum differential pressure across a filter with clean elements is five psig at normal operating temperature.

Filter Selection

The filter elements should remove particles of five microns, must be water-resistant, have a high flow rate capability with low pressure drop, possess high dirt-retention capacity, and be rupture-resistant. The clean pressure drop should not exceed five psig at 100 °F (38 °C). The elements must have a minimum collapse differential pressure of 50 psig. Pleated-paper elements are preferred—provided they meet these requirements. Usually, the pleated-paper element will yield the five psig clean drop when used in a filter that was sized to use depth-type elements. This result is due to the greater surface area of the pleated element, more than twice the area of a conventional stacked disc-type or other depth-type elements.

A differential pressure switch set to alarm when the pressure drop reaches a predetermined point protects against the loss of oil flow. In addition to the differential pressure switch, a two-way, three-port valve with a pressure gauge is piped in parallel with the differential pressure switch for accurate indication of inlet and outlet oil filter pressure. When a single transflow valve is used with a cooler-filter installation, the differential pressure switch and pressure gauge assembly should span the cooler-filter system.

Water contamination in the oil system can cause serious damage to turbomachinery, and every reasonable effort should be made to, first, prevent its entrance into the system, and second, provide suitable removal equipment if water cannot be effectively kept out. Experience indicates that designers and equipment operators can be more effective in keeping water out of the system. Since the main sources of contamination are atmospheric condensation, steam leaks, and faulty oil coolers, preventive measures should be taken.

Condensation will occur in the atmospheric vented oil system whenever the temperature in the vapor space areas drops below the dew point. This effect can take place in the return oil piping as well as the reservoir. Consoles installed in unprotected locations are more vulnerable to climatic changes than those installed inside buildings. The outside locations will be adversely affected by temperature cycles between daytime and night operations—also, by showers and sudden temperature drops due to other weather changes, especially in the fall and winter seasons. There has been great success in “drying up” oil systems by making a few simple alterations. The first step is to check the reservoir unit. The vent should be located in the very top of the reservoir. It should be free of baffles that can collect and return condensate to the reservoir, and the length should be kept as short as possible to provide a minimum of surface areas on which condensate can form. If it is necessary to run the vent up and away from the reservoir, a water trap should be provided as close to the reservoir as possible to remove any condensate formed in the vent stack. The next step is to provide and maintain an inert gas or dry-air purge on the reservoir. Only 2–5 cfh is required. The reservoir purge system will not substitute for the elimination of other water sources.

Steam and condensate leaks are the most difficult water sources to prevent in turbomachinery; however, it can be done, and every effort should be made to eliminate these sources. Obviously, the first means of prevention is to maintain the steam packing in perfect condition. Experience has shown that eventually the steam packings will leak, and steam condensate will enter the system through the bearing seals. There has also been great success in “drying up” a wet oil system. The procedure is to purge the bearing labyrinths with inert gas or dry air. One method is to drill a one-eighth-inch hole through the bearing cap and intersect the labyrinth. A one-quarter-inch diameter tube is connected to the hole in the bearing cap and to a rotometer. The labyrinth is then purged with 15 cfh (0.43 cmh) dry air or inert gas.

Another method is to install an external labyrinth with purge provisions on the bearing housings of a machine that has the necessary space to accommodate the external seal.

Removal of free water from oil systems is usually done with centrifuges or coalescer separators. Centrifuging is the most costly method in both capital outlay and operating cost. The centrifuges usually are the conventional disc-type with manual cleaning. The discs must be cleaned at least once each week with one hour required per cleaning. The coalescer separators usually require much less attention. Some separators only require element changes once a year while others may require changes at six months or three months, and in some instances once a month. The frequency appears to be related to the amount of water in the oil system. In many instances, coalescer element

changes have been reduced by the use of a prefilter in the system. This element removes the particulates (usually rust) that would restrict the two-micron coalescer element. The time required to change both the prefilter element and coalescer separator elements is less than one hour.

Cleaning and Flushing

Serious mechanical damage to turbomachinery can result from operation with dirty oil systems. It is essential that an oil system be thoroughly cleaned prior to the initial startup of a new machine, and after each overhaul of an existing machine.

Preliminary steps for the initial startup and startup after the overhaul are similar, except for the reservoir and oil requirements on the machine after an overhaul. For an overhauled machine, the oil is drained and tested for condition. If there is no water or metal changes, the oil may be used again.

Inspect the reservoir interior for rust and other deposits. Remove any rust with scrapers and wire brushes, wash down the interior with a detergent solution, and flush with clean water. Dry the interior by blowing the surfaces with dry air and use a vacuum cleaner to remove trapped liquids.

Install all new five-micron pleated-paper elements in the filters. Connect steam piping to the water side of the oil coolers for heating the oil during the flush. Remove the orifice and install jumpers at the bearings, coupling, controls, governor, and other critical parts to prevent damage from debris during the flush. Make provisions for 40-mesh telltale screens at each jumper. The conical-shaped screen is preferred, but a flat screen is acceptable. Adjust all control valves in the full-open position to allow maximum flushing flow. The effectiveness of the flush depends to a large extent on high flow velocities through the system to carry the debris into the reservoir and filters. It may be necessary to sectionalize the system to obtain maximum velocities by alternately blocking off branch lines during the flush.

Fill the reservoir with new or clean used oil. Begin the flush without telltale screens by running the pump or pumps to provide the highest possible flow rate. Heat the oil to 160 °F (71 °C) with steam on the oil cooler. Cycle the temperature between 110 °F (43 °C) and 160 °F (71 °C) to thermally exercise the pipe. Tap the piping to dislodge debris, especially along the horizontal sections. Flush through one complete temperature cycle, shut-down and install the telltale screens, and flush for an additional 30 minutes. Remove screens and check for the amount and type of debris. Repeat the preceding procedure until the screens are clean after two consecutive inspections. Observe the pressure drop across the filters during the consecutive operation. Do not allow the pressure drop to exceed 20 psig (1.4 Bar).

When the system is considered clean, empty the oil reservoir, and clean out all debris by washing with a detergent solution followed by a freshwater rinse. Dry the interior by blowing with dry air, and vacuum any freestanding water. Replace the filter elements. Remove jumpers and replace orifices. Return controls to their normal settings. Refill the oil reservoir with the same oil used in the flush if lab tests indicate it is satisfactory; otherwise, refill with new oil.

Because of the high flow velocities obtained during the flush, the previous procedure will allow the fastest possible cleanup of the oil system. The objective is to carry the debris into the reservoir and filters. The turbulence from the high flows, along with the thermal and mechanical exercising of the piping, are the main factors necessary for a fast and effective system cleanup.

Coupling Lubrication

Couplings are a very critical part of any turbomachinery. They must be carefully designed and proper lubrication must be applied. The most common methods of lubricating gear-type couplings are: (1) grease-packed, (2) oil-filled, or (3) continuous oil flow.

The grease-packed and oil-filled couplings offer similar advantages and disadvantages. The main advantage is simplicity of operation. They are also economical, easy to maintain, and the grease type resists the entry of contaminants. In addition, high tooth leading can be accommodated, since lubricants with heavy-bodied oil can be used. An important requisite for the oil-filled type is that the coupling must have an adequate static oil capacity to provide the required amount of oil to submerge the teeth when the coupling is in operation. The greatest disadvantage of these couplings is the possible loss of lubricants during operation due to defective flange gaskets, loose flange bolts, lubricant plugs, and flaws in the coupling flanges and spacers.

The lubricant of a gear coupling must withstand severe service from forces in the coupling which exceed 8000 g's. For grease-filled couplings, special-quality grease is required to prevent mating teeth wear while operating at high-g loads in a sliding load environment. This severe operating condition causes grease separation at high speeds and results in excessive wear. Tests indicate that grease separation is a function of g levels and time. Therefore, the grease coupling is not considered suitable for high-speed service, except when approved high-speed coupling grease is used, and then only for up to one year of continuous operation. Presently, new greases on the market do not separate at high speeds and may not deteriorate for three years of continuous operation.

The continuous oil-flow method is used primarily in high-speed rotating machinery. This method provides the potential for maximum continuous periods of operation at high operating speeds. The oil flow also provides cooling by carrying away heat generated within the coupling. Another important advantage is maximum reliability, since the oil supply is constant, and the loss of oil from within the coupling is not a problem as it is with oil-filled or grease-packed couplings. The main requisites for this method are: (1) provision of adequate oil flow into the coupling, (2) the oil must be absolutely clean, and (3) it must cool to carry away heat.

Some of the disadvantages of the continuous oil-flow coupling are: (1) increased cost, (2) requires supply oil and return oil piping, and (3) the entry of foreign solids with the oil will cause accelerated wear.

Foreign material in the oil is a major problem with the continuous oil-flow coupling. Since high centrifugal forces are developed within the coupling, any induced solids and water will be extracted from the oil and retained in the coupling. Abrasive wear is usually caused by the trapped sludge. In addition to the foreign abrasives, the sludge will retain the wear metal and will contribute to the coupling wear rate. Sludging has been reduced within couplings by improved oil filtration. Filters can be equipped with differential pressure alarms so that replacement can be made.

The gear-type coupling on turbomachinery can be successfully lubricated by both oil and grease methods. The grease-packed and oil-packed couplings must be absolutely oil and grease tight to prevent the loss of lubricant, and the very best high-speed coupling grease must be used. The continuous-flow type must have absolutely clean oil supplied continuously at the designed flow rate.

Lubrication Management Program

A well-planned and managed lubrication program is an important factor in the overall maintenance plan of a plant. A lubrication program includes developing a lubrication period maintenance program, sampling and testing oil, and developing specific procedures to apply lubricants. The initial step in developing a comprehensive plant lubrication program is to conduct a plant survey to determine existing lubrication practices. The survey should utilize machine drawings and external machinery inspections.

A detailed list of lubricant types and their points of application can be compiled from the results of the survey. Combining the list of lubrication types and a current schedule, a master plant lubrication schedule can be published.

A monthly lubrication schedule can then be issued to the appropriate maintenance personnel to serve as a reminder. The issuing of the lubrication schedule does not ensure its compliance, and supervisors should check to see that required lubrication is performed.

As a part of the lubrication program, oil should be periodically tested. The testing requires drawing oil from the system for a laboratory analysis. The usual tests conducted to determine the condition of oils include viscosity, pH and neutralization number, precipitation, color and odor, and a check for foreign particles in the oil. The results should be reviewed and compared with new oil characteristics to determine the life characteristics of the oil.

A program for evaluating any new lubrication products can be used to indicate the possible replacement of current lubricants. The general characteristics of new lubricants can be obtained from specifications provided by suppliers or from testing of the lubricant. The final selection of new lubricants should be made only after close observation of the lubricant in several typical plant applications. During the monthly inspections, new lubricants should be checked especially closely to ensure they are retaining their desired properties. While all lubrication applications are important to machinery health, gear couplings present special critical lubrication problems and require special attention as explained previously.

Operating experience has proven that unless a continuous program of required lubrication is followed, even the most well-designed units are sure to fail. A proper lubrication management program must incorporate a monthly lubrication schedule, an evaluation of new lubrication products, and supervision to ensure the prescribed procedures are carried out by maintenance personnel.

In the event of failures due to lubrication problems, the failures should be thoroughly analyzed to determine if they were indeed caused by lubricant failure or incorrect maintenance procedures. Once the problem has been isolated, corrective action can be initiated to prevent subsequent similar failures—whether it requires changing lubricants or procedures.

Bibliography

API Standard 614, "Lubrication, Shaft-Sealing and Control Oil Systems for Special-Purpose Applications," American Petroleum Institute, September 1973.

Clapp, A.M., "Fundamentals of Lubricating Relating to Operating and Maintenance of Turbomachinery," Proceedings of the 1st Turbomachinery Symposium, Texas A&M University, 1972.

Fuller, D.D., *Theory & Practice of Lubrication for Engineers*, Wiley Interscience, 1956.

O'Connor, J.J., and Boyd, J., eds., *Standard Handbook of Lubrication Engineering*, McGraw-Hill Book Co., 1968.

16

Spectrum Analysis

A total analysis of high-speed rotating equipment requires a complex blend of performance and vibration data. The trend toward total analysis is growing with the problems of an energy shortage and the need for maximum plant utilization. Performance analysis is essential in the efficient utilization of turbomachinery and, when coupled with vibration analysis, is an unbeatable tool as a total diagnostic system.

The real-time analyzer plays a very important role in presenting vibratory data in a manner that can lend itself to a trending data system. This important role of the spectrum analyzer will be explored in detail in this chapter. Also, the role of the spectrum analyzer will increase with a better understanding of statistical techniques in vibration analysis.

Basically, spectrum analysis transforms a displacement/time chart into an amplitude/frequency chart known as a spectrum. This analysis consists of decomposing a time-varying signal into its component pure tones. Pure tones are sinusoidal wave forms of constant frequency and amplitude. This decomposition is done digitally upon a signal by a minicomputer using the Fourier transformation or by filtering the signal.

Signals generated by high-speed machinery are very complex in nature and are generated by several forces with a net effect that masks the pure tones. The random portion of the signal, which is blended with the pure tones, is called noise. The ratio of the total amplitude (area under spectrum) to that of the noise is called the signal-to-noise (S/N) ratio. Sometimes this ratio is expressed in decibels, or db, as follows:

$$S/N \text{ ratio in db} = 20 \log_{10} \frac{S}{N} \quad (16-1)$$

For example:

$$6 \text{ db} = 2$$

$$10 \text{ db} = 3.16$$

$$20 \text{ db} = 10$$

$$40 \text{ db} = 100$$

If the S/N ratio is less than 10 db, it becomes difficult to differentiate the periodic part of the spectrum from noise.

Several types of analyzers exist today that allow a time-domain signal to be converted to a frequency-domain spectrum. The resulting spectrum of all spectrum analyzers is equivalent to the amplitude/frequency plot, which is obtained by passing the given signal across a set of constant bandwidth filters and noting the output of each filter at its center frequency.

Unfortunately, such a simple procedure cannot be used because, for adequate resolution, each filter can cover only a very narrow frequency band, and because of the cost involved. In the so-called “wave analyzer” or “tracking filter” one filter is utilized by manually incrementing the filter across the time input to determine which frequencies exhibit a large amplitude. In time-compression real-time analyzers (RTA) the filter is swept electronically across the input. The term “real time” as applied here means the instrument takes the time-domain signal and converts it to a frequency domain while the event is actually taking place. In technical terms, real time is viewed when the rate of sampling is equal to or greater than the bandwidth of the filters taking the measurements. RTAs use an analog-to-digital converter and digital circuits to speed up the data signal effectively and improve the sweeping filter scan rate, thus creating an apparent time compression. Both of the previous analyzers are basically analog instruments and, because of the characteristics of analog filtering, may be quite slow at lower frequencies.

The Fourier analyzer is a digital device based on the conversion of time-domain data to a frequency domain by the use of the fast Fourier transform. The fast Fourier transform (FFT) analyzers employ a minicomputer to solve a set of simultaneous equations by matrix methods.

Time domains and frequency domains are related through Fourier series and Fourier transforms. By Fourier analysis, a variable expressed as a function of time may be decomposed into a series of oscillatory functions (each with a characteristic frequency), which when superpositioned or summed at each time, will equal the original expression of the variable. This

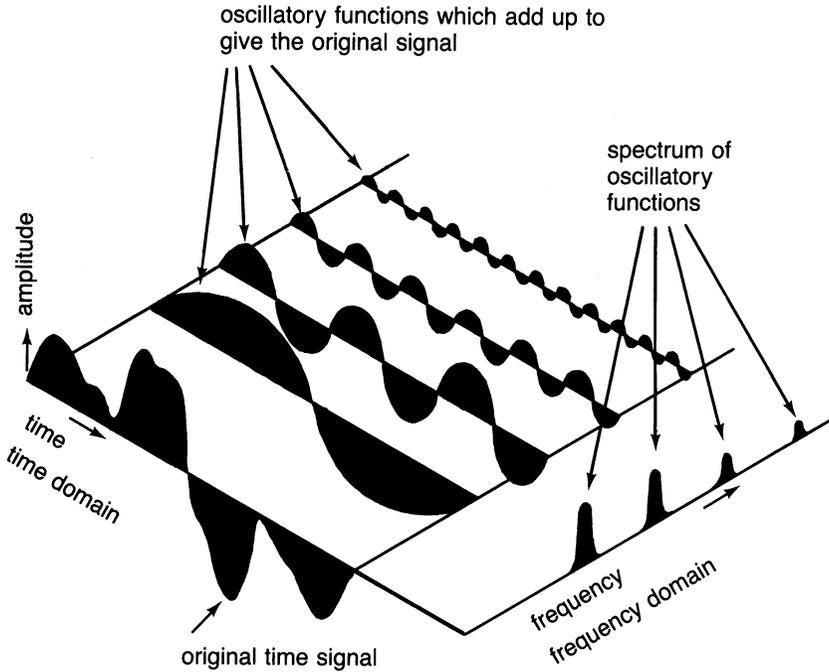


Figure 16-1. Decomposition of a time signal into a sum of oscillatory functions from which a spectrum can be obtained.

process is shown graphically in Figure 16-1. Since each of the oscillatory signals has a characteristic frequency, the frequency domain reflects the amplitude of the oscillatory function at that corresponding frequency.

The breakdown of a given signal into a sum of oscillatory functions is accomplished by application of Fourier series techniques or by Fourier transforms. For a periodic function $F(t)$ with a period t , a Fourier series may be expressed as

$$F(t) = \frac{a_0}{2} + \sum_{n=1}^{\infty} (a_n \cos n\omega t + b_n \sin n\omega t) \tag{16-2}$$

Here a and b are amplitudes of the oscillatory functions $\cos(n\omega t)$ and $\sin(n\omega t)$, respectively. The value of ω is related to the characteristic frequency f by

$$\omega = 2\pi f \tag{16-3}$$

The previous function may also be written in a complex form as

$$F(t) = \int_{-\infty}^{\infty} G(\omega)e^{i\omega t} d\omega \quad (16-4)$$

where:

$$G(\omega) = \frac{1}{2\pi} \int_{-\infty}^{\infty} F(t)e^{-i\omega t} dt \quad (16-5)$$

The function $G(\omega)$ is the exponential Fourier transform of $F(t)$ and is a function of the circular frequency ω . In practice the function $F(t)$ is not given over the entire time domain but is known from time zero to some finite time T , as shown in Figure 16-2. The time span T may be divided into K equal increments of Δt each. For computational reasons, let $K = 2^p$ where p is an integer. Also, let the circular frequency span ω_n be divided into N parts where $N = 2^q$. (In practice, N is often set equal to K .) By setting $f = K/NT$, the frequency interval $\Delta\omega$ becomes

$$\Delta\omega = 2\pi\Delta f = \frac{2\pi K}{NT} \quad (16-6)$$

Now, discrete equations analogous to Equations (16-3) and (16-4) may be defined

$$F(t_k) = \Delta\omega \sum_{n=0}^{N-1} G(\omega_n)e^{i\omega_n t_k} \quad (16-7)$$

and

$$G(\omega_n) = \frac{\Delta t}{2\pi} \sum_{k=0}^{K-1} F(t_k)e^{-i\omega_n t_k} \quad (16-8)$$

where the limits are set at 0 and $N - 1$ for computational reasons.

By using Euler identities, Equations (16-6) and (16-7) can be written

$$G(\omega_n)_{\text{real}} = \sum_{n=0}^{n-1} F(t_k) \cos(\omega_n t_k) \quad (16-9)$$

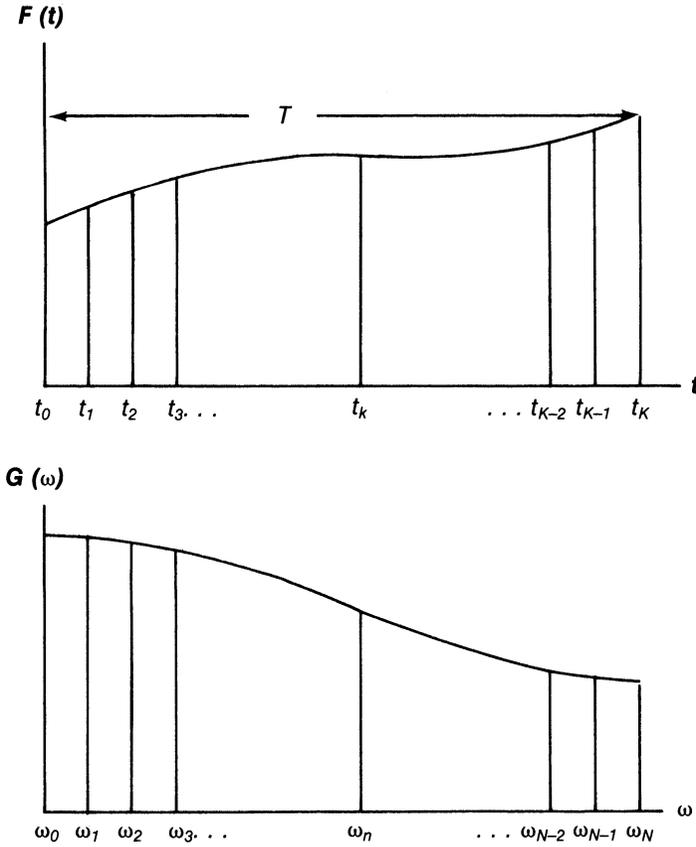


Figure 16-2. Discrete Fourier transform representation.

$$G(\omega_n)_{\text{imaginary}} = \sum_{n=0}^{n-1} F(t_k) \sin(\omega_n t_k) \tag{16-10}$$

$$F(t_k) = \Delta\omega \sum_{n=0}^{n-1} (G(\omega_n)_{\text{real}} \cos(\omega_n t_k) + G(\omega_n)_{\text{imaginary}} \sin(\omega_n t_k)) \tag{16-11}$$

Comparison of the previous equations with Equations (16-6) and (16-7) reveal that the Fourier transform is really just a Fourier series constructed over a finite interval.

The equations may be rewritten in a simpler form by making the following definitions:

$$\bar{F}_k = F(t_k) \quad (16-12)$$

$$G_n = G(\omega_n) \quad (16-13)$$

$$\omega_n = n\Delta\omega = \frac{2\pi nK}{NT} \quad (16-14)$$

$$t_K = K\Delta t \quad (16-15)$$

so that Equations (16-6) and (16-7) become

$$\bar{F}_k = \Delta\omega \sum_{n=0}^{n-1} G_n e^{(2\pi i/N)(nk)} \quad (16-16)$$

$$G_n = \frac{T}{2\pi K} \sum_{K=0}^{K-1} \bar{F}_k e^{(-2\pi i/N)(nk)} \quad (16-17)$$

If we further define

$$F_k = \frac{T}{2\pi K} \bar{F}_k \quad (16-18)$$

and

$$W = e^{-2\pi i/N}$$

we have

$$G_n = \sum_{k=0}^{K-1} F_k W^{nk} \quad (16-19)$$

or in matrix form

$$\begin{aligned} [G_n] &= [W^{(nk)}][F_k] \quad n = 0, 1, 2, \dots, N-1 \\ &\quad k = 0, 1, 2, \dots, K-1 \end{aligned} \quad (16-20)$$

The matrices $[G]$ and $[F]$ are column matrices with row numbers n and k , respectively. The matrix solution is simplified by special properties of the symmetric matrix and because the resulting values of G_n occur in complex conjugate pairs. In general, we may write

$$G_n = a_n + ib_n = |G_n|e^{i\alpha_n} \quad (16-21)$$

where:

$$|G_n| = a_n^2 + b_n^2 \quad (16-22)$$

$$\alpha_n = \tan^{-1}(b_n/a_n) \quad (16-23)$$

From the time function $F(t)$ and the calculation of $[W]$, the values of G_n may be found. One way to calculate the G matrix is by a fast Fourier technique called the Cooley-Tukey method. It is based on an expression of the matrix as a product of q square matrices, where q is again related to N by $N = 2^q$. For large N , the number of matrix operations is greatly reduced by this procedure. In recent years, more advanced high-speed processors have been developed to carry out the fast Fourier transform. The calculation method is basically the same for both the discrete Fourier transform and the fast Fourier transform. The difference in the two methods lies in the use of certain relationships to minimize calculation time prior to performing a discrete Fourier transform.

Finding the values of G_n allows the determination of the frequency-domain spectrum. The power-spectrum function, which may be closely approximated by a constant times the square of $G(f)$, is used to determine the amount of power in each frequency spectrum component. The function that results is a positive real quantity and has units of volts squared. From the power spectra, broadband noise may be attenuated so that primary spectral components may be identified. This attenuation is done by a digital process of ensemble averaging, which is a point-by-point average of a squared-spectra set.

Vibration Measurement

Successful measurement of machine vibration requires more than a transducer randomly selected, installed, and a piece of wire to carry the signal to the analyzer. When the decision to monitor vibration is made, three choices of measurement are available: (1) displacement, (2) velocity, and

(3) acceleration. These three measurement types emphasize different parts of the spectrum. To understand this peculiarity, it is necessary to consider the differences in the characteristics of each. Consider a simple harmonic vibration. The displacement, x , is given by

$$x = A \sin \omega t$$

Successive differentiation gives the expressions for velocity (\dot{x}) and acceleration (\ddot{x})

$$x = A \sin \omega t$$

$$\dot{x} = A\omega \cos \omega t$$

$$\ddot{x} = -A\omega^2 \sin \omega t$$

In actual practice, these are specified

$$\text{Displacement: peak-to-peak measure} = 2A$$

$$\text{Velocity: maximum measure} = A\omega$$

$$\text{Acceleration: maximum measure} = A\omega^2$$

It can be observed that displacement is independent of frequency, velocity is proportional to frequency, and acceleration is proportional to the square of the frequency. If the displacement and frequency are known, the velocity and acceleration can be calculated.

To measure any of the signals, a vibration transducer is used. A transducer is a device that translates some aspect of machine vibration into a time-varying voltage output that can be analyzed. The frequency range to be analyzed should be carefully considered before selecting a transducer. It should be kept in mind, however, that there is no one best sensor, and several kinds may be needed to analyze a given machine. Also, in many cases signal conditioning of the transducer signal may be required prior to analysis.

Displacement Transducers

Eddy-current proximity probes are primarily used as displacement transducers. Eddy probes generate an eddy-current field, which is absorbed by a conducting material at a rate proportional to the distance between the probe and the surface. They are often used to sense shaft motion relative to a bearing (by mounting them within the bearing itself) or to measure thrust

motions. They are generally indifferent to hostile environments, including temperatures up to 250 °F (121 °C) and are not expensive. One drawback is that shaft surface conditions and electrical runout can result in false signals. Also, the smallest displacement that can be successfully measured is limited by the S/N ratio of the system. In practice, it is difficult to measure values less than 0.0001 of an inch. If shaft displacement is being measured, the shaft runout (measured with the same pickup) should be less than the smallest measurable value. To achieve the proper shaft runout, it is necessary that the shaft be precision ground, polished, and demagnetized.

Velocity Transducers

Usual types of velocity transducers are made up of an armature mounted in a magnet. The motion of the armature in the magnet creates a voltage output proportional to the velocity of the armature. Usually, the forces being measured must be relatively great to cause a signal output. However, the signal is quite strong when mounted on the machine bearings, and amplification is usually not needed. They are very rugged but are also large and cost roughly 10 times as much as a proximity probe.

Because of damping, transfer function characteristics of the armature-magnet construction generally limit the low-frequency response to approximately 10 Hz. At the high end of the frequency range, the resonant peak of the pickup itself is the limiting factor. Thus, the useful linear bandwidth is limited. The main advantage of the velocity pickup is that it is a high-output/low-impedance device, and hence, it provides an excellent S/N ratio—even under less than ideal conditions. The major disadvantage of the velocity pickup is its sensitivity to placement. The probe is directional so that if the same force is applied horizontally or vertically, the probe will give different readings.

Acceleration Transducers

Most accelerometers consist of some small mass mounted on a piezoelectric crystal. A voltage is produced when accelerations acting on the mass create a force acting on the crystal. Accelerometers have a wide frequency response and are not excessively costly. They also are temperature resistant. Accelerometers have two main limitations. First, they are extremely low-output/high-impedance devices requiring loading impedances of at least 1 M Ω . Such requirements rule out the use of long cables. One solution has been to have an amplifier built into the pickup to provide a low-impedance/amplified signal. A power supply is required, and the weight is increased.

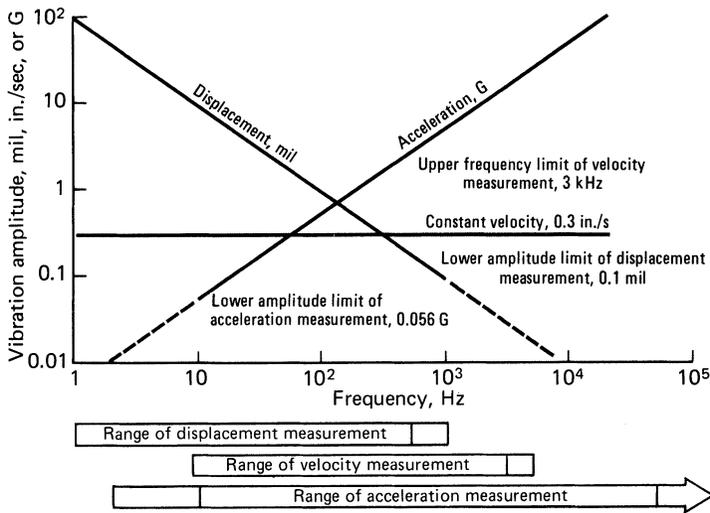


Figure 16-3. Limitations on machinery vibrations analysis systems and transducers.

The second limitation of this pickup is illustrated by an example. Acceleration of one g at 0.5 Hz represents a displacement of 100 inches. It is obvious that in spite of its wide-band response (sometimes 0.1–15 kHz), it is severely limited at the low end by a poor S/N ratio.

The transducer type used should be matched to the machine being analyzed. A knowledge of the types of problems normally encountered will benefit this selection. For instance, the noncontacting shaft displacement probe helps to correct misalignment and balancing problems but is inappropriate in analyzing gear mesh problems and blade passage frequencies. Also, if signal integration or double integration is to be carried out, the lowpass filters used to attenuate high-frequency spectra also have a highpass filter, which effectively creates a lower frequency limit (often as high as five Hz). As mentioned before, one main criterion in deciding which transducer to use is the frequency range to be analyzed. Figure 16-3 shows the frequency limitations placed on the three types of transducers discussed previously.

Dynamic Pressure Transducers

The use of dynamic pressure transducers gives early warning of problems in the compressor. The very high pressure in most of the advanced gas turbines cause these compressors to have a very narrow operating range between surge and choke. Thus, these units are very susceptible to dirt and

blade vane angles. Dynamic pressure transducers are used to obtain a spectrum where the blade and vane passing frequency are monitored. As the compressor approaches surge, the second order of the blade passing frequency ($2 \times \text{number of blades} \times \text{running speed}$) approaches the magnitude of the first order of the blade passing frequency. The early warning provided by the use of dynamic pressure measurement at the compressor exit can save major problems encountered due to tip stall and surge phenomenon.

The use of dynamic pressure transducer in the combustor section, especially in the low NO_x combustors ensures that each combustor can be burning evenly. This is achieved by controlling the fuel flow to each combustor can till the spectrums obtained from each combustor can be close to being identical. The dynamic pressure transducers when used in this application must be mounted so that the probes are not exposed to the full combustor temperatures. This can be done by the use of buffer gases. This technique has been used and found to be very effective and ensures smooth operation of the turbine.

Taping Data

For many reasons, it may be inconvenient to take the spectrum analyzer to the field each time an analysis is to be made. Often, several machines are to be analyzed at various locations. Also, a hostile environment may exist at the test site, which might result in damage to the analyzer. A way of overcoming these problems is offered by data taping. With a tape, a permanent record is made. Since each channel of the tape offers a place for data to be stored, this record may be a condensation of several inputs either from different transducers or from the same transducer at various locations. A continuous tape monitor is very beneficial. In the event of machine failure, an analysis of the playback will help diagnose the problem.

The choice of what kind of tape recorder to use is an important decision. AM tape recorders are much less expensive than FM recorders and usually have a voltage saturation limit of 20 or more volts. An FM recorder may be saturated by as little as one volt. A drawback to AM recorders is a rather high roll-off frequency of about 50 Hz (3000 rpm). Data below the roll-off frequency is attenuated and appears to be lessened in magnitude. An FM recorder has no lower frequency limit; however, it may require careful signal conditioning (attenuation or amplification) to prevent tape saturation. Usually, if the problems lie at the high frequencies, an AM recorder is the best selection. Regardless of the recorder type, a calibration of input signals is recommended using a known oscillating signal and is usually best done by following manufacturer's instructions.

The use of computers has in many cases replaced taping of the data. The use of high speed digital acquisition signals are stored directly in memory for further storing to a hard disk, and then processing it through a fast Fourier transform program.

Interpretation of Vibration Spectra

The spectrum analyzer correctly depicts the frequency content of each time-domain instant; however, the time-domain picture as well as its frequency-domain counterpart of a continuous signal change with time. Averaging is used to show which amplitudes predominate in a continuous signal. For the most part, machinery vibrations result in “stationary” signals. A stationary signal has statistical properties that do not change with time. In other words, the average of a set of time-history records is the same regardless of when that average is taken. (A stationary signal is demonstrated by a machine running at constant speed and load. Averages are also used in diagnosing startups and load changes of machinery. In this usage, averages of successive time intervals show the change in vibration levels and frequencies taking place.)

Averaging is a technique to improve the S/N ratio. Two or more successive spectra made up of both periodic and random (noise) signals are added together and then averaged. This combination results in a spectrum with a periodic component that is much the same as when viewed in the instantaneous signals but with random peaks of much less amplitude. This result occurs because the period peak stays at a fixed frequency in the spectrum, while the noise peak is fluctuating in frequency over the spectrum.

The fact that averaging removes noise-related signals is demonstrated by the instantaneous and averaged spectra shown in Figure 16-4a taken from the taped signal of a machine being diagnosed. A representation of the normal instantaneous spectra is shown in the second spectrum. An instantaneous signal clearly caused by noise was exhibited at one point in the tape and is shown in the upper spectrum. Note that the contribution of the instantaneous noise signal does not appear in the averaged signal. The large peak on the plots is the running frequency. Lesser harmonics of the running speed also appear. The importance of the instantaneous signal should not be overlooked. During startups, a long-term average may eliminate important parts of the spectra, which change because of the change in rpm. Also, nonperiodic impulses such as those caused by random impulsive loading may be masked by an average. Short averages can be used in “waterfall” graphs to show the growth of certain frequency patterns at run-up as shown in Figure 16-4b.

The frequencies of a spectrum can be divided into two parts: subharmonic and harmonic (i.e., frequencies below and above the running speed). The subharmonic part of the spectrum may contain oil whirl in the journal bearings. Oil whirl is identifiable at about one-half the running speed (as are several components) due to structural resonances of the machine with the rest of the system in which it is operating and hydrodynamic instabilities in its journal bearings. Almost all subharmonic components are independent of the running speed.

The harmonic part of the spectrum may contain multiples of running speed, blade passage frequencies (given by number of blades times the running speed), gear mesh frequencies (given by number of teeth times the running speed), and finally, solid-disc resonant frequencies of the gear discs (independent of the running speed). Roller contact bearings may add another component based on the number of rolling elements present. In addition, a once-per-revolution or first harmonic frequency is caused by mechanical imbalance. Table 16-1 shows more of the major diagnostics. To identify these frequencies with the various machine components, a baseline signature should be obtained.

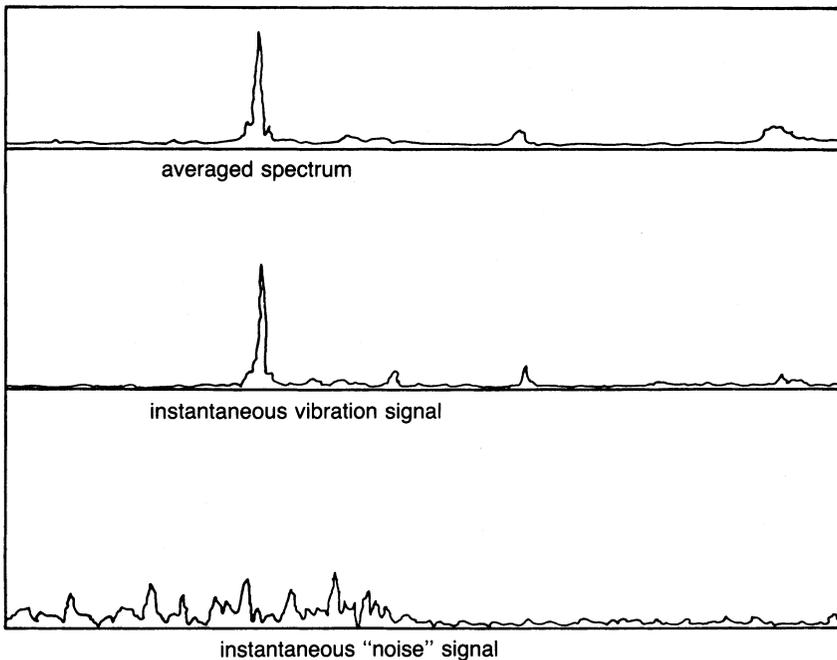


Figure 16-4a. Noise attenuation by averaging.

To be able to do effective trouble-shooting on any particular machine, it is necessary that the baseline signature of the machine be available and thoroughly analyzed. A baseline signature is the spectrum of machine vibration when the machine is operating under “normal conditions.” Generally, “normal conditions” are difficult to define and are judgmental in nature. When a machine is first installed, or after it has undergone an overhaul, a vibration spectrum should be taken and stored to serve as a “baseline” for

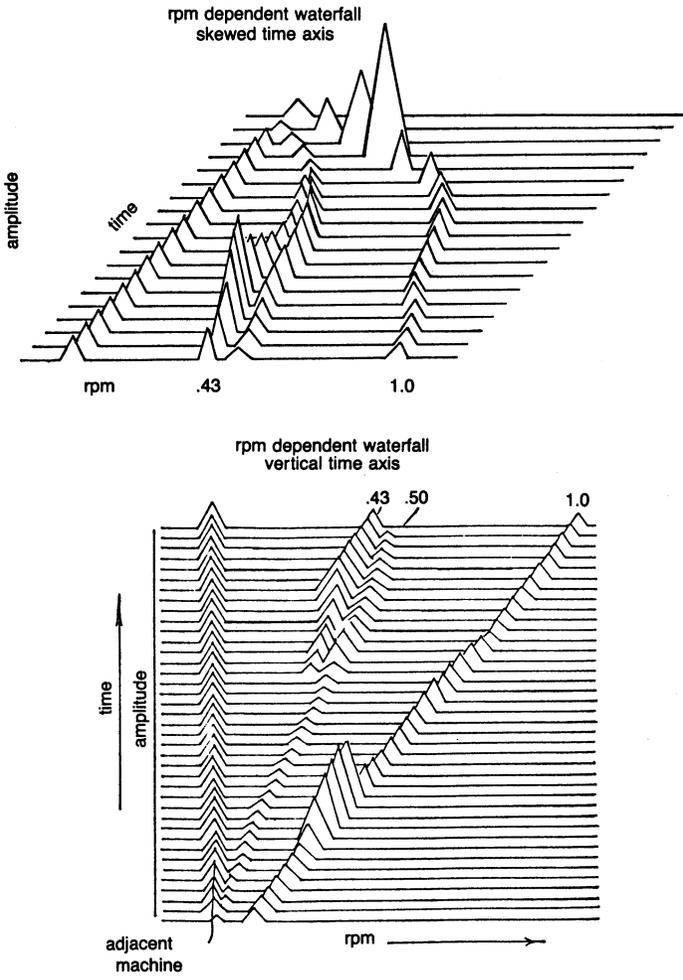


Figure 16-4b. Waterfall graph of increasing rpm.

Table 16-1
Vibration Diagnosis

| Usual Predominant Frequency* | Cause of Vibration |
|-------------------------------------|---|
| Running frequency at 0–40% | Loose assembly of bearing liner, bearing casing, or casing and support Loose rotor shrink fits Friction-induced whirl Thrust bearing damage |
| Running frequency at 40–50% | Bearing-support excitation Loose assembly of bearing liner, bearing case, or casing and support Oil whirl Resonant whirl Clearance induced vibration |
| Running frequency | Initial unbalance Rotor bow Lost rotor parts Casing distortion Foundation distortion Misalignment Piping forces Journal & bearing eccentricity Bearing damage Rotor-bearing system critical Coupling critical Structural resonances Thrust bearing damage |
| Odd frequency | Loose casing and support Pressure pulsations Vibration transmission Gear inaccuracy Valve vibration |
| Very high frequency | Dry whirl Blade passage |

* Occurs in most cases predominantly at this frequency; harmonics may or may not exist.

evaluating future spectra. When a baseline signature is determined, it should be carefully evaluated, and every component should be identified as far as possible.

First, and the most important factor to determine, is the primary or fundamental excitation frequency (i.e., frequency of the forcing function). In certain machines more than one excitation corresponds to the running

speed of the machine. In split-shaft and multispool machines there is more than one running speed.

The relationships in Table 16-1 help to further identify excitations. This information in conjunction with the baseline signature can identify the causes of sudden changes in the spectrum. However, this method runs into difficulty when a new machine is being brought up to speed. No baseline signature is available. Normal operation of the machine is not known. Information about similar machines is of limited value because of the wide variation between different samples of the same machine. This lack of knowledge is the most challenging aspect of machine vibration analysis.

For a new machine, the harmonic part of the spectrum is approximately known in its frequency content due to its relationship with the running speed. The amplitudes at these frequencies are not known. The subharmonic part, with a lot of information unrelated to the running speed, is unknown both in frequency and amplitude content. To predict some characteristics of the subharmonic spectrum, transfer-function analysis is employed.

Transfer-function analysis consists of providing an external excitation of a known variable frequency by means of a vibrator. This excitation is applied to the machine while it is stopped. The observed vibration response is a measure of the machine's structural characteristics. It helps in identifying various structural resonance frequencies and thus provides some information about the subharmonic spectrum.

During the startup of a new machine, one should try to identify all the major peaks in the real-time spectrum. If unidentifiable peaks appear, then perhaps the speed should be held constant until a cause for the peak is identified. When a completely new component shows up on the spectrum, a baseline signature is of limited help in pinpointing the cause of such a component. Generally, such an occurrence is a warning of future disaster. If the new component is erratically changing in time, it almost certainly spells trouble. On the other hand, a low-amplitude, a broad-band peak, or a set of peaks that gradually build-up over years of operation may be the result of normal aging or the settling-down process and may be completely harmless. The identification problem area is again a matter of judgment. Some insight can be gained by studying published case histories, but many times, even after a major failure, the cause of the failure cannot be positively identified. To properly utilize spectrum data as an analysis tool, one must use it in conjunction with performance factors.

Performance and vibration monitoring should be properly interfaced to achieve a level of operation free from excessive maintenance and downtime and to maximize operating efficiency at every possible point in the system.

Compressor and turbine sections can be analyzed effectively by combining vibration spectra with changes in performance data. Major problem areas in each of these components can be identified with proper monitoring and analysis.

Subsynchronous Vibration Analysis Using RTA

High-speed, flexible-shaft rotor systems, especially those that operate at more than twice the first critical speed, are prone to subsynchronous instabilities. These instabilities can be induced by various elements in the rotor system from fluid-film bearings, bushing and labyrinth seals, to aerodynamic components such as impellers, shrink fits, and shaft hysteresis. With vibration instability, the rotor's rotation provides the energy and source of rotation. In high-speed rotor systems subsynchronous instabilities are a major cause of catastrophic failures of rotor and bearing systems. The application of high-pressure reinjection in recent years has resulted in a very high incidence of problems and failures due to subsynchronous vibration. The causes of many of these problems were not identified because the conventional analog-tuned filter vibration analyzer was incapable of analyzing the problem—except when catastrophic levels of subsynchronous vibrations were reached. At this condition, machine failure was very rapid.

In the early-to-marginal stages of subsynchronous vibration the phenomenon is highly intermittent, and requires the rapid analysis and high-resolution capability of the real-time analyzer for its identification.

This study shows the analysis and identification of subsynchronous instability on a high-pressure centrifugal compressor operating at more than the first critical speed of the unit. The test plots given in Figures 16-5 through 16-8 show the vibration spectra. The bearing journal displacement in peak-to-peak mils, on the *Y* axis, is on a logarithmic scale. This scale enables identification of the low levels of subsynchronous vibrations which occur during the marginal conditions of subsynchronous instability.

Figure 16-5 shows the vibration spectrum with the machine operating at 20,000 rpm, 500 psig (34.5 Bar) suction pressure, and 1200 psig (82.7 Bar) discharge pressure. Here a synchronous peak of 0.5 mil (0.0127 mm) at 20,000 rpm due to rotor system unbalance is the only component that shows up on the spectrum plot. Figure 16-6 shows the vibration spectrum with the machine operating at 20,000 rpm and suction pressure of 500 psig (34.5 Bar) while the discharge pressure has been raised to 1250 (86.2 Bar) psig. Observe on the plot the 0.2 mil (0.00508 mm) subsynchronous component at 9000 rpm. Using the analyzer in the continuous real-time mode, this

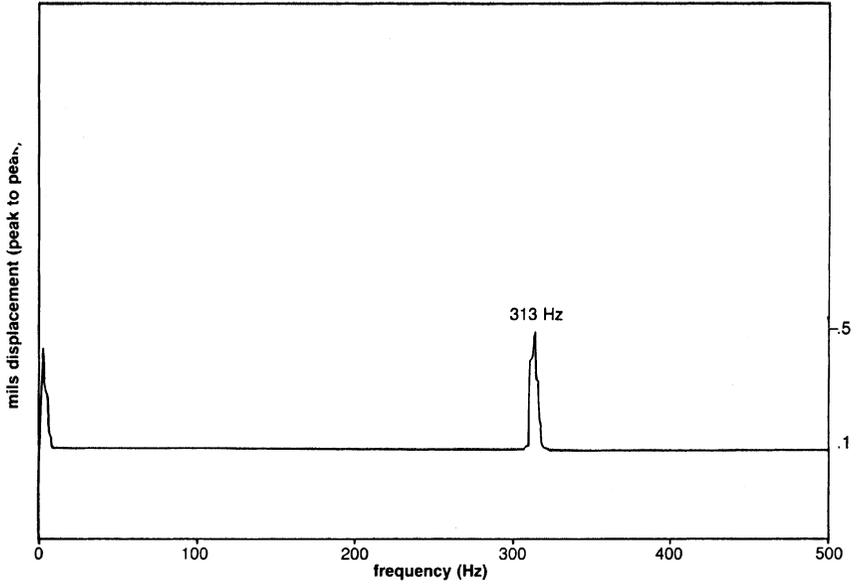


Figure 16-5. Vibration spectrum (rpm = 20,000, $P_d = 1200$ psig).

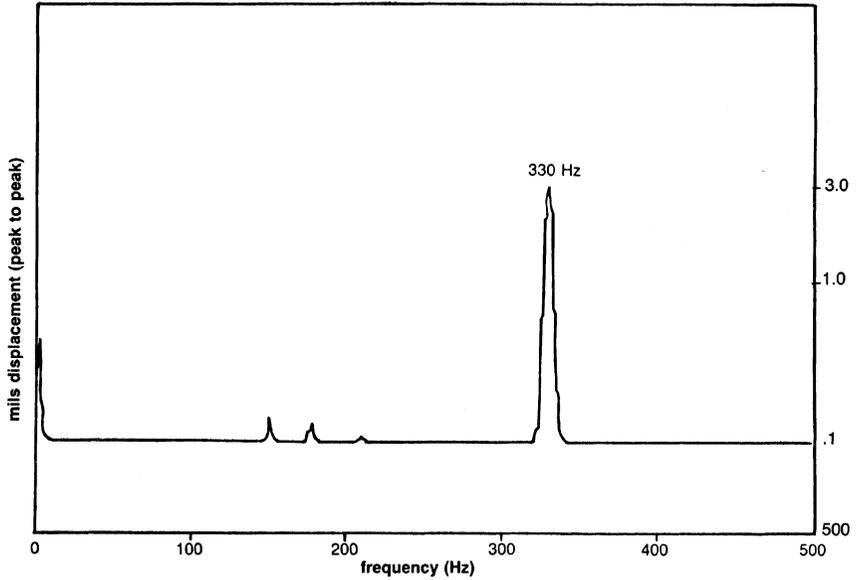


Figure 16-6. Vibration spectrum (rpm = 20,000, $P_d = 1250$ psig).

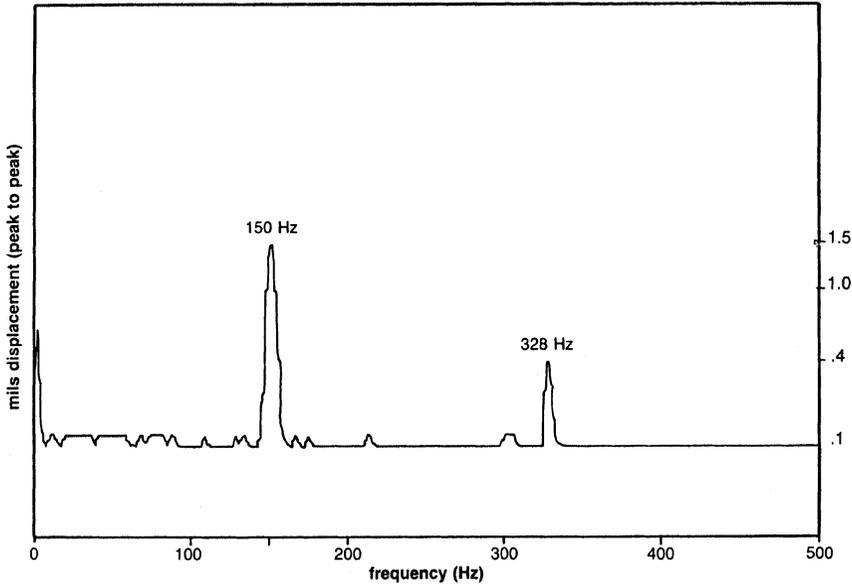


Figure 16-7. Vibration spectrum (rpm = 20,000, $P_d = 1270$ psig).

9000 rpm component was very intermittent and was captured by setting the realtime analyzer controls to the “peak hold” mode.

Figure 16-7 shows the vibration spectrum with the speed and suction pressure kept constant but with a small 20 psig increase in discharge pressure. Notice the large increase in the 9000 rpm component from 0.2 to 1.5 mil (0.0127–0.0381 mm). A further small increase in discharge pressure would have increased the subsynchronous vibrations to more than 1.0 mil (0.0254 mm) and wrecked the unit.

When the suction pressure was raised by some 50 psig (3.45 Bar) while maintaining the same discharge pressure, the unit regained its stability with the elimination of the subsynchronous component as shown in Figure 16-8. The subsynchronous instability in this machine was the result of aerodynamic excitation of the rotor systems occurring at a critical pressure rise across the machine of 770 psi differential (500–1270 psig).

Synchronous and Harmonic Spectra

The spectrum signature plots at synchronous speeds and high-frequency spectra reveal an interesting set of information. A high running speed

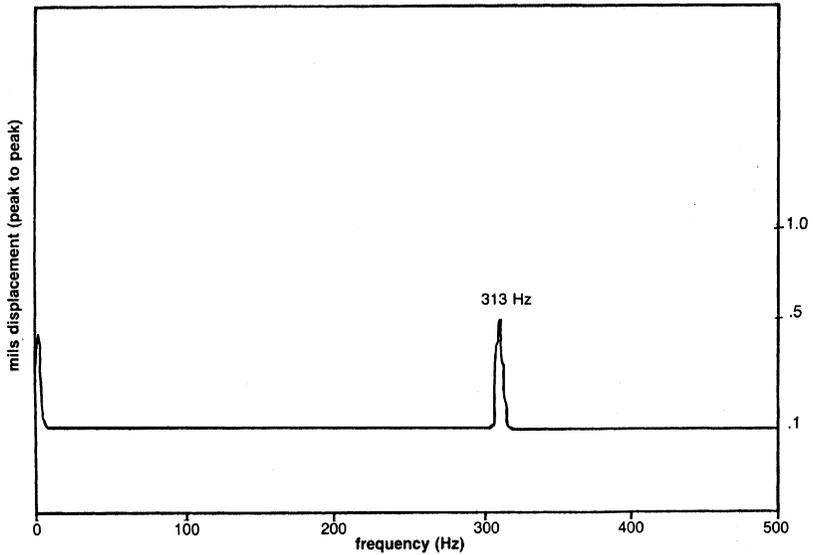


Figure 16-8. Vibration spectrum (rpm = 20,000, $P_d = 1320$ psig).

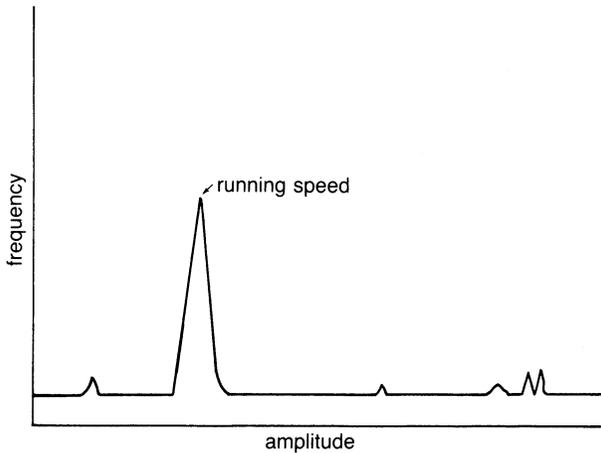


Figure 16-9. A typical unbalance signature plot.

amplitude can indicate problems such as unbalance. The spectrum showing this unbalance is in Figure 16-9. Misalignment problems can be also analyzed. Figure 16-10 shows a plot obtained from a casing-mounted pickup and the classical, high twice-per-revolution radial vibration. A high axial

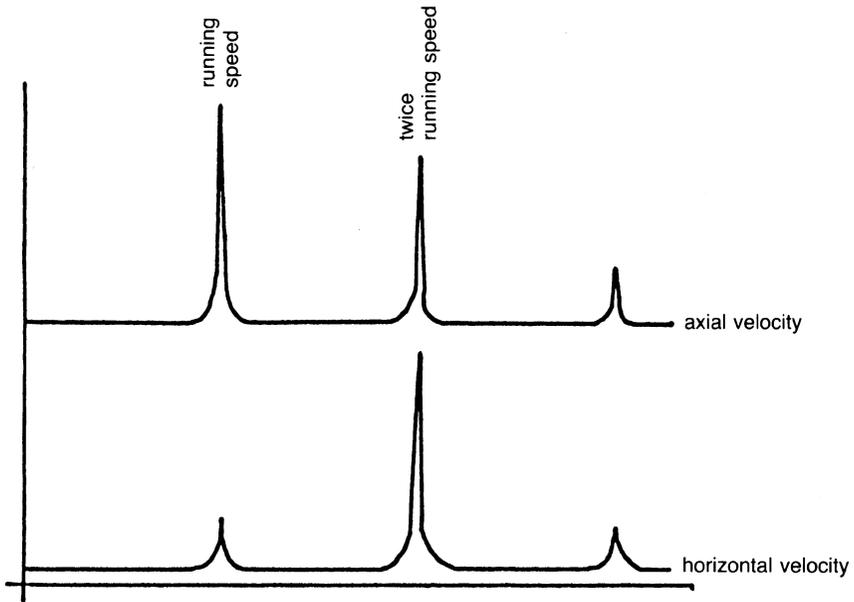


Figure 16-10. A typical misalignment signature plot.

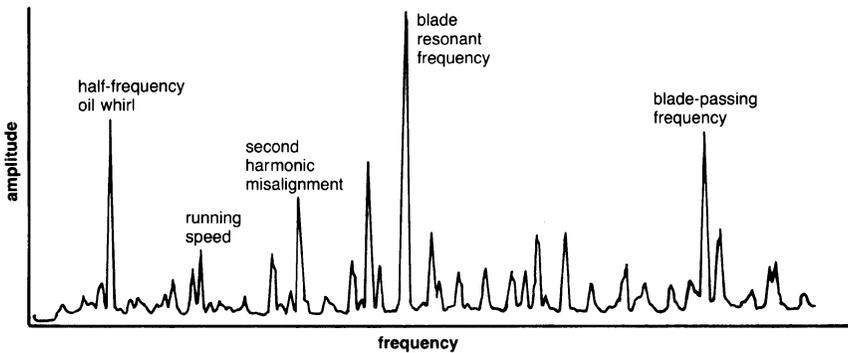


Figure 16-11. Real-time plot for a compressor shows details of critical frequencies.

vibration also exists that is usually more prominent in diaphragm-type couplings. A high-speed machinery plot is shown in Figure 16-11. To determine what the various frequency components represent, a detailed analysis of the machinery components must be known. This information consists of

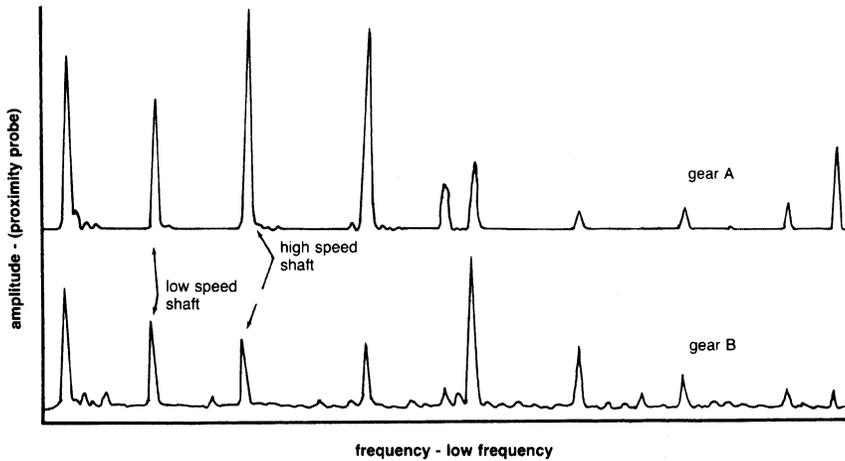


Figure 16-12. Gear box signature (low-frequency end).

the number of blades in the impeller, the number of diffusers or nozzle blades, the number of gear teeth, the resonant frequencies of the blades or casing (for antifriction bearings), the number of balls or rollers, and (for tilting-pad hydrodynamic bearings), the number of pads.

The use of accelerometers for diagnosing problems is very effective, since in many cases the high-frequency spectra give much more information than the low-frequency spectra obtained from proximity probes. An example can be seen in Figure 16-12, which shows that the two gear drives are in good mechanical condition. Figure 16-13 shows the high-frequency accelerometer signatures. These indicate a problem with gear A (a cracked or chipped tooth).

Accelerometers can also be used to detect problems with stator angles or tip stalls in axial-flow compressors. The analysis from proximity probes indicates that there is a high running-speed vibration, which can be acceptable. An analysis of the accelerometer spectrum (Figure 16-14) shows a strong frequency component of the first, second, and third harmonic of the fifth-stage stator blade. An inspection of the blades indicated cracks caused by low-stress high-cycle fatigue.

Figure 16-15 shows acoustic signatures of three jet engines of the same type installed in three different aircraft. The data were recorded with the aircraft at altitude, one engine at power and the other at flight idle. The top signature is the normal signature for this engine configuration. In the middle signature the once-per-revolution or unbalance components of the

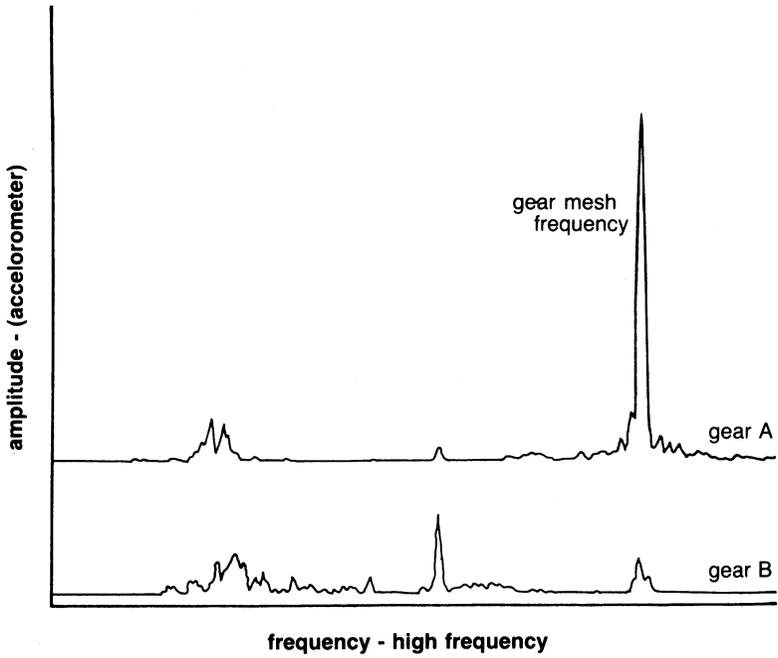


Figure 16-13. Gear box signature (high-frequency end).

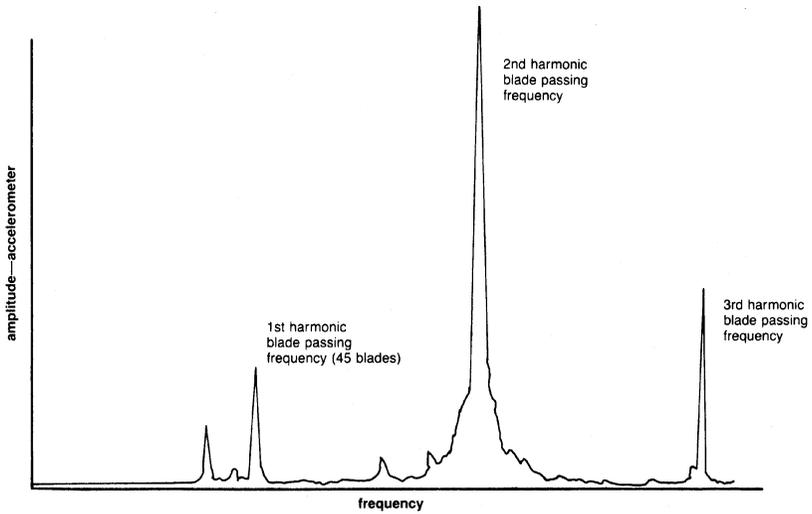


Figure 16-14. Axial-flow compressor spectrum showing blade passing frequency.

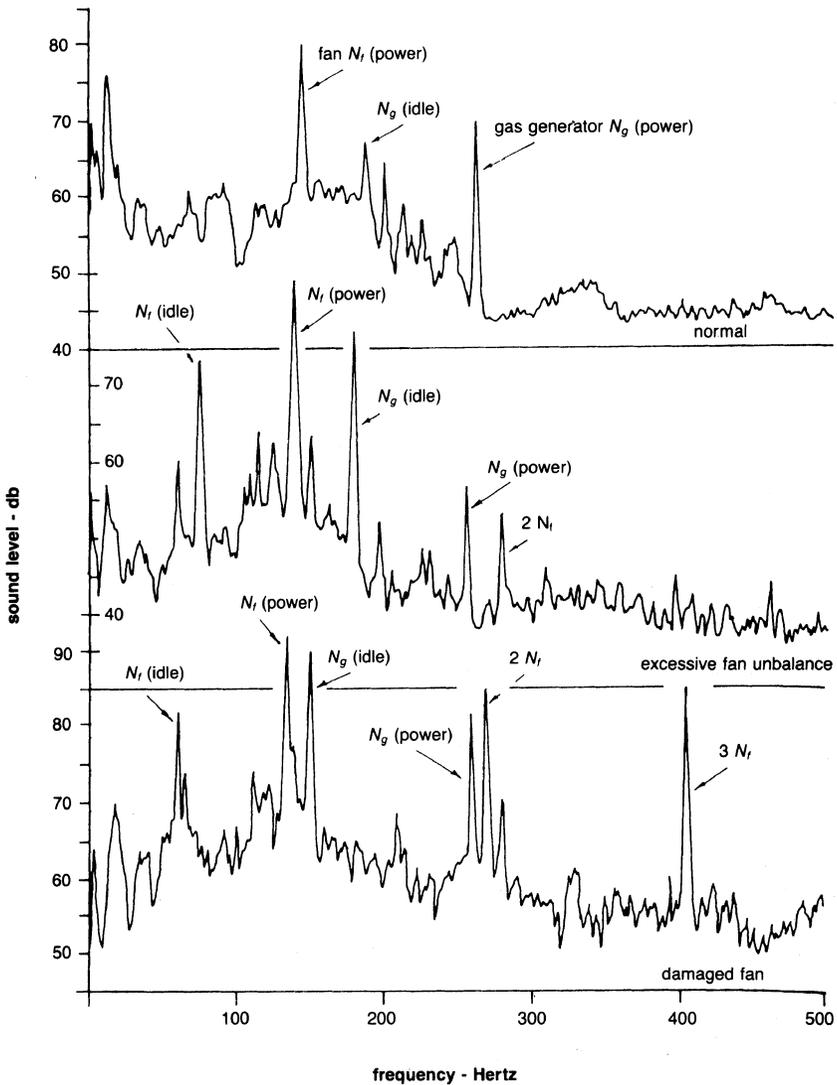


Figure 16-15. Jet engine acoustic signature.

fans on both engines are considerably greater than normal, indicating a poor fan balance. On the other hand, the once-per-revolution component of the gas generator at power is less than the norm, indicating better balance. The bottom plot shows a third engine with a fan damaged by

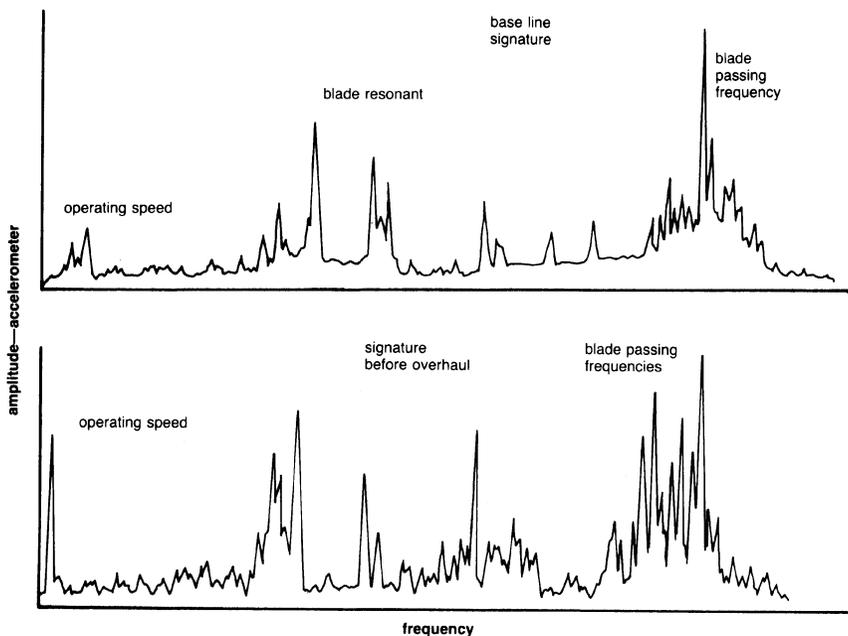


Figure 16-16. Machinery analyses showing comparison of baseline signature to signature before overhaul.

ingesting a bird on takeoff. The damaged fan has a large unbalance as shown by the size of the once-per-revolution component. In addition, the second- and third-order fan harmonics are very prominent compared to the two other signatures.

Obtaining baseline signatures is a very useful tool for detecting deterioration of an engine with time. Figure 16-16 compares the signatures of the machine when installed and after a couple of years of operation. The spectrum shows an increase in level at the high-frequency range, indicating blade flutter problems. Inspection of the unit indicated a number of cracked blades. Another example (Figure 16-17) shows the increase over time of a stator resonant frequency, indicating a high flutter of the blades. Inspection indicated cracks on that stage blade.

Spectrum analysis is a very useful tool in analyzing machinery problems; spectra in both subharmonic and high frequencies are needed to evaluate machinery problems fully.

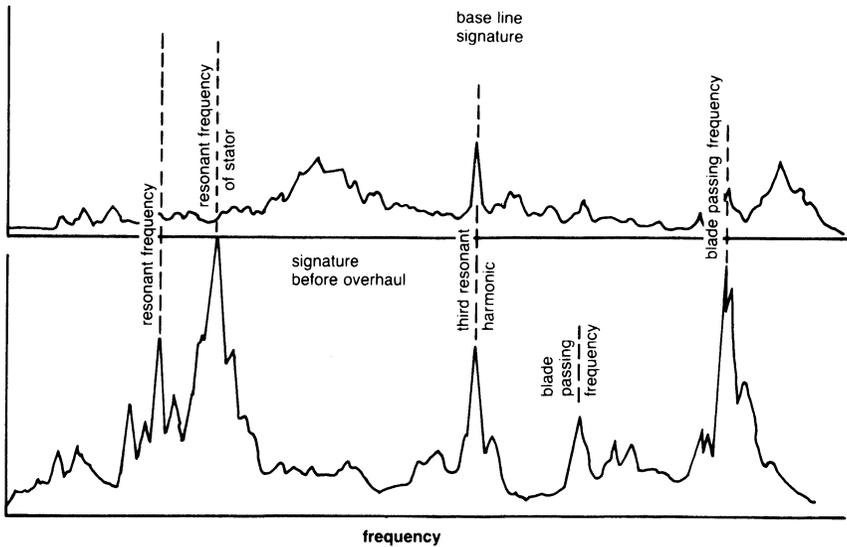


Figure 16-17. Machinery analyses showing the comparison of baseline signature to signature before overhaul.

Bibliography

- Bickel, H.J., "Calibrated Frequency Domain Measurements Using the Ubiquitous," Spectrum Analyzer, *Federal Scientific Monograph 2*, January 1970.
- Bickel, H.J., and Rothschild, R.S., "Real-Time Signal Processing in the Frequency Domain," *Federal Scientific Monograph 3*, March 1973.
- Borhaug, J.E., and Mitchell, J.S., "Applications of Spectrum Analysis to Onstream Condition Monitoring and Malfunction Diagnosis of Process Machinery," Proceedings of the 1st Turbomachinery Symposium, Texas A&M University, 1972, pp. 150-162.
- Boyce, M.P., Morgan, E., and White, G., "Simulation of Rotor Dynamics of High-Speed Rotating Machinery," Proceedings of the First International Conference in Centrifugal Compressor Technology, Madras, India, 1978, pp. 6-32.
- Lang, G.F., "The Fourier Transform . . . What It Is and What It Does," *Informal Nicolet Scientific Corporation Monograph*, December 1973.
- Lubkin, Y.J., "Lost in the Forest of Noise," *Sound and Vibration Magazine*, November 1968.
- Mitchell, H.D., and Lynch, G.A., "Origins of Noise," *Machine Design Magazine*, May 1969.

17

Balancing

Vibration problems in present-day turbomachinery are as pressing and important as those encountered in their design, manufacture, and general maintenance. Considerable amounts of precious energy go unused during machinery breakdowns, and the associated costs of machine downtime add to unproductive overheads. The modern trend of building high-speed engines requires new, dependable techniques to reduce vibrations.

Rotor Imbalance

Of the several factors that can cause vibrations in turbomachines, an unbalanced rotor stands at the top of the list. The lack of balance in a rotor may be caused by internal nonhomogeneity and/or external action. The general sources which can cause this problem are classified in the following categories:

1. Dissymmetry
2. Nonhomogeneous material
3. Eccentricity
4. Bearing misalignment
5. Shifting of parts due to plastic deformation of rotor parts
6. Hydraulic or aerodynamic unbalance
7. Thermal gradients

A certain amount of the unbalance from factors such as misalignment, aerodynamic coupling, and thermal gradients may be corrected at running speeds using modern balancing techniques; however, in most cases they are basic problems that must be initially corrected before any balancing can be

done. Rotor mass unbalance from dissymmetry, nonhomogeneous material, distortion, and eccentricity can be corrected so that the rotor can run without exerting undue forces on the bearing housings. In balancing procedures only the synchronous vibrations (vibration in which the frequency is the same as the rotor rotating speed) are considered.

In a real rotor system the amount and location of unbalances cannot always be found. The only way to detect them is with the study of rotor vibration. Through careful operation, the amount and the phase angle of vibration amplitude can be precisely recorded by electronic equipment. The relation between vibration amplitude and its generating force for an uncoupled mass station is

$$\bar{F}(t) = \bar{F}e^{i\omega t} \quad (17-1)$$

$$\bar{Y}(t) = \bar{A}e^{i(\omega t - \phi)} \quad (17-2)$$

$$\bar{A} = \frac{\bar{F}/K}{1 - \left(\frac{\omega}{\omega_n}\right)^2 + i2\xi\left(\frac{\omega}{\omega_n}\right)} \quad (17-3)$$

$$\phi = \tan^{-1} \frac{2\xi\left(\frac{\omega}{\omega_n}\right)}{1 - \left(\frac{\omega}{\omega_n}\right)^2} \quad (17-4)$$

where:

$\bar{Y}(t)$ = vibration amplitude

\bar{F} = generating force

\bar{A} = amplification factor

ϕ = phase lag between force and amplitude

From Equation (17-4), one will find that the phase lag is a function of the relative rotating speed ω/ω_n and the damping factor ξ . (See Figure 17-1.) The force direction is not the same as the maximum amplitude. Thus, for maximum benefit, the correction weight must be applied opposite to the force direction.

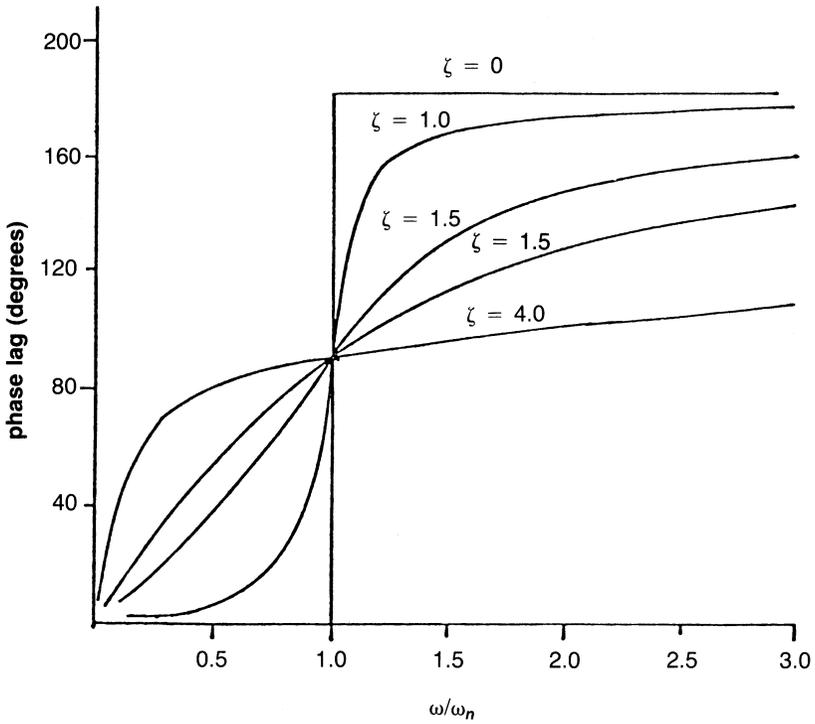


Figure 17-1. Typical phase lag between force and vibration amplitude chart.

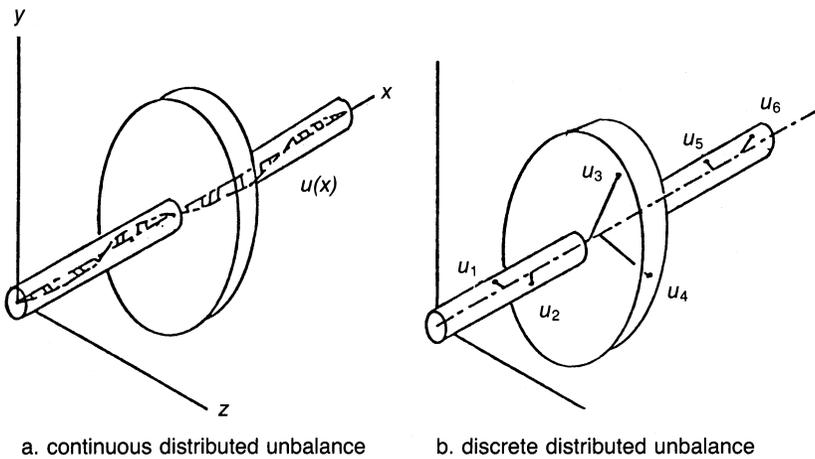
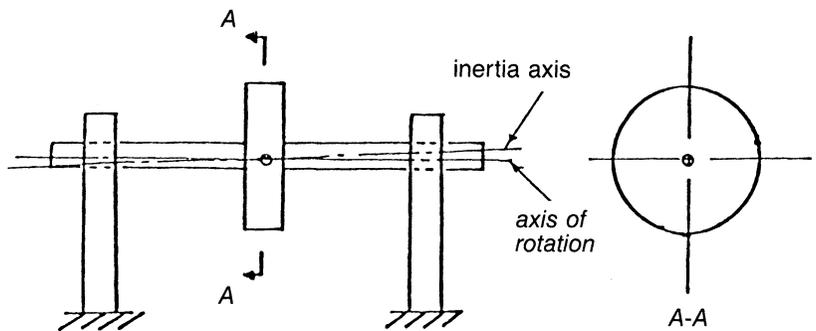


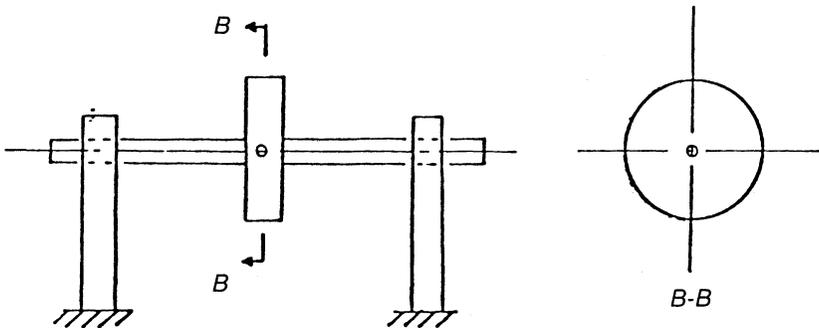
Figure 17-2. Distribution of unbalance in a rotor.

The existence of unbalance in a rotor system may be in continuous form or discrete form, as shown in Figure 17-2. Ascertaining an exact distribution is an extremely difficult, if not impossible, task by today's techniques.

For a perfectly balanced rotor, not only should the center of gravity be located at the axis of rotation, but also the inertial axis should coincide with the axis of rotation shown in Figure 17-3. This condition is almost impossible to achieve. Balancing may be defined as a procedure for adjusting the mass distribution of a rotor so that the once-per-revolution vibration motion of the journals or forces on the bearings is reduced or controlled. Balancing functions can be separated into two major areas: (1) determining the amount and location of the unbalance and (2) installing a mass or masses equal to



a. static balanced rotor



b. perfect balanced rotor

Figure 17-3. Balanced rotor.

the unbalance to counteract its effects or removing the mass of the unbalance exactly at its location.

Static techniques to determine unbalance can be performed by setting a rotor on a set of frictionless supports; the heavy point of the rotor will have a tendency to roll down. Noting the location of this point, the resultant unbalance force can be found, and the rotor can be statically balanced. Static balancing makes the center of gravity of the rotor approach the centerline of two end supports.

Dynamic balancing can be achieved by rotating the rotor either on its own supports or on an external stand. Unbalance can be detected by studying rotor vibration with various types of probes or sensors. Balancing is then achieved by placing correction weights in various planes that are perpendicular to the rotor axis. The weights reduce both the unbalanced forces and unbalanced moments. Placing the correction weights in as many planes as possible minimizes the bending moments along the shaft introduced by the original unbalance and/or the balance correction weights.

Flexible rotors are designed to operate at speeds above those corresponding to their first natural frequencies of transverse vibrations. The phase relation of the maximum amplitude of vibration experiences a significant shift as the rotor operates above a different critical speed. Hence, the unbalance in a flexible rotor cannot simply be considered in terms of a force and moment when the response of the vibration system is in-line (or in-phase) with the generating force (the unbalance). Consequently, the two-plane dynamic balancing usually applied to a rigid rotor is inadequate to assure the rotor is balanced in its flexible mode.

The best balance technique for high-speed flexible rotors is to balance them not in low-speed machines, but at their rated speed. This is not always possible in the shop; therefore, it is often done in the field. New facilities are being built that can run a rotor in an evacuated chamber at running speeds in a shop. Figure 17-4 shows the evacuation chamber, and Figure 17-5 shows the control room.

High-speed balancing should be considered for one or more of the following reasons:

1. The actual field rotor operates with characteristic mode shapes significantly different than those that occur during a standard production balance.
2. Flexible rotor balancing must be performed with the rotor whirl configuration approximating the mode in question. The operating speed(s) is in the vicinity of a major flexible mode resonance (damped critical speed). As these two speeds approach one another, a tighter

FPO

Figure 17-4. Evacuation chamber for a high-speed balancing rig. (Courtesy of Transamerica Delaval, Inc.)

FPO

Figure 17-5. Control room for high-speed balancing rig. (Courtesy of Transamerica Delaval, Inc.)

balance tolerance will be required. Those designs that have a low rotor-bearing stiffness ratio or bearings in the vicinity of mode nodal points are of special concern.

3. The predicted rotor response of an anticipated unbalance distribution is significant. This type of analysis may indicate a sensitive rotor which should be balanced at rated speed. It will also indicate which components need to be carefully balanced prior to assembly.
4. The available balance planes are far removed from locations of expected unbalance and are thus relatively ineffective at the operating speed. The rule of balancing is to compensate in the planes of unbalance when possible. A low-speed balance using inappropriate planes has an adverse effect on the high-speed operation of the rotor. In many cases, implementation of an incremental low-speed balance as the rotor is assembled will provide an adequate balance, since compensations are being made in the planes of unbalance. This is particularly effective with designs incorporating solid-rotor construction.
5. A very low-production balance tolerance is needed to meet rigorous vibration specifications. Vibration levels below those associated with a standard production-balanced rotor are often best obtained with a multiple-plane balance at the operating speed(s).
6. The rotors on other similar designs have experienced field vibration problems. Even a well-designed and constructed rotor may experience excessive vibrations from improper or ineffective balancing. This situation can often occur when the rotor has had multiple rebalances over a long service period and thus contains unknown balance distributions. A rotor originally balanced at high speed should not be rebalanced at low speed.

A wealth of technical literature concerning balancing has been published. Various phases of a variety of balancing procedures have been discussed in these papers. Jackson and Bently discuss in detail the orbital techniques. Bishop and Gladwell, as well as Lindsey, discuss the modal method of balancing. Thearle, Legrow, and Goodman discuss early forms of influence coefficient balancing. The author, Tessarzik, and Badgley have presented improved forms of the influence coefficient method that provide for the balancing of flexible rotors over a wide speed range and multiple-bending critical speeds.

Practical applications of the influence coefficient method to multiplane, multispeed balancing are presented by Badgley and the author. The separate problem of choosing balancing planes is discussed at some length by Den Hartog, Kellenberger, and Miwa for the $(N + 2)$ -plane method, and by Bishop and Parkinson in the N -plane method.

Balancing Procedures

There are three basic rotor balancing procedures: (1) orbital balancing, (2) modal balancing, and (3) multiplane balancing. These methods are subject to certain conditions that determine their effectiveness.

Orbital Balancing

This procedure is based on the observation of the orbital movement of the shaft centerline. Three signal pickups are employed, of which two probes measure the vibration amplitudes of the rotor in two mutually perpendicular directions. These two signals trace the orbit of the shaft centerline. The third probe is used to register the once-per-revolution reference point and is called the *keyphazor*. A schematic arrangement of these probes is shown in Figure 17-6.

The three signals are fed into an oscilloscope as vertical-, horizontal-, and external-intensity marker input. The keyphazor appears as a bright spot on the screen. In cases where the orbit obtained is completely circular, the maximum amplitude of vibration occurs in the direction of the keyphazor. To estimate the magnitude of the correction mass, a trial-and-error process is initiated. With the rotor perfectly balanced, the orbit finally shrinks to a

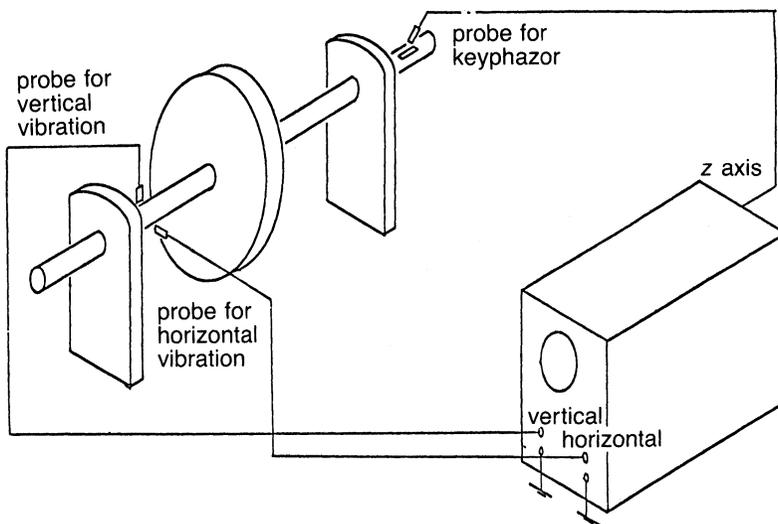


Figure 17-6. Typical arrangement for orbit.

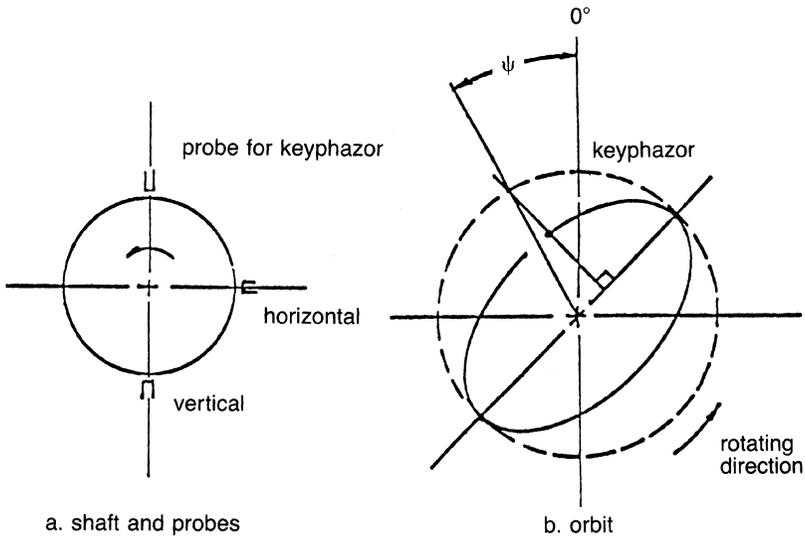


Figure 17-7. Typical probe positions and the phase angle in an elliptic orbit.

point. In the event of an elliptic orbit, a simple geometric construction allows for the establishment of the phase location of the unbalance (force). Through the keyphazor spot, a perpendicular is dropped on the major axis of the ellipse to intersect its circumcircle as shown in Figure 17-7. This intersecting point defines the desired phase angle. Correction mass is found as described earlier. It is important to note that for speeds above the first critical, the keyphazor will appear opposite the heavy point.

In the orbital method, the damping is not taken into account. Therefore, in reality, this method is effective only for very lightly damped systems. Further, as no distinction is made between the deflected mass and the centrifugal unbalance due to its rotation, the balance weights are meaningful only at a particular speed. The optimum balancing plane considered is the plane containing the center of gravity of the rotor system or, alternately, any convenient plane that allows for the orbit to be shrunk to a spot.

Modal Balancing

Modal balancing is based on the fact that a flexible rotor may be balanced by eliminating the effect of the unbalance distribution in a mode-by-mode sequence. Typical principal modes of a symmetric, uniform shaft are shown

in Figure 17-8. The deflections of a rotor at any speed may be represented by the sum of various modal deflections multiplied by constants dependent on speed

$$\bar{Y}(x, \omega) = \sum_{r=1}^{\infty} \bar{B}_r(\omega) \times \eta_r(x) \quad (17-5)$$

where $\bar{Y}(x, \omega)$ represents the amplitude of transverse vibrations, as a function of the distance along the shaft at a rotational speed ω . $\bar{B}_r(\omega)$ and $\eta_r(x)$ express, respectively, the complex coefficient at rotating speed ω and the r th principal mode.

Thus, a rotor, which has been balanced at all critical speeds, is also balanced at any other speed. For end-bearing rotors, the recommended procedure is: (1) balance the shaft as a rigid body, (2) balance for each critical speed in the operating range, and (3) balance out the remaining noncritical modes as far as possible at the running speed. Balance planes picked are the ones wherein the maximum amplitudes of vibration occur.

Modal balancing is one of the proven methods for flexible rotor balancing. Modal balancing has also been applied to problems of dissimilar lateral stiffness, hysteretic whirl, and to complex shaft-bearing problems. In many discussions on modal balancing fluid-film damping is not included. In other

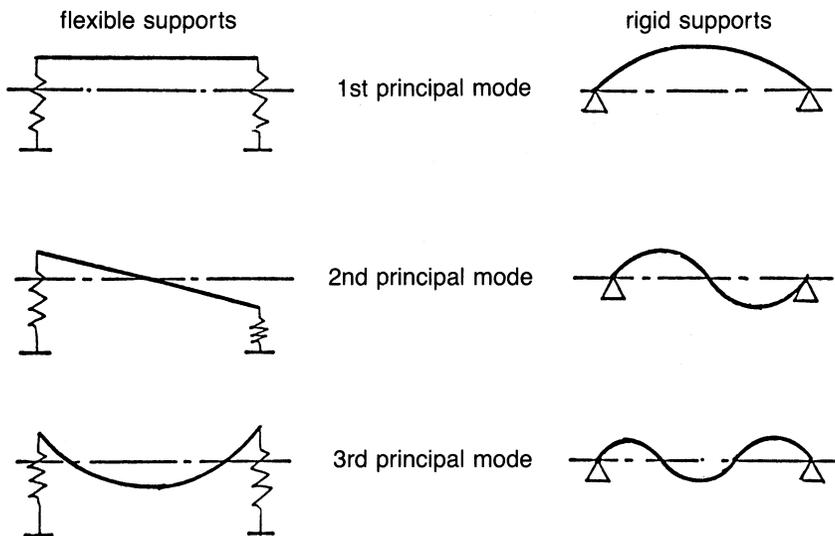


Figure 17-8. Typical principal modes for a symmetric and uniform shaft.

instances rolling-element bearing effects are neglected. In such cases, the practical usefulness of the modal method is not fully defined.

Several problems hinder the application of the modal technique to more complex systems. To use the technique, calculated information is required on the mode shapes and natural frequencies of the system to be balanced. The accuracy of the computed results depends on the capabilities of the computer program used and on the input data (dimension, coefficients, system model effectiveness) used in the calculations. In turbomachinery where system damping is significant, as with fluid-film bearings, problems arise. The mode shapes and resonant frequencies of heavily damped systems often bear little resemblance to undamped mode shapes and frequencies. The reliance of modal balancing on predicted modes and frequencies is at least an inconvenience and, without proper response programs, can be a significant disadvantage.

At present, no general-purpose modal balancing computer programs exist that are comparable in nature to the programs developed for the influence coefficient (multiplane) method. Such a program would require calculated modal amplitudes and phase angles, and that the measured amplitudes and phase angles of the rotor bearing system be balanced. The program would then be run for each separate rotor whirl mode, including the full-speed residual balance correction. At present, no general analysis suitable for programming exists.

Multiplane Balancing (Influence Coefficient Method)

Modal balancing came into being to alleviate the problems of the supercritical rotor unbalance of the steam turbine-generator industry. It combined the then available techniques for calculating response amplitudes for the various rotor vibrational modes with the available instruments for measuring actual installed vibration levels. In recent years, more systems have been designed for supercritical operation. Newer types of sensors and instruments are becoming available, making it feasible to obtain precision in amplitude and phase measurement. Minicomputers for operation on the shop floor or in balancing pits, and time-sharing terminals for in-the-field access to large computers, are now commonly available. The newest multiplane balancing techniques owe their success to advancement in these areas.

The influence coefficient method is simple to apply, and data are now easily obtainable. Consider a rotor with n discs. The method of influence coefficients provides the means for measuring the compliance characteristics of the rotor.

Let $P_1, \dots, P_j, \dots, P_n$ be the forces acting on the shaft. Then the deflection Z_i in the i -plane is given by

$$Z_i = \sum_{j=1}^n e_{ij} P_j, i = 1, \dots, n \quad (17-6)$$

This equation defines the compliance matrix $[e_{ij}]$, and the elements of the matrix are called the influence coefficients. The compliance matrix is obtained by making

$$P_j = \delta_{ij} \quad (17-7)$$

where δ_{ij} is the Kronecker delta, and measuring the deflections Z_i . As j is varied from 1 to n , each column of the compliance matrix is obtained. Once the compliance matrix is obtained, knowing the initial vibration level in each plane q_i , the system of equations

$$\sum_{j=1}^n e_{ij} F_j = q_i, i = 1, \dots, n \quad (17-8)$$

is solved for the correction forces, F_j . The correction weights can be computed from the correction forces.

In general, $2N$ sets of amplitude and phase are all that is required by the exact-point speed-balancing method. In balancing with the influence coefficient method: (1) initial unbalance amplitudes and phases are recorded, (2) trial weights are inserted sequentially at selected locations along the rotor, (3) resultant amplitudes and phases are measured at convenient locations, and (4) required corrective weights are computed and added to the system. Balance planes are obviously where the trial weights are inserted. The influence coefficients (or system parameters) can be stored for future trim balance. The method requires no foreknowledge of the system dynamic response characteristics (although such knowledge is helpful in selecting the most effective balance planes, readout locations, and trial weights).

The influence coefficient method examines relative displacements rather than absolute displacements. No assumptions about perfect balancing conditions are made. Its effectiveness is not influenced by damping, by motions of the locations at which readings are taken, or by initially bent rotors. The least-square technique for data processing is applied to find an

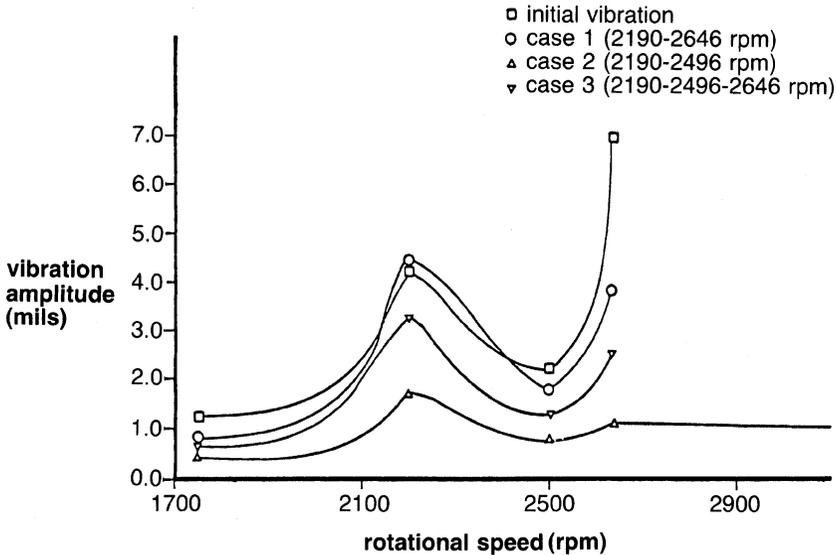


Figure 17-9. Rotor amplitudes for least-square balance.

optimum set of correction weights for a rotor that has a range of operating speeds.

A number of investigations have concerned themselves with the optimum selections of the number of balancing planes necessary to balance a flexible rotor. To perform an ideal balance on a flexible rotor, as many balancing planes as unbalances are needed. The perfect balance is either impractical or uneconomical. Two substitute approaches for deciding the number of balancing planes have been proposed.

One is the so-called N -plane approach. This approach states that only N -planes are necessary for a rotor system running over N critical speeds. The other technique, called the $(N + 2)$ -plane approach, requires two additional planes. These two additional planes are for the two-bearing system and are necessary in this school of balancing.

The N -plane is based on the concepts of the modal technique. From Equation (17-5), there are N principal modes that need to be zero for the perfect balance of a rotor, which runs through N th critical speed. Thus, N -planes located at the peaks of the principal modes will be enough for cancelling these modes. From the point of view of residual forces and moments at the support bearings, $(N + 2)$ -planes are better than N -planes.

If one can balance at design speed, that point is ideal, but there may be problems while trying to go through the various criticals. Thus, it is best to

balance the unit through the entire operation range. The number of speeds to be selected is also very important. Tests conducted show that when the points were taken at the critical speed and at a point just after the critical speed, the best balance results throughout the operating range were obtained, as seen in Figure 17-9.

Application of Balancing Techniques

Using the influence coefficient technique for multiplane balancing is simply an extension of the logic, which is “hardwired” into the standard balancing machine. This extension has been made possible by the availability of better electronics and easier access to computers.

Practical balancing may now be performed in any reasonable number of planes at virtually any reasonable number of speeds. The one-plane, low-speed balancing operation is perhaps the simplest application of the method, where a known weight at a known radial location (often in the form of wax added by hand) is used to determine balance sensitivity of the part to be balanced in a spin-up fixture. This procedure can effectively remove an unbalance force from a component. Two-plane balancing is simply an extension to permit unbalance moments as well as forces to be removed. In several instances, the sensitivities associated with these types of machines can be predetermined (the machine may be calibrated) and the values stored to permit one-start balancing. Balancing a fully assembled rotor operating in its running environment, whether rigid or flexible in nature, represents the ultimate application.

The balancing process must be in accord with the rotor dynamics, as specified by the operating environment. Unfortunately, the dynamic characteristics are often not properly recognized when the balancing procedure is specified. As a result, the unbalance distribution problem may not be identified; not enough planes may be provided; sensors may be located at nonoptimum positions, or critical speeds may be overlooked entirely. It is the responsibility of the machinery end user to satisfy himself that the manufacturer has considered:

1. The locations of the critical speeds in the running-speed range for the entire rotor system.
2. The mode shapes (problem unbalance distributions) of the rotor at the criticals.
3. The most probable distribution of unbalance in the finally installed rotor, considering manufacturing tolerances, balancing residuals after low-speed balance, assembly tolerances, etc.

4. The response of the entire rotor-bearing system to this unbalance, considering damping in bearings, joints, dampers, etc.
5. Provisions for eliminating “unbalance distribution problems” at each manufacturing step, whether by machining, low-speed balancing, or high-speed balancing.
6. Provisions for future balancing of the final rotor assembly, when and if necessary.

All of the previous steps are now commercially available at a small fraction of the cost of a replacement rotor.

Component balancing in the factory is required for a very simple reason: the mass center of the component design (or the mass center of each section of long components) does not lie on the intended axis of rotation. The problem occurs because of machining tolerances, void inclusions in the metal, etc. As a result, the component is subjected to one or more balancing steps. In the balancing operation, rotor unbalance sensitivities (interference coefficients) are determined for a sampling of rotors and stored.

Design of the production-rotor balancing process begins with an analytical optimization process, usually best conducted during system design. An unbalance-response computer program is coupled with a balancing computer program to calculate vibration amplitude as a function of unbalance. These programs yield the optimum location of vibration sensors, correction planes, and optimum balance speeds. Multiplane balancing of the rotor assembly may be done conveniently in a balancing fixture that simulates dynamically the actual environment in which the rotor will operate. A drive motor is required, and possibly a vacuum system, depending on rotor configuration and balancing speed.

It is important that final balancing corrections not be made on any components that are later to be replaced under field operation conditions. Items such as turbine wheels, which are to be replaced as balanced items during field maintenance, obviously cannot be removed and replaced without altering the assembly balance if they have been utilized for balance corrections. The balancing process design should therefore also be integrated with the maintainability design for best results.

Once the rotor system has been installed, downtime is the key cost associated with vibration. For example, it is not unusual for lost production costs to be measured in tens of thousands of dollars per day for a chemical plant compressor. Obviously, shutting down the machine to rebalance the rotor is a decision not taken lightly. The optimum approach is to determine corrections while the machine is running, and shutdown only long enough to install the trim balance weights. The multiplane balancing procedure permits

this procedure to be done with ease after the rotor sensitivities have been measured.

In field balancing (trim balancing), however, rotor speed and system temperatures are the key considerations. It will often be difficult to control speed because of process considerations; system temperatures may require hours, or even days, to stabilize. Vibration should be recorded each time the unit is stopped for trial weight insertion to determine the length of time required for thermal stabilization. Consideration of critical speed locations, vibratory mode shapes, and the like obtained by a separate rotor dynamics study can also greatly improve the results by providing better guidance to the best sensor and balancing plane locations.

Minimization of the number of startups is an important consideration because the number of starts reduces engine life. The critical aspect in this minimization is the correct selection of balance planes at the start of the process. This selection is essential because the rotor to be balanced often consists of a number of units (turbine, compressor) connected by couplings and has a great number of available correction planes. Usually, balancing is required only in one "zone" (on the turbine or at the coupling) at a particular speed. The critical location can be pinpointed almost exactly by reference to a prior analytical unbalance-response sensitivity study. Such a study, which involves the entire rotor and couplings, will indicate those planes where particular unbalance distributions, if present, will cause vibration at a particular speed. For example, a machinery train, consisting of a precisely balanced compressor with a precisely balanced coupling, will sometimes vibrate excessively at one or more speeds. This vibration usually results because the rotor assembly has one or more bending critical speeds in the running range where the mode shapes are forced by the residual unbalances left in the precision-balanced subassemblies. It must be stressed that a balanced rotor subassembly does not have zero unbalance. In reality, it has a residual unbalance distribution, which does not excite the subassembly under the balance conditions. If an analytical study does not exist, the balancing engineer must depend on vibration readings from available sensors and, ultimately, on judgment or past experience for selection of correction locations.

Once the critical zones along the rotor axis have been identified, the sensitivity factors of those planes must be calculated. If unbalance sensitivity factors of those planes must be calculated. If unbalance sensitivity factors are not available for the balance planes and sensors at the speeds of interest, trial weight runs are required. Thermal stabilization times become important, since the process can consume significant periods of time. If the sensitivities are available, then corrections may be calculated based on

vibration levels measured inservice just before shutdown, and the unit can be balanced and restarted very rapidly.

It is often tempting to try to shortcut the sensitivity factor gathering process by inserting correction weights in available planes one at a time based on hunches or one-plane vector plots. Occasionally, this shortcut will result in a balanced rotor; but more often, the opposite result is achieved. This unbalance results because the trial weights in later planes are then not the only perturbation from the “as-is” condition. Data Sheets A, B, and C show a typical process for field balancing with a computer program that employs this balancing technique.

The balancing engineer must try to maintain a balance record for each machine he balances, since in most cases the machinery system itself will often contain some nonrepeatable element. Components sensitive to thermal variations, such as dampers and bearing alignments, etc., may often cause problems. When a nonrepeatability is present, the engineer must first determine whether or not another corrective action is indicated. If not, then the balance quality that may be obtained is limited strictly by the range of the nonrepeatable element’s variability. This level of quality is difficult to ascertain without experience, either on the individual machine or on a family of similar machines. The balance engineer must balance each rotor by using mean values for each parameter, and he must keep a detailed record of the different results. This record consists, essentially, of residual unbalance experience in each case. From the standpoint of the multiplane balancing procedure, the record consists of sensitivity parameters for each machine, which are obtained as a matter of due course in the trial weight procedure.

User’s Guide for Multiplane Balancing

The following are suggested steps for balancing a rotor using a multiplane balancing technique. The steps are applicable to a specific program; however, other programs will require about the same information:

1. Choose the number of balancing planes and install an equal or greater number of proximity probes. Install a tachometer that gives a once-per-revolution pulse anywhere on the rotor. Feed the tach signal and the probe signal from one plane at a time into a phase meter to indicate the rotating speed in rpm, the vibration amplitude in peak-to-peak mils, and the phase angle of the maximum amplitude in degrees from the tach pulse.
2. Note the number of balancing planes and the balancing speed in rpm on Data Sheet A. Next, rotate the machine at a slow speed (less than

25% of balancing speed), and measure the initial runout amplitude and phase in each plane. Now, rotate the machine at the balancing speed, and measure the final vibration amplitude and phase in each plane. Record all this data on Data Sheet A.

3. Take a blank Data Sheet B. Enter the plane number. Place a trial weight at any radius and any angle in that plane. Enter these values on the sheet. Now, operate the machine at the balancing speed, and measure the vibration amplitude and phase in each plane. Repeat the procedure for each plane. (Place only one trial weight in only one plane at a time.) When finished, you should have as many Data Sheets B as the number of planes.
4. Data Sheet C describes the options available to the user. Enter the proper choice for each option.

Data Sheet A

| Number of Balancing Planes | Speed in rpm | |
|---|--------------|-------|
| | Amplitude | Phase |
| Initial Run-Out Amplitude and Phase-In-Plane | 1 | |
| | 2 | |
| | 3 | |
| | 4 | |
| | 5 | |
| Final Vibration Amplitude and Phase Before Balancing In-Plane | 1 | |
| | 2 | |
| | 2 | |
| | 4 | |
| | 5 | |

Data Sheet B

Plane _____

| Trial Weight | Radius | Angle |
|--------------|--------|-------|
| | | |
| | | |
| | | |
| | | |
| | | |
| | | |
| | | |
| | | |
| | | |
| | | |

| Vibration Amplitude and Phase In-Plane | Amplitude | Phase |
|--|-----------|-------|
| | | |
| | | |
| | | |
| | | |
| | | |
| | | |
| | | |
| | | |
| | | |
| | | |

Data Sheet C

Options

- If the same weight as the trial weight is to be used for balancing, then the program will locate radius ($NS1 = 1$). For computing the weight at a fixed radius. $NS1 = 2$.
 $NS1 =$ _____
- Radius at which balancing weights will be placed. If $NS1 = 2$, give the locating radius in each plane. (This is not applicable if $NS1 = 1$.)

| Plane No. | 1 | 2 | 3 | 4 | 5 |
|-----------|---|---|---|---|---|
| Radius | | | | | |

- If balancing is to be done to the initial run-out, then $NS2 = 1$.
If balancing is to be done to zero amplitude, $NS2 = 2$.
 $NS2 =$ _____
- If add-on weights will be used, $NS3 = 1$.
If holes will be drilled, $NS3 = 2$.
 $NS3 =$ _____
- If weights can only be placed or removed at a certain number of evenly spaced locations, $NS4 = 1$.
If they can be placed anywhere, $NS4 = 2$.
 $NS4 =$ _____
- If $NS4 = 1$, then give the number of holes and the angle to the first hole in each plane.

| Plane No. | No. of Holes | Angle of First Hole |
|-----------|--------------|---------------------|
| 1 | | |
| 2 | | |
| 3 | | |
| 4 | | |
| 5 | | |

Bibliography

- Badgley, R.H., "Recent Development in Multiplane-Multispeed Balancing of Flexible Rotors in the United States," presented at the Symposium on Dynamics of Rotors, IUTAM, Lyngby, Denmark, August 12, 1974.
- Bently Nevada Corp., "Balancing Rotating Machinery," Report 1970, Minden, Nevada.
- Bishop, R.E.D., and Parkinson, A.G., "On the Use of Balancing Machines for Flexible Rotors," ASME Paper No. 71-Vibr-73.
- Bishop, R.E.D., and Gladwell, G.M.L., "The Vibration and Balancing of an Unbalanced Flexible Rotor," *Journal of Mechanical Engineering Society*, Vol. 1, 1959, pp. 66–77.
- Boyce, M.P., "Multiplane, Multispeed Balancing of High Speed Machinery," Keio University, Tokyo, Japan, July 1977.
- Boyce, M.P., White, G., and Morgan, E., "Dynamic Simulation of a High Speed Rotor," International Conference on Centrifugal Compressors at Madras, India, February 1978.
- Den Hartog, J.P., "The Balancing of Flexible Rotors," *Air, Space, and Industr.*, McGraw-Hill, New York, 1963.
- East, J.R., "Turbomachinery Balancing Considerations," Proceedings of the 20th Turbomachinery Symposium, Texas A&M University, p. 209, 1991.
- Goodman, T.P., "A Least-Squares Method for Computing Balance Corrections," ASME Paper No. 63-WA-295.
- Jackson, C., "Using the Orbit to Balance," *Mechanical Engineering*, pp. 28–32, February 1971.
- Kellenberger, W., "Should a Flexible Rotor be Balanced in N or $(N + 2)$ Planes?" *Trans. ASME Journal of Engineering for Industry*, pp. 548–560, May 1972.
- Legrow, J.V., "Multiplane Balancing of Flexible Rotors—A Method of Calculating Correction Weights," ASME Paper No. 71-Vibr-52.
- Lindsey, J.R., "Significant Developments in Methods for Balancing High-Speed Rotors," ASME Paper No. 69-Vibr-53.
- Miwa, S., "Balancing of a Flexible Rotor (3rd Report)," *Bulletin of the ASME*, Vol. 16, No. 100, October 1973, pp. 1562–1572.
- Stroh C.G., MacKenzie J.R., Rebstock, and Jordan, "Options for Low Speed and Operating Speed Balancing of Rotating Equipment, Proceedings of the 25th Turbomachinery Symposium, Texas A&M University," p. 253, 1996.
- Tessarzik, J.M., Badgley, R.H., and Anderson, W.J., "Flexible Rotor Balancing by the Exact-Point Speed Influence Coefficient Method," Transactions

ASME, Inst. of Engineering for Industry, Vol. 94, Series B, No. 1, p. 148, February 1972.

Thearle, E.L., "Dynamic Balancing of Rotating Machinery in the Field," Trans. ASME Vol. 56, pp. 745–753, 1934.

18

Couplings and Alignment

Couplings in most turbomachines attach the driver to the driven piece of machinery. High-performance flexible couplings used in turbomachines must perform three major functions: (1) efficiently transmit mechanical power directly from one shaft to another with constant velocity, (2) compensate for misalignment without inducing high stress and with minimum power loss, and (3) allow for axial movement of either shaft without creating excessive thrust on the other.

There are three basic types of flexible couplings that satisfy these requirements. The first type is the mechanical-joint coupling. In this coupling, flexibility is accomplished by a sliding and rolling action. Mechanical-joint couplings include gear tooth couplings, chain and sprocket couplings, and slider or Oldham couplings.

The second type is the resilient-material coupling. In resilient-material couplings flexibility is a function of flexing of material. Resilient-material couplings include those that use elastomer in compression (pin and bushing, block, spider, and elastomer-annulus, metal-insert types); elastomer in shear (sandwich type, tire type); steel springs (radial leaf, peripheral coil types); and steel-disc and diaphragm couplings.

The third type is the combined mechanical and material couplings where flexibility is provided by sliding, or rolling and flexing. Combination couplings include continuous and interrupted metallic-spring grid couplings, nonmetallic gear couplings, nonmetallic chain couplings, and slider couplings that have nonmetallic sliding elements.

In choosing a coupling, the loading and speed must be known. Figure 18-1 shows the relation between coupling type, peripheral velocity coupling size, and speed. The loadings in these high-performance flexible couplings are as follows:

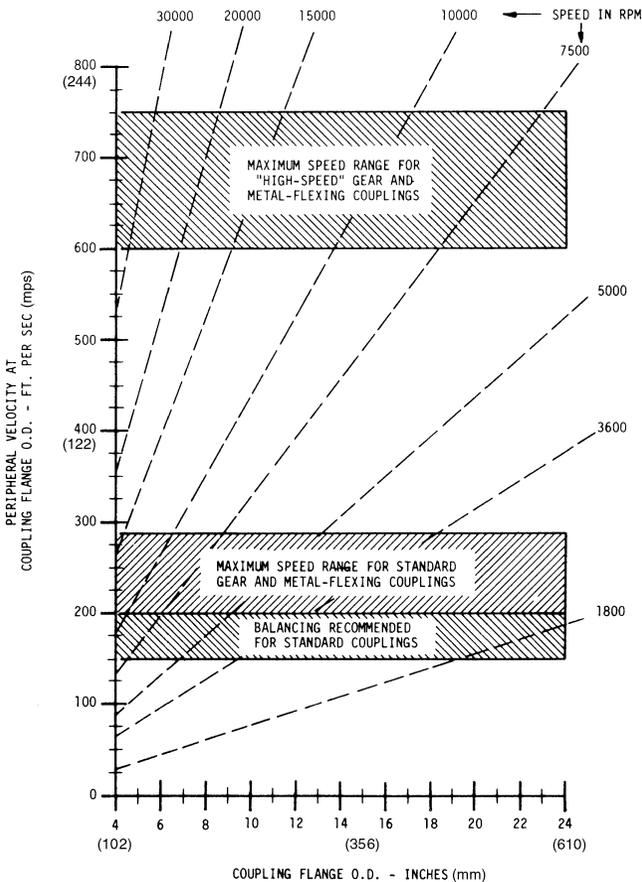


Figure 18-1. Flexible coupling operating spectrum.

1. *Centrifugal force.* Varies in importance, depending on the system speed.
2. *Steady transmitted torque.* Smooth nonfluctuating torque in electric motors, turbines, and a variety of smooth torque-absorbing load (driven) machines.
3. *Cyclically transmitted torque.* Pulsating or cyclic torque in reciprocating prime movers and load machines such as reciprocating compressors, pumps, and marine propellers.
4. *Additional cyclic torque.* Caused by machining imperfections of drive components (particularly gearing) and imbalance of rotating drive components.

5. *Peak torque, (transience)*. Caused by starting conditions, momentary shock, or overload.
6. *Impact torque*. A function of system looseness or backlash. Generally, mechanical-joint flexible couplings have inherent backlash.
7. *Misalignment loads*. All flexible couplings generate cyclic or steady moments within themselves when misaligned.
8. *Sliding velocity*. A factor in mechanical-joint couplings only.
9. *Resonant vibration*. Any of the forced vibration loads, such as cyclic or misalignment loads, may have a frequency that coincides with a natural frequency of the rotating-shaft system, or any component of the complete power plant and its foundation, and may, thus, excite vibration resonance.

The gas turbine is a high-speed, high-torque drive and requires that its coupling have the following characteristics:

1. Low-weight, low-overhung moment
2. High-speed, capacity-acceptable centrifugal stresses
3. High balancing potential
4. Misalignment capability

Table 18-1
Disc, Diaphragm, and Gear Couplings*

| | Disc | Diaphragm | Gear |
|--|---------------------|---------------------|-----------------------|
| Speed capacity | High | High | High |
| Power-to-weight ratios | Moderate | Moderate | High |
| Lubrication required | No | No | Yes |
| Misalignment capacity at high speed | Moderate | High | Moderate |
| Inherent balance | Good | Very good | Good |
| Overall diameter | Low | High | Low |
| Normal failure mode | Abrupt (fatigue) | Abrupt (fatigue) | Progressive (wear) |
| Overhung moment on machine shafts | Moderate | Moderate | Very low |
| Generated moment, misaligned, with torque | Moderate | Low | Moderate |
| Axial movement capacity | Low | Moderate | High |
| Resistance to axial movement | | | |
| Suddenly applied | High | Moderate | High |
| Gradually applied | High | Moderate | Low |

*This table is intended as a rough guide only.

Gear couplings, disc couplings, and diaphragm-type couplings are best suited for this type of service. Table 18-1 shows some of the major characteristics of these types of couplings.

Gear Couplings

A gear coupling consists of two sets of meshing gears. Each mesh has an internal and external gear with the same number of teeth. There are two major types of gear couplings that are used in turbomachinery. The first type of gear coupling has the male teeth integral with the hub as seen in Figure 18-2. In this coupling type the heat generated at the teeth flows in a different way into the shaft than it does through the sleeve to the surrounding air. The sleeve will therefore heat up and expand more than the hub. This expansion plus the centrifugal force acting on the sleeve will cause it to grow rapidly—as much as 3–4 mils more than the hub—causing an eccentricity, which can lead to a large, unbalanced force. Thus, this coupling type is more useful in low-horsepower units.

The second type of coupling, shown in Figure 18-3, has the male teeth integral with the spool. In this coupling type the same amount of heat is produced, but the hollow-bored spool will accept heat in a manner similar to the sleeve so that no differential growth occurs.

Gear couplings have a pilot incorporated into the male tooth form to support the loose member of the coupling in a concentric manner at speed, as shown in Figure 18-4.

The sliding friction coefficient is another area of evaluation in gear couplings. It produces a resistance to the necessary axial movement as rotors heat

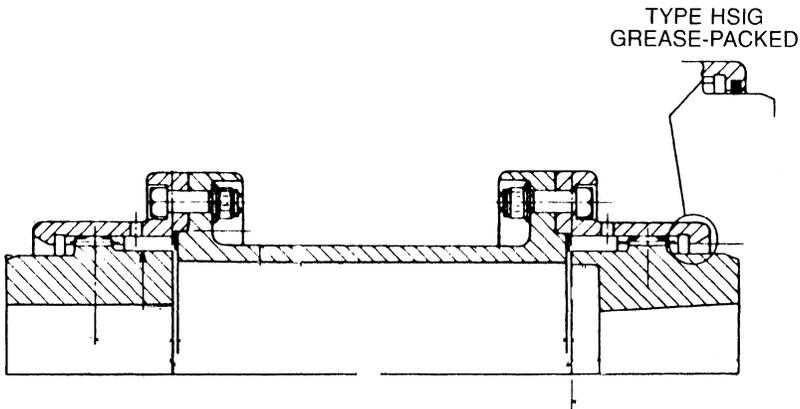


Figure 18-2. Gear coupling (male teeth integral with the hub).

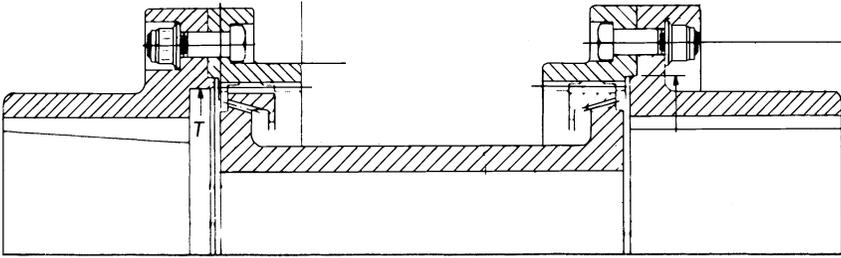


Figure 18-3. Gear coupling (male teeth integral with the spool).

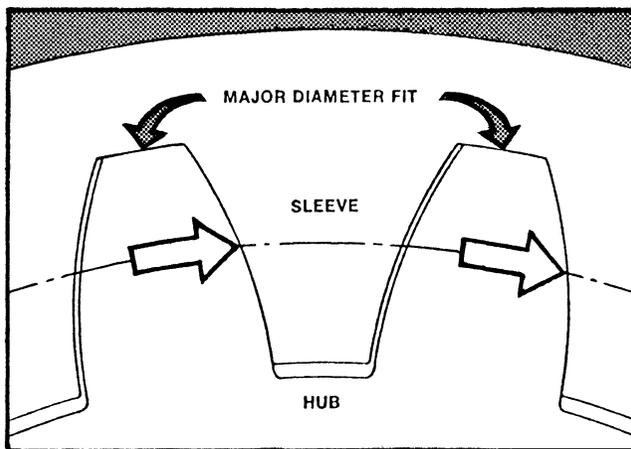


Figure 18-4. Schematic of gear used in coupling applications.

and expand. This relative sliding motion between the coupling elements takes care of the misalignment problem in gear couplings.

Relative motion between the meshing gears is oscillatory in the axial direction and has a low amplitude and a relatively high frequency. Some of the major advantages of the gear couplings are:

1. They can transmit more power per pound of steel, or per inch of diameter, than any other coupling.
2. They are forgiving; they accept errors in installation and mistreatment more readily than other types of couplings.
3. They are reliable and safe; they do not throw around pieces of metal or rubber even when they fail, and they can work longer in corrosive conditions than many other couplings.

A major disadvantage in gear couplings is the misalignment problem. Tooth-sliding velocity is directly proportional to the tooth-mesh misalignment angle and the rotational speed. Therefore, misalignment of high-speed drives must be kept to a minimum to limit sliding velocity to an acceptable value.

The coupling must be able to accommodate misalignment caused by cold startup. The physical misalignment capability of a gear-type coupling should never be considered an acceptable running condition for high-speed applications. The limits of misalignment versus operating speed are best stated on the basis of a constant, relative sliding velocity between the gear teeth.

Figure 18-5 gives recommended limits of misalignment with the system at operating temperature. The graph is based on a maximum constant sliding velocity of 1.3 inches per second and includes coupling size, speed, and the axial distance between gear meshes. Gear couplings can be more tolerant of axial growth than other coupling types.

In the disc-type couplings, the axial growth is limited by the disc deflection range, so the equipment must be adjusted with more axial accuracy than with gear couplings.

High-speed couplings must be balanced very carefully and, with a low overhung moment, the effect of coupling overhung moment is felt not only in machine bearing load but in shaft vibration.

The advantage of a reduction in overhung moment is not only to reduce bearing loads, but to minimize shaft deflection, which results in a reduction of the vibration amplitude. The reduction of the coupling overhung moment produces an upward shift in shaft critical speeds. This change in natural frequencies results in an increase in the spread between natural frequencies. For many applications, reduced overhung moment is an absolute necessity to enable the system to operate satisfactorily at the required operating speed.

The high-speed couplings have five components—usually two hubs, two sleeves, and a spacer. To obtain a proper balance, each hub should be balanced separately, then the spacer should be balanced, and finally the full coupling should be assembly balanced.

The couplings should be carefully match-marked before removal from the balancing mandrels.

Lubrication problems are a major consideration in the use of gear couplings. Relative sliding between the teeth of the hub and the sleeve requires proper lubrication to assure long component life. This sliding motion is alternative and is characterized by small amplitudes and relatively high frequencies.

Gear couplings can be either packed with lubricant or continuously lubricated. Each system has advantages and disadvantages, and the choice depends on the conditions under which the coupling works.

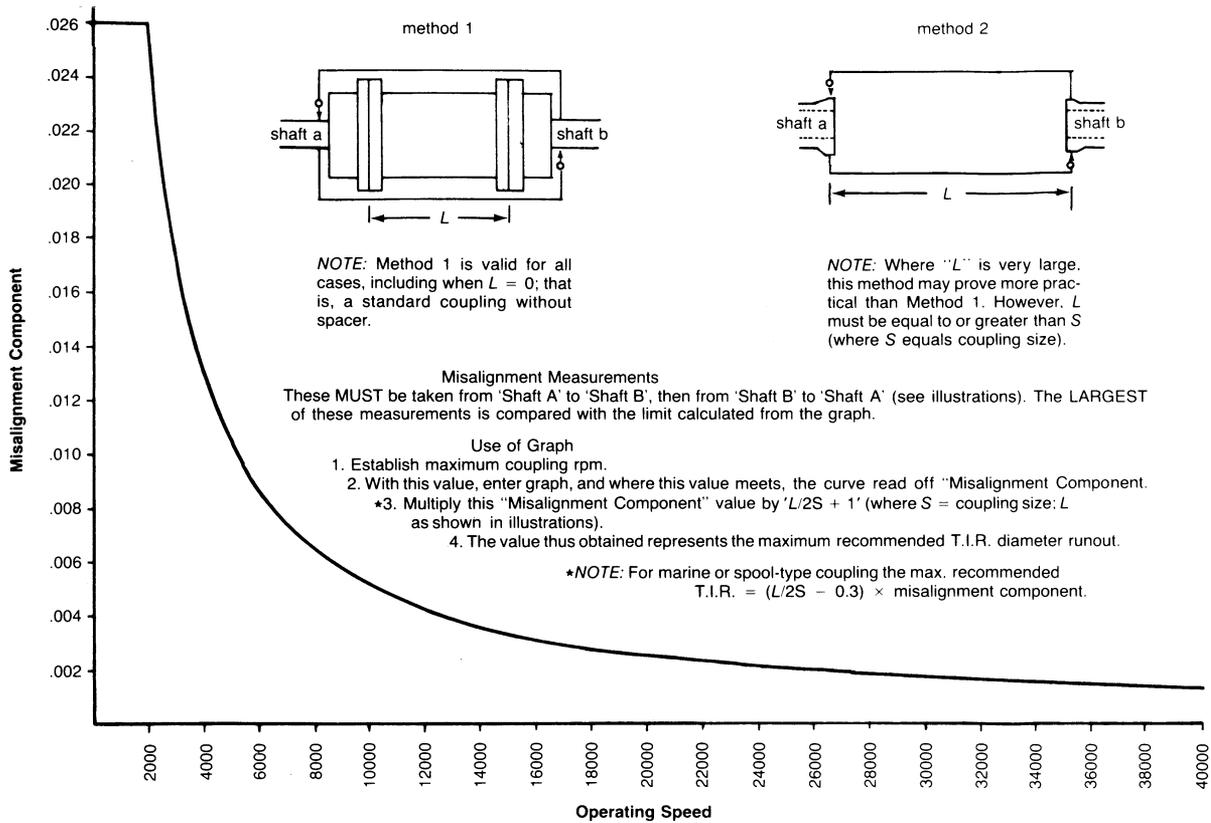


Figure 18-5. Recommended limits of misalignment vs. operating speed (Reference 3).

Oil-Filled Couplings

Very few high-performance couplings use this system because it requires large-volume couplings. It is, however, the best method of lubrication and, incidentally, the first used. Its major disadvantage is that it may leak lubricant from defective flange gaskets, etc.

Grease-Packed Couplings

Besides enabling the user to select a good lubricant, grease-packing has the advantage of sealing the coupling from the environment. The high-performance coupling works under very small misalignment and usually generates very little heat. In most cases, the couplings receive more heat from the shafts than they generate. Very few greases can work in temperatures of more than 250°F, (121°C) and for this reason grease-packed couplings cannot be installed within an enclosure that prevents the heat from dissipating. Greases also separate under large centrifugal forces. In many high-speed couplings forces exceed 8000 g's. New lubricants are appearing on the market that do not separate under high loadings.

A second disadvantage of grease lubrication is the maintenance requirement. Coupling manufacturers generally recommend relubrication every six months. There are known cases, however, where grease-packed couplings were found to be in excellent condition after two years of maintenance-free service.

Continuously Lubricated Couplings

Lubrication by continuous oil flow can represent an ideal method if there is:

1. Freedom to select the type of oil
2. Independent lube circuit

From the user's point of view, neither condition is acceptable, not only because of the added cost of an independent lube circuit, but because it is almost impossible to prevent mixing of the oil from this circuit with the lube system for the rest of the equipment.

In practice, continuously lubricated couplings are supplied with oil from the main lube system. The oil is not the best type for couplings, and also brings to the coupling a large quantity of impurities. The accumulated sludge shortens coupling life.

Sludge accumulates within a coupling for two reasons: (1) because the lubricant is not pure, and (2) because the coupling centrifuges and retains the impurities.

Very little can be done to prevent the coupling from retaining the impurities. The g forces in a coupling are very high, and the oil dam built in the sleeve configuration prevents the impurities from going over it.

Some manufacturers now offer couplings without a dam, or with sleeves provided with radial holes. Experience has shown that such couplings accumulate no sludge. The dam has, however, two useful purposes:

1. It maintains an oil level high enough to submerge the teeth completely.
2. It retains a quantity of oil within the coupling even if the lube system fails.

Removing the oil dam defeats both these features. To maintain the same performance for a damless coupling, the oil flow to the coupling should be reevaluated. Nothing can be done, however, to retain oil in the damless coupling, and some users will not accept them for this reason. A proper decision can be made only by weighing a possible coupling failure because of sludge accumulation against an accidental failure of the lube system.

Gear Coupling Failure Modes

The main causes of failure in gear couplings are wear or surface fatigue caused by lack of lubricant, incorrect lubrication, or excessive surface stresses. Component fracture caused by overload or fatigue is generally of secondary importance.

High speeds require relatively lightweight gear elements. All case-hardening procedures produce distortion—to keep this distortion to a minimum, nitriding is the preferred hardening method. This method is employed after all machinery operations are complete and no further corrections are to be made to the tooth geometry.

Nitriding permits increased tooth loading. The amount of increased capacity is not exactly known, but a 20% increase in load at 10,000–12,000 rpm has proven reliable. A further advantage of the nitrided coupling is that the coefficient of friction is lower than that for through-hardened parts. The heat from friction in the coupling decreases. More important, the transmission of axial forces is decreased by the reduced friction.

In many cases, gear shaving prior to nitriding has been used to correct or minimize small errors of tooth geometry caused by the shaping or hobbing processes.

Table 18-2
Types of Typical Gear Coupling Failures

| Standard or Sealed Lube | Continuous Lube |
|-------------------------|------------------------|
| Wear | Wear |
| Fretting corrosion | Corrosive wear |
| Worm tracking | Coupling contamination |
| Cold flow | Scoring and welding |
| Lube separation | Worm tracking |

A method of assuring nearly perfect tooth contact is to match-lap the gear teeth after nitriding. Lapping eliminates the break-in period, which otherwise takes from 70 to 120 hours. It is during the break-in period, that tooth surface distress usually occurs.

For maximum reliability, it is recommended that nitrided gear teeth be specified. Experience indicates that the extra cost of match lapping is justified.

The major failure in gear couplings is the fretting on the gear teeth. Fretting can be caused by improper lubrication. Lubrication problems can be categorized by the type of lubrication system being used. The two types of lubrication systems are the batch type and the continuous lubrication type. Table 18-2 shows some of the common problems that affect gear couplings, depending on the lube system used. Misalignment is another problem with gear couplings. Excessive misalignment can lead to any of several problems, such as tooth breakage, scoring, cold flow, wear, and pitting. Fasteners are another problem source in couplings.

Coupling fasteners should be properly heat-treated to withstand the large forces they experience in high-speed coupling applications. Fasteners should be properly torqued and, after four-to-six disassemblies, the entire fastener set should be replaced. Bolt shearing or bolt-hole elongation results from the nut bottoming out on the threads before the coupling flanges are tight, thus transmitting force through the bolt rather than through the flange faces. Bolts and nuts should be weight-balanced to very close tolerances. Table 18-3 is a diagnostic analysis of gear coupling failures.

Metal Diaphragm Couplings

The metal diaphragm coupling is relatively new in turbomachinery applications. Although the first recorded use of such a coupling dates back to 1922 on a condensing steam turbine locomotive, the contoured diaphragm did not come into wide use until the late 1950s.

Table 18-3
Diagnostic Analysis of Gear Couplings

| Damage or Stress Signs | Cause |
|--|---|
| Gear tooth surface deterioration (high rate of wear, scoring, and worm tracking) | Low oil viscosity and/or excessive misalignment |
| Gear tooth surface deterioration and overheating | Misalignment, high sliding velocity |
| Tooth breakage and wear | High misalignment angle |
| Broken hub, keys sheared | Too much shrink fit on shaft |
| Lockup-worn and broken teeth | Contaminated lubrication system, excessive misalignment |
| Worm tracking | Misalignment, separation of lubricant, low oil viscosity |
| Broken end or seal ring | Too much shaft-to-shaft spacing and misalignment |
| Galled bores | Improper removing techniques, insufficient or incorrect heating, excessive interference fit |
| Discolored bore | Improper hydraulic fit, contamination between shaft and hub |
| Fracture of components | Overload or fatigue, shock loading |
| Cold flow, wear, and fretting | High vibration |
| Bolt shearing, bolt hole elongation | Nut bottoming out on threads |
| Separation of lubricant ingredients | Centrifugal force |
| Retention of moisture impurities | Centrifugal force |
| Lubricant deterioration | High ambient temperature |

Diaphragm couplings accommodate system misalignment through flexing. Fatigue resistance is the main performance criterion. The life expectancy of a diaphragm coupling that operates within its design limits is theoretically infinite. Figure 18-6 is a photograph of a typical metal diaphragm coupling.

Figure 18-7 shows a section through a diaphragm coupling. The coupling has only five parts: two rigid hubs, one spool piece, and two alignment rings. These five parts are solidly bolted together, and misalignment is accommodated through flexing of the two diaphragms of the spool. The spool piece is made up of three separate parts: two diaphragms and a spacer tube. These parts are welded together by an electron beam.

The heart of these couplings is the flexing disc; it is manufactured from vacuum-degassed alloy steel, forged with a radial-grain orientation, and has a contoured profile machined on high-precision equipment.

The contoured profile is shown in Figure 18-8. The diaphragm undergoes axial deflection. The forces acting on the disc that are generating the stresses

FPO

Figure 18-6. Metal diaphragm coupling (one end shown). (Courtesy of Koppers Company, Inc.)

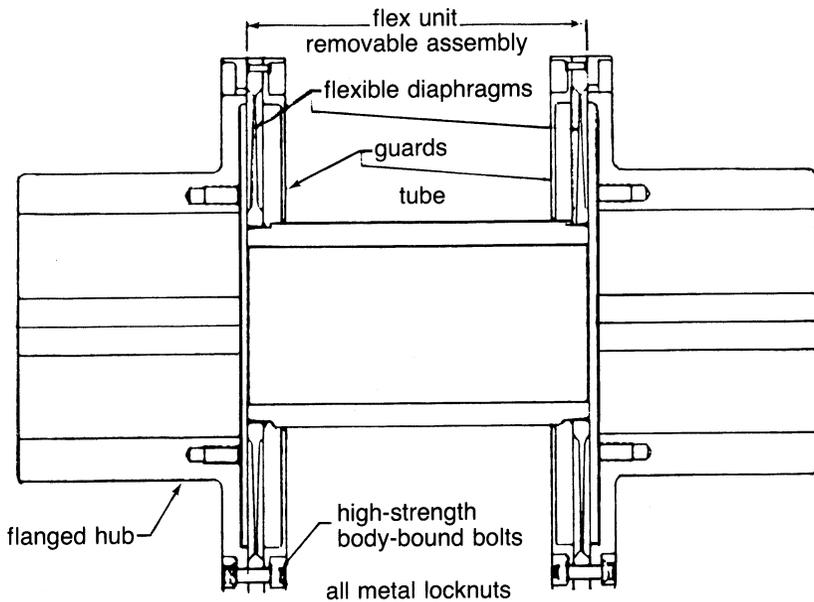


Figure 18-7. Schematic of a typical diaphragm coupling. (Courtesy of Koppers Company, Inc.)

are caused by the torque effects, centrifugal forces, and axial deflection. Standard methods for calculating centrifugal forces in a rotating disc show that both tangential and radial stresses increase rapidly with a decrease in the radius.

The stresses imposed by axial deflection are much greater at the hub than at the rim as seen in Figure 18-9. Therefore, to maintain uniform stresses in the diaphragm when all the various forces acting on the diaphragm are at their maximum, the diaphragm must be used to connect the contoured profile at both the hub and the rim to reduce stresses.

Diaphragm couplings are more susceptible to axial movement problems than gear couplings, since the diaphragm has a maximum deflection that cannot be exceeded.

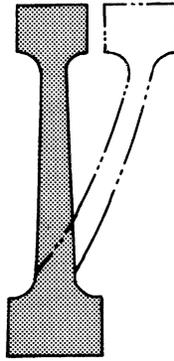


Figure 18-8. Axial deflection in a disc.

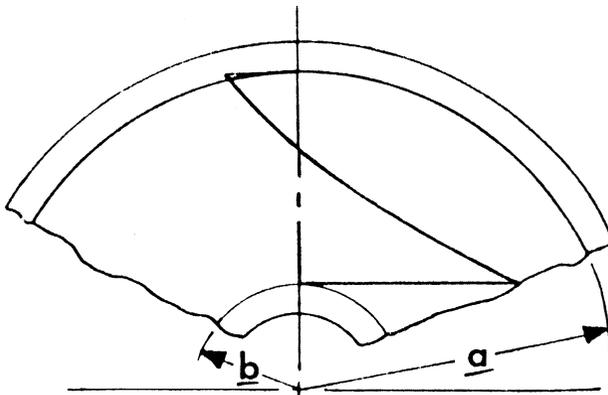


Figure 18-9. Stress distribution under axial deflection.

Theoretically, a diaphragm coupling will have no problems or failures as long as it is operated within “design limits.” The diaphragm fails from excessive torque. Two distinct modes of failure can be found—one at zero axial displacement and the other at large axial displacement. Zero axial displacement is characterized by a circular crackline that goes through the thinnest portion of the diaphragm. The crack is relatively smooth, and there is no buckling of the disc. The large axial movement and angular misalignment, which lead to disc failure, is characterized by a crackline that follows a random path from the thinnest to the thickest portion of the disc. The crackline is very irregular, and there is severe buckling of the unfailed part of the disc. Failure in this mode shows that the crackline propagates some 270° before disc buckling takes place, indicating that the torque load makes only a small contribution to the total stresses in the disc. Metal diaphragm couplings can also have problems due to corrosive action on the diaphragms. Thus, care must be taken to apply coating to protect against damage from a harsh environment.

Metal Disc Couplings

The main difference between the metal diaphragm coupling and the typical metal-flexing disc coupling is that a number of discs replace the single diaphragm between the hubs and the spacer. Figure 18-10 shows a schematic of this type of coupling. A typical metal-flexing disc coupling consists of two hubs rigidly attached by interference fit or flange bolting to the driving and driven shaft of the connected equipment. Laminated disc sets are attached to each hub to compensate for the misalignment. A spacer spans the gap between the shafts and is attached to the flexing elements at each end.

The functional requirements and characteristics of the flexing elements are to transmit rated torque as well as any system overloads without buckling or

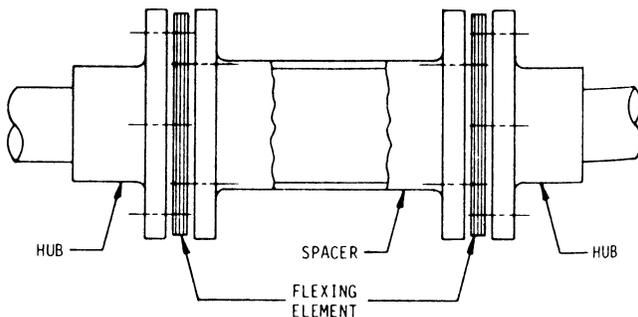


Figure 18-10. Typical metal-flexing disc coupling.

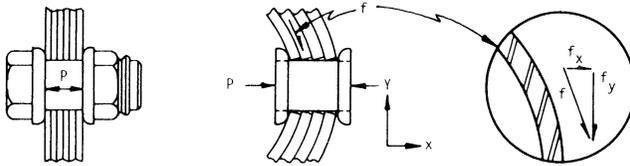


Figure 18-11. Frictional damping in a metal-disc coupling.

permanent deformation. In other words, they must possess torsional rigidity. However, under conditions of parallel, angular, and axial misalignment, the flexing element must have sufficient flexibility to accommodate these conditions without imposing excessive forces and moments on equipment shafts and bearings. Both of the previous requirements must be met while maintaining stress levels that are safely within the fatigue limit of the flexing material. Metal-flexing couplings have been known to exhibit occasional large-amplitude vibrations in the axial direction when excited at the natural frequency of the coupling.

The amount of damping present in a metal-flexing coupling is thought to be relatively small, although it is known to be greater for the laminated disc-type construction than for a coupling consisting of a single-piece membrane. The reason for the greater damping in the laminate disc configuration is that under conditions of axial movement, a microscopic amount of motion takes place between adjacent lamina, as shown in Figure 18-11. Since the element is clamped together under a bolt preload, there is a frictional force, which resists sliding.

Field experience by manufacturers and users of turbomachinery has shown that resonant axial vibration of a metal-flexing coupling can at times cause problems that are reflected through the entire drive train. With laminated disc couplings, the problem occurs only when an external forcing function exists. This condition could be a result of aerodynamic or hydraulic fluctuations in the machine train, out-of-square thrust collars, gearing inaccuracies, or electrical excitations of motor-driven equipment. It is usually possible to avoid operating the couplings at or near resonance if the condition is anticipated during the system design stage. However, such problems do not always occur until after a machine is in service. More information is needed on the nature and magnitude of external excitations.

Turbomachinery Uprates

If an existing coupling is to be replaced with a new type of coupling because of a machinery uprate, or for any other reason, there is good

justification to review, with the latest techniques, the nature of the rotating system to be coupled. Couplings, whether gear or disc-type, should not be simply picked from a catalog. Some installations are very old, and some have been revised in other ways in the field. Unfortunately, such engineering reviews are not easy to arrange with busy equipment suppliers.

Therefore, the tendency is to match the obvious characteristics of the existing coupling and see what happens. Many older designs have relatively heavy and larger-diameter shafts, and retrofits have been very successful and trouble-free. Part of this success is due to the consideration given to the retrofit by cooperating engineers of the coupling manufacturer and the rotating equipment manufacturer. A large part of the success is due to the dedication and extra effort of the first companies offering the disc coupling to ensure success.

If retrofits and new installations consume the available time of these engineers, the potential for omission increases. Therefore, more time should be allowed for the work.

Coupling application is an engineering effort involving the coupling and rotating equipment designers. The user, by the purchasing technique he employs, can aid or hinder this effort, since he chooses the basic coupling style his operations and maintenance people will work with.

In either case a good purchase specification should designate that the selection and design of the coupling must follow the rotor design work and exclude the coupling from becoming involved in competitive bids. It is simply too important an item to risk reliability for initial cost savings.

Disc couplings are used as replacements for gear couplings for two reasons: (1) the disc couplings do not require lubrication, and (2) the machinery ratings can be uprated with disc couplings.

Compressor and driver shafts often prove to be overstressed in equipment uprate situations; however, a change from conventional gear-type couplings to the more recent diaphragm coupling design can lower the shaft stress enough to avoid shaft replacement during power uprates of compressors or compressor drivers.

A close examination of how the equipment vendor arrived at his maximum allowable stress levels may frequently show that such shaft replacements can be avoided without undue risk if the coupling selection is optimized. This situation is based on the fact that gear-type couplings have the potential of inducing both torsional stresses and bending stresses in a shaft, whereas diaphragm couplings tend to induce primarily torsional stresses and insignificant bending stresses at best.

To determine if a machine's performance can be uprated without installing a large shaft, the forces acting on the shaft must be computed. The

forces acting on a shaft can be put into three separate categories: (1) torsional, (2) axial, and (3) bending forces. Torsional forces are a function of the shaft rotational speed and horsepower transmitted. They can be calculated from

$$T = \frac{63,000 \text{ (hp)}}{\text{rpm}} \quad (18-1)$$

and the torsional stress τ_T can be computed with

$$\tau_T = \frac{16T}{\pi d^3} \quad (18-2)$$

It is a generally accepted assumption that the axial stress will not exceed 20% of the torsional stress. τ_a can therefore be obtained by $\tau_a = 0.20 \tau_T$. These two stresses will be the same for either type of coupling; however, the bending stress will vary depending on which type of coupling is used.

There are three relevant bending moments caused by a gear coupling when transmitting torque with angular or parallel misalignment:

1. *Moment caused by contact-point shift.* This moment acts in the angular misalignment plane and tends to straighten the coupling. It can be expressed

$$M_c = \frac{T}{D_p/2} \times \frac{X}{2} \quad (18-3)$$

where:

T = shaft torque

D_p = gear coupling pitch diameter

X = tooth face length (Figure 18-12)

2. *Moment caused by coupling friction.* This moment acts in a plane at a right angle relative to the angular misalignment. It has the magnitude

$$M_f = T_\mu \quad (18-4)$$

where μ is the friction coefficient.

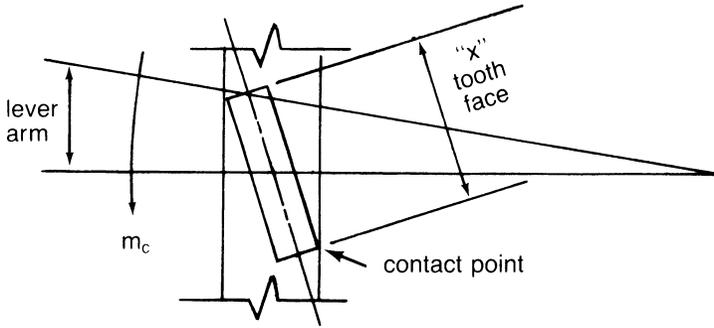


Figure 18-12. Shift in contact point.

3. *Moment caused by turning torque through a misalignment angle α .* It acts in the same direction as the friction moment M_f and can be expressed

$$M_T = T \sin \alpha \quad (18-5)$$

The total moment is the vector sum of the individual moments

$$M_{\text{total}} = \sqrt{M_c^2 + (M_f + M_T)^2} \quad (18-6)$$

The contoured diaphragm coupling causes two bending moments:

1. *Moment caused by angular misalignment.* This results in bending of the diaphragm

$$M_B = k_B \alpha \quad (18-7)$$

In this expression k_B equals the angular spring rate of the diaphragm (lb-in/degree) and α is the misalignment angle. This moment acts in the angular misalignment plane, as did M_c in the gear-coupling analysis.

2. *Moment caused by turning torque through a misalignment angle α .* It can be expressed

$$M_T = T \sin \alpha \quad (18-8)$$

The total moment is now

$$M_{\text{total}} = \sqrt{M_B^2 + M_T^2} \quad (18-9)$$

Comparing the bending moments caused by gear couplings with those resulting from contoured diaphragm couplings shows the former to be significant and the latter virtually negligible.

The cyclic bending stress imposed on a gear coupling-equipped shaft can be computed from

$$\sigma_a = \frac{M_{\text{total}} \times C}{I} \quad (18-10)$$

where:

C = shaft radius

I = shaft area moment of inertia

In addition, there is a mean tensile stress acting on the shaft cross-sectional area. This effect means stress equates to

$$\sigma_m = \frac{T\mu}{(D_p/2)(\pi C^2) \cos \Theta} \quad (18-11)$$

where Θ is the pressure angle assumed for the gear teeth.

The cycle bending stress seen by the diaphragm coupling-equipped shaft can be obtained by a rapid ratio calculation

$$\frac{\sigma_a \text{ (diaphragm coupling)}}{\sigma_a \text{ (gear coupling)}} = \frac{M_{\text{total}} \text{ (diaphragm coupling)}}{M_{\text{total}} \text{ (gear coupling)}} \quad (18-12)$$

The mean tensile stress acting on the cross-sectional area of the diaphragm coupling-equipped shaft depends on how far the diaphragm is displaced axially from its neutral rest position and the axial spring rate of the diaphragm.

For combined bending and torsion, the factor of safety can be calculated by the following relationships:

$$n = \frac{1}{\sqrt{\left(k_f \frac{\sigma_a}{\sigma_e} + \frac{\sigma_m}{\sigma_{y.p.}}\right)^2 + 3 \left(k_f' \frac{\tau_a}{\sigma_e} + \frac{\tau_m}{\sigma_{y.p.}}\right)^2}} \quad (18-13)$$

where:

σ_e = endurance limit in tension

σ_{yp} = minimum yield strength in tension

The stress concentration factor k_f results from the keyway and must be used in torsional stress calculations. Factor k'_f takes into account the shaft step; it must be used in the bending stress calculation.

Shaft Alignment

The successful alignment of a gas turbine to the unit it is driving is of great importance. A major portion of operating problems experienced in the field can often be attributed to faulty misalignment. Operating problems caused by misalignment include excessive vibration, coupling overheating, wear, and bearing failures.

Typically, misalignment problems will show up at two times rpm frequencies with axial vibrations at one and two times rpm. With diaphragm-type flexible couplings, vibrations may be somewhat suppressed, and consequently, trains using these couplings should be monitored periodically to ensure they are in alignment.

Perfect alignment—exact shaft colinearity under operating conditions—is difficult and uneconomical to attain. The degree of tolerable misalignment is a function of coupling length, size, and speed. Some companies are now specifying a minimum coupling spacer length of 18 inches, since longer coupling lengths can tolerate more misalignment.

The amount of misalignment that can be tolerated by the machine also depends on the types of journal and thrust bearings used. Tilting-pad-type bearings greatly reduce the misalignment problem. Figure 18-13 shows misalignment in both the journal and thrust bearings. The effect of misalignment on a journal bearing causes the shaft to contact the end of the bearing. Thus, journal length is a criterion in the amount of misalignment a bearing can tolerate; a shorter length obviously can tolerate more misalignment. The effect on the thrust bearing is to load up one segment of the thrust bearing arc and unload the opposite segment. This effect is more pronounced with higher loads and less flexible bearings.

The Shaft Alignment Procedure

In essence, there are three steps in any alignment procedure. These are: (1) the prealignment survey, (2) cold alignment, and (3) the hot alignment check.

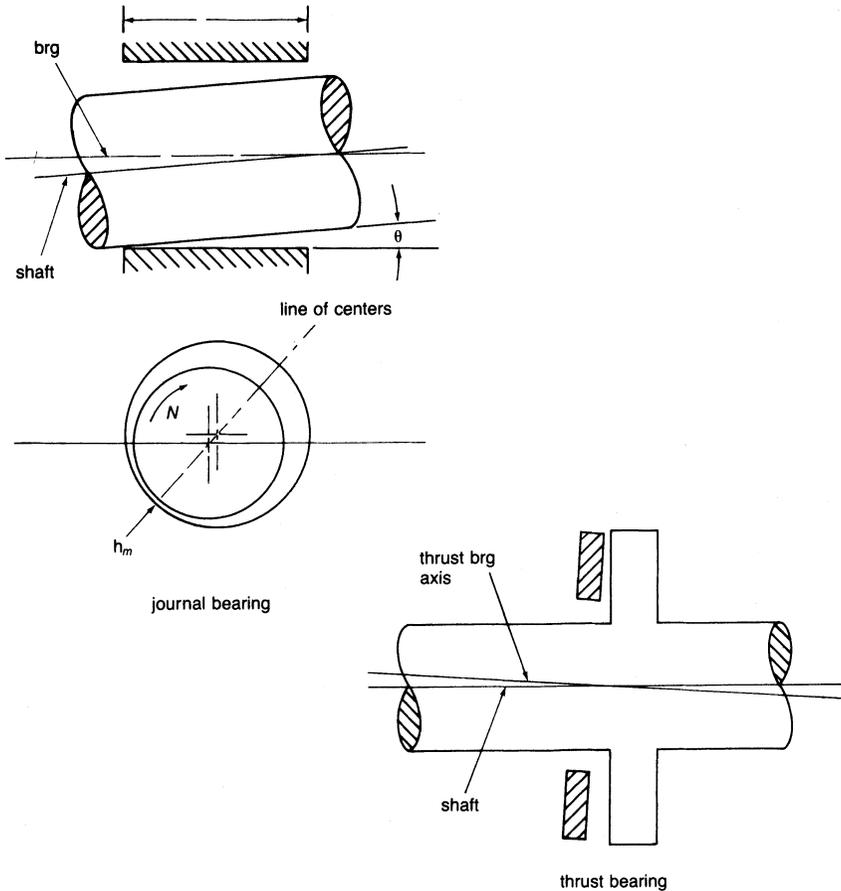


Figure 18-13. Misalignment in both journal and thrust bearings.

The prealignment survey. This survey is carried out well ahead of the cold alignment. In this survey piping, grouting, foundation bolts, shimpacks, etc., are studied and ascertained to be appropriately done and of good quality. Again, casing distortion, piping strain, misalignment of machine supports relative to the sole plate, etc. are determined, and corrections are made to ensure that these problems will not cause problems with the alignment.

Piping strain is by far the greatest problem causer, and so piping should be carefully reviewed to ensure that it is properly done according to code. Piping strains as high as 0.22 inches (0.5588 cm) have been observed.

A typical cause of piping strain occurs when two flanges do not meet and pipefitters force them together. Pipe hangers that are poorly placed or tensioned can also cause significant piping stress problems.

Cold alignment. There are two predominant techniques used for cold alignment. These are: (1) the face-OD method, and (2) the reverse-dial indicator method. Both these techniques utilize dial indicators. For high-speed turbomachinery, the reverse-dial indicator method is the superior method and should be used.

Figure 18-14 shows a face-OD indicator setup. As the name indicates, an alignment bracket is attached to one coupling hub, and face-OD readings are taken on the adjacent hub. The face and OD dial indicator readings give an indication of the angularity and offset of the shafts, respectively. The problems with this method are numerous. First, there is the problem of shaft axial float, which makes consistent readings difficult to obtain. Second, inaccuracies in the geometry of the coupling hub have to be taken into account. Third, the face diameter on which the readings are taken is relatively small, and errors are magnified over the length of the machine. The reverse-dial indicator method is shown in Figure 18-15. This method measures just the OD of the coupling hubs or shaft and eliminates the problem of shaft axial float. By spanning the entire coupling, angular misalignment is greatly magnified. For both the face-OD and reverse-dial indicator methods, it is important that sag in the alignment bracket be determined. Figure 18-16 shows a method for the determination of sag. Once the sag is determined, it

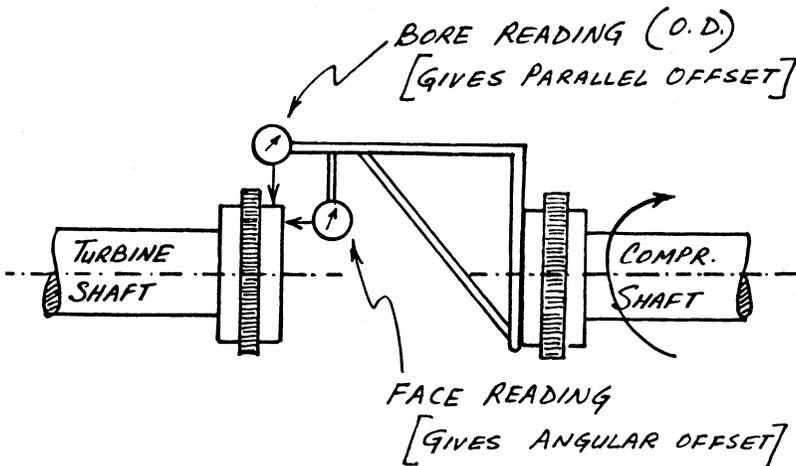


Figure 18-14. Face-OD indicator setup.

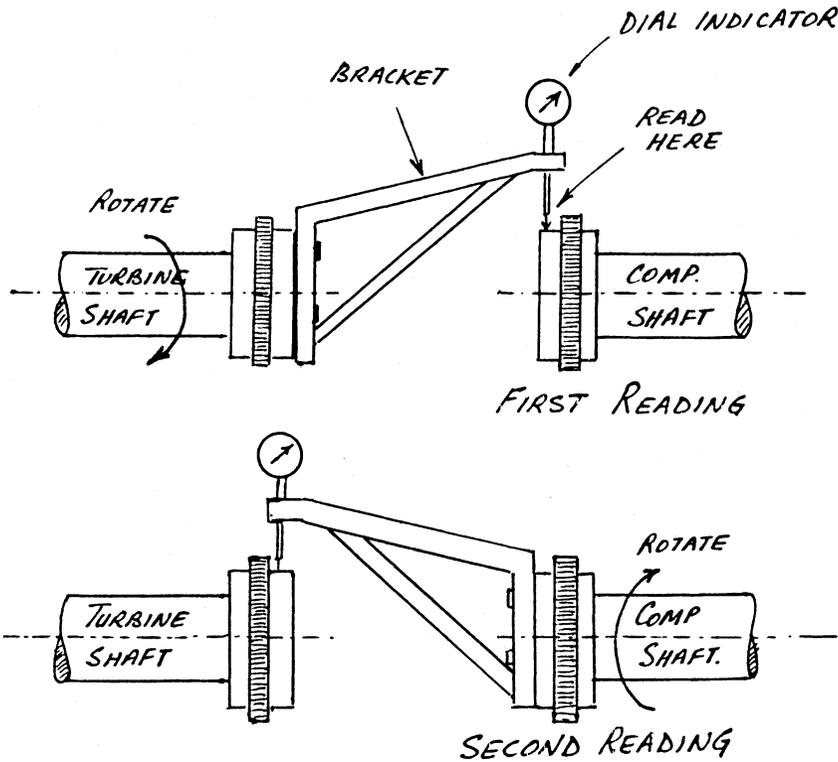


Figure 18-15. Reverse-dial indicator setup.

must be permanently stamped on the bar. The alignment bracket should be considered an important precision tool and must be stored and handled with care so that it may be reused when realignment is required.

Once the dial indicator readings are taken, a graphic plot of the two-shaft centerlines can be made on graph paper. It is at this stage that anticipated thermal growths are used in determining the shimming required to obtain shaft colinearity when the units are in the hot condition. Unfortunately, the values supplied by the manufacturers may not be accurate, and pipe strain and other external forces come into play. It is for this reason that the hot alignment check is conducted.

A simple graphic plotting exercise for the reverse-dial indicator method indicates the basic principles involved. A steam turbine compressor train is shown in Figure 18-17. Assume this train is a new installation and the manufacturer's estimated thermal growths are as indicated in Figure 18-17.

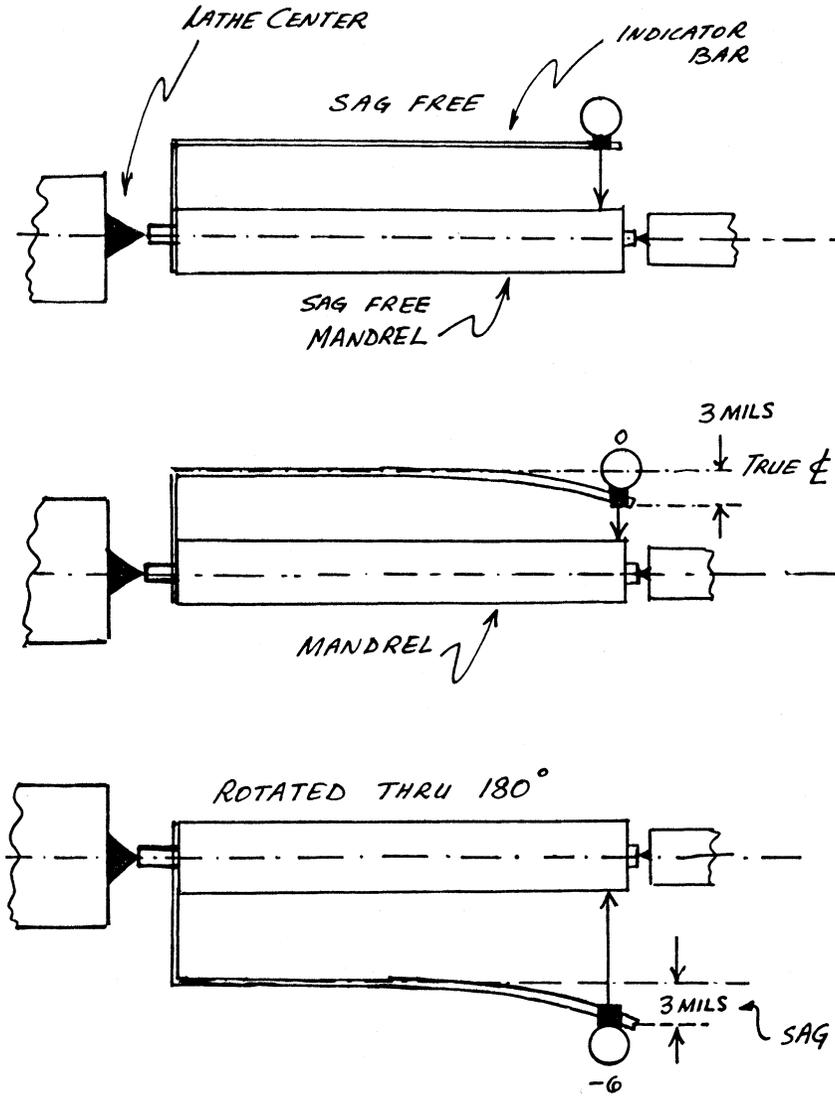


Figure 18-16. Method for determining sag.

Reverse-dial indicator readings are taken to determine the relative shaft positions. Once readings are taken, the estimated thermal growths are incorporated by shimming in the hope that a good, hot alignment can be achieved.

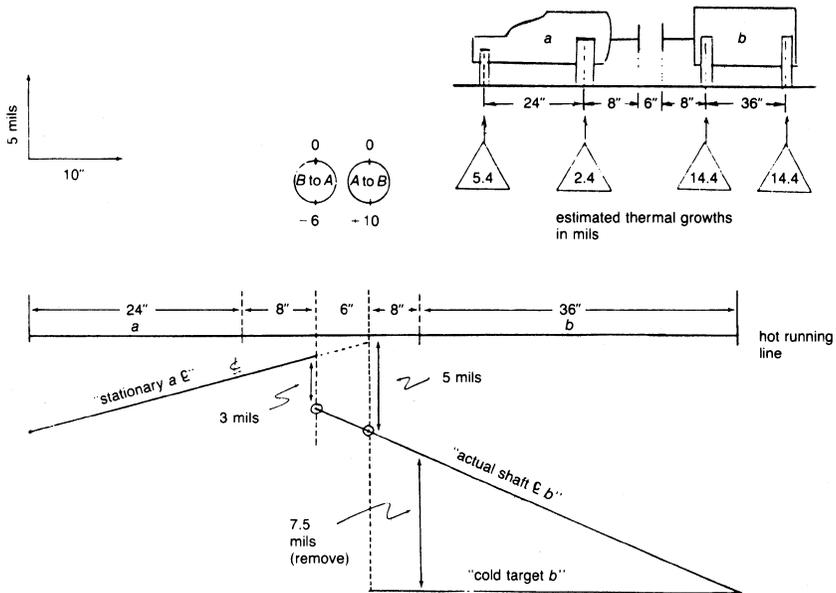


Figure 18-17. Graphic plotting for reverse-dial indicator method.

The hot alignment check is used to determine the actual thermal growth, and then the final shim changes are made if needed. This example addresses only vertical movements. Horizontal movements are obtained in a similar fashion. The graphic plot uses an amplified scale on the vertical Y axis of one inch equals five mils vertical growth, while the X axis has a scale of one inch equals 10 inches (25 cm) of train length.

In this example, it is assumed that Machine A is to be fixed, and all moves are to be conducted on Machine B. As shown in Figure 18-17, a “hot running line” is first drawn. This line is where the shafts should be when the machines are operating.

Now, using estimated thermal growth of Machines A and B, a “cold target B” line is drawn. This line is where shaft B should lie so that when hot it will be colinear with shaft A on the hot running line.

The next step is to use the dial indicator readings to determine where the shafts actually lie relative to each other. The B-to-A readings show that shaft B lies below shaft A by three mils (half-dial indicator readings) and the A-to-B reading shows that shaft A is above shaft B by five mils. Once these two points are located, shaft B can be plotted. This line is the “actual shaft B” line. Once this procedure is done, the shim changes needed can be easily found and “desired” indicator readings can be given to the millwrights.

A similar procedure is followed for horizontal movements. If the hot alignment check indicates a significant deviation from expected thermal growths and an unacceptable amount of misalignment, further shim changes can be achieved by similar plotting.

Hot alignment check. This technique attempts to determine actual alignment status when the machines are hot. When the machines are running, it is impossible to use dial indicator techniques on the shafts.

The old concept of a “hot check”—in which the units were shutdown and the coupling disassembled as quickly as possible to allow indicator readings to be taken—should not be used. Currently used, continuously lubricated couplings require significant time to disassemble during which considerable cooling occurs. Because of this factor, a number of hot alignment techniques have been developed. Optical and laser methods, proximity probe methods, and a purely mechanical means using dial indicators may be used for hot alignment checks. In all these methods, an attempt is made to use the cold position of the shaft as a benchmark and then to measure the shaft movement (or bearing housings) from the cold position to the hot position. The objective is to find the change in vertical and horizontal positions at each shaft end. Once this procedure is done along the train, the machines can be shutdown and appropriate shim changes made to attain acceptable hot alignment.

Basically, the optical method uses equipment such as alignment telescopes, jig transits, and sight levels. Instruments with built-in optical micrometers for measuring displacements from a referenced line of sight enable an accurate determination of target movements, which are mounted on the machine.

Optical alignment reference points are located on the bearing housings of the units. A jig transit is then setup at some distance from the train, and readings are taken and recorded in the vertical plane for each reference point in the train. Then the transit is moved, and a similar set of readings is taken in the horizontal plane. This procedure should be done at the same time as the reverse dial indicator readings are taken. Then, when the train is in its operating condition, another set of readings are taken. The two data sets and the cold alignment dial indicator readings enable the determination of vertical and horizontal growths of each point.

The advantages of this system are that it is accurate and, once the reference marks are on the machine, there is no need to approach the machine. However, the equipment involved is expensive and delicate, and great care has to be taken during its use. Moreover, heat waves often cause some problems in taking readings. Alignment with laser techniques has also been used, but the equipment is expensive and can be applied only in certain situations such as for a bearing alignment check. It is used primarily by

manufacturers of turbomachinery during fabrication and assembly of their units.

Proximity probes have also been used to measure machine movements. Proximity probes are mounted in special water-cooled columns and aimed at “targets” mounted on bearing housings or on other parts of the unit. Changes in the gap distances are then displayed on electrical meters. The Dodd bar system utilizes proximity probes mounted on an air-cooled bar attached between the bearings of the two machines to be aligned. The Dodd bar system allows continuous monitoring of the relative positions of the two shafts. Another system uses proximity probes located within the coupling to continuously monitor the alignment. Digital readouts of misalignment angles, etc., are available from this system.

A purely mechanical, hot alignment system utilizing dial indicators has also been developed. The system uses permanently mounted tooling balls made of stainless steel attached to the bearing housing and to the machine foundation. A spring-loaded device with a dial indicator is provided to determine accurately the distance between the two tooling balls. An inclinometer is also provided to give a measure of the angularity. Figure 18-18 shows a typical configuration. Cold readings are taken at the time when the reverse-dial indicator readings are taken, and hot readings are taken when the machine is on-line. These two sets of readings are enough to determine the vertical and horizontal movement of the shaft. The same procedure is followed at each end of the units in the train. Computations can be made either graphically or by a calculator with preprogrammed cards. Direct outputs are the degree of misalignment and the shim changes needed to correct the misalignment.

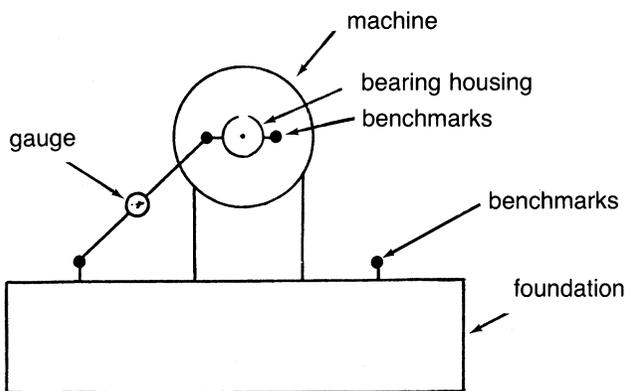


Figure 18-18. Hot alignment system with dial indicator.

It must be realized that correct alignment is of great importance in attaining high unit availability. Alignment procedures must be carefully planned, tools must be checked carefully, and, in general, great care must be taken during the alignment. The time, effort, and money spent on good alignment is well worth it.

Bibliography

- Bendix Fluid Power Corp, "Contoured Diaphragm Couplings," *Technical Bulletin*.
- Bloch, H.P., "Less Costly Turboequipment Uprates Through Optimized Coupling Section," Proceedings of the 4th Turbomachinery Symposium, Texas A&M University, pp. 149–152, 1975.
- Calistrat, M.M., and Leaseburge, G.G., "Torsional Stiffness of Interference Fit Connections," American Society of Mechanical Engineers, Pub. 72-PTG-37.
- Calistrat, M.M., and Webb, S.G., "Sludge Accumulation in Continuously Lubricated Couplings," American Society of Mechanical Engineers, 1972.
- Calistrat, M.M., "Gear Coupling Lubrication," American Society of Lubrication Engineers, 1974.
- Calistrat, M.M., "Grease Separation Under Centrifugal Forces," American Society of Mechanical Engineers, Pub. 75-PTG-3.
- Calistrat, M.M., "Metal Diaphragm Coupling Performance," Proceedings of the 5th Turbomachinery Symposium, Texas A&M University, pp. 117–123, October 1976.
- Campbell, A.J., "Optical Alignment of Turbomachinery," Proceedings of the 2nd Turbomachinery Symposium, Texas A&M Univ., pp. 8–12, 1973.
- Dodd, R.N., "Total Alignment Can Reduce Maintenance and Increase Reliability," Proceedings of the 9th Turbomachinery Symposium, Texas A&M University, pp. 123–126, 1980.
- Essinger, J.N., "Benchmark Gauges for Hot Alignment of Turbomachinery," Proceedings of the 9th Turbomachinery Symposium, Texas A&M University, pp. 127–133, 1980.
- Finn, A.E., "Instrumented Couplings: The What, the Why, and the How of the Indikon Hot Alignment Measuring System," Proceedings of the 9th Turbomachinery Symposium, Texas A&M University, pp. 135–136, 1980.
- Jackson, C.J., "Cold and Hot Alignment Techniques of Turbomachinery," Proceedings of the 2nd Turbomachinery Symposium, Texas A&M University, pp. 1–7, 1973.
- Jackson, C.J., "Alignment Using Water Stands and Eddy-Current Proximity Probes," Proceedings of the 9th Turbomachinery Symposium, Texas A&M University, pp. 137–146, 1980.

- Kramer, K., "New Coupling Applications or Applications of New Coupling Designs," Proceedings of the 2nd Turbomachinery Symposium, Texas A&M University, pp. 103–115, October 1973.
- Massey, C.R., and Campbell, A.J., "Reverse Alignment—Understanding Centerline Measurement," Proceedings of the 21st Turbomachinery Symposium, Texas A&M University, 1992, p. 189.
- Peterson, R.E., *Stress Concentration Factors*, John Wiley & Son, 1953.
- Timoshenko, S., *Strength of Materials: Advanced Theory & Problems*, 3rd ed. Van Nostrand Reinhold Pub., 1956.
- Webb, S.G., and Calistrat, M.M., "Flexible Couplings," 2nd Symposium on Compressor Train Reliability, Manufacturing Chemists Association, April 1972.
- Wilson, C.E., Jr., "Mechanisms—Design Oriented Kinematics," American Technical Society, 1969.
- Wright, J., "Which Flexible Coupling?" *Power Transmission & Bearing Handbook*, Industrial Publishing Co., 1971.
- Wright, J., "A Practical Solution to Transient Torsional Vibration in Synchronous Motor Drive Systems," American Society of Mechanical Engineers, Pub. 75-DE-15.
- Wright, J., "Which Shaft Coupling is Best—Lubricated or Non-Lubricated?" *Hydrocarbon Processing*, pp. 191–196, April 1975.

19

Control Systems and Instrumentation

Gas turbines operate over a large range of power and in many applications primarily as the driver for generators in a power complex or the driver for large compressors and pumps in petrochemical complexes, and off-shore platforms. The power and the process requirements control the operations of the plant. In the case of power plants they are usually part of a major grid and they supply the needs to meet the demand of the grid, both in power and frequency. Control systems are also closely tied up with the Distributed Control Systems (D-CS) and Condition Monitoring Systems (C-MS) with plant optimization software.

The traditional concept of maintenance in the petrochemical and the utilities industry has been undergoing a major change to ensure that equipment not only has the best availability but also is operating at its maximum efficiency. There is a consistent trend in these industries throughout the world to improve maintenance strategy from fix-as-fail to total performance based planned maintenance. In practice, this calls for on-line monitoring and condition management of all major equipment in the plant. To reach the Utopian goal of just-in-time maintenance with minor disruption in the operation of the plant requires a very close understanding of the thermodynamic and mechanical aspects of plant equipment to be able to implement predictive maintenance programs.

The benefits of total performance-based planned maintenance not only ensure the best and lowest cost maintenance program but also that the plant is operated at its most efficient point. An important supplementary effect is that the plant will be operating consistently within its environmental constraints.

Gas turbine instrumentation has expanded in the past few years from simple control systems to more complex diagnostic and monitoring systems that are designed to avert major catastrophes and operate a unit at its peak performance.

Control Systems

All gas turbines are provided with a control system by the manufacturer. The control system has three fundamental functions: startup and shutdown sequencing, steady-state control when the unit is in operation, and protection of the gas turbine.

Control systems can be an open loop or closed loop system. The open-loop system positions the manipulated variable either manually or on a programmed basis, without using any process measurements. A closed loop control system is one, which receives one or more measured process variables and then uses it to move the manipulated variable to control a device. Most combined cycle power plants have a closed loop control system.

Closed loop systems include either a feedback or feedforward, control loop or both to control the plant. In a feedback control loop, the controlled variable is compared to a set point. The difference between the controlled variable to the set point is the deviation for the controller to act on to minimize the deviation. A feedforward control system uses the measured load or set point to position the manipulated variable in such a manner to minimize any resulting deviation.

In many cases the feedforward control is usually combined with a feedback system to eliminate any offset resulting from inaccurate measurements and calculations. The feedback controller can either bias or multiply the feedforward calculation.

A controller has tuning parameters related to proportional, integrated, derivative, lag, deadtime, and sampling functions. A negative control loop will oscillate if the controller gain is too high, but if it is too low it will be ineffective. The controller must be properly related to the process parameters to ensure close-loop stability while still providing effective control. This is accomplished first by the proper selection of control modes to satisfy the requirements of the process, and second by the appropriate tuning of those modes. Figure 19-1 shows a typical block diagram for forward and feedback control.

Computers have been used in the new systems to replace analog PID controllers, either by setting set points, or lower level set points in supervisory control, or by driving valves in direct digital control. Single-station digital controllers perform PID control in one or two loops, including

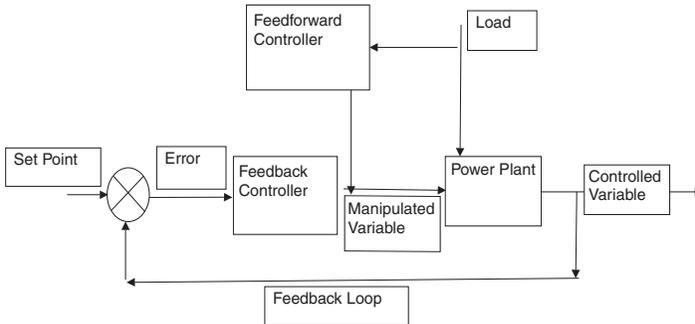


Figure 19-1. Forward and feed back control loop.

computing functions such as mathematical operations, with digital logic and alarms. D-CS provide all the functions, with the digital processor shared among many control loops. A high level computer may be introduced to provide condition monitoring, optimization, and maintenance scheduling.

The gas turbine control systems are fully automated, and ensure the safe and proper startup of the gas turbine. The gas turbine control system is complex and has a number of safety interlocks to ensure the safe startup of the turbine.

The startup speed and temperature acceleration curves as shown in Figure 19-2 are one such safety measure. If the temperature or speed are not reached in a certain time span from ignition, the turbine will be shutdown. In the early days when these acceleration and temperature curves were not used, the fuel, which was not ignited, was carried from the combustor and then deposited at the first or second turbine nozzle, where the fuel combusted which resulted in the burnout of the turbine nozzles. After an aborted start the turbine must be fully purged of any fuel before the next start is attempted. To achieve the purge of any fuel residual from the turbine, there must be about seven times the turbine volume of air that must be exhausted before combustion is once again attempted.

The gas turbine is a complex system. A typical control system with hierarchic levels of automation is shown in Figure 19-3. The control system at the plant level consists of a D-CS system, which in many new installations is connected to a condition monitoring system and an optimization system. The D-CS system is what is considered to be a plant level system and is connected to the three machine level systems. It can, in some cases, also be connected to functional level systems such as lubrication systems and fuel handling systems. In those cases, it would give a signal of readiness from those systems to the machine level systems. The condition monitoring system

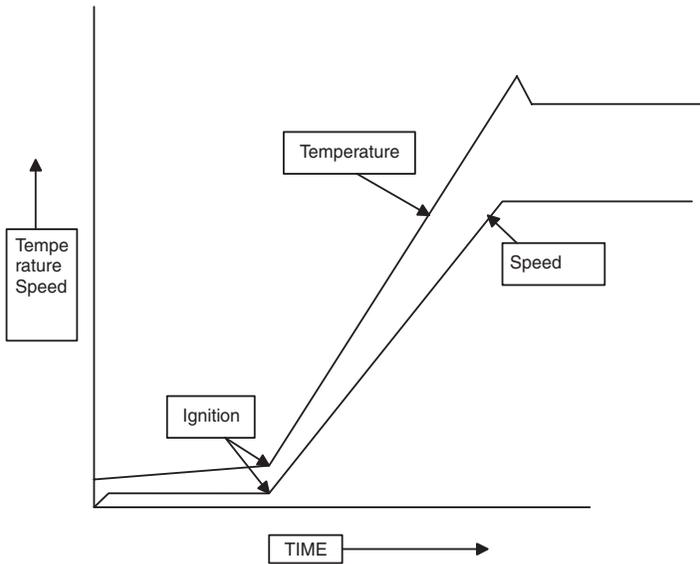


Figure 19-2. Startup characteristics of a gas turbine.

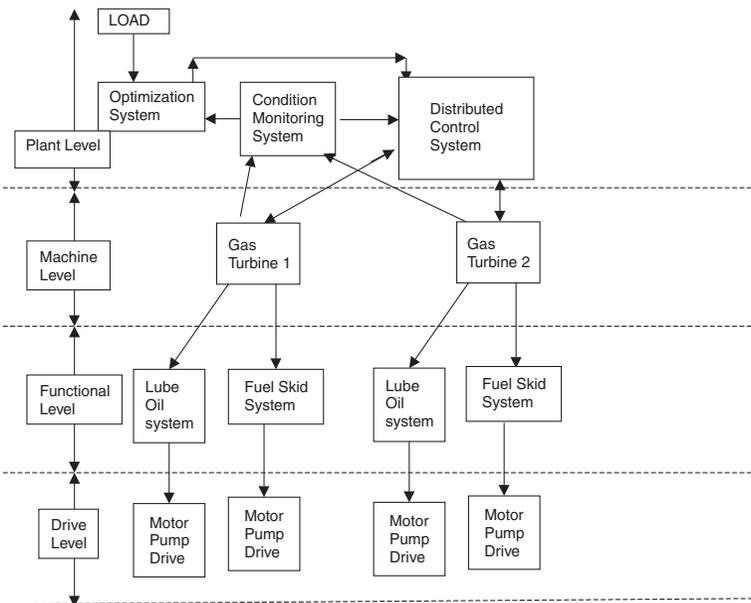


Figure 19-3. Hierarchic levels of automation.

receives all its inputs from the D-CS system, and from the steam and gas turbine controllers. The signals are checked initially for their accuracy and then a full machinery performance analysis is provided. The new performance curves produced by the condition monitoring system are then provided to the optimization system. The optimization system, usually used where multiple turbines are used, receives the load and then sends a signal to the D-CS system, which in turn sends the signal to the gas turbine for the best settings of the gas turbine to meet the load.

The gas turbine has a number of systems, it controls such as the:

1. *Lubrication skid.* The gas turbine lubrication skid is usually independent of the steam turbine skid as the lubrication oil is usually synthetic due to the high temperatures in the gas turbine. Another reason is due to water contamination of the lubrication oil from the steam turbine. It is advisable to have the lubrication system be totally independent. The gas turbine lubrication skid would report to the gas turbine controller. Since the lubrication system is also used for providing cooling, it is usually operated for about 20 minutes after the gas turbine is shutdown. The lubrication skid contains at least three pumps, two pumps in which each can provide the head required and a third pump, which is usually recommended to be a DC drive for emergency use. These pumps and their control fall under the drive level hierarchy.
2. *The fuel skid.* This could contain a gas compressor if the fuel gas pressure is low and a knockout drum for any liquid contamination that the gas may have. The requirement of fuel gas pressure is that it should be operated at a minimum of 50–70 psi (3.5–4.83 Bar) above the compressor discharge pressure. The compressor and its motor drive fall under the drive level hierarchy. In the case of liquid fuels, the skid may also contain a fuel treatment plant, which would have centrifuges, electrostatic precipitators, fuel additive pumps, and other equipment. These could be directly controlled by the D-CS system, which would then report its readiness to the gas turbine controller.

The control system requires inputs for speed determination, temperature control, flame detection, and vibration. The speed monitoring system receives an input from magnetic transducers in the form of an AC voltage with a frequency proportional to the rotational speed of the shaft. A frequency-to-voltage converter provides a voltage proportioned to speed, which is then compared to a set value. If the measured voltage is different from the reference voltage, a speed change is made. Typically, the desired speed can be manually set to a range between 80% and 105% of design speed.

The temperature control receives its signals from a series of thermocouples mounted in the exhaust. The thermocouples are normally iron-constantan or chromel-alumel fully enclosed in magnesium oxide sheaths to prevent erosion. The thermocouples are frequently mounted with one for each combustion can. The output of the thermocouples is generally averaged into two independent systems with half of the thermocouples in each group. The output of the two systems is compared and used for decisions requiring a temperature input. This redundancy protects the system against tripping if a thermocouple fails.

The protective system is independent of the control system and provides protection from over-speed, over-temperature, vibration, loss of flame, and loss of lubrication. The over-speed protection system generally has a transducer mounted on the accessory gear or shaft, and trips the gas turbine at approximately 10% of maximum design speed. The over-temperature system has thermocouples similar to the normal temperature controls with a similar redundant system. The flame detection system consists of at least two ultraviolet flame detectors to sense a flame in the combustion cans.

In gas turbines with multiple cans, the detectors are mounted in cans not equipped with spark plugs to assure flame propagation between cans during startup. Once the unit is running, more than one indicator must indicate a loss of flame to trip the machine, although the loss of flame in only one can is indicated on the annunciator panel.

Vibration protection can be based on either of the three measurement modes—acceleration, velocity, or displacement—but velocity is frequently used to provide constant trip levels throughout the operating speed range. Due to the problems encountered by velocimeters, many manufacturers, especially in aero-engines, have started using accelerometers. Two transducers are normally located on the gas turbine with additional transducers on the driven component. Vibration monitors are set to provide a warning at one vibration level with a trip at a higher level. Normally, the control system is designed to provide a warning in the event of an open-circuit, ground, or short circuit.

The gas turbine control loop controls the Inlet Guide Vanes (IGV) and the Gas Turbine Inlet Temperature (TIT). The TIT is defined as the temperature at the inlet of the first stage turbine nozzle. Presently, in 99% of the units, the inlet temperature is controlled by an algorithm, which relates the turbine exhaust temperature, or the turbine temperature after the gasifier turbine, the compressor pressure ratio, the compressor exit temperature, and the air mass flow to the turbine inlet temperature. New technologies are being developed to measure the TIT directly by the use of pyrometers and other specialized probes, which could last in these harsh environments. The TIT is controlled by the fuel flow and the IGV, which controls the total air mass

flow to the gas turbine. In a Combined Cycle Power Plant application, the turbine exhaust temperature is maintained at or near a constant down to about 40% of the load.

All power plants are synchronized to the overall grid and thus the operation of the plant at the given frequency is very important. The grid cannot stand many fluctuations of the plant frequency. It is, therefore, very important to operate the plant at its assigned frequency, which is 60 Hz in the United States and the Americas as well as many countries in the mideast. Europe and most of Asia are operating at a 50 Hz frequency. If there is a frequency change, this must be taken care of in seconds.

Frequency response will be needed outside a dead band of ± 0.1 Hz. The dead band is essential for stable operation of a plant otherwise the plant could oscillate and plant failures have occurred due to a lack of a dead band. Frequency droop is a major problem in plants due to machinery degradation. The standard droop setting is about 5%, which means that a grid frequency drop of 5% would cause an increase of the load by 100%. Gas turbines can easily take swings of 20–30% but large swings cause changes in firing temperature, which places a large strain on the hot section of the turbine. Gas turbines are rated for peak operation to about 10–15% of their base load. It is therefore suggested that the gas turbine be operated at about 95% of the base load so that there is room for adjustment.

Figure 19-4 shows the behavior of the gas turbine for changes in frequency as a stand-alone and also for changes as part of a combined cycle plant. The figure shows changes in the Gas Turbine plant (GT), the Steam Turbine plant (ST) and the Gas Turbine (GTC) and the steam turbine (STC) as part of a steam turbine plant. In a Combined Cycle Power Plant, the falling

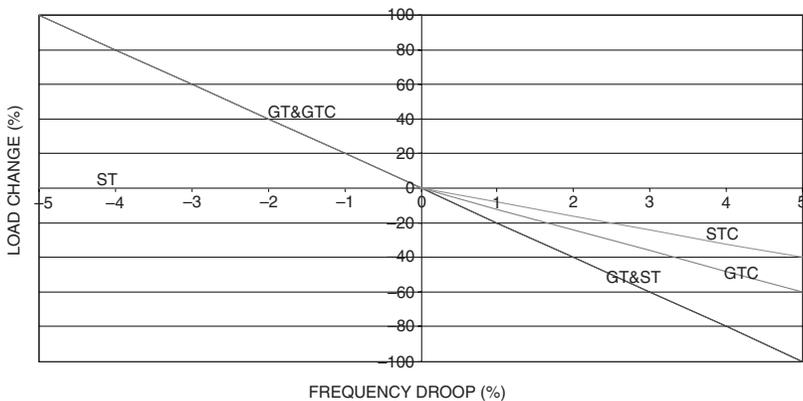


Figure 19-4. Droop curves for Combined Cycle Power Plants.

frequency is usually taken up by the GTC, by a fast change in increasing the load, since the steam turbine cannot respond fast enough. For an increasing frequency, the gas turbine and the steam turbine both can respond, thus, as shown in the figure, the gas turbine (60% load) and the steam turbine (40% load) take their appropriate change in load.

The startup and shutdown of a typical gas turbine is shown in figures 19-5 and 19-6, respectively. The time and percentages are approximate values and will vary depending upon the turbine design.

The gas turbine during the start-up is on an auxiliary drive, initially it is brought to a speed of about 1200–1500 RPM when ignition takes place and the turbine speed and temperature rise very rapidly. The bleed valves are open to prevent the compressor from surging. As the speed reaches about 2300–2500 rpm, the turbine is declutched from its start-up motor, the first set of bleed valves are closed, and then as the turbine has reached near full speed, the second set of bleed valves are closed. If the turbine is a two or three shaft turbine as is the case with aero-derivative turbines, the power turbine shaft will “break loose” at a speed of about 60% of the rated speed of the turbine.

The turbine temperature, flow, and speed increases in a very short time of about three to five minutes to the full rated parameters. There is usually a short period of time where the temperature may overshoot. If supplementary firing or steam injection for power augmentation is part of the plant system, these should be turned on only after the gas turbine has reached full flow. The injection of steam for power augmentation, if done before full load, could cause the gas turbine compressor to surge.

The shutdown of a gas turbine first requires the shutdown of the steam injection and then the opening of the bleed valves to prevent the compressor from

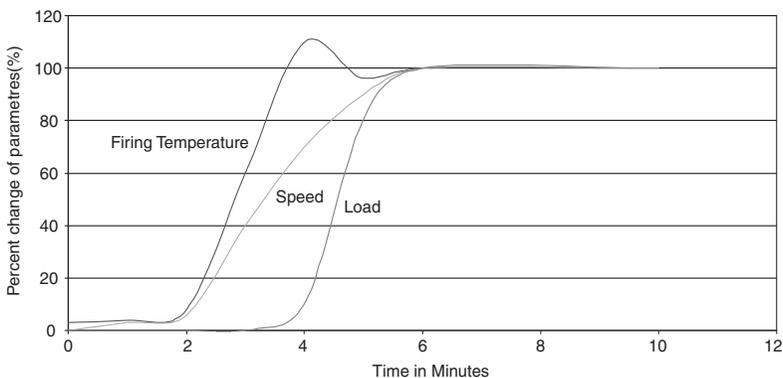


Figure 19-5. A typical startup curve for a gas turbine.

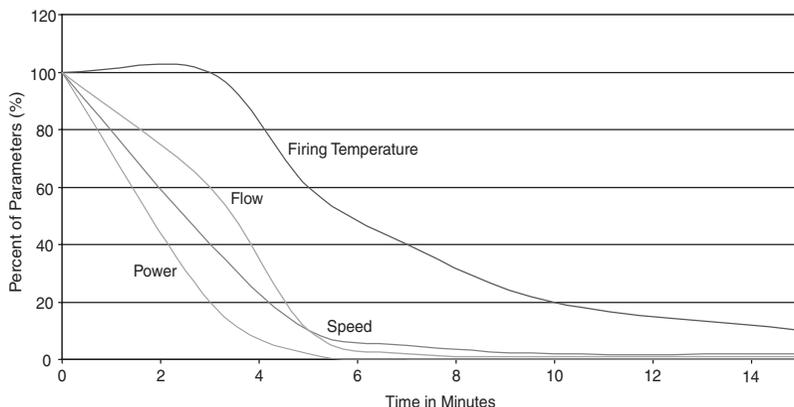


Figure 19-6. A typical shutdown curve for a gas turbine.

surging as the speed is reduced. The gas turbine, especially for frame type units, must be put on a turning gear to ensure that the turbine rotor does not bow. The lubrication systems must be on so that the lubrication can cool of the various components, this usually takes about 30–60 minutes.

Startup Sequence

One of the major functions of the combined control-protection system is to perform the startup sequence. This sequence ensures that all subsystems of the gas turbine perform satisfactorily, and the turbine does not heat too rapidly or overheat during startup. The exact sequence will vary for each manufacturer's engine, and the owner's and operator's manual should be consulted for details.

The gas turbine control is designed for remote operations to start from rest, accelerate to synchronous speed, automatically synchronize with the system, and be loaded in accordance with the start selector button depressed. The control is designed to automatically supervise and check as the unit proceeds through the starting sequence to load condition. A typical startup sequence for a large gas turbine follows:

Starting preparations. The steps necessary to prepare the services and apparatus for a typical startup are as follows:

1. Close all associated control and service breakers.
2. If the computer has been de-energized, close the computer breaker, start the computer, and enter time of day. Under normal conditions, the computer is left running continuously.

3. Place maintenance switches to "Auto."
4. Acknowledge any alarm condition.
5. Check that all lockout relays are reset.
6. Position "Remote-Local" switch to desired position.

Startup description. When the unit is prepared to start, the "Ready to Start" lamp will be lit. With local control, operating one of the following push buttons will initiate a start:

1. Load minimum start.
2. Load base-start.
3. Load peak-start.

The master contactor function will accomplish:

1. Secondary auxiliary lube pump starter energized.
2. Instrument air solenoid valve energized.
3. Combustor-shell pressure transducer line drain solenoid valve energized.

When the auxiliary lube pump builds up sufficient pressure, the circuit to close the turbine gear starter will be completed. Thirty seconds are allowed for the lube pressure to build up, or the unit will shutdown. With the signal that the turning-gear line-starter is picked up, the sequence will continue. Next, the starting-device circuit is energized if lube oil pressure is sufficient. The turning-gear motor will be turned off at about 15% speed. When the turbine has reached firing speed, the turbine overspeed trip solenoid and vent solenoid will be energized to reset. With the build up of overspeed trip oil pressure, the ignition circuit is energized.

The ignition will energize or initiate:

1. Ignition transformers.
2. Ignition time function (30 seconds allowed for establishing flame on both detectors or the unit will be shut down after several tries).
3. Appropriate fuel circuits (as determined from mode of fuel selected).
4. Atomizing air.
5. Ignition time function (to de-energize ignition at the proper time).

At approximately 50% speed, as sensed by the speed channel, the starting device is stopped. The bleed valves are closed near synchronous speed, each at a particular combustor-shell pressure. After fuel is introduced and

ignition confirmed, the speed reference is increased at a preset variable rate and will determine the fuel valve position set point. The characterized speed reference and compressor inlet temperature will provide a feed-forward signal that will approximately position the fuel valves to maintain the desired acceleration. The speed reference will be compared with the shaft-speed signal, and any error provides a calibration signal to ensure that the desired acceleration is maintained. This mode of control will be limited by maximum blade path and exhaust temperatures corresponding to the desired turbine inlet temperatures. If desired acceleration is not maintained, the unit must be shut down. This control avoids many major turbine failures.

With the advance of the turbine to idle speed, the turbine is ready to synchronize, and control is considered in synchronization. Both manual and automatic synchronizing are available locally. The unit is synchronized, and the main breaker closed. The speed reference will be switched to become a load reference. The speed/load reference will be automatically increased at a predetermined rate so that the fuel valve will be at the approximate position required for the desired load. For maintenance scheduling, the computer will count the number of normal starts and accumulate the number of hours at the various load levels.

Shutdown. Normal shutdown shall proceed in an orderly fashion. Either a local or remote request for shutdown will first reduce the fuel at a predetermined rate until minimum load is reached. The main and field breakers and the fuel valves will be tripped. In an emergency shutdown, the main and field breakers and fuel valves will be tripped immediately without waiting for the load to be reduced to minimum. All trouble shutdowns are emergency shutdowns. The turbine will coast down and as the oil pressure from the motor-driven pump drops, the DC auxiliary lube oil pump will come on. At about 15% speed, the turning-gear motor will be restarted, and when the unit coasts to turning-gear speed (about five rpm), the turning-gear over-running clutch will engage, allowing the turning-gear motor to rotate the turbine slowly. Below ignition speed, the unit may be restarted; however, the unit must be purged completely of any fuel. This is accomplished by moving through the turbine at least five times its total volume flow.

If left on turning gear, it will continue until the turbine exhaust temperature decreases to 150°F (66°C), and a suitable amount of time (up to 60 hrs) has elapsed. At this point, the turning gear and auxiliary lube oil pump will stop and the shutdown sequence is complete. On recognition of a shutdown condition, various contact status and analog values are saved (frozen) for display, if desired.

Generator protection. The generator protective relays are mounted in a switchboard, which usually houses the wattmeter and various transducers, teleductors, and optional watt-hour meters.

The basic generator protection equipment has the following items:

1. Generator differential
2. Negative sequence
3. Reverse power
4. Lockout relays
5. Generator ground relay
6. Voltage-controlled overcurrent relay

Condition Monitoring Systems

Predictive performance-based condition monitoring is emerging, as a major maintenance technique, with large reduction in maintenance costs as shown in Figure 19-7. The histogram shows that although an approximate one-third reduction in operating and maintenance (O&M) costs was achieved by moving from a “corrective,” more realistically termed a “breakdown”

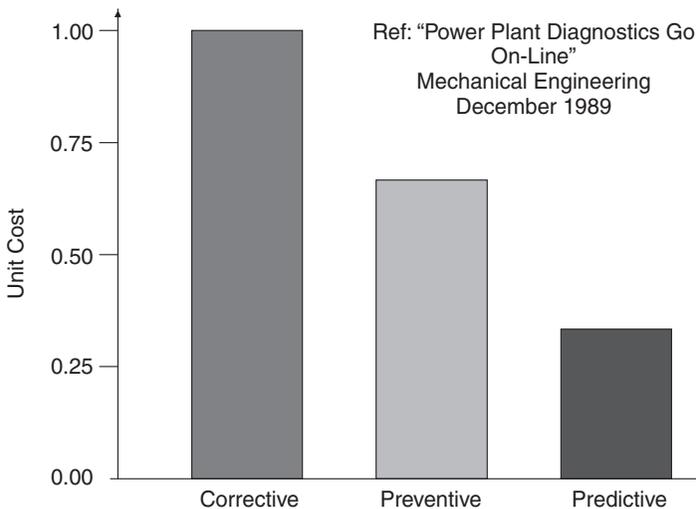


Figure 19-7. Comparison between various maintenance techniques.

or “fix as fail” repair strategy, to a “preventive” regime, this yielded only approximately half of the maximum cost savings. Although more difficult to introduce than the simple scheduling of traditional maintenance activities required for preventive action, the Electric Power Research Institute (EPRI) research showed that the introduction of “predictive” maintenance strategies could yield a further one-third reduction in O&M costs.

The introduction of the total maintenance condition monitoring system means the use of composite condition monitoring systems, which combine mechanical and performance-based analysis with corrosion monitoring. These three components are the primary building blocks that enable the introduction of a comprehensive plant-wide condition management strategy. Numerous case studies have shown that many turbomachinery operational problems can only be diagnosed and resolved by correlating the representative performance parameters with mechanical parameters.

In plant health terms, monitoring and measurement both cost money and are only half way to the real objective, which is the avoidance of cost and plant damage. Condition management makes proper use of both activities and exploits information derived from them to generate money for the plant operator. Good plant condition management, therefore, should be the objective of materials and machine health specialists.

The change has further implications: in the past, corrosion and condition monitoring were considered to be service activities, providing only a *reactive* strategy. Condition *management* embodies a *pro-active* stance on plant health. This fundamental understanding should not go unrecognized by the materials and condition monitoring specialists. Condition management is a huge opportunity for technical specialists to provide the best possible service to clients, whether internal or external. The same specialists also will be able to derive the maximum direct benefit from their expertise.

Conventional alloy selection, coating specification and failure investigation skills will always be required, as will inspection services to confirm the condition of the plant. However, the phenomenon labeled corrosion should no longer be regarded as a necessary evil as it is only a problem when out of control. The electrochemical behavior characterizing corrosion is also the means by which on-line plant health management can be achieved.

Major power plant complexes contain various types of large machinery. Examples include many types of machinery, in particular gas and steam turbines, pumps and compressors, and their effect on the Heat Recovery Steam Generators (HRSG), condensers, cooling towers, and other major plant equipment. Thus, the logical trend in condition monitoring is to multi-machine train monitoring. To accomplish this goal, an extensive database, which contains data from all machine trains along with many composite

multi-machine analysis algorithms are implemented in a systematic and modular form in a central system.

Implementation of advanced performance degradation models, necessitate the inclusion of advanced instrumentation and sensors such as pyrometers for monitoring hot section components, dynamic pressure transducers for detection of surge and other flow instabilities such as combustion especially in the new dry low NO_x combustors. To fully round out a condition monitoring system the use of expert systems in determining fault and life cycle of various components is a necessity.

The benefits of total performance based planned maintenance not only ensure the best and lowest cost maintenance program but also that the plant is operated at its most efficient point. An important supplementary effect is that the plant will be operating consistently within its environmental constraints.

The new purchasing mantra for the new utility plants is “life cycle cost” and to properly ensure that this is achieved a “total performance condition monitoring” strategy is unsurpassed.

To avoid excessive downtime and maintain availability, a turbine should be closely monitored and all data analyzed for major problem areas.

To achieve effective monitoring and diagnostics of turbomachinery, it is necessary to gather and analyze both the mechanical and aerothermal operating data from the machines. The instrumentation and diagnostics must also be custom tailored to suit the individual machines in the system, and also to meet the requirements of the end users. The reasons for this are that there can be significant differences in machines of the same type or manufacturer because of differences in installation and operation.

Requirements for an Effective Diagnostic System

1. The system must produce diagnostic and failure prediction information in a timely manner before serious problems occur on the machines monitored.
2. When equipment shutdown becomes necessary, diagnostics must be precise enough to accomplish problem identification and rectification with minimal downtime.
3. The system should be useable and understood well enough by production personnel so that an engineer is not always necessary when urgent decisions need to be made.
4. The system should be simple and reliable and cause negligible downtime for repairs, routine calibration, and checks.

5. The system must be cost effective; namely, it should cost less to operate and maintain than the expenses resulting from loss of production and machinery repairs that would have resulted if the machinery was not under monitoring and predictive surveillance.
6. System flexibility to incorporate improvements in the state of the art is desirable.
7. System expansion capabilities to accept projected increases in installed machinery or increases in the number of channels must be considered.
8. The use of excess capacity in a computer system available at the plant can result in considerable equipment cost savings. System components that mate with the existing computer system may, therefore, be a necessary prerequisite.

A condition monitoring system designed to meet these needs must be comprised of hardware and software designed by engineers with experience in machinery and energy system design, operation, and maintenance. Each system needs to be carefully tailored to individual plant and machinery requirements. The systems must obtain real-time data from the plant DCS and if required from the gas and steam turbine control systems. Dynamic vibration data is taken in from the existing vibration analysis system into a data acquisition system. The system can comprise of several high-performance networked computers depending on plant size and layout. The data must be presented using a Graphic User Interface (GUI) and include the following:

1. *Aerothermal analysis*: This pertains to a detailed thermodynamic analysis of the full power plant and individual components. Models are created of individual components, including the gas turbine, steam turbine heat exchangers, and distillation towers. Both the algorithmic and statistical approaches are used. Data is presented in a variety of performance maps, bar charts, summary charts, and baseline plots.
2. *Combustion analysis*: This includes the use of pyrometers to detect metal temperatures of both stationary and rotating components such as turbine blades. The use of dynamic pressure transducers to detect flame instabilities in the combustor especially in the new dry low NO_x applications.
3. *Vibration analysis*: This includes an on-line analysis of the vibration signals, FFT spectral analysis, transient analysis, and diagnostics. A wide variety of displays are available including orbits, cascades, bode and nyquist plots, and transient plots.

4. *Mechanical analysis*: This includes detailed analysis of the bearing temperatures, lube, and seal oil systems and other mechanical subsystems.
5. *Corrosion analysis*: On-line electrochemical sensors are being used to monitor changes in the corrosivity of flue gases especially in exhaust stacks. The progressive introduction of ever-more stringent regulations to reduce NO_x emissions has resulted in an increase in the risk of water wall tube wastage in large power boilers, refinery process heaters and municipal waste incinerators.
6. *Diagnosis*: This includes several levels of machinery diagnosis assistance available via expert systems. These systems must integrate both mechanical and aerothermal diagnostics.
7. *Trending and prognosis*: This includes sophisticated trending and prognostic software. These programs must clearly provide users to clearly understand underlying causes of operating problems.
8. *“What-if” analysis*: This program should allow the user to do various studies of plant operating scenarios to ascertain the expected performance level of the plant due to environmental and other operational conditions.

Monitoring Software

The monitoring software for every system will be different. However, all software is there to achieve one goal—it must gather data, ensure that it is correct, and then analyze and diagnose the data. Presentations must be in a convenient form and should be easily understood by plant operational personnel. All priorities must be to the data collection process. This process must not in any manner be hampered since it is the corner stone of the whole system.

A convenient *framework* within which to categorize the software could be as follows:

1. *Graphic User Interface (GUI)*—This consists of screens, which would enable the operator to easily interrogate the system and to visually see where the instruments are installed and their values at any point of time. By carefully designed screens, the operator will be able to view at a glance the relative positions of all values, thus, fully understanding the operation of the machinery.
2. *Alarm/system logs*—To fully understand a machine we have to have various types of alarms. The following are some of the suggested types of alarms:
 - a. *Instrument alarms*: These alarms are based on the instrumentation range.

- b. *Value range alarm*: These alarms are based on operating values of individual points both measured and calculated points. These alarms should be variable in that they would change with operating conditions.
 - c. *Rate of change alarm*: These alarms must be based on any rapid change in values in a given time range. This type of alarm is very useful to detect bearing problems, surge problems, and other instabilities.
 - d. *Prognostic alarms*: These alarms must be based on trends and the prognostics based on those trends. It is advisable not to have prognostics, which project in time more than the time of data that is trended.
3. *Performance maps*: These are performance maps based on design or initial tests (base lines) of the various machinery parameters. These maps, for example present how power output varies with ambient conditions, or with properties of the fuel, or the condition of the filtration system; or how close to the surge line a compressor is operating. On these maps, the present value is displayed, thus allowing the operator to determine the degradation in performance occurring in the units.
4. *Analysis programs*—These include aerothermal and mechanical analysis programs, with diagnostics and optimization programs.
- a. *Aero-thermal analysis*: Typical aero-thermal performance calculations involve the evaluation of component unit power, polytropic and adiabatic head, pressure ratio, temperature ratio, polytropic and adiabatic efficiencies, temperature profiles, and a host of other machine specific conditions under steady state as well as during transients—startups and shutdowns. This program must be tailored to individual machinery and to the instrumentation available. Data must be corrected to a base condition, so that it can be compared and trended. The base condition can vary from ISO ambient conditions, to design conditions of a compressor or pump if those conditions are very different from ISO ambient conditions. To analyze off-design operation, it is necessary to transpose values from the operating points back to the design point for comparison of unit degradation.
 - b. *Mechanical analysis*: This program must be tailored to the mechanical properties of the machine train under consideration. It should include bearing analysis, seal analysis, lubrication analysis, rotor dynamics, and vibration analysis. This includes the evaluation and correlation of bearing metal temperatures, shaft orbits, vibration

velocity, spectrum snapshots, waterfall plots, stress analysis, and material properties.

- c. *Diagnostic analysis*: This program can be part of an expert system or consist of an operational matrix, which can point to various problems. The program must include comparison of both performance and mechanical health parameters to a machine specific fault matrix to identify if a fault exists. Expert analysis modules can in many cases aid to faster fault identification but are usually more difficult to integrate into the system.
 - d. *Optimization analysis*: Optimization programs take into account many variables, such as, deterioration rate; overhaul costs, interest, and utilization rates. These programs may also be dependent on more than one machine train if the process is interrelated between various trains.
 - e. *Life cycle analysis*: The determination of the effect of the material, the temperature excursions, the number of startups and shut downs, and the type of fuel all relate to the life of hot section components.
5. *Historical data management*—This includes the data acquisition and storage capabilities. Present-day prices of storage mediums have been dropping rapidly, and systems with 80 gigabyte hard disks are available. These disks could store a minimum of five years of one-minute data for most plants. One-minute data is adequate for most steady state operation, while start-ups and shutdowns or other non steady state operation should be monitored and stored at an interval of one second. To achieve these time rates, data for steady state operation can be obtained from most plant-wide D-CS systems, and for unsteady state conditions, data can be obtained from control systems.

Implementation of a Condition Monitoring System

The implementation of a condition monitoring system in a major utilities plant requires a great deal of forethought. A major utilities plant will have a number of varied, large rotating equipment. This will consist usually of various types of prime movers such as large gas turbines, steam turbines, compressors, pumps, electric generators, and motors. The following are some of the major steps, which need to be taken to ensure a successful system installation:

1. The first decision is to decide on what equipment should be monitored on line and what systems should be monitored off-line. This requires

an assessment of the equipment in terms of both first cost and operating costs, redundancy, reliability, efficiency, and criticality.

2. Obtain all pertinent data of the equipment to be monitored. This would include details of the mechanical design and the performance design. Some of this information may be difficult to obtain from the manufacturer and will have to be calculated from data being obtained in the field or after installation during commissioning tests in a new installation. Obtaining baseline data is critical in the installation of any condition monitoring system. In most systems, it is the rate of change of parameters that are being trended not the absolute values of these points. It is also important to decide what type of alarms will be attached to the various points. Rate of change alarms must be for bearing metal temperatures especially for thrust bearings where temperature changes are critical. Prognostic alarms should be applied to critical points. Alarms randomly applied tend to slow down the system and do not provide added protection.

The following are some of the basic data that would be necessary in setting up a system:

- a. Type of gases and fluids used in the various processes. The equation of state and other thermodynamic relationship, which govern these gases and fluids.
 - b. Type of fuel used in the prime movers. If the fuel analysis is available including the fuel composition and the heating values of the fuel.
 - c. Materials used in various hot sections such as combustor liners, turbine nozzles, and blades. This includes stress and strain properties as well as Larson-Miller parameters.
 - d. Performance maps of various critical parameters such as power and heat consumption as a function of ambient conditions, pressure drop in filters, and the effect of backpressure. Compressor surge, efficiency, and head maps.
3. Determine the instrumentation, which exists, and their actual location. Location of the instrumentation from the inlet or exit of the machinery is important so that proper and effective compensation may be provided for the various measured parameters. In some cases additional instrumentation will be needed. Experience indicates that older plants require 10–20% more instrumentation depending upon the age of the plant.
 4. Once the data points have been decided, limits and alarm must be set. This is a long and challenging task, as the limits on many points are

not given in the operation manuals. In some cases, the criticality of the equipment may necessitate that the alarm threshold on certain points be lowered to give early warning of any deterioration of the system. It should be noted that since this is a condition monitoring system early alarm warnings are in most cases desirable.

5. Types of reports and summary charts should be planned to optimize the data and to present it in the most useful manner to the plant operations, and maintenance personnel.
6. The types of D-CS and the control systems available in the plant. The protocol of these systems and their relationships to the condition monitoring system. The slave or master relationship is important in setting up the protocols.
7. Diagnostics for the system requires noting any unusual characteristics of the machinery, especially in older plants, which have a history of operation inspections and overhauls.
8. Costs of operations such as fuel costs, labor costs, down time costs, overhaul hours, interest rates are necessary in computing parameters such as time of major inspections, off-line cleaning, and overhauls.

Plant Power Optimization

On-line optimization processes for large utility plants is gaining tremendous favor. Plant optimization is gaining importance with Combined Cycle Power Plants as these plants are operated over a wide range of power in day-to-day operation. On-line optimization may be defined as the place where economics, operation, and maintenance meet. At first sight, it may be imagined that process integration is not connected to condition management or inspection, and this has been the case in the past. However, there is every incentive for complete integration of all these production-related technologies, since the condition monitoring of the various components in a plant are upgraded constantly, thus the operational curves with degradation of each unit are no longer stagnant.

Process integration was developed initially as a means of optimizing the design of chemical and petrochemical process plants. Process optimization is still only a pre-construction or pre-production exercise. This is surprising because many process plants are designed for batch manufacture of a range of products, each of which will require continuously changing optimization parameters. Process optimization and re-optimization “on the fly” can enable companies to meet variations in market demand and maximize production efficiency and overall profitability.

When embodied in a modern integrated plant environment, dynamic plant health assessment, process modeling and process integration provide the means to augment plant reliability, availability and safety with maximum capacity and flexibility.

On-line Optimization Process

Figure 19-8 shows how on-line systems are configured. The system gathers data in real time. The data is gathered from either the D-CS system or from the control system. Data for startups and transients are needed from the control system since the data from the D-CS is usually updated every three to four seconds, while the control system can have very rapid loops, which are updated as often as 40 times per second. To ensure that performance data is taken at a steady state condition, since most models of the plant are steady state, the system must observe some key parameters and ensure that they are not varying. In turbines parameters, such as turbine wheel space, temperatures should be observed to be constant. This data is then checked for accuracy and errors removed. This involves simple checks against instrument operational ranges, and system operation parameter ranges. The data is then fully analyzed and various performance data checks are made. New operational and performance maps are then plotted and the system then can optimize itself against an operational model. The operational goal is to maximize the efficiency of the plant at all loads, thus the new performance maps, which show degradation of the plant are then used in the plant model to ensure that the control is at the right setting for the operation of the plant at any given time. Many maintenance practices are also based on the rate of economic return these operational maintenance practices such as an off-line compressor wash would contribute to the operations of the plant.

Many plants use off-line optimization. Off-line optimization is an open loop control system. Instead of the closed loop system, which controls the plant settings, data is provided to the operator so that he can make the decisions based on the findings of the operational data. Off-line systems are also used by engineers to design plants and by maintenance personnel to plan plant maintenance. Comparisons of the on-line systems to off-line systems can be seen in Table 19-1.

Performance evaluation is also important initially in determining that a plant meets its guarantee points and, subsequently, to ensure it continues to be operated at or near its design operating condition. Maintenance practices are being combined ever more closely with operational practices to ensure

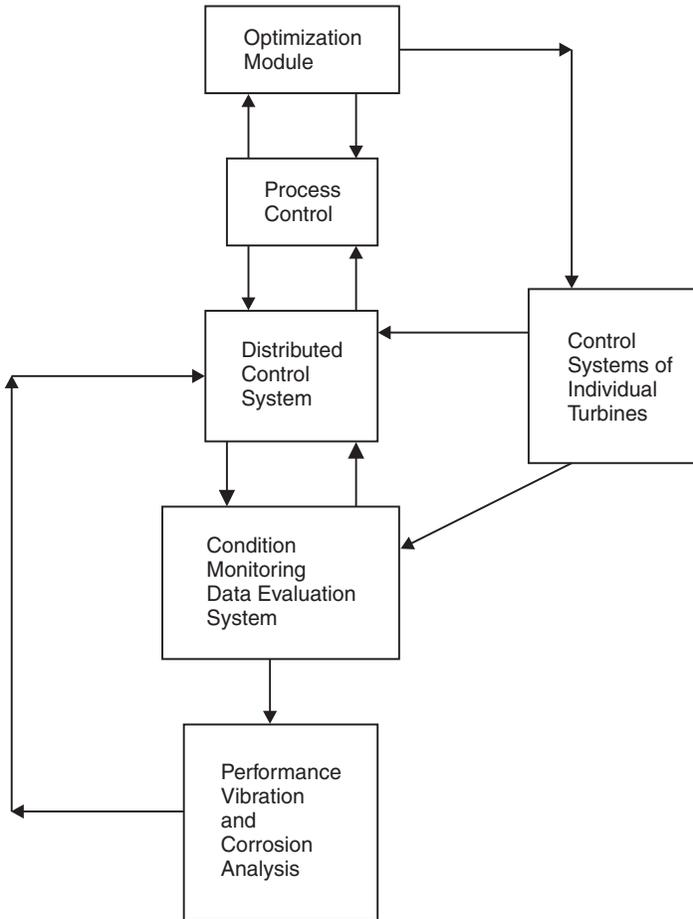


Figure 19-8. A block diagram for an on-line condition monitoring system.

that plants have the highest reliability with maximum efficiency. When a new plant is built, its cost amounts to only about 7–10% of the life cycle cost. Maintenance costs represent approximately 15–20% overall. However, operating costs, which in the case of a power plant for example, consist essentially of energy costs, make up the remainder, and amount to between 70–80% of the life cycle costs of the facility. This brings performance monitoring to the forefront as an essential tool in any type of plant condition monitoring system. Operating a plant as close as possible to its design conditions will guarantee that its operating costs will be reduced. As an

Table 19-1
Comparisons of On-line and Off-line Plant Optimization System Use

| | On-line Systems | Off-line Systems |
|------------|--|---|
| Objectives | Maximize economic benefit, operate the plant at its maximum efficiency at all operation points | Maximize economic benefit, operate the plant at its maximum efficiency at all operation points Optimize overall facilities design and investment |
| Target | Existing operating plant | Existing operating plant New facilities Facility expansion |
| Prime use | Process and maintenance operations | Process and maintenance operations Design modifications |
| Users | Operation and maintenance engineers | Operation and maintenance engineers Project and design engineers |

illustration of the opportunity cost this represents, large fossil power plants currently being commissioned range from 600–2800 MW. The fuel costs for these plants will amount to between US\$72 million and US\$168 million per annum. Therefore, savings of 1–3% of these costs can amount to an overall cost reduction of upward of US\$1 million per annum.

A change in approach is clearly necessary in order that the full benefit of integrated plant condition management and control can be recognized and exploited. Improved control and enhanced performance monitoring will enable shutdown intervals to be extended without increasing the risk of premature or unexpected failure. In turn, this will increase the confidence of operations, inspection and management personnel in the effectiveness of unified plant administration.

Life Cycle Costs

The life cycle costs of any machinery are dependent on the life expectancy of the various components, the efficiency of its operation through out its life. Figure 19-9 shows the cost distribution by the three major categories, initial costs, maintenance costs, and operating or energy costs. This figure indicates that the new costs are about 7–10% of the life cycle costs, while maintenance costs are approximately 15–20% of the life cycle costs and operating costs, which essentially consist of energy costs, make up the remainder between 70–80% of the life cycle costs of any major machinery in a utilities plant.

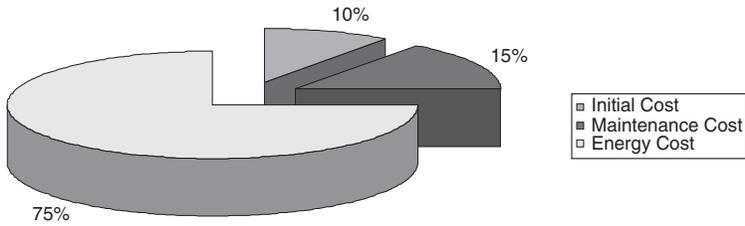


Figure 19-9. Life cycle costs for Combined Cycle Power Plants.

It is therefore clear why the new purchasing mantra for a utility plant, or for that matter of fact, for any major plant operating large machinery is “life cycle cost.”

This brings forth to the forefront performance monitoring as an essential tool in any type of plant condition monitoring system. The major costs in a life cycle are the cost of energy. Thus operating the plant as close to its design conditions guarantees that the plant will reduce its operating costs. This can be achieved by ensuring that the turbine compressor is kept clean and that the driven compressor is operating close to its maximum efficiency, which in many cases is close to the surge line. Thus knowing where the compressor is operating with respect to its surge line is a very critical component in plant operating efficiency.

The life expectancy of most hot section parts is dependent on various parameters and is usually measured in terms of equivalent engine hours. The following are some of the major parameters that effect the equivalent engine hours in most machinery, especially gas turbines:

1. Type of fuel.
2. Firing temperature.
3. Materials stress and strain properties.
4. Effectiveness of cooling systems.
5. Number of starts.
6. Number of trips.

Maintenance practices are being combined more and more with operational practices to ensure that plants have the highest reliability with maximum efficiency. This has led to the importance of performance condition monitoring as a major tool in the operation and maintenance of a plant. Life cycle costs, rightly so, now drive the entire purchasing cycle and thus the

operation of the plant. Life cycle costs, based on a 25-year life, indicate that the following are the major cost parameters:

1. Initial purchase cost of equipment is 7–10% of the overall life cycle cost.
2. Maintenance costs are about 15–20% of the overall life cycle cost.
3. Energy costs are about 70–80% of the life cycle costs.

This distribution in life cycle costs indicates that component efficiency throughout the life period of the plant is the most important factor affecting the cost of a particular machine train. Thus, monitoring the efficiency of the train and ensuring that degradation rates are slowed down ensures that the predicted life cycle costs are achieved. Performance monitoring of the entire train is a must for plants operating on life cycle cost strategies.

Performance monitoring also plays a major role in extending life, diagnosing problems, and increasing time between overhauls. On-line performance monitoring requires an in-depth understanding of the equipment being measured. Most trains are very complex in nature and thus require very careful planning in installation of these types of systems. The development of algorithms for a complex train needs careful planning, understanding of the machinery and process characteristics. In most cases, help from the manufacturer of the machinery would be a great asset. For new equipment, this requirement can be part of the bid requirements. For plants with already installed equipment, a plant audit to determine the plant machinery status is the first step.

To sum up, total performance condition monitoring systems will help the plant engineers to achieve their goals of:

1. Maintaining high availability of their machinery.
2. Minimizing degradation and maintaining operation near design efficiencies.
3. Diagnosing problems, and avoiding operating in regions, which could lead to serious malfunctions.
4. Extending time between inspections and overhauls.
5. Reducing life cycle costs.

Diagnostic System Components and Functions

1. Instrumentation and instrumentation mountings
2. Signal conditioning and amplifiers for instrumentation
3. Data transmission system (cables, telephone link-up, or microwave)

4. Data integrity checking, data selection, data normalization and storage
5. Baseline generation and comparison
6. Problem detection
7. Diagnostics generation
8. Prognoses generation
9. On-site display
10. Systems for curve plotting, documentation, and reporting

Data Inputs

Obtaining good data inputs is a fundamental requirement, since any analysis system is only as good as the inputs to the system. A full audit of the various trains to be monitored must be made to obtain optimum instrumentation selection.

The factors that need to be considered are the instrument type, its measurement range, accuracy requirements, and the operational environmental conditions. These factors must be carefully evaluated to select instruments of optimum function and cost to match the total requirements of the system. For instance, the frequency range of the vibration sensor should be adequate for monitoring and diagnostics and should match with the frequency range of analysis equipment. Sensors should be selected to operate reliably and accurately within the environmental conditions that prevail (for example, when used on high-temperature turbine casings). Resistance temperature sensors, with their higher accuracy and reliability compared to thermocouples, may be necessary for analysis accuracy and reliability. Calibration of instrumentation should be conducted on a schedule established after reliability factors have been analyzed.

All data should be checked for validity and to determine if they are within reasonable limits. Data that are beyond predetermined limits should be discarded and flagged for investigation. An unreasonable result or analysis should set up a routine for identification of possible discrepant input data.

Instrumentation Requirements

It is essential that instrumentation requirements be tailored to the requirements of the machine being monitored. However, the instrumentation requirements should exist to cover the requirements for both vibration and athermal monitoring.

Any existing instrumentation should be used if found to be adequate. While there are advantages in the use of noncontacting sensors built into

the machine for measurement of journal displacements, this instrumentation is often impossible to install in existing machinery. Suitably selected and located accelerometers can adequately cover the vibration-monitoring requirements of machinery. Accelerometers are often an essential supplement to displacement sensors to cover the higher frequencies generated by gear mesh, blade passing, rubs, and other conditions.

Typical Instrumentation (Minimum Requirements for Each Machine)

(*Note:* Locations and type of sensors depend on the type of machine under consideration.)

1. Accelerometer
 - a. At machine inlet bearing case, vertical
 - b. At the machine discharge bearing case, vertical
 - c. At machine inlet bearing case, axial
2. Process pressure
 - a. Pressure drop across filter
 - b. Pressure at compressor and turbine inlet
 - c. Pressure at compressor and turbine discharge
3. Process temperature
 - a. Temperature at compressor and turbine inlet
 - b. Temperature at compressor and turbine discharge.
4. Machine speed
 - a. Machine speed of all shafts
5. Thrust-bearing temperature
 - a. Thermocouples or resistance temperature elements embedded in front and rear thrust bearing

Desirable Instrumentation (Optional)

1. Noncontacting eddy-current vibration displacement probe adjacent to:
 - a. Inlet bearing, vertical
 - b. Inlet bearing, horizontal
 - c. Discharge bearing, vertical
 - d. Discharge bearing, horizontal
2. Noncontacting eddy-current gap-sensing probe adjacent to:
 - a. Forward face of thrust-bearing collar
 - b. Rear face of thrust-bearing collar (*Note:* The noncontacting sensor in its role of measurement of gap DC voltage is sensitive to probe

and driver temperature variations. Careful evaluation must be conducted of sensor type, its mounting, and location for this measurement.)

3. Process flow measurement at inlet or discharge of machine
4. Radial-bearing temperature thermocouple or resistance temperature element embedded in each bearing, or temperature at lube oil discharge of each bearing.
5. Lube oil pressure, temperature, and corrosion probe
6. Dynamic pressure transducer at compressor discharge for indication of flow instability
7. Fuel system (water capacitance probe, corrosion probe, and Btu detector)
8. Exhaust gas analysis
9. Torque measurement

Figures 19-10 and 19-11 show possible instrument locations for an industrial gas turbine and centrifugal compressor.

Criteria for the Collection of Aerothermal Data

Turbomachinery operating pressures, temperatures, and speeds are very important parameters. Obtaining accurate pressures and temperatures will depend not only on the type and quality of the transducers selected, but also on their location in the gas path of the machine. These factors should be carefully evaluated. The accuracy of pressure and temperature measurements required will depend on the analysis and diagnostics that need to be performed. Table 19-2 presents some criteria for selection of aerothermal instrumentation of pressure and temperature sensors for measurement of compressor efficiency. Note that the percentage accuracy requirements are more critical for temperature sensors than pressure sensors. The requirements are also dependent on the compressor pressure ratio.

Pressure Drop in Filter System

The prime design objective of the filter system is to protect the gas turbine. The performance of the gas turbine inlet-air filter system has important and far-reaching influences on overall maintenance costs, reliability, and availability of gas turbines. There are three major results of improper air filtration: (1) erosion, (2) fouling of the axial-flow compressor, and (3) corrosion of the gas turbine hot-gas path inlets. The importance of the inlet-air filter, as it relates to each of these three phenomena, can be appreciated if

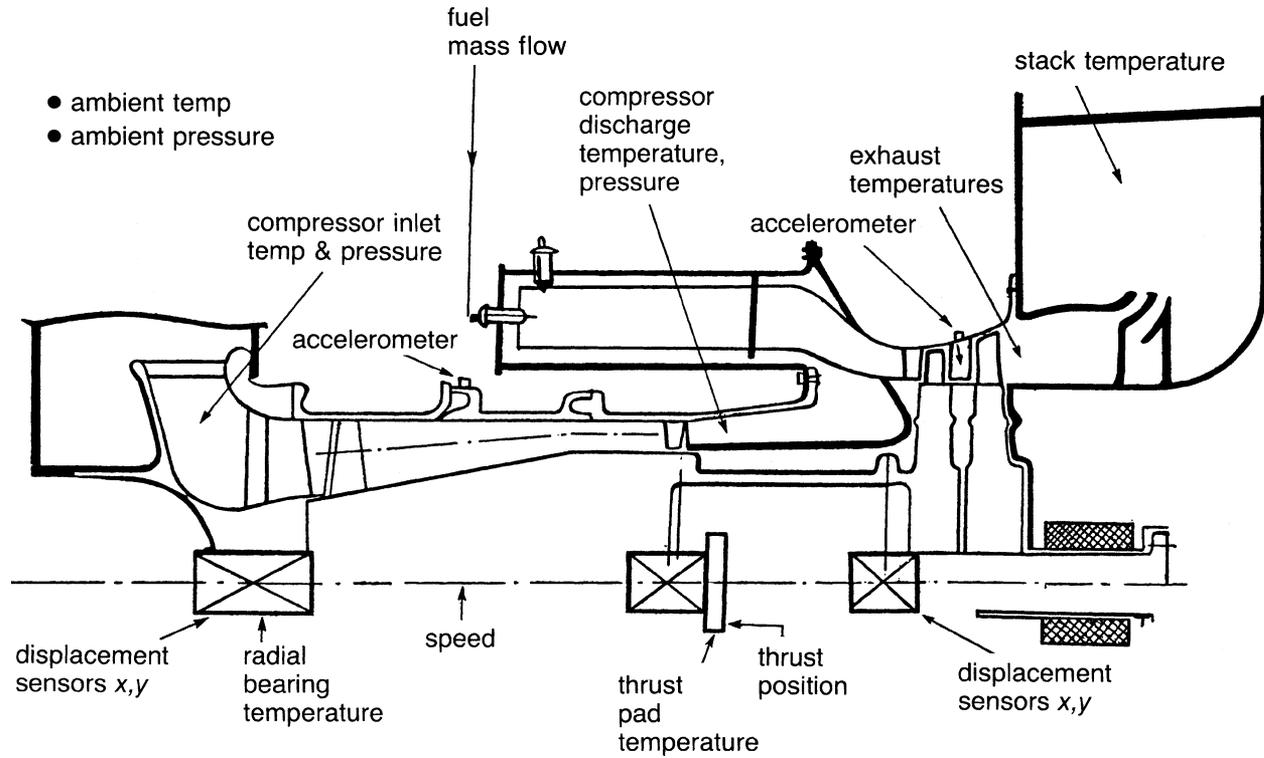


Figure 19-10. Instrumentation for monitoring and diagnostics on a gas turbine engine.

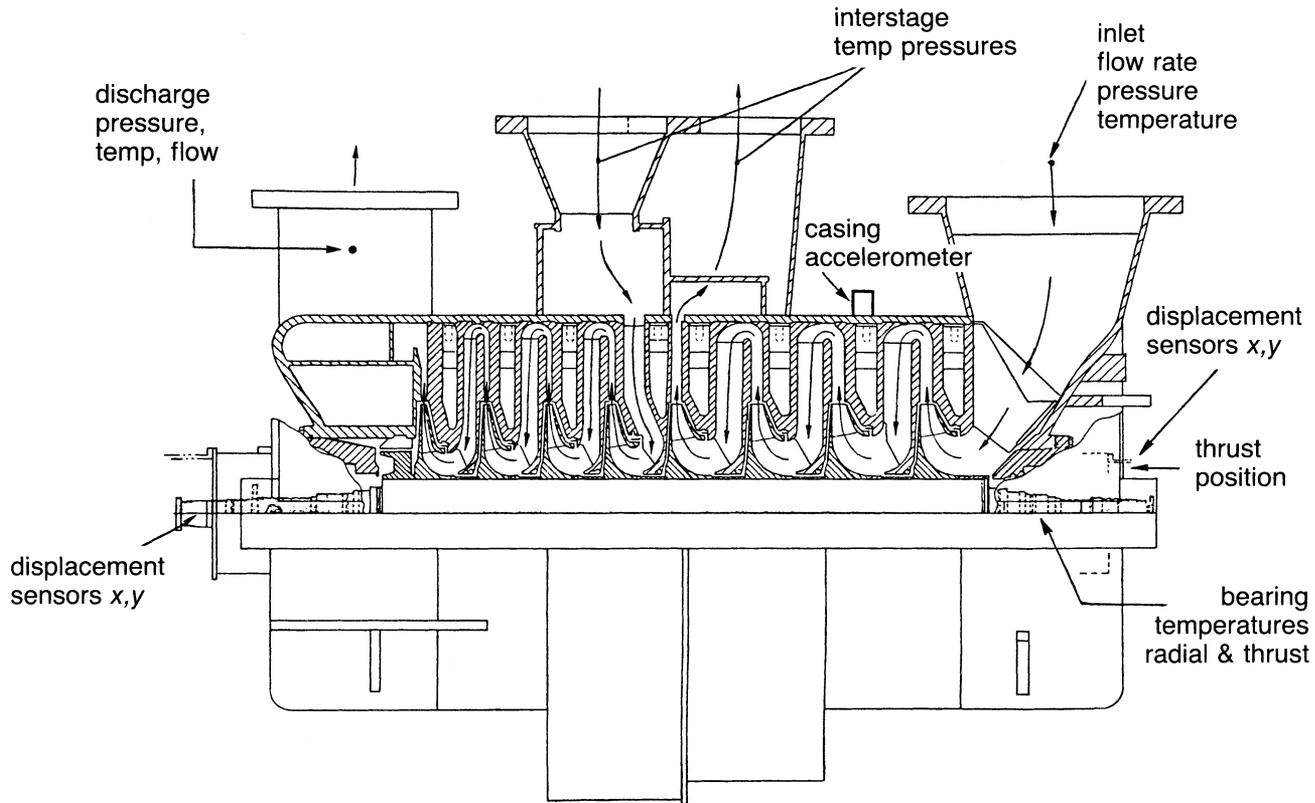


Figure 19-11. Instrumentation for monitoring and diagnostics on a centrifugal compressor.

Table 19-2
Criteria for Selection of Pressure and Temperature Sensors for
Compressor Efficiency Measurements

| Compressor Pressure Ratio P_2/P_1 | P_2 Sensitivity (%) | T_2 Sensitivity (%) |
|---|-----------------------|-----------------------|
| 6 | 0.704 | 0.218 |
| 7 | 0.750 | 0.231 |
| 8 | 0.788 | 0.240 |
| 9 | 0.820 | 0.250 |
| 10 | 0.848 | 0.260 |
| 11 | 0.873 | 0.265 |
| 12 | 0.895 | 0.270 |
| 13 | 0.906 | 0.277 |
| 14 | 0.933 | 0.282 |
| 15 | 0.948 | 0.287 |
| 16 | 0.963 | 0.290 |

Tabulation showing percent changes in P_2 and T_2 needed to cause 1/2% change in air compressor efficiency. Ideal gas equations are used.

one considers the fact that the gas turbine ingests about 7000–9000 cf (198.2179–254.8516 cm) of air per minute for every megawatt of power produced.

Temperature and Pressure Measurement for Compressors and Turbines

Temperature and pressure represent two of the major parameters measured and evaluated in a monitoring system. All gas turbine engines are equipped with sensors of this type; however, the exact number as well as their location varies considerably among manufacturers.

At each of the measurement locations, pressure probes may be attached to a harness, and these probes will direct the air flow to external pressure transducers for measurement while serving as a sheath for the appropriate thermocouple at that location (each thermocouple will be seated inside a pressure probe).

The electrical output of the thermocouple varies with temperature. This output is fed through a flexible cable to an external signal-conditioner circuit to amplify and condition the signal for interfacing to the monitoring system.

Temperature Measurement

Temperature measurement is important to gas turbine performance. Exhaust gas temperature should be monitored to avoid overheating of turbine components. Most gas turbines are equipped with a series of thermocouples in their exhausts. Measuring turbine inlet temperature directly is very useful but, because of the turbine damage that results if a thermocouple breaks and passes through the turbine blades, thermocouples are not generally installed upstream of the turbine. Bearing oil temperature is normally monitored at the discharge to ensure proper oil characteristics; however, this temperature is not an accurate indication of bearing conditions, since bearings may develop localized hot spots during operation. To measure bearing temperature accurately, transducers should be located in the bearings themselves. The temperature will indicate problems in either journal or thrust-bearings prior to damage. In addition to turbine exhaust temperatures, compressor inlet and discharge temperature measurement is necessary to evaluate compressor performance.

For most points requiring temperature monitoring, either thermocouples or resistive thermal detectors (RTDs) can be used. Each type of temperature transducer has its own advantages and disadvantages, and both should be considered when temperature is to be measured. Since there is considerable confusion in this area, a short discussion of the two types of transducers is necessary.

Thermocouples

The various types of thermocouples provide transducers suitable for measuring temperatures from -330 to 5000°F (-201 to 2760°C). The useful ranges for the various types are shown in Figure 19-12. Thermocouples function by producing a voltage proportional to the temperature difference between two junctions of dissimilar metals. By measuring this voltage, the temperature difference can be determined. It is assumed that the temperature is known at one of the junctions; therefore, the temperature at the other junction can be determined. Since the thermocouples produce a voltage, no external power supply is required to the test junction; however, for accurate measurement, a reference junction is required. For a temperature monitoring system, reference junctions must be placed at each thermocouple or similar thermocouple wire installed from the thermocouple to the monitor where there is a reference junction. Properly designed thermocouple systems can be accurate to approximately $\pm 2^{\circ}\text{F}$ ($\pm 1^{\circ}\text{C}$).

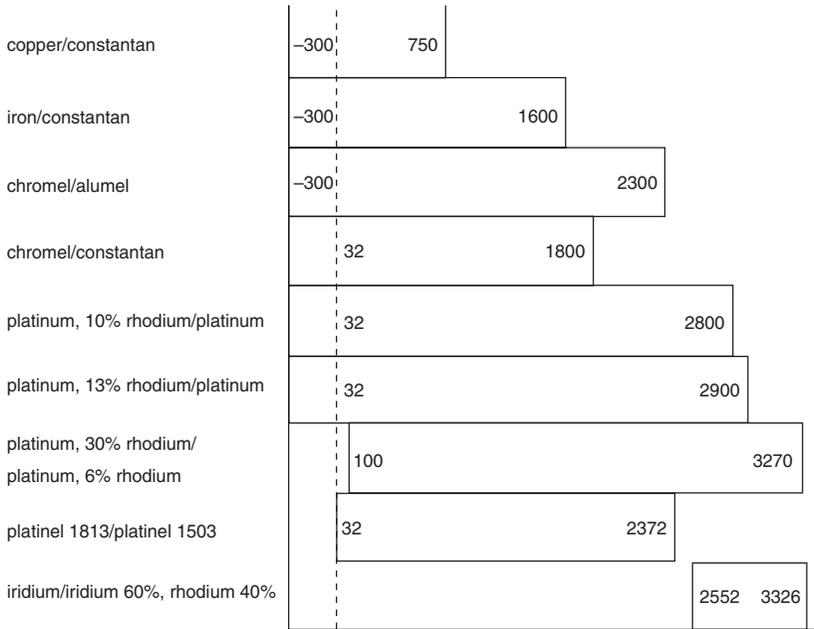


Figure 19-12. Ranges of various thermocouples.

Resistive Thermal Detectors

RTDs determine temperature by measuring the change in resistance of an element due to temperature. Platinum is generally utilized in RTDs because it is mechanically and electrically stable, resists contamination, and can be highly refined. The useful range of platinum RTDs is $-454-1832^{\circ}\text{F}$ ($-270-1000^{\circ}\text{C}$). Since the temperature is determined by the resistance in the element, any type of electrical conductor can be utilized to connect the RTD to the indicator; however, an electrical current must be provided to the RTD. A properly designed temperature monitoring system utilizing RTDs can be accurate to $\pm 0.02^{\circ}\text{F}$ ($\pm 0.01^{\circ}\text{C}$).

Pyrometers

The use of pyrometers in control of the advanced gas turbines is being investigated. Presently all turbines are controlled based on gasifier turbine exit temperatures or power turbine exit temperatures. By measuring the

blade metal temperatures of the first stage nozzles and blades, the gas turbine is being controlled at its most important parameter. In this manner, the turbine is being operated at its real maximum capability.

Gas turbines can be ordered with ports for pyrometer measurements of the first stage nozzle and blades. Pyrometers have been able to detect which blade is running hot. In a particular case a blade was found to be running about 50 °F (28 °C) hotter than the rest of the blades. The blade upon inspection was found to have its cooling passages blocked. This led to the manufacturer changing their inspection techniques.

Pressure Measurement

Almost all gas turbines are equipped with pressure-measuring devices of some type, although the number and location may vary. These transducers consist of a diaphragm and strain gauges. When pressure is applied, the deformation of the diaphragm is measured by the strain gauges. The resulting output signal varies linearly with pressure changes over the operating range.

Because of temperature constraints, the transducers, which usually do not operate above 350 °F (177 °C) are located outside the engine. A probe is then located inside to direct the air to the transducer. Most manufacturers provide probes to measure the compressor inlet pressure, compressor exit pressure, and the turbine exhaust pressure. These probes are usually located along the shroud of the machine, and therefore, the pressure readings may be slightly in error due to boundary-layer effects.

In addition to these standard locations, it is recommended that probes be located at each bleed chamber in the compressor and on each side of the air filter. These new locations are not intended to measure the unit performance, but are used to diagnose problem areas.

By using dynamic pressure probes in the bleed chamber, it is possible to detect tip stall. A pressure rake at the compressor exit enables accurate readings of exit pressure and is also helpful in the diagnosis of compressor stall.

Pressure transducers must be located outside of the engine because of temperature constraints. A pressure transducer can typically withstand temperatures up to 350 °F (177 °C), which is quite low with respect to the temperature of the points to be measured. The electrical output of the transducer will be in the mV/V range and therefore must be amplified and conditioned for interfacing to the monitor system. The locations are as follows:

1. *Compressor inlet.* Unit is constructed of Chromel-Alumel (nickel alloy) and characterized by an exposed junction consisting of a bare wire with ceramic insulation. One unit is required here.

2. *Compressor discharge.* Same as compressor inlet thermocouples. One or two units required in this area.
3. *Turbine inlet temperature.* Thermocouple is constructed of platinum-platinum rhodium with the junction enclosed with ceramic insulation. Typically, 9–12 units are required at this stage.
4. *Turbine exhaust.* Thermocouple is constructed of Chromel-Alumel with an exposed junction. Nine to 12 units are required at this stage.

Vibration Measurement

Vibration measurement is described in detail in Chapter 16. To monitor a machine for vibration problems, the use of displacement probes, velocity pickups, and accelerometers must be used to describe fully the mechanical behavior of a machine. Displacement probes measure the movement of the shaft at the location of the probe. They cannot be used very successfully to measure shaft bending away from the probe location. Displacement probes can indicate problems such as unbalance, misalignment, and some subsynchronous vibration instabilities such as oil whirl and hysteretic whirl. Accelerometers, since they are mounted on the casing, pick up the spectrum vibration problems which are transmitted from the shaft to the casing. Accelerometers are used to diagnose many problems, especially those that have a high frequency response, such as blade flutter, dry frictional whirl, surge, and gear teeth wear. Velocity pickups are used for their flat response of amplitude as a function of frequency as a go/no-go device. This means that the setting to alert the operator can be the same regardless of the speed of the unit. The role of velocity probes as a diagnostic tool is somewhat limited. The velocity pickups are very directional—they read different values for the same force if the probe is placed in a different direction.

Charts are available to convert from one type of measurement to another as shown in Figure 19-13. Many of these charts also show approximate vibration limits. The charts demonstrate the independence of velocity measurements relative to frequency, except at very low and very high frequencies where the amplitude limits are constant throughout the operating speed range. These limits are approximate—the type of machinery, casing, foundation, and bearings must be considered to determine final vibration limits.

Vibration Instrumentation Selection

The type of vibration instrumentation, its frequency ranges, its accuracy, and its location within, or on the machine, must be carefully analyzed with

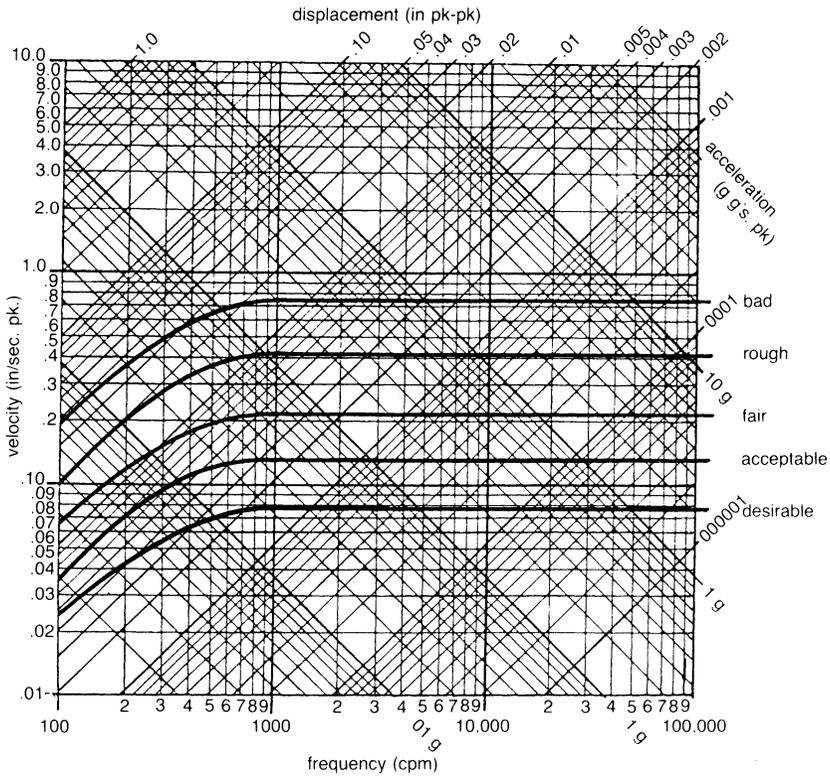


Figure 19-13. Vibration nomograph and severity chart. (Courtesy of IRD Mechanical Analysis, Inc.)

respect to the diagnostics required to be achieved. These guidelines have been previously discussed.

The displacement noncontacting eddy current sensor is most effective for monitoring and measuring vibrations near rotational and subrotational speeds. While the displacement sensor is capable of measuring vibration frequencies of more than 2 kHz, the amplitude of vibrational displacement levels that occur at frequencies above 1 kHz are extremely small, and are usually lost or buried in the noise level of the readout system. The acceleration sensor is best suited for measurements at high frequencies, such as blade-passing and gear-meshing frequencies; however, the signals at one rotational speed are usually at low acceleration levels, and may be lost in the noise level of the measurement system monitoring. Low-pass filtering and additional

amplification stages may, therefore, be necessary to bring out the rotational speed signals when measurements are made with accelerometers.

Velocity sensors, because of their limited operational frequency range (usually) from 10 Hz to 2 kHz, are not recommended for application in a diagnostic system for high-speed machinery. Velocity sensors have moving elements and are subject to reliability problems at operational temperatures of more than 250 °F (121 °C). Gas turbine engine casing temperatures are usually in the 500 °F (200 °C) level or above; hence, sensor locations must be carefully examined for temperature levels. Accelerometers for these higher temperatures are more easily available than velocity sensors. At these elevated operational temperatures, high-frequency accelerometers (20 kHz and above) are available from only a few selected manufacturers.

Selection of Systems for Analyses of Vibration Data

The overall vibration level on a machine is satisfactory for an initial or rough check. However, when a machine has a seemingly acceptable overall level of vibration, there may be hidden under this level some small levels of vibrations at discrete frequencies that are known to be dangerous. An example of this is subsynchronous instabilities in a rotor system.

In the analysis of vibration data there is often the need to transform the data from the time domain to the frequency domain or, in other words, to obtain a spectrum analysis of the vibration. The original and inexpensive system to obtain this analysis is the tuneable swept-filter analyzer. Because of inherent limitations of this system, this process, despite the use of automated sweep, is time-consuming when analyzing low frequencies. When the spectra data needs to be digitized for computer inputting, there are further limitations in capability of tuneable filter-analysis systems.

Real-time spectrum analyzers using “time compression” or the “fast Fourier transform” (FFT) techniques are used extensively for performing vibration spectrum analysis in computerized diagnostic systems. The FFT analyzers use digital-signal processing, and hence are easier to integrate with the modern digital computer. FFT analyzers are often hybrids using micro-processors and FFT-dedicated circuitry.

The FFT can be implemented in a computer using the FFT algorithm for obtaining a pure mathematical computation. While this computation is an error-free process, its implementation in a digital computer can introduce several errors. To avoid these errors, it is essential to provide signal conditioning upstream of the computer. Such signal conditioning minimizes the errors, such as aliasing and signal leakage introduced in sampling and digitizing the time domain. Such signal conditioning systems will introduce

considerable expense and complexity in effecting the mathematical FFT in a computer. The computerized FFT is also slower than a dedicated FFT analyzer. It also has limitations in frequency resolution. Hence, the use of a dedicated FFT analyzer is considered to be the most reliable and cost-effective means for performing frequency spectrum analysis and plots in a computerized system for machinery diagnostics.

Careful analysis must be made of the type of spectrum analysis systems and the computational techniques used in vibrational analysis. There are several factors that must be considered, some of which are:

1. Frequency analysis ranges
2. Single or multichannel analysis
3. Dynamic range
4. Accuracy of measurements necessary
5. Speed at which analyses are required to be made
6. System portability, especially if the analysis system is required for both lab and field use
7. Ease of integration with the host computer system

Auxiliary System Monitoring

Fuel System

Since the reliability of gas turbines in the power industry has been lower than desired in recent years because of hot-corrosion problems, techniques have been developed to detect and control the parameters that cause these problems. By monitoring the water content and corrosive contaminant in the fuel line, any changes in fuel quality can be noted and corrective measures initiated. The concept here is that Na contaminants in the fuel are caused from external sources such as seawater; thus, by monitoring water content, Na content is automatically being monitored. This on-line technique is adequate for lighter distillate fuels. For heavier fuels, a more complete analysis of the fuel should be carried out at least once a month using the batch-type system. The data should be input directly to the computer. The water and corrosion detecting systems also operate in conjunction with the batch analysis for the heavier fuels.

A Btu meter may be used in the fuel-quality system as an aid in determining turbine system efficiency. A water capacitance probe is used for detection of water in the fuel line. A water-detecting device can be incorporated into the corrosion monitoring system. This monitoring device is based on detection of changes in the dielectric constant of unknown fluid components

passing through the probe. This device provides continuous and instantaneous monitoring of the percentage of water suitable for quality or process control.

The sensor itself is based on a balanced capacitance bridge detection principle, utilizing a high-frequency oscillator with a closed-loop servo-amplitude control to assure that loading or variation in supply voltage does not affect the stability and accuracy of this instrument. Output from the bridge is directly coupled to a preamplifier to step up the detected signal to a desired level and, also, to correct for nonlinear characteristics of the water measurement. This measurement is achieved through a nonlinear feedback loop.

The corrected and amplified output is then directly coupled to a constant-current amplifier, which can provide 0–5 mA or 4–20 mA output. This type of signal termination allows the detector system to be located at a distance from the measuring point for ease of usage. This water detection system offers: (1) an accurate means of water measurement, (2) easy installation and minimum maintenance, (3) a simple two-step calibration procedure, and (4) long-term stability and dependable service.

A corrosion probe is used to monitor the corrosive condition of the fuel. This can be accomplished with a special probe which can detect metal in the lubricant.

A Btu meter is used to determine the fuel heating rate. The Btu meter is a capacitance device ideally suited to real-time on-line Btu measurement of gas turbine liquid fuel, such as naphtha, that is a valuable asset in determining turbine efficiency.

Torque Measurement

This measurement can be accomplished by using a mechanical system or various types of electronic systems. All of these systems are expensive and in many cases require repeated calibration. The mechanical system (Figure 19-14) is a three-gear, phase-related system which measures the displacement between two gears and the proportionate shaft twist. A third gear is situated so that any variations other than shaft twist will occur in the first two gears. This signal is used to eliminate errors caused by these variations.

Baseline for Machinery

Mechanical baseline. The vibration baseline for a machine can be defined as the normal or average operating condition of a machine. It can be represented on a vibration spectrum plot showing vibration frequency on

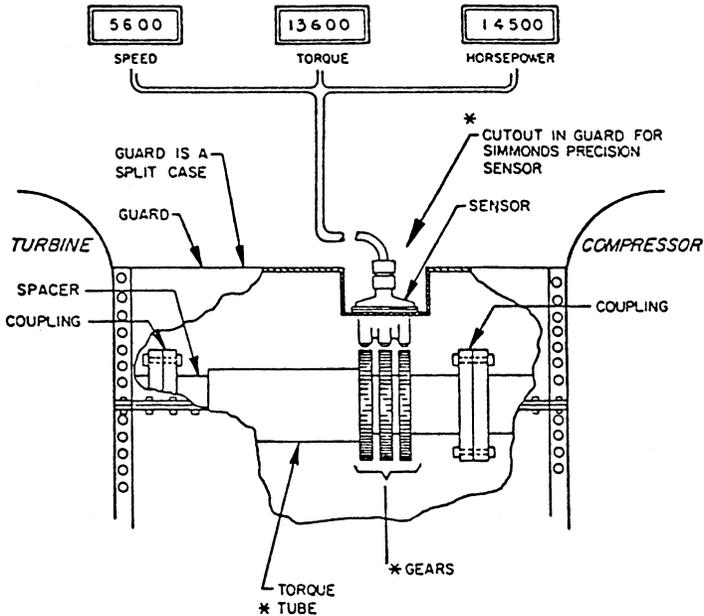


Figure 19-14. Torque meter for a gas turbine.

the X -axis and vibration amplitude (peak-to-peak displacement, peak velocity, or peak acceleration) on the Y -axis. Since the vibration spectrum will be different at different positions, the spectrum must be associated with a specific measurement position or sensor location on the machine. When portable vibration measurement equipment is used, it is essential to ensure that the sensor is relocated at exactly the same point on the machine each time vibration readings are taken. Changes of baseline with machine speed and process conditions should be investigated and, where necessary, baseline should be generated for set ranges of speeds and process conditions. When the operating vibration levels exceed the baseline levels beyond set values, an alert signal should be activated for investigation of this condition.

Aerothermal baseline. In addition to the vibration baseline spectrum, a machine also has an aerothermal performance baseline, or its normal operating point on the aerothermal characteristic. Significant deviation of the operating point beyond its base point should generate alert signals.

When a compressor operates beyond its surge margin, a danger alert should be activated. A typical compressor characteristic is presented in Figure 19-15. Some of the other monitoring and operating outputs are loss

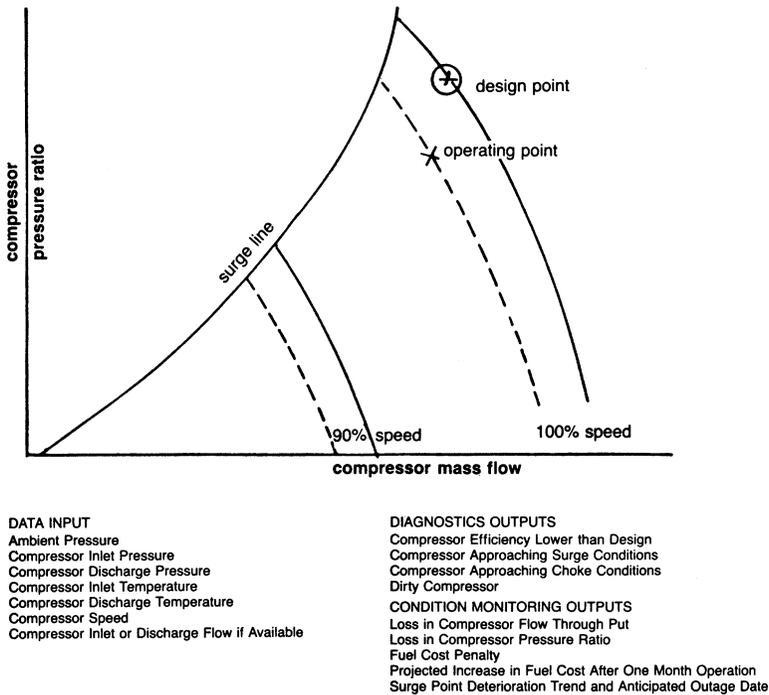


Figure 19-15. Aerothermal condition monitoring for compressors.

in compressor flow, loss in pressure ratio, and increase in operating fuel cost due to, for instance, operating at off-design conditions or with a dirty compressor.

Since aerothermal performance of compressors and turbines is very sensitive to inlet temperature and pressure variations, it is essential to normalize the aerothermal performance parameters such as flow, speed, horsepower, etc., to standard-day conditions. When these corrections to standard conditions are not applied, a performance degradation may appear to occur when in fact it was a performance change resulting merely from ambient pressure and temperature changes. Some of the equations for obtaining correction to standard-day conditions are given in Table 19-3.

Data Trending

The data received should first be corrected for sensing errors. This usually consists of sensor calibration correction.

Table 19-3
Gas Turbine Aerothermal Performance Equations
for Correction to Standard-Day Conditions

| Factors for Correction to Standard-Day Temperature & Pressure Conditions | |
|---|----------------|
| Assumed standard-day pressure | 14.7 psia |
| Assumed standard-day temperature | 60 °F (520 °R) |
| Conditions of test | |
| Inlet temperature | T_i °R |
| Inlet pressure | P_i psia |
| Corrected compressor discharge temperature = (Observed temperature) $(520/T_i)$ | |
| Corrected compressor discharge pressure = (Observed pressure) $(14.7/P_i)$ | |
| Corrected speed = (Observed speed) $\sqrt{520/T_i}$ | |
| Corrected air flow = (Observed flow) $(14.7/P_i) \sqrt{T_i/520}$ | |
| Corrected horsepower = (Observed power) $(14.7/P_i) \sqrt{T_i/520}$ | |

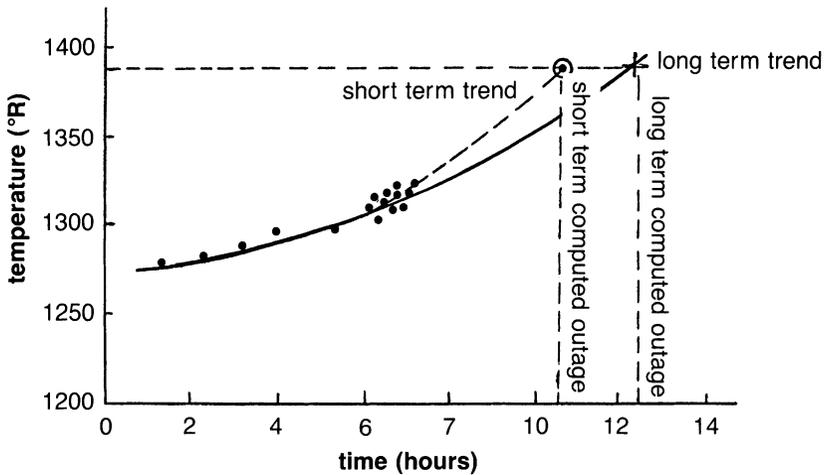


Figure 19-16. Temperature versus expected outage time.

The trending technique essentially involves evaluating the slope of a curve derived from the received data. The slope of the curve is calculated for both a long-term trend, about 168 hours, and a short-term trend, based on the last 24 hours. If the short-term slope deviates from the long-term slope beyond a set limit, it means that the rate of deterioration is changed, and the maintenance schedule will be affected. Thus, the program might take into account

the biasing of the long-term slope by the short-term slope. Figure 19-16 shows a schematic of this type of trending. Numerous statistical techniques are available for trending.

Trended data is used to obtain predictions that are helpful in the scheduling of maintenance. Referring to Figure 19-17, for example, it is possible to estimate when compressor cleaning will be necessary. This figure was prepared by recording the compressor exit temperature and pressure each day. These points are then joined, and a dotted line is projected to predict when

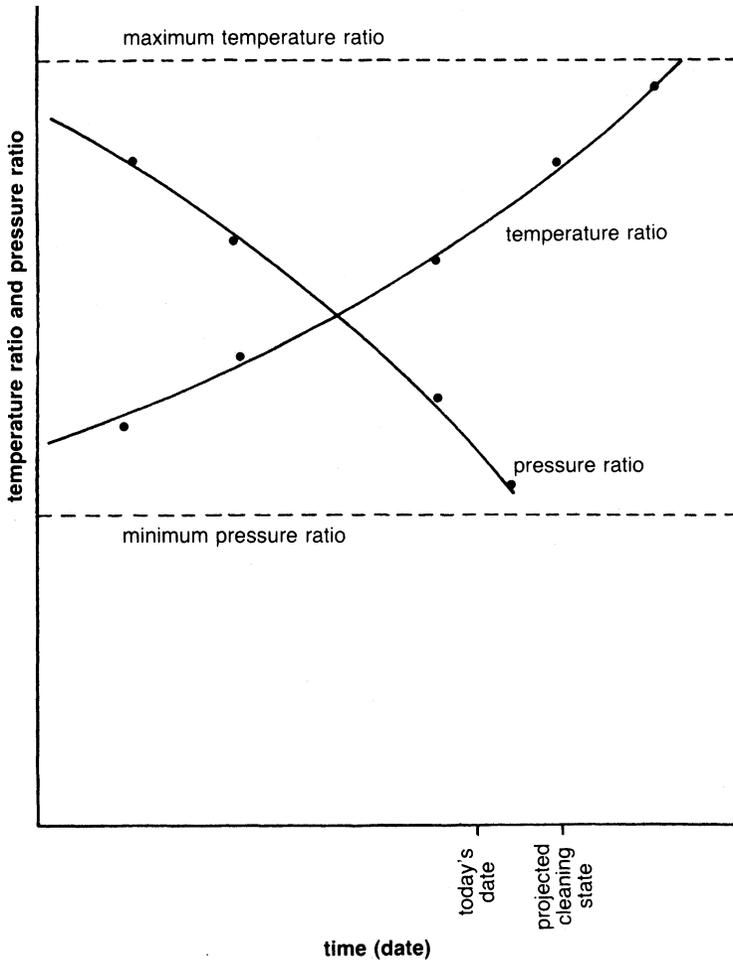


Figure 19-17. Data trending to predict maintenance schedules.

cleaning will be required. In this case, two parameters were monitored, but since their rates differed, the cleaning was based on the first parameter to reach the critical point. However, using a trend of both temperature and pressure provides a cross check on the validity of the diagnostics.

The Gas Turbine

The new gas turbines are the cornerstone of the rise of the combined cycle as the power source of the new millennium, and for many other drives for petrochemical plants. The new gas turbines have a very high-pressure ratio, a high-firing temperature, and in some cases, a reheat burner in the gas turbine. The gas turbines also have new dry low NO_x combustors. The combination of all these components has dramatically increased the thermal efficiency of the gas turbine. The gas turbine since the early 1960s has gone from efficiencies as low 15–17% to efficiencies around 45%. This has been due to the pressure ratio increase from around 7:1 to as high as 30:1, and an increase in the firing temperature from about 800 °C to about 1350 °C. With these changes, we have also seen the efficiency of the major components in the gas turbine increase dramatically. The gas turbine compressor efficiency increased from around 78–87%; the combustor efficiency from about 94–98%, and the turbine expander efficiency from about 84–92%.

The increase in compressor pressure ratio decreases the operating range of the compressor. The operating range of the compressor stretches from the surge line at the low flow end of the compressor speed line to the choke point

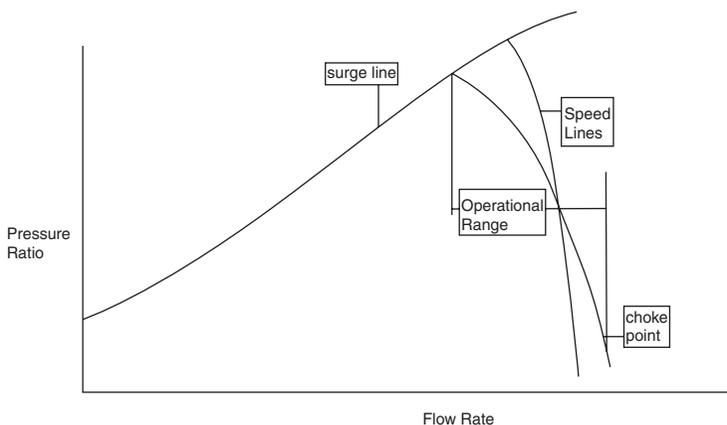


Figure 19-18. Performance map of an axial flow compressor used in most gas turbines.

Table 19-4
Effect of Various Parameters on the Output and Heat Rate

| Parameters | Parameter Change | Power Output (%) | Heat Rate Change (%) |
|---------------------------------------|---|------------------|----------------------|
| Ambient temperature | 20° F (11° C) | -6.5 | 2 |
| Ambient pressure | 4 in. H ₂ O 0.15 psi 10 mbar | 0.9 | 0.9 |
| Ambient relative humidity | 10% | -0.0002 | 0.0005 |
| Pressure drop in filter | 1 in. WC 25mm. WC | -0.5 | -0.3 |
| Increase in gas turbine back pressure | 1 in. WC 25mm. WC | -0.25 | -0.08 |

at the high flow end. As seen in Figure 19-18 the lower pressure speed line has a larger operational range than the higher-pressure speed line. Therefore, the higher-pressure ratio compressors are subject to fouling, and can result in surge problems or blade excitation problems, which lead to blade failure.

The drop in pressure ratio at the turbine inlet due to filter fouling amounts to a substantial loss in the turbine overall efficiency and the power produced. An increase in the pressure drop of about 1 in. (25 mm). WC, amounts to a drop of about 0.3% reduction in power. Table 19-4 shows the approximate changes that would occur for changes in ambient conditions; the fouling of the inlet filtration system and the increase in back pressure on the gas turbine in a combined cycle mode. These modes were selected because these are the most common changes that occur on a system in the field. It must be remembered that these are just approximations and will vary for individual power plants.

The gas turbine has to be operated at a constant speed since this is used for power generation, and any slight variation in speed could result in major problems for the grid. Thus, the control of the load has to be by controlling the fuel input, therefore the turbine firing temperature, and the inlet guide vane position, thus controlling the airflow. The effect of this is to try and maintain the exhaust temperature from the gas turbine at a relatively high value, especially in combined cycle or cogeneration plants, since this gas is used in the HRSG, and the effectiveness of the HRSG is dependent on maintaining this temperature.

The effect of compressor fouling is also very important on the overall performance of the gas turbine since it uses nearly 60% of the work generated by the gas turbine. Therefore, a 1% drop in compressor efficiency equates to nearly a 0.5% in the gas turbine efficiency and about a 0.3% drop in the overall cycle efficiency. The cleaning of these blades by on line

water washing is a very important operational requirement. In many plants, this operational procedure has contributed literally hundreds of thousands of dollars to the bottom line of the plant. It has been the experience of many plants that washing using de-mineralized water is as effective as using a detergent in on-line water wash. The practice of using abrasive cleaning by injecting walnut shells, rice, or spent catalyst is being suspended in most new plants. Where it is used, it must be carefully evaluated; rice for instance is a very poor abrasive since it shatters and tends to get into seals and bearings and into the lubrication system. Walnut shells should never be used since they tend to collect inside the HRSG system and in some cases have been noted to catch on fire. On-line water washing is not the answer to all the problems since after each wash the full power is not regained, therefore a time comes when the unit needs to be cleaned off-line. The time for off-line cleaning must be determined by calculating the loss of income in power as well as the cost of labor to do so and equate it against the extra energy costs.

The cleaning of the hot section turbine nozzles is a major problem in turbines, which use heavy liquid fuels with high vanadium content. To counteract the vanadium the fuel is treated with the addition of magnesium, which is supposed to mix with the vanadium and results in harmless fly ash. The problem occurs due to the fact that the fly ash gets collected in the turbine nozzles and reduces the turbine nozzle areas. This can be a very major problem since it collects at the rate of 5–12% per 100 hours of operation.

The life of the various hot section components of the gas turbine depends on the following operational parameters:

1. *Type of fuel.* Natural gas is the base fuel against which all other fuels are measured. The use of diesel fuel reduces the average life by about 25%, and the use of residual fuel reduces life by as much as 65%.
2. *Type of service.* Peaking service tends to reduce life by as much as 20% as compared to base load operation.
3. *Number of starts.* Each start is equivalent to about 50 hours of operation.
4. *Number of full load trips.* This is very hard on the turbine and is nearly equivalent to about 400–500 hours of operation.
5. *Type of material.* The properties of the blade and nozzle vanes are a very important factor. The new blade materials, which are the single crystal structures, have done much to help the life of these blades in the higher temperatures, which are used in these new turbines. It must be remembered that if more than about 8% of the air is used in cooling than the advantage of going to higher temperatures is lost.

The Larson-Miller parameters, which describe an alloy's stress rupture characteristics over a wide range of temperature, life, and stress, is very useful in comparing the elevated temperature capabilities of many alloys.

6. *Types of coatings.* The use of coatings in both compressor and turbines has extended the life of most of the components. Coatings are also being used on combustor liners. The new overlay coatings are more corrosion-resistant as compared to the old diffusion coatings. The coatings of the compressor are now more prevalent especially since some of the new compressors are operating at very high-pressure ratios, which translate into high exit temperatures from the compressor. Compressor coatings also tend to reduce the frictional losses and can have a very rapid payback.

Identification of Losses

The losses that are encountered in a plant can be divided into two groups, uncontrollable losses, and controllable losses. The uncontrollable losses are usually environmental conditions, such as temperature, pressure, humidity, and turbine aging. The controllable losses are those that the operator can have some degree of control over and can take corrective actions:

1. *Pressure drop across the inlet filter.* This can be remedied by cleaning or replacing the filter.
2. *Compressor fouling.* On-line water cleaning can restore part of the drop encountered.
3. *Fuel lower heating value.* In many plants, on-line fuel analyzers have been introduced to not only monitor the turbine performance but to also calculate the fuel payments, which are usually based on the energy content of the fuel.
4. *Turbine back pressure.* In this case, the operator is relatively limited since he cannot do anything about the downstream design. If there is some obstruction in the ducting to the HRSG that can be removed or if the duct has collapsed in an area the duct could be replaced.

Compressor Aerothermal Characteristics and Compressor Surge

Figure 19-19 shows a typical performance map for a centrifugal compressor, showing efficiency islands and constant aerodynamic speed lines. The total pressure ratio can be seen to change with flow and speed. Usually

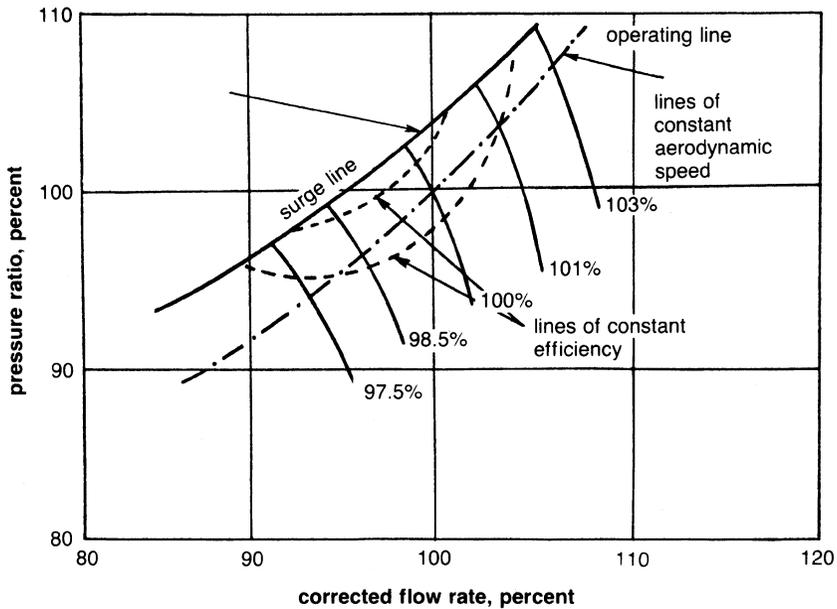


Figure 19-19. Typical compressor map.

compressors are operated on a working line separated by some safety margin from the surge line.

Compressor surge is essentially a situation of unstable operation and should, therefore, be avoided in both design and operation. Surge has been traditionally defined as the lower limit of stable operation of a compressor and involves the reversal of flow. This reversal of flow occurs because of some kind of aerodynamic instability within the system. Usually, it is a part of the compressor that is the cause of the aerodynamic instability, though it is possible that the system arrangement could be capable of magnifying this instability.

Usually, surge is linked with excessive vibration and an audible sound; yet, there have been cases in which surge problems, which are not audible, have caused failures.

Failure Diagnostics

Problem evaluation in turbomachinery is complex, but with the aid of performance and mechanical signals, solutions can be found to diagnose various types of failures. This is done by using several inputs and a matrix. A sample of some of the problems are given in the next few sections.

Compressor Analysis

Compressor analysis is done by monitoring the inlet and exit pressures and temperatures, the ambient pressure, vibration at each bearing and the pressure and temperature of the lubrication system. Table 19-5 shows the effect various parameters have on some of the major problems encountered in a compressor. Monitoring these parameters allows the detection of:

1. *Clogged air filter.* A clogged air filter may be detected by noting an increase in the pressure drop through the filter.
2. *Compressor surging.* Surge may be detected by noting a rapid increase in shaft vibration, along with a discharge pressure instability. If more than one stage is present, the probes located within the bleed air chambers are useful in locating the problem stage by checking for pressure fluctuations.
3. *Compressor fouling.* This is indicated by a decrease in pressure ratio and flow accompanied by an increase of exit temperature with time. The change in the temperature and pressure ratio tend to show a decrease in efficiency. If a change in vibration has occurred, the fouling is critical, since it indicates excessive build up of deposits on the rotor.
4. *Bearing failure.* Symptoms of bearing trouble include a loss of lubrication pressure, an increase in the temperature difference across the bearing, and an increase in vibration. If oil whirl or other bearing instabilities are present, there will be a vibration at subsynchronous frequency.

Table 19-5
Compressor Diagnostics

| | η_c | P_2/P_1 | T_2/T_1 | Mass Flow | Vibration | ΔT Bearing | Bearing Pressure | Bleed Chamber Pressure |
|-----------------|----------|-----------|-----------|-----------|--------------------|--------------------|------------------|------------------------|
| Clogged filter | | ↓ | | ↓ | | | | |
| Surge | ↑ | Variable | | ↓ | Highly fluctuating | ↑ | ↑ | Highly fluctuating |
| Fouling | ↓ | ↓ | ↑ | ↓ | ↑ | | | |
| Damaged blade | ↓ | ↓ | ↑ | ↓ | ↑ | | | Highly fluctuating |
| Bearing failure | | | | | ↑ | ↑ | ↓ | |

Combustor Analysis

In the combustor, the only two parameters that can be measured are fuel pressure and evenness of combustion noise. Turbine inlet temperatures are not usually measured due to very high temperatures and limited probe life. Table 19-6 shows the effect of various parameters on important functions of the combustor.

Table 19-6
Combustor Diagnostics

| | Fuel Pressure | Unevenness of Combustion (Sound) | Exhaust Temperature Spread | Exhaust Temperature |
|---------------------------|---------------|----------------------------------|----------------------------|---------------------|
| Clogging | ▲ | ▲ | ▲ | ▲ |
| Combustor fouling | ▲ or ▼ | ▲ | ▲ | ▼ |
| Crossover tube failure | ▲ or ▼ | — | ▲ + | — |
| Detached or cracked liner | ▲ or ▼ | ▲ | ▲ | — |

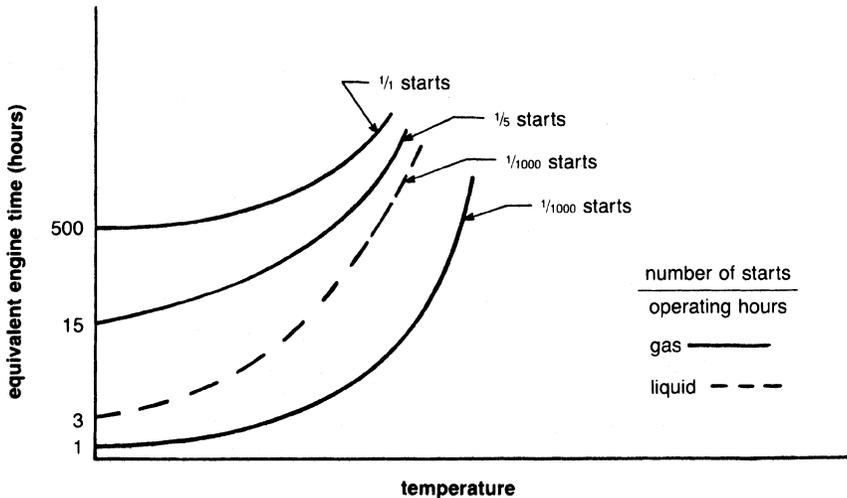


Figure 19-20. Equivalent engine time in the combustor section.

The measurement of the two parameters allows the detection of:

1. *Plugged nozzle*. This is indicated by an increase in fuel pressure in conjunction with increased combustion unevenness. This is a common problem when residual fuels are used.
2. *Cracked or detached liner*. This is indicated by an increase in an acoustic meter reading and a large spread in exhaust temperature.
3. *Combustor inspection or overhaul*. This is based on equivalent engine hours, which are based on the number of starts, fuel, and temperature. Figure 19-20 shows the effect of these parameters on the life of the unit. Note the strong effect that fuel and number of starts has on the life.

Turbine Analysis

To analyze a turbine, it is necessary to measure pressures and temperatures across the turbine, shaft vibration, and the temperature and pressure of the lubrication system. Table 19-7 shows the effect various parameters have on important functions of the turbines. Analysis of these parameters will aid in the prediction of:

1. *Turbine fouling*. This is indicated by an increase in turbine exhaust temperature. Change in vibration amplitude will occur when fouling is excessive and causes rotor imbalance.
2. *Damaged turbine blades*. This results in a large vibration increase accompanied by an increase in the exhaust temperature.
3. *Bowed nozzle*. The exhaust temperature will increase, and there may be an increase in turbine vibration.

Table 19-7
Turbine Diagnosis

| | η_t | P_3/P_4 | T_3/T_4 | Vibration | ΔT Bearing | Cooling Air Pressure | Wheel Space Temperature | Bearing Pressure |
|------------------------|----------|-----------|-----------|-----------|-----------------------|----------------------------|-------------------------------|---------------------|
| Fouling | ↓ | | ↓ | ↑ | | | ↑ | |
| Damaged blade | ↓ | | ↓ | ↑ | | | | |
| Bowed nozzle | ↓ | ↓ | ↓ | ↑ | | | ↑ | |
| Bearing failure | | | | ↑ | ↑ | | | ↓ |
| Cooling air failure | | | | | ↑ | ↓ | ↑ | |

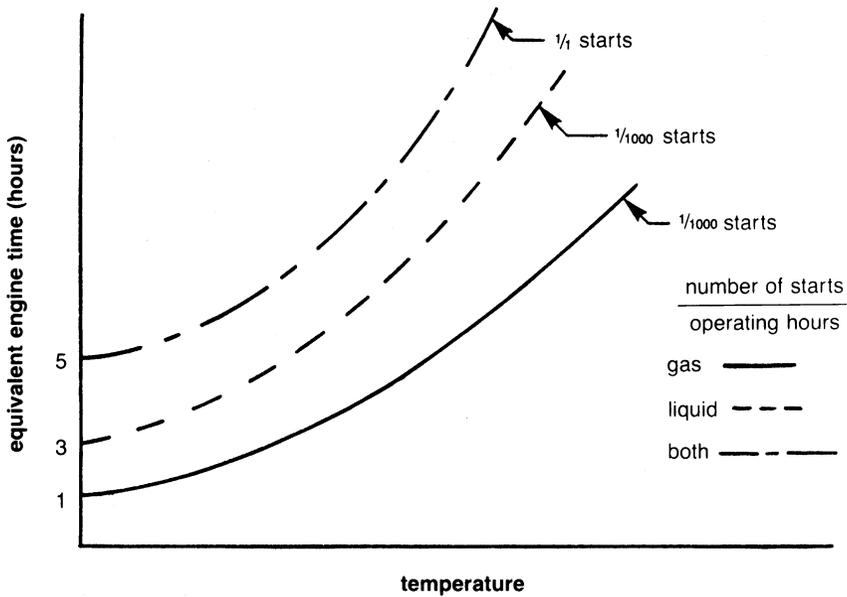


Figure 19-21. Equivalent engine time in the turbine section.

4. *Bearing failure.* The symptoms of bearing problems for a turbine are the same as for a compressor.
5. *Cooling air failure.* Problems associated with the blade cooling system may be detected by an increase in the pressure drop in the cooling line.
6. *Turbine maintenance.* This should be based on “equivalent engine time,” which is the function of temperature, type of fuel used, and number of starts. Figure 19-21 shows the correction that can be applied to running hours for intermittent-duty units with high-start/stop operation.

Turbine Efficiency

1. With the current high cost of fuel, very significant savings can be achieved by monitoring equipment operating efficiencies and correcting for operational inefficiencies. Some of these operational inefficiencies may be very simple to correct, such as washing or cleaning of the compressor on a gas turbine unit. In other cases, it may be necessary to develop a load-distribution program that achieves maximum overall efficiency of the plant equipment for a given load demand.

2. Figure 19-22 shows the significant dollar cost penalties that occur when operating a turbine at a very small percentage efficiency degradation.
3. Table 19-8 shows a load-distribution program for an 87.5-MW power station of steam turbines and gas turbines. The selection of equipment and their loading for the most efficient operation can be programmed when the efficiency of individual units are monitored. The program

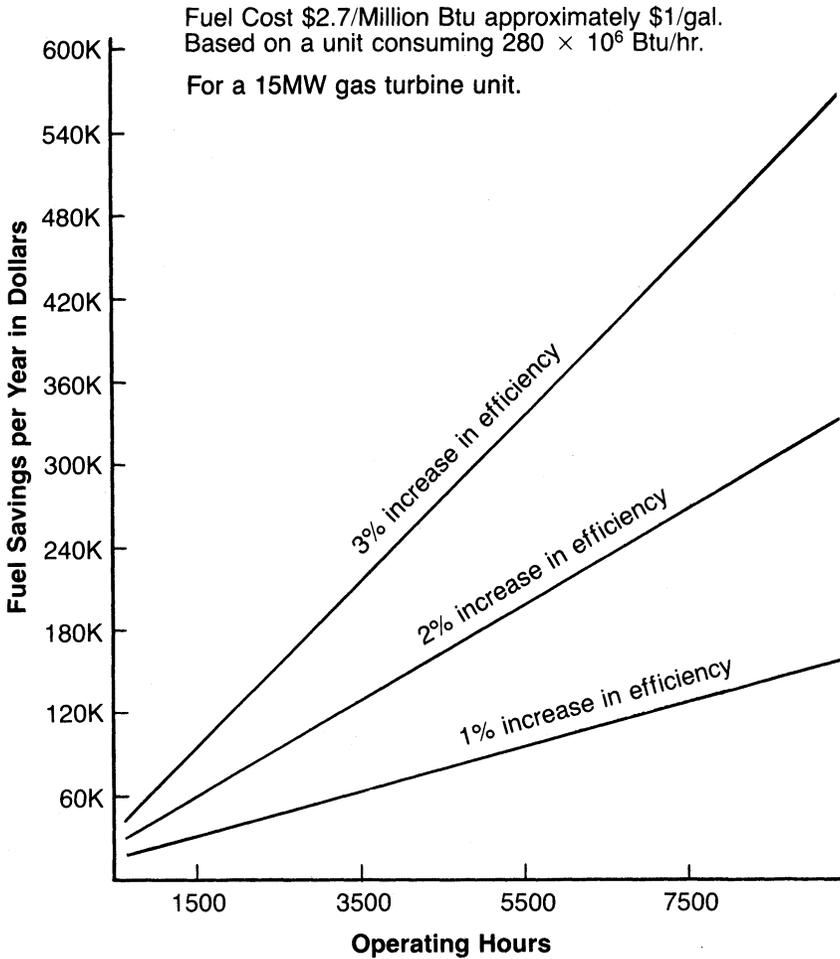


Figure 19-22. Savings versus efficiency.

**Table 19-8
Load Sharing Program Description of Utility Plant Units**

| Unit # | Design MW | Turbine Type | Efficiency at Design Output Point |
|--------|-----------|--------------|-----------------------------------|
| 1 | 2.5 | Steam | 22 |
| 2 | 2.5 | Steam | 22 |
| 3 | 5.0 | Steam | 24 |
| 4 | 5.0 | Steam | 24 |
| 5 | 5.0 | Steam | 24 |
| 6 | 7.5 | Steam | 25 |
| 7 | 15.0 | Steam | 30 |
| 8 | 15.0 | Steam | 23 |
| 9 | 15.0 | Gas | 21 |
| 10 | 15.0 | Gas | 21 |

**Combination of Units of Yield Efficient Power
Load Distribution for Different Demand Loads**

| Total Demand = | | 30.00 MW | Total Demand = | | 50.00 MW |
|--|-------|----------|------------------------------------|-------|----------|
| Total Output Supplied = | | 30.00 MW | Total Output Supplied = | | 50.00 MW |
| Units not working = | | 1 4 9 0 | Units not working = | | 1 4 0 0 |
| Unit 1 = | 0.00 | 0.00 | Unit 1 = | 0.00 | 0.00 |
| Unit 2 = | 0.00 | 0.00 | Unit 2 = | 2.50 | 22.01 |
| Unit 3 = | 2.50 | 21.00 | Unit 3 = | 5.00 | 24.50 |
| Unit 4 = | 0.00 | 0.00 | Unit 4 = | 0.00 | 0.00 |
| Unit 5 = | 5.00 | 24.50 | Unit 5 = | 5.00 | 24.50 |
| Unit 6 = | 7.50 | 25.19 | Unit 6 = | 7.50 | 25.19 |
| Unit 7 = | 15.00 | 29.91 | Unit 7 = | 15.00 | 29.81 |
| Unit 8 = | 0.00 | 0.00 | Unit 8 = | 0.00 | 0.00 |
| Unit 9 = | 0.00 | 0.00 | Unit 9 = | 0.00 | 0.00 |
| Unit 10 = | 0.00 | 0.00 | Unit 10 = | 15.00 | 21.00 |
| Maximum Overall Efficiency = 27.04 | | | Maximum Overall Efficiency = 25.02 | | |
| Power Demands = MW (Maximum demand = 87.5) | | | | | |

selects the units that should be operated to provide the powerload demand at the maximum overall efficiency of the combination of units.

Mechanical Problem Diagnostics

The advent of new, more reliable, and sensitive vibration instrumentation such as the eddy-current sensor and the accelerometer coupled with modern

technology analysis equipment (the real-time vibration spectrum analyzer and low-cost computers) gives the mechanical engineer very powerful aids in achieving machinery diagnostics.

A chart for vibration diagnosis is presented in Table 19-9. While this is a general criterion or rough guideline for diagnosis of mechanical problems, it can be developed into a very powerful diagnostic system when specific problems and their associated frequency domain vibration spectra are

Table 19-9
Vibration Diagnosis

| Usual Predominant Frequency* | Cause of Vibration |
|-------------------------------------|---|
| Running frequency at 0–40% | Loose assembly of bearing liner, bearing casing, or casing and support Loose rotor shrink fits Friction-induced whirl Thrust bearing damage |
| Running frequency at 40–50% | Bearing-support excitation Loose assembly of bearing liner, bearing case, or casing and support Oil whirl Resonant whirl Clearance induced vibration |
| Running frequency | Initial unbalance Rotor bow Lost rotor parts Casing distortion Foundation distortion Misalignment Piping forces Journal & bearing eccentricity Bearing damage Rotor-bearing system critical Coupling critical Structural resonances Thrust-bearing damage |
| Odd frequency | Loose casing and support Pressure pulsations Vibration transmission Gear inaccuracy Valve vibration |
| Very high frequency | Dry whirl Blade passage |

*Occurs in most cases predominantly at this frequency; harmonics may or may not exist.

logged and correlated in a computerized system. With the extensive memory capability of the computer system, case histories can be recalled and efficient diagnostics achieved.

Data Retrieval

In addition to being valuable as a diagnostic and analysis tool, a data retrieval program also provides an extremely flexible method of data storage and recovery. By careful design of a health monitoring system, an engineer or technician can compare the present operation of a unit with the operation of the same machine, or of another machine, under similar conditions in the past. This can be done by selecting one or several limiting parameters and defining the other parameters that are to be displayed when the limiting parameters are met. This eliminates the necessity of sifting through large amounts of data. A few examples of how this system is used are:

1. *Retrieval by time.* In this mode, the computer retrieves data taken during a specified time period, thus enabling the user to evaluate the period of interest.
2. *Retrieval by ambient temperature.* The failure of a gas turbine may occur during an unusually hot or cold period, and the operator may wish to determine how his unit functioned at this temperature in the past.
3. *Retrieval by turbine exhaust temperature.* The exhaust temperature can be an important parameter in failure investigations. An analysis of this parameter in failure investigations. An analysis of this parameter can verify the existence of a problem with either the combustor or turbine.
4. *Retrieval by vibration levels.* Inspection of data provided by this mode can be useful in determining compressor fouling, compressor or turbine blade failure, nozzle bowing, uneven combustion, and bearing problems.
5. *Retrieval by output power.* In this mode, the user should input the output power range of interest and thus obtain only data applying to that particular power setting. In this manner, he has only to consider the pertinent data to pinpoint the problem areas.
6. *Retrieval by two or more limiting parameters.* By retrieving data with limits on several parameters, the data can be evaluated and will be even further reduced. Diagnostic criteria can then be developed.

Summary

1. The monitoring of turbomachinery mechanical characteristics, such as vibrations, has been applied extensively over the past decade. The advent of the accelerometer and the real-time vibration spectrum analyzer has required a computer to match and utilize the extensive analysis and diagnostic capability of these instruments.
2. The high cost for machinery replacements and downtime makes machinery operational reliability very important; however, with the current and projected increases in fuel costs, aerothermal monitoring has become very important. Aerothermal monitoring can provide not merely increased operational efficiency for turbomachinery but, when combined with mechanical monitoring, it provides an overall, more effective system than one that monitors only the mechanical functions or aerothermal functions.
3. While there had been concern about the reliability of computer systems, they are currently receiving wide acceptance and are fast replacing analog systems.
4. The systematized application of modern technology (instrumentation, both mechanical and aerothermal and low-cost computers) and turbo-machinery engineering experience will result in the development and application of cost-effective systems.

Bibliography

- ASME, *Gas Turbine Control and Protection Systems*, B133.4 Published: 1978 (Reaffirmed year: 1997).
- Boyce, M.P., Gabriles, G.A., Meher-Homji, C.B., Lakshminarasimha, A.N., and Meher-Homji, F.J., "Case Studies in Turbomachinery Operation and Maintenance Using Condition Monitoring," Proceeding of the 22nd Turbomachinery Symposium, Dallas, Texas. September 14–16, 1993, pp. 101–12.
- Boyce, M.P., and Herrera, G., "Health Evaluation of Turbine Engines Undergoing Automated FAA Type Cyclic Testing," Presented at the SAE International Ameritech '93, Costa Mesa, California, September 27–30, 1993, SAE Paper No. 932633.
- Boyce, M.P., Gabriles, G.A., and Meher-Homji, C.B., "Enhancing System Availability and Performance in Combined Cycle Power Plants by the Use of Condition Monitoring," European Conference and Exhibition Cogeneration of Heat and Power, Athens, Greece, November 3–5, 1993.

- Boyce, M.P., "Control and Monitoring an Integrated Approach," *Middle East Electricity*, December 1994, pp. 17–20.
- Boyce, M.P., "Improving Performance with Condition Monitoring"—*Power Plant Technology Economics and Maintenance*, March/April 1996, pp. 52–55.
- Boyce, M.P., and Venema, J., "Condition Monitoring and Control Center", *Power Gen Europe in Madrid*, Spain, June 1997.
- Boyce, M.P., and Cox, W.M., "Condition Monitoring Management-Strategy", *The Intelligent Software Systems in Inspection and Life Management of Power and Process Plants in Paris*, France, August 1997.
- Boyce, M.P., "How to Identify and Correct Efficiency Losses Through Modeling Plant Thermodynamics," *Proceedings of the CCGT Generation Power Conference*, London, United Kingdom, March, 1999.
- Boyce, M.P., "Condition Monitoring of Combined Cycle Power Plants," *Asian Electricity* July/August 1999, pp. 35–36.
- Meher-Homji, C.B., Boyce, M.P., Lakshminarasimha, A.N., Whitten, J.A., and Meher-Homji, F.J., "Condition Monitoring and Diagnostic Approaches for Advanced Gas Turbines," *Proceedings of ASME Cogen Turbo Power 1993, 7th Congress and Exposition on Gas Turbines in Cogeneration and Utility*, Sponsored by ASME in participation of BEAMA, IGTI-Vol. 8 Bournemouth, United Kingdom, September 21–23, 1993, pp. 347–55.

20

Gas Turbine Performance Test

Introduction

The performance analysis of the new generation of gas turbines are complex and presents new problems, which have to be addressed. The new units operate at very high turbine firing temperatures. Thus, variation in this firing temperature significantly affects the performance and life of the components in the hot section of the turbine. The compressor pressure ratio is high which leads to a very narrow operation margin, thus making the turbine very susceptible to compressor fouling. The turbines are also very sensitive to backpressure exerted on them when used in combined cycle or cogeneration duty. The pressure drop through the air filter also results in major deterioration of the performance of the turbine.

If a life cycle analysis were conducted the new costs of a plant are about 7–10% of the life cycle costs. Maintenance costs are approximately 15–20% of the life cycle costs. Operating costs, which essentially consist of energy costs, make up the remainder, between 70–80% of the life cycle costs, of any major power plant. Thus, performance evaluation of the turbine is one of the most important parameter in the operation of a plant.

Total performance monitoring on or off line is important for the plant engineers to achieve their goals of:

1. Maintaining high availability of their machinery.
2. Minimize degradation and maintain operation near design efficiencies.
3. Diagnose problems, and avoid operating in regions, which could lead to serious malfunctions.

4. Extend time between inspections and overhauls.
5. Reduce life cycle costs.

To determine the deterioration in component performance and efficiency, the values must be corrected to a reference plane. These corrected measurements will be referenced to different reference planes depending upon the point, which is being investigated. Corrected values can further be adjusted to a transposed design value to properly evaluate the deterioration of any given component. Transposed data points are very dependent on the characteristics of the components performance curves. To determine the characteristics of these curves, raw data points must be corrected and then plotted against representative nondimensional parameters. It is for this reason that we must evaluate the turbine train while its characteristics have not been altered due to component deterioration. If component data were available from the manufacturer, the task would be greatly reduced.

Performance Codes

Performance analysis is not only extremely important in determining overall performance of the cycle but in also determining life cycle considerations of various critical hot section components.

In this chapter, a detailed technique with all the major equations governing a Gas Turbine Power Plant are presented based on the various ASME Test Codes. The following five ASME Test Codes govern the test of a Gas Turbine Power Plant:

1. ASME, Performance Test Code on Overall Plant Performance, ASME PTC 46 1996, American Society of Mechanical Engineers 1996
2. ASME, Performance Test Code on Test Uncertainty: Instruments and Apparatus PTC 19.1, 1988
3. ASME, Performance Test Code on Gas Turbines, ASME PTC 22 1997, American Society of Mechanical Engineers 1997

The ASME, Performance Test Code on Overall Plant Performance, ASME PTC 46, was designed to determine the performance of the entire heat cycle as an integrated system. This code provides explicit procedures to determination of power plant thermal performance and electrical output.

The ASME, Performance Test Code on Test Uncertainty: Instruments and Apparatus PTC 19.1 specifies procedures for evaluation of uncertainties in individual test measurements, arising from both random errors and

Table 20-1
Instrumentation Accuracy

| Measurement | Bias Uncertainty |
|------------------------------------|--|
| Temperature below 200 °F (93.3 °C) | 0.5 °F (0.27 °C) |
| Temperature above 200 °F (93.3 °C) | 1.0 °F (0.56 °C) |
| Pressure | 0.1% |
| Vacuum pressure | Absolute pressure transmitters recommended |
| Mass flow of fuel gas | 0.8% |

systematic errors, and for the propagation of random and systematic uncertainties into the uncertainty of a test results. The various statistical terms involved are defined. The end result of a measurement uncertainty analysis is to provide numerical estimates of systematic uncertainties, random uncertainties, and the combination of these into a total uncertainty with an approximate confidence level. This is especially very important when computing guarantees in plant output and plant efficiency.

The PTC 22 establishes a limit of uncertainty of each measurement required; the overall uncertainty must then be calculated in accordance with the procedures defined in ASME PTC 19.1 Measurement Uncertainty. The code requires that the typical uncertainties be within a 1.1% for the Power Output, and 0.9% in the heat rate calculations. It is very important that the post-test uncertainty analysis should be also performed to assure the parties that the actual test has met the requirement of the code.

The instrumentation will be calibrated as per the requirements of the test codes. All the instrumentation must be calibrated before a test and certified that they meet the code requirements. The ASME PTC 19 series outlines the governing requirements of all instrumentation for an ASME Performance Test to be within the governing band of uncertainty.

Table 20-1 is a very short abstract of the test measurement requirements for the performance tests; the ASME PTC 19 series should be the final governing document:

Flow Straighteners

Minimum lengths of straight pipe are required for flow-measuring devices and for certain pressure measurements. Flow straighteners and/or equalizers should be used in the vicinity of throttle valves and elbows, as shown in Figure 20-1.

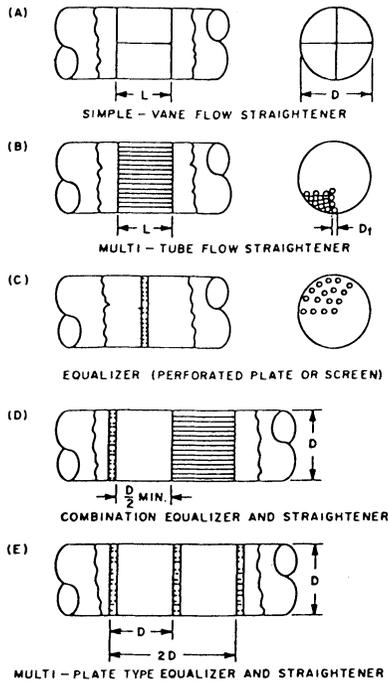


Figure 20-1. Flow equalizers and straighteners. (Power Test Code 10, *Compressors and Exhausters*, American Society of Mechanical Engineers, 1965.)

Pressure Measurement

The following types of instruments are used to make pressure measurements:

1. Bourdon tube gauges
2. Dead-weight gauges (used for calibration purposes only)
3. Liquid manometers
4. Impact tubes
5. Pitot-static tubes
6. Pressure transmitters
7. Pressure transducers
8. Barometers

Good-quality Bourdon tube test gauges are highly suitable for pressure measurements of more than 20 psi. They should be calibrated against a

deadweight tester in their normal operating range. When selecting a pressure gauge, it is important to see that the measure value is above midpoint on the scale.

Differential pressures and subatmospheric pressures should be measured by manometers with a fluid that is chemically stable when in contact with the test gas. Mercury traps should be used where necessary to prevent the manometer fluid from entering the process piping. Errors in these instruments should not exceed 0.25%.

A common failure in pressure measurement is the uncertainty of the configuration of static-pressure taps penetration through the pipe wall. This failure is another early-planning concern, since proper taps are easy to provide prior to placing the machine in service, but inspection of the taps after operation has commenced is a luxury rarely afforded the test team.

Another pitfall in pressure measurement, particularly important in flow measurement, is the potential for liquids in gauge lines. All too often gauge lines coming from overhead pipes have no provision for maintaining a liquid-free status, even though the flowing fluid may be condensible at gauge-line temperatures.

Calibration of the pressure-measuring device presents another pitfall for test crews. All too often a test is conducted through the field calculation step before bad data reveals that gauges, possibly with too large a minimum increment, were removed from the shipping carton and installed, relying on the vendor's calibration. On-site calibration of all instruments is always good insurance against a bad test.

Frequently, new machines are put into service with a "startup screen" in the compressor inlet piping to guard against the inevitable weld slag and construction debris that will remain in a new or rebuilt piping system after construction. Regardless of the age of the installation, care must be exercised to ensure that measurements defining suction or discharge conditions are not influenced by such devices.

Inlet and discharge pressures are defined as the stagnation pressures at the inlet and discharge, which are the sum of static and velocity pressures at the corresponding points. Static pressures should be measured at four stations in the same plane of the pipe as shown in the piping arrangements. Velocity pressure, when less than 5% of the pressure rise, can be computed by the formula

$$P_v = \frac{(V_{av})^2 \rho}{2g_c \times 144} = \frac{(V_{av})^2 \rho}{9266.1} \quad (20-1)$$

where V_{av} is the ratio of measured volume flow rate to the cross-sectional area of the pipe.

When the velocity pressure is more than 5% of the pressure rise, it should be determined by a pitot-tube traverse of two stations. For each station, the traverse consists of 10 readings at positions representing equal areas of the pipe cross section, as shown in Figure 20-2. The average velocity pressure P_v is given by

$$P_v = \frac{\rho \Sigma V_p^3}{288 g_c n_t V_{av}} \quad (20-2)$$

where at each traverse point

$$V_p = \sqrt{\frac{9266.1 p_v}{\rho}} \quad (20-3)$$

and n_t equals the number of traverse points.

Barometric pressure should be measured at the test site at 30-minute intervals during the test.

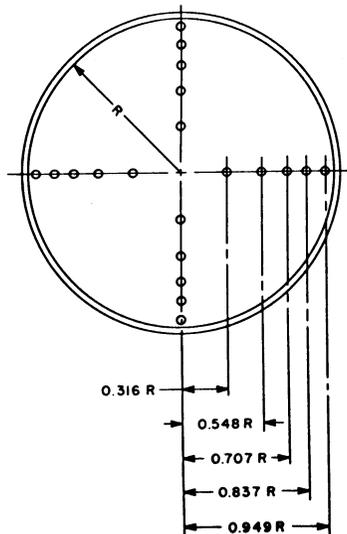


Figure 20-2. Traverse points in pipe. (Power Test Code 10, *Compressors and Exhausters*, American Society of Mechanical Engineers, 1965.)

Temperature Measurement

Temperature may be measured by any of the following instruments:

1. Mercury-in-glass thermometers
2. Thermocouples
3. Resistance thermometers
4. Thermometer wells

Thermocouples are the preferred type of instruments because of the simplicity in basic design and operation. They can attain a high level of accuracy, are suitable for remote reading, and are robust and relatively inexpensive.

Regardless of the temperature-measuring device to be used, on-site calibration of the entire measurement system is desirable. Usually, a two-point check can be made by employing frozen and boiling water. At the very least, all devices can be checked at a common temperature, preferably in the midrange of expected temperatures so that any deviant devices can be discarded. This check is particularly desirable for low-head machines where the temperature rise will be slight.

Test plans frequently are prepared on the assumption that a laboratory thermometer can replace an operating instrument in an existing thermometer well. While this change may be satisfactory, the prudent tester needs to be aware that because of the propensity of thermowells to break off and perhaps enter the machine or cause a hazardous leak, their design is compromised such that true gas temperature determination is impossible. The compromise may be to make the well short and/or to make it thick-walled. In either event the mass of metal exposed to ambient temperature may exceed that exposed to the gas, resulting in significant error if the gas temperature is much different from the ambient. High-pressure systems requiring thick-wall pipe are particularly susceptible to this fault. However, the use of a good heat-transfer fluid can minimize the error. The best gas temperature reading is attained by a calibrated fine-wire thermocouple with the junction directly exposed to the gas near the center of the flow. As deviations from this ideal are made, the potential for error is increased.

Inlet and discharge temperatures are the stagnation temperatures at the respective points and should be measured within an accuracy of 1 °F (0.55 °C). When the velocity of the gas stream is more than 125 fps (36.6 mps), the velocity effect should be included in the temperature measurement with a total temperature probe. This probe is a thermocouple with its hot junction provided with a shielded cup. The cup opening points upstream. A trade-off has to be made in a field test situation where the gas is not clean.

Flow Measurement

Gas flow through the compressor is measured by flow nozzles or other devices installed in the piping. Among the various devices are:

1. *Orifice plates.* Either the concentric orifice, eccentric orifice, or segmented orifice-type. Choice depends on the quality of the fluid handled.
2. *Venturi tubes.* These consist of a well-rounded convergent section at the entrance, a throat of constant diameter, and a divergent section. Their accuracy is high; however, installation, unless planned for in advance, is very difficult in the field.
3. *ASME flow nozzle.* These nozzles provide for accurate measurements. Their use is limited because they are not easily placed in a process plant; however, they are excellent for shop tests. Venturi meters and nozzles can handle about 60% more flow than orifice plates with varied pressure losses.
4. *Elbow flow meters.* The principle of centrifugal force at the bend is used to obtain the difference in pressure at the inside and outside of the elbow, which is then related to the discharge pressure.
5. *Turbine flow meters.* The principle of this flow meter is the computation of the revolutions of the turbine wheel in a given time frame.

Other techniques for measuring flow through the compressor include:

1. Calibrated pressure drops from the inlet flange to the eye of the firststage impeller in centrifugal compressors, when such data is available from the manufacturer.
2. A flow trace technique in which Freon is injected into the constream, and flight time between two detection points is measured.
3. Velocity traverse techniques must be used when, due to the configuration in piping, nozzles, or orifice plates, etc., cannot be used.

These techniques have been described previously in the pressure measurement section. Usually, one of the flow-measuring devices and the required instrumentation is incorporated as a part of the plant piping. The choice of technique depends on the allowable pressure drop, flow type, accuracy required, and cost.

Nozzle arrangements for various applications vary considerably. For subcritical flow measurement at the outlet end, where nozzle differential pressure p is less than the barometric pressure, flow should be measured with impact tubes and manometers as shown in Figure 20-3.

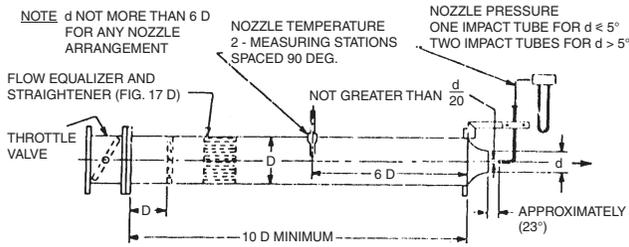


Figure 20-3. Flow nozzle for subcritical flow. (Power Test Code 10, *Compressors and Exhausters*, American Society of Mechanical Engineers, 1965.)

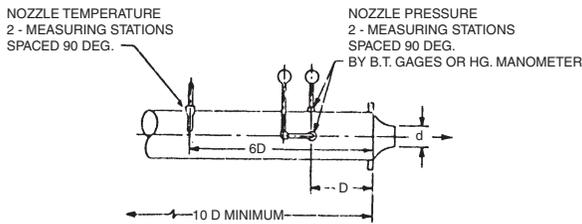


Figure 20-4. Flow nozzle, for critical flow. (Power Test Code 10, *Compressors and Exhausters*, American Society of Mechanical Engineers, 1965.)

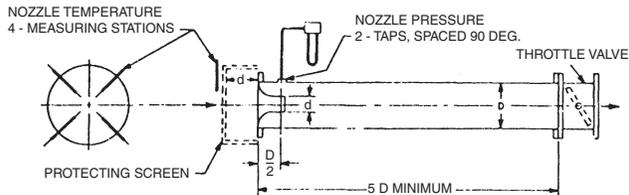


Figure 20-5. Nozzle for exhausters. (Power Test Code 10, *Compressors and Exhausters*, American Society of Mechanical Engineers, 1965.)

For critical measurement, where the drop p is more than the barometric pressure, flow should be measured with static-pressure taps upstream from the nozzle as illustrated in Figure 20-4. For exhaust measurements, differential pressure is measured at two static taps located downstream from the nozzle at the inlet as shown in Figure 20-5.

Gas Turbine Test

Before starting any performance test the gas turbine shall be run until stable conditions have been established. Stability conditions will be achieved

Table 20-2
Maximum Permissible Variation in Test Conditions

| Variables | Variation of Any Station During the Test Run |
|---|---|
| Power output (electrical) | ±2% |
| Power factor | ±2% |
| Rotating speed | ±1% |
| Barometric pressure at site | ±0.5% |
| Inlet air temperature | ±4.0 °F (± 2.2 °C) |
| Heat valve—gaseous fuel per unit volume | ±1% |
| Pressure—gaseous fuel as supplied to engine | ±1% |
| Absolute exhaust back pressure at engine | ±0.5% |
| Absolute inlet air pressure at engine | ±0.5% |
| Coolant temperature—outlet [Note (2)] | ±5.0 °F (± 2.8 °C) |
| Coolant temperature—rise [Note (2)] | ±5.0 °F (± 2.8 °C) |
| Turbine control temperature [Note (3)] | ±5.0 °F (± 2.8 °C) |
| Fuel mass flow | ±0.8% |

when continuous monitoring indicates the readings have been within the maximum permissible limits. The ASME PTC-22-test code requires that the performance test will be run as much as possible to the design test conditions as specified in the contract. The maximum permissible variation in a test run shall not vary from the computed average for that operating condition during the complete run by more than the values specified in Table 20-2. If operation conditions vary during any test run vary by more than the prescribed values in Table 20-2 than the results of that test run shall be discarded. The test run should not exceed 30 minutes and during that time the interval between readings should not exceed 10 minutes. There should be three to four test runs performed, which then could be averaged to get the final guarantee test points.

Correction factors are also provided in ASME PTC Test Code-46. The correction factors for ambient temperature, ambient pressure, and relative humidity are presented in this chapter.

The equations and performance parameters for all the major components of a power train must be corrected for ambient conditions and certain parameters must be further corrected to design conditions to accurately compute the degradation. Therefore, to fully compute the performance, and degradation of the plant and all its components, the actual, corrected, and transposed to reference conditions of critical parameters must be computed.

The overall plant needs the following parameters to be computed. The most important two parameters from an economic point of view are the computation of the power delivered and the fuel consumed to deliver

the power. The following are the parameters that need to be computed to fully understand the macro picture of the plant.

1. Overall plant system
2. Gross unit heat rate
 - a. Net unit heat rate
 - b. Gross output
 - c. Net output
 - d. Auxiliary power

Gas Turbine

The ASME, Performance Test Code on Gas Turbines, ASME PTC 22 examines the overall performance of the gas turbine. The ASME PTC 22 only examines the overall turbine and many turbines in the field are better instrumented for computation of the detail characteristics of the gas turbine. Figure 20-6 shows the desired location of the measurement points for a fully instrumented turbine. The following are the various computations required to calculate the gas turbine overall performance based on the code:

1. Gas turbine overall computation
2. Gas turbine output
3. Inlet air flow

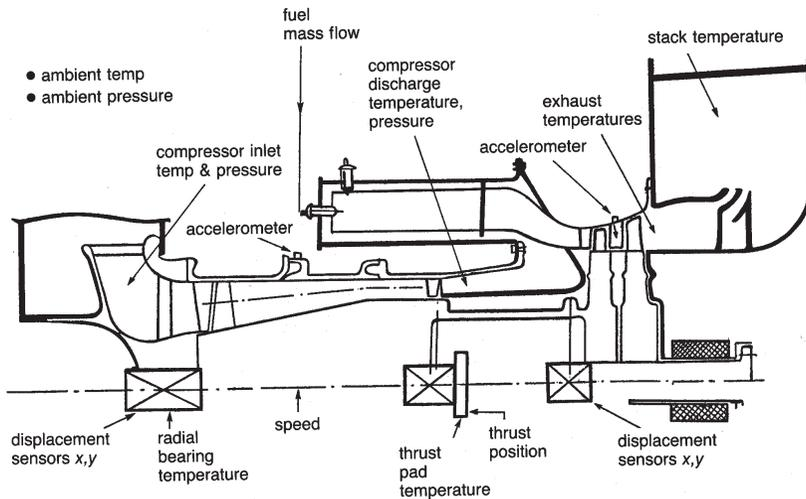


Figure 20-6. Gas turbine suggested measurement points.

4. First stage nozzle cooling flow rate
5. Total cooling flow rate
6. Heat rate
7. Expander efficiency
8. Gas turbine efficiency
9. Exhaust flue gas flow
10. Specific heat of exhaust flue gas

To further analyze, the gas turbine must be examined in its four major categories:

1. Air inlet filter
2. Compressor
3. Combustor
4. Expander turbine

Air Inlet Filter Module

Loss computation, this enables the operator to ensure that the filters are clean and that no additional losses than necessary reduce the performance of the gas turbine. The following parameters are necessary to monitor the filter:

1. Time to replace each stage of filters
2. Filter plugged index to monitor the condition of each stages of filters
3. Inlet duct air leak

Compressor Module

The compressor of a gas turbine is one of the most important components of the gas turbine. It consumes between 50–65% of the energy produced in a gas turbine. Thus fouling of the compressor can cause large losses in power and efficiency for the gas turbine. Furthermore, the fouling of the compressor also creates surge problems, which not only affects the performance of the compressor but also creates bearing problems and flame-outs. The following are some of the major characteristics that need to be calculated:

Overall Parameters of the Compressor.

1. Efficiency
2. Surge map
3. Compressor power consumption
4. Compressor fouling index

5. Compressor deterioration index
6. Humidity effects on the fouling
7. Stage deterioration

Compressor Losses. These losses are divided into two sections:

1. *Controllable Losses.* Losses, which can be controlled by the action of the operator such as:
 - a. Compressor fouling
 - b. Inlet pressure drop
2. *Uncontrollable Losses.* Losses, which cannot be controlled by the operator such as:
 - a. Ambient pressure
 - b. Ambient temperature, this, in cases of refrigerated inlets, could be controlled but in most applications is uncontrolled.
 - c. Ambient humidity
 - d. Ageing

Compressor Wash. When should the compressor be washed on-line, and when should an off-line compressor wash should be considered.

On-line Wash. This wash is done by many plants as the pressure drop decreases by more than 2%. Some plants do it on a daily basis. The water for these washes must be treated.

Off-line Wash. Figure 20-7 shows that on-line water wash will not return the power to normal thus after a number of these washes, an off-line water wash must be planned. This is a very expensive maintenance program and must be fully evaluated before it is undertaken. Chapter 12 deals with the various washes in detail.

Combustor Module

The calculation of the firing temperature is one of the most important calculations in the combined cycle performance computation. The temperature is computed using two techniques (1) Fuel Heat Rate (2) Power Balance. The following are the important parameters that need to be computed:

1. Combustor efficiency
2. Deterioration of combustor
3. Turbine inlet temperature (first stage nozzle inlet temperature)
4. Flash back monitor (for dry low NO_x combustors)
5. Specific fuel consumption

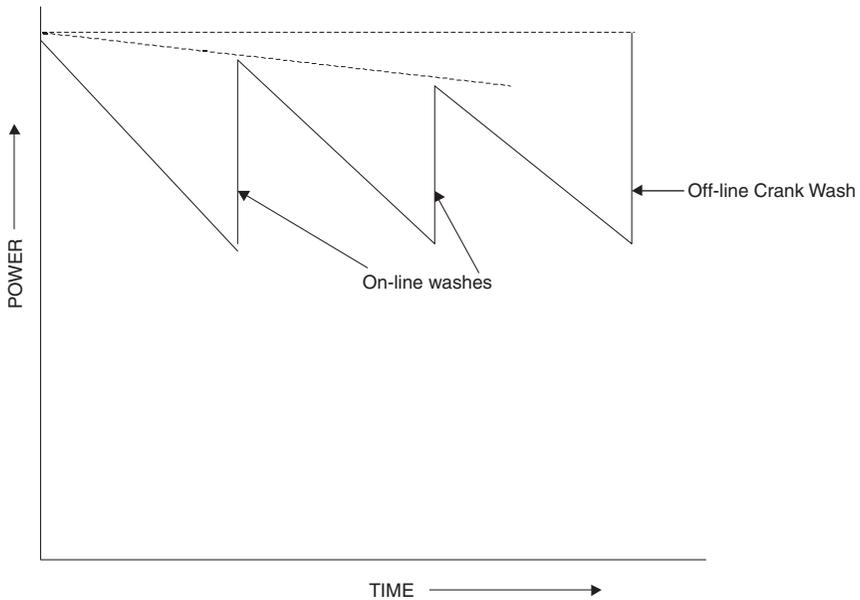


Figure 20-7. Compressor water wash characteristics.

Expander Module

The calculation of the turbine expander module depends whether or not this is a single shaft gas turbine or a multiple shaft gas turbine. In aero-derivative turbines, there are usually two or more shafts. In the latest aero-derivative turbines, there are usually two compressor sections, the LP compressor section, and the HP compressor section. This means that the turbine has three shafts; the third shaft is the power shaft. The turbines that drive the compressor section are known as the gasifier turbines, and the turbine, which drives the generator, is the power turbine. The gasifier turbine produces the work to drive the compressor.

The parameters which must be computed are:

1. Expander efficiency
2. Fouled expander parameter
3. Eroded turbine nozzle monitor parameter
4. Expander power produced
5. Deterioration monitor parameter
6. Plugged turbine nozzle monitor parameter

Life Cycle Consideration of Various Critical Hot Section Components

The life expectancy of most hot section parts is dependent on various parameters and is usually measured in terms of equivalent engine hours. The following are some of the major parameters that effect the equivalent engine hours in most machinery, especially gas turbines:

1. Type of fuel
2. Firing temperature
3. Materials stress and strain properties
4. Effectiveness of cooling systems
5. Number of starts
6. Number of trips
7. Expander Losses
 - a. Controllable losses
 - 1) Firing temperature
 - 2) Back pressure
 - 3) Turbine fouling (combustion deposits)
 - b. Uncontrollable (degradation) Losses
 - 1) Turbine ageing (increasing clearances)

Performance Curves

It is very important to form a base line for the entire power plant. This would enable the operator to determine if the section of the plant is operating below design conditions. The following performance curves should be obtained either from the manufacturer or during acceptance testing so that the in-depth study of the parameters and their interdependency with each other can be defined:

1. Gas turbine compressor inlet bell-mouth pressure differential versus air flow rate
2. Gas turbine output versus compressor inlet temperature
3. Heat rate versus compressor inlet temperature
4. Fuel consumption versus compressor inlet temperature
5. Exhaust temperature versus compressor inlet temperature
6. Exhaust flow versus compressor inlet temperature
7. The NO_x water injection rate for oil firing versus gas turbine compressor inlet temperature
8. Gas turbine generator power output and heat rate correction as result of water injection

9. Effect of water injection on generator output as a function of compressor inlet temperature
10. Effect of water injection rate on heat rate as a function of compressor inlet temperature
11. Ambient humidity corrections to generator output and heat rate
12. Power factor correction
13. Losses in generation due to fuel restriction resulting in operational constraints (e.g. temperature spread, problems on fuel stroke valve, etc.)

Performance Computations

This section deals with the equations, and techniques used to compute and simulate the various performance and mechanical parameters for the gas turbine power plant. The goals have been to be able to operate the entire power plant at its maximum design efficiency, and at the maximum power that can be obtained by the turbine without degrading the hot section life.

Gas turbine power adjustments in a utility application require that the mechanical speed must remain constant due to unacceptable consequences of frequency fluctuations. The control is obtained by IGV adjustments to reduce the flow at off-design loads and to maintain the high exhaust gas temperature.

The gas turbine efficiency drops off quickly at part load as would be expected, as the gas turbine is very dependent on turbine firing temperature and mass flow of the incoming air. The gas turbine heat rate increases rapidly at part load conditions.

The plant overall power and the heat rate are very dependent on the inlet conditions as seen in Figure 20-8, which is based on a typical gas turbine plant. The effect of temperature is the most critical component in the ambient condition variations of temperature, pressure, and humidity.

General Governing Equations

The four fundamental equations, which govern the properties of the combined cycle are the equation of state, conservation of mass, momentum and energy equations.

Equation of state

$$\frac{P}{\rho} = Z \frac{R}{MW} T \quad (20-4)$$

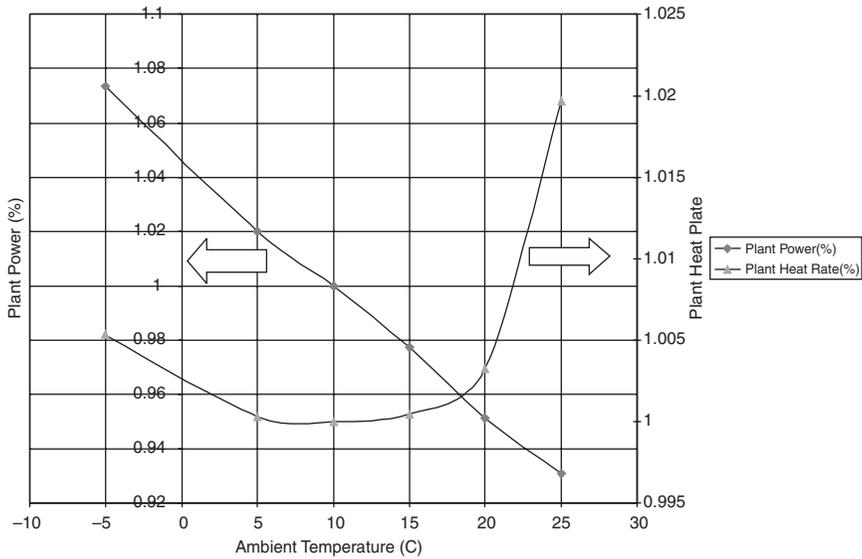


Figure 20-8. Plant conditions as a function of inlet ambient temperature.

which can also be written as:

$$\frac{P}{\rho^n} = C \tag{20-4a}$$

Where n varies from $0 \rightarrow \infty$; $n = 0, P = C$ (constant pressure process); $n = 1, T = C$ (constant temperature process); $n = \gamma \left(\gamma = \frac{C_p}{C_v} \right), S = C$ (constant entropy process); $n = \infty, V = C$ (constant volume process).

Conservation of mass

$$m = \rho AV \tag{20-5}$$

Momentum equation for a calorically and thermally perfect gas, and one in which the radial and axial velocities do not contribute to the forces generated on the rotor the Adiabatic Energy (E_{ad}) per unit mass is given as follows (Euler Turbine Equation):

$$E_{ad} = \frac{1}{g_c} (U_1 V_{\theta 1} - U_2 V_{\theta 2}) \tag{20-6}$$

Energy equation for a calorically and thermally perfect gas the Work (W) can be written as follows:

$$Q_{\text{rad}} + \Delta UE + \Delta PV + \Delta KE + \Delta PE = W \quad (20-7)$$

where ΔU is the change in the internal energy, ΔPV is the change in the flow energy, ΔKE is the change in kinetic energy, and ΔPE is the change in Potential Energy. The total enthalpy is given by the following relationship:

$$H = U + PV + KE \quad (20-8)$$

neglecting the changes in potential energy (ΔPE) and heat losses due to radiation (Q_{rad}); the work is equal to the change in total enthalpy:

$$W = H_2 - H_1 \quad (20-9)$$

In the gas turbine (Brayton cycle), the compression and expansion processes are adiabatic and isentropic processes. Thus, for an isentropic adiabatic process $\gamma = \frac{c_p}{c_v}$; where c_p and c_v are the specific heats of the gas at constant pressure and volume respectively and can be written as:

$$c_p - c_v = R \quad (20-10)$$

$$\text{where } c_p = \frac{\gamma R}{\gamma - 1} \quad \text{and} \quad c_v = \frac{R}{\gamma - 1} \quad (20-11)$$

values for air and products of combustion (400% theoretical air) are given in Appendix B. It is important to note that the pressure measured can be either Total or Static however, only Total Temperature can be measured. The relationship between total and static conditions for pressure and temperature are as follows:

$$T = T_s + \frac{V^2}{2c_p} \quad (20-12)$$

where T_s = static temperature, and V = gas stream velocity and

$$P = P_s + \rho \frac{V^2}{2g_c} \quad (20-13)$$

where P_s = static pressure and the acoustic velocity in a gas is given by the following relationship

$$a^2 = \left(\frac{\partial P}{\partial \rho} \right)_{s=c} \quad (20-14)$$

for an adiabatic process (s = entropy = constant) the acoustic speed can be written as follows:

$$a = \sqrt{\frac{\gamma g_c R T_s}{MW}} \quad (20-15)$$

where T_s = static Temperature.

The Mach Number is defined as:

$$M = \frac{V}{a} \quad (20-16)$$

it is important to note that the Mach No. is based on static temperature.

The turbine compressor efficiency and pressure ratio are closely monitored to ensure that the turbine compressor is not fouling. Based on these computations the turbine compressor is water washed with mineralized water, and if necessary adjustment of Inlet Guide Vanes (IGV) is carried out to optimize the performance of the compressor, which amounts to between 60–65% of the total work produced by the gas turbine.

The turbine firing temperature, which affects the life, power output, as well as the overall thermal efficiency of the turbine, must be calculated very accurately. To ensure the accuracy of this calculation, the turbine firing temperature is computed using two techniques. These techniques are based firstly on the fuel heat input and secondly on the turbine heat balance. Turbine expander efficiencies are computed and deterioration noted.

Gas Turbine Performance Calculation

Increase in pressure ratio and increase in the firing temperature are the two most important factors in the increase of gas turbine efficiency as can be seen from Figure 20-9. Today the large gas turbines have pressure ratios ranging from 15:1 to as high as 30:1, and firing temperatures as high as 2500 °F (2071 °C). These high-pressure ratios lead to a very narrow operational margin in the gas turbine compressor. The operating margin, between the surge line and the choke region, is reduced with increasing

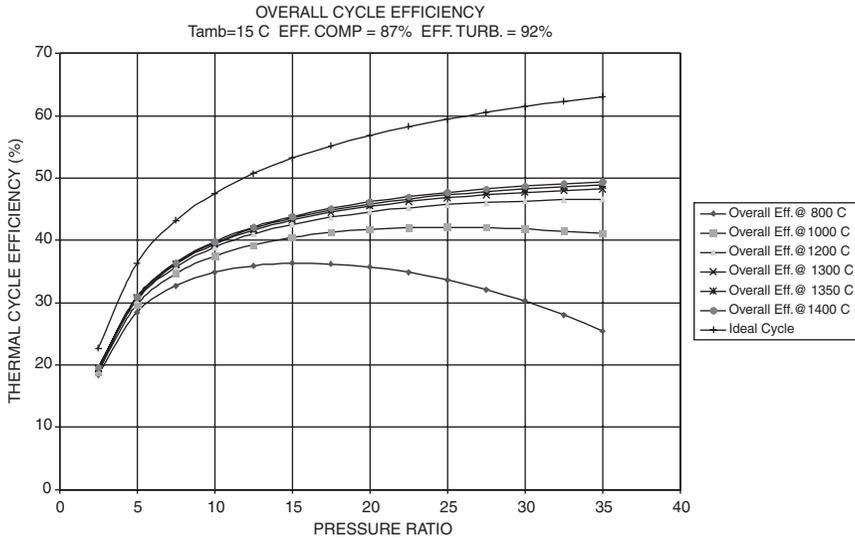


Figure 20-9. Effect of pressure ratio and firing temperature on the performance of a gas turbine.

pressure ratio. This means, in a practical sense, that the new compressors on these gas turbines are very susceptible to any fouling of the compressor, indicating that the inlet filters must be very efficient and the turbines must be performance monitored to ensure maximum operational efficiency.

The overall compressor work is calculated using the following relationship:

$$W_c = (H_{2a} - H_1) = c_{pavg} T_1 \left\{ \left(\frac{P_2}{P_1} \right)^{\left(\frac{\gamma-1}{\gamma} \right)} - 1 \right\} \tag{20-17}$$

the work per stage is calculated assuming the energy per stage is equal, this has been found to be a better assumption than assuming the pressure ratio per stage to be equal. It is necessary to know the work per stage if there is inter-stage bleed of the air for cooling or other reasons.

$$w_{stg} = \frac{(H_{2a} - H_1)}{n_{stg}} \tag{20-18}$$

where n_{stg} = number of compressor stages. The computation of the compressor total energy requirements can now be computed.

$$Pow_c = m_a w_{stg} n_1 + (m_a - m_{b1}) w_{stg} n_2 + (m_a - m_{b1} - m_{b2}) w_{stg} n_3 \dots \tag{20-19}$$

The work of the compressor under ideal conditions occurs at constant entropy. The actual work occurs with an increase in entropy thus the adiabatic efficiency can be written in terms of the total changes in enthalpy:

$$\eta_{ac} = \frac{\text{Isentropic work}}{\text{Actual work}} = \frac{(H_{2TI} - H_{1T})}{(H_{2a} - H_{1T})} \tag{20-20}$$

where H_{2TI} = total enthalpy of the gas at isentropic exit conditions, and H_{2a} = total enthalpy of the gas at actual exit conditions, and H_1 = total enthalpy of the gas at inlet conditions for a calorically perfect gas the equation can be written as:

$$\eta_{ac} = \frac{\left[\left(\frac{P_2}{P_1} \right)^{\frac{\gamma-1}{\gamma}} - 1 \right]}{\left[\frac{T_{2a}}{T_1} - 1 \right]} \tag{20-21}$$

The gas turbine compressor which produces the high pressure gas at elevated temperature uses a very large part of the turbine power produced by the gas

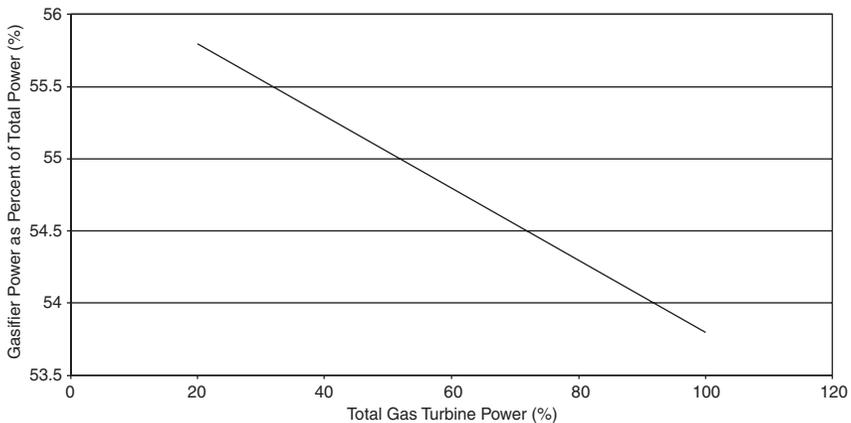


Figure 20-10. Gasifier power as a function of total gas turbine power.

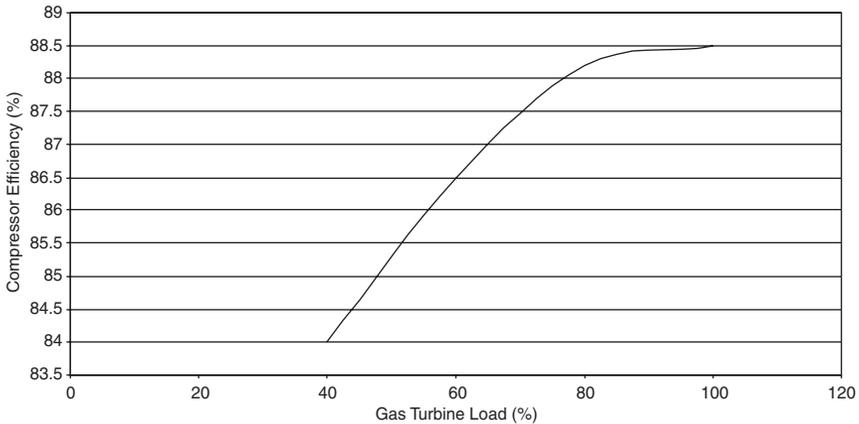


Figure 20-11. Gas turbine compressor efficiency as a function of temperature load.

turbine, this can amount to about 60% of the total power produced. Figure 20-10 shows the distribution of the gasifier power required as a function of the gas turbine load of a typical large gas turbine. The fouling of the compressor therefore is a large parasitic load on the gas turbine. Figure 20-11 shows the effect on the compressor efficiency at part load conditions. The flow and the firing temperature affect the turbine expander.

The calculation of the turbine firing temperature (T_{tit}) is based firstly on the fuel injected into the turbine and the fuel’s lower heating value (LHV). The lower heating value of the gas is one in which the H_2O in the products has not condensed. The lower heating value is equal to the higher heating value minus the latent heat of the condensed water vapor.

$$H_{\text{tit}} = \frac{(m_a - m_b)H_{2a} + m_f \eta_b LHV}{(m_a + m_f - m_b)} \tag{20-22}$$

where H_{tit} = enthalpy of the combustion gas at the firing temperature; m_a = mass of air; m_b = bleed air; m_f = mass of fuel; η_b = combustor efficiency (usually between 97–99%)

The turbine firing temperature should be computed by knowing the gas characteristics of the combustion gas. If these characteristics are known then one can use the combustion gas equations given in the ASME performance test codes 4.4 (1991) for gas turbine HRSG. Usually the gas constituents are not known so it is not a bad assumption to use the 400% theoretical air tables in the Keenan and Kaye gas tables. The following equations for

specific heat at constant pressure and the ratio of specific heats have been obtained based on the air tables based on a fuel with a mole weight of the combustion gas to be 28.9553 lb_m/pmole (kg/kgmole).

$$c_p = (-2.76 * 10^{(-10)} T^2 + 1.1528 * 10^{(-5)} T + 0.237) * C1 \quad (20-23)$$

where $C1 = 1.0$ in the U.S. units and $C1 = 4.186$ in the SI units and

$$\gamma = \frac{c_p}{\left(c_p - \frac{778.16}{MW} \right)} \quad (20-24)$$

The turbine firing temperature based on the heat balance can be also computed and must be within about 2–6 °F (1–3 °C) of each other. The heat balance relationships as they apply to the gas turbine

$$H_{tit} = \frac{\frac{Pow_c}{\eta_{mc}} + \frac{Pow_g}{\eta_{mt}} + (m_a + m_f)H_{exit}}{(m_a + m_f - \sum m_b)} \quad (20-25)$$

where Pow_c = work of the gas turbine compressor (Btu/sec, kJ/sec); Pow_g = generator output; η_{mc} = mechanical loss in the turbine compressor drive; η_{mt} = mechanical loss in the turbine process compressor drive; and H_{exit} = enthalpy at turbine exit

Split shaft gas turbines usually have temperature measurements at the gasifier turbine exit and also at the power turbine exit. From experience and also based on theoretical relationships, the temperature ratio of the temperature at the gasifier inlet (T_{tit}) and the temperature of the power turbine inlet temperature (T_{pit}) for a given geometry remains constant even though the load and ambient conditions change. It is because of this that most manufacturers limit the engine based on the power turbine inlet temperature.

$$Tr = \frac{T_{tit}}{T_{pit}} \quad (20-26)$$

This also enables equation (19) for the case of a split shaft turbine to be rewritten as:

$$H_{tit} = \frac{\frac{Pow_c}{\eta_{mc}} + (m_a + m_f - 0.6m_b)H_{pit}}{(m_a + m_f - m_b)} \quad (20-27)$$

where an assumption of 40% of the bleed flow was assumed to have entered the turbine through the cooling mechanisms of the first few stages of the turbine.

To ensure that the heat balance is accurate the following relationship indicates the accuracy of the computations. This heat balance ratio can be written as follows:

$$HB_{ratio} = \frac{\frac{Pow_c}{\eta_{mt}} + (m_a + m_f)H_{exit} - m_a H_{inlet}}{m_f * LHV} \tag{20-28}$$

this ratio should be between 0.96 and 1.04.

Figure 20-12 shows the effect of the turbine firing temperature on the turbine expander efficiency. The decrease in firing temperature reduces the absolute velocity, as also does the reduction in the mass flow, both of which occur at part load conditions. Figure 20-13 shows the variation in the firing temperature and the exhaust gas temperature as a function of the load. It is interesting to note that the firing temperature of the turbine is greatly reduced while the exhaust temperature remains nearly constant accounting for the steam turbine producing more work at low part loads.

The work produced by the gasifier turbine (W_{gt}) is equal to the gas turbine compressor work (W_c):

$$Pow_{gt} = \frac{Pow_c}{\eta_{mc}} \tag{20-29}$$

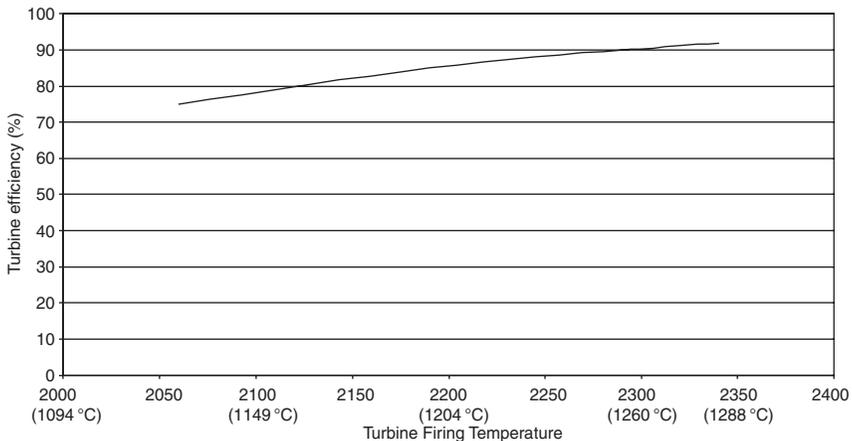


Figure 20-12. Gas turbine efficiency as a function of firing temperature.

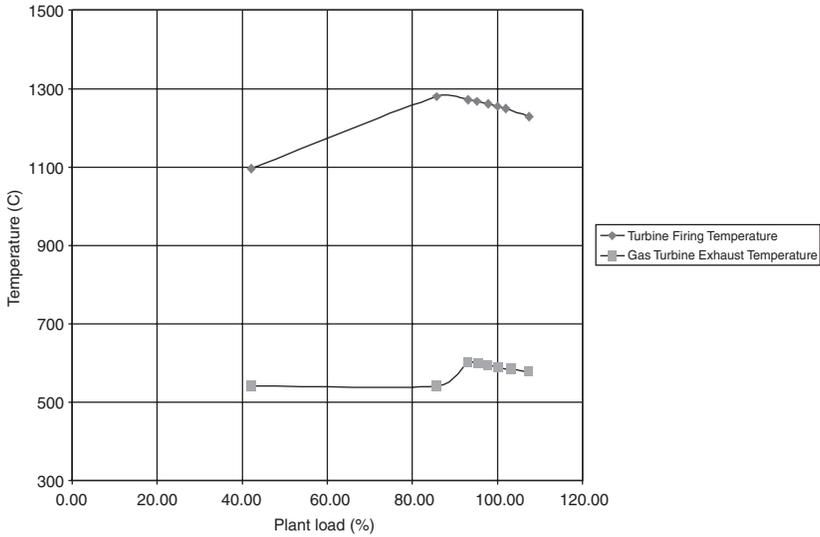


Figure 20-13. Effect of the plant load on turbine firing temperature and the turbine exhaust.

The gasifier turbine efficiency (η_{gt})

$$\eta_{gt} = \frac{H_{tit} - H_{pita}}{H_{tit} - H_{piti}} 100 \tag{20-30}$$

where H_{pita} = is the enthalpy of the gas based on the actual temperature at the exit of the gasifier turbine; H_{piti} is the enthalpy of the gas based on the ideal temperature at the exit of the gasifier turbine. To obtain this ideal enthalpy, the pressure ratio across the gasifier turbine must be known.

The pressure ratio (P_{grt}) across the turbine depends on the pressure drop (ΔP_{cb}) through the combustor. This varies in various combustor designs where a pressure drop of between 1–3% of the compressor discharge pressure.

$$P_{grt} = \frac{P_{dc}(1 - \Delta P_{cb})}{P_{dgt}} \tag{20-31}$$

where P_{dgt} is the pressure at the gasifier turbine exit. Thus, the ideal enthalpy at the gasifier turbine exit is given by

$$H_{piti} = \frac{H_{tit}}{\frac{c_{p_{tit}}}{c_{p_{pit}}} \left(P_{grt}^{\frac{\gamma-1}{\gamma}} \right)} \tag{20-32}$$

where γ is based on an average temperature across the gasifier turbine based on equation (20-24). The power turbine efficiency can be computed using equations (20-30) and (20-32).

The overall thermal efficiency of the gas turbine in a simple cycle (varies between 25–45% depending on the turbine) is computed to determine deterioration of the turbine:

$$\eta_{\text{ovt}} = \frac{\frac{Pow_g}{\eta_{\text{mt}}}}{m_f LHV} 100 \quad (20-33)$$

The heat rate can now be easily computed

$$HR = \frac{2544}{\frac{\eta_{\text{th}}}{100}} \left(\frac{\text{Btu}}{HP - hr} \right) = \frac{3600}{\frac{\eta_{\text{th}}}{100}} \left(\frac{\text{KJ}}{KW - hr} \right) \quad (20-34)$$

Gas Turbine Performance Calculations

The performance of the gas turbine is based on the basic equations in the prior section. To relate these relationships to the turbine in concern and to calculate the deterioration of different sections of the gas turbine, the values obtained must be corrected to design conditions and in some cases values would have to be transposed from off-design conditions to the design conditions. The corrected values define the engine corrected performance values. Geometric similarity such as blade characteristics, clearances, nozzle areas, and guide vane settings do not change when geometric similarity is constant. Dynamic similarity, which relates to such parameters as gas velocities, and turbine speeds, when maintained together with the geometric similarity ensures that these corrected parameters will maintain the engine performance at all operating conditions.

Corrected mass flow

$$m_{\text{acorr}} = \frac{m_a \sqrt{\frac{T_{\text{inlet}}}{T_{\text{std}}}}}{\frac{P_{\text{inlet}}}{P_{\text{std}}}} \quad (20-35)$$

where m_{acorr} is the corrected mass flow of the air entering the gas turbine inlet. These corrections are from the ambient conditions to usually the ISO conditions (14.7 psia, 60 °F, RH = 60%), (1.01 Bar, 15 °C, RH = 60%).

The corrected speed for both the gasifier and power turbine defines the corrected engine performance.

Corrected speed

$$N_{\text{corr}} = \frac{N_{\text{act}}}{\sqrt{\frac{R_g T_a}{(RT)_{\text{std}}}}} \quad (20-36)$$

Corrected temperature

$$T_{\text{corr}} = \frac{T_a}{\frac{T_{\text{inlet}}}{T_{\text{std}}}} \quad (20-37)$$

Corrected fuel flow

$$m_{\text{fcorr}} = \frac{m_f}{\left(\frac{P_{\text{inlet}}}{P_{\text{std}}}\right) / \left(\sqrt{\frac{T_{\text{inlet}}}{T_{\text{std}}}}\right)} \quad (20-38)$$

Corrected power

$$HP_{\text{corr}} = \frac{HP_{\text{act}} \frac{T_{\text{inlet}}}{T_{\text{std}}}}{\frac{P_{\text{inlet}}}{P_{\text{std}}}} \quad (20-39)$$

The above relationship has to be further modified to take into account the pressure drop in the inlet ducting, the increase in back pressure due to exhaust ducting, the off-design operation due to decrease in turbine firing temperature and decrease in speed of the power turbine. These modifications are used to calculate the transposed power (HP_{pt}) by transposing from the off-design output power at operating conditions of the turbine to the design conditions.

Transpose power output

$$\begin{aligned} HP_{\text{tp}} = & HP_{\text{corr}} + (\Delta P_c(PW_i)) + (\Delta P_e(PW)_e) \\ & + (T_{\text{dit}} - T_{\text{atit}})c_p(m_d - m_a)\eta_{\text{at}} + \left[1 + 0.45\left(1 - \frac{N_{\text{ptcorr}}}{N_{\text{ptdes}}}\right)^m\right] HP_{\text{act}} \end{aligned} \quad (20-40)$$

where ΔP_c is the pressure drop at the inlet due to the filters and evaporator in the inlet ducting, P_{wi} the power loss per inch of H_2O (mm. H_2O) drop, ΔP_e is the back pressure at the discharge due to the exhaust ducting, P_{we} the power loss per inch of H_2O (mm. H_2O) drop. The last term of the equation only applies to split shaft turbines. The power factor (m) to which the speed ratio is raised will vary with turbines; in the case of this turbine the value was $m = 0.4$

Plant Losses

The losses that are encountered in a plant can be divided into two groups, uncontrollable losses, and controllable losses. The uncontrollable losses are usually environmental conditions, such as temperature, pressure, humidity, and the turbine aging. Table 20-3 shows the approximate changes that would occur for these changes. It must be remembered that these are just approximations and will vary for individual power plants.

The controllable losses are those that the operator can have some degree of control over and can take corrective actions:

1. Pressure drop across the inlet filter. This can be remedied by cleaning or replacing the filter.
2. Compressor fouling. On-line water cleaning can restore part of the drop encountered.
3. Fuel lower heating value. In many plants on-line fuel analyzers have been introduced to not only monitor the turbine performance but to also calculate the fuel payments, which are usually based on the energy content of the fuel.

Table 20-3
Effect of Uncontrollable Losses on the Output and Heat Rate

| Parameters | Parameter Change | Power Output (%) | Heat Rate Change (%) |
|---------------------------|--|------------------|----------------------|
| Ambient temperature | 20 °F (11 °C) | -6.5 | 2 |
| Ambient pressure | 4 in. H_2O (10 mbar) (mm. H_2O) | 0.9 | 0.9 |
| Ambient relative humidity | 10% | -0.0002 | -0.0005 |
| Turbine age | First 10,000 hrs | -0.34/1000 | 0.5 |
| Turbine age | Above 10,000 hrs | -0.03 | -0.08 |

Table 20-4
Effect of Controllable Losses on the Output and Heat Rate

| Parameters | Parameter Change | Power Output (%) | Heat Rate Change (%) |
|---------------------------------------|--|------------------|----------------------|
| Compressor fouling | 2% | -1.5 | 0.65 |
| Pressure drop in filter | 1 in H ₂ O (25 mm H ₂ O) | -0.5 | -0.3 |
| Increase in gas turbine back pressure | 1 in H ₂ O (25 mm H ₂ O) | -0.25 | -0.08 |
| Lower heating value | -430 Btu/lb (-1000 kJ/kg) | 0.4 | -1.0 |
| Power factor | -0.05 | -0.14 | 0.15 |

4. Turbine back pressure. In this case, the operator is relatively limited since the operator cannot do anything about the downstream design. Unless there is some obstruction in the ducting, which can be removed, or if the duct has collapsed in a section the duct could be replaced.

Table 20-4 shows the effect of controllable losses in the output and heat rate of a typical Combined Cycle Power Plant. The gas turbine has to be operated at a constant speed for power generation, and any slight variation in speed could result in major problems for the grid. Thus, the control of the load has to be by controlling the fuel input, therefore, the turbine firing temperature, and the inlet guide vane position, thus controlling the airflow. The effect of this is to try and maintain the exhaust temperature from the gas turbine at a relatively high value since this gas is used in the HRSG, and the effectiveness of the HRSG is dependent on maintaining this temperature.

Bibliography

- ASME, Power Test Code 10 (PTC10), 1965.
- ASME, Performance Test Code on Steam Condensing Apparatus, ASME PTC 12.2 1983, American Society of Mechanical Engineers, 1983.
- ASME, Performance Test Code on Test Uncertainty: Instruments and Apparatus PTC 19.1, 1988.
- ASME, Performance Test Code on Gas Turbine Heat Recovery Steam Generators, ASME PTC 4.4 1981, American Society of Mechanical Engineers, Reaffirmed 1992.

- ASME, Gas Turbine Fuels B 133.7M Published: 1985 (Reaffirmed year: 1992).
- ASME, Performance Test Code on Overall Plant Performance, ASME PTC 46, 1996.
- ASME, Performance Test Code on Steam Turbines, ASME PTC 6, 1996.
- ASME, Performance Test Code on Atmospheric Water Cooling Equipment PTC 23, 1997.
- ASME, Performance Test Code on Gas Turbines, ASME PTC 22 1997, American Society of Mechanical Engineers, 1997.
- Boyce, M.P., Bayley, R.D., Sudhakar, V., and Elchuri, V., "Field Testing of Compressors," Proceedings of the 5th Turbomachinery Symposium, Texas A&M University, pp. 149–160, 1976.
- Boyce, M.P., "Performance Monitoring of Large Combined Cycle Power Plants," Proceedings of the ASME 1999 International Joint Power Generation Conference, San Francisco, California. Vol. 2, pp. 183–190, July 1999.
- Boyce, M.P., "Performance Characteristics of a Steam Turbine in a Combined Cycle Power Plant," Proceedings of the 6th EPRI Steam Turbine Generator/Workshop, August 1999.
- Canjar, L.N., "There's a Limit to Use of Equations of State," Petroleum Refiner, p. 113, February 1956.
- Edmister, W.C., *Applied Hydrocarbon Dynamics*, Vol. 1, Gulf Publishing Co., Houston, Texas, pp. 1–3, 1961.
- Gas Producers Association, Table of Physical Constants of Paraffin Hydrocarbons and Other Components of Natural Gas, Standard 2145–94.
- Gonzalez, Fr., Boyce, Me. P., "Solutions to Field Problems of a Gas Turbine-Axial Flow Chemical Process Compressor Train Based on Computer Simulation of the Process," Proceedings of the 28th Turbomachinery Symposium, Texas A&M University, p. 77, 1999.
- ISO, Natural Gas—Calculation of Calorific Value, Density and Relative Density International Organization for Standardization ISO 6976-1983(E).

21

Maintenance Techniques

Philosophy of Maintenance

Maintenance, defined as the “upkeep of property,” is one of the most important operations in a plant. The manufacture and maintenance of turbomachinery are totally different. The first involves the shaping and assembly of various parts to required tolerances, while the second, maintenance, involves restoration of these tolerances through a series of intelligent compromises. The crux of maintenance technique is in keeping the compromises intelligent.

Maintenance is not a glamorous procedure; however, its importance is second to none. Maintenance procedures are always controversial, since the definition of “upkeep” varies with the individual interpretation of each maintenance supervisor. The latitude of maintenance ranges from strict planning and execution, inspection and overhaul, accompanied by complete reports and accounting of costs, to the operation of machinery until some failure occurs, and then making the necessary repairs.

Modern day turbomachinery is built to last between 30–40 years. Thus, the keeping of basic maintenance records and critical data is imperative for a good maintenance program. Economic justification is always the controlling factor for any program, and maintenance practices are not different.

Maintenance costs can be minimized by, and are directly related to, good operation; likewise, better operating results can be obtained when the equipment is under the control of a planned maintenance program. Improper operation of mechanical equipment can be as much or more the cause of its deterioration and failure as is actual, normal mechanical wear. Thus, operation and maintenance go together.

Combining the practice of preventive maintenance and total quality control and total employee involvement results in an innovative system for equipment maintenance that optimizes effectiveness, eliminates breakdowns, and promotes autonomous operator maintenance through day-to-day activities. This concept known as Total Productive Maintenance (TPM) was conceived by Seiichi Nakajima and is well-documented in his book “Introduction of TPM” and is highly recommended reading for all involved in the maintenance area.

A new maintenance system is introduced based on the new mantra for the selection of all equipment “Life Cycle Cost.” This new system especially for major power plants is based on the combination of total condition monitoring, and the maintenance principles of total productive maintenance, and is called the “Performance Based Total Productive Maintenance System.”

The general maintenance system is fragmented and can be classified into many maintenance concepts. The following are five P’s of maintenance for major power plants, petro-chemical corporations, and other process type industries leading to the ultimate maintenance system:

1. Panic maintenance based on breakdowns
2. Preventive maintenance
3. Performance based maintenance
4. Performance productive maintenance
5. Performance based total productive maintenance (PTPM).

Performance based total productive maintenance consists of the following elements:

1. Performance based total productive maintenance aims to maximize equipment efficiency and time between overhaul. (overall performance effectiveness)
2. Performance based total productive maintenance aims to maximize equipment effectiveness. (overall effectiveness)
3. Performance based total productive maintenance establishes a thorough system of PM for the equipment’s entire life span.
4. Performance based total productive maintenance is implemented by various departments (engineering, operations, maintenance).
5. Performance based total productive maintenance involves every single employee, from top management to workers on the floor.
6. Performance based total productive maintenance is based on the promotions of PM through *motivation management*: autonomous small group activities.

The word “total” in “performance based *total* productive maintenance” has four meanings that describe the principal features of PTPM:

1. *Total overall performance effectiveness* indicates PTPM’s pursuit of maximum plant efficiency and minimum downtime.
2. *Total overall performance effectiveness* indicates PTPM’s pursuit of economic efficiency or profitability.
3. *Total maintenance system* includes maintenance prevention (MP) and maintainability improvement (MI) as well as preventive maintenance.
4. *Total participation of all employees* includes autonomous maintenance by operators through small group activities.

Table 21-1 shows the relationship between PTPM, productive maintenance, and preventive maintenance.

Performance based total productive maintenance eliminates the following seven major losses:

Down time:

1. Loss of time due to unnecessary overhauls based only on time intervals.
2. Equipment failure-from breakdowns.
3. Loss of time due to spare part unsuitability or insufficient spares.

Table 21-1
Benefits of Various Maintenance Systems Maintenance

| | Performance Based Total Productive Maintenance | Performance Productive Maintenance | Performance Based Maintenance | Preventive Maintenance | Panic Maintenance |
|-------------------------------------|---|---|--------------------------------------|-------------------------------|--------------------------|
| Economic efficiency | Yes | Yes | Yes | Yes | No |
| Economic and time efficiency | Yes | Yes | Yes | No | No |
| Total system efficiency | Yes | Yes | No | No | No |
| Autonomous maintenance by operators | Yes | No | No | No | No |

4. Idling and minor stoppages—due to the abnormal operation of sensors or other protective devices.
5. Reduced output—due to discrepancies between designed and actual operating conditions.

Defect:

1. Process defects—due to improper process conditions that do not meet machinery design requirements.
2. Reduced yield—from machine startup to stable production due to the inability of the machine to operate at proper design conditions.

Maximization of Equipment Efficiency and Effectiveness

High machine efficiency and availability can be attained by maintaining the health of the equipment. Total performance condition monitoring can play a major part here as it provides early warnings of potential failures and performance deterioration. Figure 21-1 shows the concept of a total performance condition monitoring system.

Pure preventive maintenance alone cannot eliminate breakdowns. Breakdowns occur due to many factors such as, design and or manufacturing errors, operational errors, and wearing out of various components. Thus, changing out components at fixed intervals does not solve the problems and in some cases adds to the problem. A study at a major nuclear power station indicated that nearly 35% of the failures occurred within a month of a major turnaround. Figure 21-2 shows the life characteristics of a major piece of turbomachinery.

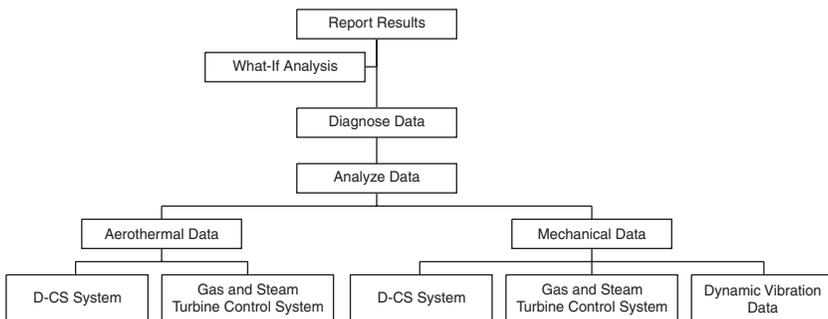
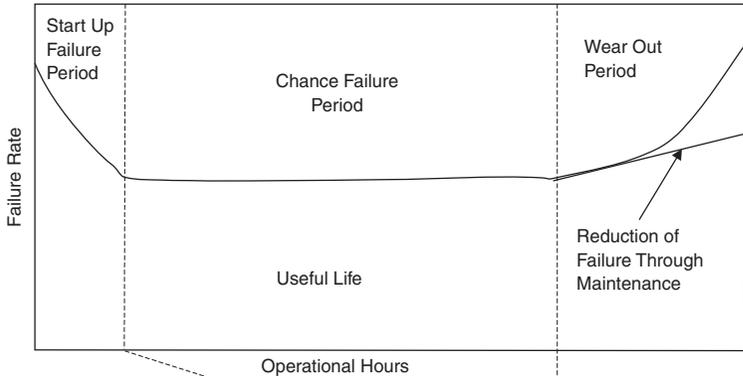


Figure 21-1. Total performance-based condition monitoring system.



| Category | Start up Failure | Chance Failure | Wear Out Failure |
|------------------|---|--------------------|--|
| Cause | Design Manufacturing Errors | Operational Errors | Wear Out |
| Counter Measures | Trial runs at acceptance and startup controls | Proper Operation | Preventive and Maintainability Improvement |
| | Maintenance Prevention | | |

Figure 21-2. Machinery life cycle characteristics.

The goal of any good maintenance program is “Zero Breakdown.” To achieve this goal, there are five counter measures. These are listed below:

1. Maintaining well-regulated basic conditions (cleaning, lubricating, and bolting).
2. Adhering to proper operating procedures.
3. Total condition monitoring (performance, mechanical, and diagnostic based).
4. Improving weaknesses in design.
5. Improving operation and maintenance skills.

The interrelationship between these five items is shown in Figure 21-3.

The division of labor between operations and maintenance is shown in Figure 21-4. It is the primary responsibility of the production department to establish and regulate basic operating conditions, and it is the primary responsibility of the maintenance department to improve defects in design. The other tasks are shared between the two departments.

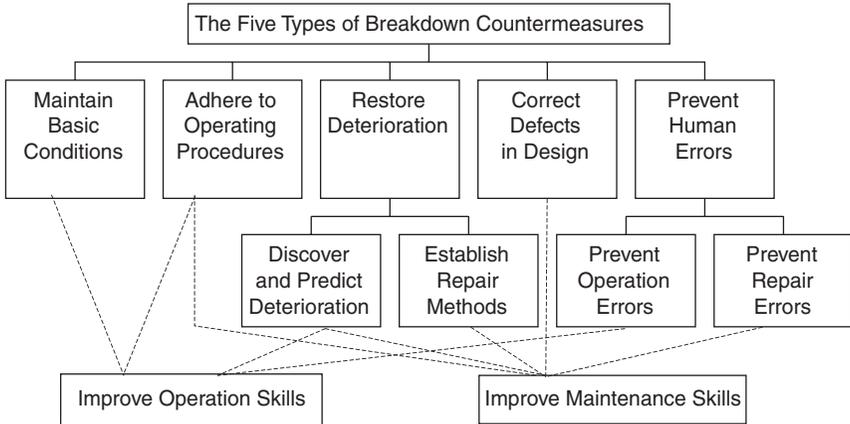


Figure 21-3. Breakdown countermeasures.

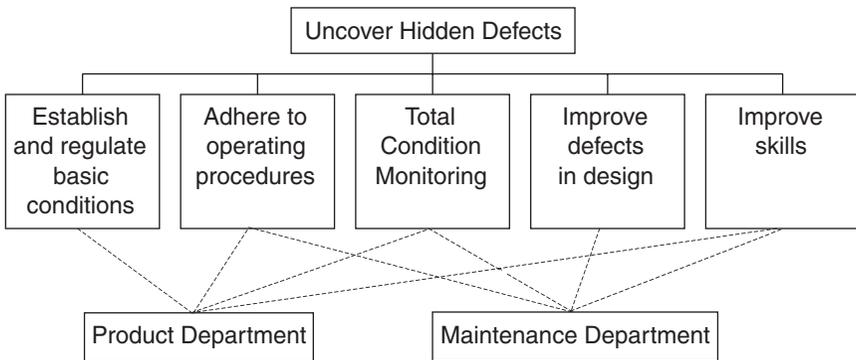


Figure 21-4. Responsibilities of the operations and maintenance departments.

The successful implementation of total productive maintenance requires:

1. Elimination of the six big losses to improve equipment effectiveness
2. An autonomous maintenance program with total condition monitoring
3. A scheduled maintenance program for the maintenance department
4. Increased skills of operations and maintenance personnel
5. An initial equipment management program

Organization Structures for a Performance Based Total Productive Maintenance Program

Typically successful implementation of PTPM in a large plant takes three years. Implementation calls for:

1. Changing peoples attitudes
2. Increasing motivation
3. Increasing competency
4. Improving the work environment

The four major categories in developing a Performance Based Total Productive Maintenance program are:

1. Preparation for the PTPM program
2. Preliminary implementation
3. PTPM implementation
4. Stabilization of the program

Implementation of a Performance Based Total Productive Maintenance

There are several steps involved in implementation of a PTPM program.

1. *Announcement of decision to implement PTPM.* A formal presentation must be made by top management introducing the concepts, goals, and benefits of PTPM. Management commitment must be made clear to all levels of the organization.
2. *Educational campaign.* The training and promotion of PTPM philosophy is a must. This is useful to reduce the resistance to change. The education should cover how PTPM will be beneficial to both the corporation and the individuals.
3. *Creation of organization to promote PTPM.* The PTPM promotional structure is based on an organizational matrix. Obviously, the optimal organizational structure would change from organization to organization.

In large corporations, PTPM promotional headquarters must be formed and staffed. Thus, any questions can be addressed here on a corporate level.

4. *Establishment of basic PTPM goals.* Establishing mottos and slogans can do this. All goals must be quantifiable and precise specifying:

- a. Target (what)
 - b. Quantity (how much)
 - c. Time Frame (when)
5. *Master plan development for PTPM.* A master plan must be created. Total condition monitoring equipment should be designed, and equipment should be purchased.
 6. *Initiation of PTPM.* This represents a “kickoff” stage. At this point, the whole staff must start to get involved.
 7. *Improvement of equipment effectiveness.* This should start with a detailed design review of the plant machinery. A performance analysis of the plant could point to a specific area known to have problems (i.e., section of plant) must be selected and focused on, project teams should be formed and assigned to each train. An analysis should be conducted that address the following:
 - a. *Define the problem.* Examine the problem (loss) carefully; compare its symptoms, conditions, affected parts, and equipment with those of similar cases.
 - b. *Do a physical analysis of the problem.* A physical analysis clarifies ambiguous details and consequences. All losses can be explained by simple physical laws. For example, if scratches are frequently produced in a process, friction or contact between two objects should be suspected. (Of the two objects, scratches will appear in the object with the weaker resistance.) Thus, by examining the points of contact, specific problem areas and contributing factors are revealed.
 - c. *Isolate every condition that might cause the problem.* A physical analysis of breakdown phenomena reveals the principles that control their occurrence and uncovers the conditions that produce them. Explore all possible causes.
 - d. *Evaluate equipment, material, and methods.* Consider each condition identified in relation to the equipment, jigs and tools, material, and operating methods involved, and draw up a list of factors that influence the conditions.
 - e. *Plan the investigation.* Carefully plan the scope and direction of investigation for each factor. Decide what to measure and how to measure it and select the datum plane.
 - f. *Investigate malfunctions.* All items planned in step 5 must be thoroughly investigated. Keep in mind optimal conditions to be achieved and the influence of slight defects. Avoid the traditional factor analysis approach; do not ignore malfunctions that might otherwise be considered harmless.

12. *Final implementation of PTPM.* This stage involves the refinement of PTPM and the formulation of new goals that meet specific corporate needs.

Maintenance Department Requirements

To ensure the success of the PTPM program, the maintenance department must be well equipped and trained. The following six basic categories are prerequisite to the proper functioning of the Maintenance Department under the PTPM:

1. Training of personnel
2. Tools and equipment
3. Condition and life assessment
4. Spare parts inventory
5. Redesign for higher machinery reliability
6. Maintenance scheduling
7. Maintenance communication
8. Inspections

Training of Personnel

Training must be the central theme. The days of the mechanic armed with a ball-peen hammer, screwdriver, and a crescent wrench are gone. More and more complicated maintenance tools must be placed in the hands of the mechanic, and he must be trained to utilize them.

People must be trained, motivated and directed so that they gain experience and develop, not into mechanics, but into highly capable technicians. While good training is expensive, it yields great returns. Machinery has grown more complex, requiring more knowledge in many areas. The old, traditional craft lines must yield before complicated equipment maintenance needs. A joint effort by craftsmen is necessary to accomplish this.

I. Type of Personnel

a. Maintenance Engineer. In most plants, the maintenance engineer is a mechanical engineer with training in the turbomachinery area. His needs are to convert what he has learned in the classroom into actual hands-on solutions. He must be well versed in a number of areas such as performance analysis, rotor dynamics, metallurgy, lubrication systems, and general shop practices. His training must be well planned so that he can pick up

Table 21-2
Performance Test Codes

| | |
|----|---|
| 1. | ASME, Performance Test Code on Overall Plant Performance, ASME PTC 46 1996, American Society of Mechanical Engineers, 1996 |
| 2. | ASME, Performance Test Code on Test Uncertainty: Instruments and Apparatus PTC 19.1, 1988 |
| 3. | ASME, Performance Test Code on Gas Turbines, ASME PTC 22 1997, American Society of Mechanical Engineers, 1997 |
| 4. | ASME, Performance Test Code on Gas Turbine Heat Recovery Steam Generators, ASME PTC 4.4 1981, American Society of Mechanical Engineers, Reaffirmed 1992 |
| 5. | ASME Gas Turbine Fuels B 133.7M Published: 1985 (Reaffirmed year: 1992) |
| 6. | ISO, Natural Gas—Calculation of Calorific Value, Density and Relative Density International Organization for Standardization ISO 6976-1983(E) |

these various areas in steps. His training must be a combination of a hands-on approach coupled with the proper theoretical background. He should be well versed in the various ASME power test codes. Table 21-2 is a listing of some of the applicable codes for gas turbine power plants. Attendance at various symposiums where users of machinery get together to discuss problems should be encouraged. It is not uncommon to find a solution to a problem at these types of round table discussions.

b. Foremen and Lead Machinist. These men are the key to a good maintenance program. They should be sent frequently to training schools to enhance their knowledge. Some plants have one foreman who is an “in-house serviceman;” he supervises no personnel, but acts as an in-house consultant on maintenance jobs.

c. Machinist/Millwright. The machinist should be encouraged to operate most of the machinery in the plant maintenance shop. By rotating him among various jobs, his learning and development is accelerated. He should then become as familiar with a large compressor as a small pump. Encouragement should be given to the machinist to learn balancing operations and to participate in the solution of problems.

Spreading around the hardest jobs develops more competent people and is the basis of any PTPM program. Restricting a man to one type of work will probably make him an expert in that area, but his curiosity and initiative, prime motivators, will eventually fade.

II. Types of Training

a. Update Training. This training is mandatory for all maintenance personnel, so that they may keep abreast of this high technology industry.

Personnel must be sent to manufacturer-conducted schools. These schools, in turn, should be encouraged to cover some basic machinery principles as well as their own machinery. In-house seminars should be provided with in-house personnel and consultants at the plant. Engineers should be sent to various schools so that they may be exposed to the latest technology.

An in-house website, cataloging experiences and special maintenance techniques should be updated and available for the entire corporation especially maintenance and operation personnel. These websites should be full of illustrations, short, and to the point.

A small library should be adjacent to the shop floor, with field drawings, written histories of equipment, catalogs, API specifications, and other literature pertinent to the machine maintenance field. Drawings and manuals should be transferred to the electronic digital media as soon as possible. Access to the Internet on the maintenance and production area computers is a must as many manufacturers post helpful operational and maintenance hints on their websites. API specifications, which govern mechanical machinery, are listed in Table 21-3.

Manufacturer instruction books are often inadequate and need to be supplemented. The re-writing of maintenance manuals on such subjects as mechanical seals, vertical pumps, hot-tapping machines, and gas and steam turbines are not uncommon. The turbine overhaul manuals transferred on CD's could consist of (1) step-by-step overhaul procedures, developed largely from the manufactures training school, (2) hundreds of photographs, illustrating the step-by-step procedures on various types of gas and steam turbines, (3) an arrow diagram showing the sequences of the procedures, and, (4) typical case histories.

Detailed drawings on CD's are developed to aid in maintenance, such as a contact seal assembly, because the "typical" dimensionless drawing supplied by the OEM is not adequate to correctly assemble the compressor seals. Many other assembly drawings should be developed to facilitate the overall maintenance program. Videotaped programs are being developed on seals, bearings, and rotor dynamics, which will be a tremendous asset to most company maintenance programs.

b. Practical Training. The engineers in the maintenance group should be encouraged to gather pertinent vibration and aerothermal data and analyze the machinery. ASME performance specifications, which govern all types of power plants and other critical equipment, are listed in Table 21-2. They should be encouraged to work closely at the various maintenance schedules and turnarounds so that they are familiar with the machinery.

Table 21-3
Mechanical Specifications

| |
|---|
| ASME Basic Gas Turbines B 133.2 Published: 1977 (Reaffirmed year: 1997) |
| ASME Gas Turbine Control and Protection Systems B133.4 Published: 1978 (Reaffirmed year: 1997) |
| ASME Gas Turbine Installation Sound Emissions B133.8 Published: 1977 (Reaffirmed: 1989) |
| ASME Measurement of Exhaust Emissions from Stationary Gas Turbine Engines B133.9 Published: 1994 |
| ASME Procurement Standard for Gas Turbine Electrical Equipment B133.5 Published: 1978 (Reaffirmed year: 1997) |
| ASME Procurement Standard for Gas Turbine Auxiliary Equipment B133.3 Published: 1981 (Reaffirmed year: 1994) |
| ANSI/API Std 610 Centrifugal Pumps for Petroleum, Heavy Duty Chemical and Gas Industry Services, 8th Edition, August 1995 (-1995) |
| API Std 613 Special Purpose Gear Units for Petroleum, Chemical and Gas Industry Services, 4th Edition, June 1995 |
| API Std 614, Lubrication, Shaft-Sealing, and Control-Oil Systems and Auxiliaries for Petroleum, Chemical and Gas Industry Services, 4th Edition, April 1999 |
| API Std 616, Gas Turbines for the Petroleum, Chemical and Gas Industry Services, 4th Edition, August 1998 |
| API Std 617, Centrifugal Compressors for Petroleum, Chemical and Gas Industry Services, 6th Edition, February 1995 |
| API Std 618, Reciprocating Compressors for Petroleum, Chemical and Gas Industry Services, 4th Edition, June 1995 |
| API Std 619, Rotary-Type Positive Displacement Compressors for Petroleum, Chemical, and Gas Industry Services, 3rd Edition, June 1997 |
| ANSI/API Std 670 Vibration, Axial-Position, and Bearing-Temperature Monitoring Systems, 3rd Edition, November 1993 |
| API Std 671, Special Purpose Couplings for Petroleum Chemical and Gas Industry Services, 3rd Edition, October 1998 |

They should be sent to special training sessions where hands-on experience can be gained.

After the completion of basic machinist training, the machinist should continue his training with on-the-job experiences. His skills should be tested, and he should be encouraged to take on different tasks.

To develop the skills of in-house personnel, as much repair work as possible should utilize plant personnel. Encouraging the participation of the machinist in the solution of difficult problems often results in the machinist seeking information on his own. References to API and ASME specifications should not be uncommon on the shop floor. Today's machinist and mechanic must be computer literate. Internet training must be provided with some basic training on word processing and spreadsheet programs.

c. Basic Machinist Training. Most of the basic training can be developed and conducted by in-plant personnel. This training can be highly detailed and tailored precisely to meet individual plant requirements. Training must be carefully planned and administered to fit the requirements of different machinery in the plant.

Many plants have a full-time training program, and personnel for conducting training at this basic level. Good maintenance practices should be inculcated into the young machinist from the beginning. He should be taught that all clearances should be carefully checked, and noted both before and after reassembly. He should learn the proper care in the handling of instrumentation, and the care in placing and removing seals and bearings. A base course on the major turbomachinery principles is a must, so there is basic understanding of what these machines do and how they function. The young machinist should also be exposed to basic machinery-related courses such as:

1. Reverse indicator alignment
2. Gas and steam turbine overhaul
3. Compressor overhaul
4. Mechanical seal maintenance
5. Bearing maintenance
6. Lubrication system maintenance
7. Single plane balancing

Tools and Shop Equipment

A mechanic must be supplied with the proper tools to facilitate his jobs. Many special tools are required for different machines, so as to ensure proper disassembly and reassembly. Torque wrenches should be an integral part of his tools, as well as of his vocabulary.

The concepts of “finger tight” and “hand tight” can no longer be applied to high-speed, high-pressure machinery. A recent major explosion at an oxygen plant, which resulted in a death, was traced back to gas leakage due to improper torquing. A good dial indicator and special jigs for taking reverse indicator dial readings is a must. The jigs must be specially made for the various compressor and turbine trains. Special gear and wheel pullers are usually necessary.

Equipment for heating wheels in the field for assembly and disassembly are needed; specially designed gas rings are often used for this purpose.

A maintenance shop should have the traditional horizontal and vertical lathes, mills, drill presses, slotters, bores, grinders, and a good balancing machine. A balancing machine can pay for itself in a very short time in

providing a fast turnaround and accurate dynamic balance. Techniques to check the balance of gear-type couplings for the large high-speed compressors and turbine drives, as a unit should be developed. This leads to the solving of many vibration related problems. High-speed couplings should be routinely check-balanced.

By dynamically balancing most parts, seal life and bearing life is greatly improved, even on smaller equipment. Dynamic balancing is needed on pump impellers, as the practice of static balance is woefully inadequate. Vertical pumps must be dynamically balanced; the long, slender shafts are highly susceptible to any unbalanced-induced vibration.

This assembly and disassembly of rotors must be in a clean area. Horses or equivalents should be available to hold the rotor. The rotor should rest on the bearing journals, which must be protected by soft packing, or the equivalent, to avoid any marring of the journals. To accomplish uniform shrink fits, the area should have provisions for heating and/or cooling. A special rotor-testing fixture should be provided; this is very useful in checking for wheel wobbles, wheel roundness, and shaft trueness. Rotors in long-term storage should be stored in a vertical position in temperature-controlled warehouses.

Spare Parts Inventory

The problem of spare parts is an inherent phase of the maintenance business. The high costs of replacement parts, delivery, and in some instances, poor quality, are problems faced daily by everyone in the maintenance field. The cost of spare parts for a major power plant or refinery runs into many millions of dollars.

The inventory of these plants can run into over 20,000 items, including over 100 complete rotor systems. The field of spare parts is changing rapidly and is much more complex than in the past. A group of plants have gotten together in a given region and formed "Part Banks."

Many pieces of equipment are made up of unitized components from several different vendors. The traditional attitude has been to look to the packaging vendor as the source of supply. Many vendors refuse to handle requests for replacement parts on equipment not directly manufactured by them. More and more specialty companies are entering the equipment parts business; some are supplying parts directly to OEM companies for resale as their "own" brand. Others supply parts directly to the end user. The end user must develop multiple sources of supply for as many parts as possible.

Gaskets, turbine carbon packing, and mechanical seal parts can be purchased from local sources. Shafts, sleeves, cast parts can be purchased from

local sources. Shafts, sleeves, cast parts such as impellers, are becoming increasingly available from specialty vendors. All this competition is causing the OEM's to alter their spare parts system to improve service and reduce prices, which is definitely a bright spot in the picture. The quality control of both OEM and some specialty houses leaves much to be desired. In turn, this causes many plants to have an in-house quality control person checking all incoming parts, a concept highly recommended.

Condition and Life Assessment

Condition and life assessment is significant for all types of plants, and especially Combined Cycle Power Plants. The most important aspect of a plant is high availability, and reliability, in some cases even more significant than higher efficiency.

The availability of a power plant is the percent of time the plant is available to generate power in any given period. The reliability of the plant is the percentage of time between planned overhauls.

The availability of a power plant is defined as

$$A = \frac{P - S - F}{P} \quad (21-1)$$

where:

P = Period of time, hours, usually this is assumed as one year, which amounts to 8,760 hours

S = Scheduled outage hours for planned maintenance

F = Forced outage hours or unplanned outage due to repair

The reliability of a power plant is defined as

$$R = \frac{P - F}{P} \quad (21-2)$$

Availability and reliability have a very major impact on the plant economy. Reliability is essential in that when the power is needed it must be there. When the power is not available it must be generated or purchased, and can be very costly in the operation of a plant. Planned outages are scheduled for non-peak periods. Peak periods is when the majority of the income is generated as usually there are various tiers of pricing depending on the demand. Many power purchase agreements have clauses, which contain capacity payments, thus making plant availability critical in the economics of the plant.

Gas turbines with the new technology, higher pressure ratio and higher firing temperature, has led to the building of large gas turbines producing

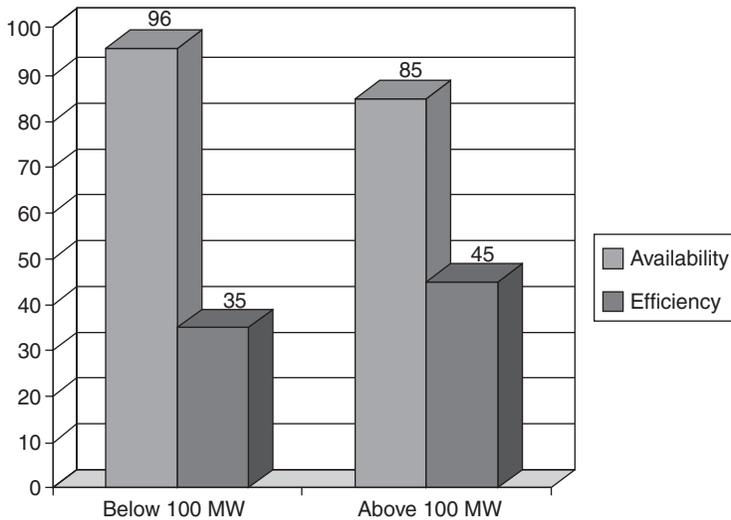


Figure 21-5. Comparison of availability and efficiency for large frame type gas turbines.

nearly 300 MW and reaching gas turbine efficiencies in the mid forties. The availability factor for units with mature technology, below 100 MW, are between 94–97%, while the bigger units above 100 MW have availability factors of 85–89%. The bigger units produce twice the output, but the availability factor has decreased from 95% to 85%. A decrease of 7–10 points for all manufacturers. Part of this decrease may be related to larger machinery taking more time to repair. It is also due to the high temperature and pressure.

The increase in unit size and complexity together with the higher turbine inlet temperature, and higher pressure ratio has lead to an increase in overall gas turbine efficiency. The increase in efficiency of 7–10% has in many cases lead to an availability decrease of the same amount or even more as seen in Figure 21-5. A 1% reduction in plant availability could cost \$500,000/yr in income on a 100 MW plant, thus in many cases offsetting gains in efficiency.

Reliability of a plant depends on many parameters, such as the type of fuel, the preventive maintenance programs, the operating mode, the control systems, and the firing temperatures.

Redesign for Higher Machinery Reliability

Low reliability of units gives rise to high maintenance costs. Low reliability is usually a greater economic factor than the high maintenance costs.

In many large power plants, refineries, and petrochemical complexes, about one-third of the failures are due to machinery failure; it is therefore necessary to redesign parts of a machine to improve reliability.

The maintenance practice of one large refinery is to replace gas turbine control systems with state-of-the-art electronics and “plug-in” concepts for ease of maintenance. These installations have been highly successful in that maintenance has been minimal, and can usually be accomplished on-stream. Another replaces all journal bearings with tilting pad bearings.

In addition, the new control systems increase turbine performance, while speed control and flexibility are greatly improved. The original design has been supplemented to include a self-contained alarm system, a semi-automatic sequential start system, and a complete trip and protection system, as well as the electronic controls. The cost of this system is substantially less than the cost of a similar device offered by the OEM on new machines.

The gas turbines major limitations on the life are the combustor cans, first stage turbine nozzles and first stage turbine blades as seen in Figure 21-6. The effect of dry Low NO_x combustors have been very negative on the availability of Combined Cycle Power Plants, especially those with dual fuel capability. Flash back problems are a very major problem as they tend to create burning in the pre-mix section of the combustor, and cause failure of the pre-mix tubes. These pre-mix tubes are also very susceptible to resonance vibrations.

Bearing failures are one of the major causes of failures in turbomachinery. The changing of various types of radial bearings from cylindrical and/or

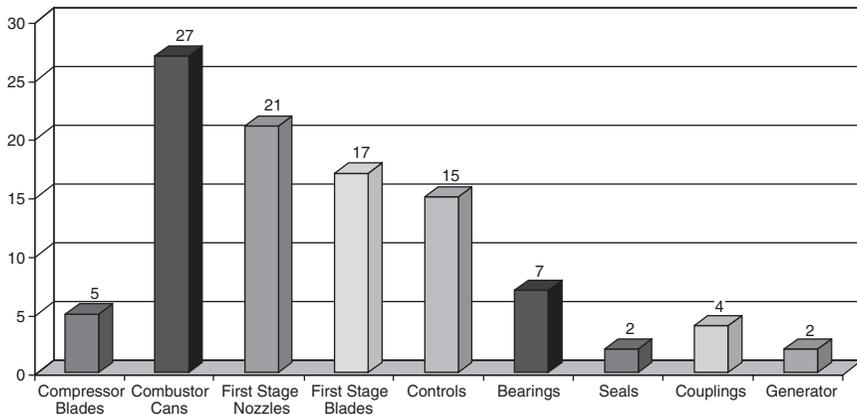


Figure 21-6. Contributions of various major components to gas turbine down time.

pressure dam babbitted sleeve bearings to tilting pad journal bearings is becoming common in the industry. In most cases, this gives better stability, eliminates oil whirl, and under misalignment condition, is more forgiving.

Thrust bearing changes, from the simple, tapered land thrust bearings to tilting pad thrust bearings with leveling links (Kingsbury type), is another area of common change. These types of bearings absorb sudden load surges and liquid slugs. Many users have changed out the inactive thrust bearing to carry the same load as the active thrust bearings. This has been the case in older gas turbines where traditionally the load carrying capacity of the inactive thrust bearing was 1/3 of the active thrust bearing. As gas turbines got older the leakages increased and the thrust forces were altered greatly leading to failures in the inactive thrust bearings.

A major plant replaces the entire large journal and thrust bearings in their main machinery to tilting pad bearings in their plant as a matter of practice.

Material changes of the babbitt are sometimes undertaken. Changing from the more common steel backed babbitted bearings to the copper alloys, with this babbitted pads, conducts surface heat away at a faster rate, thus increasing the load carrying capacity. In some instances, a 50–100% load carrying capacity improvement can be achieved. Some equipment manufacturers are offering bearing-upgrading kits for their machine in service.

Design of turbine blades to obtain higher efficiency and damping has been done. In some cases, this has improved efficiency by 8–10%, and stopped failures in these blades. Steam injection has been utilized in gas turbines to improve efficiency and to increase the power output. Redesign of various bleed-off ports has reduced tip stalls and their accompanying blade failures.

Today's machinery, which is pushing the state-of-the-art in design, needs more than "simple fixes." This is one major reason why so much redesign takes place in the field. Maintenance engineers are no longer just required to repair, they are required in many cases to make revisions. Continual improvements and updating of the machinery is required to obtain the long runs and high efficiencies desirable in today's turbomachinery.

Maintenance Scheduling

The scheduling of maintenance inspections and overhauls is an essential part of the total maintenance philosophy. As we move from "Breakdown" or "Panic" maintenance towards a *performance based total productive maintenance system*, total condition monitoring and diagnostics becomes an integral part of both operation and maintenance. Total condition monitoring and diagnostic examines both the mechanical and performance

of the machinery and then carries out diagnostics. Condition monitoring systems, which are only mechanical systems without performance inputs give less than half of the picture and can be very unreliable. Unscheduled maintenance is very costly and should be avoided. To properly schedule overhauls, both mechanical and performance data must be gathered and evaluated. As indicated earlier, we want to consider repairs during a planned “turnaround” not “random” repairs, which are frequently done on an “emergency” basis and where, due to time restraints, techniques are sometimes used, which are questionable and should only be used in emergencies.

To plan for a “turnaround,” one must be guided by the operating history of the given plant and, if it is the first “turnaround,” by conditions found in other plants utilizing the same or closely similar process and machinery. This is how the time between subsequent “turnarounds” has been extended to three years or more in many instances. By utilizing the operating history and inspection at previous “turnarounds” at this or similar installations, one can get a fair idea of what parts are most likely to be found deteriorated and, therefore, must be replaced and/or repaired, and what other work should be done to the unit while it is down. It should be pointed out that, with modern turbomachinery, items such as bearings, seals, filters and certain instrumentation, which are precision made, are seldom, if ever, repaired except in an emergency; such items are replaced with new parts.

This means that parts must be ordered in advance for the “turnaround” and other work must be planned so that the whole operation may proceed smoothly and without holdups that could have been foreseen. This usually means close collaboration with the manufacturer or consultant and the OEM (or specialty service shop) so that handling facilities, service men, parts, cleaning facilities, inspection facilities, chrome plating and/or metalizing facilities, balancing facilities, and some cases even heat treatment facilities, are available and will be open for production at the proper time required. This is the planning, which must be done in detail before the shutdown with sufficient lead-time available in order to have replacement parts available at the job site.

The old maxim “if it ain’t broke don’t fix it” is very applicable in today’s machinery. A study conducted at a major nuclear power facility found that 35% of the failures occurred after a major turnaround. This is why total condition monitoring is necessary in any performance based total productive maintenance system and leads to overhauls being planned on proper data evaluation of the machinery rather than on a fixed interval.

Maintenance Communications

It is not uncommon to hear the complaint that the maintenance department has “never been informed as to what is happening in the plant.” If this is a common complaint, the maintenance manager needs to examine the communications in his department. The following are six practical suggestions for improving communications:

1. Operation and service manuals
2. Continuous updating of drawing and print files
3. Updating of training materials
4. Pocket guides
5. Written memos, interoffice E-mails
6. Seminars
7. Website postings

Each of these items listed, if properly employed, can transmit knowledge to the person who must keep the plant’s machinery running. How well the information is transmitted depends entirely on the communication skills applied to the preparation of the materials.

Operation and Service Manuals. To be of real value to the mechanic, an operation and service manual must be indexed to permit quick location of needed information. The manual must be written in simple, straightforward language, have illustrations, sketches, or exploded views adjacent to pertinent text, and have minimum references to another page or section. Major sections or chapters should be tabbed for quick location.

Most often a mechanic or serviceman refers to a manual because of a problem. Problems seem to happen during a production run. It is essential, therefore, that he be able to find the needed information quickly. The mechanic should not be delayed by wordy, irrelevant text. The objective of any manual is to be an effective, immediate source of service information.

The assignment of a nontechnical person to write a manual is shortsighted and more costly in the long run. A well-written manual is continuously in use. Good manuals need not be complicated. In fact, the simpler the better. Manuals should be readable and understandable, whether they are compiled in-house or outside.

Drawing and Print File. A good print file is a vital tool for any maintenance organization. Reference files in a large or multi-plant company can be particularly burdensome for several reasons:

1. Prints are bulky and difficult to store properly
2. Control of use is necessary
3. Files must be kept up to date
4. Handling and distribution of new or revised prints is usually expensive.

A practical solution is to digitize the drawings and place them on CD's available to the maintenance and operation department. A good digital file reduces search time and helps the departments do a better job of keeping the machinery operating at their peak efficiency with minimal downtime.

Training Materials. Like any other written or audio-visual maintenance tool, training materials of all kinds are basically communication devices, and to be effective, should be presented in a simple straightforward, attractive, and professional manner.

Once the need for specific maintenance training has been determined, a program must be developed. If the training need applies to a proprietary machine or one that is unique to a very few industries, it might be necessary to contact companies who specialize in custom digital programs on CD's, slide/tape, movie, videotape, or written training programs. The cost may shock the uninitiated, but after shopping around, the company may find that it can recover far more than the initial cost in tangible benefits over a relatively short period.

Pocket Guide. When a new maintenance form or procedure is introduced, a quick reference pocket guide can promote understanding and accuracy. The key to effectiveness is a deliberate design to provide maximum illustrations or examples in simple language. If it cannot be prepared in-house, outside help should be sought. Professionalism is essential to good communications.

Written Memos. One of the most effective devices for improving maintenance communications is a newsletter or internal memo. The memo's success depends heavily on communicating formal tips and techniques in the mechanics language and using photos, sketches, and drawings generously to get the message across.

Everyone in the maintenance department should be encouraged to contribute ideas on a better way to do a task or a solution to a nagging problem related to the maintenance or operation of production equipment. Each contributor should be given credit by name and location for his or her effort. Very few workers can resist a bit of pride in seeing their names attached to an article that is seen by virtually everyone in the company.

Seminars and Workshops. College or industry-sponsored seminars, continuing education courses, and workshops are means of upgrading or

sharpening skills of maintenance people. Such an approach serves a twofold purpose. First, it communicates the company's good faith in the person's ability to benefit from the experience, and by acceptance, the worker shows willingness to improve his or her usefulness to the company. The seminars are very useful in disseminating knowledge. They also provide forum for gripes and meaningful solutions. Discussion groups in these seminars and workshops are very important as participants share experiences and solutions to problems. The knowledge gained from these seminars is very useful.

Inspection

As with any power equipment, gas turbines require a program of planned inspections with repair or replacement of damaged components. A properly designed and conducted inspection and preventive maintenance program can do much to increase the availability of gas turbines and reduce unscheduled maintenance. Inspections and preventive maintenance can be expensive, but not as costly as forced shutdowns. Nearly all manufacturers emphasize and describe preventive maintenance procedures to ensure the reliability of their machinery, and any maintenance program should be based on manufacturer's recommendations. Inspection and preventive maintenance procedures can be tailored to individual equipment application with references such as the manufacturer's instruction book, the operator's manual, and the preventive maintenance checklist.

Inspections range from daily checks made while the unit is operating to major inspections that require almost total disassembly of the gas turbine. Daily inspections should include (but are not limited to) the following checks:

1. Lubrication oil level
2. Oil leakage around the engine
3. Loose fasteners, pipe and tube fittings, and electrical connections
4. Inlet filters
5. Exhaust system
6. Control and monitoring system indicator lights

The daily inspection should require less than an hour to perform properly and can be made by the operator.

The interval between more thorough inspections will depend on the operating conditions of the gas turbine. Manufacturers generally provide guidelines for determining inspection intervals based on exhaust gas temperatures, type and quality of fuel utilized, and number of starts.

Table 12-2 shows time intervals for various inspections based on fuels and startups. Minor inspections should be performed after about 3000–6000 hours of operation, or after approximately 200 starts, whichever comes first. This inspection requires a shutdown for two to five days, depending on availability of parts and extent of repair work to be done. During this inspection, the combustion system and turbine should be checked.

The first minor inspection or overhaul of a turbine forms the most important datum point in its maintenance history, and it should always be made under the supervision of an experienced engineer. All data should be carefully taken and compared with the turbine erection information to ascertain if any setting changes, misalignment, or excessive wear have occurred during operation. Subsequent inspections are also of great importance, since they verify manufacturers' recommendations or help to establish maintenance trends for particular operating conditions.

When the established time for major maintenance approaches, a meeting should be arranged between the operating department and the manufacturer's engineer to discuss and arrange for the date of turbine outage. A short time before taking the turbine out of service a complete operational test should be made at zero, one-half, and normal maximum loads, preferably in the presence of the manufacturer's engineer. These tests are for reference temperatures and pressures, which will serve as a means of comparison with identical tests that should be made immediately after the unit is overhauled. The operational tests should end with an over-speed trip test to indicate whether attention should be given to the governor or tripping mechanism during the shutdown. These specific data will also serve together with the logged operational data or case history (which should be reviewed with the manufacturer's engineer) to determine the focal point or items requiring special attention or investigation:

1. Increase or change in vibration
2. Decrease in air compressor discharge pressure
3. Change in lube oil temperatures or pressure
4. Air or combustion gases blowing out at the shaft seals
5. Incorrectly reading thermocouples
6. Change in wheel space temperatures
7. Fuel oil or gas leakage
8. Fuel control valves operate satisfactorily
9. Hydraulic control oil pressures changed
10. The turbine governor "hunts"
11. Change in sound level of gear boxes

12. Overspeed devices operate satisfactorily
13. Babbitt or other material found on lubricating oil screens
14. Lube oil analysis shows corrosion factor increase
15. Change in pressure drop across heat exchangers
16. Turbogenerator reaches rated load at design ambient and exhaust temperature conditions

Preparation for shutdown should be made as complete as possible to eliminate lost time and confusion at the beginning of the job.

A list should be made of all major items that are to be inspected or repairs to be made if they are known at the time. This list should be prepared with the manufacturer's engineer present. A detailed schedule should be formulated from this list including the time allotted for the shutdown and the maintenance crew available. Plan the work with the expectation of finding the worst conditions—the unexpected work found after the machine is opened will then be compensated. This procedure will greatly reduce the possible need for costly overtime.

Tools on-site should be reviewed by the manufacturer's engineer. All special or regular equipment not on hand that is necessary or required to do any part of the work should be ordered and on-site before shutdown.

Exact outage time should be arranged, and the turbine prepared for the contracting crew or plant maintenance crew. All personnel should be on the job or available to meet the starting date.

Facilities, such as convenient air and electrical connections, should be prearranged for operating tools, etc. Sufficient hose lengths and connectors are required as well as electrical extension cords. Install air driers or water separators in the air system, since dry air is necessary for successful grit blasting of turbine parts.

Before removing turbine flange bolts or disturbing the normal turbine setting, clearance readings between the last row of turbine rotating blades and their wheel shroud should be made at both horizontal and vertical positions. Evidence of the main turbine flange spreading or warping should be checked with feeler gauges between each of the flange bolts. Elevation checks at each of the turbine supports should be made for comparison with original readings to determine if there has been movement at these points. When all outside checks have been made, structural beam supports should be placed under the turbine at the midpoints between the normal turbine supports. Screw jacks must then be used to bring pressure under the turbine until a slight deflection on dial has been reached. For this purpose, use only screw jacks, not hydraulic or lift jacks. Flange bolts can then be removed as well as the top half of the turbine casing.

Borescope Inspection

Borescope inspection is carried out because of the following benefits it can provide in the maintenance program:

1. Internal on-site visual checks without disassembly
2. External periods between scheduled inspection
3. Allows accurate planning and scheduling of maintenance actions
4. Monitors condition of internal components
5. Increased ability to predict required parts, special tools, and skilled manpower

Figure 21-7 shows the time savings one may obtain by the proper use of borescopic inspection for planned maintenance.

The borescope contains its own light source throughout the engine internal passages. Once inserted, the flexible borescope can be maneuvered to inspect the complete hot-section flow path. The results of the visual inspection can be used to assist in planning scheduled disassembly of the gas turbine. It must be remembered that a borescope is a monocular device, and it is extremely difficult to estimate size or distance. Maintenance personnel should be well trained to use a borescope effectively. Photographs, especially colored, can be utilized as a reference on the history of a machine. In addition to performing inspections while the gas turbine is not operating, some research has been conducted to develop methods for inspection during operations by providing a film of cooling air around the borescope tube. If this system is developed, it will enable visual inspections of the hot sections up to the first-stage turbine blades without shutting down the unit.

Turbomachinery Cleaning

There are at least three reasons for “on-stream” cleaning. The first is to restore the system’s capability. If the unit is a driver, its maximum horsepower will probably drop as it becomes dirty. Cleaning will restore this limit. If the machine is a dynamic compressor, fouling may reduce its head, and therefore, the maximum gas flow rate. Cleaning will restore the capacity limit.

The second reason is to increase the machine’s efficiency. In most cases, fouling will increase the fuel or power required for a certain task. The deposits change the flow contours. Removal of the deposits will restore the original profiles and the efficiency.

Cleaning also prevents failures due to abnormal operating modes. Fouling of the rotor blades on turbines can cause thrust-bearing failures. Deposits on

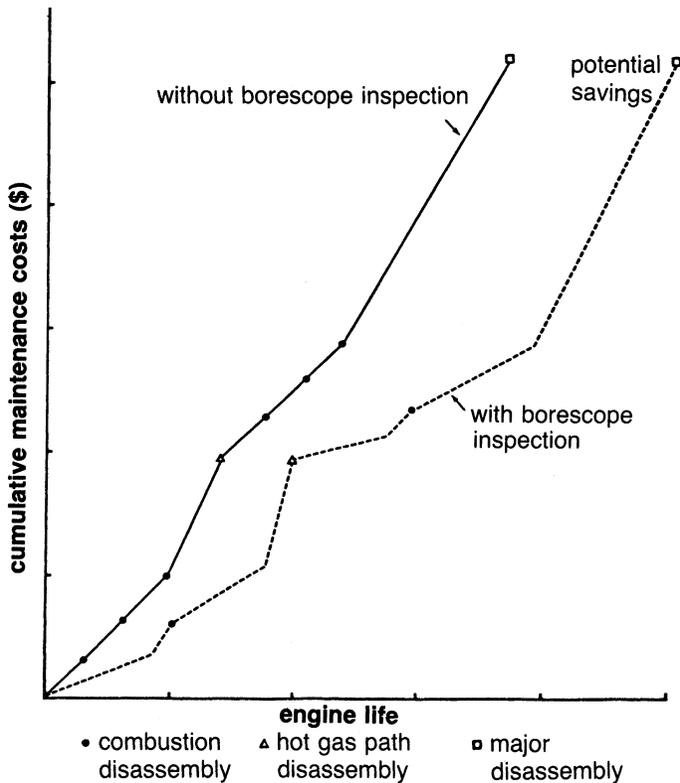


Figure 21-7. Effect on planned maintenance with usage of borescope.

turbine governor valves and trip and throttle valves are suspected of causing overspeed failures. Fouling of balance piston labyrinths and balance lines has caused thrust-bearing failures in centrifugal machines. Any rotor deposit can cause vibration from unbalance if it is not laid down uniformly or if it sluffs off nonuniformly. There can be other, similar effects which will cause failure of a unit.

Fouling Indicators

A prerequisite of a cleaning program is some kind of fouling detection system. Naturally, this system must cover the prime reason for cleaning. If the machine is a gas turbine, the prime reason may be horsepower capability, or it may be efficiency. On a centrifugal compressor, the prime reason for

cleaning may be to restore capacity, to improve efficiency, or to reduce thrust loading.

The selection of a fouling detection system will be strongly influenced by the safety and complexity of the cleaning procedure. For example, the procedure may be to throw 10 pounds of spent catalyst into the suction of a gas turbine. Or, it may involve injecting a quart of water into a single-stage mechanical-drive turbine with a 30 °F superheated inlet. In either case the risk of damage and the personnel required are low. The cleaning should be frequent and routine.

Fouling indicators include:

1. Gas turbine exhaust temperature
2. The exponent $n - 1/n$ on a compressor or gas turbine where γ is either known or is relatively constant
3. The exponent $n - 1/n$ in one section of a machine relative to another section handling the same gas
4. The pressure ratio in one section of a machine relative to another section
5. Thrust loading or thrust-bearing metal temperature
6. Balance line to suction differential pressure
7. Compressor discharge pressure and temperature
8. High vibration readings

Cleaning Techniques

There are two basic approaches to cleaning: abrasive cleaning, and solvent cleansing. Details of cleaning are given in Chapter 12. Abrasion is the simplest of the two methods, but it is usually the least effective. Figure 21-8 shows that abrasive cleaning does not bring the unit back to full performance and that there is a deterioration in the maximum performance after repeated cleanings. The more common abrasives are 1/64-inch nut shells or spent catalyst. The abrasive must have sufficient mass to achieve the momentum required to dislodge the dirt. However, high-mass particles do not follow the gas stream. Also, they are hit by the leading edge of the moving wheels and blades. Consequently, the trailing edges are not abraded. The closer the dirt is to the injection point, the less significant the asymmetrical distribution.

The abrasive must also be sufficiently tough to resist breakage on impact. Rice is a poor substitute, since it tends to shatter on impact and small particles lodge themselves in bearings and seals. Again, the closer the injection to the deposit, the less significant the toughness.

Another problem with abrasives is what happens to them after they have done the cleaning. In a simple-cycle gas turbine they will probably be burnt.

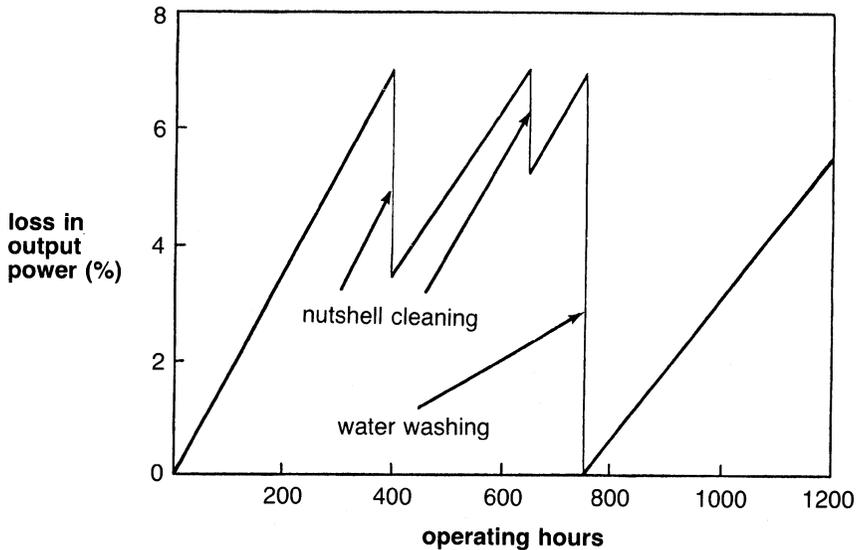


Figure 21-8. Effect of cleaning on power output.

However, in a regenerative unit they can deposit in the regenerator. Some regenerator burnouts have been attributed to these deposits. In steam systems they will probably plug up traps throughout the system.

During discussions about abrasive cleaning, the possibility of causing labyrinth damage is always raised. In fact, these apprehensions have proven groundless. No one knows why, but it could be that the particles are too big to enter the clearance space. On a centrifugal compressor, a typical radial clearance on the interstage shaft labyrinth is 0.008 inches, as compared to a particle size of 0.060 inches. The eye labyrinth has a much greater clearance, but an abrasive particle would have to make an unguided 180° turn to reach it. It is unlikely that a particle would do so.

How are the abrasives introduced into the machine? With air compressors, the abrasive can be thrown into the open suction. If the suction or point of injection is pressurized, the abrasives can be introduced with a blow pot. An eductor should be used to put the abrasive leaving the blow pot into a fluidized state before introducing it to the main gas stream. A good starting point for the injection rate is 0.1 weight percent of gas flow.

Solvent cleaning is a much more delicate technique than the brute force of abrasion. In reality, there will almost always be some abrasive action involved. The idea is to dissolve the deposit in a solvent. The solution must

then be removed from the system before the solute is redeposited. Each solvent-cleaning application presents different problems. Two methods are outlined:

1. *Water wash.* This method is used to remove deposits. Distilled water is sprayed into the air inlet at a specified rate and engine speed. This speed is normally at a reduced rpm so that the water will not flash into steam in the compressor and therefore become ineffective on the latter stages or diffuser.
2. *Detergent wash.* This method is used to remove oil and oil-like deposits. A mixture of solvent detergent and water is sprayed into the inlet while the gas turbine is being rotated by the starter. The unit is allowed to remain idle for a period of time to allow the solution to dissolve and loosen the deposits. The procedure is then repeated except that distilled water is used to flush the deposits off the compressor and out the combustor drains.*

Hot-Section Maintenance

Combustion chambers can be removed if integrally arranged with the turbine, or they can be minutely inspected for cracks or burned areas with a borescope. Short, individual cracks are not uncommon and need no immediate attention. However, if the cracks are grouped such that their continuance or the beginning of another crack could cause the loss of a piece of metal, then a repair should be made. Cracks of this nature normally can be welded with a type of welding rod recommended by the manufacturer, depending on the kind of metal involved. Burned or warped areas in combustion chambers or baskets can be cut out and new sections welded. However, burned areas should be studied with regard to location, pattern, or repetition in all chambers to determine the cause of the burning.

Individual burned areas may indicate a dirty or faulty fuel burner nozzle or misalignment of the combustion chamber. Similar burned areas in various chambers may indicate abnormally high firing temperatures during starting due to excessive fuel use. They may also be the result of “slugs” of liquids entering with the fuel gas, excessively rapid starts, or overloading of the

* Solvent wash of the hot section requires the unit to be brought down to idle speed. The metal temperatures in the unit should be around 200 °F. To achieve this temperature in a reasonable time, the unit can be run on the starter rotor. For a large turbine, the entire wash cycle will take about 16–20 hours.

turbine. The combustion chamber positions as well as the actual chambers or baskets should be permanently numbered, and a complete record should be made for each basket regarding hours of service, repairs or replacements made, and their location in the turbine at each inspection date. The basket ends, or at places where they are supported, should be inspected for excessive wear from vibration, or expansion and contraction movement. Repair of these parts should be made by cutting out and welding in new materials or replacing spring seals if necessary. The first-stage turbine stationary blades or nozzles can be superficially inspected for warps or sags by entering the turbine through the combustion chamber areas or by removing inspection plates. In certain size turbines (and by somewhat difficult maneuvering), the last row or turbine rotating blades can be inspected by entering through the turbine discharge duct. The opportunity should be taken to measure, if possible, the blade tip clearance at four points on the circumference. Comparison of these clearance readings with those at installation or at some previous time will indicate if rubs have occurred and whether or not the seal ring is warped and out of round. It will also indicate whether or not the rotor is below its original position and requires further investigation at the over-haul period.

As the hot sections become exposed, preliminary inspection for cracks or warping should be undertaken to estimate work to be done. The bearings require inspection for wear and alignment for the same reason. The transition pieces should be inspected for cracking and wear at points of contact. Wear usually occurs between the transition piece and the combustion liner sleeve, and also at the first-stage nozzle fit. The cylindrical section of the transition piece may be replaced if the wear is excessive; wear at the nozzle-end of the transition piece is more serious because it allows excessive vibration of the transition piece, which might lead to cracking. Transition pieces should be replaced if 50% of the inner or outer seal is reduced to half the original thickness. If the transition piece is in otherwise excellent condition, the seals may be ground off and replaced. The new floating seals have been found to be more reliable than the old fixed seals. Transition pieces should be replaced if cracks are found in the body.

Turbine blades should be closely inspected for erosion and cracks. The most critical areas in the turbine rotor are the fir-tree section, where the blades are attached to the rotor, and the trailing edge of the blade near the hub. The trailing edge of the turbine blade is usually the hottest section of the blade. These areas should be carefully cleaned and checked for cracks with spray penetrant. First-stage inlet vanes and rotating blades should be removed and blasted clean with a No. 200 grit aluminum oxide or other approved blasting material. They should then be inspected minutely for

cracks by means of red dye or black light. The first-stage inlet vanes will probably need attention, which can be done on the job. Vane warpage on the trailing edge, if any, can be taken out by inserting a spacer piece of correct cross-sectional area between the vanes, heating the top vane to red heat with a torch, and forging the vane edge flat with a hammer and flatter. The cracks, if less than 1.5 inches long, can be grooved out and welded, providing the crack does not run under the end-supporting rings. In this case, the vane must be removed and welded or a new vane fitted in place. As the vanes are welded, they must be continually checked for new cracks, which in turn must be grooved and welded and checked again.

While repairing the first-stage inlet vanes, the upper- and lower-vane section should be bolted or clamped together, and the entire ring should be placed on a flat, level surface, or sufficiently supported in the horizontal plane to prevent heat warpage of the ring due to heating of the vanes during their repair.

After straightening or taking out any warpage in the trailing edges of the vanes (partitions), perpendicular distances between the trailing edges of each vane and the surface of the next should be carefully measured. An average of these distances should be made and then corrected to a plus or minus percentage approved by the manufacturer. This method will help to assure equal distribution of gas flow to the first-stage rotating blades for elimination of blade vibration.

Turbine rotating blades cannot be field-repaired if they are cracked. If one or two blades are damaged mechanically, the manufacturer may recommend field repair or replacement of the damaged blades. However, if several blades are fatigue cracked, it is recommended that the entire set be replaced, since the remaining blades have been exposed to the same operating conditions and, therefore, have little fatigue life left.

Both top and bottom halves of the journal bearings should be inspected for misalignment wear as well as excessive "in-line" wear, which can occur in turbines with frequent starts. An indication of the condition of the thrust-bearings can be made by removing a small section of the turbine shaft, usually on the governor end, and axially moving or bumping the shaft. The amount of axial shaft movement will indicate the thrust clearance and, if it is found to be 0.012–0.015 inches, it can be considered normal.

If the turbine is not out of alignment, or the shaft bowed as determined by the vertical and horizontal clearance checks or the appearance of the bearing surfaces, it is not recommended that the rotor be removed. Some turbine designs, however, may require removal of the rotor to facilitate the removal of some bottom sections of the diaphragms or inlet vanes. If the rotor is

removed, special care must be taken when separating the couplings. Coupling flanges must be marked and run-out checks made for alignment so that they can be properly reassembled. However, the work should always be done under the manufacturer's supervision.

Work should be made to progress strictly in accordance with the planned flow charts, which must be constantly kept updated. Extra work and delays will probably be encountered; however, a well-planned program will include certain allowances, and little change should be required. If any significant change is encountered, the program should be revised to show the extra outage time and possible extra personnel required.

Compressor Maintenance

Besides checking the hot section, the compressor blades in axial compressors should also be inspected. The compressor inspection should be conducted to determine the mechanical and aerodynamic condition of the compressor. Most axial-flow compressors have stacked rotors with bolts extending through all the discs. The bolts should be inspected and, if any are loose, the stretch on the bolts should be determined.

Axial compressor performance is sensitive to the condition of the rotor blades. During a major inspection, all blades should be cleaned and checked for cracks with a penetrant test. If cracks are found in any blade, that blade should be replaced. Occasionally, small cracks can be blended out, but this procedure should be approved by the manufacturer.

The amount of wear on an axial-flow compressor blade is usually a function of foreign particle ingestion. Dust is the most common foreign particle. The maximum and minimum chord lengths should be recorded and reported to the manufacturer, who in turn should be able to report the performance loss occasioned by wear and the decrease in structural strength.

If the air inlet is subjected to saltwater contamination, the rotor and stator blades should be checked for pitting. Severe pitting near the blade roots may lead to structural failures. The manufacturer should be informed of severe pitting.

Stator blades are as important as rotor blades. All the same cleaning, inspection, and nondestructive test procedures should apply. It should be noted that the wear pattern is somewhat different on the stator blades. Again, the manufacturer should be informed of the wear conditions and should in turn make recommendations concerning continuous operation or replacement.

On completion of required repair and replacement, the gas turbine should be reassembled. This reassembly should be done under careful and experienced supervision to ensure all work meets established criteria. Blade clearances, bearing clearances, and spacing should be checked and recorded during assembly. Special care should be taken to ensure that the machinist uses the proper torque when tightening bolts and nuts. There is a very strong tendency for machinists to apply a torque that “feels” right rather than using a torque wrench. Torque is a very important aspect of assembly. Improper torquing can cause component warpage and distortion, especially in those components subject to high temperatures during operation.

Bearing Maintenance

With high-speed machines, simple bearing failures are rare unless they are caused by faulty alignment, distortion, wrong clearance, or dirt. More common are failures caused by vibrations and rotor whirls. Some of these originate in the bearings, others can be amplified or attenuated by the bearings, the bearing cases, and the bearing support structure.

During inspection, all journal bearings should be closely inspected. If the machine has not suffered from excessive vibrations or lubrication problems, the bearings can be reinstalled and utilized.

Four places should be checked for wear during inspection periods:

1. Babbitted shoe surface
2. Pivoting shoe surface and seat in retaining ring
3. Seal ring bore or end plates
4. The shoe thickness at the pivot point or across ball *and* socket; all shoes should be within 0.0005% of the same thickness

While being inspected, the following checks should be made:

1. All leading edges of shoes must have a uniform radius for the full length across the shoe. File the radii if necessary to obtain proper size.
2. Light scratches in the babbitt face do not necessarily require shoe replacement. If no wear is detected, scrape lightly with a sharp straight-edged scraper (plate type) to remove any upsetting caused by scratches.
3. Shoes should be replaced as *sets* only if:
 - a. Radial clearance has increased more than $1\frac{1}{2}$ mils over nominal design clearance.
 - b. Leading or lagging edges of shoes show signs of wear.

4. The tilting-pad and support-ball combination spare parts should be lapped together, making them an integral unit. When a new or used bearing is disassembled for cleaning and inspection, care should be taken not to mix the tilting-pad and support-ball combinations.
5. On reassembly, care should be taken to return the tilting-pad and support-ball combination to the original location in the support ring. Changes in clearance and concentricity can result if the tilting-pad and support-ball combination is not returned to the same location. An eccentricity of as little as one mil can cause severe vibration problems.

Clearance Checks

1. Check housing OD and ID to be sure it is round.
2. Check bore and face-end plates for nicked edges, deep scratches, or scoring. Stone or scrape if necessary, and polish with very fine aluminum oxide polishing paper.
3. Check parting-line surfaces for full contact. Stone or lap if burrs or raised edges exist.
4. Check pivoting surfaces of shoe and housing ring for scratches, scoring, or erosion. Stone if necessary.
5. For tilting-pad bearings, blue-shoe the pivot surface, and check for contact area and position. The contacting surface must be in the center only and at the bottom portion of the pivot bore in the retainer.
6. Check to be sure that pins do not bottom-out in pads.
7. For ball-and-socket designs, check to be sure the ball seats properly and solidly in the counter bore.
8. Check for shaft clearance as follows:
 - a. Select a stub mandrel in which the minimum diameter is the journal diameter plus minimum desired clearance (about $1\frac{1}{2}$ mil per inch of shaft diameter) and the larger diameter is journal diameter plus desired clearance (about 2 mils per inch of shaft diameter).
 - b. Assemble the bearing halves.
 - c. Slip the assembled bearing over the smaller diameter of the mandrel.
 - d. Tap the bearing lightly on the back of the housing and slide the bearing down on the next larger diameter.
 - e. The mandrel should be rotated and the OD of housing indicated.

Thrust-Bearing Failure

A thrust-bearing failure is one of the worst things that can happen to a machine, since it often wrecks the machine, sometimes completely. To evaluate the reliability of a thrust-bearing arrangement, we must first consider how a failure is initiated and evaluate the merits of the various designs.

Failure initiation. Failures caused by bearing overload during normal operation (design error) are rare today, but still far more thrust failures occur than one would expect, considering all the precautions taken by the bearing designer. The causes in the following list are roughly in sequence of importance:

1. *Fluid slugging.* Passing a slug of fluid through a turbine or compressor can increase the thrust to many times its normal level—even if only a few gallons are involved. Instantaneous failures of the downstream bearing may result from fluid slugging.
2. *Build-up of solids in rotor and/or stator passages (“plugging” of turbine buckets).* This problem should be noticed from performance or pressure distribution in the machine (first-stage pressure) long before the failure occurs.
3. *Off-design operation.* Especially from backpressure (vacuum), inlet pressure, extraction pressure, moisture. Many failures are caused by overload, off-design speed.
4. *Compressor surging.* Especially in double-flow machines.
5. *Gear coupling thrust.* A frequent cause of failure, especially of upstream thrust bearings. Thrust is high when alignment is perfect (friction coefficient 0.4–0.6), decreasing to a minimum when a small misalignment is present (about 0.1 at 25° angular misalignment). Friction increases rapidly again to 0.5 or more with an increase in misalignment. (These are rough numbers only, to show basic relationships.) The thrust is caused by friction in the loaded teeth that opposes thermal expansion. Therefore, thrust can get very high, since it has no relation to the normal thrust caused by pressure distribution inside the machine (for which the thrust bearing may have been dimensioned). The coupling thrust may act either way, adding to or subtracting from normal thrust. Much depends on tooth geometry and coupling quality. A straight-sided tooth can take misalignment only when the tooth fit has enough clearance to permit slanting of the male tooth inside the female teeth. For example, with vertical

misalignment, the teeth on both sides will bind when the clearance is insufficient to allow for slanting. This can cause very high thrust, sometimes one can hear a “metallic sound” building up until the rotors finally slip with a very noticeable “bump.” Then the noise and vibration are gone, at least for a while. This phenomenon, of course, is torture for the thrust bearings, and it may cause failure in either direction. Dirt in the coupling can aggravate this situation or even cause it.

6. *Dirt in oil.* A common cause of failures, especially when combined with other factors. The oil film at the end of the oil wedge is only a small fraction of a thousandths thick. If dirt goes through, it can cause the film to rupture, and the bearing may burn out. Therefore, very fine filtering of the oil is required. But the best filter is no good if maintenance personnel leave the filter or bearing case open after inspection, and the rain and sand blow in, or if they put the wet filter elements on the sandy floor, or accidentally knock holes in the elements. It happens far too often. Once a machine is wrecked, it is difficult to reconstruct.
7. *Momentary loss of oil pressure.* Sometimes encountered while switching filters or coolers.

Failure protection. Fortunately, accurate and reliable instrumentation is now available to monitor thrust bearings well enough to assure safe continuous operation and to prevent catastrophic failure in the event of an upset to the system.

Temperature sensors, such as RTDs (Resistance Temperature Detectors), thermocouples, and thermistors, can be installed directly in the thrust bearing to measure metal temperature. The installation shown in Figure 21-9 has the RTD embedded in the babbitted surface. It is in the most sensitive

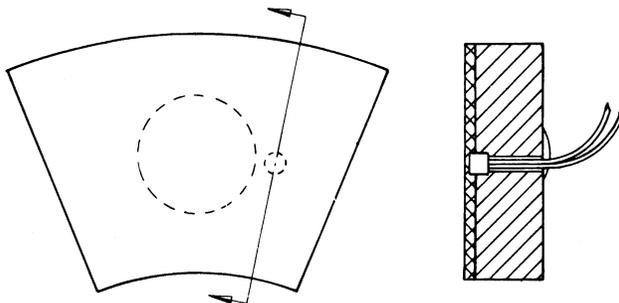


Figure 21-9. RTD embedded in bearing surface.

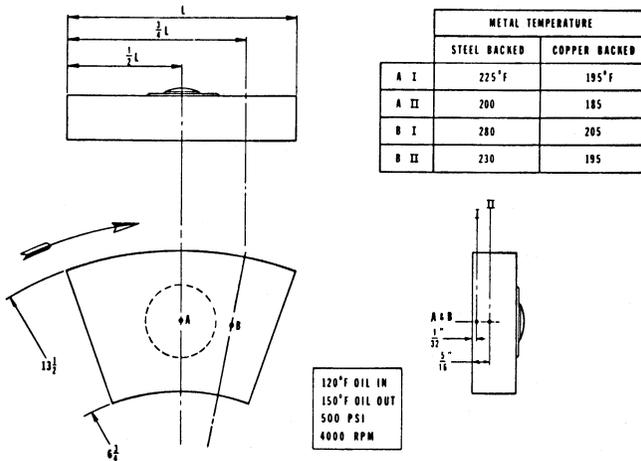


Figure 21-10. Temperature distribution in bearing surfaces.

zone of the shoe—70% from the leading edge and 50% radially. The position of the sensor is critical in establishing the safe operating limits. As long as the probe is generally in the zone of maximum temperature, it will be highly sensitive to load, although the level of temperature may vary considerably as can be seen in Figure 21-10. The temperature is also dependent on the pad-backing material. At 500 psi load, the center sensor at A-II registers 200°F while the sensor at B-I registers 280°F in a steel-backed bearing. Again, these temperatures are typical and will vary with size, type, speed, and lubrication from bearing to bearing. The difference in a copper-backed bearing can be seen to be quite significant, with A-II reading 185°F and B-I reading 205°F. The position of the sensor with respect to the surface is less significant in this bearing than in the steel-backed bearing. Again, position in the sensitive zone is important in establishing safe operating limits with respect to temperature.

Axial proximity probes are another means of monitoring rotor position and the integrity of the thrust bearing. A typical installation is shown in Figure 21-11. In this case two positions are being monitored: one at the thrust runner, and one at the end of the shaft near the centerline. This method detects thrust-collar runout and also rotor movement. In most cases this ideal positioning of the probes is not possible. Many times the probes are indexed to the rotor or other convenient locations and thus do not truly show the movement of the rotor with respect to the thrust bearing.

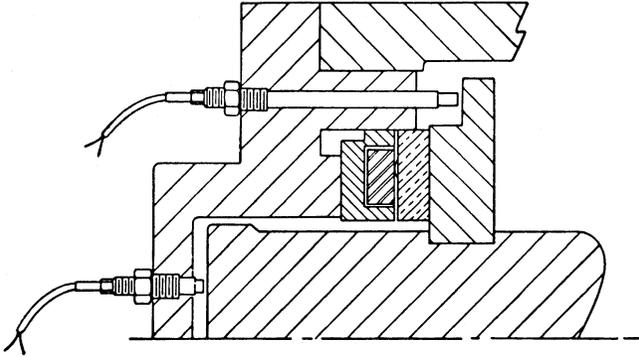


Figure 21-11. Actual probes for thrust-bearing monitoring.

A critical installation should have the metal temperature sensors in the thrust pad. Axial proximity probes may be used as a backup system. If metal temperatures are high and the rate of change of those temperatures begins to alter rapidly, thrust-bearing failure should be anticipated.

Coupling Maintenance

The major inspections should also include detailed inspections of any couplings in the train. Gear couplings should be disassembled and teeth inspected for indications of problems. The most common failures encountered with continuous lubrication-type gear couplings are:

1. Wear
2. Corrosive wear
3. Coupling contamination
4. Scoring and welding

Couplings with sealed lubrication systems tend to have wear problems similar to couplings with continuous lubrication, but they must also be checked for fretting corrosion and cold flow. These problems result from normal coupling operation. If for some reason excessive misalignment exists, additional damage can be revealed by tooth breakage, scoring, and pitting.

Disc couplings should be checked to ensure there are no cracks in the discs or connecting shaft. If damage does not exist, which can be repaired, the coupling should be rebalanced prior to installation.

Rejuvenation of Used Turbine Blades

Nature of Service Damage in Turbine Blades

Two distinct types of damage can be recognized: surface damage and internal degradation. Surface damage may be due to either mechanical impact or corrosion, and is generally confined to the blade airfoil. In both cases, light damage can be removed by blending or dressing. Blades with severe surface damage or cracks are scrapped. Some of these blades can be coated with some high-temperature coatings. When properly applied, these coatings can increase the life of the blades considerably, in some cases even more than when they were new. Recent advances in high-temperature coatings for severe hot-corrosion service has resulted in the low unit cost feature of pack cementation and the economy of electroplating to yield multiple-element coatings containing precious-metal aluminides. These coatings are available in several combinations of platinum, rhodium, and aluminum for application to cobalt- and nickel-based vanes and blades.

Internal degradation is caused by microstructural changes, which result from extended exposure at high temperature under stress. The microstructural changes are responsible for the reduction in mechanical properties. Three forms of internal degradation have been verified: (1) precipitate coarsening or overaging, (2) changes in grain boundary carbides, and (3) cavitation or void formation.

A considerable fraction of the intermediate temperature strength of nickel-based turbine blade alloys results from the fine γ' precipitate $\text{Ni}_3(\text{Al}, \text{Ti})$. The γ' particles generally coarsen as a function of time to the one-third power growth law, with a corresponding decrease in strength. Grain boundary carbide morphology and amount can also change with time. Since the alloy heat treatments, which cause carbide formation, are generally optimized for short-term properties, long-term changes in carbide structure are usually detrimental, particularly with respect to such properties as ductility and notch sensitivity. Cavitation represents the initial step in creep failure. It consists of the nucleation and growth of voids on grain boundaries. With time, the isolated voids link up to form cracks. It appears that blade material has to be near or in tertiary creep before cavitation can readily be detected by optical microscopy.

It is not known to what extent each of the previous mechanisms contributes to turbine blade degradation during service. It is also probable that each alloy will respond differently to a particular temperature/stress combination. Figure 21-12 shows the typical variation in stress/rupture life determined at 1350 °F (375 °C) with service time for forged Inconel X-750 blades.

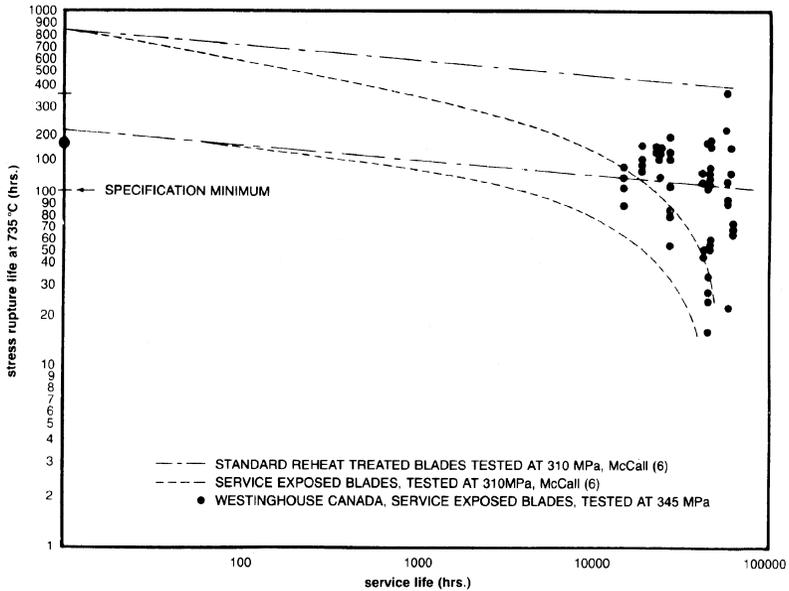


Figure 21-12. The variation of remaining stress rupture life at 1350°F (735°C) with service time in forged Inconel alloy X-750 turbine blades. (Courtesy of Westinghouse Electric Corp., Gas Turbine Div.).

Internal service damage due to precipitate coarsening and changes in grain boundary carbides should generally be reversible with conventional heat treatment involving complete solutioning followed by controlled precipitation at lower temperatures. For creep voids, it is not clear if cavitation damage can be removed by conventional heat treatment.

Normal reheat treatment can partially restore blade properties; however, it does not appear to be capable of full property recovery, although the microstructures are comparable to new blades. This shortcoming implies that cavitation may be present and was not removed by conventional reheat treatment. Hot isostatic press (HIP) processing is an alternative that ensures void removal. It has demonstrated its ability to remove even gross internal shrinkage porosity in investment castings.* The results of HIP treatment

* The HIP treatment is conducted in a five-zone furnace located in a steel pressure vessel that can be pressurized to 20,000 psi with argon and capable of temperatures of 2250°F. The blades placed inside the furnace must not be subjected to any undue loads and thus are stacked in separate tiers. Between cycles, the furnace temperature is maintained at 1470°F to obtain maximum life of the Kanthal elements. The pressurizing argon is provided by two diaphragm compressors in series and can be reclaimed at the end of each cycle.

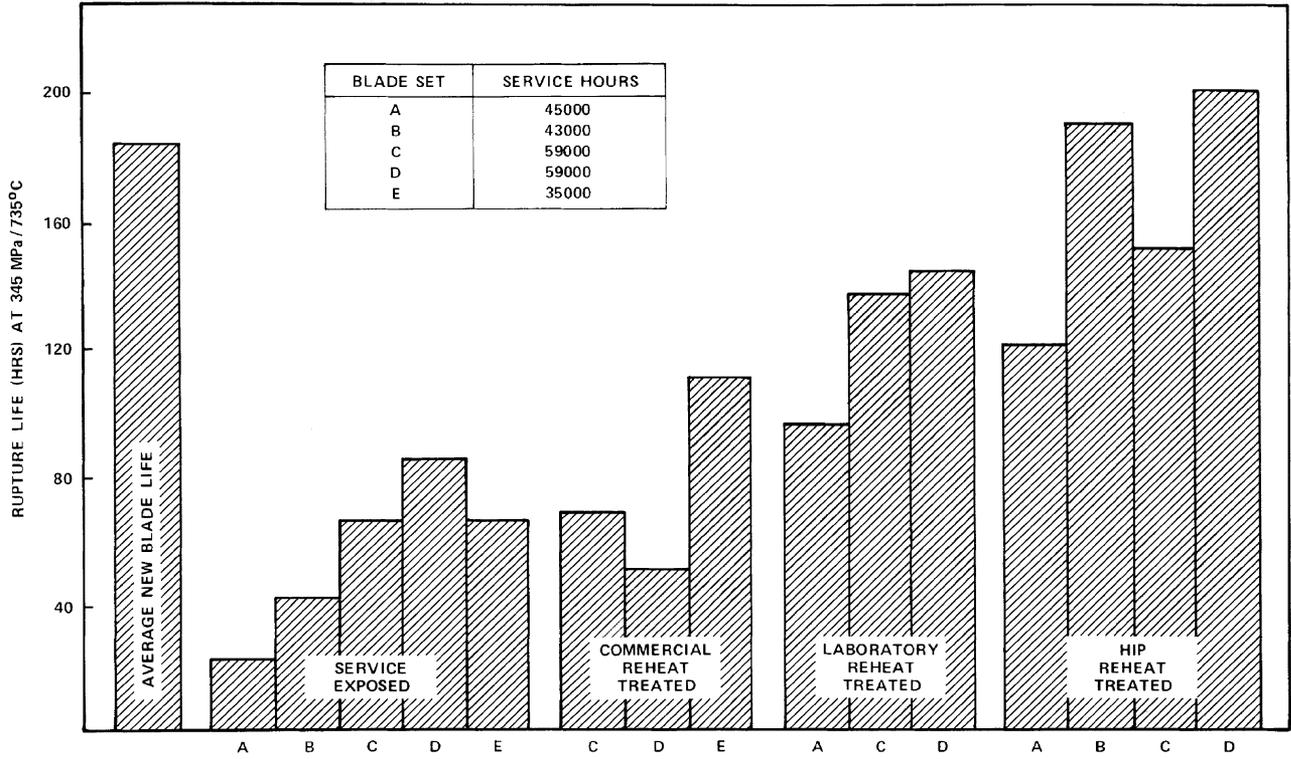


Figure 21-13. Comparison of stress rupture life at 50 ksi/1350°F (345 MPa/735°C) in service exposed, commercially reheat-treated, laboratory reheat-treated, and HIP reheat-treated used Inconel X-750 turbine blades. (Courtesy of Westinghouse Electric Corp., Gas Turbine Div.)

(Figure 21-13) clearly show that the HIP-processed material is superior to both commercial and laboratory conventional reheat-treated material. Cost estimates indicate that used blades can be rejuvenated at a fraction of the cost of a new set of blades.

Repair and Rehabilitation of Turbomachinery Foundations

In many instances, vibration problems in turbomachinery can be attributed to faulty support. Once the problem areas have been identified, correcting defects can be a logical procedure. What is novel is that this result can often be accomplished through the proper selection and application of adhesives.

Most turbomachinery is mounted on structural steel platforms sometimes referred to as base plates or skids. These platforms are then installed on a mass of concrete at the jobsite (either by direct grouting or mounting on sole plates) to become the machinery foundation. Platforms should always be considered as part of the foundation rather than as part of the machinery.

Problems with platforms fall into one or both of the following categories:

1. Improper installation
2. Insufficient mass and/or rigidity

Improper installation is not a design weakness. This defect can be corrected rather easily in the field at any time after installation. Insufficient mass or rigidity is a design weakness brought about by the complexity of the origin of vibration in high-speed rotating machinery and its sensitivity of vibration. Nevertheless, mass and rigidity can be increased in the field, but it is more of a task to do so than the mere correcting of installation defects.

Installation Defects

A typical compressor train containing a turbine and two compressor stages are shown in Figure 21-14. The I-beams on the platform are grouted to the concrete structure. When proper grouting techniques are carried out during the original installation, the grout should contact the entire lower surfaces of all longitudinal and transverse I-beams.

Cement-based grouts will not bond well to the platform load-bearing surfaces. Over a period of time, lubricating oils will severely degrade both cement grouts and concrete. This problem is further aggravated because

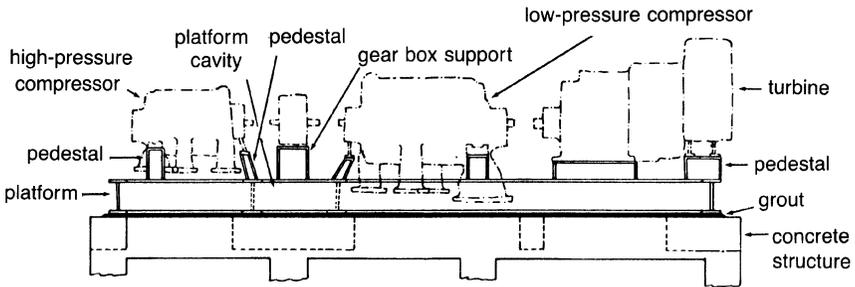


Figure 21-14. A typical compressor train containing a turbine and two compressor stages.

most platforms are not designed with oil drains. On several occasions, as much as 6–8 inches of oil has been found trapped within the platform cavities. This condition not only provides head-pressure for an increased rate of oil penetration, but also creates a severe fire hazard.

All platforms, regardless of the type of grout to be used, should be designed with oil drains. Epoxy grouts are recommended on platform installations because they provide an excellent oil barrier for the concrete below. Cement grouts should be used only for temporary installations.

When differences in vibration amplitudes can be detected between the lower flange of the platform beams and the concrete structure, the decision to bond the entire lower surfaces of the platform to the concrete structure should be made. Bonding can be accomplished using a technique known as pressure-grouting. With this technique, holes are drilled through the lower flange at locations near the web on centers of approximately 18 inches. These holes are then tapped, and ordinary grease fittings are installed. Pressure-grouting can then be carried out with either automatic injection equipment or with conventional grease guns.

Some manufacturers recommend that their platforms be installed on rails or sole plates, which have been grouted to the concrete foundation. Occasionally, the installation will be either poorly designed or the contractor will fail to clean the plates before grouting. Loss of adhesion may result in excessive vibration or movement of the plate in the grout. When this problem occurs, pressure-grouting can be accomplished with a relatively high degree of success if proper techniques are used. The following are some main points to consider when designing and grouting a sole plate:

1. Check to see that the block between the equipment base and the sole plate is adequate to transmit the load.

2. Corners on the edges of the sole plate should have at least a two-inch radius to prevent the creation of stress risers and subsequent cracking of the corners.
3. There should be a sufficient amount of aggregate in the epoxy mixture. Insufficient quantities of aggregate will lead to a layer of unfilled epoxy on the surface of the mortar. The linear coefficient of thermal expansion of the unfilled epoxy can be expected to be on the order of magnitude of $6-8 \times 10^{-5}$ inches per inch of thickness per °F. The linear coefficient of thermal expansion for the epoxy mortar below can be expected to be on the order of magnitude of 2×10^{-5} inches per inch of thickness per °F. This difference in thermal expansion rates will encourage crack propagation, particularly on cooling when the system is subjected to cyclic temperatures such as between day and night.
4. Make sure that a foamy surface does not exist immediately below the sole plate. A foamy surface is caused by an insufficient quantity of aggregate in preparing the epoxy mortar. The epoxy adhesive has a density of about nine pounds per gallon. The aggregate has a bulk density of about 14 pounds per gallon, which assumes about 25–30% voids. In preparing an epoxy mortar, the resin and hardener components are always mixed together before the addition of aggregate. When the aggregate is added to the mix, it obviously falls to the bottom and introduces air into the mix. If a soupy mortar is prepared, the air will simply rise to create a weak, foamy surface.

Increasing Mass and Rigidity

When excessive vibration is detected in the gear box of a compressor train (Figure 21-14) and is transferred to the platform below, a dampening effect can be created by increasing the rigidity of the support below. This effect can be accomplished by first filling the platform cavity and then the gear-box support with epoxy mortar.

In the case where the turbine and supports have a minimal cross section, then the ability to increase the stiffness of these pedestals is minimized. Consequently, the objective is to concentrate on increasing the mass of the pedestals. This increase is accomplished by filling the cavities with a special mortar prepared with epoxy and steel shot. The density of this special mortar can be in excess of 300 pounds per cubic foot. To inject this special mortar, a pipe has been installed in the access hole that was drilled in the side of the pedestal near the top. These same techniques can be employed to stabilize the foundations under much smaller equipment.

Large Machinery Startup Procedure

Many of these problems can be quickly resolved by deductive reasoning if sufficient care has been taken in obtaining startup data. The following are good guidelines, but they are not intended to be complete:

1. Before startup, become generally familiar with the train. Find out:
 - a. Critical speeds of the train's rotors
 - b. Operating speeds, temperatures, and pressures
 - c. Unusual operational characteristics
 - d. If all vibration monitoring systems are functioning and what are the alert and danger limits
2. For turbines, find out:
 - a. Slow roll (from one-half to three hours, depending on operational experience) to relieve rotor bow and allow for system warmup
3. At a slow-roll speed of less than 800 rpm, take the applicable slow-roll vibration data:
 - a. Gap voltages
 - b. Probe identification
 - c. Total electrical and mechanical run-out
 - d. Keyphazor relationships
 - e. Vibration values in mils, displacement, velocity, and acceleration.
4. Observe all meters, guages, sight glasses, oil temperatures, discharge temperatures, balance-line pressures, surface condenser temperature, etc.
5. Bring the machine *through* the first critical and observe the machine's performance for 15 minutes
6. Bring the machine midway between the first critical and minimum governor. Observe performance for 15 minutes.
7. Go quickly to minimum governor to ensure that the rotors go through any other criticals as easily as possible.
8. At minimum governor, get another set of vibrational readings.
9. Document all readings and observations and file for future reference with a copy sent to the unit supervisor and unit engineer.

During the startup, all vibration signals should be tape recorded. The recordings can be analyzed and plotted to provide baseline vibration data for future evaluation of machine performance.

Typical Problems Encountered in Gas Turbines

There are many types of failures associated with a gas turbine, since these units are very complex in their overall makeup. The failures in the hot section far outnumber the problems in the compressor due to the high temperatures associated with the hot section. Hot-section failures are usually connected to problems associated with fuels. Turbine failures can be very costly, the average cost runs about \$500,000 for units between 10 and 50 MW and about \$700,000 for units above 50 MW. These average failures result in downtime of between 12 and 16 weeks. The type of operation the unit experiences is a major factor in the problem. The unit has a more trouble-free operation if it is a baseload unit.

Intermittent operation and peak-load operation lead to more problems and reduce the life of many of the hot parts. Peak-load units account for only about 20% of the units above the 10 MW range. The smaller units (between 1 and 10 MW) are usually operated as standby power generators or for compressor drives mostly on offshore platforms. Small-unit repair costs average about \$55,000–\$100,000. These units are very rarely used for peaking services.

Fuel nozzles clog easily and can come loose, creating a large flow of fuel, which ignites and can lead to severe burning problems. A number of such cases has occurred in dual-fuel units. In most of these cases, the fuel nozzle loosens and comes off. Because of design constraints, the nozzle does not go through the turbine, but allows a very large amount of fuel to enter the combustor can. This fuel is then transported to the transition piece and toward the first-stage nozzles. The first-stage nozzles act as flame holders, causing the fuel to ignite and create a large flame, which burns out the first-stage nozzle and rotor blades. Figure 21-15 shows the burnt first-stage rotor blades. Note how evenly the blades have been burned. It is obvious from these photographs that the flame was angled and that the first-stage nozzle acted as a flame holder. Figure 21-16 shows the damage on the first-stage nozzle, which acted as a flame holder. Note that the retainer disc has been melted due to the intense heat.

Another common combustion problem concerns the crossover tubes. Cross-over tubes are used in can-annular combustors to assure combustion in all chambers and to equalize pressure. Many times the flow of hot gases through the crossover tubes is increased due to blocked fuel nozzles, which can lead to tube failures as shown in Figure 21-17.

Liner cracks can be caused by liquids in the fuel or blocked nozzles, which can create hot sections in the liner as seen in Figure 21-18. In many turbines, the injection of steam or water in the combustor can has been used to meet

FPO

Figure 21-15. Burnt first-stage turbine blades. Note evenness of burn.

FPO

Figure 21-16. Burnt first-stage nozzle.

FPO

Figure 21-17. Damaged crossover tubes.

NO_x emission requirements. This injection of steam reduces the temperature in the hot section, thus reducing the amount of NO_x produced. When sprayed through the fuel nozzle, this steam can impinge on the liner, thus creating a temperature gradient, which can lead to cracks. Steam injection—whether it is required for NO_x control or for extra power (5% steam by weight will produce 12% more work and increase efficiency a few percent)—must inject steam into the compressor diffuser to be safe and effective. This process will allow the steam to be fully mixed with the air before it enters the combustor, reducing the incidence of liner failures due to steam injection.

Nozzle bowing of the first-stage turbine nozzle is another common problem. Bowing can be caused by uneven combustion or loss of cooling air to the nozzle and can decrease turbine efficiency by changing the air velocity and angles leaving the nozzles. Another problem with turbine nozzles occurs with the second or downstream nozzles. This problem is due to liquids entrained in the fuels or ignition failure at startup. Liquid hydrocarbons are entrained in the fuel impinge on the turbine, causing hot spots and leading to cracked blades. Ignition failure at startup can lead to an accumulation of the fuel in pockets. When combustion finally occurs, it creates an

FPO

Figure 21-18. Cracks in a combustor liner.

explosion and/or fire where the fuel is trapped. This trapping of the fuel occurs in areas where the velocity is lower and the blades act as flame holders. Thus, the second-stage nozzles are an ideal candidate for this problem. The problem can be avoided by purging the fuel after a failure of the turbine to ignite. This function can be automatic or manual. Usually, a five-minute interval is required and at least five times the total air volume must be changed before another startup can be attempted.

Compressor problems are minimized due to the less-hostile environment in which it operates compared to a turbine. The compressor requires a good-quality, high-efficiency filter. In areas where there is a high-moisture content, a rainshield should be used in front of the high-efficiency filters. It is not uncommon to see a very high rate of erosion at the blade tips of compressors operating in sandy regions with poor or no filtration (Figure 21-19). A high-efficiency filter usually is a two-stage filter with an inertia filter for the first-stage and a bag-type filter as a second stage. The tip erosion of the blades leads to inefficiency or compressor surge.

Blade flutter and rotating stall are problems encountered in the compressor due to poor design or contamination of the blades. Changing blade angles can usually solve the problem; however, this adjustment is very

FPO

Figure 21-19. Compressor with high erosion at blade tips due to improper filtration system.

impractical. Abrasive cleaning of the compressor or a water wash usually will restore the blade surface and thus create the original design angle. In some cases, blade flutter problems are initiated due to bleed-off valves; excessive bleed-off can result in a compressor surge of the latter stages. The amount of bleed-off, which can be tolerated in most units, is between 12 and 17%.

Centrifugal compressors can have problems at the inducer and blade tips. These parts of the blade can be excited by aerodynamic forces. Blade discs can have stresses at the rotor tips, which lead to cracks. To solve this problem, the offending part is removed and a scalloped disc results as seen in Figure 21-20. This type of disc experiences some efficiency loss (about 2–4%).

Problems with blade fatigue are common. When interstage cooling is used, water from the cooler is carried over to the blades. These water particles

FPO

Figure 21-20. Scalloped rotor.

impinge against the blades and give rise to a high-stress region, usually near the blade exit. The cracks spread out from this area, and the blade initially suffers a cyclic fatigue, which leads to a rupture. Since this usually occurs in the first-stages of the casings, a serious loss is incurred as the blade debris goes downstream, wiping out everything in its path. Figure 21-21 shows a cross section of such a blade. Figure 21-22 shows the effect of the blade passing through the rest of the rotor.

Other problems experienced in compressors and turbines occur in regenerators, shafts, gearing, bearings, seals, and couplings. Problems with regenerators often occur due to a leak in the system. Abrasive cleaning of compressors, which lead to regenerators, should be confined to using spent catalyst or other nonflammable-type cleaners. Abrasive cleaners such as peanut shells and rice should be avoided, since they have a tendency to accumulate in corners where they can create hot spots or a fire that will burn through the wall. Shaft problems are usually not very common, but now and then a shaft will shear due to excessive load. This excessive load has many causes. Most often the problem results when the type of driver is changed from a turbine to a synchronous electric-motor drive. With the latter drive, very high torsional stresses are produced that can lead to shaft failures when the unit is brought from rest to design speed in seconds. Rotor bearings usually experience a type of instability called oil whirl. This phenomena has been described in detail in Chapter 5. In some cases, this problem is alleviated by a change of oil temperature, otherwise the problem requires a change in bearing design such as going to a pressure-dam bearing or in

FPO

Figure 21-21. Cross section of fatigued blade. Note chevron markings near the trailing edge indicating cyclic fatigue.

excessive cases to a tilting-pad bearing. Thrust-bearing problems are due to misalignment, or because the unit is running very close to the active thrust surface. To compensate for the thrust, a balance piston is introduced. This balance piston compensates for the aerodynamic thrust. A case in point was a four-stage rotor as shown in Figure 21-23. The air to the right of the balance piston was low-pressure air from the compressor inlet. This air was originally bled-off from the inlet to the compressor. After routine maintenance, it was decided that the air be taken from in front of the inlet air cooler rather than from behind it. This small change in pressure was enough to destabilize the system, and the rotor screwed itself into the diaphragms, creating a great loss.

Gearing problems are due to case distortion, improper gear cooling, or high backlash on the gears. Misalignment also is a great contributor to this problem. Gears should be checked for proper fit; in some cases lapping is advised. Care is always needed to prevent lapping compound from entering the lubrication system and bearings. Cooling of the high-speed gears is accomplished by directing a jet of lubrication oil on the gears as they become unmeshed. In very high-speed applications oil should be directed at the casing to reduce thermal distortion of the casing. Coupling problems are

FPO

Figure 21-22. The effect of blade failure on compressor blading.

also directly or indirectly caused by improper lubrication or a high level of misalignment. Couplings of the gear type should have a continuous lubrication system rather than be grease-packed. Grease tends to separate at high speeds; however, new greases being developed may change the whole coupling picture. In many cases, gear couplings are being replaced by disc-type couplings. This type of coupling is more forgiving of angular alignment problems and also does not require any type of lubrication. Misalignment problems in the system can often be aggravated by the piping to the system. Pipe stresses can run very high, and the unit will move, thus causing high misalignments in the system.

Seal problems can give rise to high leakages and thrust problems. The high leakages reduce the efficiency of the unit and can also lead to contamination of the lubricant. Thrust problems are created by air leakage past seals, causing an unbalance of the thrust forces on the system.

The previous problems are some of the more common types encountered on a gas turbine train. Regular and preventive maintenance is the key to a successful operation. Problems will arise, but by proper monitoring of the aerothermal and mechanical problems, preventive maintenance can often avert major or catastrophic failures.

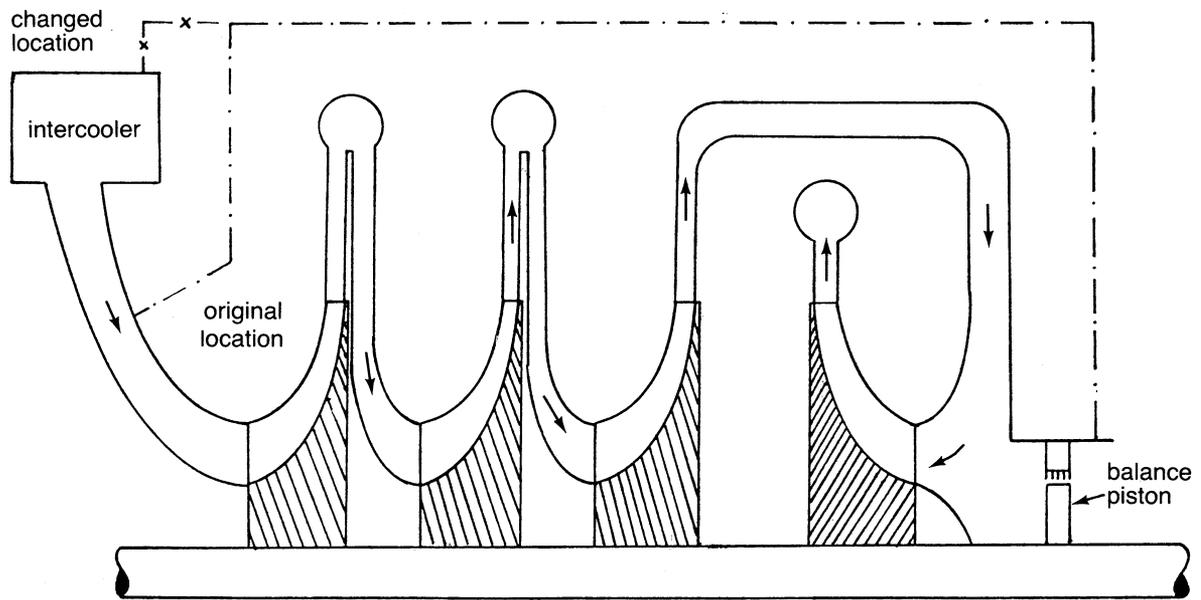


Figure 21-23. Thrust forces in a centrifugal compressor.

Bibliography

- Boyce, M.P., "Managing Power Plant Life Cycle Costs," International Power Generation, pp. 21–23, July 1999.
- Herbage, B.S., "High Efficiency Film Thrust Bearings for Turbomachinery," Proceedings of the 6th Turbomachinery Symposium, Texas A&M University, pp. 33–38, 1977.
- Meher-Homji C.B., and Gabriles G.A., "Gas Turbine Blade Failures—Causes, Avoidance, and Troubleshooting," Proceedings of the 27th Turbomachinery Symposium, Texas A&M University, pp. 129, 1998.
- Nakajima, S., "Total Productive Maintenance," Productivity Press, Inc.
- Nelson, E., "Maintenance Techniques for Turbomachinery," Proceedings of the 2nd Turbomachinery Symposium, Texas A&M University, 1973.
- Renfro, E.M., "Repair and Rehabilitation of Turbomachinery Foundation," Proceedings of the 6th Turbomachinery Symposium, Texas A&M University, pp. 107–112, 1977.
- Sohre, J., "Operating Problems with High-Speed Turbomachinery—Causes and Correction," 23rd Annual Petroleum Mechanical Engineering Conference, September 1968.
- Sohre, J., "Reliability Evaluation for Trouble-Shooting of High-Speed Turbomachinery," ASME Petroleum Mechanical Engineering Conference, Denver, Colorado.
- VanDrunen, G., and Liburdi, J., "Rejuvenation of Used Turbine Blades by Host Isostatic Processing," Proceedings of the 6th Turbomachinery Symposium, Texas A&M University, pp. 55–60, 1977.

Appendix

Equivalent Units

Abbreviations. A = angstrom, atm = standard atmosphere, 760 mm of Hg at 0°C, cal = calorie (gram), cm = centimeter, deg = degree, gal = gallon, U.S. liquid, gm (and g) = gram, gmole = gram-mole, J = joule, kcal = kilocalorie, kg = kilogram, kJ = kilojoule, km = kilometer, kW = kilowatt, l = liter, lb = avoirdupois pound, m = meter, mi = mile (U.S.) mm = millimeter, N = newton, oz = avoirdupois ounce, pmole = pound mole, pt = pint, rad = radian, rev = revolution, s = second, ton = short U.S. ton, V = volt, W = watt. Others are as usual.

LENGTH

$$12 \frac{\text{in}}{\text{ft}} \quad 6080.2 \frac{\text{ft}}{\text{naut.mi}} \quad 5280 \frac{\text{ft}}{\text{mi}} \quad 0.3937 \frac{\text{in}}{\text{cm}} \quad 30.48 \frac{\text{cm}}{\text{ft}} \quad 10^4 \frac{\text{microns}}{\text{cm}}$$

$$3 \frac{\text{ft}}{\text{yd}} \quad 1.152 \frac{\text{mi}}{\text{naut.mi}} \quad 10^{10} \frac{\text{A}}{\text{m}} \quad 2.54 \frac{\text{cm}}{\text{in}} \quad 3.28 \frac{\text{ft}}{\text{m}} \quad 1.609 \frac{\text{km}}{\text{mi}}$$

AREA

$$144 \frac{\text{in}^2}{\text{ft}^2} \quad 43,560 \frac{\text{ft}^2}{\text{acre}} \quad 640 \frac{\text{acres}}{\text{mi}^2} \quad 10.76 \frac{\text{ft}^2}{\text{m}^2} \quad 929 \frac{\text{cm}^2}{\text{ft}^2} \quad 6.452 \frac{\text{cm}^2}{\text{in}^2}$$

VOLUME

$$1728 \frac{\text{in}^3}{\text{ft}^3} \quad 7.481 \frac{\text{gal}}{\text{ft}^3} \quad 43,560 \frac{\text{ft}^3}{\text{acre} - \text{ft}} \quad 3.7854 \frac{\text{l}}{\text{gal}} \quad 28.317 \frac{\text{l}}{\text{ft}^3} \quad 35.31 \frac{\text{ft}^3}{\text{m}^3}$$

$$231 \frac{\text{in}^3}{\text{gal}} \quad 8 \frac{\text{pt}}{\text{gal}} \quad 10^3 \frac{\text{l}}{\text{m}^3} \quad 61.025 \frac{\text{in}^3}{\text{l}} \quad 10^3 \frac{\text{cm}^3}{\text{l}} \quad 28,317 \frac{\text{cm}^3}{\text{ft}^3}$$

DENSITY

$$1728 \frac{\text{lb}/\text{ft}^3}{\text{lb}/\text{in}^3} \quad 32.174 \frac{\text{lb}/\text{ft}^3}{\text{slug}/\text{ft}^3} \quad 0.51538 \frac{\text{gm}/\text{cm}^3}{\text{slug}/\text{ft}^3} \quad 16.018 \frac{\text{kg}/\text{m}^3}{\text{lb}/\text{ft}^3} \quad 1000 \frac{\text{kg}/\text{m}^3}{\text{gm}/\text{cm}^3}$$

ANGULAR

$$2\pi = 6.2832 \frac{\text{rad}}{\text{rev}} \quad 57.3 \frac{\text{deg}}{\text{rad}} \quad \frac{1}{2\pi} \frac{\text{rpm}}{\text{rad/min}} \quad 9.549 \frac{\text{rpm}}{\text{rad/sec}}$$

TIME

$$60 \frac{\text{s}}{\text{min}} \quad 3600 \frac{\text{s}}{\text{hr}} \quad 60 \frac{\text{min}}{\text{hr}} \quad 24 \frac{\text{hr}}{\text{day}}$$

SPEED

$$88 \frac{\text{fpm}}{\text{mph}} \quad 0.6818 \frac{\text{mph}}{\text{fps}} \quad 0.5144 \frac{\text{m/s}}{\text{knot}} \quad 0.3048 \frac{\text{m/s}}{\text{fps}} \quad 0.44704 \frac{\text{m/s}}{\text{mph}}$$

$$1.467 \frac{\text{fps}}{\text{mph}} \quad 1.152 \frac{\text{mph}}{\text{knot}} \quad 1.689 \frac{\text{fps}}{\text{knot}} \quad 152.4 \frac{\text{cm/min}}{\text{ips}}$$

FORCE, MASS

$$16 \frac{\text{oz}}{\text{lb}_m} \quad 32.174 \frac{\text{lb}_m}{\text{slug}} \quad 444,820 \frac{\text{dynes}}{\text{lb}_f} \quad 2.205 \frac{\text{lb}_m}{\text{kg}} \quad 9080665 \frac{\text{N}}{\text{kg}_f}$$

$$1000 \frac{\text{lb}_f}{\text{kip}} \quad 32.174 \frac{\text{poundals}}{\text{lb}_f} \quad 980.665 \frac{\text{dynes}}{\text{gm}_f} \quad 14.594 \frac{\text{kg}}{\text{slug}} \quad 4.4482 \frac{\text{N}}{\text{lb}_f}$$

$$2000 \frac{\text{lb}_m}{\text{ton}} \quad 7000 \frac{\text{grains}}{\text{lb}_m} \quad 453.6 \frac{\text{gm}}{\text{lb}_m} \quad 10^5 \frac{\text{dynes}}{\text{N}} \quad 1 \frac{\text{kilopond}}{\text{kg}}$$

$$14.594 \frac{\text{kg}}{\text{slug}} \quad 28.35 \frac{\text{gm}}{\text{oz}} \quad 453.6 \frac{\text{gmole}}{\text{pmole}} \quad 907.18 \frac{\text{kg}}{\text{ton}} \quad 1000 \frac{\text{kg}}{\text{metric ton}}$$

PRESSURE

$$14.696 \frac{\text{psi}}{\text{atm}} \quad 101,325 \frac{\text{N/m}^2}{\text{atm}} \quad 13.6 \frac{\text{kg}}{\text{mm Hg}(0^\circ\text{C})} \quad 51.715 \frac{\text{mm Hg}(0^\circ\text{C})}{\text{psi}} \quad 47.88 \frac{\text{N/m}^2}{\text{psf}}$$

$$29.921 \frac{\text{in Hg}(0^\circ\text{C})}{\text{atm}} \quad 10^5 \frac{\text{N/m}^2}{\text{bar}} \quad 13.57 \frac{\text{in H}_2\text{O}(60^\circ\text{F})}{\text{in Hg}(60^\circ\text{F})} \quad 703.07 \frac{\text{kg/m}^2}{\text{psi}} \quad 6894.8 \frac{\text{N/m}^2}{\text{psi}}$$

$$33.934 \frac{\text{ft H}_2\text{O}(60^\circ\text{F})}{\text{atm}} \quad 14.504 \frac{\text{psi}}{\text{bar}} \quad 0.0361 \frac{\text{psi}}{\text{in H}_2\text{O}(60^\circ\text{F})} \quad 0.0731 \frac{\text{kg/cm}^2}{\text{psi}} \quad 760 \frac{\text{torr}}{\text{atm}}$$

780 Gas Turbine Engineering Handbook

$$1.01325 \frac{\text{bar}}{\text{atm}} \quad 10^6 \frac{\text{dynes/cm}^2}{\text{bar}} \quad 0.4898 \frac{\text{psi}}{\text{in Hg}(60^\circ\text{F})} \quad \frac{9.869}{10^7} \frac{\text{atm}}{\text{dyne/cm}^2} \quad 133.3 \frac{\text{N/m}^2}{\text{torr}}$$

$$33.934 \frac{\text{ft H}_2\text{O}(60^\circ\text{F})}{\text{atm}} \quad 760 \frac{\text{mm Hg}(0^\circ\text{C})}{\text{atm}} \quad 406.79 \frac{\text{in H}_2\text{O}(39.2^\circ\text{F})}{\text{atm}} \quad 0.1 \frac{\text{dyne/cm}^2}{\text{N/m}^2} \quad 1.0332 \frac{\text{kg/cm}^2}{\text{atm}}$$

ENERGY AND POWER

$$778.16 \frac{\text{ft} - \text{lb}}{\text{Btu}} \quad 2544.4 \frac{\text{Btu}}{\text{hp} - \text{hr}} \quad 5050 \frac{\text{hp} - \text{hr}}{\text{ft} - \text{lb}} \quad 1 \frac{\text{J}}{\text{W} - \text{s}} \frac{\text{J}}{\text{N} - \text{m}} \quad 0.01 \frac{\text{bar} - \text{dm}^3}{\text{J}}$$

$$550 \frac{\text{ft} - \text{lb}}{\text{hp} - \text{s}} \quad 42.4 \frac{\text{Btu}}{\text{hp} - \text{min}} \quad 1.8 \frac{\text{Btu/lb}}{\text{cal/gm}} \quad 1 \frac{\text{kW} - \text{s}}{\text{kJ}} \quad \frac{16.021}{10^{12}} \frac{\text{J}}{\text{MeV}}$$

$$33,000 \frac{\text{ft} - \text{lb}}{\text{hp} - \text{min}} \quad 3412.2 \frac{\text{Btu}}{\text{kW} - \text{hr}} \quad 1800 \frac{\text{Btu/pmole}}{\text{kcal/gmole}} \quad 1 \frac{\text{V} - \text{amp}}{\text{W} - \text{s}} \quad \frac{1.6021 \text{ erg}}{10^{12} \text{ eV}}$$

$$737.562 \frac{\text{ft} - \text{lb}}{\text{kW} - \text{s}} \quad 56.87 \frac{\text{Btu}}{\text{kW} - \text{min}} \quad 2.7194 \frac{\text{Btu}}{\text{atm} - \text{ft}^3} \quad 10^7 \frac{\text{ergs}}{\text{J}} \quad \frac{11.817 \text{ ft} - \text{lb}}{10^{12} \text{ MeV}}$$

$$1.3558 \frac{\text{J}}{\text{ft} - \text{lb}} \quad 251.98 \frac{\text{cal}}{\text{Btu}} \quad 4.1868 \frac{\text{kJ}}{\text{kcal}} \quad 3600 \frac{\text{kJ}}{\text{kW} - \text{hr}} \quad 0.746 \frac{\text{kW}}{\text{hp}}$$

$$1.055 \frac{\text{kJ}}{\text{Btu}} \quad 101.92 \frac{\text{kg} - \text{m}}{\text{kJ}} \quad 0.4300 \frac{\text{Btu/pmole}}{\text{J/gmole}} \quad 860 \frac{\text{cal}}{\text{W} - \text{hr}} \quad 1.8 \frac{\text{Btu}}{\text{chu}}$$

ENTROPY, SPECIFIC HEAT, GAS CONSTANT

$$1 \frac{\text{Btu/pmole} - ^\circ\text{R}}{\text{cal/gmole} - \text{K}} \quad 1 \frac{\text{Btu/lb} - ^\circ\text{R}}{\text{gal/cm} - \text{K}} \quad 1 \frac{\text{Btu/lb} - ^\circ\text{R}}{\text{kcal/kg} - \text{K}} \quad 0.2389 \frac{\text{Btu/pmole} - ^\circ\text{R}}{\text{J/gmole} - \text{K}} \quad 4.187 \frac{\text{kJ/kg} - \text{K}}{\text{Btu/lb} - ^\circ\text{R}}$$

UNIVERSAL GAS CONSTANT

$$1545.32 \frac{\text{ft} - \text{lb}}{\text{pmole} - ^\circ\text{R}} \quad 8.3143 \frac{\text{kJ}}{\text{kmole} - \text{K}} \quad 0.7302 \frac{\text{atm} - \text{ft}^3}{\text{pmole} - ^\circ\text{R}} \quad 82.057 \frac{\text{atm} - \text{cm}^3}{\text{gmole} - \text{K}}$$

$$1.9859 \frac{\text{Btu}}{\text{pmole} - ^\circ\text{R}} \quad 1.9859 \frac{\text{cal}}{\text{gmole} - \text{K}} \quad 10.731 \frac{\text{psi} - \text{ft}^3}{\text{pmole} - ^\circ\text{R}} \quad 83.143 \frac{\text{bar} - \text{cm}^3}{\text{gmole} - \text{K}}$$

$$8.3143 \frac{\text{J}}{\text{gmole} - \text{K}} \quad 8.3149 \times 10^7 \frac{\text{erg}}{\text{gmole} - \text{K}} \quad 0.08206 \frac{\text{atm} - \text{m}^3}{\text{kgmole} - \text{K}} \quad 0.083143 \frac{\text{bar} - \text{l}}{\text{gmole} - \text{K}}$$

Newton's proportionality constant k (as a conversion unit)

$$32.174\text{fps}^2 \left(\frac{\text{lb}}{\text{slug}} \right) \quad 386.1 \text{ ips}^2 \left(\frac{\text{lb}}{\text{p sin}} \right) \quad 9.80665 \frac{\text{m}}{\text{s}^2} \left(\frac{\text{N}}{\text{kg}} \right) \quad 980.665 \frac{\text{cm}}{\text{s}^2} \left(\frac{\text{dynes}}{\text{gm}} \right)$$

MISCELLANEOUS CONSTANTS

| | | |
|---|---|--|
| Speed of light | Avogadro Constant | Planck Constant |
| $c = 2.9979 \times 10^8 \frac{\text{m}}{\text{s}}$ | $N_A = 6.02252 \times 10^{23} \frac{\text{molecules}}{\text{gmole}}$ | $h = 6.6256 \times 10^{-34} \text{J-s}$ |
| Boltzmann Constant | Gravitational Constant | Normal mole volume |
| $k = 1.38054 \times 10^{-23} \frac{\text{J}}{\text{K}}$ | $G = 6.670 \times 10^{-11} \frac{\text{N} \cdot \text{m}^2}{\text{kg}^2}$ | $2.24136 \times 10^{-2} \frac{\text{m}^3}{\text{gmole}}$ |

Index

A

- Absolute velocity, 46, 119, 120, 240, 292, 323, 345, 715
- Absorption cooling systems, 99
- Acceleration transducers, 566–7
- ACCP (Advanced Combined Cycle Power Plants), 5
- Acoustic signature, 579
- Acoustic speed, 115
- Adiabatic efficiency, 122–4
- Aerodynamic
 - cross-coupling effect, 209–10
 - whirl, 209–10
- Aerothermal equations, 117–22
- Aerothermodynamics, turbomachine, 112–17
- Air,
 - angle, 259, 260, 294, 339
 - injection of compressed, 101–5
 - inlet angle, 279, 305
 - outlet angle, 279
 - turning angle, 279
- Air inlet filter module, 703
- Air pollution problems, 392–403
- Aircraft propulsion, 142–3
- Airfoil theory, elementary, 280–2
- Airfoils, laminar-flow, 283–4
- Air-standard Brayton Cycle.
 - See Brayton Cycle
- Alignment
 - and couplings, 605–33
 - cold, 624, 626–30
 - Dodd bar system, 631
 - face-OD method, 626–7
 - graphic plotting, 627, 629
 - hot check, 624, 630–2
 - optical, 630–1
 - prealignment survey, 625–6
 - proximity probe method, 630
 - reverse-dial indicator
 - method, 626, 630, 631
 - sag, 626
- American Gear Manufacturers Association (AGMA) standards
 - AGMA 2, 531
 - AGMA 211, 534
 - AGMA 163, 421
- Amplification factor, 158
- Amplitude factor (gas turbines), 189–90
- Analysis
 - dimensional, 125–30
 - spectrum, 558–83
 - theoretical and actual cycle, 58–111
- Angle of attack, 240, 279, 281–2
- API (American Petroleum Institute) standards, 141, 151
 - API 614, 155
 - API 616, 151
 - API 618, 154
 - API 619, 154
 - API 670, 155
 - API 671, 155
 - API 677, 154
- ASME (American Society of Mechanical Engineers), 141, 151
- Aspect ratio, 278
- Asymmetric flexibility, 203
- Asymmetrical stage, 297–9
- Atmospheric tanks, 462–3
- Auxiliary system monitoring, 671–7
 - baseline for machinery, 672–4
 - data trending, 674–7
 - fuel system, 671–2
 - torque measurement, 672
- Availability 14, 737–8
- Axial-flow compressors, 28–30, 275–318
 - cascade test, 284–290
 - deviation rule, 303
 - diffusion factor, 300
 - incidence rule, 301
 - laminar-flow airfoils, 283
 - losses, 313
 - nomenclature, 276–9
 - performance characteristics of, 311–13

- radial equilibrium, 299–300
 - reaction degree of, 294–9
 - stall analysis of, 313–17
 - velocity triangles, 292–4
 - Axial-flow turbines, 337–69
 - axial velocity, 340
 - stall analysis, 313–17
 - cooled-turbine aerodynamics, 362–3
 - impulse turbine, 344–8
 - reaction turbine, 348–51
 - turbine blade cooling concepts, 351–4
 - convection cooling, 353
 - film cooling, 353
 - impingement cooling, 353
 - transpiration cooling, 353–4
 - water/steam cooling, 354
 - turbine blade cooling design, 354–62
 - convection and impingement
 - cooling/strut insert design, 354
 - film and convection cooling design, 354–8
 - multiple small-hole design, 359
 - steam-cooled turbine blades, 361–2
 - transpiration cooling design, 358–9
 - water-cooled turbine blades, 359–61
 - turbine geometry, 337–44
 - degree of reaction, 340–1
 - utilization factor, 341
 - velocity diagrams, 342–4
 - work factor, 341–2
 - turbine losses, 363–7
- B**
- Balancing, 584–604
 - application of balancing
 - techniques, 597–600
 - balancing procedures, 591–7
 - high-speed, 588–90
 - modal, 592–4
 - multiplane, 594–7
 - orbital, 591–2
 - procedures, 591–7
 - modal balancing, 592–4
 - multiplane balancing, 594–7
 - orbital balancing, 591–2
 - rotor imbalance, 584–90
 - techniques, 597–600
 - user's guide for multiplane, 600–2
 - user's guide for multiplane
 - balancing, 600–2
 - Barrel compressor casings, 268
 - Baseline
 - aerothermal, 673–4
 - mechanical (vibration), 672–3
 - Baseline signature, 571–2, 582
 - Bearing and shaft instabilities, 487–8
 - Bearing design
 - factors affecting thrust, 489–93
 - principles, 479–83
 - Bearing maintenance, 755–60
 - clearance checks, 756
 - thrust-bearing failure, 757–60
 - Bearing materials, 486–7
 - Bearings, 469
 - journal, 476–9
 - rolling, 469–6
 - thrust, 488–94
 - tilting-pad journal, 483–6
 - Bearings, Journal, 476–94
 - coefficient of friction curve, 482
 - design
 - factors, 478
 - principles, 479
 - leading edge lock-up, 485
 - lubrication modes, 479–83
 - materials, 486–7
 - parasitic load, 478
 - preload, 483–6
 - types, 476–8
 - ZN/P* curve, 481–2
 - Bearings Roller 469–76
 - design
 - factors, 469
 - principles, 471–5
 - wear 475
 - Bearing Thrust 488–94
 - Design 488–91
 - factors affecting thrust, 489–93
 - principles, 479–83
 - Bearing and shaft instabilities, 487–8
 - Bearing maintenance, 755–60
 - clearance checks, 756
 - thrust-bearing failure, 757–60
 - Bending critical speed, 195
 - Bernoulli equation, 281
 - Blade and cascade nomenclature, 196–8

- Blade axial Compressor
 - Camberline, 278–9
 - Carter's rule, 303
 - Cascades, 276–9
 - Casing treatment, 288–291
 - cascade nomenclature, 276–9
 - Cascade testing, 284–8
 - inlet angle, 279
 - material, 427
 - outlet angle, 279
 - tip speed, 120, 293
 - treatment, 285
 - stall, individual, 311
 - Blade Turbines
 - cooling concepts, 351–4
 - convection, 354
 - film, 354
 - impingement, 354
 - transpiration, 358–9
 - water, 359–60
 - cooling design, 354
 - convection and impingement, 354
 - film and convection, 354–8
 - multiple small-hole, 359
 - transpiration, 358–9
 - water cooled, 359–60
 - corrosion, 418–22
 - fatigue, 771
 - flutter, 771
 - life, 418–19
 - materials, 422–5
 - passage frequencies, 570
 - rejuvenation of used turbine, 761–4
 - Blades
 - compressor, 427
 - rejuvenation of used turbine, 761–4
 - Borescope inspection, 747
 - Boundary-layer development, 239–40
 - Brayton cycle, 58–68
 - regeneration effect, 63–5
 - Pressure effect, 61–3
 - Temperature Effect, 61–3
 - Brayton-Rankine cycle, 84–5
 - Bushing seals, 499–501
- C**
- C-MS (Condition Monitoring Systems), 634
 - CAES (Compressed Air Energy Storage Cycle), 93–5
 - Camberline, 278
 - Campbell diagram, 211–16
 - Carbon monoxide, 392
 - Carnot cycle, 66, 76
 - Carter's rule, 303
 - Cascade nomenclature, blade and, 276–9
 - Cascade tests, 284–92
 - energy increases, 289–92
 - Catalytic combustion, 403–8
 - features of, 404–6
 - Catalytic combustion design, 406–8
 - CCPP (Combined Cycle Power Plant), 5
 - Centrifugal compressors, 221–74
 - components, 223–49
 - causes of slip in impellers, 238–41
 - centrifugal sections of impellers, 237–8
 - diffusers, 243–6
 - Euler equation, 119, 227, 230, 293
 - IGVs (inlet guide vanes), 229–32
 - impellers, 232–5
 - inducers, 236–7
 - scroll, 247–9
 - Stanitz slip factor, 243
 - Stodola slip factor, 241–3
 - volute, 247–9
 - compressor surge, 254–66
 - performance, 249–54
 - process, 266–72
 - process centrifugal compressors, 266–72
 - Centrifugal flow compressors, 30–2
 - Ceramics, 428–9
 - CFC (Chlorofluorocarbons), 99
 - Choke, 131, 255
 - Choke point, 29
 - Chordline, 278–9
 - Classic flutter, 311
 - Cleaning, turbomachinery, 747–51
 - CO (carbon monoxide), 392
 - Coatings, 49–50, 429–35
 - future, 434–5
 - shroud, 434
 - Combustion, 373–5
 - catalytic, 403–8
 - chamber design, 375–81
 - combustion and dilution, 380
 - film cooling of liner, 380–1
 - flame stabilization, 379–80

- features of catalytic, 404–6
- terms, 372–3
 - equivalence ratio, 372
 - lower heating value, 373
 - pressure drop, 373
 - profile factor, 372
 - reference velocity, 372
 - stoichiometric proportions, 372
 - traverse number, 372
- Combustor arrangements, typical, 36–40, 386–92
 - annular, 36
 - can-annular, 36
 - external combustor
 - (experimental), 37–40
 - side combustors, 36–7
 - tubular, 36–7
- Combustors, 33–6, 370–408
 - air pollution problems, 392–403
 - carbon monoxide, 392
 - dry low NO_x combustor, 397–403
 - oxides of nitrogen, 392–7
 - smoke, 392
 - unburnt hydrocarbons, 392
 - catalytic combustion, 403–8
 - catalytic combustor design, 406–8
 - features of catalytic combustion, 404–6
 - catalytic combustor design
 - catalytic reactor, 407–8
 - main fuel injector, 407
 - preburner, 407
 - combustion, 373–5
 - combustion chamber design, 375–81
 - combustion terms, 372–3
 - design considerations
 - combustion liners, 384–5
 - cross-sectional area, 383
 - length, 383
 - liner holes, 384
 - pressure drop, 383
 - reliability of combustors, 385–6
 - transition pieces, 385
 - volumetric heat-release rate, 383–4
 - Wobbe Index, 383
 - dry low NO_x, 397–403
 - fuel atomization and ignition, 381–6
 - combustor design considerations, 383–6
 - ignition, 381–6
 - modules, 704
 - reliability of, 385–6
 - typical combustor arrangements, 386–92
- Communications, maintenance, 742–4
- Compliance matrix, 595
- Components, major gas turbine, 26–40
 - combustors, 33–6
 - compressors, 26–32
 - regenerators, 32–3
 - typical combustor arrangements, 36–40
- Compressed Air Energy Storage Cycle (CAES), 93–5
- Compressed air, injection of, 101–5
- Compressibility effect, 115–17
- Compressors, 26–32
 - axial-flow, 28–30, 275–318
 - blade and cascade nomenclature, 276–9
 - cascade test, 284–92
 - compressor stall, 308–11
 - degree of reaction, 294–9
 - deviation rule, 303–8
 - diffusion factor, 300
 - elementary airfoil theory, 280–2
 - incidence rule, 301–3
 - laminar-flow airfoils, 283–4
 - performance characteristics of axial-flow compressors, 311–13
 - radial equilibrium, 299–300
 - stall analysis of axial-flow compressors, 313–17
 - velocity triangles, 292–4
 - centrifugal, 221–74
 - centrifugal flow, 30–2
 - maintenance, 754–5
 - modules, 703–4
 - performance characteristics, 112, 130–2
 - aerothermal equations, 117–22
 - dimensional analysis, 125–30
 - efficiencies, 122–5
 - performance characteristics of
 - axial-flow, 311–13
 - process centrifugal, 266–72
 - stall analysis of axial-flow, 313–17
 - stalls, 308–11
 - individual blade stall, 311
 - rotating stall, 308–11
 - stall flutter, 311
 - surges, 254–66, 680–1
 - washing, 455–6

- Compressors, aerothermal characteristics, 680–1
- Compressors, blades, 427
- Condition monitoring system,
 - implementation of, 651–6
 - on-line optimization process, 654–6
 - plant power optimization, 653–4
- Condition monitoring systems, 645–9
- Continuity equation, 117
- Control systems, 635–45
 - and instrumentation, 634–91
 - auxiliary system monitoring, 671–7
 - condition monitoring systems, 645–9
 - failure diagnostics, 681–7
 - implementation of condition monitoring system, 651–6
 - life cycle costs, 656–4
 - mechanical problem diagnostics, 687–9
 - monitoring software, 649–51
 - pressure measurement, 667–8
 - temperature measurement, 665–7
 - vibration measurement, 668–71
 - startup sequence, 642–5
 - generator protection, 645
 - shutdown, 644
 - starting preparations, 642–3
 - startup description, 643–4
- Control systems and instrumentation,
 - gas turbine, 677–81
 - compressor aerothermal characteristics and compressor surge, 680–1
 - identification of losses, 680
- Cooling systems, absorption, 99
- Cooley-Tukey method, 564
- COP (coefficient of performance), 99
- Coriolis acceleration, 252
- Coriolis circulation, 239
- Corrosion, 418–22
- Costs, life cycle, 656–64
- Coupling lockkeys, 522
- Coupling lockup, 528
- Coupling maintenance, 760
- Couplings
 - and alignment, 605–33
 - shaft alignment, 624–32
 - turbomachinery uprates, 619–24
 - continuously lubricated, 612–13
 - failure modes, 613–14
 - functions, 605
 - gear, 608–14
 - grease-packed, 612
 - lock keys, 522
 - lock up, 528
 - metal diaphragm, 614–18
 - metal disc, 618–19
 - oil-filled, 612
- Creep and rupture, 413–15
- Critically damped system, 184–5
- Critical speed calculations, 195–8
- Critical speed map, 194
- Curtis turbine, 345–6
- Cycle analysis
 - actual, 68–85
 - Brayton-Rankine cycle, 84–5
 - evaporative regenerative cycle, 81–4
 - intercooled regenerative reheat cycle, 76–7
 - intercooled simple cycle, 73–5
 - regenerative cycle, 72–3
 - reheat cycle, 76
 - simple cycle, 68–70
 - split-shaft simple cycle, 70–2
 - steam injection cycle, 77–81
 - summation of, 85–7
 - theoretical and actual, 58–111
 - actual cycle analysis, 68–85
 - Brayton cycle, 58–68
 - CAES (Compressed Air Energy Storage Cycle), 93–5
 - general overview of combined cycle plants, 87–93
 - power augmentation, 95–105
 - summation of cycle analysis, 85–7
 - summation of power augmentation systems, 105–10
 - theoretical and actual, power augmentation
 - combination of evaporative and refrigerated inlet systems, 99–101
 - injection of compressed air, steam, or water, 96
 - injection of compressed air, steam, or water for increasing power, 101–5
 - inlet cooling, 96
 - inlet cooling techniques, 96–9
 - mid compressor flashing of water, 101–3
 - thermal energy storage systems, 101
- Cycle plants, general overview
 - of combined, 87–93

Energy Distribution, 88
 HRSG, 90–3
 Load Sharing, 89
 Cycle, steam injection, 77–81
 Cyclic fatigue, 416–17

D

D-CS (Distributed Control Systems),
 634, 653, 654
 Damped system, 182–6
 critically, 184–5
 critically damped system, 184–5
 overdamped system, 184
 underdamped system, 185–6
 Damping factor, 184, 585
 Data
 retrieval, 689
 taping, 568–9
 trending, 674–7
 Deflection angle, *See* Air turning angle
 Degrees of freedom, 179
 Degree of reaction, 294, 325, 340
 Deviation
 angle, 303
 rule, 303–8
 Diagnostics, 681, 687–9
 combustors, 682–4
 compressors, 683–4
 mechanical problems, 687–89
 turbines, 684–5
 Diagnostic system(s)
 aerothermal data collection, 661
 components and functions, 658–9
 data inputs, 659
 data retrieval, 689
 instrumentation, 659–60
 requirements of, 647–8
 vibration instrumentation, 668–70
 Diagrams
 Campbell, 211–16
 impulse, 343–4
 symmetrical, 344
 zero exit swirl, 343
 Diffusers, 243–6
 Diffusion factor, 300
 Dimensional analysis, 125–30
 Flow Coefficient, 127

Pressure Coefficient, 127
 Reynolds Number, 127
 Specific Speed, 126
 Wobbe Index, 383
 Discrete Fourier transform.
See Fourier transformation
 Displacement transducers, 565–6
 DLE (Dry Low Emissions), 394,
 397, 398, 400, 402
 DLN (Dry Low NO_x), 394
 DOE (Department of Energy), 44
 Drag coefficient, 281
 Dry-friction whirl, 207–8
 Dry gas seals, 515–19
 Dry low NO_x combustor, 397–403
 DS (directional solidification), 49, 424
 Ductility and fracture, 415–16
 Dynamic pressure transducers, 567–8

E

Economic Comparisons, 8
 Economic Cycles, 6–9
 Economics, fuel, 41–2, 456–8
 Economic, prime movers, 3–5
 Efficiencies, 122–3
 adiabatic efficiency, 122–4
 polytropic efficiency, 124–5
 Efficiency
 adiabatic, 122–4
 polytropic, 124–5
 Electric tracing, 462
 Electromechanical systems and
 analogies, 198–211
 forces acting on rotor bearing system, 200–1
 rotor bearing system instabilities, 201–4
 self-excited instabilities, 204–11
 Elementary airfoil theory, 280–1
 attack, angle of, 280–2
 components of, 281
 Elevated tanks, 463
 Elgi leakage formulae, 498
 Enclosures, 147
 Energy equation, 121–2
 Environmental effects, 43–4
 EPA (Environmental Protection
 Agency), 84, 393
 EPRI (Electric Power Research
 Institute), 646

- Equations
 - aerothermal, 117–22
 - continuity equation, 117
 - energy equation, 121–2
 - momentum equation, 118–21
 - state 113–14
- Equipment, maximization of efficiency and effectiveness, 725–7
- Euler
 - turbine equation, 119–21, 227, 230, 293, 323, 348
 - work distribution, 232
- Eulerian motion, 113
- identities, 561
- Evaporative regenerative cycle, 81–4
- Expander module, 705

- F**
- Face seals, 501–7
- Failure diagnostics, 681–7
 - combustor analysis, 683–4
 - compressor analysis, 682
 - turbine analysis, 684–5
 - turbine efficiency, 685–7
- Fast Fourier transform. *See* Fourier transformation
- Fatigue
 - cyclic, 416–17
 - thermal, 417–18
- FFT (fast Fourier transform), 559, 670, 671
- Flexible shaft, 192–5
- Flow coefficient, 127
- Fluid-film lubrication. *See* Bearings
- Fluids. *See* Aerothermodynamics
- Fixed roof tanks, 463–4
- Fixed seal rings, 501
- Flexible supports, 193–5
- Floating roof tanks, 464
- Floating seal rings, 501
- Flow straighteners, 694–700
 - flow measurement, 699–700
 - pressure measurement, 695–7
 - temperature measurement, 698
- Flutter, 582
- FOD (foreign object damage), 432
- Forced vibrations, 186–9
- Foundations, 765
- Fouling indicators, 748–9
- Forgings and nondestructive testing, 427–9
- Fourier transformation, 559
 - Cooley-Tukey method, 564
- Fracture, and ductility, 415–16
- Frame type heavy-duty gas turbines, 16–18
- Free system, undamped, 181–2
- Frequency, natural, 189
- Frequency domain, 559
- Fuel economics, 456–8
- Fuel properties, 443–7
- Fuel specifications, 440–3
- Fuel treatment, 447–52
- Fuel type, 40–2
- Fuels, 436–65
 - ash content, 441
 - availability, 440
 - carbon residue, 441, 444
 - cleanliness, 440–1, 454–5
 - cleaning of turbine components, 454–6
 - corrosivity, 440
 - deposition and fouling tendencies, 440
 - economics, 456–8
 - flash point, 443
 - gaseous, 436, 441
 - heating value, 440
 - heavy, 452–6
 - inhibitors, 450
 - liquid, 436–7, 442–3
 - luminosity, 444
 - operating experience, 458
 - pour point, 441
 - properties, 443–7
 - specific gravity, 444
 - specifications, 440–3
 - sulfur content, 442
 - treatment, 447–52
 - heat tracing of piping systems, 459–61
 - heavy, 452–3
 - heavy fuels, 452–3
 - operating experience, 458–9
 - storage of liquids, 462–5
 - type of, 146–7
 - types of heat-tracing systems, 461–2
- Fuel atomization and ignition, 381–3
- Fuel monitoring system
 - Btu meter, 671–2
 - water content monitor, 671–2
- Fuel system fouling, 452

- Fuel treatment, 334–9
 - centrifugal separators, 448–9
 - electrostatic separators, 448–9
- Frequency domain, 559
- G**
- Gas composition, effects of, 261–2
- Gaseous fuels. *See* Fuels
- Gas, ideal, 113–15 *See* Aerothermodynamics
- Gas turbine applications, variables for, 141–8
- Gas turbine components, major, 26–40
- Gas turbines
 - aircraft-derivative, 18–20
 - application of mechanical standards to, 156–75
 - categories of, 16–26
- design considerations, 11–15
- frame type heavy-duty, 16–18
- increasing work output of simple cycle, 65–8
- industrial type, 20–2
- materials, 422–7
- overview of, 3–57
 - categories of gas turbines, 16–26
 - coatings, 49–50
 - environmental effects, 43–4
 - fuel type, 40–2
 - gas turbine cycle in cogeneration mode, 3–9
 - gas turbine cycle in combined cycle, 3–9
 - gas turbine design considerations, 11–15
 - gas turbine heat recovery, 50–3
 - gas turbine performance, 9–11
 - major gas turbine components, 26–40
 - materials, 48–9
 - supplementary firing of heat recovery systems, 54–6
 - turbine expander section, 44–7
- performance calculations, 710–19
- performance tests, 692–721
- performances, 9–11
- power turbine, 15–21, 55
- problems, 768–76
- reliability factor, 14
- serviceability, 14
- shaft alignment, 624–31
- shutdown, 644
- small, 16, 22–4, 28, 30
- startup, 642–3, 767
- tests, 700–2
- Gearbox
 - alignment, 535–6
 - baseplate, 536
 - bearing types, 529–30
 - installation and operation, 535–7
 - oil system, 536–7
 - spray nozzles, 537
- Gear coupling failure modes, 613–14
- Gear couplings, 608–14
- Gear design, factors affecting, 524–32
 - gear accuracy, 529
 - gear housings, 531
 - helix angle, 526–8
 - lubrication, 531–2
 - pressure angle, 525–6
 - scoring, 528–9
 - service factor, 530–1
 - tooth hardness, 528
 - types of bearings, 529–30
- Gear types, 522–4
- Gears, 163–6, 521–38
 - factors affecting gear design, 524–32
 - gear types, 522–4
 - installation and initial operation, 535–7
 - manufacturing processes, 532–5
 - gear noise, 534–5
 - gear rating, 533–4
 - grinding, 533
 - hobbing, 532
 - hobbing and lapping, 533
 - hobbing and shaving, 532
 - housings, 531
 - installation and initial operation, 535–7
 - lubrication, 531–2
 - manufacturing processes, 532–5
 - noise, 534–5
 - overlap ratio, 527
 - pressure angle, 525–6
 - rating, 533–4
 - scoring, 528
 - service factor, 530–1
 - standards. *See* AGMA
 - tooth hardness, 528
 - types, 522–4
- Gear mesh frequencies, 570

Goodman Diagram, 417
 Grease-packed couplings, 612
 GUIs (Graphical User Interfaces), 648

H

H-S diagram, 325
 Half-frequency whirl, 487
 Harmonic motion, 180–1
 Heat-recovery steam generators, 50–3
 Heat recovery, gas turbine, 50–3
 Heat recovery systems, supplementary
 firing of, 54–6
 instrumentation and controls, 55–6
 Heat tracing of piping systems, 459–61
 Heat-tracing systems, types of, 461–2
 electric tracing, 462
 stream tracing systems, 461–2
 Heavy fuels, 452–3
 Helmholtz vorticity law, 239
 Horizontally split casings, 266–7
 Hot corrosion mechanism, 418, 420, 443
 Hot-section maintenance, 751–4
 Hot section wash, 454–5
 HP (High Pressure Section), 92–5
 HPP (Hybrid Power Plants), 5
 HRSGs (Heat Recovery Steam Generators),
 50, 51, 58, 88, 89, 92, 104, 147, 646, 680
 Hub-to-tip ratio. *See* Aspect ratio
 Hydrocarbons, unburnt, 392
 Hysteretic whirl, 206–7

I

Ideal gas, 113–15
 Ignitor plug, 382–3
 IGV (Inlet Guide Vanes), 90, 710
 IGVs (inlet guide vanes), 223, 229–32
 Impeller fabrication, 269–72
 electron beam technique, 271
 materials, 271–2
 slot welding technique, 271
 Impeller fabrication, 269–72
 Impellers, Design 223–41
 inlet guide vanes 223, 229–32
 causes of slip in, 238–41
 boundary-layer development, 239–40
 Coriolis circulation, 239
 leakage, 240

 number of vanes, 240
 vane thickness, 240
 centrifugal sections of, 237–8
 Impulse diagrams, 343–4
 Impulse turbines, 344–8
 Incidence rule, 301–3
 Inducers, 236–7
 camberlines, 236, 278–9
 inlet (impeller eye), 230
 systems, 225
 Inlet guide vanes, 229–32
 nonprewhirl, 230
 prewhirl, 229–32
 types, 229–32
 Influence coefficient method, 594
 See also Balancing
 Inlet cooling techniques, 96–9
 evaporative cooling of turbines, 96–8
 refrigerated inlets for
 gas turbines, 98–9
 Instrumentation, control
 systems and, 634–91
 Intercooled regenerative
 reheat cycle, 76–7
 Intercooled simple cycle, 73–5
 Intercooling and
 reheat effects, 65–8
 IP (Intermediate Pressure Section), 92, 93
 Isentropic efficiency, 327–28
 Isentropic flow. *See* Compressibility

J

Journal bearings, 476–9

K

Karman vortices, 311
 Keyphazor, 591
 Kronecker delta, 595

L

Labyrinth seals, 495–99
 Laminar-flow airfoils, 283–4
 Lagrangian motion, 113
 Larson-Miller parameters, 414–16,
 424–5, 680

Lift coefficient, 279
 LCC (life cycle costs), 730
 LCF (low-cycle fatigue), 49, 424
 Li-Br (lithium-bromide), 99
 Life cycle costs, 656–64
 criteria for collection of
 aerothermal data, 661
 data inputs, 659
 desirable instrumentation, 660–1
 diagnostic system components
 and functions, 658–9
 instrumentation requirements, 659–60
 pressure drop in filter system, 661–4
 pressure measurement for
 compressors and turbines, 664
 temperature measurement for
 compressors and turbines, 664
 typical instrumentation, 660
 Liner cooling, 378–80
 air-film method, 380
 Liquid fuels. *See* Fuels
 Liquids, storage of, 462–5
 atmospheric tanks, 462–3
 elevated tanks, 463
 fixed roof tanks, 463–4
 floating roof tanks, 464
 open tanks, 463
 pressure tanks, 464–5
 Low-stress high-cycle fatigue, 579
 Losses
 rotor, 250–3
 stator, 253–4
 Losses, axial, 424–5
 LP (Low Pressure Section), 92–5
 Lubrication, 541–57
 Alarms, 547
 basic oil system, 541–8
 lubrication oil system, 542–7
 seal oil system, 547–8
 cleaning and flushing, 553–4
 coupling lubrication, 554–5
 filter selection, 551–3
 lubricant selection, 549
 lubrication management program, 555–6
 nitrogen purge, 542
 reservoir retention time, 542
 oil contamination, 550–1
 oil sampling and testing, 549–50
 systems, 166–8, 541–7

M

Mach number, 30–2, 115–17
 Relative
 Machinery startup
 procedures, large, 767
 Maintenance
 bearing, 755–60
 clearance checks, 756
 thrust-bearing failure, 757–60
 communications, 742–4
 compressor, 754–5
 coupling, 760
 hot-section, 751–4
 philosophy of, 722–31
 implementation of productive
 maintenance, 728–31
 maintenance department
 requirements, 731
 maximization of equipment efficiency
 and effectiveness, 725–7
 organization structures for maintenance
 program, 728
 scheduling, 740–1
 Maintenance techniques, 722–77
 bearing maintenance, 755–60
 compressor maintenance, 754–5
 coupling maintenance, 760
 hot-section maintenance, 751–4
 large machinery startup procedure, 767
 philosophy of maintenance, 722–31
 rejuvenation of used turbine blades, 761–4
 repair and rehabilitation of turbomachinery
 foundations, 764–7
 tools and shop equipment, 735–47
 borescope inspection, 747
 condition and life assessment, 737–8
 inspection, 744–6
 maintenance communications, 742–4
 maintenance scheduling, 740–1
 redesign for higher machinery reliability,
 738–40
 spare parts inventory, 736–7
 training of personnel, 731–5
 type of personnel, 731–2
 type of training, 732–5
 turbomachinery cleaning, 747–51
 typical problems encountered in gas
 turbines, 768–76

- Materials, 48–9, 411–35
 - bearing, 486–7
 - coatings, 429–35
 - future coatings, 434–5
 - shroud coatings, 434
 - compressor blades, 427
 - forgings and nondestructive testing, 427–9
 - gas turbine, 422–7
 - turbine wheel alloys, 425–7
 - gas turbine materials, 422–7
 - general metallurgical behaviors in gas turbines, 413–22
 - corrosion, 418–22
 - creep and rupture, 413–15
 - cyclic fatigue, 416–17
 - ductility and fracture, 415–16
 - thermal fatigue, 417–18
 - Goodman diagram, 417
 - Larson-Miller Parameters, 416–18
 - Mechanical drives, 143
 - Mechanical parameters, 150–6
 - Mechanical seal selection and application, 507–11
 - Mechanical seals, 501–7
 - Mechanical standards
 - application to gas turbine, 156–75
 - gears, 163–6
 - lubrication systems, 166–8
 - vibration measurements, 168–75
 - and performance, 141–77
 - application of mechanical standards to gas turbine, 156–75
 - mechanical parameters, 150–6
 - variables for gas turbine application, 141–8
 - Meridional
 - plane, 232–5
 - velocity, 120, 240
 - Metal diaphragm couplings, 614–18
 - Metal disc couplings, 618–19
 - Metallurgical behaviors
 - creep and rupture, 413–15
 - cycle fatigue, 416–17
 - ductility and fracture, 415–16
 - thermal fatigue, 417–18
 - corrosion, 418
 - MI (maintainability improvement), 724
 - Misalignment, 203, 578
 - Micro-turbines, 24–6
 - Modal balancing, 592–4
 - Modules
 - air inlet filter, 703
 - combustor, 704
 - compressor, 703–4
 - expander, 705
 - Momentum equation, 118–21
 - Monitoring and diagnostic systems, 647–9
 - Monitoring software, 649–51
 - MP (maintenance prevention), 724
 - Multiplane balancing, 594–7
 - user's guide for, 600–2
 - MVT (multi-venturi tube) fuel, 407
- ## N
- Na₂SO₄ (sodium sulfate), 429
 - NACA (National Advisory Committee for Aeronautics), 279, 284, 304
 - NASA (National Aeronautics and Space Administration), 279, 362
 - Natural frequency, 189
 - Newtonian approach, 183, 186
 - Nitrogen, oxides of, 392–7
 - Noncontacting seals, 494–501
 - Nondestructive testing, forgings and, 427–9
 - NO_x combustor, dry low, 397–403
 - NO_x (nitrogen oxides), 15, 43–4, 55, 392–7, 403, 404, 700
 - NO_x prevention, basis for, 395–7
 - Nozzle
 - bowing, 770
 - efficiency, 325–6
 - vanes, 321–3
- ## O
- O&M (operation and maintenance), 99, 645
 - OEM (original equipment manufacturer), 736, 737
 - Oil
 - contamination, 550–1
 - coolers, 545–6
 - sampling and testing, 549–550
 - Oil-filled couplings, 612
 - Oil system, associated, 513–14

- Oil whirl, 206–10, 488, 570
- On-line optimization process, 654–6
- Open tanks, 463
- Optimum pressure ratio, 61
- Oscillatory function, 559–60
- Orbital balancing, 591–2
- OTSG (Once Through Steam Generators), 51
- Overdamped system, 184
- Oxidation, 418–21
- Oxides of nitrogen (NO_x), 392–7, 403, 404

- P**
- Performance
 - centrifugal compressor, 249–54
 - rotor losses, 250–3
 - stator losses, 253–4
 - characteristics
 - compressor, 112, 130–2
 - turbine, 112, 132–3
 - characteristics of axial-flow compressors, 311–13
 - codes, 693–4
 - curves, 706–7
 - gas turbine, 9–11
 - and mechanical standards, 141–77
 - performance standards, 148–50
 - variables for gas turbine application, 141–8
 - of radial-inflow turbine, 332–5
 - standards, 148–50
- Performance computation, gas turbine, 134–40
- Performance test, gas turbine,
 - 692–721, 702–6
 - air inlet filter module, 703
 - combustor module, 704
 - compressor module, 703–4
 - expander module, 705
 - flow straighteners, 694–700
 - gas turbine test, 700–2
 - life cycle and hot section components, 706
 - performance codes, 693–4
 - performance computations, 707–19
 - gas turbine performance calculations, 710–19
 - general governing equations, 707–10
 - performance curves, 706–7
 - plant losses, 719–20
- Periodic
 - loading, 204
 - motion, 180
- Phase angle, 180–1
- Piping systems, heat tracing of, 459–61
- Pitch, 279
- Pitot-tube traverse, 697
- Plant
 - locations, 144
 - losses, 719–20
 - power optimization, 653–4
- Plant operation mode: base or peaking, 147
- Polytropic
 - Compression, 124
 - efficiency, 124–5
 - head, 127
- Power augmentation, 95–105
- Power augmentation systems, summation of, 105–10
- Power generation, 143–4
- Power, injection of compressed air, steam, or water for increasing, 101–5
 - combination of evaporative cooling and steam injection, 104–5
 - injection of humidified and heated compressed air, 102–3
 - injection of steam in combustor of gas turbines, 104
 - injection of water or steam at gas turbine compressor exit, 103–4
 - mid-compressor flashing of water, 101–2
- Power-spectrum function, 564
- Pressure
 - coefficient, 127
 - measurement, 667–8
 - ratio, 3, 9–12, 14, 16, 20, 23, 26–7, 30, 32, 35, 47
 - static, 23, 114
 - total, 24, 115
- Pressure tanks, 464–5
- Pretwist angle, 279
- Prew whirl, 231–2
 - control vortex, 232
 - forced vortex, 231
 - free-vortex, 231
- Problem diagnostics, mechanical, 687–9
- Problems, air pollution, 392–403
- Problems, noise, 335

- Process centrifugal compressors, 266–72
 - casing material, 266
 - classification, 266–7
 - compressor configuration, 268–9
 - impeller fabrication, 269–72
- Propulsion, aircraft, 142–3
- PTPM (performance based total productive maintenance), 723–4, 729–31
- Pyrometers, 666–7

- Q**
- Quasi-three-dimensional flow, 232, 333

- R**
- Radial equilibrium, 299–300
- Radial-inflow turbines, 319–36
 - advantages, 319
 - cantilever-type, 320–1
 - description, 320–3
 - design, 329
 - losses, 330–2
 - mixed-flow, 320–2
 - noise problems in, 335
 - performance of, 332–5
 - performance of radial-inflow turbine, 332–5
 - problems, 335
 - theory, 323–8
 - turbine design considerations, 329–30
- Ratteau turbine, 345, 346
- Reaction turbine, 348–51
- Real-time analyzer (RTA), 558, 559, 574
- Recuperative heat exchanger, 22, 65
- Regenerative cycle, 72–3
- Regenerators, 32–3
- Reheat cycle, 76
 - intercooled regenerative, 76–7
- Reheat effects, intercooling and, 65–8
- Reheat factors, 328
- Relative
 - eddy motion, 241–3
 - Mach number, 230–2
 - velocity, 119–120, 292
- Reliability, 14, 737–8
- Residual fuels, 437
- Resistive thermal detectors (RTD), 665
- Reversible adiabatic flow, 113
- Reynolds number, 126, 127, 223, 320, 483
- RGT (Recuperative Gas Turbine), 5
- Rigid-body critical, 194
- Rigid supports, 192–3
- Ring seals, 499–501
- Rolling bearings, 469–76
- Roof tanks
 - fixed, 463–4
 - floating, 464
- Rotating machines, application to, 192–5
 - flexible supports, 193–5
 - rigid supports, 192–3
- Rotating stall, 308–11
- Rotor bearing systems
 - critical speed calculations for, 195–8
 - forces acting on, 200–1
 - forces applied to rotor, 201
 - forces generated by rotor motion, 201
 - forces transmitted to casing and foundations, 200–1
 - instabilities, 201–4
 - forced (resonant) vibration, 203–4
 - periodic loading, 204
- Rotor dynamics, 178–217
 - application to rotating machines, 192–5
 - Campbell diagram, 211–16
 - critical speed calculations for rotor bearing systems, 195–8
 - electromechanical systems and analogies, 198–211
 - mathematical analysis, 178–92
 - damped system, 182–6
 - design considerations, 189–92
 - forced vibrations, 186–9
 - undamped free system, 181–2
- Rotor efficiency, 326
- Rotor imbalance, 584–91
- Rotor losses, 250–3
 - clearance loss, 252
 - diffusion-blading loss, 251
 - disc friction loss, 250–1
 - incidence loss, 250
 - shock in rotor losses, 250
 - skin friction loss, 252
- Rotors, whirl from fluid trapped in, 210–11
- RTAs (real-time analyzers), 559
 - subsynchronous vibration analyses using, 574–6
- RTDs (resistive thermal detectors), 493, 665, 666

- Rules
 - deviation, 303–8
 - incidence, 301–3
 - Runaway speed, 329
 - Rupture, creep and, 413–15
- S**
- SCGT (Simple Cycle Gas Turbine), 5
 - Scroll, 247–9
 - Seal rings
 - fixed, 501
 - floating, 501
 - Seal selection and application,
 - mechanical, 507–11
 - arrangement considerations, 509–10
 - balance, 503
 - buffering, 505
 - components, 502
 - differential thermal expansion, 501
 - Elgi leakage formulae, 498
 - equipment, 510
 - face combinations, 510
 - fixed seal rings, 501
 - floating seal rings, 501
 - gland plate 510–11
 - labyrinth, 495–9
 - leakage, 497–500
 - main seal body, 511
 - mechanical face, 371–6
 - miscellaneous product considerations, 509
 - noncontacting, 494–5
 - oil system, 513–4, 547
 - product, 507–8
 - ring (bushing), 499–500
 - secondary packing, 510
 - selection and application, 507–8
 - systems, 511–13
 - windback type, 499
 - Seal systems, 511–13
 - Seals, 469, 493–4
 - associated oil system, 513–14
 - bushing, 499–501
 - dry gas, 515–19
 - dry gas seal degradation, 517–19
 - dry gas seal materials, 517
 - dry gas seal systems, 517
 - operating range, 516–17
 - face, 501–7
 - labyrinth, 495–9
 - mechanical, 501–7, 507–11
 - noncontacting, 494–501
 - ring, 499–501
 - Self-acting bearing, 479
 - Self-excited instabilities, 204–11
 - aerodynamic whirl, 209–10
 - dry-friction whirl, 207–8
 - hysteretic whirl, 206–7
 - oil whirl, 208–9
 - whirl from fluid trapped in rotor, 210–11
 - Shaft alignment, 624–32
 - procedure, 624–32
 - cold alignment, 626–30
 - hot alignment check, 630–2
 - prealignment survey, 625–6
 - Shaft instabilities, bearing and, 487–8
 - Shop equipment, tools and, 735–47
 - Shrouded impeller, 269
 - Shroud coatings, 434
 - Signal-to-noise ratio, 558–9, 566–7, 569
 - Simple harmonic vibration, 565
 - Site configuration, 144
 - Slip factor
 - Stanitz, 243
 - Stodola, 241–3
 - Smoke, 392
 - Software, monitoring, 649–51
 - Solidity, 279
 - Specific
 - diameter, 127
 - speed, 126
 - Specifications, fuel, 440–3
 - Specification, Gas Turbine, 172–3
 - Specifications, Centrifugal Compressor, 173–5
 - Spectrum analysis, 558–83
 - interpretation of vibration spectra, 569–74
 - subsynchronous vibration
 - analysis using RTA, 574–6
 - synchronous and harmonic spectra, 576–83
 - taping data, 568–9
 - vibration measurement, 564–8
 - Split-shaft simple cycle, 70–2
 - ST (Steam Turbine Plant), 5
 - ST (Steam Turbine plant), 640

- Stall
 - analysis of axial-flow compressors, 313–17
 - compressor, 308–11
 - flutter, 311
 - individual blade, 311
 - rotating, 308–11
 - Standards
 - Mechanical, 150–71
 - Performance, 148–50
 - Stanitz slip factor, 243
 - Startup
 - procedure, 642–3
 - sequence, 642
 - techniques, 147
 - Static
 - pressure, 113
 - temperature, 114
 - Stator losses, 253–4
 - exit loss, 254
 - recirculating loss, 253
 - vaned diffuser loss, 254
 - vaneless diffuser loss, 254
 - wake-mixing loss, 253
 - STC (steam turbine), 640
 - Steam injection cycle, 77–81
 - Steam, injection of, 101–5
 - Stodola slip factor, 241–3
 - Stone walling, 131, 255
 - Stream tracing systems, 461–2
 - Subsynchronous vibration, 574–6
 - Sulfidation, 418, 442, 444
 - Supports
 - flexible, 193–5
 - rigid, 192–3
 - Surface temperatures, 404–6
 - Surge, compressor, 254–66, 680–1
 - dynamic, 264
 - effects of gas composition, 261–2
 - effects of surge, 262–3
 - external causes, 262–3
 - static, 263
 - surge detection and control, 263–6
 - Surge detection and control, 263–6
 - Swirl diagram, zero exit, 343
 - Symmetrical diagram, 344
 - Systems
 - absorption cooling, 99
 - combination of evaporative and refrigerated inlet, 99–101
 - control, 634–91
 - critical speed calculations for
 - rotor bearing, 195–8
 - critically damped, 184–5
 - damped, 182–6
 - dry gas seal, 517
 - electromechanical, 198–211
 - forces acting on rotor bearing system, 200–1
 - rotor bearing system instabilities, 201–4
 - self-excited instabilities, 204–11
 - heat tracing of piping, 459–61
 - lubrication, 166–8
 - overdamped, 184
 - seal, 511–13
 - stream tracing, 461–2
 - summation of power augmentation, 105–10
 - supplementary firing of heat recovery, 54–6
 - thermal energy storage, 101
 - types of heat-tracing, 461–2
 - undamped free, 181–2
 - underdamped, 185–6
- T**
- Tangential velocity, 247
 - Tanks
 - atmospheric, 462–3
 - elevated, 463
 - fixed roof, 463–4
 - floating roof, 464
 - open, 463
 - pressure, 464–5
 - Taping data, 568–9
 - Tape recorders, 568–9
 - AM, 568
 - FM, 568
 - roll-off frequency, 568
 - Taylor Series, 124,
 - TBCs (Thermal Barrier Coatings), 384, 385, 403
 - Temperature
 - measurement, 665–7
 - pyrometers, 666–7
 - RTDs (resistive thermal detectors), 666
 - thermocouples, 665–6
 - ratio, 12

- static, 113
 - total, 113
 - Temperatures, surface, 404–6
 - Testing, forgings and nondestructive, 427–9
 - Tests
 - cascade, 284–92
 - gas turbine, 700–2
 - gas turbine performance, 692–721
 - Thermal fatigue, 417–18
 - Thermocouples, 665–6
 - Three-dimensional theory, 232
 - Thrust-bearings, 488–9
 - designs, 489–93
 - failure, 757–8
 - power losses, 493
 - temperature monitoring systems, 493, 758–60
 - Tilting-pad journal bearings, 483–6
 - Tip
 - clearance loss, 365–6
 - speed, 319
 - speed ratio, 329
 - Tools and shop equipment, 735–47
 - Torque. *See* Couplings
 - Torque measurement, 662
 - Torsional forces, 621–4
 - Total
 - pressure, 113
 - temperature, 115
 - TPM (Total Productive Maintenance), 723
 - Tracing, electric, 462
 - Tracking filter, 559
 - Transducers
 - acceleration, 566–7
 - displacement, 565–6
 - dynamic pressure, 567–8
 - velocity, 566
 - Transfer function analysis, 573
 - Triangles, velocity, 292–4
 - Trouble-shooting, 571
 - Turbine blades, rejuvenation of
 - used turbine blades, 761–4
 - Turbine components, cleaning of, 454–6
 - compressor washing, 455–6
 - hot section wash, 454–5
 - Turbines
 - radial-inflow
 - turbine design considerations, 329–30
 - reaction, 348–51
 - Turbines; *See also* Micro-turbines
 - axial-flow, 337–69
 - expander sections
 - axial-flow turbines, 46–7
 - mixed-flow turbine, 44–6
 - radial-inflow turbine, 44
 - impulse, 344–8
 - performance characteristics, 112, 132–3
 - aerothermal equations, 117–22
 - efficiencies, 122–5
 - gas turbine performance
 - computation, 134–40
 - turbomachine aerothermodynamics, 112–17
 - radial-inflow, 319–36
 - description, 320–3
 - noise problems in, 335
 - performance of radial-inflow turbine, 332–5
 - theory, 323–8
 - turbine design considerations, 329–30
 - wheel alloys, 425–7
 - Turbomachine aerothermodynamics, 112–17
 - compressibility effect, 115–17
 - dimensional analysis, 125–30
 - ideal gas, 113–15
 - Turbomachinery
 - cleaning, 747–51
 - cleaning techniques, 749–51
 - fouling indicators, 748–9
 - foundations, repair and rehabilitation of, 764–7
 - increasing mass and rigidity, 766–7
 - installation defects, 764–6
 - uprates, 619–24
- ## U
- UHC (unburnt hydrocarbon), 392
 - Unbalances, 189–92
 - sources of, 584–7
 - Unburnt hydrocarbons, 392
 - Undamped free system, 181–2
 - Underdamped system, 185–6
 - Uprates Couplings, 619–24
 - Utilization factor, 324

V

- Vanadium, 418, 422, 436–8
- Vaporized fuel oil (VFO), 436, 451–2
- Variables for gas turbine application, 141–8
 - enclosures, 147
 - gas turbine size and efficiency, 144–6
 - plant location, 144
 - plant operation mode: base or peaking, 147
 - site configuration, 144
 - start-up techniques, 147
 - type of application, 142–4
 - type of fuel, 146–7
- Velocity diagrams, 342–4
 - impulse diagram, 343–4
 - symmetrical diagram, 344
 - zero exit swirl diagram, 343
- Velocity transducers, 566
- Velocity triangles, 292–4
 - absolute, 46, 117–20
 - axial, 340
 - diagrams axial compressors, 292–300
 - diagrams axial turbine, 340–50
 - diagrams centrifugal compressors, 229–31
 - diagrams radial turbine, 324–30
 - impulse diagram, 343–4
 - meridional, 229–31,
 - relative, 46, 117–20, 229–31, 339–44
- Vibration measurement, 168–75,
 - 564–8, 668–71
 - acceleration transducers, 566–7
 - displacement transducers, 565–6
 - dynamic pressure transducers, 567–8
 - forced, 203–7
 - instrumentation, 167–71, 668–70
 - monitoring system, 537
 - selection of systems for analysis of
 - vibration data, 670–1
 - severity charts, 490

- velocity transducers, 566
- vibration instrumentation selection,
 - 668–70

- Vibration measurements,
- Vibration spectra, interpretation
 - of, 569–74
- Vibrations, forced, 186–9
- Viscous damping, 182, 183
- Volute, 247–9

W

- Wash, hot section, 454–5
- Washing, compressor, 455–6
- Water, injection of, 101–5
- Wheel alloys, turbine, 425–7
 - 12 Cr alloys, 426–7
 - A286 alloy, 427
 - alloy 706 nickel-based alloy, 425
 - alloy 718 nickel-based alloy, 425
 - Cr-Mo-V alloy, 425–6

Whirl

- aerodynamic, 209–10
- dry-friction, 207–8
- from fluid trapped in rotor, 210–11
- hysteretic, 206–7
- oil, 208–9

Wobbe Index, 383

Work factor, 337, 341–2

Y

Yttrium, 433

Z

- Zero exit swirl diagram, 343
- Zero pre whirl, 229

About the Author



Dr. Meherwan P. Boyce, P.E., Fellow ASME & IDGTE; has over 35 years of experience in the field of Turbomachinery in both industry and academia. His industrial experience covers twenty years as Chairman and CEO of Boyce Engineering International, and five years as a designer of compressors and turbines for gas turbines for various gas turbine manufacturers. His academic experience covers a fifteen year period, which includes the position of Professor of Mechanical Engineering at Texas A&M University and Founder of the Turbomachinery Laboratories and the Turbomachinery Symposium, which is now in its thirtieth year. He is the

author of several books including *Gas Turbine Engineering Handbook* (Gulf Professional Publishing), *Cogeneration and Combined Cycle Power Plants* (ASME Press), and *Centrifugal Compressors, A Basic Guide* (PennWell Books). He is a contributor to several handbooks; his latest contribution is to the *Perry's Chemical Engineering Handbook Seventh Edition* (McGraw Hill) in the areas of transport and storage of fluids, and gas turbines. Dr. Boyce has taught over 100 short courses around the world attended by over 3,000 students representing over 400 companies. He is a consultant to the aerospace, petrochemical and utility industries globally, and is a much-requested speaker at universities and conferences throughout the world.

Dr. Boyce has authored more than 100 technical papers and reports on Gas Turbines, Compressors Pumps, Fluid Mechanics, and TurboMachinery. He is a Fellow of the ASME, and the Institute of Diesel and Gas Turbine Engineers, U.K., and member of SAE, NSPE and several other professional and honorary societies. He is also a registered professional engineer in Texas.

Dr. Boyce received a B.S. and M.S. in mechanical engineering from the South Dakota School of Mines and Technology and the State University of New York, respectively, and a Ph.D. (aerospace & mechanical engineering) from the University of Oklahoma.

